R-08-99

Fracture mineralogy Laxemar

Site descriptive modelling SDM-Site Laxemar

Henrik Drake
Isochron Geoconsulting HB

Eva-Lena Tullborg
Terralogica AB

December 2009

Svensk Kärnbränslehantering AB
Swedish Nuclear Fuel
and Waste Management Co

Box 250, SE-101 24 Stockholm
Phone +46 8 459 84 00

ISSN 1402-3091
SKB Rapport R-08-99

Fracture mineralogy Laxemar

Site descriptive modelling SDM-Site Laxemar

Henrik Drake
Isochron Geoconsulting HB

Eva-Lena Tullborg
Terralogica AB

December 2009

Keywords: Fracture mineralogy, Geochemistry, Geochronology, Stable isotopes, Fluid inclusions, Redox, U-series disequilibrium.

Executive summary

Detailed investigations of fracture minerals and wall rock alteration have been carried out as part of the site characterisation programme during 2003 to 2007 in the Laxemar-Simpevarp area. The results have been published in a number of SKB P-reports, in scientific journals and as conference abstracts. This report summarises and evaluates the data obtained during the detailed fracture mineralogical studies conducted as part of the site investigations.

One aim of the detailed fracture mineralogical studies has been to describe the low to moderate temperature geological and palaeohydrogeological evolution in the Laxemar-Simpevarp area. Furthermore, to contribute to the conceptual geological understanding of the site and to provide input to hydrogeochemical modelling.

Thin sections and samples of fracture surfaces from more than 300 fractures have been prepared from drill cores from 30 cored boreholes. Fracture fillings or individual minerals have been analysed, for example for geochemistry, stable isotopes and fluid inclusions, in order to distinguish different fracture filling generations and their formation conditions. Radiometric $^{40}Ar/^{39}Ar$ dating has been carried out to provide time constraints on the different generations and, with help of palaeo-stress indications from orientations of carefully selected fractures, to relate these to specific geological events. This information has contributed to the understanding of the geological, hydrogeological and hydrogeochemical evolution of the site.

These investigations have revealed a relative sequence of fracture fillings consisting of six generations as shown in Figure S-1. Most of the fracture fillings in the area are very old (Proterozoic to Palaeozoic) and only small amount of fracture minerals may possibly be Quaternary. The signatures of most of the generations suggest precipitation during a long time span including varying conditions. The characteristics of these generations are:

- Generation 1 is an epidote- and quartz-rich mylonite associated with deformation zones and formed during the early geological history of the area. A minimum age close to c. 1,773 Ma, when the rock cooled below ~500°C is suggested, based on formation temperature estimates.
- Generation 2 is cataclasite of at least two different varieties, sometimes with semi-ductile features and formed during the early geological history of the area. The observed semi-ductile features suggest formation close to 300–350°C, inferring either 1) formation prior to 1,620 Ma when the rock initially cooled below 300°C and/or 2) formation related to the intrusions at Götemar and Uthammar or at a slightly earlier thermal event.
- Generation 3 consists of a sequence of at least three different mineral parageneses in sealed fractures, and occasionally of greisen. Main minerals are calcite, quartz, chlorite, fluorite, pyrite, muscovite, epidote, prehnite and laumontite. The most probable scenario is that Generation 3 minerals formed during a prolonged time period where the latest and main pulse of precipitation was related to the intrusion of the Götemar and Uthammar granites. This is supported by $^{40}Ar/^{39}Ar$ plateau ages of greisen and the characteristically altered and red-stained wall rock of about 1,424–1,417 Ma. Generation 3 calcite and pyrite show hydrothermal and inorganic $\delta^{13}C$, $\delta^{18}O$, and $\delta^{34}S$ signatures, homogenization temperatures (T_h) of c. 195–370°C. Large variation in salinity, trace element chemistry, and T_h suggest varying formation conditions. This generation is related to more intense wall rock alteration than younger generations.
- Generation 4 mainly includes calcite, adularia, laumontite, chlorite, quartz, illite and hematite. Generation 4 minerals are found in thin sealed fractures cross-cutting Generation 3 fillings but are difficult to distinguish from these due to similar mineralogy and appearance. However, they have slightly different stable isotope and fluid inclusion signatures (although also of hydrothermal origin with inorganic signatures), as well as chlorite chemistry. They are interpreted to be formed later than c. 1,400 Ma, but prior to 710 ± 78 Ma. Generation 4 may be of Sveconorwegian age as indicated by a $^{40}Ar/^{39}Ar$ adularia age of c. 989 Ma. This generation is not very distinct and not as widespread as Generations 3 and 5.

- The oldest Generation 5 fillings were probably formed in relation to the Caledonian orogeny. These calcite-dominated fillings were formed from warm brine fluids (c. 80–145°C) at c. 440–400 Ma. Other minerals include adularia, fluorite, pyrite (and other sulphides), gypsum, barite, zeolites, hematite, clay minerals, chlorite and REE-carbonate. These fillings were formed in dominantly WNW-ESE trending, subvertical fractures, which correlate to the maximum compressive stress during the Caledonian orogeny. Calcite show organic $\delta^{13}C$ signatures, T_h of 80–145°C, high salinities and lower $^{87}Sr/^{86}Sr$ (also in gypsum), and lower $\delta^{18}O$ than the present groundwater. Formation from descending organic-rich fluids influenced by Palaeozoic sediments or Palaeozoic seawater may be proposed. The relatively high formation temperatures may also be influenced by subsidence due to thick overlying sediments.
- Late Palaeozoic to recent, possibly Quaternary minerals (mainly calcite, pyrite, clay minerals and goethite) are difficult to differentiate from each other and are therefore discussed collectively. Calcite and pyrite show organic and microbial influence at temperatures below 110°C, occasionally with closed system signatures. $\delta^{18}O$ and $^{87}Sr/^{86}Sr$ values show that some of these calcites may have formed from fluids in equilibrium with waters similar to present groundwaters at ambient temperatures. Formation from waters with different $\delta^{18}O$ values and salinities, such as fresh and brackish water, is indicated. The frequency of low $\delta^{13}C$ and biogenically (and microbially) modified $\delta^{34}S$ decreases with depth. In general, the information obtained for the youngest minerals (also including clay minerals and goethite) of this generation agree with the understanding of the site /SKB 2006b/. Although major hydrological and hydrochemical fluctuations during recent low-temperature conditions are indicated, the amounts of minerals precipitated or dissolved during these conditions have been relatively small, at least at depths greater than about 100 m.

Mapping of fractures and fracture minerals has been carried out routinely on all drill cores recovered during the site investigations and the resulting data have been used here to obtain a statistical overview of the variation of fracture mineralogy with depth in water conducting fractures, deformation zones, different fracture and rock domains and with respect to fracture orientation. Fracture minerals provide buffer capacity in terms of pH (mainly calcite) and redox (mainly Fe[II] minerals such as chlorite, clay minerals and pyrite) and therefore the distribution of these minerals are of utmost importance for the assessment of longterm safety.

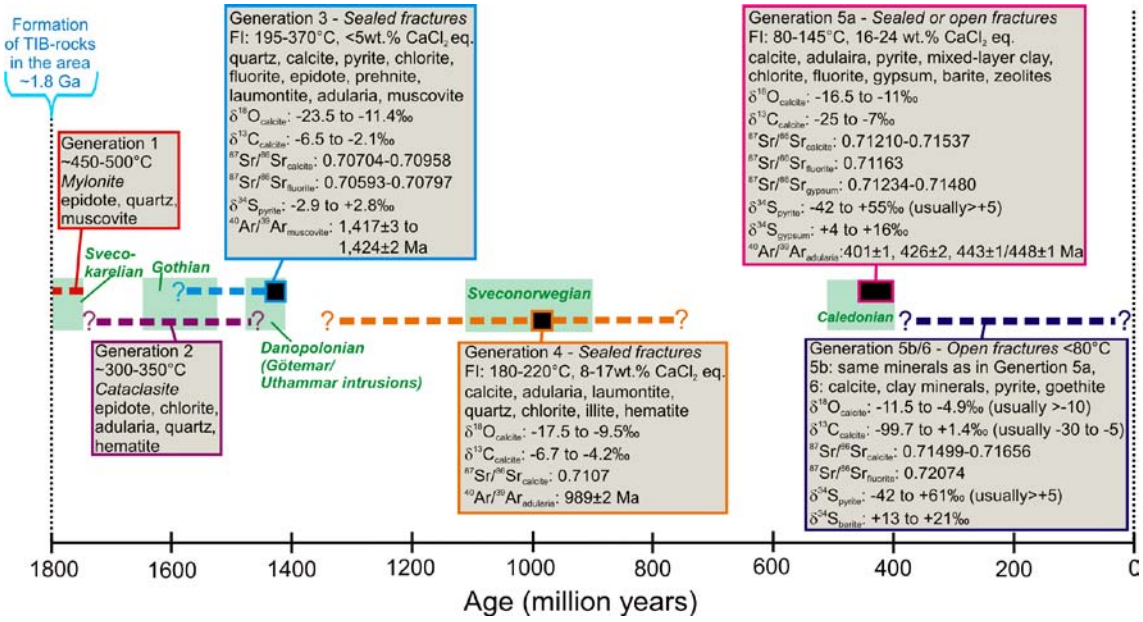

Figure S-1. *Summary of the fracture mineralogical data from the Laxemar-Simpevarp area, in chronological order, with orogenies and nearby intrusions indicated (in green). Time ranges from /Åhäll 2001, Roberts 2003, Bingen et al. 2008/. "FI"= fluid inclusion.*

Calcite and chlorite are by far the most common fracture minerals in the Laxemar-Simpevarp area, and these are especially frequent in the open fractures. These minerals dominate in all of the different rock domains, fracture domains, deformation zones and in hydraulically conductive fractures. Clay minerals, pyrite and hematite are also most frequently found in open fractures. Epidote, adularia, quartz and prehnite are more frequent in sealed fractures. Additional minerals, for example, gypsum, are found in less than 1% of the fractures. About 2.5% of the open fractures do not contain any macroscopically visible fracture minerals. These are more frequent towards the ground surface and may possibly be young. Chlorite and calcite show no distinct variation with depth. Exceptions are the lower amount of calcite (and slightly lower amount of chlorite) in the uppermost 10–20 m, and slightly lower amounts of calcite below about –800 m above sea level. The former depletion is probably related to near surface dissolution, and the latter decline for calcite marks the shift to a less dynamic hydraulic system with limited precipitation of calcite spanning in time from the Palaeozoic to recent. Clay minerals and the hydrothermal minerals epidote, prehnite, quartz, hematite and adularia show no systematic variation in occurrence with depth. Pyrite is a common mineral in open fractures at most depths, although there is a clear decrease in frequency near the surface due to oxidative dissolution of pyrite. Gypsum is absent in most boreholes, but when present it is generally restricted to open fractures in isolated sections with low fracture frequency and low transmissivity at depths greater than –350 m above sea level.

The frequency of most of the minerals is similar in the different rock domains and fracture domains. However, some variations exist, especially between the rock domains, and these are apparently mainly related to the difference in wall rock chemistry.

Fracture filling material from hydraulically conductive fractures has been analysed to provide input to the hydrogeochemical modelling and conceptual hydrogeochemical understanding of the site. Analyses include mineralogical composition, geochemistry, uranium series disequilibrium (USD), and stable isotopes. Special attention has been paid to the behaviour of chemical analogues for radionuclides and to redox-sensitive elements. The chemical analyses of individual fracture minerals and bulk fracture fillings confirm the mineralogy determined from the mapping, and identification using XRD and microscopy. The chemical analyses, in combination with XRD and microscopy investigations, have revealed information on the association of certain elements to specific minerals, and the abundance of minerals and elements in the fracture fillings.

Mineralogy, geochemistry, porosity and redox capacity of red-stained, hydrothermally altered wall rock, which is a common feature adjacent to many fractures in the Laxemar-Simpavarp area, have been studied and compared with fresh, unaltered rock. The results show that the Fe^{3+}/Fe_{tot} ratio in the oxide phase is higher in the red-stained samples whereas the Fe^{3+}/Fe_{tot} ratio in the silicate phase is largely similar in the wall rock and the reference rock. Because most of the Fe is hosted in the silicate phase the decrease in reducing capacity (Fe^{2+}), if any, in the red-stained wall rock is very small and not as high as macroscopic observations suggest. Instead, the mineralogical changes in combination with the modest oxidation and formation of minute hematite grains in porous secondary minerals in pseudomorphs after plagioclase, have produced the red staining.

The position of the redox front in the near surface bedrock has been investigated using mineralogical, chemical and uranium series decay analyses of fracture coatings from a series of closely spaced relatively short core-drilled boreholes. The analyses show that the redox front at these drill sites is generally positioned at about 20 m (+/–5 m) depth below the ground surface. The main features of the redox front generally include a shift from mainly goethite to mainly pyrite in the fractures, from positive Ce-anomalies to slightly negative or insignificant Ce-anomalies in the bulk fracture coatings, and from a state of mainly removal of U to mainly deposition of U in the bulk fracture coatings (Figure S-2). Leaching of calcite in open fractures in the upper 20–30 m further support past infiltration of very dilute recharge waters which probably had relatively low pH and may at least have been partly loaded with oxygen. Localised percolation of oxidising groundwater to depths that otherwise have experienced reduced conditions is shown by occasional signs of U removal at depths between 35 and 55 m, seen in intervals of high transmissivity. In fracture coatings below 55 m depth, U was not removed preferentially with respect to Th during the last 100 ka and, therefore, U was likely present in its more insoluble reduced form. Although penetration of glacial waters to great depths has been confirmed in the area /SKB 2006b/, the current work supports the modelling carried out by /Guimerà et al. 1999/ and conclusions drawn by /Gascoyne 1999/ that these glacial waters

were not oxidising at repository depth. Instead, oxygen in the recharge water is generally consumed within the upper 20 m (+/–5 m), the corresponding penetration reaching slightly greater depth in fractures or shear zones of high transmissivity ($T \geq 1 \cdot 10^{-7}$ m^2/s).

An updated compilation of mineralogical and geochemical data of rocks previously presented in /Drake et al. 2006/ for SR-Can is included as an appendix in the present report.

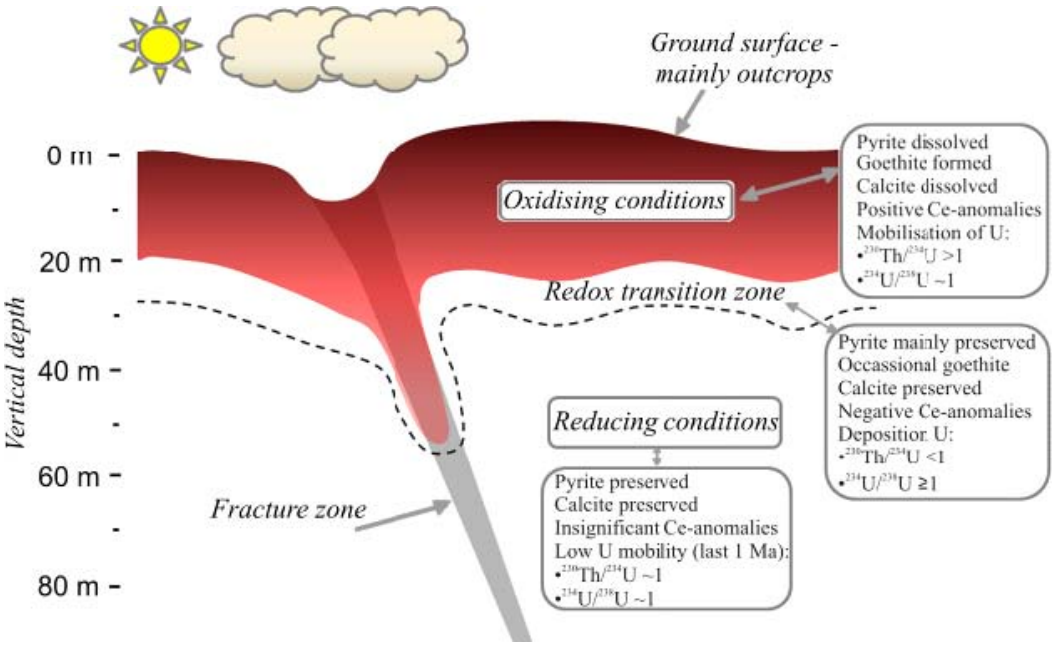

Figure S-2. *Tentative sketch model of the near-surface redox front in the Laxemar-Simpevarp area, Sweden. The different fields represent the depth intervals where mineralogical, geochemical and U-series analyses of fracture coatings indicate Quaternary oxidising condition, reducing conditions or a transition zone between these two.*

Contents

Appendices attached on CD

1 Introduction, objectives and concepts

1.1 Introduction and objectives

The Swedish Nuclear Fuel and Waste Management Company (SKB) is carrying out site investigations at Forsmark and Oskarshamn in Sweden with the objective of finding a suitable location for a final, deep-seated repository for spent nuclear fuel. Studies of the fracture mineralogy in the Laxemar area (comprising the Simpevarp and the Laxemar subareas, Figure 1-1), have been carried out as part of the Oskarshamn site investigation programme from 2003 to 2007. The results of these studies have been published in numerous SKB P- and R-reports, peer-reviewed papers summarised in a PhD thesis, and included in abstract volumes to scientific conferences (Table 1-1). The objective of the present report is to summarise and evaluate the comprehensive data set obtained during the detailed fracture mineralogical studies. An updated compilation of mineralogical and geochemical data of rocks previously presented in /Drake et al. 2006/ for SR-Can is also attached as an appendix to the report (Appendix 1).

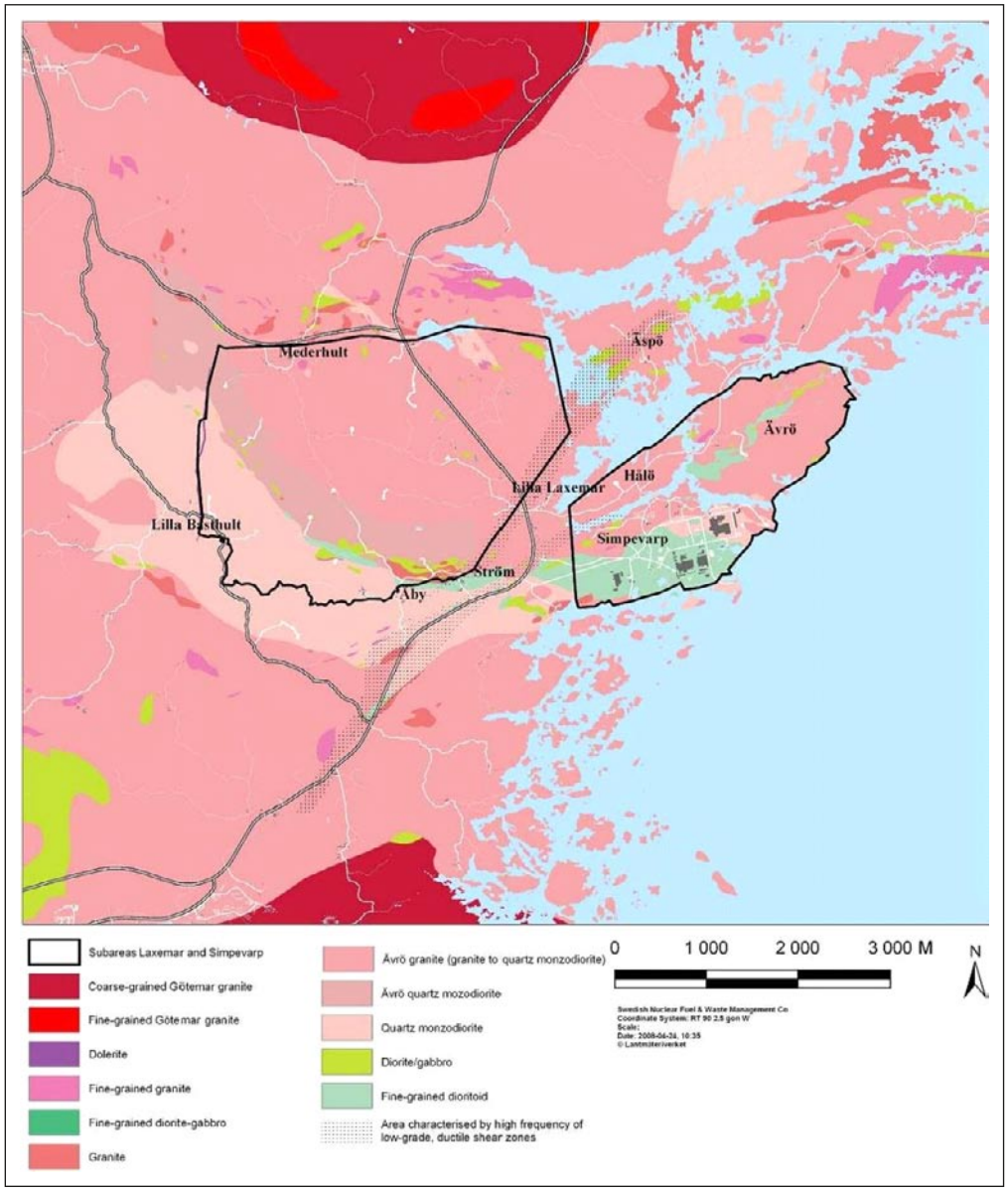

Figure 1-1. *Map showing the bedrock geology of the region with the Laxemar subarea (left) and Simpevarp subarea (right) encircled. Map based on the SKB GIS database, per 23rd April, 2008.*

Table 1-1. Publications related to detailed investigations of fracture minerals and wall rock alteration related to site investigations in the Laxemar area.

SKB P- and R-reports

P-04-250 /Drake and Tullborg 2004/. Oskarshamn site investigation. Fracture mineralogy and wall rock alteration, Results from drill core KSH01A+B.

P-05-174 /Drake and Tullborg 2005/. Oskarshamn site investigation. Fracture mineralogy and wall rock alteration, Results from drill cores KAS04, KA1755A and KLX02.

P-06-04 /Drake and Tullborg, 2006a/. Oskarshamn site investigation. Fracture mineralogy of the Götemar granite, Results from drill cores KKR01, KKR02 and KKR03.

P-06-03 /Drake and Tullborg 2006b/. Oskarshamn site investigation. Fracture mineralogy and wall rock alteration, Results from drill core KSH03A+B.

P-06-02 /Drake and Tullborg 2006c/. Oskarshamn site investigation. Mineralogical, chemical and redox features of red-staining adjacent to fractures, Results from drill core KLX04.

P-06-01 /Drake and Tullborg 2006d/. Oskarshamn site investigation. Mineralogical, chemical and redox features of red-staining adjacent to fractures, Results from drill cores KSH01A+B and KSH03A+B.

R-06-109 /Drake et al. 2006/. Mineralogy and geochemistry of rocks and fracture fillings from Forsmark and Oskarshamn: Compilation of data for SR-Can.

P-07-27 /Drake et al. 2007a/. Oskarshamn site investigation. $^{40}Ar/^{39}Ar$ dating of fracture minerals.

P-07-74 /Drake and Tullborg 2007a/. Oskarshamn site investigation. Fracture mineralogy. Results from drill cores KLX03, KLX04, KLX06, KLX07A, KLX08 and KLX10A.

P-08-44 /Drake and Tullborg 2008a/. Oskarshamn site investigation. Detecting the near surface redox front in crystalline rock. Results from drill cores KLX09B-G and KLX11B-F.

P-08-12 /Drake and Tullborg 2008b/. Oskarshamn site investigation. Fracture mineralogy. Results from drill core KLX15A.

P-08-11 /Drake and Tullborg 2008c/. Oskarshamn site investigation. Mineralogy in water conducting zones. Results from drill cores KLX13A and KLX17A with additional fracture mineralogical data from drill cores KLX14A, KLX19A, KLX20A and KLX26A.

P-08-42 /Drake and Tullborg 2008d/. Oskarshamn site investigation. Mineralogy in water conducting zones. Results from boreholes KLX07A+B and KLX08.

P-08-41 /Drake and Tullborg 2008e/. Oskarshamn site investigation. Mineralogy in water conducting zones. Results from boreholes KLX03, KLX04, KLX06, KSH01A+B, KSH02 and KSH03A.

P-09-15 /Drake and Tullborg 2009b/. Oskarshamn site investigation, Investigations of goethite-bearing fractures in cored boreholes Laxemar subarea.

Peer reviewed papers

/Drake and Tullborg 2007b/. Paleohydrogeology of the Simpevarp area, southeastern Sweden, as evidenced by stable isotopes in fracture minerals. *In* Bullen T.D. and Wang Y. (eds), *Water-Rock Interaction. Proceedings of the 12th international symposium on water-rock interaction. WRI-12, Kunming, China, 31 July–5 August 2007*. Taylor and Francis, London, 723–726.

/Drake et al. 2008/. Red-staining of the wall rock and its influence on the reducing capacity around water conducting fractures. *Applied geochemistry,* 23, 1898–1920.

/Tullborg et al. 2008/. Palaeohydrogeology: A methodology based on fracture mineral studies. *Applied Geochemistry,* 23, 1881–1897.

/Drake and Tullborg 2009a/. Paleohydrogeological events recorded by stable isotopes, fluid inclusions and trace elements in fracture minerals in crystalline rock, Simpevarp area, SE Sweden. *Applied Geochemistry.* 24. 715–732.

/Drake et al. 2009a/. Detecting the near surface redox front in crystalline bedrock using fracture mineral distribution, geochemistry and U-series disequilibrium. *Applied Geochemistry.* 24. 1023–1039.

/Drake et al. 2009b/. Distinguished multiple events of fracture mineralisation related to far-field orogenic effects in Paleoproterozoic crystalline rocks, Simpevarp area, SE Sweden. *Lithos.* 110, 37–49.

Licentiate Thesis

/Drake 2006/. Fracture fillings and red-stained wall rock in the Simpevarp are, SE Sweden. *Earth Sciences Centre, University of Gothenburg, Publ. A102.*

Doctoral Thesis

/Drake 2008/. Proterozoic to Quaternary events of fracture mineralisation and oxidation in SE Sweden. *Earth Sciences Centre, University of Gothenburg, Publ. A120.*

Abstracts in conference volumes

/Drake et al. 2004/. Fracture fillings and wall rock alteration – results from borehole KSH01, Simpevarp and KFM01, Forsmark, *GFF: The 26th Geological Winter Meeting, Abstract volume,* vol. 126, p. 170.

/Drake and Tullborg 2006e/. Hydrothermal red-staining adjacent to fractures in granodioritic to dioritic rock, Simpevarp, south-east Sweden. *Bulletin of the Geological Society of Finland, Special Issue 1. P.* 26.

/Drake et al. 2007b/. $^{40}Ar/^{39}Ar$ ages of fracture fillings in crystalline Precambrian bedrock, Sweden. *Geophysical Research Abstracts* 9, 02289, SRef-ID 1607-7962/gra/EGU2007-A-02289.

/Drake and Tullborg 2008f/. Paleohydrogeological evidences from stable isotopes, fluid inclusions and trace elements in fracture minerals in crystalline rock, Simpevarp area, south-eastern Sweden. In N.A. Wahl (ed), *28th Nordic Geological Winter Meeting. Jan 7–10, 2008, Aalborg-Denmark*. Aalborg University. p 105.

/Drake and Tullborg 2008g/. Detection of the near surface redox front in crystalline bedrock. In N.A. Wahl (ed), *28th Nordic Geological Winter Meeting. Jan 7–10, 2008, Aalborg-Denmark*. Aalborg University. p. 32.

/Drake and Tullborg 2008h/. Detection of the near-surface redox front in crystalline bedrock, Sweden, IGC 33, Oslo Norway, abstract volume. Abstract number HYH07708L.

One aim of the detailed fracture mineralogical studies has been to describe the low to moderate temperature (below ~400ºC), post-metamorphic geological and palaeohydrogeological evolution in the Laxemar area and thereby contribute to a better conceptual geological understanding of the site and to provide input to hydrogeochemical modelling. The main part of this evolution, comprising several generations of fracture fillings, occurred in the brittle regime of the crust, although the oldest deformation in the area was ductile.

Mapping of fractures and fracture minerals has been carried out routinely on all drill cores recovered during the site investigations and the resulting data have been used here in more detailed fracture mineralogical studies. These include an evaluation of the variation in fracture mineralogy: 1) with depth, 2) in water conducting fractures, 3) in deformation zones and sections of crushed rock, 4) in different fracture domains, 5) in different rock domains, and 6) with fracture orientation. The concept of rock domains and fracture domains is briefly described in Section 1.2. The variation of fracture mineralogy in open and sealed fractures versus depth is studied (see also Section 3.6.5 in /Wahlgren et al. 2008/) both for each individual borehole and collectively for all boreholes. The orientations of fractures outside deformation zones (DZ), bearing different fracture minerals, have also been evaluated based on fracture domains. The fracture mineralogy within the deformation zones and in sections of crushed rock is discussed briefly (see also /Wahlgren et al. 2008/).

Fracture filling material, preferably selected from hydraulically conductive fractures, have been analysed to provide input to the hydrogeochemical modelling and conceptual hydrogeochemical understanding of the site. Analyses include mineralogical composition, geochemistry, uranium series disequilibrium (USD), and stable isotopes.

The mineralogy, geochemistry, porosity and redox capacity of red-stained, hydrothermally altered wall rock, which is a common feature adjacent to many fractures in the Laxemar area, have been studied and are compared with fresh, unaltered rock.

The position of the redox front in the near surface bedrock has been investigated using mineralogical, chemical and uranium series equilibrium (USD) analyses of fracture coatings in a series of closely spaced boreholes which were core drilled from the ground surface.

1.2 Rock domain, fracture domain and deformation zone concepts

A rock domain refers to a rock volume in which rock units that show specifically similar composition, grain size, texture, degree of bedrock homogeneity, and degree and style of ductile deformation have been combined and distinguished from each other. The term rock domain is used in the 3D geometric modelling work and different rock domains at Laxemar are referred to as RSMxxx. The major groups of rocks in Laxemar are mainly distinguished on the basis of their composition, grain size, texture and relative age. Rock units shown along with deformation zones on the bedrock geological map of the local model area (Figure 1-2) are distinguished on the basis of the character of the dominant rock type. Figure 1-3 shows a three dimensional model for rock domains in the regional model volume. The three dominant rock domains are RSMD01, RSMM01 and RSMA01. The RSMD01 domain is strongly dominated by equigranular, medium-grained quartz monzodiorite, which is estimated to constitute c. 89% of the domain volume. The RSMM01 domain is dominated by the commonly medium-grained and finely porphyritic Ävrö quartz monzodiorite, including granodioritic to granitic compositions (Ävrö granodiorite). Together, these two compositional varieties constitutes c. 75% of the domain, out of which Ävrö quartz monzodiorite constitutes c. 50% and Ävrö granodiorite c. 25%. The dominant rock type in the RSMA01 domain is the Ävrö granite, i.e. in its use as the collective term for a commonly medium-grained and finely porphyritic rock that varies in composition between quartz monzodiorite, granodiorite and granite.

Fracturing is described in terms of fracture domains instead of rock domains. Fracture domains provide a large-scale conceptual framework for describing spatial heterogeneity in rock fracturing. A fracture domain refers to a rock volume outside deformation zones in which rock units show similar fracture intensity characteristics, and is mainly used in the discrete fracture network modelling work /La Pointe et al. 2008/. Fracture domains at Laxemar are denoted FSMxx. The Laxemar subarea has been divided into six fracture domains /Wahlgren et al. 2008/ and a map of the surface extensions of these fracture domains is shown in Figure 1-4.

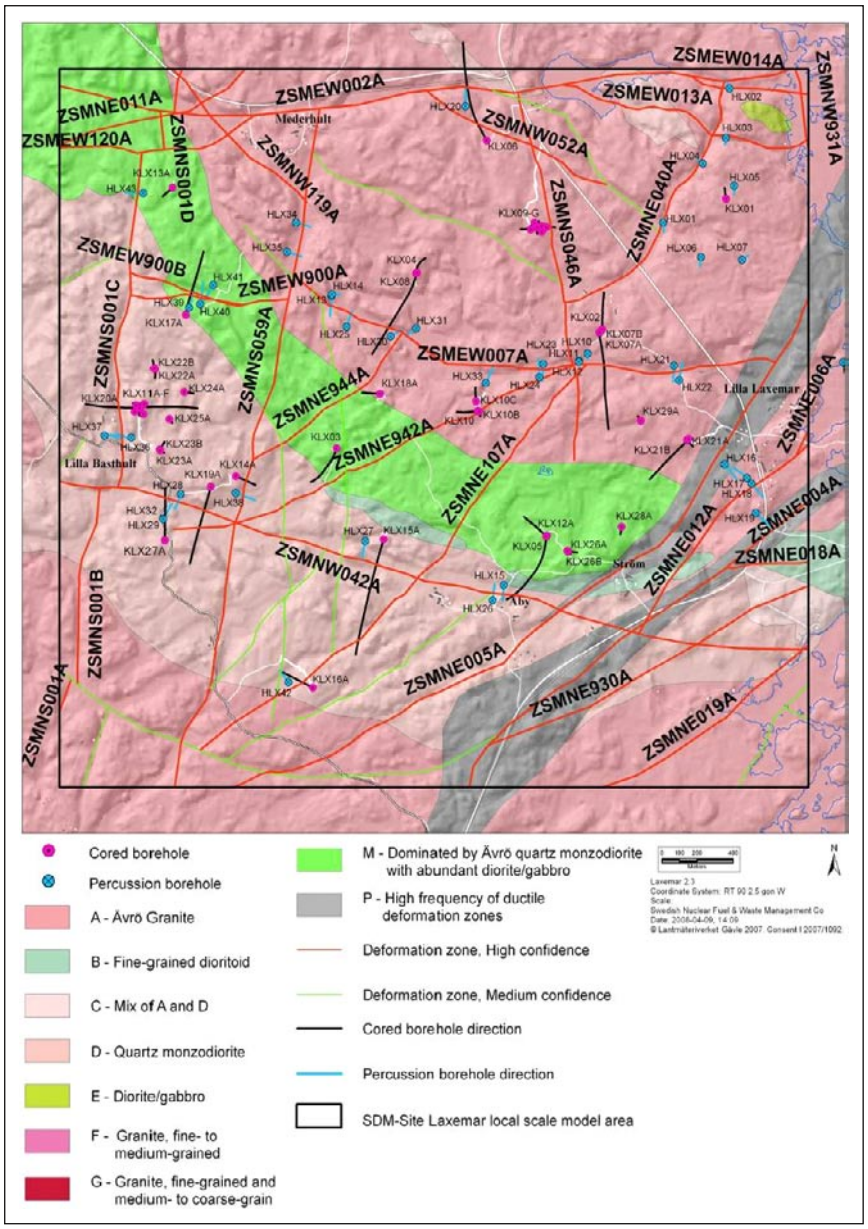

Figure 1-2. *An overview of the deformation zones and rock domains modelled deterministically in the Laxemar local model area, from /Wahlgren et al. 2008/.*

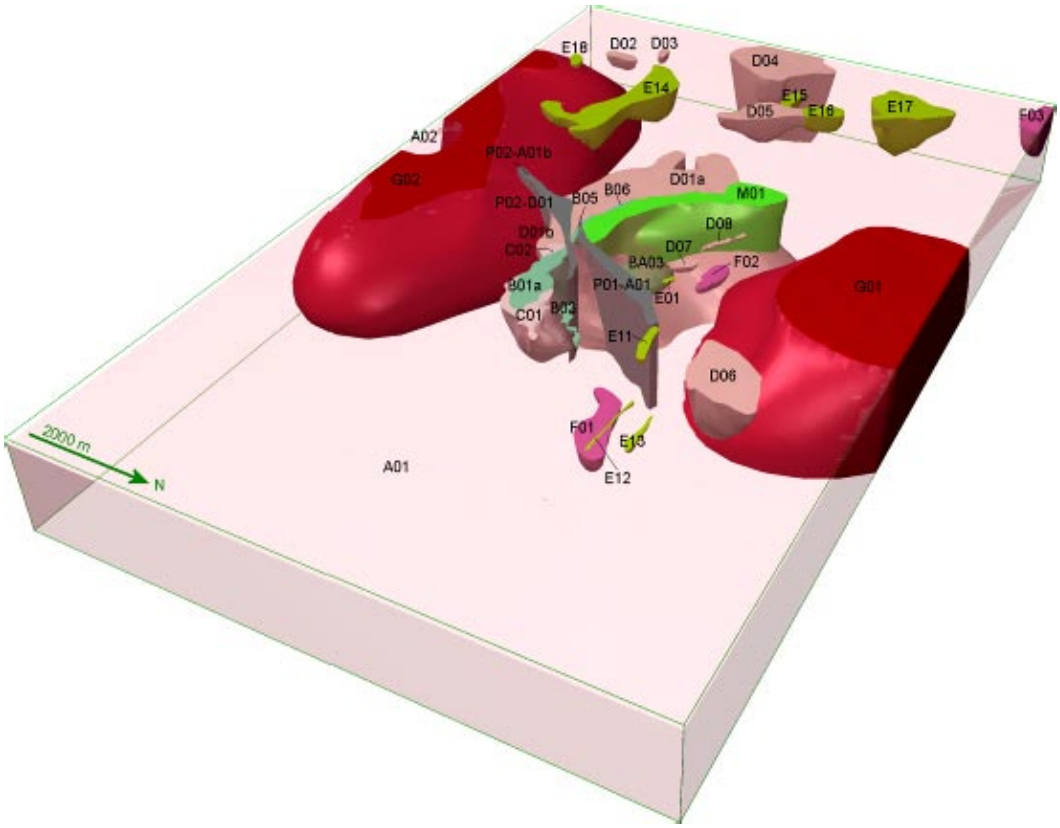

Figure 1-3. *Three-dimensional model for rock domains in the regional model volume viewed to the south-west. The prefix RSM has been excluded in the denomination of the rock domains. From /Wahlgren et al. 2008/.*

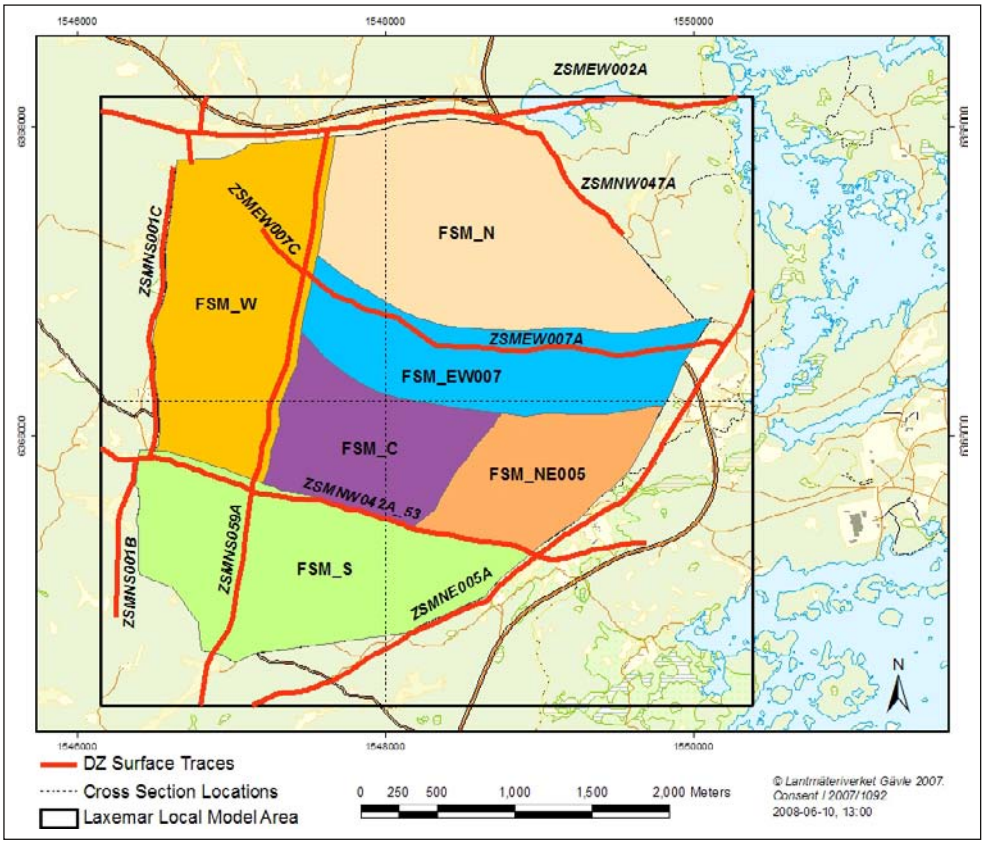

Figure 1-4. *Illustration of the SDM Site Laxemar Fracture Domain Model, from /La Pointe et al. 2008/.*

Fracture domain FSM_EW007 represents a volume of rock on the south side and on the north side of deformation zone ZSMEW007A. Most open fractures appear to strike in a WNW direction. Both fracture intensity and orientation have been interpreted as being affected by the E-W striking deformation zone ZSMEW007A. Fracture domain FSM_NE005 is characterised by a significant increase in the relative intensity of N-S striking sealed fractures, relative to the rest of the Laxemar local model area. Fracture domain FSM_W has a dominance of north-south strike is noted in both subvertically dipping and subhorizontal fractures. Fracture domain FSM_C is dominated by sealed N-S striking fractures in a fashion similar to FSM_W, and open WNW striking fractures. Fracture domain FSM_N is dominated by subhorizontal fractures, but lacks the dominant open WNW fractures observed in FSM_C. Fracture domain FSM_S represents the rock volume south of zone ZSMNW042A. The definition of this rock volume as a separate fracture domain is highly uncertain due to the lack of data from this volume of rock.

Deformation zone is employed as a general notation of an essentially 2D structure characterised by ductile or brittle deformation, or a combination of the two. Those deformation zones which are possible to correlate between the surface (lineament with a length >1,000 m) and an interpreted borehole intercept, or alternatively between one or more borehole intercepts, or exhibit an interpreted true thickness >10 m are modelled deterministically (Figure 1-2). Deformation zones at Laxemar are denoted ZSM followed by two to eight letters or digits.

From a fracture mineralogical point of view, it is important to evaluate possible differences in fracture mineral frequency between the different domains. Therefore, statistical analyses of fracture mineralogy have been carried out based on the fracture domain and rock domain concept. Furthermore, an analysis of fracture mineralogical frequencies in deformation zones and minor deformation zones (MDZ) has been carried out.

2 Methods and available data

2.1 Opening remarks

During the detailed fracture mineralogical studies, thin sections (30 μm thick rock slices) and fracture surface samples from more than 300 fractures (about 120 thin sections and 185 fracture surface samples) have been prepared from 30 drill cores (Table 2-1 and Figure 2-1). The samples have been analysed mainly by binocular microscopy, petrographic microscopy under polarised light and SEM-EDS (Scanning Electron Microscope equipped with an Energy Dispersive Spectrometer).

Sample descriptions and detailed methodology, e.g. analytical details, such as detection limits are presented in /Drake and Tullborg 2004, 2005, 2006a, b, c, d, 2007a, 2008a, b, c, d, e, 2009a, b, Drake et al. 2006, 2007a, 2009a, b/.

X-ray diffraction (XRD) has been applied on samples containing clay minerals, especially in water conducting fractures. The XRD detection limit for a mineral depends on the specific mineral in question, its degree of crystallinity and other minerals present in the sample. As a rough estimate, the detection limit for a mineral phase is generally in the order of a few vol.%.

Mineral specific chemical analyses have been carried out using SEM-EDS on thin sections and ICP-MS on leachates of calcite and gypsum. Other analyses carried out on the fracture minerals include bulk geochemical analyses, stable isotope analyses ($\delta^{13}C$ and $\delta^{18}O$ in calcite; $\delta^{34}S$ in pyrite, barite and gypsum; $^{87}Sr/^{86}Sr$ in calcite, gypsum and fluorite), fluid inclusions (calcite and quartz), radiometric geochronology ($^{40}Ar/^{39}Ar$ in adularia and muscovite) and U-series disequilibrium (bulk samples). Boremap data from the drill core mapping have been used to evaluate mineral frequency and the orientation of fractures filled with specific minerals.

The $\delta^{18}O$ of calcite reflects the $\delta^{18}O$ of the groundwater from which it precipitated as well as the formation temperature /e.g. Veizer 1983/, and the $\delta^{18}O$ value in the precipitation fluid reflects its origin (e.g. marine or meteoric water). However, water-rock interaction (i.e. potential oxygen shift) may also have an influence on the $\delta^{18}O$ value, especially under hydrothermal conditions /e.g. Truesdell and Hulston 1980/. In contrast to $\delta^{18}O$, $\delta^{13}C$ is not very temperature dependent and influence from interaction with the crystalline wall rock is generally insignificant. Instead, the $\delta^{13}C$ in calcite reflects the $\delta^{13}C$ of the carbon sources involved (e.g. dissolved CO_2 or CH_4) /Ohmoto and Rye 1979/. The $\delta^{34}S$ value in sulphides and sulphates is, for example, used to distinguish between magmatic/hydrothermal and lower temperature precipitates, between microbial from thermochemical reduction of sulphate, and to trace the origin of the sulphate /e.g. Hoefs 2004/. The $^{87}Sr/^{86}Sr$-ratios of calcite and gypsum reflect the ratio of the waters from which they precipitated. The $^{87}Sr/^{86}Sr$-ratios of dissolved Sr in groundwater are mainly controlled by water-rock interactions and, therefore, by the isotopic compositions of the strontium bearing minerals in the wall rock which will increase over time in response to ^{87}Rb decay /Faure 1986, McNutt 2000/. The $^{87}Sr/^{86}Sr$-ratios can therefore be used to distinguish different fracture filling generations and determine whether some of these might be formed in equilibrium with the present groundwater at the site /Tullborg et al. 2008/.

Fluid inclusion analyses of calcite and quartz provide constraints on the formation temperature, salinity and composition of the formation fluid. The trace element composition of calcite can give information of redox conditions, formation temperature, and fluid composition /Möller and Morteani 1983, Tullborg et al. 2008/.

Geochemical analyses of bulk fracture fillings have been applied on material from currently hydraulically conductive fractures and zones in order to evaluate element mobility and deposition. These analyses serve as a complement (i.e. background data) to the chemical analyses of groundwater and hydrogeochemical modelling. The geochemistry of fracture coatings depends on the fluid from which they precipitated, as well as the chemical exchange during water-rock interaction and microbial processes. Special attention has been paid to the behaviour of chemical analogues for radionuclides (e.g. Cs, Sr, U, Th and REE) and on redox sensitive elements (e.g. Fe, Ce, Mn and U), with respect to their variation with depth, their stability over time and their association to specific minerals.

Table 2-1. Details of cored boreholes from the Laxemar subarea, Simpevarp subarea and Äspö used in the detailed fracture mineralogical studies. Boreholes KLX05, KLX09, KLX10B, KLX10C, KLX11A, KLX16A, KLX18A, KLX21A–KLX25A, KLX26B–KLX29A have not been sampled and have been evaluated using Boremap data only. Data extracted from Sicada (Data delivery SICADA_08_107). The locations of the sampled boreholes are shown in Figure 2-1.

Borehole	Borehole length (m)*	Start of cored borehole (m)#	Length of casing to ground surface (m)	Top of casing to bedrock (m)	Soil cover (m)	Elevation (m.a.s.l. at top of casing)	Inclination (°)	Bearing (°)
Laxemar								
KLX02	1,700,50	202,95	0,400			18,40	–85	357
KLX03	1,000,42	100,35	0,100	1,10	1,00	18,49	–75	199
KLX04	993,49	100,35	0,100	2,00	1,90	24,09	–85	1
KLX05	1,000,16	100,30	0,100	0,10	0,00	17,63	–65	190
KLX06	994,94	100,30	0,100	1,10	1,00	17,68	–65	330
KLX07A	844,73	100,46	0,200	0,70	0,50	18,47	–60	174
KLX07B	200,13		0,100	0,60	0,50	18,38	–85	174
KLX08	1,000,41	100,33	0,300	3,10	2,80	24,31	–61	199
KLX09	880,38	100,60	0,120	0,77	0,65	23,45	–85	267
KLX09B	100,22		0,300	2,48	2,18	23,61	–90	21
KLX09C	120,05		0,300	0,30	0,00	23,75	–60	160
KLX09D	121,02		0,300	2,48	2,18	23,10	–60	270
KLX09E	120,00		0,300	0,30	0,00	22,16	–60	339
KLX09F	152,30		0,300	0,30	0,00	19,57	–60	91
KLX09G	100,10		0,300	0,30	0,00	19,63	–61	85
KLX10	1,001,20	100,60	0,120	0,42	0,30	18,28	–85	251
KLX10B	50,25		0,300	0,30	0,00	18,15	–60	170
KLX10C	146,25		0,300	0,30	0,00	16,93	–60	352
KLX11A	992,29	100,06	0,150	0,85	0,70	27,14	–77	90
KLX11B	100,20		0,300	1,21	0,91	27,27	–90	136
KLX11C	120,15		0,300	0,30	0,00	27,19	–61	159
KLX11D	120,35		0,300	0,30	0,00	25,57	–59	269
KLX11E	121,30		0,300	0,30	0,00	22,65	–61	336
KLX11F	120,05		0,300	0,30	0,00	24,46	–61	89
KLX12A	602,29	100,57	0,150	1,70	1,55	17,74	–75	316
KLX13A	595,85	99,86	0,150	1,15	1,00	24,15	–82	224
KLX14A	176,27		0,300	3,20	2,90	16,35	–50	112
KLX15A	1,000,43	76,13	0,300	2,50	2,20	14,59	–54	199
KLX16A	433,55		0,300	2,50	2,20	18,85	–65	294
KLX17A	701,08	65,42	0,150	1,50	1,35	27,63	–61	11
KLX18A	611,28	99,93	0,300	0,80	0,50	21,01	–82	271
KLX19A	800,07	99,33	0,300	0,60	0,30	16,87	–58	197
KLX20A	457,92	99,91	0,300	1,00	0,70	27,24	–50	271
KLX21B	858,78	99,41	0,300	3,30	3,00	10,68	–71	225
KLX22A	100,45		0,300			21,97	–60	179
KLX22B	100,25		0,300			21,57	–61	344
KLX23A	100,15		0,300	0,30	0,00	22,26	–61	29
KLX23B	50,27		0,300	0,30	0,00	22,32	–61	121
KLX24A	100,17		0,300	0,30	0,00	21,29	–59	98
KLX25A	50,24		0,300	0,30	0,00	22,84	–59	146
KLX26A	101,14		0,300	0,30	0,00	15,63	–60	93
KLX26B	50,37		0,300	0,30	0,00	15,82	–60	137
KLX27A	650,56	75,60	0,150	4,40	4,40	16,98	–65	1
KLX28A	80,23		0,300	2,85	2,55	10,05	–60	190
KLX29A	60,25		0,300	0,30	0,00	13,63	–61	321
Simpevarp								
KSH01A	1,003,00	100,24	0,000		1,40	5,32	–80	174
KSH01B	100,25		0,240	1,59	1,35	5,20	–88	178
KSH02	1,001,11	65,85	0,100	3,10	3,00	5,48	–86	331
KSH03A	1,000,70	100,60	0,180	0,18	0,00	4,15	–59	126
KSH03B	100,86		0,110	0,11	0,00	4,08	–64	129
Äspö								
KA1755A	320,58				0,00	–237,77		
KAS04	480,98	100,70			0,00	11,69	–60	129

*Length along borehole inclination, #If uppermost part of the borehole is hammer drilled and lacks core.

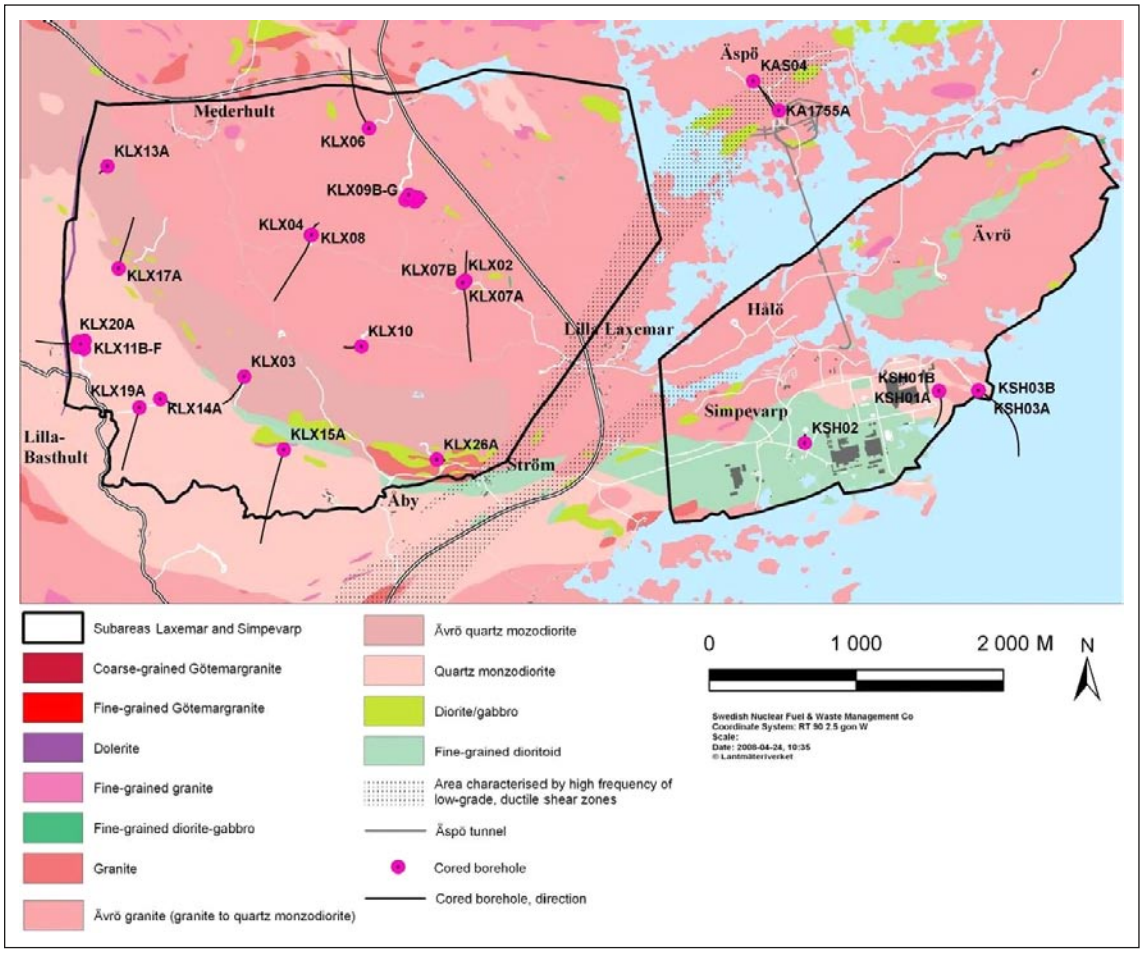

Figure 2-1. *Geological map of the Laxemar and Simpevarp subareas showing boreholes sampled for detailed fracture mineralogical studies.*

$^{40}Ar/^{39}Ar$ dating of fracture minerals has been carried out in the Laxemar area in order to provide radiometric ages to different fracture filling generations /Drake et al. 2007a/. A major problem with radiometric dating of fracture minerals is that minerals commonly used for radiometric dating of rocks, e.g. zircon, titanite, monazite, baddeleyite, are very rare in the fracture systems. However, K-bearing minerals suitable for radiometric $^{40}Ar/^{39}Ar$ dating are present in the Laxemar fractures, although in rather small amounts and not in all generations. Dating has been applied successfully to muscovite and adularia (hornblende, illite and apophyllite samples were less successful) which were sampled based on the interpreted relative sequence of fracture mineralisations.

The uranium decay series nuclides (^{238}U, ^{234}U and ^{230}Th) can be applied, for example, to study the mobility of uranium during the last 1 Ma. This provides information on recent redox conditions at different depths, for example, removal of uranium under oxidising conditions at the near surface and redeposition under reducing conditions at greater depths. In the simplest case, secular equilibrium (activity ratio ≈1) between the nuclides in the uranium decay series indicates that no significant mobilisation or deposition has occurred during the last 1 Ma.

Fracture orientations have been obtained using BIPS (Borehole Image Processing System) /e.g. Gustafsson and Gustafsson 2007/, a method used for imaging 360° of the borehole wall obtained from lowering a digital high resolution TV-camera (resolution ~1.0 mm) into the borehole. During the BIPS-based mapping of the drill core, the orientation of fractures and other structures are imported to the Boremap™ software mapping file. To visualise these fracture orientations with different minerals, data obtained from the drill core mapping have been extracted from SKB's Sicada database and plotted in stereographic contoured plots using a Terzhagi correction. In this report, only fractures outside the deformation zones are analysed.

2.1.1 Confidence in the mapping data

The detailed fracture mineralogical studies provide an overview of the fracture mineralogy in the area but do not provide a fully covering statistical basis due to time and cost constraints. Samples for detailed studies are chosen to solve specific issues or to provide sufficient material to carry out combined analyses from a single fracture filling. For frequency analysis of fracture minerals, quantitative data obtained from the drill core mapping are extracted from SKB's Sicada database and processed. The mapping is based on ocular inspection, which is partly subjective. A comparative evaluation study between the different mapping crews from the two sites (Forsmark and Laxemar) has been carried out /Glamheden and Curtis 2006/, showing that there are crew-related differences in the mapping, but because there has been continuity in the mapping at each site, the variation in fracture mineral frequency is considered to be representative. There is high confidence that all major fracture mineral phases at Laxemar have been identified, especially since the mineralogical studies have been carried out in close collaboration with the drill core mapping geologists at the site.

Evaluation of the representativity of the Boremap fracture mineral data extracted from Sicada has greatly benefited from the close collaboration and communication with the drill core mapping geologists. The Boremap data is well organised and impressive with only a few exceptions:

a) Prehnite is easily mistaken for epidote or a mixture between epidote and quartz and may therefore in places be both underestimated and overestimated in the Boremap data. Communication with the drill core mapping geologists and subsequent analyses of specific fractures suggest that prehnite is greatly underestimated in the drill core mapping of KLX02–KLX07B (and in all drill cores from the Simpevarp subarea).

b) Hematite-stained adularia was mapped as hematite in the earliest boreholes (especially KLX02 and KLX03 and in all the drill cores from the Simpevarp subarea). Furthermore, even very small amounts of hematite discolour the fracture coating which may mask other minerals (e.g. adularia or chlorite) which in turn will be underestimated.

c) Different clay minerals are not distinguished during the drill core mapping, and it is also probable that clay minerals are partly lost during drilling operations. In the early stages of the mapping programme, open fractures including clay minerals were often mapped as chlorite only. Therefore, the frequency of clay minerals in the core mapping can be regarded as an absolute minimum.

d) The identification of calcite is most reliable during the mapping because even small volumes are detected by HCl which is added to the fracture surface or filling. Other minerals are therefore probably underestimated compared with calcite.

e) About 20% of the sealed fractures contain insufficient mineral volumes for identification. These are referred to as "non-visible mineral". These fractures are commonly identified by a thin zone of related hydrothermally altered, mostly red-stained wall rock. The minerals sealing these fractures, probably mostly quartz, calcite, epidote, chlorite, prehnite and K-feldspar, are therefore underestimated in the mapping of sealed fractures.

f) Only four fracture minerals (including wall rock alteration) can be listed in the Boremap mapping file due to the interface of the mapping program. Additional mapping data may be listed in the comment file, but this is not linked to the main mapping data file in Sicada (p_fract_core). Open fractures commonly include a higher number of identified minerals, not uncommonly more than four, than thin sealed fractures. Therefore, some minerals in open fractures and especially wall rock alteration adjacent to open fractures are underestimated in the mapping data. This is also shown by the unrealistically high amount of sealed fractures with altered wall rock compared with open fractures with altered wall rock.

It should be noted that the uncertainties of the mapping data have been reduced as the site investigations have progressed. This can be attributed to updating the mapping crew with results from detailed SEM-EDS, microscopy and XRD investigations of specific fracture minerals. Furthermore, the mapping crew has alternated during the site investigations and this change of staff members may have resulted in inconsistencies in the mapping data.

2.1.2 Sampling

The amounts of fracture minerals are usually very limited due to the drill core diameter (c. 50 mm) which represents a very small part of the actual fracture surface, and due to the usually very thin coatings. Therefore, it is difficult to obtain representative samples for analyses of the fracture material especially when it comes to separate mineral phases. The spatial extent of the fractures is virtually impossible to evaluate and therefore to obtain representative data for fractures of different length is not possible. The location of each cored borehole sampled during the fracture mineralogical studies is shown in Figure 2-1.

Sampling for detailed fracture mineral studies has been focused on addressing different tasks in the site descriptive modelling work (e.g. hydrogeochemistry and geology). The tasks include:

- *Mineralogical identification;* sampling has usually been initiated by the drill core mapping geologists. Binocular microscopy, XRD and/or SEM-EDS analyses have been performed on these samples.
- *Samples selected for study of mineral paragenesis*; ideally these samples should show a complex mineralogy and preferably contain several generations of fracture minerals (parageneses) representing a relative sequence of mineralisation. Cross-cutting relations have been of special interest for this purpose. Thin sections and/or fracture surface samples have been prepared from these samples and subsequently studied using binocular microscopy, petrographic microscopy and SEM-EDS.
- *Palaeohydrogeological studies; preferably open, and ideally water-conducting fractures coated with calcite, pyrite, gypsum or barite which can be selected for analyses of stable isotopes ($\delta^{13}C$, $\delta^{18}O$, $\delta^{34}S$ and $^{87}Sr/^{86}Sr$) and trace elements, etc*. Minerals from open fractures are preferred because they may have precipitated recently (i.e. in a time frame of relevance for the safety assessment of a nuclear fuel repository), as oppose to the usually Palaeozoic or older minerals in sealed fractures. Furthermore, minerals in open fractures also contribute to the hydrogeochemical interpretations and modelling of the present groundwater system. A large depth variety in the sample set has been prioritised. Special emphasis was put on sampling of calcite crystals of different morphologies because this has been applied successfully in several other studies to distinguish between different salinities in the formation water /e.g. Folk 1974, Milodowski et al. 2002, 2005/. However, at other sites this relationship has been less obvious (e.g. at Forsmark, Sweden /Sandström et al. 2008/. Sealed fractures have also been used in the palaeohydrogeological investigations, especially regarding fillings older than Palaeozoic age.
- *Hydraulically conductive fractures have been sampled based on Posiva Flow Log anomalies* (PFL) /cf. Sokolnicki and Väisäsvaara 2006/. SEM-EDS and XRD analyses, geochemical analyses of bulk fracture fillings, and uranium-series disequilibrium analyses have been carried out on these samples. Fractures containing high amounts of fracture coatings have been prioritised in order to carry out all the above analyses adequately. The main focus has been to sample fractures corresponding to sections sampled for groundwater chemistry. These fractures are *currently* hydraulically conductive, but do not necessarily represent previously hydrologically active fractures, or future conductive fractures (flow channels) for that matter. Calcite samples from the hydraulically conductive sections have also been analysed for stable isotopes and are included in the palaeohydrogeological interpretations.
- *Detection of the near surface redox front, i.e. the shift from oxidising conditions in near surface groundwater to reducing conditions in groundwater at greater depths and its stability over time*; open fractures were sampled from the ground surface down to 115 m vertical depth from a number of closely spaced boreholes. Sampling was focused on fractures with large amounts of coatings (for SEM-EDS, XRD, bulk geochemistry, and U-series analyses) and/or containing pyrite, goethite or calcite; $\delta^{13}C$, $\delta^{18}O$ and $^{87}Sr/^{86}Sr$ in calcite and $\delta^{34}S$ in pyrite have also been analysed. Thin sections of wall rock samples have been studied using optical microscope and SEM-EDS in order to investigate the extension of the weathering into the wall rock. The distribution of goethite, pyrite and calcite in open fractures was obtained from the mapping data stored in the SKB database (Sicada).
- *Red staining of the wall rock and its influence on the reducing capacity around water conducting fractures*; red-stained, hydrothermally altered wall rock samples have been compared with relatively unaltered reference samples from within 0.1 to 1 m distance from the red-stained rock. These investigations were carried out in order to describe and interpret the differences in mineralogy (thin sections; petrographic microscopy and SEM-EDS), geochemistry (whole rock analyses), redox properties (Mössbauer spectroscopy) and porosity between hydrothermally altered wall rock and relatively fresh rock.

In the selected drill core samples, the relative sequence of formation of the fracture minerals has been established based on cross-cutting relations (in macro scale Figure 1-2a, and in micro scale Figure 1-2a) and/or overgrowth (Figure 2-3). From this initial data set a more general relative sequence of fracture mineralisations has emerged. The sequence has then been slightly modified as more knowledge became available and the data set expanded during the site investigations /e.g. Drake and Tullborg 2004, 2005, 2006b, 2007a, Drake et al. 2007a/. In the latest model, the number of fracture mineral generations (parageneses) is six /Drake and Tullborg 2008b/. Only small modifications have been made to the sequence of fracture mineral generations since the preliminary Laxemar 1.2 geological model /SKB 2006a/ was defined, implying a high degree of stability in the established sequence. The sequence represents geological and/or hydrogeological events that succeeded each other in time. It has been used as a basis for radiometric dating of fracture minerals and interpretation of the formation conditions during precipitation, for example, based on mineral stabilities, stable isotopes and fluid inclusions.

In this report, specific samples are generally designated according to their borehole length. In diagrams where depth variations are presented, elevation is in meters above sea level (m.a.s.l.). Exceptions are in sections where vertical depths trends near the ground surface are studied (e.g. about the near-surface redox front). This is because boreholes are drilled from different elevations, which can vary by up to almost 30 m and important trends in the near-surface interval may be overlooked if elevation (m.a.s.l.) is used.

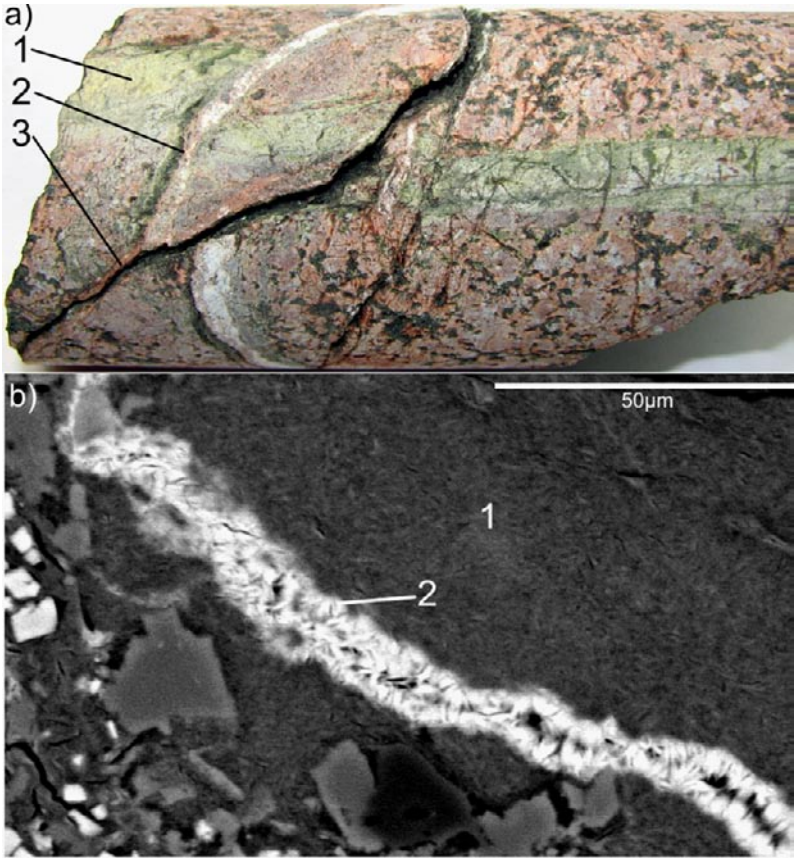

Figure 2-2. *Cross-cutting relations. a) Photograph of three generations of fractures in drill core KLX13A: 1) epidote, 2) calcite, adularia and laumontite in a fracture off-setting 1 and 3) an open fracture cross-cutting and off-setting both 1 and 2. b) Back-scattered SEM-image (BSE) of two generations of fracture fillings containing Mg-rich chlorite, adularia and apatite (1), cut by a fracture filled with Fe–rich chlorite (2). Drill core KSH01A: 208 m borehole length.*

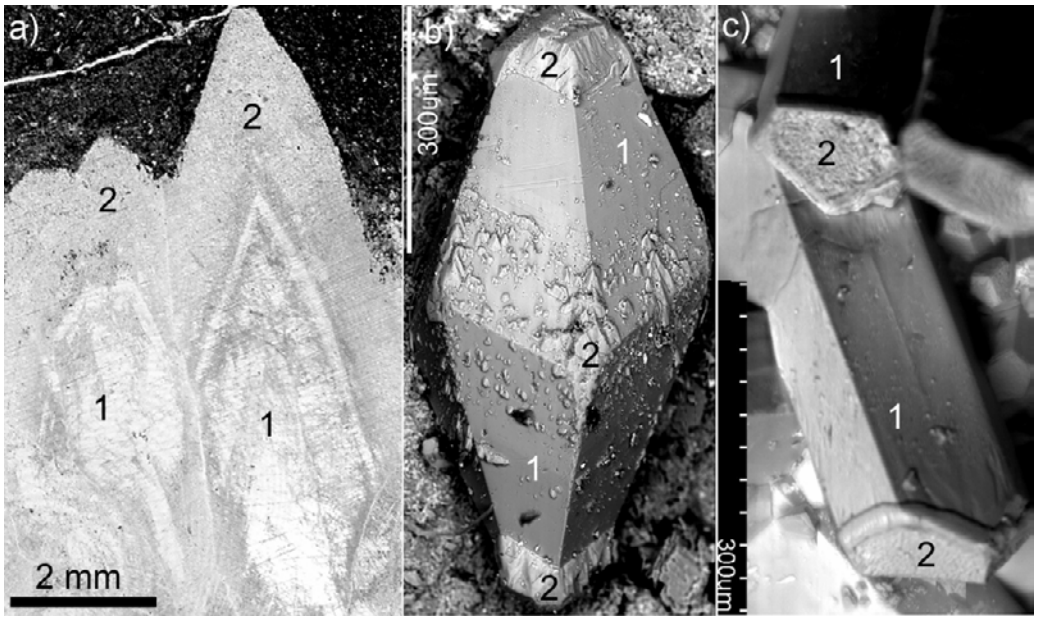

Figure 2-3. *Overgrowths of older calcite by younger calcite. a) Photomicrograph of two generations of scalenohedral calcite (1 and 2), drill core KLX08: 772 m borehole length. b) BSE-image of a scalenohedral crystal (1) overgrown by younger calcite (2) with higher Mn-content (brighter) drill core KLX07A: 272 m, borehole length. b) Needle-shaped crystals (very long c-axis, 1), overgrown by younger, nailhead-shaped crystals (very short c-axis, 2), drill core KLX08: 218 m,borehole length.*

2.2 Sicada data

The data discussed in this report are available in P-reports (Table 1-1) and in the SKB database Sicada and can be traced by their activity plan number (AP number). The drill core mapping data, used for evaluation of fracture mineral distributions, are available in Sicada.

3 Fracture minerals

3.1 Fracture minerals

The fracture minerals identified in the Laxemar area are presented in alphabetical order below. SEM-EDS and XRD data referred to are published in /Drake and Tullborg 2004, 2005, 2006a, b, 2007a, 2008a, b, c, d, e/. Chemical formulae are from /Deer et al. 1992/. The frequency of different fracture minerals shows large variation and the relative frequency can be summarised as follows: calcite and chlorite » epidote, quartz and clay minerals > pyrite > hematite, adularia and prehnite » zeolites (see also Chapter 7). Other minerals (e.g. gypsum, muscovite, amphibole, talc, and goethite) have only been found as minor occurrences but can be more frequent in certain intervals. However, the absolute volumes of each mineral in the specific fractures vary widely. A mapping campaign of the actual volumes of fracture minerals of interest for safety assessment considerations has recently been carried out and the results are quantified in /Löfgren and Sidborn, in preparation/ and the results will be used for modelling included in the forthcoming SR-Site process report. Qualitative XRD analyses have been carried out to identify unknown minerals, especially clay minerals, and also to complement the geochemical analyses of material from hydraulically conductive fractures (and crushed zones). The latter commonly contain fine-grained material including fragments of wall rock together with a fraction of clay-sized particles. The most abundant minerals identified by XRD in these samples are K-feldspar, quartz, plagioclase, calcite, chlorite, clay minerals and subordinate hematite and epidote. The fine fraction (<10 μm) of most samples are dominated by chlorite and clay minerals.

The identified fracture minerals in the Laxemar-Simpevarp area, in alphabetic order, with a short description of each mineral, are:

Albite (Na-Plagioclase) $NaAlSi_3O_8$ is usually found only in trace amounts in the fractures, normally in paragenesis with adularia, quartz ± calcite. However, albite is quite common as fragments in cataclasite, mylonite, as angular clasts in fracture filling sandstone and in pseudomorphs after plagioclase in hydrothermally altered wall rock. It is generally difficult to macroscopically distinguish between albite and adularia.

Amphibole, usually *hornblende* $(Na,K)_{0–1}Ca_2(Mg,Fe,Al)_5Si_{6–7.5}Al_{2–0.5}O_{22}(OH)_2$, occurs in a limited number of sealed fractures with red-stained, hydrothermally altered wall rock. It is especially abundant in KLX08 and to a lesser degree in KLX06 and KSH01A. The paragenesis includes epidote, K-feldspar, chlorite prehnite, quartz and calcite.

Analcime $Na[AlSi_2O_6].H_2O$ is a Na-zeolite which has only been found in two samples (one from Simpevarp subarea; in borehole KSH01A and one from Laxemar subarea; in borehole KLX17A, Figure 3-1) but these samples are dominated by analcime. The crystals are usually euhedral white to transparent trapezohedral crystals. Both of the occurrences identified include paragenetic, euhedral harmotome.

Apatite $Ca_5(PO_4)_3(OH,F,Cl)$ is an accessory mineral in the intact rocks in the area, but it also occurs in minor amounts in fractures together with e.g. quartz, adularia and chlorite (Figure 3-2).

Apophyllite $(K,Na)Ca_4[Si_8O_{20}](F,OH).8H_2O$ is a very brittle and soft hydrothermal sheet silicate with white to silvery surface (Figure 3-3). In the Laxemar subarea it occurs as either fluoroapophyllite or natroapophyllite and is commonly associated with gypsum.

Barite $BaSO_4$ is a sulphate mineral which commonly occurs as euhedral crystals in open fractures together with calcite, fluorite, pyrite and zeolites (Figure 3-4). The mineral is frequently observed using back-scatter SEM-EDS (due to its high density) but the amount of barite in each sample is usually quite small and it has only been identified with XRD in a few samples.

Calcite $CaCO_3$ is, along with chlorite, the most common fracture mineral in the Laxemar area and it is found in several parageneses representing different generations. Its formation conditions range from greenschist facies to the ambient groundwater conditions of recent times. Calcite of Palaeozoic age or younger is commonly found together with fluorite, sulphides ± sulphates. Crystal morphologies may vary, probably partly based on the fluid salinity, and e.g. c-axis elongated crystals (cf. Figure 3-5) indicate precipitation from saline or brackish water whereas c-axis flattened crystals indicate precipitation from fresh water /cf. Milodowski et al. 1998a, b, 2005/. Calcite generally shows low contents of Mg, Fe, whereas the Mn contents may be elevated (up to 4 wt.% MnO), especially in Phanaerozoic calcite.

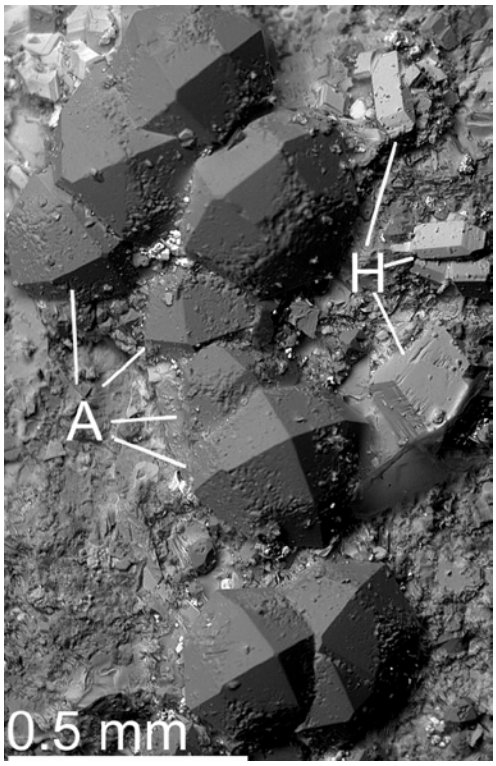

Figure 3-1. *Back-scattered SEM-image of euhedral analcime (A) and harmotome (H) on a fracture surface from borehole KLX17A, borehole length about 431 m.*

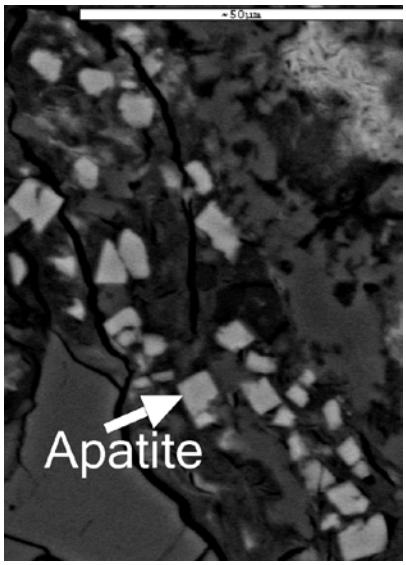

Figure 3-2. *Back-scattered SEM-image of apatite in a fracture filling. Other minerals are adularia and chlorite. From borehole KSH01A, borehole length about 208 m. Scale bar in the upper right corner is 50 µm.*

Figure 3-3. *Back-scattered SEM-image of an apophyllite fracture coating. From borehole KLX03, borehole length about 970 m. Scale bar in the upper left corner is 200 µm.*

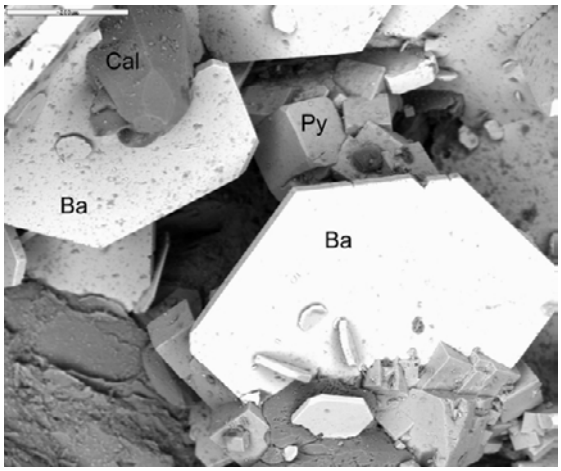

Figure 3-4. *Back-scattered SEM-image of barite (Ba), calcite (Cal) and pyrite (Py) in an open fracture. Scale bar in the upper left corner is 200 µm. From borehole KLX03, borehole length about 457 m.*

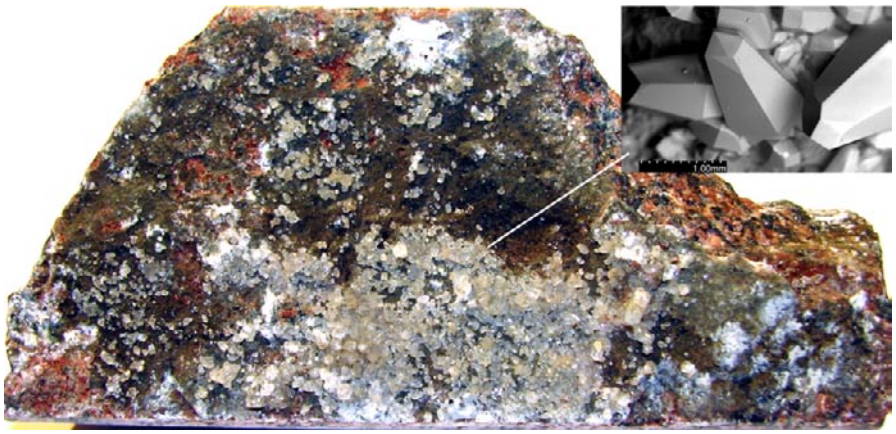

Figure 3-5. *Euhedral (scalenohedral) calcite in an open fracture (inserted close-up image is a back-scattered SEM-image) from borehole KLX15A, borehole length about 1,000 m. Drill core diameter is 50 mm (=height of image). Scale marker in the SEM-image is 1 mm.*

Chalcopyrite ($CuFeS_2$) occurs in the Laxemar area as small grains together with pyrite, sometimes in old (Proterozoic), sealed fractures but usually in younger (Palaeozoic) coatings in open fractures.

Chlorite $(Mg,Fe,Mn,Al)_{12}[(Si,Al)_8O_{20}](OH)_{16}$ is next to calcite, the most common fracture mineral in the Laxemar area. Chlorite can form at temperatures below 400°C. Continuous solid solution extends from Mg-rich chlorite (clinochlore) to Fe-rich chlorite (chamosite). Mg-, Mg-Fe- and Fe-rich chlorites have been identified in the Laxemar area in sealed (Figure 3-16) and open (Figure 3-6) fractures of several different generations. The occurrence of K, Na and Ca in many of the chlorite samples, mainly from open fractures, indicates ingrowths with clay minerals, mostly corrensite.

Epidote $Ca_2Al_2O.(Al,Fe)_3OH[Si_2O_7][SiO_4]$ is green and mainly occurs in sealed fractures. It is normally found at temperatures above 200°C but has been reported in active geothermal systems at temperatures below 200°C /Bird et al. 1984, Bird and Spieler 2004/. Epidote also occurs as a product of the hydrothermal alteration (saussuritisation) of plagioclase and along fractures. In the Laxemar subarea it is found in mylonite, cataclasite or in sealed brittle fractures together with quartz, fluorite and calcite (Figure 3-7).

Fluorite CaF_2 is a cubic, sometimes yellow (Figure 3-8a) but usually dark violet (Figure 3-8b) mineral. Fluorite in greisen may be red as well. Fluorite is found both in old sealed hydrothermal fractures along with epidote, calcite and quartz (Figure 3-7) but is also found in younger (Palaeozoic, Figure 3-8) sealed or open fractures, often together with calcite, pyrite and smaller amounts of galena and barite.

Galena PbS is mainly found as anhedral crystals on fracture surfaces or in sealed fractures. The mineral usually occurs with pyrite, calcite and fluorite.

Figure 3-6. *Fracture coating dominated by chlorite. The older filling is predominantly made up of calcite coated by hematite-stained adularia. KLX15A, borehole length about 570 m. Drill core diameter is 50 mm.*

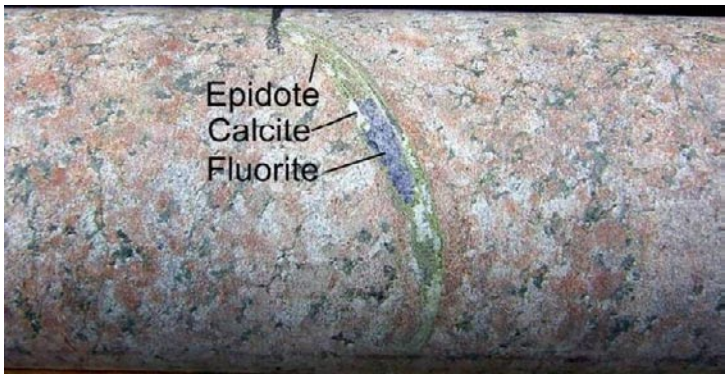

Figure 3-7. *Sealed fracture filled by epidote, calcite and fluorite. From borehole KLX06, borehole length about 315 m. Drill core diameter is 50 mm.*

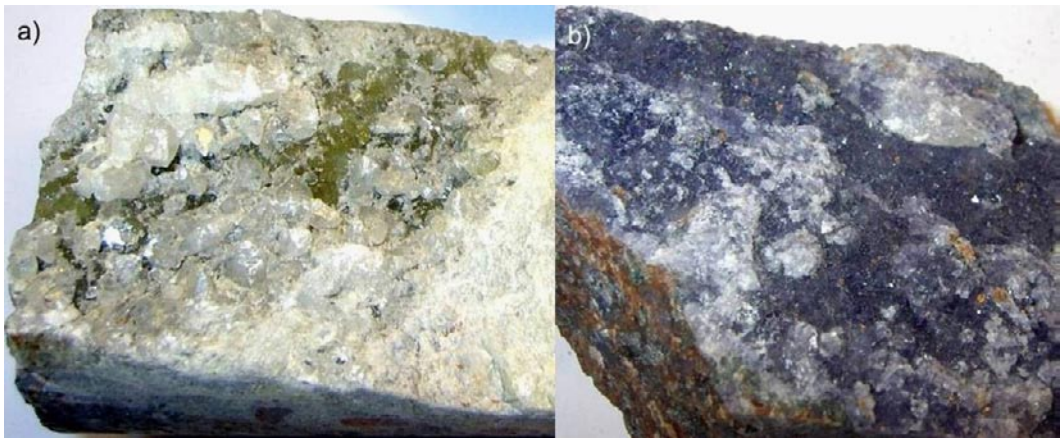

Figure 3-8. *Open fractures coated with fluorite (a: yellow; b: violet) and calcite (grey to white). a) From borehole KLX06, borehole length about 814 m. b) From borehole KLX04, borehole length about 925 m. Drill core diameter is 50 mm. Drill core diameter is 50 mm.*

Goethite FeOOH commonly occurs as a weatering product (oxidation) of Fe(II)-bearing minerals such as magnetite and pyrite. It gives the coating a yellow to brownish (rust-) red colour (Figure 3-9). It is most common in near surface fractures exposed to oxygen-rich fluids (see Section 6.2). However, despite goethite's ability to colour the fracture surface, the absolute volume of goethite in these fractures is commonly very small (below or close to the detection limit for XRD).

Gypsum $CaSO_4 2H_2O$ is a soft and easily dissolved sulphate. It is present in some fractures in the Laxemar subarea (e.g. KLX03, KLX06, KLX08, KLX10, KLX12A and KLX17A, Figure 3-10), mainly at depths greater than –500 m above sea level, occasionally accompanied by apophyllite, calcite, pyrite, fluorite, barite and rarely celestine.

Harmotome $Ba_2[Al_4Si_{12}O_{32}].12H_2O$ is a Ba-zeolite which usually occurs as small euhedral crystals in open fractures (Figure 3-1) with barite, calcite (usually scalenohedral), pyrite, chlorite, clay minerals and other zeolites. It is a low temperature zeolite with stability temperatures that are somewhat lower than that of laumontite, although the stability field of harmotome has not been as extensively studied as that of laumontite. Harmotome has not been identified in fractures at depths greater than –430 m above sea level, but is generally limited to the upper 300 m. SEM-EDS analyses show that the harmotome in the Laxemar area contains detectable contents of Na and K.

Hematite Fe_2O_3 occurs frequently in the Laxemar fractures but the amount of hematite in each fracture is relatively low (often below the XRD detection limit). In open fractures, it is present mostly as minute grains covering other fracture minerals, giving the coating a red to brown colour (Figure 3-11). It is also found within K-feldspar and laumontite crystals, giving these minerals a reddish colour. Euhedral hematite crystals with metallic lustre have also been found in a few fractures. Hematite has commonly partly replaced magnetite in hydrothermally altered wall rock.

Figure 3-9. *Near surface fracture coated by, for example, goethite. From borehole KLX09E, borehole length about 1 m. Drill core diameter is 50 mm.*

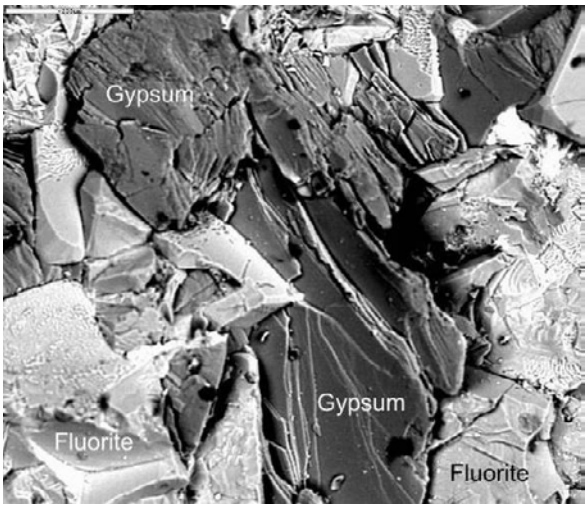

Figure 3-10. *Back-scattered SEM-image of gypsum and fluorite crystals on a fracture surface. Scale bar in the upper left corner is 200 µm. From borehole KLX06, borehole length about 789 m.*

Figure 3-11. *Fracture surface covered with hematite. The white fracture filling is older calcite. From borehole KLX04, borehole length about 674 m. Drill core diameter is 50 mm.*

K-feldspar $KAlSi_3O_8$ is usually present along fractures in its low temperature form adularia. The colour is either brick red due to hematite staining or grey (sometimes light greenish). Paragenesis includes calcite, quartz, laumontite, illite, chlorite and hematite. Microcline is found within wall rock fragments in breccias and cataclasites.

Laumontite $Ca_4[Al_8Si_{16}O_{48}]\cdot 16H_2O$ is the most common zeolite in the Laxemar subarea and is abundant in some of the deformation zones (e.g. the Mederhult zone, (ZSMEW002A, cf. Figure 1-2), cf. Figure 3-12). It is white coloured, but may be red-stained by minute hematite crystals. The stability field of laumontite is c. 150–250ºC /Liou et al. 1985/.

Muscovite $K_2Al_4[Si_6Al_2O_{20}](OH,F)_4$ is found in fracture fillings (e.g. in greisen in KLX06 close to the Götemar granite, Figure 3-13), in mylonite and as sericite in hydrothermally altered wall rock, for example, in red-stained rock.

Prehnite $Ca_2(Al,Fe)[AlSi_3O_{10}](OH)_2$ is a hydrothermal mineral often associated with calcite and fluorite. It is commonly bright greyish green to grey or white. It is formed at temperatures below 280°C (at P<3 ka), /Frey et al. 1991/. The low-temperature alteration of prehnite may produce laumontite or chlorite and clay minerals. In the Laxemar subarea it is associated with red-stained wall rock (Figure 3-14).

Pyrite FeS_2 occurs in many open fractures as small euhedral, cubic crystals (Figure 3-15) but is also found as anhedral, occasionally coarse-grained crystals together with calcite and quartz in sealed fractures or related to greisen alteration (Figure 3-13).

Figure 3-12. *Laumontite and calcite in sealed fractures in borehole KLX06, borehole length about 400 m. Drill core diameter is 50 mm.*

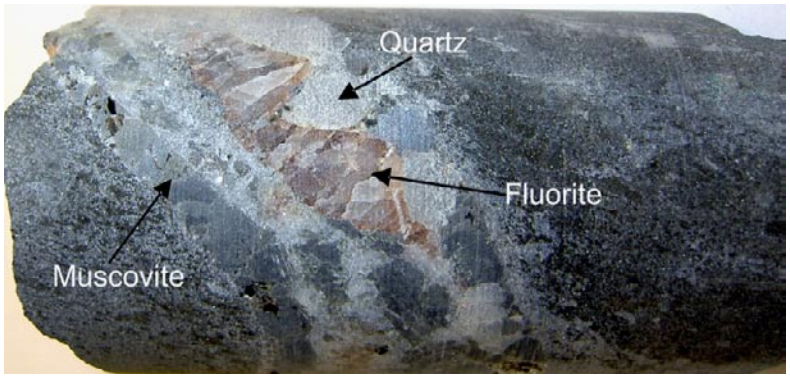

Figure 3-13. *Muscovite, quartz and fluorite in greisen fractures in borehole KLX06, borehole length about 572 m. Drill core diameter is 50 mm.*

Figure 3-14. *Fracture filled with prehnite. Note the red colour of the wall rock due to hydrothermal alteration. From borehole KLX07A, borehole length about 227 m. Drill core diameter is 50 mm.*

Quartz SiO_2 is found in several fracture filling generations, in both sealed (Figure 3-16, also in greisen) and open fractures. In the latter case, quartz may be euhedral.

REE-carbonate (probably bastnäsite) $(Ce,La,Y)CO_3F$ is Palaeozoic or younger and is found in paragenesis with calcite, fluorite, sulphides and sulphates (Figure 3-17). The mineral is frequently observed using back-scatter SEM-EDS (due to its high density) but the amount of REE-carbonate in each sample is quite small and it has only been identified with XRD (best fit is bastnäsite) in a few samples.

Sphalerite (ZnS) has been found in minor amounts in both open and sealed fractures and is commonly associated with pyrite, galena and chalcopyrite, in calcite- (fluorite-) rich fillings.

Talc $Mg_6[Si_8O_{20}](OH)_4$ almost exclusively occurs in open fractures in dolerites, especially in KLX20A, where it is slickensided, indicative of shearing.

Figure 3-15. *Back-scattered SEM-image of cubic pyrite crystals coating an open fracture, borehole KLX03, borehole length about 266 m.*

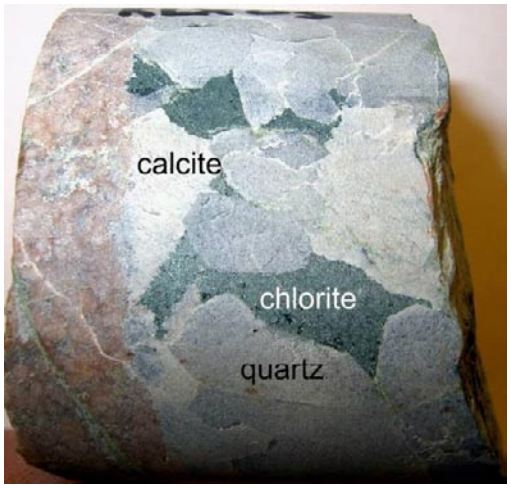

Figure 3-16. *Fracture filling with chlorite (arrow), calcite (white) and quartz (grey). KLX03, borehole length about 730 m. Drill core diameter is 50 mm.*

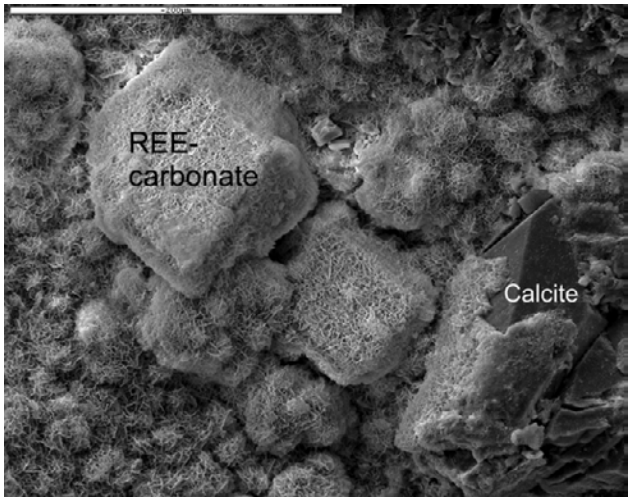

Figure 3-17. *Back-scattered SEM-image of calcite covered with REE-carbonate, from borehole KSH01A: 289 m.*

Clay minerals:

Illite $K_{1.5–1.0}Al_4[Si_{6.5–7}Al_{1.5–1.0}O_{20}](OH)_4$ occurs as micro- to cryptocrystalline, micaceous flakes and is often formed as an alteration product of mica or K-feldspar. Illite is together with corrensite the most frequently found clay mineral in the Laxemar subarea.

The smectite group $(½Ca,Na)_{0.7}(Al,Mg,Fe)_{4(or\ 6)}[(Si,Al)_8O_{20}](OH)_4.nH_2O$ is a group of swelling clay minerals taking up water or organic molecules between their structural layers. They also show marked cation exchange properties /Deer et al. 1992/. Smectite has been identified in the Laxemar area, commonly in mixed-layer clay; illite/smectite or chlorite/smectite (corrensite).

Saponite $(½Ca,Na)_{0.33}(Mg,Fe)_3(Si,Al)_4O_{10}(OH)_2.4H_2O$ is a variety of swelling smectite which has been identified in the Laxemar area, both as individual crystals and in mixed-layer clay; illite/smectite or chlorite/smectite (corrensite).

Vermiculite $(Mg,Ca)_{0.6–0.9}(Mg,Fe,Al)_{6.0}[(Si,Al)_8O_{20}](OH)_4.nH_2O$ is similar to smectite and is a constitutuent in corrensite, which is one of the most common clay minerals in the Laxemar area.

Kaolinite $Al_4[Si_4O_{10}](OH)_8$ has only been identified by XRD in one borehole (KLX11F at about 13 m vertical depth).

Mixed-layer clay

Mixed-layer clay (Figure 3-18) is the term usually applied to clays having alternating layers of e.g. illite/smectite or chlorite/smectite-vermiculite.

Mixed-layer clay – Corrensite $(Ca,Na,K)(Mg,Fe,Al)_9(Si,Al)_8O_{20}(OH)_{10}.nH_2O$ is a mixed-layer clay with layers of chlorite and smectite/vermiculite, usually in a ratio of 1:1. It is usually found together with chlorite. XRD analyses show irregular ordering in the layering of many of the corrensite samples, either due to alteration or due to that it has not reached perfect corrensite crystallinity. Corrensite is commonly swelling and is very common in the water conducting fractures in the Laxemar subarea (Figure 3-19).

Mixed-layer clay – illite/smectite is usually swelling and is commonly identified in XRD analyses from the Laxemar area, although it is not as common as corrensite or the corrensite-like minerals (Figure 3-20). The ratio between the illite and smectite layers varies due to degree of re-crystallisation and the illite component increases with increasing formation temperature.

Separation of different clay minerals was not possible during the drill core mapping and therefore no estimation of the relative frequency of these minerals exists. However, the XRD data can be used to make a rough estimation (Figure 3-20, including chlorite present in the fine fraction; <10 µm).

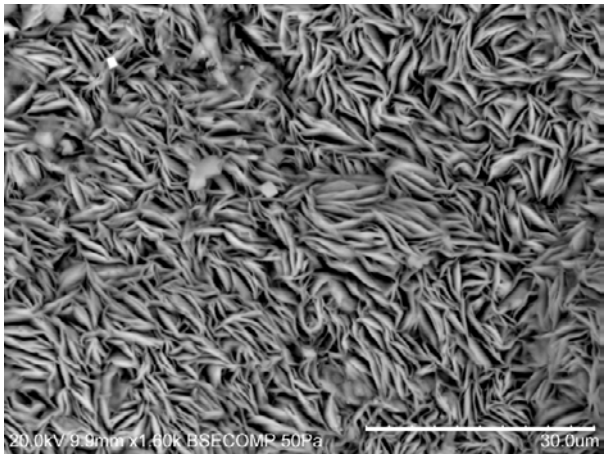

Figure 3-18. *Back-scattered SEM-image showing mixed-layer clay on a fracture surface from KLX08, borehole length about 108 m. Scale bar in the lower right corner is 30 µm.*

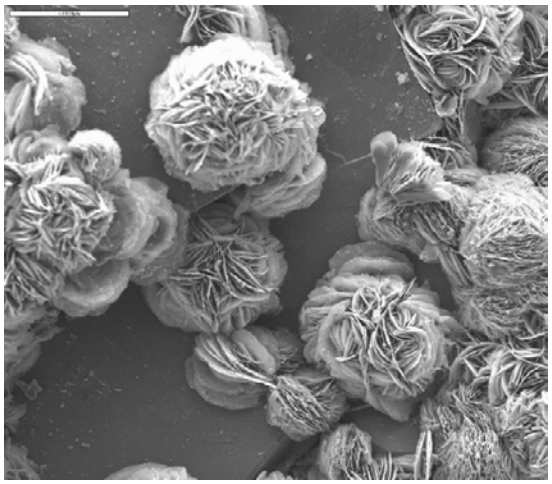

Figure 3-19. *Back-scattered SEM-image of spherulitic corrensite aggregates on a fracture surface from borehole KLX06, borehole length about 831 m. Scale bar in the upper left corner is 200 µm.*

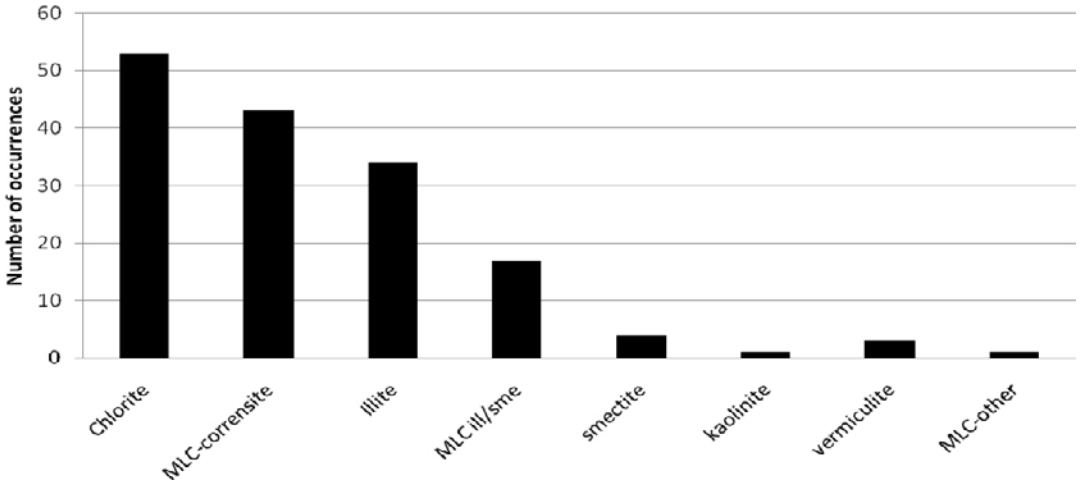

Figure 3-20. *Histogram showing number of fractures where clay minerals and chlorite have been identified by XRD-analysis of bulk fracture filling material in the fine fraction (<10 µm). MLC = mixed-layer clay, sme = smectite, ill = illite. Total number of samples analysed is 68.*

Additional information is also gained from SEM-EDS studies and from the examination of the drill cores during sampling for the detailed mineralogical studies. From this information it is evident that corrensite is the most common clay mineral followed by illite and illite/smectite mixed-layer clay. Non-mixed smectite, vermiculite and kaolinite, as well as unidentified mixed-layer clay have also been observed, but only in a few samples.

Rare minerals occasionally identified

Fracture minerals titanite ($CaTi[SiO_4](O,OH,F)$), celestine ($SrSO_4$), Ti-oxide (rutile and/or anatase; TiO_2), topaz, U-rich silicate (possibly coffinite; $U(SiO_4)_{1-x}(OH)_{4x}$), Ce-oxide (possibly cerianite; $(Ce,Th)O_2$), Mn-oxide, W-rich mineral (possibly wolframite; $(Fe,Mn)WO_4$), serpentine group minerals (e.g. antigorite; $(Mg,Fe)_3Si_2O_5(OH)_4$, and chrysotile; $Mg_3Si_2O_5(OH)_4$), biotite ($K(Mg,Fe)_3[AlSi_3O_{10}](OH,F)_2$), pumpellyite ($Ca_2MgAl_2(SiO_4)(Si_2O_7)(OH)_2\cdot(H_2O)$), magnetite ($Fe_3O_4$), argentite ($Ag_2S$), sylvite (KCl), halite (NaCl), native gold, native copper and Zn-oxide have been identified in a small number of fractures, usually using SEM-EDS (e.g. <5 µm grains of gold) or XRD (e.g. serpentine group minerals).

3.2 Concluding remarks

It can be stated with confidence that all major fracture mineral phases have been identified within the Laxemar area. However, there are some minor uncertainties in the mapping data. Detailed SEM-EDS, microscopy and XRD investigations have revealed the existing fracture minerals including minor phases and these data have been used to support the mapping and therefore, the uncertainties in the mapping have been reduced as the site investigations have progressed. The frequency of different fracture minerals shows large variation and the relative frequency can be summarised as follows: calcite and chlorite » epidote, quartz and clay minerals > pyrite > hematite, adularia and prehnite » zeolites. Other minerals have generally only been observed in minor amounts but can be more frequent in certain intervals (e.g. gypsum, muscovite, amphibole, talc, and goethite). However, the absolute volumes of each mineral in the specific fractures vary widely.

XRD analyses of presently water conducting fractures show that the relative clay mineral frequency in these structures is in order: corrensite (or similar mixed-layer clay) > illite > mixed layered illite/smectite. Other clay minerals have also been identified, but only in a few samples. The only carbonate identified apart from calcite is a REE-carbonate, probably bastnäsite according to the XRD spectrum, which is found in small amounts on many fracture surfaces. The sulphate minerals identified are gypsum, barite and very rarely celestine. Pyrite is the dominant sulphide, but chalcopyrite, galena, sphalerite and trace amounts of some other sulphides have also been identified. Zeolites are dominated by laumontite and harmotome but analcime has also been identified.

4 Sequence of fracture mineralisations

Detailed studies of cross-cutting fracture mineral relations (cf. Figure 2-2. Figure 2-3 and Section 2.1.2) in a large number of samples have, along with palaeohydrogeological studies (Chapter 5), resulted in the establishment of a relative chronological sequence of fracture filling generation. An estimation of formation temperatures for each generation can be interpreted from the stability temperatures of specific minerals or the mineral paragenesis. The Ca-silicates epidote-prehnite and laumontite have similar chemical compositions but precipitate under different, slightly overlapping, temperatures. Epidote normally precipitates above 200°C /Bird et al. 1984, Bird and Spieler 2004/, prehnite at about 200 to 280°C /Frey et al. 1991/ and laumontite at about 150 to 250°C /Liou et al. 1985/. Temperature information to constrain the formation conditions of each generation has also been obtained from fluid inclusion analyses (see Section 5.2 for details). Stable isotope values and trace element concentrations, may also provide temperature constraints, e.g. microbial or organic signatures indicate low temperature conditions (below ~150–100°C, see e.g. Sections 5.1, and 5.5).

The ages of the ca 1.80 Ga rock units belonging to the Transscandinavian Igneous Belt (TIB) in the Laxemar area are well established (ca 1.80 Ga TIB rocks) /Wahlgren et al. 2004, 2006a/, and provide a maximum age of the fractures. Younger rocks are the Götemar and Uthammar granites aged 1.45–1.44 Ga /Åhäll 2001/, N-S striking dolerite dykes aged 0.9 Ga /Wahlgren et al. 2007/ and Cambrian sandstone fractures /Alm and Sundblad 2002, Röshoff and Cosgrove 2002, Drake and Tullborg 2006a, b, 2008a/.

A summary of the sequence of fracture mineralisations is presented in Table 4-1 and Figure 4-1. Drill core samples used for $^{40}Ar/^{39}Ar$ geochronology and their resulting $^{40}Ar/^{39}Ar$-spectra are shown in Figure 4-2 and Figure 4-3. Detailed descriptions of the different fracture mineral generations are presented in Sections 4.1 to 4.7.

The preferred orientations of fractures filled with minerals of different generations can reveal palaeo-stress information for the time of formation and can thus help to relate the generations to specific events and also help to distinguish between different generations. However, such a linkage is not easily observed in the Laxemar area because the fractures are extensively reactivated and the orientations of early formed shear zones have also influenced the orientation of the fractures /cf. Talbot and Riad 1988, Munier and Talbot 1993, Drake and Tullborg 2004, 2007a, Viola and Venvik Ganerod 2007/.

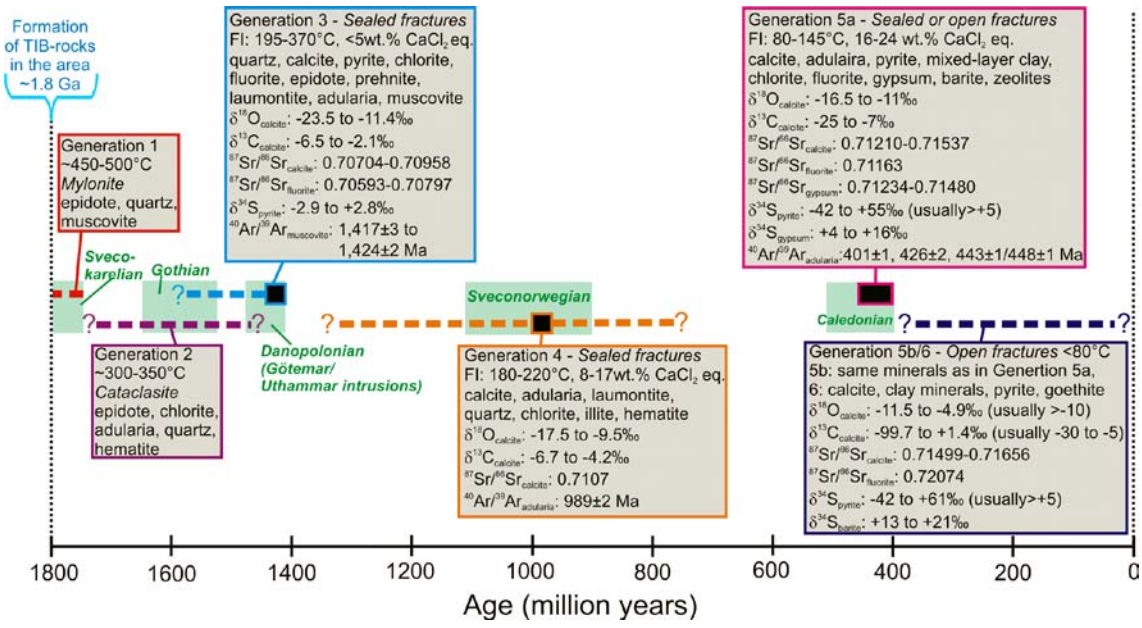

Figure 4-1. *Summary of the fracture mineralogical data from the Laxemar area, in chronological order, with orogenies and nearby intrusions (indicated in green). Time ranges from /Åhäll 2001, Roberts 2003, Bingen et al. 2008/. "FI"= fluid inclusion.*

Table 4-1. Characteristics of each fracture mineral generation.

	Dominating minerals	Formation temperature[1] (°C)	Fluid Salinity[1] (wt.% $CaCl_2$ eq.)	$\delta^{18}O$ in calcite (‰PDB)	$\delta^{13}C$ in calcite (‰PDB)	$^{87}Sr/^{86}Sr$ in calcite, fluorite, and gypsum	$\delta^{34}S$ in pyrite, barite, gypsum (‰CDT)	Radiometric ages[2] (Ma)
Generation 1 *Mylonite*	epidote, quartz, muscovite	(450–500[3])	n.a.	n.a.	n.a.	n.a.	n.a.	(1,406 ± 3[4])
Generation 2 *Cataclasite*	epidote, chlorite, adularia, quartz, hematite	n.a.	n.a.	n.a.	n.a.	n.a.	n.a.	n.a.
Generation 3 *Coarse-grained, Sealed fractures*	quartz, calcite, pyrite, chlorite, epidote, prehnite, laumontite, adularia, muscovite	~200 to 370	1 to 20 (usually <5)	–23.5 to –11.4 (usually <–16)	–6.5 to –2.1	cc: 0.70704–0.70958 fl: 0.70593–0.70797 (outlier: 0.74681)	py: –2.9 to +2.8	1,417 ± 3[5] 1,423 ± 3[6] 1,424 ± 2[6] 1,424 ± 2[6]
Generation 4 *Thin, sealed fractures*	calcite, adularia, laumontite, quartz, chlorite, illite, hematite	~180 to 220[7]	8 to 17[7]	–17.5 to –9.5	–6.7 to –4.2	0.7107[7]	n.a.	989 ± 2[8]
Generation 5a *Sealed or open fractures*	calcite, adularia, Pyrite[11], MLC[12], chlorite, fluorite, sulphates[13], zeolites[14]	~80–145	16 to 24	–16.5 to –11 (sometimes higher)	–25 to –7 (mainly –16 to –9)	cc: 0.71210–0.71537 fl: 0.71163[7] gy: 0.71234–0.71480	py: –42 to +55[9] (usually >+5) gy: +4 to +16	401 ± 1[10] 426 ± 2[10] 443 ± 1/448 ± 1[10]
Generation 5b/6 *Open fractures*	5b: same as 5a. 6: calcite, clay minerals, pyrite, goethite	<80	n.a.	–11.5 to –4.9 (usually >–10)	–99.7 to +1.4 (usually –30 to –5)	cc: 0.71499–0.71656[15] fl: 0.72074[7]	py: –42 to +61[9] (usually >+5) ba: +13 to +21	n.a.

[1)] Based on fluid inclusion analyses of calcite and quartz, [2)] Based on $^{40}Ar/^{39}Ar$ dating of adularia and muscovite, [3)] Based on textural observations /Lundberg and Sjöström 2006/, [4)] Represents resetting of the Ar-system in the muscovite, [5)] Muscovite in altered wall rock, [6)] Muscovite in greisen fractures, [7)] Based on a single sample, [8)] May represent resetting of the Ar-system in the adularia, [9)] No clear subdivision of pyrite of Generation 5a and 5b/6 have been possible, Götemar granite pyrite has +13.2 to +60.8(‰CDT), [10)] Fracture-filling adularia. [11)]Other sulphides are chalcopyrite, galena and sphalerite, [12)] Mixed-layer clay; e.g. corrensite and interstratified illite/smectite, [13)] Includes barite, gypsum and rarely celestine, [14)]Mainly harmotome but also analcime and laumontite. [15)] Calcite in Götemar granite fractures has $^{87}Sr/^{86}Sr$-ratios of 0.71598–0.71695 (Generation 5a) and 0.71717–0.71726 (Generation 5b/6).

Abbreviations: cc = calcite, fl = fluorite, py = pyrite, gy = gypsum, ba = barite.

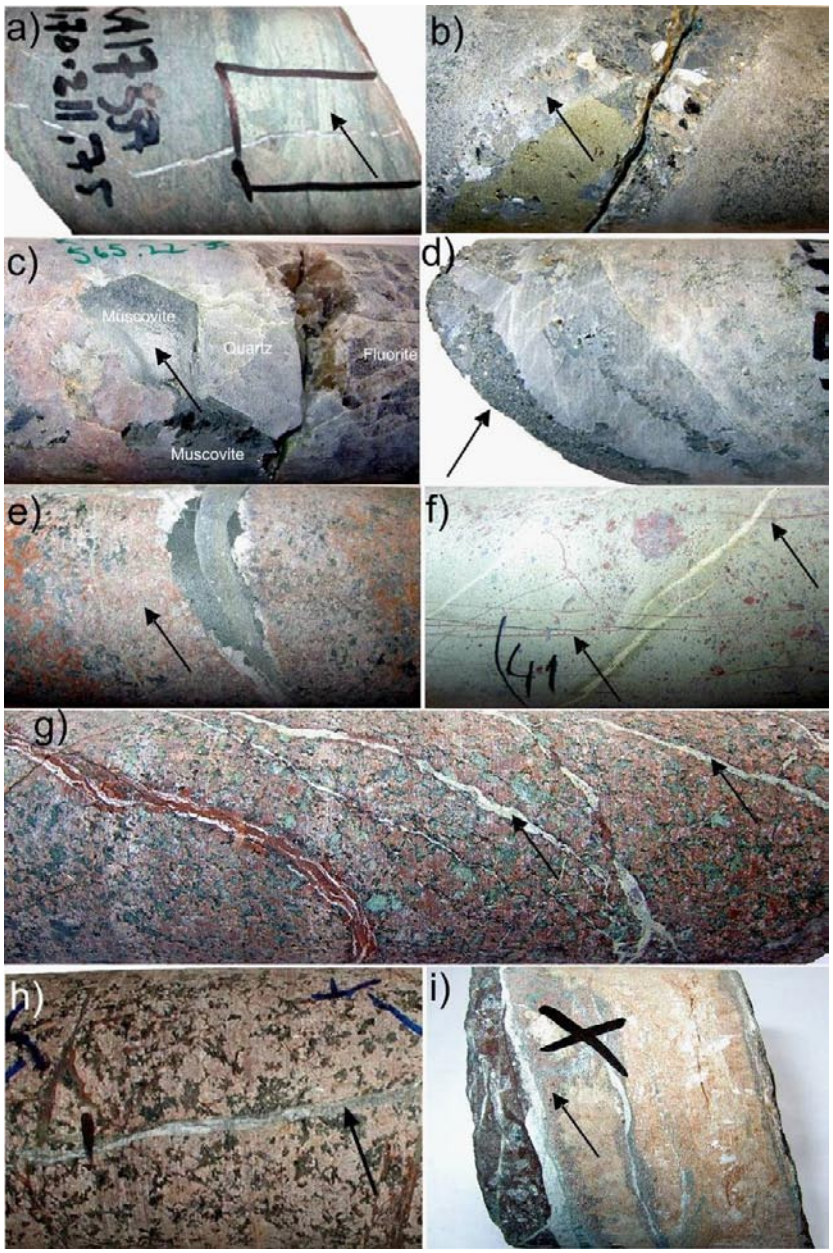

Figure 4-2. *Samples yielding $^{40}Ar/^{39}Ar$ plateau ages (arrow indicates the minerals dated). a) Muscovite in mylonite of the Äspö shear zone (ZSMNE005A), borehole KA1755A: 211 m borehole length. The mylonite is cross-cut by a fracture filled with calcite, fluorite and hematite (probably of Generation 3). b–d) Coarse-grained muscovite in sub-horizontal greisen fractures, KLX06: 535 m borehole length (b, orientation of broken fracture through the filling: 183°/12°), 565 m (c, upper rim: 329°/34°; lower rim: 331°/26°) and 595 m (d, upper rim: 213°/15°; lower rim: 228°/16°), respectively. e) Muscovite/sericite in altered, bleached/red-stained wall rock adjacent to a fracture (upper fracture rim: 100°/6°; lower rim: 92°/25°) filled with Generation 3 minerals, KLX03: 722 m borehole length. f) Adularia in numerous parallel fractures cutting through epidote-dominated mylonite/cataclasite, KSH03A: 863 m borehole length. g) Adularia with calcite and hematite in numerous sub-parallel fractures (dominant orientations: 272°/80°, 280°/72° and 279°/66°), KSH03B: 15 m borehole length. h) Adularia with calcite, chlorite, and sulphides in fractures cutting through cataclasite (fracture orientations are deviating; cutting cataclasite: 41°/70°; reactivating cataclasite: e.g. 100°/15°, 128°/24° and 3°/18°), KSH01A: 257 m borehole length. i) Adularia in a section characterised by reactivated fractures with fillings of several generations (orientation of the specific adularia fracture is 196°/45°), KSH03A: 181 m borehole length. $^{40}Ar/^{39}Ar$ spectra for these samples are presented in Figure 4-3.*

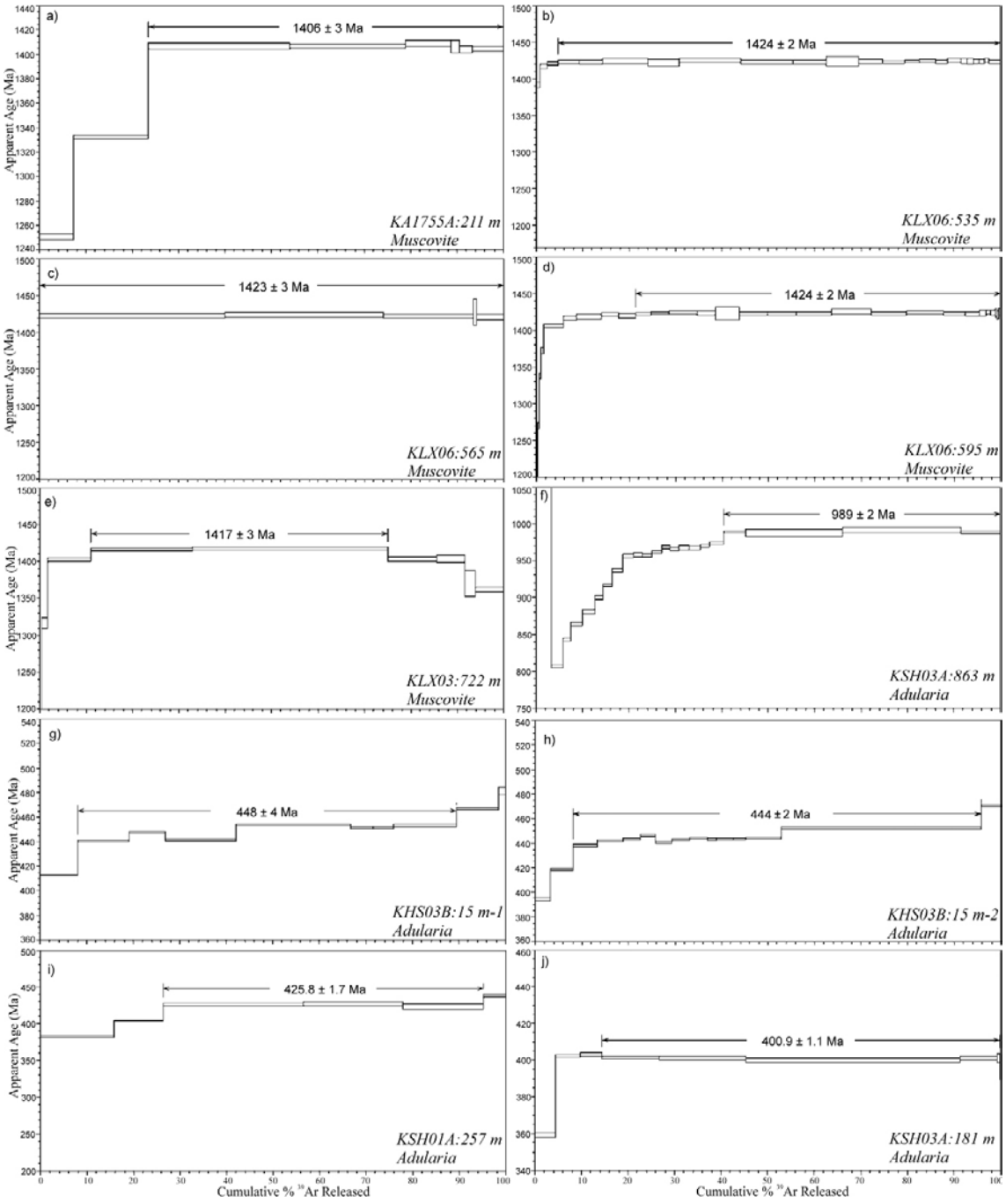

Figure 4-3. *$^{40}Ar/^{39}Ar$ spectra of the samples shown in Figure 4-2. Note that g) and h) represent two splits from the same sample. All of these samples fit the criteria of /Dalrymple and Lanphere 1971/ for defining plateau ages; specified as the presence of at least three contiguous incremental heating steps with statistically indistinguishable ages and constituting greater than 50% of the total ^{39}Ar released during the experiment.*

Since the most common fracture minerals occur in several fracture filling generations, and especially since the degree of reactivation is very high, it is difficult to interpret preferred fracture orientations of the different generations /Munier and Talbot 1993, Drake and Tullborg 2004, 2007a/. A few minerals, such as gypsum, which is only present in one generation, has been shown to reveal palaeostress information, if obviously reactivated fractures (distinguished by the presence of older minerals and wall rock alteration) are excluded /Drake and Tullborg 2007a/. Furthermore, different fracture orientations dominate in different fracture domains within the Laxemar subarea /Wahlgren et al. 2008/, partly assumed to be associated with the orientations of older deformation zones which have influenced the formation

of newly formed fractures nearby. Therefore, two approaches of stereographic projections (stereo plots) are used to interpret the dominant fracture orientations for the most common minerals and thus the fracture filling generations:

1) An extensive analysis in which the orientation of all fractures containing a certain mineral is plotted on a fracture domain basis, separating sealed and open fractures (mainly due to the frequent fracture reactivations in the area). The most important plots are shown next to the generation they mainly represent in order to trace differences in orientations of each generation in the different fracture domains (all plots are shown in Appendix 2).
2) A more detailed and selective analysis including minerals interpreted to be of special importance for palaeostress analysis. The data set for each of these minerals is limited in an attempt to reveal primary fracture orientations which are not inherited from older fractures or influenced by adjacent deformation zones. This subset of data is mainly chosen to eliminate reactivated fractures, i.e. fractures including old hydrothermal minerals or extensive wall rock alteration are left out when analysing low-temperature generations and vice versa and these orientations are shown separately in Section 4.8. All of the stereographic projections show Fisher concentrations as a percentage of the total number of poles per 1.0% of stereonet area. Terzaghi corrections have been applied to compensate for the effects of borehole orientations. Fracture domain FSM_S is excluded due to the scarcity of data from this domain (only one borehole).

4.1 Generation 1

Mylonites of Generation 1 are present in the major deformation zones such as ZSMNE005A (the Äspö shear zone) and ZSMEW002A (the Mederhult zone, Figure 4-4), but also in minor deformation zones. The mylonites are dominated by epidote and quartz, occasionally with abundant muscovite, chlorite and albite and often with minor amounts of K-feldspar, calcite and trace amounts of titanite, zircon and apatite. These fine-grained minerals represent the first mineralisation in the area. The mylonites have been reactivated and are cross-cut by several generations of cataclasites and brittle fractures. The mineral assemblage of epidote-chlorite-albite suggests formation during greenschist facies conditions. The most prominent ductile shear zones are sub-vertical and strike N-S, NE-SW and E-W /Wahlgren et al. 2006b/. Formation temperatures have been interpreted from micro-structures to be c. 450–500°C /Lundberg and Sjöström 2006/. A minimum age close to c. 1.77 Ga /Söderlund et al. 2008/, when the rock cooled below ~500°C, is thus suggested. Furthermore, field observations indicate a close temporal relationship between the formation of the TIB-rocks and the ductile shear zones /Lundberg and Sjöström 2006/. Two different mylonite varieties of similar age have been identified in the Äspö shear zone /Munier and Talbot 1993/. $^{40}Ar/^{39}Ar$-dating of muscovite in mylonite from Äspö shear zone yielded a plateau age of 1,406 ± 3 Ma (Figure 4-2a and Figure 4-3a) and this age is much younger than expected and probably does not represent the ductile deformation. Instead, the age probably reflects cooling below 350°C after resetting of the $^{40}Ar/^{39}Ar$-system in relation to the nearby intrusions. The $^{40}Ar/^{39}Ar$ system in the dated mylonite may be particularly disturbed by a cross-cutting Generation 3 fracture (Figure 4-2a), which is probably related to circulation of Götemar-related hydrothermal fluids, of a later stage than the greisen (see Section 4.3 below). The ductile shear zones are definitely older than the c. 1.45 Ga Götemar granite /Nisca 1987, Talbot and Riad 1988, Munier and Talbot 1993, Cruden 2008/.

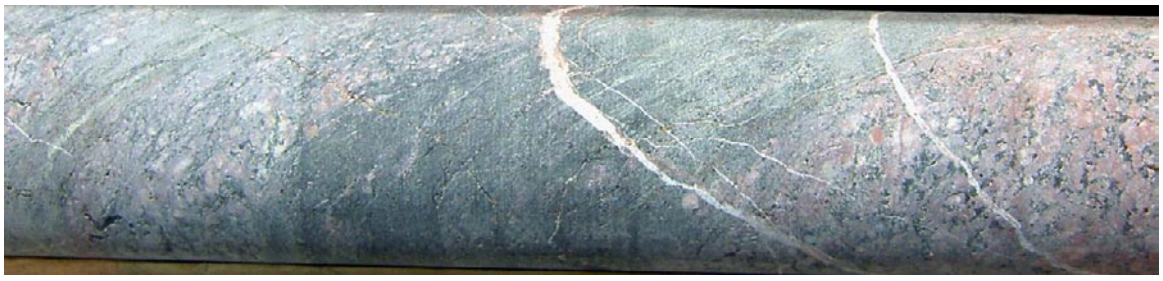

Figure 4-4. *Photograph of mylonite of Generation 1 cross cut by younger fractures filled with calcite. KLX06, borehole length, about 373 m. Deformation zone ZSMEW002A. Drill core diameter is 50 mm.*

The direction of the maximum compressive stress was approximately N-S to NNW-SSE (with related ductile shortening in this direction) during the formation of the ductile shear zones in the area, probably in the late stages of the Svecokarelian orogeny, at >1,750 Ma /Lundberg and Sjöström 2006, Wahlgren et al. 2006b, Stephens and Wahlgren 2008/.

The orientations of fractures filled with e.g. epidote and quartz are therefore discussed in Section 4.3 on fracture fillings of Generation 3.

4.2 Generation 2

Cataclasite of Generation 2 is very common in the deformation zones, especially in the Simpevarp subarea, e.g. in ZSMNE024A in KSH03A, but also exists in the Laxemar subarea, e.g. in ZSMEW007A in KLX04. Several varieties exist and these can be divided into two main types, which both show occasional semi-ductile features. The oldest type; Generation 2a, is a green coloured cataclasite rich in epidote, quartz, chlorite, with minor amounts of K-feldspar and albite (Figure 4-5a–b). The younger Generation 2b is a reddish brown cataclasite rich in K-feldspar, chlorite, quartz, hematite, albite and subordinate illite (Figure 4-5a–d). The colour of the Generation 2b fillings is due to discolouration of the feldspars and chlorite by very small amounts of hematite. The only chlorite sample analysed is of Fe-Mg-type (Figure 4-6), similarly to the chlorite of Generation 3 and chlorite in hydrothermally altered wall rock. The observed semi-ductile features suggest formation close to the brittle-ductile transition at about 300–350°C (corresponds to depths of at least 10 km in granitic rock /Davis and Reynolds 1996/). Because the cataclasites often have reactivated ductile shear zones the orientation of these has influenced the orientation of most Generation 2 structures. The cataclasite has not been dated but two main alternatives on the formation of the cataclasites may be proposed based on the

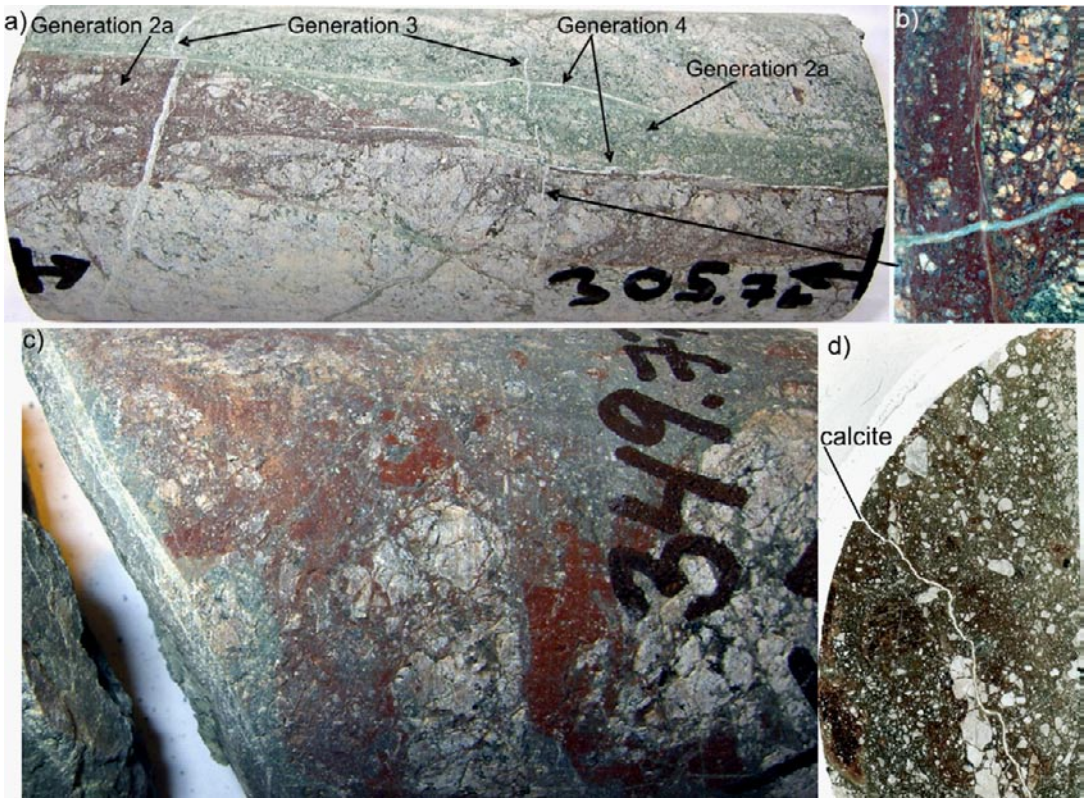

Figure 4-5. *a–b) Photograph of drill core and polished rock chip (b) of sample KSH03A: 305 m borehole length, showing green-coloured cataclasite of Generation 2a and red coloured cataclasite of Generation 2b. Both of the cataclasite types have been cut by calcite veins of Generation 3 and 4. c–d) Photograph (c) and scanned thin section (d) of drill core sample KLX04: 349 m borehole length (deformation zone ZSMEW007A), showing cataclasite of Generation 2b cut by a thin fracture filled with calcite. Drill core diameter is ~50 mm.*

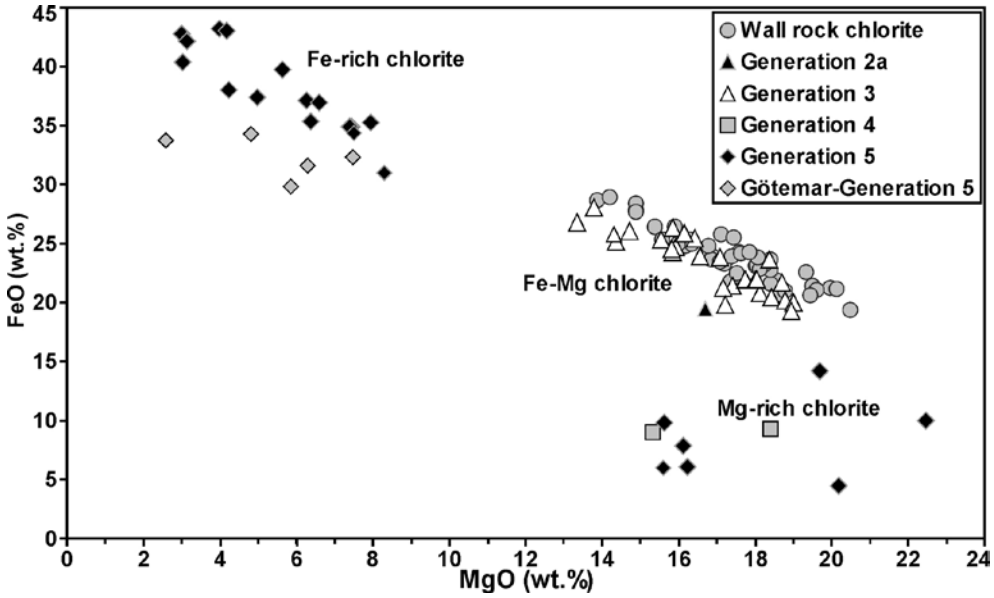

Figure 4-6. *FeO versus MgO in chlorite of different fracture filling generations and from altered wall rock. Composition of Generation 5 chlorite from the Götemar granite is also shown. From /Drake et al. 2009b/.*

formation temperatures: 1) formation in association with the Gothian orogeny (mainly effecting southwestern Sweden and Norway /cf. Bingen et al. 2008/), prior to 1,620 Ma when the rock initially cooled below 300°C and 2) formation related to the intrusions at Götemar and Uthammar or at a slightly earlier thermal event /cf. Page et al. 2007/.

Cataclasite is much less common than younger brittle, dilation fractures with similar mineralogy. The orientations of fractures filled with e.g. epidote, quartz, hematite, chlorite and K-feldspar (adularia) are therefore discussed in relation to younger fracture fillings.

4.3 Generation 3

Generation 3 consists of a sequence of at least three different mineral parageneses (sub-generations 3a, 3b and 3c) and occasionally of greisen, found in cross-cutting fractures formed at gradually lower formation temperatures, as suggested by the stability temperatures of the dominant Ca-Al-silicates; epidote (Generation 3a, Figure 4-7), prehnite (3b, Figure 4-8), and laumontite (3c, Figure 4-8) /Bird et al. 1984, Frey et al. 1991, Bucher and Frey 2002, Bird and Spieler 2004/. The gradually lower formation temperatures are also confirmed by homogenisation temperatures from fluid inclusion

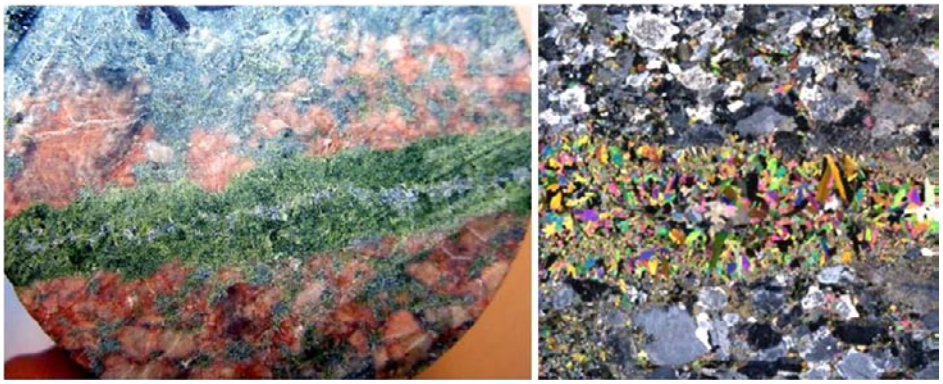

Figure 4-7. *Photograph (left) and thin section viewed with crossed polars (right) of a Generation 3 fracture filled with euhedral epidote (green) with calcite and quartz (white) in the centre of the fracture. Drill core sample KLX02, 525 m borehole length. The wall rock shows heterogeneous red staining adjacent to the fracture.*

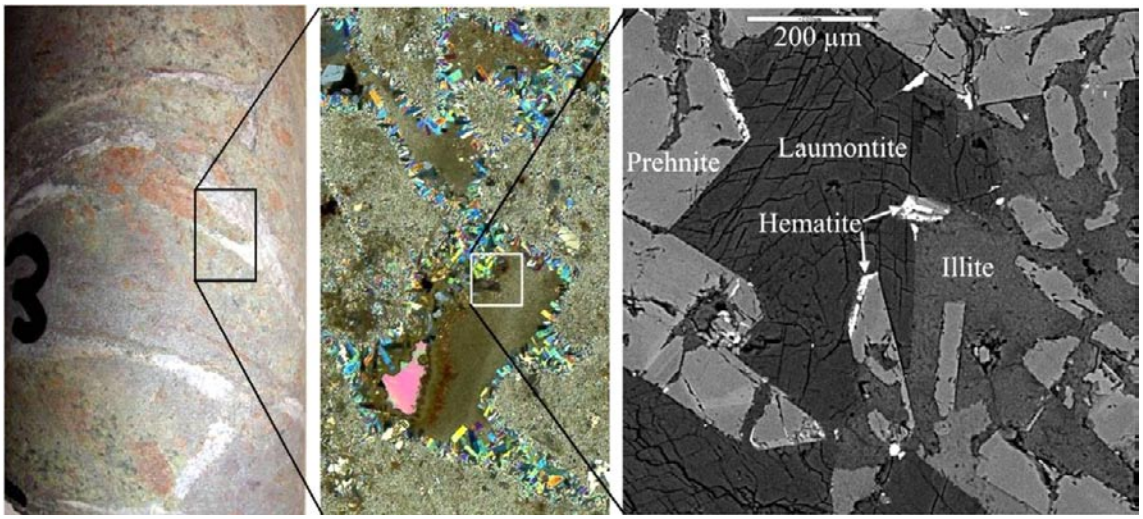

Figure 4-8. *Photograph of the drill core (left), photomicrograph (centre) and BSE-image (right) of a sample dominated by fracture fillings of Generation 3. Euhedral prehnite is the oldest mineral and coats the walls of the fractures and cavities. Subsequently, prehnite has been partly dissolved and partly replaced by laumontite, which has grown on the expense of prehnite as temperatures decreased during the fracture filling event. Illite, calcite, adularia and hematite are other minerals post-dating prehnite in the fractures, and prehnite is found as fragments within these later fillings. Drill core sample KLX04: 322 m borehole length.*

analyses of quartz and calcite that range from ~370 to 195°C (lowest for the laumontite paragenesis and highest for the epidote paragenesis, see Section 5.2 and Figure 5-5). However, these (including the greisen) are interpreted to be nearly coeval and formed under similar conditions, based on stable isotopes in calcite ($\delta^{18}O$, $\delta^{13}C$ and $^{87}Sr/^{86}Sr$) and pyrite ($\delta^{34}S$), (see Chapter 5). This is also indicated by mineral replacements of old Generation 3 minerals by younger Generation 3 minerals during the sealing of the fractures (Figure 4-8 and Figure 4-9). These fillings are often coarse-grained and the crystals are occasionally euhedral (Figure 4-7 and Figure 4-8). There are many indications of

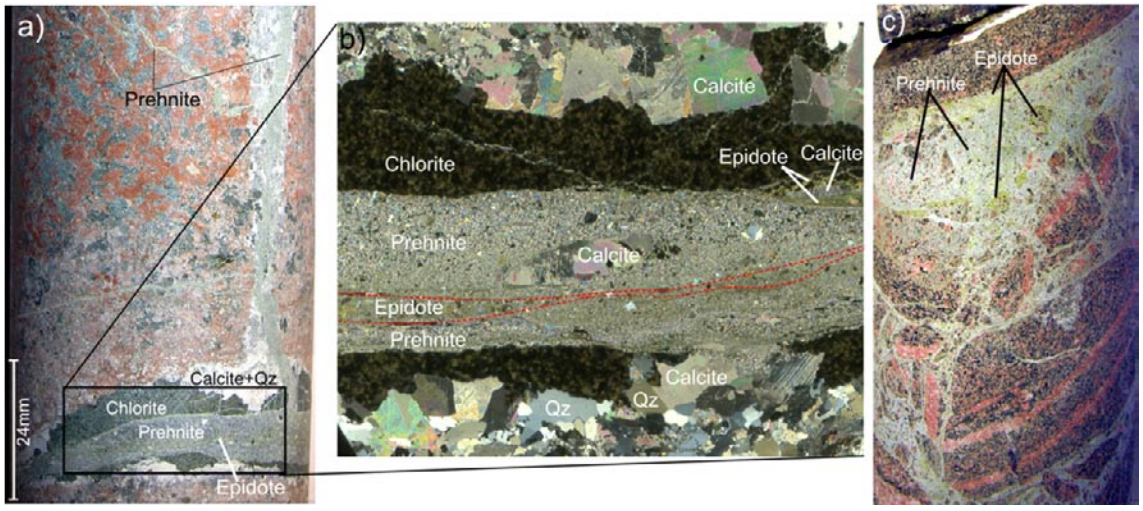

Figure 4-9. *Photograph (a) and scanned thin section (b, crossed polars) of a Generation 3 fracture filled with calcite, quartz (Qz), chlorite, epidote and prehnite. Prehnite and epidote is formed somewhat later than the other minerals and seem to be formed in the same event. Alternatively, prehnite was formed slightly later than epidote since epidote is found as fragments in the prehnite filling. Drill core KLX03, borehole length ~722 m. c) Network of sealed fractures filled with prehnite and older epidote, which shows either that older fractures filled with epidote have been reactivated and filled with prehnite with remnants of epidote as fragments or the fractures were initially partly filled with epidote but as the temperatures (and/or pressure) dropped during the fracture filling event, prehnite formed instead of epidote. Drill core KLX17A, borehole length ~315 m.*

association between Generation 3 and the intrusions of the Götemar and Uthammar granites nearby (U-Pb ages 1452 +11/–9 Ma and 1441 +5/–3 Ma /Åhäll 2001/, respectively), although many of these fracture fillings, especially epidote-dominated Generation 3a fillings, are probably older than the granites, as indicated by a few observations of cross-cutting epidote fractures of which the youngest is interpreted to be related to the nearby granites. These granites have earlier been interpreted to be anorogenic /Kresten and Chyssler 1976, Åberg et al. 1984, Kornfält et al. 1997/. However, recent studies of /Čečys and Benn 2007, Bogdanova et al. 2008, Brander and Söderlund 2008/ indicate that these and other coeval granites in south Sweden and at Bornholm are associated with the Danopolonian orogeny in the south. Consequently, many of the Generation 3 fillings would also have been formed as a far-field effect of this orogeny.

Chlorite is of Fe-Mg type (Figure 4-6) like the chlorite in the altered and red-stained wall rock. The Fe-content in epidote is higher in Generation 3 than in the older generations. This indicates lower formation temperatures of Generation 3 epidote compared with older epidote, since Fe^{3+} incorporation in epidote increases with decreasing temperatures /Liou et al. 1983/.

Fracture-controlled greisen /cf. Stemprok 1987/ is widespread in horizontal to sub-horizontal fractures (Figure 3-13 and Figure 4-2b–d) below the Mederhult zone in borehole KLX06, close to the Götemar granite. The fracture minerals are coarse-grained (cm-sized crystals) quartz, muscovite, fluorite, pyrite and calcite, with smaller amounts of topaz, Fe-Mg-chlorite and trace amounts of e.g. rutile, albite, zircon, and sulphides (Cu, Zn, As, Sn, Sb and Fe-bearing). The wall rock shows high degree of sericitisation. Greisen also crops out within the TIB rocks close to the Götemar granite contact /Kresten and Chyssler 1976/. Greisen-like parageneses are also found in fractures at about –900 m above sea level in borehole KLX10. Muscovite from three coarse-grained greisen fillings (Figure 4-2b–d) from borehole KLX06 yielded $^{40}Ar/^{39}Ar$ ages of between 1,423 ± 3 Ma and 1,424 ± 2 Ma (Figure 4-3b–d). These ages are very close to a biotite $^{40}Ar/^{39}Ar$ age (1,421 ± 4 Ma) from the Götemar granite /Page et al. 2007/. The ages represent the cooling of the muscovite below ~350°C.

The Generation 3 fractures are commonly bordered by intensely altered, red-stained wall rock (Figure 4-7a and Figure 4-9a). This alteration has caused breakdown of biotite, plagioclase and magnetite and formation of chlorite, albite, adularia and hematite (see Section 6.1). The red-staining also shows strong spatial association to deformation zones (Generation 1 and 2) but is mainly associated with Generation 3 fractures. The relation between Generation 3 fractures and the extensive wall rock alteration in the area is strengthened by similar chlorite compositions (Figure 4-6), e.g. since chlorite compositions vary with temperature /Cathelineau 1988/. A high degree of fluid-rock interaction is indicated by an oxygen shift in the $\delta^{18}O$ values in calcite (see Section 5.1) as well as by the widespread wall rock alteration (red-staining). The features of this wall rock alteration vary somewhat within the area. In the northern and southernmost parts of the Laxemar subarea (the areas adjacent to the Götemar and Uthammar granites, respectively), the wall rock is more often bleached along the fracture due to heavy sericitisation in contrast to formation of secondary adularia in the red-stained rock. Further away from the fracture, the bleached, sericitised rock grades into red-stained rock with a higher adularia/sericite ratio. The frequency of fractures with sericitised rock also increases significantly with increased depths. The tendency of increased wall rock sericitisation towards the Uthammar- and Götemar granites, both vertically and horizontally suggests influence on the rock within the area by the adjacent granites, which is reasonable since these granites have great extents in the subsurface /cf. Cruden 2008/. Closer to the granites greisenisation is the dominant wall rock alteration. The chemical features of the characteristic red staining alteration adjacent to Generation 3 fractures also indicate association to the intrusions and post-magmatic circulation of the Götemar and Uthammar granites /Drake et al. 2008/. Sericite/muscovite from the sericitised and red-stained wall rock adjacent, and related, to a Generation 3 fracture yielded an $^{40}Ar/^{39}Ar$ age of 1,417 ± 3 Ma (Figure 4-2e and Figure 4-3e) which represents a minimum age of the fracture filling. The age represents the cooling of the sericite/muscovite below ~350°C. This ages is similar to a biotite $^{40}Ar/^{39}Ar$ age (1,421 ± 4 Ma) from the Götemar granite /Page et al. 2007/ and suggests relation between Generation 3 and the nearby granite intrusions. The wall rock age may alternatively be related to a repeated heating event associated with the intrusions of the nearby granites, but nevertheless represents a rough minimum age of Generation 3.

Generation 3a consists of dominantly quartz, epidote, chlorite, calcite, pyrite and fluorite and subordinate K-feldspar, muscovite and amphibole, mainly hornblende (e.g. Figure 3-7 and Figure 4-7). The muscovite content increases towards the Götemar granite, especially related to greisen.

Generation 3b consists of prehnite, calcite and subordinate fluorite and K-feldspar and is often found in reactivated Generation 3a fractures (Figure 4-9). The prehnite crystals are often partially dissolved and replaced by younger minerals (Figure 4-8).

Generation 3c consists dominantly of calcite, laumontite, adularia, chlorite, quartz, illite, hematite, and minor amounts of albite and fluorite (e.g. Figure 3-12 and Figure 4-10a). Laumontite has often partially replaced older prehnite (Figure 4-8) and epidote. In the deepest part of the Mederhult zone-ZSMEW002A (closest to the Götemar granite), most of the epidote in the mylonite as well as most of the wall rock plagioclase have been replaced by laumontite (Figure 4-10b). The laumontite alteration in the lower part of the Mederhult zone is another indication that Generation 3 mainly formed in association with hydrothermal circulation related to the intrusion of the Götemar granite. This extensive alteration and the rarely observed greisenisation within the Laxemar subarea suggest that the Mederhult zone acted as a barrier for hydrothermal fluids from the Götemar granite.

Although the data set is very variable, an attempt to visualise the preferred fracture orientations of fractures filled with Generation 3 fillings by using sealed fractures filled with epidote (Figure 4-11), muscovite (Figure 4-12) and prehnite (Figure 4-13) has been applied since these minerals are dominantly found in Generation 3 fillings. Amphibole is also a characteristic Generation 3a mineral but is only found at great depths in borehole KLX08, therefore it is not included in the fracture domain based fracture orientation analysis, but is plotted separately in Section 4.8. Sealed fractures with altered wall rock and no visible filling are also interpreted to belong to Generation 3 mainly (Figure 4-14). Pyrite (Figure 4-15), quartz (Figure 4-16), fluorite (Figure 4-17) and laumontite (Figure 4-18) are found in other generations as well, but considering sealed fractures only they dominantly belong to Generation 3. Fractures sealed with calcite and chlorite are also very common in Generation 3 but these minerals are too common in sealed fractures of other generations to allow any reasonable interpretations to be carried out (see Appendix 2 for plots of these fractures).

Fractures with Generation 3 minerals are dominantly sub-horizontal and/or steep and N-S (NNE-SSW to NNW-SSE) trending and the patterns differ slightly between the different fracture domains and between different minerals. These trends are for example also evident when only prehnite fractures with red-stained wall rock are considered (Section 4.8), or when only sealed fractures with red-stained wall rock are considered (Figure 4-14). Occasional clusters of other fracture directions,

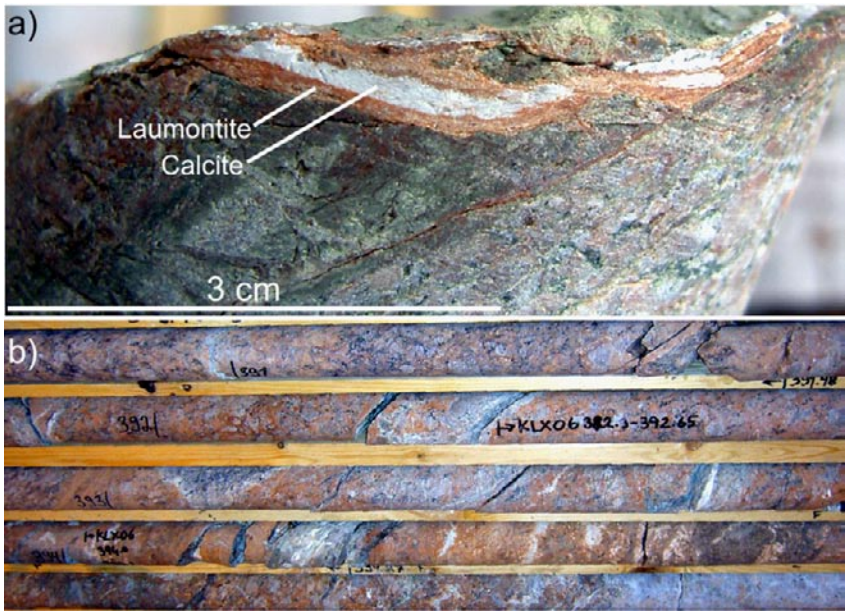

Figure 4-10. *a) Characteristic laumontite-calcite filled fracture of Generation 3c. Drill core KLX04. b) Photograph of a drill core section with intense laumontite-dominated alteration (orange coloured). The alteration is both localised to older epidote-rich mylonites in which epidote is replaced by laumontite and to the mylonite wall rock, in which most of the primary plagioclase is replaced by laumontite, while e.g. K-feldspar augens (perthite) have remained virtually unaltered. Drill core KLX06, ~391–396 m borehole length. Width of photograph is about 1 m.*

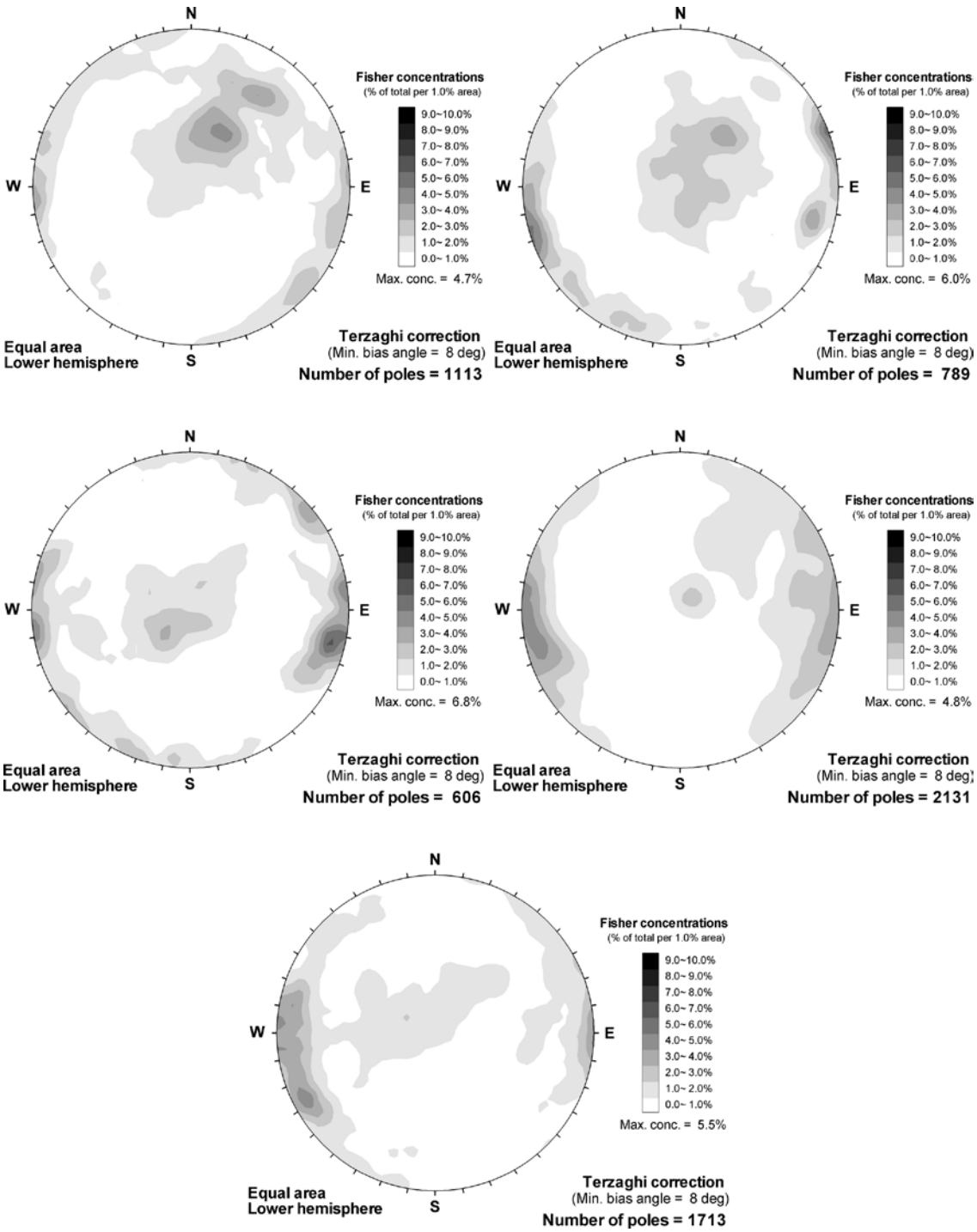

Figure 4-11. *Orientation of sealed epidote fractures in fracture domains FSM_C, FSM_EW007, FSM_N, FSM_NE005 and FSM_W (from upper left to lower right). Fisher concentrations are shown as a percentage of the total number of poles per 1.0% of stereonet area. A Terzaghi correction has been applied to compensate for borehole orientations.*

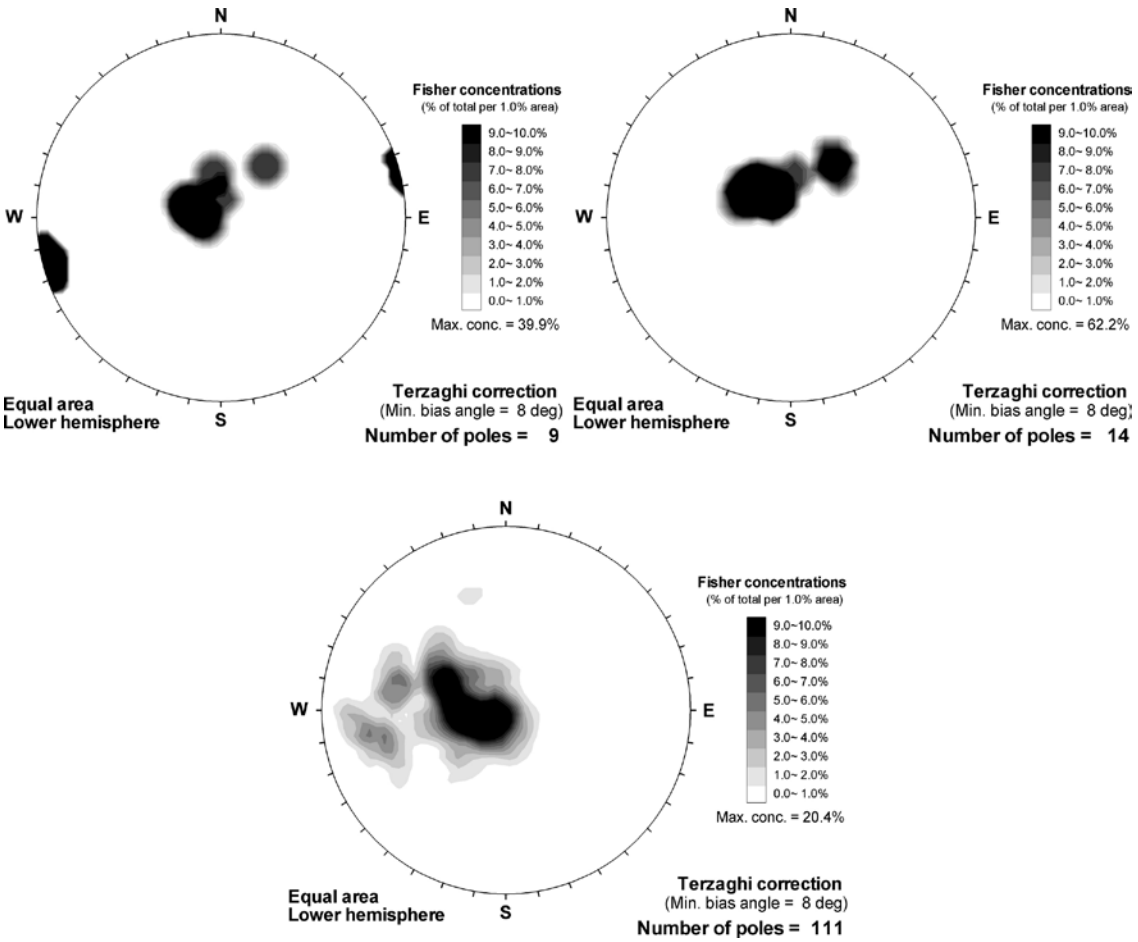

Figure 4-12. *Orientation of sealed muscovite fractures in fracture domains FSM_C, FSM_EW007, and FSM_N (from left to right). No muscovite in any FSM_NE005 and FSM_W fractures.*

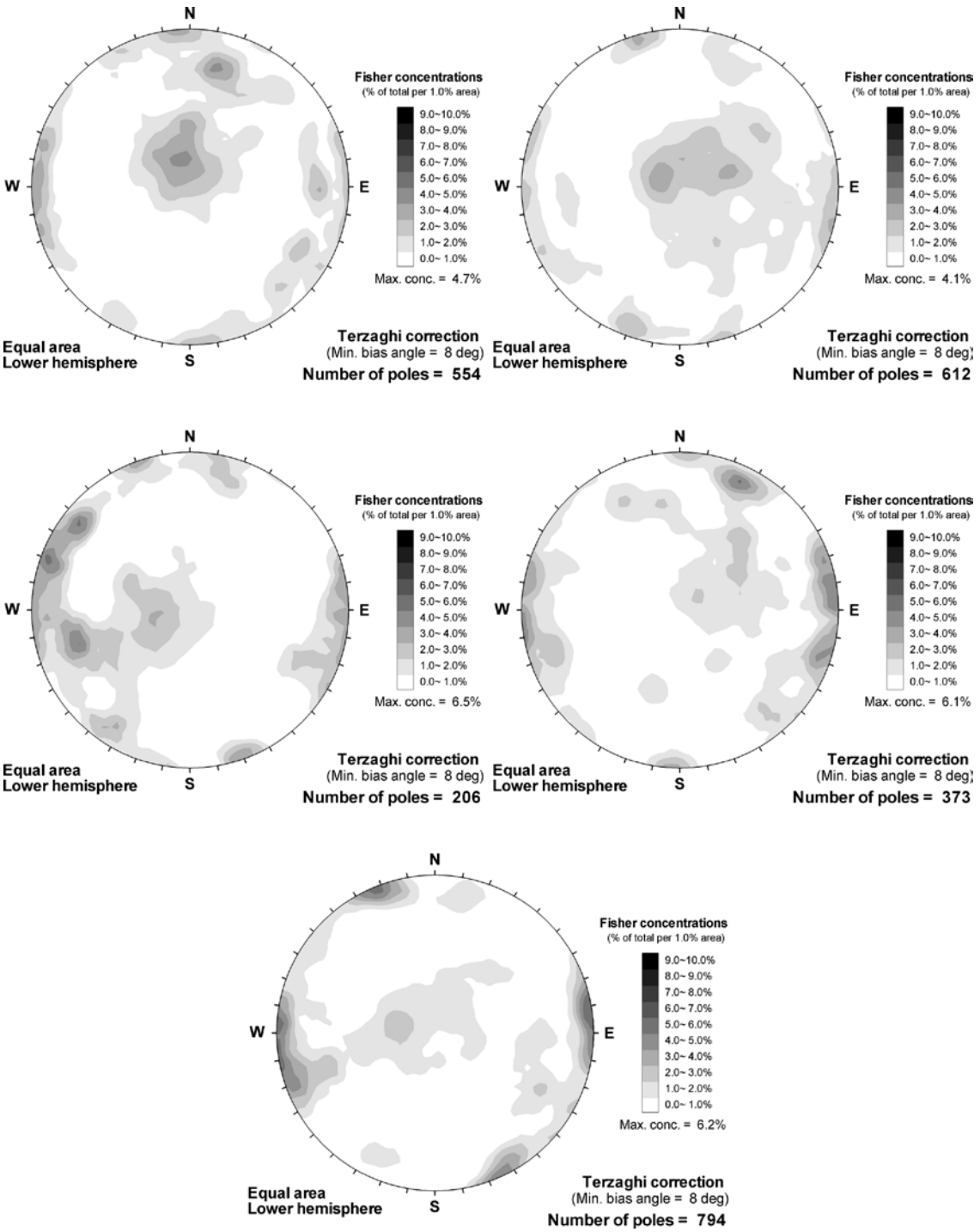

Figure 4-13. *Orientation of sealed prehnite fractures in fracture domains FSM_C, FSM_EW007, FSM_N, FSM_NE005 and FSM_W (from upper left to lower right). A Terzaghi correction has been applied to compensate for borehole orientations.*

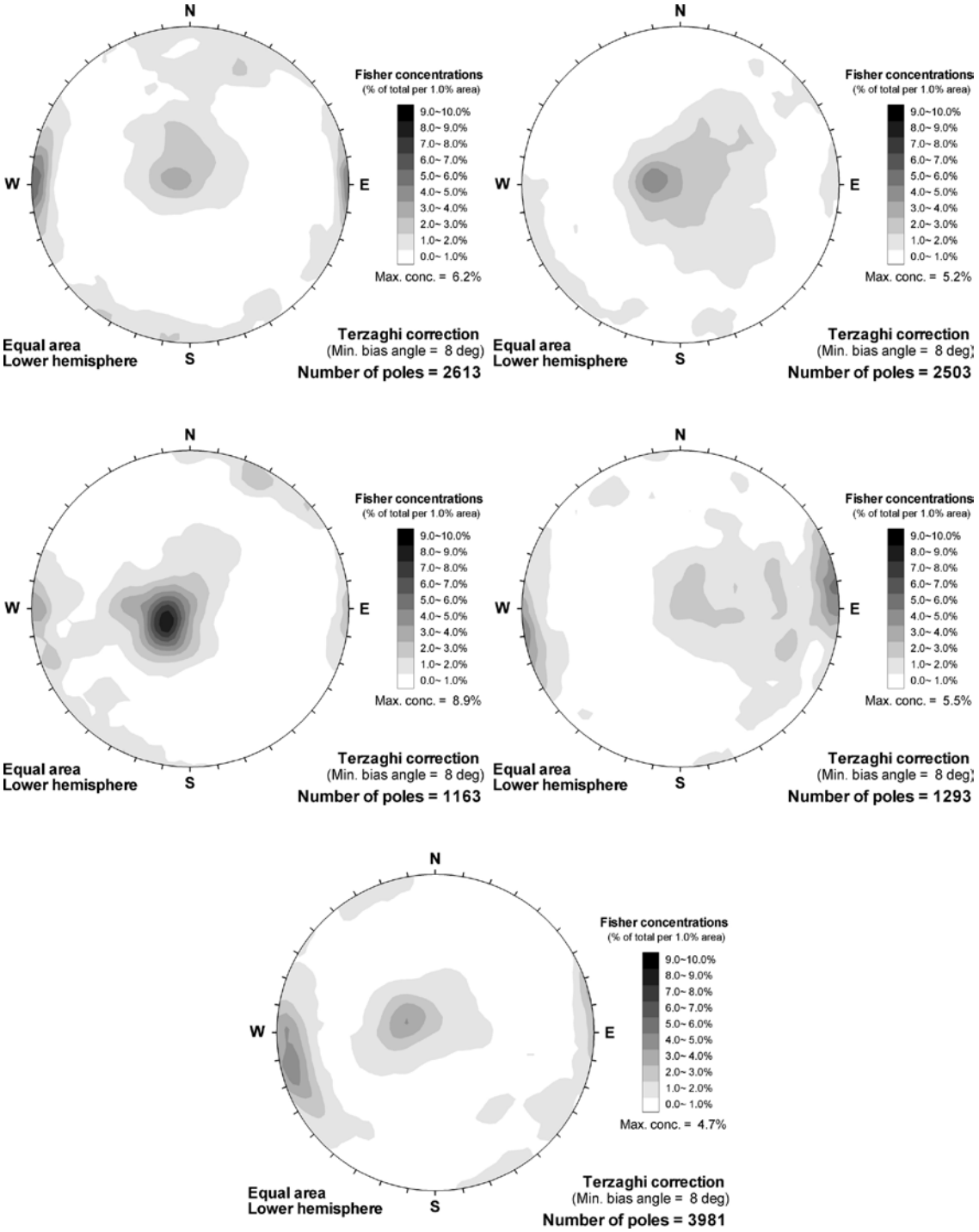

Figure 4-14. *Orientation of sealed fractures with altered wall rock but with no visible filling (see Figure 7-2) in fracture domains FSM_C, FSM_EW007, FSM_N, FSM_NE005 and FSM_W (from upper left to lower right). A Terzaghi correction has been applied to compensate for borehole orientations.*

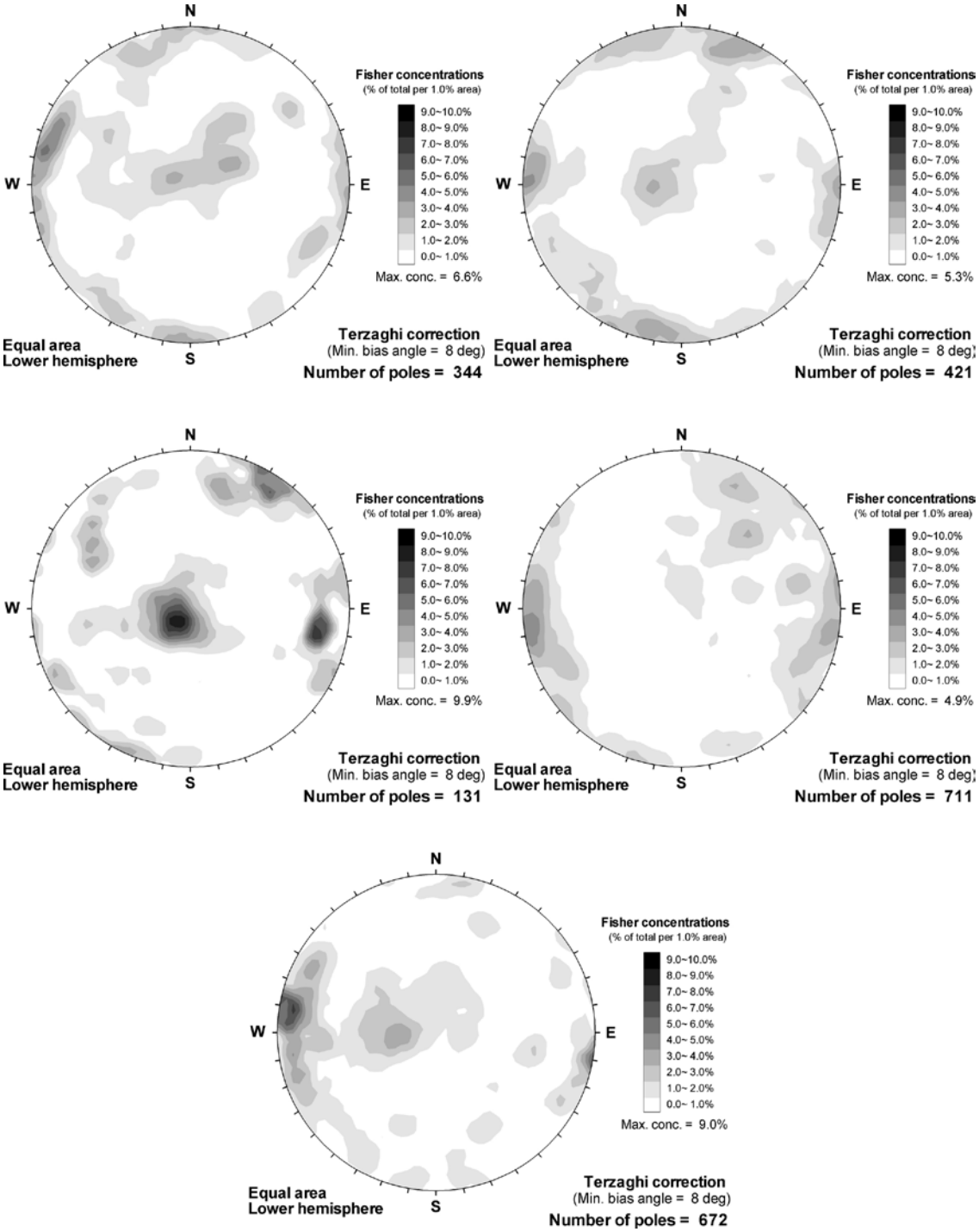

Figure 4-15. *Orientation of sealed pyrite fractures in fracture domains FSM_C, FSM_EW007, FSM_N, FSM_NE005 and FSM_W (from upper left to lower right). A Terzaghi correction has been applied to compensate for borehole orientations.*

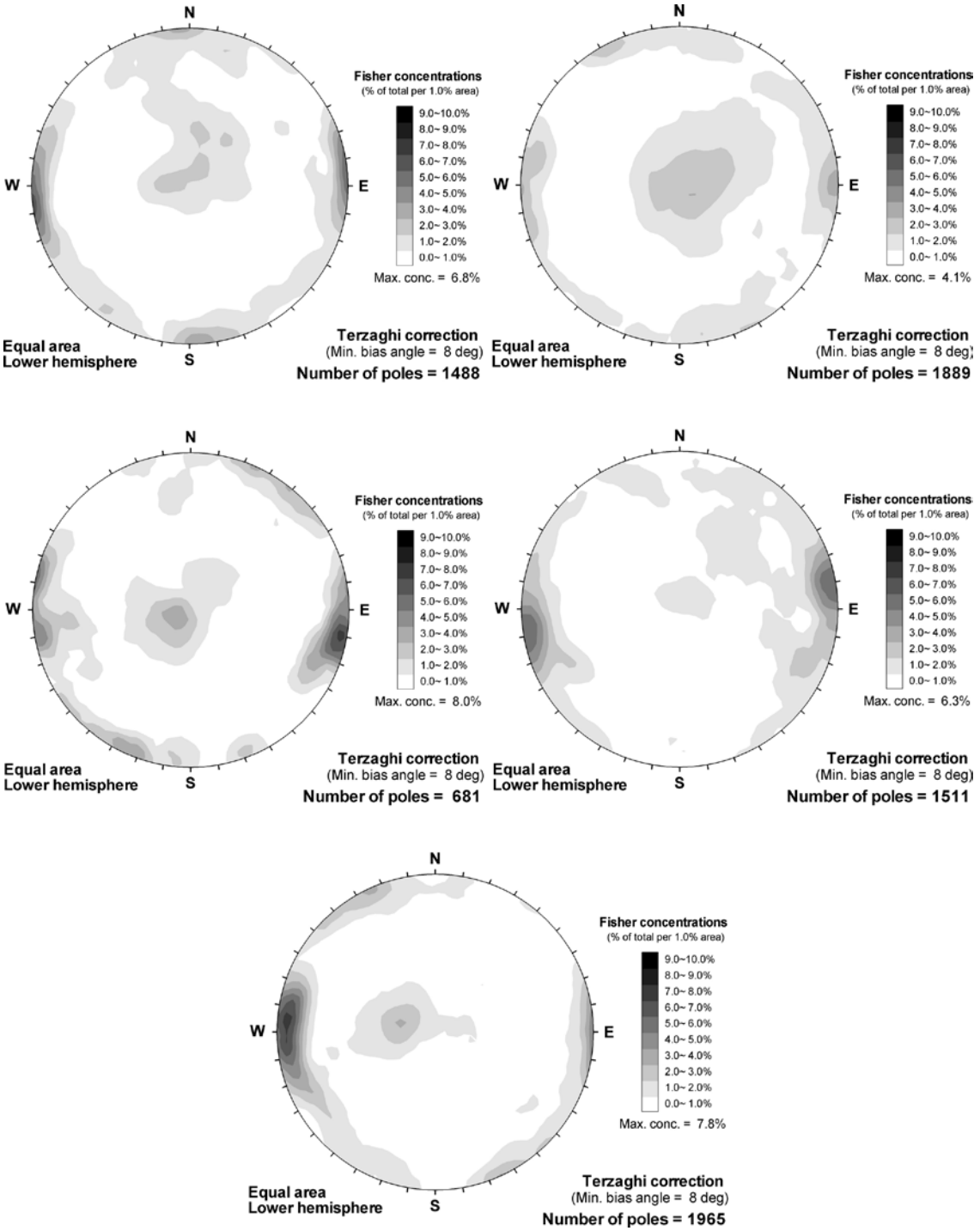

Figure 4-16. *Orientation of sealed quartz fractures in fracture domains FSM_C, FSM_EW007, FSM_N, FSM_NE005 and FSM_W (from upper left to lower right). A Terzaghi correction has been applied to compensate for borehole orientations.*

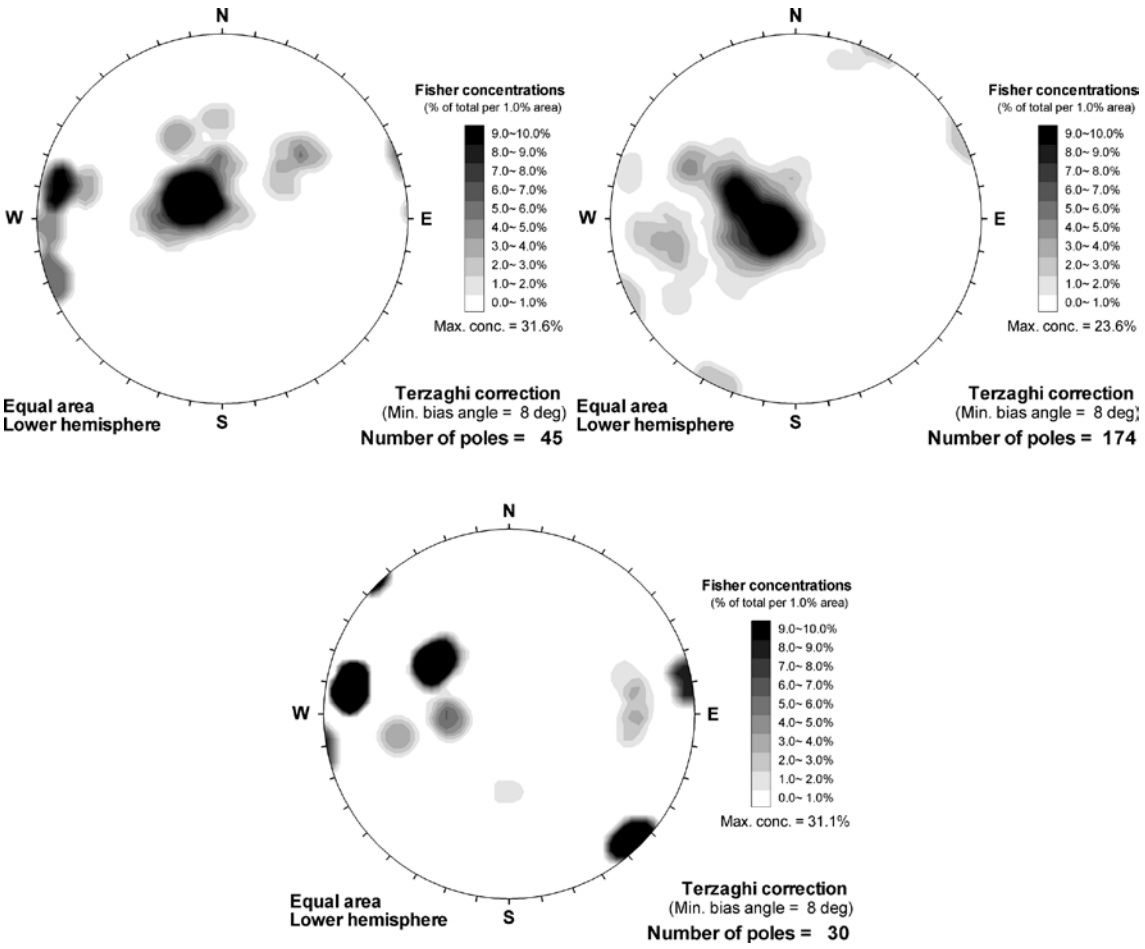

Figure 4-17. *Orientation of sealed fluorite fractures in fracture domains FSM_EW007, FSM_N, and FSM_W (from left to right). Fluorite concentrations in domains FSM_C (3 poles) and FSM_NE005 (6 poles) are too low for any interpretations. A Terzaghi correction has been applied to compensate for borehole orientations.*

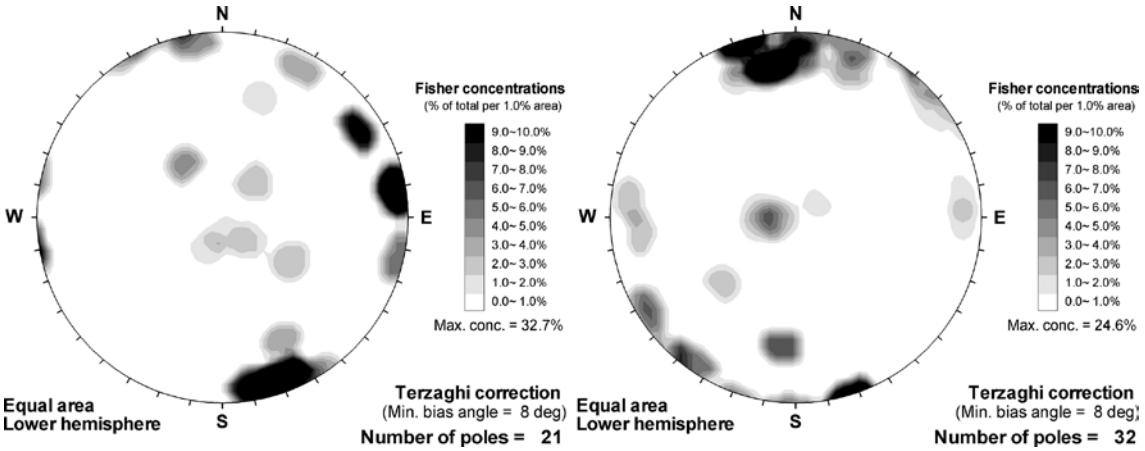

Figure 4-18. *Orientation of sealed laumontite fractures in fracture domains FSM_EW007 (left) and FSM_N (right). Laumontite concentrations in domains FSM_C, FSM_NE005 and FSM_W are too low for any interpretations. A Terzaghi correction has been applied to compensate for borehole orientations.*

e.g. E-W trending with moderate to sub-vertical dips, also exist. Some of these deviations may be due to reactivation of fractures and due to that the mineral plotted, e.g. quartz and pyrite, may be younger than Generation 3. Amphibole and greisen related muscovite and fluorite are, for example, dominantly found in sub-horizontal fractures (cf. Section 4.8 and FSM_N in Figure 4-12 and Figure 4-17). These are mainly associated with the intrusion and related hydrothermal circulation of the Götemar granite. A wide variety of scenarios may be suggested for the formation of the roughly N-S (NNE-SSW to NNW-SSE) trending fractures filled with Generation 3 minerals: e.g. 1) reactivation pre-existing, roughly N-S trending fractures, possibly formed during the waning stages of the Svecokarelian orogeny, during the intrusions of the nearby granites, and 2) Formation as a direct far-field stress effect of the Danopolonian orogeny in the south /Bogdanova et al. 2001, 2008/, although the features of this orogeny and its influence on adjacent areas are still rather poorly defined, and furthermore, main shortening directed ENE-WSW or NE-WS has been proposed, /Čečys and Benn 2007, Bogdanova et al. 2008/. A set of N-S trending fractures carrying euhedral epidote and quartz fillings have also been reported from Äspö /Munier and Talbot 1993/. The most likely scenario is that Generation 3 minerals have precipitated during a prolonged period of time at different events with the latest and probably main pulse of precipitation related to the intrusion of the Götemar and Uthammar granites. These intrusions affected the area with the opening of new fractures and reactivation of older fractures and deformation zones, intense wall rock alteration (red-staining, sericitisation and greisenisation) and precipitation of e.g. epidote, prehnite and subsequently laumontite as suggested by the $^{40}Ar/^{39}Ar$-ages of greisen and altered wall rock.

Laumontite fractures are dominantly steep and E-W trending (Figure 4-18) and therefore deviate somewhat from other Generation 3 minerals. However, laumontite has only been mapped in a few fractures (probably underestimated) and is also found in other generations. Furthermore, the majority of the E-W trending laumontite fractures are from the proximity of the roughly E-W trending deformation zones ZSMEW007A and ZSMEW002A in fracture domains FSM_EW007 and FSM_N, respectively. The orientations of these fractures are probably partly influenced by the orientations of these pre-existing zones.

The most probable scenario is that some of the oldest Generation 3a fracture fillings, especially epidote-dominated, are older than the Götemar and Uthammar granites, while the major part of the prehnite- and laumontite-dominated fracture fillings (Generation 3b and 3c) and a large part of the epidote-dominated fractures (Generation 3a) precipitated during a prolonged event with gradually lower temperatures in relation to the intrusions and associated post-magmatic circulation of these granites. This means that the Generation 3 minerals generally represent precipitation under different conditions during a single prolonged and complex tectonothermal event. This suggestion is based on geochronology, wall rock alteration, stable isotopes, geochemistry (see also Chapter 5) and the observations of gradual transitions between epidote and prehnite (Figure 4-9) and prehnite and laumontite (Figure 4-8), which indicate a rather long depositional history. The oldest epidote fillings commonly lack paragenetic calcite and no distinction of pre- and syn-Götemar Generation 3a fracture fillings based on stable isotopes have therefore been possible discern.

4.4 Generation 4

Generation 4 consists of calcite, adularia, laumontite, chlorite, quartz, illite and hematite. Albite, apatite and illite-dominated mixed-layer clay may be present as well. The fillings are commonly thin, fine-grained and sometimes cataclastic and reddish brown (Figure 4-19). Based on the mineralogy and appearance only, Generation 4 fillings are not easily distinguishable from Generation 3 fillings in the absence of any cross-cutting relationships. However, they can be separated by stable isotope and fluid inclusion signatures (cf. Chapter 5). Furthermore, the chlorite is Mg-rich (similar to Generation 5, Figure 4-6) in contrast to Generation 3. Generation 4 fracture fillings (and cataclasites) are interpreted to be formed later than c. 1.4 Ga, assuming that this is the minimum age of Generation 3, but before the Cambrian sandstone fractures (see Section 4.5). The hydrothermal signatures from stable isotopes and homogenisation temperatures from fluid inclusions in calcite (mainly >200°C, cf. Chapter 5) suggest that these minerals were formed prior to 710 ± 78 Ma, when the rock temperatures cooled below c. 200°C, as shown by titanite fission track ages /Tullborg et al. 1996/. Generation 4 may be of Sveconorwegian age, as indicated by the $^{40}Ar/^{39}Ar$ age of adularia in borehole KSH03A (989 ± 2 Ma, Figure 4-3f and Figure 4-4f). However, this age may also represent resetting of the adularia during the Sveconorwegian orogeny (E-W directed compressive stress), as shown by reset $^{40}Ar/^{39}Ar$ biotite ages of c. 928 Ma from the same borehole in deformation zone ZSMNE024A /Page et al. 2007/.

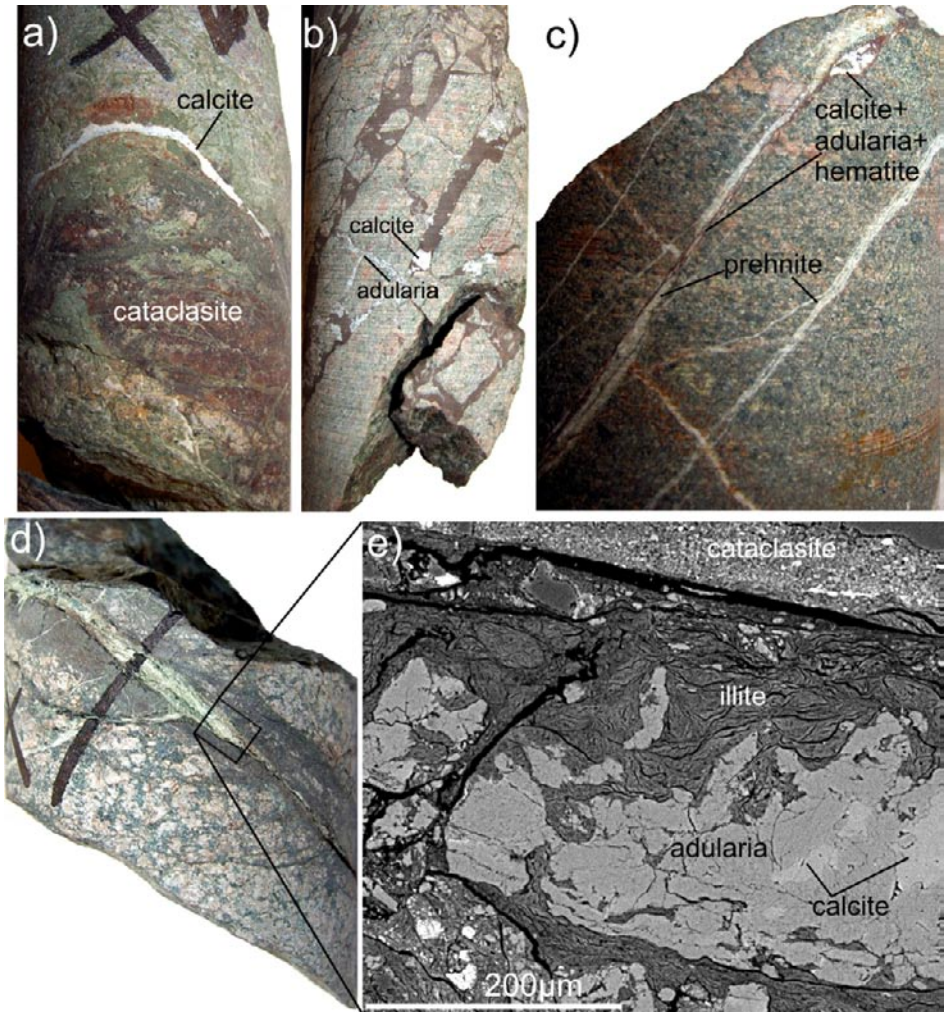

Figure 4-19. *Characteristic fillings of Generation 4. a) Calcite of Generation 4 in a fracture cutting through cataclasite of Generation 2, drill core sample KLX04: 346 m borehole length. b) Fractures filled with calcite, adularia and a brick red (partly cataclastic), very fine-grained fracture filling consisting of e.g. adularia, chlorite, hematite and wall rock fragments. Drill core sample KLX13A: 497 m borehole length. c) Calcite, adularia and hematite of Generation 4 in fractures reactivating prehnite-filled fractures of Generation 3. Drill core sample KLX04: 878 m borehole length. d) Cataclasite of Generation 2 reactivated by a Generation 4 fracture. Drill core sample KSH03A, 245 m borehole length. e) BSE close-up of (d) showing illite, adularia and calcite of Generation 4.*

This indicates that deformation zone ZSMNE024A, as well as fractures in the surrounding wall rock, were reactivated and injected by hydrothermal fluids as a far-field effect of the Sveconorwegian orogeny in south-western Sweden. Sveconorwegian K-Ar model ages have been obtained from K-feldspar in shear zones at Äspö, although these have been interpreted to be cooling ages associated with the nearby Götemar and Uthammar intrusions /Maddock et al. 1993/. Furthermore, the intrusion of N-S oriented, c. 0.9 Ga dolerites in the westernmost part of the Laxemar subarea indicates E-W oriented extension during a late stage of the Sveconorwegian orogeny /Wahlgren et al. 2007/. Therefore, Sveconorwegian brittle reactivation and formation of new fractures are expected in the area. However, apart from the $^{40}Ar/^{39}Ar$ ages in KSH03A and the dolerites, there is no sufficient evidence of extensive reactivation of the Laxemar area and the effect of Sveconorwegian brittle deformation in this area is largely unknown. It is noted that Sveconorwegian shear zone reactivation and extensive brittle fracturing have been identified in southern Finland /Heeremans and Wijbrans 1999/ and at Forsmark, central Sweden /Sandström et al. 2006a/, respectively, i.e. in two areas far away from the Sveconorwegian orogene.

4.5 Cambrian sandstone in bedrock fractures

Cambrian sandstone has been observed in a few sub-vertical, near-surface fractures in the Laxemar area, e.g. surface observations at the Simpevarp peninsula /Drake and Tullborg 2006b, Stephens and Wahlgren 2008/ and at drill site KLX11, striking mainly ENE /Cronquist et al. 2006, Viola and Venvik Ganerod 2007/, and in cored boreholes KLX11C, D and E at 25–100 m vertical depths, striking mainly NW /Drake and Tullborg 2008a/. These occurrences indicate that the present bedrock surface is close to the sub-Cambrian denudation surface, the sub-Cambrian peneplane, which dips gently to the east. A fragment of relatively well preserved Cambrian sandstone is also found at 230 m depth in the NE-striking deformation zone ZSMNE024A in borehole KSH03A (at c. 230 m vertical depths) /Drake and Tullborg 2006b/. The sandstone fillings are found in close spatial relation to Generation 5 fillings. However, the latter cut the sandstone and fill the pore space of the sandstone, a feature also observed in fractures filled with Cambrian sandstone within the Götemar granite /Alm and Sundblad 2002, Drake and Tullborg 2006a/. The sandstone fractures thus provide an early Palaeozoic age marker between Generation 4 and Generation 5. Sandstone in drill core samples shallower than 30 m is better preserved than in the fractures from greater depths, which show small amounts of, often fragmented, clasts and high amounts of chlorite and clay minerals. Wall rock fragments are common within the sandstone. The clasts are usually better preserved and larger in the centre of the fractures (highest flow velocity), and more angular and fine-grained towards the wall rock (lower flow velocity, Figure 4-20).

According to /Röshoff and Cosgrove 2002/, these textures indicate that the sandstone has been forcefully injected downwards as unconsolidated, fluidised sediment with a high internal fluid pressure. The clasts are also increasingly fragmented with depth. High fluid pressures in the sandstone might have been built up in the Lower Cambrian sediments due to the load of overlying Palaeozoic sedimentary successions covering southern Sweden. The fluidised sediments were then forcefully injected into sub-vertical, probably pre-existing, bedrock fractures when these were re-activated during early Palaeozoic tectonic events. Cambrian sandstone fractures in the coastal region around Simpevarp generally follow the orientation of the basement fracture sets with dominant directions in NNE-SSW to ENE-WSW

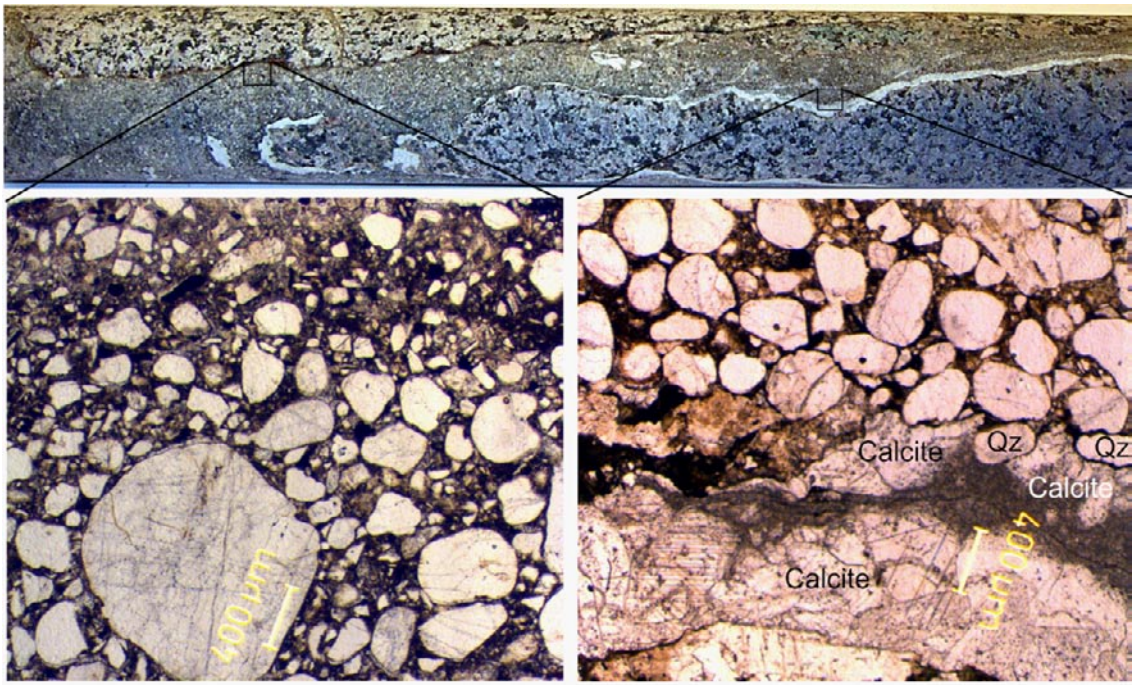

Figure 4-20. *Photograph (upper image) and photomicrographs (lower images) of a steep fracture (orientation: upper rim 142°/71°; lower rim 135°/74°) filled with Cambrian sandstone, as well as with calcite and fluorite of Generation 5. The left photomicrograph shows the gradual fragmentation and decrease in grain size of the sandstone clasts from the central part of the filling (lower rim of image) to the wall rock contact (upper rim of the image). The right photomicrograph shows the contact between the sandstone and the adjacent fracture filled with calcite (and fluorite, not shown in the image). Quartz clasts (Qz) are found within the calcite filling which suggests that the sandstone predates the calcite filling, which is also supported by observations of calcite and fluorite filling the pore space of the sandstone. Drill core KLX11D, borehole length ~30 m.*

/Nordenskjöld 1944, Kresten and Chyssler 1976, Talbot et al. 1988, Munier and Talbot 1993, Alm and Sundblad 2002, Röshoff and Cosgrove 2002/. The mainly NNE-SSW to ENE-WSW -striking sandstone fractures in the Simpevarp area and adjacent areas may have been formed in relation to NW-SE directed extension associated with the opening of the Iapetus Ocean, as proposed by /Munier and Talbot 1993/. The somewhat varying orientations of the sandstone fractures might be due to e.g. emplacement during periods of interchanged least and greatest principal stress directions or due to influence of bordering deformation zones /cf. Wahlgren et al. 2008/. Hydrostatic stresses may also have been high enough to reactivate randomly oriented sub-vertical fractures, assuming small horizontal differential stress /cf. Röshoff and Cosgrove 2002/.

4.6 Generation 5

Generation 5 consists of minerals precipitated at low-temperature conditions and is dominated by calcite with adularia, chlorite, fluorite, hematite, quartz, pyrite, barite, gypsum and corrensite. Apophyllite, harmotome, REE-carbonate (probably bastnäsite), galena, illite, chalcopyrite and laumontite occur occasionally, while e.g. sphalerite, U-silicate (possibly coffinite), apatite, Ti-oxide, albite and analcime, sylvite, celestine and Zn-oxide are very rare. Generation 5 fillings are found in both open (Figure 4-21a–d) and sealed or partly sealed fractures (Figure 4-21e–f), commonly with fresh wall rock if not in reactivated fractures. Although no major mineralogical subdivision of Generation 5 fillings have been distinguishable, stable isotopes (mainly $\delta^{18}O$), trace element chemistry and fluid inclusion studies of fracture minerals of Generation 5 show that these can be separated into two groups: Generation 5a) formed at 80–145°C (which probably represents the peak temperatures during the Palaeozoic) and Generation 5b) formed at even lower temperatures, ranging into formation conditions similar to the present, cf. Chapter 5. They both show organic and possibly microbial influence (especially 5b), which suggests that they are precipitated from descending organic-rich waters, possibly from overlying sediments /Drake and Tullborg 2007b/. Morphologically, calcite of Generation 5b (and 6) shows large variation in crystal shapes; c-axis elongated (scalenohedral), pronounced c-axis elongated (needle-shaped), short c-axis (equant), and c-axis flattened (nailhead-shaped) crystals (see Section 4.7). Generation 5 chlorite shows both older Mg- and younger Fe-rich varieties (Figure 4-6). The Fe-rich variety is also found in Generation 5 fractures in the Götemar granite /Drake and Tullborg 2006a/. Adularia from sealed Generation 5a fractures in boreholes KSH01A (in a minor deformation zone), KSH03A (in deformation zone ZSMNE0024A) and KSH03B yielded $^{40}Ar/^{39}Ar$ ages of 425.7 ± 1.7 Ma, 400.9 ± 1.1 Ma, and 444 ± 2/448 ± 4 Ma (2 splits from the same sample), respectively (Figure 4-2g–i and Figure 4-3g–j). A couple of minor mineralogical separations can also be made between Generation 5a and 5b since most fluorite, laumontite, adularia, gypsum (based $^{87}Sr/^{86}Sr$-ratios), apophyllite and galena have precipitated along with Generation 5a calcite, while harmotome and analcime (only found in the upper 430 m) and most of the barite (grown on top of Generation 5a calcite) belong to Generation 5b. Gypsum generally appears in open fractures at depths greater than –500 m above sea level, in sections with low fracture frequency and fresh wall rock, but seldom in older re-activated fractures. If calcium sulphate was precipitated during the peak temperatures during the Palaeozoic it precipitated in the form of anhydrite, which in such case has been transformed to gypsum at lower temperatures. Gypsum is the only relatively abundant mineral found exclusively in Generation 5. These fractures are mostly found in fracture domain FSM_C in which they are almost exclusively sub-vertical and WNW-ESE trending both for sealed and open fractures (Figure 4-22 and Figure 4-23). Gypsum is also found in open fractures in FSM_NE005 and FSM_W in which they have more irregular, but mainly sub-vertical fractures trending NE-SW, N-S and NW-SE (Figure 4-22), but these gypsum occurrences are not as certain as those in FSM_N which have been identified using SEM-EDS and XRD. The dominance of steep to sub-vertical WNW-ESE trending gypsum fractures is further strengthened when fractures with older minerals and wall rock alteration are excluded (see Section 4.7). Generation 5a calcite is mainly scalenohedral (c-axis elongated, Figure 4-21b).

Generation 5b and Generation 6 can be separated mineralogically, i.e. Generation 5b includes minerals (e.g. laumontite and barite) unlikely to have been precipitated during recent groundwater conditions, in contrast to the Generation 6 fillings. However, Generation 5b and Generation 6 are difficult to separate using stable isotopes because precipitation in these fractures have been episodic over several hundred million years, at gradually lower temperatures, probably starting in the late Palaeozoic (Generation 5b) and continuing until the Quaternary (Generation 6). The stable isotope signatures in calcite and pyrite overlap and are mostly in the range of the present groundwaters (see Chapter 5).

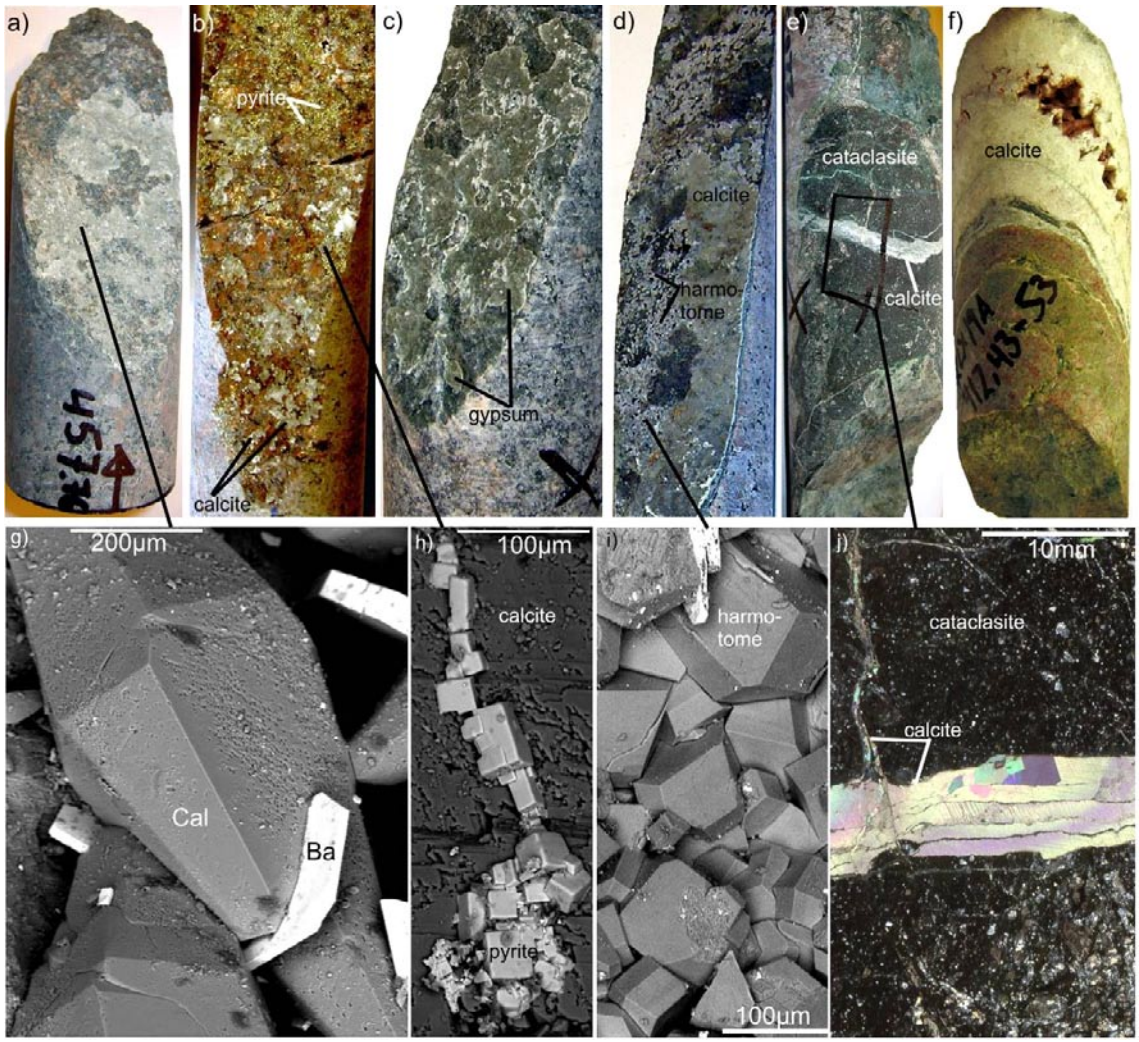

Figure 4-21. *Characteristic fracture fillings and coatings of Generation 5. Pictures a-f represent photographs of drill core samples, whereas pictures g–i represent BSE-images and j scanned thin section (crossed polars). a) KLX03: 457 m borehole length, fracture coated by e.g. barite and scalenohedral (c-axis elongated) calcite, close-up in (g). b) KLX07A: 373 m borehole length, fracture coated by calcite and pyrite, close up in (h) and in Figure 2-3b. c) KLX08: 795 m borehole length, fracture coated by gypsum. d) KLX09D: 23 m borehole length, fracture coated by calcite and harmotome, close up in (i). e) KSH03A: 220 m borehole length, Generation 5 calcite in a sealed fracture cutting through older cataclasite. The frame shows the position of (j). The main fracture (trending E-W in (j)) is made up of at least five parallel fractures filled by calcite crystals "elongated" parallel to the fracture wall, occasionally as continuous single crystals through the width of the thin section (c. 2 cm). Thin bands of adularia are found between these parallel calcite fractures. A younger fracture (trending N-S in (j)) is filled with calcite and barite and belongs to a later stage of Generation 5. f) KLX19A: 419 m borehole length, fracture partly sealed with calcite. The remaining void holds centimetre-sized scalenohedral calcite crystals coated by hematite. The diameter of the drill core is ~5 cm.*

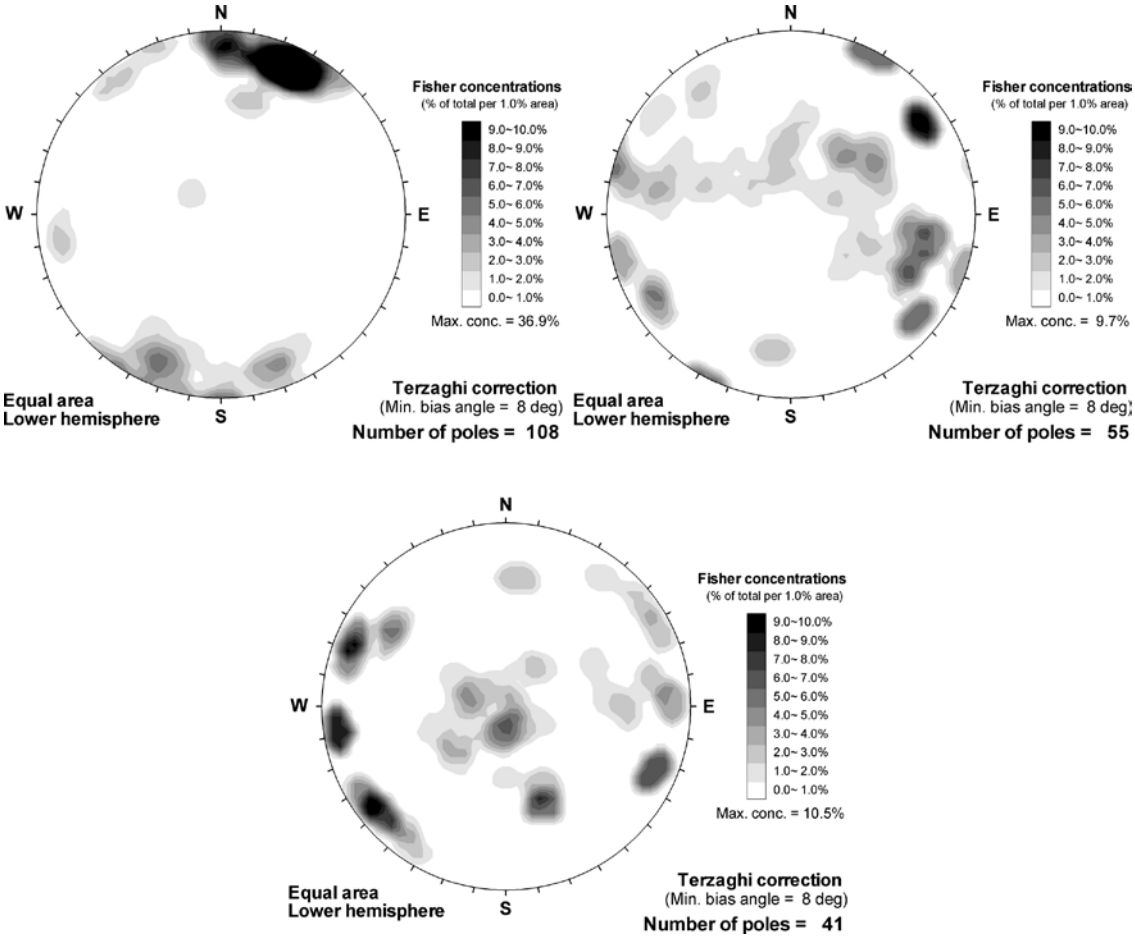

Figure 4-22. *Orientation of open fractures with gypsum in fracture domains FSM_C, FSM_NE005 and FSM_W (from left to right). No gypsum in open fractures in domain FSM_EW007 and only one occurrence in FSM_N. A Terzaghi correction has been applied to compensate for borehole orientations.*

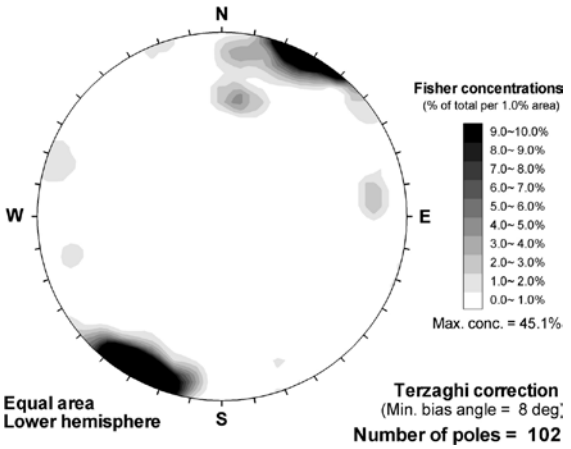

Figure 4-23. *Orientation of sealed fractures with gypsum in fracture domains FSM_C. Domains FSM_NE005, FSM_W, FSM_EW007 and FSM_N have too few gypsum fractures for any interpretations. A Terzaghi correction has been applied to compensate for borehole orientations.*

The most abundant Generation 5 minerals calcite, fluorite, adularia, chlorite and pyrite are present in several generations and the mapping data can therefore not be successfully used to evaluate the fracture orientations. Open fractures containing calcite, pyrite, hematite or clay minerals may however, be of mainly Generation 5 origin. These are shown in Figure 4-24, Figure 4-25, Figure 4-26 and Figure 4-27 show very similar patterns for each fracture domain: FSM_C, FSM_EW007 show mostly sub-vertical E-W to WNW-ESE trending fractures, FSM_N show similar patterns but with a higher frequency of sub-horizontal fractures, while FSM_NE005 and FSM_W show more scattered orientations, with clusters of e.g. sub-horizontal fractures and steep NE-SW and N-S trending fractures.

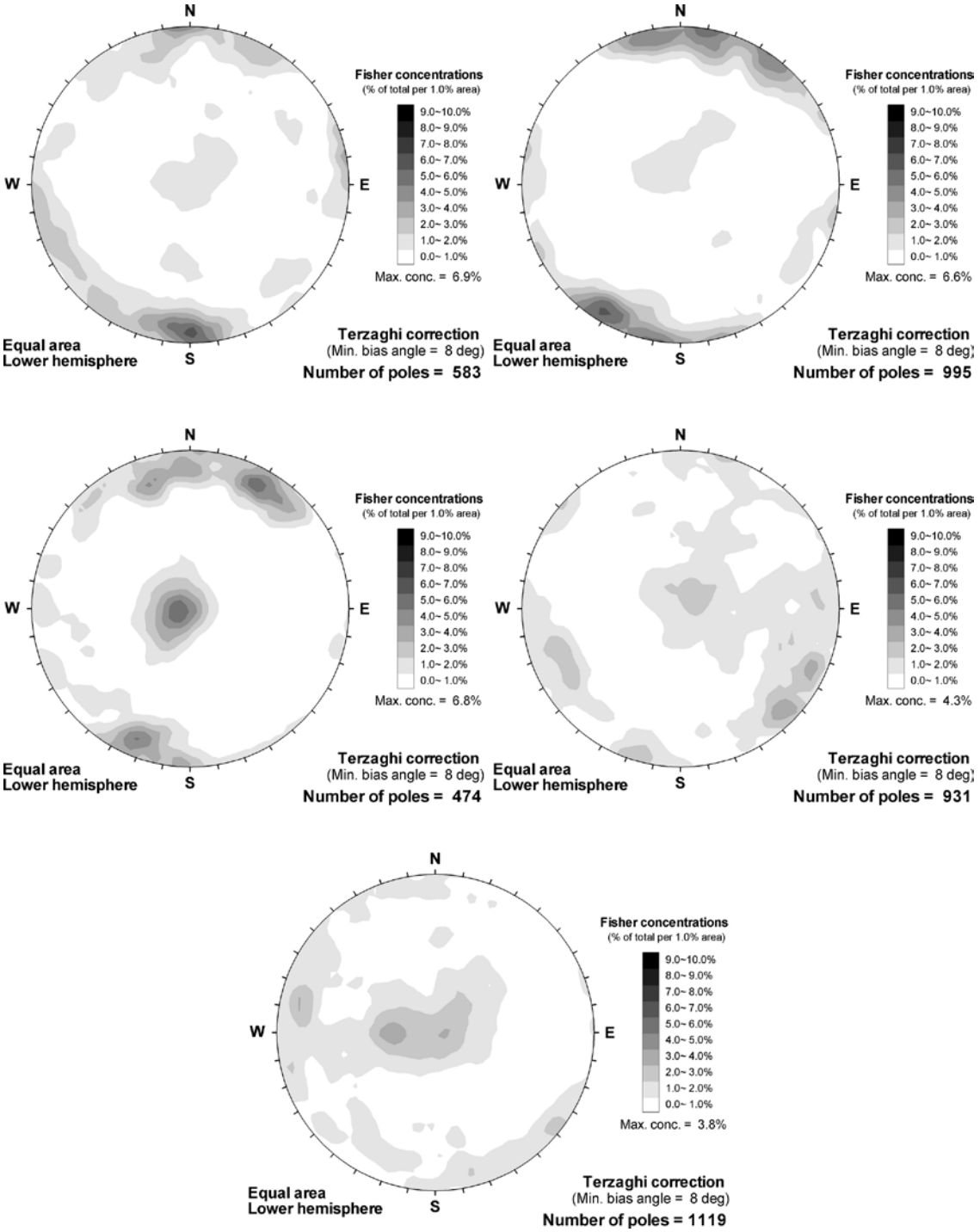

Figure 4-24. *Orientation of open fractures with pyrite in fracture domains FSM_C, FSM_EW007, FSM_N, FSM_NE005 and FSM_W (from upper left to lower right). A Terzaghi correction has been applied to compensate for borehole orientations.*

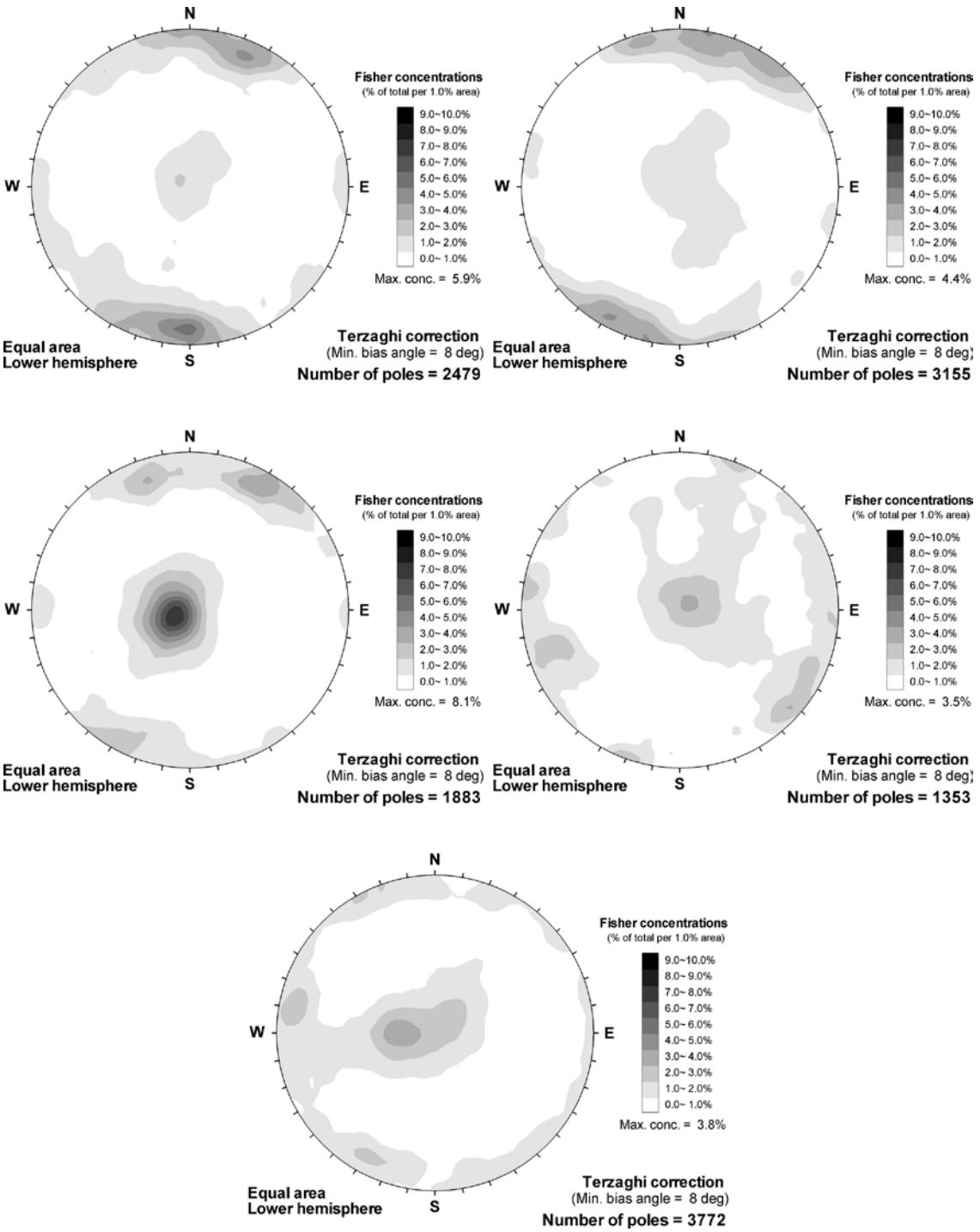

Figure 4-25. *Orientation of open fractures with calcite in fracture domains FSM_C, FSM_EW007, FSM_N, FSM_NE005 and FSM_W (from upper left to lower right). A Terzaghi correction has been applied to compensate for borehole orientations.*

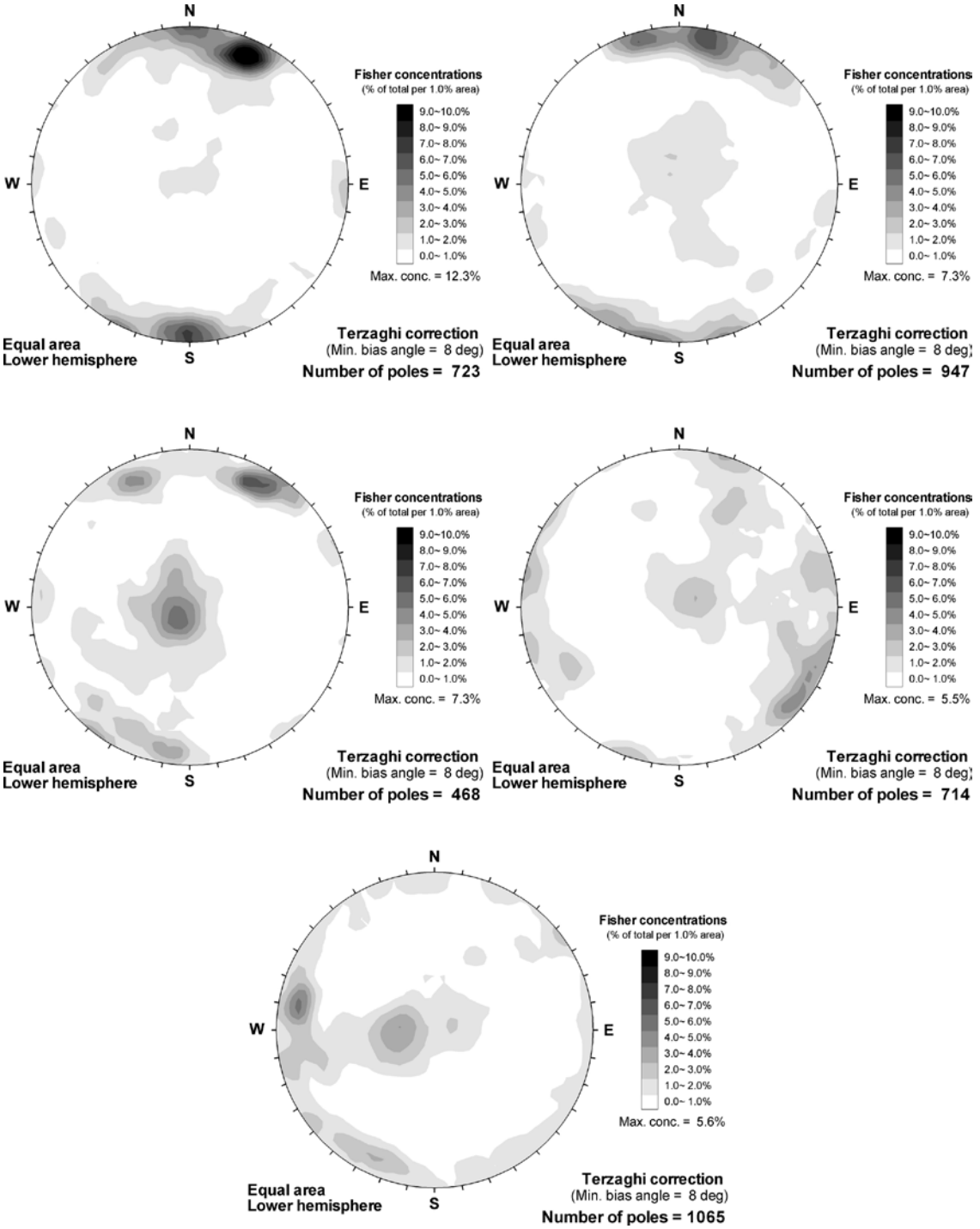

Figure 4-26. *Orientation of open fractures with clay minerals in fracture domains FSM_C, FSM_EW007, FSM_N, FSM_NE005 and FSM_W (from upper left to lower right). A Terzaghi correction has been applied to compensate for borehole orientations.*

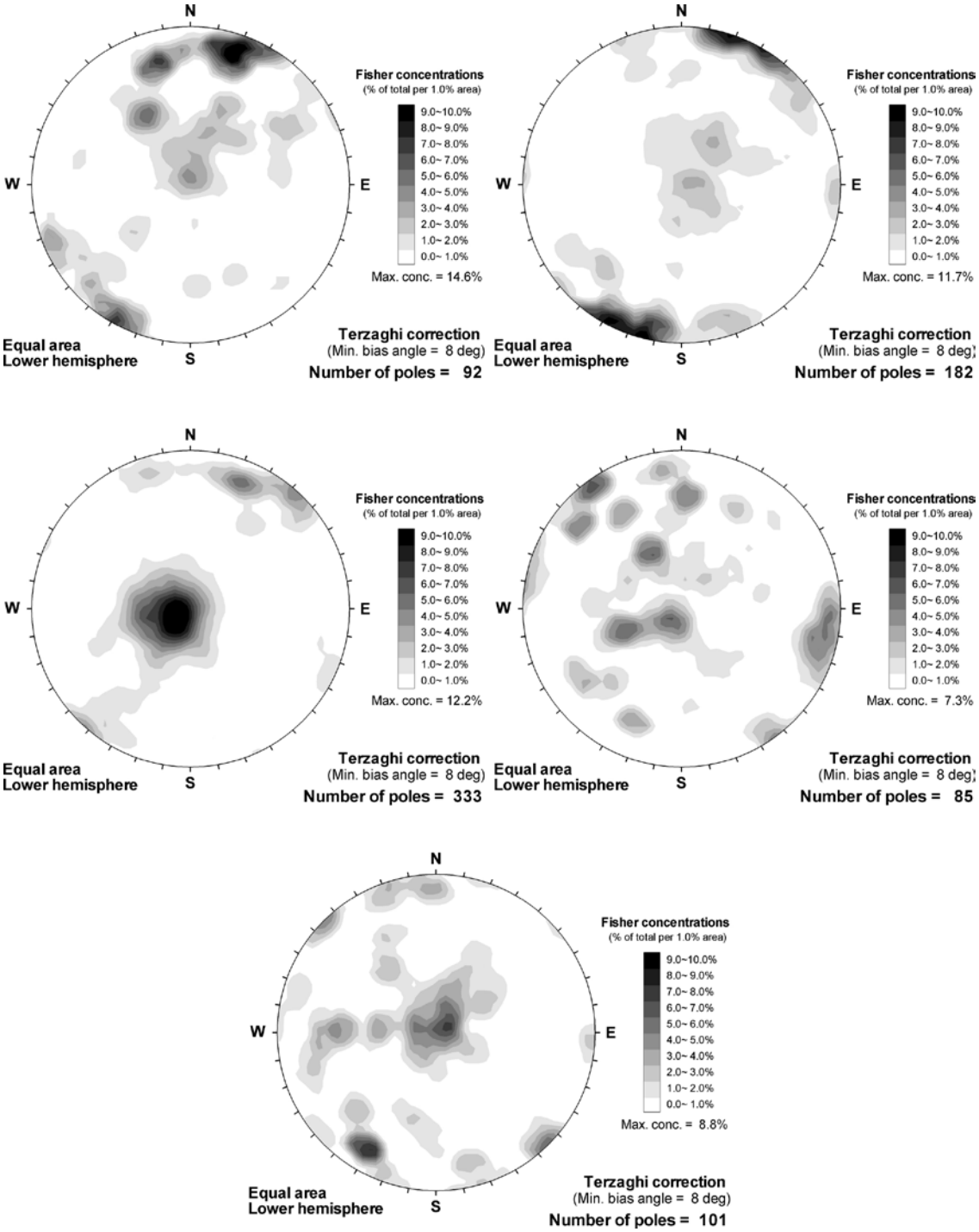

Figure 4-27. *Orientation of open fractures with hematite in fracture domains FSM_C, FSM_EW007, FSM_N, FSM_NE005 and FSM_W (from upper left to lower right). A Terzaghi correction has been applied to compensate for borehole orientations.*

The mapping was not focused on separation of different generations. Therefore, detailed investigations of the drill cores and of e.g. thin sections have been carried out in order to distinguish Generation 5 fractures (see Section 4.7). These specific fractures are mainly sub-vertical with dominantly E-W to ESE-WNW directions. Palaeozoic reactivation of most of the deformation zones in the area, as well as of the dolerite dyke in western part of the Laxemar subarea, is evidenced by the presence Generation 5 fillings.

The ages obtained from adularia of Generation 5a (Figure 4-3g–j) overlap with the Scandinavian Caledonian (SC) orogeny in the northwest (at ~510–400 Ma with the main Laurentia-Baltica collision event at ~430–400 Ma /e.g. Gee 1975, Fossen and Dunlap 1998, Roberts 2003/) and with the slightly older North German-Polish Caledonian (NGPC) orogeny in the south (at ~443 Ma /Ziegler 1985a, b, Torsvik and Rehnström 2003/). The Generation 5a minerals are formed from 80–145°C, brine type fluids with organic, and possibly microbial, influence (see Chapter 5). It is therefore suggested that they have at least partly been precipitated from descending, organic-rich, fluids from overlying, organic-rich, Cambrian-Silurian sediments /Drake and Tullborg 2007b/, as evidenced by asphaltite in Palaeozoic fillings at Forsmark, central Sweden /Sandström et al. 2006b/. Similar warm brine precipitates have been described from outcrops throughout the Baltic shield /e.g. Mattsson 1962, Carlsson and Holmqvist 1968, Kresten and Chyssler 1976, Bergman and Lindberg 1979, Rickard et al. 1979, Johansson 1984, Alm and Sundblad 2002, Kendrick et al. 2005/ and from drill core samples at adjacent Äspö /Tullborg 2003/. The ages of the Generation 5a adularia are consistent with less precise Sm/Nd-ages (~440–400 Ma) of calcite and fluorite fillings from the Swedish east coast (e.g. at Götemar), southern Finland and along the SC front /Alm et al. 2005/, as well as with $^{40}Ar/^{39}Ar$-ages of K-feldspar (~430–425 Ma) in Pb-Zn mineralisations along the SC front /Kendrick et al. 2005/. The Götemar fracture fillings have been shown to be the equivalent to Generation 5a within the Laxemar and Simpevarp subareas /Drake and Tullborg 2006a/, whereas signs of older brittle deformation are rare and ductile structures are absent /Drake and Tullborg 2006a/, which suggests that Precambrian brittle fracturing have not been extensive within this granite (cf. Generation 4).

Caledonian, ~440–420 Ma, reactivation of shear zones nearby (at Äspö) has previously been documented by /Maddock et al. 1993/ and also in southern Finland /Mertanen 2004/.

The dominant orientations of the Generation 5a fractures and especially the invariable orientations of fractures containing gypsum (mainly WNW-ESE, Figure 4-24 to Figure 4-27 and Figure 4-33 in section 4.7) correlate to the maximum compressive stress direction during the SC orogeny in the far northwest and are therefore interpreted to be formed or reactivated as a far-field response to this orogeny. Similar orientations have been documented for post-Ordovician fractures at the nearby island of Öland /Milnes and Gee 1992/ and fractures cross-cutting Cambrian sandstone dykes in SE Sweden /Nordenskjöld 1944/. Other orientations, e.g. NNE-SSW to ENE-WSW, dominate the Götemar granite fractures of Generation 5a /Alm and Sundblad 2002/. These may be related to extension parallel to the SC orogeny, possibly during the migration of a foreland basin and related foreland bulge, migrating from northwest to southeast /Bassett 1985, Baarli 1990, Sliaupa et al. 2006/. Alternatively, the fracture opening orientations were influenced by compression related to the NGPC orogeny in the south or by interplay between this and the SC. However, the NGPC orogeny have probably not been as influential for the structural evolution of the area as the SC in the NW, as there was stronger tectonism at the continent-continent collision between Laurentia and Baltica than between the "softer" transpressional collision of Avalonia and Baltica /Sliaupa 1999, Sliaupa et al. 2006, cf. Torsvik and Rehnström 2003/. Later, strong SE directed compressive stresses in the Late Silurian and Early Devonian initiated reverse faulting along ancient basement faults striking NE and ENE in the Baltic Basin (at c. 415–410 Ma) /Puura and Vaher 1997, Puura et al. 1999, Sliaupa 1999, Brangulis and Kanevs 2002, Sliaupa et al. 2006/. The Generation 5a fractures with these directions may also have been initiated or reactivated during this period. The deviant fracture directions between the fracture domains in the Laxemar subarea and in adjacent areas (e.g. Götemar) might reflect influence by pre-existing fracture sets and deformation zones in the different crustal blocks, or local differences in the stress field of these rock blocks (cf. the sandstone fractures in Section 4.5). They possibly also reflect the varying stress field during the different phases of the Caledonian orogenies. Hydraulic fracturing induced by heavy sedimentary load may have played a role as well (cf. Section 4.5). The orientation of these fractures depends on the maximum horizontal stress situation, which may vary slightly between different rock blocks. However, there is also the less likely possibility that Generation 5a minerals have been formed in every fracture orientation and that minerals in other fracture directions than those currently observed were completely dissolved due to subsequently changed stress situations.

Palaeozoic sedimentary successions are absent in the Laxemar area. However, the thickness of sedimentary successions related to the Caledonian foreland basin have been estimated to be about 2,500–4,000 m in the Laxemar area, using e.g. thermal modelling /Middleton et al. 1996/ and apatite fission track ages /Larson et al. 1999/ in correlation with apatite (U-Th)/He ages /Söderlund et al. 2005, cf. Larson et al. 2006/. However, significant subsidence related to the NGPC in the south

influenced the development of the thick Palaeozoic sedimentary successions in the Baltic basin /Poprawa et al. 1999, Puura et al. 1999/ and probably also in southern Sweden /Lazauskiene et al. 2002/. This is indicated by the thicker modelled Palaeozoic sedimentary cover in the Laxemar area compared that modelled for central Sweden (<2 km) /Cederbom et al. 2000, Cederbom 2001/ and is also suggested from the relatively high homogenisation temperatures of the Generation 5a fluid inclusions (~80–145°C) /Alm and Sundblad 2002, Milodowski et al. 2005, Drake and Tullborg 2009a/. Furthermore, the organic stable isotope signatures in the fracture fillings indicate formation from descended fluids, probably of sedimentary origin. An additional explanation for the elevated homogenisation temperatures involves "upbulging" of the lithosphere in the extensional tectonic foreland regime accompanying the SC collision, as argued by /Alm et al. 2005/ but isotopic evidences for ascending hot fluids from this event are lacking (Chapter 5).

The Palaeozoic sedimentary successions were then successively eroded away (and are indicatively found in the Baltic basin /Plink-Björklund and Björklund 1999, Pontén and Plink-Björklund 2007/. Generation 5b minerals were precipitated intermittently in the bedrock fractures during these conditions of gradually lower temperatures, following the uplift related to this erosion, ranging into ambient temperatures similar to the recent conditions. Precipitation from saline, brackish as well as fresh water with organic and microbial influence is indicated /Tullborg 2003, Milodowski et al. 2005, Drake and Tullborg 2009a/, cf. Chapter 5.

4.7 Generation 6

Generation 6 consists of calcite, pyrite, clay minerals and goethite (near surface) in open fractures. Typical examples are shown in Figure 4-28 and Figure 4-29. Some of these coatings may have been precipitated recently (Quaternary) and the calcites show stable isotope signatures and morphologies (Figure 4-30) which indicate possible precipitation from saline, brackish or fresh water similar to the present groundwater at the site /Drake and Tullborg 2007b/. Pyrite and calcite are mainly absent in the upper 20–40 m, whereas goethite is mainly found at these depths and rarely deeper in water conducting fractures /Drake and Tullborg 2008a/ (cf. Sections 6.2.1.1 and 7.5). Fracture coatings in water conducting fractures often consist of loose and clay-rich coatings. Most of these fracture coatings contain quartz, K-feldspar and albite in addition to calcite, chlorite and clay minerals. Altered wall rock fragments

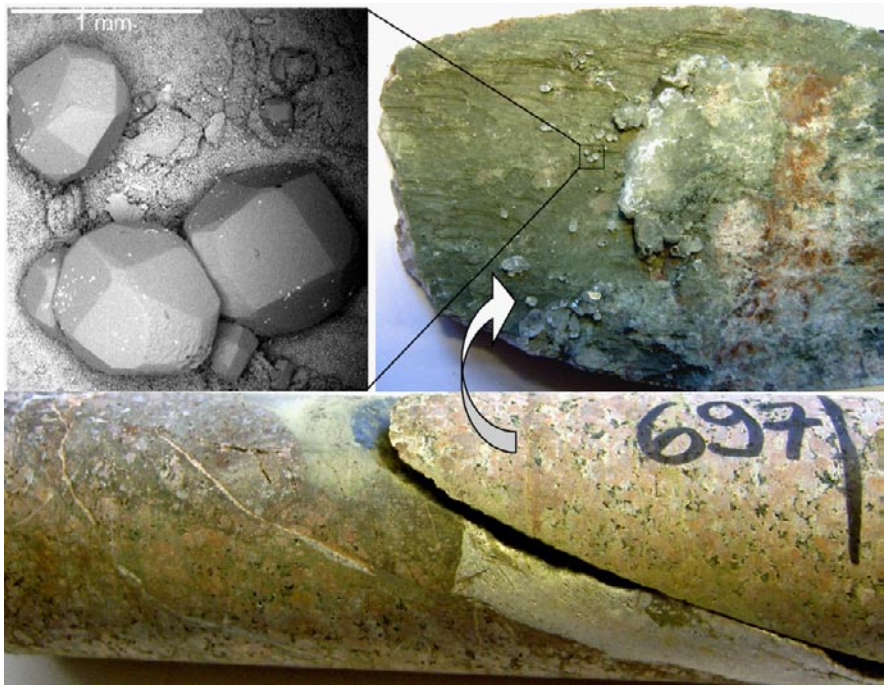

Figure 4-28. *Photograph of the drill core (bottom, sample KLX07A 697 m borehole length) and the fracture surface (upper right), as well as a BSE-image (upper left) of equant calcite crystals on the striated fracture surface coated by chlorite and clay minerals. The diameter of the drill core is ~50 mm.*

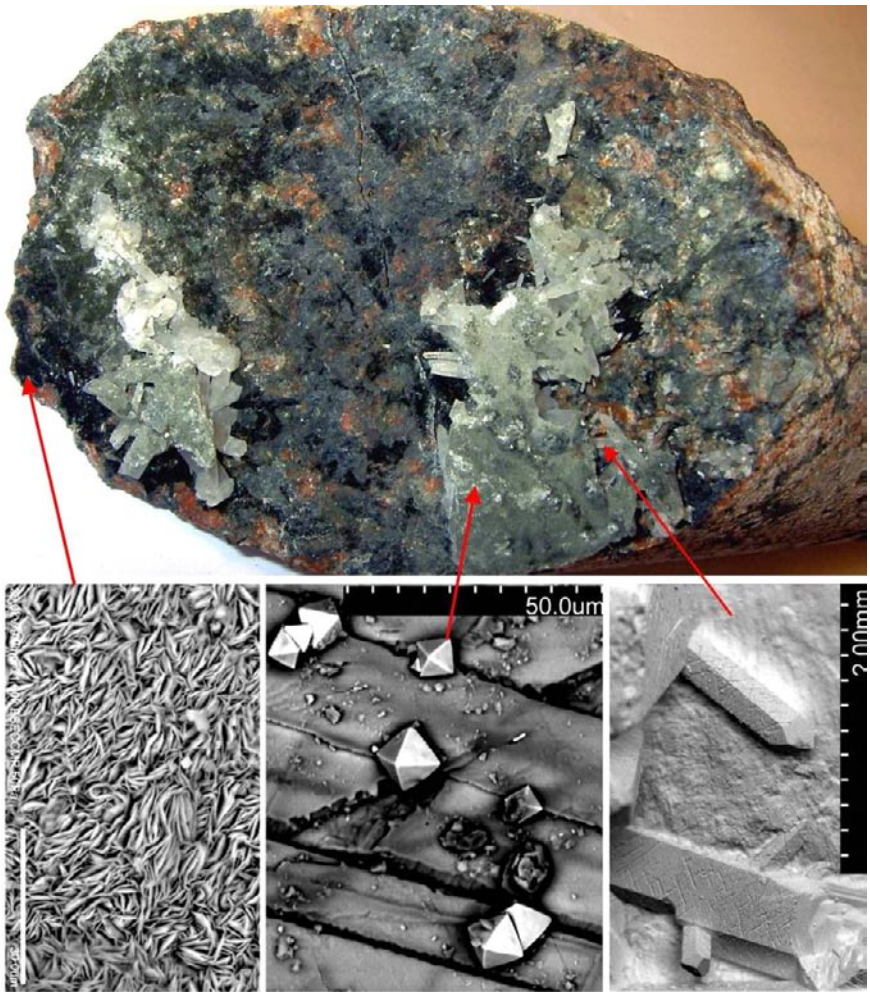

Figure 4-29. *Photograph of drill core KLX08, borehole length 108 m (top) with close-up BSE-images (below) of clay minerals (left), pyrite grown on calcite (centre) and needle-shaped calcite (right). The diameter of the drill core is ~50 mm.*

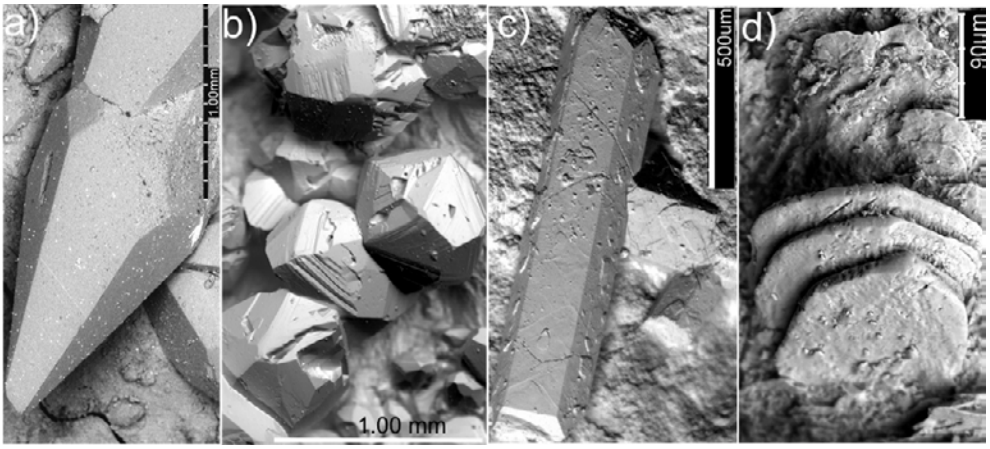

Figure 4-30. *BSE-images of calcite of different morphologies. a) scalenohedral (c-axis elongated), from drill core KLX07A, borehole length 346 m. b) equant (short c-axis/round), from drill core KLX17A, borehole length 315 m. c) needle-shaped (very elongated c-axis), from drill core KLX08, borehole length 108 m. d) nailhead-shaped (very short c-axis) from drill core KLX09F, borehole length 77 m. Scale bars are indicated in the images.*

dominate the gouge material and it is therefore probable that most of the sampled quartz and feldspars come from these rock fragments or from the fracture walls. Swelling clays like corrensite and mixed-layer clays of illite/smectite type are common. The combination of $\delta^{18}O$ and crystal morphologies of the youngest calcite have shown that the fresh-saline water interface has changed considerably over time /Drake and Tullborg 2009a/. Most of the presently water conducting fracture systems were activated or reactivated during the Palaeozoic and have probably been water pathways ever since. This is exemplified by the presence of both Palaeozoic calcite and later low temperature precipitates on the same fracture surfaces, cf. studies from Äspö /Tullborg et al. 1999/. However, the detailed flow paths have changed through time and past groundwaters have left precipitates from which the different groundwater regimes now can be traced. Organic influence and closed system microbial activity are indicated by very low $\delta^{13}C$, extreme variation in $\delta^{34}S$ and trace element compositions, consistent with descending fluids, as shown by a decrease in organically influenced fracture fillings with increased depth (see Chapter 5).

The finding of pyrite crystals in the outermost layers of the fracture coatings are in agreement with the present reducing groundwater chemistry /SKB 2006b/. However, above the redox front (at c. 20–40 m depth), recent oxidation is evidenced by the lack of pyrite and abundant goethite in the open fractures, and further strengthened by positive Ce-anomalies and U-series disequilibrium in the bulk fracture coatings, see Chapter 6. Based on the U-series isotopes, this corresponds to conditions prevailing during the Quaternary. Dissolution of calcite in the upper tenths of metres is consistent with alteration caused by descending weakly acidic and oxidising fluids.

Generation 6 minerals calcite, clay minerals and pyrite are found in open fractures with minerals from other generations as well. They are therefore not suitable as definite evidence of preferred fracture orientations (see Generation 5). However, in most fracture domains, open fractures with these minerals are mainly sub-vertical and strike E-W to mainly WNW-ESE or are sub-horizontal, although clusters of other orientations are present as well. The dominant fracture orientations (WNW-ESE) correspond fairly well to the prevailing NW-directed maximum horizontal stress /Bjarnason et al. 1989, Lee et al. 1994/. Furthermore, the dominance of sub-vertical, roughly WNW-ESE trending fractures, as well as of sub-horizontal to gently dipping fractures, is also shown to be the main orientations for open fractures containing goethite (Figure 4-31) and for open fractures without visible fracture minerals (Figure 4-32). The former is interpreted to be mainly of Generation 6 origin and the latter may be of late origin as well. In particular, sub-horizontal fractures with no coating in the upper part of the bedrock may be formed as a response to pressure release, e.g. associated with deglaciation. It should be noted that many of the fractures of these types are not shown in these plots because they are from the uppermost part of the boreholes which lack BIPS images and thus lack correct orientation measurements. Several of the fractures without visible fracture minerals may be drilling or mapping artefacts. In order to understand the geological importance of the fractures with no visible minerals, further analysis of the Boremap data, detailed microscopic examination of the fracture surfaces and evaluation of groundwater chemistry regarding dissolution/precipitation of minerals under present conditions are needed.

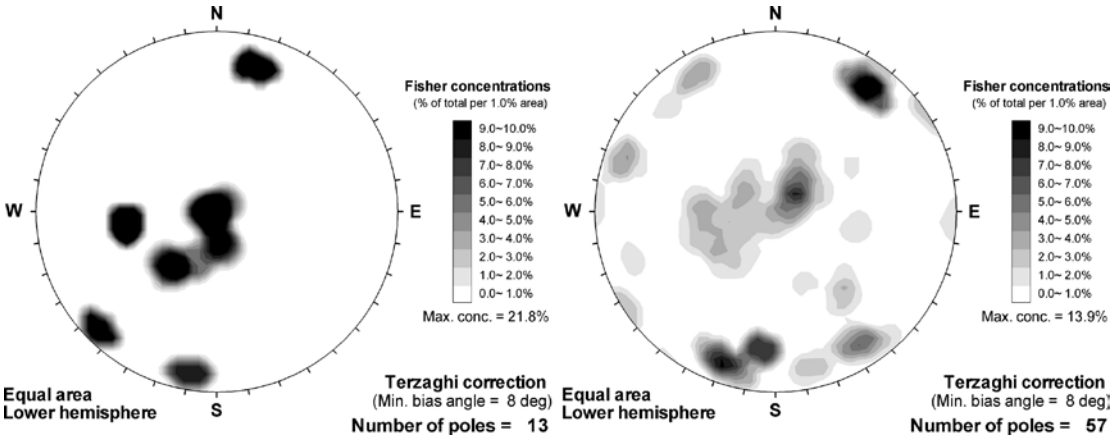

Figure 4-31. *Orientation of open fractures with goethite in fracture domains, FSM_N (left) and FSM_W (right). The goethite occurrences in FSM_EW007, FSM_C and FSM_NE005 are too few for any interpretations. A Terzaghi correction has been applied to compensate for borehole orientations.*

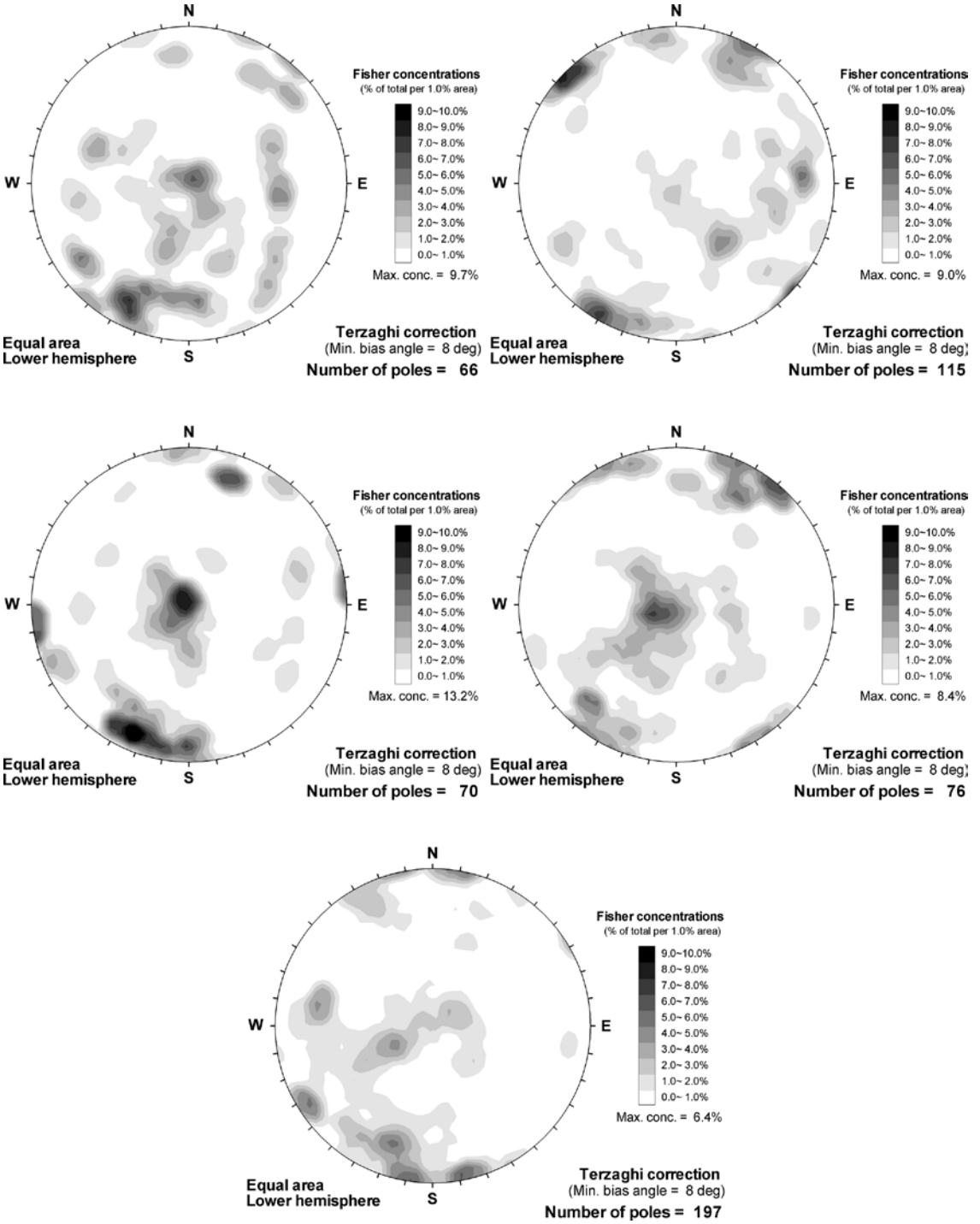

Figure 4-32. *Orientation of open fractures without visible fracture minerals in fracture domains FSM_C, FSM_EW007, FSM_N, FSM_NE005 and FSM_W (from upper left to lower right). A Terzaghi correction has been applied to compensate for borehole orientations.*

4.8 Analyses of orientation of selected fractures

As stated in the beginning of this chapter, since many of the minerals, e.g. calcite and chlorite are found in several generations and because reactivation of fractures may result in misleading interpretations of the fracture orientations, special care must be taken when selecting the minerals for fracture orientation interpretation. To avoid the influence on the fracture orientations by major deformation zones, borehole sections intersecting these zones are generally excluded. Preferred features include minerals (or a mineral paragenesis) that only exist in one generation. This subset of data is mainly chosen to

eliminate reactivated fractures, e.g. fractures including old hydrothermal minerals or extensive wall rock alteration are left out when analysing low-temperature generations and vice versa. Inconsistencies in the mapping are also taken into account, e.g. epidote and prehnite were not effectively distinguished in boreholes KLX02–07B or in the boreholes from the Simpevarp subarea. A selection of stereographic plots, based on these conditions is shown in Figure 4-33 (these differ from those shown in Sections 4.3, 4.6 and 4.7, as stated above). These indicate that greisen fractures (represented by muscovite) in KLX06 and amphibole-filled fractures in KLX08 (Generation 3) are mainly sub-horizontal (Figure 4-33a, d). Epidote and prehnite-dominated fractures of Generation 3 are dominantly sub-vertical and c. N-S oriented as well as sub-horizontal (Figure 4-33b, c). Gypsum of Generation 5 is dominantly found in sub-vertical fractures trending WNW-ESE to NW-SE (Figure 4-33f). Additionally, since the Boremap data provide no information on different generations, fractures containing Generation 5 fillings exclusively were distinguished macroscopically or with microscope or SEM-EDS from cored boreholes KLX03, 04, 05, 06, 07A, 08, 09A, 09D–F, 10, 10C, 11C, 11E, 14A, 19A, 20A, 26A (Figure 4-33e). These fractures are mainly sub-vertical and trend WNW-ESE (E-W to NW-SE), but the orientations of these fractures vary more than those containing gypsum.

In conclusion, the fracture orientations of these subsets are more distinct than when using the entire data set for the fracture domains.

4.9 Concluding remarks

Investigation of cross-cutting fractures has, with some support from palaeohydrogeological studies (Chapter 5), revealed a relative sequence of fracture fillings consisting of six generations.

- Generation 1 is an epidote- and quartz-rich mylonite formed during the early geological history of the area, although it has experienced later brittle reactivation. The mylonites are mainly associated with deformation zones and are often accompanied by wall rock alteration. $^{40}Ar/^{39}Ar$-dating of muscovite in mylonite from Äspö shear zone yielded a plateau age of c. 1,406 Ma. However, this age probably represents cooling below 350°C after resetting of the $^{40}Ar/^{39}Ar$-system caused by influence from the Götemar-Uthammar intrusions nearby. The $^{40}Ar/^{39}Ar$ system in the dated mylonite may be particularly disturbed by a cross-cutting Generation 3 fracture. Instead, a minimum age close to c. 1,773 Ma, when the rock cooled below ~500°C, is suggested, based on formation temperature estimates. The shear zones are definitely older than the c. 1,450 Ma Götemar granite. The direction of the maximum compressive stress was approximately N-S to NNW-SSE during the formation of the ductile shear zones in the area, probably in the late stages of the Svecokarelian orogeny at >1,750 Ma.
- Generation 2 is cataclasite of at least two different varieties, sometimes with semi-ductile features. Both were formed during the early geological history of the area, although both have experienced later re-activation. The cataclasites are mainly associated with deformation zones and the older ductile shear zones have influenced the orientation of many Generation 2 structures. The observed semi-ductile features suggest formation close to 300–350°C. The formation temperatures suggest either 1) formation prior to 1,620 Ma when the rock initially cooled below 300°C and/or 2) formation related to the intrusions at Götemar and Uthammar or at a slightly earlier thermal event.
- Generation 3 consists of a sequence of at least three different mineral parageneses in sealed fractures, and occasionally of greisen. Major minerals are calcite, quartz, chlorite, fluorite, pyrite, muscovite, epidote, prehnite and laumontite. The latter three replace or cut each other in chronological order and a prolonged deposition event is indicated. The generation is interpreted to be related to the intrusions of the Götemar and Uthammar granites but many of the fillings are probably older. These granites have been interpreted to be associated with the Danopolonian orogeny in the south and consequently the Generation 3 fillings would also have been formed as a far-field effect of this orogeny. $^{40}Ar/^{39}Ar$ plateau ages of greisen and the characteristically altered and red-stained wall rock of about 1,424–1,417 Ma indicate the association of a major part of this generation to the nearby intrusions. Generation 3 fillings are dominantly found in sealed sub-horizontal fractures and/or steep fractures trending N-S (NNE-SSW to NNW-SSE) although the patterns differ slightly between the different fracture domains and between different minerals. Greisen fractures related to the intrusion and post-magmatic circulation of the Götemar granite are mainly sub-horizontal. The many roughly N-S (NNE-SSW to NNW-SSE) trending fractures filled with Generation 3 minerals may alternatively suggest formation during the waning stages of the Svecokarelian orogeny when

maximum compressive stress was N-S to NNW-SSE directed. However, these fractures may also have been formed or been reactivated in relation to the nearby granite intrusions and filled with Generation 3 minerals. Formation as a direct far-field stress effect of the Danopolonian orogeny in the south may also be suggested for these fractures but the features of this orogeny and its influence on adjacent areas are still rather poorly defined. The most probable scenario is that Generation 3 minerals formed during a prolonged period of time at different events with the latest and major pulse of precipitation related to the intrusion of the Götemar and Uthammar granites. The latter affected the area with opening of new fractures and reactivation of fractures and deformation zones, intense wall rock alteration and precipitation of e.g. epidote, prehnite and subsequently laumontite.

- Generation 4 mainly includes calcite, adularia, laumontite, chlorite, quartz, illite and hematite. Generation 4 minerals are found in thin sealed fractures cross-cutting Generation 3 fillings but are difficult to distinguish from these due to similar mineralogy and appearance. However, they have slightly different stable isotope and fluid inclusion signatures, as well as chlorite chemistry. They are interpreted to be formed later than c. 1,400 Ma, but prior to 710 ± 78 Ma. Generation 4 may be Sveconorwegian in age as indicated by a $^{40}Ar/^{39}Ar$ adularia age of c. 989 Ma, although this age may also represent resetting of the adularia during this orogeny, as shown by reset $^{40}Ar/^{39}Ar$ ages for biotite of c. 928 Ma from the same borehole. Furthermore, the intrusion of N-S oriented, c. 0.9 Ga dolerites in the westernmost part of the Laxemar subarea indicates E-W directed late Sveconorwegian extension. However, apart from the mentioned $^{40}Ar/^{39}Ar$ ages and the dolerite intrusion, no sufficient evidence of extensive Sveconorwegian fracturing of the Laxemar area has been traced. Although Generation 4 may be largely Sveconorwegian, it is not very distinct and not as widespread as Generations 3 and 5.
- Cambrian sandstone is present in a few sub-vertical, near-surface fractures in the Laxemar area. The sandstone textures indicate forceful injection downwards as fluidised sediment with a high internal fluid pressure, possibly built up by overlying Palaeozoic sedimentary successions. In the coastal areas around the Laxemar area the dominating fracture orientations are NNE-ENE and might be related to a NW-SE directed extension event.
- The oldest of fillings of Generation 5 were probably formed in relation to the Caledonian orogeny. These calcite dominated fillings were formed from warm brine fluids (c. 80–145°C) at c. 440–400 Ma. Other minerals include adularia, fluorite, pyrite, gypsum, barite, zeolites, hematite, clay minerals, chlorite, chalcopyrite, galena, sphalerite and REE-carbonate. These fillings were formed in dominantly WNW-ESE (E-W to NW-SE) trending fractures with sub-vertical dips, and these orientations correlate to the maximum compressive stress during the Caledonian orogeny. These fillings precipitated from organic-rich fluids, probably influenced by descending waters from overlying sediments. The relatively high formation temperatures may also be influenced by subsidence due to thick overlying sediments. Younger fillings of Generation 5 precipitated during gradually lower temperatures as the overlying sedimentary successions were successively eroded, shown by the changing stable isotope compositions and chemical compositions, which grade into Generation 6 signatures.
- Generation 6 consists of fracture coatings which may have been precipitated recently, i.e. during the Quaternary. These include clay minerals, calcite, goethite above the redox front and pyrite below the redox front. U-series measurements suggest that U present on fracture coatings has been dissolved above the redox front and deposited mainly below the redox front within the last 1 Ma. Generation 6 minerals are not easily distinguished from the youngest Generation 5 fillings which have overlapping stable isotope signatures and trace element compositions. The stable isotope composition of these minerals (mainly calcite) shows that they may have been precipitated from waters with similar signatures to the present ground water at the site. The calcite crystals show large variation in morphologies, which indicate precipitation from different types of water. Open fractures without visible coatings may be recent, e.g. connected to unloading, but may also be the result of reactivation of fractures with very small amounts of fracture minerals that have been dissolved or flushed away. In order to understand the geological importance of these fractures, further analysis of the Boremap data, detailed microscopic examination of the fracture surfaces and evaluation of groundwater chemistry regarding dissolution/precipitation of minerals under present conditions are needed (and have been initiated). Open fractures with Generation 6 minerals, or without any minerals, are mainly sub-vertical and strike E-W to mainly WNW-ESE or are sub-horizontal. The dominant fracture orientations correspond fairly well to the dominantly prevailing maximum horizontal stress and sub-horizontal fractures in the upper part may be formed as a response to pressure release, e.g. related to deglaciation.

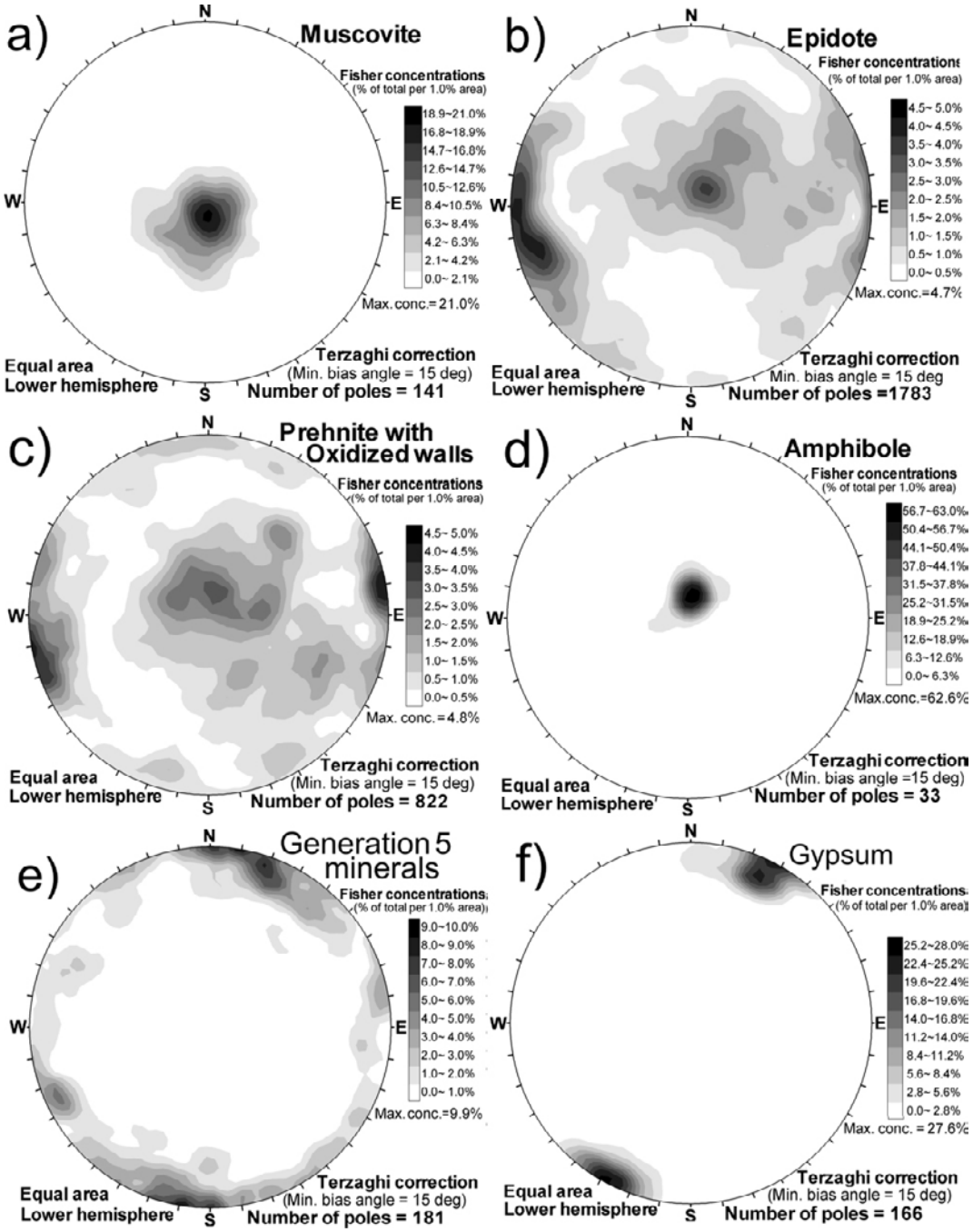

Figure 4-33. *Orientations of fractures containing specific minerals. a) Muscovite in greisen fractures in borehole KLX06 north of ZSMEW002A. b) Epidote-dominated (mapped as the most abundant in Boremap) sealed fractures in boreholes KLX08, 09A–B, 10, 12A, 13A, 14A, 17A, 18A, 21B, except fractures including prehnite or zeolites. c) Prehnite-dominated sealed fractures with red-stained wall rock in KLX08, 09A–B, 10, 12A, 13A, 14A, 17A, 18A, 21B, except fractures including epidote or zeolites. d) Amphibole in sealed fractures (only present in KLX08). e) Generation 5 minerals, confirmed with microscope or hand lens, in open or sealed fractures in KLX03, 04, 05, 06, 07A, 08, 09A, 09D–F, 10, 10C, 11C, 11E, 14A, 19A, 20A, 26A. Re-activated fractures containing minerals older than Generation 5 are excluded. f) Gypsum in open and sealed fractures in KLX03, 08, 10, except in fractures containing epidote, fluorite, prehnite, feldspars or fractures with altered wall rock. A Terzaghi correction has been applied to compensate for borehole orientations.*

5 Stable isotopes, calcite geochemistry and fluid inclusions

Since stable carbon and oxygen isotope analyses can be carried out on very small sample volumes (150–200 µg), a relatively large number (222) of $\delta^{18}O$ and $\delta^{13}C$ analyses of calcite have been carried out. Larger sample volumes are needed for $^{87}Sr/^{86}Sr$ (30–40 mg) and trace element analyses and thus a smaller number of samples (c. 70 and 28, respectively), have been analysed. 41 samples have been analysed for $\delta^{34}S$ and fluid inclusions have been analysed in 12 samples. In this chapter, all depths are shown as vertical depth from the ground surface, in order to perform best possible evaluation of depth trends. All samples are therefore shown and discussed according to their vertical depths which have been extracted from the Sicada (data delivery Sicada_08_062).

For a detailed description of the different generations, see Chapter 4. Detailed descriptions of the analysed calcite and pyrite samples are available in the P-reports listed in Table 1-1.

A small number of samples from KSH01A-B from the earliest phase of the site investigations are excluded because they include calcite of mixed generations (as a consequence of discrete cross-cutting relations, old hydrothermal calcite was in-mixed with younger calcite in the analyses) which gives unrepresentative results for these small number of samples only. Results from earlier studies at Äspö HRL and KLX01–02 /Wallin and Peterman 1999, Bath et al. 2000, Milodowski et al. 2005/ are included in most of the figures for comparison. It should be noted that these were generally not sampled in as detailed a manner as at the current site investigations and may thus include mixed generations. Götemar granite samples of Generation 5a and 5b/6 /Drake and Tullborg 2006a/ are also included and show similar signatures as coeval samples from within the subareas.

5.1 Carbon and oxygen isotopes

Very large variations in isotope ratios are observed for both $\delta^{13}C$ (–99.7 to +1.4‰) and $\delta^{18}O$ (–23.5 to –4.9‰) in calcite (Figure 5-1), and the variability in these isotope systems far exceeds analytical error and thus reflects natural variability. The isotopic signatures of the different generations are listed in Table 4-1. In summary, and as shown in Figure 5-1, calcite of Generation 3 and 4 show similarly high and quite homogeneous $\delta^{13}C$ values of –6.5 to –2‰, whereas the $\delta^{18}O$ values show larger variation and Generation 3 includes $\delta^{18}O$ values down to –23.5‰. As stated above, calcite of Generation 5a and Generation 5b/6 are distinguished by their $\delta^{18}O$ signatures. Generation 5a calcites have lower $\delta^{13}C$ values (mainly –16 to –9‰) and a more restricted span in $\delta^{18}O$ (–16.5 to –11‰) compared with Generations 3 and 4. Calcite of Generation 5b/6 have higher $\delta^{18}O$ than older calcite and much more extreme variation in $\delta^{13}C$ (–99.7 to +1.4‰).

Variation in $\delta^{18}O$ and $\delta^{13}C$ values between different crystals from the same fracture surface is commonly less then 1‰ ($\delta^{18}O$) and 3‰ ($\delta^{13}C$), but variations of up to 8.7‰ ($\delta^{18}O$) and 50‰ ($\delta^{13}C$), also exist. No distinct separation in stable isotope composition related to crystal morphology has been possible to establish, except some scalenohedral crystals which show extremely low $\delta^{13}C$ values (Figure 5-2). There is also a small difference in median $\delta^{18}O$ values of the crystals with different morphology, of which nailhead has the lowest values and scalenohedral has the highest values.

Variation of $\delta^{13}C$ values with vertical depth is shown in Figure 5-3. Calcite of Generation 3, 4 and 5a generally show no systematic $\delta^{13}C$ variation with depth, although there is a low frequency of Generation 3 and 4 calcites in the upper part of the bedrock. Furthermore, Generation 5a calcite with $\delta^{13}C$-values below –11.5‰ are not found at depths greater than 800 m. In accordance with samples from Äspö and KLX01 and 02, extreme $\delta^{13}C$ values in Generation 5b/6 are most frequent in the upper part of the bedrock, at ~25–200 m. However, very low $\delta^{13}C$ values, mainly in scalenohedral crystals, are found down to c. 670 m in the Laxemar subarea. $\delta^{13}C$ values higher than –3‰ are found in the upper 107 metres. Calcite of Generation 5b/6 lacks $\delta^{13}C$ values below –13.5‰ at depths greater than 800 m.

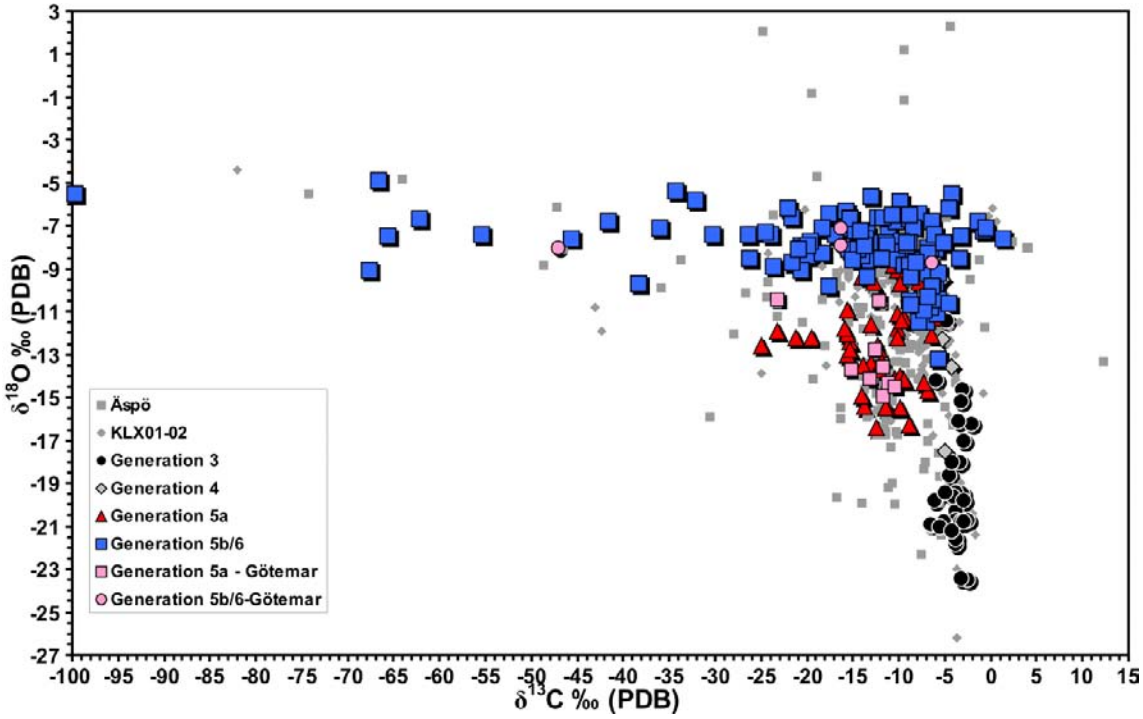

Figure 5-1. *$\delta^{18}O$ versus $\delta^{13}C$ in fracture filling calcite of different generations from the Laxemar and Simpevarp subareas and from the Götemar granite. Calcite samples from Äspö and KLX01–02 /Tullborg et al. 1999, Wallin and Peterman 1999, Bath et al. 2000, Milodowski et al. 2005/ are also shown but are not separated into different generations. Analytical errors are within the size of the symbols.*

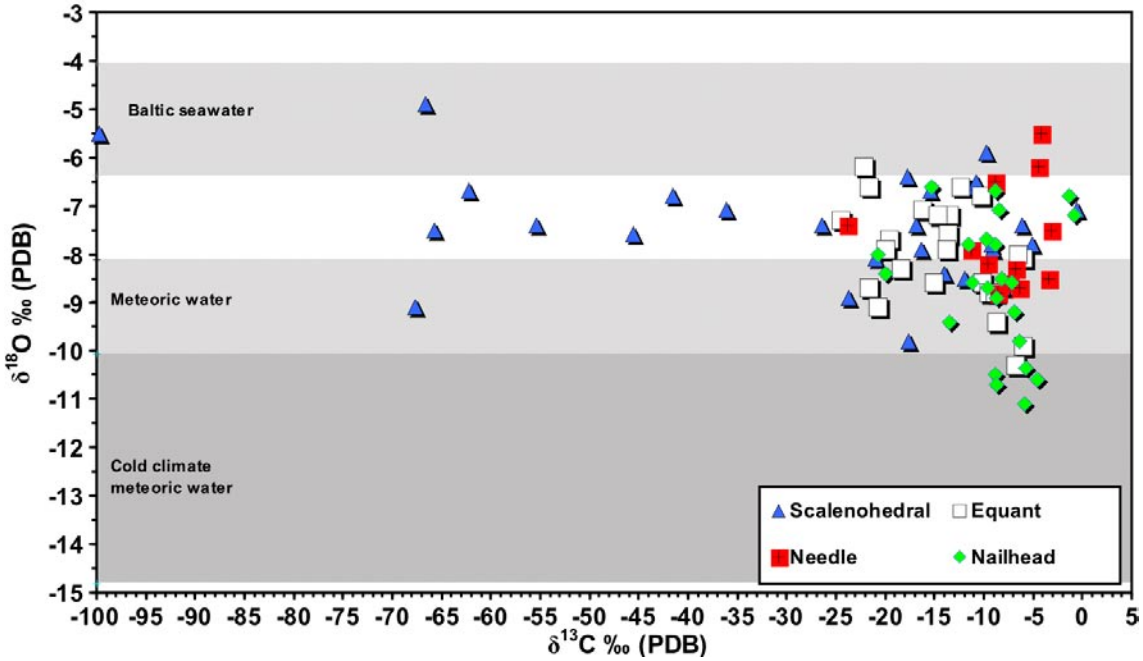

Figure 5-2. *$\delta^{13}C$ versus $\delta^{18}O$ in fracture filling calcite of Generation 5b/6 with defined morphology. Samples are from the Laxemar and Simpevarp subareas, and additionally from the Götemar granite. Shaded areas represent calcite precipitated in equilibrium with present day Baltic seawater and meteoric water as well as cold climate meteoric water at 7–15°C using fractionation factors from /O'Neil et al. 1969/ and the Laxemar 2.3 groundwater data set, defined by the extended data freeze per November 30, 2007 (extracted from Sicada). Analytical errors are within the size of the symbols.*

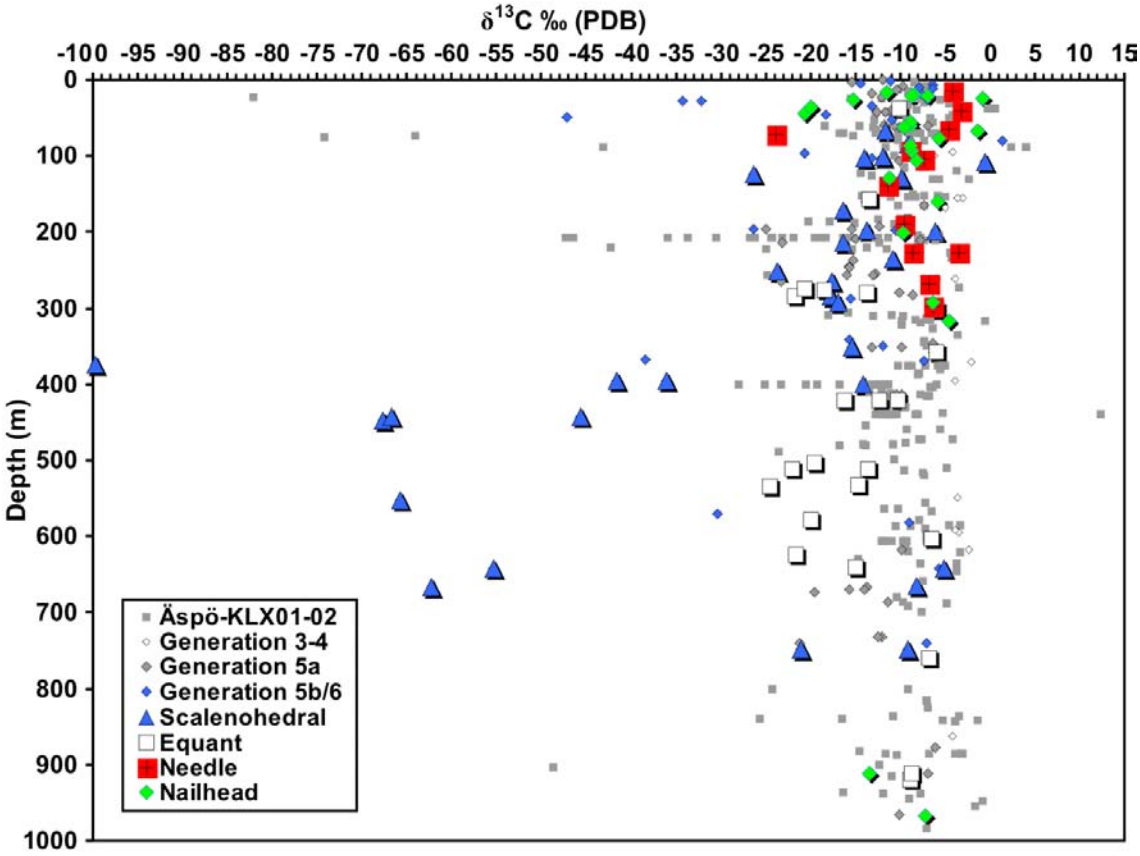

Figure 5-3. *$\delta^{13}C$ versus vertical depth in fracture filling calcite of Generations 3–4, 5 and 5b/6 from the Laxemar subarea, the Simpevarp subarea and from the Götemar granite. Morphologies of calcite of Generation 5b/6 are indicated where observed. Calcite samples from Äspö and KLX01–02, Laxemar /Tullborg et al. 1999, Wallin and Peterman 1999, Bath et al. 2000, Milodowski et al. 2005/ are also shown but are not separated into different generations. Analytical errors are within the size of the symbols.*

Variation of $\delta^{18}O$ values with vertical depth is shown in Figure 5-4. Shaded areas in this figure represent calcite precipitated in equilibrium with present-day Baltic seawater and meteoric water, as well as cold climate meteoric water, at temperatures increasing linearly from 7 ± 2°C near the ground surface to 18 ± 2°C at 1,000 m depth; using fractionation factors from /O'Neil et al. 1969/ and groundwater and temperature data from the Laxemar 2.3 groundwater data set, defined by the extended data freeze per November 30, 2007 (extracted from Sicada). $\delta^{18}O$ signatures in calcite of Generation 3, 4 and 5a generally show no systematic variation with depth, although there is low frequency of Generation 3 and 4 calcites in the upper part of the bedrock. For the Generation 5b/6 calcites, there are some trends in the data set, e.g. the slightly decreasing values with depths. The highest values (>–6‰) are mainly found in the upper 100 m and occasionally at greater depths, e.g. at 370–440 m. The number of calcite occurrences of Generation 5a and 5b/6 is very small at depths greater than 800 m and those present lack $\delta^{18}O$ values higher than 8.6‰. Needle-shaped and nailhead-shaped calcite crystals are mainly found in fractures from depths down to 300 m, except for a few nailhead-shaped crystals at great depths in highly transmissive fractures in KLX04. Equant and scalenohedral crystals are more evenly distributed with depth.

5.2 Fluid inclusions

Calcite of Generation 3, 4, 5a and 5b/6 and quartz of Generation 3, have been analysed for fluid inclusions (Figure 5-5). However, the only sample of Generation 5b/6 (needle-shaped) prepared for analysis did not contain any inclusions. The inclusions observed mainly consisted of single phase liquid inclusions or two-phase aqueous liquid and vapour inclusions of variable size (mainly 5–25 µm, occasionally larger; 20–50 µm) that were often in clusters. Homogenisation temperatures (T_h) and temperature of

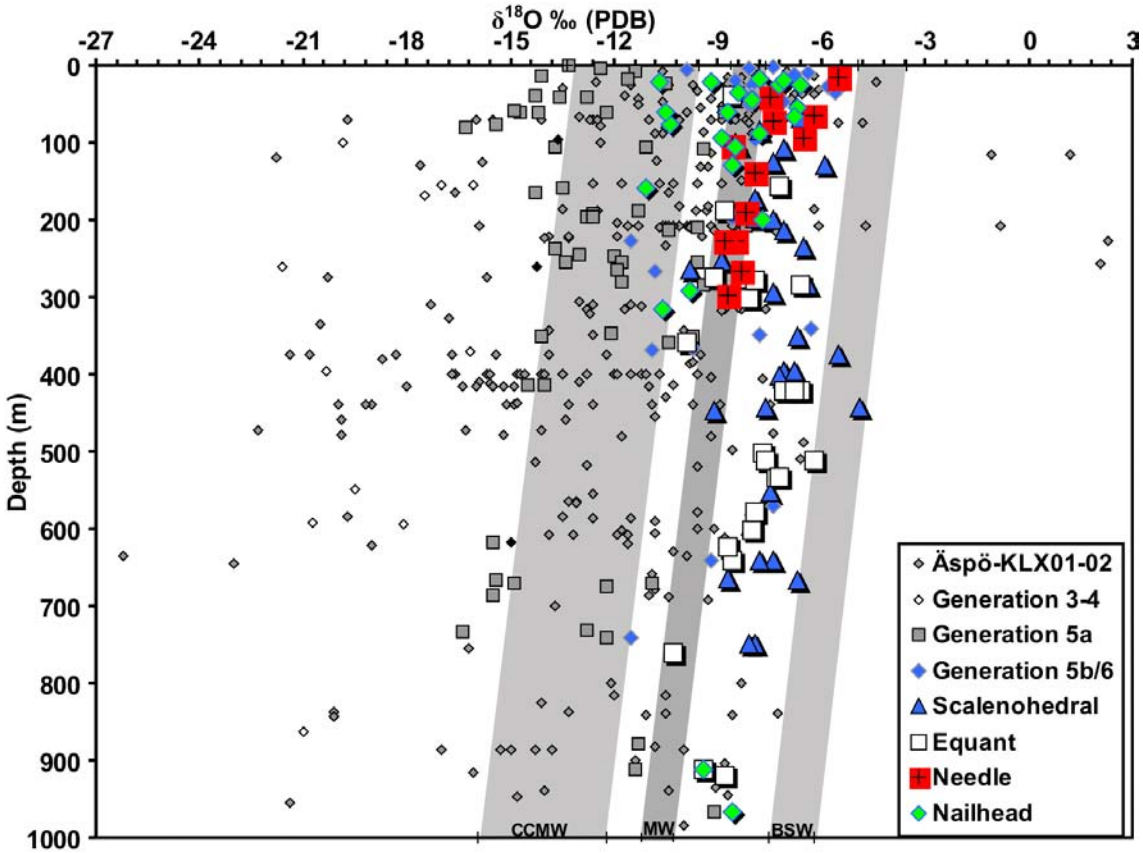

Figure 5-4. *$\delta^{18}O$ versus vertical depth in fracture filling calcite of Generations 3–4, 5 and 5b/6 from the Laxemar subarea, the Simpevarp subarea and from the Götemar granite. Morphologies of calcite of Generation 5b/6 are indicated where observed. Calcite samples from Äspö and KLX01–02, Laxemar /Tullborg et al. 1999, Wallin and Peterman 1999, Bath et al. 2000, Milodowski et al. 2005/ are also shown but are not separated into different generations. Shaded areas represent calcite precipitated in equilibrium with present-day Baltic seawater (BSW) and meteoric water (MW) as well as cold climate meteoric water (CCMW) at temperatures increasing linearly from 7 ± 2°C near the ground surface to 18 ± 2°C at 1,000 m depth, and using fractionation factors from /O'Neil et al. 1969/ and the Laxemar 2.3 groundwater data set, defined by the extended data freeze per November 30, 2007 (extracted from Sicada). Analytical errors are within the size of the symbols.*

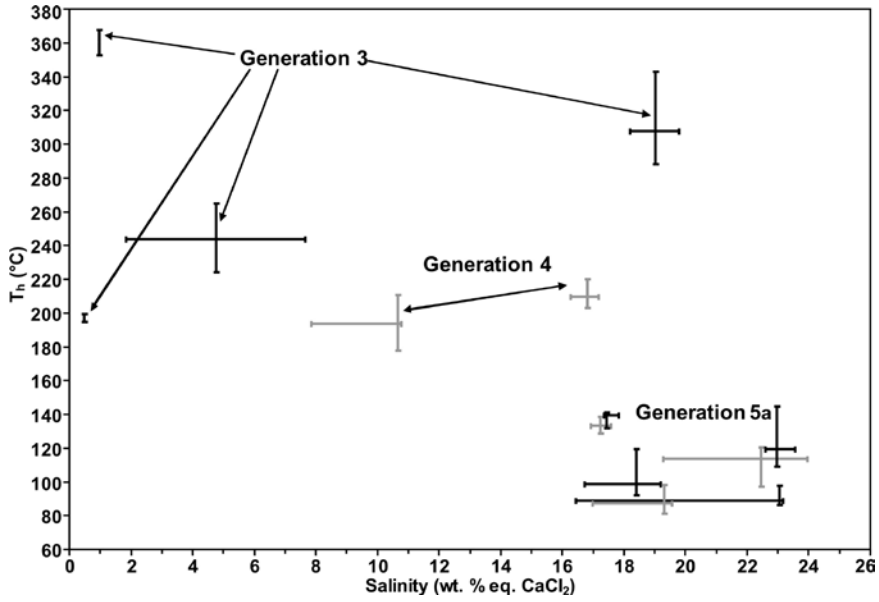

Figure 5-5. *Homogenisation temperature (T_h) vs. salinity (wt. % eq. $CaCl_2$) for primary fluid inclusions in calcite and quartz. The range of T_h and salinity is shown with lines for each sample and the intersections of the lines represent the median values. Two populations are shown for the single Generation 4 sample. The figure is adopted from /Drake and Tullborg 2009a/. Colour variations are used in order to distinguish better between different samples.*

final ice melting (T_m) were analysed for the two-phased inclusions at room temperature. Reactivation of the fractures is common and therefore, resetting of earlier formed inclusions and formation of secondary inclusions has most likely occurred. This is demonstrated by closely spaced inclusions with similar appearance, but with very different salinities and/or T_h. It is difficult to recognise secondary inclusions by appearance only, although inclusions found along twin planes or sealed micro-fractures are recognised as secondary according to the criteria of /Roedder 1981/. However, for most of the samples it was possible to distinguish primary from secondary inclusions, considering the highest T_h population to be primary. Temperature of first ice melting (T_{fm}) was only detected in highly saline inclusions. Other inclusions had too low optical contrast between ice and liquid. T_{fm} was mainly –50 to –60°C, indicative of a mixed NaCl-$CaCl_2$-H_2O type brine (eutectic at –52°C) of unknown $CaCl_2$/($NaCl+CaCl_2$)-ratio /Crawford 1981, Shepherd et al. 1985/. Furthermore, the brown colouration observed in the moderately to highly saline inclusions upon freezing is typical for NaCl-$CaCl_2$ ($\pm MgCl_2$) fluids /Shepherd et al. 1985/. However, the most saline inclusions (T_m: c. –25°C) indicate a dominance of $CaCl_2$ over NaCl /e.g. Milodowski et al. 2005/. Therefore, the salinities are given as wt.% eq. $CaCl_2$, in accordance with earlier fluid inclusion studies of fracture minerals in the area /Alm and Sundblad 2002, Milodowski et al. 2005/.

Fluid inclusions in calcite and quartz of Generation 3 generally show low to moderate salinities (<1 wt.% eq. $CaCl_2$ in two samples and c. 2–8 wt.% eq. $CaCl_2$ in one sample, Figure 5-5) and relatively high T_h with a large spread between samples (c. 195–370°C) depending on paragenesis; highest temperature with epidote and lowest with laumontite. One sample of Generation 3 calcite shows very high salinity (c. 18–20 wt.% eq. $CaCl_2$) and high T_h (c. 290–340°C), which infer a $\delta^{18}O_{H2O}$ of 2.4 to 4.0‰ utilising fractionation factors from /O'Neil et al. 1969/. The single calcite sample of Generation 4 shows two populations of fluid inclusions with different salinities but overlapping T_h (mostly lower than in Generation 3). Generation 5a calcite shows T_h of c. 80–145°C and salinities of c. 17–24 wt.% eq. $CaCl_2$. Calculated $\delta^{18}O_{H2O}$ is commonly 1–4‰ but two samples yield $\delta^{18}O_{H2O}$ of a few per mil below zero.

5.3 Strontium isotopes

The $^{87}Sr/^{86}Sr$-ratios in analysed calcites increase with age and are positively correlated to $\delta^{18}O$ (Figure 5-6, Table 4-1 and Table 5-1). The $^{87}Sr/^{86}Sr$-ratios in the groundwater and in calcite of Generation 5a and 5b/6, varies with wall rock composition and are mainly higher in Ävrö granite (5a: >0.7132 and 5b/6: 0.7152–0.7166) than in quartz monzodiorite or dioritoid (5a: <0.7132 and 5b/6: 0.7150–0.7160, respectively). Calcite of Generation 5b/6 has $^{87}Sr/^{86}Sr$-ratios within the range of the present groundwater. The $^{87}Sr/^{86}Sr$-ratios of calcite of Generation 5b/6 is, however, much higher than those of Baltic Seawater. No distinct separation in $^{87}Sr/^{86}Sr$-ratios related to crystal morphology has been possible to establish. Older calcite is generally lower in $^{87}Sr/^{86}Sr$ than the present groundwater. Gypsum of Generation 5a has $^{87}Sr/^{86}Sr$-ratios within the range of the $^{87}Sr/^{86}Sr$-ratios of coeval calcite. Calcite from the Götemar granite has higher $^{87}Sr/^{86}Sr$-ratios than calcite of the same generation within the Laxemar and Simpevarp subareas. This is related to the highly different $^{87}Sr/^{86}Sr$-ratios of the wall rocks /Drake and Tullborg 2007a/ (Table 5-1).

The $^{87}Sr/^{86}Sr$-ratios of the three major, and coeval, rock types in the Laxemar area (Ävrö granite, quartz monzodiorite and fine-grained dioritoid, Table 4-1) vary due to their Rb/Sr- ratio /Drake et al. 2006, Drake and Tullborg 2007a/. The younger Götemar granite, on the other hand, has much higher $^{87}Sr/^{86}Sr$-values then these rocks, due to its higher Rb/Sr-ratios and higher initial $^{87}Sr/^{86}Sr$-values /Åberg 1978, Alm et al. 2005, Drake et al. 2006, Drake and Tullborg 2007a /. Although information on the initial $^{87}Sr/^{86}Sr$-ratios in the rocks from in the Laxemar area is lacking, the current $^{87}Sr/^{86}Sr$-ratios of these rocks are considerably higher than the initial $^{87}Sr/^{86}Sr$-ratios (0.7040–0.7081) of coeval TIB-granites and porphyries in southern Sweden /Åberg 1978/. The present $^{87}Sr/^{86}Sr$-ratio of the Götemar granite is much higher than its initial $^{87}Sr/^{86}Sr$-ratio of 0.7079 ± 0.0063 /Åberg 1978/.

The association between $^{87}Sr/^{86}Sr$-ratios and $\delta^{18}O$ values (Figure 5-6), is in contrast to some samples from Äspö, which, however, might involve several generations of calcite within the same sample.

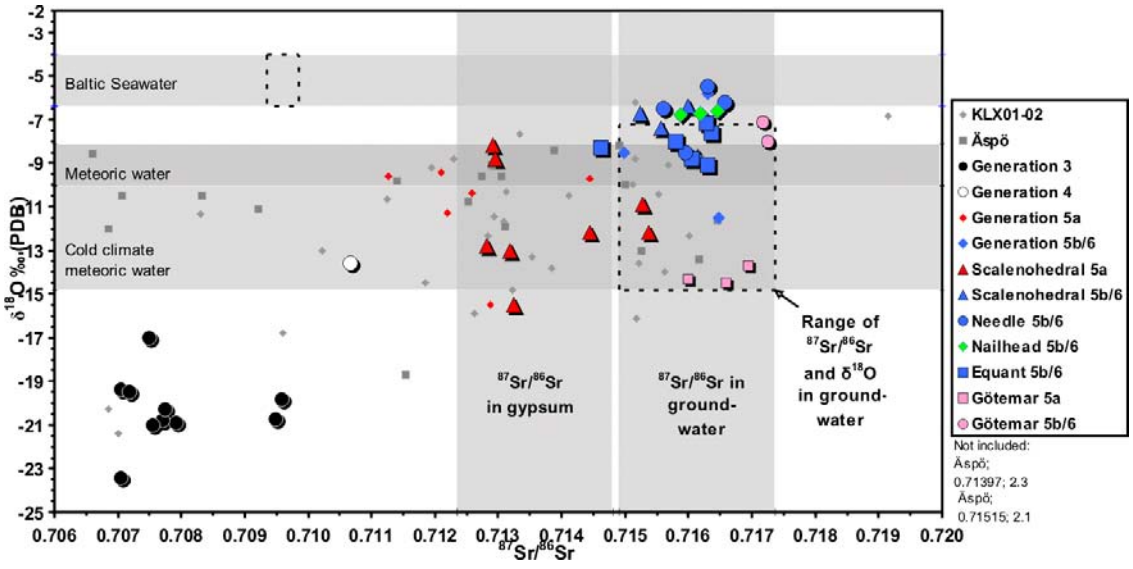

Figure 5-6. *$^{87}Sr/^{86}Sr$ ratio versus $\delta^{18}O$ in fracture filling calcite from the Laxemar subarea, the Simpevarp subarea and from the Götemar granite. Crustal morphologies are indicated where observed. Calcite samples from Äspö and KLX01–02 /Tullborg et al. 1999, Wallin and Peterman 1999, Bath et al. 2000, Milodowski et al. 2005/ are also shown but are not separated into different generations. Shaded areas (y-axis) represent calcite precipitated in equilibrium with present-day Baltic seawater and meteoric water as well as cold climate meteoric water at 7–15°C, using fractionation factors from /O'Neil et al. 1969/ and the Laxemar 2.3 groundwater data set, defined by the extended data freeze per November 30, 2007 (extracted from Sicada). Shaded areas (x-axis) represent the range in $^{87}Sr/^{86}Sr$ in gypsum of Generation 5a as well as of the present groundwater in the Laxemar and Simpevarp subareas. Stippled areas represent the isotopic composition of the Baltic Seawater as well as of the present groundwater in the Laxemar and Simpevarp subareas. Analytical errors are within the symbol size.*

Table 5-1. Compilation of Ca/Sr (by weight) and $^{87}Sr/^{86}Sr$-ratios in different generations of calcite, gypsum, fluorite, rock types and different water types in the Laxemar area. Rock data have been extracted from Sicada (data deliveries Sicada_08_071, Sicada_08_071_2 and Sicada_08_071_3), and water chemistry has been obtained from the Laxemar 2.3 groundwater data set, defined by the extended data freeze per November 30, 2007 (extracted from Sicada). Rock type 501044 hosts of the majority of the sampled fractures in the Laxemar subarea.

Samples	Ca/Sr				$^{87}Sr/^{86}Sr$			
Fracture minerals	Number of samples	Range	Mean	Standard deviation	Number of samples	Range	Mean	Standard deviation
Generation 3 calcite	7	609–1,482	1,162	334	14	0.7070–0.7096	0.70788	0.00092
Generation 3 fluorite	0	–	–	–	3	0.7059–0.7080[1]	0.70689	0.00102
Generation 4 calcite	0	–	–	–	1	0.7107	–	–
Generation 5a calcite	12	4,861–10,756	7,148	1,519	14	0.7113–0.7154	0.71326	0.00121
-in 501036-section	8	4,861–7,236	6,453	876	6	0.7113–0.7132	0.71242	0.00071
-in 501044-section	1	8,427			4	0.7132–0.7154	0.71458	0.00098
Generation 5a gypsum	6	1,005–1,758	1,379	260	7	0.7123–0.7148	0.71367	0.00090
Generation 5a fluorite	0				1	0.7116		
Generation 5b/6 calcite	9	3,307–10,282	5,676	2,318	20	0.7150–0.7166	0.71595	0.00052
-in 501036-section	2	4,071–10,282	7,772	–	3	0.7150–0.7160	0.71551	0.00050
-in 501044-section	5	3,307–7,666	4,789	1,707	14	0.7152–0.7166	0.71613	0.00037
Generation 5b/6 fluorite	0	–	–	–	1	0.7207	–	–
Rock types								
Ävrö granite (501044)	62	15.8–36.8	25.5	3.4	1	0.7160	–	–
Quartz monzodiorite (501036)	28	50.3–74.2	59.6	6.3	1	0.7135	–	–
Fine-grained dioritoid (501030)	15	20.7–109	67.0	18.4	1	0.7151	–	–
Götemar granite	2	116–183	150	–	2	0.9761–0.9781	0.97712	–
Waters								
Surface waters-Laxemar	694	16–397	223	52.0	65	0.7186–0.7263	0.72149	0.00191
Lake water-Laxemar	285	176–226	196	16	16	0.7205–0.7280	0.72256	0.00219
Groundwater-Laxemar	275	35–230	67	32	117	0.7149–0.7175[2]	0.71567	0.00058
Groundwater-Simpevarp	67	26–128	63	16	6	0.7149–0.7160[3]	0.71540	0.00033
Baltic Sea Water	438	58–86	67	3.4	46	0.7094–0.7104	0.70950	0.00020

[1)] Outlier of 0.7468 excluded
[2)] Outlier of 0.7210 excluded
[3)] Outlier of 0.7115 excluded

5.4 Trace elements in calcite

Fe and Mg show low concentrations, below 0.2%, and no systematic variation; neither with depths nor between the different generations. The largest calcite trace element variations are those of Sr, Mn and rare earth elements (REE). The Sr content is higher in Generation 3 (215–450 ppm) than in Generation 5a and 5b/6 (mainly c. 50–75 ppm) and this trend corresponds to a decrease in $^{87}Sr/^{86}Sr$ (Figure 5-7), which is in accordance with earlier studies from Äspö HRL and KLX01–02 /Wallin and Peterman 1999, Bath et al. 2000, Milodowski et al. 2005/. 1/Sr versus $^{87}Sr/^{86}Sr$ for Palaeozoic calcite and younger (Figure 5-8) do not show any significant mixing trends. However, a possible diffuse trend might be indicated in the association of decreasing 1/Sr with increasing $^{87}Sr/^{86}Sr$-ratios in the $^{87}Sr/^{86}Sr$-interval from 0.7150 to 0.7165, although this is partly defined by calcite samples of unknown age, purity and type, adopted from earlier studies (i.e. mixing of different generations within the same sample). The Mn content is mainly lower in Generation 3 (c. 20–3,900 ppm) than in Generation 5a and 5b/6, in which it generally decreases with increasing depth (Figure 5-9). Mn contents above 5,000 ppm are only found in the upper 360 m. No elevated Th or U concentrations have been found in the calcite; the concentrations of both elements are usually below 0.2 ppm, although U concentrations may be up to 1.6 ppm occasionally. U concentrations of up to 3.8 ppm is documented in Generation 5a calcite from the U-rich Götemar granite /Drake and Tullborg 2007a/.

The Ca/Sr-ratio in groundwater samples from cored and percussion boreholes from the Laxemar subarea is 35–230 (26–128 in the Simpevarp subarea; data from the Laxemar 2.3 groundwater data set defined by the extended data freeze per November 30, 2007, extracted from Sicada) (Table 5-1). Calcite of Generation 3 shows Ca/Sr-ratios of 609–1,482, whereas the calcite of Generation 5a and Generation 5b/6 show higher ratios: 4,861–10,756 and 3,307–10,282, respectively. A compilation of the Ca/Sr-ratios and $^{87}Sr/^{86}Sr$-ratios in different calcite generations, waters and rocks is presented in Table 5-1.

Calcite of Generation 3 generally has lower rare earth elements (REE) concentrations and different chondrite-normalised REE patterns than younger calcite. They differ also from REE pattern of the wall rock (Figure 5-10). Two different REE patterns have been recognised in Generation 3 calcite (Figure 5-10a): 1) heavy rare earth elements (HREE) enrichment (calcite in paragenesis with epidote) and 2) low but varying REE contents (calcite in paragenesis with prehnite or laumontite). Both of these

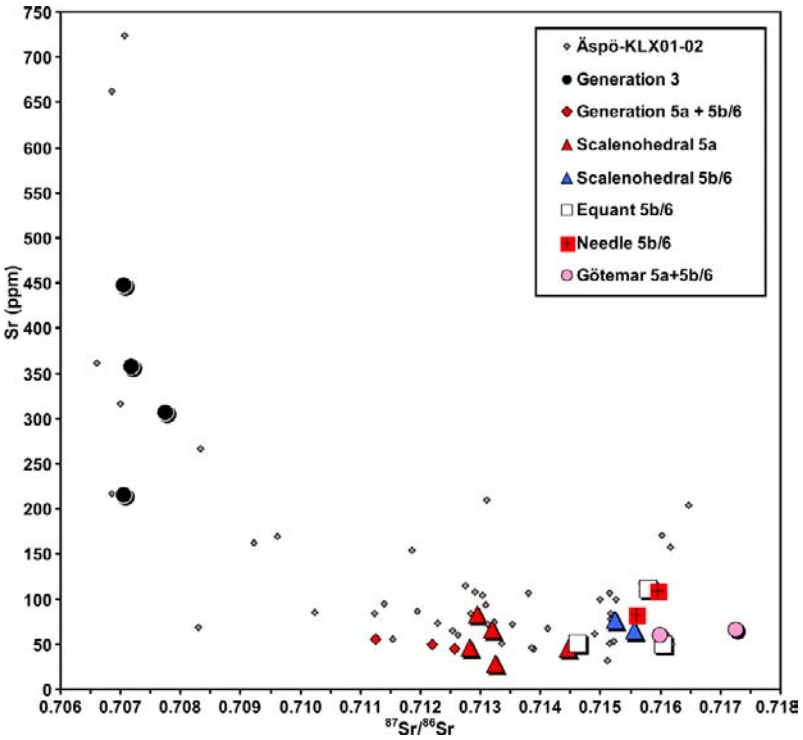

Figure 5-7. *Sr (ppm) versus $^{87}Sr/^{86}Sr$ in calcite, with morphologies indicated where observed. Götemar granite samples are plotted separately. Samples from Äspö and KLX01–02 /Wallin and Peterman 1999, Bath et al. 2000, Milodowski et al. 2005/ are shown as background but are not separated into different generations.*

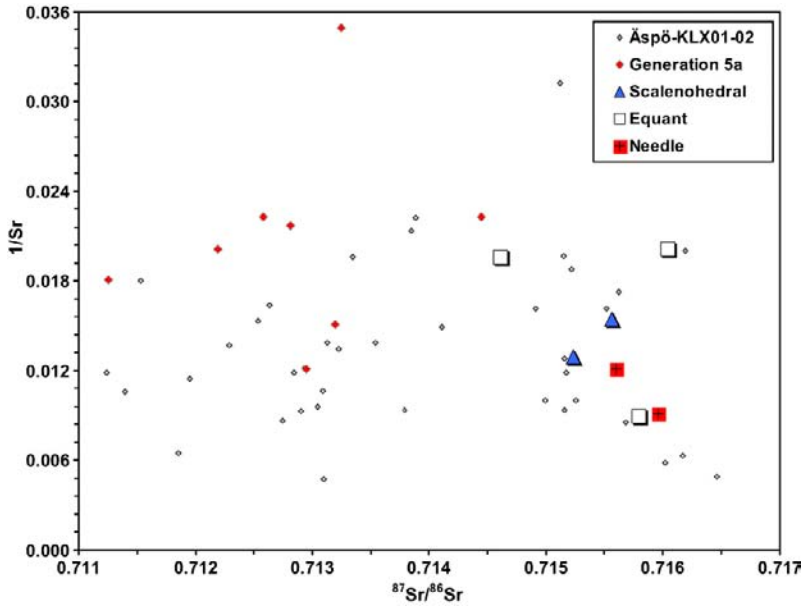

Figure 5-8. *1/Sr (ppm) versus $^{87}Sr/^{86}Sr$ in fracture filling calcite of Generation 5a and 5b/6, with morphologies indicated where observed (for Generation 5b/6). Samples from Äspö and KLX01–02 /Wallin and Peterman 1999, Bath et al. 2000, Milodowski et al. 2005/ are shown as background but are not separated into different generations.*

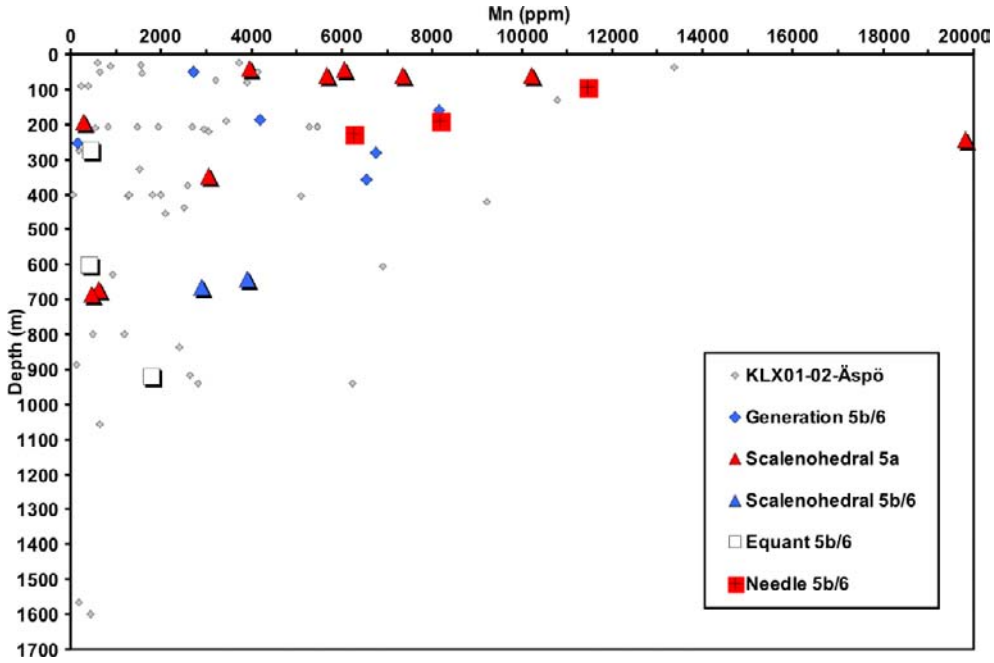

Figure 5-9. *Mn in calcite versus vertical depth, for Generation 5a and 5b/6, with morphologies indicated where observed. Samples from Äspö and KLX01–02 /Tullborg et al. 1999, Bath et al. 2000, Milodowski et al. 2005/ are also shown but are not separated into different generations.*

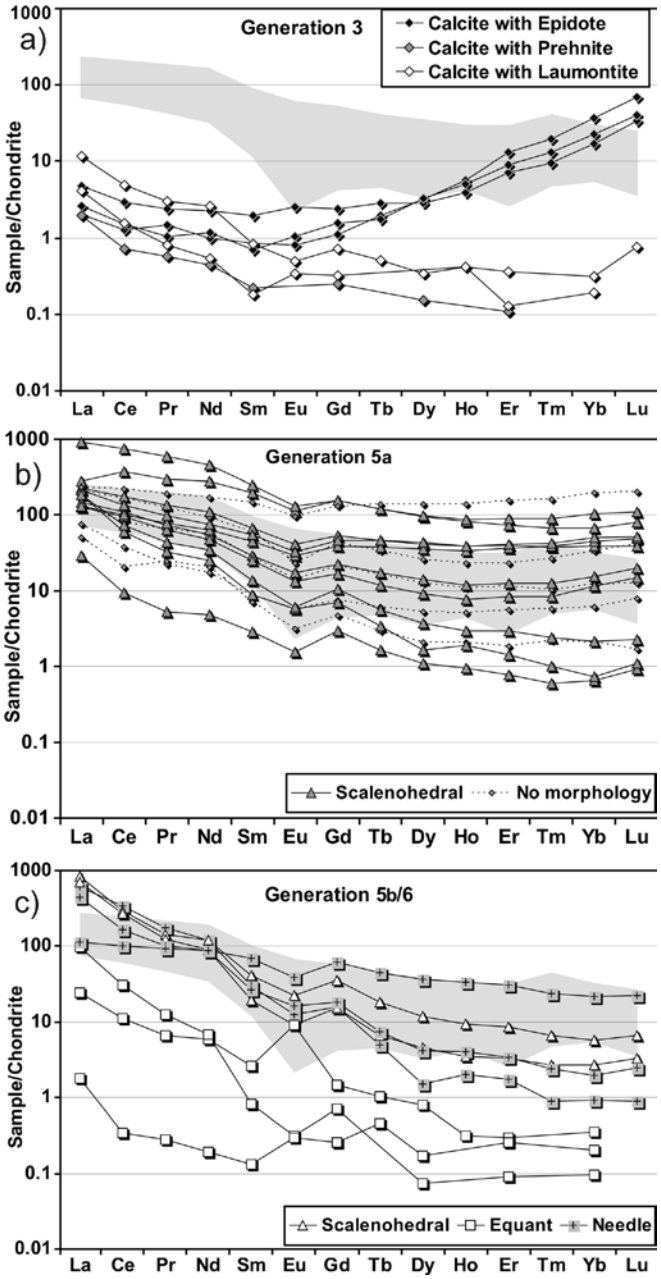

Figure 5-10. *Chondrite-normalised REE patterns for calcite of a) Generation 3 (with paragenetic mineralogy indicated), b) Generation 5a and c) Generation 5b/6. Range of the REE patterns for the rocks in this area is also indicated /Alm et al. 2005, Drake et al. 2006/. Chondrite values are from /Evansen et al. 1978/.*

patterns have similar light rare earth elements (LREE) concentrations. Calcite of Generation 5a has highly variable REE contents although most of the samples show values within the range of the REE contents of the wall rock. Most of the samples show flat REE patterns, generally similar to those of the wall rock (Figure 5-10b). Two samples show significant LREE enrichment. Calcite of Generation 5b/6 has highly variable REE contents, and more significant LREE enrichment, compared with the wall rock and older calcite (Figure 5-10c), except for one sample of needle-shaped calcite with flat REE pattern. Equant calcite has lower REE contents than needle-shaped and scalenohedral calcite, but the number of analyses is small. Calcite of Generation 5a and 5b/6 shows small negative Eu anomalies, except one sample with a significant positive Eu anomaly.

5.5 Sulphur isotopes

Pyrite of Generation 3, including those in greisen, has $\delta^{34}S$ of –3 to +3‰ (Figure 5-11, Table 4-1) Gypsum of Generation 5a (+4 to +16‰) and barite of Generation 5b/6 (+13 to +21‰) show slightly more varied positive $\delta^{34}S$ values, while pyrite of Generation 5b/6 shows large variation in $\delta^{34}S$ values (–42 to +61‰). However, most pyrite analysed has similar $\delta^{34}S$ values as gypsum and barite. Exceptions are the very high $\delta^{34}S$ values in pyrite at 100–275 m (+27 to +61‰) of which the highest values are from the Götemar granite (Laxemar maximum is c. +54‰). Another exception is the very low $\delta^{34}S$ at 707 m (–42‰). The isotopic difference between barite and pyrite ($\Delta\delta^{34}S_{ba\text{-}py}$) from the same fracture surface is +15.7, +0.4 and –5.8‰. The difference within single pyrite samples of Generation 5b/6 is as large as 6.5‰. Generation 5a and 5b/6 sulphides and sulphates from the Laxemar area show similar trends in $\delta^{34}S$ values with depths as the $\delta^{34}S(SO_4)$ in the groundwater in the Laxemar subarea, i.e. high but variable values in the upper 300 m followed by decreasing values with depths.

5.6 Discussion

5.6.1 Generation 3

Based solely on $\delta^{13}C$ and $\delta^{18}O$ values (–6.5 to –2.1‰ and $\delta^{18}O$; –23.5 to c. –16‰, respectively), two distinctly different origins are possible for Generation 3 calcite: 1) precipitation from a glacial meltwater source at low temperatures (cf. sub-glacial carbonate in /Larson and Tullborg 1984, SKB 2006b/) or 2) precipitation under hydrothermal conditions. Based on mineral paragenesis (e.g. co-precipitation with epidote, prehnite and muscovite and greisen alteration) and the typical hydrothermal alteration features of the wall rock adjacent to Generation 3 fractures, a hydrothermal/magmatic origin is strongly supported and is further supported by the homogenisation temperatures of the fluid inclusions (c. 195–370°C). These observations are in accordance with earlier observations of

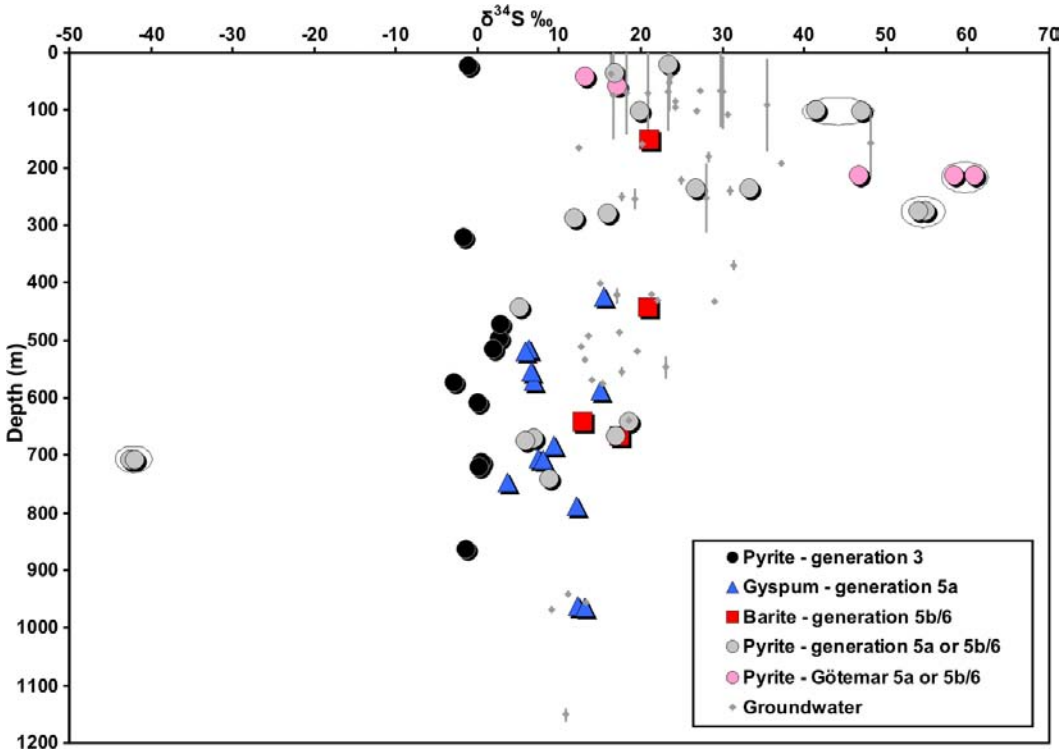

Figure 5-11. *$\delta^{34}S$ in fracture filling pyrite, gypsum and barite versus vertical depth. Samples are from the Laxemar and Simpevarp subareas and from the Götemar granite (plotted separately). Encircled values are two analyses of material from the same fracture surface. $\delta^{34}S$ in groundwater samples are also shown and y-axis bars define the borehole length of each section sampled (data from the Laxemar 2.3 groundwater data set, defined by the extended data freeze per November 30, 2007, extracted from Sicada). Analytical errors are within the size of the symbols.*

hydrothermal calcite from Äspö and from earlier studies in the Laxemar area (boreholes KLX01 and KLX02) /Tullborg et al. 1999, Wallin and Peterman 1999, Tullborg 2003, Milodowski et al. 2005/, at other sites in Sweden /e.g. Larson and Tullborg 1983, 1984, Eliasson et al. 1989, Fritz et al. 1989, Sandström and Tullborg 2007/ and in Finland and Canada /Frape et al. 1992, Blyth et al. 2000/. Furthermore, pyrite of Generation 3 also shows typical hydrothermal/magmatic $\delta^{34}S$ signatures in the narrow range of –3 to +3 ‰ (Figure 5-11) /cf. Ohmoto and Rye 1979, Field and Fifarek 1985/, which differ significantly from the highly varying $\delta^{34}S$ signatures of younger pyrite. The large range in $\delta^{18}O$ is interpreted to be, at least partly, due to varying degrees of water-rock interaction, which have increased the $\delta^{18}O$ of the fluid /e.g. Truesdell and Hulston 1980/. Other possible explanations include successively lower formation temperatures and boiling. The low amount of hydrothermal calcite in the upper 50 metres is most likely due to later dissolution and re-crystallisation. Such dissolution may have influenced the composition of the groundwater and of younger (re-crystallised) calcite.

The wide range in T_h indicates that Generation 3 minerals have formed during a long time period of decreasing temperatures. The two main explanations for the large variation in fluid inclusion salinities are: a) variable degree of water-rock interaction of the fluids as suggested by $\delta^{18}O$ in calcite, or b) different origins of the fluids, such as magmatic/hydrothermal (e.g. Götemar granite intrusion related), input of marine water, or brine developed through prolonged water-rock interaction.

Calcite $^{87}Sr/^{86}Sr$-ratios are lower than those in the present groundwater, in the wall rock or in younger calcite (Figure 5-6, Table 5-1). This further indicates that these fillings are formed early in the history of the rock, when $^{87}Sr/^{86}Sr$-ratios were closer to the initial ratios of the rock. The high concentration of Sr in Generation 3 calcite is probably associated with extensive hydrothermal alteration of the wall rock (especially alteration of primary plagioclase) adjacent to Generation 3 fractures /cf. Tullborg 1995, Drake et al. 2008, and Section 6.1/, and/or high precipitation rates /Pingitore and Eastman 1986/. Similar Sr contents have been reported for hydrothermal calcite at Äspö and in the Laxemar area (Figure 5-6) /Landström and Tullborg 1995, Wallin and Peterman 1999, Tullborg 2003/. None of the subsequent lower temperature fracturing events resulted in extensive wall rock alteration and Sr release from the wall rock. The large difference in REE contents and/or patterns between calcite of Generation 3 and younger calcite indicates formation from fluids of different compositions. Two different REE patterns are distinguished for Generation 3 calcite (Figure 5-10a) and these patterns represent samples of different parageneses. However, all of these samples have similar wall rock chemistry and isotope composition (C, O, Sr). The different REE-trends may be due to differences in complexation, e.g. with ligands such as CO_3^{2-}, OH^- and F^- which form stronger complexes with HREEs than with LREEs /Bau and Möller 1992/. Other explanations include different degrees of precipitation of the fluid, i.e. the amount of remaining ligands in the fluid capable of transporting the HREEs /Möller and Morteani 1983/.

5.6.2 Generation 4

Generation 4 minerals are more difficult to characterise and distinguish mineralogically than Generation 3. The few samples analysed generally show somewhat higher $\delta^{18}O$ than Generation 3 but similar $\delta^{13}C$ (Figure 5-1). This indicates a hydrothermal origin for Generation 4 in common with Generation 3 but with slightly lower formation temperatures, which is also supported by fluid inclusion results (Figure 5-5). The two salinity populations of fluid inclusions in calcite of Generation 4 (based on a single sample) with similar T_h suggest mixing of two different fluids, such as brine and a more dilute fluid. The calculated high $\delta^{18}O_{H2O}$ of 4.8–7.1‰, suggests prolonged water-rock interaction.

5.6.3 Generation 5a

Calcite of Generation 5a has $\delta^{18}O$ and $\delta^{13}C$ values ranging from –16.5 to –11‰ and –16 to –9‰, respectively. Salinites of fluid inclusions ranges from c. 17–24 wt.% eq. $CaCl_2$ and T_h of c. 80–145°C. This corresponds to precipitation from “warm brine” fluids, which has also been determined from studies of calcite at Äspö and in the Laxemar area /Tullborg et al. 1999, Tullborg 2003, Milodowski et al. 2005/, as well as at Olkiluoto, Finland /Blyth et al. 2000/, and from studies of fluorite from the Götemar granite /Alm and Sundblad 2002/. Based on fluid inclusions and $\delta^{18}O$ values calcite of Generation 5a is interpreted to have formed during the period of peak temperatures during the Palaeozoic. The low $\delta^{13}C$ (down to –25‰) is indicative of contribution of biogenic carbon /Wigley et al. 1978, Ohmoto and Goldhaber 1997, Tullborg et al. 1999/. The organic input probably originated

from descending waters from overlying, organic-rich sediments. One possible source may be alum shale, similarly proposed for asphaltite formation in Palaeozoic fractures in crystalline rock at Forsmark /Sandström et al. 2006b/. Organic influence is also indicated by LREE-enrichment in a few calcites (Figure 5-10b, see Section 5.6.4 for more detailed information on this process). However, most of the Generation 5a calcite has flat REE patterns, similar to and mostly in the range of the wall rock REE-patterns. This suggests e.g. bicarbonate complexation of the REE /cf. Landström and Tullborg 1995, Tullborg et al. 1999/, which are dominantly wall rock derived, and that there has not been any significant REE fractionation compared with the wall rock. However, the REE concentrations in the calcites vary more than in the wall rock due to varying degree of water-rock interaction. Microbial influence is also indicated by occasionally high Mn contents in calcite (Figure 5-9, cf. Section 5.6.4). The small negative Eu anomalies in calcite are probably inherited from the wall rock signature /Drake et al. 2006/.

Fluid inclusion salinities of Generation 5a calcite are much higher than the salinity of the present groundwater at the site, which at most is 8 wt.% total dissolved $CaCl_2$-dominated salts at 1,400 m depth in KLX02 /SKB 2006b/. The wide range in fluid inclusion salinities, $^{87}Sr/^{86}Sr$ and $\delta^{18}O_{H2O}$ may be due to: 1) variable degree of water-rock interaction and/or 2) influence by descending marine water or water from overlying Cambrian-Silurian sediments of marine origin. The former possibility has probably been the most important for the $^{87}Sr/^{86}Sr$-ratios which are considerably higher in Generation 5a calcite and gypsum than for Phanaerozoic seawater ($^{87}Sr/^{86}Sr$: 0.707–0.7095 /Veizer et al. 1999/). This is also indicated by correlation between $^{87}Sr/^{86}Sr$-ratios in calcite and the $^{87}Sr/^{86}Sr$-ratios (as well as Rb concentrations) of the wall rock. The highly varying $^{87}Sr/^{86}Sr$-ratios are probably also due to a relatively long time span of precipitation. The positive covariation of $^{87}Sr/^{86}Sr$ with $\delta^{18}O$ in calcite indicates gradually lower formation temperatures of the different generations, in accordance with /Tullborg et al. 1999, Wallin and Peterman 1999, Bath et al. 2000, Tullborg 2003, Milodowski et al. 2005/.

Gypsum and possibly some of the barite is Palaeozoic and their $\delta^{34}S$ compositions overlap with $\delta^{34}S$ of Palaeozoic seawater sulphate /Strauss 1997/ which suggests precipitation from descending seawater or fluids from presently eroded Palaeozoic sediments. The $\delta^{34}S$ values of the sulphates decrease with depth and below 500 m they are generally lower than Palaeozoic seawater. Possible explanations for $\delta^{34}S$ values at depths below 500 m include formation from a mixture of marine waters and water of non-marine origin with a long residence time in the bedrock.

5.6.4 Generation 5b/6

Most of the Generation 5b/6 calcite has $\delta^{13}C$ in the range of –30 to –5‰ (Figure 5-1), typical for descending biogenic CO_2, produced by breakdown of organic material. The very low $\delta^{13}C$ values (<–30‰) in some calcites suggest microbial breakdown of organic matter *in situ*, which produces bicarbonate during non-equilibrium conditions, resulting in low $\delta^{13}C$ values /cf. Tullborg et al. 1999/. This probably excludes a deep methane source for these extreme $\delta^{13}C$ values. These calcites are found both in the upper part of the bedrock aquifer (27–200 m, Figure 5-3) in accordance with similar findings at Äspö /Tullborg 2003/, but also deeper; down to c. 670 m, but only in the Laxemar subarea. Explanations for the low $\delta^{13}C$ values at great depths in the Laxemar subarea include possible input of organic-rich water to greater depth in this recharge area compared with the discharge area /cf. SKB 2006b/. The low $\delta^{13}C$-calcites are of scalenohedral morphology, which, according to /Milodowski et al. 2002, 2005/, is indicative of formation from saline water. High $\delta^{13}C$ values (>–3‰) are only found in the upper 107 m, compatible with a marine origin, in accordance with /Tullborg et al. 1991, Wallin and Peterman 1999/, or biogenic modification of $\delta^{13}C$, e.g. microbial breakdown of organic matter. The absence of low $\delta^{13}C$ values (<–13.5‰) and high $\delta^{18}O$ (>–8‰) below 800 m in calcite of Generation 5b/6 (and 5a) indicates a decrease in organic material supply, a change to a less hydraulically dynamic system, and a depth limit of major marine and organic input. Calcite with very low $\delta^{13}C$ is absent in the upper 27 m probably due to open system conditions, which prevents extreme values to develop and may also be due to influence of high $\delta^{13}C$ values from dissolved older calcite. *In situ* microbial activity is presently evident in the bedrock groundwater /Pedersen et al. 1997, SKB 2006b, Hallbeck and Pedersen 2008/ and the depths of calcite with very low $\delta^{13}C$ values correspond with the depths of the highest HCO_3 contents in the groundwater, indicative of decreasing influence of organically-fuelled microbes with depth. In general, the information obtained for the youngest minerals of this generation agree with the understanding of the site /SKB 2006b/.

Generation 5b/6 calcite shows generally higher $\delta^{18}O$ values than those of Generation 5a suggesting lower formation temperatures. The large isotopic variation of calcites precipitated on the same fracture surface indicates that these fractures have been intermittently water conducting during different periods with varying conditions.

Unlike older calcite, many of the Generation 5b/6 calcites have $\delta^{18}O$ values in the range of calcite precipitated in equilibrium with present meteoric recharge water (c. –10 to –8‰) or brackish Baltic seawater (c. –6.5 to –4‰) at ambient temperatures of 7–15°C (Figure 5-2, Figure 5-6). Calculations are made using groundwater data from the Laxemar 2.3 groundwater data set, defined by the extended data freeze per November 30, 2007 (extracted from Sicada) and fractionation factors from /O'Neil et al. 1969/. The limits for the range in $\delta^{18}O$ of these waters are quite diffuse due to the high temperature sensitivity of the isotopic fractionation factor and may thus vary over several per mil due to temperature fluctuations in the post-glacial period. Variations in $\delta^{18}O$ values in the calcites analysed are influenced by the hydrological conditions at the time of formation, e.g. the repeated glaciations-deglaciations and transgressions-regressions during the Quaternary era. Furthermore, because the area is located at the Baltic Sea coast, large changes in both salinity and $\delta^{18}O$ in groundwater during the Quaternary have occurred. The recorded distribution of groundwaters with different chemistry and origins at the site has most probably occurred at several earlier periods during the Quaternary. Relation between calcite crystal morphology and salinity of the fluid from which the calcite precipitated is indicated by the highly saline fluid inclusions in scalenohedral calcite of Generation 5a. The variation in $\delta^{18}O$ values in calcite of all morphologies as well as the fact that all morphologies (except needle) are found both near surface and at great depths (Figure 5-3 and Figure 5-4), might be a result of the typically large changes in salinity and $\delta^{18}O$ related to glaciation-deglaciation /SKB 2006b/. Many of the Generation 5b/6 calcites have $\delta^{18}O$ values in the range of calcite precipitated in equilibrium with meteoric water at ambient temperatures (Figure 5-2and Figure 5-4), an origin which is also supported by these being dominantly nailhead-shaped, in agreement with earlier studies at Äspö and in the Laxemar area /e.g. Tullborg 2003/. Calcite that trend towards precipitation in equilibrium with Baltic seawater at ambient temperatures is mostly present in the upper 100 m but also at greater depths (down to ~500 m) in deformation zones (Figure 5-2 and Figure 5-4). Note that the span for the temperatures in Figure 5-4 is quite narrow and is based on the present temperatures in the boreholes. If the span of c. –6.5 to –4‰ $\delta^{18}O$ and the interval 7–15°C is used for all depths this field includes mainly samples from the upper 100 m. This calcite is dominantly scalenohedral and occasionally equant, supporting precipitation from saline or brackish water. An exception concerning morphology is the needle-shaped crystals which are interpreted to be precipitated from meteoric water under strong organic influence and the c-axis elongation of the needle-shaped crystals do therefore not reflect the salinity of the fluid, in contrast to scalenohedral crystals. In contrast, needle-shaped calcite has been observed in fresh water environments associated with biomineralisation and this crystal morphology has been controlled by biological processes (A.E. Milodowski, personal communication, 2007) and a fresh water $\delta^{18}O$-signature is also evident for most samples showing needle-shaped crystals.

Brackish seawater intrusion has probably occurred repeatedly during the Quaternary. This is in agreement with hydrochemical observations of Littorina seawater in pockets down to at least 500 m depth at Äspö and Simpevarp, suggesting that saline Baltic seawater descended due to density turnover until it reached water of similar salinity, which in turn might have been a mixture of very saline, glacial and older meteoric water /SKB 2006b/. However, below 500 m, the dominance of scalenohedral and equant crystals with $\delta^{18}O$ values lower than typical Baltic seawater signatures indicate that these calcites are precipitated from water of older deep saline origin. No potential precipitates from pure glacial meltwaters have been identified. However, potential precipitates from; a) meteoric water during a slightly colder climate than the present, or b) a temperate meteoric water with a glacial component, have been identified and these are dominantly of fresh water, nailhead-shaped type (Figure 5-2 and Figure 5-4). Low temperature precipitates of pure marine origin (oceanic $\delta^{18}O$: –3 to +3‰), such as those observed at nearby Äspö (Figure 5-1 and Figure 5-4) have not been found in the Laxemar area.

$^{87}Sr/^{86}Sr$-ratios in calcite of Generation 5b/6 vary with the wall rock compositions. The Generation 5b/6 calcites might have precipitated in equilibrium with the present-day groundwater because of the similar range in $^{87}Sr/^{86}Sr$-ratios, in contrast to most of the older calcite and all older gypsum. The $^{87}Sr/^{86}Sr$-ratios of calcite of Generation 5b/6 are considerably higher than those of the present Baltic seawater (Figure 5-6, Table 1-1), which is in agreement with a rapid change of the $^{87}Sr/^{86}Sr$-ratio in intruding marine waters caused by water-rock interaction and especially ion exchange along the flow paths, as suggested by /Peterman and Wallin 1999/. The large variation in $^{87}Sr/^{86}Sr$-ratios is probably also an

effect of prolonged precipitation for this generation. Because the range in $^{87}Sr/^{86}Sr$-ratios for calcite of different morphologies overlaps, no relative chronological distinction of these different types can be identified. However, scalenohedral crystals generally have slightly lower $^{87}Sr/^{86}Sr$-ratios than the other types and might therefore be slightly older than those. Calcite with $^{87}Sr/^{86}Sr$-ratios higher than in the present groundwater is not observed. Simple mixing trends of two end members, usually displayed by a distinct trend between 1/Sr and $^{87}Sr/^{86}Sr$ /Wallin and Peterman 1999, Tullborg 2003/, are not obvious in the calcites, which may indicate Sr contribution from various sources, possibly including dissolved older calcite.

Radioactive Sr is one of the possible nuclides that may be mobilised in case of canister failure. Immobilisation of Sr by co-precipitation in carbonates can possibly increase Sr retention. However, calcite precipitated at low precipitation rates (such as under the present conditions in the Laxemar area) only incorporates small amounts of Sr /Morse and Bender 1990/. Significant deposition of Sr by incorporation during ongoing precipitation of calcite is therefore less probable.

The large variation in Mn content in calcite of Generation 5b/6, and also in Generation 5a, and the decrease in Mn contents with depth (Figure 5-9), is in agreement with earlier studies at Äspö and in the Laxemar area /Tullborg 2003/. This variation in Mn content is probably due to the varying redox conditions, as Mn^{2+} can be incorporated in calcite under reducing conditions. Possible explanations for the high Mn content at shallow to intermediate depth are sub-surface microbial Mn reduction of organic material, by which Mn^{2+} remains in solution and can be incorporated in calcite /Tullborg 2003/. Mn^{2+} is effectively bound in complexes with organic colloids in groundwater /Pourret et al. 2007/ and may thus be enriched in descending organic-rich waters. Cathodoluminescence studies of young calcite in this area have shown complex growth zonation with rims or sections with different Mn contents /Milodowski et al. 2005/. The REE patterns of Generation 5a and 5b/6 are overlapping and this indicates precipitation during similar conditions for some of these calcites, as suggested by the $\delta^{18}O$ values. Most of the Generation 5b/6 calcite show significant LREE enrichment (and HREE depletion) compared with the wall rock. This may indicate REE associated with organic material and possibly microbial breakdown of organic material /Pedersen et al. 1997/, resulting in LREE-enrichment in the fluids, as suggested by /e.g. Landström and Tullborg 1995/. Because this organic material, at least in recent times, is derived from the soil zone, which contains high LREE enrichment in the near-surface groundwater in the Laxemar area /Rönnback et al. 2008/, high La/Yb-ratios are commonly concentrated near the surface and decrease with depth, which is also mirrored in the calcite in the upper 200 m at Äspö /Bath et al. 2000/. However, very high La/Yb-ratios in calcite are found deeper in the Laxemar subarea, in accordance with earlier studies /Tullborg 2003/. These observations are in agreement with findings of calcite with very low $\delta^{13}C$ values at greater depths in the recharge area compared with the discharge area.

The $\delta^{34}S$ values in the sulphates decrease with depth. The few analysed barite samples of Generation 5b/6 have $\delta^{34}S$ values which overlap with those of the present groundwater /SKB 2006b/. The two barite samples from the upper 500 m show marine $\delta^{34}S$ signatures, whereas the $\delta^{34}S$ values of the two barite samples from depths greater than 500 m, show lower values, which indicates input of other sulphur sources, e.g. from dissolved Palaeozoic gypsum. Pyrite of Generation 5b/6 has $\delta^{34}S$ values generally within the range of gypsum and barite, except at 100–275 m and 707 m depth. Several processes may explain the $\delta^{34}S$ values measured in pyrite. These include 1) abiotic thermochemical sulphate reduction (TSR), at temperatures above 100°C, /Machel et al. 1995/) of parental sulphate with $\delta^{34}S$ similar to that of gypsum (and possibly barite) in the Palaeozoic, as TSR commonly involves negligible S-isotope fractionation /Orr 1974/ and 2) bacterial sulphate reduction (BSR) at temperatures below 110ºC /Jorgensen et al. 1992/. The very high $\delta^{34}S$ values in pyrite at 100–275 m depth is probably due to closed system BSR (Rayleigh distillation) causing disequilibrium /e.g. Ohmoto and Goldhaber 1997/, in accordance with observations from Äspö /Wallin 1992, Pedersen et al. 1997/, and is also indicated by the large variation in $\delta^{34}S$ values between different samples and the quite large spread in $\delta^{34}S$ values within single samples /McKibben and Eldridge 1994, Ohmoto and Goldhaber 1997/. These depths correspond to where anaerobic sulphate reduction is the dominant current microbial process and where the highest $\delta^{34}S$ values in dissolved sulphate (up to +48‰, Figure 5-11), indicative of closed system BSR in the groundwater are observed /SKB 2006b/. Therefore, these pyrites may have formed during conditions similar to the present. The high $\delta^{34}S$ values in the pyrite may be a late stage product in a BSR process /McKibben and Eldridge 1994, Ohmoto and Goldhaber 1997/. However, heavy $\delta^{34}S$ values in barite related to the heavy $\delta^{34}S$ values in pyrite are not observed, which indicates that pyrite and barite are not co-genetic, as also indicated by $\Delta\delta^{34}S_{ba\text{-}py}$ /cf. Hoefs 2004/. Because the present groundwater is not saturated with respect to barite, recent barite formation is not expected.

5.7 Concluding remarks

The isotope record, chemistry and fluid inclusion in the analysed fracture minerals show gradually changing palaeohydrogeological signatures with time, such as successively lower temperature, increased organic and microbial influence and more radiogenic Sr. Conclusions can be summarised as follows:

- Generation 3 calcite and pyrite show hydrothermal and inorganic $\delta^{13}C$, $\delta^{18}O$, and $\delta^{34}S$ signatures, T_h c. 195–370°C and low salinities. This generation is probably related to the intrusions of the nearby granites at Götemar and Uthammar and possible to some older events as well. The large variation in salinity, trace element chemistry, and T_h suggest varying formation conditions. This generation is related to more intense wall rock alteration than younger generations.
- Generation 4 fillings are difficult to distinguish based on paragenesis only, but the isotopic and fluid inclusion results suggest a hydrothermal origin, with inorganic signatures similar to those of Generation 3. However, formation temperatures were slightly lower during this less significant event. This generation is suggested to have been formed during the Sveconorwegian, and the circulations of fluid are probably related to the intrusion of dolerite dykes during this period.
- Palaeozoic Generation 5a calcite show organic $\delta^{13}C$ signatures, T_h of 80–145°C, high salinities and lower $^{87}Sr/^{86}Sr$ (also in gypsum), and lower $\delta^{18}O$ than the present groundwater. High Mn content and partial LREE-enrichment also suggests organic and possibly microbial influence. Formation from descending organic-rich fluids influenced by Palaeozoic sediments or Palaeozoic seawater may be a possible scenario.
- Late Palaeozoic to recent, possibly Quaternary, Generation 5b/6 calcite and pyrite show organic and microbial influence at temperatures below 110°C, occasionally with closed system signatures. $\delta^{18}O$ and $^{87}Sr/^{86}Sr$ values show that some of these calcites may have formed from fluids in equilibrium with waters similar to present groundwaters at ambient temperatures. Formation from waters with different $\delta^{18}O$ values and salinities, such as fresh and brackish water, is indicated, as is also suggested by the different crystal morphologies of calcite. Low temperature oceanic or pure glacial precipitates have not been identified within the site investigation area. The frequency of low $\delta^{13}C$ and biogenically (and microbial) modified $\delta^{34}S$ decreases with depth and the microbially influenced $\delta^{13}C$ is found deeper in the recharge area (Laxemar subarea) than in the discharge area (exemplified by results from the Simpevarp subarea). In general, the information obtained for the youngest minerals of this generation agree with the understanding of the site /SKB 2006b/.
- Most of the fracture fillings in the area are very old (Proterozoic to Palaeozoic) and only small amount of fracture minerals may possibly be Quaternary. The signatures of most of the generations suggest precipitation during a long time span with varying conditions. Late Palaeozoic calcite is difficult to separate from recent calcites and these are usually found in the same fracture systems, indicating that these have been intermittently water conducting from the Palaeozoic and onwards. However, the exact position of the flow channels may have varied over time along the fracture planes.
- It is evident that the Sr isotope ratios in the groundwaters are determined by *in situ* water-rock interaction processes and original isotope ratios, especially in marine waters that have intruded in the past, have not survived.
- Although major hydrological/hydrochemical fluctuations during recent low-temperature conditions are indicated, the amounts of minerals precipiatated or dissolved during these conditions have been relatively small, at least at depths greater than about 100 m.

6 Redox

An important task in the safety assessment of a potential repository for the disposal of nuclear waste in crystalline bedrock is to demonstrate that reducing conditions can be maintained for a long period of time /Gascoyne 1999, Puigdomenech et al. 2001/. This is because 1) oxygen may harm the copper-steel canisters in which the used fuel is contained and 2) in case of canister leakage, oxidising conditions may increase the mobility of several radionuclides in the repository, especially U. Oxidising conditions in surface waters and near-surface groundwaters generally change to reducing conditions in deeper groundwaters. A scenario which may introduce oxidising water to great depth in the bedrock is glacial melt-water intrusion triggered by high hydraulic heads underneath a continental ice sheet /cf. Boulton et al. 2001/. Such water can be assumed to contain more dissolved oxygen than the present recharge water, mainly due to dissolution of air bubbles trapped in ice into glacial melt water /cf. Glynn et al. 1999/ and elevated pressure beneath the melting ice /e.g. Guimerà et al. 1999/. Furthermore, the organic buffer may be severely reduced below the ice /Puigdomenech et al. 2001/. The extent and potential for dissolved oxygen to migrate to great depth in such a glacial scenario has been debated and different model approaches give very different results /cf. Glynn and Voss 1999, Glynn et al. 1999, Gascoyne 1999, Guimerà et al. 1999/. Oxygen will also be introduced into the repository during the construction phase. Dissolved oxygen originally present is consumed through inorganic (mainly Fe^{2+}) and organic reactions along the flow paths /Puigdomenech et al. 2001/. Fracture minerals and the wall rock participate in these reactions /e.g. Rivas-Perez et al. 2003/ and studies of these can reveal past and present redox conditions, and the reducing capacity remaining. For example, complete oxidation of pyrite and formation of goethite is an indicator of the position of the redox front within the fracture-flow system.

Two different studies with focus on Precambrian as well as recent redox features in the fractures and in the wall rock have been carried out during the site investigations:

1. Hydrothermally altered, red-stained (supposedly oxidised), wall rock have been compared with fresh rock nearby, and differences in mineralogy, mineral and whole rock chemistry and especially in reducing capacity, have been determined /Drake et al. 2008/. The results are summarised in Section 6.1.
2. Detection of the position of the recent near surface redox front has been investigated based on mineralogical, geochemical and U-series disequilibrium analyses of mineral coatings along open fractures /Drake and Tullborg 2008a/. The results are presented in Section 6.2.

6.1 Red-stained wall rock

Red-stained, hydrothermally altered rock is a common feature adjacent to fractures in the Laxemar area. Almost 50% of the sealed fractures in the Laxemar subarea are bordered by red-stained wall rock (Figure 7-1). Red-stained rock is commonly thought to represent a distinct zone of altered, oxidised rock but relevant analyses are seldom performed. Red-stained wall rock from boreholes KLX04, KSH01A and KSH03A+B, have been compared with fresh rock nearby in order to detect differences in mineralogy, mineral and whole rock chemistry and especially in reducing capacity, determined by Mössbauer spectroscopy /Drake et al. 2008/. It is of importance in the safety assessment to show that Fe^{2+} is available in the bedrock and along the fractures in order to provide enough reducing capacity, e.g. in a glacial scenario when oxygenated water may descend to great depths. One of the tasks is therefore to determine how much reducing capacity, i.e. Fe^{2+} that remains in the red-stained wall rock compared with fresh rock.

6.1.1 Mineralogy

The main mineralogical features of the red staining and hydrothermal alteration are pseudomorphic replacements of plagioclase by a paragenesis of albite, K-feldspar, sericite, Fe-oxide, prehnite and epidote (Figure 6-1), of biotite by chlorite (Figure 6-2), and of magnetite by hematite (Figure 6-3).

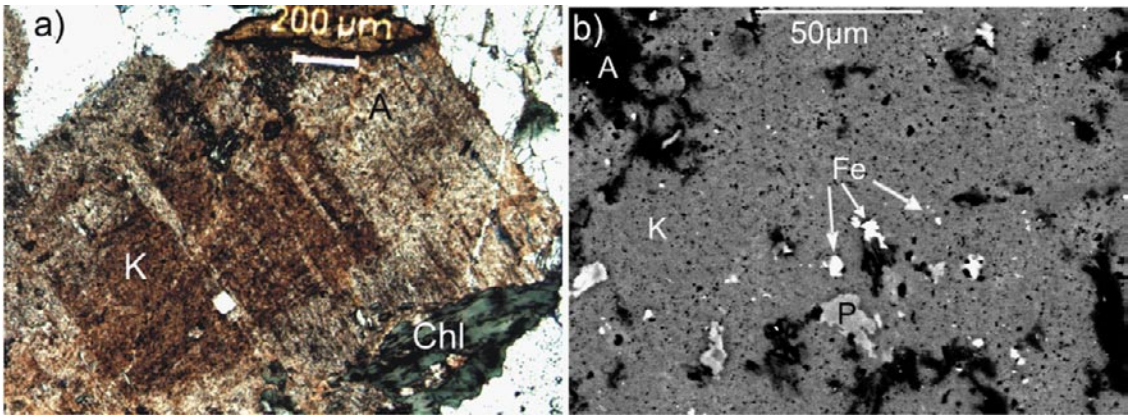

Figure 6-1. *Mineralogical features of red-stained feldspars. a) Photomicrograph of a red-stained pseudomorph after plagioclase occupied by albite (A) and more intensively coloured K-feldspar (K).Also shown is chlorite (Chl) that has replaced biotite. From drill core KLX04, borehole length 108 m. B) BSE-image of highly porous K-feldspar (K) with Fe-oxide inclusions (Fe) in a plagioclase pseudomorph (P = prehnite). Scale bar is 50 µm. From drill core KSH03B, borehole length 82 m.*

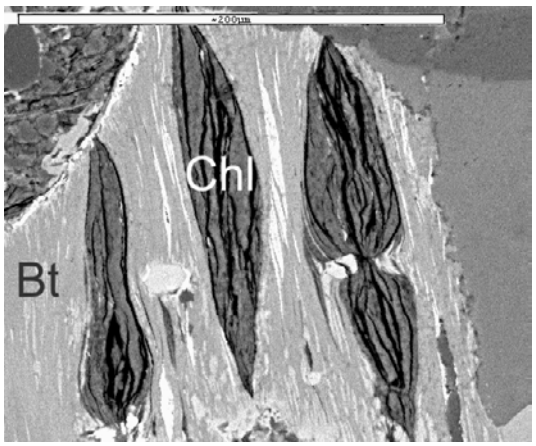

Figure 6-2. *BSE-image of biotite (Bt) partly replaced by chlorite (Chl). From drill core KSH03A borehole length 128 m.*

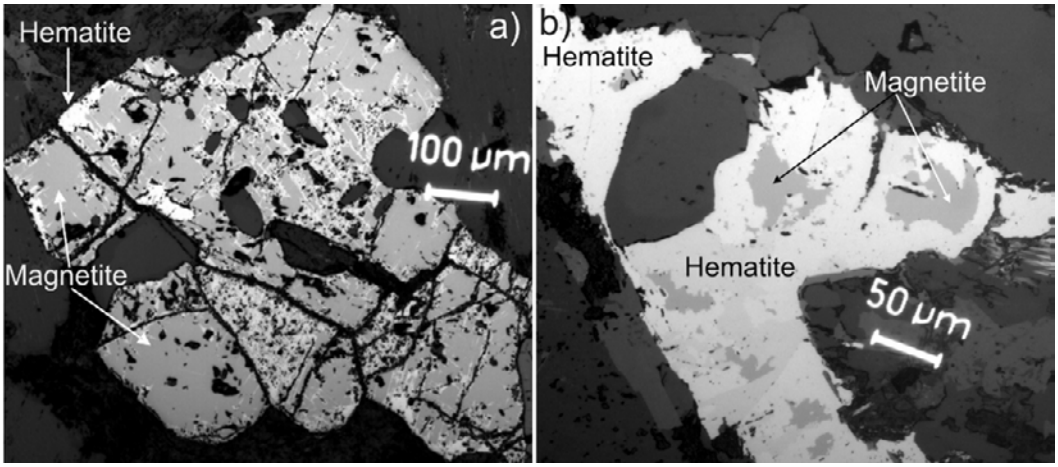

Figure 6-3. *Reflective light photomicrographs of a) magnetite with low amount of hematite in the reference rock, drill core KLX04, borehole length 153 m. and b) hematite replacing magnetite in the red-stained rock, drill core KSH03A, borehole length 372 m.*

Increased intragranular porosity and higher amounts of micro-fractures are also evident in the red-stained rock. The colour intensity of the red staining is most prominent where minute Fe-oxide inclusions are present in porous secondary minerals, particularly in K-feldspar in the pseudomorphs after plagioclase (Figure 6-1). However, Fe_{tot} contents in the altered plagioclase crystals/pseudomorphs are only slightly higher in the red-stained rock compared with the reference rock. The pseudomorphs after plagioclase in the red-stained samples are more porous than the plagioclase crystals in the reference samples. The hydrothermal alteration reaches further from the fracture than the red staining, shown by biotite and plagioclase alteration in the reference samples, in accordance with /Landström et al. 2001/.

6.1.2 Chemistry

The red staining has resulted in changes in concentrations of different elements related to the changes in mineralogy. The element mobility has been determined using the isocon mass balance calculation method of /Grant 1986/, for each sample pair. Analysed elements not discussed below are considered to have remained more or less constant during alteration, although re-distribution *in situ* is proposed for some of these.

Small scale mobility of Al is evidenced. The depletion of Al_2O_3 in the red-stained rock is mainly related to break-down of the anorthite-content in plagioclase, which is replaced mainly by albite and K-feldspar. Crystallisation of secondary prehnite, epidote and chlorite in the altered rock is insufficient to fix all excess Al, which is also included in formation of prehnite, chlorite and epidote in the fractures.

CaO and Sr are mainly depleted in the red-stained rock compared with the reference rock, mainly due to the alteration of plagioclase and partly due to the alteration of hornblende. The excess CaO and Sr is involved in the formation of secondary prehnite and smaller amounts of epidote in plagioclase pseudomorphs, voids and in micro-fractures in the red-stained rock. This growth of Ca- and Sr-rich secondary minerals like epidote which has shown preferential uptake of Sr is generally not enough to make up for the loss of CaO and Sr. Much of the CaO and Sr is involved in formation of prehnite, epidote and calcite in fractures.

Fe_{tot}, MgO, MnO, TiO_2, Cr, Sc, V and Y are mainly found in biotite, chlorite, hornblende, augite, magnetite, hematite, titanite and epidote. These elements (except Cr which is depleted in the red-stained rock due to replacement of magnetite by hematite) generally show very small changes (<5% change) between the red-stained rock and the reference rock. These elements are either fixed in minerals resistant to alteration (titanite) or in secondary minerals (e.g. chlorite). It is thus proposed that the main part of the Fe_{tot} involved in the red staining is redistributed within the rock and does not originate from the hydrothermal fluids.

The enrichment of K_2O, Ba and Rb in the red-stained rock is related to extensive growth of secondary K-feldspar (adularia) and sericite in pseudomorphs after plagioclase. Because biotite is often partially replaced by chlorite in the reference samples, the K_2O-content in these samples may already be depleted. The depletion of Cs is related to the chloritisation of biotite. Because Cs concentrations are higher in biotite than in K-feldspar /De Albuquerque 1975/, break down of biotite will result in excess Cs that is not entirely incorporated in secondary K-feldspar. Na_2O is commonly moderately enriched in the red-stained rock as a result of albitisation of plagioclase.

Higher Loss on Ignition (LOI) in the red-stained rock compared with the reference rock principally indicates a higher amount of "crystal-bound" water (including OH-groups) due to the presence of secondary mineral phases (e.g. chlorite, sericite and prehnite).

The U content is generally somewhat higher and the Th content is generally lower in the red-stained rock compared with the reference rock. The F-content is generally higher in the red-stained rock than in the reference rock.

6.1.3 Mössbauer spectroscopy

The difference in Fe^{3+}/Fe_{tot}-ratio of the red-stained rock compared with the reference rock is considerably smaller than macroscopic observations suggest (Figure 6-4), and the average Fe^{3+}/Fe_{tot}-ratio is only 0.023 higher in the red-stained samples than in the reference samples when comparing each sample pair. This enrichment is mainly related to the replacement of magnetite by hematite and the generally

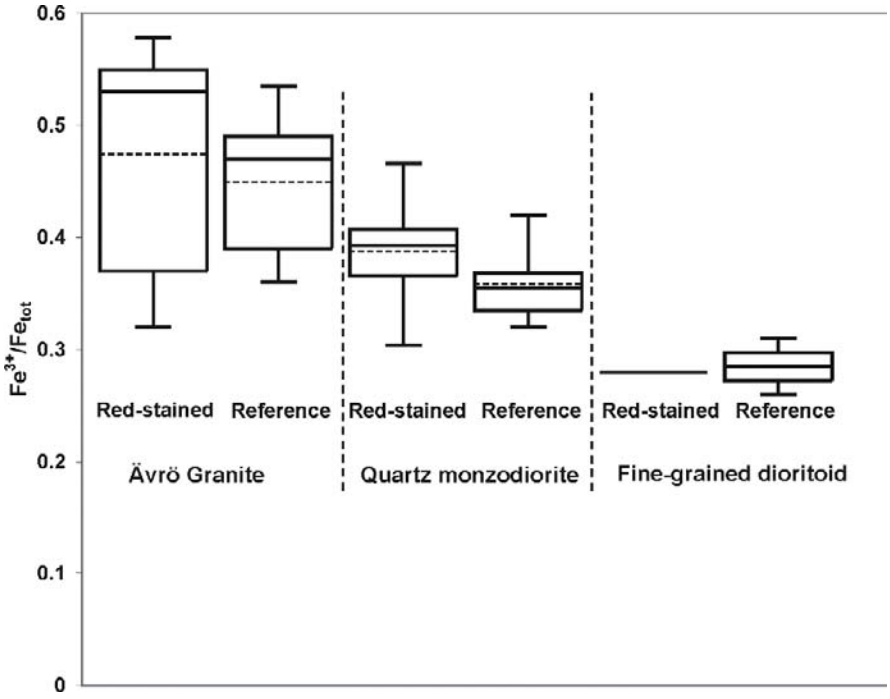

Figure 6-4. *Box-and-whisker plots of Fe^{3+}/Fe_{tot}-ratios for Ävrö granite, quartz monzodiorite and fine-grained dioritoid, for both reference and red-stained samples. The box represents the interquartile that represents 50% of the values. The whiskers are lines (upper and lower quartile) that extend from the box to the highest and lowest values. The lines across the box indicate the median and average (stippled).Figure adopted from /Drake et al. 2008/. Number of samples: Ävrö granite: red-stained 9, reference 9; quartz monzodiorite: red-stained 6, reference 6; fine-grained dioritoid: red-stained 1, reference 2.*

slightly higher epidote content in the red-stained rock. The replacement of magnetite by hematite is also shown by the lower magnetic susceptibility of the red-stained rock compared with the unaltered rock /Mattsson et al. 2004/. However, because most of the Fe in the rock is contained in the silicate phases which show fairly constant Fe^{3+}/Fe_{tot} contents, the total change in Fe^{3+}/Fe_{tot} between the red-stained rock and the unaltered rock is not as high as susceptibility measurements suggest.

The higher Fe^{3+}/Fe_{tot}-ratio in the red-stained samples is also partly related to the replacement of biotite by chlorite. The surprisingly small change in Fe^{3+}/Fe_{tot}-ratios partly depends on the high epidote content in a large number of reference rock samples, which may give even higher Fe^{3+}/Fe_{tot}-ratios in these samples than in the red-stained rock. The epidote influence is clearly shown by the highest Fe^{3+}/Fe_{tot}-ratio in the epidote-rich Ävrö granite. The high Fe^{3+}/Fe_{tot}-ratio in this rock type is also due to the lower contents of biotite, chlorite and hornblende compared with quartz monzodiorite and fine-grained dioritoid. The broader range in the Fe^{3+}/Fe_{tot}-ratios in the Ävrö granite samples is due to the large variation in composition of this rock type compared with the other rock types. In epidote-poor samples, the Fe^{3+}/Fe_{tot}-ratio is commonly slightly enriched due to replacement of biotite by chlorite, which has been shown to have somewhat higher Fe^{3+}/Fe_{tot}-ratios than biotite at the adjacent Äspö HRL /Tullborg 1995/, although the Fe^{3+}/Fe_{tot}-ratio is generally below 0.3 in chlorite.

Fine-grained dioritoid has lower Fe^{3+}/Fe_{tot}-ratios than quartz monzodiorite due to lower content of oxides and epidote. The higher total Fe^{3+}/Fe_{tot}-ratio in the reference rock than in the red-stained rock of fine-grained dioritoid is rather misleading due to sample inhomogeneity.

The Fe^{2+} content is generally very similar and the average value for all of the samples shows a very small depletion (0.03 wt.%) of the Fe^{2+} content in the red-stained rock. The average Fe^{2+}-content is considerably higher in quartz monzodiorite (3.8 wt.%) and fine-grained dioritoid (3.7 wt.%) than in Ävrö granite samples (1.7 wt.%) which has lower Fe-Mg silicate contents and higher epidote contents. The redox capacity of the major rock types in the area is compiled in Appendix 1.

6.1.4 Concluding remarks

The results, as summarised in Figure 6-5, show that the red-stained rock adjacent to the fractures displays major changes in mineralogy; biotite, plagioclase and magnetite have been altered and chlorite, K-feldspar, albite, sericite, prehnite, epidote and hematite have been formed. The changes in chemistry are however moderate; K-enrichment, Ca-depletion and constant Fe_{tot} are documented. The Fe^{3+}/Fe_{tot} ratio in the oxide phase is higher in the red- stained samples whereas the Fe^{3+}/Fe_{tot} ratio in the silicate phase is largely similar in the wall rock and the reference samples. Because most of the Fe is hosted in the silicate phase the decrease in reducing capacity (Fe^{2+}), if any, in the red-stained wall rock is very small and not as high as macroscopic observations suggest. Instead, the mineralogical changes in combination with the modest oxidation and formation of minute hematite grains in porous secondary minerals in pseudomorphs after plagioclase have produced the red staining. Increased porosity is also characteristic for the red-stained rock. Moderate alteration in the macroscopically fresh reference rock shows that the hydrothermal alteration reaches further from the fracture than the red-staining. The increase in porosity in the red-stained rock may result in enhanced retention of radionuclides due to an increased retention capacity close to the fracture.

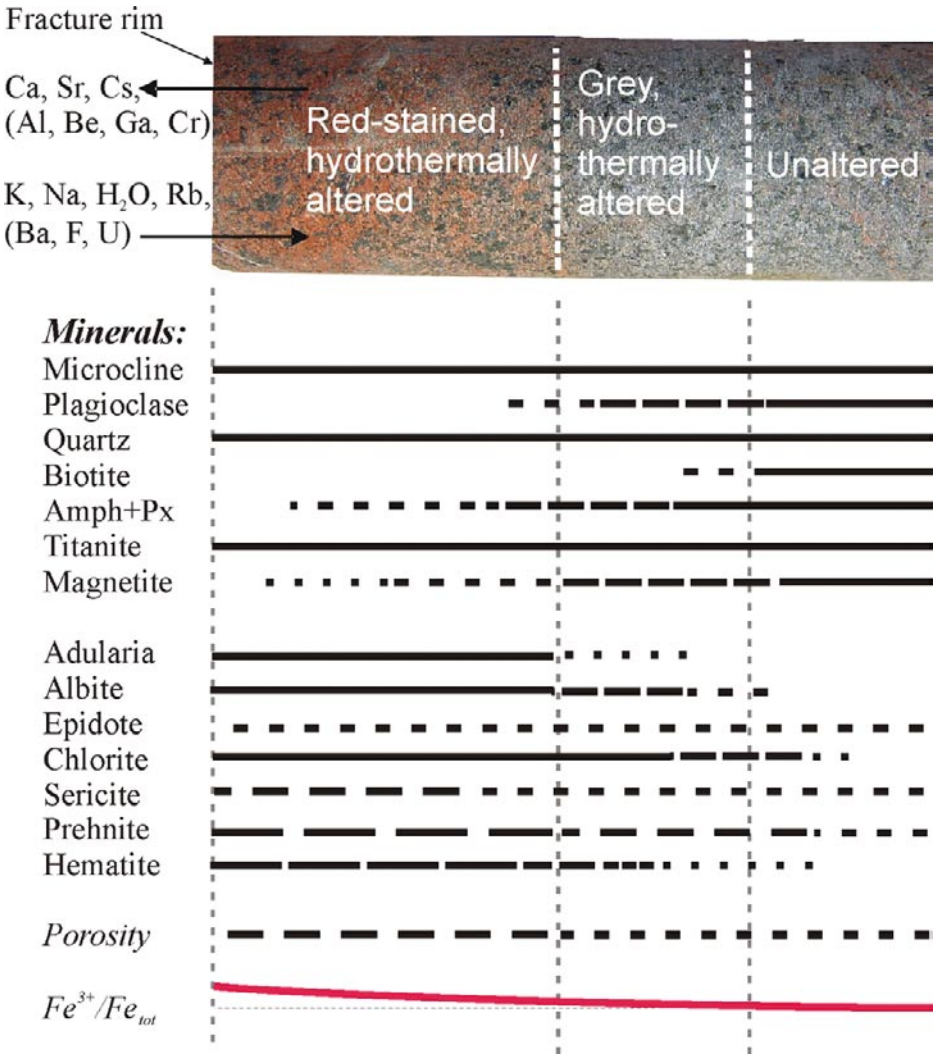

Figure 6-5. *Tentative sketch of the major features of the red stained wall rock compared with the reference rock nearby, which is either partly hydrothermally altered but not red-stained or unaltered rock, indicated by the stippled lines on the drill core photograph /Drake et al. 2008/. The fracture rim is at the left side of the sketch (common fracture minerals are prehnite, chlorite, epidote, calcite, quartz and fluorite). Arrows indicate which element that is enriched or depleted in the red-stained rock compared with the reference rock. The horizontal lines (partly stippled) show where the major minerals occur adjacent to the fracture, as well as the difference in porosity (including micro-fractures). The lowermost line illustrates the change in* Fe^{3+}/Fe_{tot} *relative to a reference line.*

6.2 Near surface redox front

Redox-sensitive minerals, elements and isotopes can be used to detect the redox front /Landström et al. 2001, Tullborg et al. 2008/, i.e. the depths to which the reducing capacity in the fractures is significantly decreased, exemplified by complete oxidation of pyrite and formation of goethite, i.e. oxidising conditions dominate totally in the analysed samples near the ground surface shown by all methods used. Below the redox front there is a transition zone where oxidising and reducing conditions have varied over time /cf. Perez del Villar et al. 2002, Yoshida et al. 2006, Arcos et al. 2008/, especially when fractures in low porosity crystalline rocks, and especially those with significant amounts of Fe^{2+}, are considered. Potential low-temperature oxidation effects are, in areas like Laxemar, usually limited to water-conducting fractures (or fracture zones) and their close vicinity. In these cases, the only way to recognise a redox front is by using microscopy to evaluate mineralogical effects due to oxidation, and to examine the behaviour of redox-sensitive elements, in fracture coatings and in the adjacent wall rock.

Information about the recent redox front position in the shallow bedrock and its stability over time is important for the understanding of the potential maximum penetration depth of descending oxidising waters.

The present study, presented in /Drake and Tullborg 2008a, Drake et al. 2009a/, has been carried out on samples of fracture coatings from 11 closely spaced, ~100 m deep, boreholes from two different drill sites (KLX09 and KLX11, Figure 2-1). The ground surface is located about 20–27 metres above sea level. The main focus has been to detect the redox front using mineralogical (distribution of redox-sensitive minerals), geochemical (redox-sensitive elements, e.g. Ce, Mn and Fe) and U-series isotope investigations of mineral coatings along open fractures (and to a lesser degree the migration of the redox front into the wall rock adjacent to near surface fractures). Detailed analyses of Fe(III)/Fe(II) and Fe isotopes on fracture coating Fe-oxides, are presently being carried out on samples from the same boreholes and will be reported in /Dideriksen et al. 2009/.

Redox-sensitive Fe-minerals such as pyrite, Fe-oxides and Fe-oxyhydroxides (e.g. goethite) can be used to detect the redox front /cf. Landström and Tullborg 1989, Landström et al. 2001/, as shown by detailed mapping of the distribution of these minerals in redox front studies at Äspö close to the Laxemar area, at other sites in southern Sweden /Eliasson et al. 1989, Tullborg 1997/, and in Spain /Perez del Villar et al. 2002/. In these studies, the redox front position was recognised at various depths (down to 100 m) depending on local topography (affecting recharge/discharge), as well as fracture frequency and orientations. Oxidation of pyrite, precipitation of goethite, and associated dissolution of calcite were observed near the surface. In areas with a thick soil cover, signs of recent oxidative alteration may not be seen in the bedrock because the groundwater may be reduced by the time it enters the bedrock (i.e. the redox front is in the soil).

In situ measurements of Eh (potentiometric) in boreholes can be technically very difficult and are usually completely unreliable in the near surface region. Moreover, sampling of groundwater close to the surface usually results in mixing of surface waters and shallow groundwaters and the interpretation of the redox-sensitive element concentrations in the groundwater may therefore be inadequate /SKB 2006b/. Instead, redox conditions can be evaluated with better depth control using redox-sensitive elements like Ce and U in minerals deposited along the fracture flow paths. Since oxidised Ce(IV) is less mobile than Ce(III), lake and stream waters usually show negative Ce-anomalies /cf. Vaniman and Chipera 1996, Dia et al. 2000, Rönnback et al. 2008/.

Although the position of the redox front can be inferred from the distribution of redox-sensitive minerals and elements, this information provides no time constraints to whether the redox front corresponds to the present conditions or not. However, measurements of radionuclides in the U-series decay chain (^{238}U-^{234}U-^{230}Th), can be used to derive time constraints for oxidising and reducing conditions in the bedrock fractures, as shown at the adjacent Äspö site /Tullborg et al. 2003/, and in other areas /e.g. Smellie et al. 1986, Gascoyne and Cramer 1987, MacKenzie et al. 1992, Griffault et al. 1993, Suksi and Rasilainen 2002, Min et al. 2005/. Disequilibria in the decay chain ^{238}U-^{234}U-^{230}Th indicate redistribution (removal or deposition) of uranium within the last 1 Ma and after such perturbation, the system will, if kept unperturbed, gradually return towards a state of secular equilibrium in which the activity ratios (AR) equal unity /Osmond and Ivanovich 1992, Scott et al. 1992, Gascoyne et al. 2002/. Oxidation of U(IV) to the more mobile U(VI) usually results in leaching of bulk U at shallow depths /e.g. Landström et al. 2001/ and since both ^{238}U and ^{234}U are leached by oxidative fluids and are much more mobile than Th, recent removal of U (oxidising conditions) results in $^{234}U/^{238}U$ AR ~1

and $^{230}Th/^{234}U$ AR >1 in the solid phase. Under reducing conditions at greater depths, ^{234}U, is more likely present in the oxidised state of U(VI), relative to ^{238}U, and is leached more easily than ^{238}U /e.g. Suksi and Rasilainen, 2002/. In addition, ^{234}U is generated by alpha decay and thus occupies a radiation-damaged site that is more susceptible to leaching than the site of ^{238}U /e.g. Gascoyne et al. 2002/. The degree of disequilibrium tends to decrease with depth due to more stagnant groundwater flow conditions /e.g. Suksi 2001, Tullborg et al. 2003/. The redox zone position varies due to short and long term variations in groundwater conditions, e.g. annual variations in groundwater chemistry and land uplift, respectively. Therefore, deposition and removal of U from fluids with different redox conditions may have occurred at a specific depth over very long time periods. The fractured bedrock constitutes a very heterogeneous system with large variations in amount of fracture coating material and fracture transmissivities. Furthermore, flow paths have probably varied over time and it is not expected that different elements and minerals should respond uniformly to changes in redox conditions (e.g. Ce-anomalies can not automatically be assumed to correspond to the U mobilisation or deposition). Furthermore, the results from the different methods may represent signatures from different time periods each represented by a specific penetration depth. Short periods with weakly oxidising conditions may not be detected when analysing fracture coatings, in contrast to signs of long time periods of stable conditions, either reducing or oxidising.

In this section, all samples are referred to by their vertical depth from the ground surface for clarity.

6.2.1 Results and discussion

6.2.1.1 Mineralogy

The fracture coatings consist of a mixture of minerals, usually including chlorite, clay minerals (e.g. illite, smectite or mixed layer-clay; corrensite or smectite/illite), calcite, quartz, K-feldspar, plagioclase, hematite, goethite and pyrite. Quartz, K-feldspar and plagioclase are mainly wall rock fragments included in the fracture coating. Accessory fracture minerals include REE-carbonate (probably bastnäsite), barite, zeolites (harmotome and laumontite), chalcopyrite, epidote and trace amounts of a U-silicate (possibly coffinite). Near the surface, Ce- and Mn-oxide are identified in a few samples. SEM investigations show that chlorite and clay minerals as well as calcite, hematite, goethite, pyrite and REE-carbonate are generally the outermost minerals of the fracture coating. Because most of the fracture filling hematite in the Laxemar area is interpreted to have been formed under different conditions than those at present, based on its paragenesis of relatively high-temperature minerals /Drake and Tullborg 2005/ and its Fe-isotope values and degree of crystallinity /Dideriksen et al. 2007, 2009/, interpretation of recent redox conditions based on Fe(III)-minerals is mainly based on goethite.

Mapping data and SEM-EDS investigations reveal that the distribution of calcite and the redox-sensitive minerals goethite and pyrite, varies with depth (Figure 6-7, Figure 6-8 and Figure 6-9). Goethite is preferentially found in the upper 10–25 m of the boreholes although depths vary between the boreholes and it may be absent in some boreholes (e.g. KLX09G). Occasionally goethite is found as deep as c. 80 m, where it is associated with highly transmissive fractures (transmissivity $T > 1 \cdot 10^{-6}$ m^2/s) and/or highly fractured intervals with more than 20 fractures/m. Goethite occurrences below 80 m are rare. On the contrary, pyrite is absent in the fractures shallower than 10 to 25 m. The distribution of pyrite and goethite in open fractures shows that the redox front is generally located at about 15–20 m depth below the ground surface. This is in accordance with preliminary results of detailed Fe-oxide studies (Mössbauer spectroscopy, SEM and XRD) in these boreholes, which indicate that Fe-oxides at 0–20 m depth are recent and of low temperature origin, while deeper Fe-oxides are either older low temperature precipitates or hydrothermal /Dideriksen et al. 2009/. Overlapping occurrences of pyrite and goethite slightly deeper than 15–20 m depth in some boreholes indicate a redox transition zone over which the redox front has varied spatially over time, but also indicate flow path heterogeneity in the fracture system. The uppermost occurrences of pyrite (10–20 m depth) are generally partly altered, which indicates an ongoing slow downward migration of the redox front and/or a zone where the conditions change with seasonal and annual variations (Figure 6-6e–h). Above the redox front the wall rock is affected by oxygenated water as shown by replacement of pyrite by goethite and alteration of biotite (Figure 6-6a–d). This alteration is most common within a distance of 1 mm from the fracture but may locally extend up to 2 cm into the wall rock. Furthermore, wall rock biotite is replaced by secondary minerals; e.g. chlorite and goethite, particularly at the fracture rim. Penetration of oxidising fluids into the wall rock adjacent to near-surface fractures is evidenced by red-coloured micro-fractures (filled with goethite, chlorite and/or clay minerals).

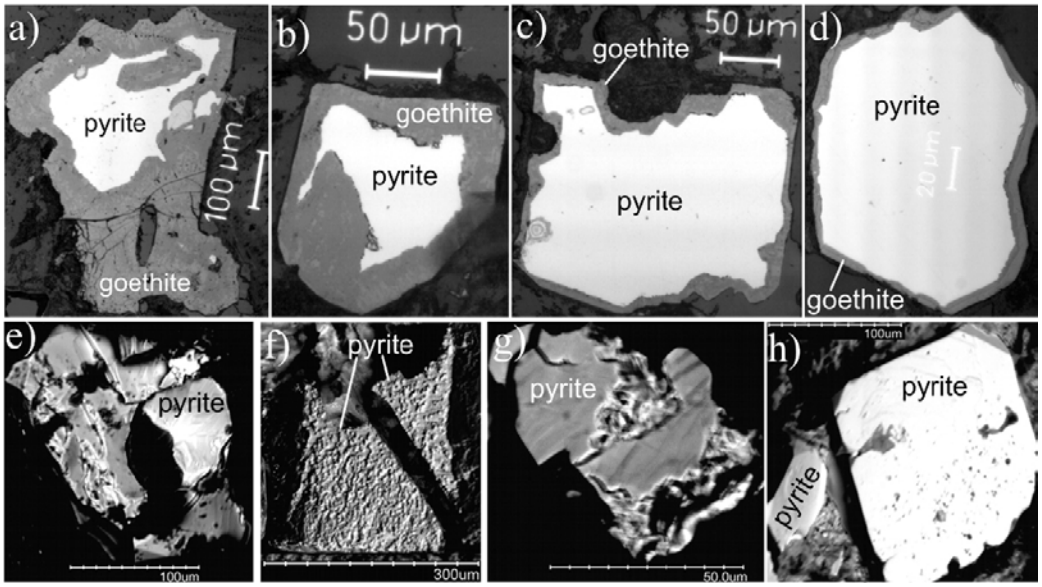

Figure 6-6. *Thin section photomicrographs in reflective light (a–d), and back-scattered SEM-images (e–l). (a–d) Wall rock pyrite increasingly replaced by goethite with decreased distance from the fracture (a) 0.4 mm from the fracture, (b) 4 mm, (c) 10 mm, and (d) 17 mm, sample KLX11F:2.0 m vertical depth). (e–g) Altered pyrite crystals on fracture surfaces; (e) KLX09B:10.5 m vertical depth, (f) KLX09D:17.3 m vertical depth, and (g) KLX11F:17.7 m vertical depth. (h) A rather fresh pyrite crystal (right) and a slightly more altered pyrite crystal (left) on a fracture surface at 19.9 m vertical depth (KLX09D).*

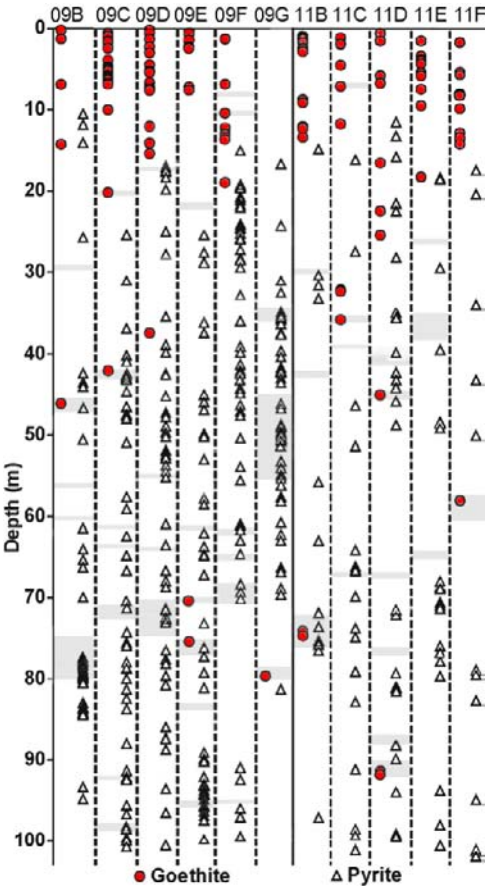

Figure 6-7. *Occurrence of goethite (circles) and pyrite (tringles) in open fractures in the KLX09B–G and KLX11B–F shown as vertical depth from the ground surface (each symbol equals one fracture). Shaded areas are intervals with highly transmissive fractures ($T>1\cdot10^{-6}$ m²/s and/or highly fractured sections (>20 fractures/m).*

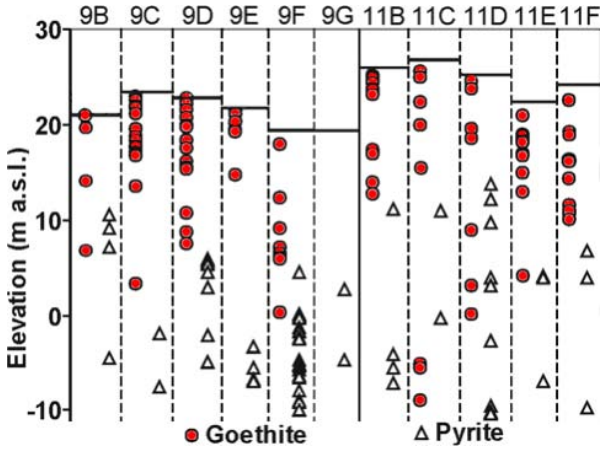

Figure 6-8. *The uppermost occurrences of goethite (circles) and pyrite (triangles) in KLX09B–G and KLX11B–F relative to elevation.*

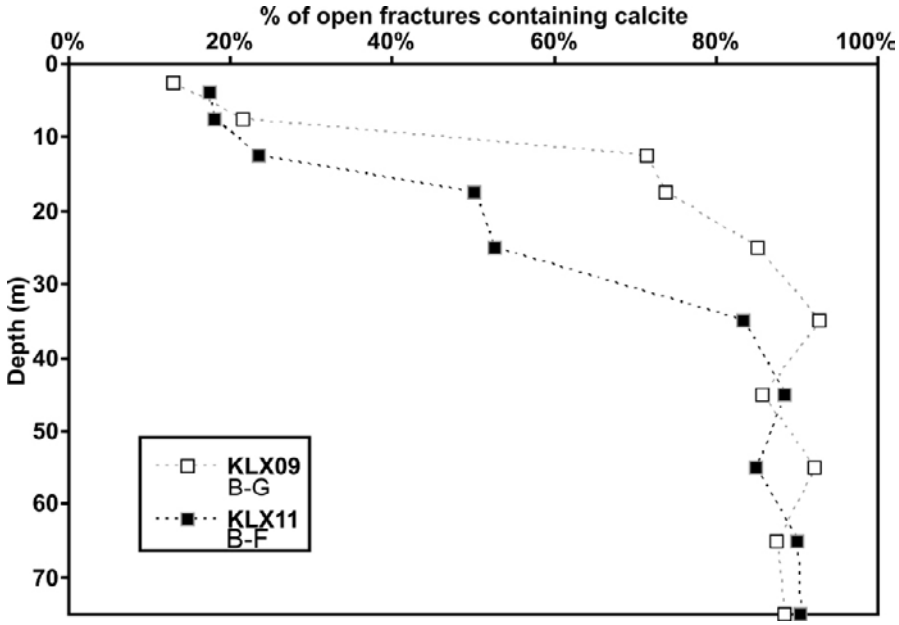

Figure 6-9. *Percent of open fractures containing calcite vs. depth. The depth intervals are 10 m (except in the upper 20 m: 5 m intervals). The trend of 80–95% calcite containing fractures continuous down to 100 m (not included in the graph). No mapping was carried out on the uppermost 2.8 m of the KLX11B–F boreholes and this interval is thus missing in the graph.*

Fracture frequency and orientation, soil cover and differences in reducing capacity of the fracture minerals and the wall rock may be partly responsible for variations in redox front elevation/depth. Redox fronts in the KLX09B–G boreholes are at slightly deeper relative to KLX11B–F boreholes and are considered being a consequence of that the greater fracture frequency in KLX09B–G wall rock has allowed a greater flux of oxidising water to penetrate to depth.

Calcite coats 80–95% of the fractures below c. 20–30 m depth but is much less abundant in fractures above this depth. Only 10–20% of open fractures contain calcite in the uppermost 10 m. Textural evidence of calcite dissolution has been observed in samples from the upper 25 metres. The smaller percentage of open fractures containing calcite in the upper 20 to 25 m is interpreted to the result of calcite dissolution as a result of infiltration of very dilute recharge waters which probably have relatively low pH and may at least partly be loaded with oxygen. Deeper in the bedrock, the pH values of fracture water are higher and solutions become saturated to oversaturated with respect to calcite /SKB 2006b/ allowing precipitation of recent calcite.

6.2.1.2 Chemistry

Most of the analysed fracture coatings have higher concentrations of e.g. Fe, K, Mg, Mn, Be, Cs and Rb than the wall rock, probably partly due to the extensive alteration of biotite in the wall rock /cf. Drake et al. 2008/ and that these elements are enriched in chlorite and clay minerals which dominate most of the fracture coatings. Excess Fe is also associated with hematite, goethite, pyrite and epidote. Mn is also associated with Mn-oxide near the surface. REE is mainly associated with REE-rich carbonate, calcite and wall rock derived titanite and zircon and rarely to Ce-oxide. Around 50% of the samples have higher U contents than the wall rock. U is related to U-rich silicate and wall rock derived apatite, zircon and titanite but may also be incorporated in amorphous phases in fracture coatings and in altered wall rock /cf. Drake et al. 2008/. Most element concentrations in bulk fracture coatings do not show obvious trends with depth (including the redox sensitive Fe). Exceptions are Ca and U which are depleted near surface (and U enriched at great depths), and Mn and the light rare earth elements (LREE), which show elevated concentrations in a number of fracture coating samples near the surface (<20 m), compared with the deeper samples (>20 m). U and Th concentrations are both usually 3 to 10 ppm and U concentrations of above 10 ppm are only found in samples below 11 m depth. The elevated U contents in some samples at depths greater than 11 m (>15 ppm, down to 71 m, cf. ^{238}U vs. depth in Figure 6-13) might be due to deposition of U, mobilised at or near the surface and transported into the fracture system as mobile U(VI) mostly stabilised as carbonate complexes. At greater depths and reducing conditions this U is deposited either due to reduction and/or due to changes in HCO_3^- concentration /cf. SKB 2006b/. Furthermore, Cs concentrations are elevated at depths greater than 50 m. The much higher Cs contents in most samples below 50 m relative to samples above 50 m is probably due to the presence of crush-zones containing increased amounts of chlorite and especially clay minerals with relatively high sorption affinities for Cs /Grütter et al. 1986, Landström and Tullborg 1995/. A small number of samples (mostly below 30 m) have much higher Ca concentrations than in the wall rock, while most fracture coating samples above 10 m have Ca contents that are lower than or similar to the wall rock, in accordance with the apparent calcite dissolution near the surface, although CaO is related to other phases as well (e.g. epidote, wall rock fragments of plagioclase, and the abundant mixed-layer clay corrensite with up to 3 wt.% CaO /Drake et al. 2006/), which makes the depletion in CaO less distinct than the calcite distribution with depth. Mn concentrations in the bulk fracture coatings are highly variable near the surface and there is a slight decrease with increasing depth and very high Mn contents are evident in two fracture coating samples containing Mn-oxide or -oxyhydroxide and Mn-rich clay minerals/chlorite above 10 m depth, indicating the presence of Mn(IV). Most of the fracture coating samples have much higher Cs concentrations than in the wall rock and the highest concentrations are found in samples below 50 m depth, mainly in clay mineral- (e.g. mixed-layer clay of illite/smectite-type) and chlorite-rich samples. LREE are within the range of the wall rock for most samples. However, a couple of near surface samples (<20 m depth) have higher LREE concentrations (La, Ce, Pr, Nd and Sm) than in the wall rock and these samples contain, possibly Palaeozoic, REE-carbonate coatings, rich in Ce, La, Nd and Y /cf. Drake and Tullborg 2005/, and Ce-oxide in one of the samples. Most samples from 0–20 m depth show positive Ce-anomalies (up to 1.52 Ce_{CN}/Ce_{CN}*, Figure 6-10). The positive Ce-anomalies in fracture minerals within the upper 20 m suggest that Ce(III) has been oxidised to Ce(IV) and scavenged by goethite and/or Mn-oxide as described by /Landström and Tullborg 1995, Vaniman and Chipera 1996, Bau 1999, Takahashi et al. 2000/. These positive Ce-anomalies compliment strong negative Ce-anomalies measured in near surface groundwater in the area /Rönnback et al. 2008/. Positive Ce-anomalies in the fracture coatings are created through near surface weathering which results in dissolution of Ce(III) and the other REE. Subsequent accumulation of Ce(IV) in the solid phase is either due to sorption of the REE onto fracture coating goethite, at which Ce(III) is partly oxidised to Ce(IV) leading to preferential desorption of Ce(III) and the other REE compared with Ce(IV) as suggested by /Bau 1999/, or due to oxidation of Ce(III) to Ce(IV) in the aqueous phase followed by preferred sorption of highly adsorptive Ce(IV) relative to other REE onto fracture coatings (e.g. goethite) /Takahashi et al. 2000/. The depth distribution of the positive Ce-anomalies in the bulk fracture coatings is similar to the distribution of goethite, and is thus in good agreement with the redox front position determined by redox sensitive minerals. As a consequence of the preferential precipitation of Ce(IV) above 20 m, fractures in the interval 20–70 m, where the conditions change to reducing, show slightly negative Ce-anomalies. At depths greater than 70 m this effect is no longer visible.

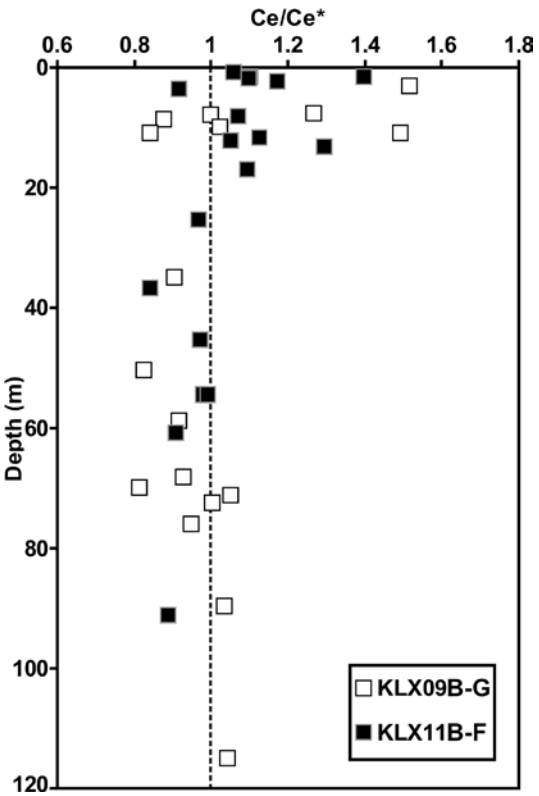

Figure 6-10. *Ce-anomalies (Ce/Ce*) vs. depth (Ce* = $(La)^{1/2}(Pr)^{1/2}$) for bulk fracture coating samples from KLX09B–G and KLX11B–F. Concentrations are chondrite normalised, using chondrite data from /Evansen et al. 1978/.*

6.2.1.3 U-series disequilibrium

U-series disequilibrium in most of the samples suggests extensive water-rock interaction at least within the last 100 ka. However, a low number of samples show AR near secular equilibrium which indicates insignificant water-rock interaction. Only two of the samples (KLX09D:75.9 m, KLX11F:1.9 m), show secular equilibrium, indicating negligible water-rock interaction within the last 1 Ma, in these specific fractures. Although there is scatter in the data set, mainly because of the heterogeneity of the fracture system (variation in transmissivity and amount of fracture coating material) some depth related trends of recent U mobilisation can be discerned. Based on $^{234}U/^{238}U$ and $^{230}Th/^{238}U$ AR (cf. the Thiel diagram /Thiel et al. 1983/ in Figure 6-11) most of the samples from the upper 20 m in the bedrock indicate a complex pattern of deposition and mobilisation during the last ~300 ka (probably as a result of changing conditions, including a shift in redox conditions and related variations in bicarbonate and organic content). Only two samples are consistent with simple removal of bulk U (KLX11E: 16.9 m and KLX11E: 3.7 m, i.e. plot in "Uranium removal sector" in Figure 6-11). Some of the samples originating from levels shallower than 20 m $^{230}Th/^{234}U$ ratios are close to unity and do not contain any goethite, which suggests that these fractures have not been open to oxidising water recently. A majority of the samples from depth greater than 35 m show deposition of U either as one single continuous process or as deposition during several occasions. However, the $^{234}U/^{238}U$ and $^{230}Th/^{238}U$ AR in two of the deeper samples (KLX11E: 36.7 m and KLX11D: 54.5 m vertical depth) indicate that both deposition and removal of U have occurred in these fractures. Higher degree of bulk dissolution of U, probably from oxidising groundwater circulation, in the upper 20 m is indicated by $^{234}U/^{238}U$ AR close to 1 and $^{230}Th/^{234}U > 1$ (Figure 6-11 and Figure 6-12). Fracture coatings from below 55 m tend to have $^{230}Th/^{234}U < 1$ and $^{234}U/^{238}U > 1$, which is consistent with the concept of long-term deposition rather than removal of U under reducing hydrologic conditions (Figure 6-12) /Landström et al. 1989, Tullborg et al. 2003/. Furthermore, bulk removal of U during oxidising conditions near the surface and redeposition of U at greater depths is also possibly indicated by the higher ^{238}U activities in samples from depths greater than 20 m, especially in highly transmissive fractures (Figure 6-13), and by that the samples with the very lowest ^{238}U activities also have the highest $^{230}Th/^{234}U$ AR (>1.5, Figure 6-14). Excess of ^{234}U in the deeper samples may be due to preferential leaching of ^{234}U relative to ^{238}U, due to that ^{234}U is more

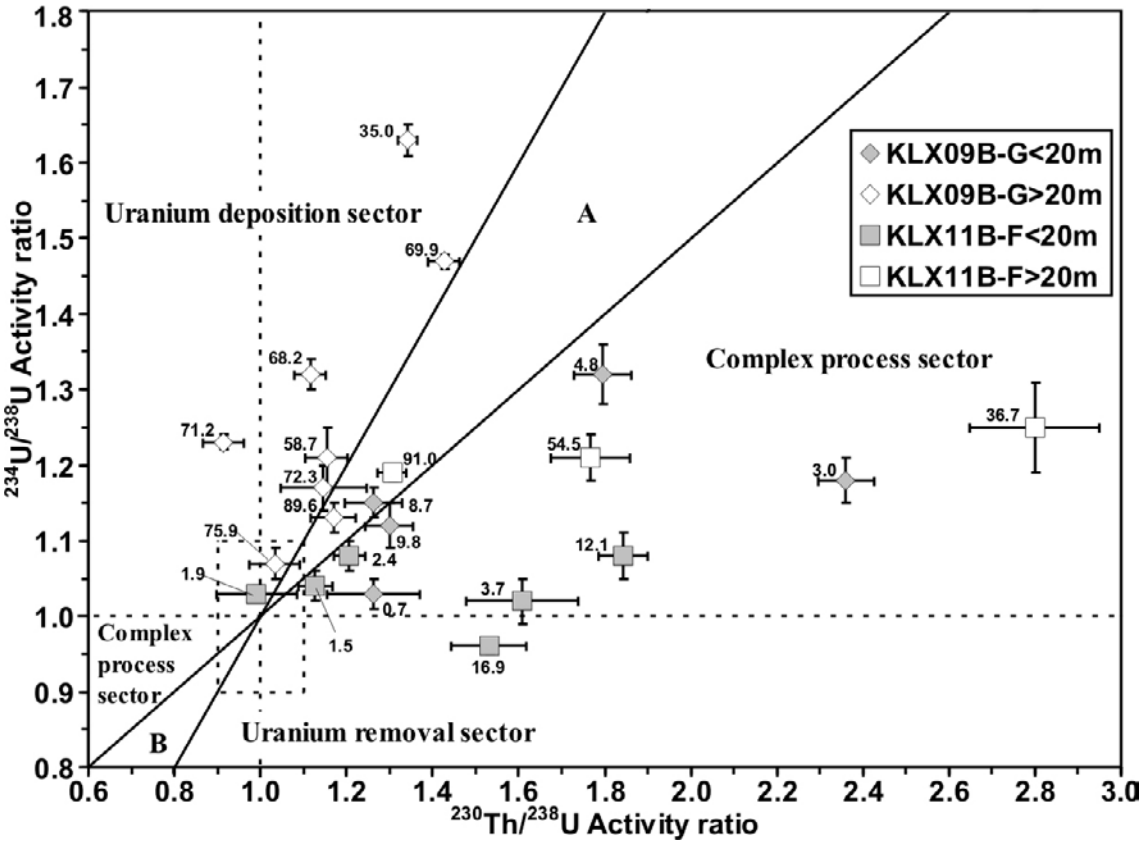

Figure 6-11. *Thiel diagram of uranium decay series for bulk fracture surface samples from KLX09B–G and KLX11B–F, separated by depths (after /Thiel et al. 1983/). Horizontal and vertical lines are shown for $^{230}Th/^{238}U = 1$ and the $^{234}U/^{238}U = 1$, respectively. The box of 1.0 ± 0.1 indicates secular equilibrium of $^{230}Th/^{238}U$ and $^{234}U/^{238}U$ within the conservative analytical error of 10%. Errors are in 1σ (sometimes within the size of the symbols, e.g. for $^{234}U/^{238}U$ AR in sample KLX11E: 16.9 m). A and B are forbidden sectors for any single continuous process. Complex process sector is forbidden for any single process. The "forbidden sectors" indicate samples that have suffered complicated U transport.*

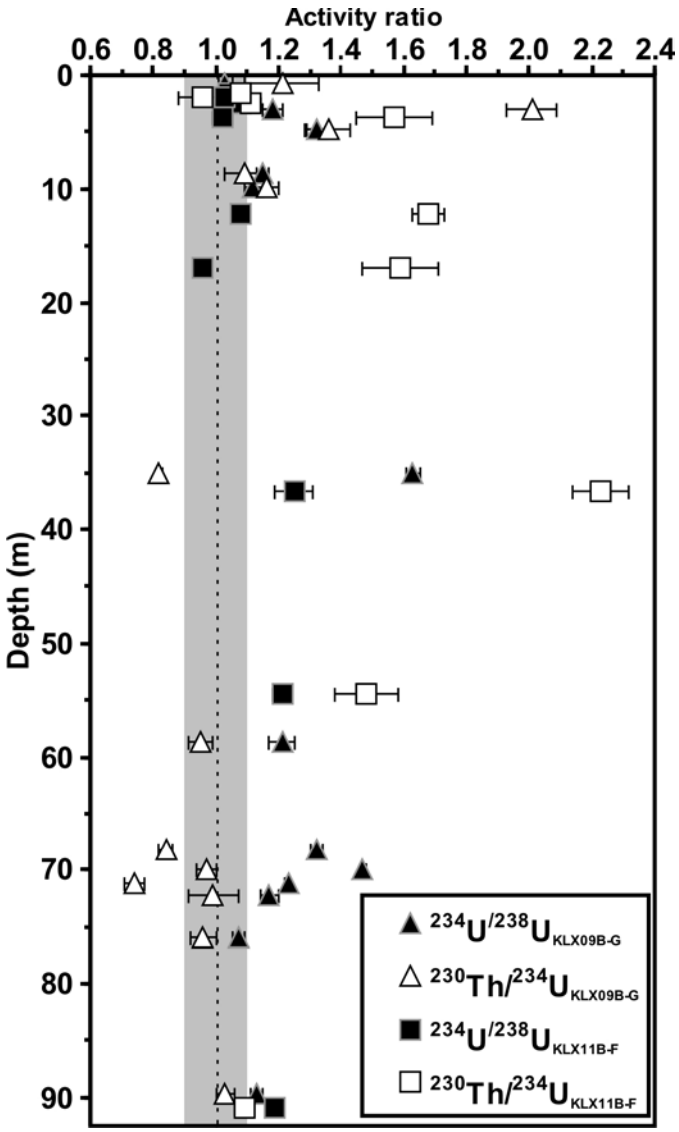

Figure 6-12. *Activity ratios of $^{234}U/^{238}U$ and $^{230}Th/^{234}U$ (with errors) vs. depth for for bulk fracture coating samples from boreholes KLX09B–G and KLX11B–F. Errors are in 1σ (sometimes within the size of the symbols). Shaded area indicates secular equilibrium 1.0 ± 0.1.*

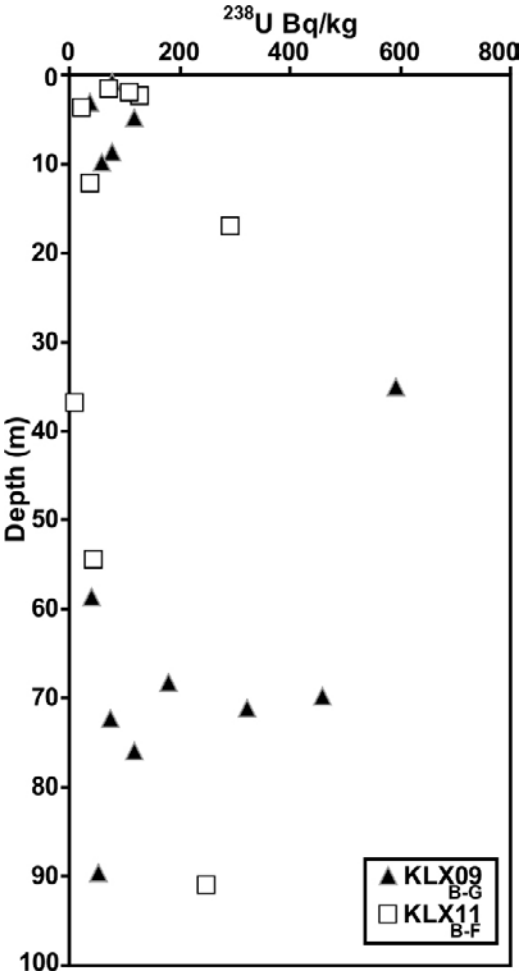

Figure 6-13. *Activity of ^{238}U vs. depth for bulk fracture coating samples from boreholes KLX09B–G and KLX11B–F. Errors (1σ) are within the size of the symbols.*

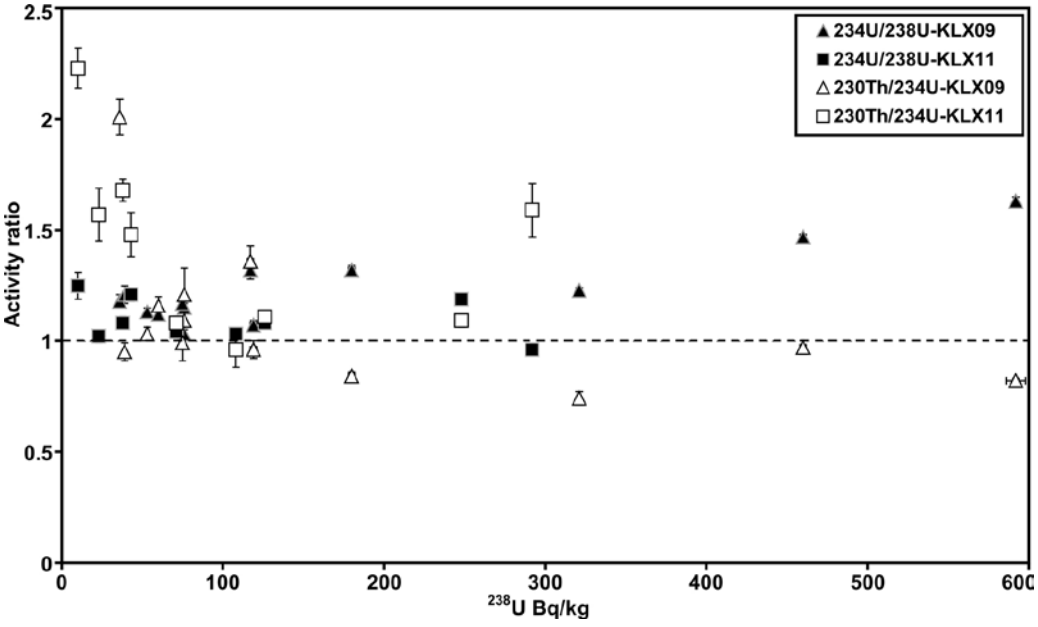

Figure 6-14. *Activity ratios of $^{234}U/^{238}U$ and $^{230}Th/^{234}U$ vs. activity of ^{238}U (with errors, 1σ, sometimes within the size of the symbols) for bulk fracture coating samples from boreholes KLX09B–G and KLX11B–F.*

likely present in the oxidised and more easily leached state of U(VI), relative to ^{238}U /e.g. Suksi and Rasilainen 2002/, and/or because of alpha recoil effects that makes more ^{234}U susceptible to leaching than the site of ^{238}U /e.g. Gascoyne et al. 2002/.

The results indicate that recent U oxidation (within 300 ka) has preferentially taken place in the upper 20 m of the boreholes and locally down to 55 m along fractures with high transmissivity. At depths below 55 m recent U deposition (within 1 Ma) under reducing conditions is evident while more stagnant reducing conditions prevail below 80 m. However, a couple of samples between 55–80 m show $^{230}Th/^{234}U \sim 1$, suggesting rather stagnant recent conditions in this interval as well.

6.2.2 Concluding remarks

The location of the redox front shows at what depths oxygenated groundwater associated with varying Quaternary hydrologic conditions (including subglacial or periglacial environments) were able to reach before oxygen was consumed by fracture minerals reactions and organic redox buffering. The analyses show that the redox front at two drill sites in the Laxemar area is generally positioned at about 15–20 m depth. The main features of the redox front are shown in Figure 6-15. These are generally shown by a shift from:

1) mainly goethite to mainly pyrite in the fractures,
2) positive Ce-anomalies to slightly negative or insignificant Ce-anomalies,
3) mainly removal of U to mainly deposition of U.

Leaching of calcite in open fractures in the upper 20–30 m further support infiltration of very dilute recharge waters which probably have relatively low pH and may at least partly be loaded with oxygen /SKB 2006b/. Scattered goethite occurrences down to c. 80 m and occasional signs of U removal at depths between 35 and 55 m (indicated by $^{230}Th/^{234}U$ AR >1), both occur in intervals of high transmissivity, facilitating localised percolation of oxygenated groundwater to depths that otherwise experience reduced conditions. Values of $^{230}Th/^{234}U$ AR that are near or below 1.0 in the sampled fracture coatings below 55 m depth imply that U was not removed preferentially with respect to Th during the last 100 ka and, therefore, that U was likely present in its more insoluble reduced form. Although penetration of glacial waters to great depths has been confirmed in the area /SKB 2006b/, this study supports the modelling carried out by /Guimerà et al. 1999/ and conclusions drawn by /Gascoyne 1999/ that these glacial waters were not oxidising at repository depth. Instead, oxygen in the recharge water is generally consumed within the upper 20 m (+/–5 m) and to slightly greater depth in fractures or shear zones with high transmissivity ($T \geq 1 \cdot 10^{-7}$ m^2/s).

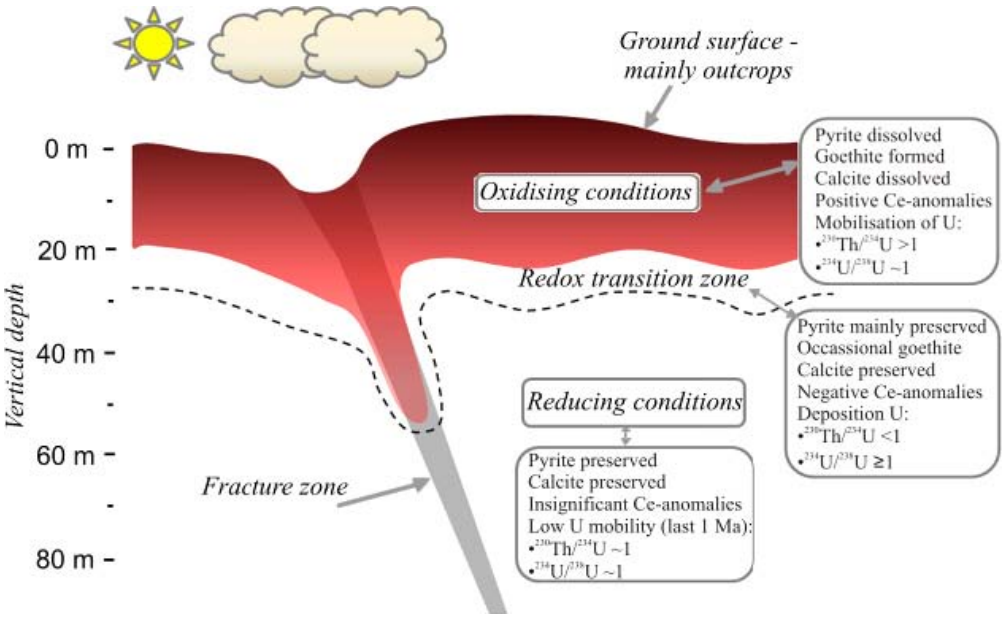

Figure 6-15. *Tentative sketch model of the near-surface redox front in the Laxemar area. The different fields represent the depth intervals where mineralogical, geochemical and U-series analyses of fracture coatings indicate Quaternary oxidising condition, reducing conditions or a transition zone between these two.*

7 Distribution of fracture minerals

The statistical analysis of the frequencies of various fracture minerals is based on Boremap data from the drill core mapping (stored in Sicada). Even though most of the minerals have been mapped with high confidence, detailed microscopy and X-ray diffraction studies have shown that some minerals are over- or underestimated in the database (see also Section 2.1.1). For instance, fractures mapped as only chlorite-bearing often include clay minerals such that the clay mineral frequency may therefore be somewhat underestimated in the mapping. Especially hematite is overrepresented due to its ability to discolour or stain other minerals like chlorite and feldspars, i.e. hematite is identified in many fractures but the amount in each filling is generally below 1%. Calcite, in contrast, is mapped with high accuracy due to the use of HCl to acertain identification.

The total number of open and sealed fractures in boreholes KLX02–29A is ~101,000 (including fractures within deformation zones), of which 67% are sealed fractures and 33% are open fractures. Sealed network sections (2,348) and sections of crushed rock (477) have been left out of this statistical analysis of mineral frequency, because the number of fractures in each og these sections is not known. It should be noted that the mapping gives only the frequency of fractures carrying a specific mineral and not the amount of the mineral in the fracture. A mapping campaign, devoted to mapping volumes of specific minerals of interest for the modelling of redox and pH buffering has been made, and the results are quantified in /Löfgren and Sidborn in preparation/.

The most common fracture minerals in the Laxemar subarea are, as mentioned above, calcite and chlorite, which dominate in both sealed and open fractures (Figure 7-1) but occur more frequently in the latter ones. It should be noted that Figure 7-1 gives frequencies of open as well as sealed

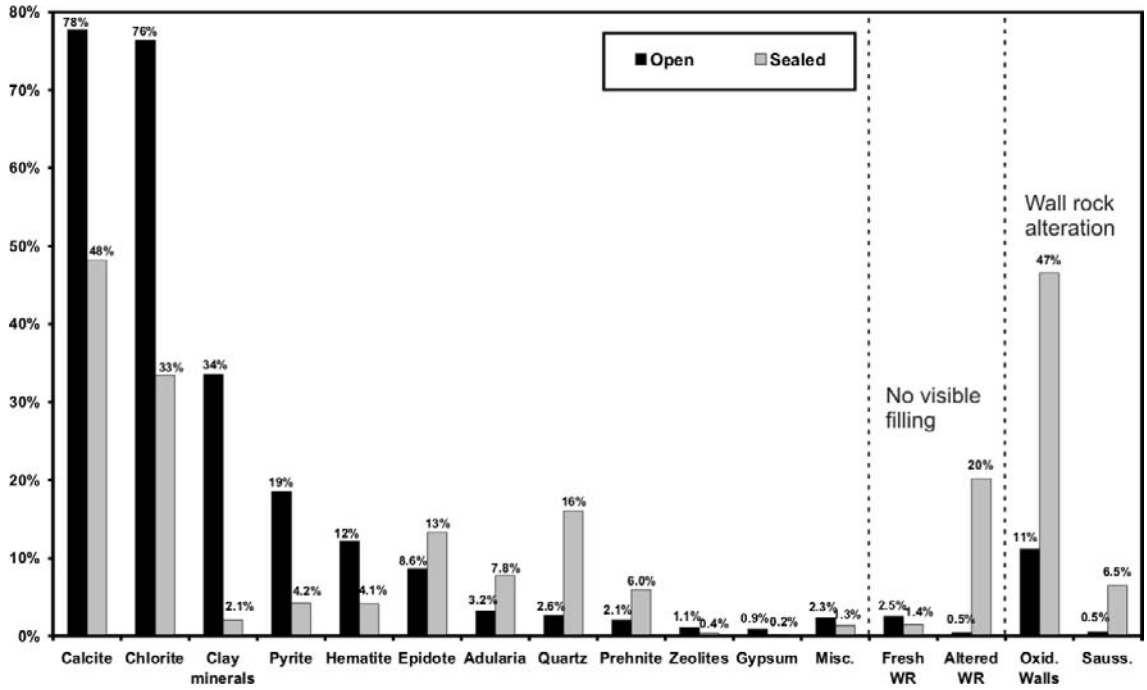

Figure 7-1. *Relative frequency of fractures (open as well as sealed) filled or coated with specific minerals (several minerals are usually found in the same fracture). Data are from the Boremap mapping from KLX02–KLX29A, excluding crush zones and sealed network. "Adularia" includes "red feldspar" and "white feldspar". Zeolites include minerals mapped as "laumontite" and "zeolites". "Misc." includes fluorite, muscovite, sericite, talc, chalcopyrite, sphalerite, sulphides, amphibole, goethite, apophyllite, barite and biotite. "No visible filling – Fresh WR" is mapped as "Broken fractures with a fresh appearance and no mineral fill" in the Boremap mapping. "No visible filling – Altered WR" is mapped as "oxidised walls", "fractures with epidotised-saussuritised walls" or "bleached fracture walls" without any visible fracture minerals. Wall rock alteration "Oxid. Walls"and "Sauss" show frequency of fractures with oxidised (red stained) and saussuritised wall rock, respectively.*

fractures containing each mineral and not the number of fractures. For instance, calcite is found in 78% of the open fractures and in 48% of the sealed fractures, but the number of open, calcite-bearing fractures is less (26,088) than the number of sealed, calcite-bearing fractures (31,166). Clay minerals, pyrite and hematite are also most frequently found in open fractures, whereas epidote, adularia, quartz and prehnite are more frequent in sealed fractures. Additional minerals identified are zeolites (mainly laumontite and harmotome) and gypsum (mainly in open fractures). Muscovite (mainly in KLX06), fluorite, goethite (mainly near surface), amphibole (mainly in KLX08), talc (mainly in KLX20A), other sulphides, barite and apophyllite each occur in less than 0.6% of the fractures (plotted as "Misc." in Figure 7-2). A large part of the sealed fractures (~ 20%) are narrow with altered wall rock but with no visible filling (i.e. microscopic fracture minerals can be assumed, Figure 7-2, "No visible filling – Altered WR" in Figure 7-1). Fractures with no visible filling associated with fresh wall rock are relatively rare (2.5% of the open fractures, "No visible filling – Fresh WR" in Figure 7-1). Considering all fractures, a large number of fractures have altered wall rock, usually red stained and/or saussuritised ("Oxid. walls" and "Sauss." in Figure 7-1). However, wall rock alteration is probably underestimated in the mapping data due to the mapping procedure (i.e. limitations in number of mapable observations for each fracture in the Boremap system).

7.1 Occurrences of fracture minerals in deformation zones and sections of crushed rock

Crushed zones are mapped separately during the drill core mapping and often represent zones characterised by high transmissivity. The fracture mineralogy of these crush zones is shown for boreholes KLX02 through to KLX29A in Figure 7-3. In this figure, each crush zone is represented as a single occurrence and the width of the section is not accounted for. Notable differences between the mineralogy between crush zones and ordinary fractures (cf. Figure 7-1) are the higher frequency of chlorite, clay minerals, calcite, hematite, goethite and the lower contents of pyrite in the crushed sections. The higher frequency of hematite and lower frequency of pyrite is related to enhanced circulation of oxidising hydrothermal fluids in the crushed zones, which have been more water-conductive than single fractures in general. In near-surface crushed zones, goethite is present and pyrite is depleted because the crushed zones are more commonly water conducting compared with ordinary fractures and therefore the downward percolation of oxidising fluids is enhanced in these zones.

The fracture mineralogy in deformation zones, the latter interpreted as a part of the extended single hole interpretation, is shown for boreholes KLX02 through to KLX29A in Figure 7-4. Similarly to the crushed sections, deformation zones show higher frequencies of clay minerals and hematite and lower contents of pyrite compared with fractures in the rock mass in general.

Figure 7-2. *Photograph of a drill core sample with a typical, hardly visible, sealed fracture with no visible fill but with altered wall rock /Drake et al. 2006/. These fractures are presented as "No visible filling – Altered WR" in Figure 7-1 and as "NVF-AWR" in Figure 7-6 and in Figure 7-9. Drill core diameter is 50 mm.*

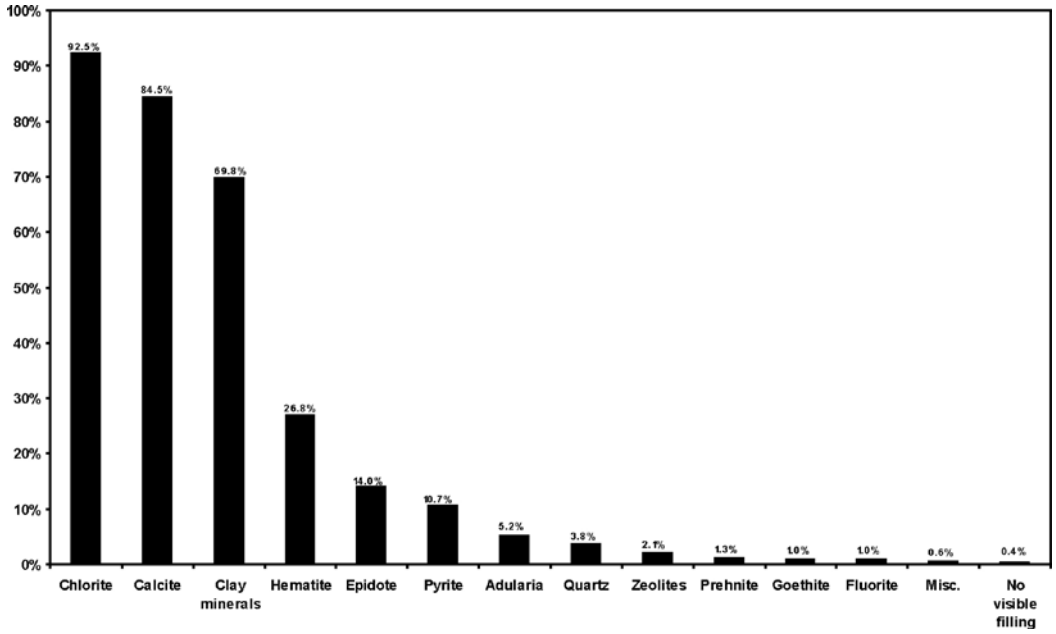

Figure 7-3. *Histogram of relative abundance of fracture minerals in crush zones as inferred from boreholes KLX02 through to KLX29A as the percentage of fractures containing a given mineral. The total number of crush zones is 477. Adularia also includes albite. "Misc." includes gypsum, barite and chalcopyrite, each accounting for about 0.2%.*

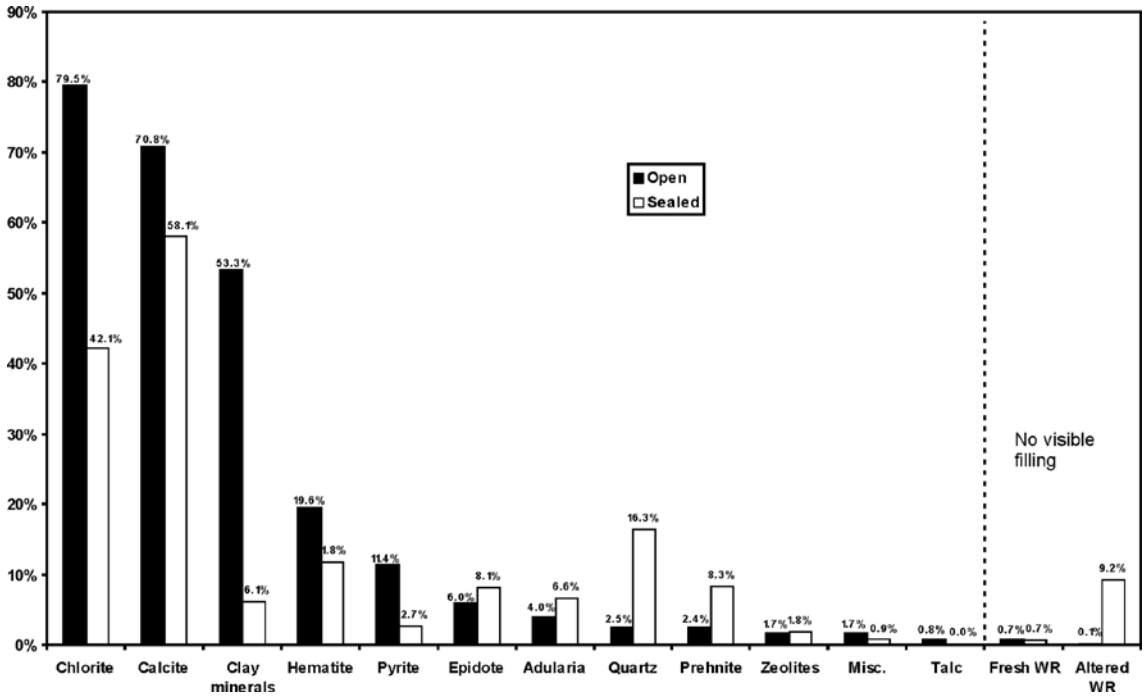

Figure 7-4. *Histogram of fracture minerals in open and sealed fractures found in the deformation zones interpreted in the ESHI (extended single hole interpretation). Data from KLX02–KLX29A, number of open fractures = 10,427, number of sealed fractures = 7,869. Adularia also includes albite. "Misc." includes muscovite, sericite, chalcopyrite, sphalerite, sulphides, amphibole, goethite, fluorite, gypsum and apophyllite.*

7.2 Occurrences of fracture minerals in different rock domains

The distributions of the most important fracture minerals, fractures with no visible filling and the dominant wall rock alteration features in rock domains RSM_A01, RSM_D01 and RSM_M01 (cf. Figure 1-2 and Figure 1-3), hereafter denoted as A01, D01 and M01, respectively, are shown in Figure 7-5, Figure 7-6 and Figure 7-7. The frequency of occurrence of most of the minerals (e.g. clay minerals and

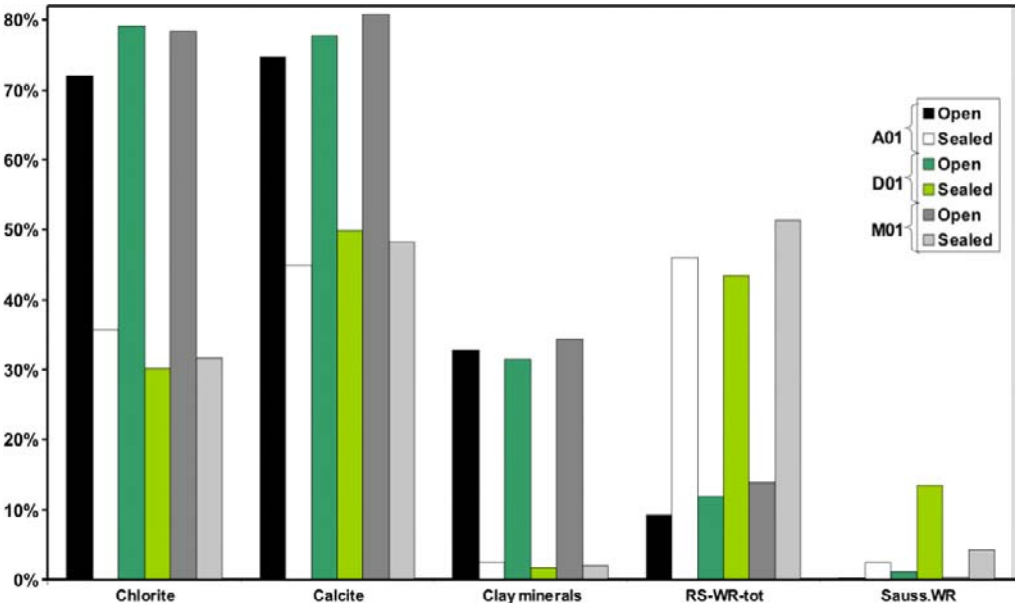

Figure 7-5. *Frequency of open and sealed fractures (open includes partly open) with chlorite, calcite or clay minerals (several minerals are usually found in the same fracture) for rock domains RSM_A01, RSM_D01 and RSM_M01. Also shown is the frequency of fractures with red-stained (RS-WR-tot) or saussuritised (Sauss-WR) wall rock.*

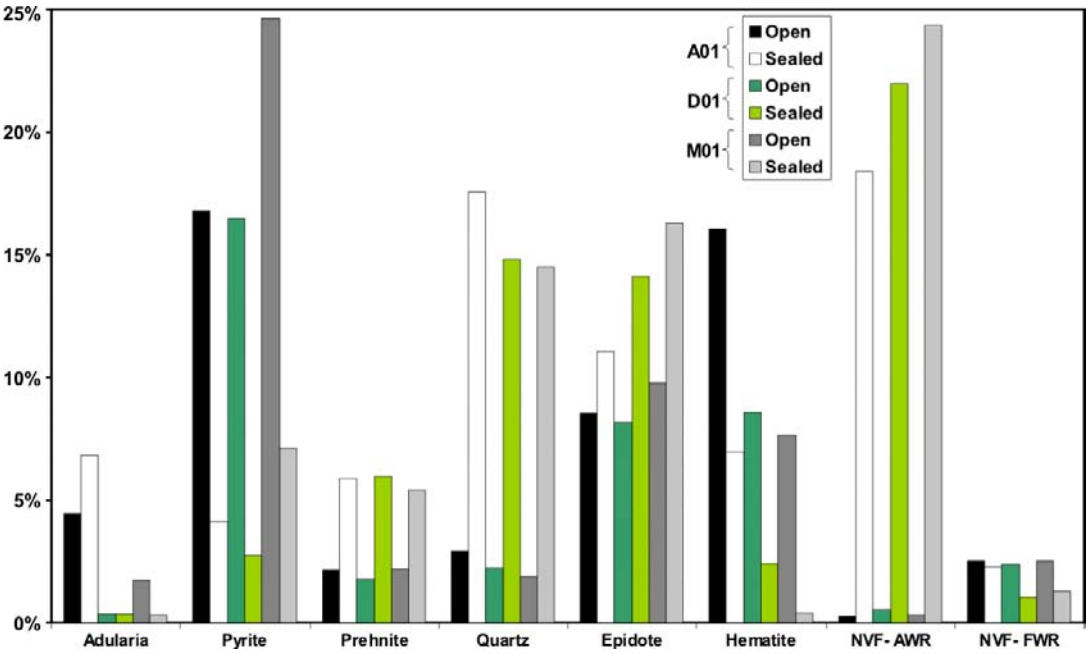

Figure 7-6. *Frequency of open and sealed fractures (open includes partly open) with adularia, pyrite, prehnite, quartz, epidote and hematite (several minerals are usually found in the same fracture) for rock domains RSM_A01, RSM_D01 and RSM_M01. Also shown is the frequency of fractures with no visible filling with either altered (NVF-AWR) or fresh (NVF-FWR) wall rock. Adularia includes minerals mapped as "red feldspar" and "white feldspar".*

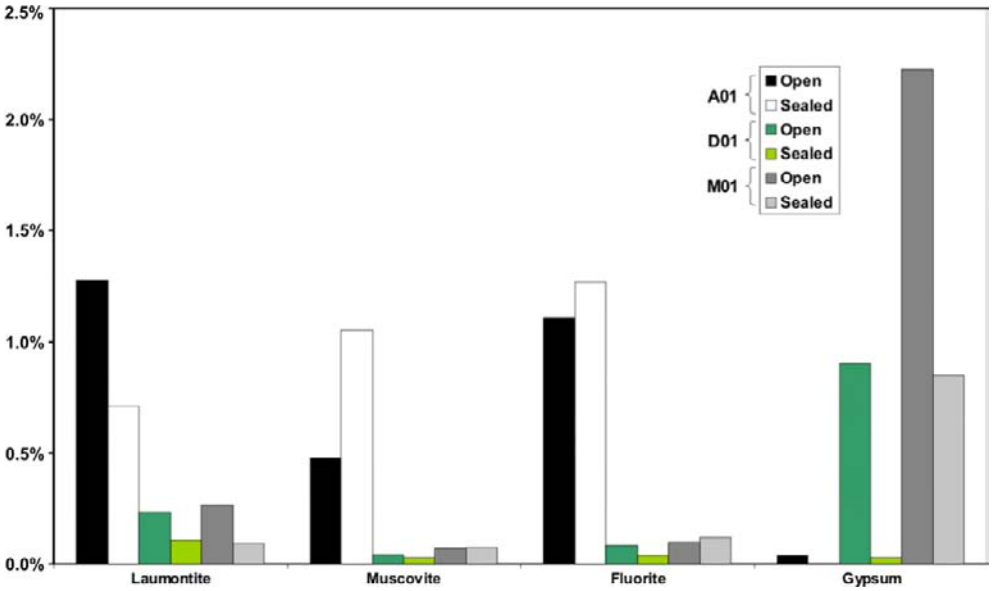

Figure 7-7. *Frequency of open and sealed fractures (open includes partly open) with laumontite, muscovite, gypsum and fluorite (several minerals are usually found in the same fracture) for rock domains RSM_A01, RSM_D01 and RSM_M01.*

prehnite), and of fractures without visible fracture minerals with fresh wall rock, is similar in the different rock domains. However, some variations exist and these are mainly related to the difference in chemistry and mineralogy of the dominant rock types characterising the different rock domains. A01 is dominated by Ävrö granite (mainly Ävrö granodiorite), M01 is dominated by Ävrö quartz monzodiorite and some diorite/gabbro, while D01 is dominated by quartz monzodiorite. Generally, the dominant rock type in the A01 domain has higher concentrations of SiO_2, K_2O and lower concentrations of Fe_2O_3, MgO, MnO, CaO and somewhat lower Al_2O_3 concentrations than the rock types in the other two domains which are compositionally more similar. Analogous mineralogical differences are the higher contents of quartz and K-feldspar and lower contents of biotite, amphibole, pyroxene, plagioclase and opaques. Furthermore, the plagioclase is more CaO-rich in the M01 and D01 domains than in A01 (see Appendix 1 for chemical and mineralogical composition of the rock types).

Noteworthy fracture mineral frequency differences related to rock chemistry are the lower amount of chlorite, calcite, epidote and higher amounts of adularia and quartz in domain A01 compared with the other domains (Figure 7-5 and Figure 7-6). These differences correlate very well to the higher MgO (chlorite), Fe_2O_3 (chlorite and epidote), CaO (calcite and epidote), in D01 and M01, and higher K_2O (adularia) and SiO_2 (quartz and possibly adularia) in A01. Another noteworthy difference is the higher amounts of gypsum in D01 and especially in M01 than in A01 (Figure 7-7). This may correlate to the difference in CaO content between the rock types in these domains, but it may alternatively be explained by more intense dissolution of gypsum in A01 than in the other domains. The amount of laumontite is generally low in most boreholes except in KLX06 in which approximately 150 fractures carry this mineral. These occurrences are dominantly found in close relation to the ZSMEW002A ("the Mederhult zone") and are probably formed during late stage hydrothermal circulation of fluids related to the Götemar intrusion (cf. Section 4.3). Laumontite is also common in relation to ZSMEW007A which, together with ZSMEW002A, explain the relatively high frequency of laumontite in domain A01 (Figure 7-7). Fluorite and muscovite are more frequent in domain A01 because of their relation to the A01 adjacent to the Götemar intrusion and influenced by its post-magmatic circulation (Figure 7-7). Furthermore, these minerals are preferentially found in the A01 boreholes located closest to the Götemar granite (i.e. KLX06, KLX09 and KLX09B–G).

The relatively high frequencies of pyrite in M01 and of hematite in A01 are more difficult to explain (Figure 7-6). This domain has a much higher number of drill cores covering the upper 100 m than the other domains and this may explain the slightly higher pyrite frequency since pyrite is, at least in the Palaeozoic, believed to be partly formed from descending fluids emanating from overlying sediments (cf. Sections 4.6, 5.6.3 and 5.6.4). Explanations for the high hematite frequency in A01 include: 1) this

domain includes the largest portion of boreholes drilled in the early stages of the site investigations when the overestimation of hematite in the core mapping was not yet recognised (cf. Section 2.1.1), and 2) this domain includes deformation zones with particularly numerous hematite-bearing fractures (e.g. ZSMEW002A in KLX06 (Figure 7-23c).

Fractures with saussuritised wall rock are fewer in number than those with red-stained wall rock and seem to be related to rock domain D01 (Figure 7-5) where this alteration feature is quite common.

7.3 Occurrences of fracture minerals in different fracture domains

The distribution in fracture domains FSM_C, FSM_EW007, FSM_N, FSM_NE005 and FSM_W (cf. Figure 1-4), of the most important fracture minerals, fractures with no visible filling and the dominant wall rock alteration features, is shown in (Figure 7-8, Figure 7-9 and Figure 7-10). Fracture domain FSM_S is not discussed due to the lack of data. The differences in fracture mineral frequency between the different fracture domains are not as apparent as between the rock domains in Section 7.1. Instead, the wall rock chemistry seems to have been more influential on the fracture mineralogy of the area than the different fracture intensity characteristics of the fracture domains. For instance, this is shown by the fact that differences in mineral frequency between different fracture domains can be explained mainly by differences in the dominant rock chemistry between these fracture domains. For example, since fracture domains FSM_EW007 and FSM_N are dominated by rock domain A01 rock types, and the other fracture domains are dominated by either rock domain D01 or M01 (or all three for fracture domain FSM_W), the same trends characterised by lower amounts of calcite, chlorite, epidote and higher amounts of adularia and quartz, as seen in rock domain A01 compared with M01 and D01, are evident when the corresponding fracture domains are compared. However, even though the separation into fracture domains evens out the frequency differences for some minerals, other differences than those related to the rock domains can be distinguished.

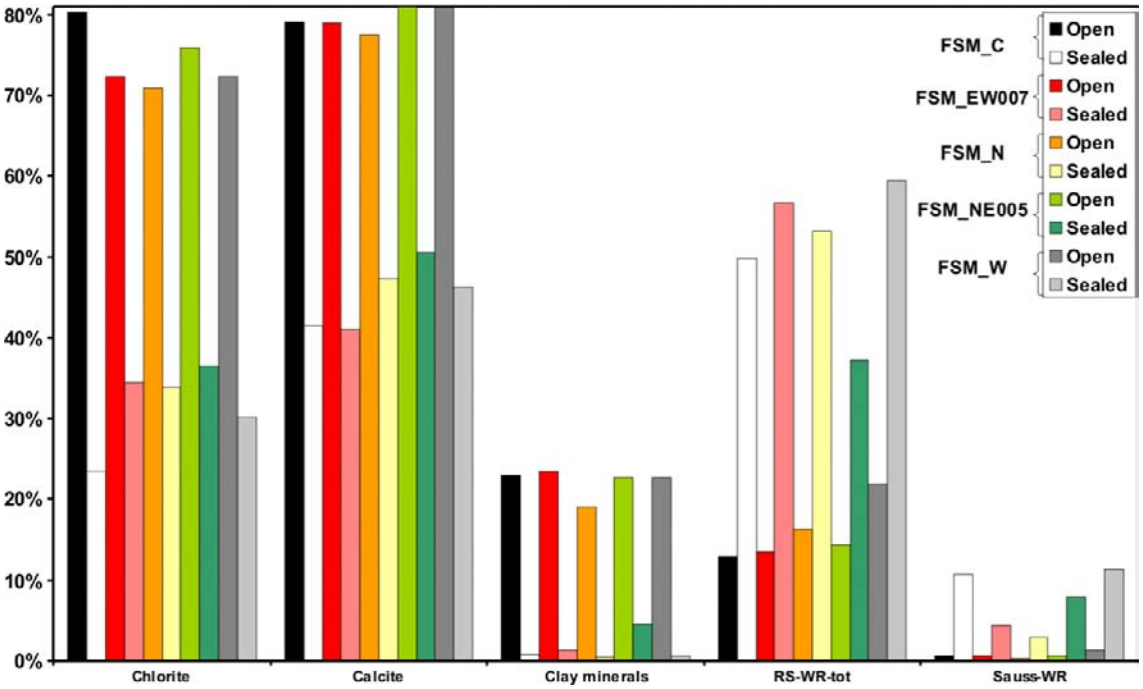

Figure 7-8. *Frequency of open and sealed fractures (open includes partly open) with chlorite, calcite or clay minerals (several minerals are usually found in the same fracture) for fracture domains FSM_C, FSM_EW007, FSM_N, FSM_NE005 and FSM_W. Also shown is the frequency of fractures with red-stained (RS-WR-tot) or saussuritised (Sauss-WR) wall rock.*

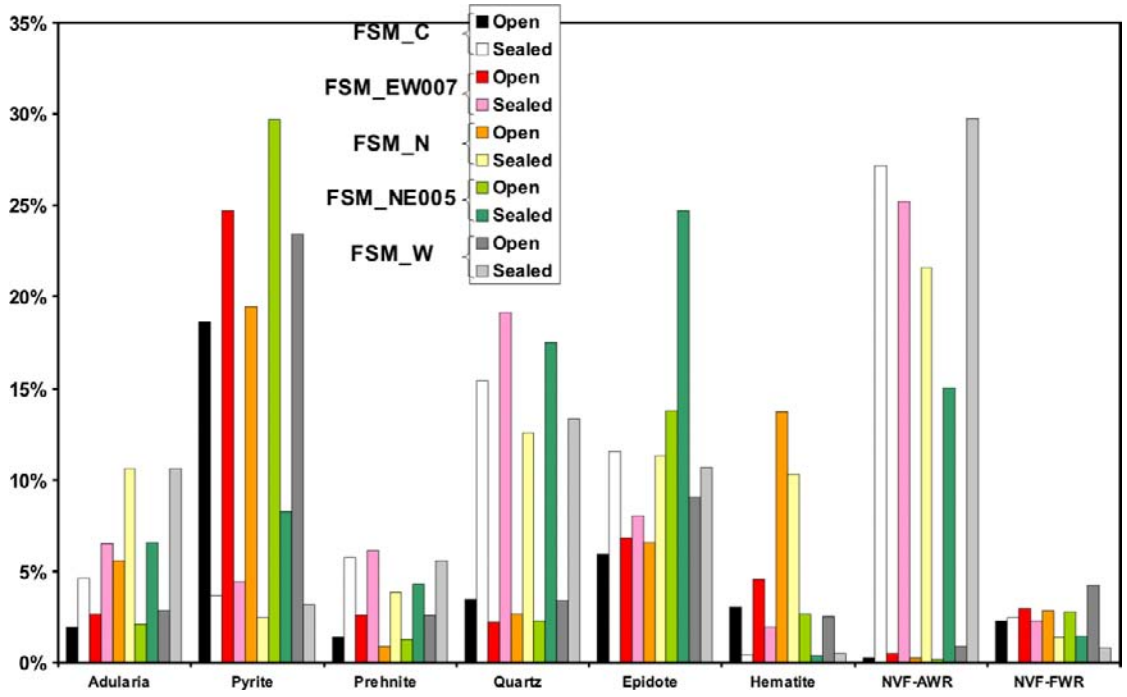

Figure 7-9. *Frequency of open and sealed fractures (open includes partly open) with adularia, pyrite, prehnite, quartz, epidote and hematite (several minerals are usually found in the same fracture) for fracture domains FSM_C, FSM_EW007, FSM_N, FSM_NE005 and FSM_W. Also shown is the frequency of fractures with no visible filling with either altered (NVF-AWR) or fresh (NVF-FWR) wall rock. Adularia includes minerals mapped as "red feldspar" and "white feldspar".*

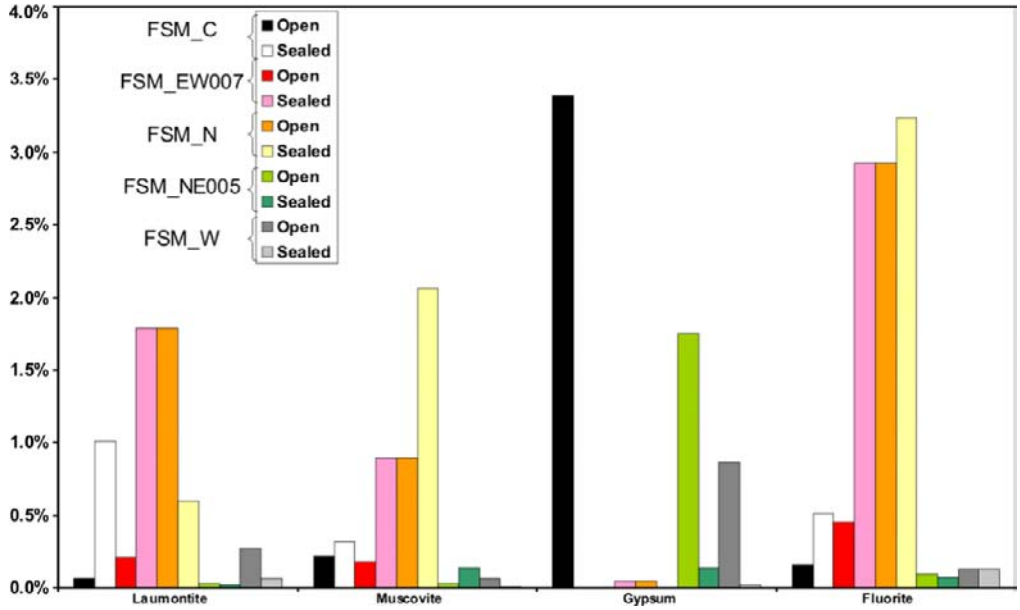

Figure 7-10. *Frequency of open and sealed fractures (open includes partly open) with laumontite, muscovite, gypsum and fluorite (several minerals are usually found in the same fracture) for fracture domains FSM_C, FSM_EW007, FSM_N, FSM_NE005 and FSM_W.*

Prehnite and clay minerals are apparently more related to fracture domain FSM_EW007 than to FSM_N, while an opposite trend is shown for adularia and hematite (Figure 7-8 and Figure 7-9). These separations within the A01 domain were not evident in the analysis on a rock domain basis. Epidote, on the other hand, is apparently most frequent in fracture domain FSM_NE005, a domain highly influenced by the epidote-rich deformation zone ZSMNE005 with a significant ductile component. This domain also seems to be least affected by red staining (Figure 7-8 and Figure 7-9).

Laumontite, muscovite and fluorite seem to be almost as common in fracture domain FSM_EW007 as in FSM_N. However, in contrast to RSM_A01, FSM_N does not include KLX06, which is the borehole with the highest amount of these minerals (Figure 7-10). Gypsum is mainly related to FSM_C (Figure 7-10), and especially to deep sections of boreholes KLX03, KLX08 and KLX10.

7.4 Variation of fracture mineral frequency with depth

Analysis of variation in fracture mineralogy with depth has been carried out using two different approaches: 1) collective analysis of all open and sealed fractures, respectively, from all cored boreholes (KLX02–29A) in the Laxemar subarea, and 2) analysis of sealed, open and total number of fractures on a borehole by borehole basis. The discussion in this section is mainly based on the collective plots for each mineral, with additional examples from representative distributions in specific boreholes (all plots are presented in Appendix 3). Fractures in sections of crushed rock and in sealed network sections are not included in the collective plots. This is because their quantification using the parameters to define these sections (i.e. number of fractures/m) gives very significant peaks of occurrence in these specific sections and these peaks are not representative for the overall depth distribution of each mineral, thus disturbing the general picture from which interpretations are drawn. These sections are, however, included in the plots for each specific borehole. The collective distribution plots show the relative frequency of each mineral (calcite, chlorite, clay minerals, adularia+albite [mapped as adularia, red feldspar and white feldspar], epidote, prehnite, hematite, pyrite, goethite, quartz, gypsum) as well as for fractures with no visible filling. This gives the percent of each mineral of each fracture type (sealed or open) within each 10 m vertical depth interval. Open fractures also include fractures mapped as partly open fractures.

The number of sealed fractures in the uppermost tens of metres is underrepresented due to the lack of BIPS images for these cored sections, since drill core mapping is generally only carried out in sections with corresponding BIPS images. The total number of mapped drill core metres for each 10 m depth interval in cored boreholes KLX02 through to KLX29A is shown in (Figure 7-11). However, some sections without corresponding BIPS images have been mapped (mainly for redox front studies). In these cases mainly open fractures have been mapped and sealed fractures have been omitted, resulting in them being underrepresented in the mapping data for these intervals. The sections were only open fractures have been mapped are included in the plots because they provide important information of near surface processes (e.g. redox related). The amount of potentially very young empty fractures is higher in this interval as well.

The boreholes are often inclined and are of variable length and deeper intervals are represented by fewer metres of core than the upper 500–600 m, which is clearly shown in Figure 7-11 and in a plot of the total number of sealed or open fractures within each 10 m depth interval (Figure 7-13). The 20 to 30 m above sea level interval is also only represented by a small number of drill cores. Consequently, the intervals with relatively few metres of drill core give less statistically representative results for each mineral.

Figure 7-13 shows the depth variation of the fracture frequency of open, sealed and the total number of fractures, in sections with corresponding BIPs images, and excluding sections classified as deformation zones based on the extended single hole interpretation (ESHI). Sections below 680 m vertical depths are excluded because the number of mapped drill core metres is relatively small (<100 m of drill core/10 m vertical depth interval) and this number constantly decreases with increased depth from this point (cf. Figure 7-11). It is shown in Figure 7-13 that:

- The frequency of all fractures with increasing depth is relatively constant at about 5–6 fractures/m, but an increase to 6–7 fractures/m is indicated in the uppermost 70–80 metres.
- The fracture frequency of sealed fractures is normally 4 ± 1 fracture/m. However, in the uppermost 10 metres a decrease in fracture frequency of sealed fractures is indicated, and a slightly increased trend is indicated at vertical depths greater than 600 m.
- The fracture frequency of open fractures shows some depth related variations. The frequency is normally between 1–2 fractures/m below 100 m vertical depth with higher frequencies at shallower depths between 40 and 100 m vertical depth (normally ~2 fractures/m) and in the uppermost 40 metres were there is a gradual increase towards the ground surface to ~3 fractures/m.

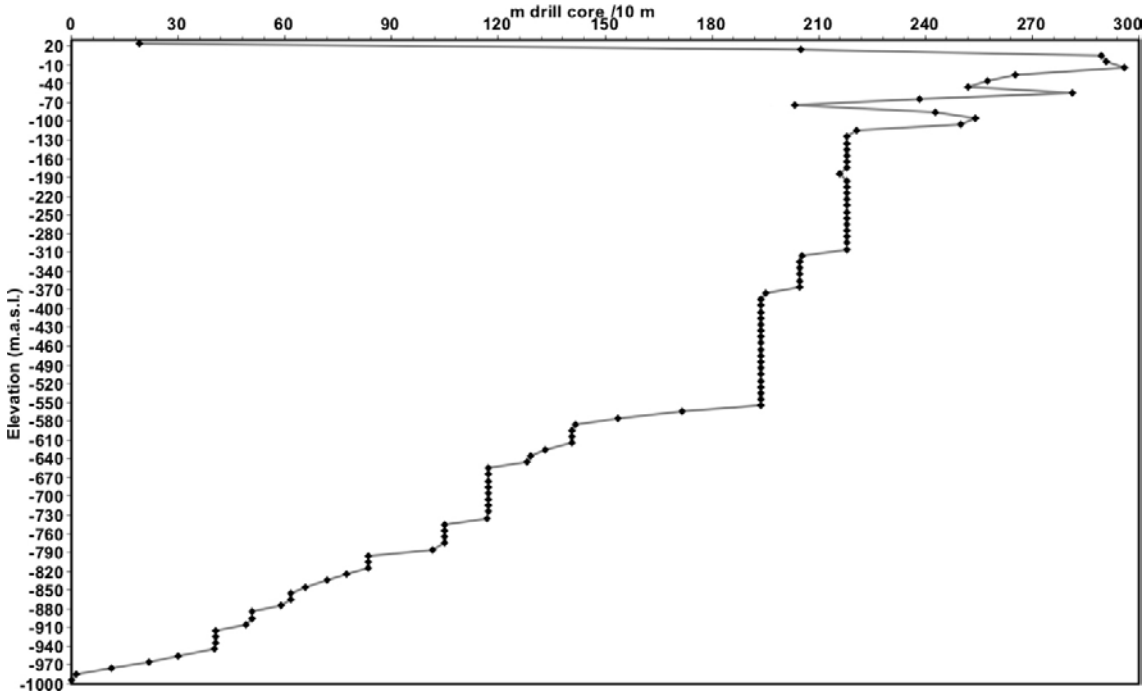

Figure 7-11. *Mapped drill core metres/10 m elevation intervals for cored boreoles KLX02–29A. This plot also includes data for sections without BIPS coverage. If sections lacking BIPS are excluded the number of metres of core in the intervals 30–20 m above sea level and 20–10 m above sea level are approximately 10 and 154, respectively. The inclination of the boreholes has been corrected for.*

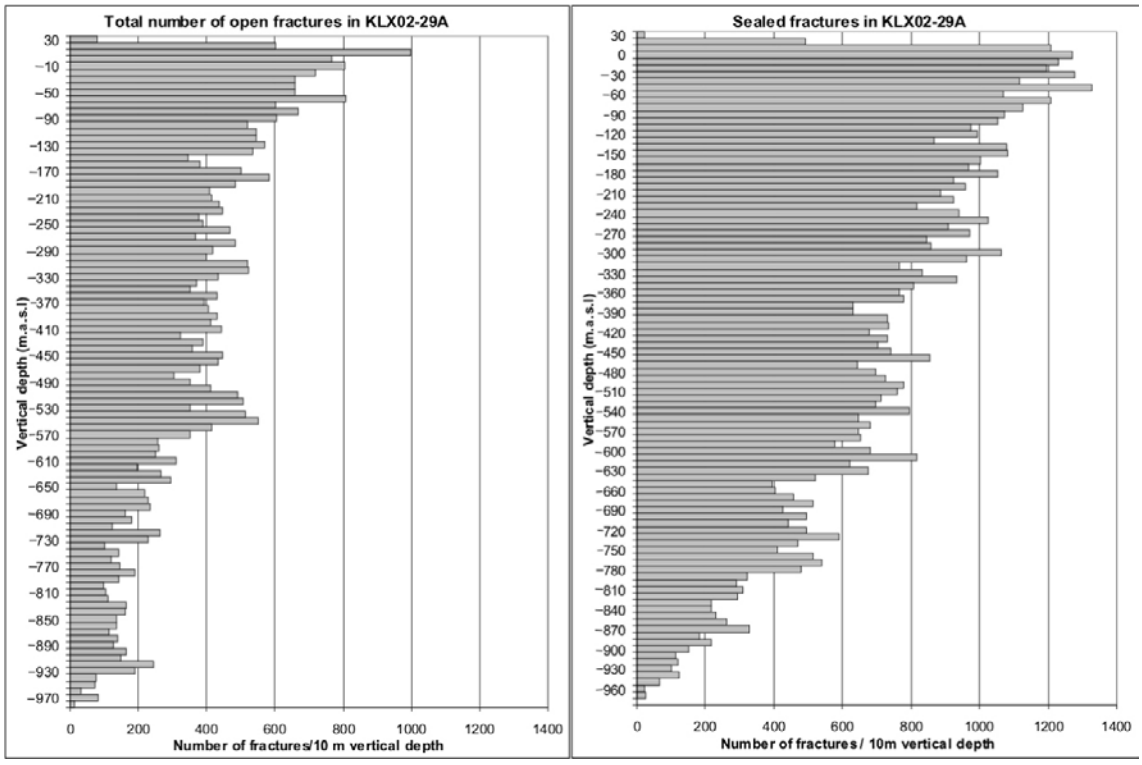

Figure 7-12. *Total number of open fractures and sealed fractures, respectively, for each 10 m vertical depth interval from cored boreholes KLX02–29A in the Laxemar subarea. Note that the number of sealed fractures in the uppermost tens of metres is underrepresented due to the lack of BIPS images for these cored sections. Drill core mapping is generally only carried out in sections with corresponding BIPS images. However, some sections without corresponding BIPS images have been mapped (mostly for redox front studies). In these cases, mainly only open fractures have been mapped and sealed fractures have been omitted which makes them underrepresented in the mapping data for these intervals.*

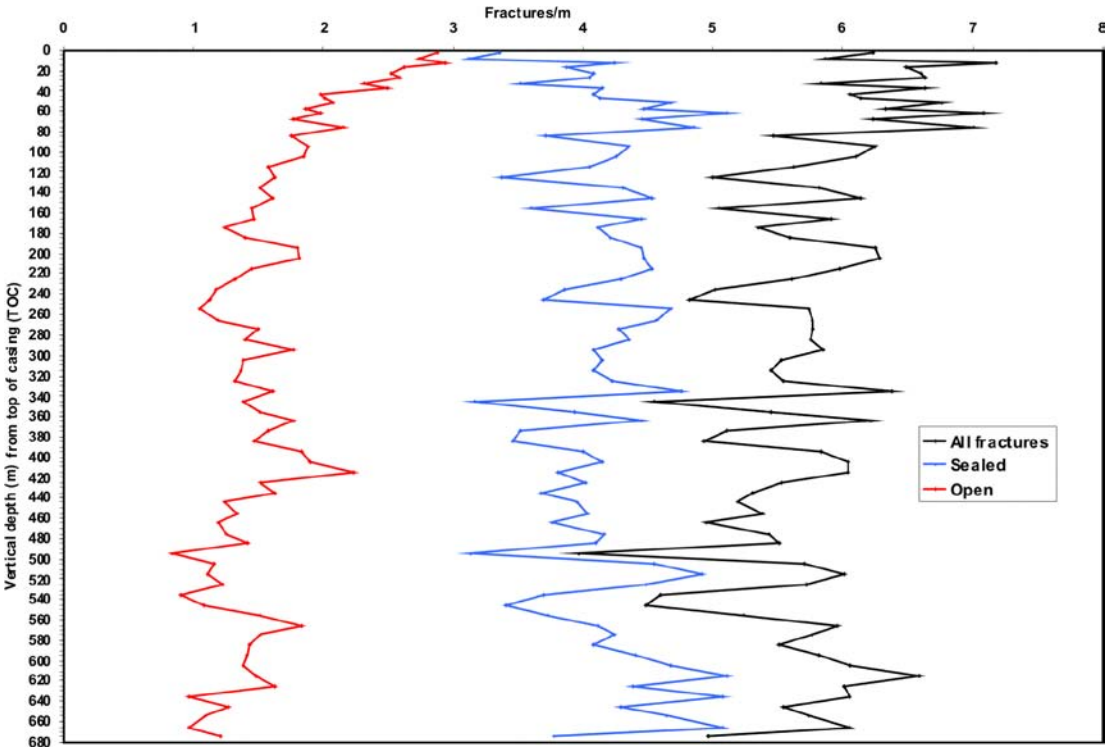

Figure 7-13. *Variation in fracture frequency of open fractures, sealed fractures and the total number of fractures, calculated for 10 m vertical depth intervals (5 m intervals in the upper 70 metres) in cored boreholes KLX03–29A. Only sections with corresponding BIPS images are used and sections classified as deformation zones based on the extended single hole interpretation (ESHI) have been excluded. The inclination of the boreholes has been corrected for.*

For the borehole by borehole based plots, the occurrences of each specific mineral in open and sealed fractures together with the total number of fractures have been analysed. The group of open fractures also includes partly open fractures and fractures from crush zones and the group of sealed fractures includes sealed networks. Fractures in deformation zones and possible deformation zones, based on the single hole interpretation, are also included. Calcite, chlorite, clay minerals, adularia+albite (mapped as adularia, red feldspar and white feldspar), epidote, prehnite, hematite, pyrite, goethite, quartz, gypsum, as well as fractures with no visible filling (divided into fractures with fresh or altered wall rock, respectively) have been studied. Furthermore, the variation of hydrothermal wall rock alteration features, i.e. red staining and saussuritisation, has been analysed. Additionally, for a limited number of boreholes, the occurrence of talc (mainly related to fractures in dolerite) and muscovite (mainly related to greisen fractures), have been analysed. About 2,100 mineral distribution plots from 46 boreholes have been generated. These show the frequency of occurrence of a particular mineral in a particular type of fracture, as well as the overall frequency of occurrence of this fracture type, in 10 m vertical depth intervals along a borehole. However, most of the relative mineral frequencies and wall rock alteration features show no variation with depth, although exceptions exist and a number of these are discussed below together with the general distribution of the specific minerals in the collective plots of all boreholes.

Except for the lower frequency of calcite in the uppermost 10–20 metres, and slightly lower frequency below about –800 m.a.s.l, the most common fracture minerals chlorite and calcite show no distinctive variation with depth (Figure 7-14 and Figure 7-15). The lower frequency in calcite mentioned above is suggested to be related to near surface dissolution caused by the downward percolation of diluted water unsaturated in respect of calcite /Drake and Tullborg 2008a/ (cf. Section 6.2.1.1); a small decline shown for chlorite within the same interval may also be related to near surface dissolution. The decline of calcite at depths below c. –800 m above sea level marks the shift to a less hydraulically conductive interval where Palaeozoic to recent calcite precipitation has been limited (cf. Section 5.6.4). Furthermore, slightly elevated calcite frequency is indicated in the –10 to –50 m above sea level interval. This may correspond to preferential precipitation of calcite from descending fluids in this interval (cf. Figure 5-4) during Palaeozoic and possibly Quaternary times. Subsequent dissolution has decreased the amount of calcite at shallower levels.

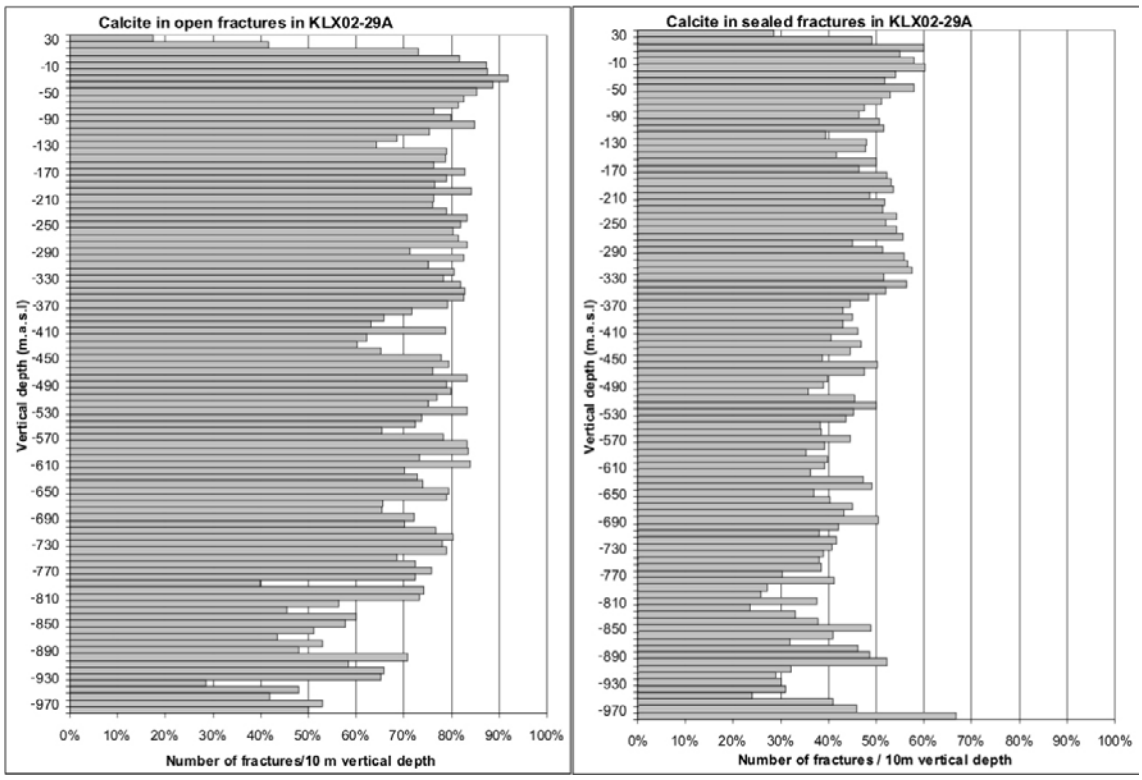

Figure 7-14. *Relative frequency of calcite in open as well as sealed fractures for each 10 m vertical depth interval from cored boreholes KLX02–29A.*

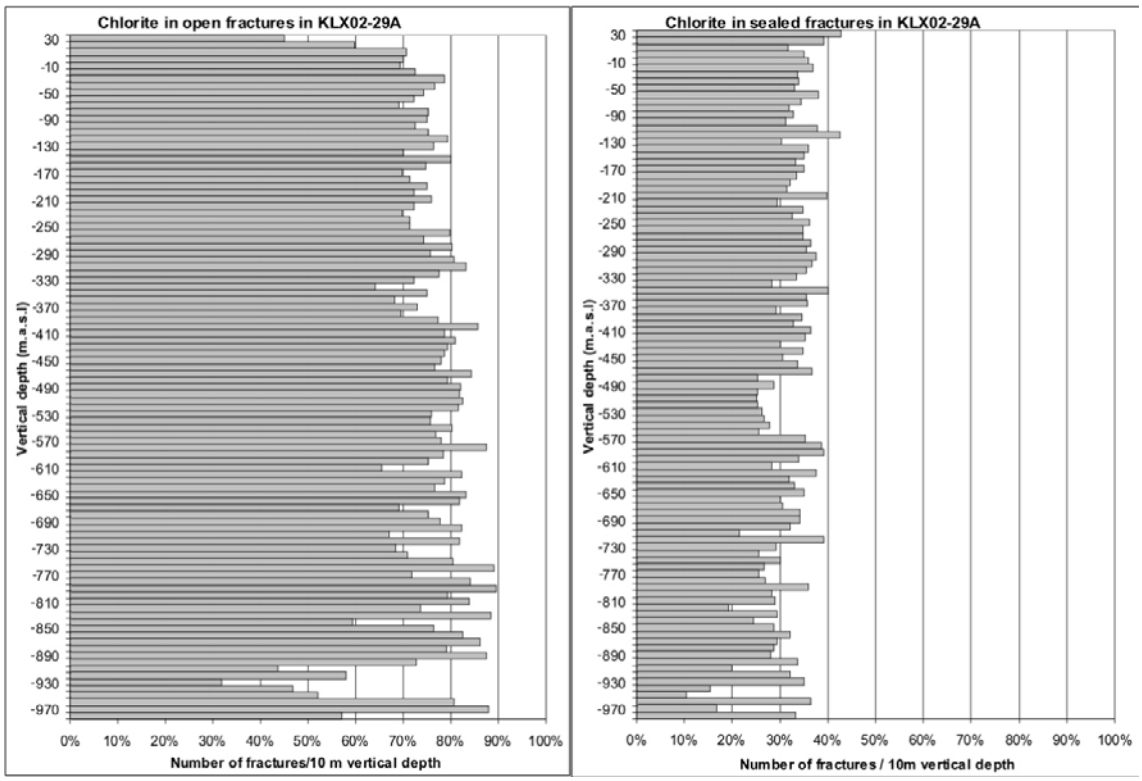

Figure 7-15. *Relative frequency of chlorite in open as well as sealed fractures for each 10 m vertical depth interval from cored boreholes KLX02–29A.*

Examples of representative calcite and chlorite borehole distributions are shown in Figure 7-16a and Figure 7-16b, for KLX03 and KLX08, respectively. The frequency of occurrence of these minerals generally follows the variation in the total fracture frequency and these minerals are common in deformation zones, for example, in ZSMEW946A in KLX03 (vertical depth: –680 to 700 m above sea level) and in ZSMEW007A (–105 to 153 and –160 to –235 m.a.s.l), and ZSMEW946A (–388 to –395 m.a.s.l) in KLX08. The trend of decreasing calcite frequency in the uppermost tens of metres is exemplified by KLX09D in Figure 7-16c).

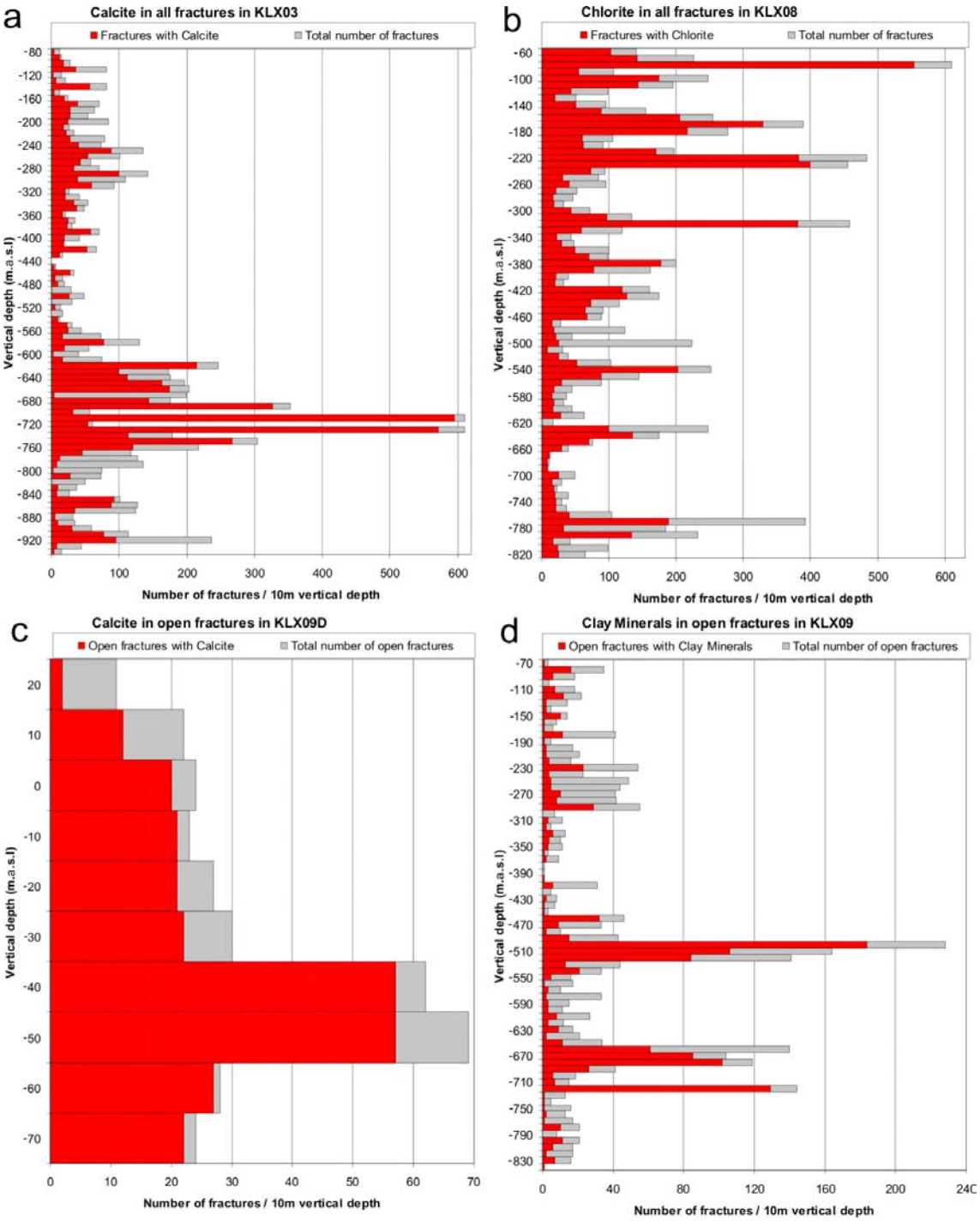

Figure 7-16. *Variation with depth of calcite (a) and chlorite (b) along all fractures in KLX03 and KLX08, respectively. Calcite (c) along open fractures versus depth in KLX09D (excluding the near surface part which lacks BIPS) and (d) clay minerals along open fractures in KLX09. The total number of fractures of the specific fracture type per 10 m borehole interval is also shown.*

Clay minerals are found in 34% of the open fractures, which makes them the third most frequent mineral occurrence in these fractures. The frequency of clay minerals in sealed fractures is, however, very small, mainly below 5%. Their frequency of occurrence generally follows the variation in frequency of occurrence of open fractures with depth (Figure 7-17), although the relative frequency is commonly higher in deformation zones. Clay minerals are overrepresented in sealed fractures in the uppermost interval which only includes a small number of mapped fractures. Similarly, clay minerals are probably underrepresented in fractures below about –950 m above sea level. Examples of high clay mineral frequency in deformation zones are DZ10 based on single hole interpretation (–492 to –526 m.a.s.l) and ZSMEW007A+ZSMNW928A (–653 to 693 m.a.s.l) in KLX09, shown Figure 7-16d.

Similarly to clay minerals, hematite does not vary systematically with depth and is occasionally frequent in open fractures in deformation zones (Figure 7-18), exemplified by ZSMEW002A in KLX06 (Figure 7-23c). The occurrence of hematite suggests oxidising formation conditions mainly of hydrothermal origin and does not reflect current ambient groundwater conditions /Drake and Tullborg 2004, Dideriksen et al. 2007/. It should be noted that the amount of hematite along these open fractures is very low, commonly below 1 vol.%.

The hydrothermal minerals epidote and prehnite of Generation 3 (cf. Section 4.3), show no systematic variation in occurrence with depth (Figure 7-19 and Figure 7-20). A similar erratic distribution with depth is observed for quartz which also dominantly belongs to Generation 3 (Figure 7-21). Examples of representative borehole distributions of epidote and prehnite from boreholes KLX11A and KLX21B are shown in Figure 7-23a, b. Adularia, which is mainly of hydrothermal origin, is also evenly distributed with depth (Figure 7-22), although increased frequency is found in open fractures at great depth, closely related to the intersection of deformation zone ZSMEW007A in borehole KLX04.

Pyrite is a common mineral in open fractures at most depths, although there is a clear decrease in frequency near the surface and also at depths below about –800 m above sea level (Figure 7-24), although the latter might be more uncertain due to the small amount of mapped core in this interval.

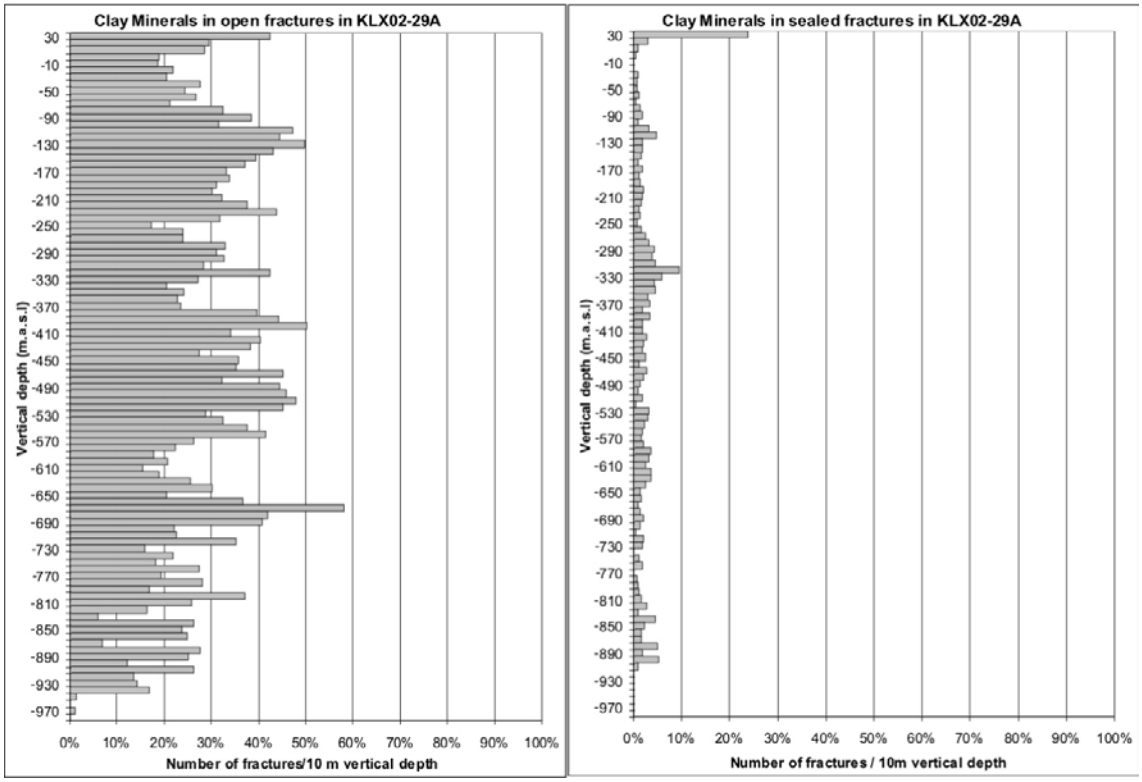

Figure 7-17. *Relative frequency of clay minerals in open as well as sealed fractures for each 10 m vertical depth interval from cored boreholes KLX02–29A.*

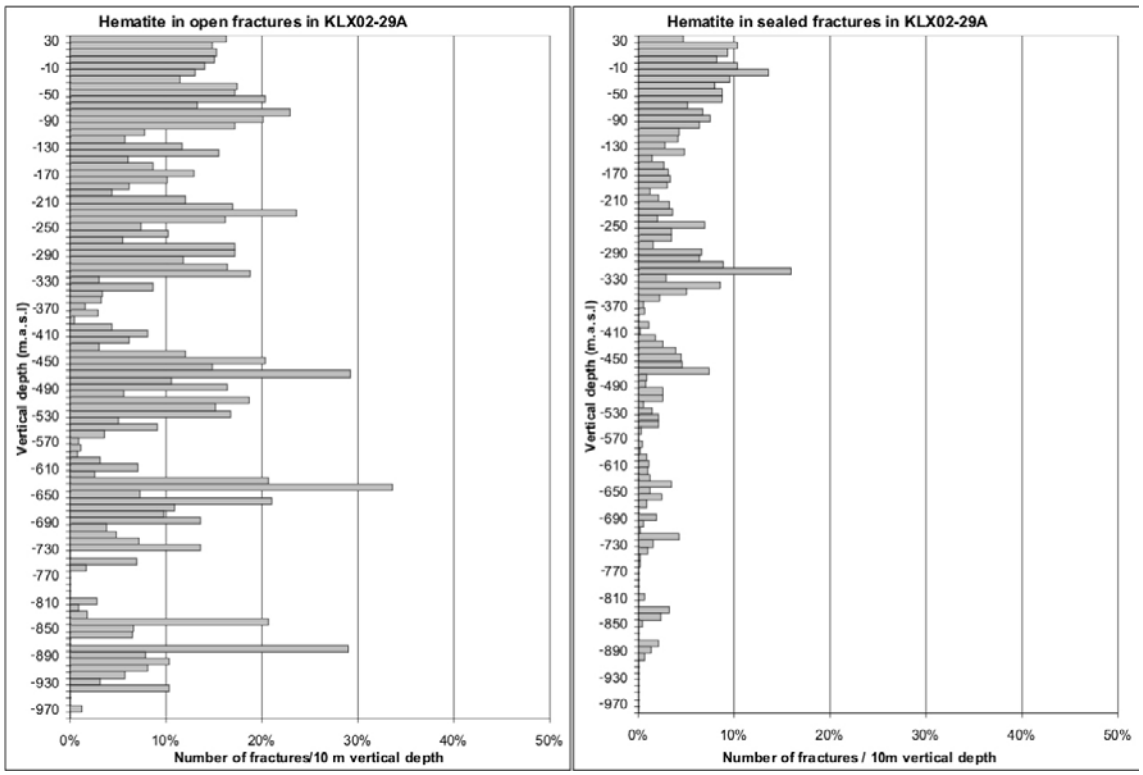

Figure 7-18. *Relative frequency of hematite in open as well as sealed fractures for each 10 m vertical depth interval from cored boreholes KLX02–29A.*

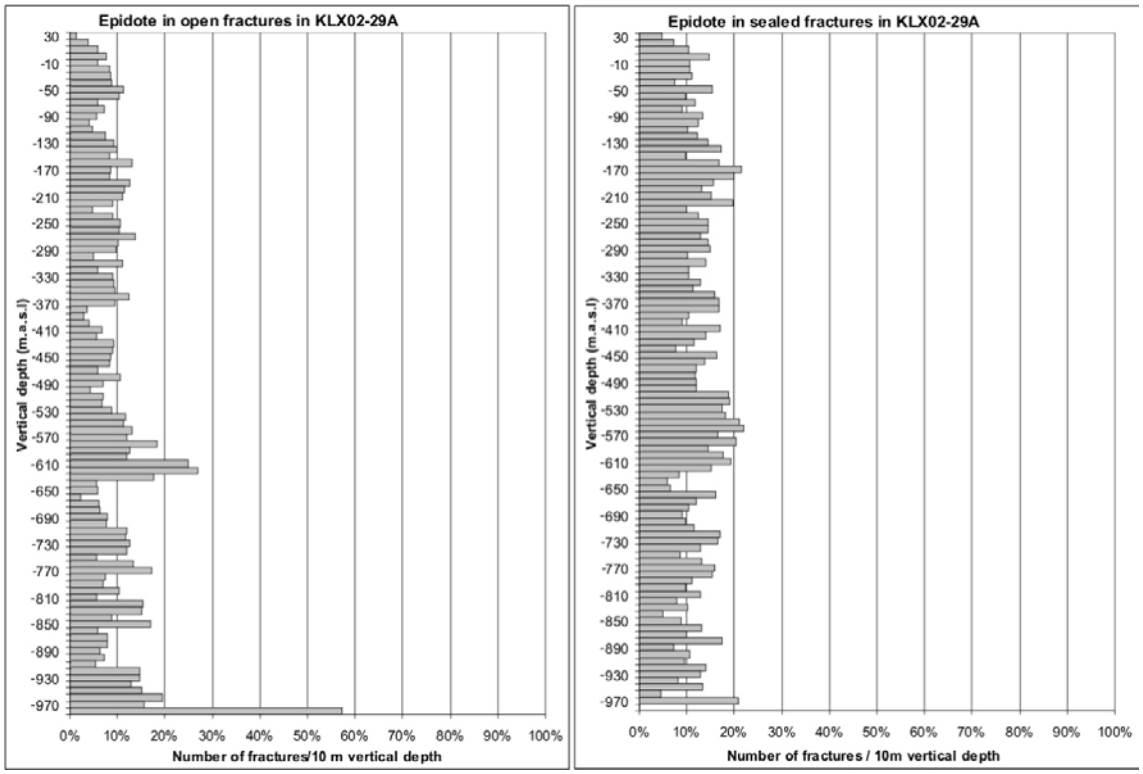

Figure 7-19. *Relative frequency of epidote in open as well as sealed fractures for each 10 m vertical depth interval from cored boreholes KLX02–29A.*

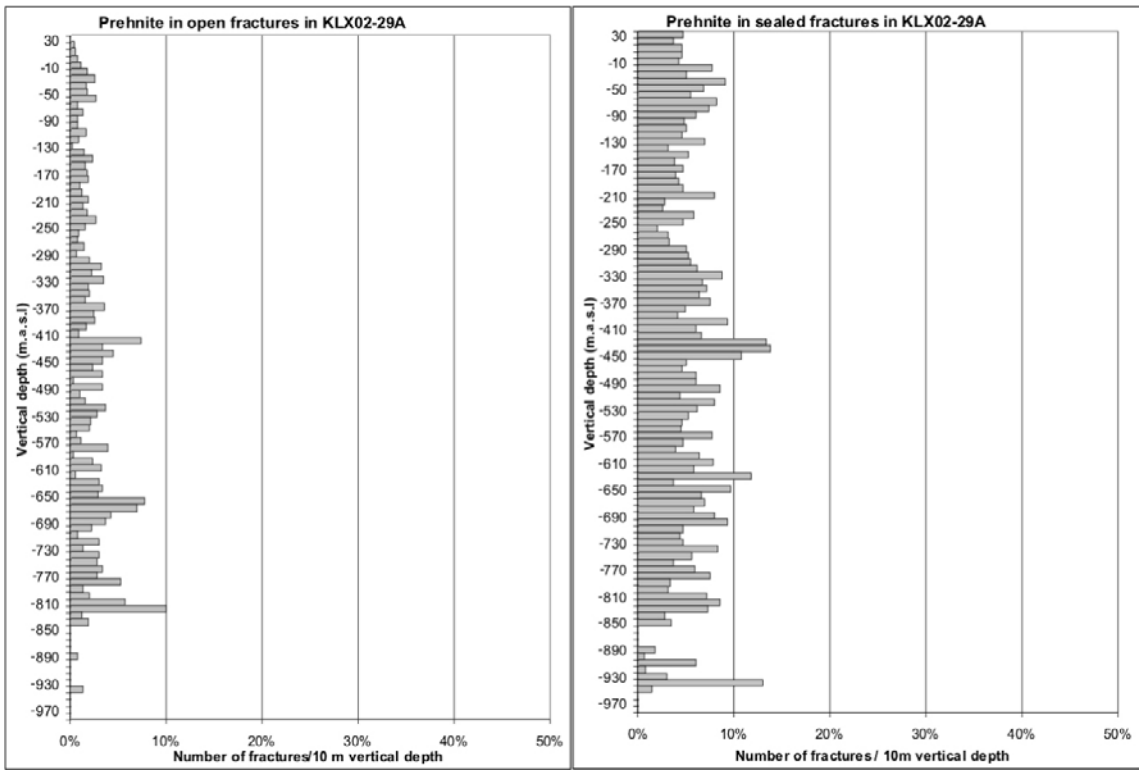

Figure 7-20. *Relative frequency of prehnite in open as well as sealed fractures for each 10 m vertical depth interval from cored boreholes KLX02–29A.*

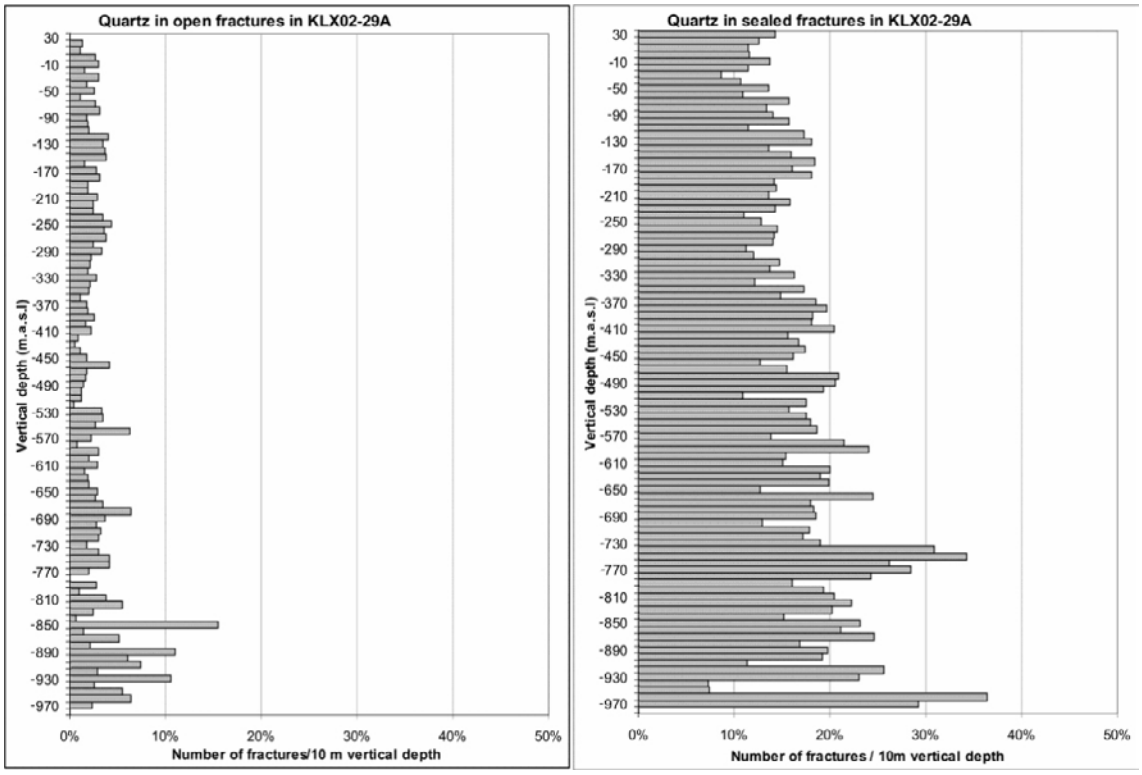

Figure 7-21. *Relative frequency of quartz in open as well as sealed fractures for each 10 m vertical depth interval from cored boreholes KLX02–29A.*

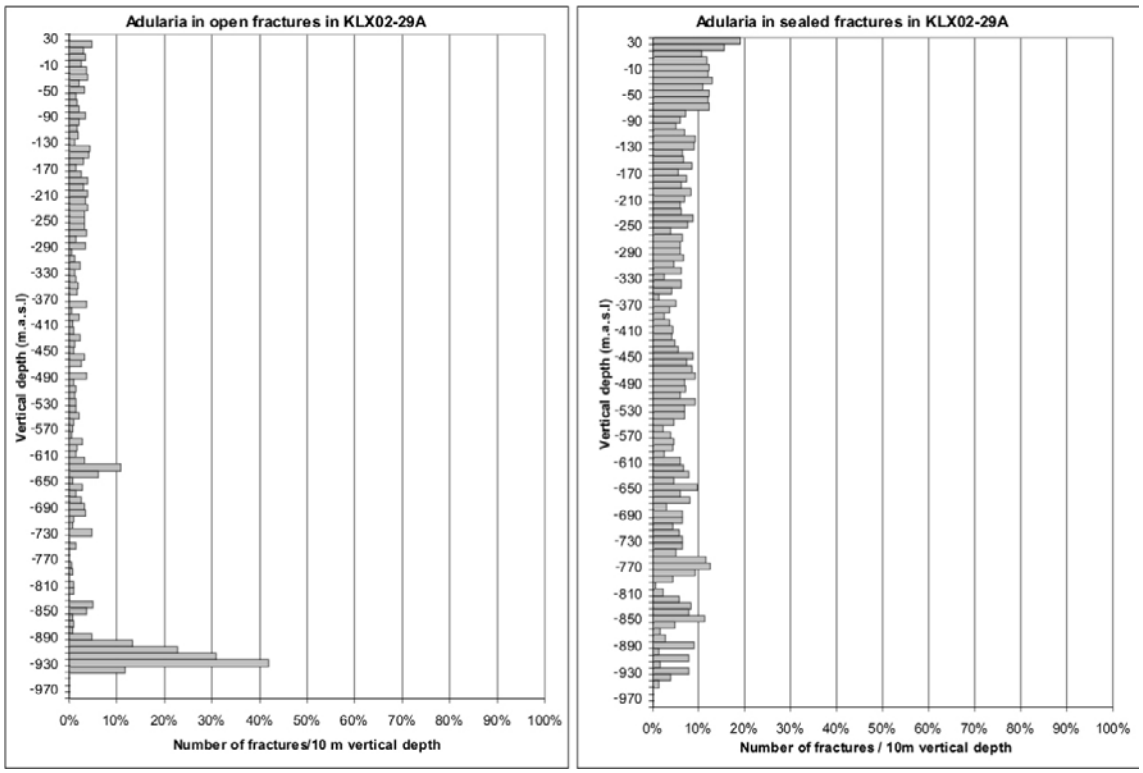

Figure 7-22. *Relative frequency of adularia (including albite) in open as well as sealed fractures for each 10 m vertical depth interval from cored boreholes KLX02–29A.*

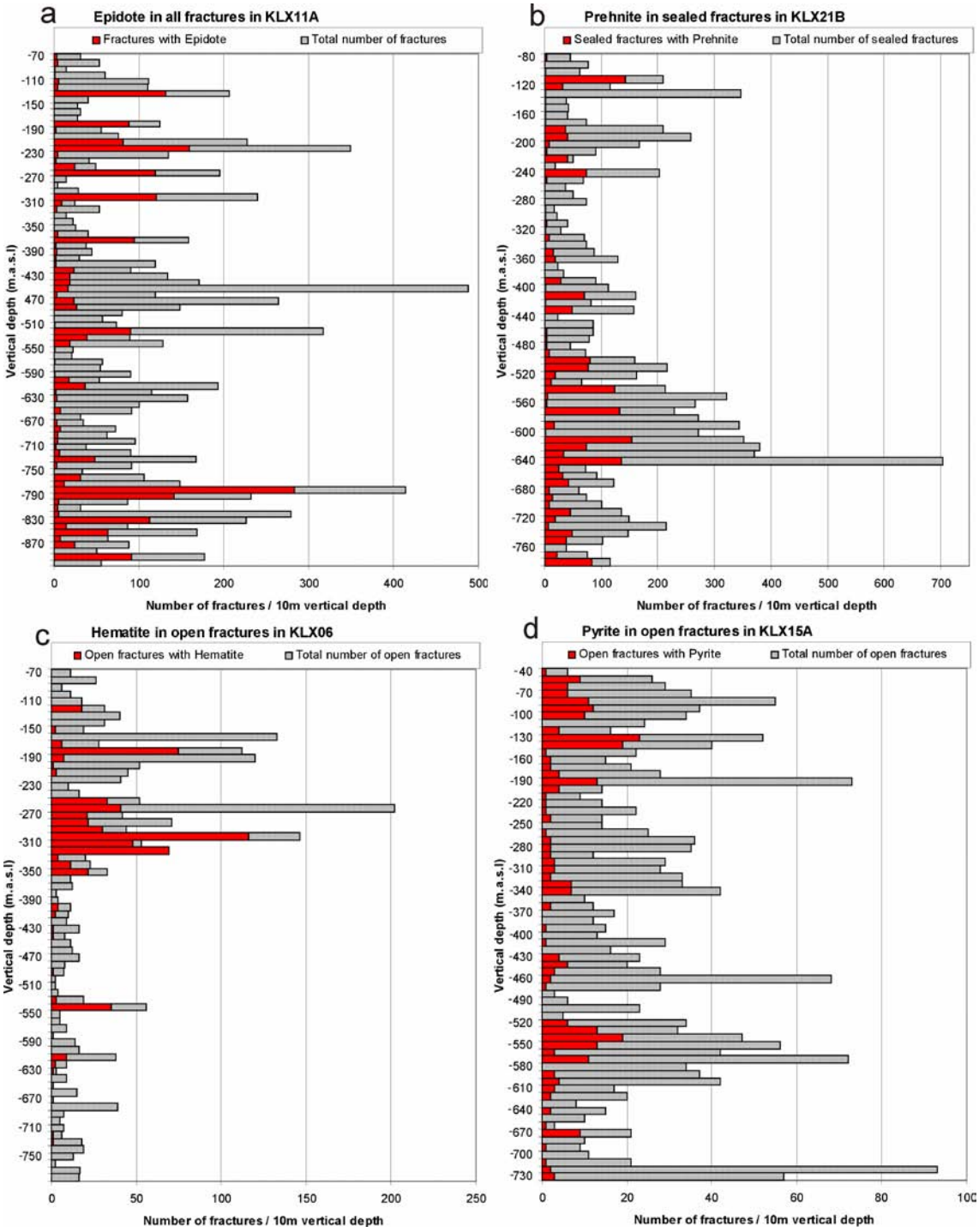

Figure 7-23. *Variation with depth of epidote (a) along all fractures in KLX11A, prehnite (b) along sealed fractures in KLX21B, hematite (c) and, pyrite (d) along open fractures in KLX06 and KLX15A, respectively. The total number of fractures of the specific fracture type per 10 m borehole interval is also shown.*

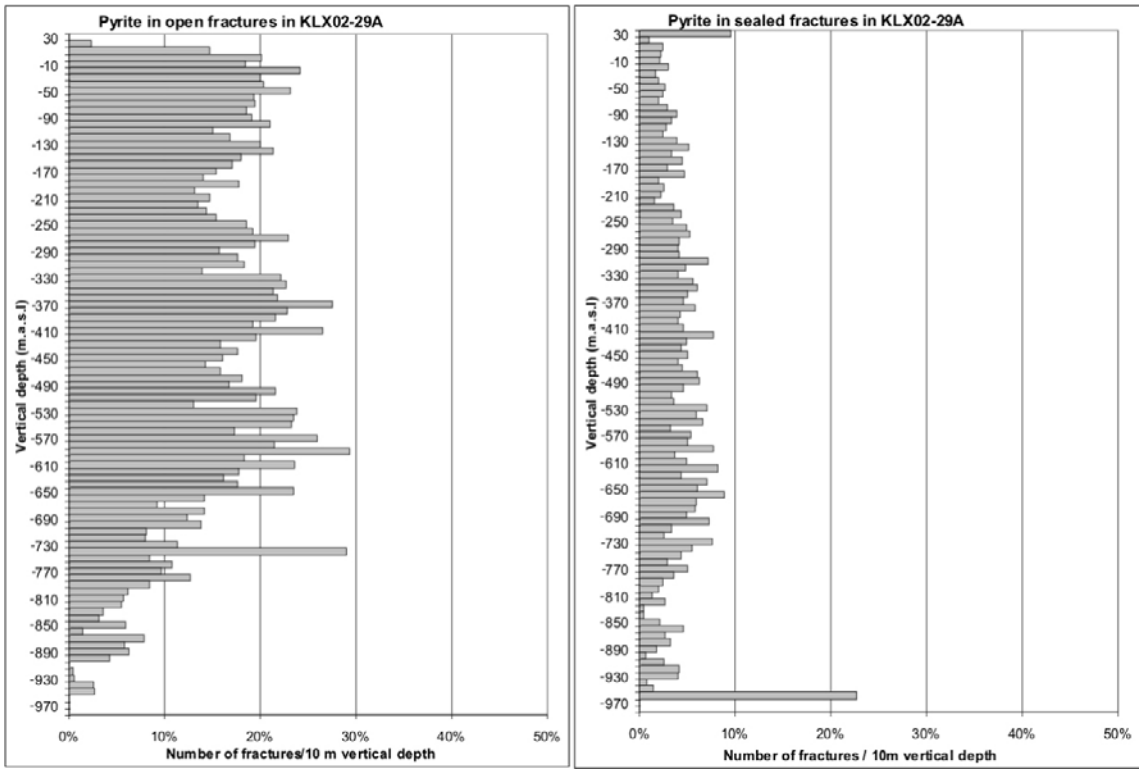

Figure 7-24. *Relative frequency of pyrite in open as well as sealed fractures for each 10 m vertical depth interval from cored boreholes KLX02–29A.*

In the interval between these two exceptions the frequency of pyrite varies with the fracture frequency, exemplified in borehole KLX15A in Figure 7-23d. The frequency of pyrite-bearing sealed fractures is lower (Figure 7-24), and the few major anomalies are from depth intervals underrepresented in cored boreholes. The near surface decrease in pyrite frequency in open fractures is due to near surface oxidative dissolution of pyrite (cf. Section 6.2.1.1). This dissolution of pyrite is accompanied by formation of goethite in open fractures during oxidising conditions in the same interval (Figure 7-25) and the distribution of these minerals indicates the location of a recent near surface redox front /cf. Drake and Tullborg 2008a/. Scattered occurrences of goethite are found at greater depths as well, indicating potential of, although very limited (see /Drake and Tullborg 2009b/ for details), low-temperature intrusion oxidants in open fractures to depths greater than about –300 m above sea level, although these occurrences are not associated with flowing fractures detected by PFL.

Borehole examples of this near surface redox transition are shown for cored borehole KLX26A in Figure 7-26. The indicated decrease in pyrite distributions in open fractures at depths greater than about –800 m above sea level might, similarly to calcite, be due to a shift to a less hydraulically conductive interval at depths below –800 m above sea level, where Palaeozoic and later mineral precipitation (mostly influenced by descending fluids) is indicated to have been limited (cf. Section 5.6.4).

Gypsum of Generation 5 is present in 0.9% of the open fractures and in 0.2% of the sealed fractures (Figure 7-1). It is absent in most boreholes and the greatest occurrences are restricted to open fractures in isolated sections with low fracture frequency and low transmissivity at depths greater than –350 m.a.s.l (Figure 7-27), for example, in KLX03 (–490 to 620 m.a.s.l), KLX08 (Figure 7-28c), KLX10 (–940 to –960 m.a.s.l), KLX12A (mainly –390 to –460 m.a.s.l) and KLX17A (–360 to –390 and –540 to –560 m.a.s.l). All of these occurrences have been confirmed using XRD and/or SEM-EDS, in contrast to more shallow occurrences associated with less confidence (especially since gypsum is not easily distinguished from apophyllite and barite in the core mapping). The present distribution of gypsum is interpreted to not represent the original distribution of mineral precipitates /Drake and Tullborg 2007a/. Instead, the present distribution indicates dissolution at depths above –350 m above sea level and in highly transmissive zones. The deeper groundwaters in the Laxemar area are relatively rich in SO_4^{2-} which is attributed to dissolution of gypsum /cf. SKB 2006b/.

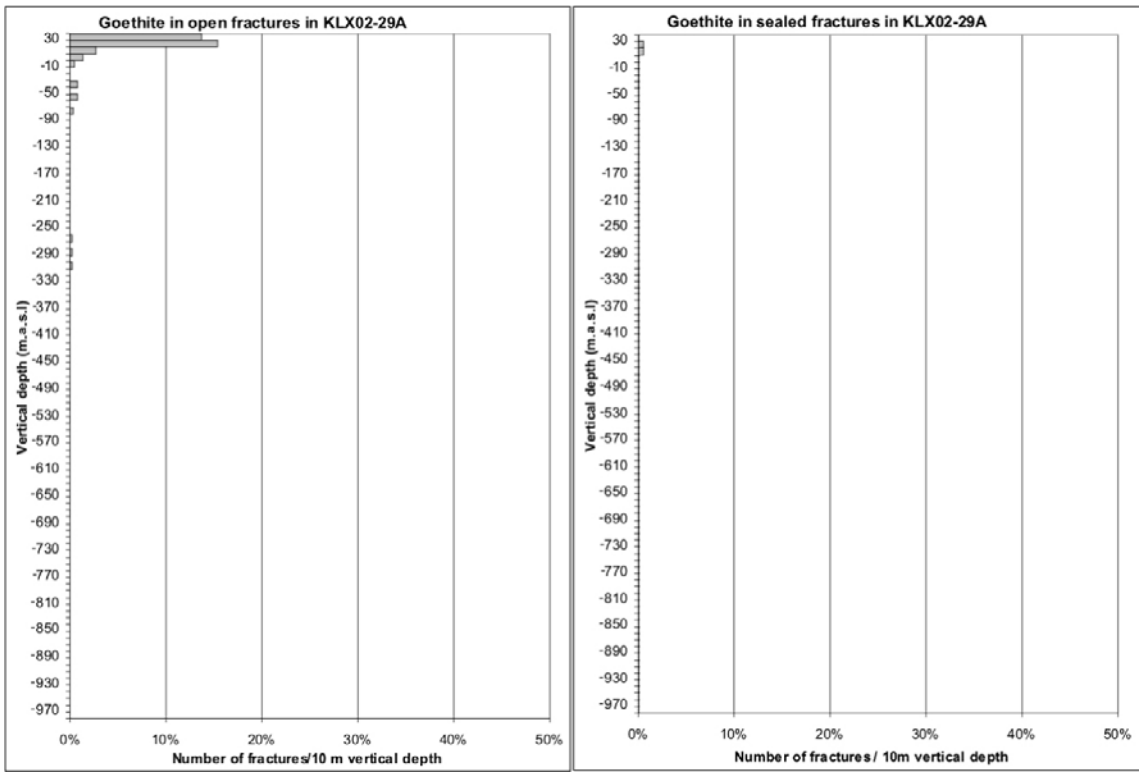

Figure 7-25. *Relative frequency of goethite in open as well as sealed fractures for each 10 m vertical depth interval from cored boreholes KLX02–29A.*

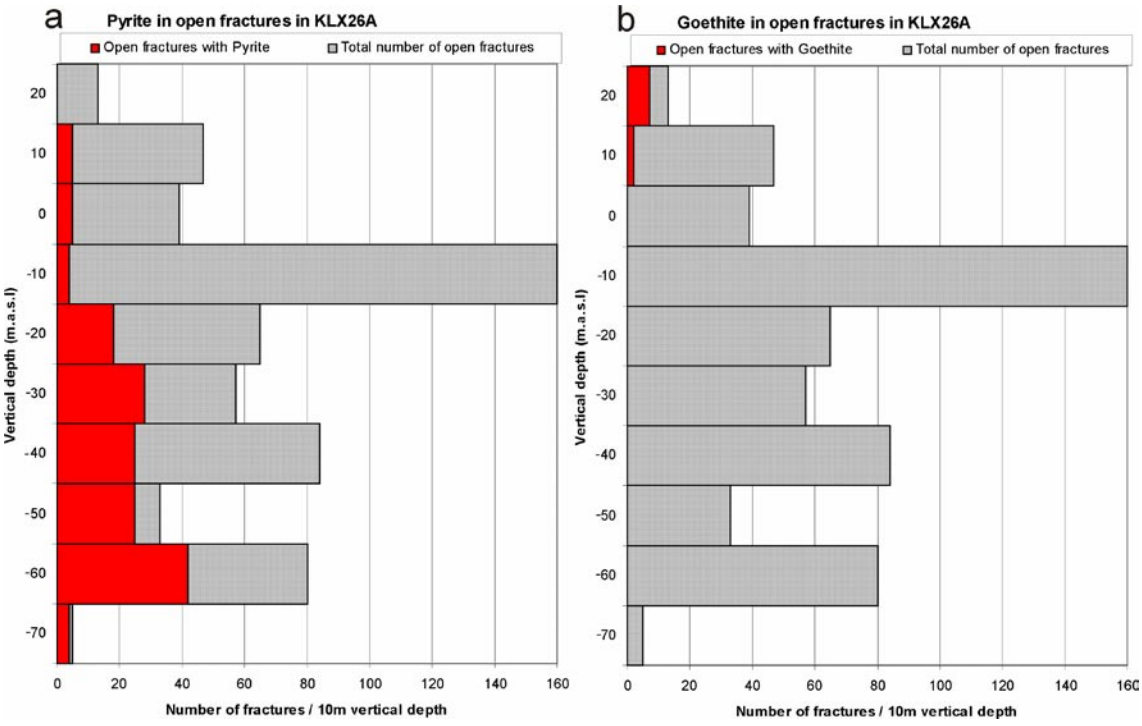

Figure 7-26. *Variation with depth of pyrite (a) and goethite (b) along open fractures in KLX26A. The total number of open fractures/10 m borehole interval is also shown.*

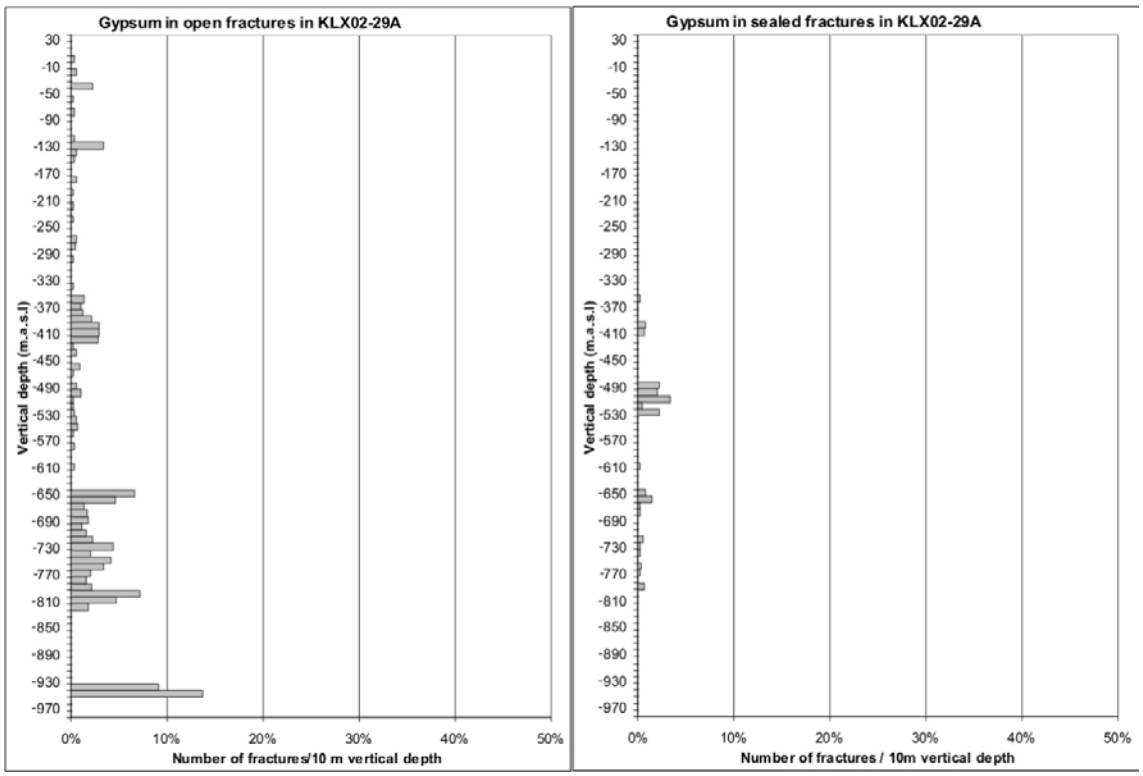

Figure 7-27. *Relative frequency of gypsum in open as well as sealed fractures for each 10 m vertical depth interval from cored boreholes KLX02–29A.*

A couple of other minerals also occur in limited sections in specific boreholes only. Talc, for instance, is only found in open fractures within the dolerite dyke in borehole KLX20A (Figure 7-28a). The most significant occurrence of muscovite is associated with greisen fractures in KLX06, below deformation zone ZSMEW002A (<–360 m above sea level). These fractures are mainly sub-horizontal (Figure 4-33a) and are most probably associated with the intrusion and post-magmatic circulation of the Götemar granite /Drake and Tullborg 2007a/ (see also Section 4.3). An interesting feature is that the greisen alteration appears to have been halted at the deformation zone ZSMEW002A and greisen alteration within the Laxemar subarea is quite rare.

Open fractures that do not contain any mineral coating and have fresh wall rock are commonly low in number and are scattered throughout most of the boreholes which are cored from 100 m borehole length and deeper, exemplified by the variation with depth in KLX15A in Figure 7-28d. However, the boreholes cored from the ground surface reveal an increase of this fracture type towards the ground surface as shown in Figure 7-29. Furthermore, in KLX04, the relative occurrence of these fractures is elevated within deformation zones based on single hole interpretation (at about –320 to –350 m above sea level in DZ6B and about –880 to –950 m above sea level in ZSMEW007A). Potentially, these fractures may be recently formed and are therefore of considerable interest. However, a number of uncertainties need to be addressed concerning these open fractures devoid of any mineral coating. These are:

- The mineral coating or filling is so thin that it has not been possible to identify any mineral along the fracture and has therefore been documented as a fracture devoid of minerals.
- The fracture has initially contained a mineral coating or filling, but this has been removed during aggressive drilling activity. However, the drill core quality in the Laxemar area is generally good.
- The fracture may have been generated in conjunction with the drilling activity (mainly hydraulic jacking or heat-induced effects during sharpening of drill bit by turning off the flushing water), or during subsequent handling of the core/core boxes, but was not excluded from the Sicada database.

In order to understand the geological significance of these fractures, a detailed study has been initiated and is currently ongoing.

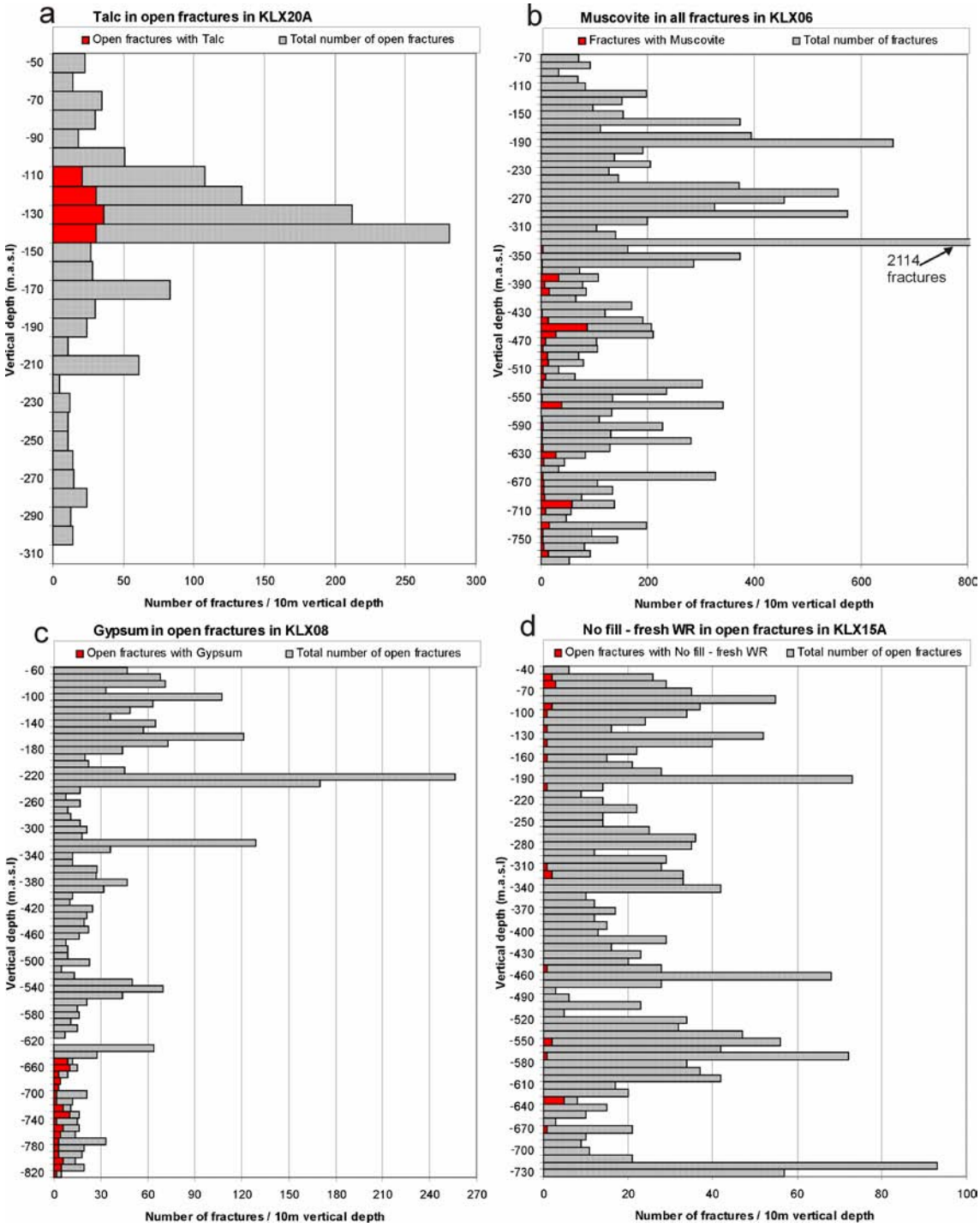

Figure 7-28. *Variation with depth of talc (a) along open fractures in KLX20A, muscovite (b, note that the x-axis has been cut) along all fractures in KLX06, gypsum (c) along open fractures in KLX08, and open fractures without any visible filling and with fresh wall rock (d) in KLX15A. The total number of fractures of the specific fracture type per 10 m borehole interval is also shown.*

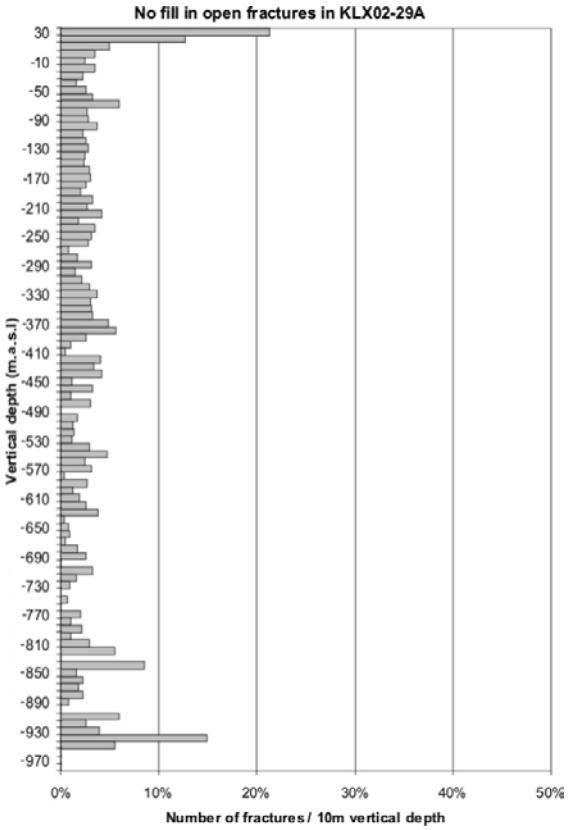

Figure 7-29. *Relative frequency of open fractures without visible fracture minerals for each 10 m vertical depth interval from cored boreholes KLX02–29A. Fractures from KLX02 are excluded because this borehole is drilled with conventional drilling technique which infers higher amounts of drilling induced fractures, grinding of drill core pieces and flushing away of loose fracture minerals.*

7.5 Distribution of clay minerals with depth

The depth distribution of clay minerals analysed with XRD is shown in Figure 7-30. The main clay mineral phases, mixed-layer clay of corrensite type or illite/smectite type and illite, are found at most depths from the ground surface to the maximum depths documented. However, illite and mixed-layer clay of illite/smectite are not as common at depths below –600 m above sea level, although the confidence in this trend is low since only a small number of samples have been analysed. Only a few samples with pure smectite (n=4), pure vermiculite (n=3) and kaolinite (n=1) have been identified, showing that these clay minerals are rare in the Laxemar subarea. The former two are distributed from the ground surface to great depths, while the only kaolinite sample documented is from a fracture near the ground surface. More detailed mapping of the occurrence of clay minerals is needed to confirm the few indicated depth related distribution anomalies.

7.6 Fracture mineralogy in hydraulically conductive fractures

Hydraulically conductive fractures have been distinguished using the Posiva Flow Log (PFL) /cf. Sokolnicki and Kristiansson 2007/, and are hereafter denoted as PFL-fractures. Only a small number of the open fractures are connected well enough to have a measurable transmissivity (PFL-fractures), and most open fractures may not be hydraulically connected. The variation of the fracture mineralogy of the open or partly open PFL-fractures in the Laxemar subarea, including fractures in deformation zones, have been analysed in this work. If several fractures exist in a PFL-section, the “best choice” fracture is chosen, i.e. the fracture which is interpreted to have the highest transmissivity in the PFL-section, as reported in the Sicada database. The distribution of PFL-fractures containing calcite and chlorite are shown in Figure 7-31, clay minerals and fractures with no visible filling are shown in Figure 7-32, and pyrite and goethite, from all cored boreholes from the Laxemar subarea, are shown in Figure 7-33. Also included in these figures is the total number of open or partly open fractures.

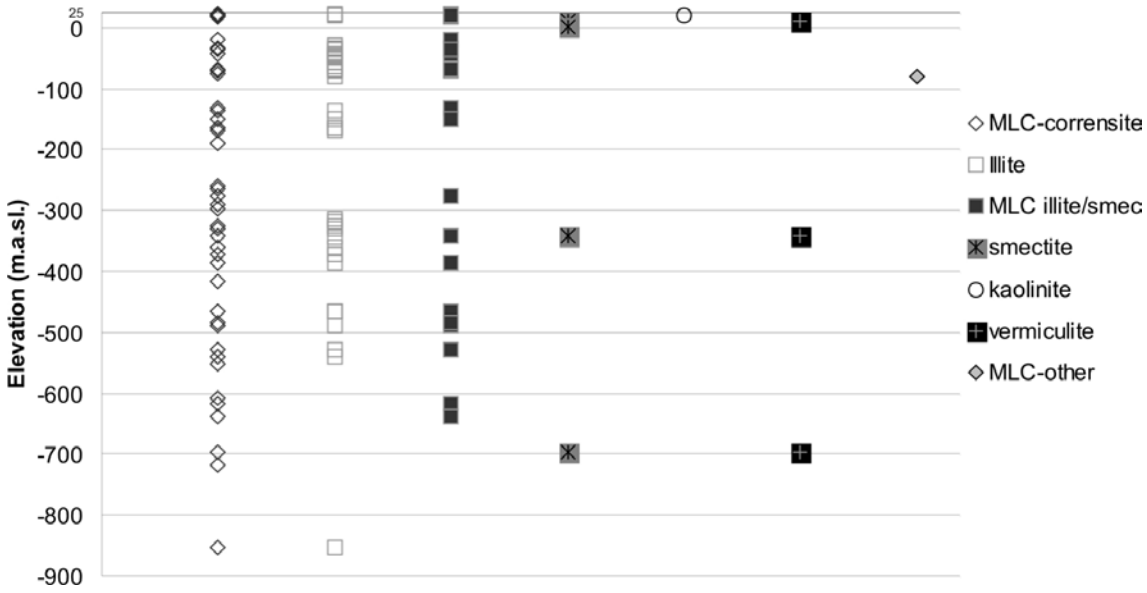

Figure 7-30. *Depth distribution of different clay minerals identified by XRD.*

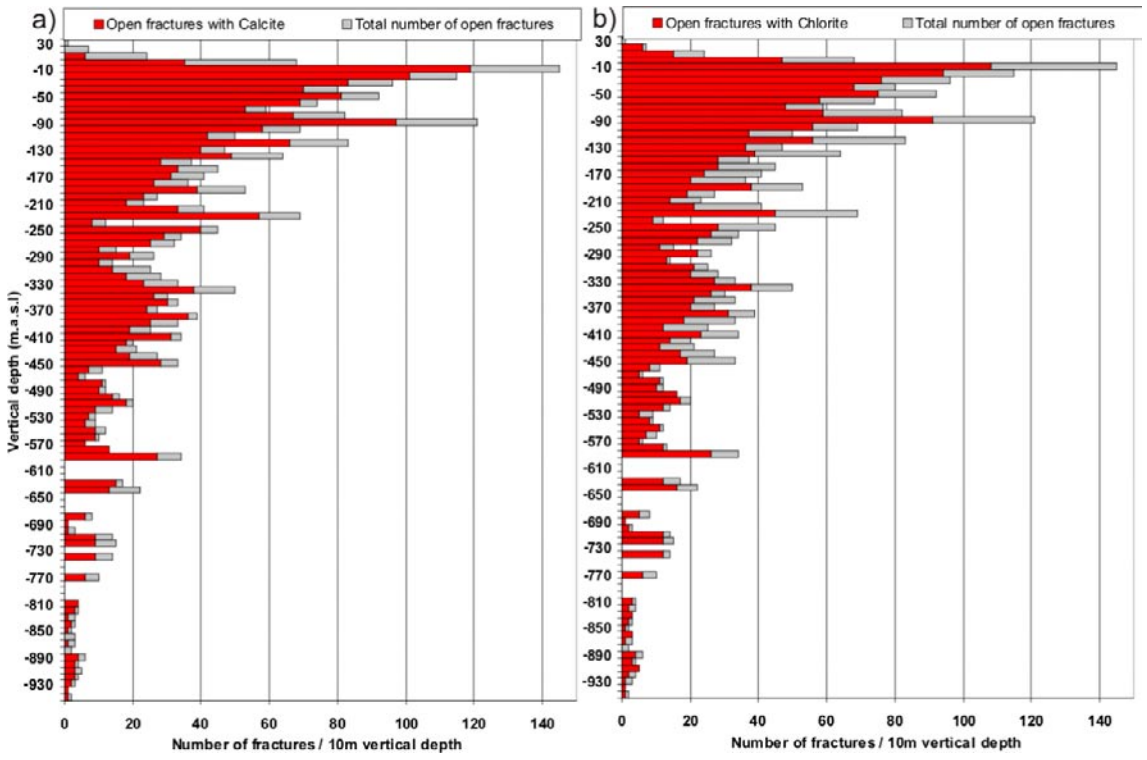

Figure 7-31. *Variation with depth of calcite (a) and chlorite (b) along open PFL-fractures in KLX02–29A. The total number of open fractures per 10 m borehole interval is also shown.*

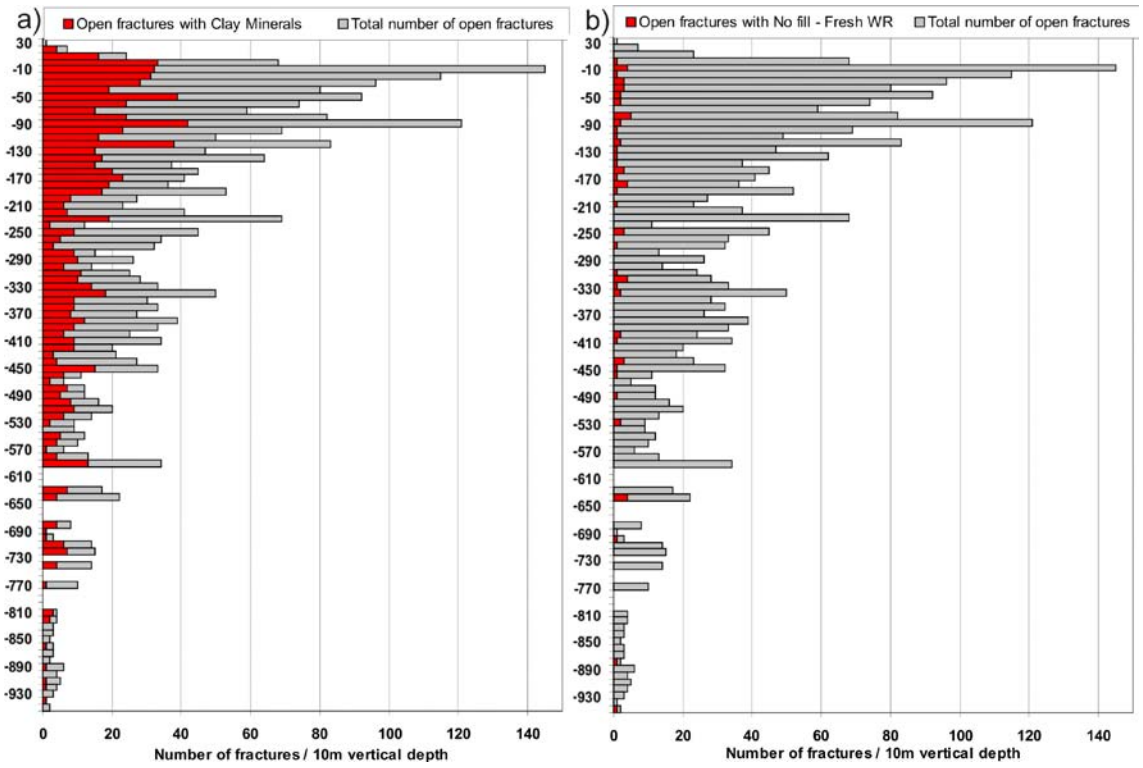

Figure 7-32. *Variation with depth (elevation m above sea level) of clay minerals (a) along open PFL-fractures in KLX02–29A. Fractures without visible fracture minerals and with fresh wall rock are shown in (b). The total number of open fractures per 10 m borehole interval is also shown.*

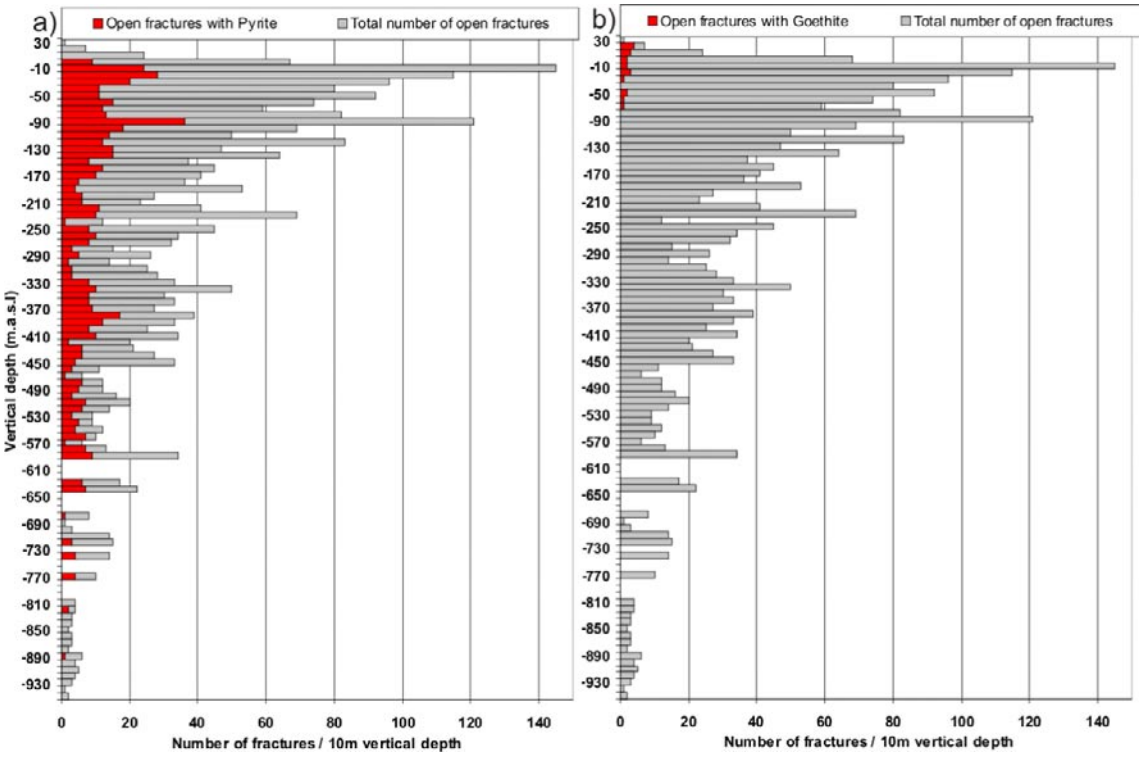

Figure 7-33. *Variation with depth of pyrite (a) and goethite (b) along open PFL-fractures in KLX02–29A. The total number of open fractures per 10 m borehole interval is also shown.*

Many of the presently water conducting fractures are coated by fracture minerals of Palaeozoic origin or sometimes older, in addition to possible recent precipitates /Drake and Tullborg 2008c, d, e/. This shows that the present groundwater flow occurs along fractures where fluids also circulated during the Palaeozoic and/or during earlier times. The number of PFL-fractures decreases with depth (cf. Figure 7-31, and /Rhén et al. 2009/). However, the dominance of near-surface PFL-fractures may be slightly exaggerated due to the preferential length and projection of the boreholes, for example, many shallow boreholes have been oriented specifically towards deformation zones. The limited number of PFL-fractures in the 0 to 30 m above sea level interval is mainly due to the fact that the uppermost part of the boreholes are generally not flow logged /cf. Sokolnicki and Väisäsvaara 2006, Sokolnicki and Kristiansson 2007/. In addition, there is a lack of confidence of mineral frequency from depths greater than –600 m above sea level due to the relatively low amount of PFL-fractures.

The frequency of calcite and chlorite is very high in the PFL-fractures (Figure 7-31), and largely in accordance with the amount of these minerals in open fractures (Figure 7-14 and Figure 7-15). The frequency of calcite and chlorite generally follow the frequency of the PFL-fractures with depth, although there is a clear decrease in the calcite frequency in the upper 30 m related to near surface dissolution (cf. Sections 6.2.1.1 and 7.4).

Clay minerals are the third most common fracture mineral (after calcite and chlorite) in hydraulically conductive fractures. In general, clay minerals also show similar frequency in PFL-fractures as in open fractures and the frequency of these minerals usually varies with the frequency of the PFL-fractures with depth (Figure 7-32a). However, clay mineral frequency is low below –600 m above sea level but, as stated above, the confidence of the mineral frequency at these depths is also quite low. The frequency of potentially young PFL-fractures without visible fracture mineral coatings show small variation with depth (Figure 7-32b), although there are fewer fractures below –530 m above sea level. The trend of increasing frequency of fractures devoid of mineral coatings towards the surface, as shown in Figure 7-29, including all open fractures, is not identified for the PFL-fractures. This is, at least partly, because the shallow depths where the empty fractures are dominantly found are not covered by the differential flow log measurements.

Regarding the redox sensitive minerals pyrite and goethite, a similar trend is seen for the PFL-fractures (Figure 7-33) as was earlier shown for all open fractures (Figure 7-24 and Figure 7-25), namely the depletion of pyrite and formation of goethite above the redox front in the upper tens of metres of the bedrock and occasionally at greater depths. A notable observation is the consistently high frequency of pyrite below the redox front down to depths of at least about –600 m above sea level in the hydraulically conductive fractures (Figure 7-33a).

Other common minerals such as epidote, quartz, prehnite and hematite, generally do not show any significant variation with depth in the PFL-fractures.

7.7 Concluding remarks

Calcite and chlorite are by far the most common fracture minerals in the Laxemar area, and these are especially frequent in the open fractures. These minerals dominate in all of the different rock domains, fracture domains, deformation zones and in hydraulically conductive fractures. Clay minerals, pyrite and hematite are also most frequently found in open fractures and are also frequent in hydraulically conductive fractures, whereas epidote, adularia, quartz and prehnite are more frequent in sealed fractures. Additional minerals, for example, gypsum, are found in less than 1% of the fractures. Wall rock alteration is common, especially adjacent to sealed fractures. 2.5% of the open fractures without wall rock alteration do not contain any macroscopically visible fracture minerals. These fractures may possibly be young and become more frequent towards the ground surface. Further studies are, however, needed to understand the significance of these fractures.

The frequency of most of the minerals is similar in the different rock domains, for example. clay minerals and prehnite as well as fractures without visible fracture minerals. However, some variations exist and these are apparently mainly related to the difference in chemistry and mineralogy of the dominant rock types in the different rock domains. Noteworthy fracture mineral frequency differences are the lower amounts of chlorite, calcite, epidote and gypsum and higher amounts of adularia and quartz in rock domain A01 compared with the other rock domains.

The difference in fracture mineral frequency between the different fracture domains is not as apparent as between the rock domains. Instead, the wall rock chemistry seems to have influenced the fracture mineralogy to a higher degree than the different fracture intensity characteristics of the fracture domains.

Chlorite and calcite show no distinct variation with depth. Exceptions are the lower amount of calcite (and slightly lower amount of chlorite) in the uppermost 10–20 m, and slightly lower amounts of calcite below about –800 m above sea level. The former depletion is probably related to near surface dissolution, and the latter decline for calcite marks the shift to a less dynamic hydraulic system with limited precipitation of calcite spanning in time from the Palaeozoic to recent. The frequency of clay minerals and hematite generally do not show any distinct variation with depth, although the relative frequency is commonly higher in deformation zones. Different clay minerals appear to be evenly distributed with depths. The hydrothermal minerals epidote and prehnite of Generation 3 show no systematic variation in occurrence with depth. Similar invariable depth distributions are shown for quartz and adularia, both mainly of hydrothermal origin. Pyrite is a common mineral in open fractures at most depths, although there is a clear decrease in frequency near the surface due to oxidative dissolution of pyrite. This dissolution is accompanied by formation of goethite in open fractures during oxidising conditions in the same depth interval and the distribution of these minerals indicates the location of the recent near surface redox front. Gypsum is absent in most boreholes and the largest occurrences identified are generally restricted to open fractures in isolated sections with low fracture frequency and low transmissivity at depths greater than –350 m above sea level.

8 Fracture filling geochemistry

The fracture filling geochemistry has been determined by:

1) Mineral specific SEM-EDS analyses or ICP-MS analyses of specific mineral grains or leachates of pure mineral aggregates. The former gives the major and minor chemical composition while the latter gives the trace element composition as well.
2) ICP-AES/QMS analyses of entire fracture fillings scraped off from the fracture surface. This gives both the major and trace element composition of the fracture coatings, although the samples consist of a mixture of minerals.

8.1 Geochemistry of selected fracture minerals

The geochemistry of selected fracture minerals from the Laxemar area is based on SEM-EDS analyses of individual mineral phases in thin section or more rarely directly on freely growing crystals on sawn-off fracture surfaces /Drake and Tullborg 2004, 2005, 2006b, 2007a, 2008e/. Trace element analyses of calcite and gypsum have been carried out by ICP-MS /Drake and Tullborg 2004, 2007a/.

Calcite

Calcite is a relatively pure $CaCO_3$ with low contents of FeO and MgO (usually below 0.1 wt.%). However, MnO contents are occasionally highly elevated with concentrations of up to 4 wt.%, although the median concentration is ~0.3 wt.%. The Sr content varies between different generations. The most abundant calcite in open fractures (Generation 5 and 6), generally has Sr concentrations between ~30–100 ppm, whereas concentrations between 215–450 ppm have been detected in Generation 3 calcite. Both U and Th contents are low, usually below 0.2 ppm. Besides calcite, a REE-rich carbonate (probably bastnäsite) rich in, for example, La, Ce, Nd, Y and F, has been identified in both open and sealed fractures. The calcite geochemistry is discussed in detail in Section 5.4.

Chlorite and corrensite

Chlorite and the most common clay mineral corrensite are the most important Fe^{2+} bearing fracture minerals in the Laxemar area. Measurements from Äspö show Fe^{3+}/Fe_{tot} ratios of 0.329 to 0.437 in chlorite /Tullborg 1995/. The FeO (representing total Fe) and MgO contents in the analysed chlorite vary widely between the different generations, for example old hydrothermal (Generation 3) chlorite has 13.5–20.5 wt.% MgO and 19–29 wt.% FeO with younger Mg-rich chlorite having 15–22.5 wt.% MgO and 4.5–10 wt.% FeO. The youngest and most common chlorite in open fractures is Fe-rich and has ~2–7 wt.% MgO and 31–46 wt.% FeO. Corrensite usually has FeO contents of about 30–35 wt.% but this content varies widely and the range can be up to 15–53 wt.%; the MgO content varies between 2–12 wt. %. Minor amounts of CaO, K_2O and Na_2O are commonly observed in corrensite. MnO contents are usually between 0.1–0.3 wt.% in corrensite and between 0.3–0.7 wt.% in chlorite.

Epidote and prehnite

The iron-phase in epidote and prehnite is almost exclusively Fe^{3+}. The Fe_2O_3 content in epidote varies between 12–18 wt. % and the CaO content is ~ 21–23 wt%. The MnO content generally varies between 0.1–0.8 wt.% but a Mn-rich variety of epidote has also been identified. The Fe_2O_3 content in prehnite is between 0.6–9.2 wt%.

Zeolites

Laumontite has a CaO content between 10–12 wt.% and the FeO content is usually below 0.1 wt.%. Laumontite may include up to 1.0 wt.% Na_2O or K_2O. The Ba-zeolite harmotome includes up to 3 wt. % Na_2O, 1.0 wt.% K_2O and 0.3 wt.% CaO in addition to BaO, Al_2O_3, SiO_2 and water. Analcime consists of Na_2O, Al_2O_3 and SiO_2 and water only.

Sulphides

Pyrite of pure FeS_2 composition is the dominant sulphide mineral and constitutes more than 99% of all the sulphides. Other sulphides present are chalcopyrite, galena and sphalerite and very rarely argentite and arsenopyrite.

Sulphates

Barite is of quite pure $BaSO_4$ composition and ICP-MS analyses of gypsum leachates show that the trace element content is usually low. The only notable trace element concentrations are Fe contents which are between 0.1–0.2 wt.% and Sr contents which are between 130–220 ppm. Celestine is very rare and no analysis has been carried out.

Adularia and albite

Adularia sometimes has elevated BaO contents of up to 0.9 wt.%. Albite is of pure composition and has a very low CaO content (<0.2 wt.%).

8.2 Geochemistry of bulk fracture filling material

K, Cs, Rb, Ba

K^+, Rb^+ and Cs^+ have similar valence and ionic size and therefore behave similarly; they are mainly hosted in K-feldspar, micas and clay minerals. Ba^{2+} is similar to K^+ in ionic size and is preferentially incorporated into K-feldspar in granitic rocks /De Albuquerque 1975/. Rb, Ba and Cs show positive correlation with K_2O in the fracture fillings (Figure 8-1 and Figure 8-2), although samples enriched in specific minerals may show anomalies for one or more of these elements. The main K-bearing phases in the Laxemar area are adularia, illite and other clay minerals. Muscovite, apophyllite, harmotome and hornblende also contain potassium but are either not very frequent or contain very small amounts of potassium. The main Ba-bearing fracture minerals in the Laxemar area are barite, harmotome (Ba-zeolite) and adularia; adularia contains less Ba than barite and harmotome but is more abundant. XRD and SEM-EDS analyses show that all samples with Ba concentrations above 5,000 ppm contain harmotome or barite (Figure 8-1), and samples moderately enriched in Ba compared with the wall rock are commonly rich in adularia.

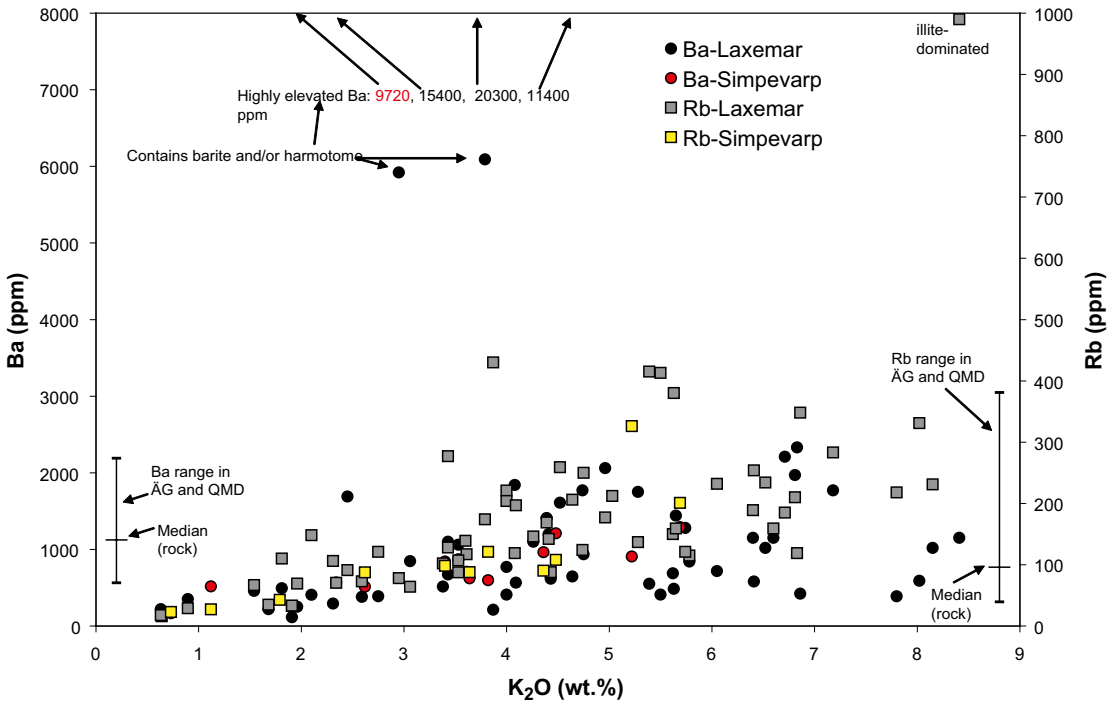

Figure 8-1. Ba (left y-axis) and Rb (right y-axis) versus K_2O in bulk fracture fillings. Vertical bars indicate the compositional span and median in Ävrö granite (ÄG) and quartz monzodiorite (QMD).

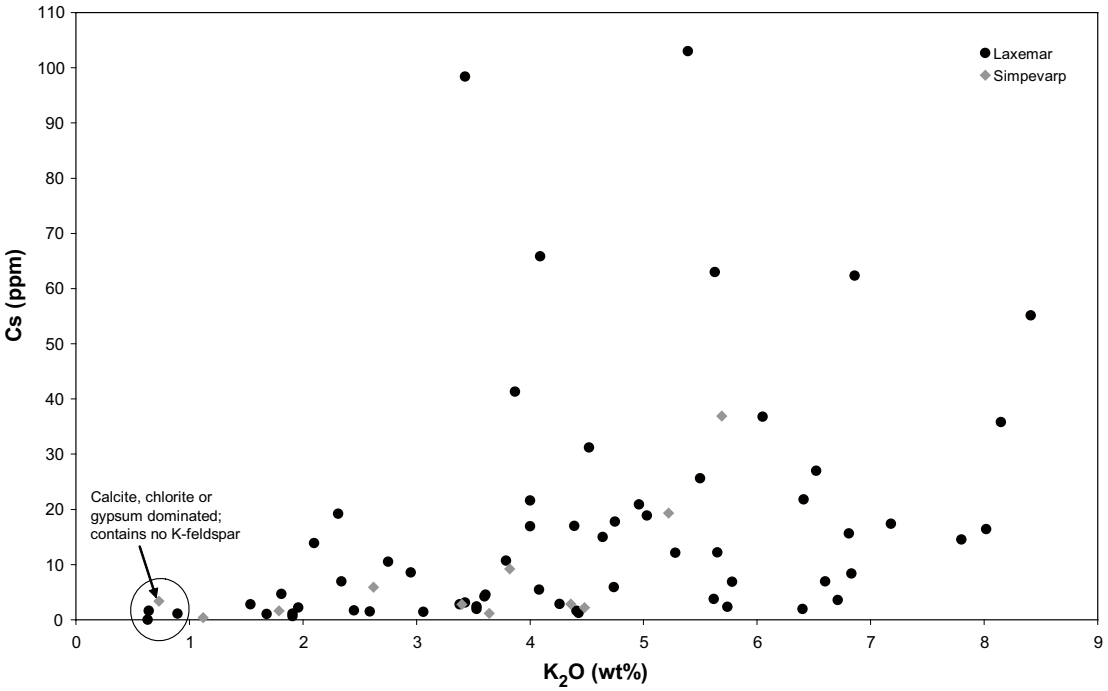

Figure 8-2. *Cs versus K_2O in bulk fracture filling material. The Cs content in Ävrö granite and quartz monzodiorite in the Laxemar area varies between 0.6 and 3 ppm.*

Cs is enriched in many of the samples compared with the wall rock (Figure 8-2). Samples with very low Cs and K_2O concentrations are either dominated by calcite, gypsum or chlorite but contain no K-feldspar. The samples with very high Cs concentrations are also quite K_2O- and Rb-rich (Figure 8-3). K-bearing clay minerals, such as illite and mixed-layer clay, are the most likely sinks for the large Rb^+ and especially Cs^+ ion in the fracture systems during present conditions. This is supported by samples with Cs concentrations of above ~40 ppm all containing illite and/or mixed-layer clays (Figure 8-3); the most Rb-rich sample is completely dominated by illite.

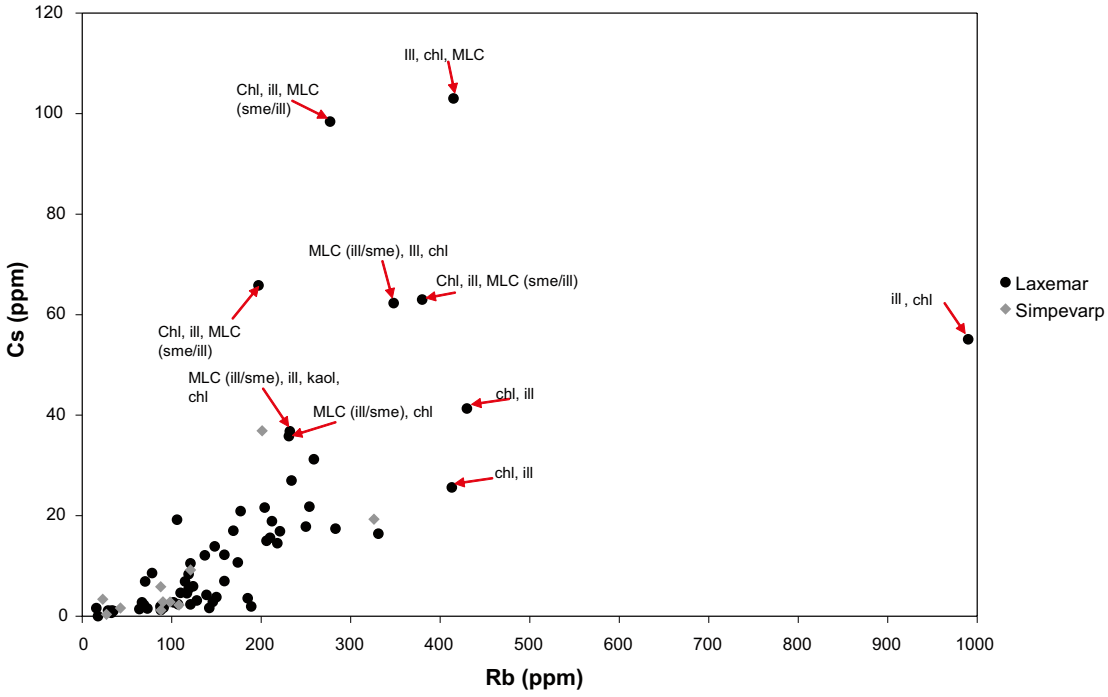

Figure 8-3. *Rb versus Cs in bulk fracture filling material. Relevant fracture minerals (identified by XRD) are indicated on samples with elevated concentrations. Chl = chlorite, Ill = illite, kaol = kaolinite, MLC = mixed-layer clay, Sme = smectite. Minerals in brackets next to MLC indicate its main composition.*

Samples with high Ba concentrations (>5,000 ppm) are only found down to –170 m above sea level (Figure 8-4), which is in accordance with the near surface concentration of Ba-zeolite /cf. Drake and Tullborg 2004, 2007a/.

No significant trends can be seen when Cs and Rb is plotted against elevation; any variation seen is probably due to variations in the abundance of clay minerals (Figure 8-5 and Figure 8-6). However, since the Cs concentrations are much higher in the fracture coatings than in the wall rock, it is indicated that Cs has been has been mobilised from the wall rock, for example, as a result of biotite alteration, and has been retained in the fracture minerals.

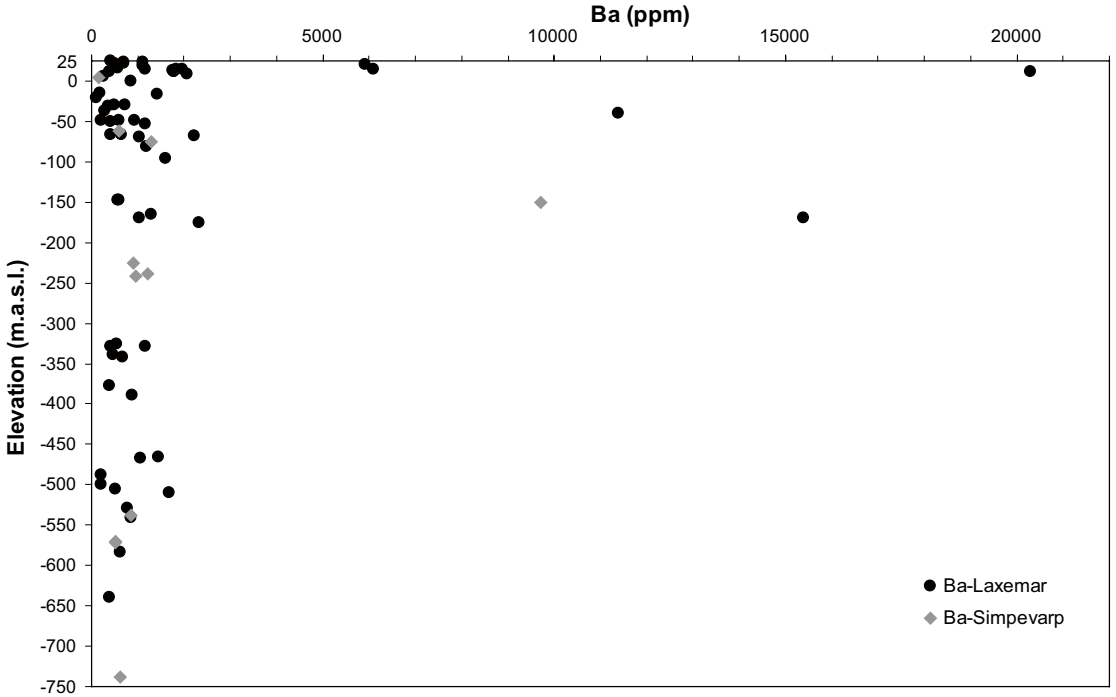

Figure 8-4. *Ba versus depth (elevation) in bulk fracture fillings.*

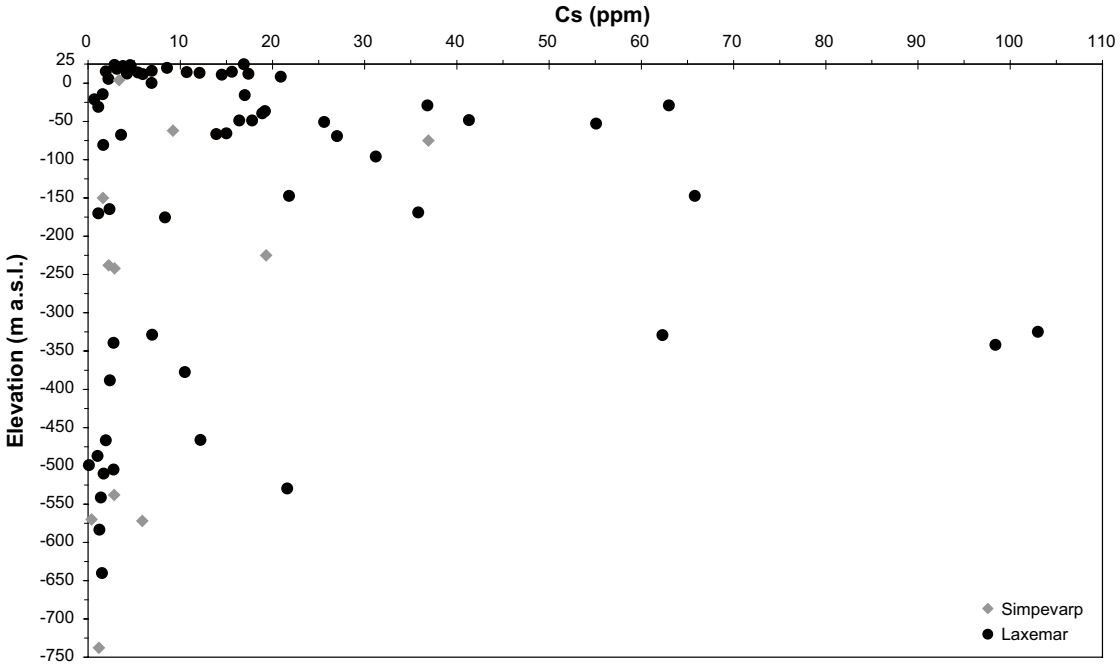

Figure 8-5. *Cs versus depth (elevation) in bulk fracture fillings.*

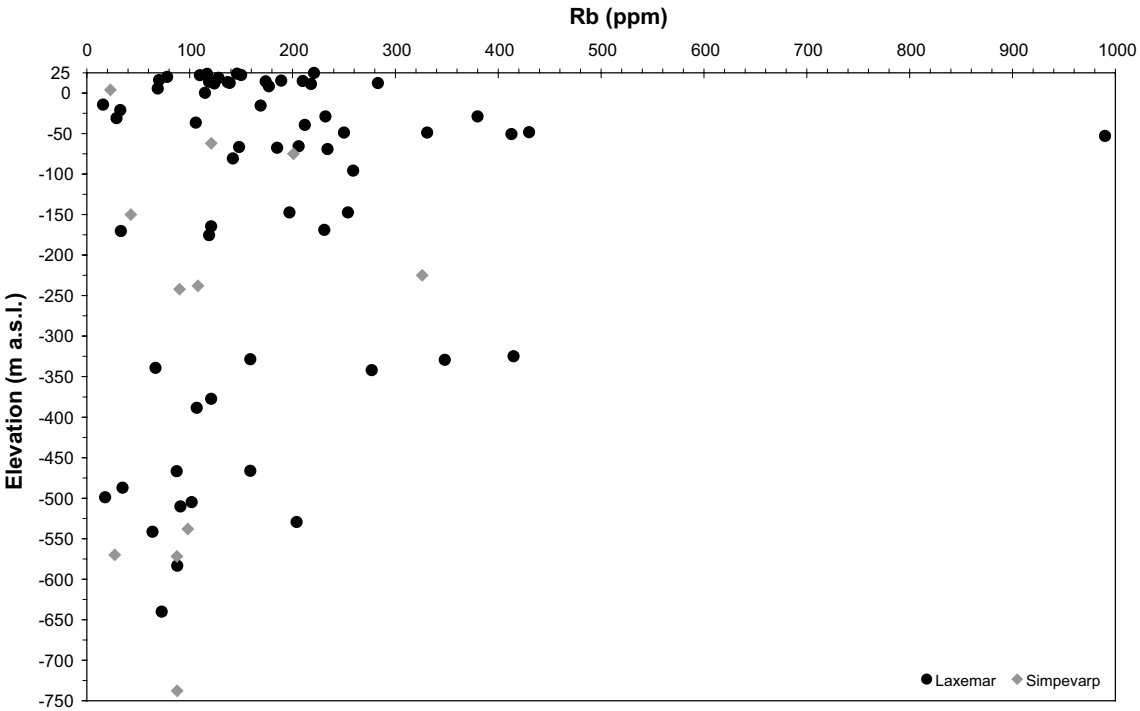

Figure 8-6. *Rb versus depth (elevation) in bulk fracture fillings.*

Na, Ca, Sr

Albite is the main Na-bearing fracture mineral with analcime and hornblende containing minor amounts of sodium. Na^+ is also incorporated in small amounts in smectite which occurs in mixed-layer clay, mainly in corrensite or interlayered with illite, but also as a pure clay mineral. In addition, small amounts of Na^+ are incorporated in apophyllite, harmotome and laumontite.

The main Ca-bearing mineral is calcite. Ca-Al-silicates are also abundant, especially epidote, prehnite and partly laumontite; minor Ca-bearing phases identified are fluorite, apophyllite, apatite and gypsum, and small amounts of Ca^{2+} are incorporated in smectite and vermiculite. The correlation between Ca^{2+} and Sr^{2+} differs between samples dominated by different minerals. Samples rich in calcite, fluorite or gypsum (high CaO content) show low Ca^{2+}/Sr^{2+} ratios, whereas mainly epidote-rich samples with low concentrations of CaO show much higher Sr^{2+} contents (and thus much higher Ca^{2+}/Sr^{2+} ratios (Figure 8-7)). Calcite usually has low Sr concentrations (30–100 ppm), although hydrothermal calcite has up to 450 ppm (cf. section 5.4 and /Drake and Tullborg 2009a/). Samples with a high content of mixed-layer clay also indicate a high affinity for Sr^{2+}, but this may also be related to the other minerals in the sample.

Fracture filling Ca/Sr-ratios indicate enrichment or depletion of Sr compared with the wall rock and groundwater. Figure 8-8 shows that the Ca/Sr-ratios of the fracture fillings overlap with those of the wall rock but are commonly higher, especially when compared with the two main rock types in the Laxemar subarea (501046 and 501056). In general, the groundwater has a somewhat higher and wider range in ratios than the wall rock, and most Ca/Sr-ratios of the fracture fillings overlap with those of the groundwater and/or the wall rock. Samples with lower ratios are usually epidote-rich and samples with higher ratios are commonly rich in calcite, gypsum or fluorite, of which the calcite dominated samples are found in the upper approximately 500 m of the bedrock. These calcites with highly elevated Ca/Sr-ratios are probably Palaeozoic or younger, i.e. the calcite types with low strontium concentrations (cf. Section 5.4), showing that the mobility at low temperatures is higher for calcium compared with strontium and/or temperature-related fractionation between calcite and the fluid.

The near surface groundwaters from the overburden show higher Ca/Sr-ratios (around 200–300) whereas the ratios for groundwaters in the percussion boreholes from the upper 100 m of the bedrock show ratios around 120–220, and the groundwaters from levels deeper than 100 m in cored boreholes show even lower ratios of around 110–130 (values calculated from the Laxemar 2.3 groundwater

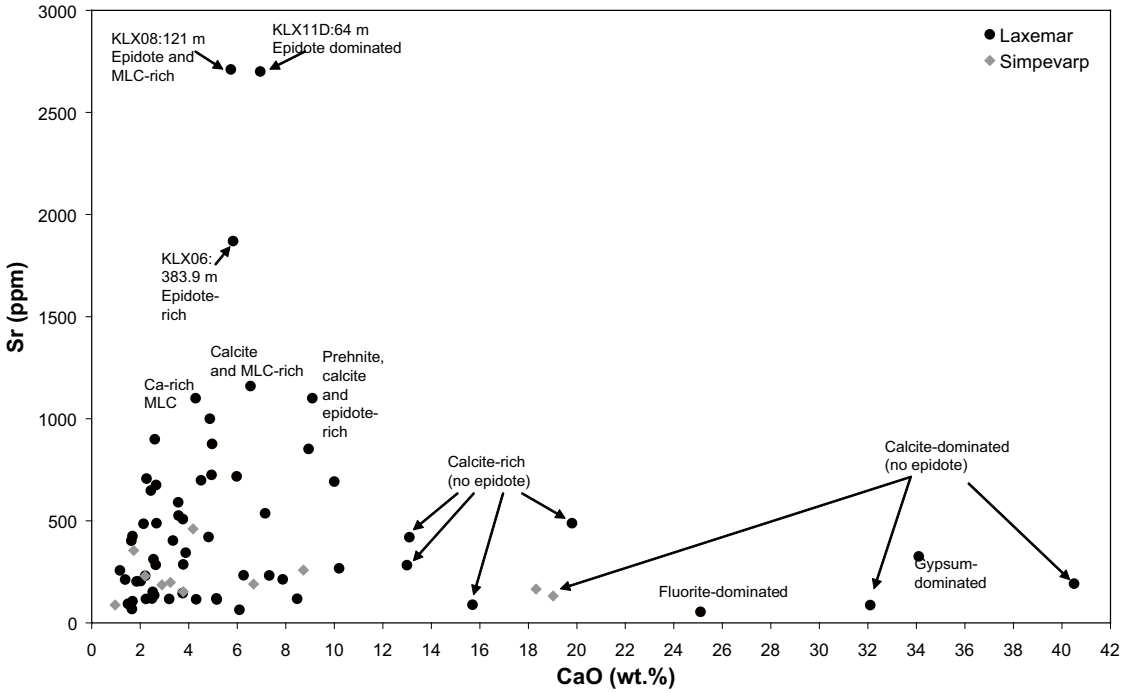

Figure 8-7. *CaO (wt%) versus Sr (ppm) in bulk fracture fillings. Relevant fracture minerals (identified by XRD) are indicated on samples with elevated concentrations. MLC = mixed-layer clay.*

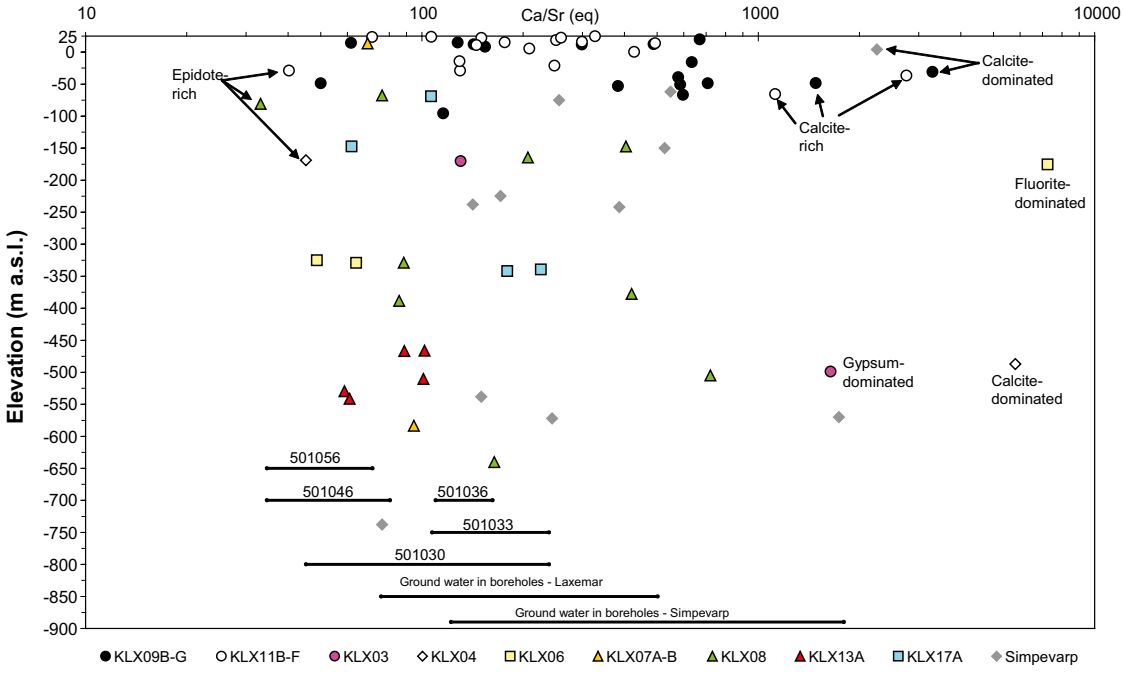

Figure 8-8. *The Ca/Sr ratio (based on equivalents) in bulk fracture fillings versus depth (elevation). The horizontal lines represent the ranges in Ca/Sr-ratios in the most abundant rock types in the Laxemar area; 501056: Ävrö granodiorite, 501046: Ävrö quartz monzodiorite, 501036: quartz monzodiorite, 501033: diorite to gabbro, 501030: fine-grained dioritoid, as well as the Ca/Sr-ratios in groundwater samples from cored boreholes in the Laxemar and Simpevarp subareas.*

data set, defined by the extended data freeze per November 30, 2007, extracted from Sicada). This indicates a higher influence on the Ca/Sr-ratios from calcite dissolution in the thin Quaternary overburden and in the very uppermost part of the bedrock than at greater depth. The Ca/Sr-ratios in the deeper groundwaters are probably more controlled by water-rock interaction, probably mainly ion exchange but also alteration of silicate minerals.

Fe, Mg, Mn

Most of the iron in the Laxemar area is hosted in chlorite and in the clay minerals, mainly Fe-rich corrensite, but also in other types of mixed-layer clay and to a lesser extent illite. Pyrite is an important and frequently observed Fe^{2+}-bearing mineral but the volumes are still small, especially in single fractures. Less common sulphides like chalcopyrite also carry iron, but in negligible volumes. Fe-bearing phases of ferric iron (Fe^{3+}) are mainly epidote and prehnite in addition to hematite and goethite, but the latter are usually found only in trace amounts on the fracture coatings (seldom >1 vol.%).

The generally positive correlation between iron and magnesium shows that iron is, as pointed out above, mainly hosted in mangnesium carrying minerals like chlorite and clay minerals (dominantly corrensite or illite) in the fracture system (Figure 8-9. MgO is also hosted in talc and, for example, antigorite, but this mineral only appears sporadically. The variation in Fe/Mg-ratios in the fracture fillings is generally related to the variation of these elements in chlorite and corrensite. However, samples with very high iron and fairly low magnesium contents commonly have a significant hematite and/or goethite component. Increased amounts of chlorite and clay minerals generally correlate with significantly higher amounts of iron and magnesium in the fracture coatings than in the dominant rock types forming the wall rocks (Figure 8-9). There are no significant depth related trends for Fe_2O_3 (representing total iron), except for the elevated concentrations found in some of the near surface samples which are rich in hematite and/or goethite.

Manganese shows a positive correlation with iron suggesting its presence in chlorite and clay minerals (Figure 8-11) and, in similarity with iron and magnesium, it is highly enriched in most fracture fillings compared with the dominating rock types (0.05–0.14 wt.% MnO). The highest MnO concentrations are found in the upper ~50–100 m of bedrock (Figure 8-12), and especially in the upper approximately 10 m in samples containing Mn-oxide (or Mn-oxyhydroxide) and Mn-rich mixed-layer clay. The MnO concentration in one of these samples is as high as 6.27 wt.%. Possible explanations for the elevated manganese contents near the surface are microbial manganese reduction of organic material /Tullborg 2003/. Mn^{2+} is effectively bound in complexes with organic colloids in groundwater /Pourret et al. 2007/ and may thus be enriched in downward percolating organic-rich groundwaters. In the Laxemar area, the number of Mn reducers in groundwater show a large variation but the three borehole sections with the highest number of manganese-reducing bacteria are all from the upper 500 m /Hallbeck and Pedersen 2008/.

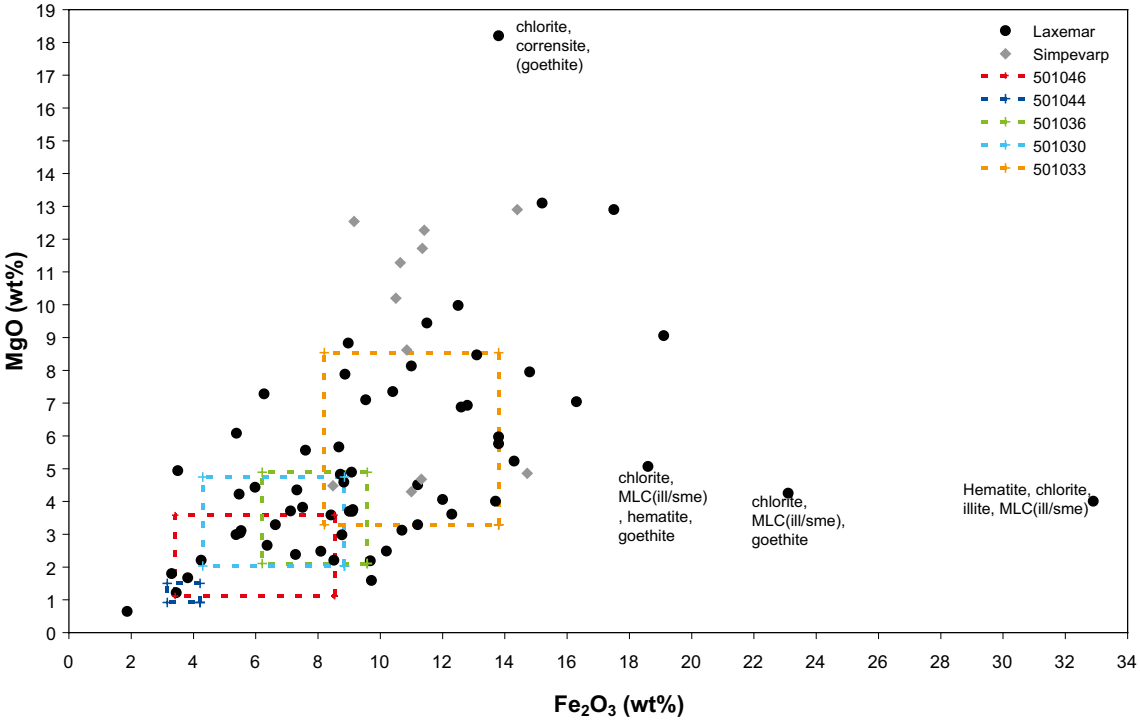

Figure 8-9. *Fe_2O_3 (representing total iron) versus MgO for fracture filling samples. The dashed coloured boxes indicate the compositional span in the dominant rock types of the area.*

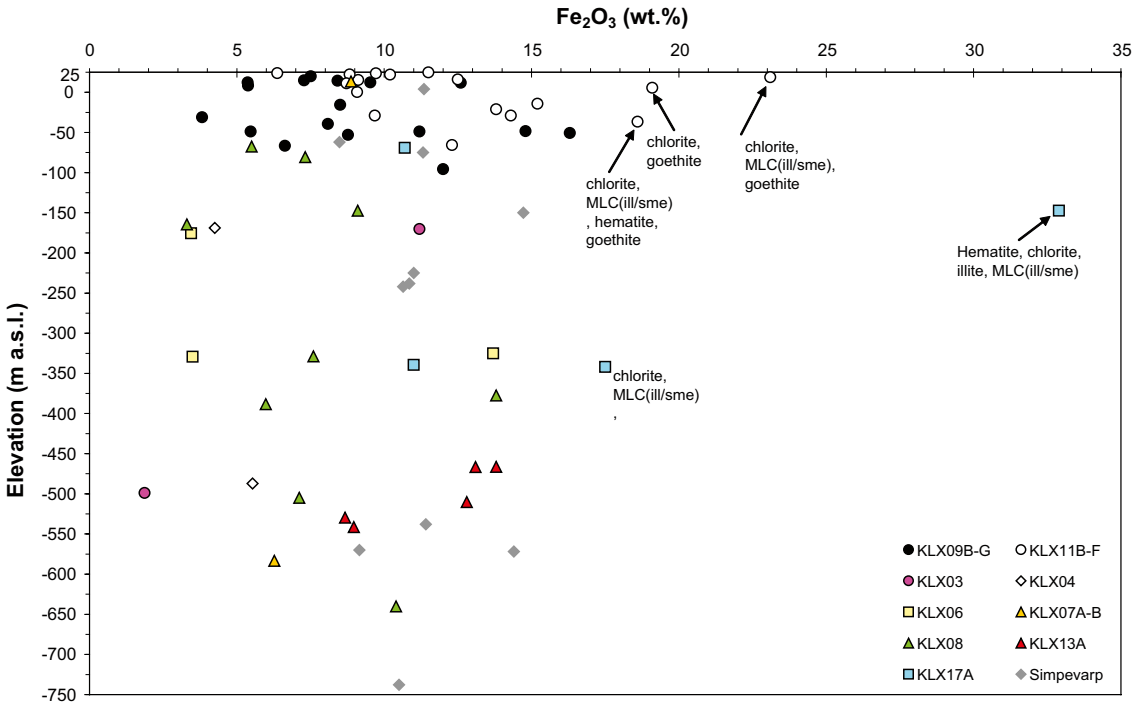

Figure 8-10. *Fe_2O_3 (representing total iron) in fracture fillings versus depth (elevation).*

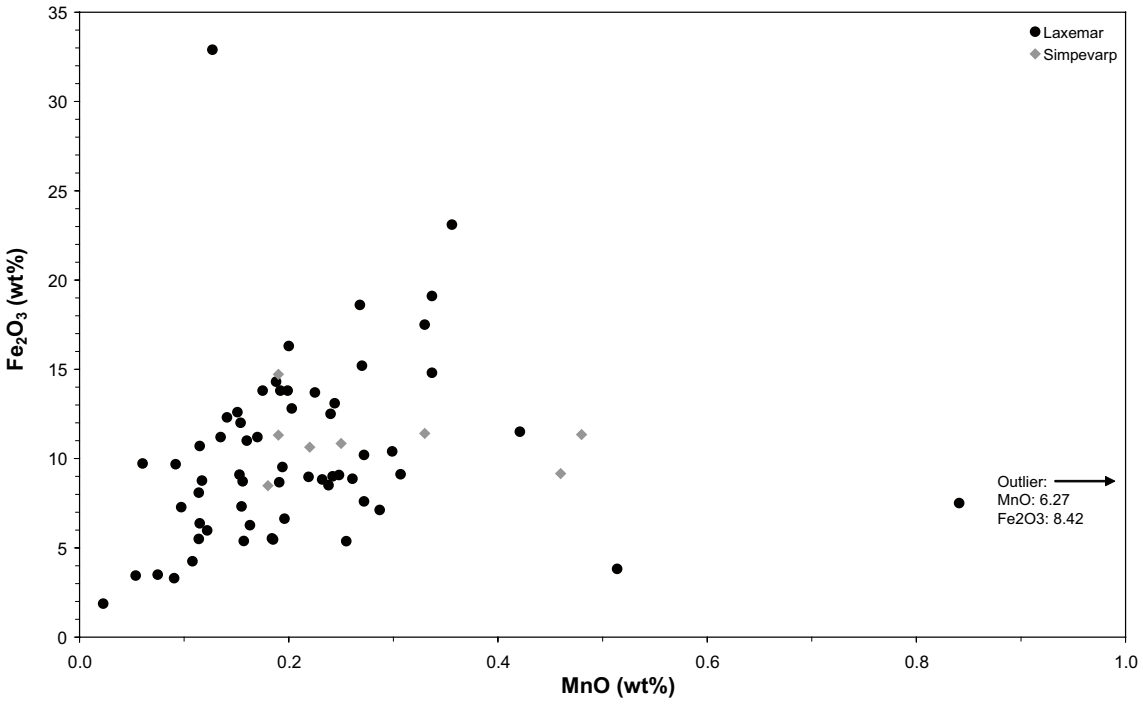

Figure 8-11. *Fe_2O_3 (representing total iron) versus MnO for fracture filling samples. One sample highly enriched in MnO plots outside the area shown.*

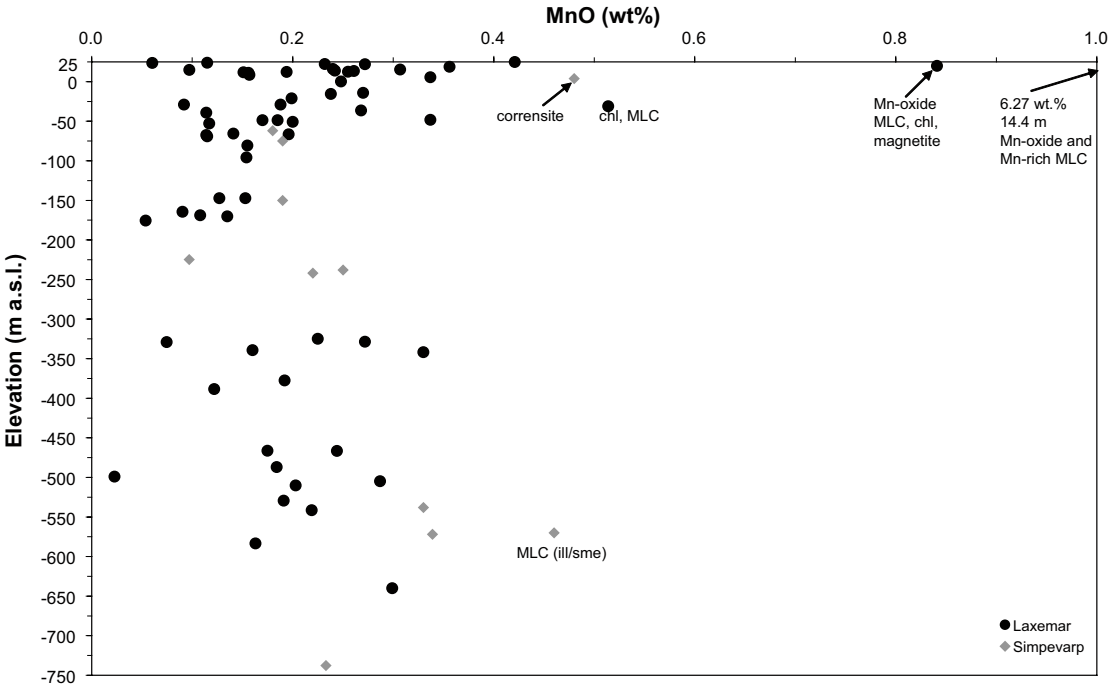

Figure 8-12. *MnO in fracture fillings versus depth (elevation). The dominating rock types in the area have MnO concentrations of 0.05–0.14 wt.%.*

U, Th

The uranium content in bulk fracture fillings varies from 0.8–43 ppm and thorium concentrations are from 0.26–27 ppm (except in two samples of 103 and 263 ppm) (Figure 8-13). Most of the fracture fillings have thorium concentrations within the range of that seen for the wall rock, whereas a significant number of samples have higher uranium concentrations than the wall rock. Th/U-ratios are mainly within the range of the the wall rock ratios, but usually below the wall rock median ratios (Figure 8-14). This is mainly due to the commonly higher uranium contents in the fracture fillings compared with the wall rock, as shown in Figure 8-13. The high uranium concentrations in many fracture fillings probably partly represent redeposited uranium at depths below the redox front, whereas samples from above the redox front, which is usually 15–20 m below the ground surface, have low uranium concentrations (Figure 8-15, cf. Section 6.2).

REEs

Chondrite normalised REE patterns for the fracture fillings analysed are shown in Figure 8-16 for near surface samples (down to –80 m above sea level) and in Figure 8-17 for samples from greater depths (chondrite values used are from /Evansen et al. 1978/). The REE patterns and the REE concentrations are generally very similar to those of the wall rock indicating that the REEs are mainly derived from the wall rock and that this leaching has been fairly uniform for all of the REEs. For instance, the slightly negative Eu anomalies have been inherited from the wall rock signature /cf. Drake et al. 2006/. However, many fracture filling samples, particularly from shallow depths (Figure 8-16), show enrichment of the light rare earth elements (LREEs) compared with the wall rock, and this is clearly visible in the plot of La/Yb ratios versus depth in Figure 8-18. The La/Yb ratios are generally within the range of those of the wall rock, but constrained to a group of LREE-enriched samples close to the surface. These samples either contain REEs and carbonate, young calcite or, more rarely, Ce-oxide. The LREE enrichment might be due to the association of REEs to organic material and possibly microbial breakdown of organic material, resulting in LREE-enrichment in the near surface groundwater (cf. Section 5.6.4).

As shown in Section 6.1.2 and in Figure 8-19, a couple of near surface samples show significant positive Ce anomalies, indicating oxidation of Ce^{3+} to Ce^{4+}, either at the fracture surface or in the groundwater. Subsequent preferred desorption of other REEs compared with the less mobile Ce(IV) from the fracture surface, or preferential precipitation Ce^{4+} on the fracture surfaces, has resulted in positive Ce anomalies. The very negative anomalies at greater depths belong to samples with very low LREE content and are therefore very uncertain.

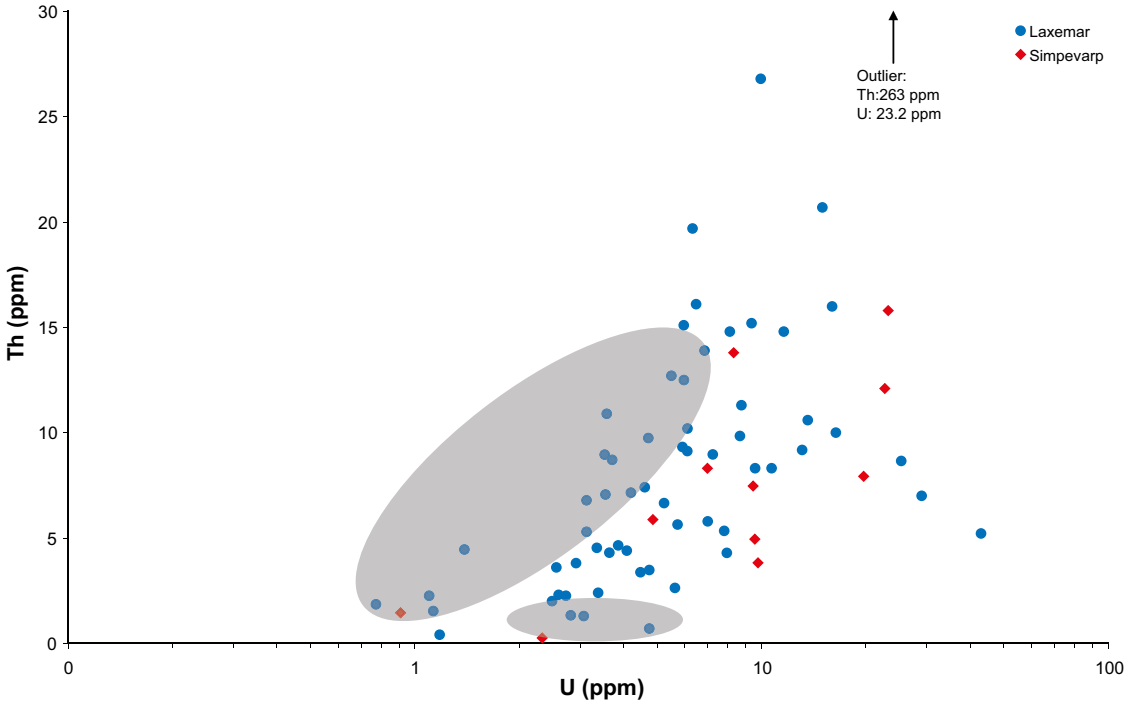

Figure 8-13. *Th versus U in fracture fillings. The shaded areas show the compositional distribution of the dominant rock types; quartz monzodiorite, Ävrö granodiorite, and Ävrö quartz monzodiorite.*

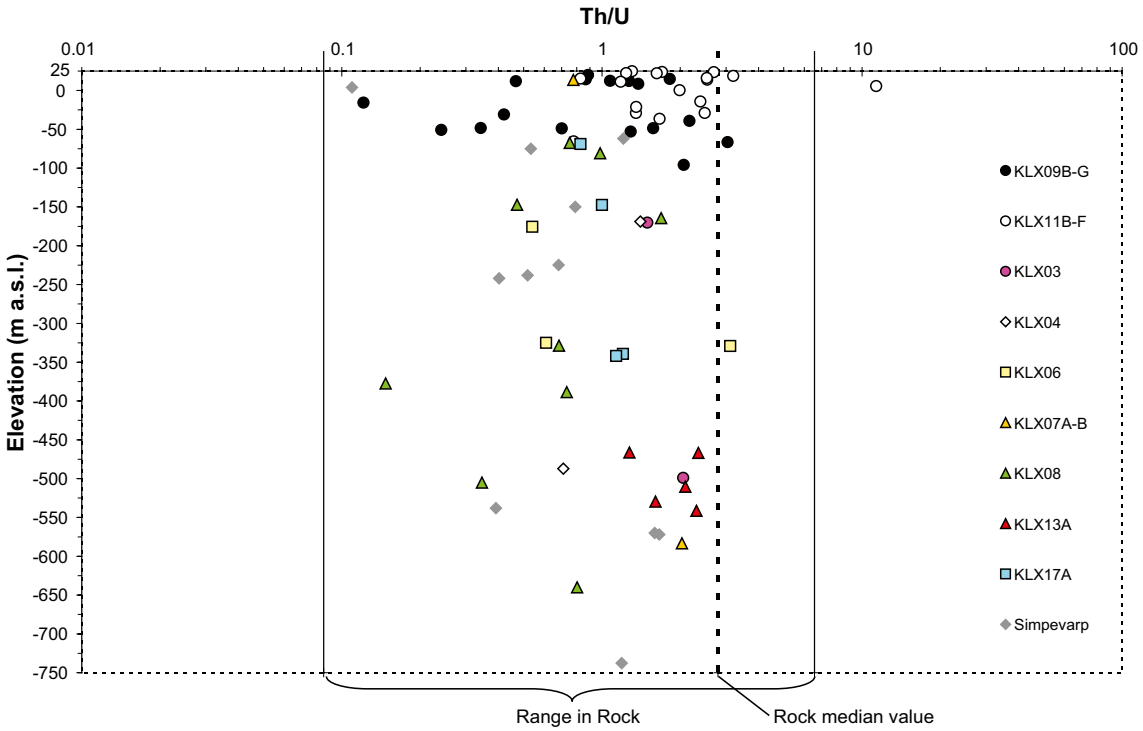

Figure 8-14. *Th/U-ratio (by weight) versus depth (elevation). The range and median of ratios for the dominant rock types (quartz monzodiorite, Ävrö granodiorite, and Ävrö quartz monzodiorite) are indicated.*

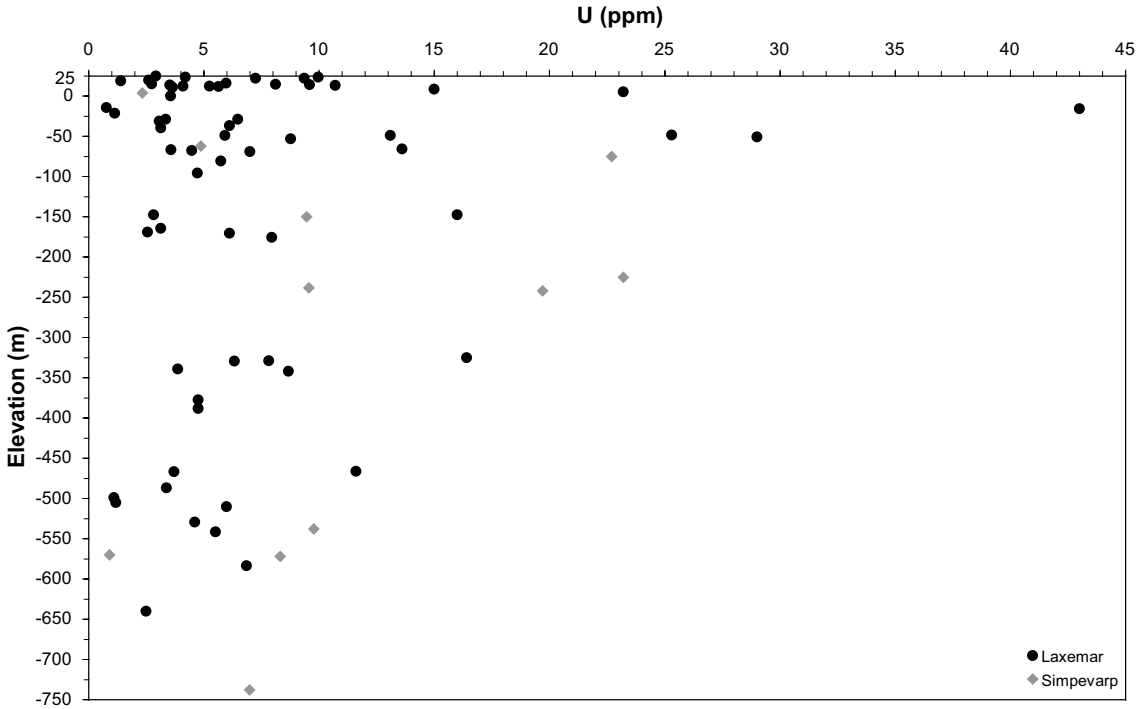

Figure 8-15. *U concentrations in fracture fillings versus depth (elevation).*

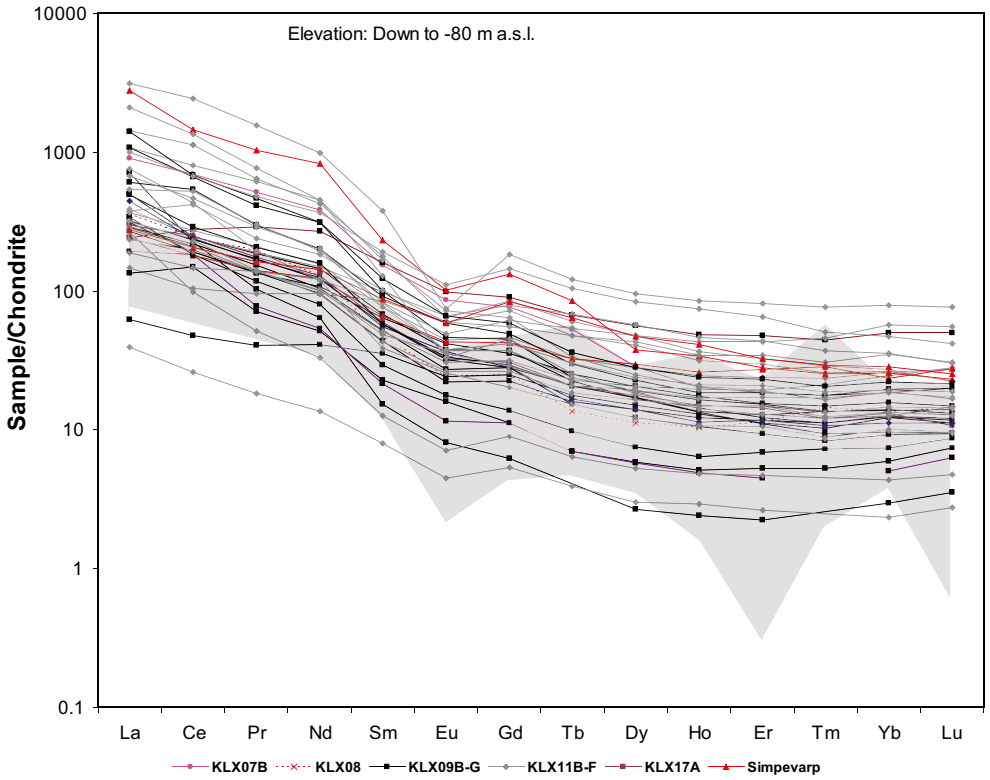

Figure 8-16. *Chondrite normalised REE patterns for fracture fillings from depths above –80 m above sea level. The shaded area represents the composition of the main rock types in the Laxemar area (quartz monzodiorite, Ävrö granodiorite, and Ävrö quartz monzodiorite).*

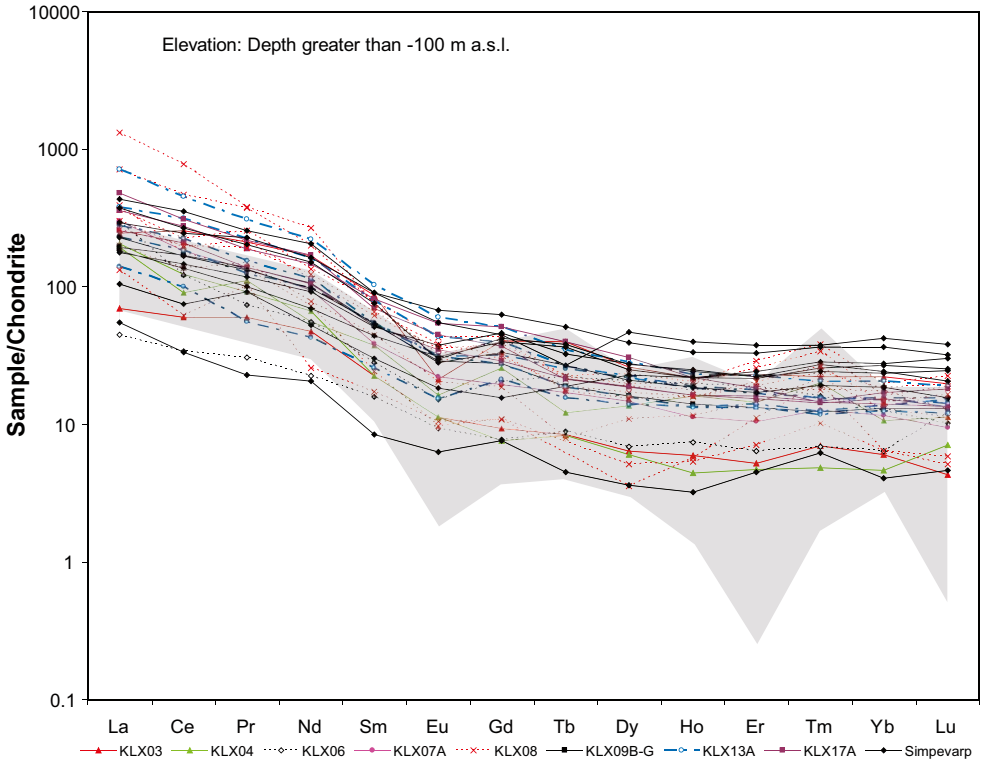

Figure 8-17. *Chondrite normalised REE patterns for fracture fillings from below –100 m above sea level. The shaded area represents the composition of the main rock types (Ävrö quartz monzodiorite, Ävrö granodiorite and quartz monzodiorite).*

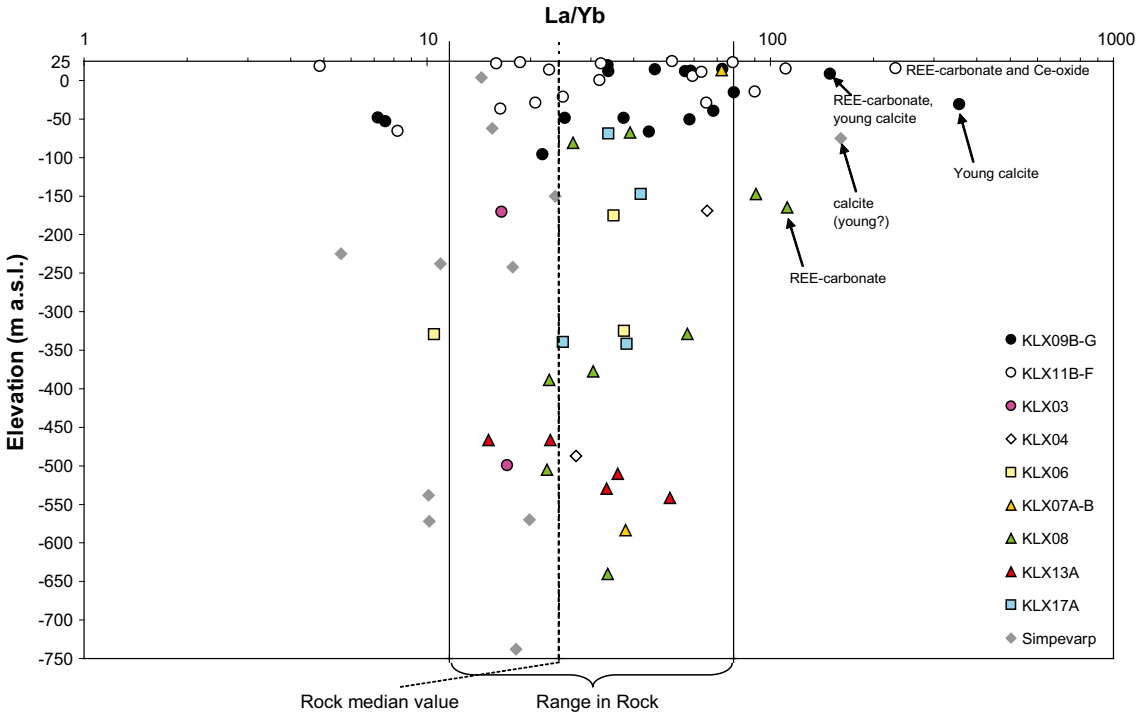

Figure 8-18. *La/Yb ratio in fracture fillings versus depth (elevation). The range and median of ratios for the main rocks types (quartz monzodiorite, Ävrö granodiorite, and Ävrö quartz monzodiorite) are indicated.*

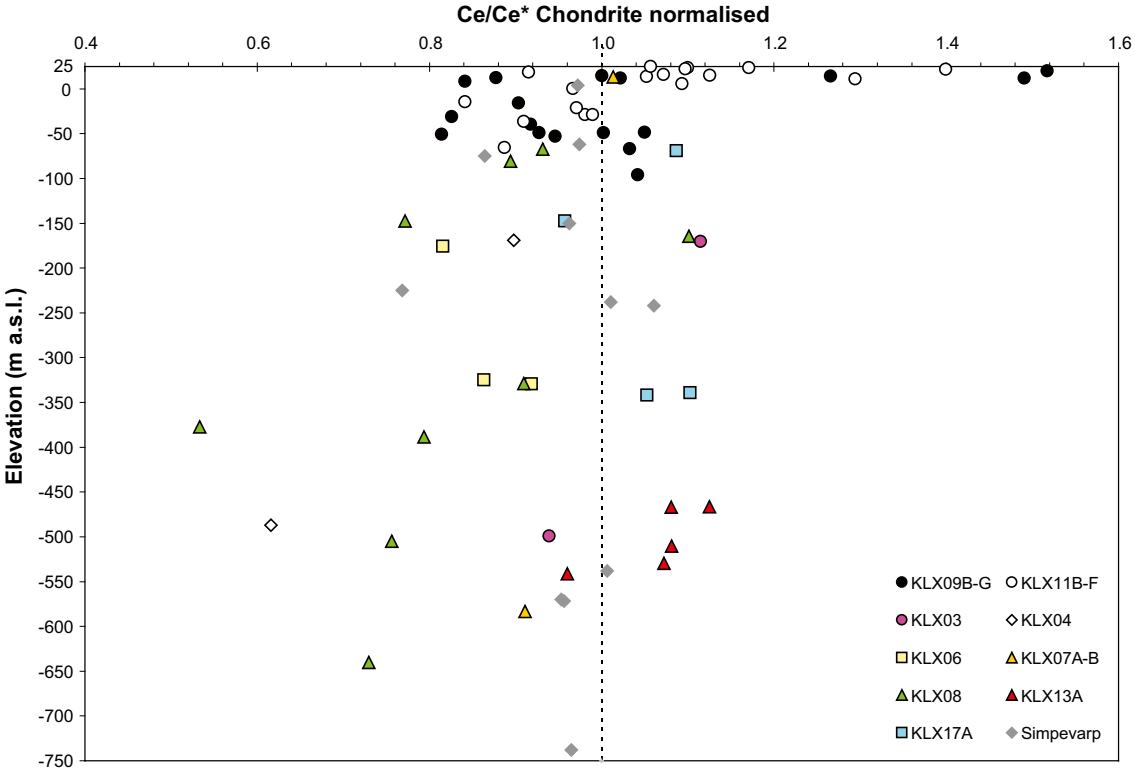

Figure 8-19. *Ce anomalies (chondrite normalised Ce/Ce*) in fracture fillings versus depth (elevation). Ce* = (La·Pr)$^{0.5}$.*

8.3 U-series analyses of fracture coatings in water conducting fractures

In this section, U-series analyses of fracture coatings from water conducting fractures are presented (compiled in Appendix 4). Vertical depth is used in the figures to facilitate comparison with samples from the redox front studies (Section 6.2), namely KLX09B–G and KLX11B–F, included in Figure 8-20 through to Figure 8-22. Figure 8-20 shows very low ^{238}U activities near the surface, i.e. above the redox front. Below the redox front there is an increase in the ^{238}U activities up to nearly 600 Bq/kg with a subsequent gradual decrease with depth. Bulk removal of U is further evidenced by a large portion of the samples with low ^{238}U having high ^{230}Th/^{234}U activity ratios (>1.5, Figure 8-21).

As shown in Section 6.2, most of the samples from the upper 20 m in the bedrock, i.e. above the redox front, indicate oxidative removal of U, probably during the last ~100 ka, as shown by the activity ratios ^{230}Th/^{234}U »1 and ^{234}U/^{238}U ~1. A majority of the samples from greater depths show deposition of U (^{230}Th/^{234}U <1 and ^{234}U/^{238}U >1) or, more commonly, no significant disequilibrium (Figure 8-22). The deposition of uranium is in accordance with other indicators of reducing conditions /SKB 2006b/ at these depths, and the insignificant disequilbrium indicates rather stagnant groundwater conditions.

The Thiel diagram in Figure 8-23 shows samples from 20–1,000 m vertical depth. Samples from KLX09B–G and KLX11B–F are excluded for readability but are plotted in Figure 6-11, which shows that samples above the redox front indicate U removal and deeper samples generally indicate U deposition or stable reducing conditions. In Figure 8-23 most samples are close to or at seqular equilibrium (activity ratios of 1.0 ± 0.1) indicating negligible recent mobilisation of U and rather stagnant and reducing groundwater conditions. It can be concluded that significant recent (post-glacial) uranium deposition indicated by activity ratios ^{234}U/^{238}U >1 and ^{230}Th/^{238}U «1 is not detected, whereas some deposition (in the time frame of some hundreds of thousands of years) has occurred, as shown by ^{234}U/^{238}U >1 and ^{230}Th/^{238}U >1. Some of these samples are also affected by later leaching of U (which may or may not be caused by sample disturbances, see below). A number of samples show close to secular equilibria ratios but still show ^{234}U/^{238}U <1 and ^{230}Th/^{238}U <1; this may be the result of small amounts of U removal during mainly reducing conditions. Two samples at depths of 316 and 401 m

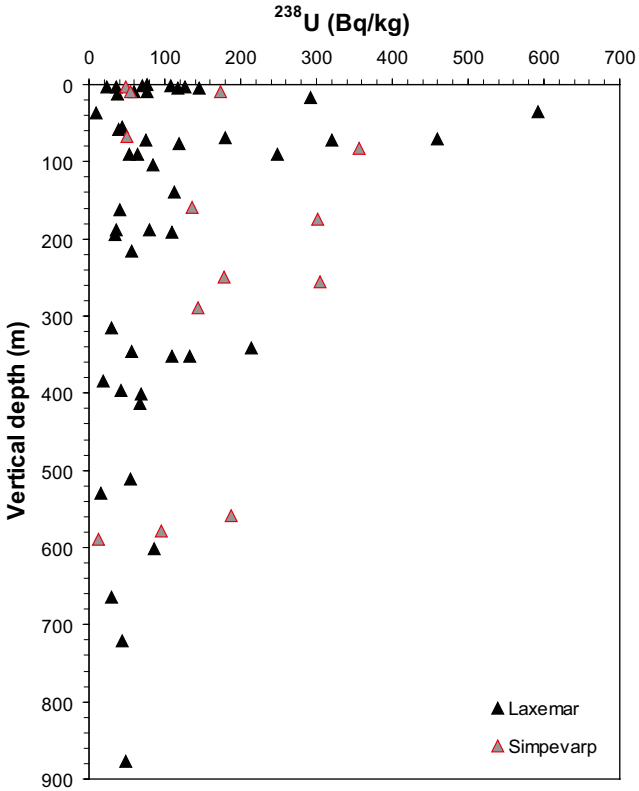

Figure 8-20. *Activity of ^{238}U vs. depth for fracture coating samples.*

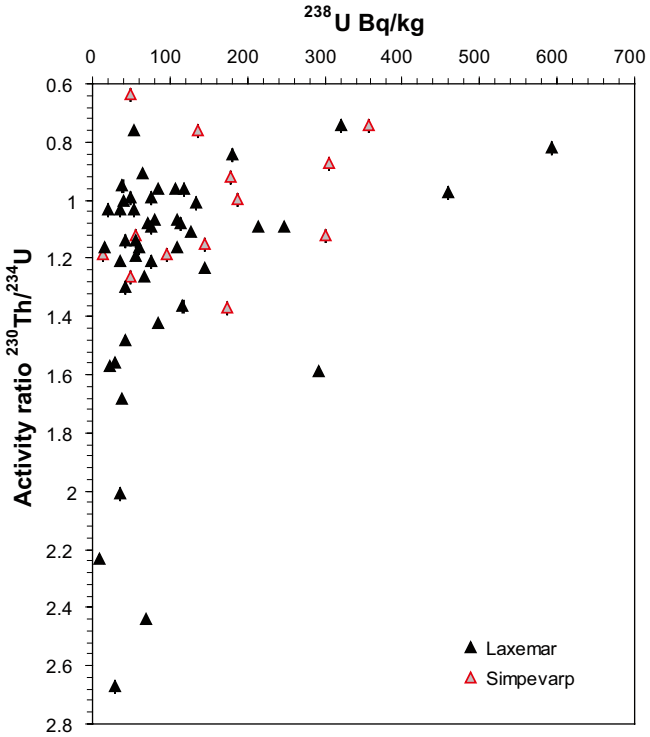

Figure 8-21. *Activity ratios of $^{230}Th/^{234}U$ vs. activity of ^{238}U for fracture coating samples.*

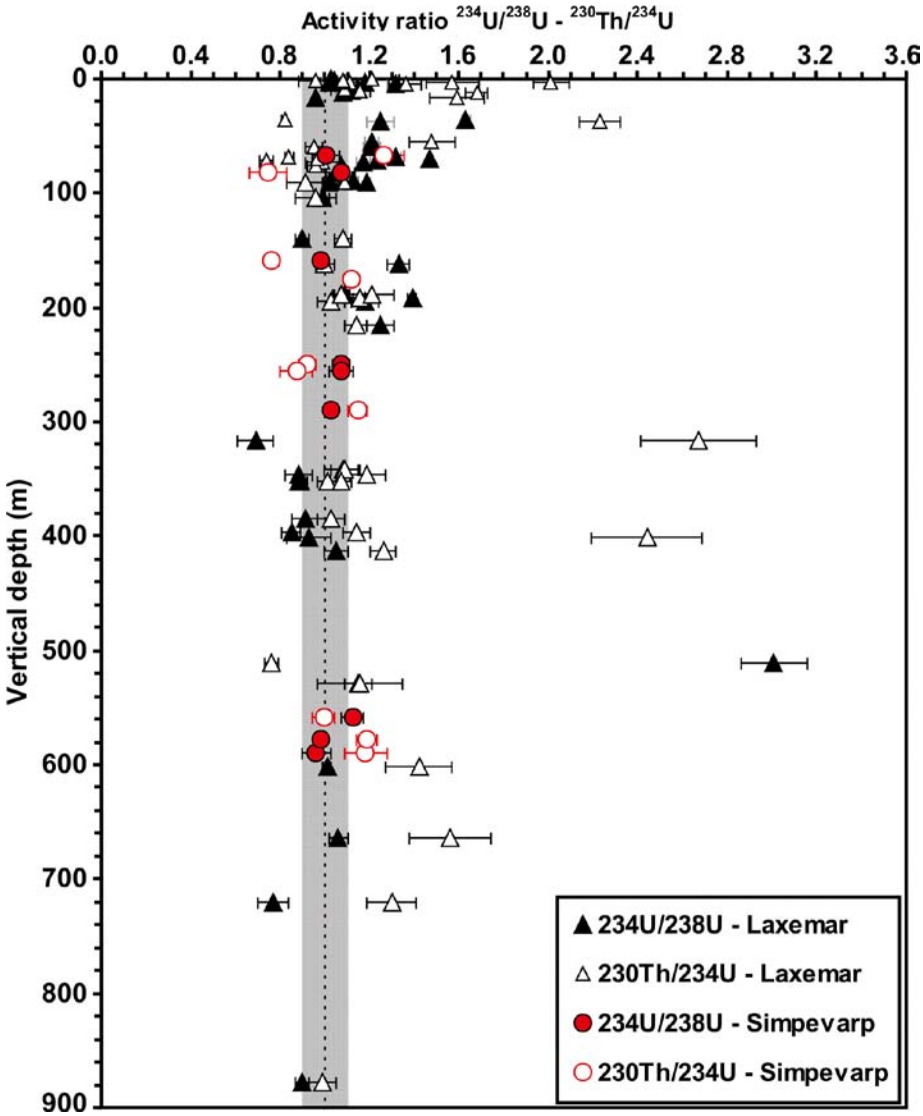

Figure 8-22. *Activity ratios of $^{234}U/^{238}U$ and $^{230}Th/^{234}U$ (with errors) versus depth for fracture coating samples. The shaded area indicates secular equilibrium 1.0 ± 0.1.*

deviate significantly from the rest by $^{230}Th/^{234}U$ >2 activity ratios. The $^{234}U/^{238}U$ ratio for one of these samples (KLX08: 465 m core length) is close to 1, typical for recent uranium removal during oxidising conditions. Taking into account the stable reducing conditions in the groundwaters at great depth /Gimeno et al. 2009/, together with the absence of goethite, recent oxidation at 400 m depth seems less probable. One large uncertainty with the present set of samples is the possible oxidation and leaching of uranium caused by the handling of the cores after drilling and before sampling; for example, the drill cores are wetted by water during several core mapping occasions and HCl is used routinely for detecting calcite. Even if HCL is only applied on small spots it may, in the worst case, lead to severe leaching of uranium. The possibility of sample disturbances must therefore be considered, especially for the few samples that significantly deviate from the general trends and even more so if the uranium contents in these fracture coatings are low (which is usually the case).

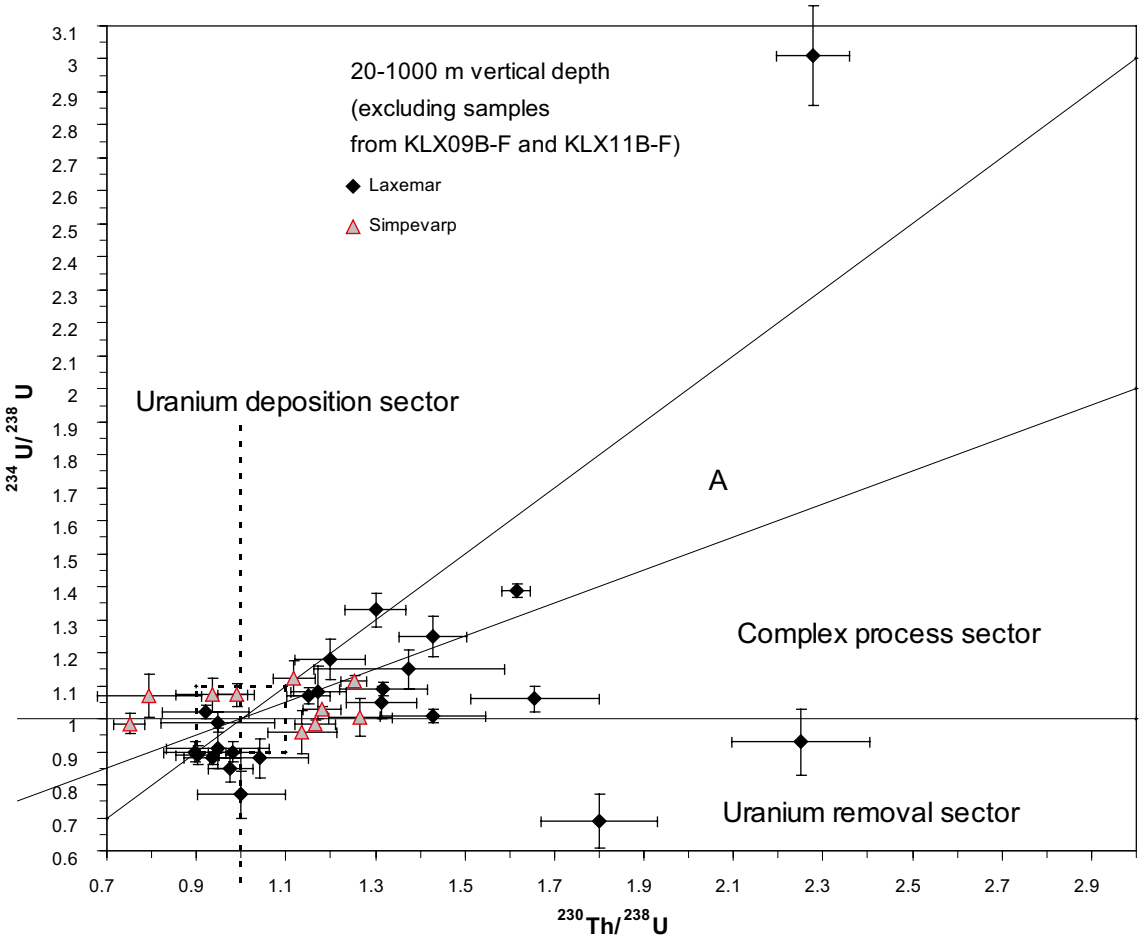

Figure 8-23. *Thiel diagram of uranium decay series for samples from the Laxemar and Simpevarp subareas representing 20–1,000 m vertical depth (after /Thiel et al. 1983/). Samples from KLX09B–G and KLX11B–F are excluded but are shown in Figure 6-11. A and B are forbidden sections for any single continuous process. The complex process sector is forbidden for any single process.*

8.4 Concluding remarks

The chemical analyses of individual fracture minerals and bulk fracture fillings confirm the mineralogy determined from the mapping, and identification using XRD and microscopy. The chemical analyses, in combination with XRD and microscopy investigations, have revealed information on the association of certain elements to specific minerals, and the abundance of minerals and elements in the fracture fillings. Useful information on the behaviour of trace elements such as redox indicating elements and radionuclide analoges is also gained.

Selected elements and their main associated minerals are listed below:

K Adularia, illite, clay minerals, (muscovite, apophyllite, harmotome, hornblende).

Cs Mixed-layer clay (e.g. illite/smectite), illite.

Rb Illite, mixed-layer clay, (adularia, muscovite).

Ba Adularia, barite, harmotome.

Na Albite, (smectite, analcime, apophyllite, mixed-layer clay).

Ca Calcite, epidote, prehnite, (laumontite, fluorite, gypsum, corrensite, apophyllite).

Sr Epidote, (prehnite, laumontite, corrensite, calcite, fluorite, gypsum, celestine).

Fe Chlorite, corrensite, pyrite, hematite, epidote, (prehnite, illite, chalcopyrite, goethite).

Mg Chlorite, corrensite, illite, (talc, antigorite).

Mn Mn-rich mixed-layer clay, Mn-oxide, chlorite.

U U-rich silicate, apatite and wall rock derived zircon and titanite.

REEs REE-carbonate, calcite, and wall rock derived titanite and zircon (Ce-oxide).

Significant uranium leaching is generally only detected in fracture coating samples from the uppermost 20 m, or slightly deeper. This uranium is deposited at slightly greater depth, at reducing conditions. A large number of samples at greater depths show low uranium mobility, taken into account the generally low uranium content and the low deviation in activity ratios (~1.0 ± 0.2). However, some samples indicate recent oxidising conditions at great depth, but taking into account the stable reducing conditions in the groundwaters at these depths /Gimeno et al. 2009/, together with the absence of goethite, recent oxidation seems less probable. One large uncertainty with the present set of samples is the possible oxidation and leaching of uranium caused by the handling of the cores after drilling and before sampling.

9 Acknowledgements

We would like to thank Carl-Henric Wahlgren (SGU) and Peter Hultgren (SKB) for support and constructive discussions during the work with the detailed fracture mineralogy. The drill core mapping geologists Jan Ehrenborg, Peter Dahlin, Vladislav Stejskal, Kalle Matsson and co workers, are thanked for their important input and assistance during sampling. Johan Öhman and Ola Forssberg (Golder Associates) are thanked for producing the stereographic projections and Martin Stigsson (SKB) for help with the figures for fracture mineral depth-relations. Seppo Gehör (University of Oulu) is thanked for his assistance during the fluid inclusion studies. Owe Gustavsson (University of Gothenburg) is acknowledged for carrying out stable isotope analyses and ICP-MS analyses on calcite. Sven Åke Larson (University of Gothenburg) is thanked for comments on the manuscript and Björn Sandström (University of Gothenburg) for discussions regarding the fracture mineralogy of the Forsmark site. Zell Peterman, Russell Alexander and Anders Winberg, are thanked for their constructive reviews.

Brangulis A J, Kanevs S, 2002. Latvijas tektonika. State Geological Survey of Latvia. Riga, Latvia (*in Latvian*).

Bucher K, Frey M, 2002. Petrogenesis of Metamorphic Rocks. Springer-Verlag, Berlin, Germany, 341 p.

Carlsson L, Holmqvist A, 1968. Ett nytt fynd av sandstensgångar i Västervikstrakten. GFF, 90, 519–528.

Cathelineau M, 1988. Cation site occupancy in chlorites and illites as a function of temperature, Special issue devoted to some papers read at the sixth meeting of the European Clay Groups. Mineralogical Society, London, UK, p. 471–485.

Čečys A, Benn K, 2007. Emplacement and deformation of the ca 1.45 Ga Karlshamn granitoid pluton, southeastern Sweden, during ENE-WSW Danopolonian shortening. International Journal of Earth Sciences, 96, 397–414.

Cederbom C, 2001. Phanerozoic, pre-Cretaceous thermotectonic events in southern Sweden revealed by fission track thermochronology. Earth and Planetary Science Letters, 188, 199–209.

Cederbom C, Larson S Å, Tullborg E-L, Stiberg J P, 2000. Fission track thermochronology applied to Phanerozoic thermotectonic events in central and southern Sweden. Tectonophysics, 316, 153–167.

Crawford M L, 1981. Phase Equilibria in aqeuous fluid inclusions. In: L.S. Hollister and M. Crawford, L (Editors), Short course handbook, Fluid inclusions: applications to petrology Mineralogical Association of Canada, Calgary, Canada, 304 pp.

Cronquist T, Forssberg O, Hansen L M, Koyi S, Vestgård J, Wikholm M, 2006. Oskarshamn site investigation. Detailed outcrop mapping on drillsite KLX11. SKB P-06-06, Svensk Kärnbränslehantering AB.

Cruden A R, 2008. Emplacement mechanisms and structural influences of a younger granite intrusion into older wall rocks – a principal study with application to the Götemar and Uthammar granites. Site descriptive modelling, SDM-Site Laxemar, SKB R-08-138, Svensk Kärnbränslehantering AB.

Dalrymple G B, Lanphere M A, 1971. $^{40}Ar/^{39}Ar$ technique of K-Ar dating: a comparison with the conventional technique, Earth and Planetary Science Letters, 12, 300–308.

Davis G H, Reynolds S J, 1996. Structural geology of rocks and regions. John Wiley, New York, USA, 776 pp.

De Albuquerque C A R, 1975. Partition of trace elements of co-existing biotite, muscovite and potassium feldspar of granitic rocks, northern Portugal. Chemical Geology, 16, 89–108.

Deer W A, Howie R A, Zussman J, 1992. An introduction to the rock-forming minerals. Pearson Education Limited, Harlow, UK, 696 pp.

Dia A, Gruau G, Olivie L G, Riou C, Molenat J, Curmi P, 2000. The distribution of rare earth elements in groundwaters; assessing the role of source-rock composition, redox changes and colloidal particles. Geochimica et Cosmochimica Acta, 64, 4131–4151.

Dideriksen K, Christiansen B C, Baker J A, Frandsen C, Balic-Zunic T, Tullborg E-L, Mørup S, Stipp S L S, 2007. Fe-oxide fracture-fillings as a palæo-temperature and -redox indicator: Structure, crystal form, REE content and Fe isotope composition. Chemical Geology, 244, 330–343.

Dideriksen K, Christiansen B C, Frandsen C, Balic-Zunic T, Mørup S, Stipp S L S, 2009. Paleo-redox boundaries in fractured granite. Geochimica et Cosmochimica Acta *(submitted)*.

Drake H, 2006. Fracture fillings and red-stained wall rock in the Simpevarp are, SE Sweden. Licentiate thesis. Earth Sciences Centre, University of Gothenburg, Publ. A102, Gothenburg, Sweden.

Drake H. 2008. Proterozoic to Quaternary events of fracture mineralisation and oxidation in SE Sweden. Doctoral thesis. Earth Sciences Centre, University of Gothenburg, Publ. A120. Gothenburg, Sweden.

Drake H, Tullborg E-L, 2004. Oskarshamn site investigation. Fracture mineralogy and wall rock alteration, results from drill core KSH01A+B. SKB-P-04-250, Svensk Kärnbränslehantering AB.

Drake H, Tullborg E-L, 2005. Oskarshamn site investigation. Fracture mineralogy and wall rock alteration, results from drill cores KAS04, KA1755A and KLX02. SKB P-05-174, Svensk Kärnbränslehantering AB.

Drake H, Tullborg E-L, 2006a. Oskarshamn site investigation. Fracture mineralogy of the Götemar granite. Results from drill cores KKR01, KKR02 and KKR03. SKB P-06-04, Svensk Kärnbränslehantering AB.

Drake H, Tullborg E-L, 2006b. Oskarshamn site investigation. Fracture mineralogy, Results from drill core KSH03A+B. SKB P-06-03, Svensk Kärnbränslehantering AB.

Drake H, Tullborg E-L, 2006c. Oskarshamn site investigation. Mineralogical, chemical and redox features of red-staining adjacent to fractures, Results from drill core KLX04. SKB P-06-02, Svensk Kärnbränslehantering AB.

Drake H, Tullborg E-L, 2006d. Oskarshamn site investigation. Mineralogical, chemical and redox features of red-staining adjacent to fractures, Results from drill cores KSH01A+B and KSH03A+B. SKB P-06-01, Svensk Kärnbränslehantering AB.

Drake H, Tullborg E-L, 2006e. Hydrothermal red-staining adjacent to fractures in granodioritic to dioritic rock, Simpevarp, south-east Sweden. Bulletin of the Geological Society of Finland, Special Issue 1. P. 26.

Drake H, Tullborg E-L, 2007a. Oskarshamn site investigation. Fracture mineralogy, Results from drill cores KLX03, KLX04, KLX06, KLX07A, KLX08 and KLX10A. SKB P-07-74, Svensk Kärnbränslehantering AB.

Drake H, Tullborg E-L, 2007b. Paleohydrogeology of the Simpevarp area, southeastern Sweden, as evidenced by stable isotopes in fracture minerals. In: T.D. Bullen and Y. Wang (Editors), Water-rock Interaction: Proceedings of the 12th International Symposium on Water-Rock Interaction, Kunming, China, 31 July–5 August 2007. Taylor and Francis, London, UK, 723–726.

Drake H, Tullborg E-L, 2008a. Oskarshamn site investigation. Detecting the near surface redox front in crystalline rock. Results from drill cores KLX09B-G and KLX11B-F. SKB P-08-44, Svensk Kärnbränslehantering AB.

Drake H, Tullborg E-L, 2008b. Oskarshamn site investigation. Fracture mineralogy. Results from drill core KLX15A. SKB P-08-12, Svensk Kärnbränslehantering AB.

Drake H, Tullborg E-L, 2008c. Oskarshamn site investigation. Mineralogy in water conducting zones. Results from drill cores KLX13A and KLX17A with additional fracture mineralogical data from drill cores KLX14A, KLX19A, KLX20A and KLX26A. SKB P-08-11, Svensk Kärnbränslehantering AB.

Drake H, Tullborg E-L, 2008d. Oskarshamn site investigation. Mineralogy in water conducting zones. Results from boreholes KLX07A+B and KLX08. SKB P-08-42, Svensk Kärnbränslehantering AB.

Drake H, Tullborg E-L, 2008e. Oskarshamn site investigation. Mineralogy in water conducting zones. Results from boreholes KLX03, KLX04, KLX06, KSH01A+B, KSH02 and KSH03A. SKB P-08-41, Svensk Kärnbränslehantering AB.

Drake H, Tullborg E-L, 2008f. Paleohydrogeological evidences from stable isotopes, fluid inclusions and trace elements in fracture minerals in crystalline rock, Simpevarp area, south-eastern Sweden. In N.A. Wahl (editor), 28th Nordic Geological Winter Meeting. Jan 7–10, 2008, Aalborg-Denmark. Aalborg University. p 105.

Drake H, Tullborg E-L, 2008g. Detection of the near surface redox front in crystalline bedrock. In N.A. Wahl (editor), 28th Nordic Geological Winter Meeting. Jan 7–10, 2008, Aalborg-Denmark. Aalborg University. p. 32.

Drake H, Tullborg E-L, 2008h. Detection of the near-surface redox front in crystalline bedrock, Sweden, IGC 33, Oslo Norway, abstract volume. Abstract number HYH07708L.

Drake H, Tullborg E-L, 2009a. Paleohydrogeological events recorded by stable isotopes, fluid inclusions and trace elements in fracture minerals in crystalline rock, Simpevarp area, SE Sweden. Applied Geochemistry. 24. 715–732.

Drake H, Tullborg E-L, 2009b. Oskarshamn site investigation, Investigations of goethite-bearing fractures in cored boreholes Laxemar subarea. SKB-P-09-15, Svensk Kärnbränslehantering AB.

Drake H, Savolainen M, Tullborg, E-L, 2004. Fracture fillings and wall rock alteration – results from borehole KSH01, Simpevarp and KFM01, Forsmark, GFF: The 26th Geological Winter Meeting, Abstract volume, vol. 126, p. 170.

Drake H, Sandström B, Tullborg E-L, 2006. Mineralogy and geochemistry of rocks and fracture fillings from Forsmark and Oskarshamn: Compilation of data for SR-Can. SKB R-06-109, Svensk Kärnbränslehantering AB.

Drake H, Page L, Tullborg E-L, 2007a. Oskarshamn site investigation, $^{40}Ar/^{39}Ar$ dating of fracture minerals. SKB-P-07-27, Svensk Kärnbränslehantering AB.

Drake H, Sandström B, Page L, Tullborg E-L, 2007b. $^{40}Ar/^{39}Ar$ ages of fracture fillings in crystalline Precambrian bedrock, Sweden. Geophysical Research Abstracts 9, 02289, SRef-ID 1607-7962/gra/EGU2007-A-02289.

Drake H, Tullborg E-L, Annersten H, 2008. Red-staining of the wall rock and its influence on the reducing capacity around water conducting fractures. Applied Geochemistry, 23: 1898–1920.

Drake H, Tullborg E-L, MacKenzie A B, 2009a. Detecting the near surface redox front in crystalline bedrock using fracture mineral distribution, geochemistry and U-series disequilibrium. Applied Geochemistry. 24. 1023–1039.

Drake H, Tullborg E-L, Page L, 2009b. Distinguished multiple events of fracture mineralisation related to far-field orogenic effects in Paleoproterozoic crystalline rocks, Simpevarp area, SE Sweden. Lithos. 110, 37–49.

Eliasson T, Tullborg E-L, Landström O, 1989. Fracture filling mineralogy and geochemistry at the Swedish HDR research site. In: R. Baria (Editor), Camborne School of Mines International Hot Dry rock Conference. Robertson Scientific Publications, London, UK, pp. 425–435.

Evansen N M, Hamilton P J, O'Nions R K, 1978. Rare Earth Abundances in Chondritic Meteorites. Geochimica et Cosmochimica Acta, 42: 1199–1212.

Faure G, 1986. Stable isotope geochemistry, 2nd ed. John Wiley and Sons, New York, USA, 589 pp.

Field C W, Fifarek R H, 1985. Light stable-isotopes systematics in the epithermal environment. Reviews in Economic Geology, 2, 99–128.

Folk R L, 1974. The natural history of crystalline calcium carbonate; effect of magnesium content and salinity. Journal of Sedimentary Petrology, 44, 40–53.

Fossen H, Dunlap W J, 1998. Timing and kinematics of Caledonian thrusting and extension collapse, southern Norway; evidence from $^{40}Ar/^{39}Ar$ thermochronology. Journal of Structural Geology, 20, 765–781.

Frape S K, Blyth A R, Jones M G, Blomqvist R, Tullborg E L, McNutt R H, McDermott F, Ivanovich M, 1992. A comparison of calcite fracture mineralogy and geochemistry for the Canadian and Fennoscandian shields. In: Y.K. Kharaka, Maest, A.S. (Editor), Proceedings of the 7th International Symposium on Water-Rock Interaction. A.A. Balkema, Rotherdam, The Netherlands, pp. 787–791.

Frey M, de Capitani C, Liou J G, 1991. A new petrogenetic grid for low-grade metabasites, Sixth meeting of the European Union of Geosciences. Blackwell Scientific Publications, Oxford, UK, pp. 106.

Fritz P, Fontes J C, Frape S K, Louvat D, Michelot J L, Balderer W, 1989. The isotope geochemistry of carbon in groundwater at Stripa. Geochimica et Cosmochimica Acta, 53, 1765–1775.

Gascoyne M, 1999. Long-term maintenance of reducing conditions in a spent nuclear fuel repository. A re-examination of critical factors. SKB R-99-41, Svensk Kärnbränslehantering AB.

Gascoyne M, Cramer J J, 1987. History of actinide and minor element mobility in an Archean granitic batholith in Manitoba, Canada. Applied Geochemistry, 2, 37–53.

Gascoyne M, Miller N H, Neymark L A, 2002. Uranium-series disequilibrium in tuffs from Yucca Mountain, Nevada, as evidence of pore-fluid flow over the last million years. Applied Geochemistry, 17, 781–792.

Gee D G, 1975. A tectonic model for the central part of the Scandinavian Caledonides. American Journal of Science, 275, 468–515.

Gimeno M J, Auqué L F, Gómez J B, Acero P, 2009. Water-rock interaction modelling and uncertainties of mixing modelling. Site descriptive modelling SDM-Site Laxemar. SKB R-08-110, Svensk Kärnbränslehantering AB.

Glamheden R, Curtis P, 2006. Comparative evaluation of core mapping results for KFM06C and KLX07B. SKB R-06-55, Svensk Kärnbränslehantering AB.

Glynn P D, Voss C I, 1999. Geochemical Characterization of Simpevarp Ground Waters near the Äspö Hard Rock Laboratory, Swedish Nuclear Power Inspectorate (SKI), SKI report 96:29, Stockholm, Sweden, 210 p.

Glynn P D, Voss C I, Provost A M, 1999. Deep penetration of oxygenated meltwaters from warm based ice-sheets into the Fennoscandian Shield. Proceedings of the NEA/OECD Workshop on "Use of Hydrochemical Information in Testing Groundwater Flow Models". Borgholm, Sweden, Sept 1–3, 1997. OECD/NEA, Paris, France.

Grant J A, 1986. The isocon diagram; a simple solution to Gresens' equation for metasomatic alteration. Economic Geology and the Bulletin of the Society of Economic Geologists, 81, 1976–1982.

Griffault L Y, Gascoyne M, Kamineni C, Kerrich R, Vandergraaf T T, 1993. Actinide and rare earth element characteristics of deep fracture zones in the Lac du Bonnet granitic batholith, Manitoba, Canada. Geochimica et Cosmochimica Acta, 57, 1181–1202.

Grütter A, von Gunten H R, Rössler E, 1986. Sorption, desorption, and isotope exchange of cesium (10^{-9}–10^{-3} M) on chlorite. Clays and Clay Minerals, 34, 677–680.

Guimerà J, Duro L, Jordana S, Bruno J, 1999. Effects of ice melting and redox front migration in fractured rocks of low permeability. SKB-TR-99-19, Svensk Kärnbränslehantering AB.

Gustafsson J, Gustafsson C, 2007. Oskarshamn site investigation, RAMAC, BIPS and deviation logging in boreholes KLX17A and HLX43. SKB P-07-12, Svensk Kärnbränslehantering AB.

Hallbeck L, Pedersen K, 2008. Explorative analyses of microbes, colloids, and gases together with microbial modeling Site description model SDM-Site Laxemar. SKB P-08-109, Svensk Kärnbränslehantering AB.

Heeremans M, Wijbrans J, 1999. Late Proterozoic tectonic events in southern Finland, constrained by $^{40}Ar/^{39}Ar$ incremental heating and single spot fusion experiments on K-feldspars. Terra Nova, 11, 216–222.

Hoefs J, 2004. Stable Isotope Geochemistry; 5th edition. Springer-Verlag, Berlin, Germany, 244 pp.

Johansson Å, 1984. Fluid inclusion and stable isotope studies on some Caledonian sulfide-bearing veins in Sweden. Economic Geology and the Bulletin of the Society of Economic Geologists, 79, 1736–1748.

Jorgensen B B, Isaksen M F, Jannasch H W, 1992. Bacterial sulfate reduction above 100°C in deep-sea hydrothermal vent sediments. Science, 258, 1756–1757.

Kendrick M A, Burgess R, Harrison D, Bjorlykke A, 2005. Noble gas and halogen evidence for the origin of Scandinavian sandstone-hosted Pb-Zn deposits. Geochimica et Cosmochimica Acta, 69, 109–129.

Kornfält K A, Persson P O, Wikman H, 1997. Granitoids from the Äspo area, southeastern Sweden; geochemical and geochronological data. GFF, 119, 109–114.

Kresten P, Chyssler J, 1976. The Götemar Massif in south-eastern Sweden; a reconnaissance survey. Geologiska Föreningen i Stockholm Förhandlingar, 98, 155–161.

La Pointe P, Fox A, Hermanson J, Öhman J, 2008. Site Descriptive Modeling, SDM Site Laxemar. Geological discrete fracture network model for the Laxemar site. SKB R-08-55, Svensk Kärnbränslehantering AB.

Landström O, Tullborg E L, 1989. The influence of fracture mineral/groundwater interaction on the mobility of U, Th, REE and other trace elements in different redox environments, Water-rock interaction; WRI-6. International Association of Geochemistry and Cosmochemistry and Alberta Research Council Sub-Group on Water-Rock Interaction, Edmonton, Canada, pp. 413–416.

Landström O, Tullborg E-L, 1995. Interactions of trace elements with fracture filling minerals from the Äspö Hard Rock Laboratory. SKB TR-95-13, Svensk Kärnbränslehantering AB. Landström O, Smellie J, Tullborg E-L, 1989. Mineralogical and geochemical studies of fracture-infillings in drillcore KLJ 01, chapter 9. In: G. Bäckblom and R. Stanfors (Editors), Interdisciplinary study of post-glacial faulting in the Lansjärv ares northern Sweden 1986–1988. SKB TR-89-31, Svensk Kärnbränslehantering AB.

Landström O, Tullborg E-L, Eriksson G, Sandell Y, 2001. Effects of glacial/post-glacial weathering compared with hydrothermal alteration – implications for matrix diffusion. Results from drillcore studies in porphyritic quartz monzodiorite from Äspö SE Sweden. SKB R-01-37, Svensk Kärnbränslehantering AB.

Larson S Å, Tullborg E-L, 1983. Stable isotope evidence on the origin of calcite fissure infillings within the Svecokarelian Province of Sweden, In: Kitano Y (ed.), Extended abstracts; 4th International Symposium on Water-Rock Interaction, Misasa, Japan, on August 29–September 8, 1983, pp. 265–268. Elsevier, Amsterdam, The Netherlands.

Larson S Å, Tullborg E-L, 1984. Stable isotopes of fissure-filling calcite from Finnsjön, Uppland, Sweden. Lithos, 17, 117–125.

Larson S Å, Tullborg E-L, Cederbom C, Stiberg J P, 1999. Sveconorwegian and Caledonian foreland basins in the Baltic Shield revealed by fission-track thermochronology. Terra Nova, 11, 210–215.

Larson S Å, Cederbom C E, Tullborg E L, Stiberg J P, 2006. Apatite fission track and (U-Th)/ He data from Fennoscandia; an example of underestimation of fission track annealing in apatite; discussion. Earth and Planetary Science Letters, 248, 561–568.

Lazauskiene J, Stephenson R, Sliaupa S, van Wees J D, 2002. 3-D flexural modelling of the Silurian Baltic Basin. Tectonophysics, 346, 115–135.

Lee M, Hewitt T, Stillborg B, 1994. Rock stress measurement and laboratory testing of rock. SKB PR-25-94-02, Svensk Kärnbränslehantering AB.

Liou J G, Kim H S, Maruyama S, 1983. Prehnite – epidote equilibria and their petrologic applications. Journal of Petrology, 24, 321–342.

Liou J G, Maruyama S, Cho M, 1985. Phase equilibria and mixed parageneses of metabasites in low-grade metamorphism, Diagenesis and low-temperature metamorphism. Mineralogical Society, London, UK, pp. 321–333.

Löfgren M, Sidborn M, in preparation. Statistical analysis of results from the quantitative mapping of fracture minerals in Laxemar. Site descriptive modelling – complementary studies. SKB R-09-31, Svensk Kärnbränslehantering AB.

Lundberg E, Sjöström H, 2006. Oskarshamn site investigation. Kinematic analysis of ductile and brittle/ductile shear zones in Simpevarp and Laxemar subarea. SKB P-06-118, Svensk Kärnbränslehantering AB.

MacKenzie A B, Scott R D, Linsalata P, Miekeley N, 1992. Natural decay series studies of the redox front system in the Pocos de Caldas uranium mineralization. Journal of Geochemical Exploration, 17, 289–322.

McKibben M A, Eldridge C S, 1994. Micron-scale isotopic zoning in minerals; a record of large-scale geologic processes. Mineralogical Magazine, 58A, 587–588.

McNutt R H, 2000. Strontium Isotopes. In: P. Cook and A.L. Herczeg (Editors), Environmental tracers in subsurface hydrology. Kluwer Academic Publishers, pp. 233–260.

Machel H G, Krouse H R, Sassen R, 1995. Products and distinguishing criteria of bacterial and thermochemical sulfate reduction. Applied Geochemistry, 10, 373–389.

Maddock R H, Hailwood E A, Rhodes E J, Muir Wood R, 1993. Direct fault dating trials at the Äspö Hard Rock Laboratory. SKB TR-93-24, Svensk Kärnbränslehantering AB.

Mattsson Å, 1962. Morphologische Studien in Südschweden und auf Bornholm über die nichtglaziale Formenwelt der Felsenskulptur. Lund Studies in Geography, Ser. A. Physical Geography, 20.

Mattsson H, Thunehed H, Triumf C-A, 2004. Oskarshamn site investigation. Compilation of petrophysical data from rock samples and in situ gamma-ray spectrometry measurements. Stage 2 – 2004 (including 2002). SKB P-04-294, Svensk Kärnbränslehantering AB.

Mertanen S, 2004. Middle Proterozoic – Paleozoic tectono-thermal reactivation of the crust in southern Finland and northwestern Russia – paleomagnetic evidences. In: C. Ehlers et al. (Editors), Litosphere 2004 – Third symposium on the structure, composition and evolution of the litosphere in Finland. Institute of Seismology, University of Helsinki, Report S-45, Helsinki, Finland.

Middleton M F, Tullborg E L, Larson S A, Bjorklund L, 1996. Modelling of a Caledonian foreland basin in Sweden; petrophysical constraints, First Nordic symposium on Petrophysics. Gothenburg, Sweden, Elsevier Science, Oxford, UK, pp. 407–413.

Milnes A G, Gee D G, 1992. Bedrock stability in southeastern Sweden. Evidence from fracturing in the Ordovician limestones of northern Öland. SKB TR-92-2-3, Svensk Kärnbränslehantering AB.

Milodowski A E, Gillespie M R, Pearce J M, Metcalfe R, 1998a. Collaboration with the SKB EQUIP programme; Petrographic characterisation of calcites from Äspö and Laxemar deep boreholes by scanning electron microscopy, electron microprobe and cathodoluminescence petrography, WG/98/45C. British Geological Survey, Keyworth, Nottingham, UK.

Milodowski A E, Gillespie M R, Naden J, Fortey N J, Shepherd T J, Pearce J M, Metcalfe R, 1998b. The petrology and paragenesis of fracture mineralization in the Sellafield area, west Cumbria. Proceedings of the Yorkshire Geological Society, 52, 215–241.

Milodowski A E, Fortey N J, Gillespie M R, Pearce J M, Hyslop E K, 2002. Synthesis report on the mineralogical characteristics of fractures from the Nirex boreholes in the Sellafield area. British Geological Survey Technical Report WG/98/8, British Geological Survey, Keyworth, Nottingham, UK.

Milodowski A E, Tullborg E-L, Buil B, Gomez P, Turrero M-J, Haszeldine S, England G, Gillespie M R, Torres T, Ortiz J E, Zacharias J, Silar J, Chvatal M, Strnad L, Sebek O, Bouch J E, Chenery S R, Chenery C, Shepherd T J, McKervey J A, 2005. Application of Mineralogical, Petrological and Geochemical tools for Evaluating the Palaeohydrogeological Evolution of the PADAMOT Study Sites. PADAMOT Project Technical Report WP2. Nirex Limited, Harwell, UK, 228 pp.

Min M, Peng X, Wang J, Osmond J K, 2005. Uranium-series disequilibria as a means to study recent migration of uranium in a sandstone-hosted uranium deposit, NW China. Applied Radiation and Isotopes, 63, 115–125.

Morse J W, Bender M L, 1990. Partition coefficients in calcite; examination of factors influencing the validity of experimental results and their application to natural systems. Chemical Geology, 82, 265–277.

Munier R, Talbot C J, 1993. Segmentation, fragmentation and jostling of cratonic basement in and near Äspo, Southeast Sweden. Tectonics, 12, 713–727.

Möller P, Morteani G, 1983. On the geochemical fractionation of rare earth elements during the formation of Ca-minerals and its application to problems of the genesis of ore deposits. In: S.S. Augustithis (Editor), The significance of trace elements in solving petrogenetic problems and controversies. Theophrastus Publ., Athens, Greece, pp. 747–791.

Nisca D H, 1987. Aerogeophysical interpretation: bedrock and tectonic analysis. SKB PR-25-87-04, Svensk Kärnbränslehantering AB.

Nordenskjöld C E, 1944. Morfologiska studier inom övergångsområdet mellan Kalmarslätten och Tjust, Meddelanden från Lunds universitets geografiska institution. *(in Swedish)*.

O'Neil J R, Clayton R N, Mayeda T K, 1969. Oxygen isotope fractionation in divalent metal carbonates. Journal of Chemistry and Physics, 51, 5547–5558.

Ohmoto H, Rye R O, 1979. Isotopes of sulfur and carbon, 2nd ed. In: H.L. Barnes (Editor), Geochemistry of hydrothermal ore deposits. John Wiley and Sons, New York, USA.

Ohmoto H, Goldhaber M B, 1997. Sulfur and carbon isotopes, 3rd ed. In: H.L. Barnes (Editor), Geochemistry of hydrothermal ore deposits. John Wiley and Sons, New York, USA.

Orr W L, 1974. Changes in Sulfur Content and Isotopic Ratios of Sulfur during Petroleum Maturation; Study of Big Horn Basin Paleozoic Oils. AAPG Bulletin, 58, 2295–2318.

Osmond J K, Ivanovich M, 1992. Uranium-series mobilization and surface hydrology.; 2nd ed. In: M. Ivanovich and R.S. Harmon (Eds.), Uranium-series disequilibrium; applications to Earth, marine, and environmental sciences. Oxford Scientific Publications, Oxford. UK.

Page L, Söderlund P, Wahlgren C-H, 2007. Oskarshamn site investigation. $^{40}Ar/^{39}Ar$ and (U-Th)/He Geochronology of samples from the cored boreholes KSH03A, KSH03B, KLX01, KLX02 and the access tunnel to the Äspö Hard Rock Laboratory. SKB P-07-160, Svensk Kärnbränslehantering AB.

Pedersen K, Ekendahl S, Tullborg E-L, Furnes H, Thorseth I, Tumyr O, 1997. Evidence of ancient life at 207 m depth in a granitic aquifer. Geology, 25, 827–830.

Perez del Villar L, Bruno J, Campos R, Gomez P, Cozar J S, Garralon A, Buil B, Arcos D, Carretero G, Ruiz Sanchez Porro J, Hernan P, 2002. The uranium ore from Mina Fe (Salamanca, Spain) as a natural analogue of processes in a spent fuel repository. Chemical Geology, 190, 395–415.

Peterman Z E, Wallin B, 1999. Synopsis of strontium isotope variations in groundwater at Äspo, southern Sweden. Applied Geochemistry, 14, 939–951.

Pingitore N E, Jr., Eastman M P, 1986. The coprecipitation of Sr^{2+} with calcite at 25°C and 1 atm. Geochimica et Cosmochimica Acta, 50, 2195–2203.

Plink-Björklund P, Björklund L, 1999. Sedimentary response in the Baltic Devonian Basin to post-collisional events in the Scandinavian Caledonides. GFF, 121, 79–80.

Pontén A, Plink-Björklund P, 2007. Depositional environment in an extensive tide-influenced delta plain, Middle Devonian Gauja Formation, Devonian Baltic Basin. Sedimentology, 54, 969–1006.

Poprawa P, Sliaupa S, Stephenson R, Lazauskiene J, 1999. Late Vendian-early Palaeozoic tectonic evolution of the Baltic Basin; regional tectonic implications from subsidence analysis. Tectonophysics, 314, 219–239.

Pourret O, Dia A, Davranche M, Gruau G, Hénin O, Angée M, 2007. Organo-colloidal control on major- and trace-element partitioning in shallow groundwaters: Confronting ultrafiltration and modelling. Applied Geochemistry, 22, 1568–1582.

Puigdomenech I, Ambrosi J-P, Eisenlohr L, Lartigue J-E, Banwart S A, Bateman K, Milodowski A E, West J M, Griffault L, Gustafsson E, Hama K, Yoshida H, Kotelnikova S, Pedersen K, Michaud V, Trotignon L, Rivas Perez J, 2001. O_2 depletion in granitic media. The REX project. SKB-TR-01-05, Svensk Kärnbränslehantering AB.

Puura V, Vaher R, 1997. Cover structure. In: A. Raukas and A. Teedumäe (Editors), Geology and Mineral Resources of Estonia. Estonian Academy Publishers, Tallinn, Estonia, pp. 166–167.

Puura V, Floden T, Monkevicius A, Vaher R, 1999. Late Caledonian compressional tectonics in the intracratonic Baltic Basin, European Union of Geosciences conference abstracts; EUG 10. Cambridge Publications, Cambridge, UK, pp. 286.

Rhén I, Forsmark T, Hartley L, Jackson P, Roberts D, Swan D, Gylling B, 2009. Hydrogeological conceptualisation and parameterisation, Site descriptive modelling SDM-Site Laxemar. SKB R-08-78, Svensk Kärnbränslehantering AB.

Rickard D T, Willden M Y, Marinder N E, Donnelly T H, 1979. Studies on the genesis of the Laisvall sandstone lead-zinc deposit, Sweden. Economic Geology, 74, 1255–1285.

Rivas-Perez J, Tullborg E-L, Banwart S A, 2003. The kinetics of O_2(aq) reduction during oxidative weathering of naturally occurring fracture minerals in groundwater. Mineralogical Magazine, 67, 399–414.

Roberts D, 2003. The Scandinavian Caledonides; event chronology, palaeogeographic settings and likely modern analogues. Tectonophysics, 365, 283–299.

Roedder E, 1981. Origin of fluid inclusions and changes that occur after trapping. In: L.S. Hollister and M. Crawford, L (Eds.), Short course handbook, Fluid inclusions: applications to petrology Mineralogical Association of Canada, Calgary, Canada, pp. 304.

Rönnback P, Åström M, Gustafsson J-P, 2008. Comparison of the behaviour of rare earth elements in surface waters, overburden groundwaters and bedrock groundwaters in two granitoidic settings, Eastern Sweden. Applied Geochemistry, 23, 1862–1880.

Röshoff K, Cosgrove J, 2002. Sedimentary dykes in the Oskarshamn-Västervik area – A study of the mechanism of formation. SKB R-02-37, Svensk Kärnbränslehantering AB.

Sandström B, Tullborg E-L, 2007. Paleohydrogeological events in Forsmark, central Sweden, recorded by stable isotopes in calcite and pyrite. In: T.D. Bullen and Y. Wang (Eds.), Water-rock Interaction: Proceedings of the 12th International Symposium on Water-Rock Interaction, Kunming, China, 31 July–5 August 2007. Taylor and Francis Ltd, London, UK, pp. 773–776.

Sandström B, Page L, Tullborg E-L, 2006a. Forsmark site investigation. $^{40}Ar/^{39}Ar$ (adularia) and Rb-Sr (adularia, prehnite, calcite) ages of fracture minerals. SKB P-06-213, Svensk Kärnbränslehantering AB.

Sandström B, Tullborg E-L, de Torres T, Ortiz J E, 2006b. The occurrence and potential origin of asphaltite in bedrock fractures, Forsmark, central Sweden. GFF, 128, 234–242.

Sandström B, Tullborg E-L, Smellie J A T, MacKenzie A B, 2008. Fracture mineralogy of the Forsmark site, SDM-Site Forsmark. SKB R-08-102, Svensk Kärnbränslehantering AB.

Scott R D, MacKenzie A B, Alexander W R, 1992. The interpretation of ^{238}U-^{234}U-^{230}Th-^{226}Ra disequilibria produced by rock-water interaction. Journal of Geochemical Exploration. 46, 323–343.

Shepherd T J, Rankin A H, Alderton D H M, 1985. A Practical Guide to Fluid Inclusion Studies, Blackie, Glasgow, UK, 239 pp.

SKB, 2006a. Preliminary site description, Laxemar subarea – version 1.2. SKB-R-06-10, Svensk Kärnbränslehantering AB.

SKB, 2006b. Hydrogeochemical evaluation, Preliminary site description Laxemar subarea – version 1.2. SKB-R-06-12, Svensk Kärnbränslehantering AB.

Sliaupa S, 1999. Far-field stress transmission effect in the structural evolution of Baltic Basin during the early Palaeozoic, European Union of Geosciences conference abstracts; EUG 10. Cambridge Publications, Cambridge, UK, pp. 286.

Sliaupa S, Fokin P, Lazauskiene J, Stephenson R A, 2006. The Vendian-early Paleozoic sedimentary basins of the East European Craton. In: D.G. Gee and R.A. Stephenson (Editors), European lithosphere dynamics. Geological Society, London, UK, pp. 449–462.

Smellie J A T, Mackenzie A B, Scott R D, 1986. An analogue validation study of natural radionuclide migration in crystalline rocks using uranium-series disequilibrium studies. Chemical Geology, 55, 233–254.

Söderlund P, Juez L J, Page L, Dunai T J, 2005. Extending the time range of apatite (U-Th)/He thermochronometry in slowly cooled terranes; Palaeozoic to Cenozoic exhumation history of southeast Sweden. Earth and Planetary Science Letters, 239, 266–275.

Söderlund P, Page L, Söderlund U, 2008. ^{40}Ar–^{39}Ar biotite and hornblende geochronology from the Oskarshamn area, SE Sweden: discerning multiple Proterozoic tectonothermal events. Geological Magazine, 145, 790–799.

Sokolnicki M, Väisäsvaara J, 2006. Oskarshamn site investigation. Difference flow logging of boreholes KLX09B-F Subarea Laxemar. SKB P-06-199, Svensk Kärnbränslehantering AB.

Sokolnicki M, Kristiansson S, 2007. Oskarshamn site investigation. Difference flow logging of boreholes KLX11B-F. SKB-P-07-74, Svensk Kärnbränslehantering AB.

Stemprok M, 1987. Greisenization (a review). Geologische Rundschau, 76, 169–175.

Stephens M., Wahlgren C-H, 2008. Bedrock evolution, in B. Söderbäck, (Ed.), Geological evolution, palaeoclimate and historical development of the Forsmark and Laxemar-Simpevarp areas, Site descriptive modelling, SDM-Site. SKB R-08-19, Svensk Kärnbränslehantering AB.

Strauss H, 1997. The isotopic composition of sedimentary sulfur through time. Palaeogeography Palaeoclimatology Palaeoecology, 132, 97–118.

Suksi J, 2001. Natural uranium as a tracer in radionuclide geosphere transport studies. PhD- thesis. Report series in Radiochemistry 16/2001, University of Helsinki, Helsinki, Finland, 152 pp.

Suksi J, Rasilainen K, 2002. Isotope fractionation of U in rocks reflecting redox conditions around a groundwater flow route. Mat. Res. Soc. Symp., 663 Scientific basis for Nuclear Waste Management: 961–969.

Takahashi Y, Shimizu H, Kagi H, Yoshida H, Usui A, Nomura M, 2000. A new method for the determination of Ce^{III}/Ce^{IV} ratios in geological materials; application for weathering, sedimentary and diagenetic processes. Earth and Planetary Science Letters, 182, 201–207.

Talbot C, Riad L, 1988. Natural fractures in the Simpevarp area. SKB PR-25-87-03, Svensk Kärnbränslehantering AB.

Talbot C, Riad L, Munier R, 1988. The geological structures and tectonic history of Äspö, SE Sweden. SKB PR-25-88-05, Svensk Kärnbränslehantering AB.

Thiel K, Vorwerk R, Saager R, Stupp H D, 1983. ^{235}U fission tracks and ^{238}U-series disequilibria as a means to study Recent mobilization of uranium in Archaean pyritic conglomerates. Earth and Planetary Science Letters, 65, 249–262.

Torsvik T H, Rehnström E F, 2003. The Tornquist Sea and Baltica-Avalonia docking. Tectonophysics, 362, 67–82.

Truesdell A H, Hulston J R, 1980. Isotopic evidence on environments of geothermal systems. In: P. Fritz, Fontes, J.C. (Editor), Handbook of environmental isotope geochemistry; vol. 1, The terrestrial environment, A. Elsevier, Amsterdam. The Netherlands.

Tullborg E-L, 1995. Chapter 4. Mineralogical/Geochemical Investigations in the Fracture Zone. In: S. Banwart (Editor), The Redox experiment in block scale. SKB PR-25-95-06, Svensk Kärnbränslehantering AB, pp. 81–101.

Tullborg E-L, 1997. Recognition of low-temperature processes in the Fennoscandian Shield. Doctoral Thesis, Göteborg University, Gothenburg, Sweden, 35 pp.

Tullborg E-L, 2003. Palaeohydrogeological evidences from fracture filling minerals – Results from the Äspö/Laxemar area. Materials Research Society Symposium, 807, Scientific basis for Nuclear Waste Management XXVII, 873–878.

Tullborg E-L, Wallin B, Landström O, 1991. Hydrogeochemical studies of fracture minerals from water conducting fractures and deep groundwaters at Äspö. SKB PR-25-90-01, Svensk Kärnbränslehantering AB.

Tullborg E-L, Larson S Å, Stiberg J P, 1996. Subsidence and uplift of the present land surface in the southeastern part of the Fennoscandian Shield. GFF, 118, 126–128.

Tullborg E-L, Landström O, Wallin B, 1999. Low-temperature trace element mobility influenced by microbial activity; indications from fracture calcite and pyrite in crystalline basement. Chemical Geology, 157, 199–218.

Tullborg E-L, Smellie J, Mackenzie A B, 2003. The use of natural uranium decay series studies in support of understanding redox conditions at potential radioactive waste disposal sites. Materials Research Society Symposium, 807, Scientific basis for Nuclear Waste Management XXVII, 571–576.

Tullborg E-L, Drake H, Sandström B, 2008. Palaeohydrogeology: A methodology based on fracture mineral studies. Applied Geochemistry, 23, 1881–1897.

Vaniman D T, Chipera S J, 1996. Paleotransport of lanthanides and strontium recorded in calcite compositions from tuffs at Yucca Mountain, Nevada, USA. Geochimica et Cosmochimica Acta, 60, 4417–4433.

Veizer J, 1983. Trace elements and isotopes in sedimentary carbonates. Reviews in Mineralogy and Geochemistry, 11, 265–299.

Veizer J, Ala D, Azmy K, Bruckschen P, Buhl D, Bruhn F, Carden G A F, Diener A, Ebneth S, Godderis Y, Jasper T, Korte C, Pawellek F, Podlaha O G, Strauss H, 1999. $^{87}Sr/^{86}Sr$, $\delta^{13}C$ and $\delta^{18}O$ evolution of Phanerozoic seawater. Chemical Geology, 161, 59–88.

Viola G, Venvik Ganerod G, 2007. Oskarshamn site investigation. Structural analysis of brittle deformation zones in the Simpevarp-Laxemar area, Oskarshamn, southeast Sweden. SKB P-07-41, Svensk Kärnbränslehantering AB.

Wahlgren C-H, Ahl M, Sandahl K-A, Berglund J, Petersson J, Ekström M, Persson P-O, 2004. Oskarshamn site investigation. Bedrock mapping 2003 – Simpevarp subarea. Outcrop data, fracture data, modal and geochemical classification of rock types, bedrock map, radiometric dating. SKB P-04-102, Svensk Kärnbränslehantering AB.

Wahlgren C-H, Bergman T, Ahl M, Ekström M, 2006a. Oskarshamn site investigation. Modal and geochemical analyses of drill core samples 2006 and updated bedrock map of the Laxemar subarea. Classification of rock types in KLX08, KLX10, KLX11A, KLX12A, KLX18A and KLX20A. SKB P-06-279, Svensk Kärnbränslehantering AB.

Wahlgren C-H, Hermanson J, Forssberg O, Curtis P, Triumf C-A, Drake H, Tullborg E-L, 2006b. Geological description of rock domains and deformation zones in the Simpevarp and Laxemar subareas. Preliminary site description Laxemar subarea – version 1.2. SKB R-05-69, Svensk Kärnbränslehantering AB.

Wahlgren C-H, Bergman T, Ahl M, Ekström M, Page L, Söderlund U, 2007. Oskarshamn site investigation. Modal and geochemical analyses of drill core samples 2007 and $^{40}Ar/^{39}Ar$ dating of a dolerite. Classification of rock types in KLX15A, KLX16A, KLX19A, KLX20A and KLX21B. SKB P-07-191, Svensk Kärnbränslehantering AB.

Wahlgren C-H, Curtis P, Hermanson J, Forssberg O, Öhman J, Drake H, Fox A, Triumf C-A, Mattsson H, Thunehed H, 2008. Geology Laxemar, Site descriptive modelling, SDM-Site Laxemar. SKB R-08-54, Svensk Kärnbränslehantering AB.

Wallin B, 1992. Sulphur and Oxygen isotope evidence from dissolved sulphates in groundwater and sulphide sulphur in fissure fillings at Äspö, Southeastern Sweden. SKB PR-25-92-08, Svensk Kärnbränslehantering AB.

Wallin B, Peterman Z, 1999. Calcite fracture fillings as indicators of palaeohydrogeology at Laxemar at the Äspö Hard Rock Laboratory, southern Sweden. Applied Geochemistry, 14, 953–962.

Wigley T M L, Plummer L N, Pearson F J Jr, 1978. Mass transfer and carbon isotope evolution in natural water systems. Geochimica et Cosmochimica Acta, 42, 1117–1140.

Yoshida H, Yamamoto K, Yogo S, Murakami Y, 2006. An analogue of matrix diffusion enhanced by biogenic redox reaction in fractured sedimentary rock. Journal of Geochemical Exploration, 90, 134–142.

Ziegler P A, 1985a. Late Caledonian framework of Western and Central Europe, The Caledonide Orogen; Scandinavia and related areas; Vol 1. John Wiley and Sons, Chichester, UK.

Ziegler P A, 1985b. Caledonian, Acadian-Ligerian, Bretonian, and Variscan orogens; is a clear distinction justified?, The Caledonide Orogen; Scandinavia and related areas; Vol 2. John Wiley and Sons, Chichester, UK.

Åberg G, 1978. Precambrian geochronology of south-eastern Sweden. Geologiska Föreningens i Stockholm Förhandlingar, 100, 125–154.

Åberg G, Löfvendahl R, Levi B, 1984. The Götemar granite-isotopic and geochemical evidence for a complex history of an anorogenic granite. Geologiska Föreningen i Stockholm Förhandlingar, 106, 327–333.

Åhäll K-I, 2001. Åldersbestämning av svårdaterade bergarter i sydöstra Sverige. SKB R-01-60, Svensk Kärnbränslehantering AB (in Swedish).

Appendix 1

Mineralogy, geochemistry, porosity and redox properties of rocks from the Laxemar subarea, with additional data from the Simpevarp subarea: Compilation of data for SR-Can

A1.1 Introduction

This appendix is a compilation of the data available in April 2008 of geochemistry, mineralogy, porosity and redox properties of the main rock types from the Laxemar subarea, as a part of the site investigation programme. Additional data from the Simpevarp subarea are included in some sections. The appendix is an update of the data compiled by /Drake et al. 2006/, but is more focused on the Laxemar subarea. The data have been extracted from the SKB database Sicada, via deliveries Sicada_08_071, Sicada_08_071_2 and Sicada_08_071_3 (delivered in April 2008).

A1.2 Rock mass

The bedrock in the Laxemar subarea has been divided into different rock domains. A rock domain refers to a rock volume in which rock units that show similar composition, grain size, degree of bedrock homogeneity, and degree and style of ductile deformation have been combined and distinguished from each other /Munier et al. 2003, Wahlgren et al. 2006c/. Each domain has been assigned a list of properties including rock domain ID, dominant rock type, subordinate rock types, degree of homogeneity, metamorphism/alteration and mineral fabric /Wahlgren et al. 2006c/. The domains RSMA01, RSMM01 and RSMD01 dominate the local model volume where the repository target volume is located /Wahlgren et al. 2008/. The rock types described in this data compilation are the rock types occurring in these domains, although data from adjacent domains have been included for some rock types.

The bedrock in the Laxemar subarea is dominated by *Ävrö granite (granite to quartz monzodiorite,* rock code 501044, subdivided into *Ävrö quartz monzodiorite*, rock code 501046 and *Ävrö granodiorite*, rock code 501056) and *quartz monzodiorite* (rock code 501036). Subordinate rock types are *fine-grained dioritoid* (rock code 501030), *fine-grained granite* (rock code 511058), *pegmatite* (rock code 501061), *diorite/gabbro* (rock code 501033), *granite* (rock code 501058), *fine-grained diorite-gabbro rock* (rock code 505102), and *dolerite* (rock code 501027) /Wahlgren et al. 2008/. The proportion of these rock types in each of the domains is listed in Table A1-1 and a two dimensional model at the surface for rock domains in the Laxemar local model area is shown in Figure A1-1.

Descriptions of the major rock types and the subordinate rock types are presented in the following sections.

Table A1-1. Quantitative estimates of the proportions of different rock types in the rock domains A01, M01, and D01. No division of Ävrö granite 501044 into 501046 and 501056 is made but 501046 dominates RSMM01 and 501056 dominates RSMA01. Numbers are based on /Wahlgren et al. 2008/.

Code (SKB)	Name	Domain (RSM)		
		A01 (%)	M01 (%)	D01 (%)
501044	Ävrö granite	82	75	1.1
501036	Quartz monzodiorite	1.8	0.4	89
501030	Fine-grained dioritoid	3.1	0.4	0.3
501058	Granite	3.4	2.0	0.4
511058	Fine-grained granite	4.1	4.7	5.0
501033	Diorite/gabbro	0.3	16	0.1
501027	Dolerite	–	–	2.1
501061	Pegmatite	0.4	0.5	1.5
505102	Fine-grained diorite-gabbro	5.7	1.8	1.8

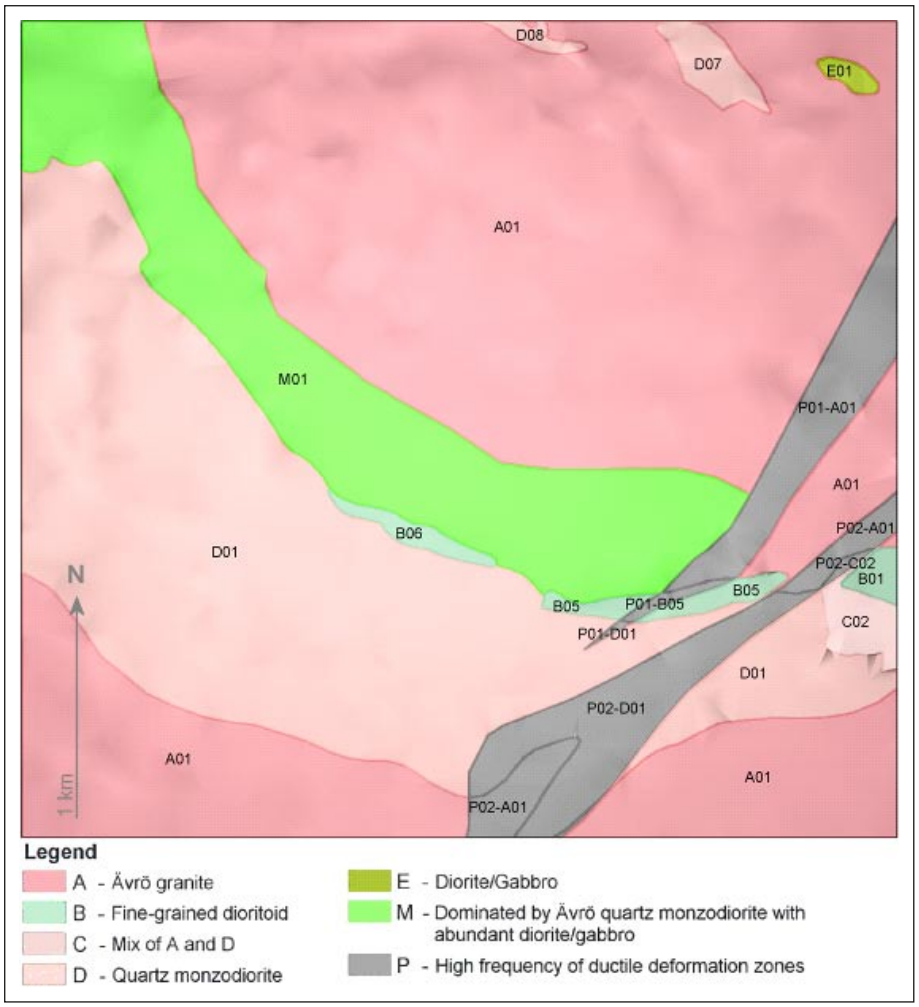

Figure A1-1. *Two dimensional model at the surface for rock domains in the Laxemar local model area. For reasons of simplicity, the prefix RSM has been excluded in the denomination of the rock domains. Figure adopted from /Wahlgren et al. 2008/.*

A1.2.1 Description and mineralogy rock types

The following section is a description of the rock type characteristics compiled from drill core and field data /Wahlgren et al. 2004, 2005, 2006a, b, c, 2007, Drake and Tullborg, 2006a, b, Adl-Zarrabi 2007, Janson et al. 2007/. The rocks are mostly well preserved and more or less undeformed, but a weak foliation is locally developed.

The mineralogical composition of the major and subordinate rock types is based on point counting. Most of the rock types are presented collectively for the Simpevarp and Laxemar subareas, in order to obtain a larger data set. However, Ävrö granite, have been divided into Ävrö granite and Ävrö quartz monzodiorite in the Laxemar subarea, in contrast to in the Simpevarp subarea /Wahlgren et al. 2006b/. Ävrö granite data from the Simpevarp subarea are thus not included in the compilation.

Some discrepancy exists between how the data have been reported into Sicada; minerals occurring only as minor components have either been reported as <0.2 vol.%, <1 vol.%, 0 vol.% or not reported at all. Where the occurrence of a mineral has been assign a value of <0.2 or <1 vol% in the Sicada data, a numeric value of 0.1 vol.% has been used for the calculation of median and standard deviation values since the resolution of the point counting is 0.2 vol.%. This results in a minor bias in the data when the occurrence of a mineral is close to the resolution limit of 0.2 vol.%.

The pyrite content is commonly not counted separately during the point counting but falls under the opaque mineral group. See /Drake et al. 2006/ for estimates of the pyrite content and grain-sizes.

Short descriptions of the texture and mineralogy of the rock types in the Laxemar area are listed below, divided into major and subordinate rock types. Modal composition of hydrothermally altered, red-stained rock adjacent to fractures is also shown for the major rock types and Fine-grained dioritoid.

A1.2.1.1 Major rock types

Ävrö granite – rock code 501044

Ävrö granitdiorite – rock code 501056

Ävrö quartz monzodiorite – rock code 501046

The Ävrö granite comprises a suite of commonly medium-grained, porphyritic rocks that vary in composition from quartz monzodiorite to granite, including granodioritic, tonalitic, quartz dioritic and quartz monzonitic varieties. In the Laxemar subarea, the Ävrö granite can be subdivided into two populations defined by their quartz content, one richer in quartz (Table A1-2, >20 vol.% quartz; the *Ävrö granodiorite*, rock code 501056, is common in domain RSMA01) and one with a lower quartz content (Table A1-3, <20 vol.% quartz, rock code 501046, the *Ävrö quartz monzodiorite*, which dominates and constitute c. 75% of the RSMM01 domain). Division of these rock types in the boreholes is based on density (501056: <2,710 kg/m^3 and 501046: >2,710 kg/m^3). Apart from the higher quartz content, the Ävrö granodiorite has somewhat higher contents of K-feldspar but lower contents of biotite, amphibole, plagioclase and opaques than the Ävrö quartz monzodiorite.

Table A1-2. Modal composition of Ävrö granodiorite (501056), vol. % (N=47).

Mineral	Median	St.dev.	Min	Max
Apatite	<0.2	n.a.	0	0.6
Biotite	8.0	1.7	3.0	11.8
Calcite	<0.2	n.a.	0	0.6
Chlorite	<0.2	n.a.	0	1.0
Epidote	1.4	0.9	0.2	4.4
Amphibole	<0.2	0.4	0	2.4
K-feldspar	22.8	5.0	13.2	34.6
Muscovite	<0.2	n.a.	0	1.0
Opaque	0.8	0.4	<0.2	1.6
Plagioclase	40.2	4.5	28.2	50.2
Prehnite	<0.2	n.a.	0	0.4
Quartz	24.8	3.2	20.6	31.8
Titanite	0.6	0.3	<0.2	1.8
Zircon	<0.2	n.a.	0.2	0.2

Table A1-3. Modal composition of Ävrö quartz monzodiorite, (501046) vol.% (N=45).

Mineral	Median	St.dev.	Min	Max
Apatite	0.4	0.3	0.0	1.0
Biotite	12.2	4.0	7.2	24.8
Calcite	<0.2	0.6	0.0	3.8
Chlorite	<0.2	0.3	0.0	1.4
Epidote	0.8	1.9	0.0	6.8
Amphibole	3.4	2.9	0.0	11.2
K-feldspar	9.8	7.6	0.6	30.0
Opaque	1.2	0.8	0.2	3.6
Plagioclase	54.2	6.9	44.4	68.0
Prehnite	<0.2	n.a.	0.0	0.4
Pyroxene	<0.2	1.2	0.0	7.2
Quartz	11.8	3.4	4.2	19.8
Titanite	1.0	0.5	0.2	2.0
Zircon	<0.2	n.a.	0.0	0.4

Quartz monzodiorite – rock code 501036

The quartz monzodiorite is a grey to reddish grey, medium-grained, equigranular to weakly porphyritic rock with relatively restricted compositional range (Table A1-4). The rock is dominated by plagioclase. The contents of biotite and amphibole are generally higher than in the Ävrö granite and Ävrö quartz monzodiorite. The RSMD01 domain is strongly dominated by the quartz monzodiorite.

A1.2.1.2 Subordinate rock types

Fine-grained dioritoid – rock code 501030

The fine-grained dioritoid is a unequigranular rock with up to 3 mm large megacrysts of hornblende and plagioclase (locally pyroxene and biotite occur as megacrysts). Most of the hornblende megacrysts are interpreted to be secondary after pyroxene. This rock is a major rock type in the Simpevarp subarea (central and southern part of the Simpevarp peninsula and central Ävrö) and a subordinate rock type in the Laxemar subarea, where it occurs as minor bodies in the southern part of the subarea, particularly along the contact zone between the Ävrö quartz monzodiorite (RSMM01) and the quartz monzodiorite (RSMD01). For one sample from borehole KSH02, altered plagioclase was counted as "sericite" (otherwise the appearance of sericite is only commented). In this compilation these sericite counts have been added to the plagioclase group in Table A1-5.

Table A1-4. Modal composition of quartz monzodiorite, vol.% (501036, N=44, 37 from the Laxemar subarea).

Mineral	Median	St.dev.	Min	Max
Apatite	0.2	0.3	0.0	1.0
Biotite	14.2	7.4	6.6	49.0
Calcite	<0.2	n.a.	0.0	2.2
Chlorite	<0.2	n.a.	0.0	1.2
Epidote	0.6	3.7	0.0	14.8
Amphibole	9.8	8.4	0.0	41.0
K-feldspar	10.8	5.3	0.0	19.8
Muscovite	<0.2	n.a.	0.0	2.6
Opaque	1.2	0.6	0.2	2.8
Plagioclase	45.9	6.4	19.4	56.2
Prehnite	<0.2	n.a.	0.0	0.2
Pyroxene	<0.2	2.2	0.0	8.2
Quartz	12.8	3.3	5.0	19.4
Titanite	0.4	0.7	0.0	3.2
Zircon	<0.2	n.a.	0.0	0.2

Table A1-5. Modal composition of fine-grained dioritoid, vol.% (501030, N=24, 3 from the Laxemar subarea).

Mineral	Median	St.dev.	Min	Max
Apatite	<0.2	n.a.	0.0	0.8
Biotite	15.2	9.5	0.0	43.8
Calcite	<0.2	0.5	0.0	2.0
Chlorite	<0.2	4.3	0.0	16.0
Epidote	1.6	2.8	0.0	10.0
Amphibole	2.2	5.7	0.0	20.0
K-feldspar	10.2	6.5	0.4	22.8
Muscovite	<0.2	n.a.	0.0	1.2
Opaque	1.2	0.9	0.1	3.4
Plagioclase	49.0	9.7	27.8	65.6
Prehnite	<0.2	n.a.	0.0	0.8
Pyroxene	<0.2	5.3	0.0	22.0
Quartz	8.7	5.5	0.8	22.2
Olivine	<0.2	n.a.	0.0	1.4
Titanite	0.4	0.6	0.0	1.8
Zircon	<0.2	n.a.	0.0	0.2

Diorite/gabbro – rock code 501033
Diorite/gabbro occurs as scattered minor bodies and enclaves, particularly in the Ävrö granite in the Laxemar subarea and its immediate surroundings. The most prominent occurrence of diorite/gabbro is the concentration along the contact zone between the Ävrö quartz monzodiorite and the quartz monzodiorite in the southern part of the Laxemar subarea (rock domain RSMM01: 16% diorite/gabbro). Modal composition is shown in Table A1-6.

Fine-grained granite – rock code 511058
Fine-grained granite is a common subordinate rock type in the Laxemar and Simpevarp subareas (4–5% of RSMA01, RSMM01 and RSMD01). It occurs as dykes of various thickness (generally 0.1–1 m), but also as veins and minor, irregular bodies in the other rock types. The rock is dominated by plagioclase, K-feldspar and quartz, with biotite, epidote, chlorite and titanite as minor constituents. The modal content is based on samples from the Simpevarp subarea only (Table A1-7).

Granite – rock code 501058
Scattered minor bodies of red to greyish red, medium- to coarse-grained granite (501058) occur in the Laxemar and Simpevarp subareas. It occurs as mixed and mingled, diffusely delimited small occurrences in the Ävrö granite (e.g. 3.4% of RSMA01). This rock type has higher plagioclase content and lower K-feldspar content (highly varying) than the fine-grained granite (Table A1-8).

Table A1-6. Modal composition of diorite/gabbro, vol.% (N=18, 14 from the Laxemar subarea).

Mineral	Median	St.dev.	Min	Max
Apatite	0.2	0.2	0.0	0.6
Biotite	15.4	9.6	0.0	44.6
Calcite	<0.2	0.2	0.0	0.4
Chlorite	<0.2	1.6	0.0	6.2
Epidote	1.2	4.3	0.0	18.2
Amphibole	20.4	15.1	5.2	62.6
K-feldspar	0.2	1.9	0.0	6.2
Opaque	2.5	2.1	0.8	9.2
Plagioclase	45.9	13.6	3.6	55.6
Prehnite	<0.2	n.a.	0.0	0.8
Pyroxene	0.3	13.8	0.0	54.0
Quartz	7.3	4.5	0.0	16.0
Titanite	0.2	1.1	0.0	3.8
Zircon	<0.2	n.a.	0.0	0.4

Table A1-7. Modal composition of fine-grained granite, vol.% (N=8, 2 from Laxemar subarea).

Mineral	Median	St.dev	Min	Max
Quartz	24.8	3.8	22.2	33.0
K-feldspar	31.3	4.0	26.0	39.8
Plagioclase	31.3	5.8	25.8	42.8
Chlorite	1.2	1.6	0.0	3.8
Biotite	3.5	3.9	0.0	10.8
Opaque	0.6	0.5	0.0	1.4
Epidote	1.4	1.9	0.0	5.2
Titanite	1.0	0.8	0.0	2.0
Amphibole	<0.2	0.1	0.0	0.4
Muscovite	0.4	1.3	0.0	4.0
Calcite	<0.2	0.1	0.0	0.2

Table A1-8. Modal composition of granite, vol.% (501058, N=3, only Laxemar subarea).

Mineral	Median	St.dev	Min	Max
Quartz	27.8	3.7	26.2	33.2
K-feldspar	16.6	11.8	3.0	26.4
Plagioclase	41.0	4.9	38.4	47.8
Chlorite	0.2	9.9	0	17.2
Biotite	6.2	3.6	0	6.2
Opaque	1.0	0.8	0.2	1.8
Epidote	0.2	0.8	0.0	1.4
Titanite	0.2	0.0	0.2	0.2
Muscovite	0.4	1.5	0.4	3.0
Prehnite	<0.2	0.1	0.0	0.2

Pegmatite – rock code 501066
Pegmatite frequently occurs as less than 0.3 m thick dykes. No modal analysis has been carried out on this rock type.

Fine-grained diorite-gabbro – rock code 505102
Locally, a fine-grained diorite-gabbro rock occurs as sheets, dykes or minor bodies (e.g. 5.7% in RSMA01). Modal composition is shown in Table A1-9.

Dolerite – rock code 501027
Dolerite occurs as dykes in KLX14A, KLX19A and KLX20A in the western part of the Laxemar subarea. Only two samples have been analysed for their modal compositions (Table A1-10).

A1.2.1.3 Hydrothermally altered rock adjacent to fractures

Differences in mineralogy between the red-stained rock and fresh rock have been reported by /Drake and Tullborg 2006a, b/. The red-stained, hydrothermally altered Ävrö granite, quartz monzodiorite and fine-grained dioritoid adjacent to fractures have experienced replacement of plagioclase by

Table A1-9. Modal composition of fine-grained diorite-gabbro, vol.% (505102, N=3; 2 from Laxemar subarea).

Mineral	Median	St.dev	Min	Max
Quartz	11.6	4.8	5.6	15.0
K-feldspar	<0.2	1.2	0.0	2.0
Plagioclase	32.6	12.0	29.8	51.8
Biotite	19.4	12.4	10.2	34.8
Opaque	1.6	1.7	0.8	4.0
Epidote	1.8	1.9	0.0	3.8
Titanite	2.0	3.7	0.0	7.2
Amphibole	20.4	9.7	12.8	32.0

Table A1-10. Modal composition of dolerite (501027), Laxemar subarea. In vol. %.

Borehole	KLX19A	KLX20A
Sample	532.97m	193.37 m
Apatite	<0.2	<0.2
Biotite	0	1.6
Chlorite	<0.2	0
Olivine	2.2	8.6
Opaque	6.0	4.8
Plagioclase	59.0	69.0
Pyroxene	11.8	11.4
Serpentine*	16.2*	4.6*

*includes iddingsite

K-feldspar, albite, sericite, epidote and prehnite. Biotite has been replaced by chlorite. Magnetite is partially or completely replaced by hematite. Primary pyrite is commonly partially altered or completely replaced. Mineralogical composition of red-stained Ävrö granite from Simpevarp and Laxemar subareas (not divided into Ävrö granodiorite and Ävrö quartz monzodiorite), fine-grained dioritoid, Simpevarp subarea and quartz monzodiorite, Simpevarp subarea is shown in Table A1-11, Table A1-12 and Table A1-13.

A1.2.2 Geochemistry

The geochemistry of the dominating rock types (Ävrö granodiorite, Ävrö quartz monzodiorite, quartz monzodiorite, fine-grained dioritoid and diorite/gabbro) as well as dolerite in the Laxemar subarea (including Simpevarp subarea for quartz monzodiorite, fine-grained dioritoid) is described below. Chemical composition of hydrothermally altered, red-stained rock adjacent to fractures is also listed for the major rock types and Fine-grained dioritoid.

Table A1-11. Mineralogical composition of red-stained Ävrö granite (501044), KLX04, Laxemar subarea (vol.%, N=6).

Mineral	Median	St.dev	Min	Max
Quartz	20.0	9.1	5.8	30.1
K-feldspar	15.0	8	11.5	30.2
Altered K-feldspar	0.6	0.4	0.2	1.2
Saussuritized Plagioclase	41.0	7.3	36.7	56.1
Plagioclase	1.4	9.1	0.3	23.7
Chlorite	7.8	5.3	3.7	17.6
Biotite	<0.2	1.3	0	3.1
Opaque	1.5	0.8	0.4	2.6
-Pyrite	<0.1		0	0.19
Epidote	2	1.3	0.5	3.8
Titanite	1.1	0.4	0.7	1.7
Hornblende	<0.2	2.4	0	6.0
Prehnite	1.1	0.8	0.3	2.3
Calcite	0.5	0.3	0.2	1.0
Voids	0.5	0.3	0.1	0.9

Table A1-12. Mineralogical composition of red-stained quartz monzodiorite (501036) from KSH03A+B, Simpevarp subarea (vol.%, N=6).

Mineral	Median	St.dev	Min	Max
Quartz	10.7	4.9	3.1	15.9
K-feldspar	5.4	4.9	1.4	13.3
Altered K-feldspar	<0.2	0.6	0.3	1.6
Saussuritized Plagioclase	50.3	3.0	47.0	54.5
Plagioclase	0.7	2.4	0.2	6.2
Chlorite	11.0	3.8	9.1	17.0
Biotite	0.3	0.6	0.1	1.8
Opaque	2.0	0.8	1.6	3.6
-Pyrite				<0.1
Epidote	1.3	0.8	1.0	3.2
Titanite	0.4	0.3	<0.2	0.9
Hornblende*	11.7	5.4	6.7	18.3
Prehnite	2.7	2.0	0.6	6.3
Voids	0.2	0.9	0.0	2.2

*=includes additional augite.

Table A1-13. Range in modal composition of two red-stained fine-grained dioritoid (501030) samples, KSH01A, Simpevarp subarea (vol.%).

Mineral	Min	Max
Quartz	14.0	28.6
K-feldspar	11.0	14.0
Altered K-feldspar	0.3	0.7
Saussuritized Plagioclase	36.4	48.4
Plagioclase	0.6	1.8
Chlorite	13.4	14.4
Biotite	1.0	1.4
Opaque*	0.3	1.2
-Pyrite	<0.1	<0.1
Epidote	0.3	0.8
Titanite	<0.1	<0.1
Amphibole*	0.7	6.5
Prehnite	1.2	2.7
Voids	0.1	0.3

*=includes hornblende, actinolite and augite.

A1.2.2.1 Ävrö granodiorite (501056) and Ävrö quartz monzodiorite (501046)

The geochemistry of Ävrö granodiorite (rock code 501056) and Ävrö quartz monzodiorite (501046) is summarized in Table A1-14 and Table A1-15. The subdivision of these rock types is made based on the modal quartz content and only geochemical analyses from samples with a known modal content are used in this compilation. The geochemistry of the Ävrö granodiorite, is characterized by a quite high SiO_2 content (median: 68.3 wt.%), which is higher than in Ävrö quartz monzodiorite (median 59.8 wt.%). Generally, Ävrö granodiorite has higher concentrations of K_2O, Rb, Th and U than the Ävrö quartz monzodiorite. The other elements (Table A1-14 and Table A1-15) have higher concentrations in Ävrö quartz monzodiorite.

A1.2.2.2 Quartz monzodiorite (501036)

The quartz monzodiorite (rock code 501036, Table A1-16, values from both the Laxemar and Simpevarp subareas) has quite similar chemical composition as the Ävrö quartz monzodiorite due to similar mineralogy (the difference between these is based on texture mainly). However, some notable chemical differences exist, e.g. higher contents of Fe_2O_3, CaO, MgO, MnO, TiO_2, Co, Cr and lower contents of SiO_2, Al_2O_3, Na_2O, Ba and Sr in the quartz monzodiorite than in the Ävrö quartz monzodiorite. These chemical differences are mainly related to the somewhat different mineralogical compositions. The main mineralogical difference between these two rock types are the higher content of biotite and amphibole and the lower content of plagioclase in the quartz monzodiorite. Furthermore, the REE patterns of the quartz monzodiorite are more flat, with lower LREE contents and higher MREE and HREE contents, than those of the Ävrö quartz monzodiorite.

A1.2.2.3 Fine-grained dioritoid (501030)

The median and standard deviation calculations of fine-grained dioritoid are based on 14 whole rock samples, all of which are from the Simpevarp subarea (Table A1-17). This is because no representative chemical analysis of this rock type has been carried out in the Laxemar subarea. Most of the major elements in the fine-grained dioritoid show similar contents as in the quartz monzodiorite, although the fine-grained dioritoid has slightly lower contents of SiO_2, Al_2O_3, Fe_2O_3, MnO, Na_2O, Ba, Co, Cr, Sr, and REE:s and slightly higher contents of MgO, Rb, Th and U. Some of these differences may be related to the slightly different mineralogy of these rock types, e.g. slightly higher contents of biotite and plagioclase but lower median contents of amphibole and quartz, and occasionally very much higher pyroxene contents in the fine-grained dioritoid compared to the quartz monzodiorite.

10 References

Alm E, Sundblad K, 2002. Fluorite-calcite-galena-bearing fractures in the counties of Kalmar and Blekinge, Sweden. SKB R-02-42, Svensk Kärnbränslehantering AB.

Alm E, Sundblad K, Huhma H, 2005. Sm-Nd isotope determinations of low-temperature fluorite-calcite-galena mineralization in the margins of the Fennoscandian Shield. SKB R-05-66, Svensk Kärnbränslehantering AB.

Arcos D, Pérez del Villar L, Bruno J, Domènech C, 2008. Geochemical modelling of the weathering zone of the ”Mina Fe” U deposit (Spain): a natural analogue for nuclear spent fuel alteration and stability processes in radwaste disposal. Applied Geochemistry 23, 807–821.

Baarli B G, 1990. Peripheral bulge of a foreland basin in the Oslo region during the Early Silurian. Palaeogeography, Palaeoclimatology, Palaeoecology, 7–8, 149–161.

Bassett M G, 1985. Silurian stratigraphy and facies development in Scandinavia, The Caledonide Orogen; Scandinavia and related areas; Vol 1. John Wiley and Sons, Chichester, UK.

Bath A, Milodowski A, Ruotsalainen P, Tullborg E-L, Cortés Ruiz A, Aranyossy J-F, 2000. Evidences from mineralogy and geochemistry for the evolution of groundwater systems during the quaternary for use in radioactive waste repository safety assessment (EQUIP project). EUR report 19613 EN. European Commission, Luxembourg, Luxembourg, 157 p.

Bau M, 1999. Scavenging of dissolved yttrium and rare earths by precipitating iron oxyhydroxide; experimental evidence for Ce oxidation, Y-Ho fractionation, and lanthanide tetrad effect. Geochimica et Cosmochimica Acta, 63, 67–77.

Bau M, Möller P, 1992. Rare Earth Element Fractionation in Metamorphogenic Hydrothermal Calcite, Magnesite and Siderite. Mineralogy and Petrology, 45, 231–246.

Bergman L, Lindberg B, 1979. Phanerozoic veins of galena in the Åland rapakivi area, southwestern Finland. Bulletin of the Geological Society of Finland, 51, 55–62.

Bingen B, Andersson J, Söderlund U, Möller C, 2008. The Mesoproterozoic in the Nordic countries, Episodes, 31, 29–34.

Bird D K, Spieler A R, 2004. Epidote in geothermal systems, Epidotes. Mineralogical Society of America and Geochemical Society, Washington, DC, USA, pp. 235–300.

Bird D K, Schiffman P, Elders W A, Williams A E, McDowell S D, 1984. Calc-silicate mineralization in active geothermal systems. Economic Geology, 79, 671–695.

Bjarnason B, Leijon B, Strindell, Öhman T, 1989. Rock stress measurements in boreholes KAS02, KAS03 and KS06 on Äspö. SKB PR-25-89-17, Svensk Kärnbränslehantering AB.

Blyth A, Frape S, Blomqvist R, Nissinen P, 2000. Assessing the past thermal and chemical history of fluids in crystalline rock by combining fluid inclusion and isotopic investigations of fracture calcite. Applied Geochemistry, 15, 1417–1437.

Bogdanova S V, Page L, Skridlaite G, Taran L N, 2001. Proterozoic tectonothermal history in the western part of the East European Craton: $^{40}Ar/^{39}Ar$ geochronological constraints. Tectonophysics, 339, 39–66.

Bogdanova S V, Bingen B, Gorbatschev R, Kheraskova T N, Kozlov V I, Puchkov V N, Volozh Y A, 2008. The East European Craton (Baltica) before and during the assembly of Rodinia. Precambrian Research, 160, 23–45.

Boulton G S, Zatsepin S, Maillot B, 2001. Anlysis of groundwater flow beneath ice sheets. SKB TR-01-06, Svensk Kärnbränslehantering AB.

Brander L, Söderlund U, 2008. Mesoproterozoic (1.47–1.44 Ga) orogenic magmatism in Fennoscandia; Baddeleyite U-Pb dating of a suite of massif-type anothosite in S. Sweden. International Journal of Earth Sciences, 98, 499–516.

Table A1-14. Chemical composition of Ävrö granodiorite (501056) from Laxemar subarea (N=34).

Element		Median	St.dev.	Min	Max
SiO_2	wt. %	68.3	1.0	65.4	69.7
Al_2O_3	wt. %	15.1	0.4	14.4	15.8
CaO	wt. %	2.6	0.3	1.3	3.3
Fe_2O_3	wt. %	3.6	0.3	3.2	4.2
K_2O	wt. %	4.2	0.2	3.8	4.8
MgO	wt. %	1.3	0.1	0.9	1.5
MnO	wt. %	0.06	0.01	0.05	0.11
Na_2O	wt. %	3.7	0.2	3.2	4.5
P_2O_5	wt. %	0.18	0.02	0.14	0.22
TiO_2	wt. %	0.47	0.05	0.36	0.59
Total	wt. %	99.5	1.4	95.8	101.7
LOI	wt. %	0.6	0.2	0.1	1.1
Ba	mg/kg	1,115	244	887	2,080
Be	mg/kg	2.4	0.2	1.6	2.8
Co	mg/kg	<6	n.a.	<6	9.4
Cr	mg/kg	22.3	15.7	5.0	66.5
Cu	mg/kg	18.4	16.8	3.0	103
Ga	mg/kg	23.3	21.8	7.2	79.3
Hf	mg/kg	4.0	1.0	1.4	5.8
Mo	mg/kg	<2	n.a.	<2	6.7
Nb	mg/kg	8.4	1.3	5.1	11.2
Ni	mg/kg	16.4	8.2	<10	33.6
Rb	mg/kg	98.0	48.6	64.7	272
Sc	mg/kg	5.4	1.1	2.7	8.5
Sn	mg/kg	2.0	5.1	<1	20.4
Sr	mg/kg	712	116	422	1,170
Ta	mg/kg	0.8	0.2	0.3	1.3
Th	mg/kg	9.2	4.0	0.5	16.3
U	mg/kg	3.1	1.1	1.3	5.3
V	mg/kg	45.6	4.8	29.7	54.6
W	mg/kg	<0.3	n.a.	<0.3	3.1
Y	mg/kg	17.0	2.8	9.3	21.3
Zn	mg/kg	53.5	14.9	40.6	120
Zr	mg/kg	184	21.2	147	228
La	mg/kg	38.7	8.6	18.6	55.5
Ce	mg/kg	80.6	16.2	36.6	111
Pr	mg/kg	9.23	2.02	4.20	11.8
Nd	mg/kg	32.1	6.4	15.7	44.5
Sm	mg/kg	4.85	1.13	1.82	6.80
Eu	mg/kg	0.92	0.36	0.13	1.29
Gd	mg/kg	3.25	0.83	0.85	4.39
Tb	mg/kg	0.51	0.11	0.17	0.69
Dy	mg/kg	2.53	0.64	0.86	3.67
Ho	mg/kg	0.50	0.14	0.09	0.70
Er	mg/kg	1.39	0.54	0.05	2.15
Tm	mg/kg	0.21	0.11	<0.1	0.46
Yb	mg/kg	1.35	0.41	0.61	2.09
Lu	mg/kg	0.23	0.07	0.02	0.39

Table A1-15. Chemical composition of Ävrö quartz monzodiorite (501046) from Laxemar subarea (N=28).

Element		Median	St.dev.	Min	Max
SiO_2	wt. %	59.8	3.1	55.4	69.1
Al_2O_3	wt. %	17.5	0.8	14.9	18.1
CaO	wt. %	4.5	0.7	2.6	5.9
Fe_2O_3	wt. %	5.8	1.0	3.4	8.5
K_2O	wt. %	3.3	0.5	2.3	4.5
MgO	wt. %	2.4	0.5	1.1	3.6
MnO	wt. %	0.09	0.02	0.05	0.14
Na_2O	wt. %	4.4	0.3	3.7	4.7
P_2O_5	wt. %	0.36	0.07	0.17	0.43
TiO_2	wt. %	0.83	0.14	0.45	1.06
Total	wt. %	99.2	1.3	96.3	101.5
LOI	wt. %	0.7	0.2	0.5	1.2
Ba	mg/kg	1,695	353	564	2,190
Be	mg/kg	2.5	0.6	1.6	4.0
Co	mg/kg	10.1	3.7	5.9	22.4
Cr	mg/kg	36.5	23.1	15.0	108
Cu	mg/kg	28.6	35.7	3.0	203
Ga	mg/kg	26.5	30.2	5.9	124
Hf	mg/kg	5.3	1.2	2.5	7.3
Mo	mg/kg	<2	n.a.	<2	3.2
Nb	mg/kg	9.5	2.6	3.8	16.0
Ni	mg/kg	25.1	10.5	5.0	50.3
Rb	mg/kg	85.0	59.8	39.3	381
Sc	mg/kg	9.1	2.4	5.0	18.6
Sn	mg/kg	3.0	3.5	<1	17.2
Sr	mg/kg	1,330	223	662	1,530
Ta	mg/kg	0.9	0.3	0.3	1.6
Th	mg/kg	5.8	2.8	0.4	12.4
U	mg/kg	2.4	1.6	0.9	7.0
V	mg/kg	86	18.2	40.0	132
W	mg/kg	0.6	0.2	<0.3	0.9
Y	mg/kg	22.0	4.1	12.4	35.6
Zn	mg/kg	98.0	41.4	52.2	231
Zr	mg/kg	266	44.9	179	377
La	mg/kg	49.5	7.5	28.3	59.5
Ce	mg/kg	108.0	19.4	67.0	139
Pr	mg/kg	13.5	2.49	7.56	16.5
Nd	mg/kg	52.2	9.7	30.7	62.4
Sm	mg/kg	7.64	1.79	3.64	10.3
Eu	mg/kg	1.48	0.44	0.65	1.98
Gd	mg/kg	4.98	1.18	1.96	7.04
Tb	mg/kg	0.69	0.31	0.18	2.00
Dy	mg/kg	3.64	0.72	1.71	4.64
Ho	mg/kg	0.70	0.28	0.43	1.98
Er	mg/kg	1.88	0.64	0.29	3.55
Tm	mg/kg	0.38	0.23	0.14	1.42
Yb	mg/kg	1.78	0.43	0.92	2.72
Lu	mg/kg	0.30	0.09	0.12	0.53

Table A1-16. Chemical composition of quartz monzodiorite (501036, N=37, 28 from the Laxemar subarea).

Element		Median	St.dev.	Min	Max
SiO_2	wt. %	58.7	2.2	50.7	61.7
Al_2O_3	wt. %	16.2	0.5	15.1	17.2
CaO	wt. %	5.2	0.7	4.0	7.1
Fe_2O_3	wt. %	7.6	0.9	6.2	9.7
K_2O	wt. %	3.3	0.3	2.4	3.9
MgO	wt. %	2.7	0.6	2.1	4.9
MnO	wt. %	0.12	0.01	0.10	0.16
Na_2O	wt. %	3.4	0.2	2.9	3.7
P_2O_5	wt. %	0.34	0.05	0.26	0.49
TiO_2	wt. %	1.00	0.09	0.86	1.34
Total	wt. %	98.2	1.4	96.2	100.9
LOI	wt. %	0.7	0.3	0.2	1.8
Ba	mg/kg	1,020	148	700	1,310
Be	mg/kg	2.3	0.2	1.9	2.7
Co	mg/kg	15.4	3.8	9.9	26.2
Cr	mg/kg	49.9	28.0	<10	135
Cu	mg/kg	25.9	20.6	6.3	121
Ga	mg/kg	25.3	29.8	<1	154
Hf	mg/kg	5.4	1.9	1.8	9.4
Mo	mg/kg	<2	n.a.	<2	3.7
Nb	mg/kg	10.8	3.1	8.0	20.7
Ni	mg/kg	21.2	10.0	<10	52.8
Rb	mg/kg	94.9	43.9	54.8	225
Sc	mg/kg	17.3	2.3	12.5	23.5
Sn	mg/kg	2.4	1.3	<1	5.3
Sr	mg/kg	644	113	504	1,150
Ta	mg/kg	0.9	0.2	0.4	1.3
Th	mg/kg	6.5	1.7	3.4	9.9
U	mg/kg	2.1	0.8	0.7	4.0
V	mg/kg	114	26.3	81.9	200
W	mg/kg	1.1	0.5	<0.3	2.0
Y	mg/kg	32.1	3.7	18.2	37.9
Zn	mg/kg	95.9	18.0	76.5	166
Zr	mg/kg	234	58.0	115	394
La	mg/kg	40.7	8.1	29.2	75.1
Ce	mg/kg	91.1	17.9	59.9	157
Pr	mg/kg	10.50	3.64	1.00	18.5
Nd	mg/kg	40.5	6.4	30.4	68.4
Sm	mg/kg	7.18	1.55	3.50	11.3
Eu	mg/kg	1.72	0.43	0.49	2.08
Gd	mg/kg	6.12	1.61	0.62	8.95
Tb	mg/kg	0.88	0.28	0.10	1.24
Dy	mg/kg	4.84	1.04	2.41	7.10
Ho	mg/kg	1.01	0.22	0.40	1.34
Er	mg/kg	2.78	1.11	0.10	3.76
Tm	mg/kg	0.46	0.19	0.10	1.10
Yb	mg/kg	3.02	0.67	0.83	3.46
Lu	mg/kg	0.37	0.11	0.08	0.51

Table A1-17. Chemical composition of fine-grained dioritoid (501030, N=14, only Simpevarp subarea).

Element		Median	St.dev.	Min	Max
SiO_2	wt. %	58.0	2.3	56.6	63.3
Al_2O_3	wt. %	16.0	0.4	15.5	17.0
CaO	wt. %	5.2	1.0	3.1	7.4
Fe_2O_3	wt. %	7.3	1.2	4.3	8.9
K_2O	wt. %	3.3	0.6	2.6	4.3
MgO	wt. %	2.8	0.7	2.0	4.8
MnO	wt. %	0.12	0.01	0.08	0.14
Na_2O	wt. %	3.3	0.3	2.8	3.9
P_2O_5	wt. %	0.31	0.06	0.27	0.47
TiO_2	wt. %	1.00	0.15	0.66	1.25
Total	wt. %	98.9	1.4	95.7	100.6
LOI	wt. %	0.8	0.8	0.0	3.2
Ba	mg/kg	935	322	682	1,980
Be	mg/kg	2.4	0.3	1.5	2.8
Co	mg/kg	13.7	4.7	<6	22.3
Cr	mg/kg	16.1	36.7	10.0	107
Cu	mg/kg	17.2	15.5	7.9	54
Ga	mg/kg	32.4	19.6	26.2	81.9
Hf	mg/kg	6.3	1.2	3.6	7.7
Mo	mg/kg	<2	n.a.	<2	<5
Nb	mg/kg	12.0	2.0	7.4	15.6
Ni	mg/kg	13.5	8.0	10.0	33.3
Rb	mg/kg	103	19.6	72.1	144
Sc	mg/kg	16.8	3.8	7.7	25.3
Sn	mg/kg	1.9	2.3	1.0	8.3
Sr	mg/kg	543	144	455	1,060
Ta	mg/kg	1.2	0.3	0.7	1.8
Th	mg/kg	6.7	3.0	4.1	14.0
U	mg/kg	3.2	1.2	1.6	5.6
V	mg/kg	114	30.5	67.2	179
W	mg/kg	1.0	0.9	<0.3	3.8
Y	mg/kg	34.7	6.4	19.3	47.4
Zn	mg/kg	86.6	14.3	77.0	125
Zr	mg/kg	262	47.8	192	350
La	mg/kg	36.3	5.9	30.4	54.2
Ce	mg/kg	77.8	12.4	65.1	118
Pr	mg/kg	8.68	4.81	1.00	14.7
Nd	mg/kg	35.8	7.3	26.6	58.7
Sm	mg/kg	6.50	1.56	3.30	9.10
Eu	mg/kg	1.53	0.71	0.37	2.77
Gd	mg/kg	6.09	2.67	1.32	11.3
Tb	mg/kg	0.86	0.43	0.10	1.58
Dy	mg/kg	5.16	1.59	2.67	9.50
Ho	mg/kg	0.99	0.30	0.58	1.78
Er	mg/kg	2.48	1.65	0.10	5.04
Tm	mg/kg	0.34	0.19	0.10	0.65
Yb	mg/kg	2.64	0.95	1.29	5.15
Lu	mg/kg	0.37	0.12	0.12	0.67

A1.2.2.4 Diorite/gabbro (501033)

The median and standard deviation calculations are based on 11 whole rock samples, all from the Laxemar subarea (Table A1-18). This rock has relatively high concentrations of Fe_2O_3, MgO, TiO_2, Co, Cr, Ni, Sc and V and low concentrations of e.g. SiO_2, K_2O, Na_2O, Ba, Sr, U, Th and LREE:s compared to the rocks described above.

Table A1-18. Chemical composition of diorite/gabbro (501033), Laxemar subarea (N=11).

Element		Median	St.dev.	Min	Max
SiO_2	wt. %	54.0	4.1	44.9	56.5
Al_2O_3	wt. %	16.4	1.2	14.3	18.0
CaO	wt. %	7.8	1.7	5.8	11.0
Fe_2O_3	wt. %	9.8	1.7	8.2	13.8
K_2O	wt. %	2.4	0.7	1.1	3.0
MgO	wt. %	4.8	1.8	3.3	8.5
MnO	wt. %	0.15	0.02	0.13	0.20
Na_2O	wt. %	3.4	0.5	2.3	3.8
P_2O_5	wt. %	0.41	0.26	0.22	1.19
TiO_2	wt. %	1.1	0.40	0.87	2.4
Total	wt. %	98.4	2.3	95.8	102.3
LOI	wt. %	0.9	0.5	0.5	1.9
Ba	mg/kg	917	302	305	1,230
Be	mg/kg	2.0	0.3	1.6	2.7
Co	mg/kg	26.5	8.3	19.6	42.8
Cr	mg/kg	110	160	45	563
Cu	mg/kg	16.9	42.7	7	156
Ga	mg/kg	16.6	6.8	<1	27.5
Hf	mg/kg	4.4	2.0	0.9	7.2
Mo	mg/kg	<2	n.a.	<2	<6
Nb	mg/kg	10.9	3.1	5.7	18.0
Ni	mg/kg	41.6	33.9	20.4	129
Rb	mg/kg	69	24.7	18	91.5
Sc	mg/kg	23.3	7.6	17.7	43.1
Sn	mg/kg	<20	n.a.	<20	<20
Sr	mg/kg	765	109	638	1,040
Ta	mg/kg	0.5	0.3	0.3	1.1
Th	mg/kg	2.6	2.0	<0.1	7.7
U	mg/kg	1.1	0.7	0.0	2.7
V	mg/kg	173	41.1	128	253
W	mg/kg	0.5	0.3	<0.4	1.0
Y	mg/kg	31.2	7.6	23.2	47.9
Zn	mg/kg	121	904	92	3,120
Zr	mg/kg	186	80.0	91	361
La	mg/kg	34.6	9.1	27.0	57.8
Ce	mg/kg	82.1	20.1	65	139
Pr	mg/kg	11.0	3.31	5.6	19.3
Nd	mg/kg	43.5	13.6	33.0	84.1
Sm	mg/kg	7.24	2.73	4.90	15.0
Eu	mg/kg	2.00	0.63	1.22	3.74
Gd	mg/kg	6.57	2.06	4.1	10.6
Tb	mg/kg	0.98	0.35	0.39	1.70
Dy	mg/kg	5.75	1.26	4.06	7.79
Ho	mg/kg	1.11	0.27	0.74	1.74
Er	mg/kg	3.15	1.01	1.32	5.16
Tm	mg/kg	0.47	0.12	0.31	0.72
Yb	mg/kg	2.42	0.55	1.86	3.60
Lu	mg/kg	0.31	0.10	0.16	0.47

A1.2.2.5 Dolerite (501027)

Only two geochemical analyses have been carried out on dolerite (Table A1-19). The concentrations of most of the elements in these two samples are very similar which indicates that the dolerite has rather homogeneous composition. This rock generally has slightly lower contents of SiO_2, K_2O, Ba, Sr, Th, U, and LREE:s, and higher contents of Fe_2O_3, MgO, TiO_2, Co, Ni, V and HREE:s compared to diorite/gabbro (501033), which has higher contents of amphibole but lower contents of e.g. opaques, pyroxene and olivine.

Table A1-19. Chemical composition of dolerite – rock code 501027, Laxemar subarea.

Element		KLX19A:532.97 m	KLX20A:193.37 m
SiO_2	wt. %	49.4	49.8
Al_2O_3	wt. %	16.4	16.5
CaO	wt. %	7.3	7.3
Fe_2O_3	wt. %	12.8	12.9
K_2O	wt. %	1.3	1.4
MgO	wt. %	5.3	5.4
MnO	wt. %	0.1	0.2
Na_2O	wt. %	3.5	3.5
P_2O_5	wt. %	0.6	0.7
TiO_2	wt. %	2.9	2.9
Total	wt. %	99.7	100.5
LOI	wt. %	0.5	0.1
Ba	mg/kg	393	415
Be	mg/kg	1.4	1.4
Co	mg/kg	41.2	40.9
Cr	mg/kg	60	61
Cu	mg/kg	25.0	31.3
Ga	mg/kg	19.0	18.8
Hf	mg/kg	5.6	5.4
Mo	mg/kg	2.4	2.6
Nb	mg/kg	18.1	17.8
Ni	mg/kg	69.6	71.6
Rb	mg/kg	30	29.2
Sc	mg/kg	17.7	17.9
Sn	mg/kg	3.8	3.8
Sr	mg/kg	528	543
Ta	mg/kg	0.9	0.9
Th	mg/kg	1.5	1.4
U	mg/kg	0.5	0.6
V	mg/kg	213	212
W	mg/kg	0.6	0.6
Y	mg/kg	32.3	32.4
Zn	mg/kg	124	125
Zr	mg/kg	229	231
La	mg/kg	24.2	24.1
Ce	mg/kg	57.0	56.4
Pr	mg/kg	7.7	7.56
Nd	mg/kg	33.6	33.3
Sm	mg/kg	7.49	7.52
Eu	mg/kg	2.29	2.34
Gd	mg/kg	7.34	7.19
Tb	mg/kg	1.08	1.05
Dy	mg/kg	6.25	6.45
Ho	mg/kg	1.21	1.21
Er	mg/kg	3.31	3.25
Tm	mg/kg	0.45	0.44
Yb	mg/kg	2.83	2.84
Lu	mg/kg	0.41	0.40

A1.2.2.6 Hydrothermally altered rock adjacent to fractures

Differences in chemistry and mineralogy between the red-stained rock and fresh rock have been reported by /Drake and Tullborg 2006a, b/ and are summarized in /Drake et al. 2006/. In summary, the red-stained, hydrothermally altered Ävrö granite, quartz monzodiorite and fine-grained dioritoid adjacent to fractures have higher concentrations of K_2O, Na_2O and Rb and lower concentrations of CaO, Al_2O_3 and Sr than in the fresh rock. This is due to replacement of plagioclase by K-feldspar and albite in the red-stained rock. The Cs content is lower in the red-stained rock due to replacement of biotite by chlorite. Higher LOI values of the red-stained rock compared to the fresh rock is due to the formation of secondary water-bearing minerals like chlorite, sericite, epidote and prehnite. However, the Fe_2O_3 content in the red-stained rock is about the same in the red-stained rock and in the fresh rock. The S content is generally lower in the red-stained rock compared to the fresh rock due to oxidation of primary pyrite. However, the S content is enriched in some red-stained samples due to formation of pyrite in the rock after the red-staining event. The content of the REE:s remains constant in the red-stained rock compared to the fresh rock.

A1.2.3 Porosity

Porosity measurements have been carried out on the rock types at Simpevarp and Laxemar within several different studies (e.g. geology and transport). All determinations consider connected porosity and are measured with water saturation technique. However, the methods used in different studies differ in terms of e.g. sample selection, sample size, water saturation time and drying time. The terminology used varies as well and the porosity measured is presented as effective, open or connected, of which the latter is preferred in this compilation. The porosity results from the Geology and Transport studies are compiled below.

A1.2.3.1 Geology

The porosity of surface samples and drill core samples from the Simpevarp and Laxemar subareas has been measured as a part of the petrophysical parametrization and are presented for the dominant rock types of each rock domain in Table A1-23.

A1.2.3.2 Transport

Compiled porosity analyses from the Transport programme /Selnert et al. 2009/ are listed in Table A1-24 (subdivided based on amount of micro-fractures) and Table A1-25 (subdivided based on alteration intensity). The samples have also been subdivided into samples inside or outside deformation zones.

A1.2.4 Redox – Whole rock

Mössbauer analyses of relatively unaltered as well as red-stained rock have been carried out on Ävrö granite from borehole KLX04, Laxemar subarea, and on Ävrö granite, quartz monzodiorite and fine-grained dioritoid from boreholes KSH01A and KSH03A+B, Simpevarp subarea (Table A1-26) /Drake and Tullborg 2006a, b/. No division of the Ävrö granite samples into Ävrö granodiorite and Ävrö quartz monzodiorite has been carried out.

A generally small increase of Fe^{3+}/Fe_{tot} in the red-stained rock compared to the unaltered rock is shown. The mean Fe^{3+}/Fe_{tot} content is 2.3% higher in the red-stained rock (mean Fe^{3+}/Fe_{tot} content: 43.0%) compared with the relatively unaltered rock (mean Fe^{3+}/Fe_{tot} content: 40.7%). This increase is related to the partial or complete replacement of magnetite by hematite and subordinately the replacement of biotite by chlorite and the general increase of epidote in the red-stained rock compared to the unaltered rock. The Fe^{3+}/Fe_{tot} content in the oxide phase is almost always higher in the red-stained rock than in the unaltered rock due to partial replacement of magnetite by hematite, which is in agreement with lower susceptibility of red-stained rock compared to unaltered rock /Mattsson et al. 2005/. However, since most of the Fe in the rock is contained in the silicate phase which has fairly unchanged Fe^{3+}/Fe_{tot}, the total change in Fe^{3+}/Fe_{tot} contents between the red-stained rock and the unaltered rock is not as high as susceptibility measurements suggest.

Table A1-20. Chemical composition of red-stained, hydrothermally altered Ävrö granite (501044), KLX04, Laxemar subarea (N=6).

Element		Median	St.dev.	Min	Max
SiO_2	wt. %	67.5	4.78	57.7	68.9
Al_2O_3	wt. %	15.2	1.28	14.6	17.6
CaO	wt. %	2.48	0.80	1.65	3.89
Fe_2O_3	wt. %	3.36	1.21	3.02	5.77
K_2O	wt. %	4.07	0.47	3.16	4.56
MgO	wt. %	1.38	0.67	1.22	2.73
MnO	wt. %	0.06	0.02	0.06	0.11
Na_2O	wt. %	3.93	0.64	3.82	5.45
P_2O_5	wt. %	0.19	0.11	0.16	0.40
TiO_2	wt. %	0.49	0.23	0.42	0.97
Total	wt. %	1.3	0.38	1.1	2.1
LOI	wt. %	98.3	0.56	97.2	98.6
Ba	mg/kg	1,135	190	1,050	1,570
Be	mg/kg	2.72	0.35	2.44	3.38
Co	mg/kg	<6	2.60	<6	11.4
Cr	mg/kg	58.9	8.14	51.6	70
Cs	mg/kg	1.95	0.47	1.7	2.98
Cu	mg/kg	17.7	9.27	8.62	29.4
F	wt. %	0.14	0.06	0.09	0.23
Ga	mg/kg	26.2	3.25	24.4	32.9
Hf	mg/kg	6.5	0.64	5.87	7.57
Mo	mg/kg	<2	n.a.	4.06	4.06
Nb	mg/kg	10.84	3.16	8.47	15.5
Ni	mg/kg	18.4	4.22	14.2	24.8
Rb	mg/kg	119	18.0	101	149
S	mg/kg	52.6	68.1	17.6	198
Sc	mg/kg	5.24	2.54	4.78	10.5
Sn	mg/kg	2.28	0.55	1.86	3.21
Sr	mg/kg	705	222	593	1,180
Ta	mg/kg	1.06	0.29	0.80	1.56
Th	mg/kg	16.4	2.68	13.1	20.1
U	mg/kg	5.58	1.78	3.72	8.95
V	mg/kg	45.8	25.4	40.7	96.8
W	mg/kg	2.67	0.98	2.03	4.65
Y	mg/kg	17.6	5.29	15.2	27.7
Zn	mg/kg	71.4	24.3	48.8	104
Zr	mg/kg	221	36.3	181	277
La	mg/kg	41.0	11.0	35.2	61.4
Ce	mg/kg	90.3	30.3	80.2	146
Pr	mg/kg	10.0	3.95	9.01	17.5
Nd	mg/kg	34.9	15.6	29.7	62.7
Sm	mg/kg	5.22	2.42	4.39	10
Eu	mg/kg	1.00	0.47	0.74	1.81
Gd	mg/kg	3.79	1.02	2.21	5.1
Tb	mg/kg	0.74	0.27	0.64	1.25
Dy	mg/kg	3.43	0.94	2.68	4.87
Ho	mg/kg	0.66	0.16	0.59	0.98
Er	mg/kg	1.82	0.54	1.7	2.86
Tm	mg/kg	0.36	0.07	0.26	0.48
Yb	mg/kg	1.92	0.47	1.68	2.73
Lu	mg/kg	0.30	0.08	0.25	0.45

Table A1-21. Chemical composition of red-stained, hydrothermally altered quartz monzodiorite (501036), KSH03A+B, Simpevarp subarea (N=6).

Element		Median	St.dev.	Min	Max
SiO_2	wt. %	53.1	3.77	51.1	60.7
Al_2O_3	wt. %	16.0	0.55	15	16.7
CaO	wt. %	5.43	1.71	2.98	7.33
Fe_2O_3	wt. %	8.89	1.37	6.61	10.3
K_2O	wt. %	3.32	0.46	3.18	4.39
MgO	wt. %	3.88	0.73	2.77	5
MnO	wt. %	0.15	0.02	0.12	0.16
Na_2O	wt. %	3.82	0.24	3.55	4.13
P_2O_5	wt. %	0.42	0.10	0.32	0.61
TiO_2	wt. %	1.14	0.15	0.98	1.4
Total	wt. %	2.1	0.56	1.7	3.3
LOI	wt. %	97.6	0.66	96.1	97.9
Ba	mg/kg	1,095	200	868	1,380
Be	mg/kg	1.75	0.20	1.51	2.05
Co	mg/kg	14.5	2.97	10.3	18.4
Cr	mg/kg	111	14.12	95.3	136
Cs	mg/kg	1.37	0.79	0.44	2.27
Cu	mg/kg	28.9	7.60	12.3	33.4
F	wt. %	0.13	0.04	0.09	0.2
Ga	mg/kg	13	1.00	10.9	13.6
Hf	mg/kg	4.65	0.86	2.86	5.32
Mo	mg/kg	<2	n.a.	<2	<2
Nb	mg/kg	8.62	1.80	6.69	11.5
Ni	mg/kg	17.9	5.62	5.65	21
Rb	mg/kg	81.8	26.01	68.9	134
S	mg/kg	524	465	15.5	1,000
Sc	mg/kg	22.1	2.82	15.9	23.1
Sn	mg/kg	<1	n.a.	<1	2.13
Sr	mg/kg	426	101	329	618
Ta	mg/kg	0.65	0.16	0.41	0.84
Th	mg/kg	3.03	1.19	2.13	5.13
U	mg/kg	1.76	0.49	1.31	2.44
V	mg/kg	151	28.6	92.3	168
W	mg/kg	0.63	0.27	0.55	1.05
Y	mg/kg	31.5	2.13	28.7	34.3
Zn	mg/kg	74.6	17.24	60.1	108
Zr	mg/kg	201	52.6	113	260
La	mg/kg	36.2	3.48	33.8	42.8
Ce	mg/kg	80.7	6.19	76.7	91.6
Pr	mg/kg	10.1	0.71	9.17	11.1
Nd	mg/kg	40.5	2.75	38.4	46.1
Sm	mg/kg	5.08	0.91	4.74	7.21
Eu	mg/kg	1.63	0.19	1.3	1.86
Gd	mg/kg	5.13	0.64	4.71	6.3
Tb	mg/kg	0.77	0.06	0.67	0.85
Dy	mg/kg	4.28	0.32	3.78	4.69
Ho	mg/kg	0.87	0.07	0.79	0.97
Er	mg/kg	2.06	0.19	1.88	2.34
Tm	mg/kg	0.33	0.06	0.29	0.44
Yb	mg/kg	2.02	0.25	1.76	2.4
Lu	mg/kg	0.27	0.04	0.23	0.33

Table A1-22. Range in chemical composition of two red-stained fine-grained dioritoid (501030) samples, KSH01A, Simpevarp subarea.

Element		Min	Max
SiO_2	wt. %	59.0	60.7
Al_2O_3	wt. %	15.1	15.4
CaO	wt. %	3.44	5.26
Fe_2O_3	wt. %	7.25	7.39
K_2O	wt. %	3.25	3.54
MgO	wt. %	2.6	2.78
MnO	wt. %	0.10	0.11
Na_2O	wt. %	3.47	3.65
P_2O_5	wt. %	0.27	0.29
TiO_2	wt. %	0.98	0.99
Total	wt. %	2.0	2.3
LOI	wt. %	97.7	97.9
Ba	mg/kg	529	616
Be	mg/kg	1.79	2.2
Co	mg/kg	11.3	13.6
Cr	mg/kg	118	133
Cs	mg/kg	0.95	0.99
Cu	mg/kg	16.2	28.4
F	wt. %	0.13	0.13
Ga	mg/kg	10.7	11.5
Hf	mg/kg	5.56	7.1
Mo	mg/kg	<2	<2
Nb	mg/kg	8.28	10.1
Ni	mg/kg	2.82	2.84
Rb	mg/kg	81.5	83.8
S	mg/kg	77.4	87.6
Sc	mg/kg	17.5	18.4
Sn	mg/kg	<1	3.92
Sr	mg/kg	234	237
Ta	mg/kg	0.74	0.97
Th	mg/kg	5.86	7.64
U	mg/kg	2.65	3.42
V	mg/kg	103	119
W	mg/kg	0.65	0.89
Y	mg/kg	32.1	40.8
Zn	mg/kg	59.6	79.8
Zr	mg/kg	243	296
La	mg/kg	35.4	36.3
Ce	mg/kg	76.9	85.7
Pr	mg/kg	9.65	11.3
Nd	mg/kg	35.5	40.2
Sm	mg/kg	4.45	6.6
Eu	mg/kg	1.34	1.36
Gd	mg/kg	5.28	5.81
Tb	mg/kg	0.85	0.95
Dy	mg/kg	4.21	5.97
Ho	mg/kg	0.89	1.18
Er	mg/kg	2.44	3.2
Tm	mg/kg	0.40	0.48
Yb	mg/kg	2.4	2.77
Lu	mg/kg	0.35	0.41

Table A1-23. Porosity (%) of the dominant rock types in the rock domains in the Laxemar local model area. Data from /Wahlgren et al. 2008/. Values from RSMB01 are also valid for RSMB05 and RSMB06.

Rock domain	Rock type	Porosity (%) Mean value ± std	Number of samples
RSMA01	Ävrö granite (501044)	0.66 ± 0.14	15
RSMB01	Fine-grained dioritoid (501030)	0.33 ± 0.08	9
RSMD01	Quartz monzodiorite (501036)	0.52 ± 0.12	12
RSME01	Diorite to gabbro (501033)	0.19 ± 0.14	11
RSMM01	Ävrö quartz monzodiorite (501046)	0.57 ± 0.18	10
RSMM01	Diorite/gabbro (501033)	0.30 ± 0.10	4

Table A1-24. Porosities (vol. %) of different rock types from the Laxemar-Simpevarp areas, the median min and max values from the numbers (N) of samples involved in the study. The division of samples in inside or outside deformation zones (DZ) is based on the extended single hole interpretation (ESHI). Data from /Selnert et al. 2009/.

Rock type (SKB code)		All rock samples				Samples without visible open micro fractures				Samples with visible open micro fractures			
	Inside or outside DZ	Median	Min	Max	N	Median	Min	Max	N	Median	Min	Max	N
Fine-grained dioritoid (501030)	Outside	0.15	0.00	1.49	76	0.12	0.00	1.49	59	0.21	0.08	1.33	17
	Inside	0.12	0.04	0.75	18	0.09	0.04	0.41	13	0.31	0.07	0.75	5
Diorite/gabbro (501033)	Outside	0.06	0.05	0.06	2	0.06	0.05	0.06	2	–	–	–	0
	Inside	–	–	–	0	–	–	–	0	–	–	–	0
Quartz monzodiorite (501036)	Outside	0.13	0.00	1.32	61	0.13	0.00	1.32	59	0.30	0.12	0.47	2
	Inside	0.77	0.17	1.59	10	0.78	0.17	1.59	9	0.45	–	–	1
Ävrö quartz monzodiorite (501046)	Outside	0.35	0.05	0.80	45	0.34	0.05	0.80	44	0.58	–	–	1
	Inside	0.28	0.15	1.45	10	0.27	0.15	0.42	8	1.29	1.12	1.45	2
Ävrö granodiorite (501056)	Outside	0.29	0.13	0.99	41	0.27	0.13	0.58	34	0.36	0.15	0.99	7
	Inside	0.39	0.17	0.89	15	0.37	0.17	0.89	14	0.63	–	–	1
Granite (501058)	Outside	0.61	0.38	0.84	2	0.61	0.38	0.84	2	–	–	–	0
	Inside	0.76	–	–	1	0.76	–	–	1	–	–	–	0
Pegmatite (501061)	Outside	0.02	–	–	1	–	–	–	0	0.02	–	–	1
	Inside	–	–	–	0	–	–	–	0	–	–	–	0
Fine-grained diorite-gabbro (505102)	Outside	0.19	0.03	0.22	8	0.19	0.03	0.22	8	–	–	–	0
	Inside	0.33	0.05	1.15	4	0.33	0.05	1.15	4	–	–	–	0
Fine-grained granite (511058)	Outside	0.24	0.07	1.15	26	0.24	0.07	0.40	23	0.20	0.20	1.15	3
	Inside	0.14	0.05	0.25	4	0.16	0.13	0.25	3	0.05	–	–	1

Table A1-25. Porosities (vol. %) of some different rock types from the Laxemar and Simevarp areas based on the alteration of the samples. The alteration analyses based on the binocular inspection of the individual drill core samples. The division of samples in inside or outside deformation zones (DZ)is based on the extended single hole interpretation (ESHI). Data from /Selnert et al. 2009/. N=number of samples.

Rock type (SKB code)	Outside/Inside DZ		Median	Min	Max	N
Fine-grained dioritoid (501030)	Outside	All samples	0.15	0.00	1.49	76
		Medium or strong alteration	0.84	0.21	1.33	3
		Without medium or strong alteration	0.13	0.00	1.49	73
	Inside	All samples	0.12	0.04	0.75	18
		Medium or strong alteration	0.47	0.19	0.75	2
		Without medium or strong alteration	0.11	0.04	0.41	16
Quartz monzodiorite (501036)	Outside	All samples	0.13	0.00	1.32	61
		Medium or strong alteration	–	–	–	0
		Without medium or strong alteration	0.13	0.00	1.32	61
	Inside	All samples	0.77	0.17	1.59	10
		Medium or strong alteration	0.83	0.45	1.59	8
		Without medium or strong alteration	0.25	0.17	0.34	2
Ävrö quartz monzodiorite	Outside	All samples	0.35	0.05	0.80	45
(501046)		Medium or strong alteration	0.80	–	–	1
		Without medium or strong alteration	0.34	0.05	0.60	44
	Inside	All samples	0.28	0.15	1.45	10
		Medium or strong alteration	0.28	0.15	1.45	6
		Without medium or strong alteration	0.28	0.27	0.42	4
Ävrö granodiorite (501056)	Outside	All samples	0.29	0.13	0.99	41
		Medium or strong alteration	0.34	0.15	0.99	5
		Without medium or strong alteration	0.29	0.13	0.58	36
Ävrö granodiorite (501056)	Inside	All samples	0.39	0.17	0.89	15
		Medium or strong alteration	0.52	0.17	0.79	3
		Without medium or strong alteration	0.37	0.22	0.89	12
Fine-grained diorite-gabbro (505102)	Outside	All samples	0.19	0.03	0.22	8
		Medium or strong alteration	–	–	–	0
		Without medium or strong alteration	0.19	0.03	0.22	8
	Inside	All samples	0.33	0.05	1.15	4
		Medium or strong alteration	–	–	–	0
		Without medium or strong alteration	0.33	0.05	1.15	4
Granite	Outside	All samples	0.24	0.07	1.15	26
(511058)		Medium or strong alteration	0.64	0.12	1.15	2
		Without medium or strong alteration	0.24	0.07	0.40	24
	Inside	All samples	0.14	0.05	0.25	4
		Medium or strong alteration	–	–	–	0
		Without medium or strong alteration	0.14	0.05	0.25	4

Table A1-26. Schematic summary of the changes in Fe3+/Fetot-ratios and related mineralogy in the different rock types. Values in brackets are average values. Data from KSH01A, KSH03A+B and KLX04 /Drake and Tullborg 2006a, b/.

Sample†	Silicates				Oxides					Total			
	Biotite (vol.%)	Chlorite (vol.%)	Epidote (vol.%)	Fe^{3+}/Fe_{tot} silicate(%)	Oxides [a] (vol.%)	Magnetite (vol.%)[b]	Hematite (vol.%) [b]	Mt+Hem† (vol.%) [b]	Fe^{3+}/Fe_{tot} oxide (%)	Fe^{3+}/Fe_{tot} total (%)	Fe_{tot} (wt.%)[c]	Fe^{2+}_{tot} (wt.%)	Fe^{3+}_{tot} (wt.%)
Dioritoid	6.7–15.4 (11.1)	0.8–6.7 (3.8)	0.1–0.2 (0.15)	20–22.6 (21.3)	0.6–0.7 (0.65)	60–72.7 (66.4)	10–18.2 (14.1)	9.1–30 (19.5)	62–65 (63.5)	26–31 (28.5)	5.10–5.52 (5.31)	3.77–3.81 (3.79)	1.33–1.71 (1.52)
Unaltered[d]													
Dioritoid red-stained	1–1.4 (1.2)	13.4–14.4 (13.9)	0.3–0.8 (0.6)	12–23 (17.5)	0.3–1.2 (0.72)	16.7–25 (20.8)	0–25 (12.5)	50–83.3 (66.7)	69.4*	28*	5.07*	3.65*	1.42*
QMD Unaltered[d]	0.3–11.8 (4.4)	0.9–17.2 (10.4)	0.1–1.4 (0.5)	15–25 (21.6)	0.3–3.2 (1.8)	2–100 (72.8)	0–9.8 (2.9)	0–88.2 (24.3)	62–100 (74.2)	32–42 (35.9)	4.65–7.00 (6.20)	2.93–4.69 (3.97)	1.73–2.85 (2.22)
QMD red-stained	0.1–1.8 (0.6)	9.1–17.7 (12.5)	1–3.2 (1.6)	16.5–31 (23.5)	0.6–3.6 (1.9)	0–80 (22.8)	7.1–32.3 (15.8)	0–92.9 (61.5)	72–100 (85.2)	30.4–46.6 (38.8)	4.62–7.20 (6.12)	3.22–4.62 (3.72)	1.41–3.25 (2.40)
Ävrö granite Unaltered[d]	0.6–12 (5.2)	0.6–11.5 (4.8)	0.2–10.3 (3.6)	19–44 (32.9)	0.6–1.8 (1.3)	0–100 (45.7)	0–31.8 (7.4)	0–90.9 (46.4)	65–89 (75.6)	36.0–53.5 (44.9)	2.06–3.90 (3.07)	1.12–2.23 (1.70)	0.8–1.71 (1.36)
Ävrö granite red-stained	0–3.1 (0.4)	3.8–17.6 (8.4)	0.5–9.4 (3.4)	20–52 (33.0)	0.3–2.7 (1.3)	0–100 (26.3)	10–76.9 (28.5)	0–83.3 (43.8)	66–100 (84.2)	32.0–57.8 (47.8)	2.11–4.04 (3.06)	1.03–2.54 (1.60)	0.78–2.21 (1.46)

†: Abbreviations:

Dioritoid = fine-grained dioritoid (rock type 501030).

QMD = quartz monzodiorite (rock type 501036).

Ävrö granite = rock type 501044 (not divided into 501056 and 501046).

Mt+Hem = magnetite partially replaced by hematite.

* = Based on one sample.

[a] = Magnetite and hematite (ilmenite is excluded).

[b] = % of counted oxide vs. total counts of magnetite, hematite and magnetite+hematite.

[c] = Fe_2O_3 multiplied by 0.6995.

[d] = Includes partially altered but not red-stained samples.

The most important Fe^{2+}-bearing minerals (low Fe^{3+}/Fe_{tot}-ratio) in the rocks in the Simpevarp area are chlorite, biotite, magnetite and subordinately hornblende and augite. Most important Fe^{3+} bearing minerals are magnetite ($Fe^{3+}/Fe_{tot} = 0.667$), hematite ($Fe^{3+}/Fe_{tot} = 1$) and epidote ($Fe^{3+}/Fe_{tot} \approx 1$). Pyrite is also an important Fe^{2+}-bearing mineral but it is only found in either minor or trace amounts (below 0.26 vol%, mean value is below 0.1 vol%).

The total Fe^{2+} content is higher and the Fe^{3+}/Fe_{tot}-ratio is lower in quartz monzodiorite and fine-grained dioritoid compared to Ävrö granite. This is mainly due to the higher amount of Fe-Mg silicates and the lower amount of epidote in the quartz monzodiorite and fine-grained dioritoid compared to the Ävrö granite. It should also be noted that the Ävrö granite samples with a more quartz monzodioritic composition have lower Fe^{3+}/Fe_{tot} ratios and higher Fe^{2+} contents than the Ävrö granite samples with a more granodioritic/granitic composition. The Ävrö granite also show a much larger variation in Fe^{3+}/Fe_{tot} compared to quartz monzodiorite and fine-grained dioritoid (although the Ävrö granite samples are more numerous).

Fine-grained dioritoid samples (N=2) are from KSH01A, Simpevarp subarea. Quartz monzodiorite samples (N=10) are from KSH03A+B, Simpevarp subarea. Ävrö granite samples (N=19) are from KLX04, Laxemar subarea and KSH03A, Simpevarp subarea, respectively. Pyrite is commonly present in very small amounts in the samples (generally below 0.26 vol. %, mean value is below 0.1 vol. %) and is not included in Table A1-26. However, both point-counting and whole rock chemical analyses show that pyrite and sulfur is generally depleted in the red-stained rock compared to the reference rock (exceptions occur).

A1.3 References

Adl-Zarrabi B, 2007. Oskarshamn site investigation. Borehole KLX03, KLX05, KLX07, KLX10 and KLX11A. Thermal properties of rocks using calorimeter and TPS method, and mineralogical composition by modal analysis. SKB-P-07-62, Svensk Kärnbränslehantering AB.

Drake H, Tullborg E-L, 2006a. Oskarshamn site investigation. Mineralogical, chemical and redox features of red-staining adjacent to fractures, Results from drill cores KSH01A+B and KSH03A+B. SKB-P-06-01, Svensk Kärnbränslehantering AB.

Drake H, Tullborg E-L, 2006b. Oskarshamn site investigation. Mineralogical, chemical and redox features of red-staining adjacent to fractures, Results from drill core KLX04. SKB-P-06-02, Svensk Kärnbränslehantering AB

Drake H, Sandström B, Tullborg E-L, 2006. Mineralogy and geochemistry of rocks and fracture fillings from Forsmark and Oskarshamn: Compilation of data for SR-Can. SKB-R-06-109, Svensk Kärnbränslehantering AB.

Janson T, Ljunggren B, Bergman T, 2007. Oskarshamn site investigation. Modal analyses on rock mechanical specimens. Specimens from borehole KLX03, KLX04, KQ0064G, KQ0065G, KF0066A and KF0069A. SKB-P-07-03, Svensk Kärnbränslehantering AB.

Mattsson H, Thunehed H, Keisu M, 2005. Oskarshamn site investigation. Interpretation of geophysical borehole measurements and compilation of petrophysical data from KLX01, KLX03, KLX04, HLX21, HLX22, HLX23, HLX24, HLX25, HLX26, HLX27 and HLX28. SKB-P-05-34, Svensk Kärnbränslehantering AB.

Munier R, Stenber L, Stanfors R, Milnes A G, Hermanson J, Triumf C-A, 2003. Geological Site Descriptive Model. A strategy for the model development during site investigations. SKB-R-03-07, Svensk Kärnbränslehantering AB

Selnert E, Byegård J, Widestrand H, Carlsten S, Döse C, Tullborg E-L, 2009. Bedrock transport properties. Data evaluation and retardation model. Site descriptive modelling SDM-Site Laxemar, SKB-R-08-100, Svensk Kärnbränslehantering AB.

Wahlgren C-H, Ahl M, Sandahl K-A, Berglund J, Petersson J, Ekström M, Persson P-O, 2004. Oskarshamn site investigation. Bedrock mapping 2003 - Simpevarp subarea. Outcrop data, fracture data, modal and geochemical classification of rock types, bedrock map, radiometric dating. SKB-P-04-102, Svensk Kärnbränslehantering AB.

Wahlgren C-H, Bergman T, Persson Nilsson K, Eliasson T, Ahl M, Ekström M, 2005. Oskarshamn site investigation. Bedrock map of the Laxemar subarea and surroundings. Description of rock types, modal and geochemical analyses, including the cored boreholes KLX03, KSH03 and KAV01. SKB-P-05-180, Svensk Kärnbränslehantering AB.

Wahlgren C-H, Bergman T, Ahl M, Ekström M, 2006a. Oskarshamn site investigation. Modal and geochemical analyses of drill core samples 2005 - Classification of rock types in KLX03, KLX04, KLX06, KLX07A, KLX07B, KLX08 and KLX10. SKB-P-06-05, Svensk Kärnbränslehantering AB.

Wahlgren C-H, Bergman T, Ahl M, Ekström M, 2006b. Oskarshamn site investigation. Modal and geochemical analyses of drill core samples 2006 and updated bedrock map of the Laxemar subarea. Classification of rock types in KLX08, KLX10, KLX11A, KLX12A, KLX18A and KLX20A. SKB-P-06-279, Svensk Kärnbränslehantering AB.

Wahlgren C-H, Hermanson J, Forssberg O, Curtis P, Triumf C-A, Drake H, Tullborg E-L, 2006c. Geological description of rock domains and deformation zones in the Simpevarp and Laxemar subareas. Preliminary site description Laxemar subarea - version 1.2. SKB-R-05-69, Svensk Kärnbränslehantering AB

Wahlgren C-H, Bergman T, Ahl M, Ekström M, Page L, Söderlund U, 2007. Oskarshamn site investigation. Modal and geochemical analyses of drill core samples 2007 and 40Ar/39Ar dating of a dolerite. Classification of rock types in KLX15A, KLX16A, KLX19A, KLX20A and KLX21B. SKB-P-07-191, Svensk Kärnbränslehantering AB.

Wahlgren C-H, Curtis P, Hermanson J, Forssberg O, Öhman J, Drake H, Fox A, Triumf C-A, Mattsson H, Thunehed H, 2008. Geology Laxemar, Site descriptive modelling, SDM-Site Laxemar. SKB-R-08-54, Svensk Kärnbränslehantering AB.

Appendix 2

Compilation of orientations of fractures with specific minerals separated by fracture domain

A2.1 Introduction

This appendix is a compilation of the data available in April 2008 of drill core mapping data. Fractures bearing certain minerals have been divided into sealed and open fractures and separated into fracture domains FSM_C, FSM_EW007, FSM_N, FSM_NE005 and FSM_W. Fracture domain FSM_S is excluded due to the low amount of data from this domain. The stereographic projections are divided into fracture poles as well as Fisher concentrations as a percentage of the total number of poles per 1.0 % of stereonet area. Contours have been set to 10% for consistency. Terzaghi corrections have been applied to compensate for borehole orientations. Minerals mapped as “white feldspar”, and “red feldspar” have been added to the adularia data set. Fractures without any visible minerals have been divided into fractures with wall rock alteration (labelled “No fill - Altered WR”) and fractures without wall rock alteration (labelled “No fill - Fresh WR”).

A2.2 Stereographic plots

Fracture orientations of fractures from fracture domains FSM_C, FSM_EW007, FSM_N, FSM_NE005 and FSM_W (in order) are shown below divided into sealed and open fractures for each specific mineral.

FSM_C

Adularia

Open Fractures

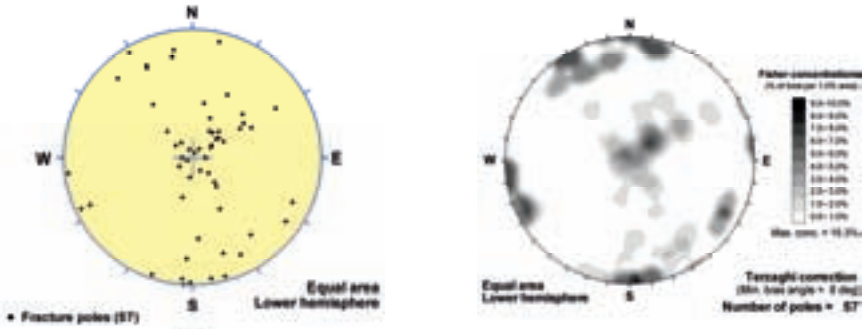

Sealed Fractures

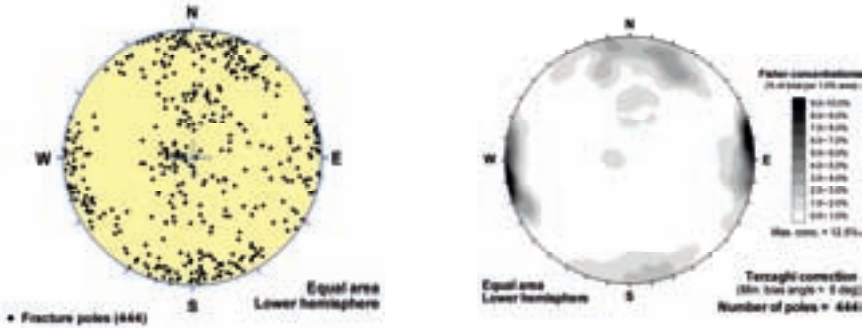

Calcite

Open Fractures

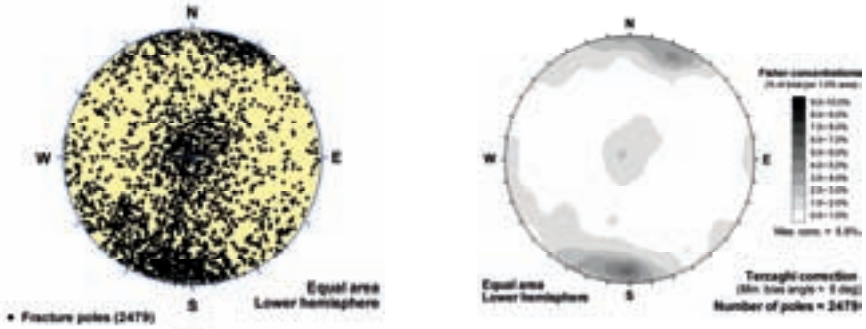

Sealed Fractures

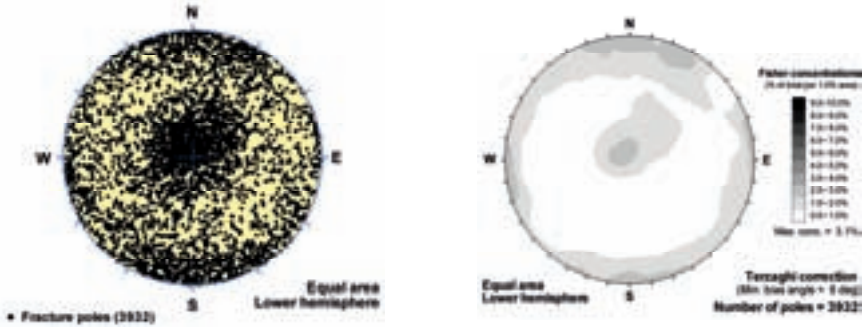

FSM_C

Chlorite

Open Fractures

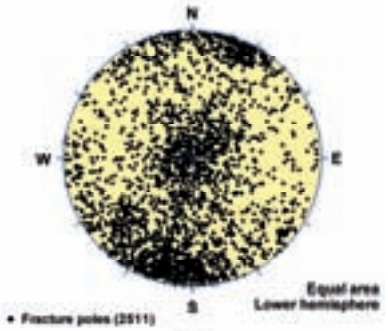

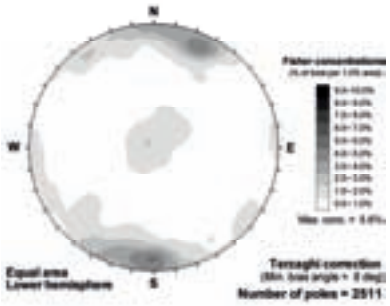

Sealed Fractures

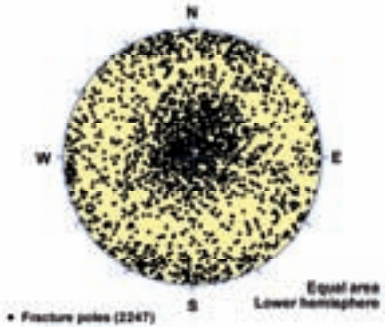

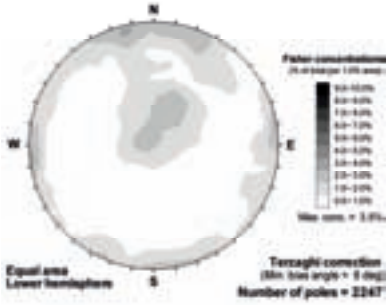

Clay Minerals

Open Fractures

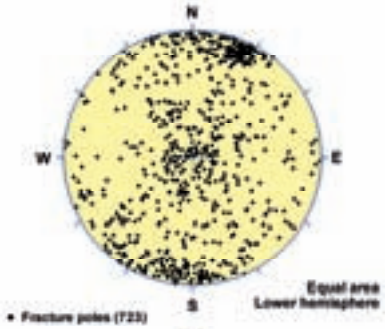

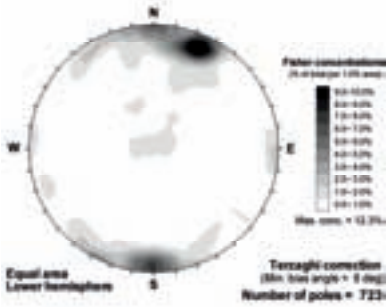

Sealed Fractures

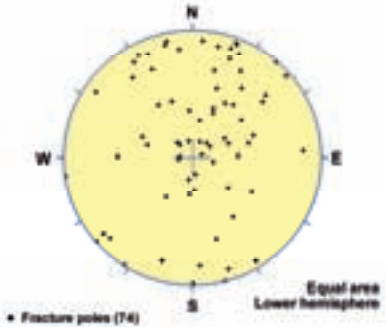

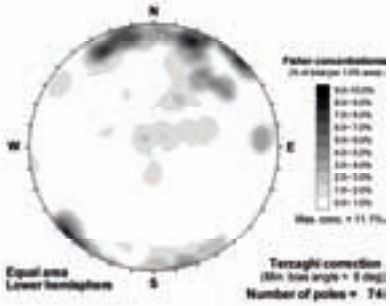

FSM_C

Epidote

Open Fractures

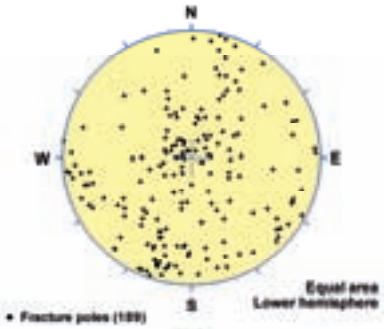

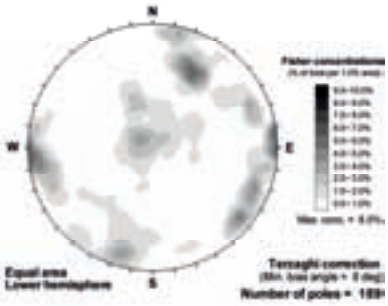

Sealed Fractures

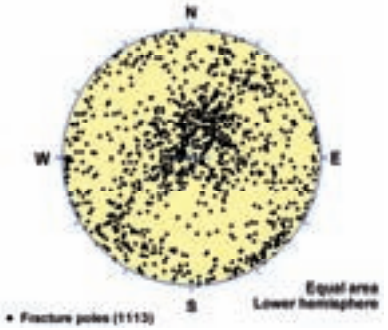

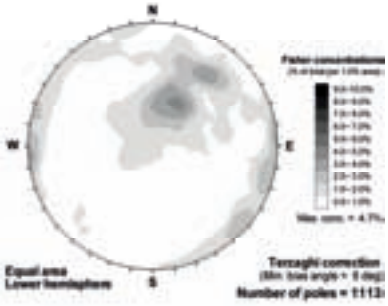

Fluorite

Open Fractures

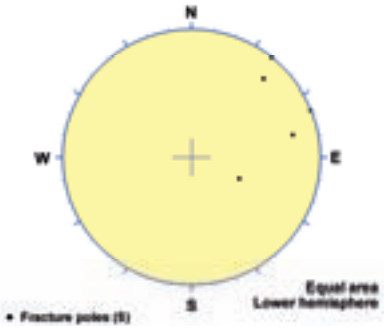

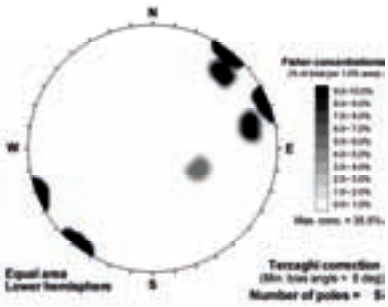

Sealed Fractures

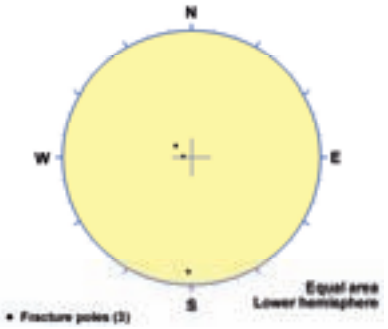

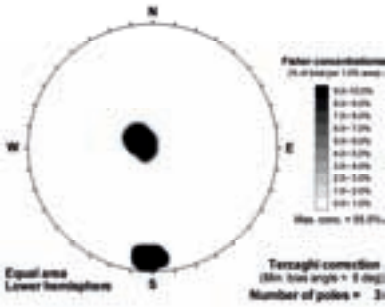

FSM_C

Goethite

Open Fractures

Sealed Fractures

Gypsum

Open Fractures

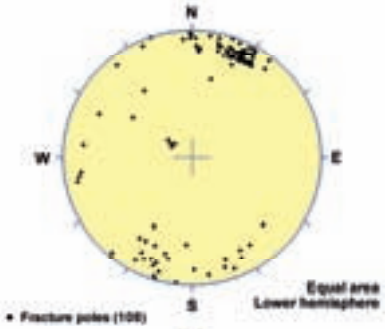

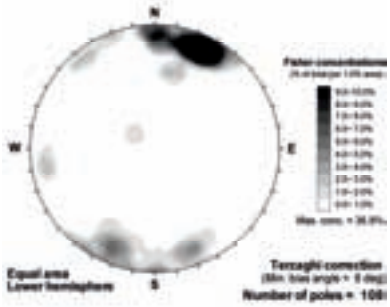

Sealed Fractures

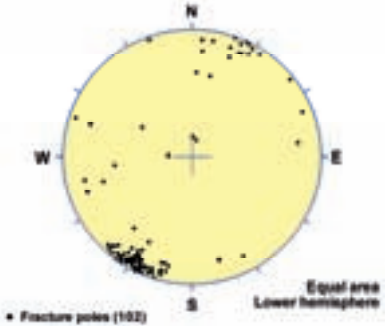

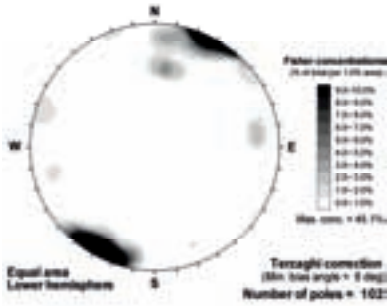

FSM_C

Hematite

Open Fractures

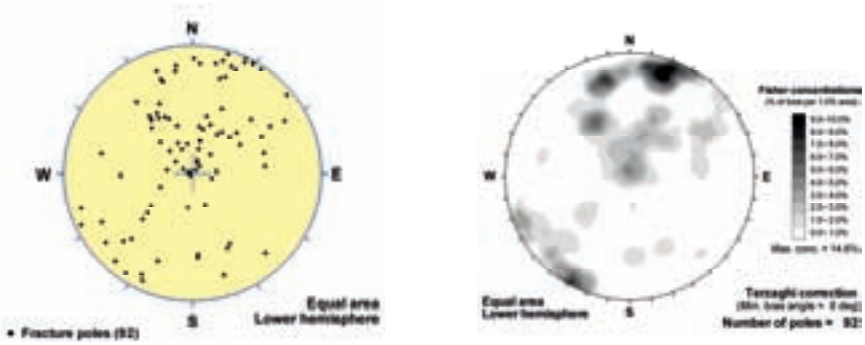

Sealed Fractures

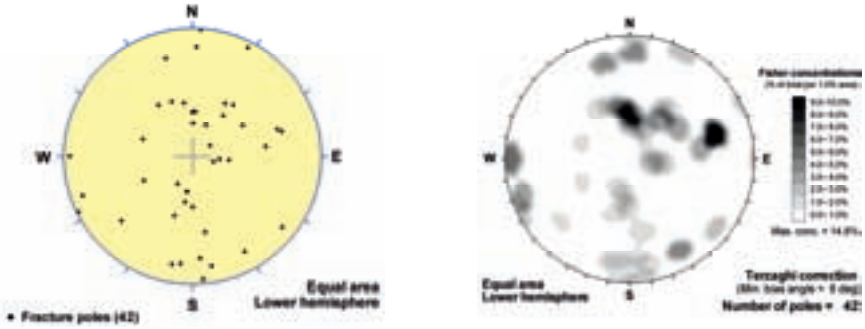

Laumontite

Open Fractures

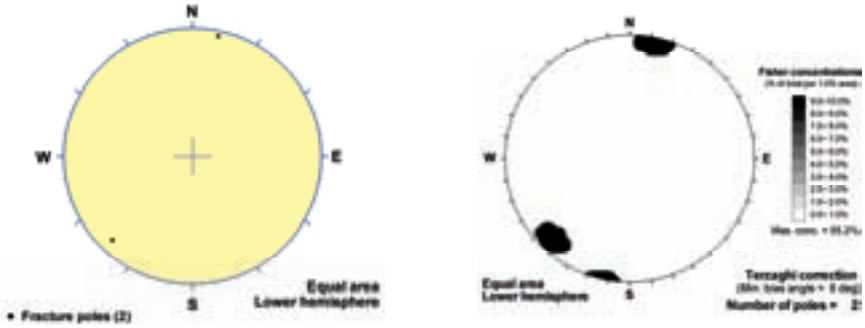

Sealed Fractures

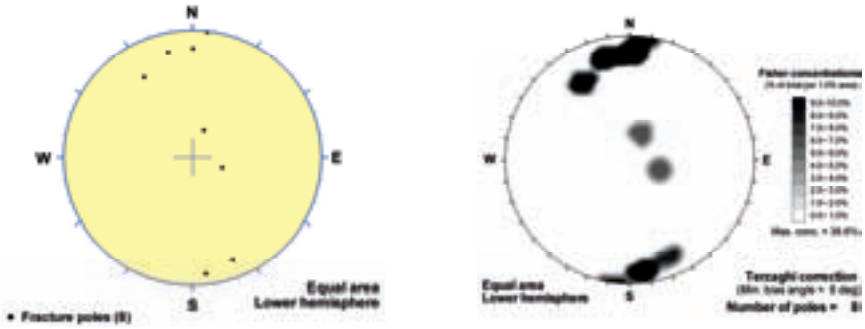

FSM_C

Muscovite

Open Fractures

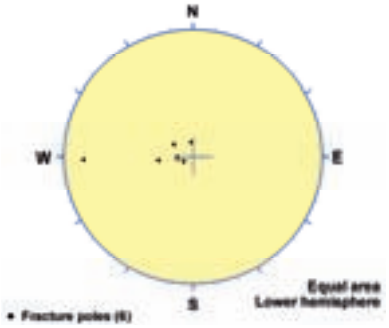

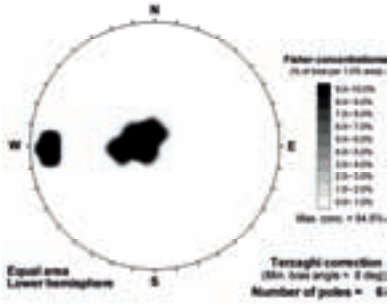

Sealed Fractures

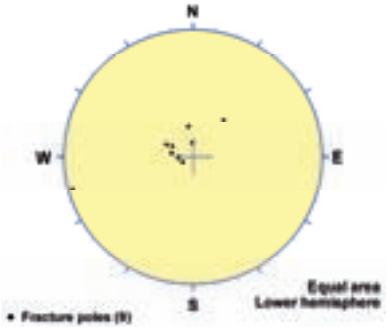

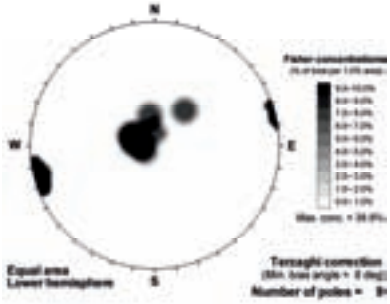

Prehnite

Open Fractures

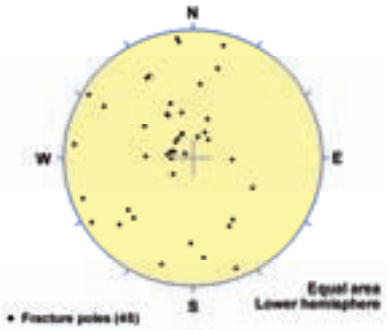

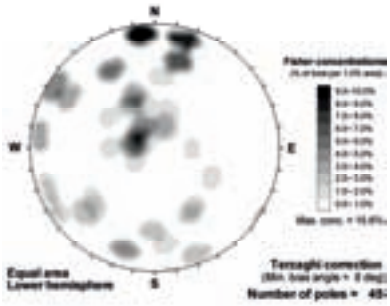

Sealed Fractures

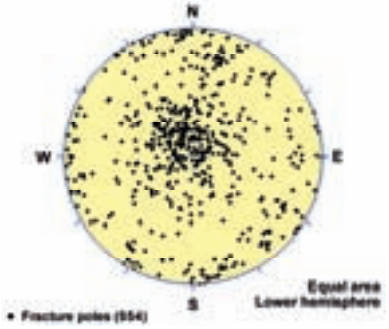

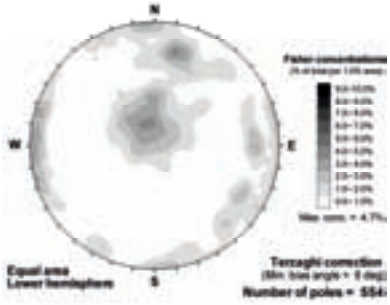

FSM_C

Pyrite

Open Fractures

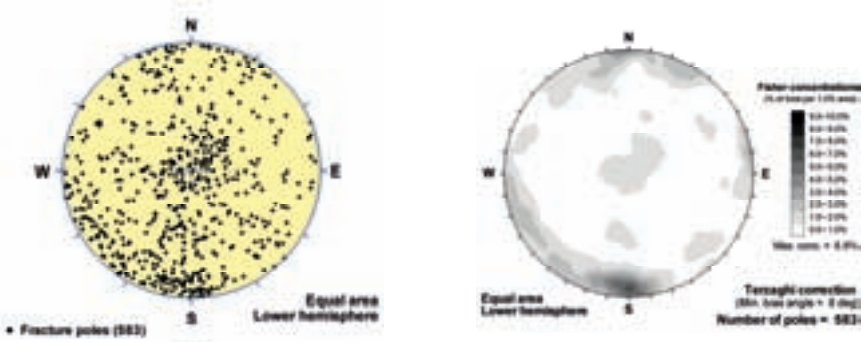

Sealed Fractures

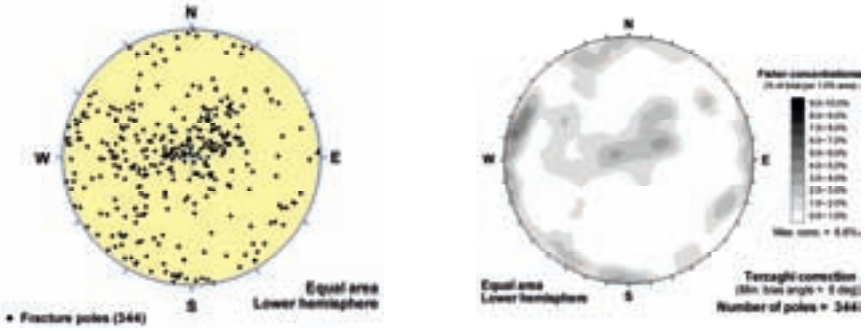

Quartz

Open Fractures

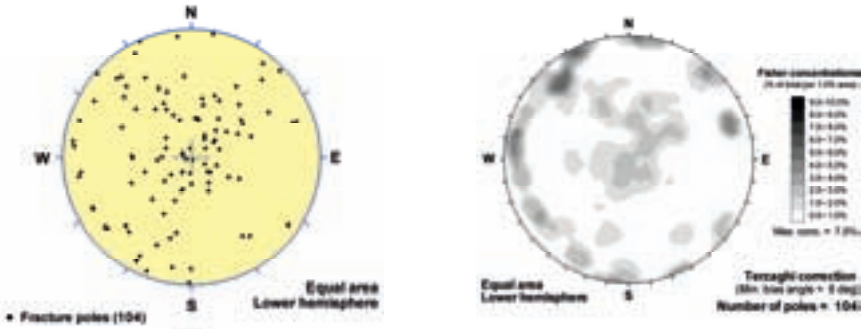

Sealed Fractures

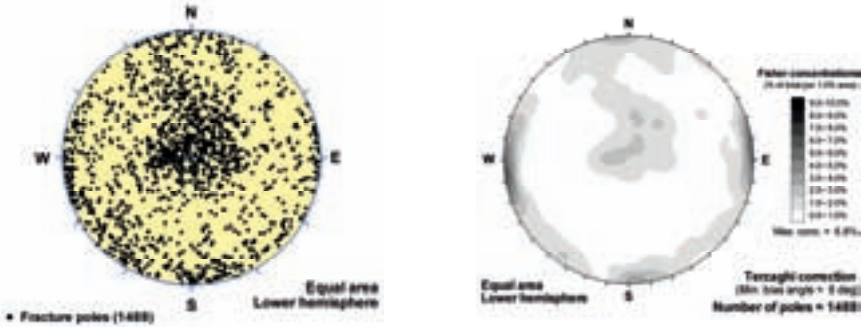

FSM_C

No fill - Altered WR

Open Fractures

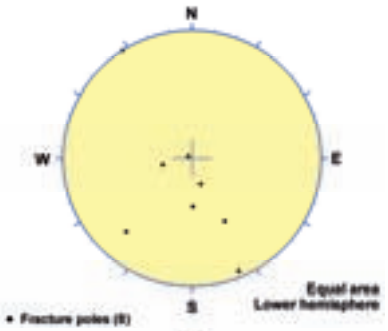

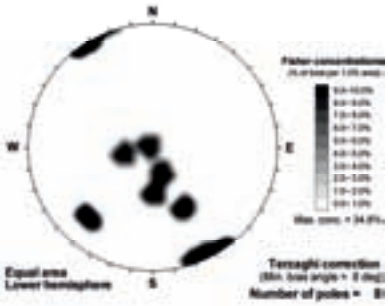

Sealed Fractures

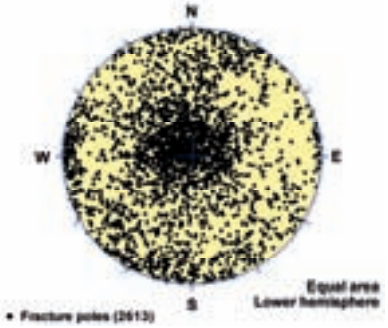

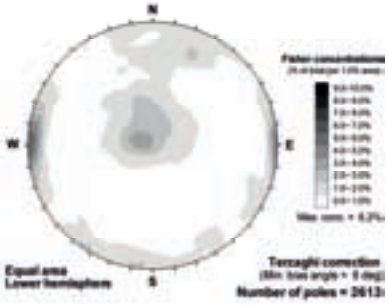

No fill - Fresh WR

Open Fractures

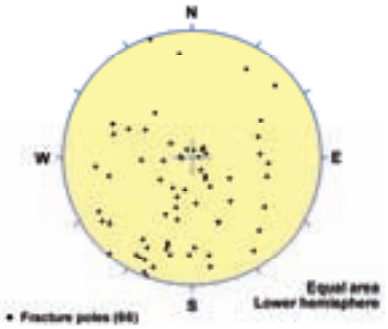

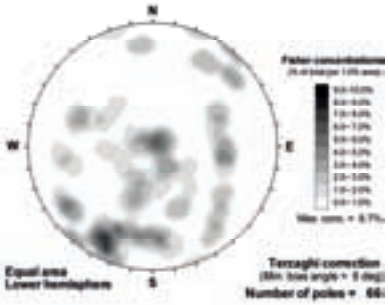

Sealed Fractures

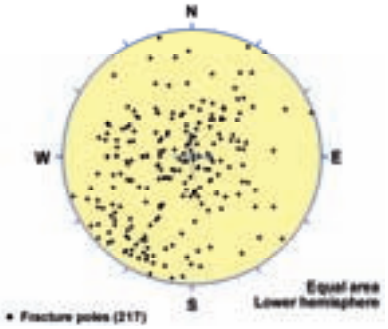

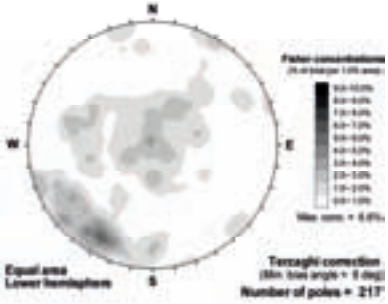

FSM_EW007

Adularia

Open Fractures

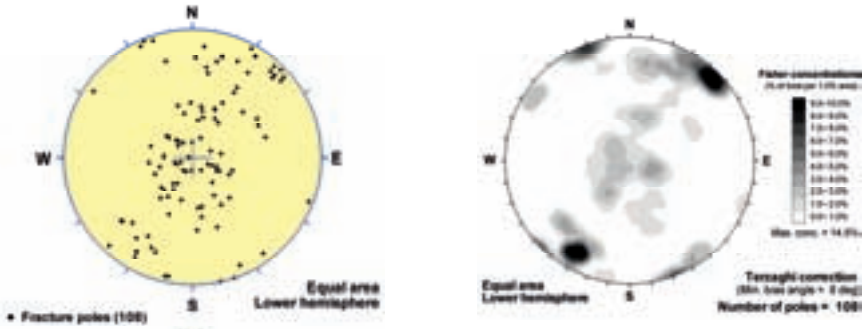

Sealed Fractures

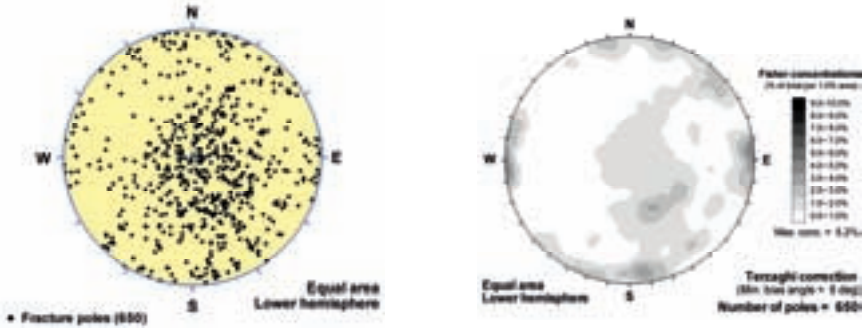

Calcite

Open Fractures

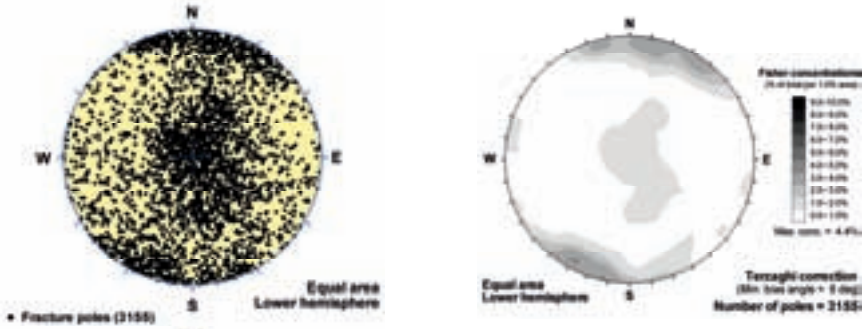

Sealed Fractures

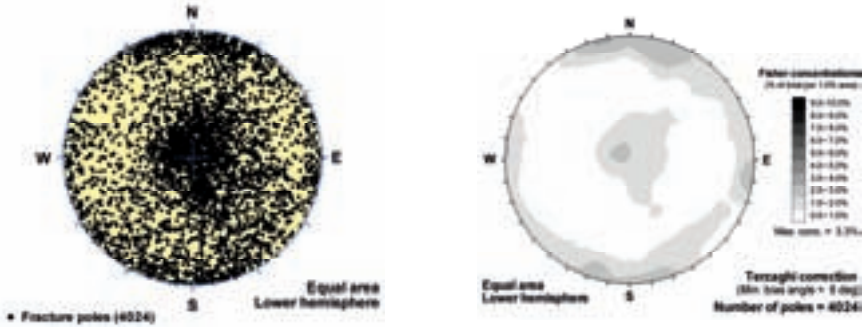

FSM_EW007

Chlorite

Open Fractures

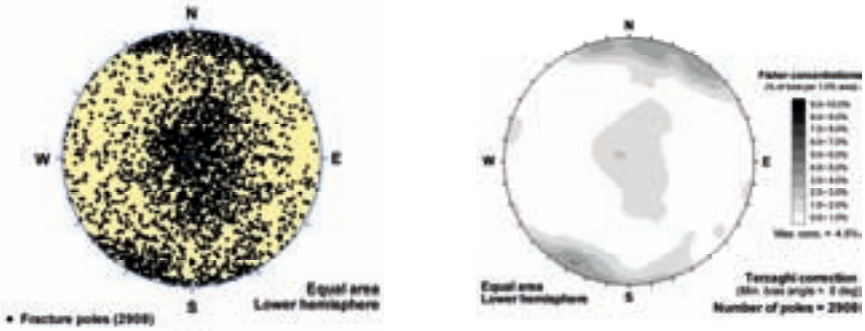

Sealed Fractures

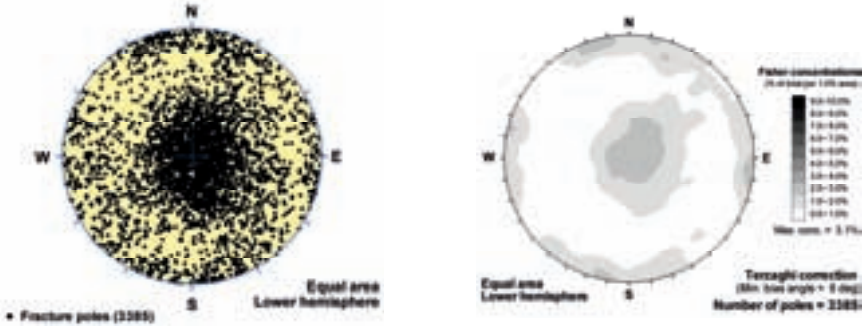

Clay Minerals

Open Fractures

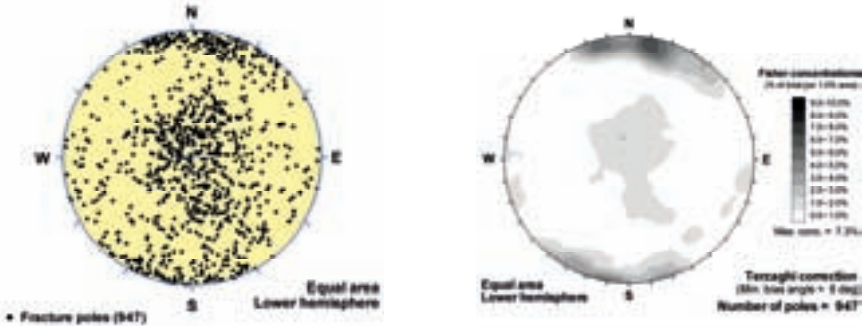

Sealed Fractures

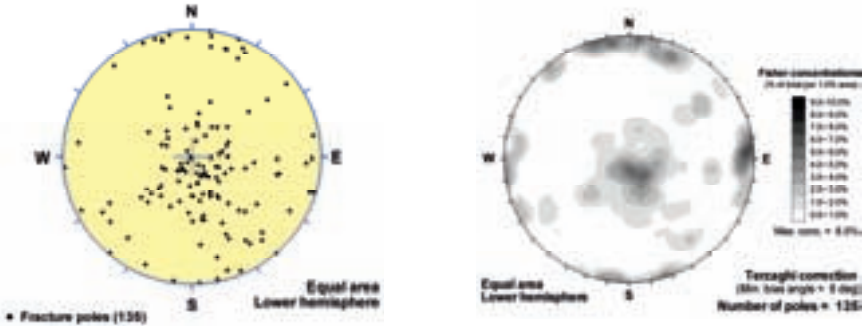

FSM_EW007

Epidote

Open Fractures

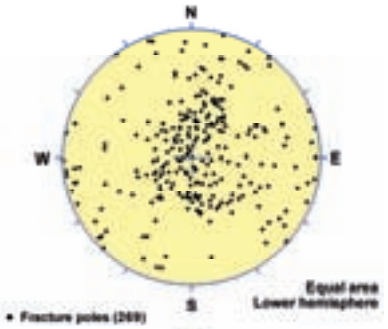

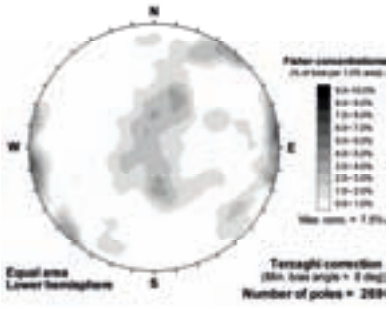

Sealed Fractures

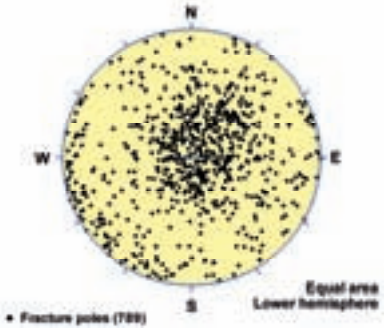

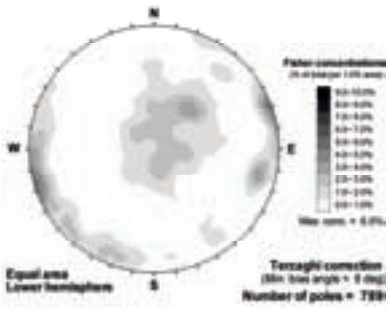

Fluorite

Open Fractures

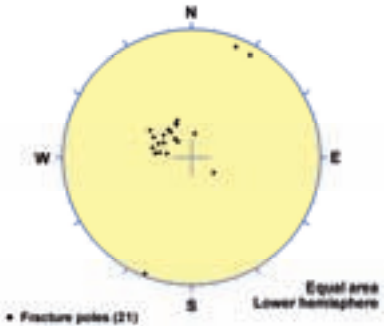

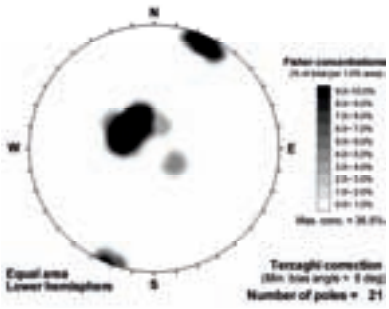

Sealed Fractures

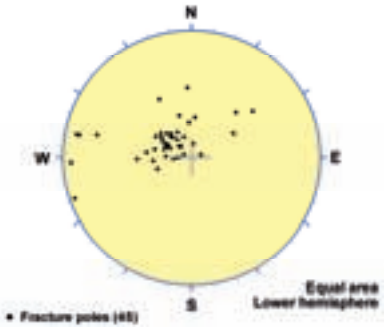

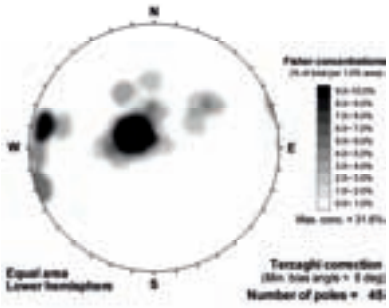

FSM_EW007

Goethite

Open Fractures

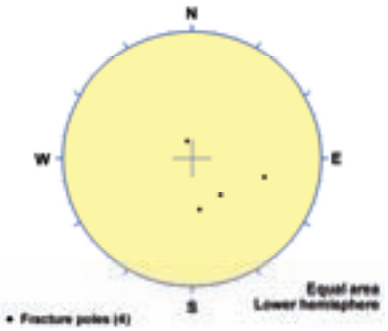

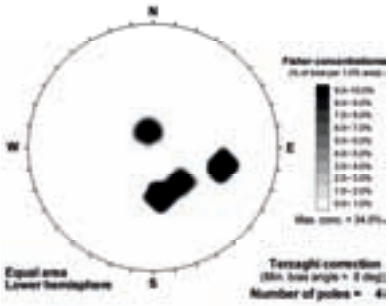

Sealed Fractures

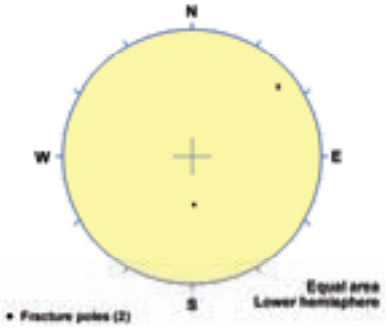

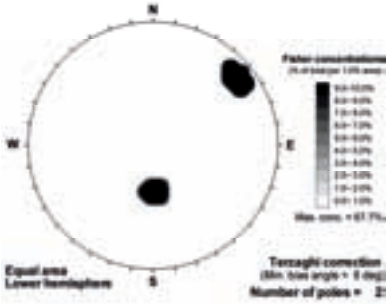

Gypsum

Open Fractures

Sealed Fractures

FSM_EW007

Hematite

Open Fractures

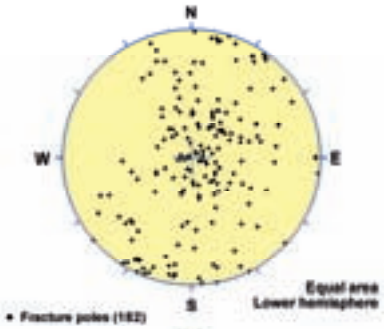

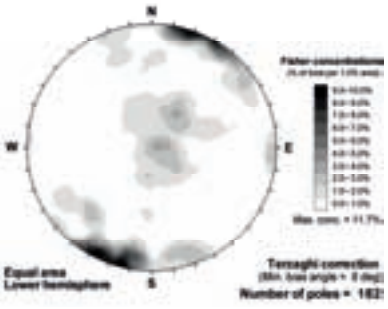

Sealed Fractures

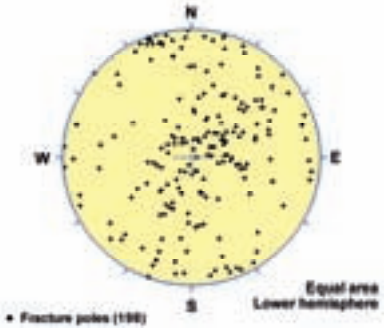

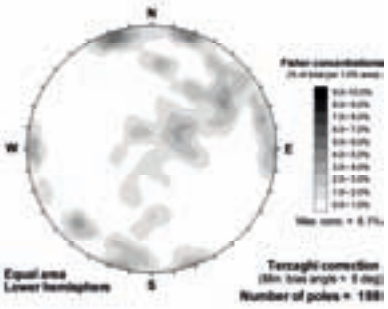

Laumontite

Open Fractures

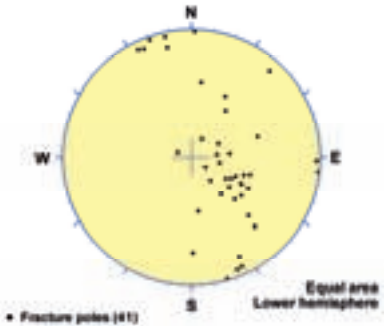

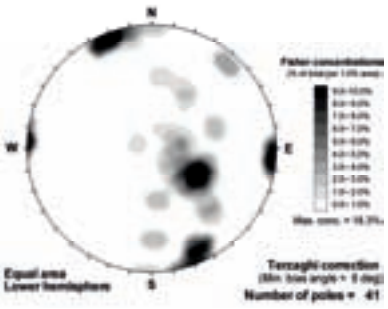

Sealed Fractures

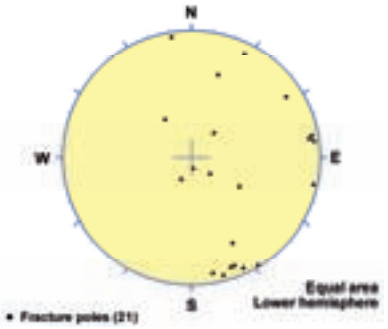

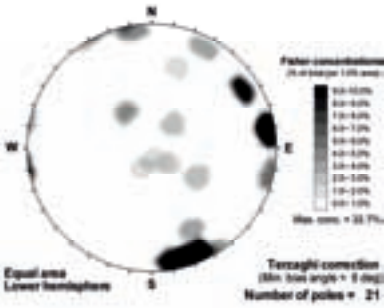

FSM_EW007

Muscovite

Open Fractures

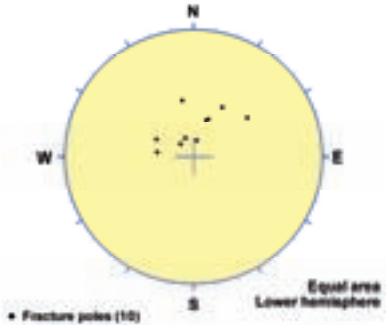

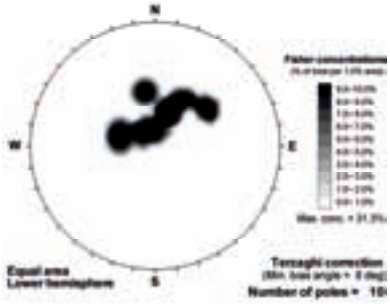

Sealed Fractures

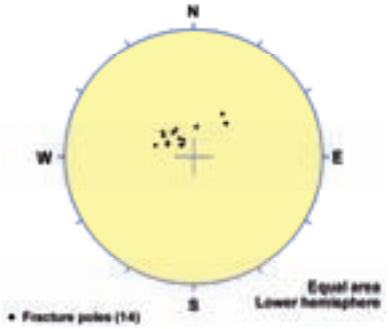

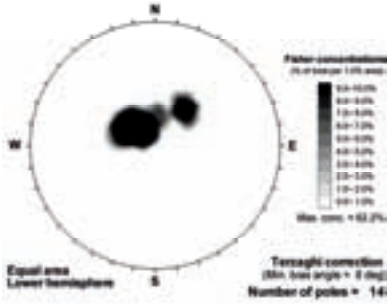

Prehnite

Open Fractures

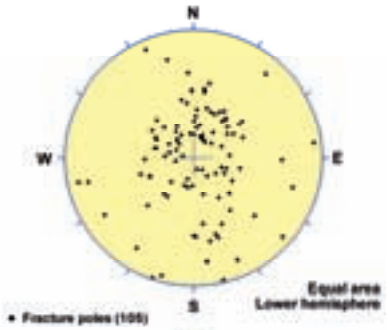

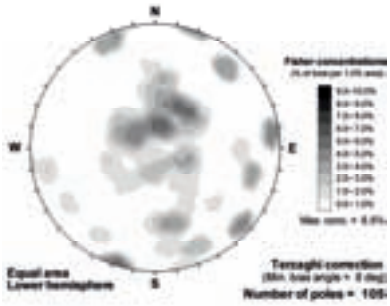

Sealed Fractures

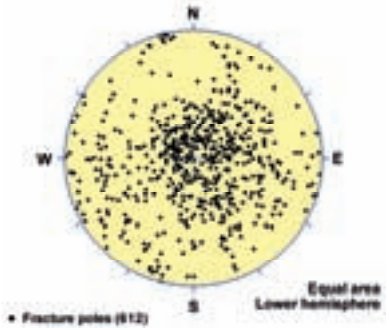

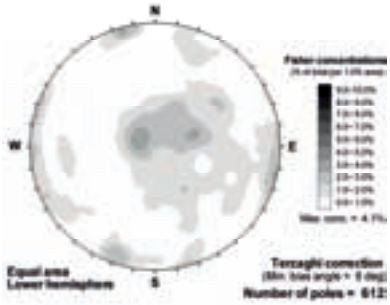

FSM_EW007

Pyrite

Open Fractures

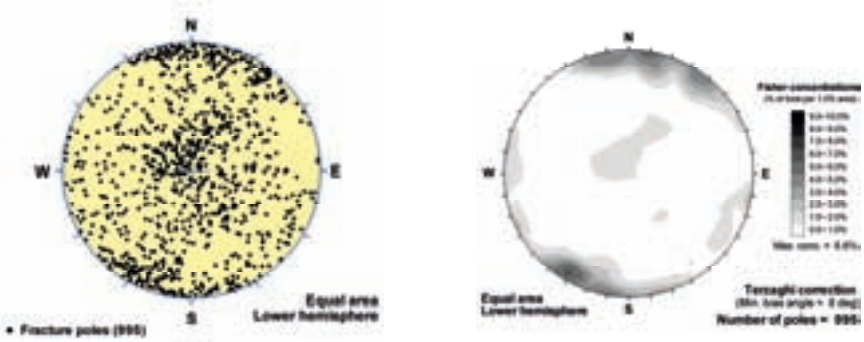

Sealed Fractures

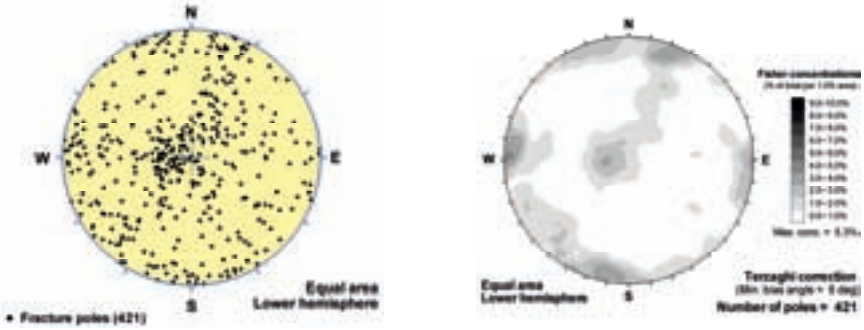

Quartz

Open Fractures

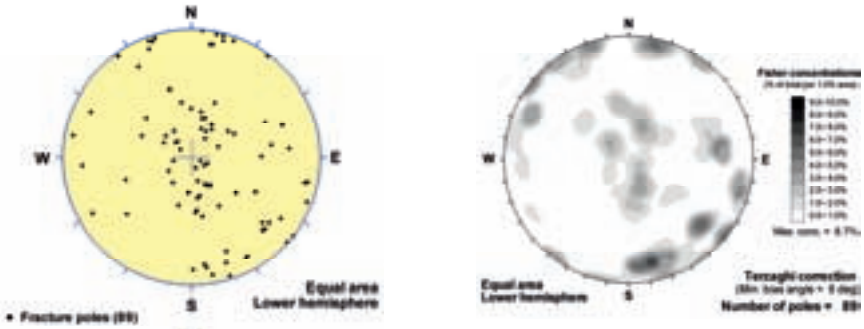

Sealed Fractures

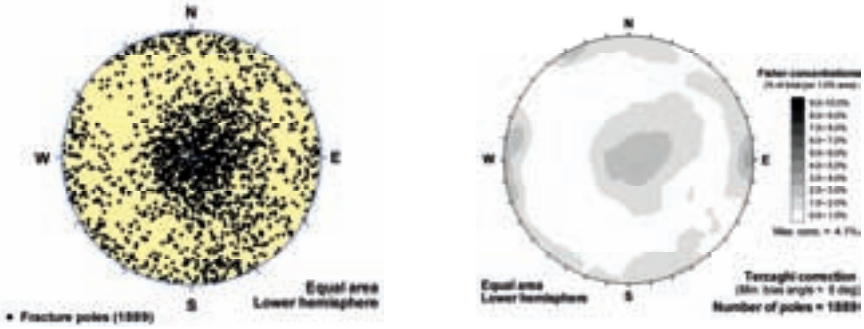

FSM_EW007

No fill - Altered WR

Open Fractures

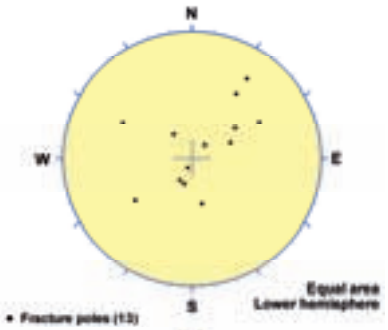

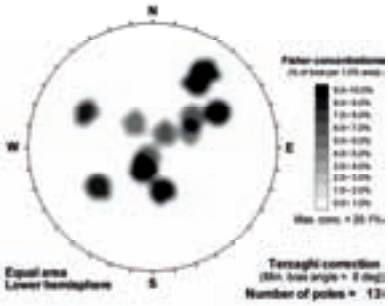

Sealed Fractures

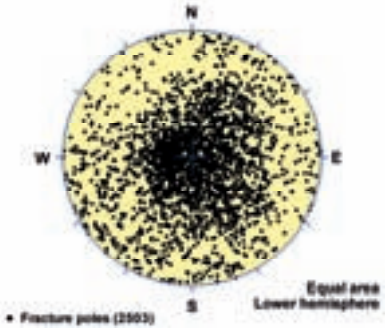

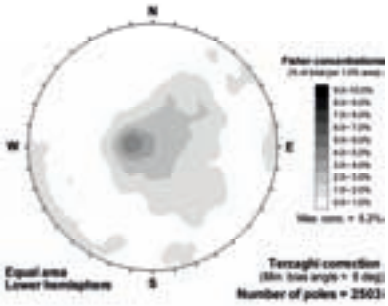

No fill - Fresh WR

Open Fractures

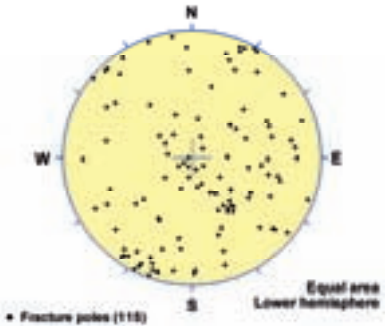

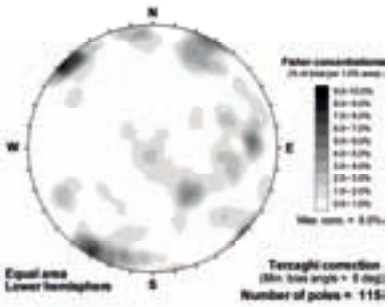

Sealed Fractures

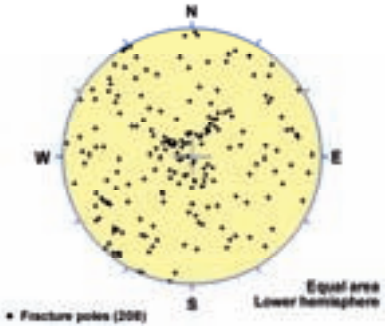

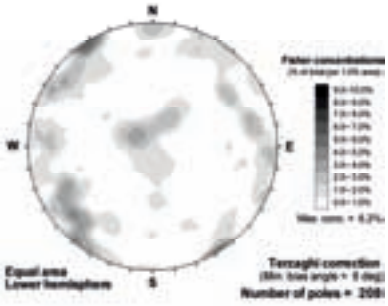

FSM_N

Adularia

Open Fractures

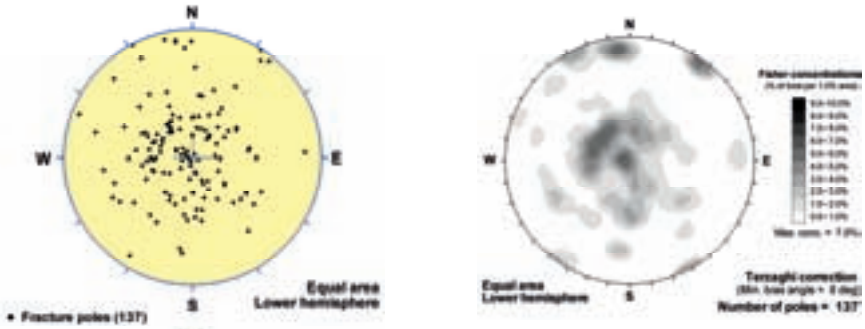

Sealed Fractures

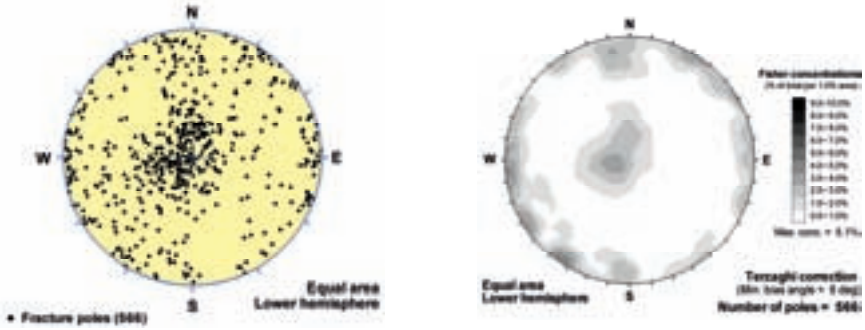

Calcite

Open Fractures

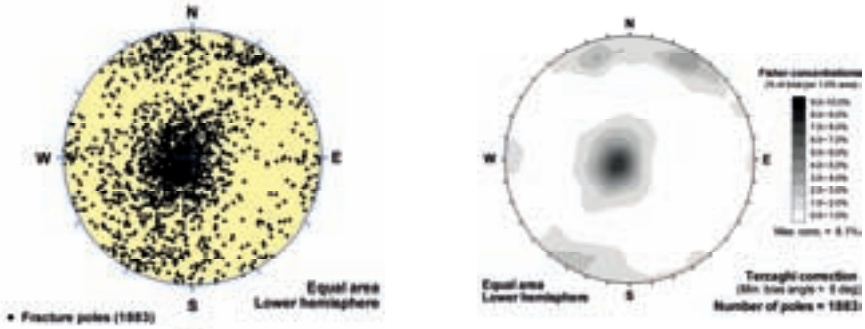

Sealed Fractures

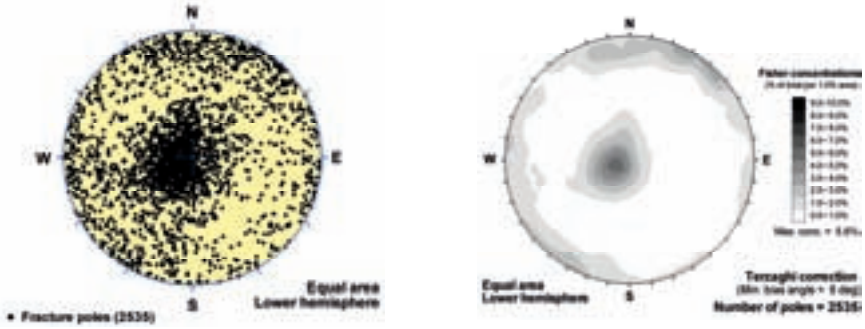

FSM_N

Chlorite

Open Fractures

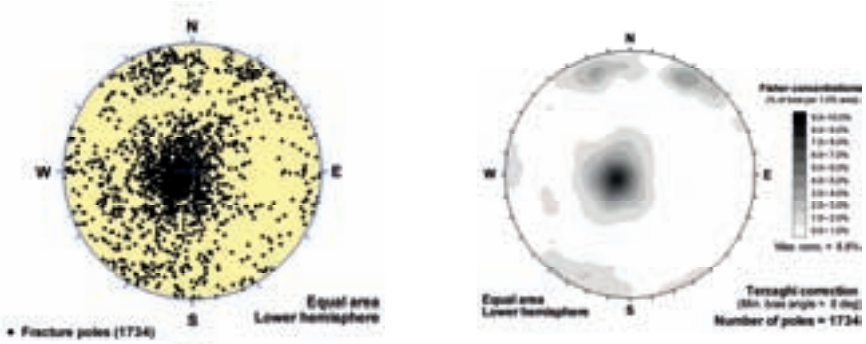

Sealed Fractures

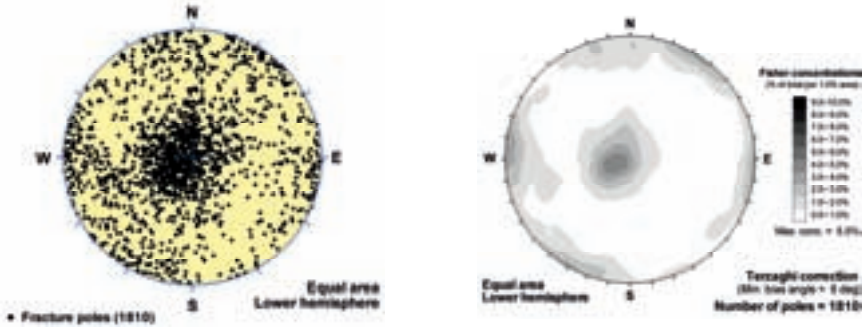

Clay Minerals

Open Fractures

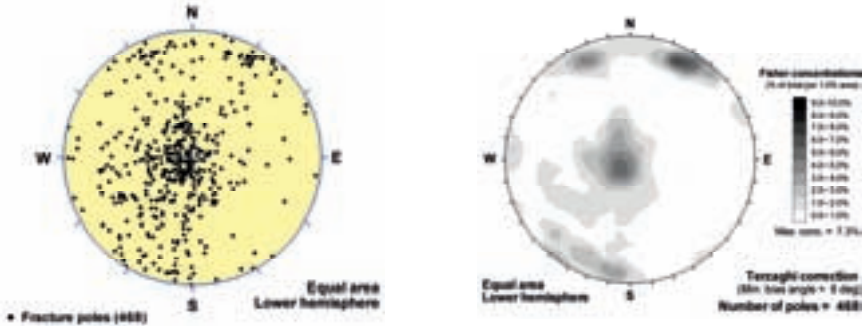

Sealed Fractures

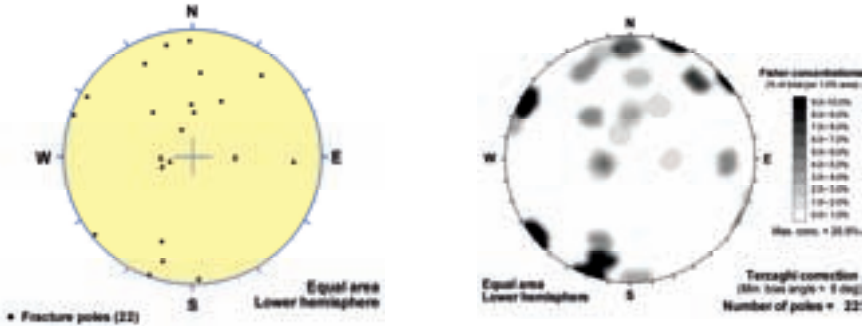

FSM_N

Epidote

Open Fractures

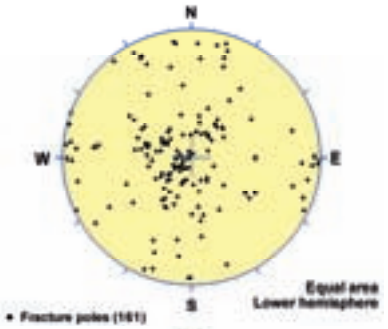

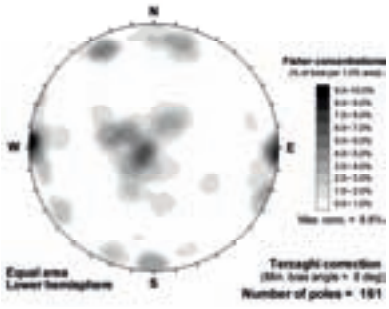

Sealed Fractures

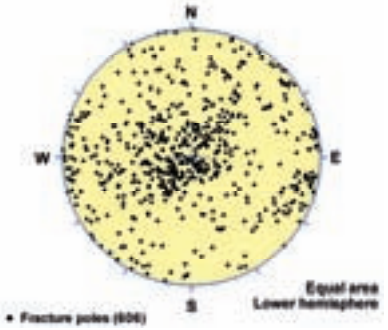

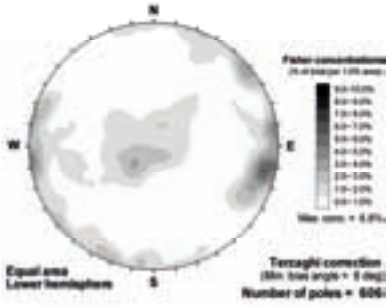

Fluorite

Open Fractures

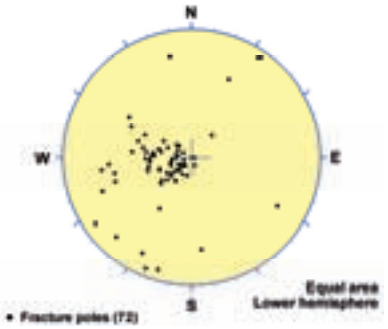

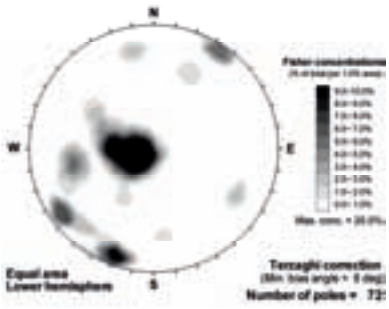

Sealed Fractures

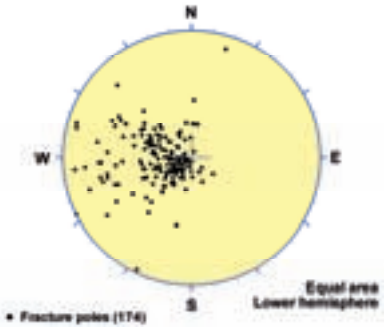

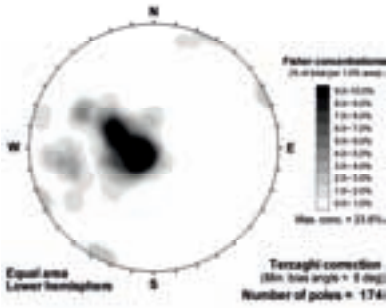

FSM_N

Goethite

Open Fractures

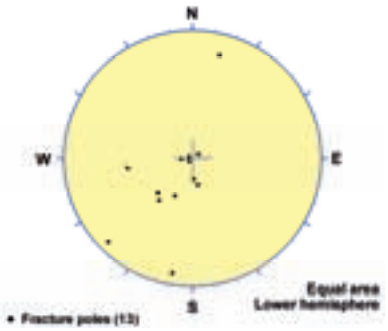

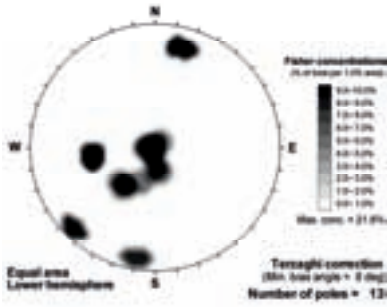

Sealed Fractures

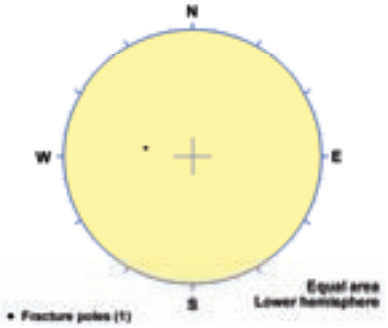

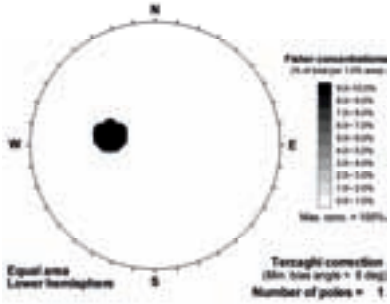

Gypsum

Open Fractures

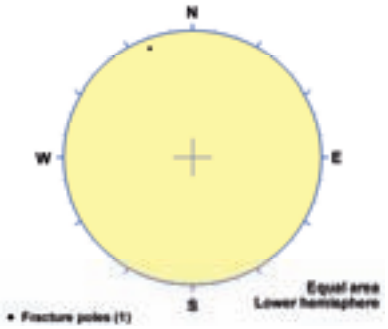

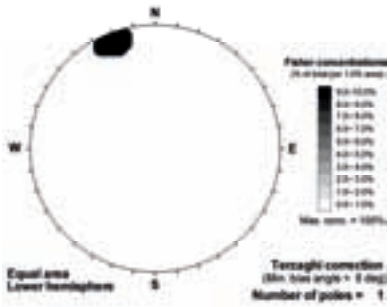

Sealed Fractures

FSM_N

Hematite

Open Fractures

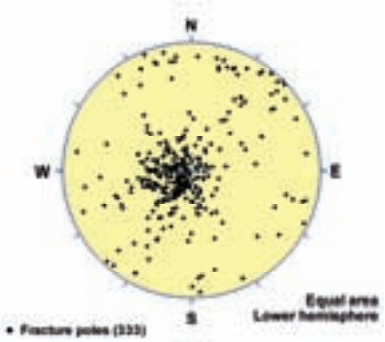

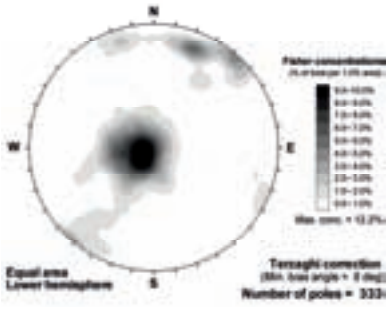

Sealed Fractures

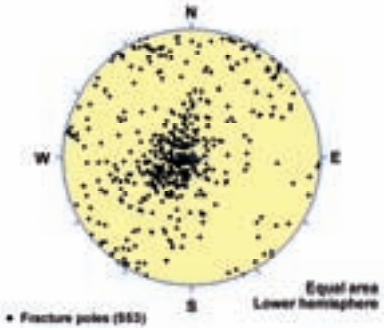

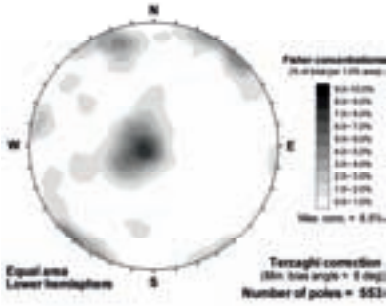

Laumontite

Open Fractures

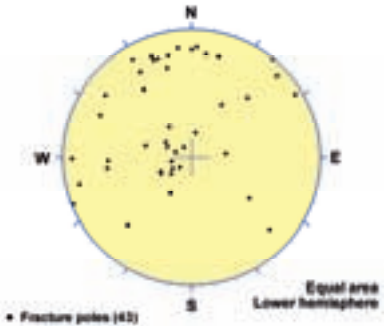

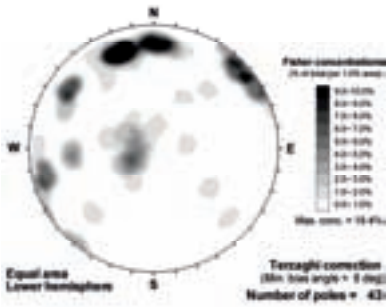

Sealed Fractures

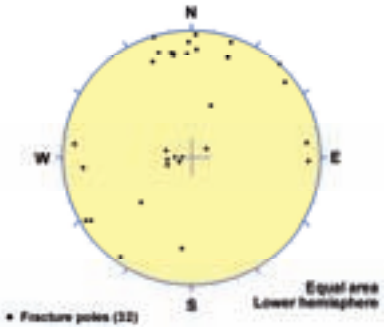

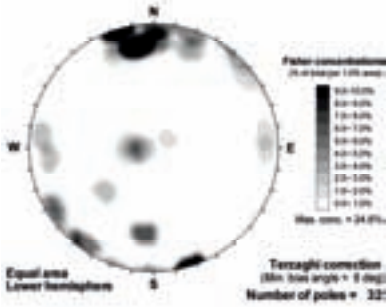

FSM_N

Muscovite

Open Fractures

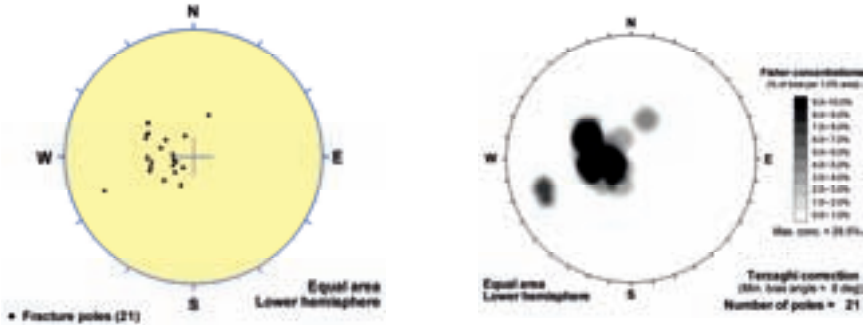

Sealed Fractures

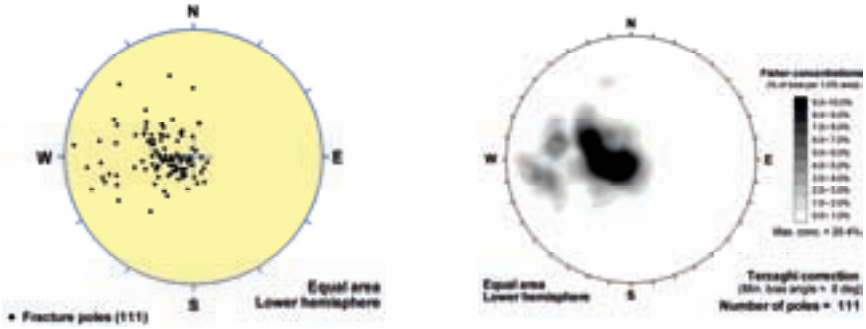

Prehnite

Open Fractures

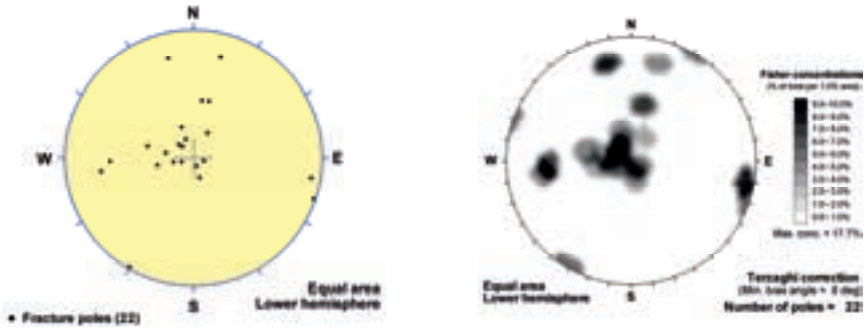

Sealed Fractures

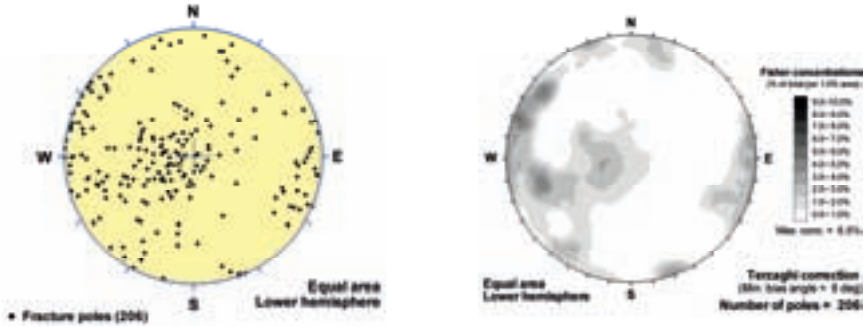

FSM_N

Pyrite

Open Fractures

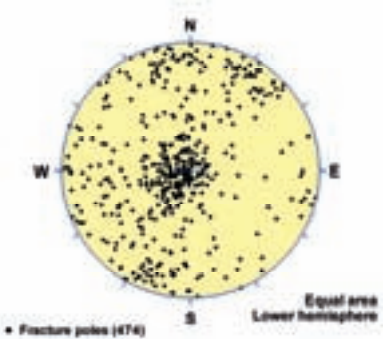

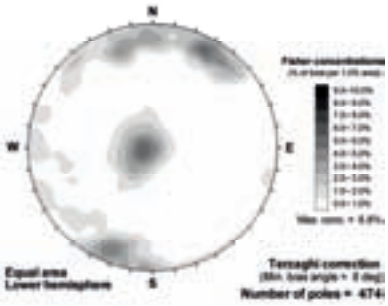

Sealed Fractures

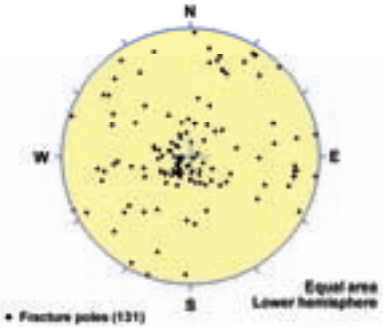

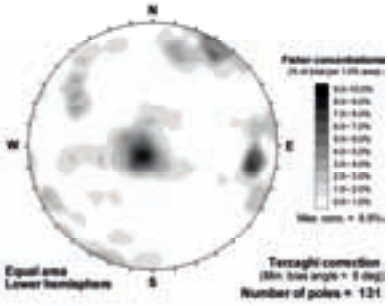

Quartz

Open Fractures

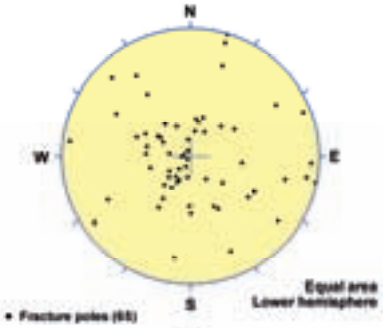

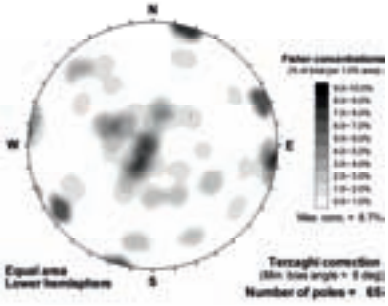

Sealed Fractures

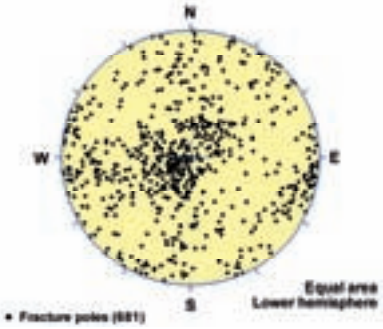

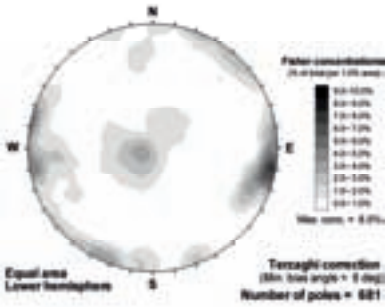

FSM_N

No fill - Altered WR

Open Fractures

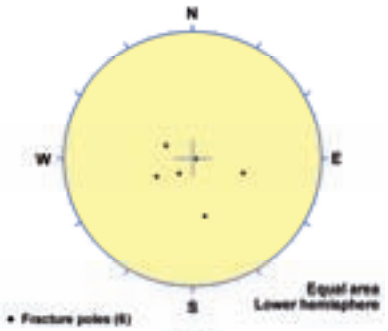

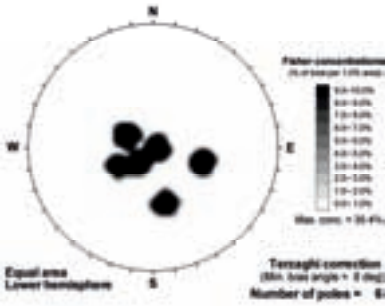

Sealed Fractures

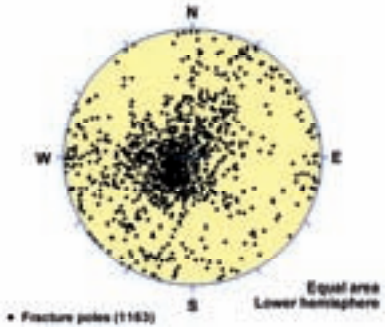

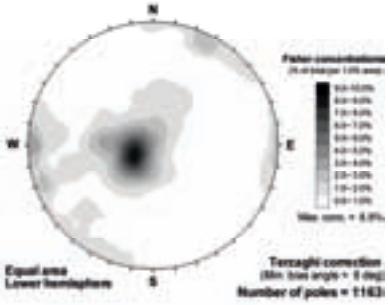

No fill - Fresh WR

Open Fractures

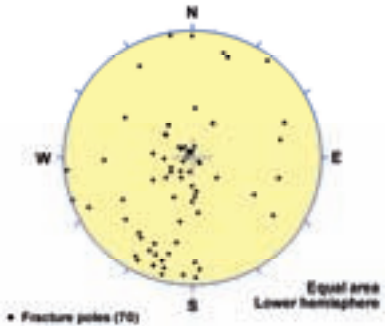

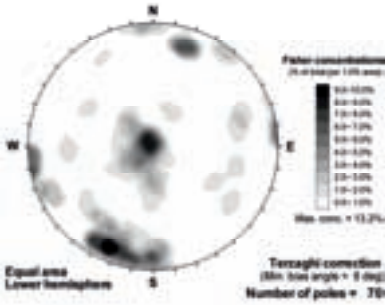

Sealed Fractures

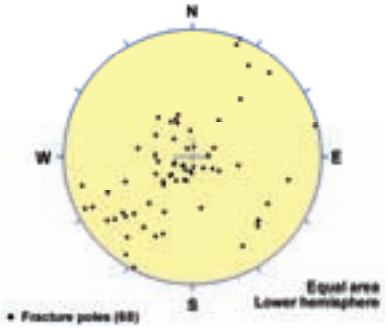

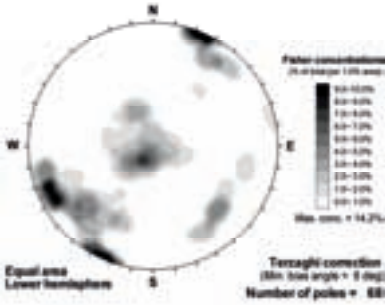

FSM_NE005

Adularia

Open Fractures

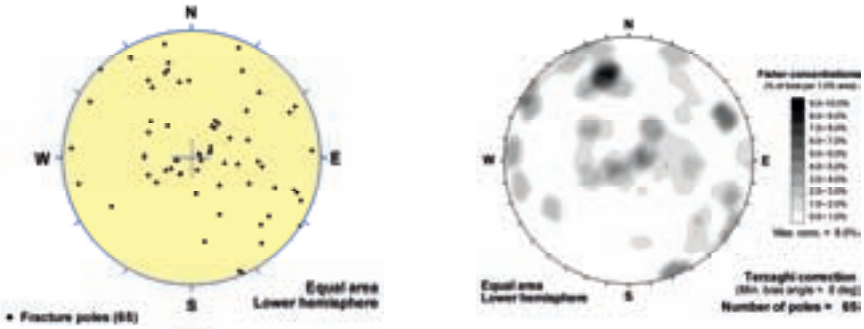

Sealed Fractures

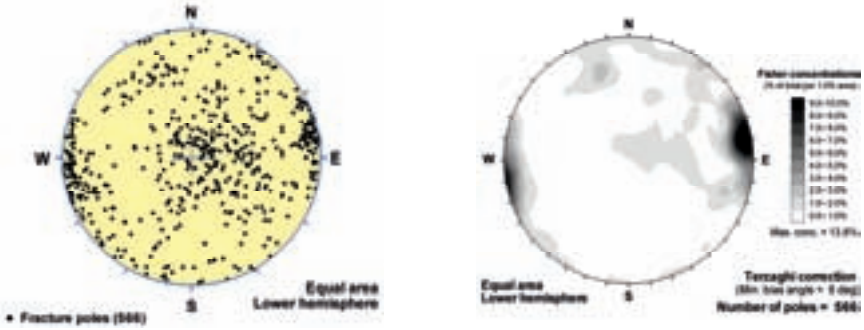

Calcite

Open Fractures

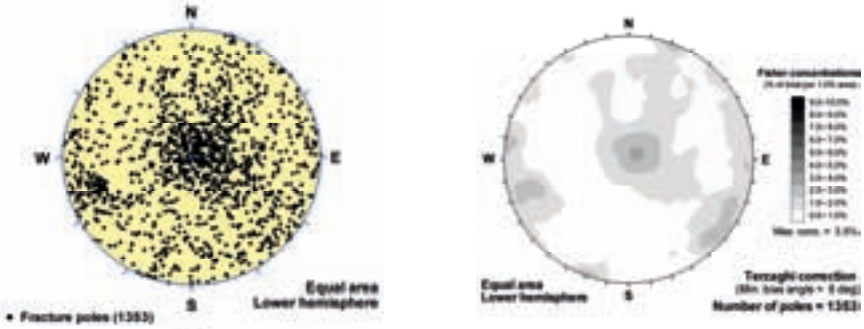

Sealed Fractures

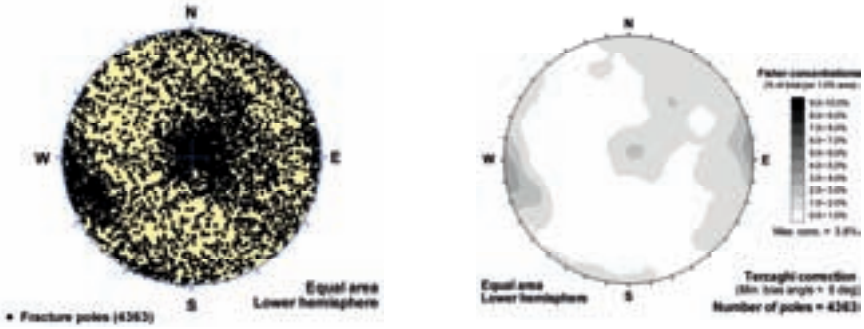

FSM_NE005

Chlorite

Open Fractures

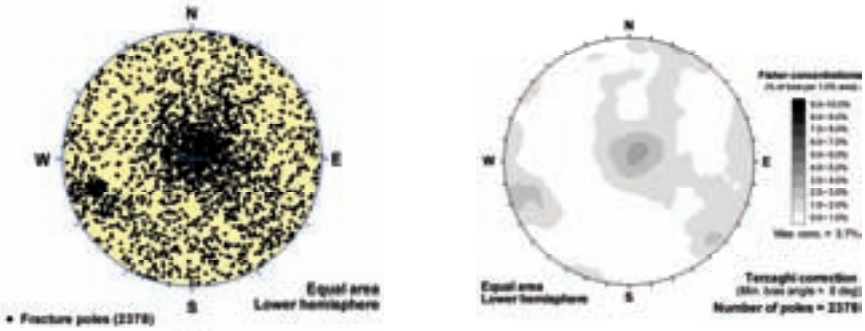

Sealed Fractures

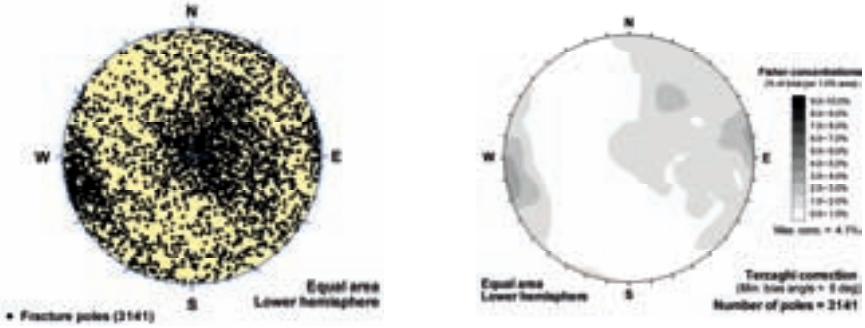

Clay Minerals

Open Fractures

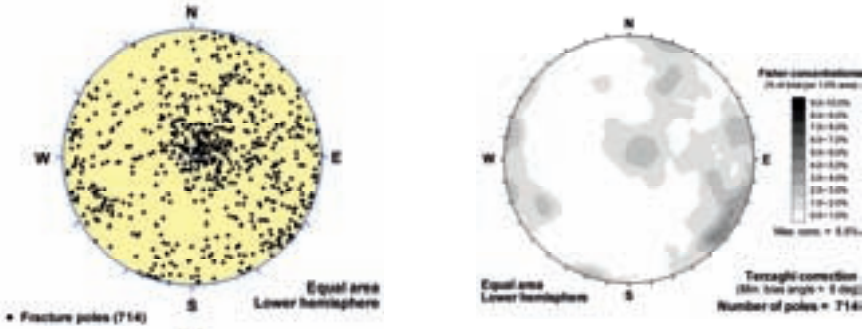

Sealed Fractures

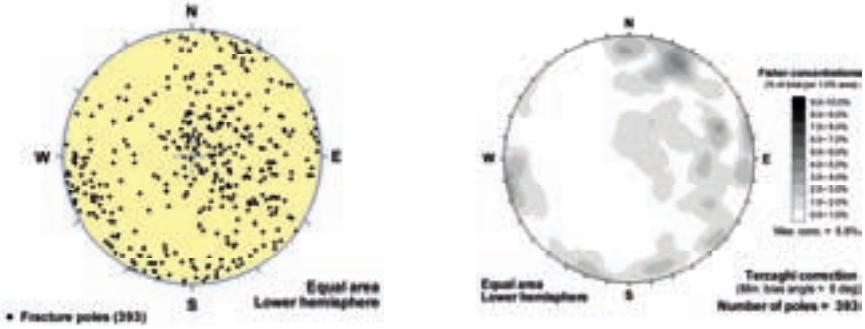

FSM_NE005

Epidote

Open Fractures

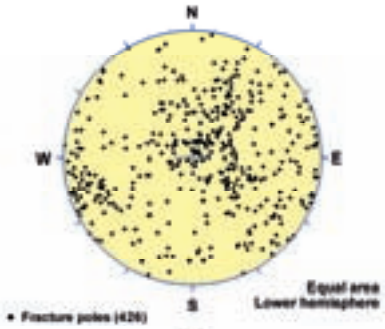

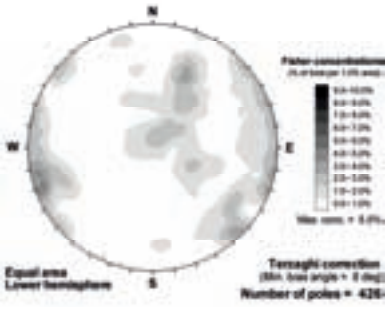

Sealed Fractures

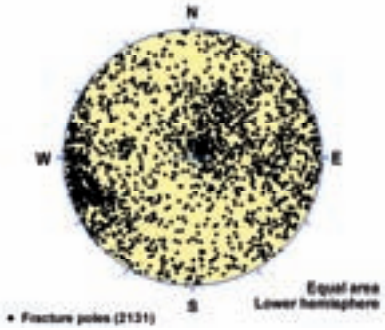

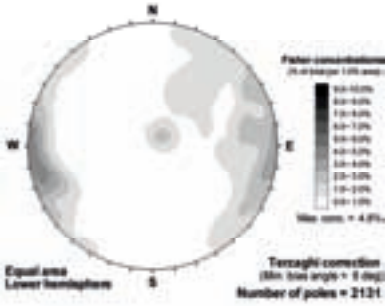

Fluorite

Open Fractures

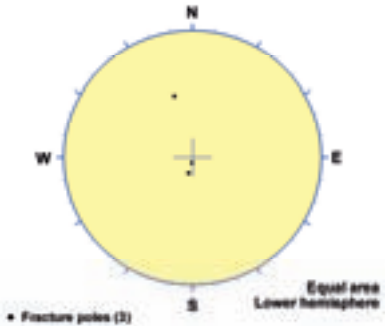

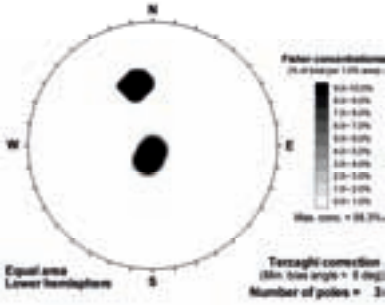

Sealed Fractures

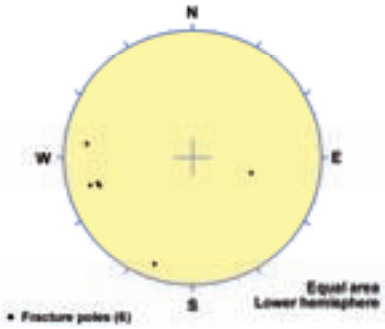

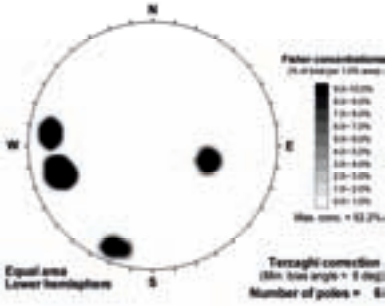

FSM_NE005

Goethite

Open Fractures

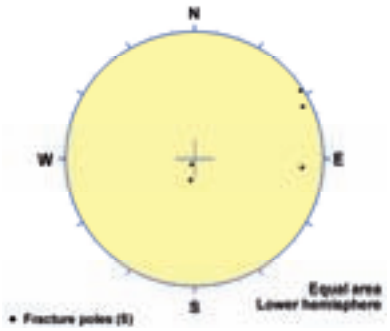

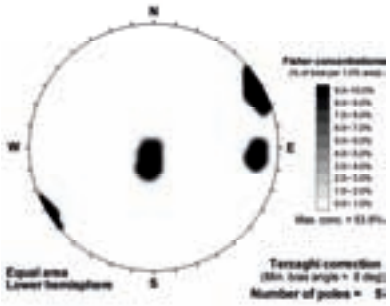

Sealed Fractures

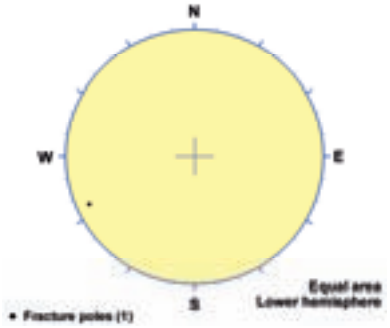

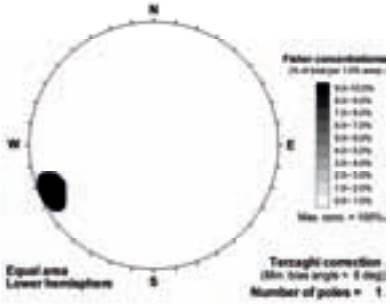

Gypsum

Open Fractures

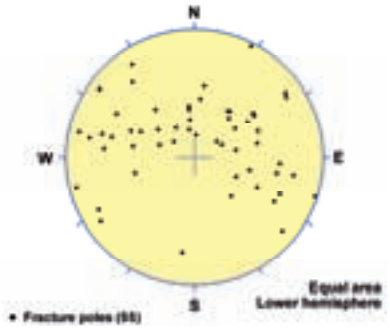

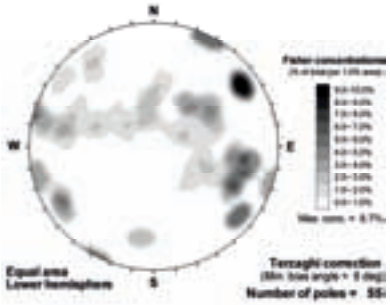

Sealed Fractures

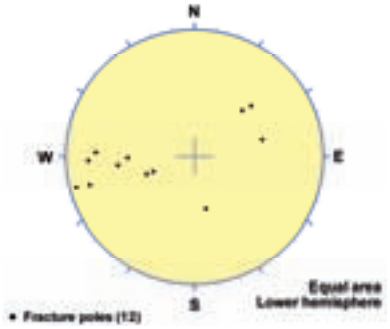

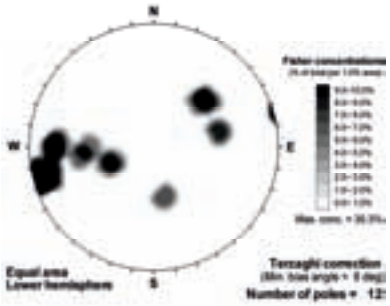

FSM_NE005

Hematite

Open Fractures

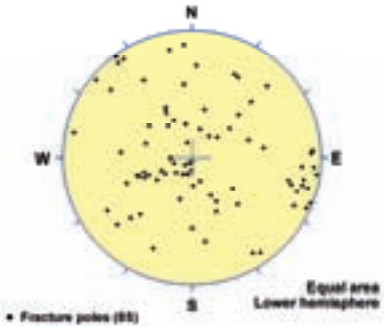

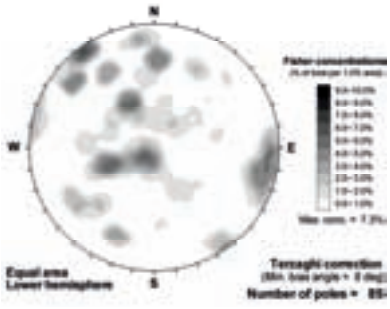

Sealed Fractures

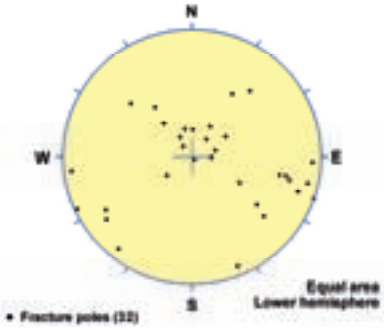

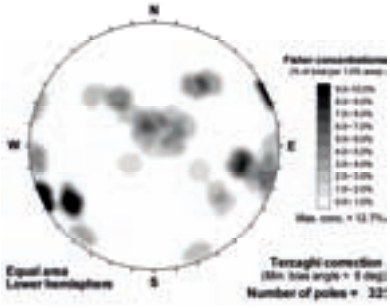

Laumontite

Open Fractures

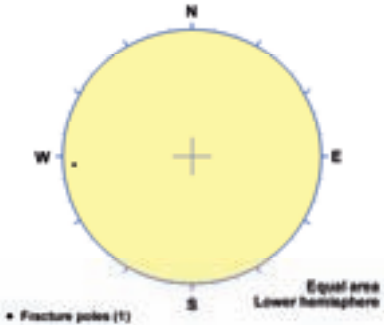

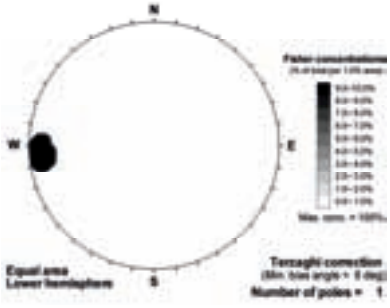

Sealed Fractures

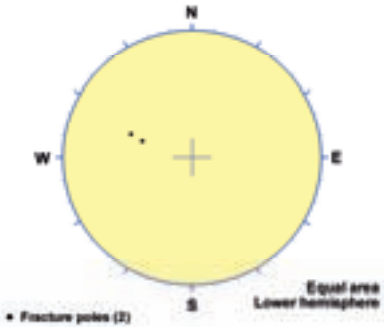

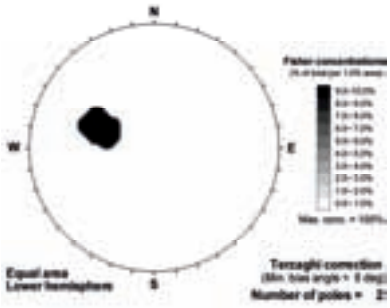

FSM_NE005

Muscovite

Open Fractures

Sealed Fractures

Prehnite

Open Fractures

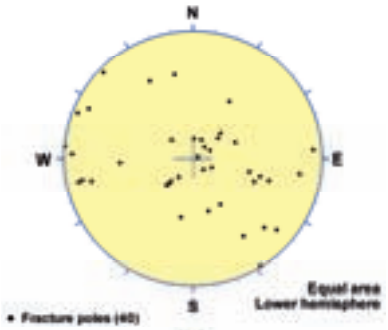

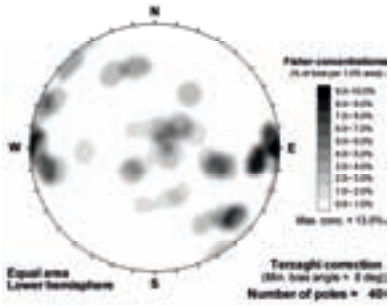

Sealed Fractures

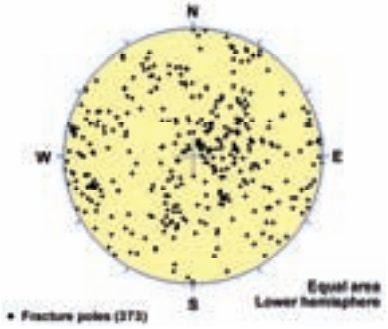

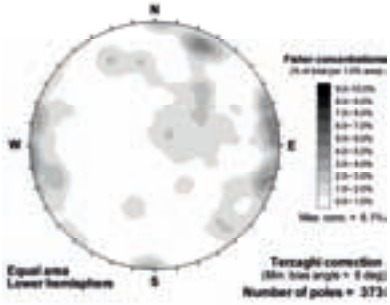

FSM_NE005

Pyrite

Open Fractures

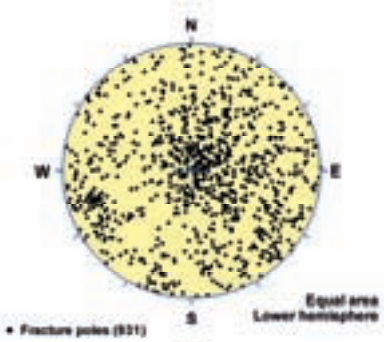

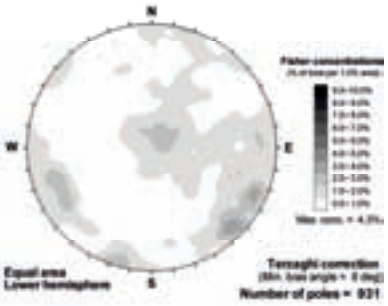

Sealed Fractures

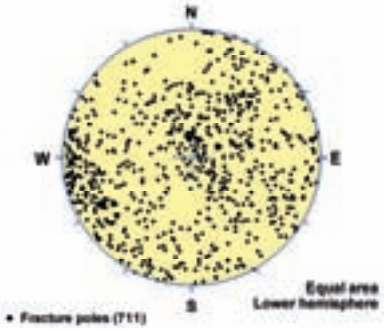

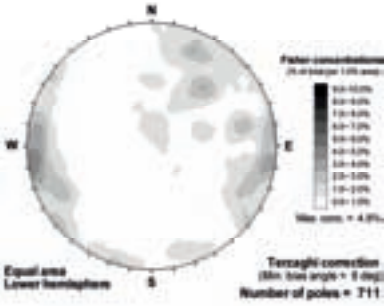

Quartz

Open Fractures

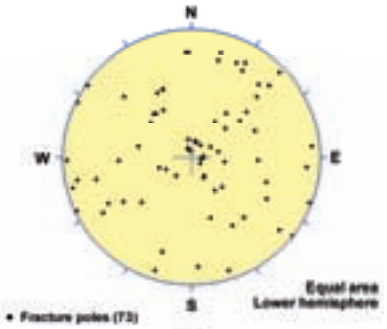

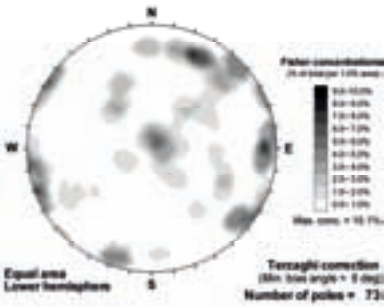

Sealed Fractures

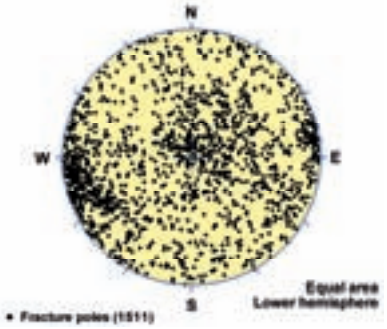

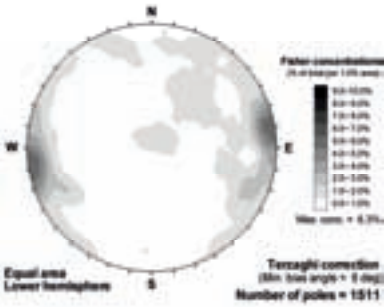

FSM_NE005

No fill - Altered WR

Open Fractures

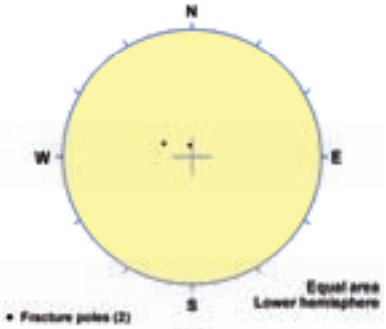

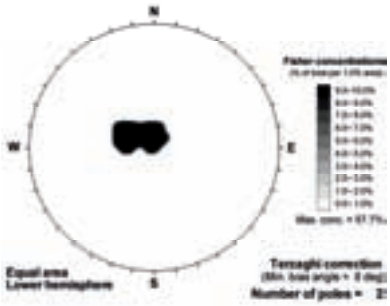

Sealed Fractures

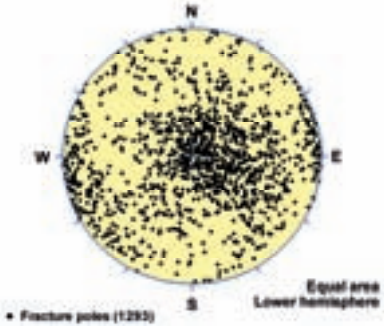

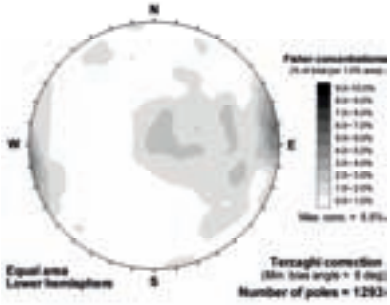

No fill - Fresh WR

Open Fractures

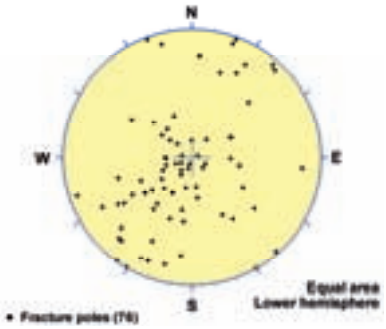

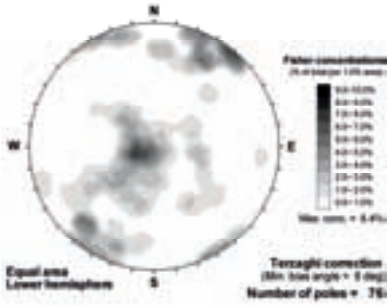

Sealed Fractures

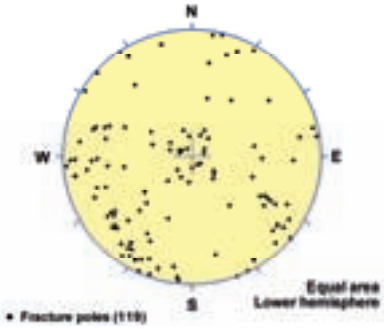

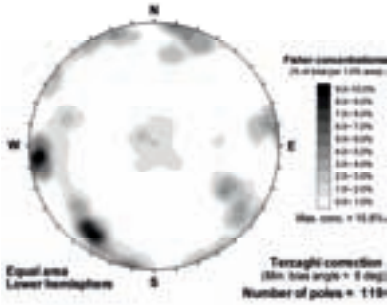

FSM_W

Adularia

Open Fractures

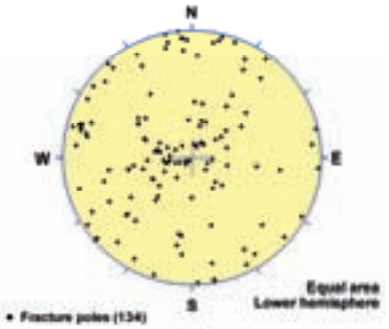

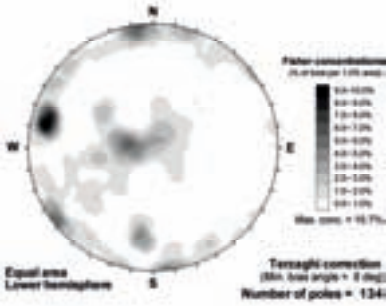

Sealed Fractures

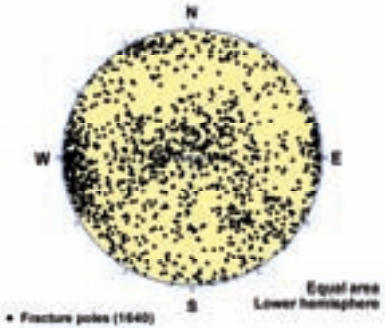

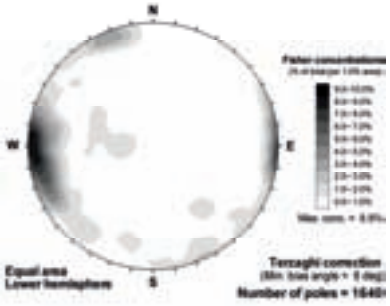

Calcite

Open Fractures

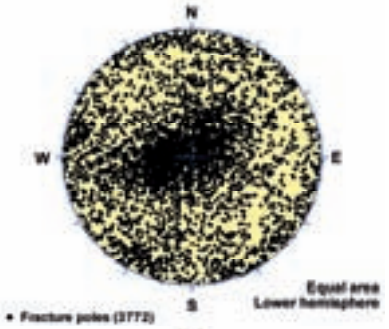

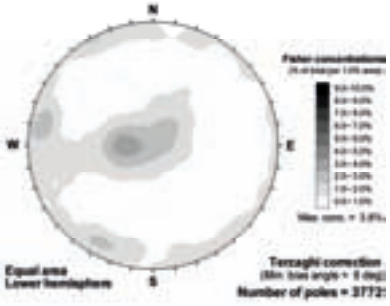

Sealed Fractures

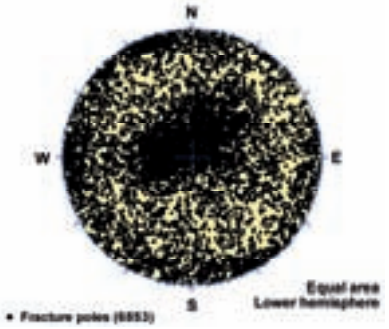

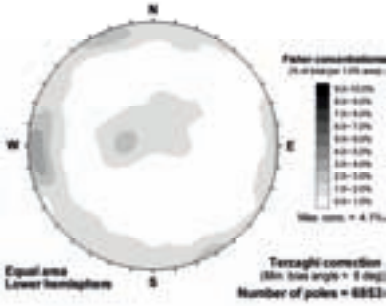

FSM_W

Chlorite

Open Fractures

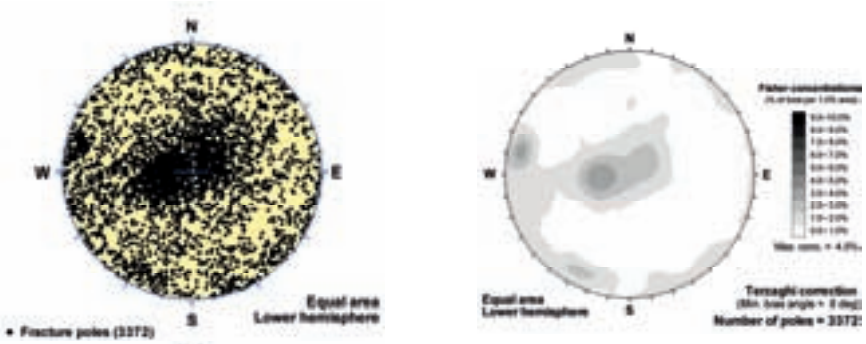

Sealed Fractures

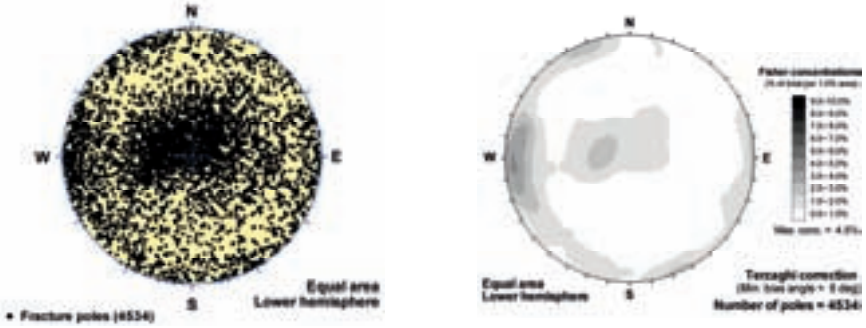

Clay Minerals

Open Fractures

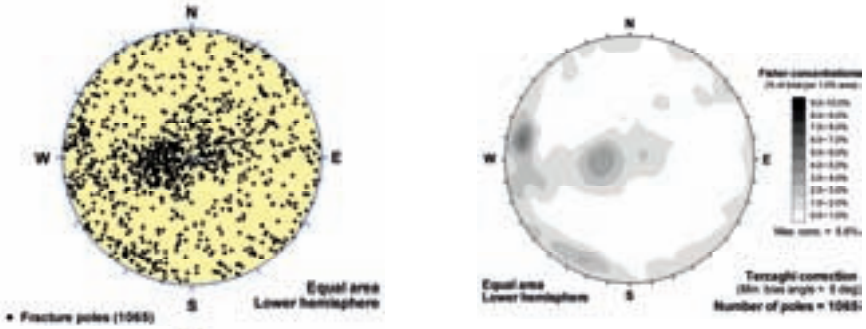

Sealed Fractures

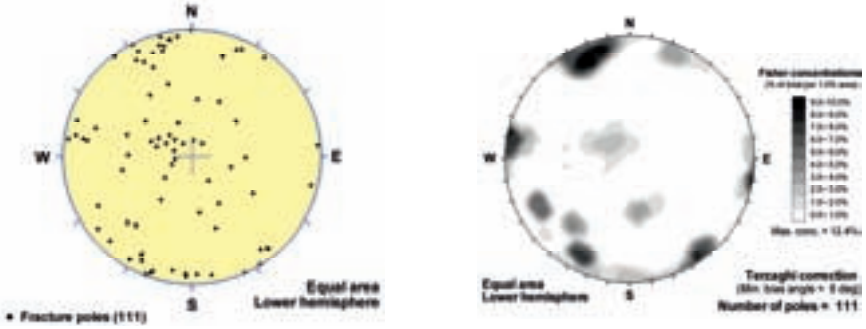

FSM_W

Epidote

Open Fractures

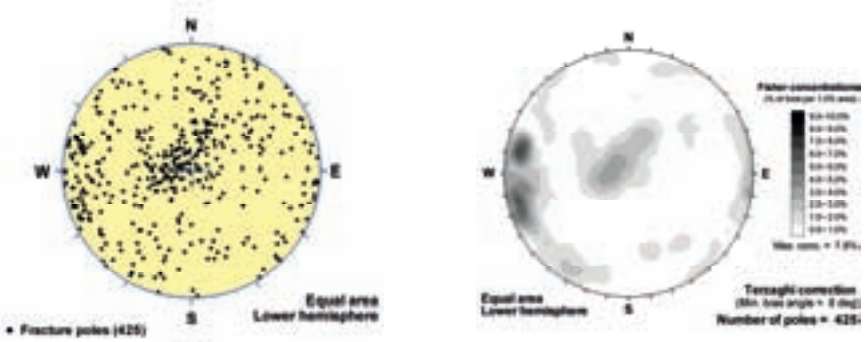

Sealed Fractures

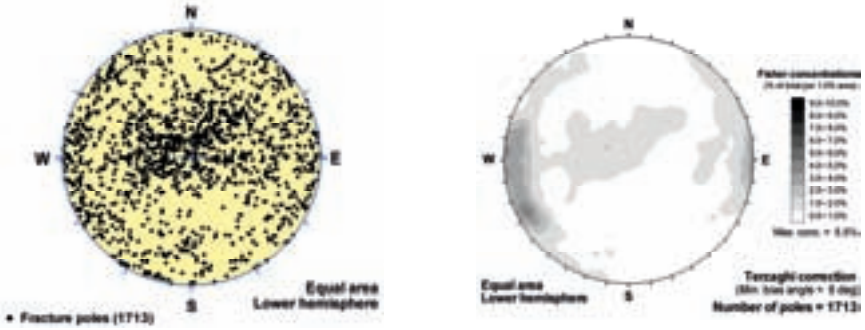

Fluorite

Open Fractures

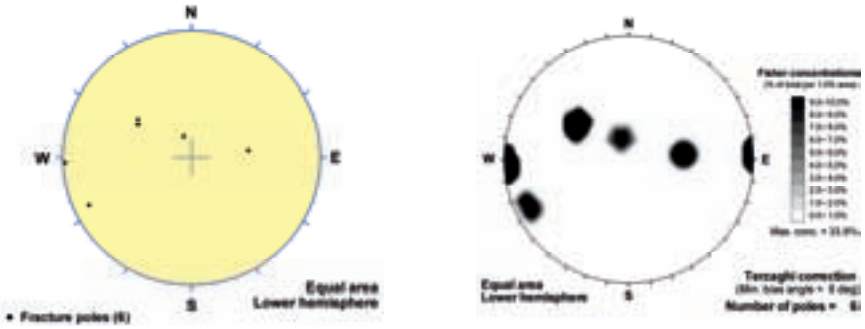

Sealed Fractures

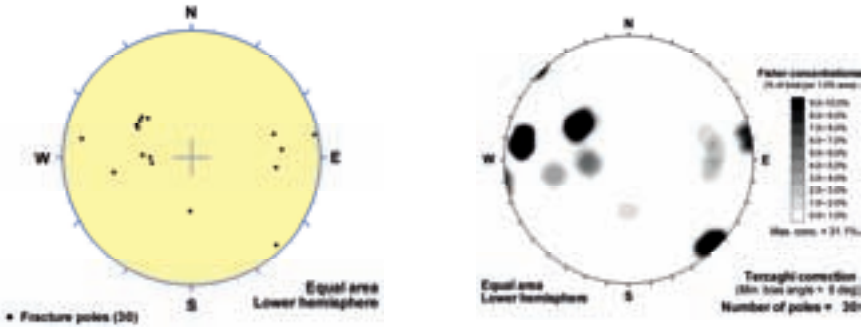

FSM_W

Goethite

Open Fractures

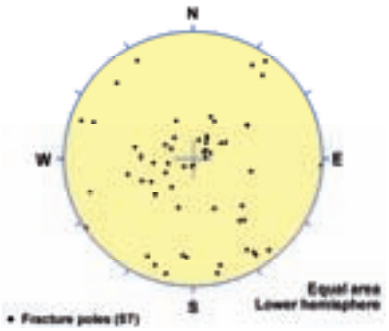

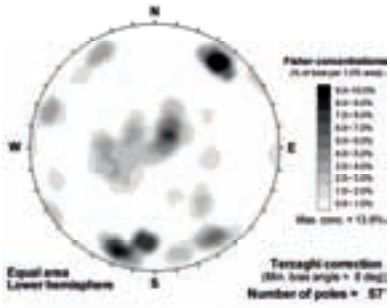

Sealed Fractures

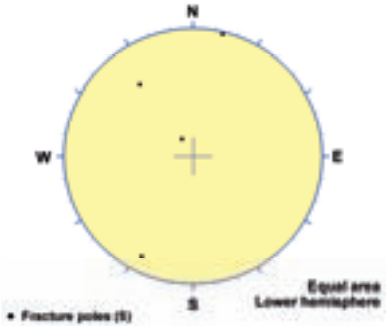

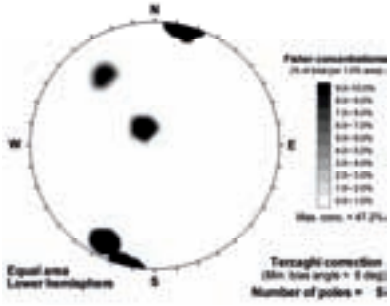

Gypsum

Open Fractures

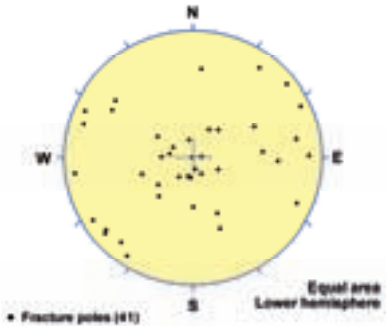

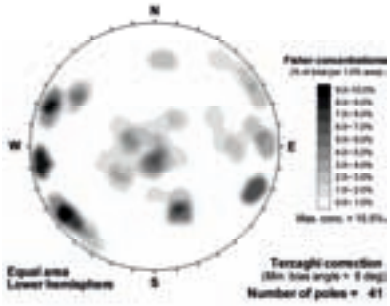

Sealed Fractures

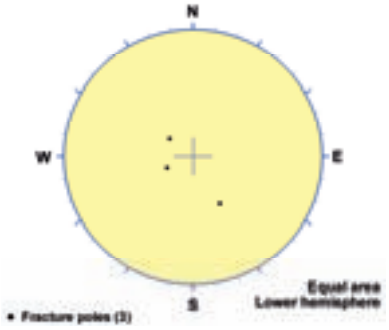

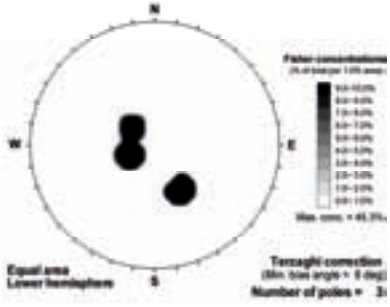

FSM_W

Hematite

Open Fractures

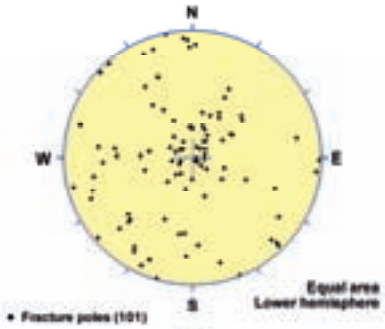

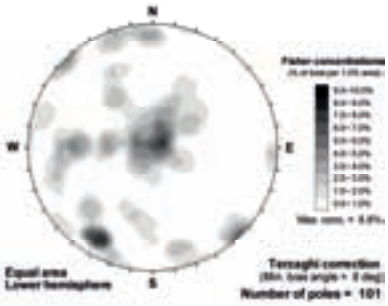

Sealed Fractures

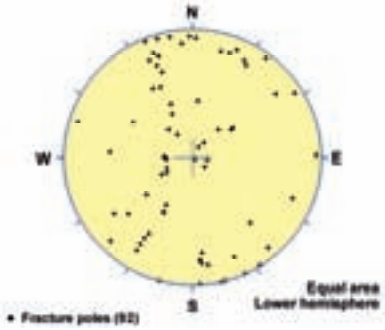

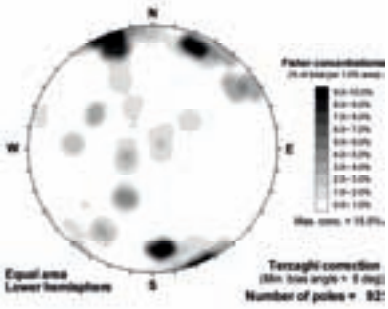

Laumontite

Open Fractures

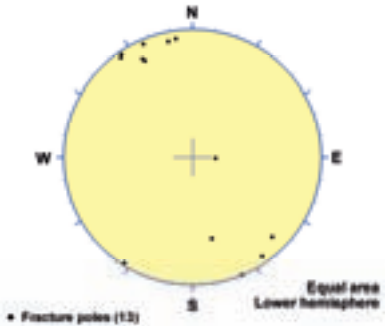

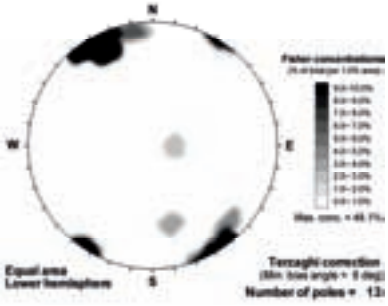

Sealed Fractures

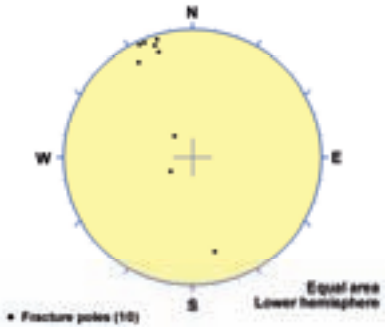

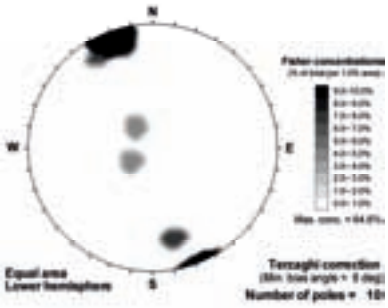

FSM_W

Muscovite

Open Fractures

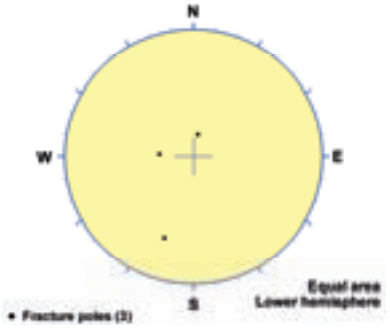

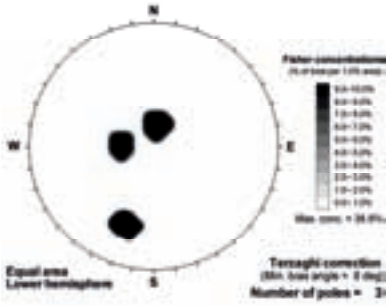

Sealed Fractures

Prehnite

Open Fractures

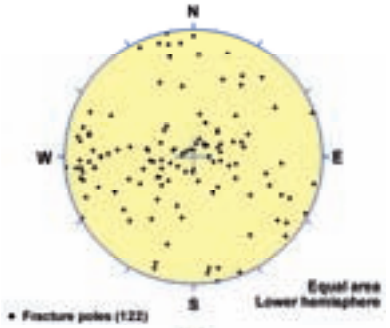

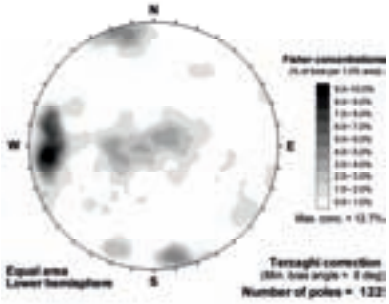

Sealed Fractures

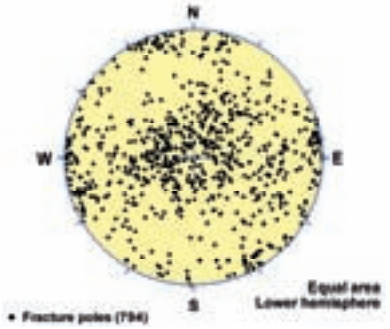

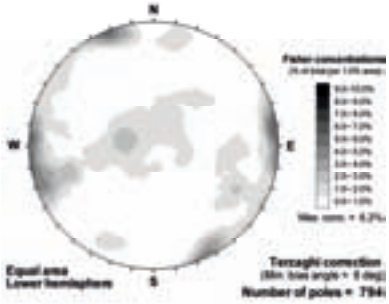

FSM_W

Pyrite

Open Fractures

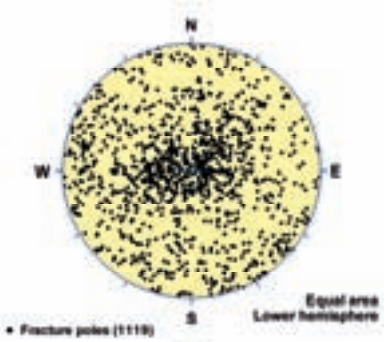

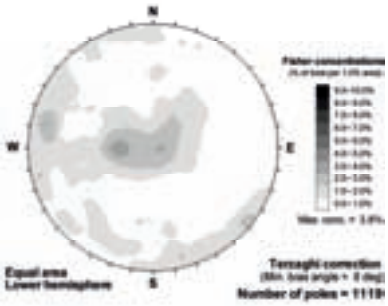

Sealed Fractures

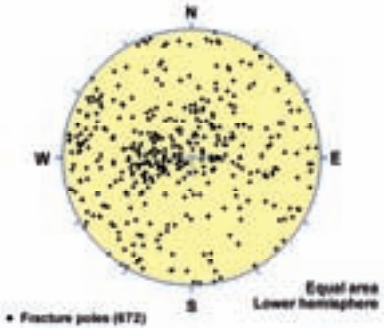

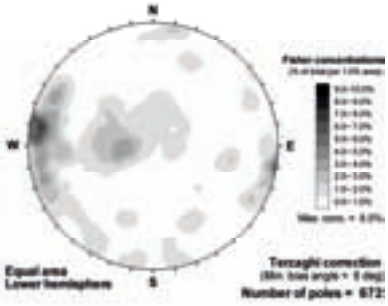

Quartz

Open Fractures

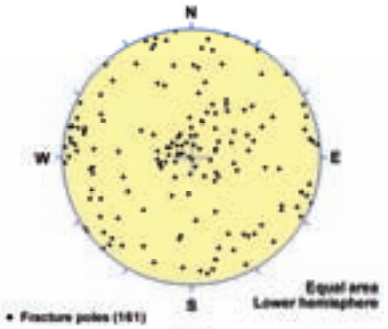

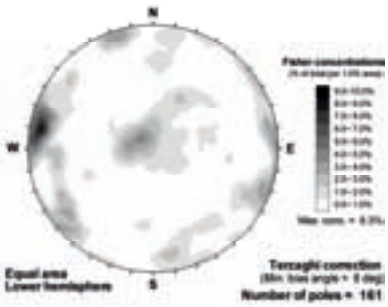

Sealed Fractures

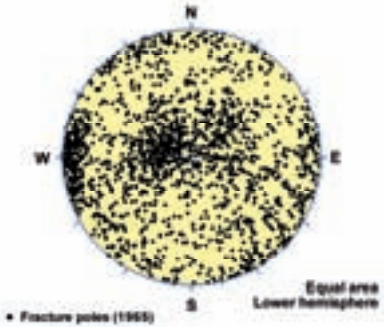

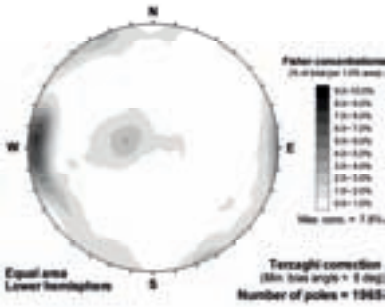

FSM_W

No fill - Altered WR

Open Fractures

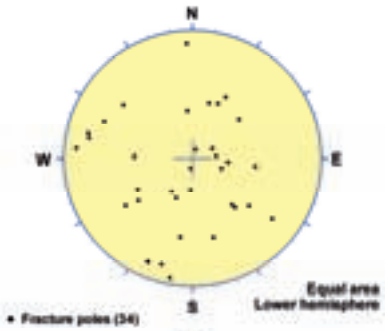

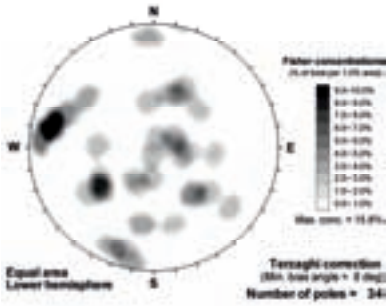

Sealed Fractures

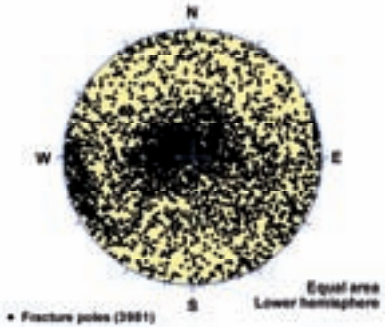

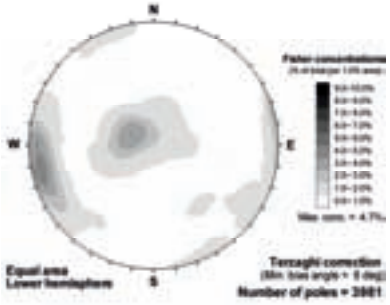

No fill - Fresh WR

Open Fractures

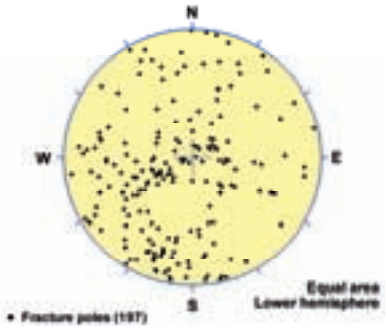

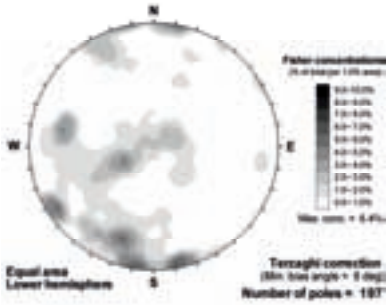

Sealed Fractures

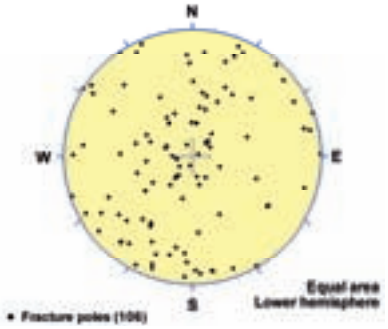

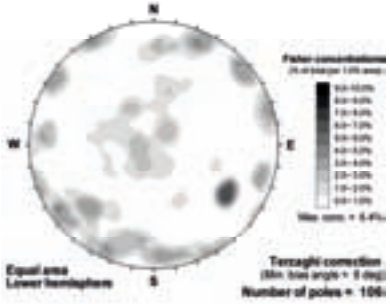

Appendix 3

Variation of fracture mineral frequencies versus depth

This appendix is a compilation of the data available in April 2009 of drill core mapping data. Fractures carrying certain minerals have been divided into sealed fractures, open fractures and total amount of fractures and plotted versus depth on a borehole by borehole basis and are plotted together with the depth distribution of all fractures of each fracture type. Fractures in deformation zones, in sections of crushed rock and in sections mapped as sealed network are included as well. Minerals mapped as “white feldspar”, “red feldspar” and “adularia” are presented collectively as “adularia+albite”. Other minerals included in the analysis are calcite, chlorite, clay minerals, epidote, goethite, gypsum, hematite, prehnite, pyrite and quartz. Fractures without any visible minerals have been divided into fractures with wall rock alteration (labelled “No fill - altered WR”) and fractures without wall rock alteration (labelled “No fill - fresh WR”).

KLX02

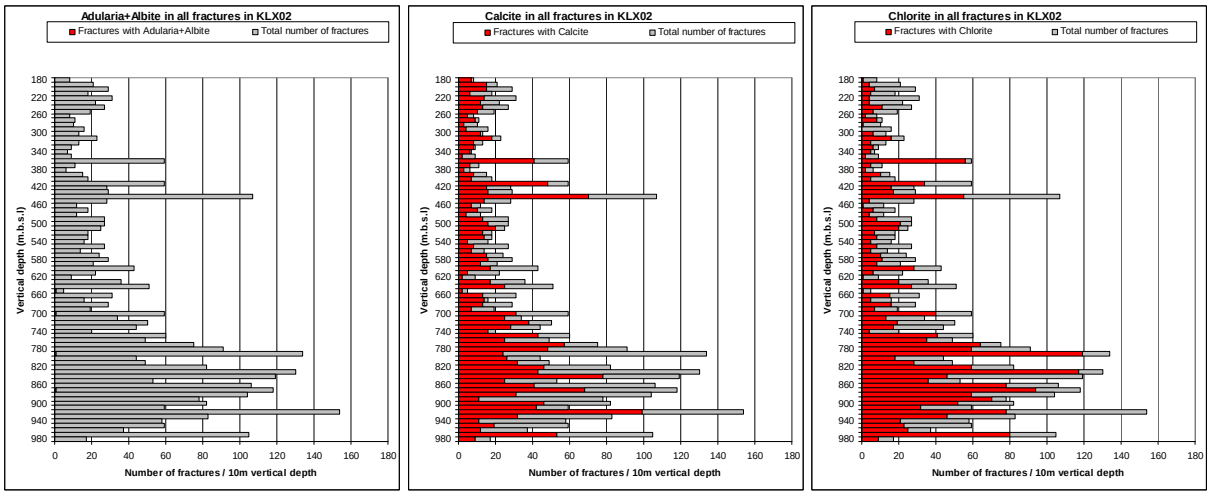

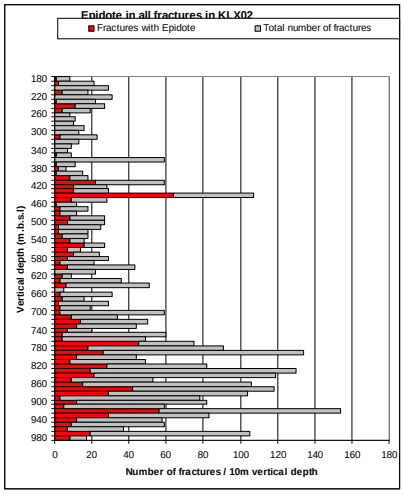
Epidote in all fractures in KLX02
Fractures with Epidote
Total number of fractures
Vertical depth (m.b.s.l)
Number of fractures / 10m vertical depth

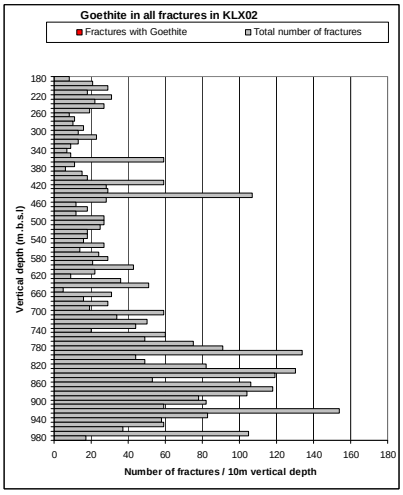
Goethite in all fractures in KLX02
Fractures with Goethite
Total number of fractures
Vertical depth (m.b.s.l)
Number of fractures / 10m vertical depth

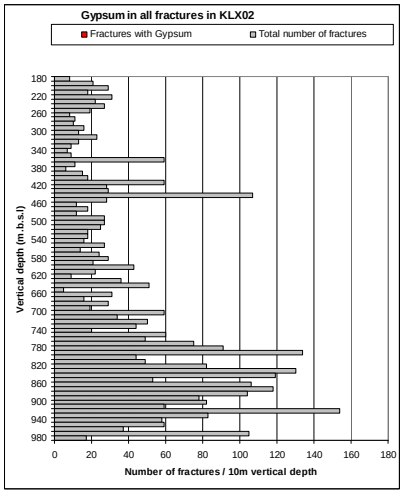
Gypsum in all fractures in KLX02
Fractures with Gypsum
Total number of fractures
Vertical depth (m.b.s.l)
Number of fractures / 10m vertical depth

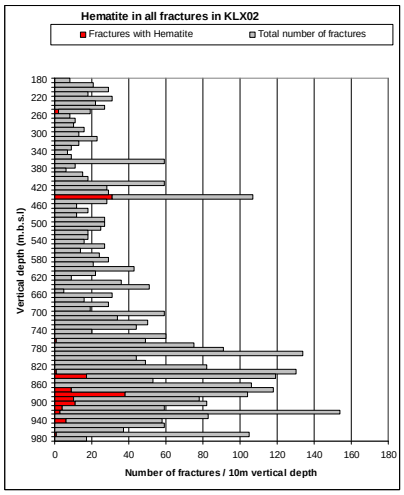
Hematite in all fractures in KLX02
Fractures with Hematite
Total number of fractures
Vertical depth (m.b.s.l)
Number of fractures / 10m vertical depth

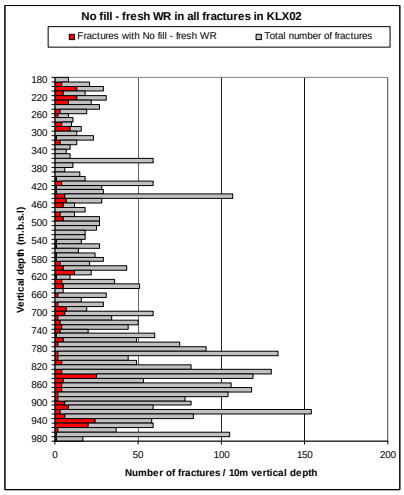
No fill - fresh WR in all fractures in KLX02
Fractures with No fill - fresh WR
Total number of fractures
Vertical depth (m.b.s.l)
Number of fractures / 10m vertical depth

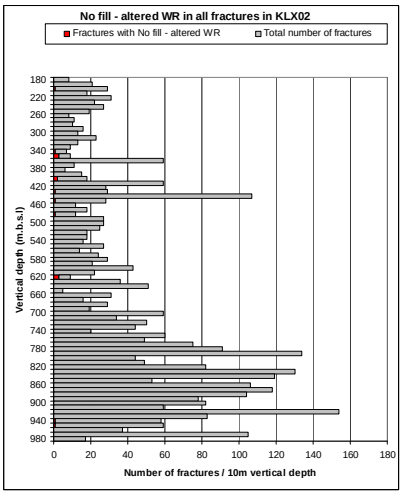
No fill - altered WR in all fractures in KLX02
Fractures with No fill - altered WR
Total number of fractures
Vertical depth (m.b.s.l)
Number of fractures / 10m vertical depth

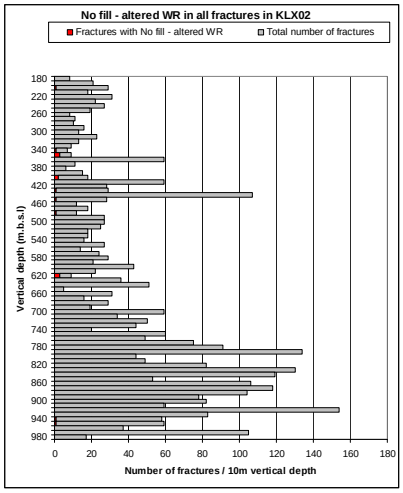
No fill - altered WR in all fractures in KLX02
Fractures with No fill - altered WR
Total number of fractures
Vertical depth (m.b.s.l)
Number of fractures / 10m vertical depth

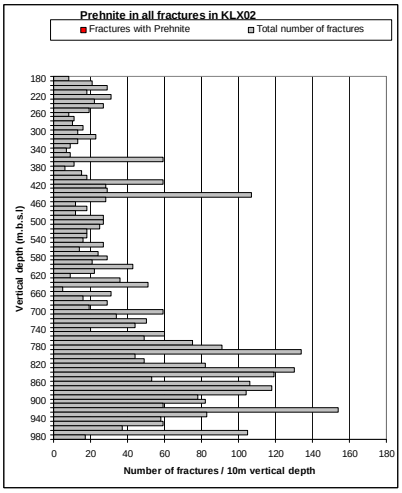
Prehnite in all fractures in KLX02
Fractures with Prehnite
Total number of fractures
Vertical depth (m.b.s.l)
Number of fractures / 10m vertical depth

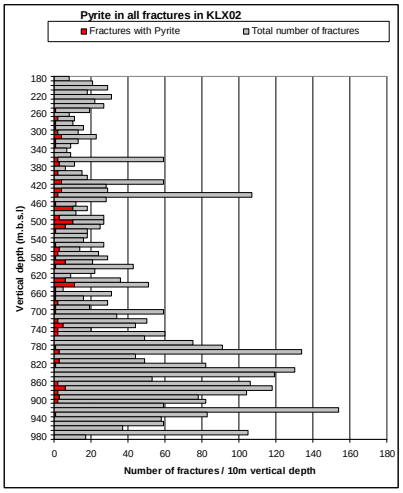
Pyrite in all fractures in KLX02
Fractures with Pyrite
Total number of fractures
Vertical depth (m.b.s.l)
Number of fractures / 10m vertical depth

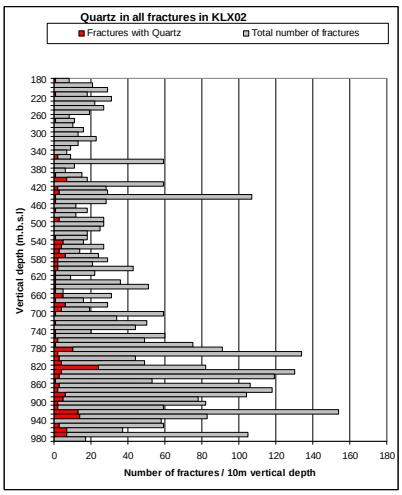
Quartz in all fractures in KLX02
Fractures with Quartz
Total number of fractures
Vertical depth (m.b.s.l)
Number of fractures / 10m vertical depth

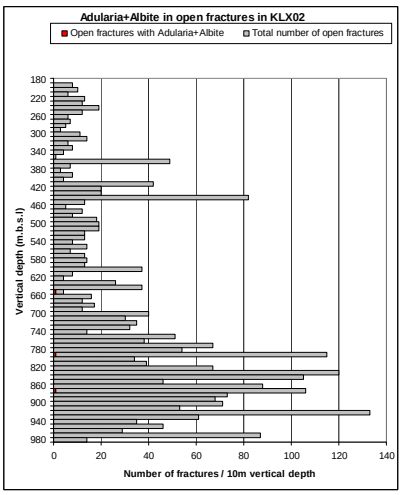
Adularia+Albite in open fractures in KLX02
Open fractures with Adularia+Albite
Total number of open fractures
Vertical depth (m.b.s.l)
Number of fractures / 10m vertical depth

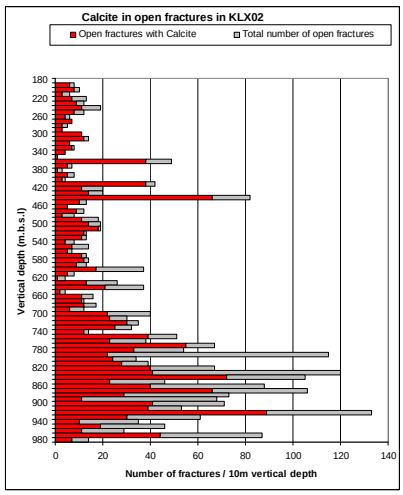
Calcite in open fractures in KLX02
Open fractures with Calcite
Total number of open fractures
Vertical depth (m.b.s.l)
Number of fractures / 10m vertical depth

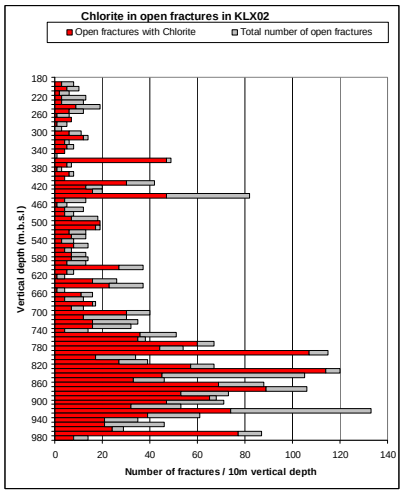
Chlorite in open fractures in KLX02
Open fractures with Chlorite
Total number of open fractures
Vertical depth (m.b.s.l)
Number of fractures / 10m vertical depth

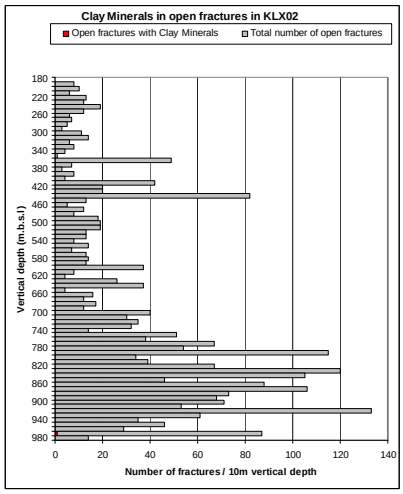
Clay Minerals in open fractures in KLX02
Open fractures with Clay Minerals
Total number of open fractures
Vertical depth (m.b.s.l)
Number of fractures / 10m vertical depth

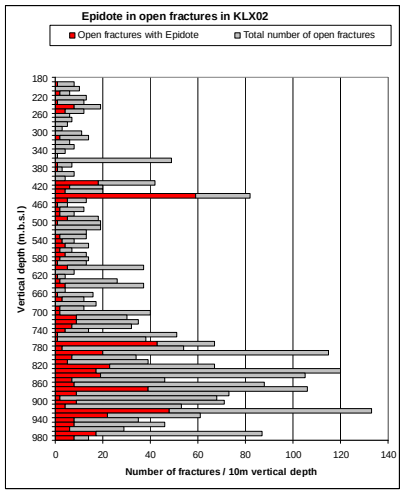
Epidote in open fractures in KLX02
Open fractures with Epidote
Total number of open fractures
Vertical depth (m.b.s.l)
Number of fractures / 10m vertical depth

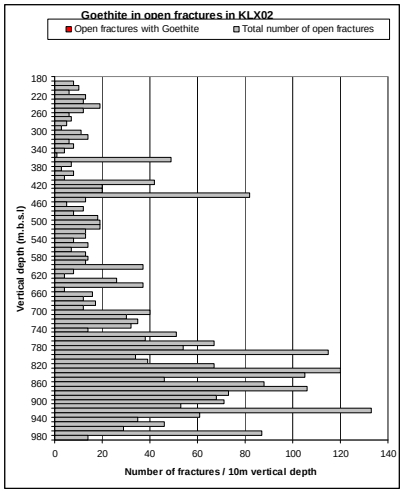
Goethite in open fractures in KLX02
Open fractures with Goethite
Total number of open fractures
Vertical depth (m.b.s.l)
Number of fractures / 10m vertical depth

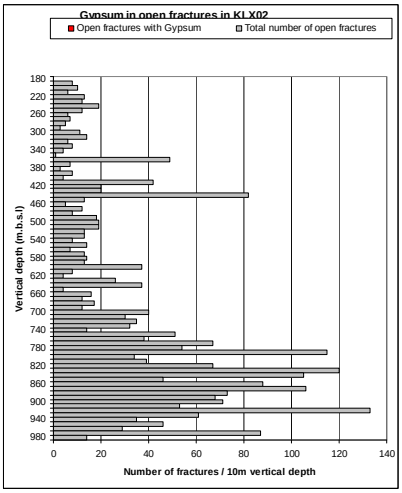
Gypsum in open fractures in KLX02
Open fractures with Gypsum
Total number of open fractures
Vertical depth (m.b.s.l)
Number of fractures / 10m vertical depth

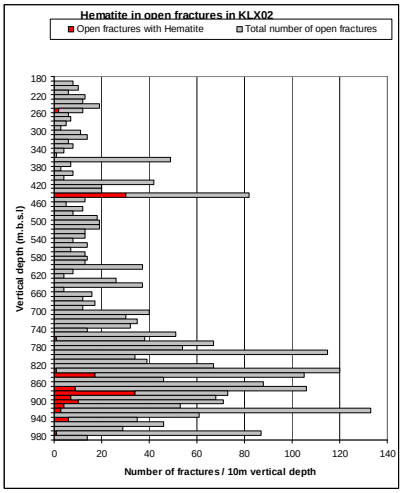
Hematite in open fractures in KLX02
Open fractures with Hematite
Total number of open fractures
Vertical depth (m.b.s.l)
Number of fractures / 10m vertical depth

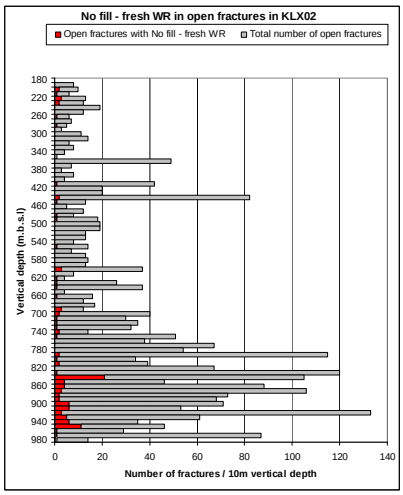
No fill - fresh WR in open fractures in KLX02
Open fractures with No fill - fresh WR
Total number of open fractures
Vertical depth (m.b.s.l)
Number of fractures / 10m vertical depth

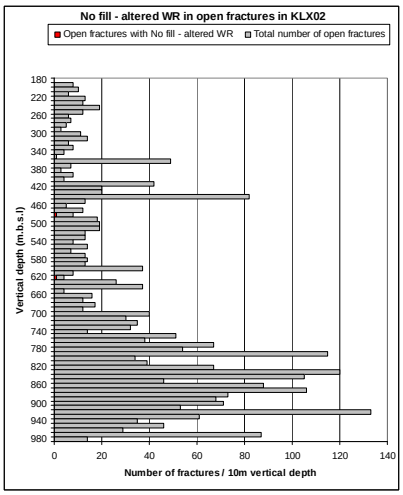
No fill - altered WR in open fractures in KLX02
Open fractures with No fill - altered WR
Total number of open fractures
Vertical depth (m.b.s.l)
Number of fractures / 10m vertical depth

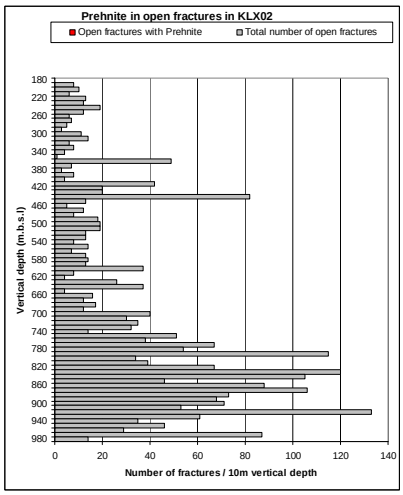
Prehnite in open fractures in KLX02
Open fractures with Prehnite
Total number of open fractures
Vertical depth (m.b.s.l)
Number of fractures / 10m vertical depth

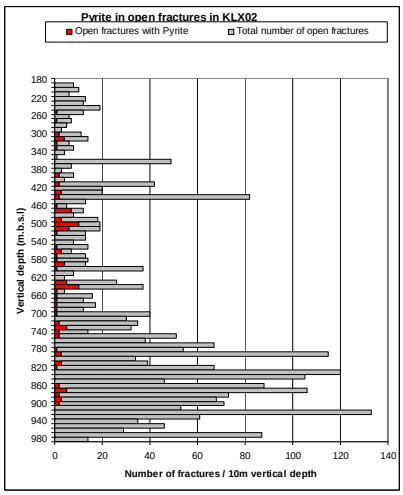
Pyrite in open fractures in KLX02
Open fractures with Pyrite
Total number of open fractures
Vertical depth (m.b.s.l)
Number of fractures / 10m vertical depth

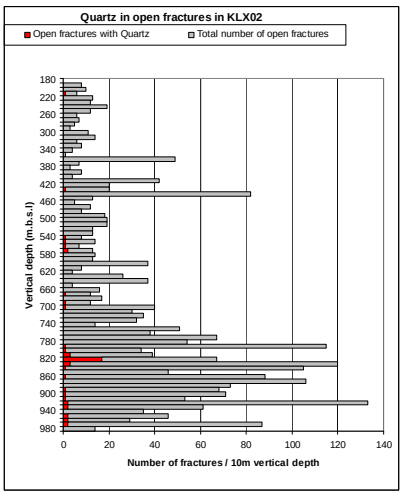
Quartz in open fractures in KLX02
Open fractures with Quartz
Total number of open fractures
Vertical depth (m.b.s.l)
Number of fractures / 10m vertical depth

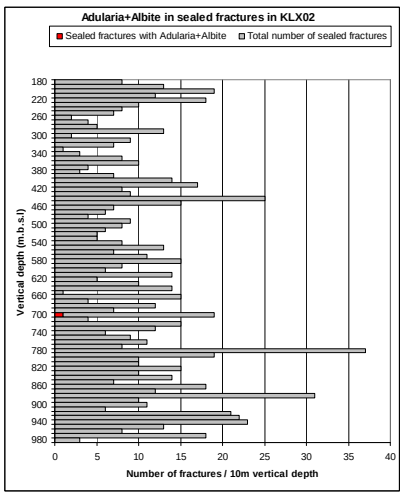
Adularia+Albite in sealed fractures in KLX02
Sealed fractures with Adularia+Albite
Total number of sealed fractures
Vertical depth (m.b.s.l)
Number of fractures / 10m vertical depth

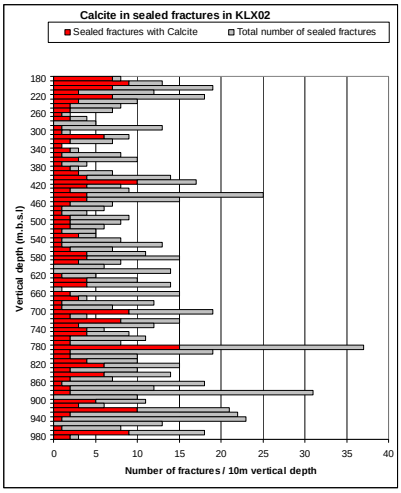
Calcite in sealed fractures in KLX02
Sealed fractures with Calcite
Total number of sealed fractures
Vertical depth (m.b.s.l)
Number of fractures / 10m vertical depth

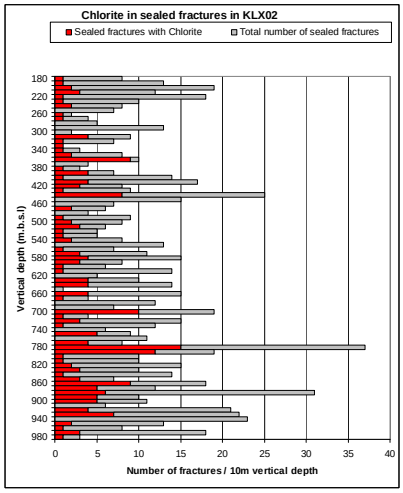
Chlorite in sealed fractures in KLX02
Sealed fractures with Chlorite
Total number of sealed fractures
Vertical depth (m.b.s.l)
Number of fractures / 10m vertical depth

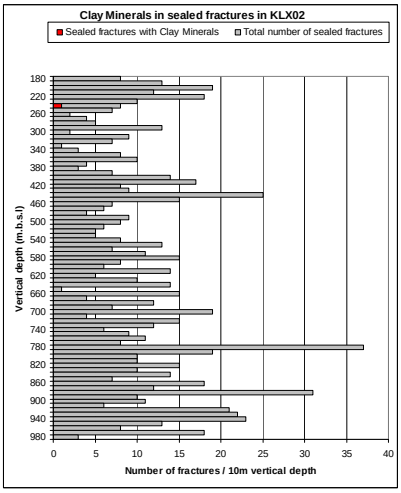
Clay Minerals in sealed fractures in KLX02
Sealed fractures with Clay Minerals
Total number of sealed fractures
Vertical depth (m.b.s.l)
Number of fractures / 10m vertical depth

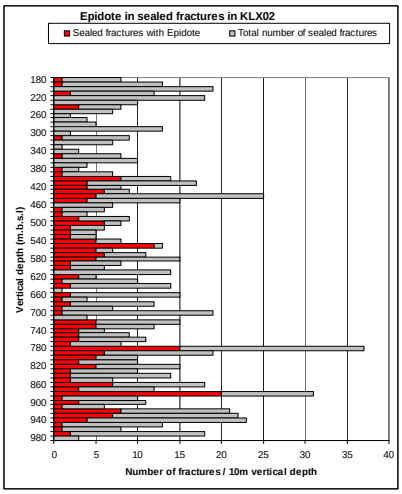
Epidote in sealed fractures in KLX02
Sealed fractures with Epidote
Total number of sealed fractures
Vertical depth (m.b.s.l)
Number of fractures / 10m vertical depth

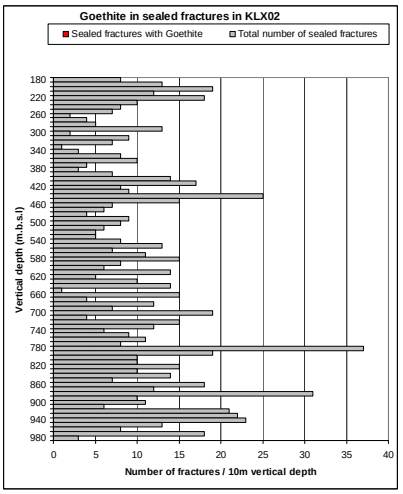
Goethite in sealed fractures in KLX02
Sealed fractures with Goethite
Total number of sealed fractures
Vertical depth (m.b.s.l)
Number of fractures / 10m vertical depth

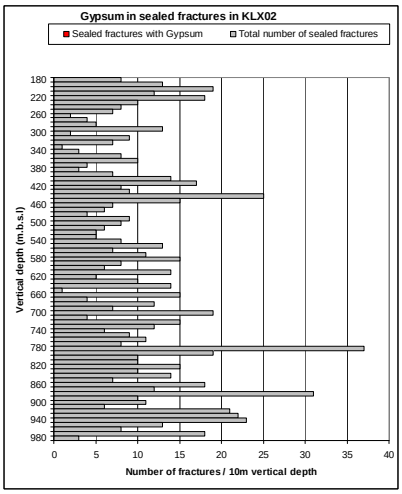
Gypsum in sealed fractures in KLX02
Sealed fractures with Gypsum
Total number of sealed fractures
Vertical depth (m.b.s.l)
Number of fractures / 10m vertical depth

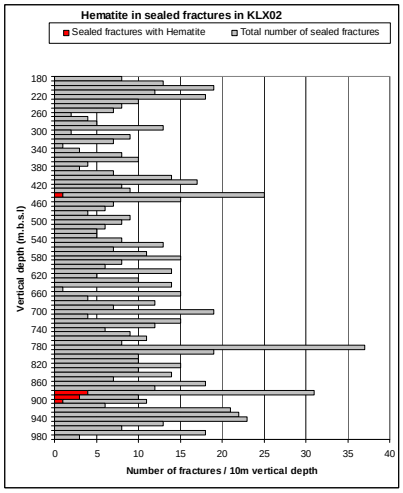
Hematite in sealed fractures in KLX02
Sealed fractures with Hematite
Total number of sealed fractures
Vertical depth (m.b.s.l)
Number of fractures / 10m vertical depth

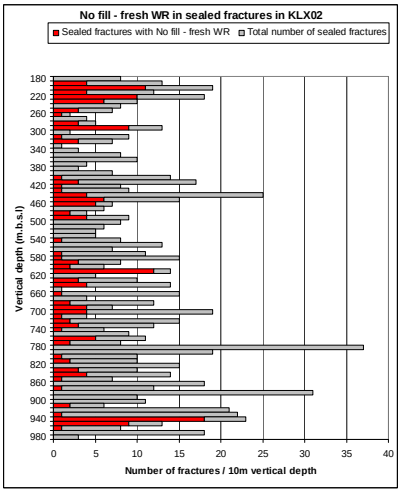
No fill - fresh WR in sealed fractures in KLX02
Sealed fractures with No fill - fresh WR
Total number of sealed fractures
Vertical depth (m.b.s.l)
Number of fractures / 10m vertical depth

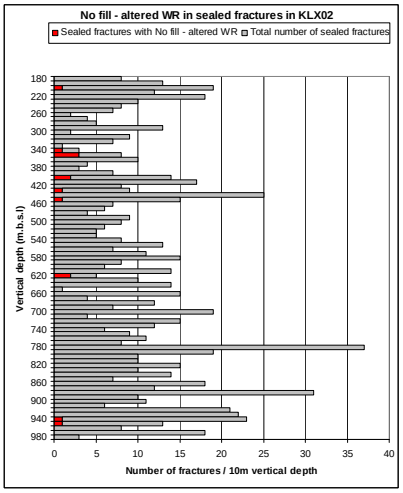
No fill - altered WR in sealed fractures in KLX02
Sealed fractures with No fill - altered WR
Total number of sealed fractures
Vertical depth (m.b.s.l)
Number of fractures / 10m vertical depth

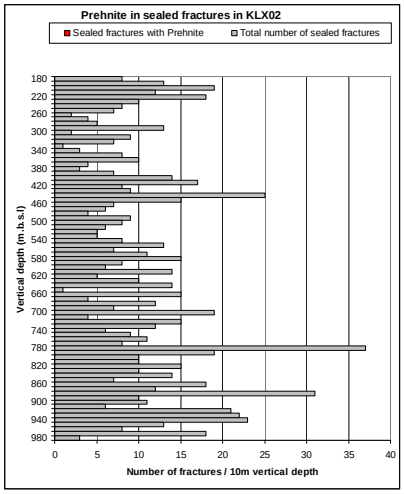
Prehnite in sealed fractures in KLX02
Sealed fractures with Prehnite
Total number of sealed fractures
Vertical depth (m.b.s.l)
Number of fractures / 10m vertical depth

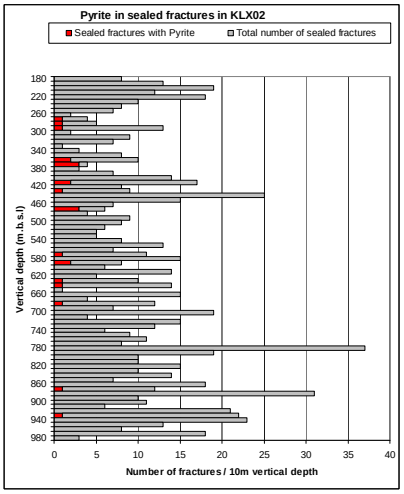
Pyrite in sealed fractures in KLX02
Sealed fractures with Pyrite
Total number of sealed fractures
Vertical depth (m.b.s.l)
Number of fractures / 10m vertical depth

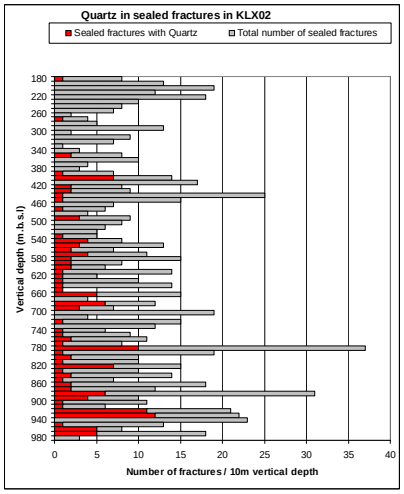
Quartz in sealed fractures in KLX02
Sealed fractures with Quartz
Total number of sealed fractures
Vertical depth (m.b.s.l)
Number of fractures / 10m vertical depth

KLX03

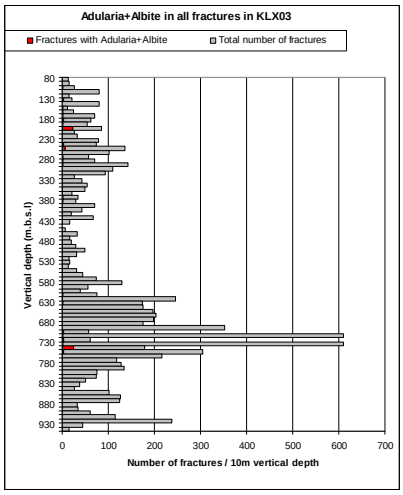
Adularia+Albite in all fractures in KLX03
Fractures with Adularia+Albite
Total number of fractures
Vertical depth (m.b.s.l)
Number of fractures / 10m vertical depth

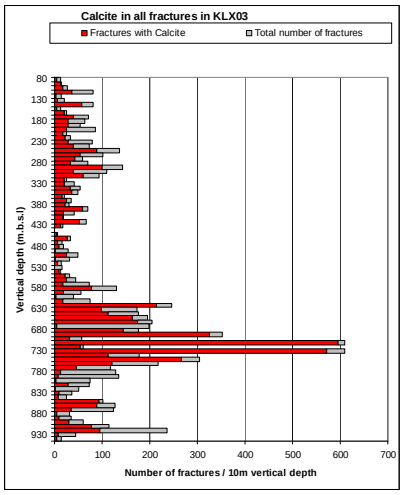
Calcite in all fractures in KLX03
Fractures with Calcite
Total number of fractures
Vertical depth (m.b.s.l)
Number of fractures / 10m vertical depth

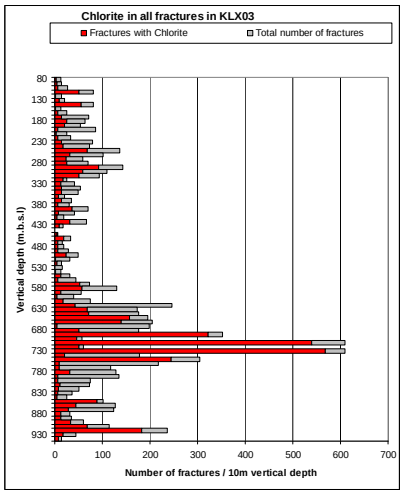
Chlorite in all fractures in KLX03
Fractures with Chlorite
Total number of fractures
Vertical depth (m.b.s.l)
Number of fractures / 10m vertical depth

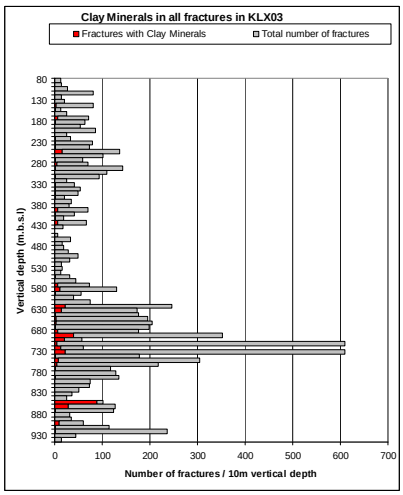
Clay Minerals in all fractures in KLX03
Fractures with Clay Minerals
Total number of fractures
Vertical depth (m.b.s.l)
Number of fractures / 10m vertical depth

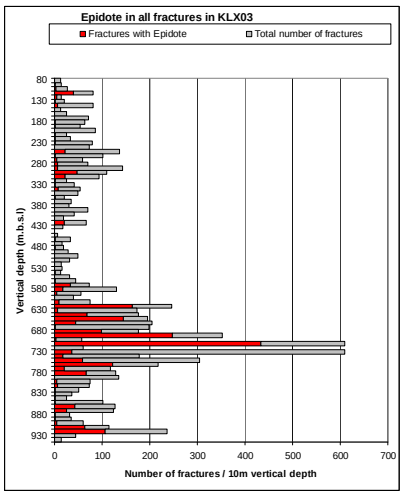
Epidote in all fractures in KLX03
Fractures with Epidote
Total number of fractures
Vertical depth (m.b.s.l)
Number of fractures / 10m vertical depth

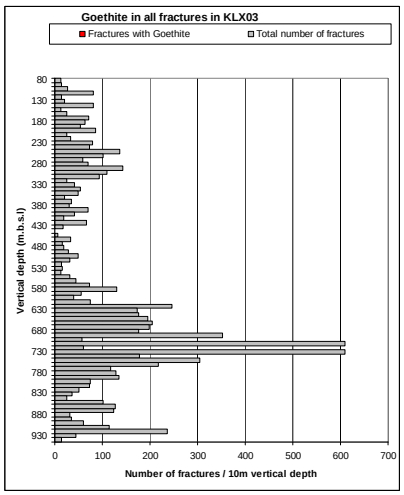
Goethite in all fractures in KLX03
Fractures with Goethite
Total number of fractures
Vertical depth (m.b.s.l)
Number of fractures / 10m vertical depth

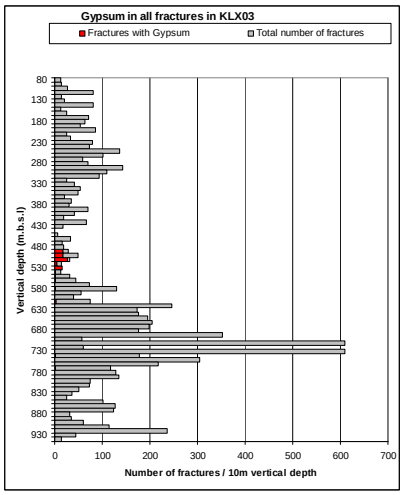
Gypsum in all fractures in KLX03
Fractures with Gypsum
Total number of fractures
Vertical depth (m.b.s.l)
Number of fractures / 10m vertical depth

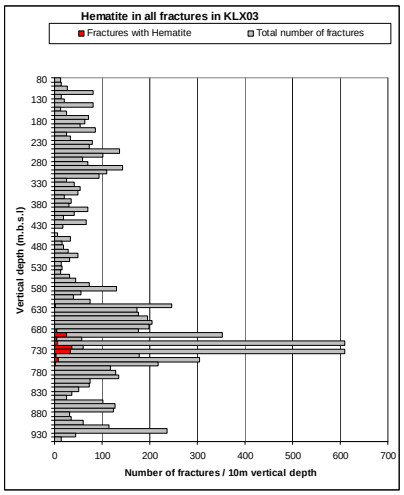
Hematite in all fractures in KLX03
Fractures with Hematite
Total number of fractures
Vertical depth (m.b.s.l)
Number of fractures / 10m vertical depth

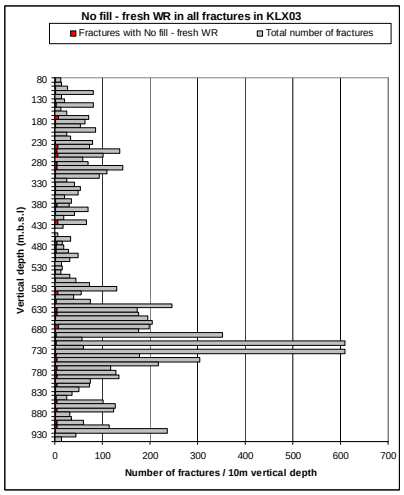
No fill - fresh WR in all fractures in KLX03
Fractures with No fill - fresh WR
Total number of fractures
Vertical depth (m.b.s.l)
Number of fractures / 10m vertical depth

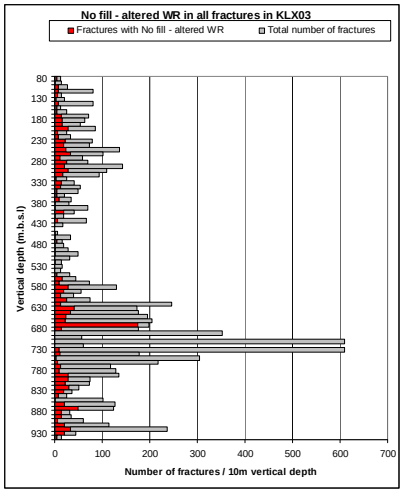
No fill - altered WR in all fractures in KLX03
Fractures with No fill - altered WR
Total number of fractures
Vertical depth (m.b.s.l)
Number of fractures / 10m vertical depth

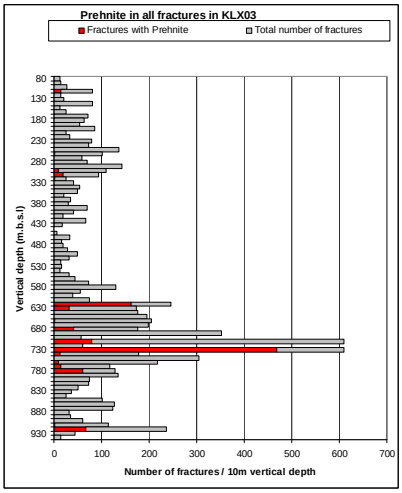
Prehnite in all fractures in KLX03
Fractures with Prehnite
Total number of fractures
Vertical depth (m.b.s.l)
Number of fractures / 10m vertical depth

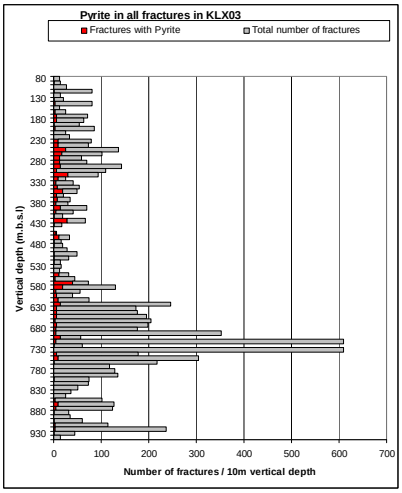
Pyrite in all fractures in KLX03
Fractures with Pyrite
Total number of fractures
Vertical depth (m.b.s.l)
Number of fractures / 10m vertical depth

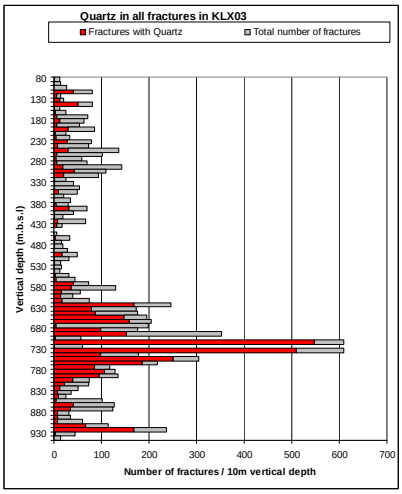
Quartz in all fractures in KLX03
Fractures with Quartz
Total number of fractures
Vertical depth (m.b.s.l)
Number of fractures / 10m vertical depth

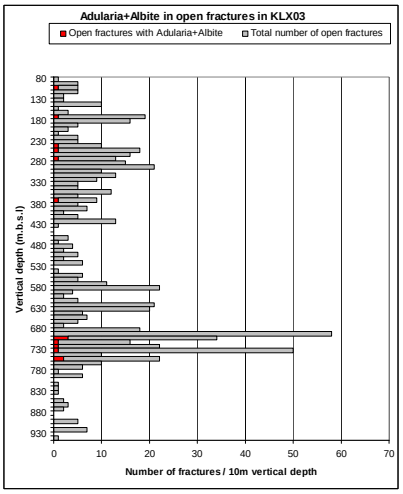
Adularia+Albite in open fractures in KLX03
Open fractures with Adularia+Albite
Total number of open fractures
Vertical depth (m.b.s.l)
Number of fractures / 10m vertical depth

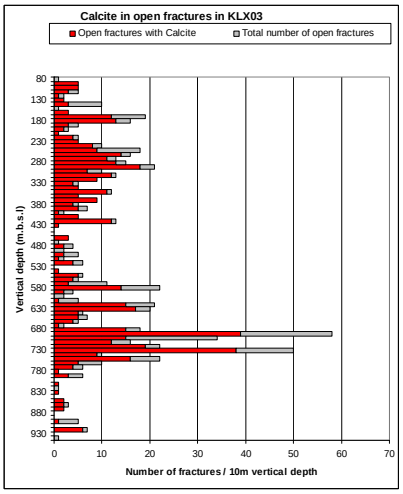
Calcite in open fractures in KLX03
Open fractures with Calcite
Total number of open fractures
Vertical depth (m.b.s.l)
Number of fractures / 10m vertical depth

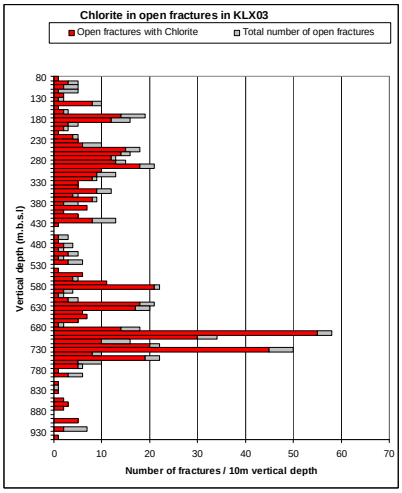
Chlorite in open fractures in KLX03
Open fractures with Chlorite
Total number of open fractures
Vertical depth (m.b.s.l)
Number of fractures / 10m vertical depth

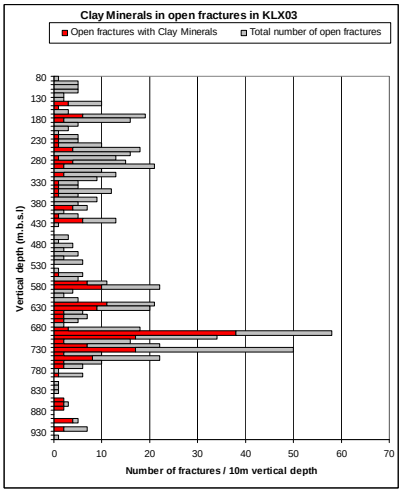
Clay Minerals in open fractures in KLX03
Open fractures with Clay Minerals
Total number of open fractures
Vertical depth (m.b.s.l)
Number of fractures / 10m vertical depth

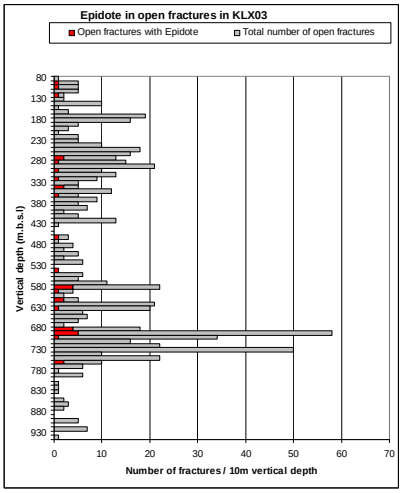
Epidote in open fractures in KLX03
Open fractures with Epidote
Total number of open fractures
Vertical depth (m.b.s.l)
Number of fractures / 10m vertical depth

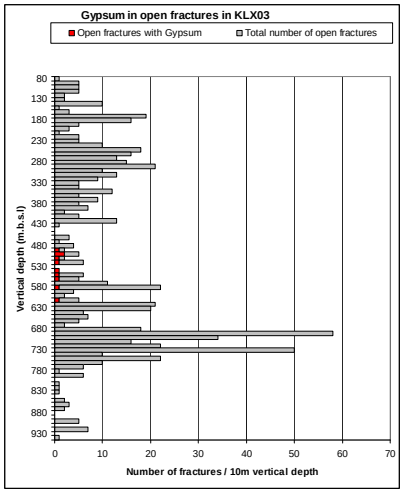
Gypsum in open fractures in KLX03
Open fractures with Gypsum
Total number of open fractures
Vertical depth (m.b.s.l)
Number of fractures / 10m vertical depth

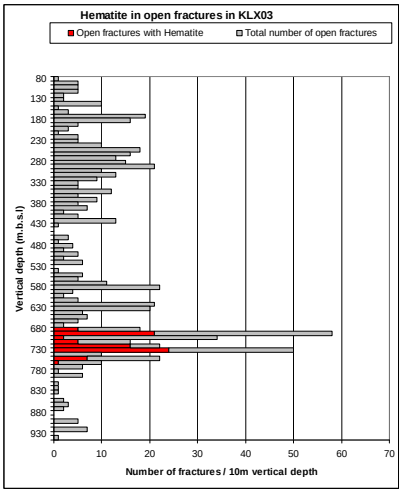
Hematite in open fractures in KLX03
Open fractures with Hematite
Total number of open fractures
Vertical depth (m.b.s.l)
Number of fractures / 10m vertical depth

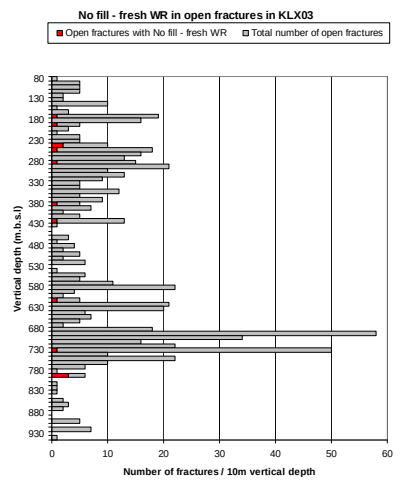
No fill - fresh WR in open fractures in KLX03
Open fractures with No fill - fresh WR
Total number of open fractures
Vertical depth (m.b.s.l)
Number of fractures / 10m vertical depth

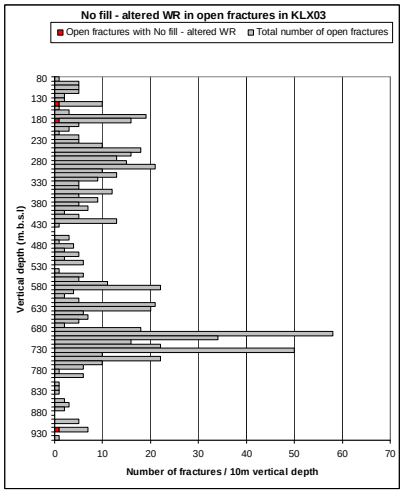
No fill - altered WR in open fractures in KLX03
Open fractures with No fill - altered WR
Total number of open fractures
Vertical depth (m.b.s.l)
Number of fractures / 10m vertical depth

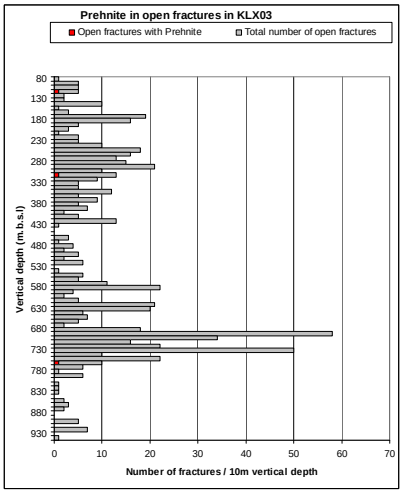
Prehnite in open fractures in KLX03
Open fractures with Prehnite
Total number of open fractures
Vertical depth (m.b.s.l)
Number of fractures / 10m vertical depth

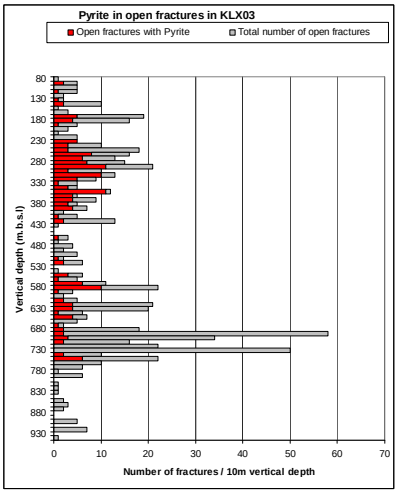
Pyrite in open fractures in KLX03
Open fractures with Pyrite
Total number of open fractures
Vertical depth (m.b.s.l)
Number of fractures / 10m vertical depth

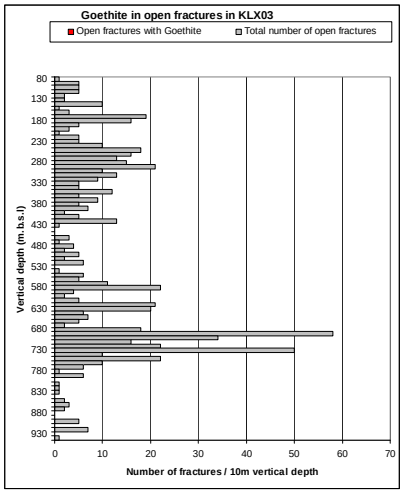
Goethite in open fractures in KLX03
Open fractures with Goethite
Total number of open fractures
Vertical depth (m.b.s.l)
Number of fractures / 10m vertical depth

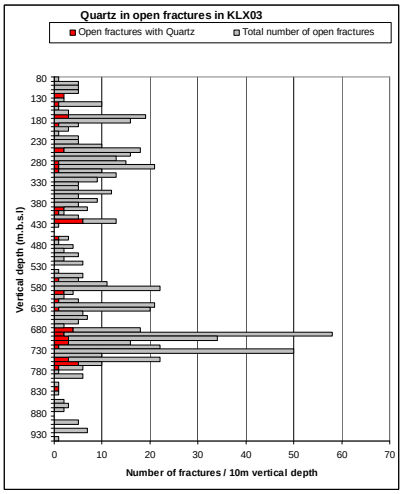
Quartz in open fractures in KLX03
Open fractures with Quartz
Total number of open fractures
Vertical depth (m.b.s.l)
Number of fractures / 10m vertical depth

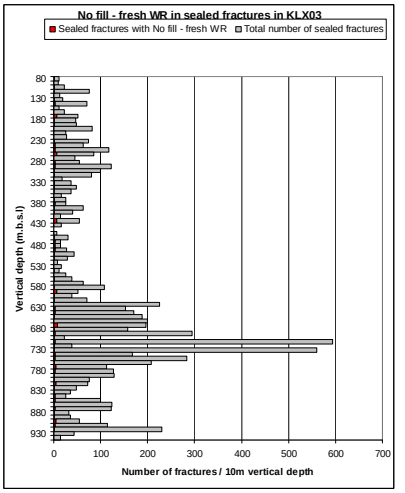
No fill - fresh WR in sealed fractures in KLX03
Sealed fractures with No fill - fresh WR
Total number of sealed fractures
Vertical depth (m.b.s.l)
Number of fractures / 10m vertical depth

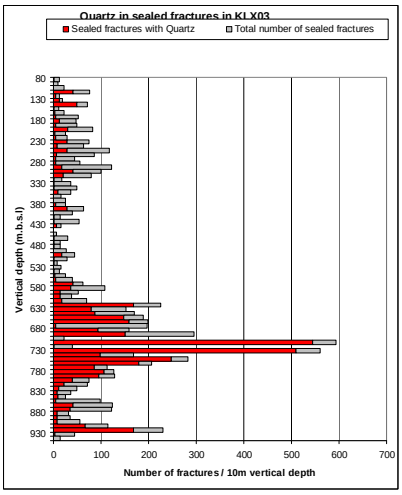
Quartz in sealed fractures in KLX03
Sealed fractures with Quartz
Total number of sealed fractures
Vertical depth (m.b.s.l)
Number of fractures / 10m vertical depth

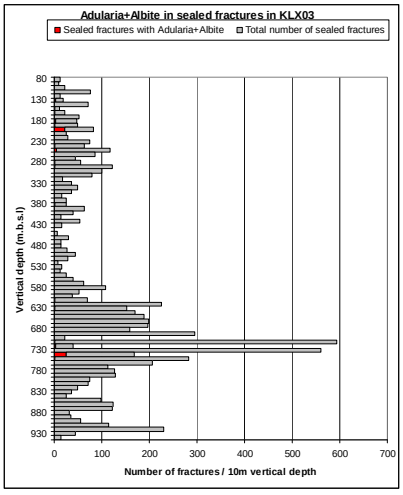
Adularia+Albite in sealed fractures in KLX03
Sealed fractures with Adularia+Albite
Total number of sealed fractures
Vertical depth (m.b.s.l)
Number of fractures / 10m vertical depth

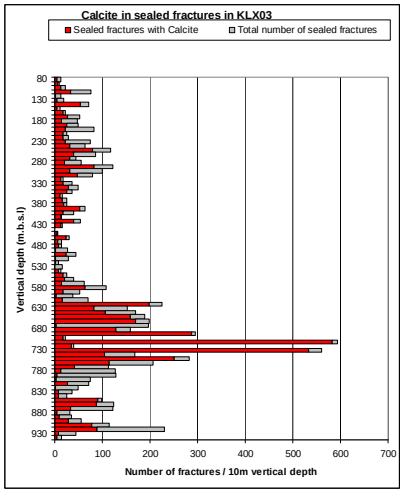
Calcite in sealed fractures in KLX03
Sealed fractures with Calcite
Total number of sealed fractures
Vertical depth (m.b.s.l)
Number of fractures / 10m vertical depth

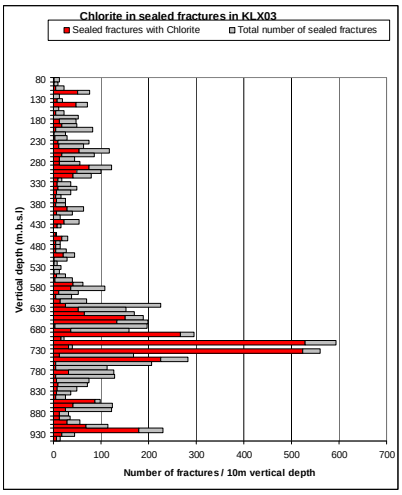
Chlorite in sealed fractures in KLX03
Sealed fractures with Chlorite
Total number of sealed fractures
Vertical depth (m.b.s.l)
Number of fractures / 10m vertical depth

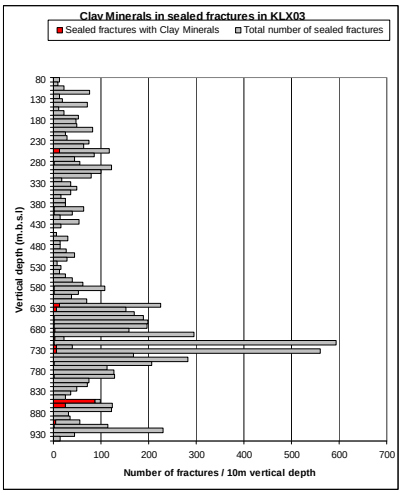
Clay Minerals in sealed fractures in KLX03
Sealed fractures with Clay Minerals
Total number of sealed fractures
Vertical depth (m.b.s.l)
Number of fractures / 10m vertical depth

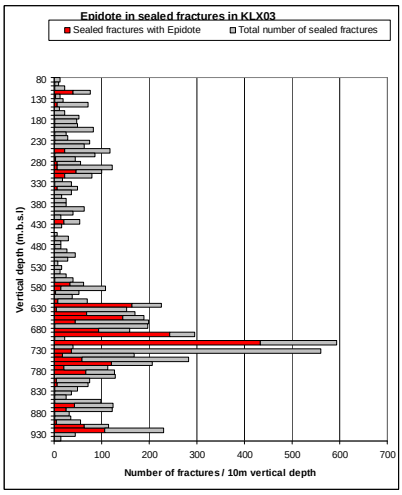
Epidote in sealed fractures in KLX03
Sealed fractures with Epidote
Total number of sealed fractures
Vertical depth (m.b.s.l)
Number of fractures / 10m vertical depth

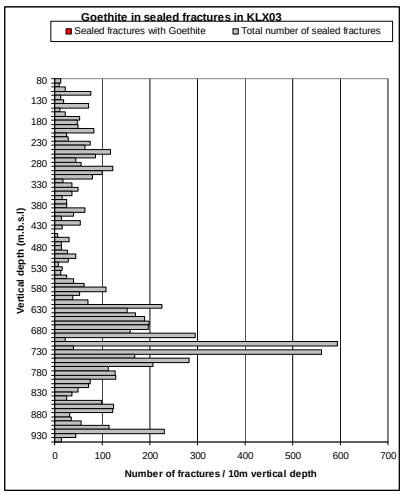
Goethite in sealed fractures in KLX03
Sealed fractures with Goethite
Total number of sealed fractures
Vertical depth (m.b.s.l)
Number of fractures / 10m vertical depth

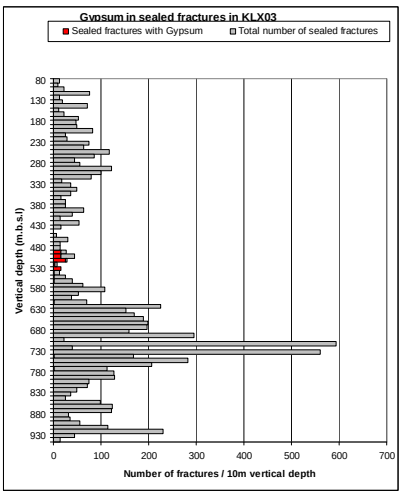
Gypsum in sealed fractures in KLX03
Sealed fractures with Gypsum
Total number of sealed fractures
Vertical depth (m.b.s.l)
Number of fractures / 10m vertical depth

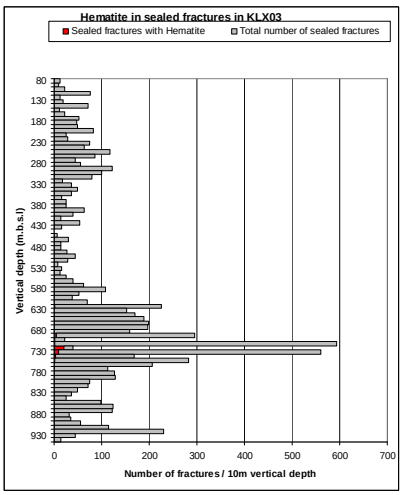
Hematite in sealed fractures in KLX03
Sealed fractures with Hematite
Total number of sealed fractures
Vertical depth (m.b.s.l)
Number of fractures / 10m vertical depth

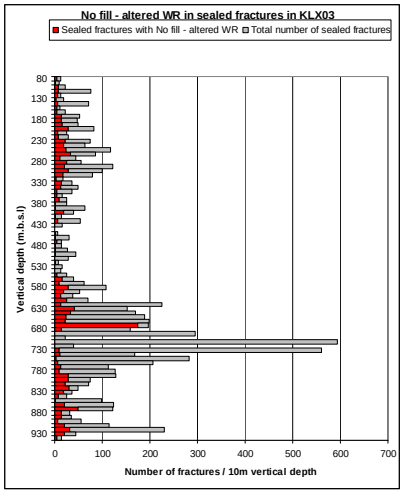
No fill - altered WR in sealed fractures in KLX03
Sealed fractures with No fill - altered WR
Total number of sealed fractures
Vertical depth (m.b.s.l)
Number of fractures / 10m vertical depth

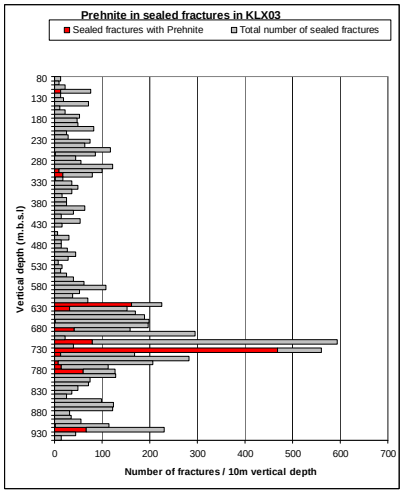
Prehnite in sealed fractures in KLX03
Sealed fractures with Prehnite
Total number of sealed fractures
Vertical depth (m.b.s.l)
Number of fractures / 10m vertical depth

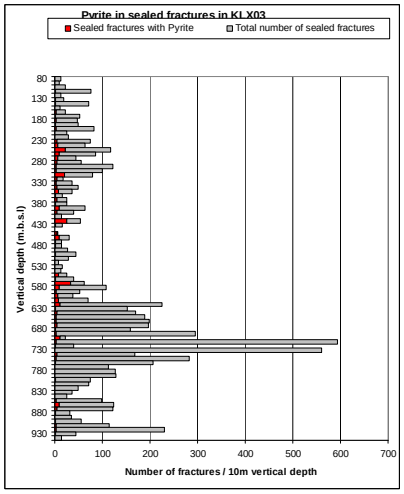
Pyrite in sealed fractures in KLX03
Sealed fractures with Pyrite
Total number of sealed fractures
Vertical depth (m.b.s.l)
Number of fractures / 10m vertical depth

KLX04

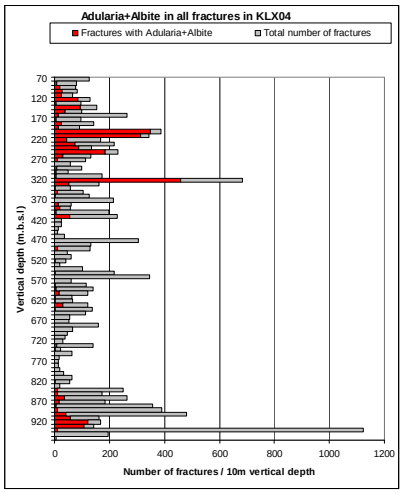
Adularia+Albite in all fractures in KLX04
Fractures with Adularia+Albite
Total number of fractures
Vertical depth (m.b.s.l)
Number of fractures / 10m vertical depth

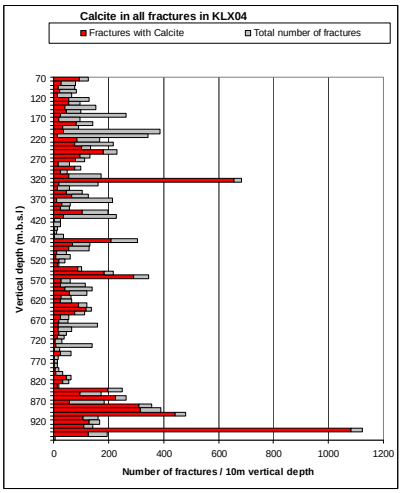
Calcite in all fractures in KLX04
Fractures with Calcite
Total number of fractures
Vertical depth (m.b.s.l)
Number of fractures / 10m vertical depth

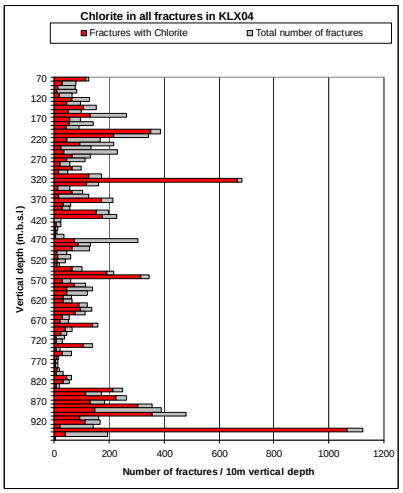
Chlorite in all fractures in KLX04
Fractures with Chlorite
Total number of fractures
Vertical depth (m.b.s.l)
Number of fractures / 10m vertical depth

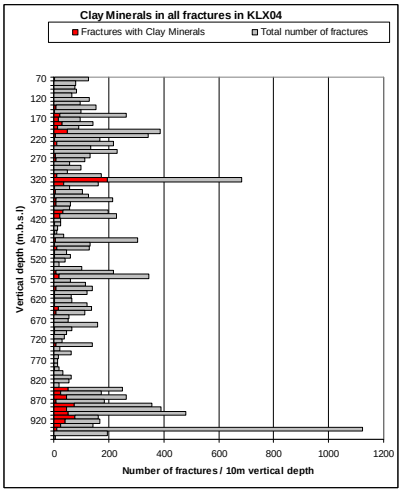
Clay Minerals in all fractures in KLX04
Fractures with Clay Minerals
Total number of fractures
Vertical depth (m.b.s.l)
Number of fractures / 10m vertical depth

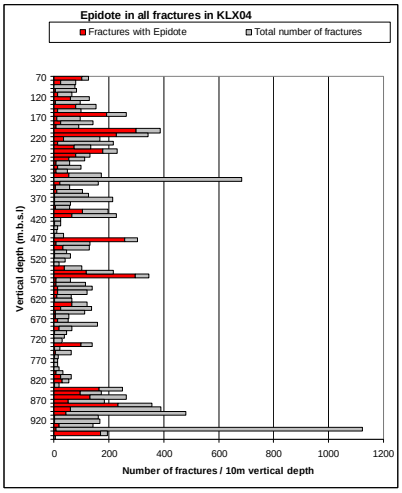
Epidote in all fractures in KLX04
Fractures with Epidote
Total number of fractures
Vertical depth (m.b.s.l)
Number of fractures / 10m vertical depth

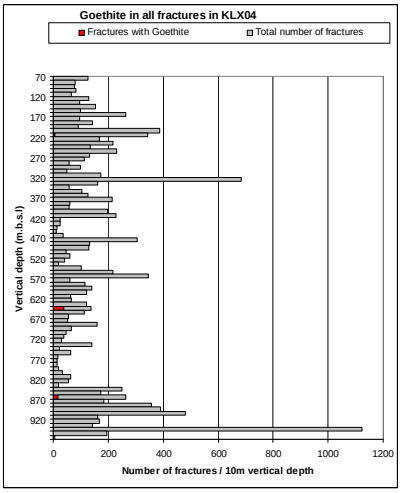
Goethite in all fractures in KLX04
Fractures with Goethite
Total number of fractures
Vertical depth (m.b.s.l)
Number of fractures / 10m vertical depth

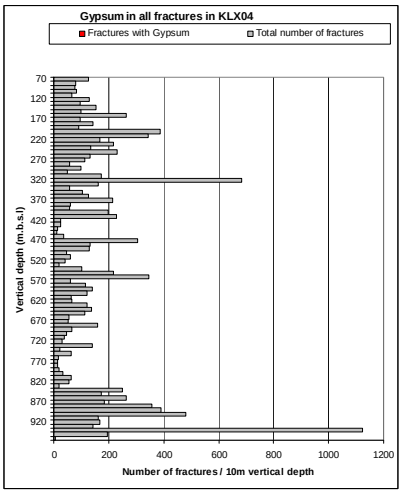
Gypsum in all fractures in KLX04
Fractures with Gypsum
Total number of fractures
Vertical depth (m.b.s.l)
Number of fractures / 10m vertical depth

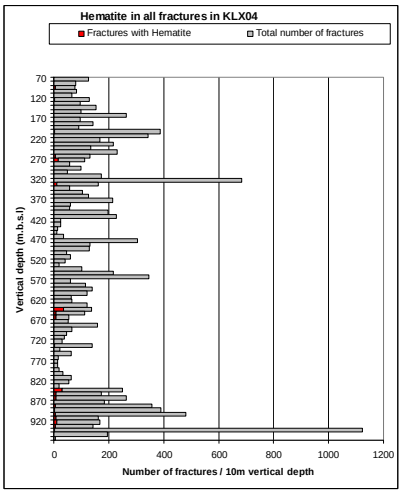
Hematite in all fractures in KLX04
Fractures with Hematite
Total number of fractures
Vertical depth (m.b.s.l)
Number of fractures / 10m vertical depth

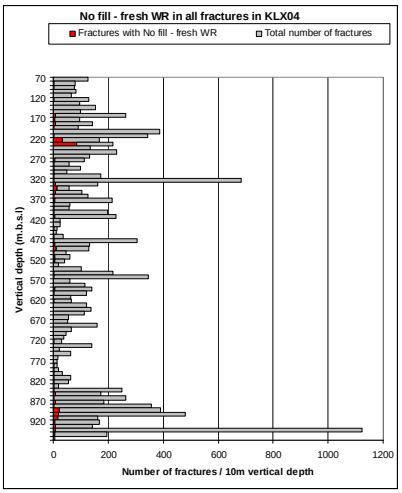
No fill - fresh WR in all fractures in KLX04
Fractures with No fill - fresh WR
Total number of fractures
Vertical depth (m.b.s.l)
Number of fractures / 10m vertical depth

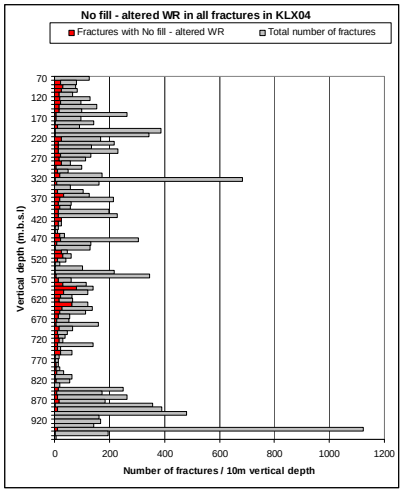
No fill - altered WR in all fractures in KLX04
Fractures with No fill - altered WR
Total number of fractures
Vertical depth (m.b.s.l)
Number of fractures / 10m vertical depth

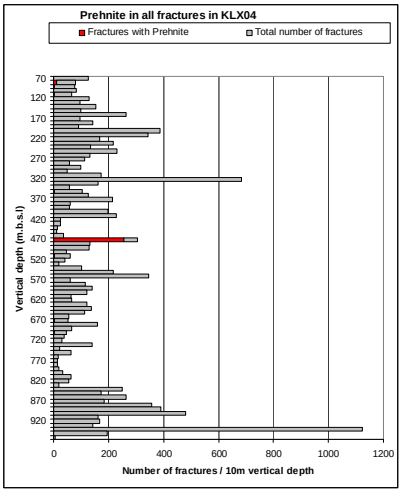
Prehnite in all fractures in KLX04
Fractures with Prehnite
Total number of fractures
Vertical depth (m.b.s.l)
Number of fractures / 10m vertical depth

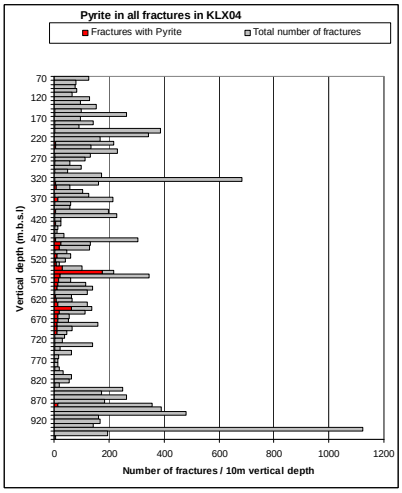
Pyrite in all fractures in KLX04
Fractures with Pyrite
Total number of fractures
Vertical depth (m.b.s.l)
Number of fractures / 10m vertical depth

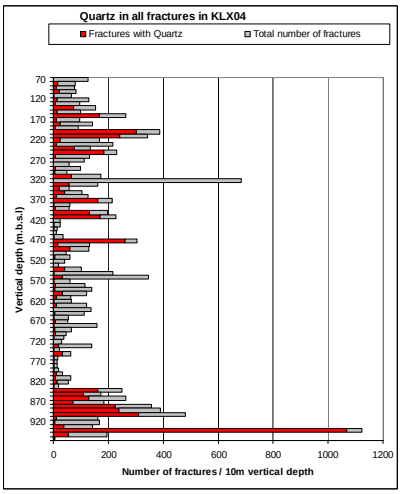
Quartz in all fractures in KLX04
Fractures with Quartz
Total number of fractures
Vertical depth (m.b.s.l)
Number of fractures / 10m vertical depth

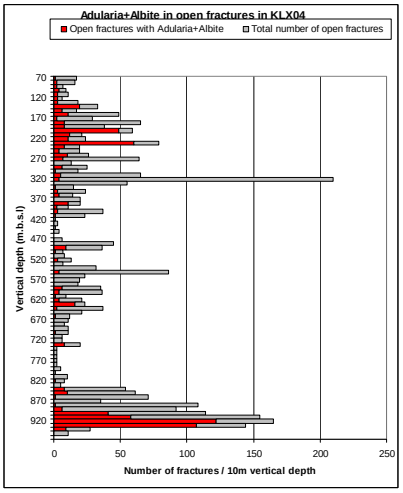
Adularia+Albite in open fractures in KLX04
Open fractures with Adularia+Albite
Total number of open fractures
Vertical depth (m.b.s.l)
Number of fractures / 10m vertical depth

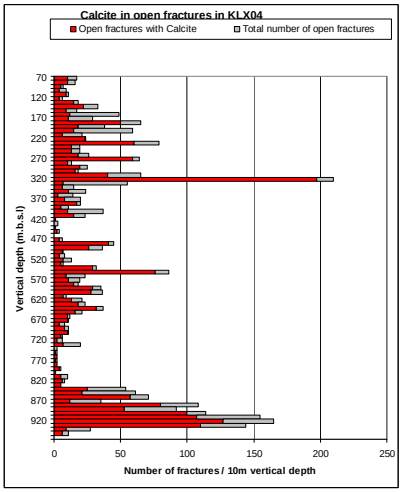
Calcite in open fractures in KLX04
Open fractures with Calcite
Total number of open fractures
Vertical depth (m.b.s.l)
Number of fractures / 10m vertical depth

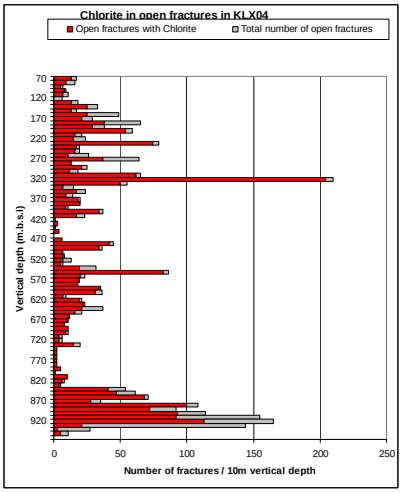
Chlorite in open fractures in KLX04
Open fractures with Chlorite
Total number of open fractures
Vertical depth (m.b.s.l)
Number of fractures / 10m vertical depth

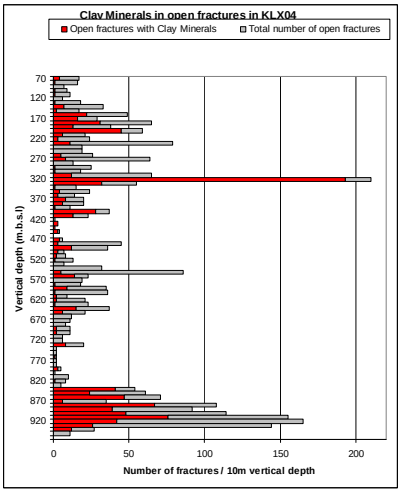
Clay Minerals in open fractures in KLX04
Open fractures with Clay Minerals
Total number of open fractures
Vertical depth (m.b.s.l)
Number of fractures / 10m vertical depth

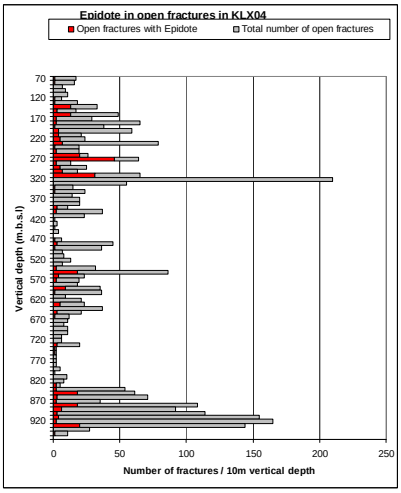
Epidote in open fractures in KLX04
Open fractures with Epidote
Total number of open fractures
Vertical depth (m.b.s.l)
Number of fractures / 10m vertical depth

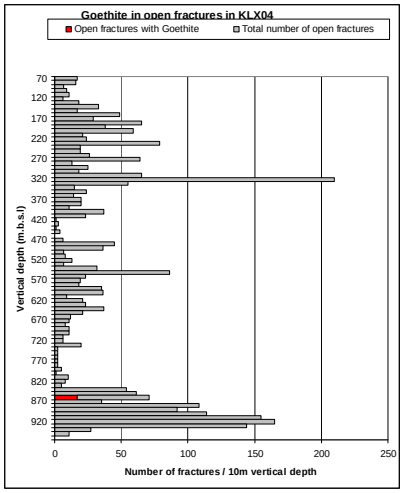
Goethite in open fractures in KLX04
Open fractures with Goethite
Total number of open fractures
Vertical depth (m.b.s.l)
Number of fractures / 10m vertical depth

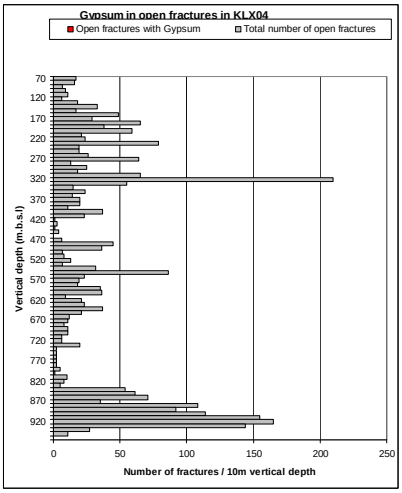
Gypsum in open fractures in KLX04
Open fractures with Gypsum
Total number of open fractures
Vertical depth (m.b.s.l)
Number of fractures / 10m vertical depth

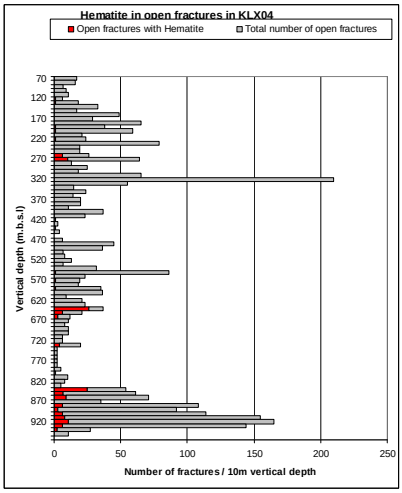
Hematite in open fractures in KLX04
Open fractures with Hematite
Total number of open fractures
Vertical depth (m.b.s.l)
Number of fractures / 10m vertical depth

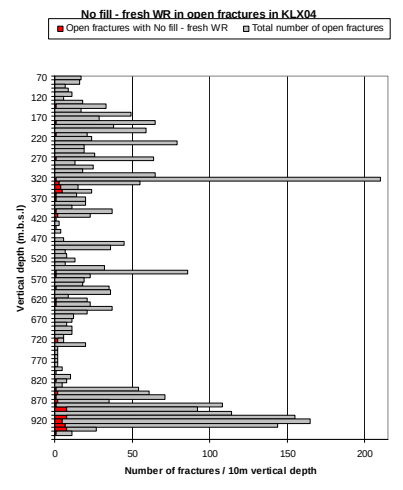
No fill - fresh WR in open fractures in KLX04
Open fractures with No fill - fresh WR
Total number of open fractures
Vertical depth (m.b.s.l)
Number of fractures / 10m vertical depth

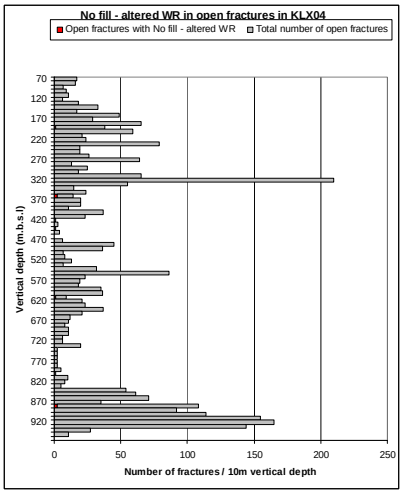
No fill - altered WR in open fractures in KLX04
Open fractures with No fill - altered WR
Total number of open fractures
Vertical depth (m.b.s.l)
Number of fractures / 10m vertical depth

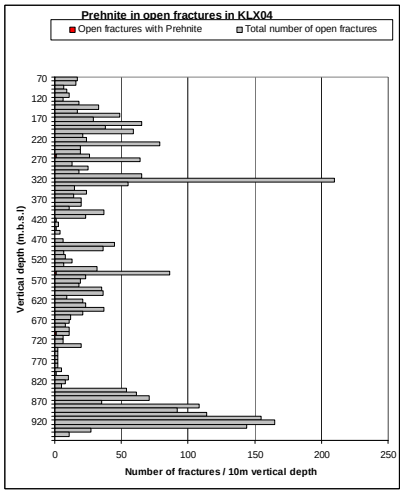
Prehnite in open fractures in KLX04
Open fractures with Prehnite
Total number of open fractures
Vertical depth (m.b.s.l)
Number of fractures / 10m vertical depth

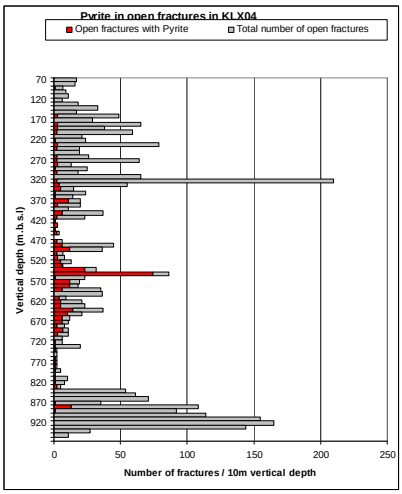
Pyrite in open fractures in KLX04
Open fractures with Pyrite
Total number of open fractures
Vertical depth (m.b.s.l)
Number of fractures / 10m vertical depth

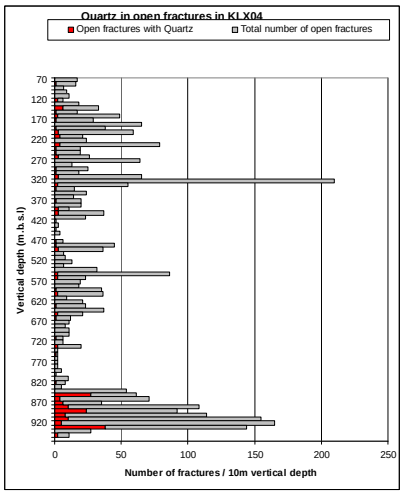
Quartz in open fractures in KLX04
Open fractures with Quartz
Total number of open fractures
Vertical depth (m.b.s.l)
Number of fractures / 10m vertical depth

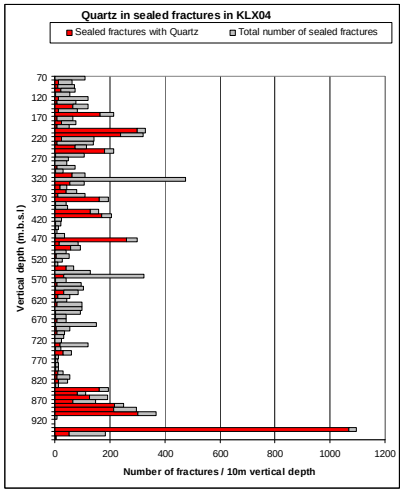
Quartz in sealed fractures in KLX04
Sealed fractures with Quartz
Total number of sealed fractures
Vertical depth (m.b.s.l)
Number of fractures / 10m vertical depth

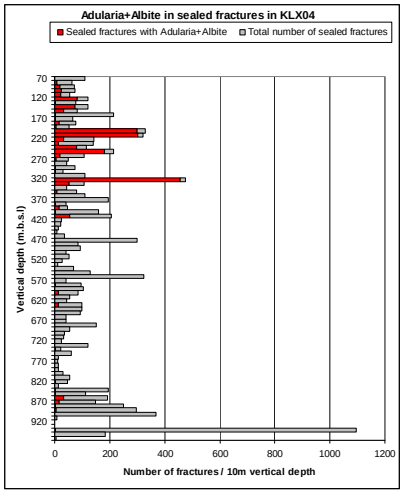
Adularia+Albite in sealed fractures in KLX04
Sealed fractures with Adularia+Albite
Total number of sealed fractures
Vertical depth (m.b.s.l)
Number of fractures / 10m vertical depth

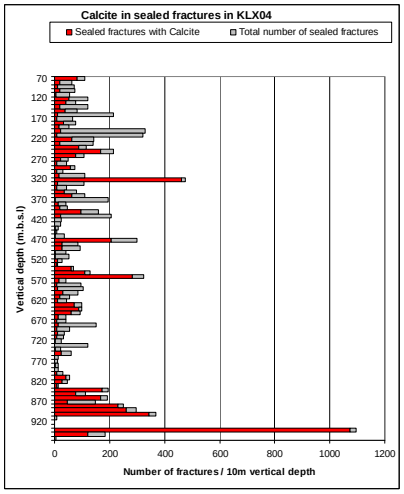
Calcite in sealed fractures in KLX04
Sealed fractures with Calcite
Total number of sealed fractures
Vertical depth (m.b.s.l)
Number of fractures / 10m vertical depth

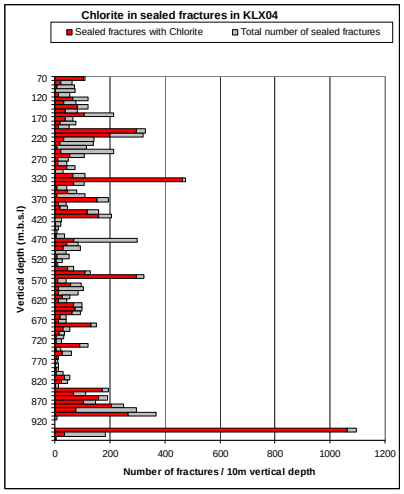
Chlorite in sealed fractures in KLX04
Sealed fractures with Chlorite
Total number of sealed fractures
Vertical depth (m.b.s.l)
Number of fractures / 10m vertical depth

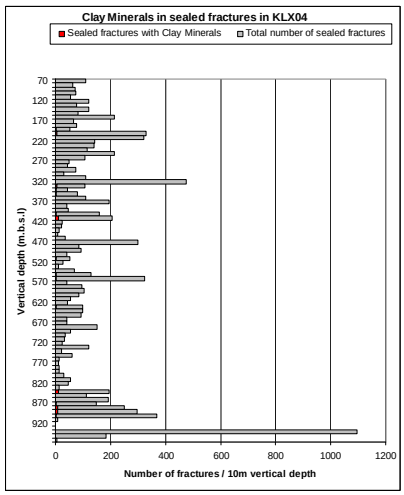
Clay Minerals in sealed fractures in KLX04
Sealed fractures with Clay Minerals
Total number of sealed fractures
Vertical depth (m.b.s.l)
Number of fractures / 10m vertical depth

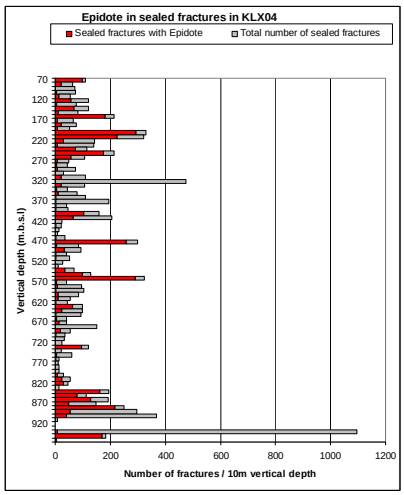
Epidote in sealed fractures in KLX04
Sealed fractures with Epidote
Total number of sealed fractures
Vertical depth (m.b.s.l)
Number of fractures / 10m vertical depth

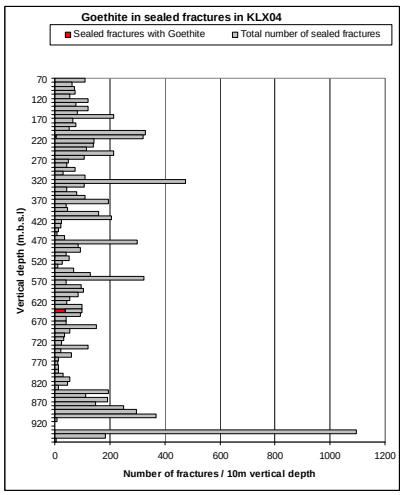
Goethite in sealed fractures in KLX04
Sealed fractures with Goethite
Total number of sealed fractures
Vertical depth (m.b.s.l)
Number of fractures / 10m vertical depth

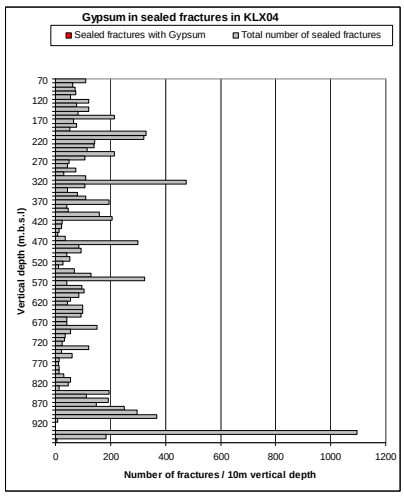
Gypsum in sealed fractures in KLX04
Sealed fractures with Gypsum
Total number of sealed fractures
Vertical depth (m.b.s.l)
Number of fractures / 10m vertical depth

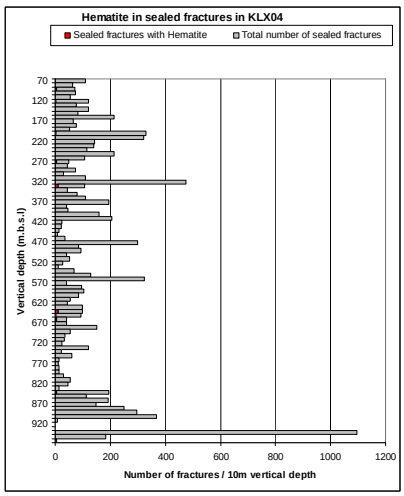
Hematite in sealed fractures in KLX04
Sealed fractures with Hematite
Total number of sealed fractures
Vertical depth (m.b.s.l)
Number of fractures / 10m vertical depth

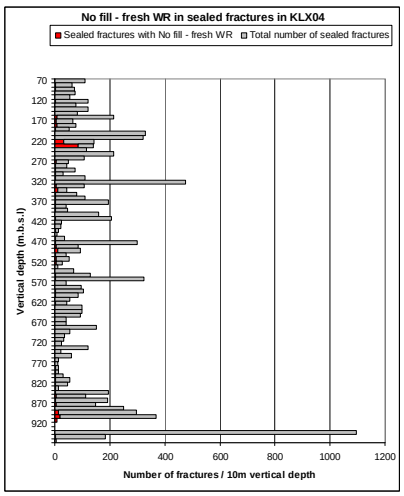
No fill - fresh WR in sealed fractures in KLX04
Sealed fractures with No fill - fresh WR
Total number of sealed fractures
Vertical depth (m.b.s.l)
Number of fractures / 10m vertical depth

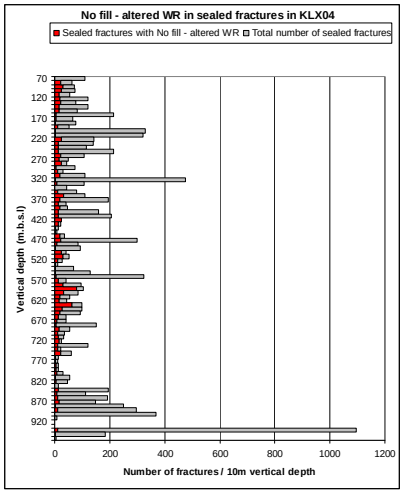
No fill - altered WR in sealed fractures in KLX04
Sealed fractures with No fill - altered WR
Total number of sealed fractures
Vertical depth (m.b.s.l)
70
120
170
220
270
320
370
420
470
520
570
620
670
720
770
820
870
920
0
200
400
600
800
1000
1200
Number of fractures / 10m vertical depth

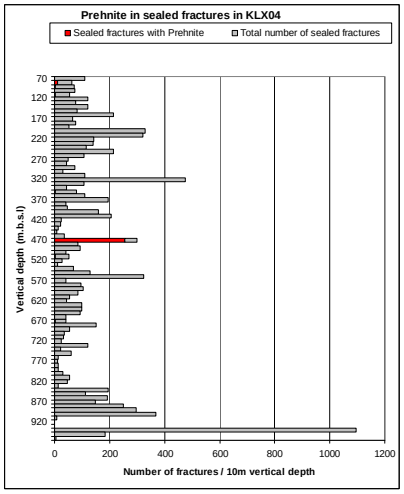
Prehnite in sealed fractures in KLX04
Sealed fractures with Prehnite
Total number of sealed fractures
Vertical depth (m.b.s.l)
70
120
170
220
270
320
370
420
470
520
570
620
670
720
770
820
870
920
0
200
400
600
800
1000
1200
Number of fractures / 10m vertical depth

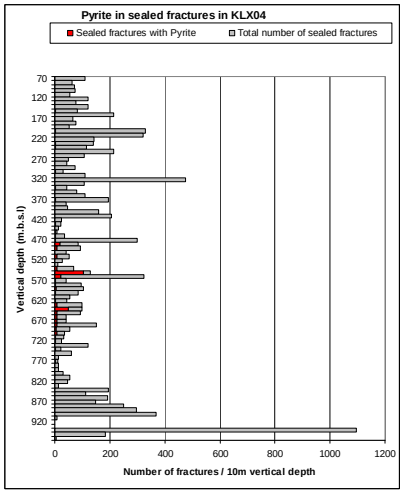
Pyrite in sealed fractures in KLX04
Sealed fractures with Pyrite
Total number of sealed fractures
Vertical depth (m.b.s.l)
70
120
170
220
270
320
370
420
470
520
570
620
670
720
770
820
870
920
0
200
400
600
800
1000
1200
Number of fractures / 10m vertical depth

KLX05

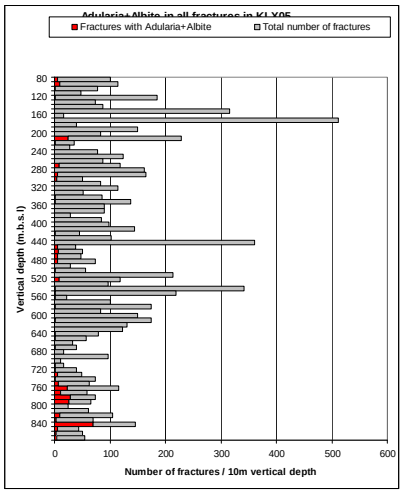
Fractures with Adularia+Albite
Total number of fractures
Vertical depth (m.b.s.l)
Number of fractures / 10m vertical depth

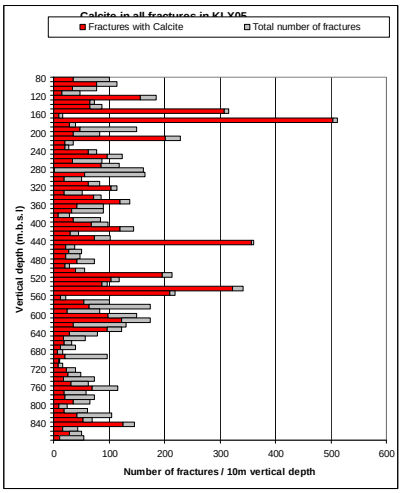
Fractures with Calcite
Total number of fractures
Vertical depth (m.b.s.l)
Number of fractures / 10m vertical depth

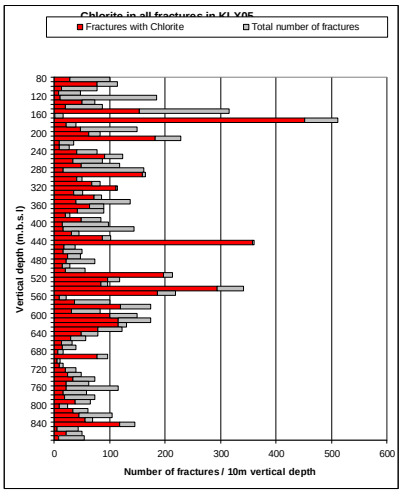
Fractures with Chlorite
Total number of fractures
Vertical depth (m.b.s.l)
Number of fractures / 10m vertical depth

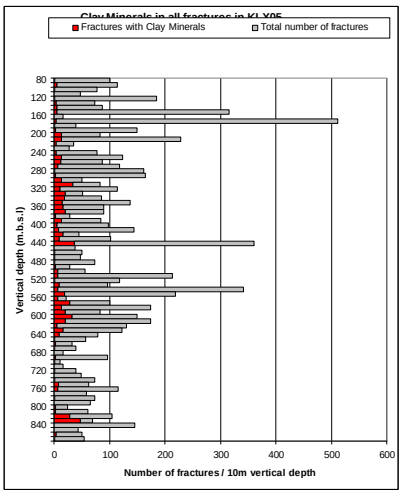
Fractures with Clay Minerals
Total number of fractures
Vertical depth (m.b.s.l)
Number of fractures / 10m vertical depth

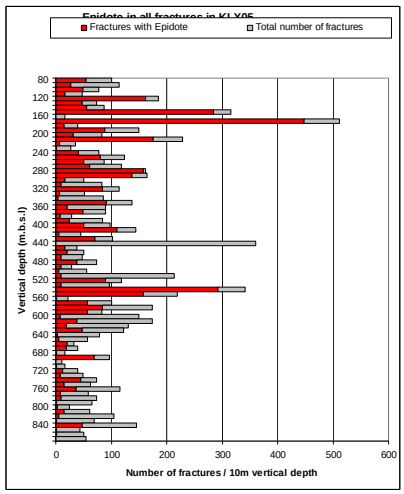
Fractures with Epidote
Total number of fractures
Vertical depth (m.b.s.l)
Number of fractures / 10m vertical depth

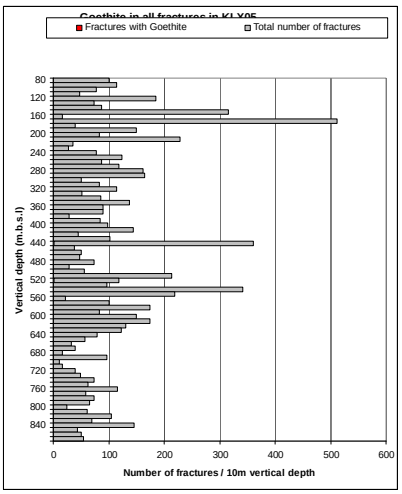
Fractures with Goethite
Total number of fractures
Vertical depth (m.b.s.l)
Number of fractures / 10m vertical depth

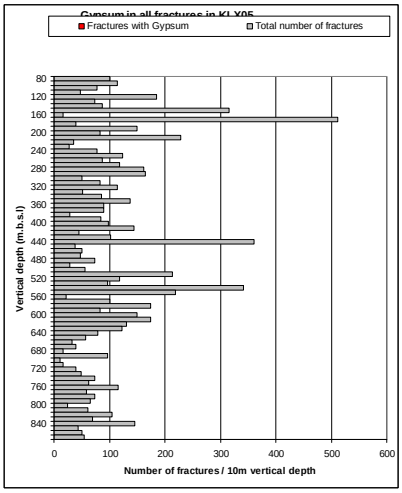
Fractures with Gypsum
Total number of fractures
Vertical depth (m.b.s.l)
Number of fractures / 10m vertical depth

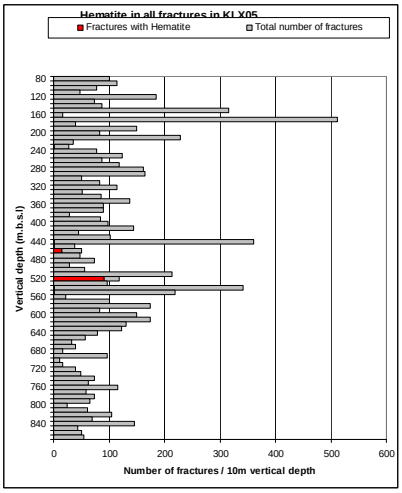
Fractures with Hematite
Total number of fractures
Vertical depth (m.b.s.l)
Number of fractures / 10m vertical depth

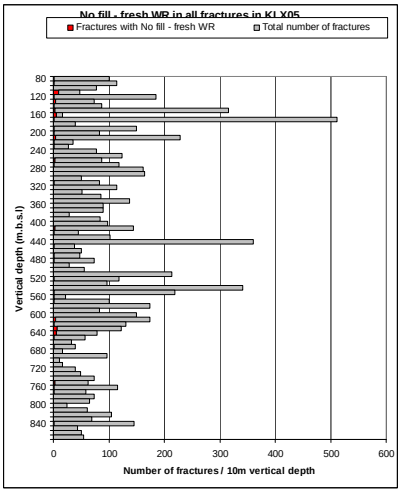
Fractures with No fill - fresh WR
Total number of fractures
Vertical depth (m.b.s.l)
Number of fractures / 10m vertical depth

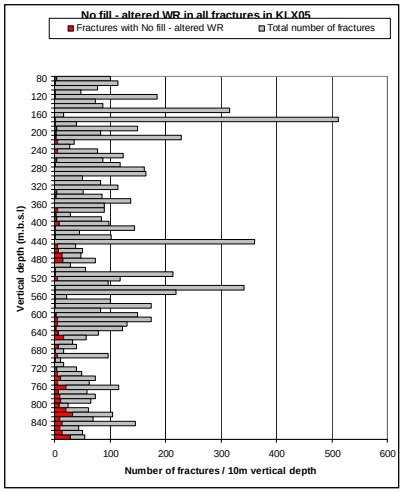
No fill - altered WR in all fractures in KLX05
Fractures with No fill - altered WR
Total number of fractures
Vertical depth (m.b.s.l)
Number of fractures / 10m vertical depth

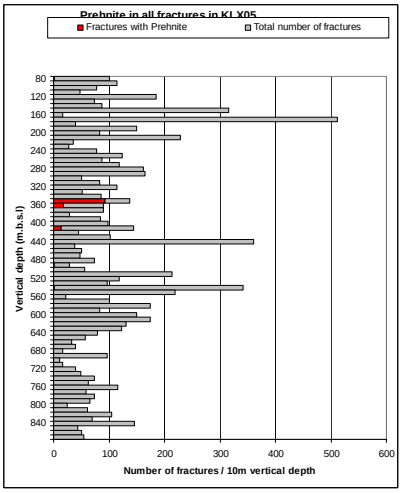
Prehnite in all fractures in KLX05
Fractures with Prehnite
Total number of fractures
Vertical depth (m.b.s.l)
Number of fractures / 10m vertical depth

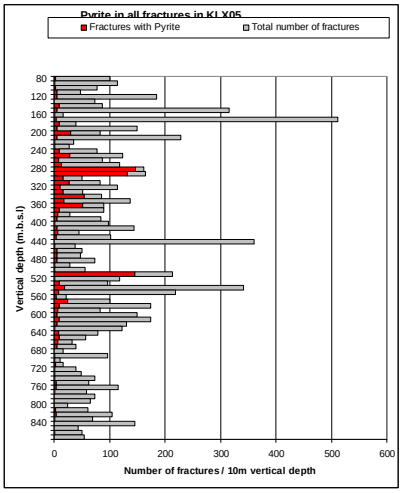
Pyrite in all fractures in KLX05
Fractures with Pyrite
Total number of fractures
Vertical depth (m.b.s.l)
Number of fractures / 10m vertical depth

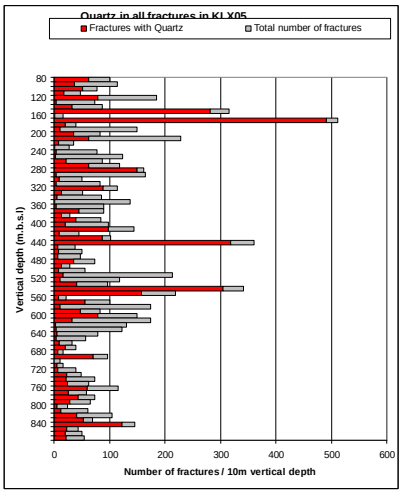
Quartz in all fractures in KLX05
Fractures with Quartz
Total number of fractures
Vertical depth (m.b.s.l)
Number of fractures / 10m vertical depth

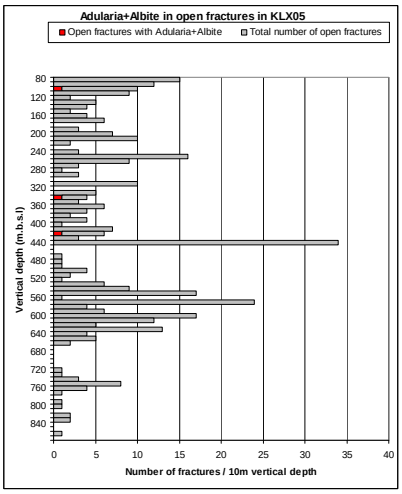
Adularia+Albite in open fractures in KLX05
Open fractures with Adularia+Albite
Total number of open fractures
Vertical depth (m.b.s.l)
Number of fractures / 10m vertical depth

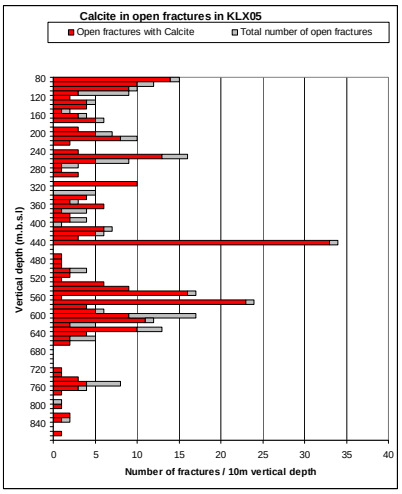
Calcite in open fractures in KLX05
Open fractures with Calcite
Total number of open fractures
Vertical depth (m.b.s.l)
Number of fractures / 10m vertical depth

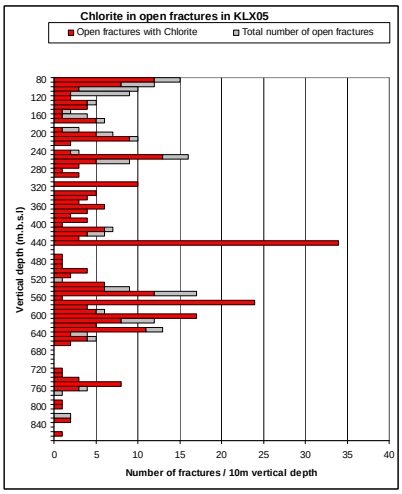
Chlorite in open fractures in KLX05
Open fractures with Chlorite
Total number of open fractures
Vertical depth (m.b.s.l)
Number of fractures / 10m vertical depth

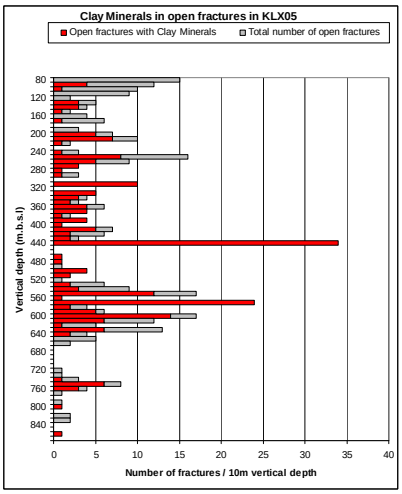
Clay Minerals in open fractures in KLX05
Open fractures with Clay Minerals
Total number of open fractures
Vertical depth (m.b.s.l)
Number of fractures / 10m vertical depth

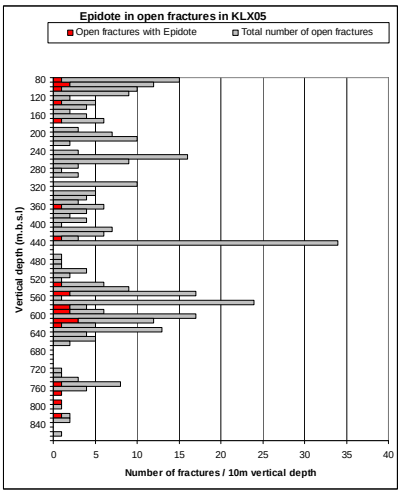
Epidote in open fractures in KLX05
Open fractures with Epidote
Total number of open fractures
Vertical depth (m.b.s.l)
Number of fractures / 10m vertical depth

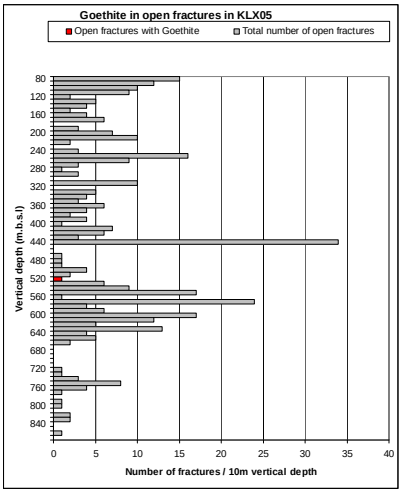
Goethite in open fractures in KLX05
Open fractures with Goethite
Total number of open fractures
Vertical depth (m.b.s.l)
Number of fractures / 10m vertical depth

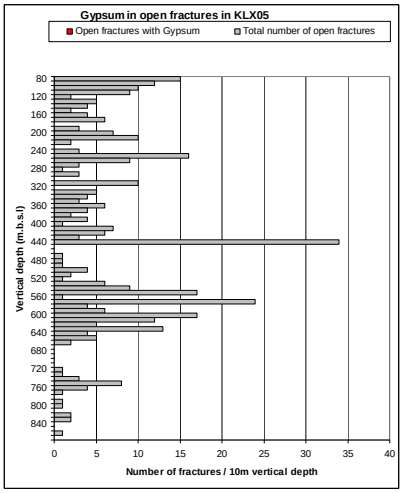
Gypsum in open fractures in KLX05
Open fractures with Gypsum
Total number of open fractures
Vertical depth (m.b.s.l)
Number of fractures / 10m vertical depth

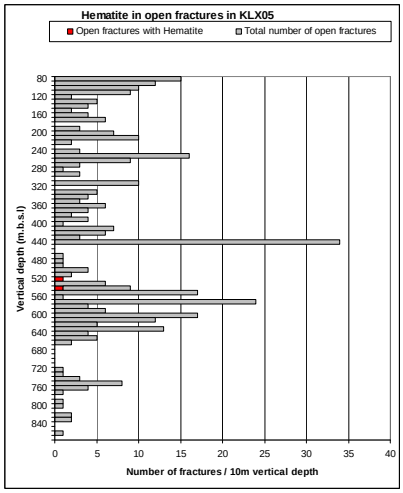
Hematite in open fractures in KLX05
Open fractures with Hematite
Total number of open fractures
Vertical depth (m.b.s.l)
Number of fractures / 10m vertical depth

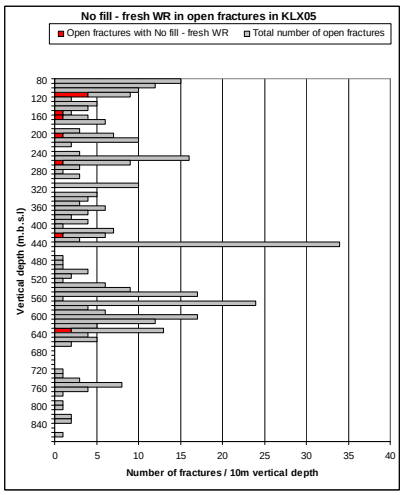
No fill - fresh WR in open fractures in KLX05
Open fractures with No fill - fresh WR
Total number of open fractures
Vertical depth (m.b.s.l)
Number of fractures / 10m vertical depth

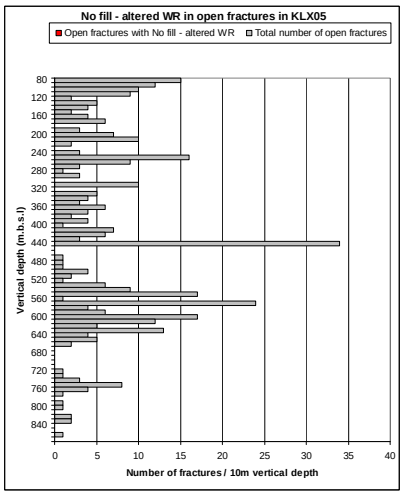
No fill - altered WR in open fractures in KLX05
Open fractures with No fill - altered WR
Total number of open fractures
Vertical depth (m.b.s.l)
Number of fractures / 10m vertical depth

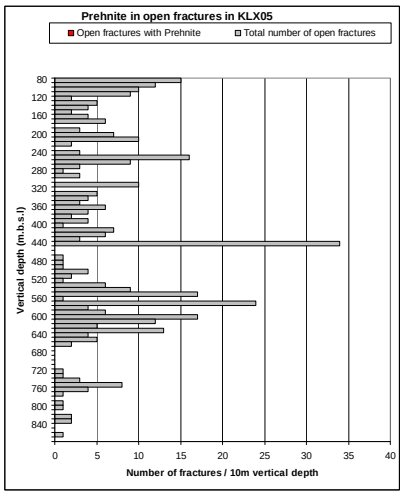
Prehnite in open fractures in KLX05
Open fractures with Prehnite
Total number of open fractures
Vertical depth (m.b.s.l)
Number of fractures / 10m vertical depth

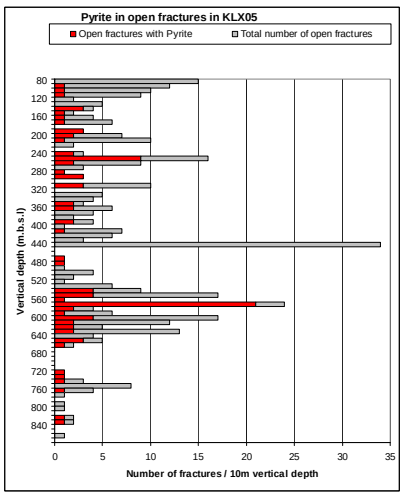
Pyrite in open fractures in KLX05
Open fractures with Pyrite
Total number of open fractures
Vertical depth (m.b.s.l)
Number of fractures / 10m vertical depth

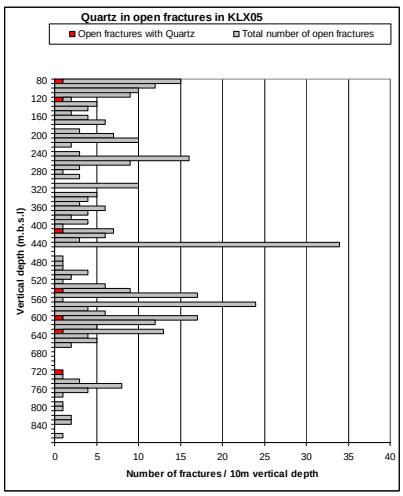
Quartz in open fractures in KLX05
Open fractures with Quartz
Total number of open fractures
Vertical depth (m.b.s.l)
Number of fractures / 10m vertical depth

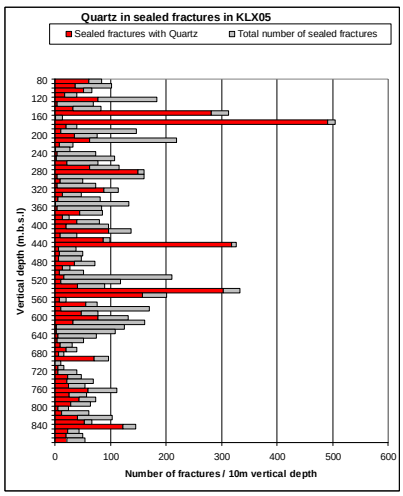
Quartz in sealed fractures in KLX05
Sealed fractures with Quartz
Total number of sealed fractures
Vertical depth (m.b.s.l)
Number of fractures / 10m vertical depth

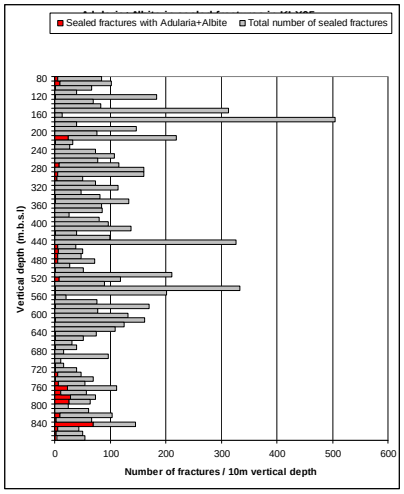
Sealed fractures with Adularia+Albite
Total number of sealed fractures
Vertical depth (m.b.s.l)
Number of fractures / 10m vertical depth

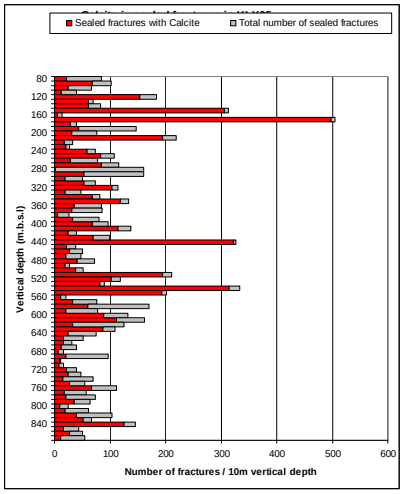
Sealed fractures with Calcite
Total number of sealed fractures
Vertical depth (m.b.s.l)
Number of fractures / 10m vertical depth

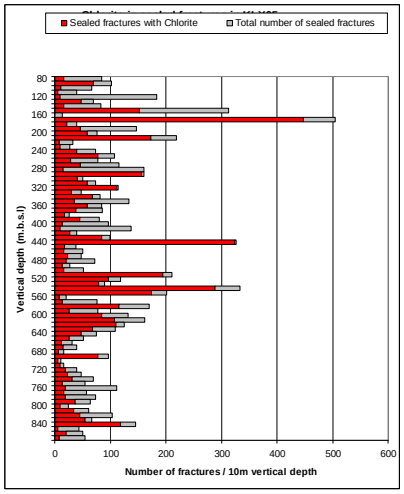
Sealed fractures with Chlorite
Total number of sealed fractures
Vertical depth (m.b.s.l)
Number of fractures / 10m vertical depth

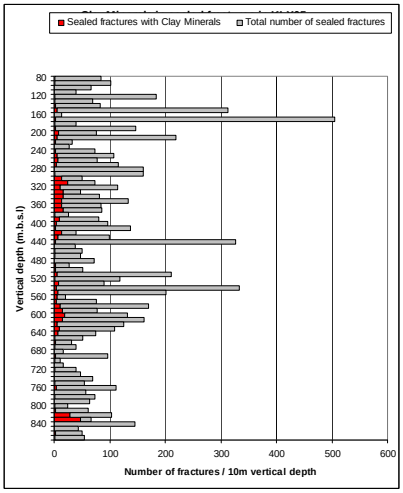
Sealed fractures with Clay Minerals
Total number of sealed fractures
Vertical depth (m.b.s.l)
Number of fractures / 10m vertical depth

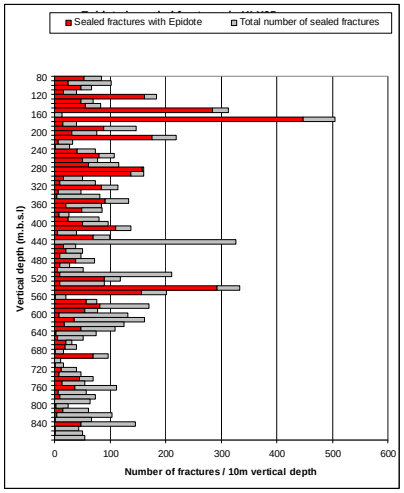
Sealed fractures with Epidote
Total number of sealed fractures
Vertical depth (m.b.s.l)
Number of fractures / 10m vertical depth

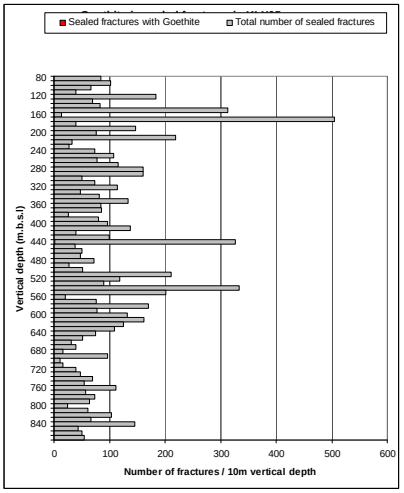
Sealed fractures with Goethite
Total number of sealed fractures
Vertical depth (m.b.s.l)
Number of fractures / 10m vertical depth

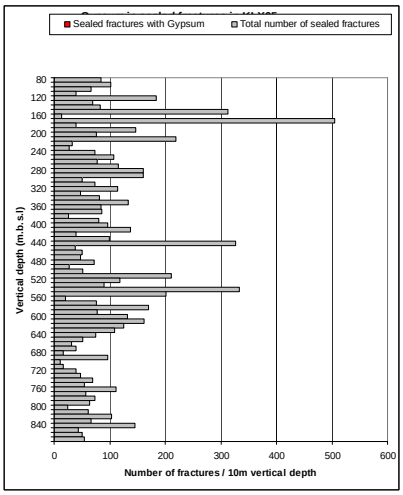
Sealed fractures with Gypsum
Total number of sealed fractures
Vertical depth (m.b.s.l)
Number of fractures / 10m vertical depth

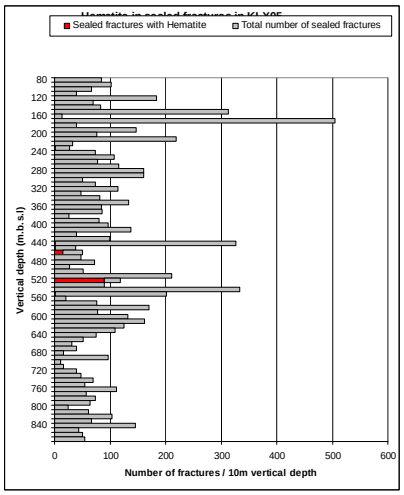
Sealed fractures with Hematite
Total number of sealed fractures
Vertical depth (m.b.s.l)
Number of fractures / 10m vertical depth

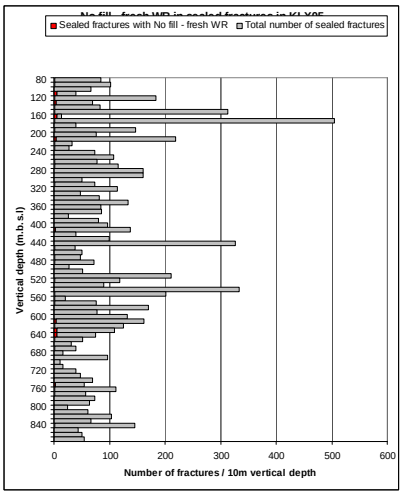
Sealed fractures with No fill - fresh WR
Total number of sealed fractures
Vertical depth (m.b.s.l)
Number of fractures / 10m vertical depth

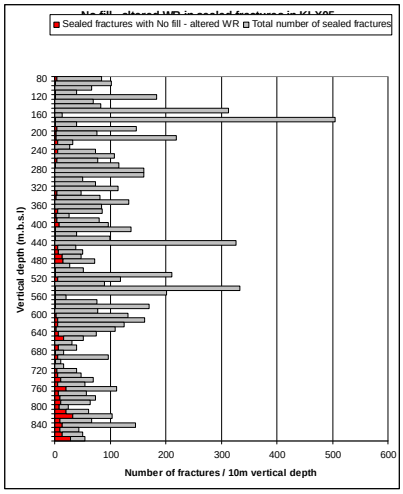
Sealed fractures with No fill - altered WR
Total number of sealed fractures
Vertical depth (m.b.s.l)
Number of fractures / 10m vertical depth

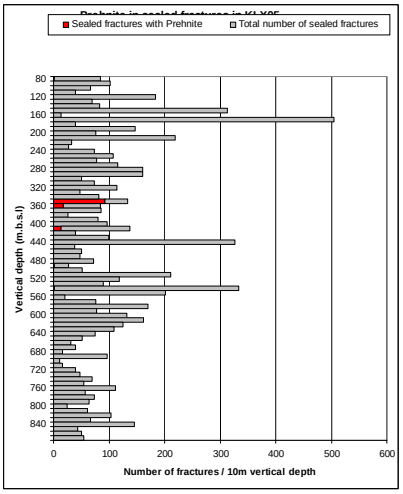
Sealed fractures with Prehnite
Total number of sealed fractures
Vertical depth (m.b.s.l)
Number of fractures / 10m vertical depth

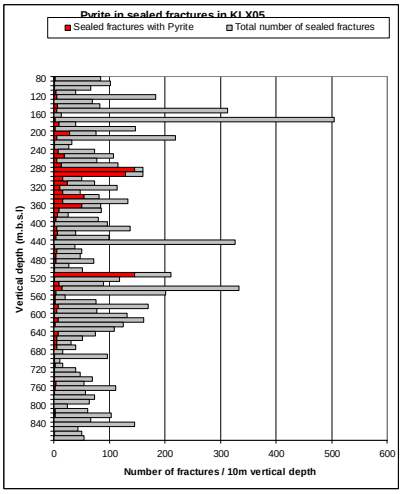
Pyrite in sealed fractures in KLX05
Sealed fractures with Pyrite
Total number of sealed fractures
Vertical depth (m.b.s.l)
Number of fractures / 10m vertical depth

KLX06

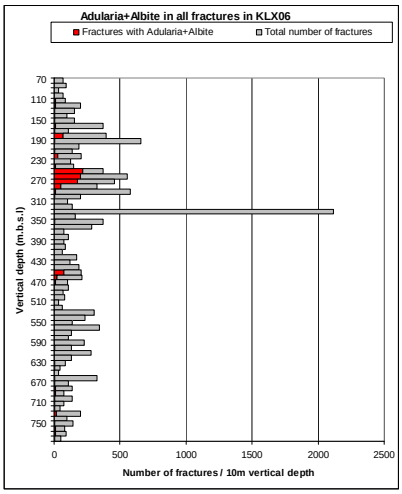
Adularia+Albite in all fractures in KLX06
Fractures with Adularia+Albite
Total number of fractures
Vertical depth (m.b.s.l)
Number of fractures / 10m vertical depth

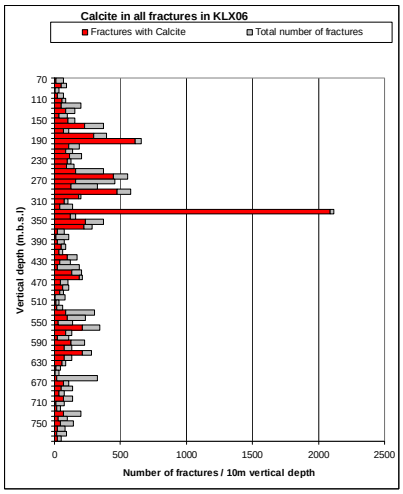
Calcite in all fractures in KLX06
Fractures with Calcite
Total number of fractures
Vertical depth (m.b.s.l)
Number of fractures / 10m vertical depth

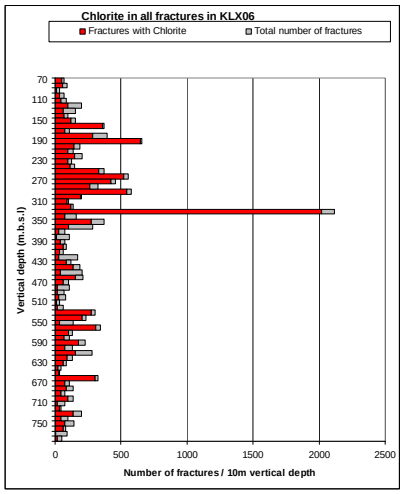
Chlorite in all fractures in KLX06
Fractures with Chlorite
Total number of fractures
Vertical depth (m.b.s.l)
Number of fractures / 10m vertical depth

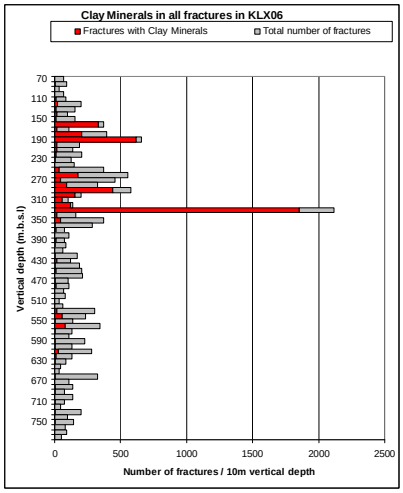
Clay Minerals in all fractures in KLX06
Fractures with Clay Minerals
Total number of fractures
Vertical depth (m.b.s.l)
Number of fractures / 10m vertical depth

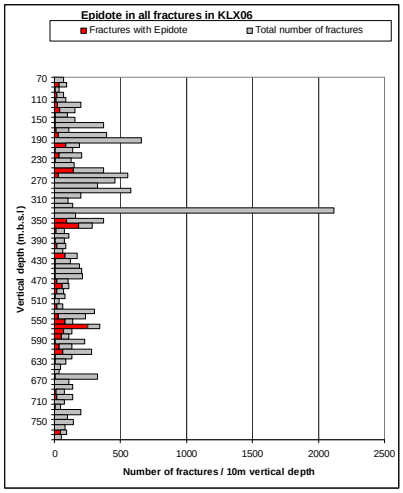
Epidote in all fractures in KLX06
Fractures with Epidote
Total number of fractures
Vertical depth (m.b.s.l)
Number of fractures / 10m vertical depth

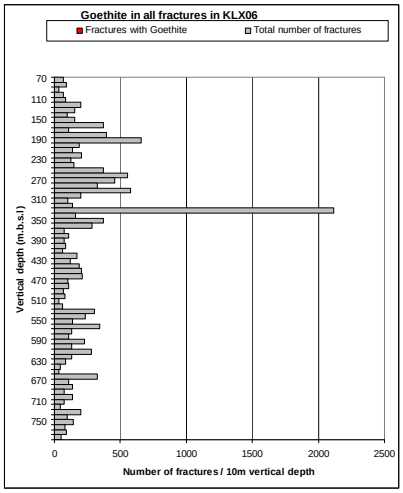
Goethite in all fractures in KLX06
Fractures with Goethite
Total number of fractures
Vertical depth (m.b.s.l)
Number of fractures / 10m vertical depth

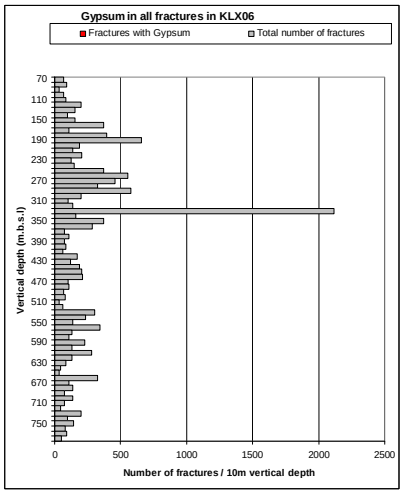
Gypsum in all fractures in KLX06
Fractures with Gypsum
Total number of fractures
Vertical depth (m.b.s.l)
Number of fractures / 10m vertical depth

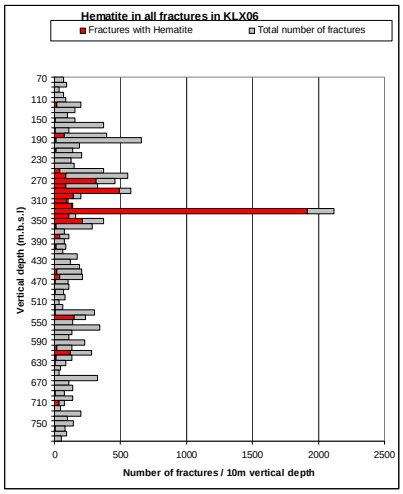
Hematite in all fractures in KLX06
Fractures with Hematite
Total number of fractures
Vertical depth (m.b.s.l)
Number of fractures / 10m vertical depth

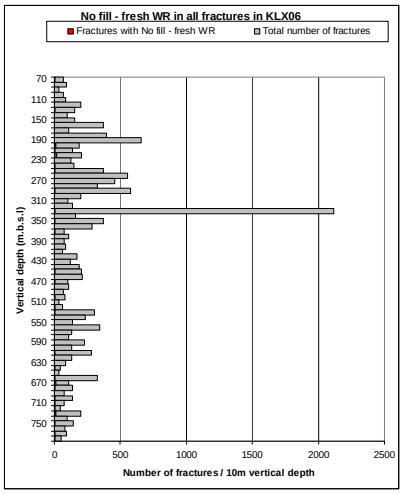
No fill - fresh WR in all fractures in KLX06
Fractures with No fill - fresh WR
Total number of fractures
Vertical depth (m.b.s.l)
Number of fractures / 10m vertical depth

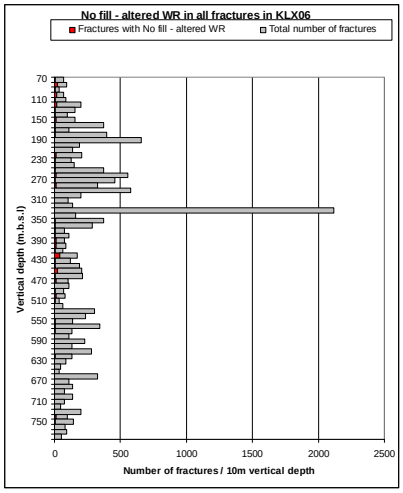
No fill - altered WR in all fractures in KLX06
Fractures with No fill - altered WR
Total number of fractures
Vertical depth (m.b.s.l)
Number of fractures / 10m vertical depth

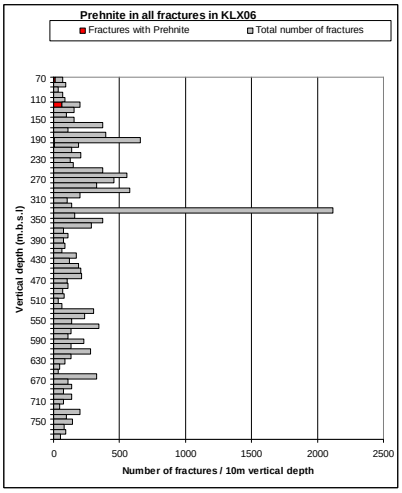
Prehnite in all fractures in KLX06
Fractures with Prehnite
Total number of fractures
Vertical depth (m.b.s.l)
Number of fractures / 10m vertical depth

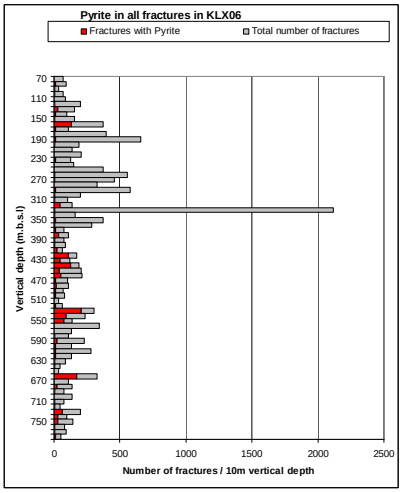
Pyrite in all fractures in KLX06
Fractures with Pyrite
Total number of fractures
Vertical depth (m.b.s.l)
Number of fractures / 10m vertical depth

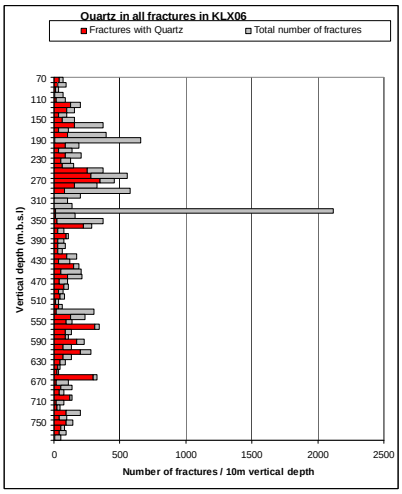
Quartz in all fractures in KLX06
Fractures with Quartz
Total number of fractures
Vertical depth (m.b.s.l)
Number of fractures / 10m vertical depth

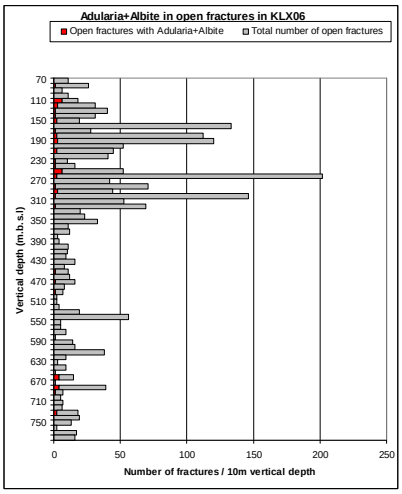
Adularia+Albite in open fractures in KLX06
Open fractures with Adularia+Albite
Total number of open fractures
Vertical depth (m.b.s.l)
Number of fractures / 10m vertical depth

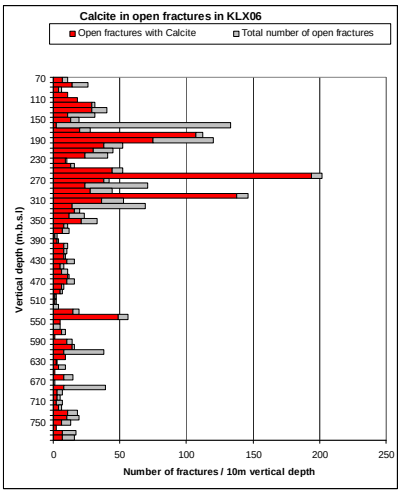
Calcite in open fractures in KLX06
Open fractures with Calcite
Total number of open fractures
Vertical depth (m.b.s.l)
Number of fractures / 10m vertical depth

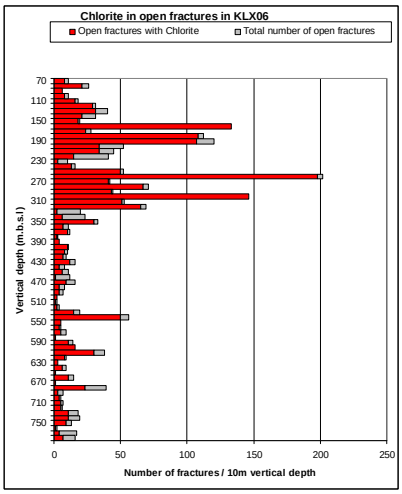
Chlorite in open fractures in KLX06
Open fractures with Chlorite
Total number of open fractures
Vertical depth (m.b.s.l)
Number of fractures / 10m vertical depth

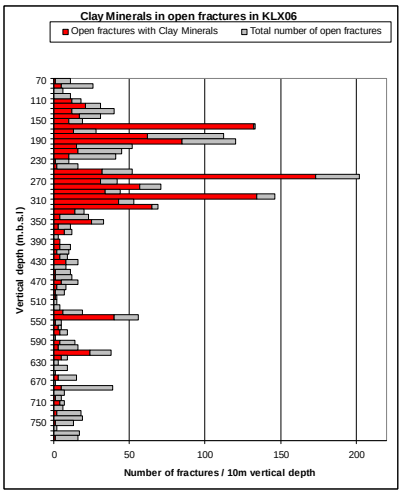
Clay Minerals in open fractures in KLX06
Open fractures with Clay Minerals
Total number of open fractures
Vertical depth (m.b.s.l)
Number of fractures / 10m vertical depth

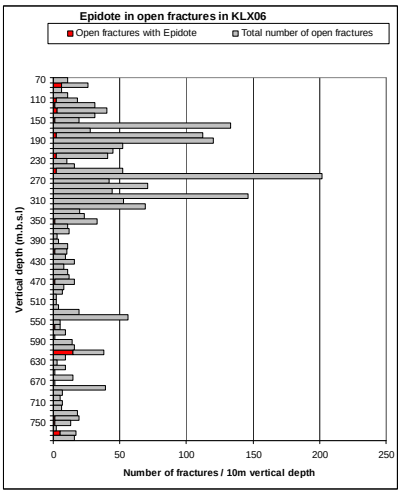
Epidote in open fractures in KLX06
Open fractures with Epidote
Total number of open fractures
Vertical depth (m.b.s.l)
Number of fractures / 10m vertical depth

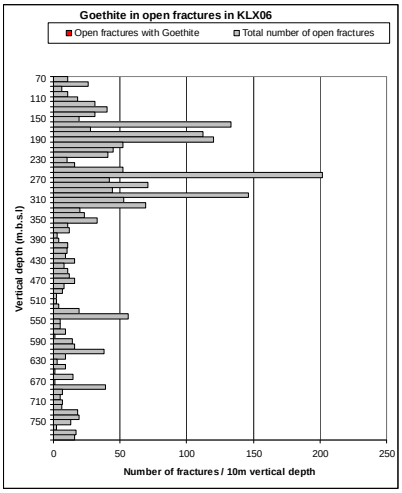
Goethite in open fractures in KLX06
Open fractures with Goethite
Total number of open fractures
Vertical depth (m.b.s.l)
Number of fractures / 10m vertical depth

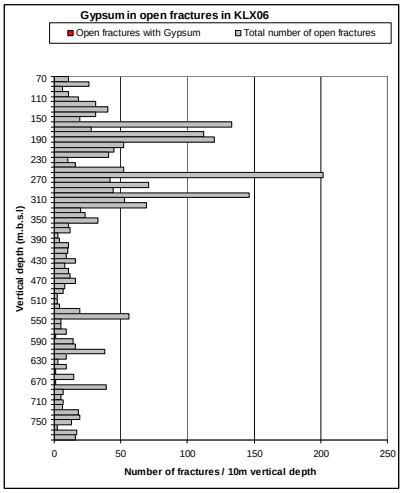
Gypsum in open fractures in KLX06
Open fractures with Gypsum
Total number of open fractures
Vertical depth (m.b.s.l)
Number of fractures / 10m vertical depth

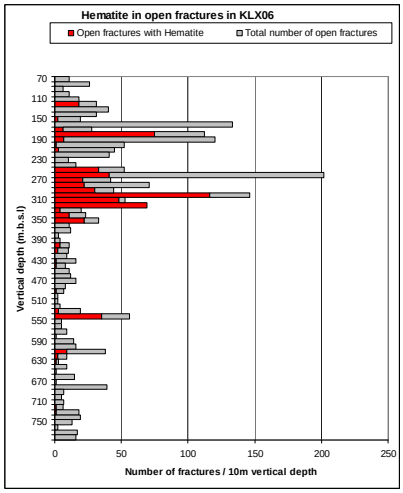
Hematite in open fractures in KLX06
Open fractures with Hematite
Total number of open fractures
Vertical depth (m.b.s.l)
Number of fractures / 10m vertical depth

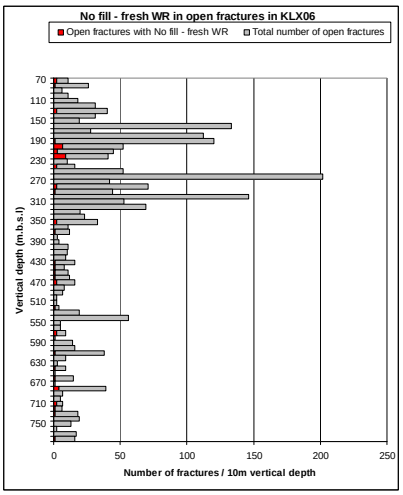
No fill - fresh WR in open fractures in KLX06
Open fractures with No fill - fresh WR
Total number of open fractures
Vertical depth (m.b.s.l)
Number of fractures / 10m vertical depth

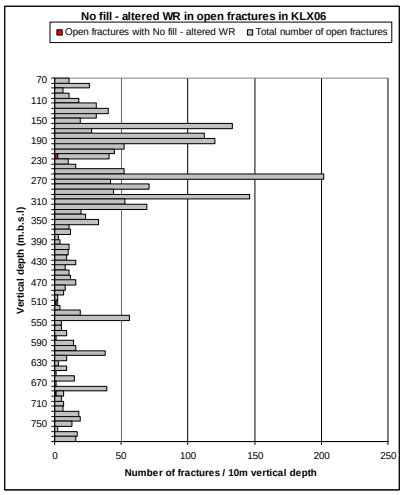
No fill - altered WR in open fractures in KLX06
Open fractures with No fill - altered WR
Total number of open fractures
Vertical depth (m.b.s.l)
Number of fractures / 10m vertical depth

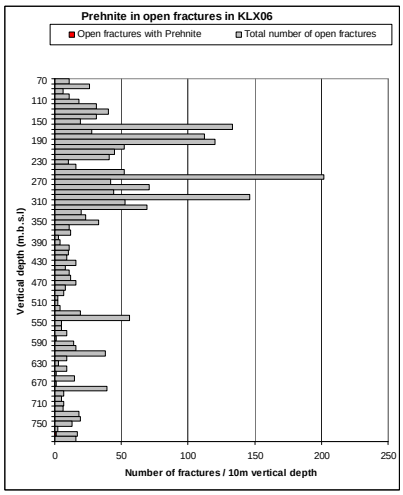
Prehnite in open fractures in KLX06
Open fractures with Prehnite
Total number of open fractures
Vertical depth (m.b.s.l)
Number of fractures / 10m vertical depth

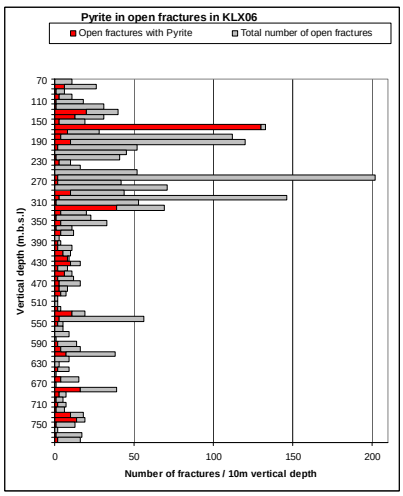
Pyrite in open fractures in KLX06
Open fractures with Pyrite
Total number of open fractures
Vertical depth (m.b.s.l)
Number of fractures / 10m vertical depth

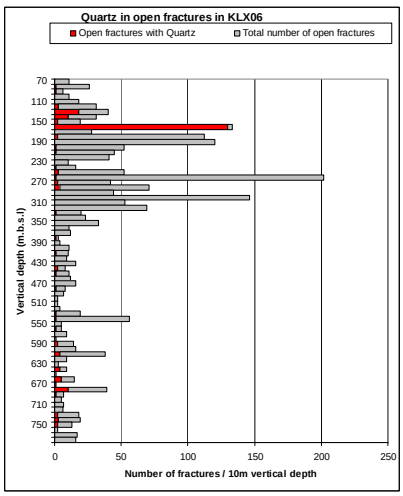
Quartz in open fractures in KLX06
Open fractures with Quartz
Total number of open fractures
Vertical depth (m.b.s.l)
Number of fractures / 10m vertical depth

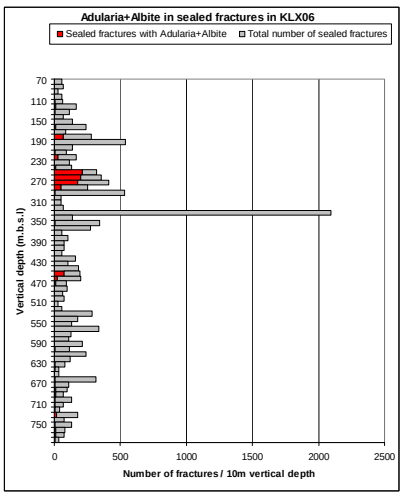
Adularia+Albite in sealed fractures in KLX06
Sealed fractures with Adularia+Albite
Total number of sealed fractures
Vertical depth (m.b.s.l)
Number of fractures / 10m vertical depth

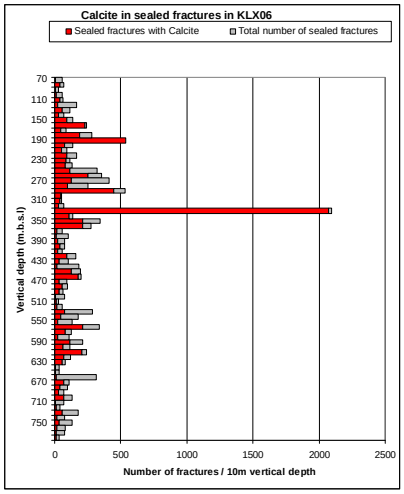
Calcite in sealed fractures in KLX06
Sealed fractures with Calcite
Total number of sealed fractures
Vertical depth (m.b.s.l)
Number of fractures / 10m vertical depth

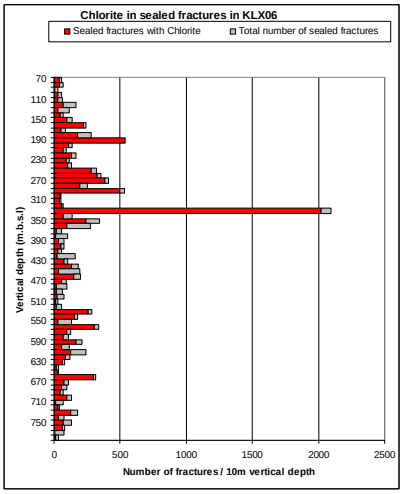
Chlorite in sealed fractures in KLX06
Sealed fractures with Chlorite
Total number of sealed fractures
Vertical depth (m.b.s.l)
Number of fractures / 10m vertical depth

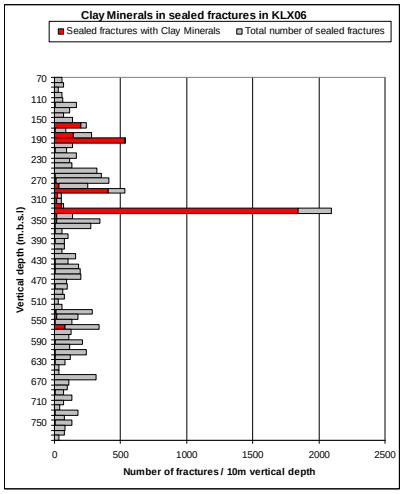
Clay Minerals in sealed fractures in KLX06
Sealed fractures with Clay Minerals
Total number of sealed fractures
Vertical depth (m.b.s.l)
Number of fractures / 10m vertical depth

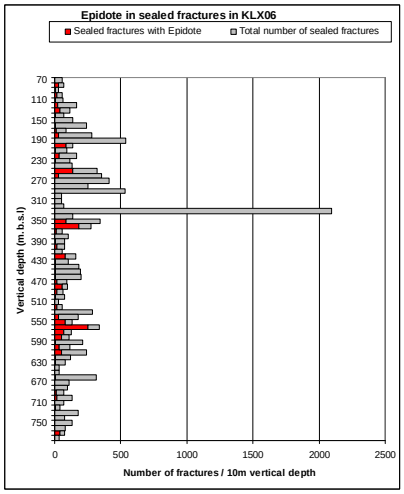
Epidote in sealed fractures in KLX06
Sealed fractures with Epidote
Total number of sealed fractures
Vertical depth (m.b.s.l)
Number of fractures / 10m vertical depth

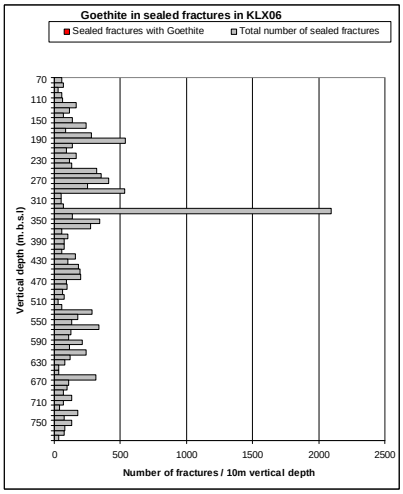
Goethite in sealed fractures in KLX06
Sealed fractures with Goethite
Total number of sealed fractures
Vertical depth (m.b.s.l)
Number of fractures / 10m vertical depth

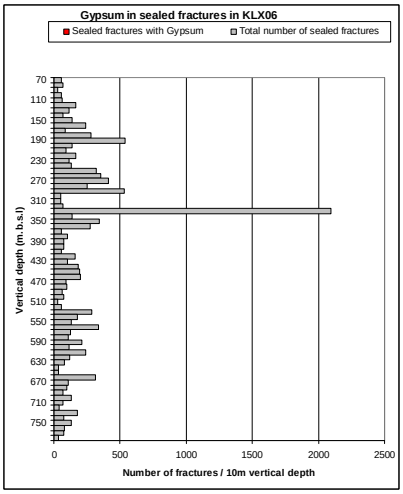
Gypsum in sealed fractures in KLX06
Sealed fractures with Gypsum
Total number of sealed fractures
Vertical depth (m.b.s.l)
Number of fractures / 10m vertical depth

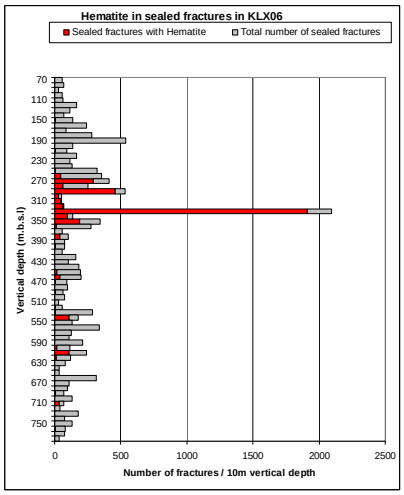
Hematite in sealed fractures in KLX06
Sealed fractures with Hematite
Total number of sealed fractures
Vertical depth (m.b.s.l)
Number of fractures / 10m vertical depth

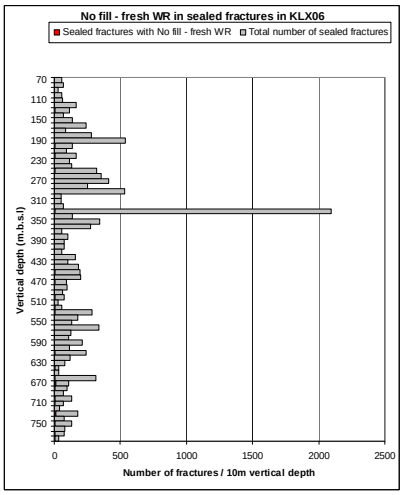
No fill - fresh WR in sealed fractures in KLX06
Sealed fractures with No fill - fresh WR
Total number of sealed fractures
Vertical depth (m.b.s.l)
Number of fractures / 10m vertical depth

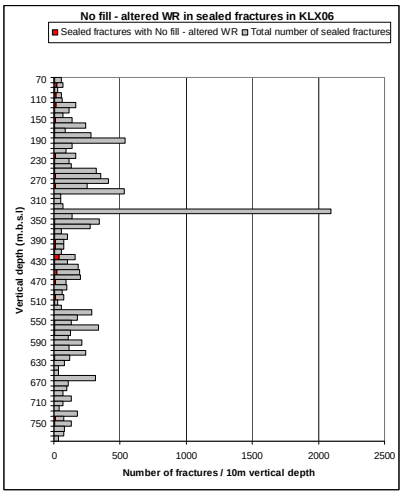
No fill - altered WR in sealed fractures in KLX06
Sealed fractures with No fill - altered WR
Total number of sealed fractures
Vertical depth (m.b.s.l)
Number of fractures / 10m vertical depth

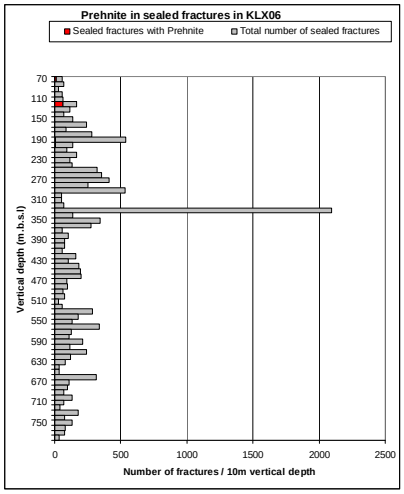
Prehnite in sealed fractures in KLX06
Sealed fractures with Prehnite
Total number of sealed fractures
Vertical depth (m.b.s.l)
70
110
150
190
230
270
310
350
390
430
470
510
550
590
630
670
710
750
0
500
1000
1500
2000
2500
Number of fractures / 10m vertical depth

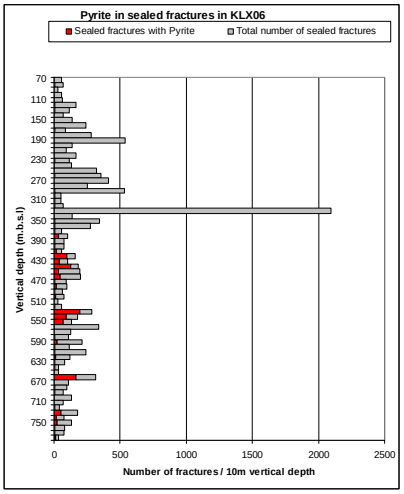
Pyrite in sealed fractures in KLX06
Sealed fractures with Pyrite
Total number of sealed fractures
Vertical depth (m.b.s.l)
70
110
150
190
230
270
310
350
390
430
470
510
550
590
630
670
710
750
0
500
1000
1500
2000
2500
Number of fractures / 10m vertical depth

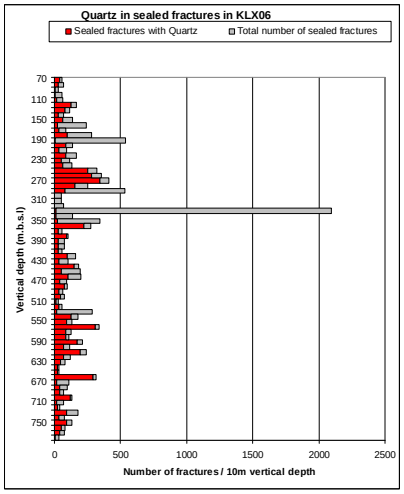
Quartz in sealed fractures in KLX06
Sealed fractures with Quartz
Total number of sealed fractures
Vertical depth (m.b.s.l)
70
110
150
190
230
270
310
350
390
430
470
510
550
590
630
670
710
750
0
500
1000
1500
2000
2500
Number of fractures / 10m vertical depth

KLX07A

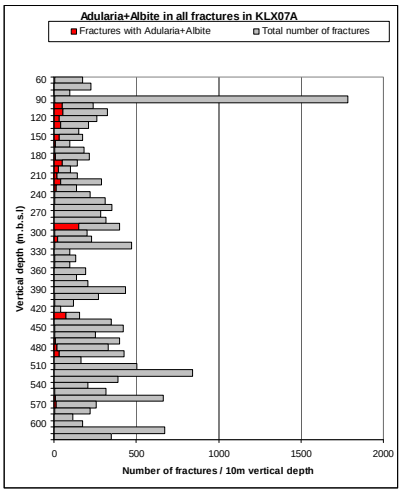
Adularia+Albite in all fractures in KLX07A
Fractures with Adularia+Albite
Total number of fractures
Vertical depth (m.b.s.l)
Number of fractures / 10m vertical depth

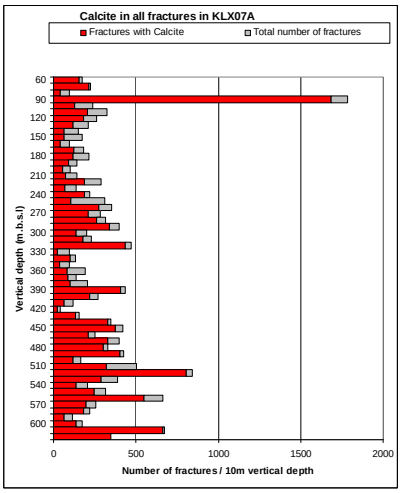
Calcite in all fractures in KLX07A
Fractures with Calcite
Total number of fractures
Vertical depth (m.b.s.l)
Number of fractures / 10m vertical depth

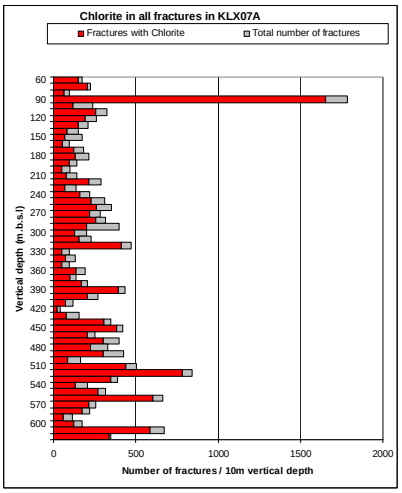
Chlorite in all fractures in KLX07A
Fractures with Chlorite
Total number of fractures
Vertical depth (m.b.s.l)
Number of fractures / 10m vertical depth

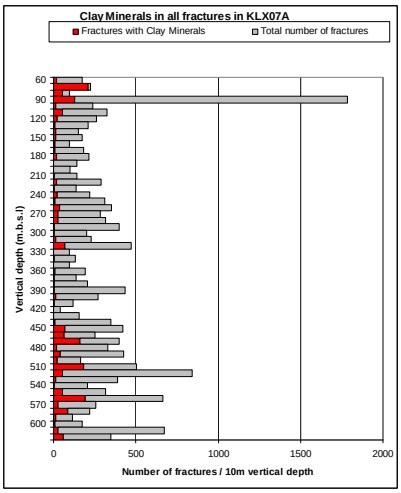
Clay Minerals in all fractures in KLX07A
Fractures with Clay Minerals
Total number of fractures
Vertical depth (m.b.s.l)
Number of fractures / 10m vertical depth

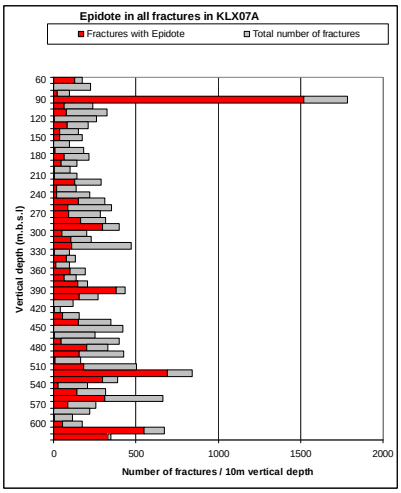
Epidote in all fractures in KLX07A
Fractures with Epidote
Total number of fractures
Vertical depth (m.b.s.l)
Number of fractures / 10m vertical depth

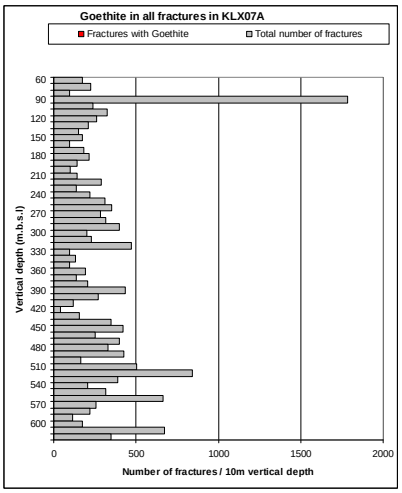
Goethite in all fractures in KLX07A
Fractures with Goethite
Total number of fractures
Vertical depth (m.b.s.l)
Number of fractures / 10m vertical depth

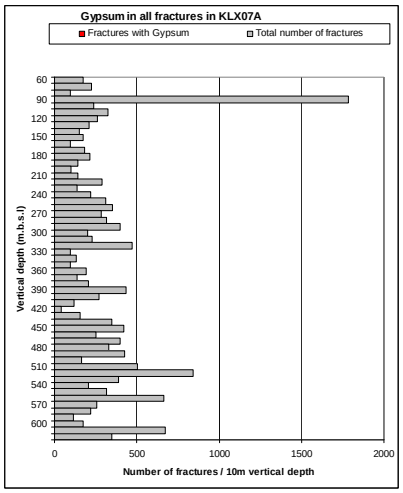
Gypsum in all fractures in KLX07A
Fractures with Gypsum
Total number of fractures
Vertical depth (m.b.s.l)
Number of fractures / 10m vertical depth

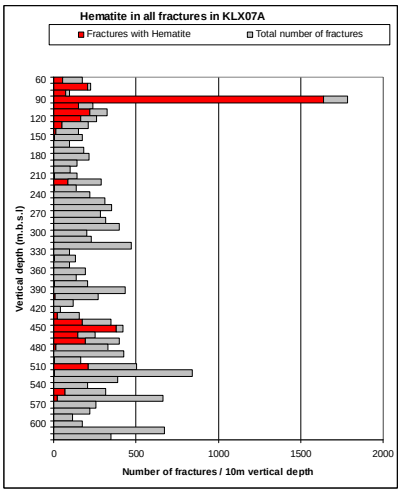
Hematite in all fractures in KLX07A
Fractures with Hematite
Total number of fractures
Vertical depth (m.b.s.l)
Number of fractures / 10m vertical depth

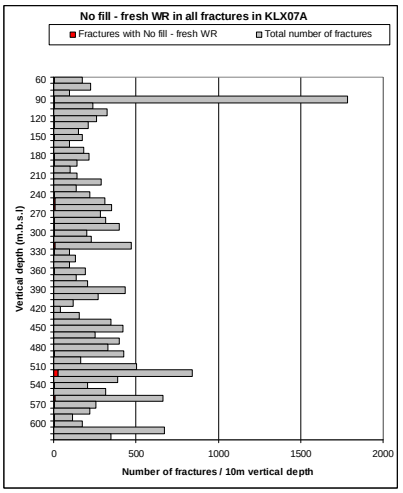
No fill - fresh WR in all fractures in KLX07A
Fractures with No fill - fresh WR
Total number of fractures
Vertical depth (m.b.s.l)
Number of fractures / 10m vertical depth

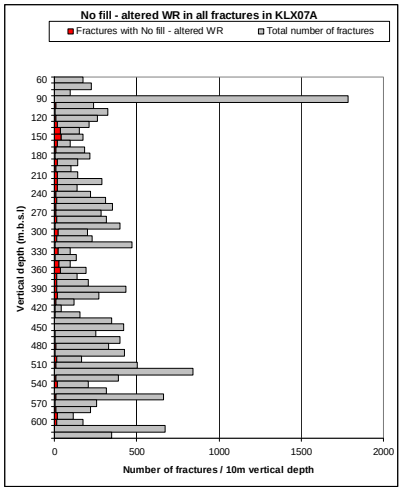
No fill - altered WR in all fractures in KLX07A
Fractures with No fill - altered WR
Total number of fractures
Vertical depth (m.b.s.l)
Number of fractures / 10m vertical depth

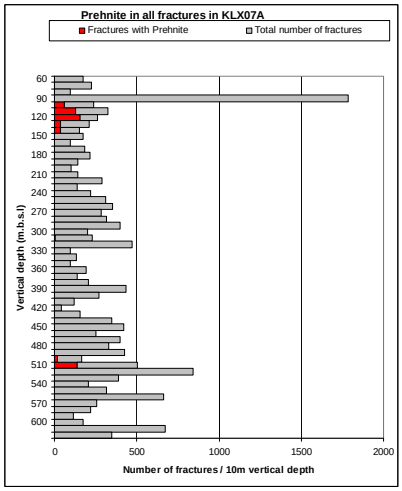
Prehnite in all fractures in KLX07A
Fractures with Prehnite
Total number of fractures
Vertical depth (m.b.s.l)
Number of fractures / 10m vertical depth

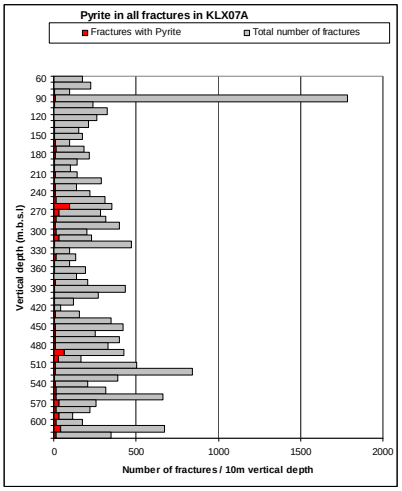
Pyrite in all fractures in KLX07A
Fractures with Pyrite
Total number of fractures
Vertical depth (m.b.s.l)
Number of fractures / 10m vertical depth

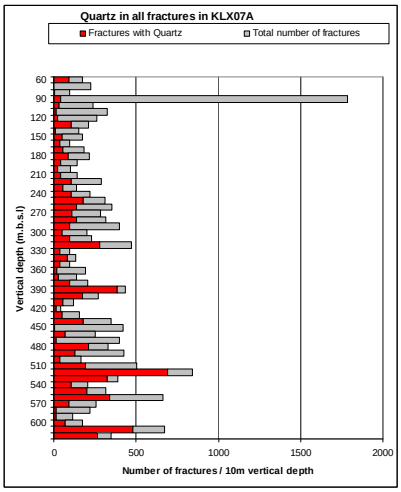
Quartz in all fractures in KLX07A
Fractures with Quartz
Total number of fractures
Vertical depth (m.b.s.l)
Number of fractures / 10m vertical depth

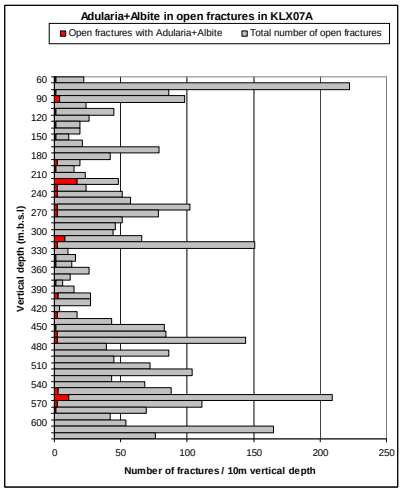
Adularia+Albite in open fractures in KLX07A
Open fractures with Adularia+Albite
Total number of open fractures
Vertical depth (m.b.s.l)
Number of fractures / 10m vertical depth

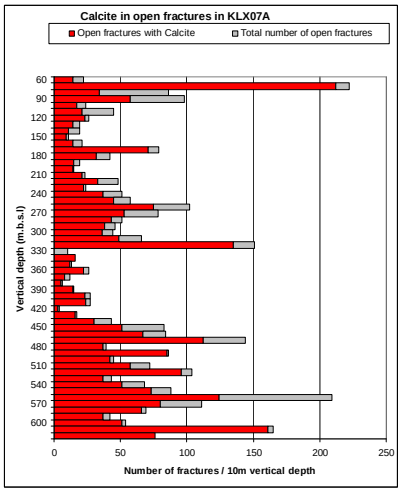
Calcite in open fractures in KLX07A
Open fractures with Calcite
Total number of open fractures
Vertical depth (m.b.s.l)
Number of fractures / 10m vertical depth

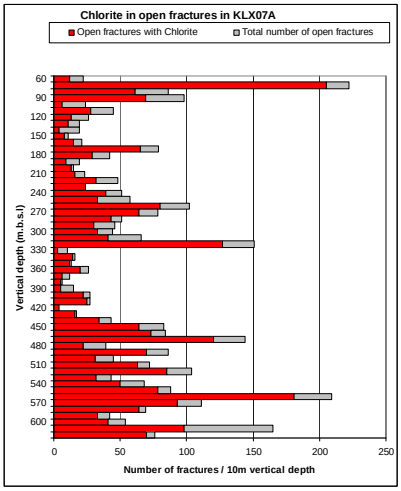
Chlorite in open fractures in KLX07A
Open fractures with Chlorite
Total number of open fractures
Vertical depth (m.b.s.l)
Number of fractures / 10m vertical depth

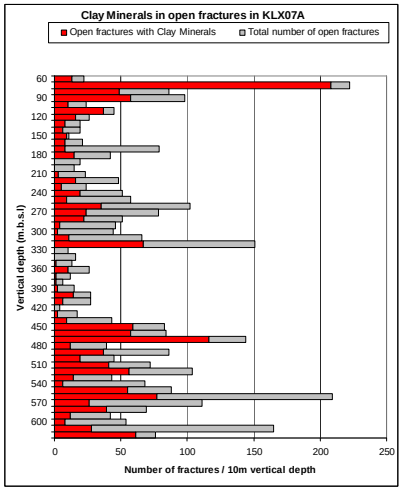
Clay Minerals in open fractures in KLX07A
Open fractures with Clay Minerals
Total number of open fractures
Vertical depth (m.b.s.l)
Number of fractures / 10m vertical depth

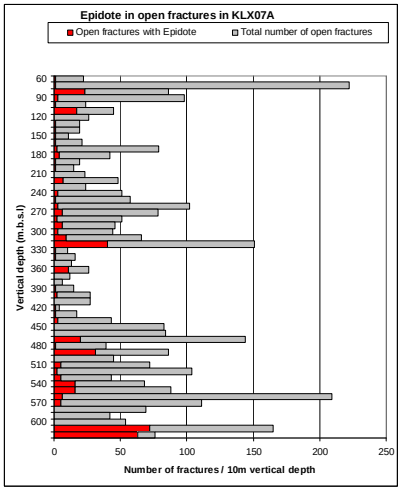
Epidote in open fractures in KLX07A
Open fractures with Epidote
Total number of open fractures
Vertical depth (m.b.s.l)
Number of fractures / 10m vertical depth

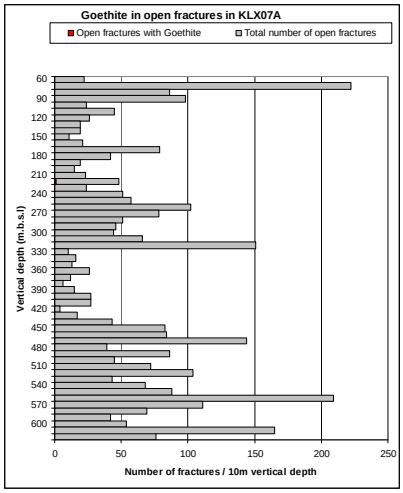
Goethite in open fractures in KLX07A
Open fractures with Goethite
Total number of open fractures
Vertical depth (m.b.s.l)
Number of fractures / 10m vertical depth

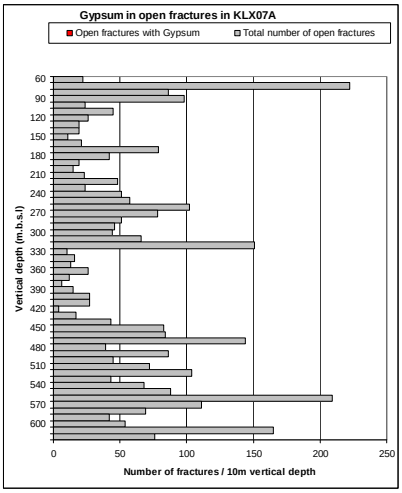
Gypsum in open fractures in KLX07A
Open fractures with Gypsum
Total number of open fractures
Vertical depth (m.b.s.l)
Number of fractures / 10m vertical depth

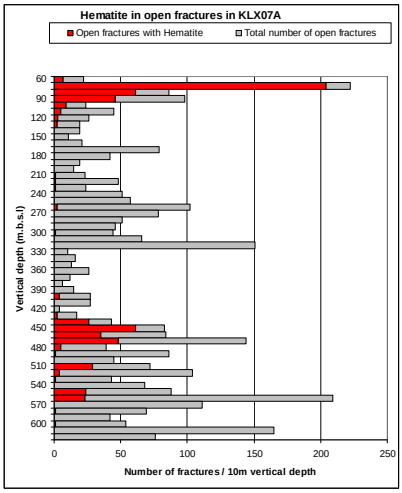
Hematite in open fractures in KLX07A
Open fractures with Hematite
Total number of open fractures
Vertical depth (m.b.s.l)
Number of fractures / 10m vertical depth

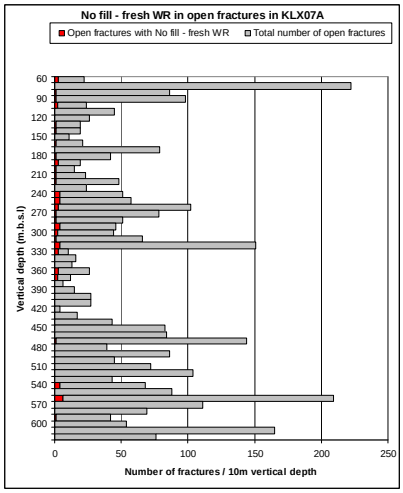
No fill - fresh WR in open fractures in KLX07A
Open fractures with No fill - fresh WR
Total number of open fractures
Vertical depth (m.b.s.l)
Number of fractures / 10m vertical depth

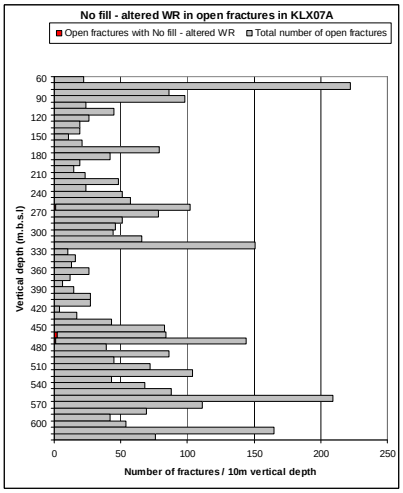
No fill - altered WR in open fractures in KLX07A
Open fractures with No fill - altered WR
Total number of open fractures
Vertical depth (m.b.s.l)
Number of fractures / 10m vertical depth

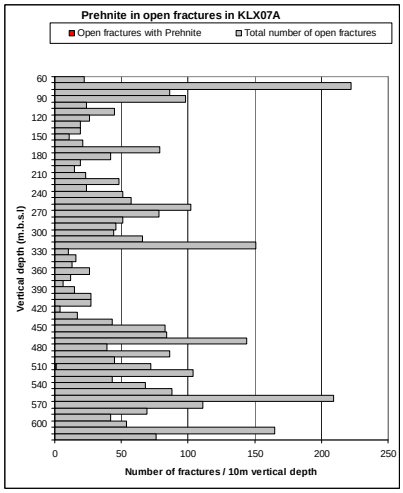
Prehnite in open fractures in KLX07A
Open fractures with Prehnite
Total number of open fractures
Vertical depth (m.b.s.l)
Number of fractures / 10m vertical depth

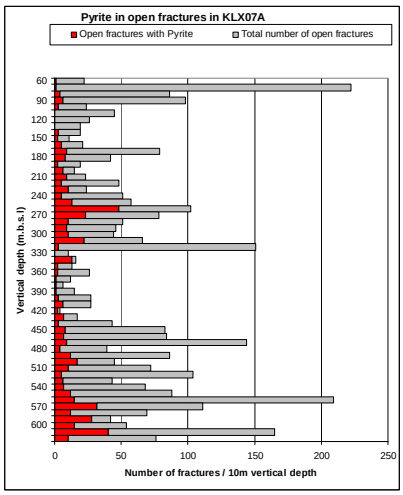
Pyrite in open fractures in KLX07A
Open fractures with Pyrite
Total number of open fractures
Vertical depth (m.b.s.l)
Number of fractures / 10m vertical depth

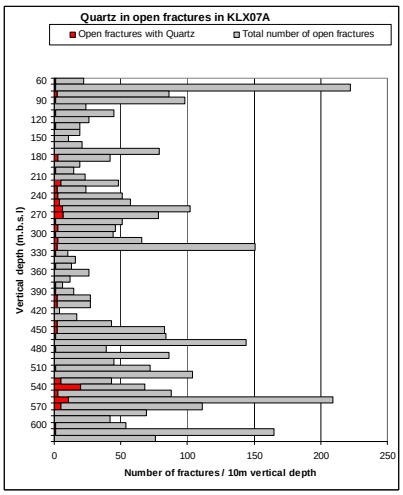
Quartz in open fractures in KLX07A
Open fractures with Quartz
Total number of open fractures
Vertical depth (m.b.s.l)
Number of fractures / 10m vertical depth

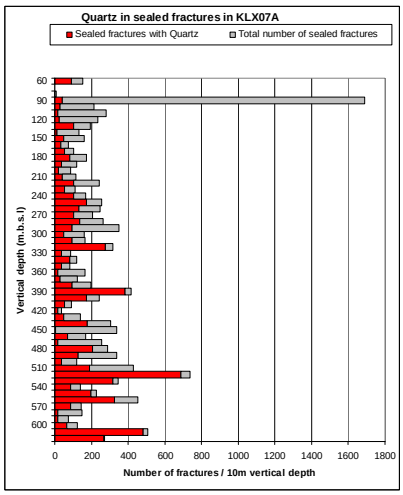
Quartz in sealed fractures in KLX07A
Sealed fractures with Quartz
Total number of sealed fractures
Vertical depth (m.b.s.l)
Number of fractures / 10m vertical depth

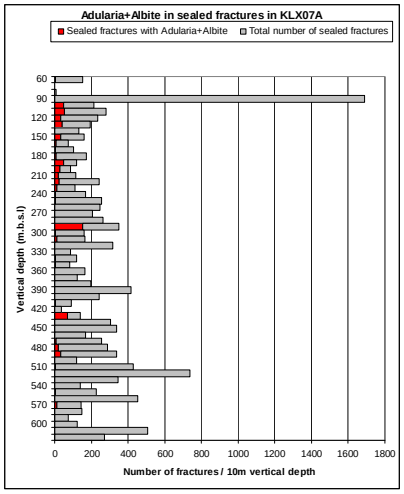
Adularia+Albite in sealed fractures in KLX07A
Sealed fractures with Adularia+Albite
Total number of sealed fractures
Vertical depth (m.b.s.l)
Number of fractures / 10m vertical depth

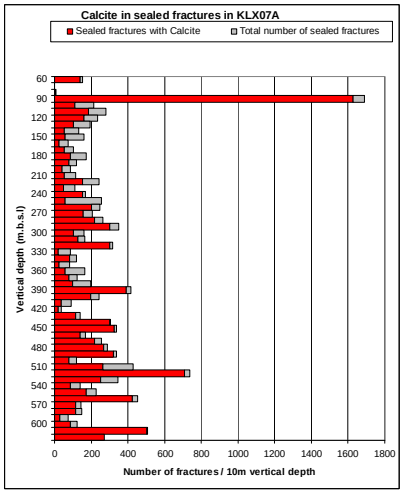
Calcite in sealed fractures in KLX07A
Sealed fractures with Calcite
Total number of sealed fractures
Vertical depth (m.b.s.l)
Number of fractures / 10m vertical depth

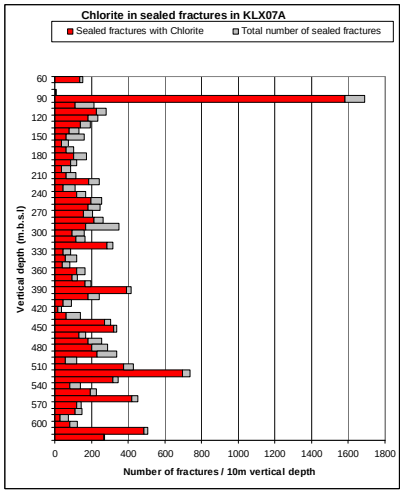
Chlorite in sealed fractures in KLX07A
Sealed fractures with Chlorite
Total number of sealed fractures
Vertical depth (m.b.s.l)
Number of fractures / 10m vertical depth

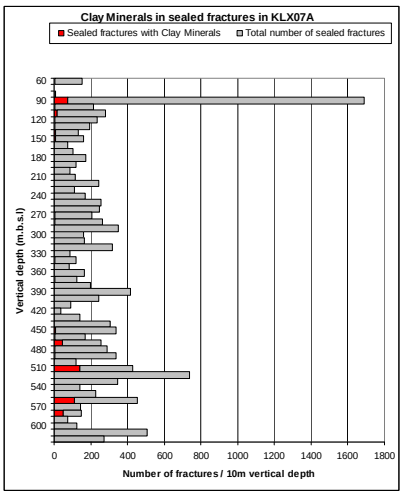
Clay Minerals in sealed fractures in KLX07A
Sealed fractures with Clay Minerals
Total number of sealed fractures
Vertical depth (m.b.s.l)
Number of fractures / 10m vertical depth

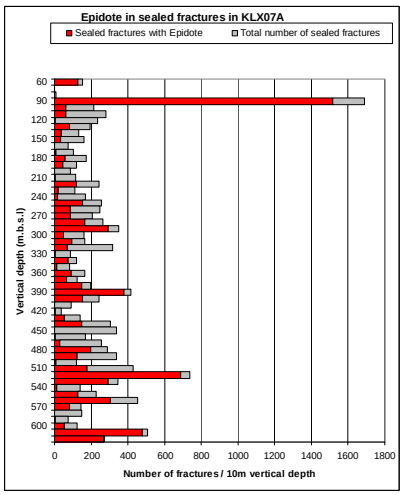
Epidote in sealed fractures in KLX07A
Sealed fractures with Epidote
Total number of sealed fractures
Vertical depth (m.b.s.l)
Number of fractures / 10m vertical depth

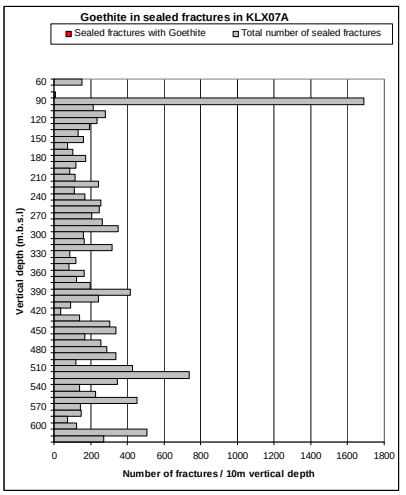
Goethite in sealed fractures in KLX07A
Sealed fractures with Goethite
Total number of sealed fractures
Vertical depth (m.b.s.l)
Number of fractures / 10m vertical depth

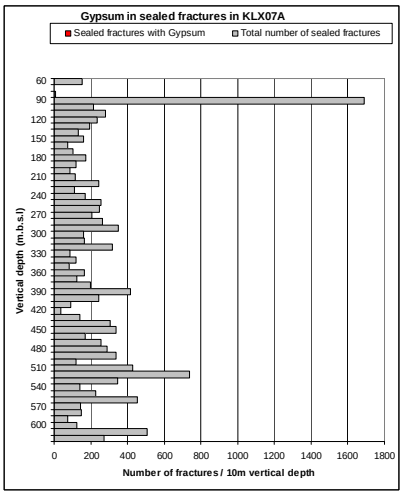
Gypsum in sealed fractures in KLX07A
Sealed fractures with Gypsum
Total number of sealed fractures
Vertical depth (m.b.s.l)
Number of fractures / 10m vertical depth

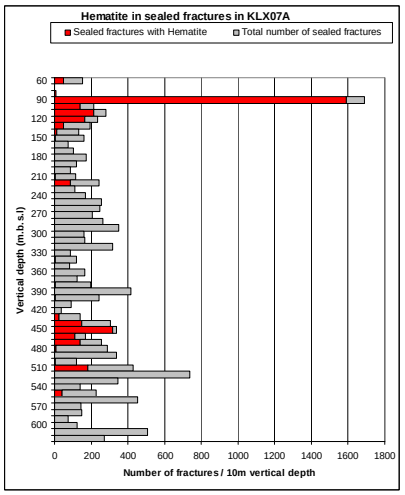
Hematite in sealed fractures in KLX07A
Sealed fractures with Hematite
Total number of sealed fractures
Vertical depth (m.b.s.l)
Number of fractures / 10m vertical depth

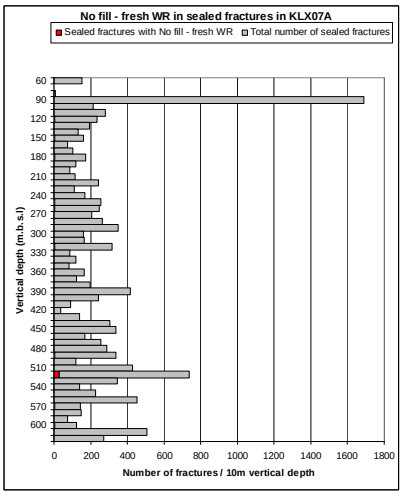
No fill - fresh WR in sealed fractures in KLX07A
Sealed fractures with No fill - fresh WR
Total number of sealed fractures
Vertical depth (m.b.s.l)
Number of fractures / 10m vertical depth

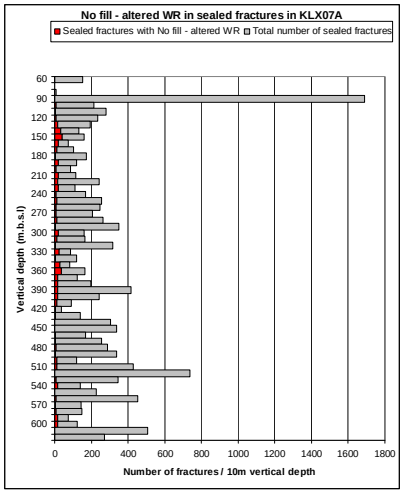
No fill - altered WR in sealed fractures in KLX07A
Sealed fractures with No fill - altered WR
Total number of sealed fractures
Vertical depth (m.b.s.l)
Number of fractures / 10m vertical depth

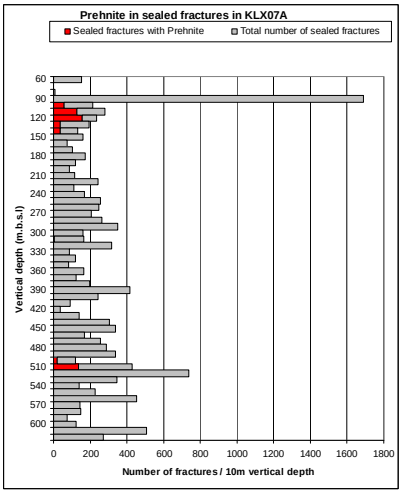
Prehnite in sealed fractures in KLX07A
Sealed fractures with Prehnite
Total number of sealed fractures
Vertical depth (m.b.s.l)
Number of fractures / 10m vertical depth

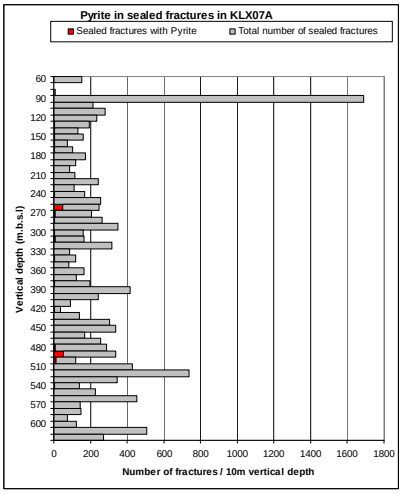
Pyrite in sealed fractures in KLX07A
Sealed fractures with Pyrite
Total number of sealed fractures
Vertical depth (m.b.s.l)
Number of fractures / 10m vertical depth

KLX07B

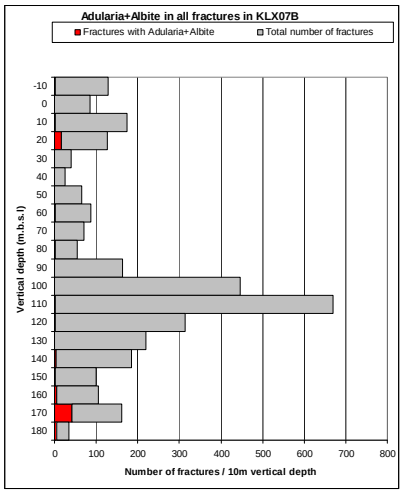
Adularia+Albite in all fractures in KLX07B
Fractures with Adularia+Albite
Total number of fractures
Vertical depth (m.b.s.l)
Number of fractures / 10m vertical depth

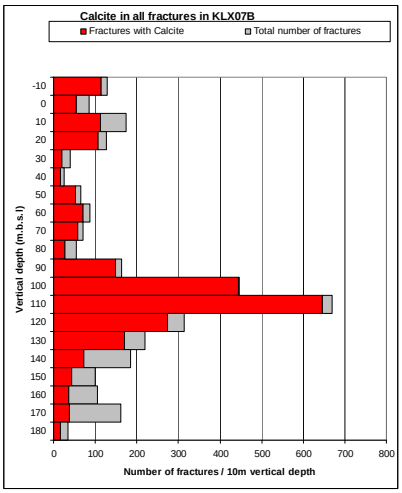
Calcite in all fractures in KLX07B
Fractures with Calcite
Total number of fractures
Vertical depth (m.b.s.l)
Number of fractures / 10m vertical depth

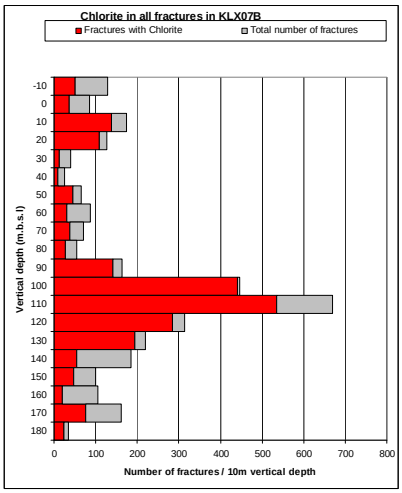
Chlorite in all fractures in KLX07B
Fractures with Chlorite
Total number of fractures
Vertical depth (m.b.s.l)
Number of fractures / 10m vertical depth

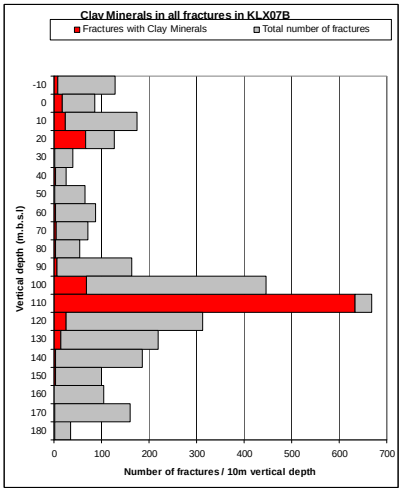
Clay Minerals in all fractures in KLX07B
Fractures with Clay Minerals
Total number of fractures
Vertical depth (m.b.s.l)
Number of fractures / 10m vertical depth

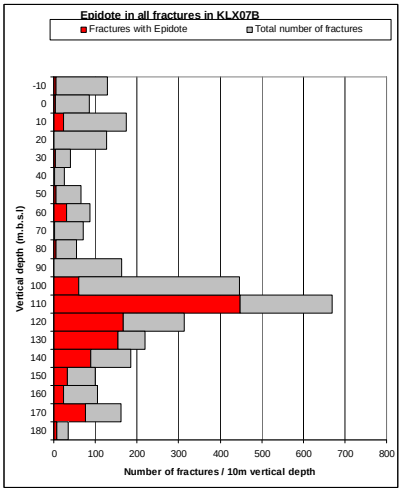
Epidote in all fractures in KLX07B
Fractures with Epidote
Total number of fractures
Vertical depth (m.b.s.l)
Number of fractures / 10m vertical depth

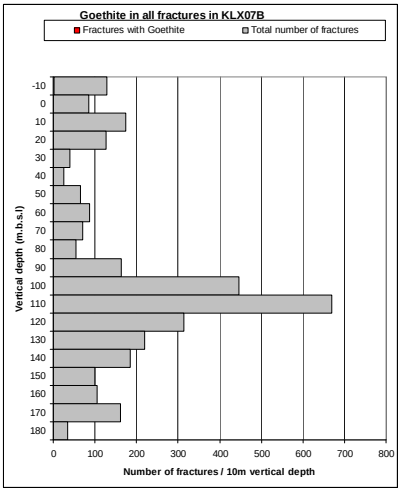
Goethite in all fractures in KLX07B
Fractures with Goethite
Total number of fractures
Vertical depth (m.b.s.l)
Number of fractures / 10m vertical depth

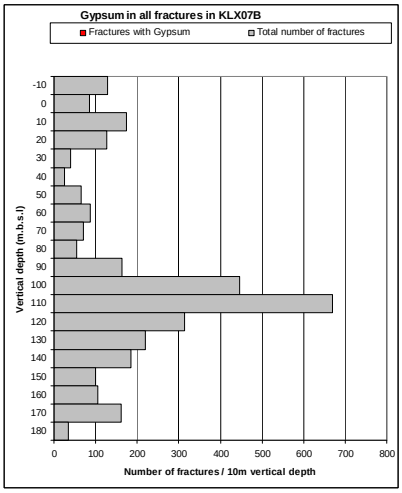
Gypsum in all fractures in KLX07B
Fractures with Gypsum
Total number of fractures
Vertical depth (m.b.s.l)
Number of fractures / 10m vertical depth

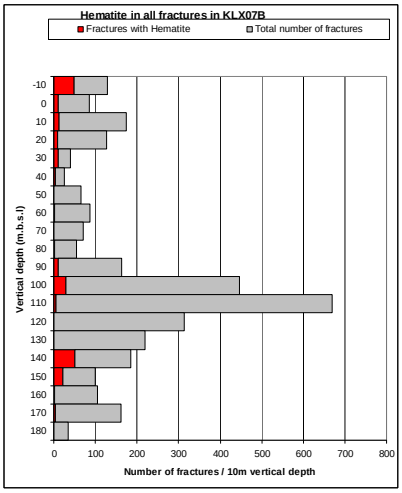
Hematite in all fractures in KLX07B
Fractures with Hematite
Total number of fractures
Vertical depth (m.b.s.l)
Number of fractures / 10m vertical depth

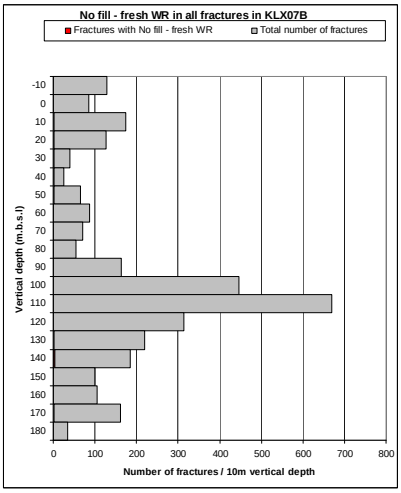
No fill - fresh WR in all fractures in KLX07B
Fractures with No fill - fresh WR
Total number of fractures
Vertical depth (m.b.s.l)
Number of fractures / 10m vertical depth

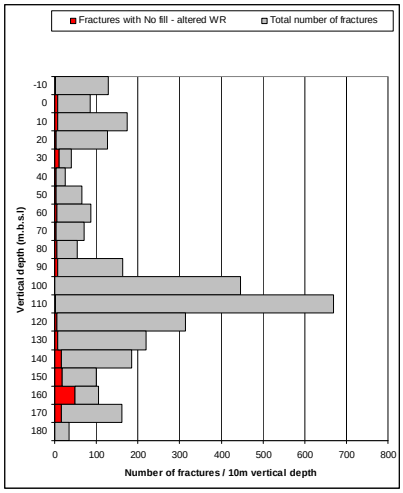
Fractures with No fill - altered WR
Total number of fractures
Vertical depth (m.b.s.l)
Number of fractures / 10m vertical depth

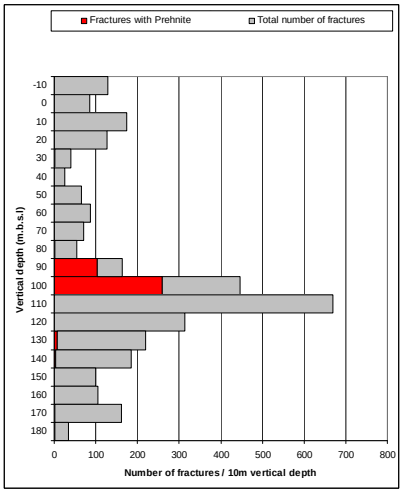
Fractures with Prehnite
Total number of fractures
Vertical depth (m.b.s.l)
Number of fractures / 10m vertical depth

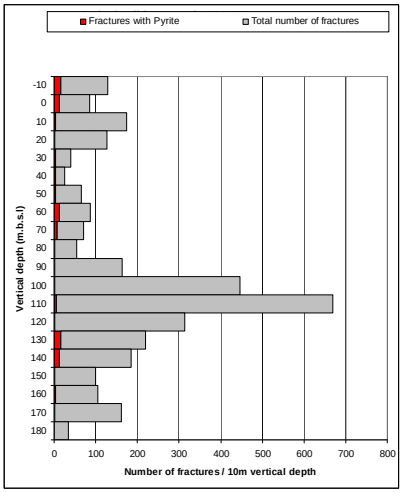
Fractures with Pyrite
Total number of fractures
Vertical depth (m.b.s.l)
Number of fractures / 10m vertical depth

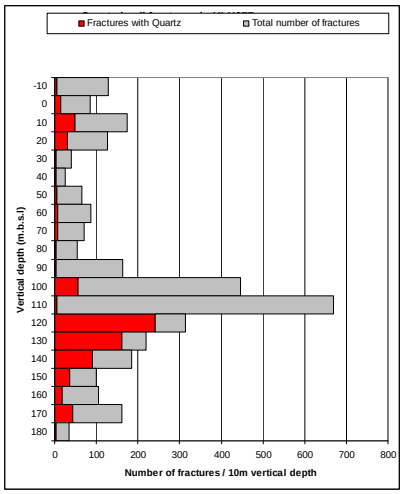
Fractures with Quartz
Total number of fractures
Vertical depth (m.b.s.l)
Number of fractures / 10m vertical depth

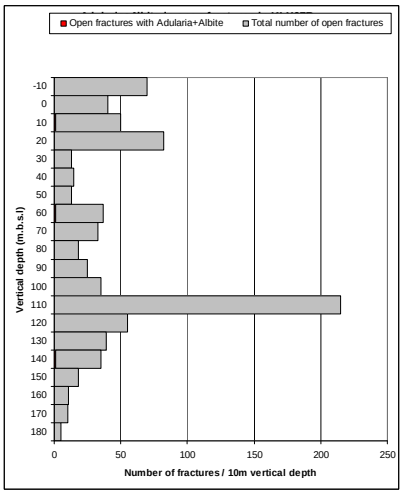
Open fractures with Adularia+Albite
Total number of open fractures
Vertical depth (m.b.s.l)
Number of fractures / 10m vertical depth

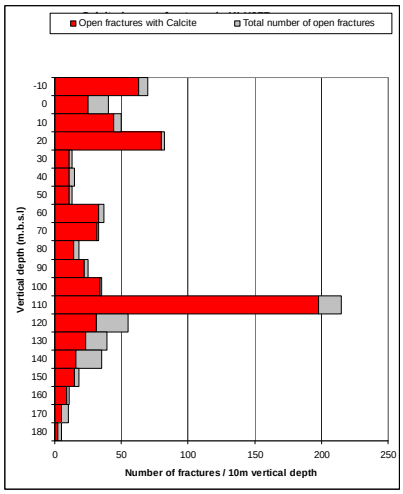
Open fractures with Calcite
Total number of open fractures
Vertical depth (m.b.s.l)
Number of fractures / 10m vertical depth

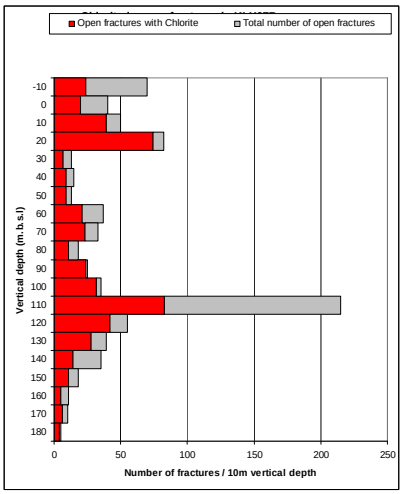
Open fractures with Chlorite
Total number of open fractures
Vertical depth (m.b.s.l)
Number of fractures / 10m vertical depth

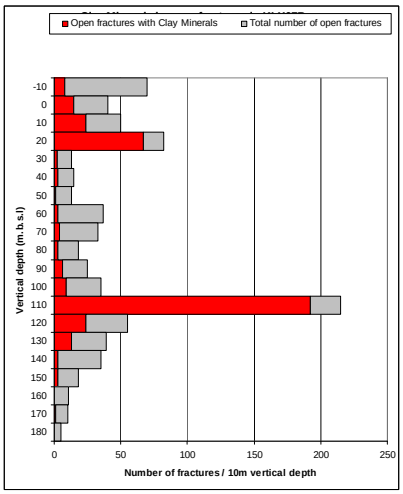
Open fractures with Clay Minerals
Total number of open fractures
Vertical depth (m.b.s.l)
Number of fractures / 10m vertical depth

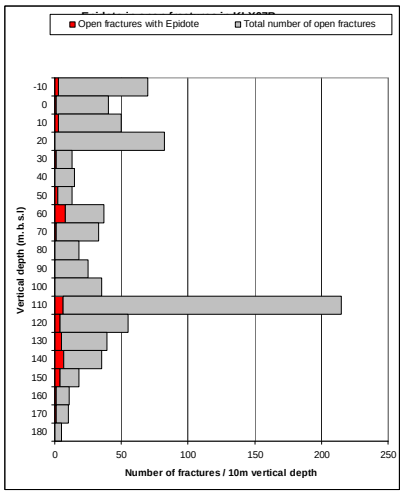
Open fractures with Epidote
Total number of open fractures
Vertical depth (m.b.s.l)
Number of fractures / 10m vertical depth

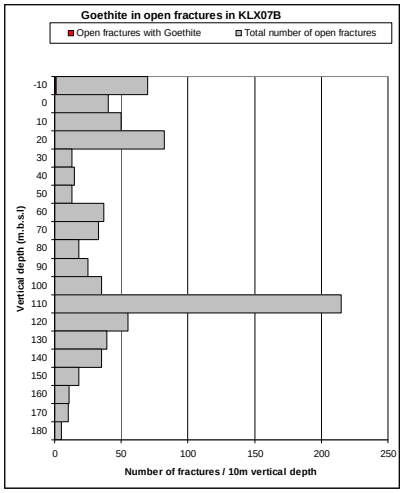
Goethite in open fractures in KLX07B
Open fractures with Goethite
Total number of open fractures
Vertical depth (m.b.s.l)
Number of fractures / 10m vertical depth

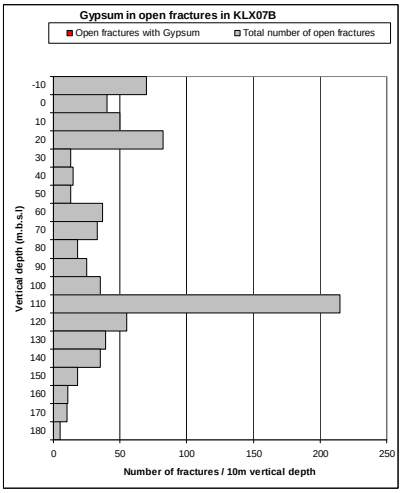
Gypsum in open fractures in KLX07B
Open fractures with Gypsum
Total number of open fractures
Vertical depth (m.b.s.l)
Number of fractures / 10m vertical depth

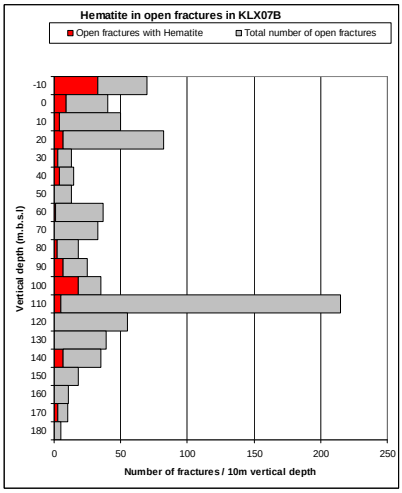
Hematite in open fractures in KLX07B
Open fractures with Hematite
Total number of open fractures
Vertical depth (m.b.s.l)
Number of fractures / 10m vertical depth

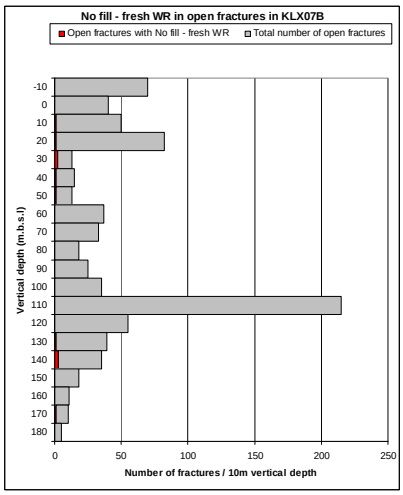
No fill - fresh WR in open fractures in KLX07B
Open fractures with No fill - fresh WR
Total number of open fractures
Vertical depth (m.b.s.l)
Number of fractures / 10m vertical depth

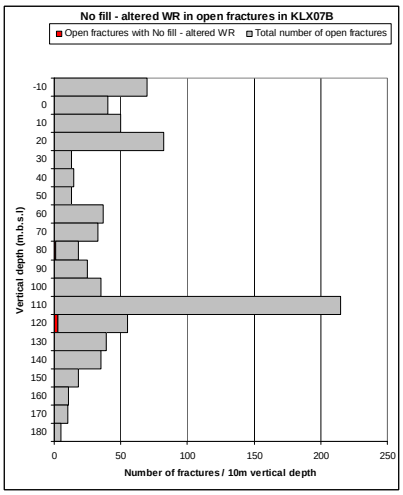
No fill - altered WR in open fractures in KLX07B
Open fractures with No fill - altered WR
Total number of open fractures
Vertical depth (m.b.s.l)
Number of fractures / 10m vertical depth

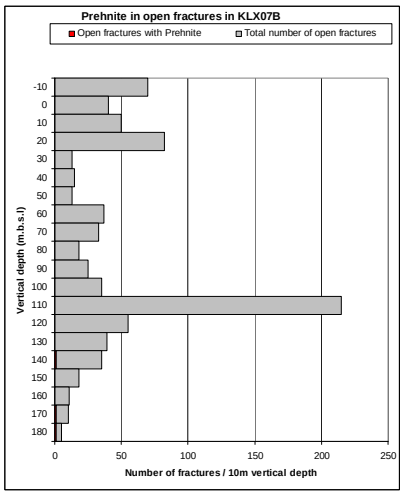
Prehnite in open fractures in KLX07B
Open fractures with Prehnite
Total number of open fractures
Vertical depth (m.b.s.l)
Number of fractures / 10m vertical depth

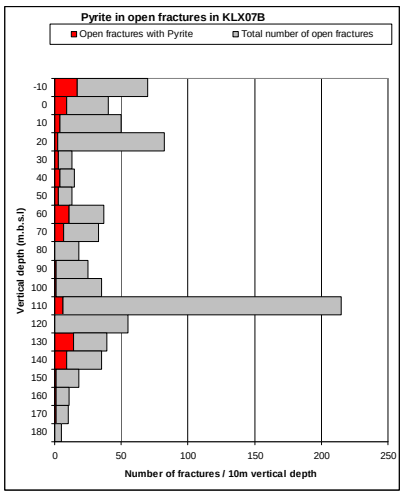
Pyrite in open fractures in KLX07B
Open fractures with Pyrite
Total number of open fractures
Vertical depth (m.b.s.l)
Number of fractures / 10m vertical depth

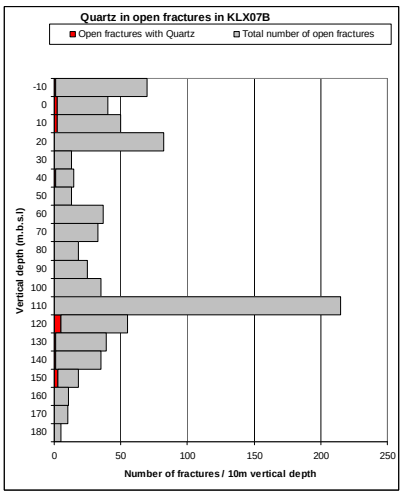
Quartz in open fractures in KLX07B
Open fractures with Quartz
Total number of open fractures
Vertical depth (m.b.s.l)
Number of fractures / 10m vertical depth

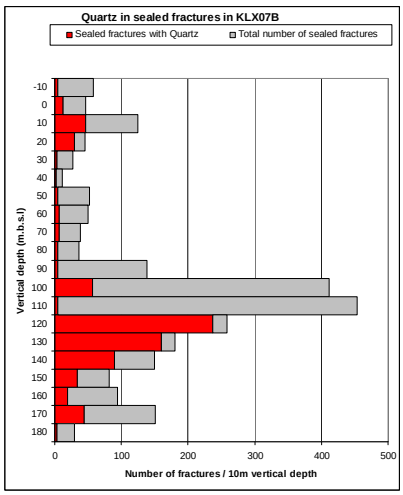
Quartz in sealed fractures in KLX07B
Sealed fractures with Quartz
Total number of sealed fractures
Vertical depth (m.b.s.l)
Number of fractures / 10m vertical depth

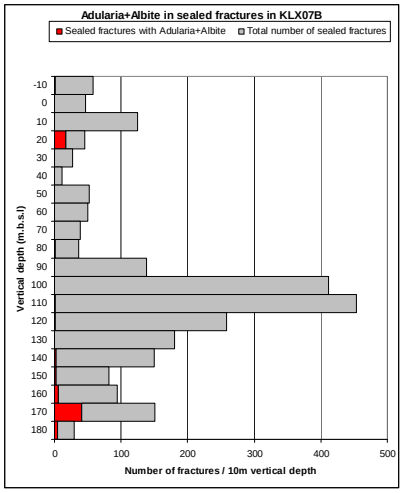
Adularia+Albite in sealed fractures in KLX07B
Sealed fractures with Adularia+Albite
Total number of sealed fractures
Vertical depth (m.b.s.l)
Number of fractures / 10m vertical depth

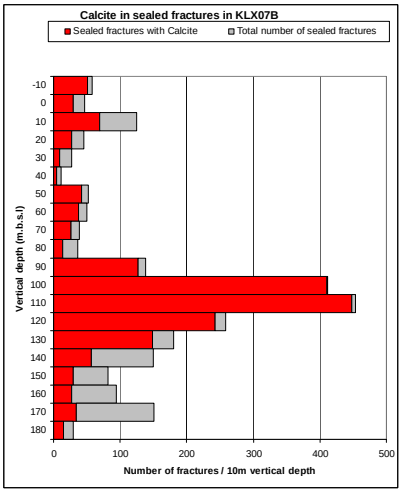
Calcite in sealed fractures in KLX07B
Sealed fractures with Calcite
Total number of sealed fractures
Vertical depth (m.b.s.l)
Number of fractures / 10m vertical depth

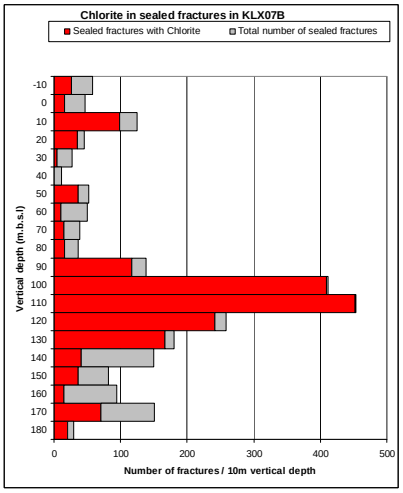
Chlorite in sealed fractures in KLX07B
Sealed fractures with Chlorite
Total number of sealed fractures
Vertical depth (m.b.s.l)
Number of fractures / 10m vertical depth

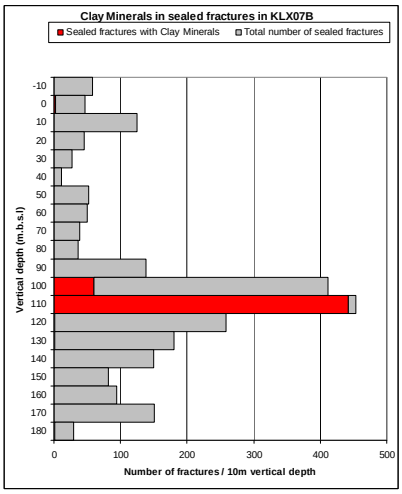
Clay Minerals in sealed fractures in KLX07B
Sealed fractures with Clay Minerals
Total number of sealed fractures
Vertical depth (m.b.s.l)
Number of fractures / 10m vertical depth

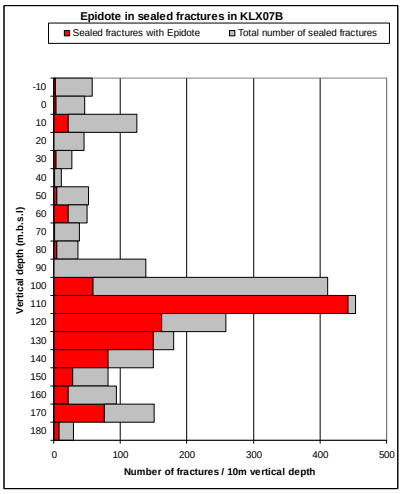
Epidote in sealed fractures in KLX07B
Sealed fractures with Epidote
Total number of sealed fractures
Vertical depth (m.b.s.l)
Number of fractures / 10m vertical depth

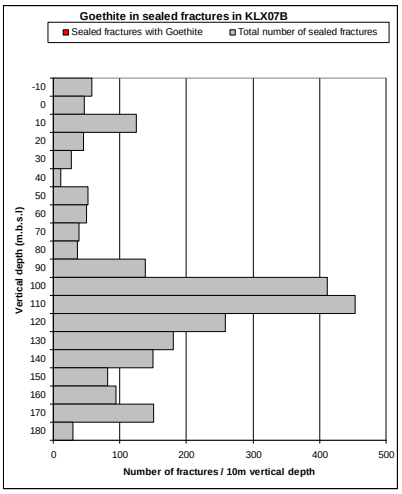
Goethite in sealed fractures in KLX07B
Sealed fractures with Goethite
Total number of sealed fractures
Vertical depth (m.b.s.l)
Number of fractures / 10m vertical depth

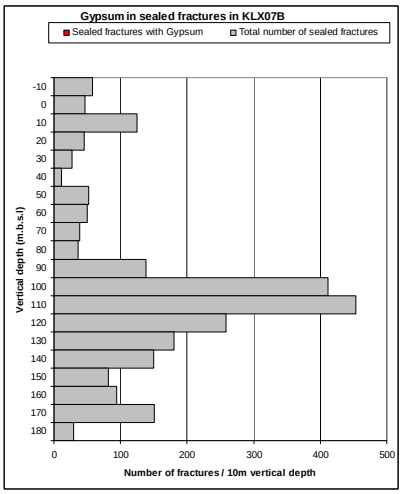
Gypsum in sealed fractures in KLX07B
Sealed fractures with Gypsum
Total number of sealed fractures
Vertical depth (m.b.s.l)
Number of fractures / 10m vertical depth

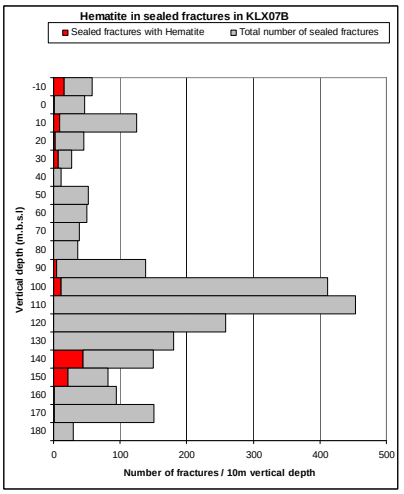
Hematite in sealed fractures in KLX07B
Sealed fractures with Hematite
Total number of sealed fractures
Vertical depth (m.b.s.l)
Number of fractures / 10m vertical depth

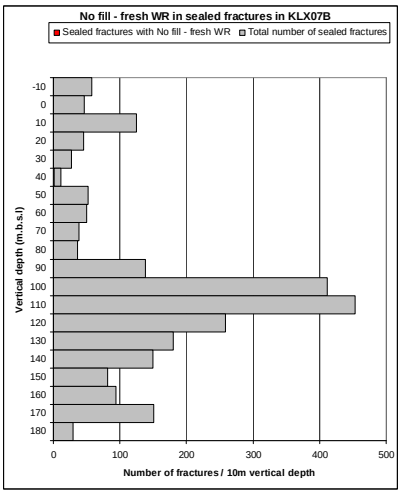
No fill - fresh WR in sealed fractures in KLX07B
Sealed fractures with No fill - fresh WR
Total number of sealed fractures
Vertical depth (m.b.s.l)
Number of fractures / 10m vertical depth

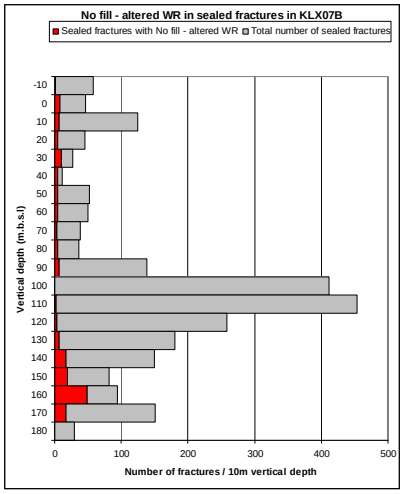
No fill - altered WR in sealed fractures in KLX07B
Sealed fractures with No fill - altered WR
Total number of sealed fractures
Vertical depth (m.b.s.l)
-10
0
10
20
30
40
50
60
70
80
90
100
110
120
130
140
150
160
170
180
0
100
200
300
400
500
Number of fractures / 10m vertical depth

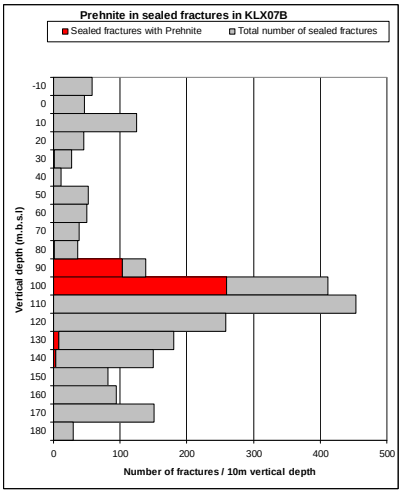
Prehnite in sealed fractures in KLX07B
Sealed fractures with Prehnite
Total number of sealed fractures
Vertical depth (m.b.s.l)
-10
0
10
20
30
40
50
60
70
80
90
100
110
120
130
140
150
160
170
180
0
100
200
300
400
500
Number of fractures / 10m vertical depth

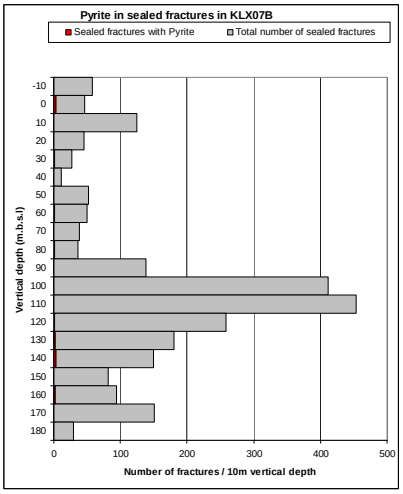
Pyrite in sealed fractures in KLX07B
Sealed fractures with Pyrite
Total number of sealed fractures
Vertical depth (m.b.s.l)
-10
0
10
20
30
40
50
60
70
80
90
100
110
120
130
140
150
160
170
180
0
100
200
300
400
500
Number of fractures / 10m vertical depth

KLX08

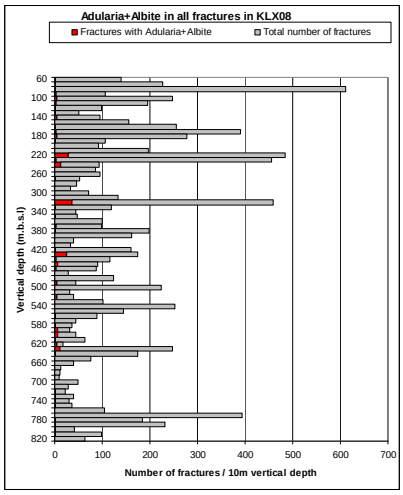
Adularia+Albite in all fractures in KLX08
Fractures with Adularia+Albite
Total number of fractures
Vertical depth (m.b.s.l)
Number of fractures / 10m vertical depth

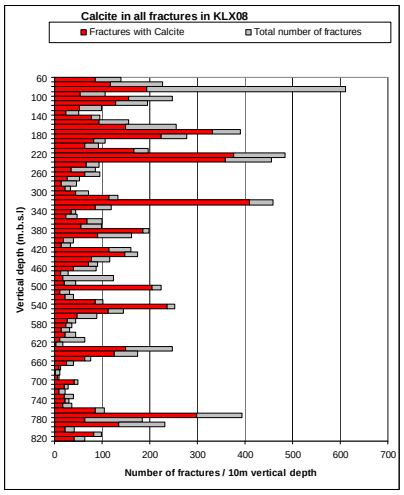
Calcite in all fractures in KLX08
Fractures with Calcite
Total number of fractures
Vertical depth (m.b.s.l)
Number of fractures / 10m vertical depth

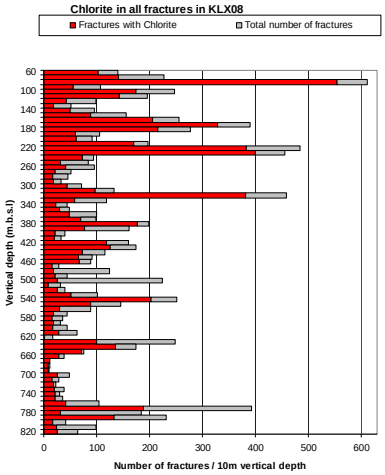
Chlorite in all fractures in KLX08
Fractures with Chlorite
Total number of fractures
Vertical depth (m.b.s.l)
Number of fractures / 10m vertical depth

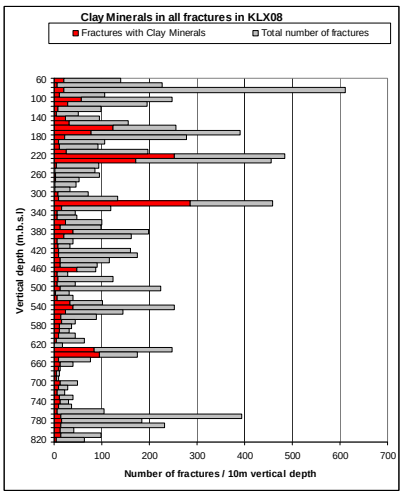
Clay Minerals in all fractures in KLX08
Fractures with Clay Minerals
Total number of fractures
Vertical depth (m.b.s.l)
Number of fractures / 10m vertical depth

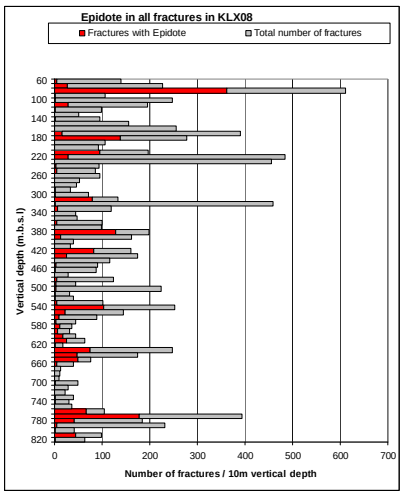
Epidote in all fractures in KLX08
Fractures with Epidote
Total number of fractures
Vertical depth (m.b.s.l)
Number of fractures / 10m vertical depth

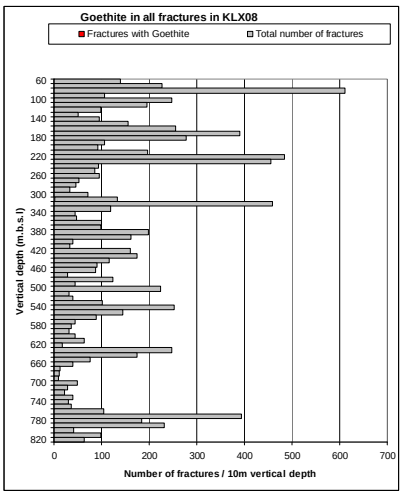
Goethite in all fractures in KLX08
Fractures with Goethite
Total number of fractures
Vertical depth (m.b.s.l)
Number of fractures / 10m vertical depth

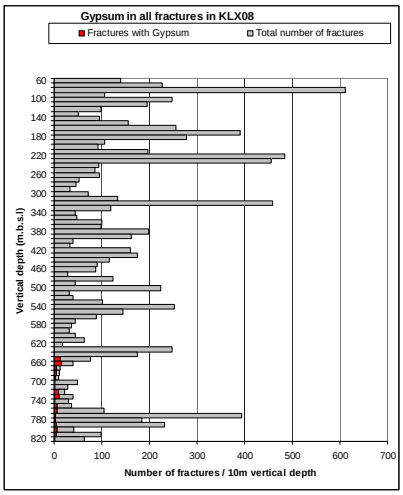
Gypsum in all fractures in KLX08
Fractures with Gypsum
Total number of fractures
Vertical depth (m.b.s.l)
Number of fractures / 10m vertical depth

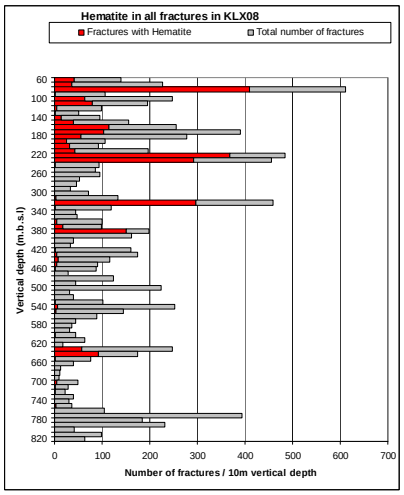
Hematite in all fractures in KLX08
Fractures with Hematite
Total number of fractures
Vertical depth (m.b.s.l)
Number of fractures / 10m vertical depth

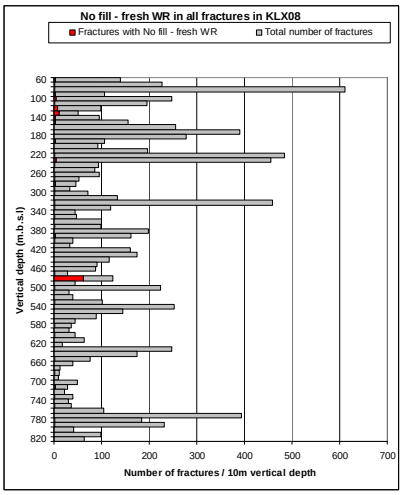
No fill - fresh WR in all fractures in KLX08
Fractures with No fill - fresh WR
Total number of fractures
Vertical depth (m.b.s.l)
Number of fractures / 10m vertical depth

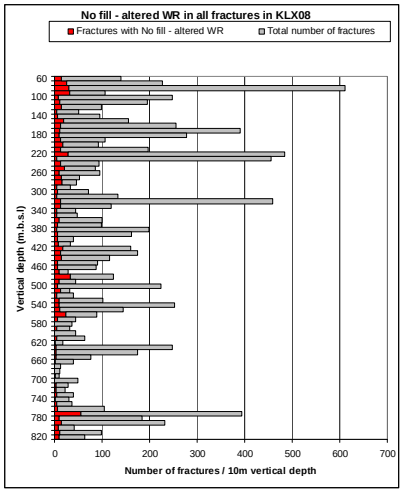
No fill - altered WR in all fractures in KLX08
Fractures with No fill - altered WR
Total number of fractures
Vertical depth (m.b.s.l)
Number of fractures / 10m vertical depth

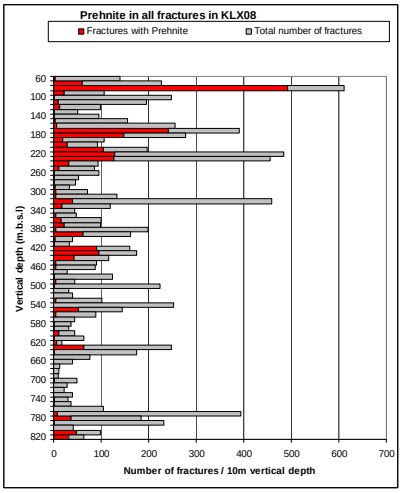
Prehnite in all fractures in KLX08
Fractures with Prehnite
Total number of fractures
Vertical depth (m.b.s.l)
Number of fractures / 10m vertical depth

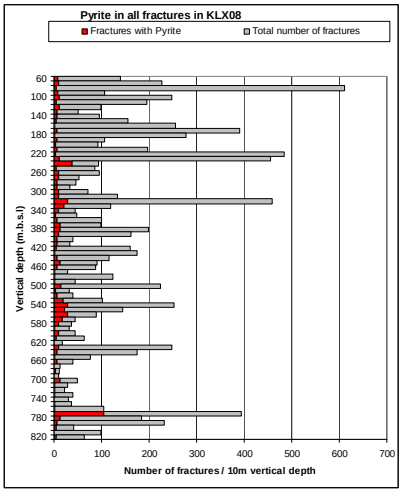
Pyrite in all fractures in KLX08
Fractures with Pyrite
Total number of fractures
Vertical depth (m.b.s.l)
Number of fractures / 10m vertical depth

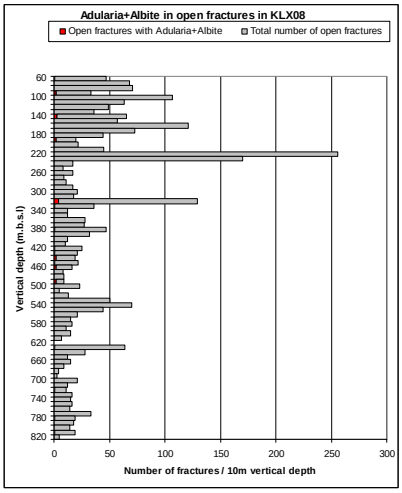
Adularia+Albite in open fractures in KLX08
Open fractures with Adularia+Albite
Total number of open fractures
Vertical depth (m.b.s.l)
Number of fractures / 10m vertical depth

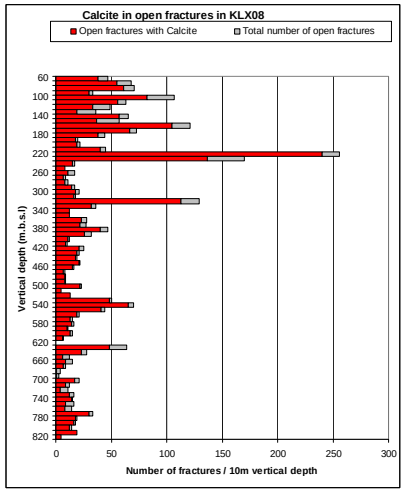
Calcite in open fractures in KLX08
Open fractures with Calcite
Total number of open fractures
Vertical depth (m.b.s.l)
Number of fractures / 10m vertical depth

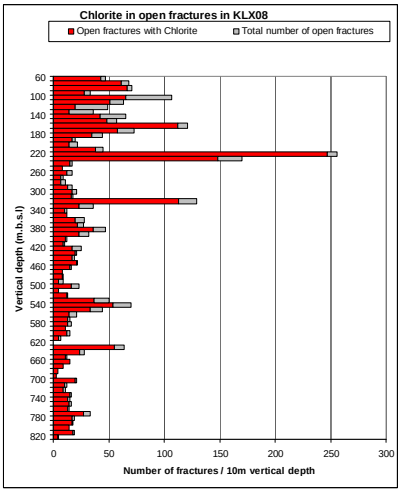
Chlorite in open fractures in KLX08
Open fractures with Chlorite
Total number of open fractures
Vertical depth (m.b.s.l)
Number of fractures / 10m vertical depth

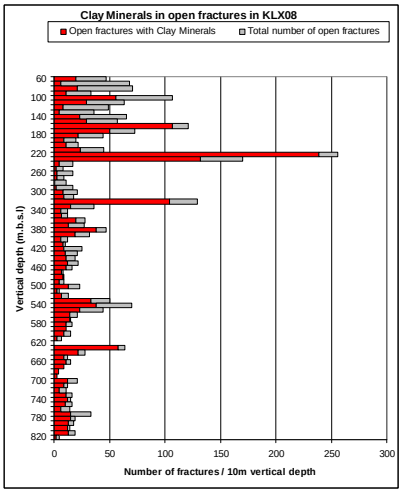
Clay Minerals in open fractures in KLX08
Open fractures with Clay Minerals
Total number of open fractures
Vertical depth (m.b.s.l)
Number of fractures / 10m vertical depth

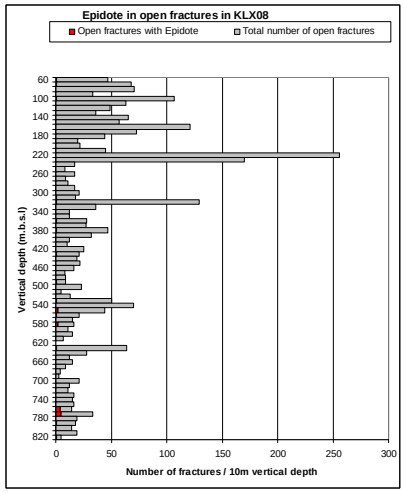
Epidote in open fractures in KLX08
Open fractures with Epidote
Total number of open fractures
Vertical depth (m.b.s.l)
Number of fractures / 10m vertical depth

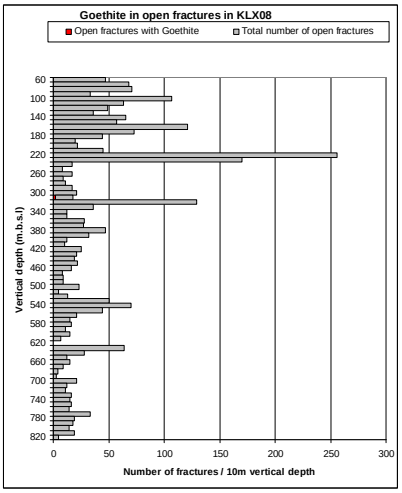
Goethite in open fractures in KLX08
Open fractures with Goethite
Total number of open fractures
Vertical depth (m.b.s.l)
Number of fractures / 10m vertical depth

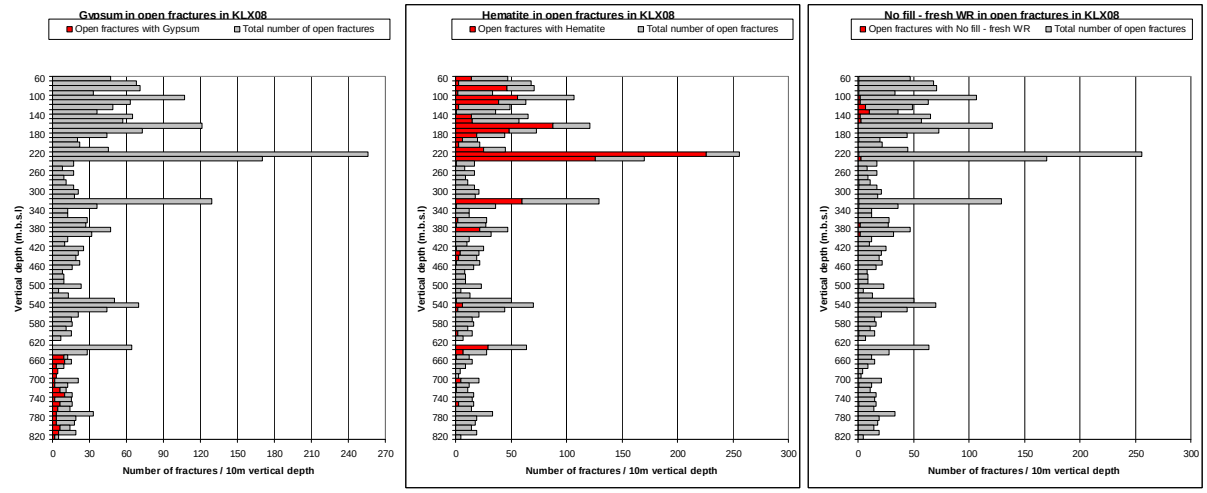
Gypsum in open fractures in KLX08
Open fractures with Gypsum
Total number of open fractures
Hematite in open fractures in KLX08
Open fractures with Hematite
Total number of open fractures
No fill - fresh WR in open fractures in KLX08
Open fractures with No fill - fresh WR
Total number of open fractures
Vertical depth (m.b.s.l)
Number of fractures / 10m vertical depth

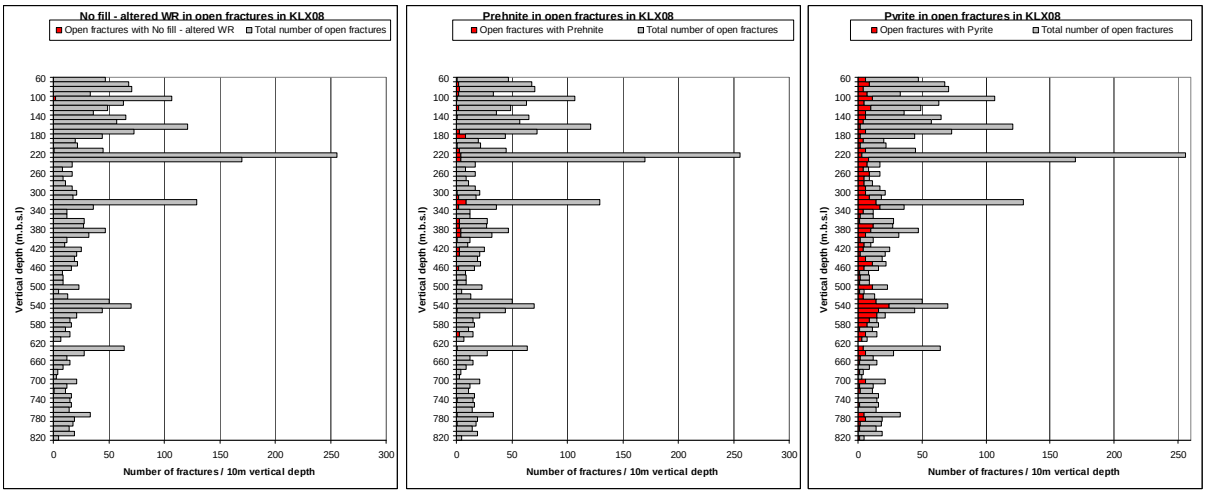
No fill - altered WR in open fractures in KLX08
Open fractures with No fill - altered WR
Total number of open fractures
Prehnite in open fractures in KLX08
Open fractures with Prehnite
Total number of open fractures
Pyrite in open fractures in KLX08
Open fractures with Pyrite
Total number of open fractures
Vertical depth (m.b.s.l)
Number of fractures / 10m vertical depth

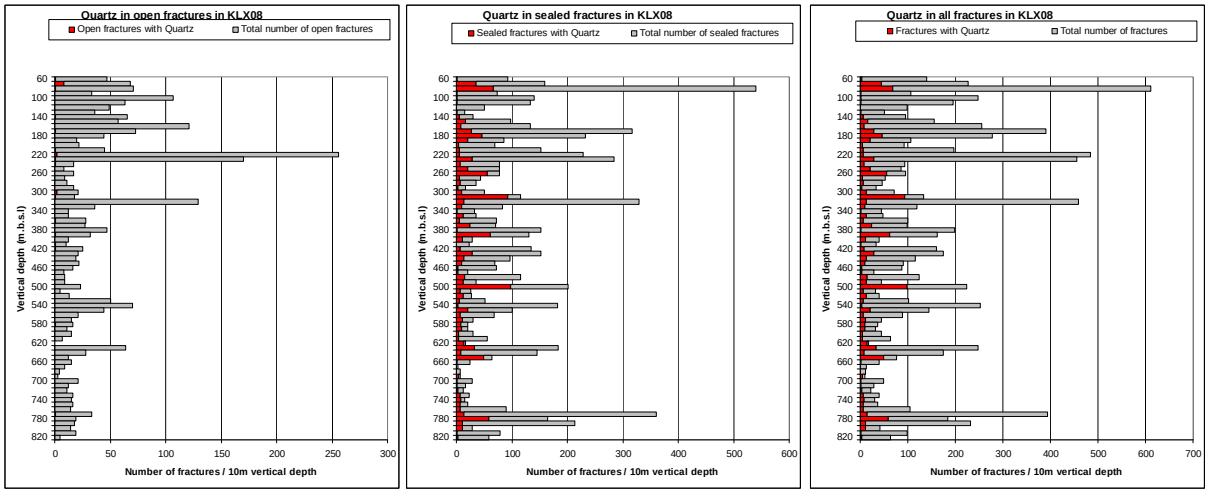
Quartz in open fractures in KLX08
Open fractures with Quartz
Total number of open fractures
Quartz in sealed fractures in KLX08
Sealed fractures with Quartz
Total number of sealed fractures
Quartz in all fractures in KLX08
Fractures with Quartz
Total number of fractures
Vertical depth (m.b.s.l)
Number of fractures / 10m vertical depth

i

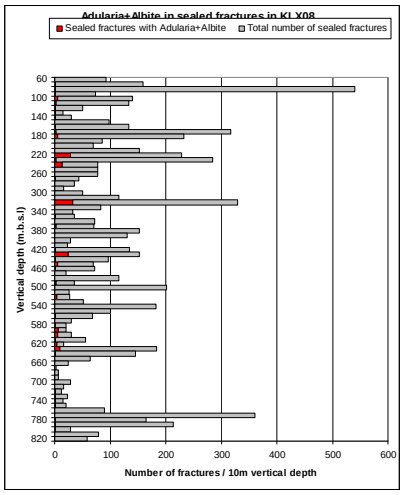
Adularia+Albite in sealed fractures in KLX08
Sealed fractures with Adularia+Albite
Total number of sealed fractures
Vertical depth (m.b.s.l)
Number of fractures / 10m vertical depth

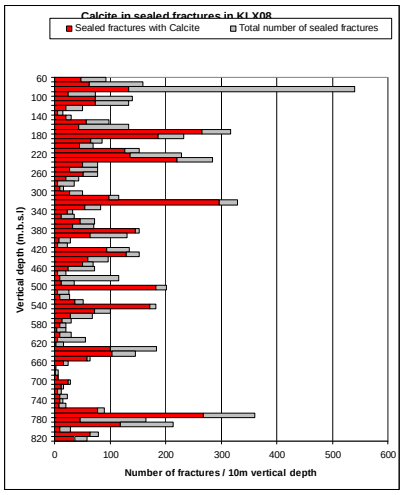
Calcite in sealed fractures in KLX08
Sealed fractures with Calcite
Total number of sealed fractures
Vertical depth (m.b.s.l)
Number of fractures / 10m vertical depth

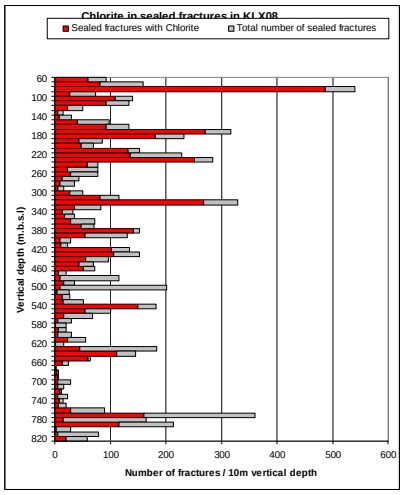
Chlorite in sealed fractures in KLX08
Sealed fractures with Chlorite
Total number of sealed fractures
Vertical depth (m.b.s.l)
Number of fractures / 10m vertical depth

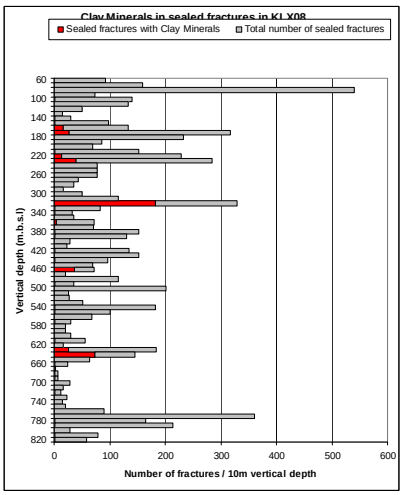
Clay Minerals in sealed fractures in KLX08
Sealed fractures with Clay Minerals
Total number of sealed fractures
Vertical depth (m.b.s.l)
Number of fractures / 10m vertical depth

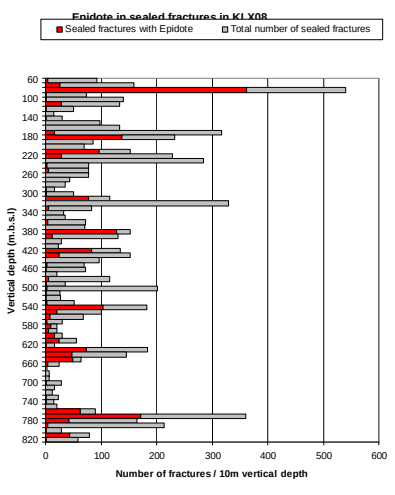
Epidote in sealed fractures in KLX08
Sealed fractures with Epidote
Total number of sealed fractures
Vertical depth (m.b.s.l)
Number of fractures / 10m vertical depth

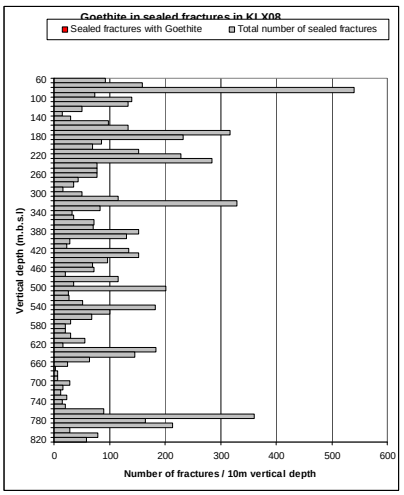
Goethite in sealed fractures in KLX08
Sealed fractures with Goethite
Total number of sealed fractures
Vertical depth (m.b.s.l)
Number of fractures / 10m vertical depth

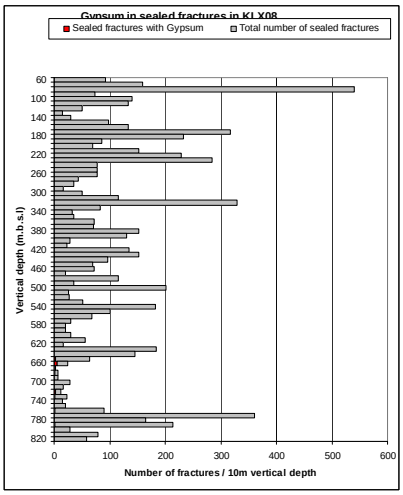
Gypsum in sealed fractures in KLX08
Sealed fractures with Gypsum
Total number of sealed fractures
Vertical depth (m.b.s.l)
Number of fractures / 10m vertical depth

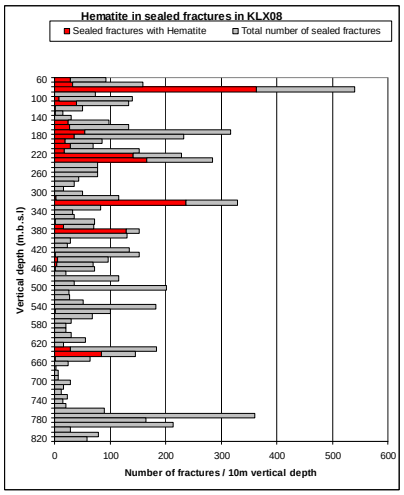
Hematite in sealed fractures in KLX08
Sealed fractures with Hematite
Total number of sealed fractures
Vertical depth (m.b.s.l)
Number of fractures / 10m vertical depth

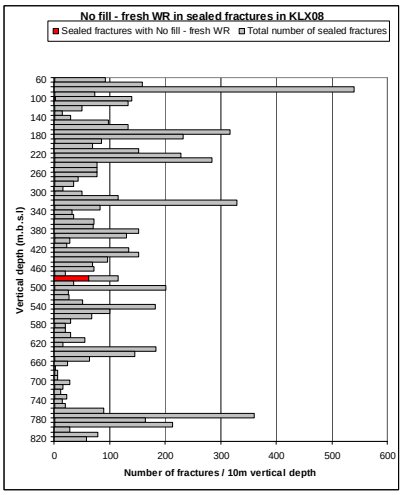
No fill - fresh WR in sealed fractures in KLX08
Sealed fractures with No fill - fresh WR
Total number of sealed fractures
Vertical depth (m.b.s.l)
Number of fractures / 10m vertical depth

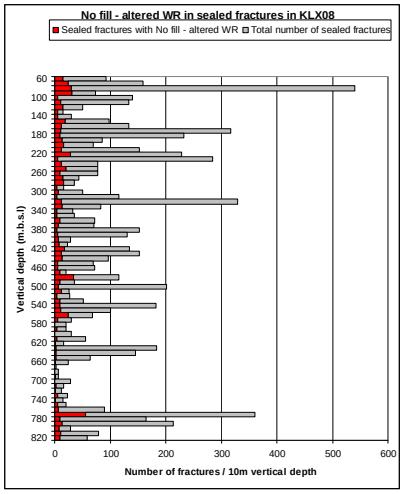
No fill - altered WR in sealed fractures in KLX08
Sealed fractures with No fill - altered WR
Total number of sealed fractures
Vertical depth (m.b.s.l)
Number of fractures / 10m vertical depth

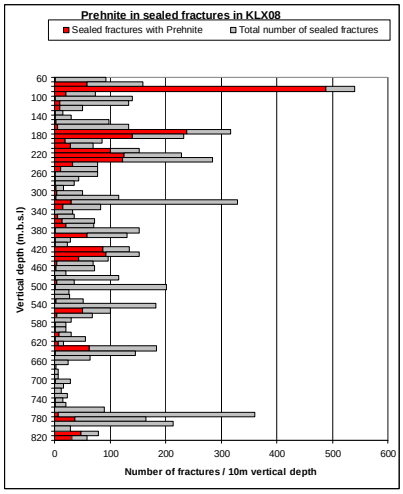
Prehnite in sealed fractures in KLX08
Sealed fractures with Prehnite
Total number of sealed fractures
Vertical depth (m.b.s.l)
Number of fractures / 10m vertical depth

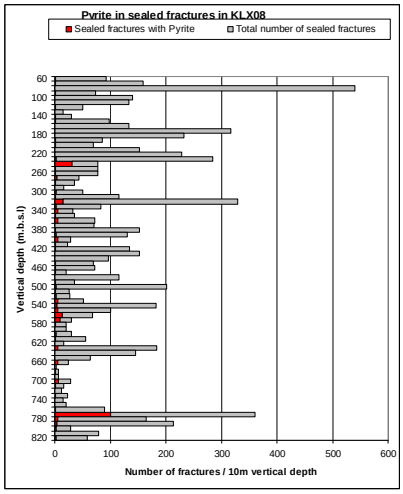
Pyrite in sealed fractures in KLX08
Sealed fractures with Pyrite
Total number of sealed fractures
Vertical depth (m.b.s.l)
Number of fractures / 10m vertical depth

KLX09

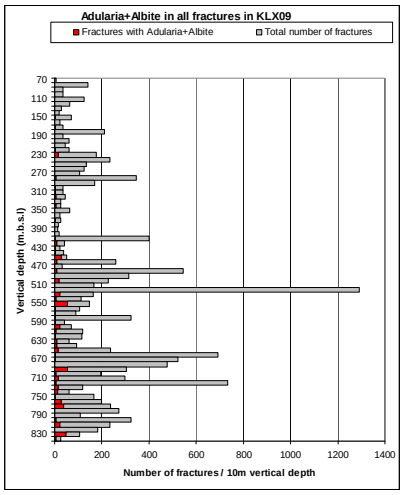
Adularia+Albite in all fractures in KLX09
Fractures with Adularia+Albite
Total number of fractures
Vertical depth (m.b.s.l)
Number of fractures / 10m vertical depth

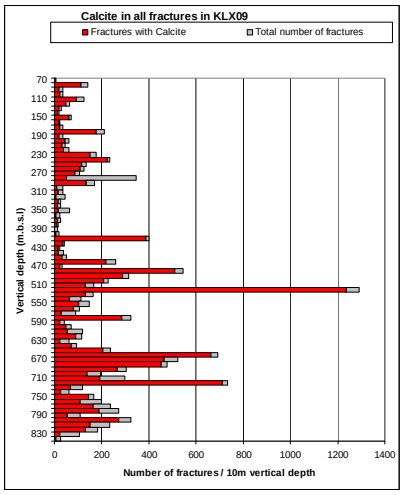
Calcite in all fractures in KLX09
Fractures with Calcite
Total number of fractures
Vertical depth (m.b.s.l)
Number of fractures / 10m vertical depth

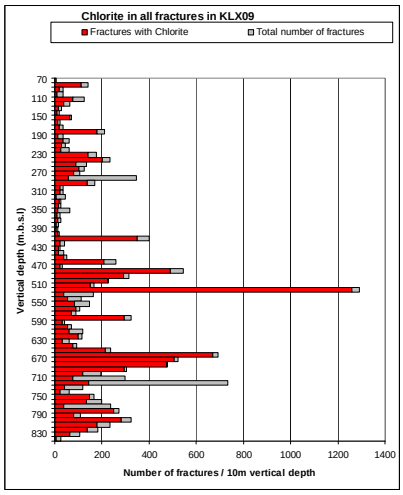
Chlorite in all fractures in KLX09
Fractures with Chlorite
Total number of fractures
Vertical depth (m.b.s.l)
Number of fractures / 10m vertical depth

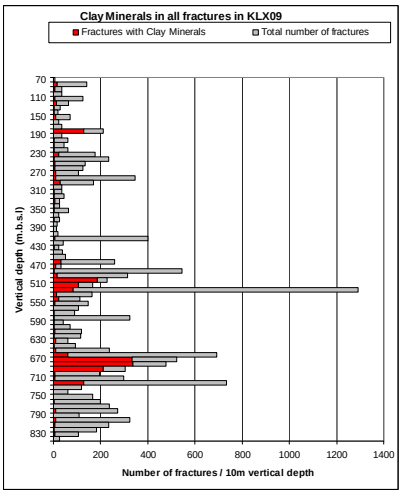
Clay Minerals in all fractures in KLX09
Fractures with Clay Minerals
Total number of fractures
Vertical depth (m.b.s.l)
Number of fractures / 10m vertical depth

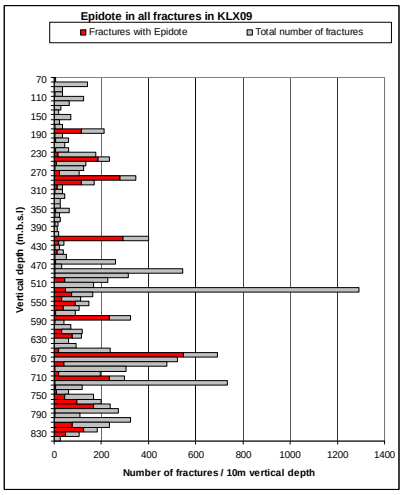
Epidote in all fractures in KLX09
Fractures with Epidote
Total number of fractures
Vertical depth (m.b.s.l)
Number of fractures / 10m vertical depth

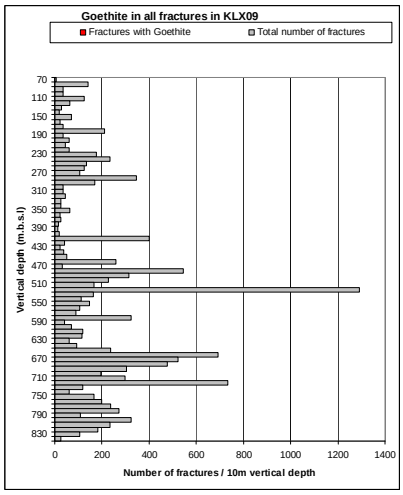
Goethite in all fractures in KLX09
Fractures with Goethite
Total number of fractures
Vertical depth (m.b.s.l)
Number of fractures / 10m vertical depth

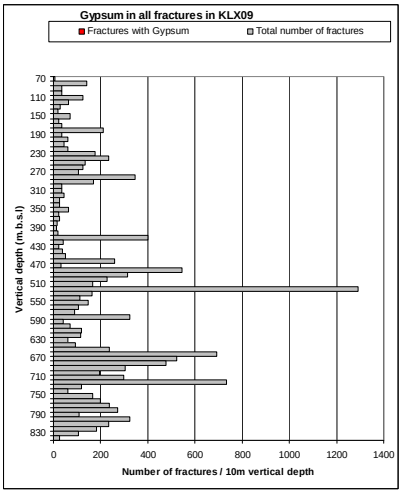
Gypsum in all fractures in KLX09
Fractures with Gypsum
Total number of fractures
Vertical depth (m.b.s.l)
Number of fractures / 10m vertical depth

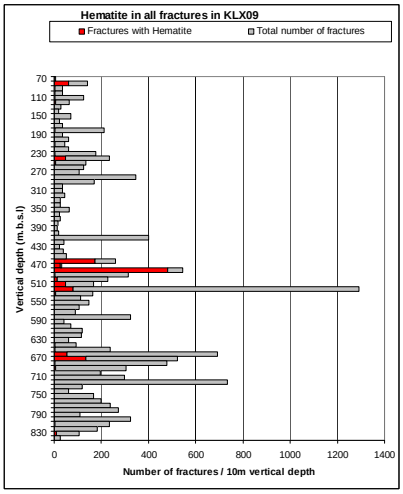
Hematite in all fractures in KLX09
Fractures with Hematite
Total number of fractures
Vertical depth (m.b.s.l)
Number of fractures / 10m vertical depth

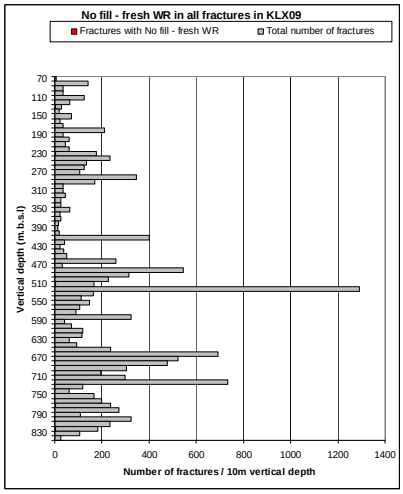
No fill - fresh WR in all fractures in KLX09
Fractures with No fill - fresh WR
Total number of fractures
Vertical depth (m.b.s.l)
Number of fractures / 10m vertical depth

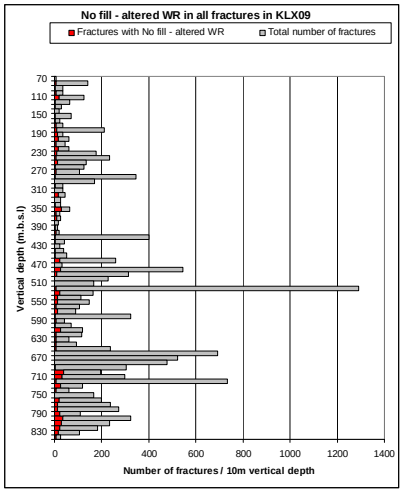
No fill - altered WR in all fractures in KLX09
Fractures with No fill - altered WR
Total number of fractures
Vertical depth (m.b.s.l)
Number of fractures / 10m vertical depth

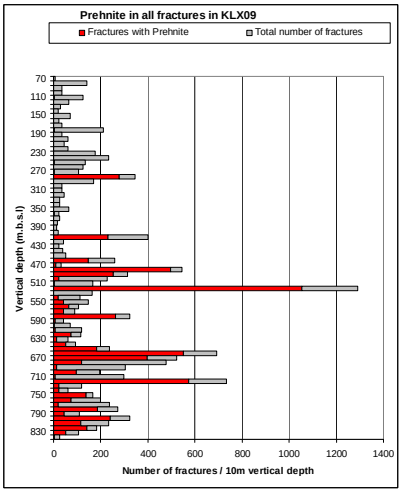
Prehnite in all fractures in KLX09
Fractures with Prehnite
Total number of fractures
Vertical depth (m.b.s.l)
Number of fractures / 10m vertical depth

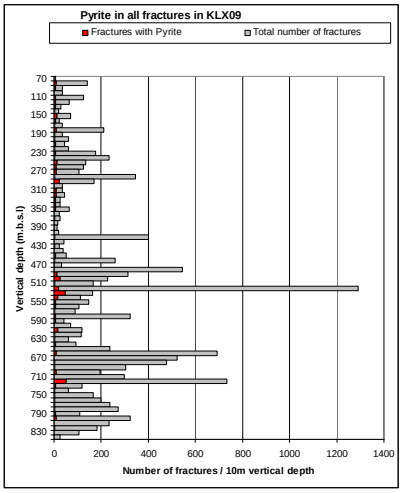
Pyrite in all fractures in KLX09
Fractures with Pyrite
Total number of fractures
Vertical depth (m.b.s.l)
Number of fractures / 10m vertical depth

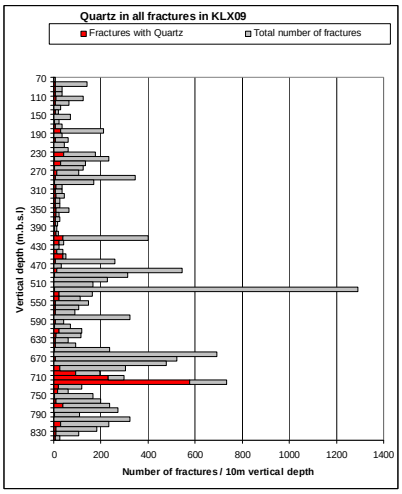
Quartz in all fractures in KLX09
Fractures with Quartz
Total number of fractures
Vertical depth (m.b.s.l)
Number of fractures / 10m vertical depth

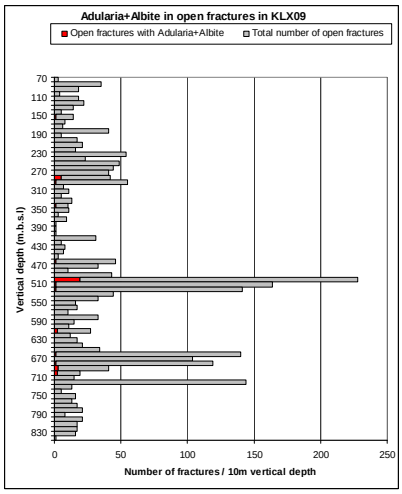
Adularia+Albite in open fractures in KLX09
Open fractures with Adularia+Albite
Total number of open fractures
Vertical depth (m.b.s.l)
Number of fractures / 10m vertical depth

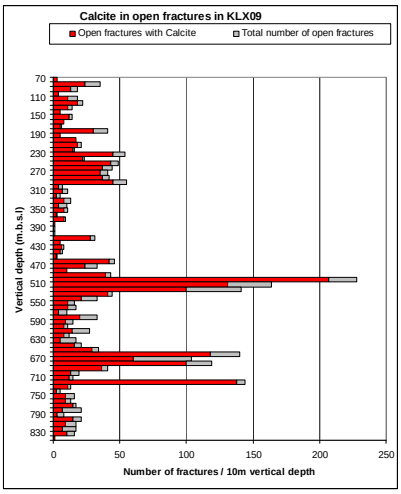
Calcite in open fractures in KLX09
Open fractures with Calcite
Total number of open fractures
Vertical depth (m.b.s.l)
Number of fractures / 10m vertical depth

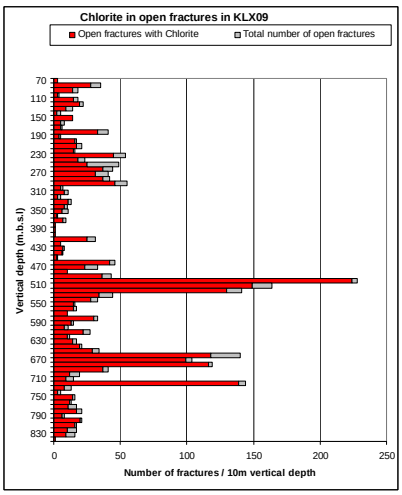
Chlorite in open fractures in KLX09
Open fractures with Chlorite
Total number of open fractures
Vertical depth (m.b.s.l)
Number of fractures / 10m vertical depth

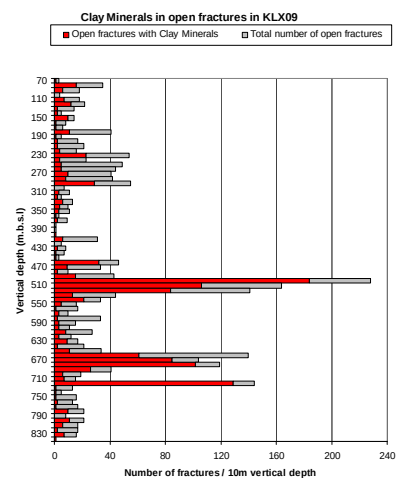
Clay Minerals in open fractures in KLX09
Open fractures with Clay Minerals
Total number of open fractures
Vertical depth (m.b.s.l)
Number of fractures / 10m vertical depth

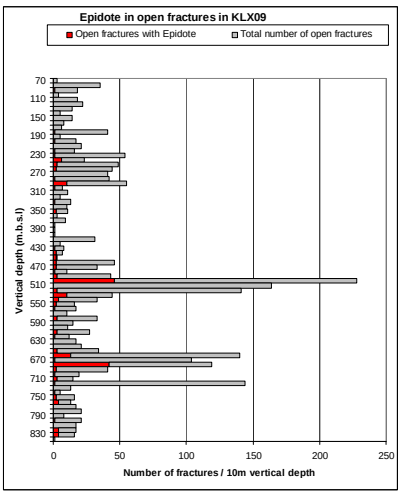
Epidote in open fractures in KLX09
Open fractures with Epidote
Total number of open fractures
Vertical depth (m.b.s.l)
Number of fractures / 10m vertical depth

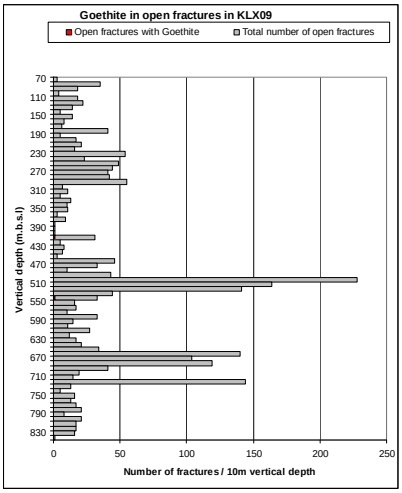
Goethite in open fractures in KLX09
Open fractures with Goethite
Total number of open fractures
Vertical depth (m.b.s.l)
Number of fractures / 10m vertical depth

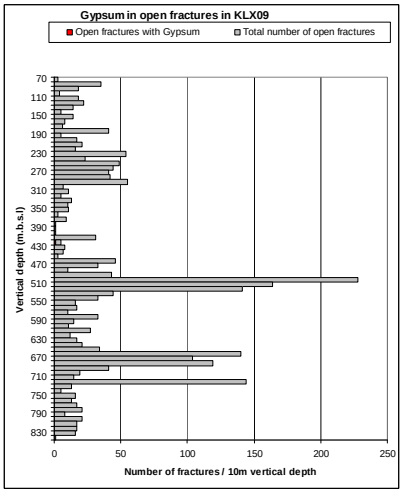
Gypsum in open fractures in KLX09
Open fractures with Gypsum
Total number of open fractures
Vertical depth (m.b.s.l)
Number of fractures / 10m vertical depth

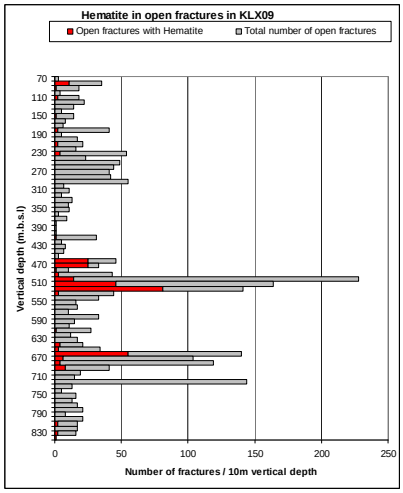
Hematite in open fractures in KLX09
Open fractures with Hematite
Total number of open fractures
Vertical depth (m.b.s.l)
Number of fractures / 10m vertical depth

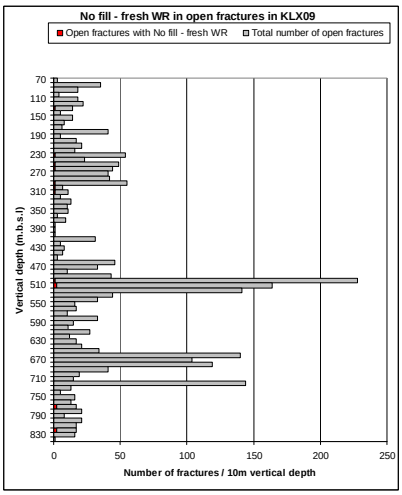
No fill - fresh WR in open fractures in KLX09
Open fractures with No fill - fresh WR
Total number of open fractures
Vertical depth (m.b.s.l)
Number of fractures / 10m vertical depth

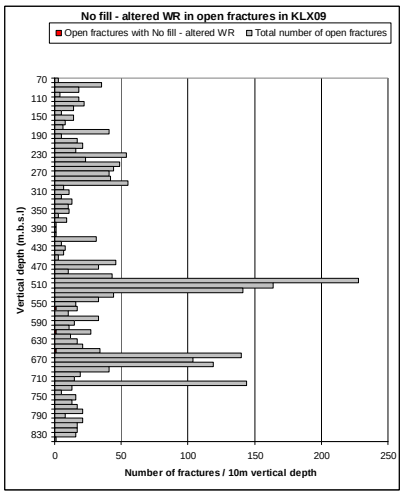
No fill - altered WR in open fractures in KLX09
Open fractures with No fill - altered WR
Total number of open fractures
Vertical depth (m.b.s.l)
Number of fractures / 10m vertical depth

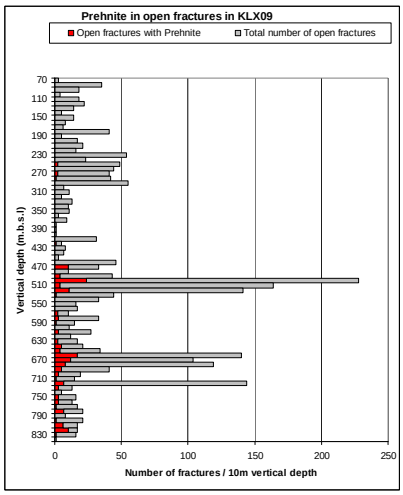
Prehnite in open fractures in KLX09
Open fractures with Prehnite
Total number of open fractures
Vertical depth (m.b.s.l)
Number of fractures / 10m vertical depth

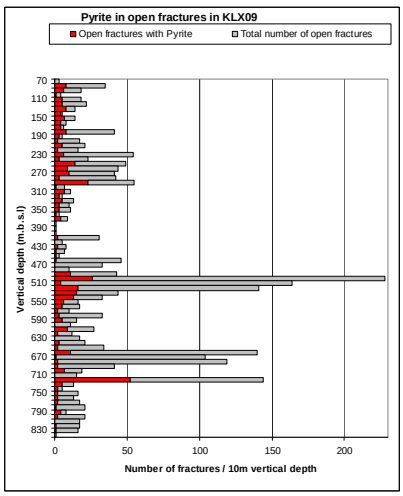
Pyrite in open fractures in KLX09
Open fractures with Pyrite
Total number of open fractures
Vertical depth (m.b.s.l)
Number of fractures / 10m vertical depth

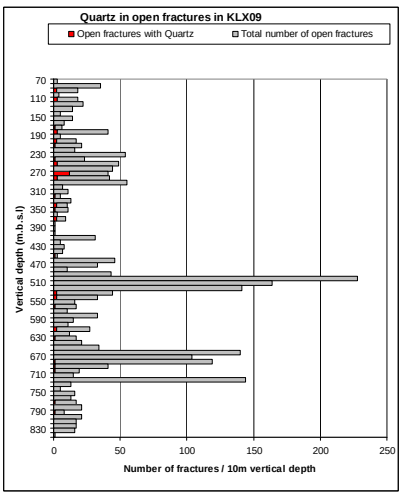
Quartz in open fractures in KLX09
Open fractures with Quartz
Total number of open fractures
Vertical depth (m.b.s.l)
Number of fractures / 10m vertical depth

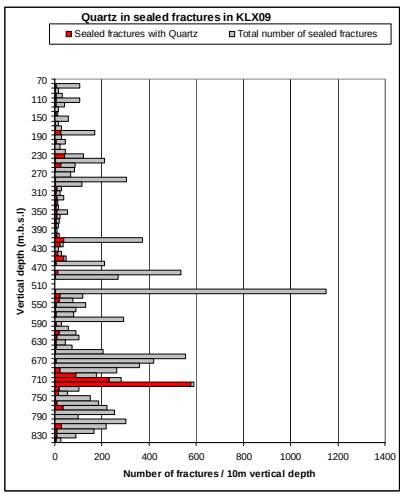
Quartz in sealed fractures in KLX09
Sealed fractures with Quartz
Total number of sealed fractures
Vertical depth (m.b.s.l)
Number of fractures / 10m vertical depth

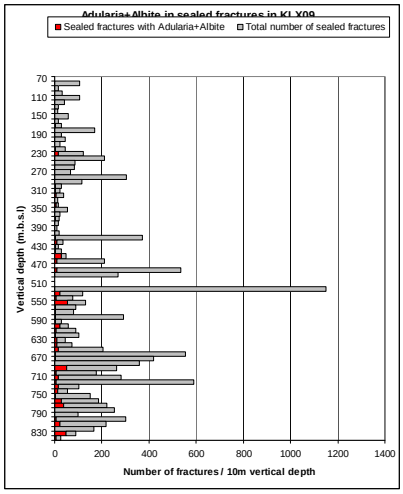
Adularia+Albite in sealed fractures in KLX09
Sealed fractures with Adularia+Albite
Total number of sealed fractures
Vertical depth (m.b.s.l)
Number of fractures / 10m vertical depth

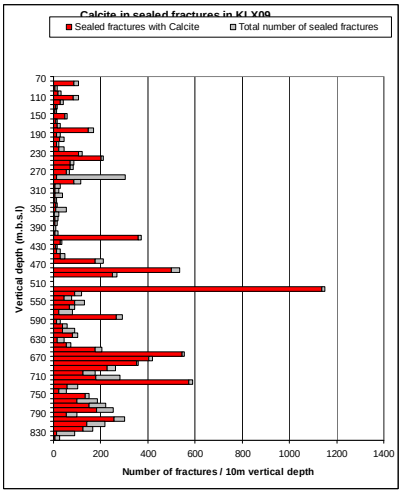
Calcite in sealed fractures in KLX09
Sealed fractures with Calcite
Total number of sealed fractures
Vertical depth (m.b.s.l)
Number of fractures / 10m vertical depth

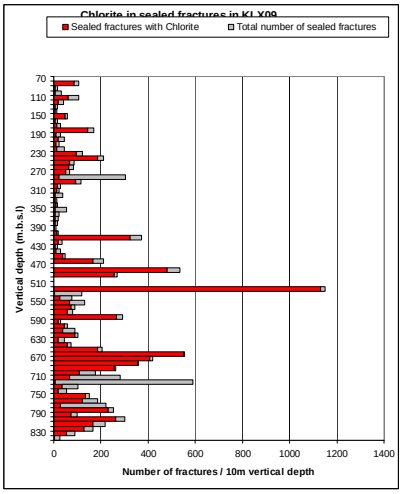
Chlorite in sealed fractures in KLX09
Sealed fractures with Chlorite
Total number of sealed fractures
Vertical depth (m.b.s.l)
Number of fractures / 10m vertical depth

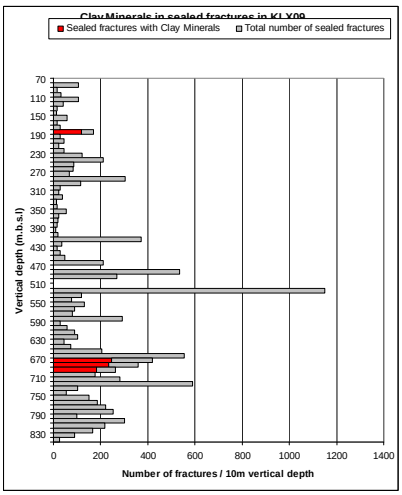
Clay Minerals in sealed fractures in KLX09
Sealed fractures with Clay Minerals
Total number of sealed fractures
Vertical depth (m.b.s.l)
Number of fractures / 10m vertical depth

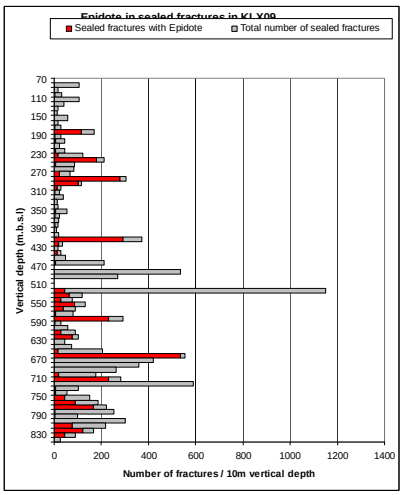
Epidote in sealed fractures in KLX09
Sealed fractures with Epidote
Total number of sealed fractures
Vertical depth (m.b.s.l)
Number of fractures / 10m vertical depth

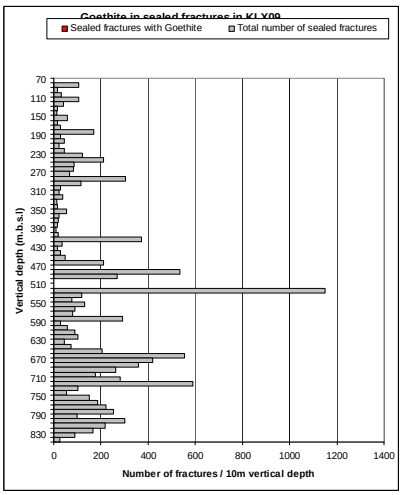
Goethite in sealed fractures in KLX09
Sealed fractures with Goethite
Total number of sealed fractures
Vertical depth (m.b.s.l)
Number of fractures / 10m vertical depth

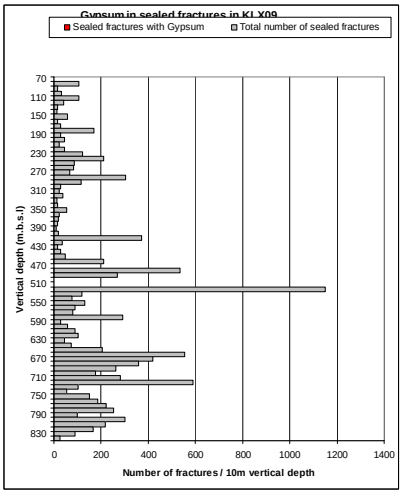
Gypsum in sealed fractures in KLX09
Sealed fractures with Gypsum
Total number of sealed fractures
Vertical depth (m.b.s.l)
Number of fractures / 10m vertical depth

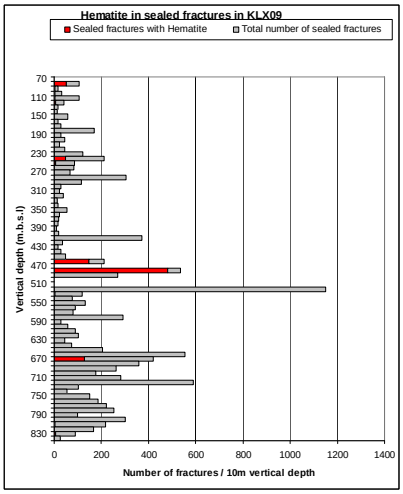
Hematite in sealed fractures in KLX09
Sealed fractures with Hematite
Total number of sealed fractures
Vertical depth (m.b.s.l)
Number of fractures / 10m vertical depth

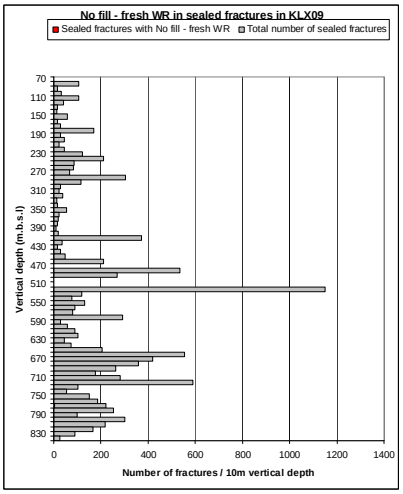
No fill - fresh WR in sealed fractures in KLX09
Sealed fractures with No fill - fresh WR
Total number of sealed fractures
Vertical depth (m.b.s.l)
Number of fractures / 10m vertical depth

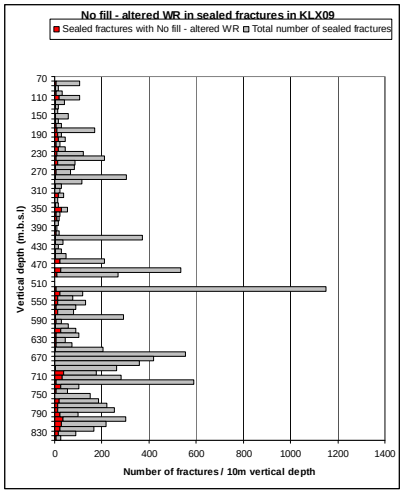
No fill - altered WR in sealed fractures in KLX09
Sealed fractures with No fill - altered WR
Total number of sealed fractures
Vertical depth (m.b.s.l)
Number of fractures / 10m vertical depth

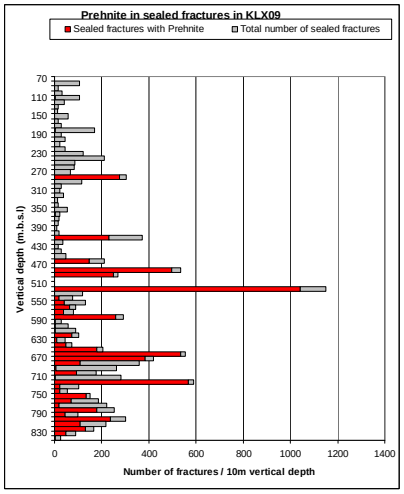
Prehnite in sealed fractures in KLX09
Sealed fractures with Prehnite
Total number of sealed fractures
Vertical depth (m.b.s.l)
Number of fractures / 10m vertical depth

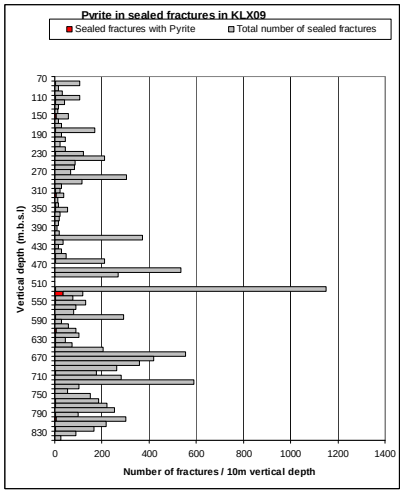
Pyrite in sealed fractures in KLX09
Sealed fractures with Pyrite
Total number of sealed fractures
Vertical depth (m.b.s.l)
Number of fractures / 10m vertical depth

KLX09B

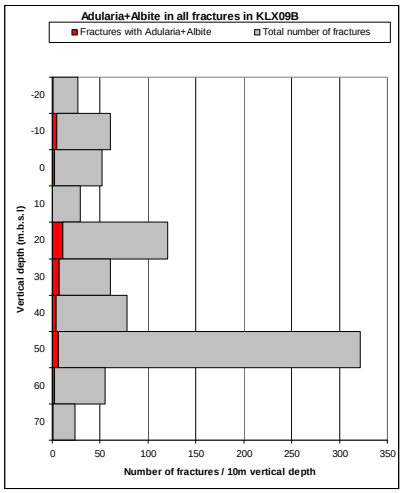
Adularia+Albite in all fractures in KLX09B
Fractures with Adularia+Albite
Total number of fractures
Vertical depth (m.b.s.l)
Number of fractures / 10m vertical depth

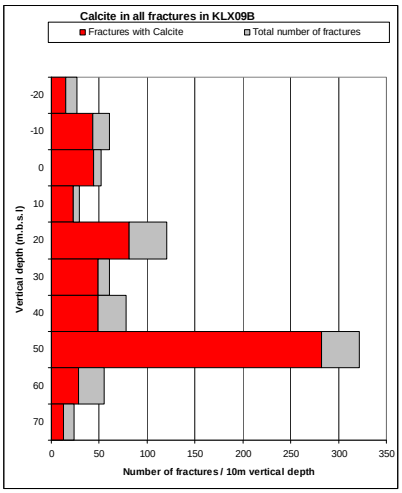
Calcite in all fractures in KLX09B
Fractures with Calcite
Total number of fractures
Vertical depth (m.b.s.l)
Number of fractures / 10m vertical depth

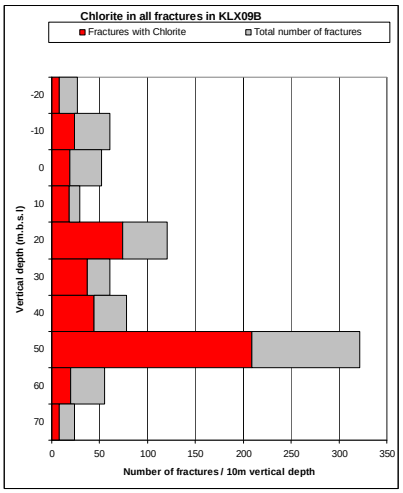
Chlorite in all fractures in KLX09B
Fractures with Chlorite
Total number of fractures
Vertical depth (m.b.s.l)
Number of fractures / 10m vertical depth

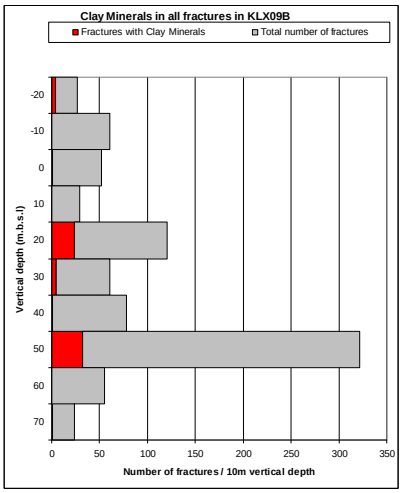
Clay Minerals in all fractures in KLX09B
Fractures with Clay Minerals
Total number of fractures
Vertical depth (m.b.s.l)
Number of fractures / 10m vertical depth

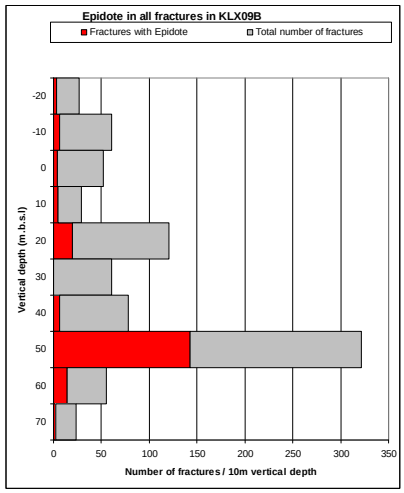
Epidote in all fractures in KLX09B
Fractures with Epidote
Total number of fractures
Vertical depth (m.b.s.l)
Number of fractures / 10m vertical depth

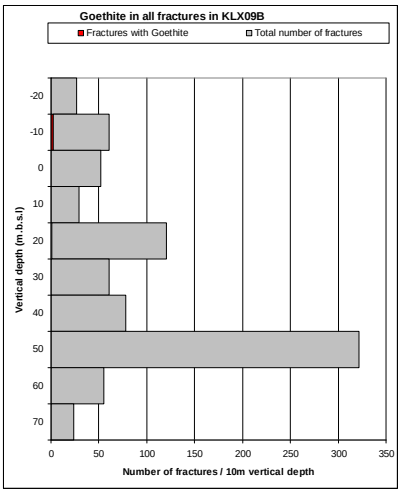
Goethite in all fractures in KLX09B
Fractures with Goethite
Total number of fractures
Vertical depth (m.b.s.l)
Number of fractures / 10m vertical depth

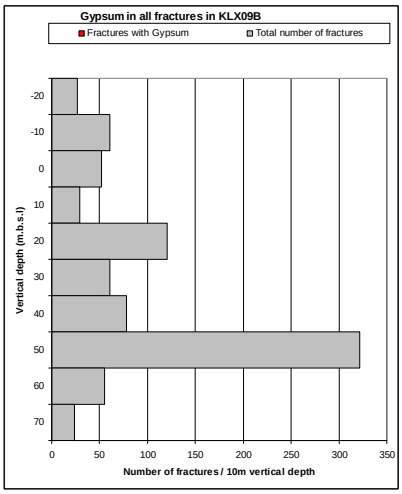
Gypsum in all fractures in KLX09B
Fractures with Gypsum
Total number of fractures
Vertical depth (m.b.s.l)
Number of fractures / 10m vertical depth

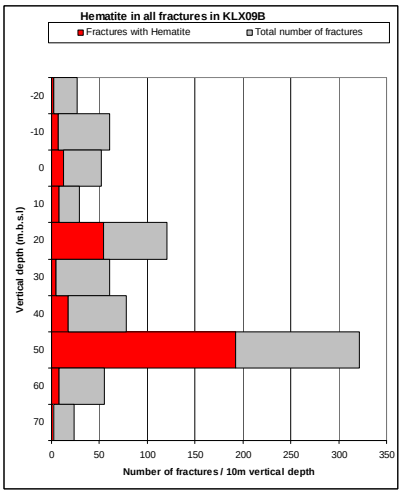
Hematite in all fractures in KLX09B
Fractures with Hematite
Total number of fractures
Vertical depth (m.b.s.l)
Number of fractures / 10m vertical depth

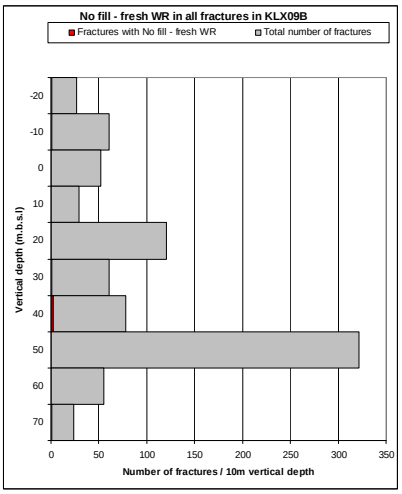
No fill - fresh WR in all fractures in KLX09B
Fractures with No fill - fresh WR
Total number of fractures
Vertical depth (m.b.s.l)
Number of fractures / 10m vertical depth

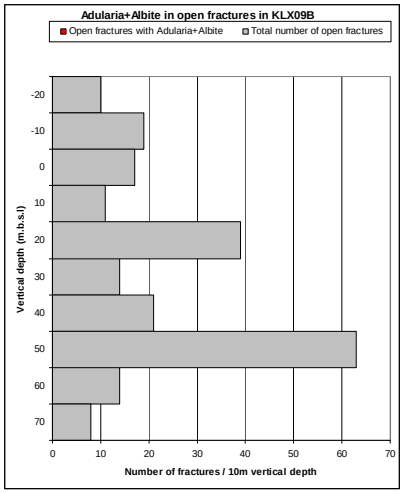
Adularia+Albite in open fractures in KLX09B
Open fractures with Adularia+Albite
Total number of open fractures
Vertical depth (m.b.s.l)
Number of fractures / 10m vertical depth

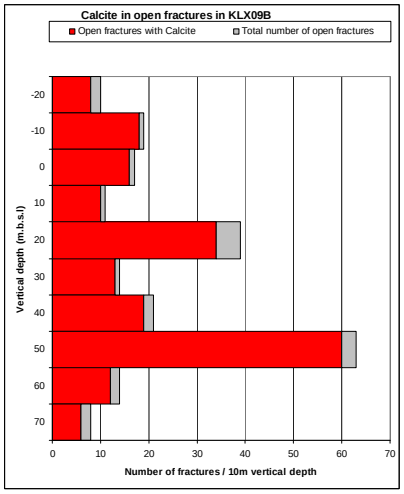
Calcite in open fractures in KLX09B
Open fractures with Calcite
Total number of open fractures
Vertical depth (m.b.s.l)
Number of fractures / 10m vertical depth

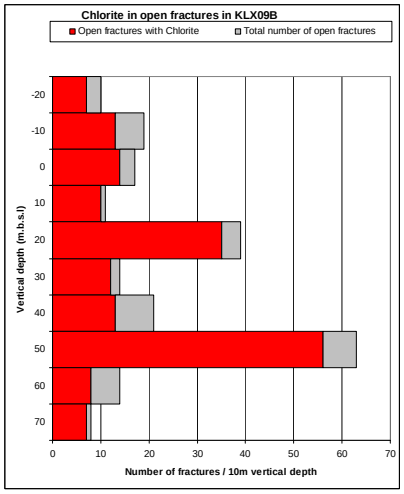
Chlorite in open fractures in KLX09B
Open fractures with Chlorite
Total number of open fractures
Vertical depth (m.b.s.l)
Number of fractures / 10m vertical depth

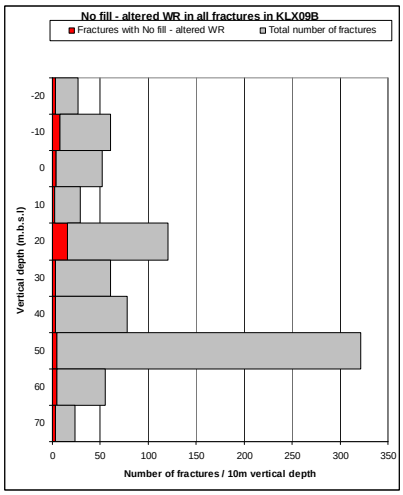
No fill - altered WR in all fractures in KLX09B
Fractures with No fill - altered WR
Total number of fractures
Vertical depth (m.b.s.l)
Number of fractures / 10m vertical depth

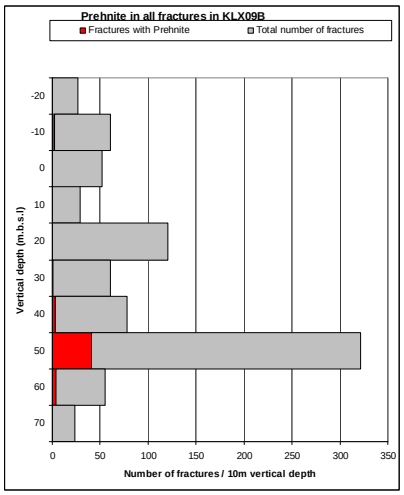
Prehnite in all fractures in KLX09B
Fractures with Prehnite
Total number of fractures
Vertical depth (m.b.s.l)
Number of fractures / 10m vertical depth

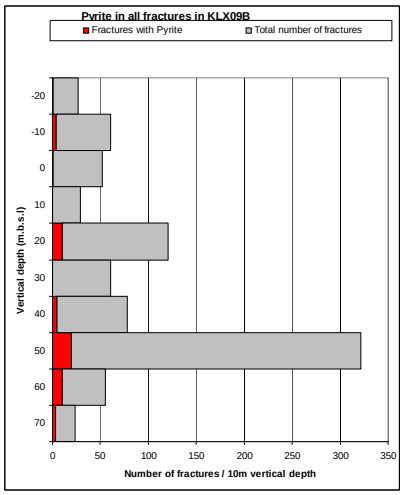
Pyrite in all fractures in KLX09B
Fractures with Pyrite
Total number of fractures
Vertical depth (m.b.s.l)
Number of fractures / 10m vertical depth

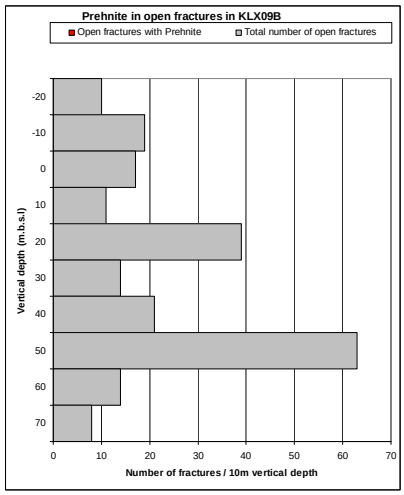
Prehnite in open fractures in KLX09B
Open fractures with Prehnite
Total number of open fractures
Vertical depth (m.b.s.l)
Number of fractures / 10m vertical depth

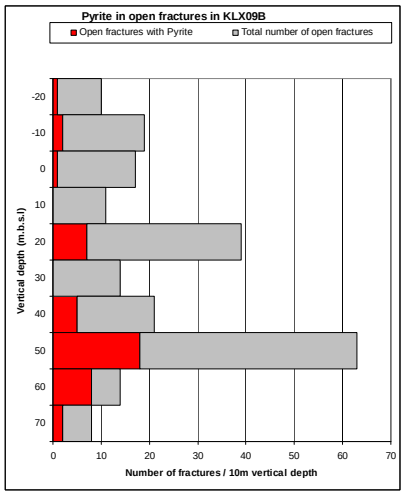
Pyrite in open fractures in KLX09B
Open fractures with Pyrite
Total number of open fractures
Vertical depth (m.b.s.l)
Number of fractures / 10m vertical depth

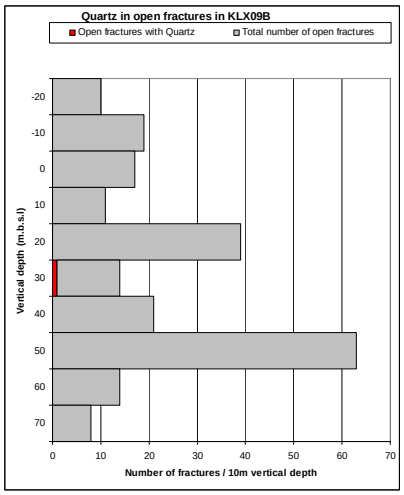
Quartz in open fractures in KLX09B
Open fractures with Quartz
Total number of open fractures
Vertical depth (m.b.s.l)
Number of fractures / 10m vertical depth

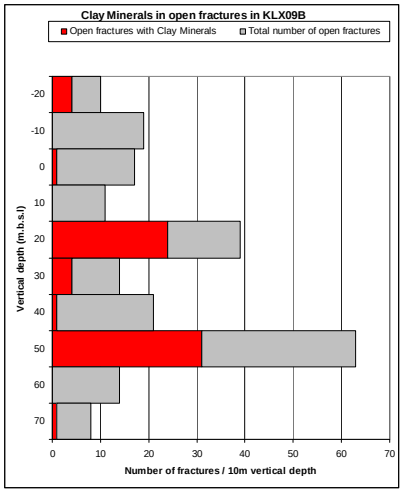
Clay Minerals in open fractures in KLX09B
Open fractures with Clay Minerals
Total number of open fractures
Vertical depth (m.b.s.l)
Number of fractures / 10m vertical depth

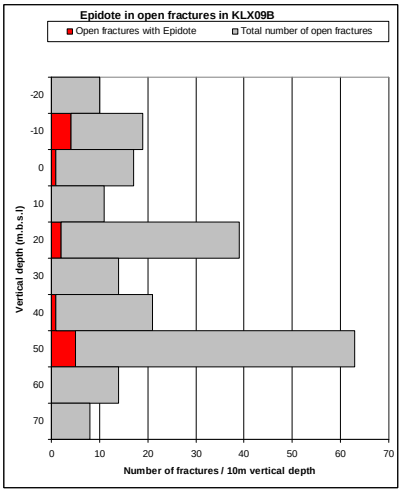
Epidote in open fractures in KLX09B
Open fractures with Epidote
Total number of open fractures
Vertical depth (m.b.s.l)
Number of fractures / 10m vertical depth

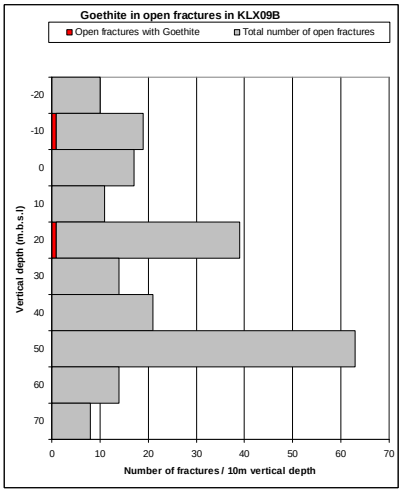
Goethite in open fractures in KLX09B
Open fractures with Goethite
Total number of open fractures
Vertical depth (m.b.s.l)
Number of fractures / 10m vertical depth

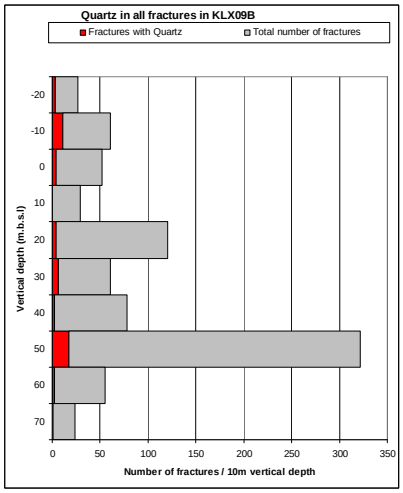
Quartz in all fractures in KLX09B
Fractures with Quartz
Total number of fractures
Vertical depth (m.b.s.l)
Number of fractures / 10m vertical depth

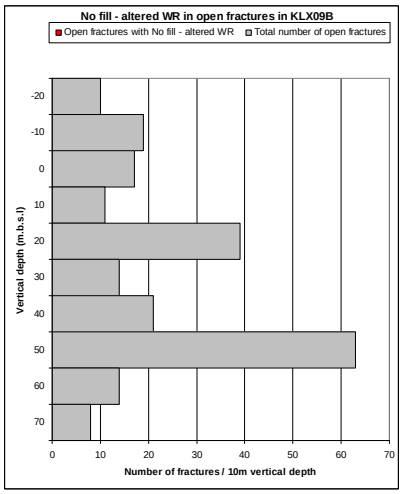
No fill - altered WR in open fractures in KLX09B
Open fractures with No fill - altered WR
Total number of open fractures
Vertical depth (m.b.s.l)
Number of fractures / 10m vertical depth

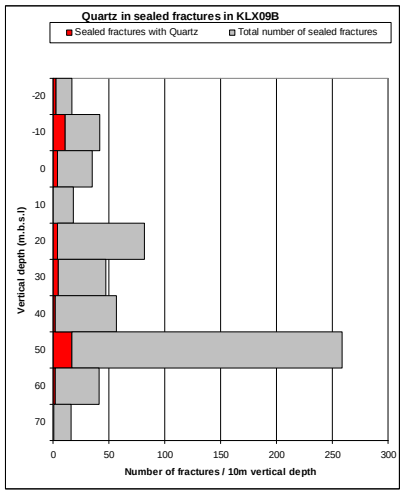
Quartz in sealed fractures in KLX09B
Sealed fractures with Quartz
Total number of sealed fractures
Vertical depth (m.b.s.l)
Number of fractures / 10m vertical depth

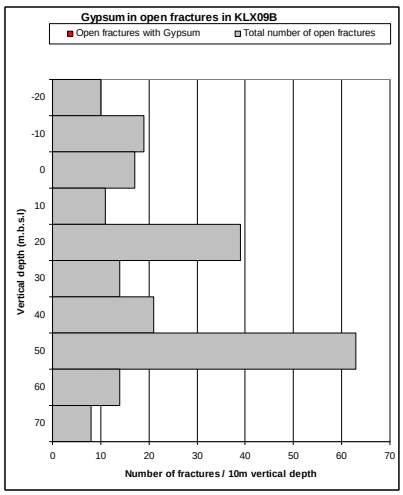
Gypsum in open fractures in KLX09B
Open fractures with Gypsum
Total number of open fractures
Vertical depth (m.b.s.l)
Number of fractures / 10m vertical depth

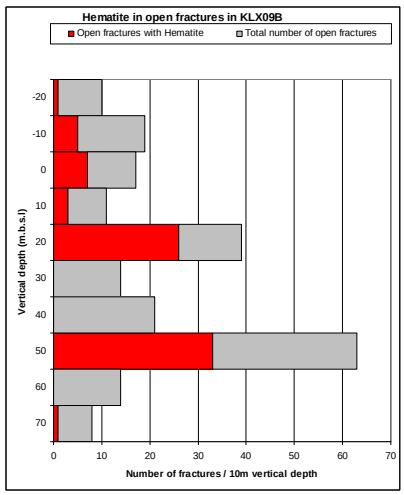
Hematite in open fractures in KLX09B
Open fractures with Hematite
Total number of open fractures
Vertical depth (m.b.s.l)
Number of fractures / 10m vertical depth

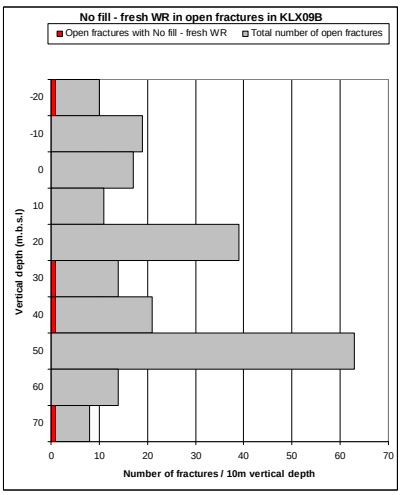
No fill - fresh WR in open fractures in KLX09B
Open fractures with No fill - fresh WR
Total number of open fractures
Vertical depth (m.b.s.l)
Number of fractures / 10m vertical depth

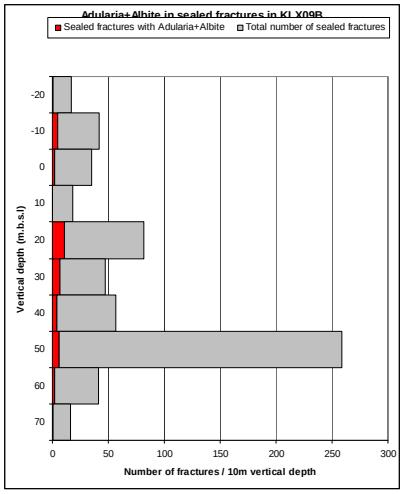
Adularia+Albite in sealed fractures in KLX09B
Sealed fractures with Adularia+Albite
Total number of sealed fractures
Vertical depth (m.b.s.l)
Number of fractures / 10m vertical depth

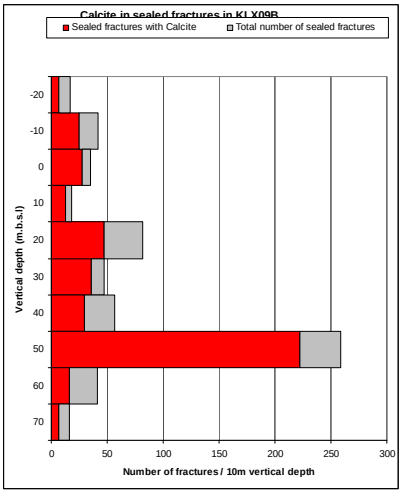
Calcite in sealed fractures in KLX09B
Sealed fractures with Calcite
Total number of sealed fractures
Vertical depth (m.b.s.l)
Number of fractures / 10m vertical depth

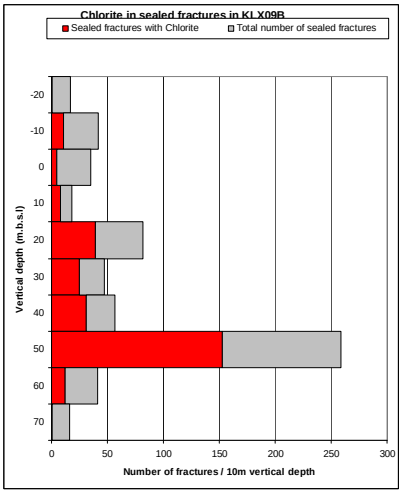
Chlorite in sealed fractures in KLX09B
Sealed fractures with Chlorite
Total number of sealed fractures
Vertical depth (m.b.s.l)
Number of fractures / 10m vertical depth

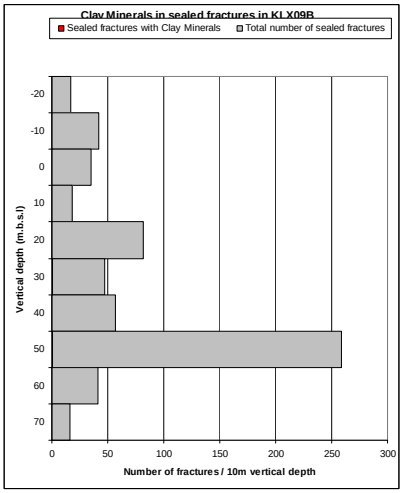
Clay Minerals in sealed fractures in KLX09B
Sealed fractures with Clay Minerals
Total number of sealed fractures
Vertical depth (m.b.s.l)
Number of fractures / 10m vertical depth

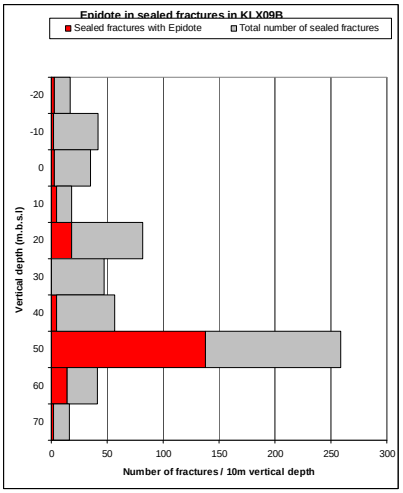
Epidote in sealed fractures in KLX09B
Sealed fractures with Epidote
Total number of sealed fractures
Vertical depth (m.b.s.l)
Number of fractures / 10m vertical depth

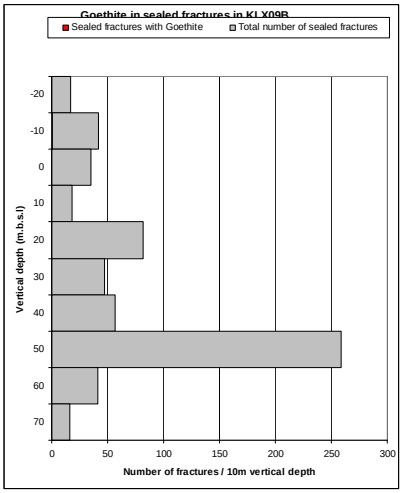
Goethite in sealed fractures in KLX09B
Sealed fractures with Goethite
Total number of sealed fractures
Vertical depth (m.b.s.l)
Number of fractures / 10m vertical depth

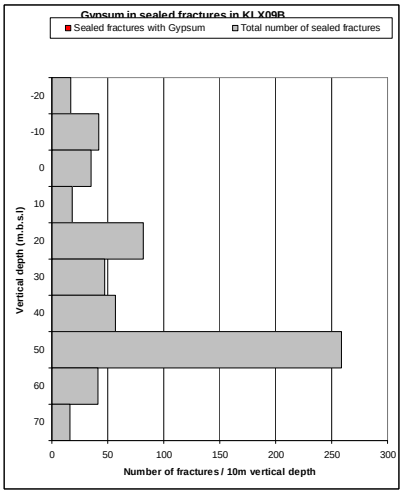
Gypsum in sealed fractures in KLX09B
Sealed fractures with Gypsum
Total number of sealed fractures
Vertical depth (m.b.s.l)
Number of fractures / 10m vertical depth

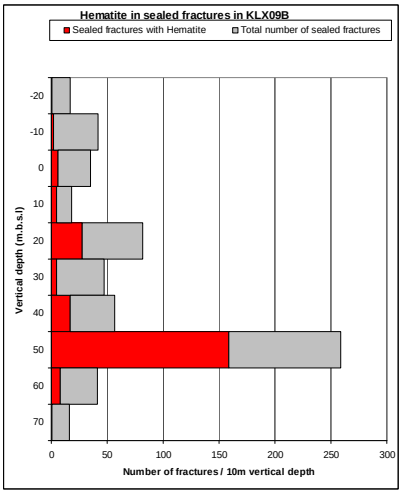
Hematite in sealed fractures in KLX09B
Sealed fractures with Hematite
Total number of sealed fractures
Vertical depth (m.b.s.l)
Number of fractures / 10m vertical depth

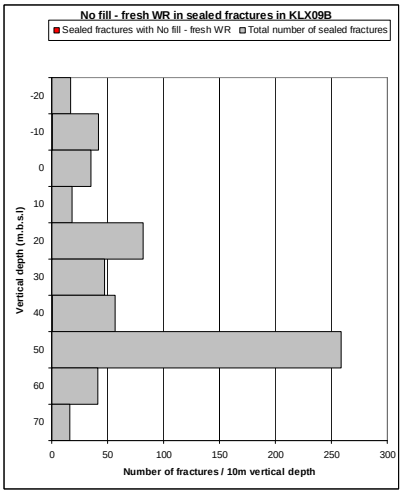
No fill - fresh WR in sealed fractures in KLX09B
Sealed fractures with No fill - fresh WR
Total number of sealed fractures
Vertical depth (m.b.s.l)
Number of fractures / 10m vertical depth

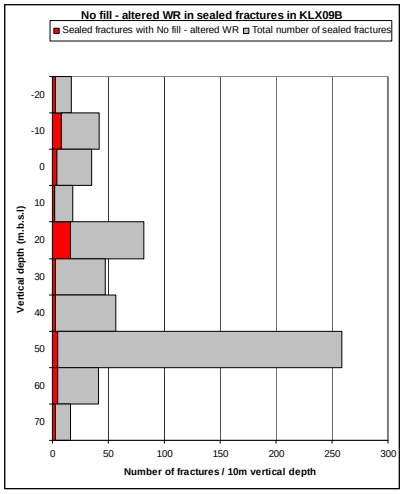
No fill - altered WR in sealed fractures in KLX09B
Sealed fractures with No fill - altered WR
Total number of sealed fractures
Vertical depth (m.b.s.l)
-20
-10
0
10
20
30
40
50
60
70
0
50
100
150
200
250
300
Number of fractures / 10m vertical depth

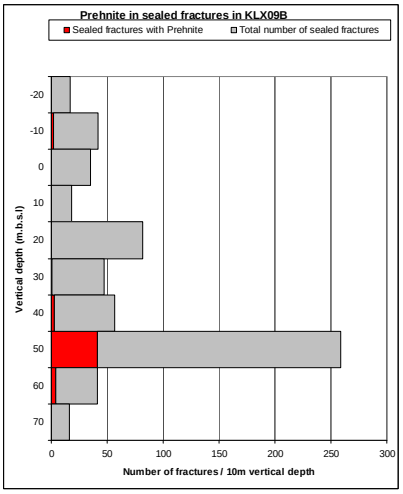
Prehnite in sealed fractures in KLX09B
Sealed fractures with Prehnite
Total number of sealed fractures
Vertical depth (m.b.s.l)
-20
-10
0
10
20
30
40
50
60
70
0
50
100
150
200
250
300
Number of fractures / 10m vertical depth

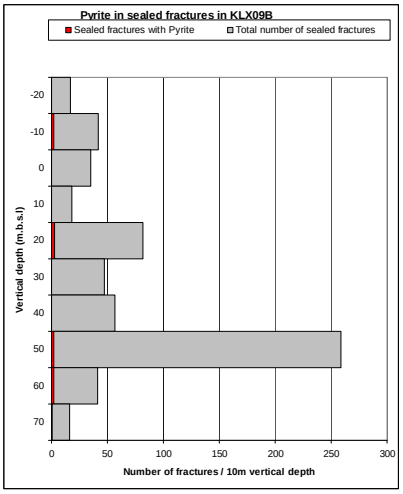
Pyrite in sealed fractures in KLX09B
Sealed fractures with Pyrite
Total number of sealed fractures
Vertical depth (m.b.s.l)
-20
-10
0
10
20
30
40
50
60
70
0
50
100
150
200
250
300
Number of fractures / 10m vertical depth

KLX09C

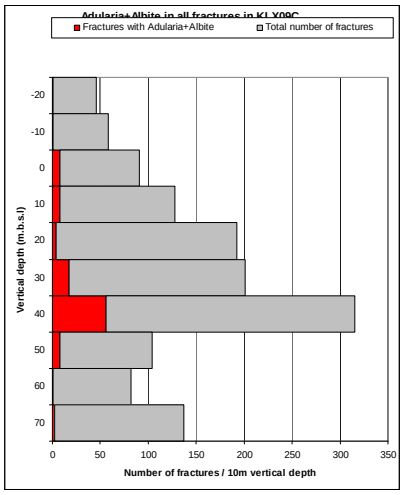
Fractures with Adularia+Albite
Total number of fractures
Vertical depth (m.b.s.l)
Number of fractures / 10m vertical depth

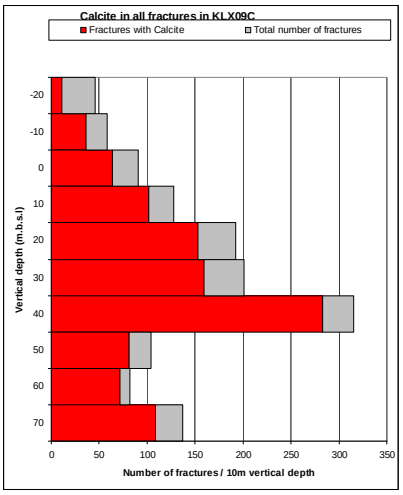
Calcite in all fractures in KLX09C
Fractures with Calcite
Total number of fractures
Vertical depth (m.b.s.l)
Number of fractures / 10m vertical depth

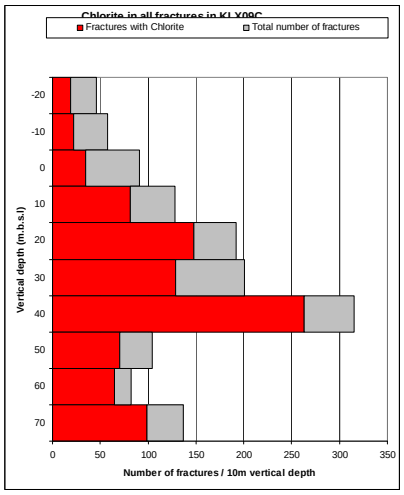
Fractures with Chlorite
Total number of fractures
Vertical depth (m.b.s.l)
Number of fractures / 10m vertical depth

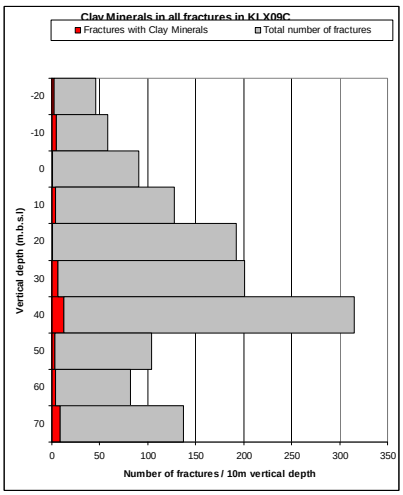
Fractures with Clay Minerals
Total number of fractures
Vertical depth (m.b.s.l)
Number of fractures / 10m vertical depth

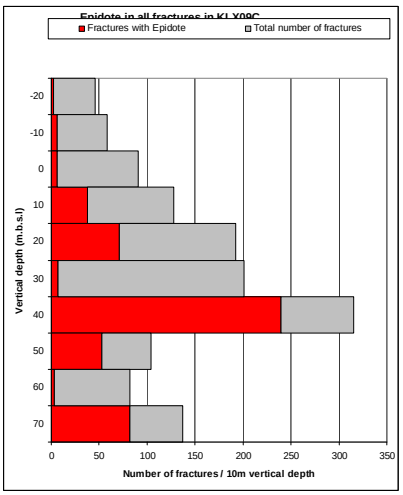
Fractures with Epidote
Total number of fractures
Vertical depth (m.b.s.l)
Number of fractures / 10m vertical depth

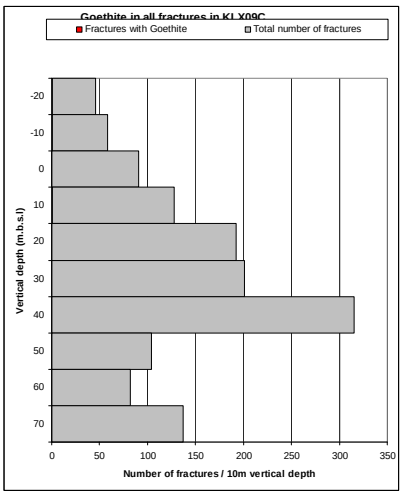
Fractures with Goethite
Total number of fractures
Vertical depth (m.b.s.l)
Number of fractures / 10m vertical depth

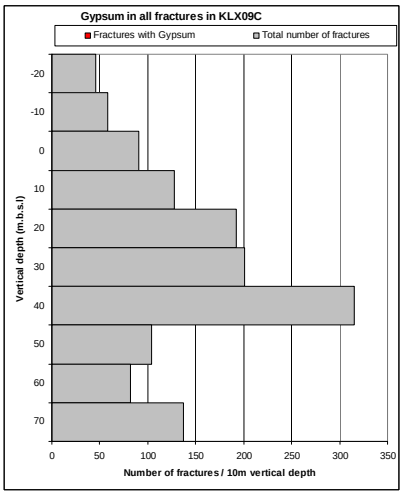
Gypsum in all fractures in KLX09C
Fractures with Gypsum
Total number of fractures
Vertical depth (m.b.s.l)
Number of fractures / 10m vertical depth

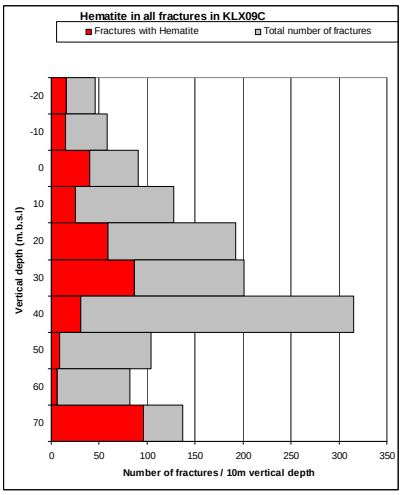
Hematite in all fractures in KLX09C
Fractures with Hematite
Total number of fractures
Vertical depth (m.b.s.l)
Number of fractures / 10m vertical depth

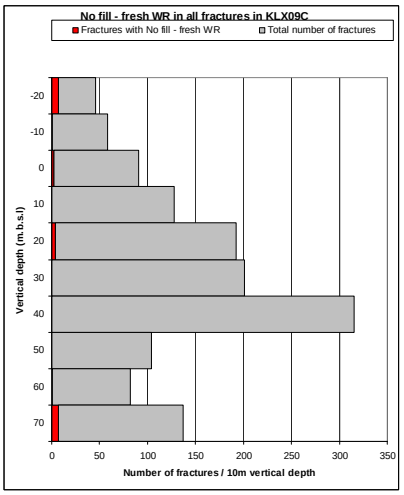
No fill - fresh WR in all fractures in KLX09C
Fractures with No fill - fresh WR
Total number of fractures
Vertical depth (m.b.s.l)
Number of fractures / 10m vertical depth

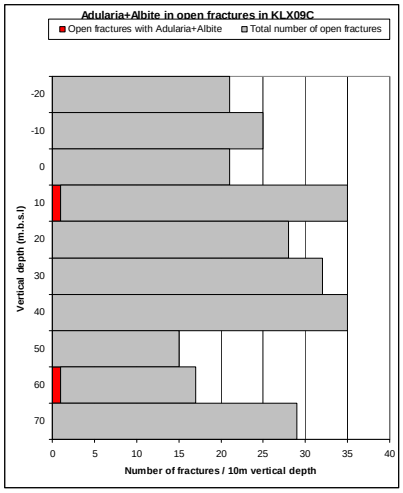
Adularia+Albite in open fractures in KLX09C
Open fractures with Adularia+Albite
Total number of open fractures
Vertical depth (m.b.s.l)
Number of fractures / 10m vertical depth

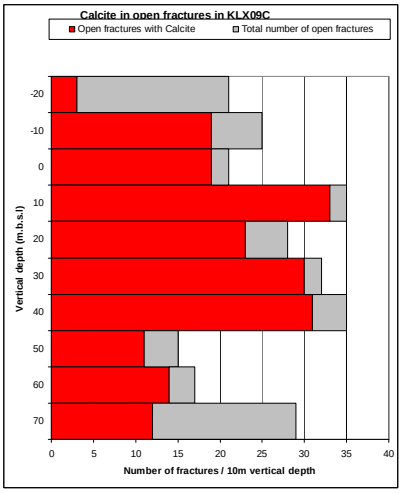
Calcite in open fractures in KLX09C
Open fractures with Calcite
Total number of open fractures
Vertical depth (m.b.s.l)
Number of fractures / 10m vertical depth

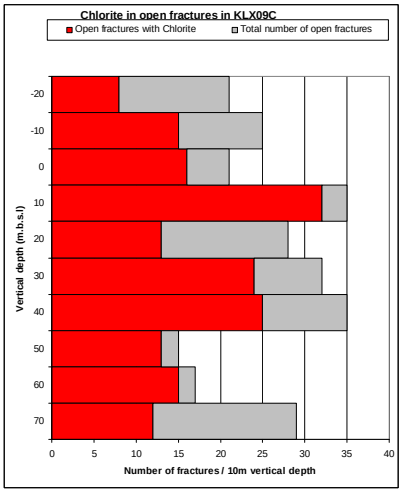
Chlorite in open fractures in KLX09C
Open fractures with Chlorite
Total number of open fractures
Vertical depth (m.b.s.l)
Number of fractures / 10m vertical depth

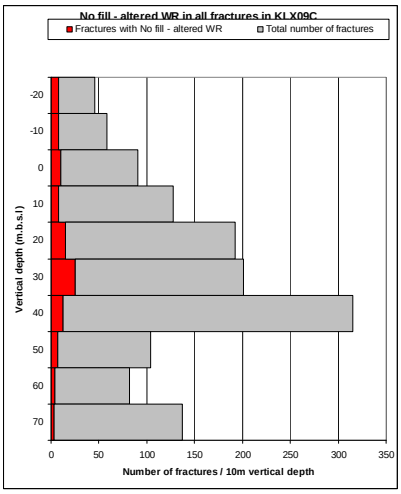
No fill - altered WR in all fractures in KLX09C
Fractures with No fill - altered WR
Total number of fractures
Vertical depth (m.b.s.l)
Number of fractures / 10m vertical depth

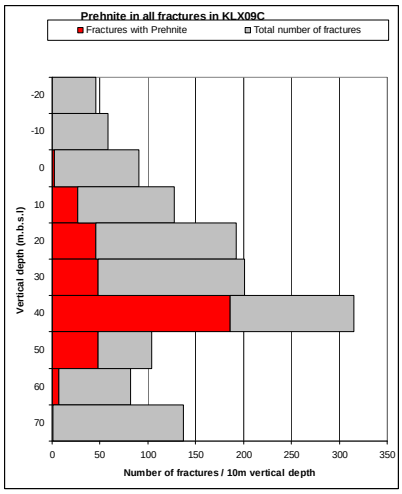
Prehnite in all fractures in KLX09C
Fractures with Prehnite
Total number of fractures
Vertical depth (m.b.s.l)
Number of fractures / 10m vertical depth

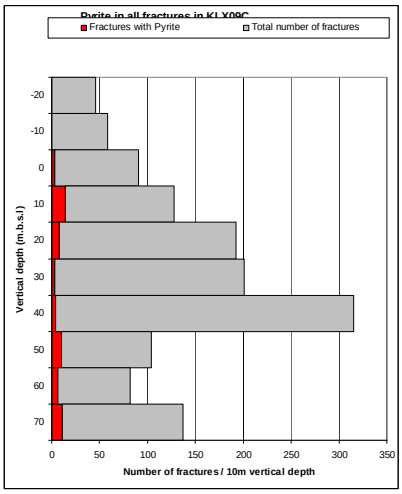
Pyrite in all fractures in KLX09C
Fractures with Pyrite
Total number of fractures
Vertical depth (m.b.s.l)
Number of fractures / 10m vertical depth

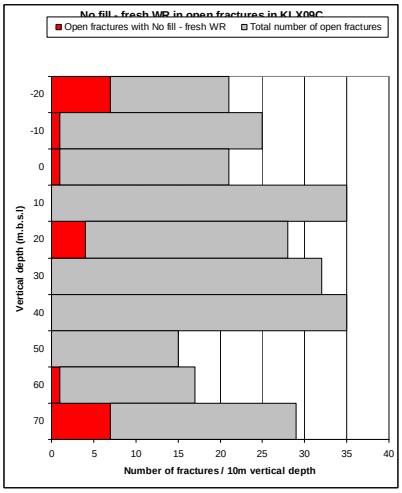
No fill - fresh WR in open fractures in KLX09C
Open fractures with No fill - fresh WR
Total number of open fractures
Vertical depth (m.b.s.l)
Number of fractures / 10m vertical depth

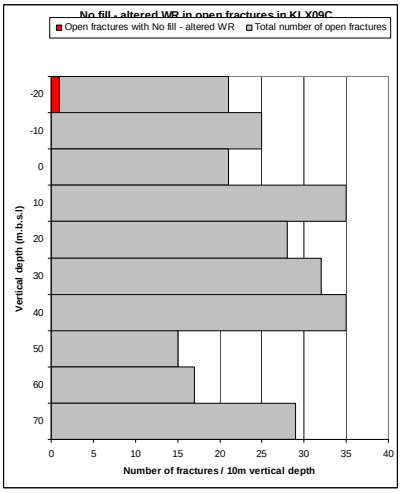
No fill - altered WR in open fractures in KLX09C
Open fractures with No fill - altered WR
Total number of open fractures
Vertical depth (m.b.s.l)
Number of fractures / 10m vertical depth

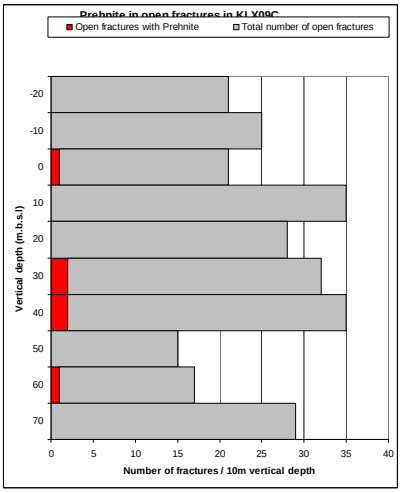
Prehnite in open fractures in KLX09C
Open fractures with Prehnite
Total number of open fractures
Vertical depth (m.b.s.l)
Number of fractures / 10m vertical depth

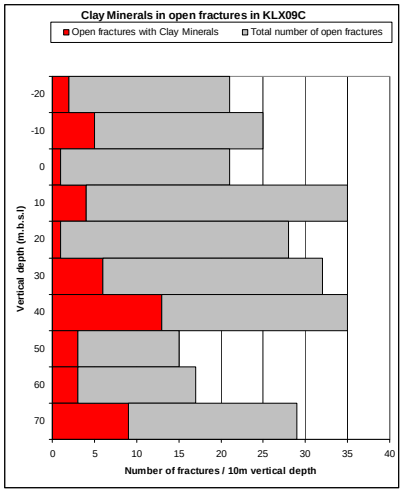
Clay Minerals in open fractures in KLX09C
Open fractures with Clay Minerals
Total number of open fractures
Vertical depth (m.b.s.l)
Number of fractures / 10m vertical depth

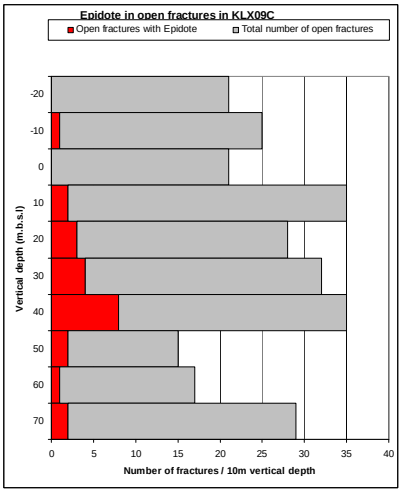
Epidote in open fractures in KLX09C
Open fractures with Epidote
Total number of open fractures
Vertical depth (m.b.s.l)
Number of fractures / 10m vertical depth

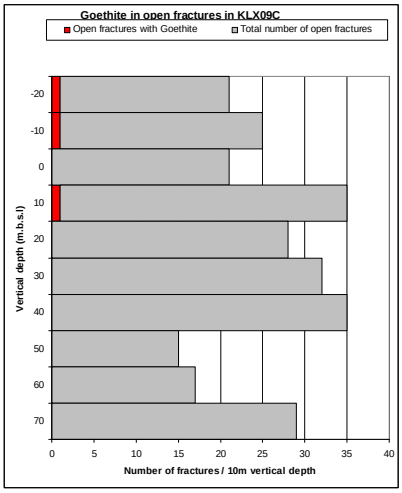
Goethite in open fractures in KLX09C
Open fractures with Goethite
Total number of open fractures
Vertical depth (m.b.s.l)
Number of fractures / 10m vertical depth

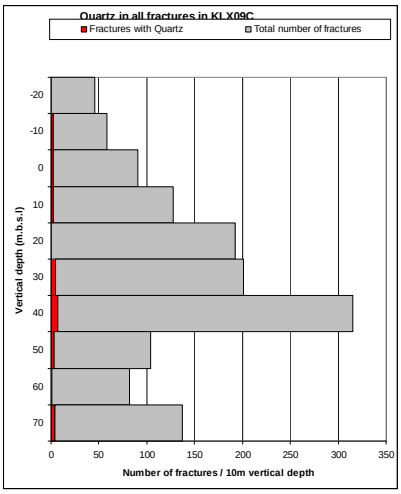
Quartz in all fractures in KLX09C
Fractures with Quartz
Total number of fractures
Vertical depth (m.b.s.l)
Number of fractures / 10m vertical depth

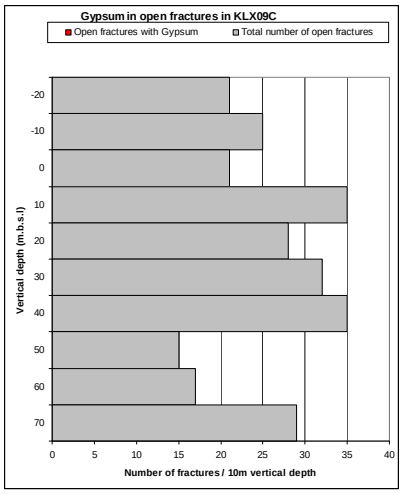
Gypsum in open fractures in KLX09C
Open fractures with Gypsum
Total number of open fractures
Vertical depth (m.b.s.l)
Number of fractures / 10m vertical depth

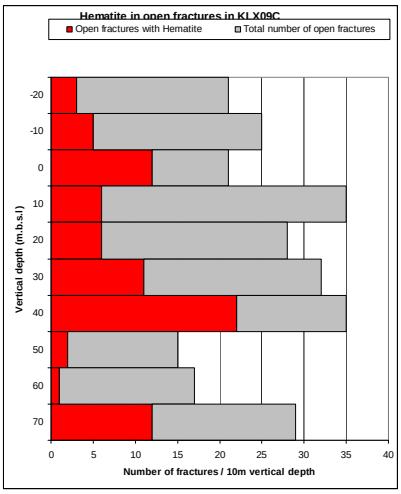
Hematite in open fractures in KLX09C
Open fractures with Hematite
Total number of open fractures
Vertical depth (m.b.s.l)
Number of fractures / 10m vertical depth

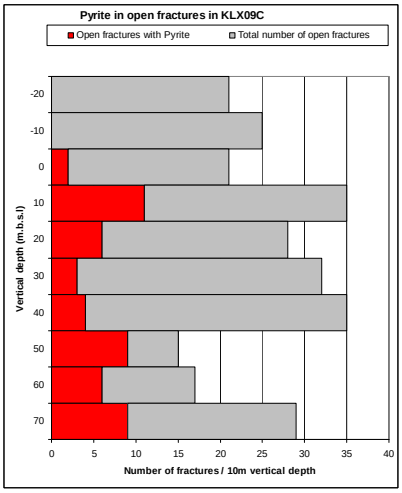
Pyrite in open fractures in KLX09C
Open fractures with Pyrite
Total number of open fractures
Vertical depth (m.b.s.l)
Number of fractures / 10m vertical depth

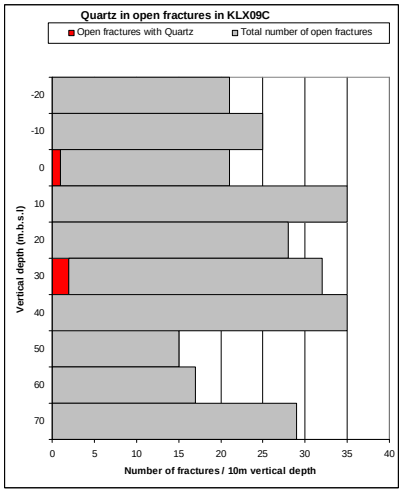
Quartz in open fractures in KLX09C
Open fractures with Quartz
Total number of open fractures
Vertical depth (m.b.s.l)
Number of fractures / 10m vertical depth

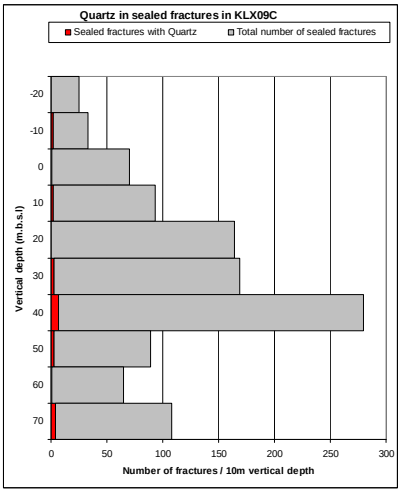
Quartz in sealed fractures in KLX09C
Sealed fractures with Quartz
Total number of sealed fractures
Vertical depth (m.b.s.l)
Number of fractures / 10m vertical depth

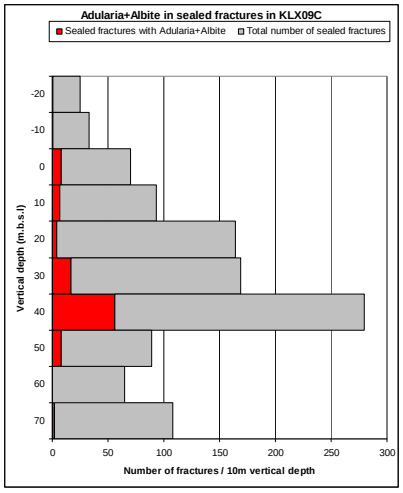
Adularia+Albite in sealed fractures in KLX09C
Sealed fractures with Adularia+Albite
Total number of sealed fractures
Vertical depth (m.b.s.l)
Number of fractures / 10m vertical depth

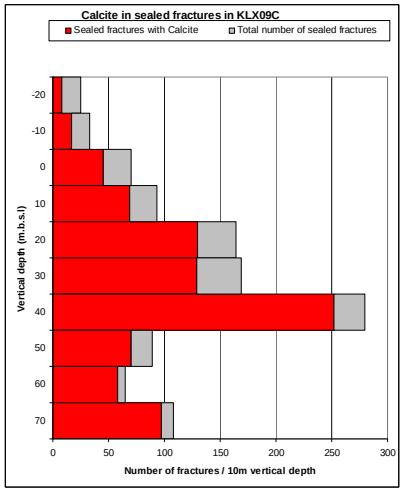
Calcite in sealed fractures in KLX09C
Sealed fractures with Calcite
Total number of sealed fractures
Vertical depth (m.b.s.l)
Number of fractures / 10m vertical depth

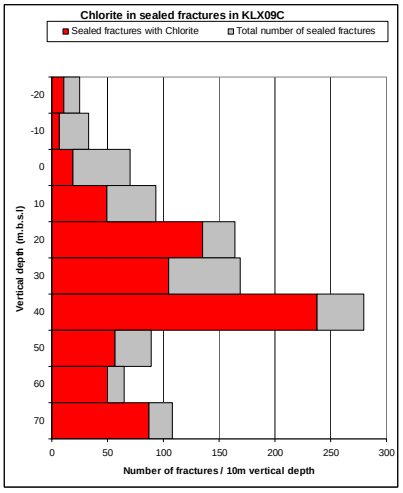
Chlorite in sealed fractures in KLX09C
Sealed fractures with Chlorite
Total number of sealed fractures
Vertical depth (m.b.s.l)
Number of fractures / 10m vertical depth

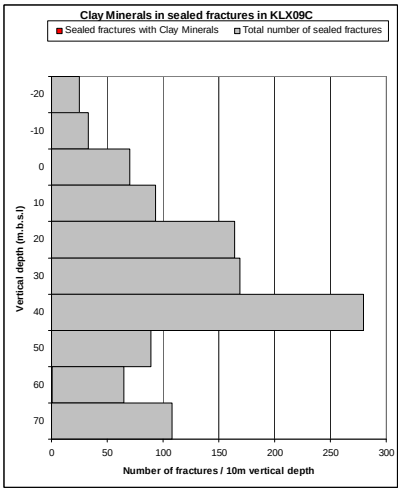
Clay Minerals in sealed fractures in KLX09C
Sealed fractures with Clay Minerals
Total number of sealed fractures
Vertical depth (m.b.s.l)
Number of fractures / 10m vertical depth

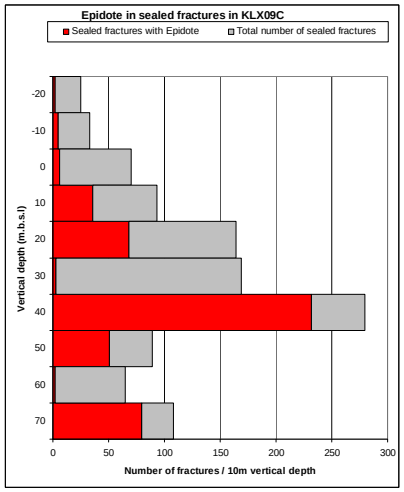
Epidote in sealed fractures in KLX09C
Sealed fractures with Epidote
Total number of sealed fractures
Vertical depth (m.b.s.l)
Number of fractures / 10m vertical depth

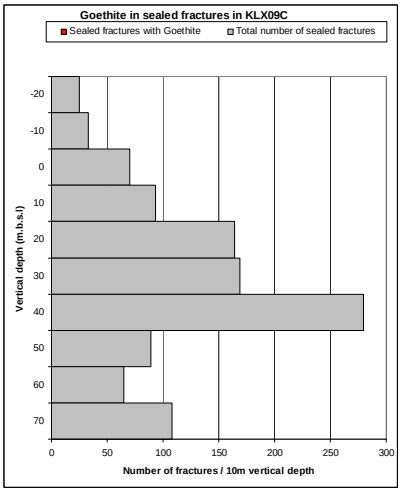
Goethite in sealed fractures in KLX09C
Sealed fractures with Goethite
Total number of sealed fractures
Vertical depth (m.b.s.l)
Number of fractures / 10m vertical depth

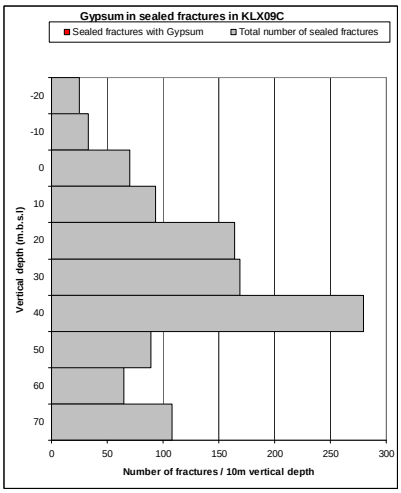
Gypsum in sealed fractures in KLX09C
Sealed fractures with Gypsum
Total number of sealed fractures
Vertical depth (m.b.s.l)
Number of fractures / 10m vertical depth

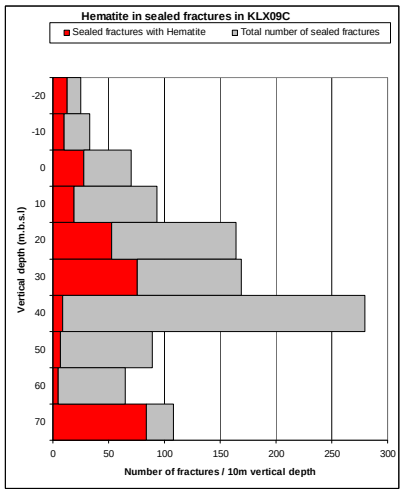
Hematite in sealed fractures in KLX09C
Sealed fractures with Hematite
Total number of sealed fractures
Vertical depth (m.b.s.l)
Number of fractures / 10m vertical depth

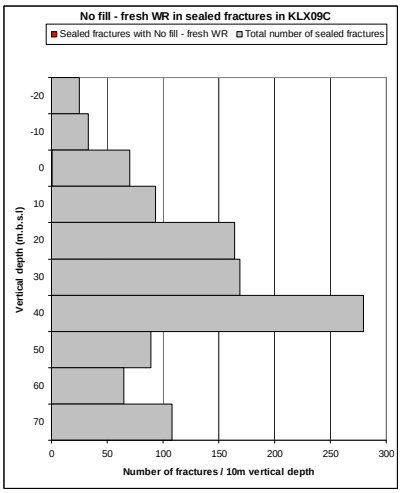
No fill - fresh WR in sealed fractures in KLX09C
Sealed fractures with No fill - fresh WR
Total number of sealed fractures
Vertical depth (m.b.s.l)
Number of fractures / 10m vertical depth

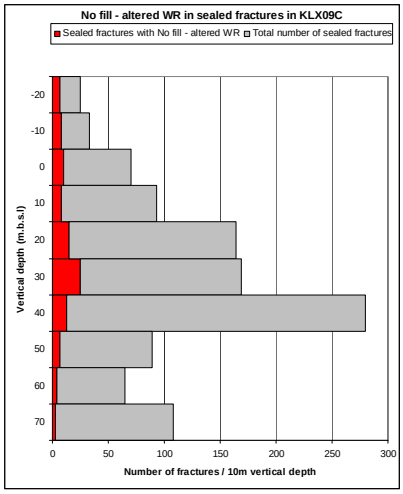
No fill - altered WR in sealed fractures in KLX09C
Sealed fractures with No fill - altered WR
Total number of sealed fractures
Vertical depth (m.b.s.l)
-20
-10
0
10
20
30
40
50
60
70
0
50
100
150
200
250
300
Number of fractures / 10m vertical depth

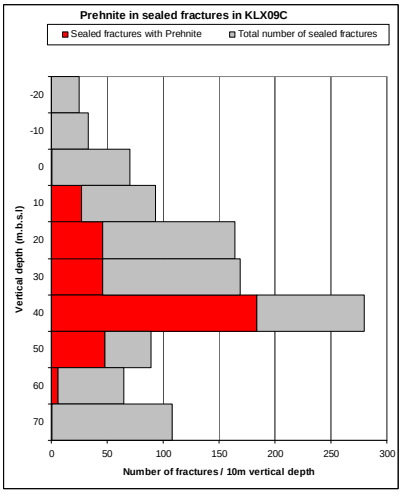
Prehnite in sealed fractures in KLX09C
Sealed fractures with Prehnite
Total number of sealed fractures
Vertical depth (m.b.s.l)
-20
-10
0
10
20
30
40
50
60
70
0
50
100
150
200
250
300
Number of fractures / 10m vertical depth

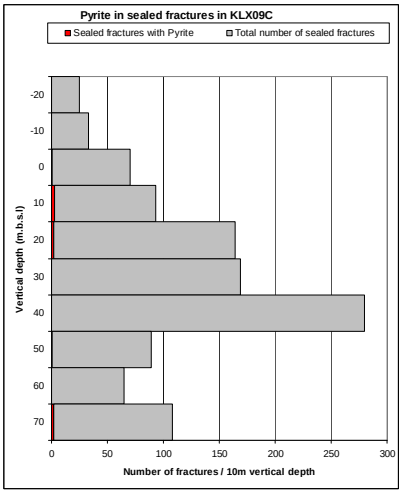
Pyrite in sealed fractures in KLX09C
Sealed fractures with Pyrite
Total number of sealed fractures
Vertical depth (m.b.s.l)
-20
-10
0
10
20
30
40
50
60
70
0
50
100
150
200
250
300
Number of fractures / 10m vertical depth

KLX09D

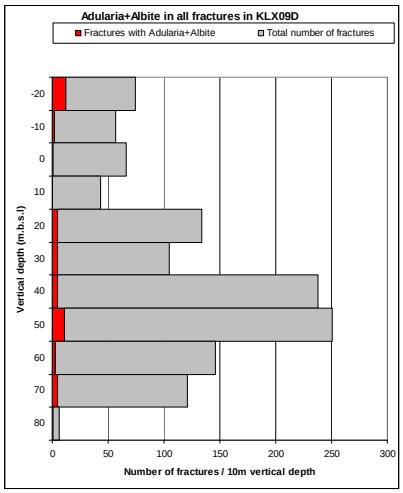
Adularia+Albite in all fractures in KLX09D
Fractures with Adularia+Albite
Total number of fractures
Vertical depth (m.b.s.l)
Number of fractures / 10m vertical depth

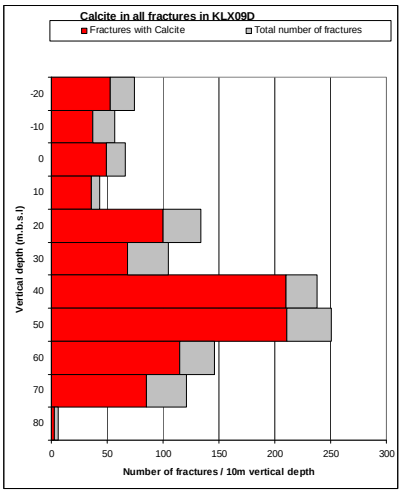
Calcite in all fractures in KLX09D
Fractures with Calcite
Total number of fractures
Vertical depth (m.b.s.l)
Number of fractures / 10m vertical depth

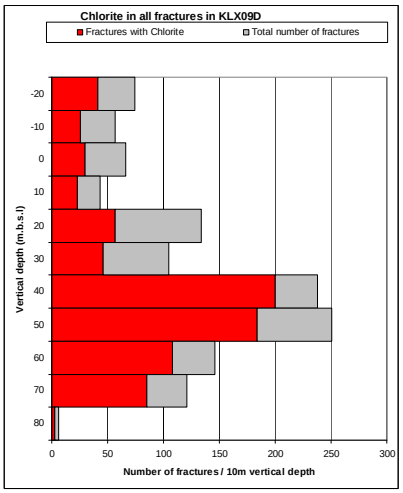
Chlorite in all fractures in KLX09D
Fractures with Chlorite
Total number of fractures
Vertical depth (m.b.s.l)
Number of fractures / 10m vertical depth

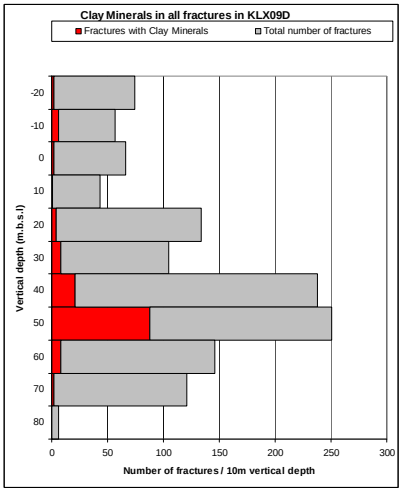
Clay Minerals in all fractures in KLX09D
Fractures with Clay Minerals
Total number of fractures
Vertical depth (m.b.s.l)
Number of fractures / 10m vertical depth

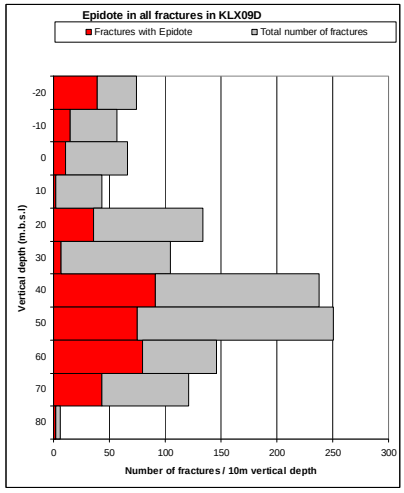
Epidote in all fractures in KLX09D
Fractures with Epidote
Total number of fractures
Vertical depth (m.b.s.l)
Number of fractures / 10m vertical depth

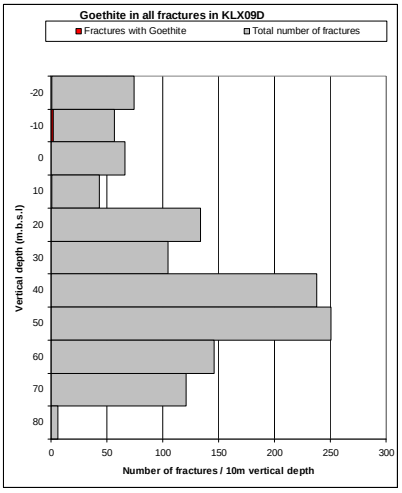
Goethite in all fractures in KLX09D
Fractures with Goethite
Total number of fractures
Vertical depth (m.b.s.l)
Number of fractures / 10m vertical depth

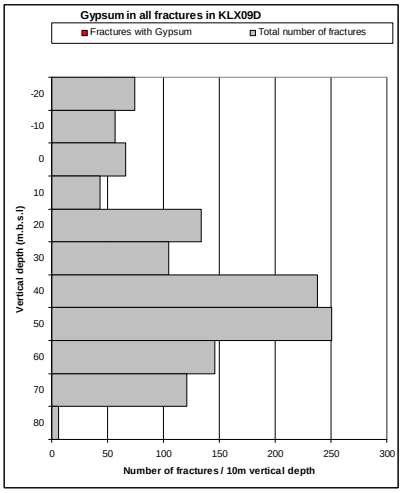
Gypsum in all fractures in KLX09D
Fractures with Gypsum
Total number of fractures
Vertical depth (m.b.s.l)
Number of fractures / 10m vertical depth

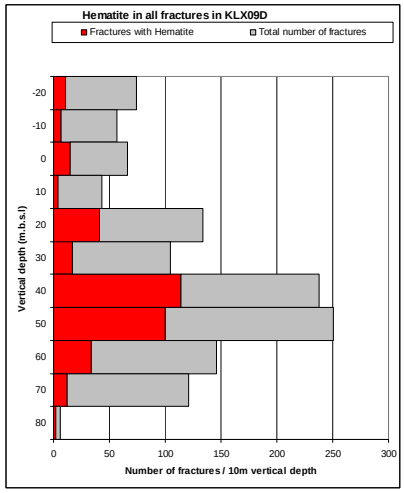
Hematite in all fractures in KLX09D
Fractures with Hematite
Total number of fractures
Vertical depth (m.b.s.l)
Number of fractures / 10m vertical depth

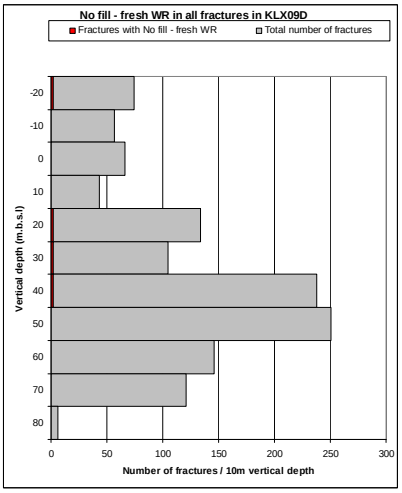
No fill - fresh WR in all fractures in KLX09D
Fractures with No fill - fresh WR
Total number of fractures
Vertical depth (m.b.s.l)
Number of fractures / 10m vertical depth

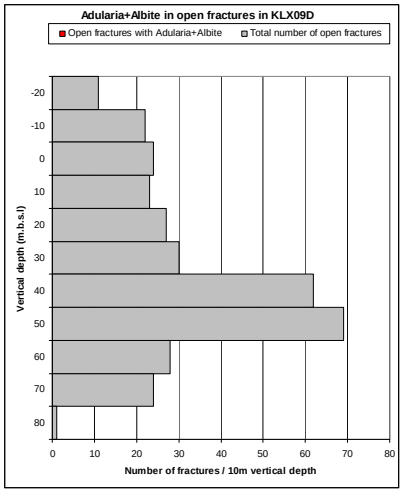
Adularia+Albite in open fractures in KLX09D
Open fractures with Adularia+Albite
Total number of open fractures
Vertical depth (m.b.s.l)
Number of fractures / 10m vertical depth

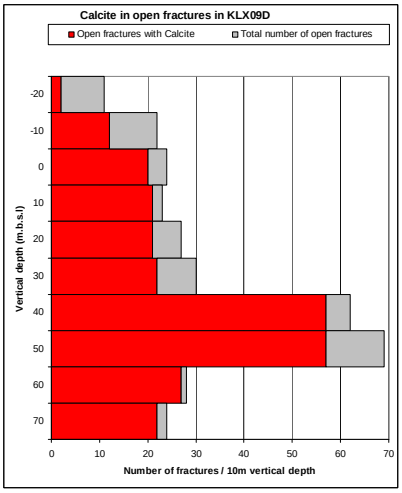
Calcite in open fractures in KLX09D
Open fractures with Calcite
Total number of open fractures
Vertical depth (m.b.s.l)
Number of fractures / 10m vertical depth

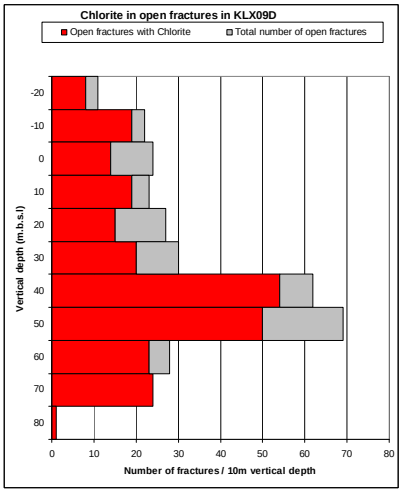
Chlorite in open fractures in KLX09D
Open fractures with Chlorite
Total number of open fractures
Vertical depth (m.b.s.l)
Number of fractures / 10m vertical depth

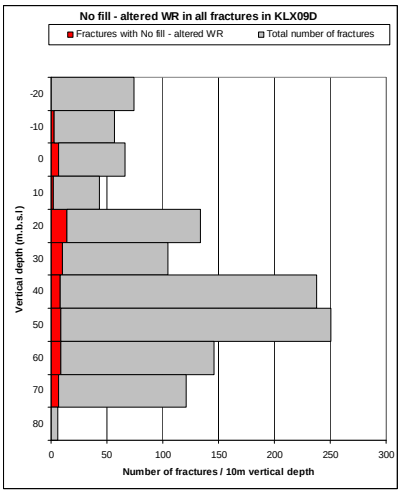
No fill - altered WR in all fractures in KLX09D
Fractures with No fill - altered WR
Total number of fractures
Vertical depth (m.b.s.l)
Number of fractures / 10m vertical depth

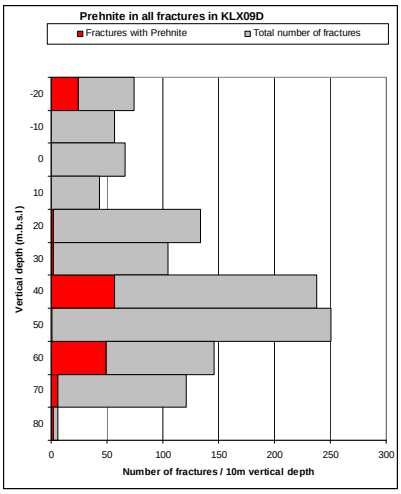
Prehnite in all fractures in KLX09D
Fractures with Prehnite
Total number of fractures
Vertical depth (m.b.s.l)
Number of fractures / 10m vertical depth

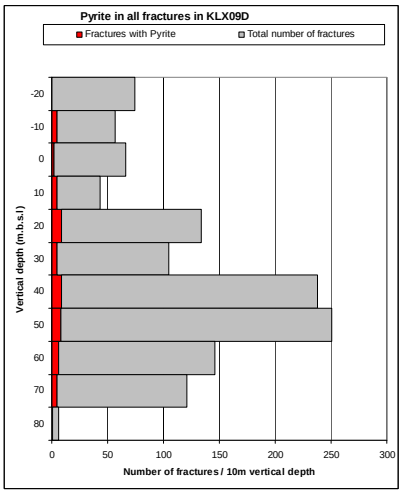
Pyrite in all fractures in KLX09D
Fractures with Pyrite
Total number of fractures
Vertical depth (m.b.s.l)
Number of fractures / 10m vertical depth

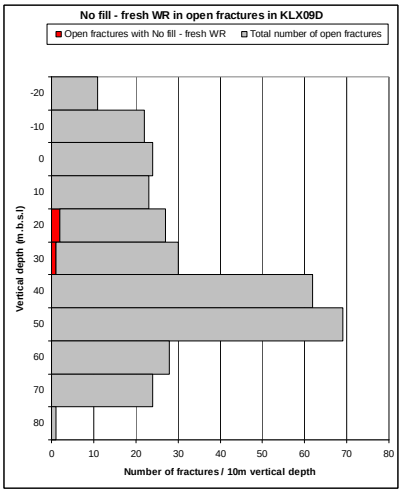
No fill - fresh WR in open fractures in KLX09D
Open fractures with No fill - fresh WR
Total number of open fractures
Vertical depth (m.b.s.l)
Number of fractures / 10m vertical depth

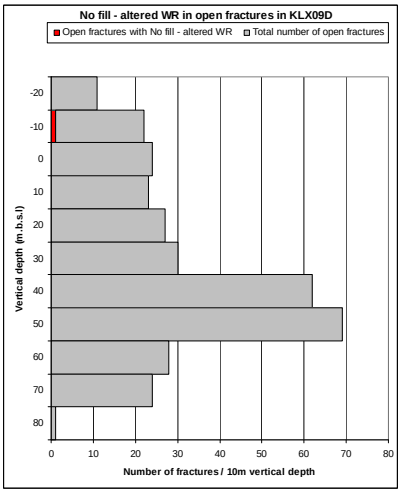
No fill - altered WR in open fractures in KLX09D
Open fractures with No fill - altered WR
Total number of open fractures
Vertical depth (m.b.s.l)
Number of fractures / 10m vertical depth

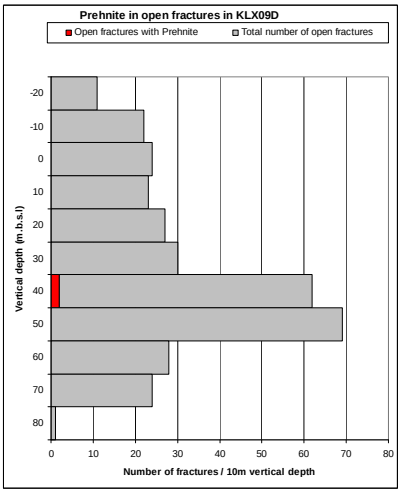
Prehnite in open fractures in KLX09D
Open fractures with Prehnite
Total number of open fractures
Vertical depth (m.b.s.l)
Number of fractures / 10m vertical depth

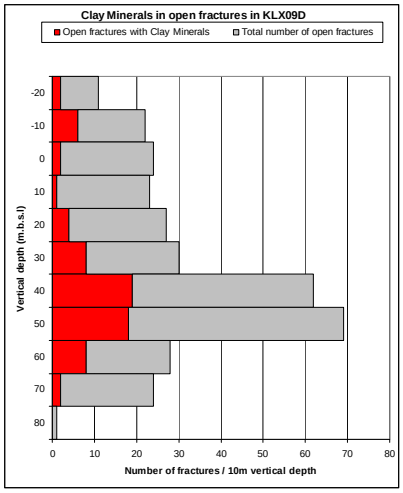
Clay Minerals in open fractures in KLX09D
Open fractures with Clay Minerals
Total number of open fractures
Vertical depth (m.b.s.l)
Number of fractures / 10m vertical depth

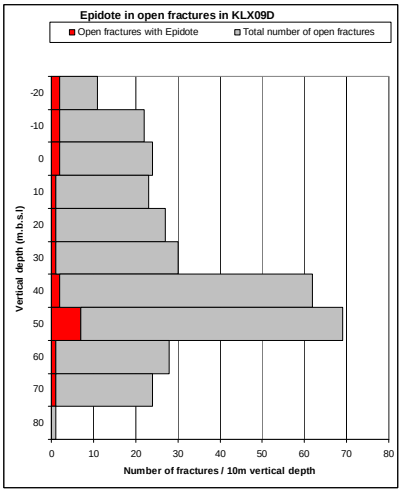
Epidote in open fractures in KLX09D
Open fractures with Epidote
Total number of open fractures
Vertical depth (m.b.s.l)
Number of fractures / 10m vertical depth

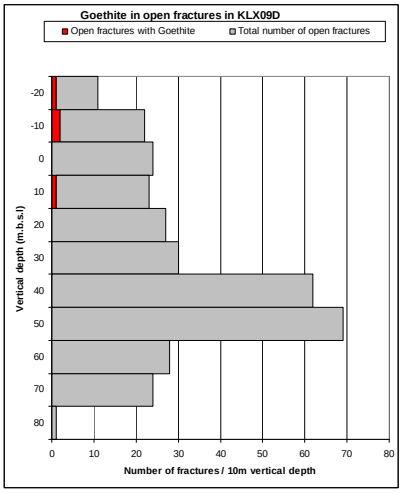
Goethite in open fractures in KLX09D
Open fractures with Goethite
Total number of open fractures
Vertical depth (m.b.s.l)
Number of fractures / 10m vertical depth

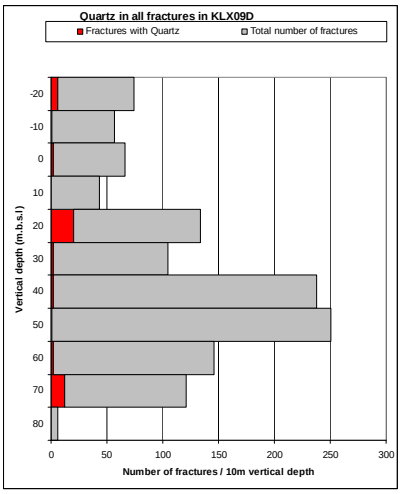
Quartz in all fractures in KLX09D
Fractures with Quartz
Total number of fractures
Vertical depth (m.b.s.l)
Number of fractures / 10m vertical depth

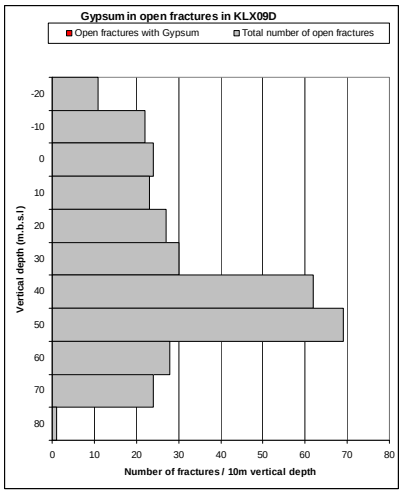
Gypsum in open fractures in KLX09D
Open fractures with Gypsum
Total number of open fractures
Vertical depth (m.b.s.l)
Number of fractures / 10m vertical depth

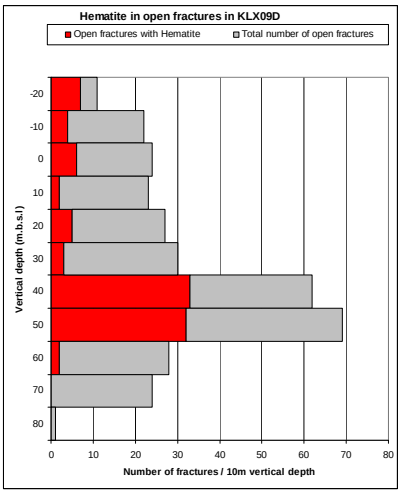
Hematite in open fractures in KLX09D
Open fractures with Hematite
Total number of open fractures
Vertical depth (m.b.s.l)
Number of fractures / 10m vertical depth

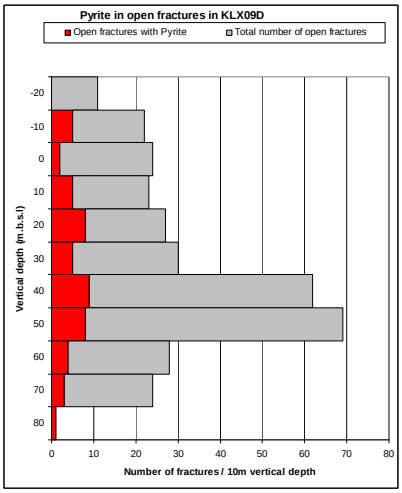
Pyrite in open fractures in KLX09D
Open fractures with Pyrite
Total number of open fractures
Vertical depth (m.b.s.l)
Number of fractures / 10m vertical depth

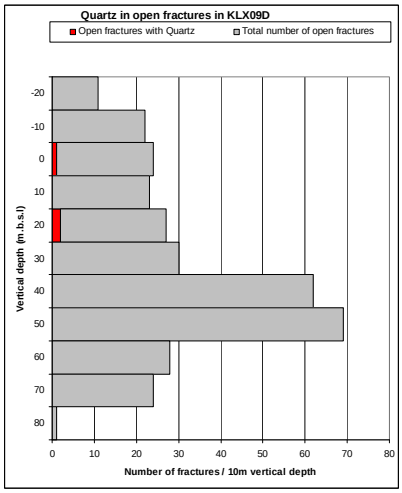
Quartz in open fractures in KLX09D
Open fractures with Quartz
Total number of open fractures
Vertical depth (m.b.s.l)
Number of fractures / 10m vertical depth

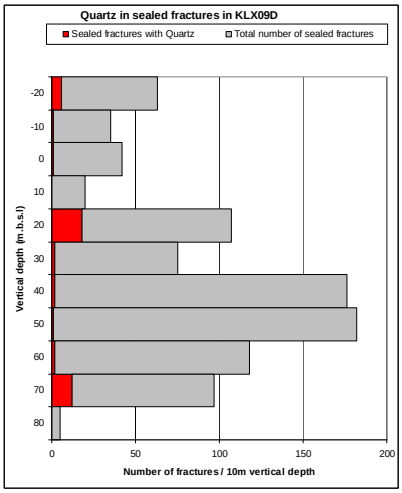
Quartz in sealed fractures in KLX09D
Sealed fractures with Quartz
Total number of sealed fractures
Vertical depth (m.b.s.l)
Number of fractures / 10m vertical depth

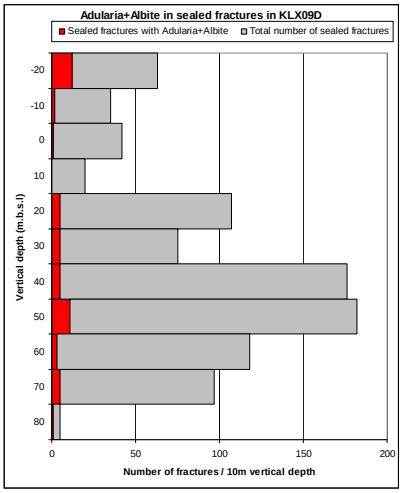
Adularia+Albite in sealed fractures in KLX09D
Sealed fractures with Adularia+Albite
Total number of sealed fractures
Vertical depth (m.b.s.l)
Number of fractures / 10m vertical depth

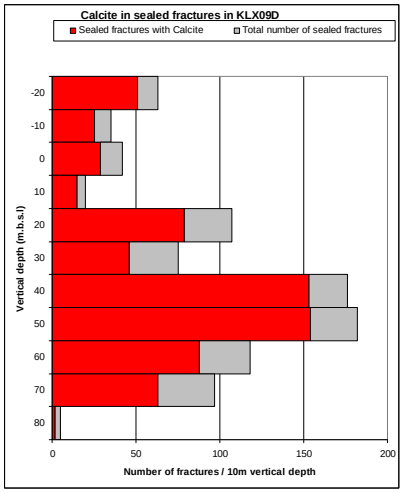
Calcite in sealed fractures in KLX09D
Sealed fractures with Calcite
Total number of sealed fractures
Vertical depth (m.b.s.l)
Number of fractures / 10m vertical depth

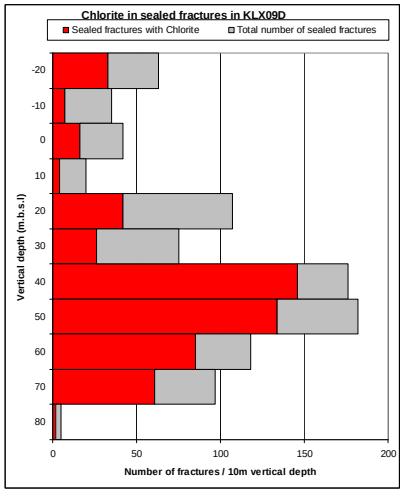
Chlorite in sealed fractures in KLX09D
Sealed fractures with Chlorite
Total number of sealed fractures
Vertical depth (m.b.s.l)
Number of fractures / 10m vertical depth

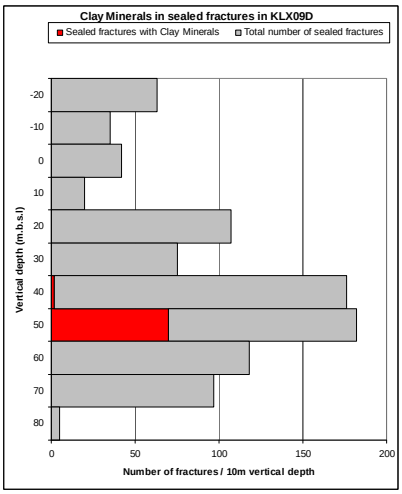
Clay Minerals in sealed fractures in KLX09D
Sealed fractures with Clay Minerals
Total number of sealed fractures
Vertical depth (m.b.s.l)
Number of fractures / 10m vertical depth

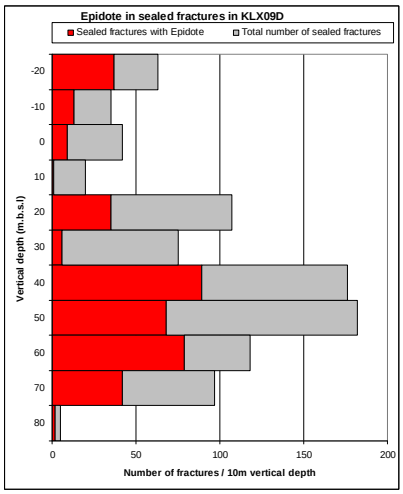
Epidote in sealed fractures in KLX09D
Sealed fractures with Epidote
Total number of sealed fractures
Vertical depth (m.b.s.l)
Number of fractures / 10m vertical depth

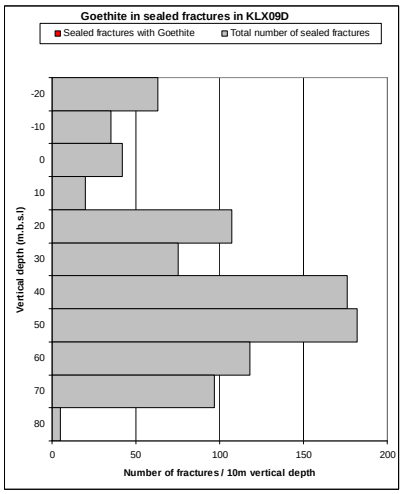
Goethite in sealed fractures in KLX09D
Sealed fractures with Goethite
Total number of sealed fractures
Vertical depth (m.b.s.l)
Number of fractures / 10m vertical depth

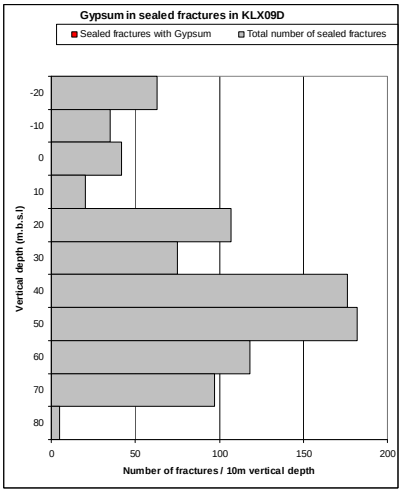
Gypsum in sealed fractures in KLX09D
Sealed fractures with Gypsum
Total number of sealed fractures
Vertical depth (m.b.s.l)
Number of fractures / 10m vertical depth

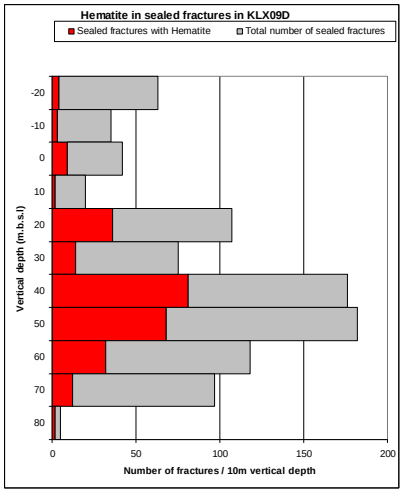
Hematite in sealed fractures in KLX09D
Sealed fractures with Hematite
Total number of sealed fractures
Vertical depth (m.b.s.l)
Number of fractures / 10m vertical depth

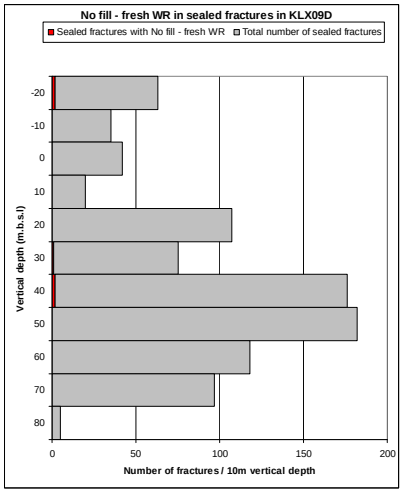
No fill - fresh WR in sealed fractures in KLX09D
Sealed fractures with No fill - fresh WR
Total number of sealed fractures
Vertical depth (m.b.s.l)
Number of fractures / 10m vertical depth

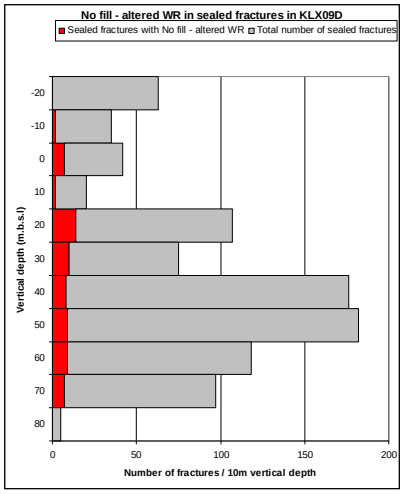
No fill - altered WR in sealed fractures in KLX09D
Sealed fractures with No fill - altered WR
Total number of sealed fractures
Vertical depth (m.b.s.l)
-20
-10
0
10
20
30
40
50
60
70
80
0
50
100
150
200
Number of fractures / 10m vertical depth

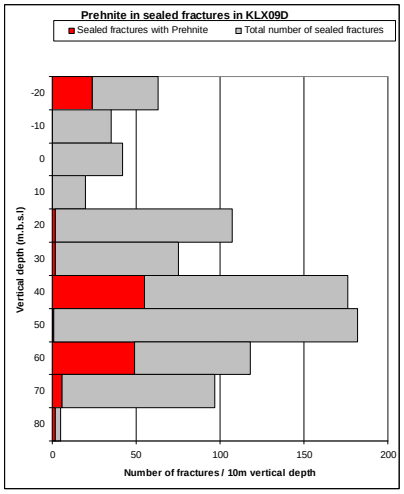
Prehnite in sealed fractures in KLX09D
Sealed fractures with Prehnite
Total number of sealed fractures
Vertical depth (m.b.s.l)
-20
-10
0
10
20
30
40
50
60
70
80
0
50
100
150
200
Number of fractures / 10m vertical depth

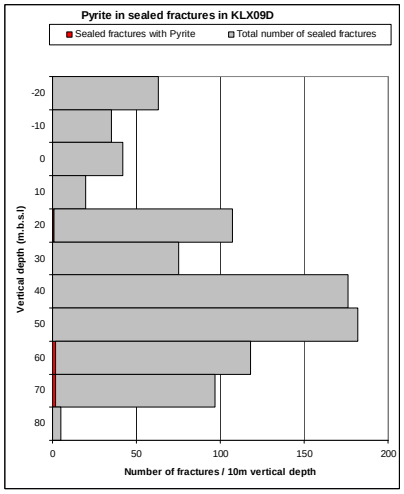
Pyrite in sealed fractures in KLX09D
Sealed fractures with Pyrite
Total number of sealed fractures
Vertical depth (m.b.s.l)
-20
-10
0
10
20
30
40
50
60
70
80
0
50
100
150
200
Number of fractures / 10m vertical depth

KLX09E

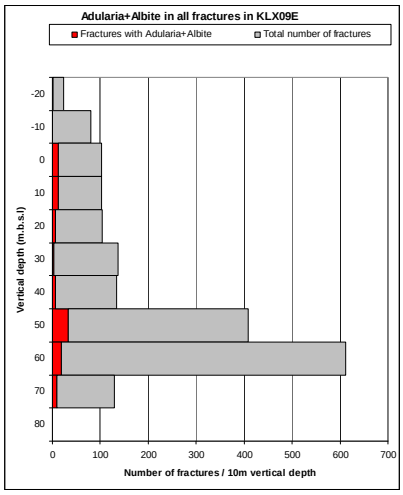
Adularia+Albite in all fractures in KLX09E
Fractures with Adularia+Albite
Total number of fractures
Vertical depth (m.b.s.l)
Number of fractures / 10m vertical depth

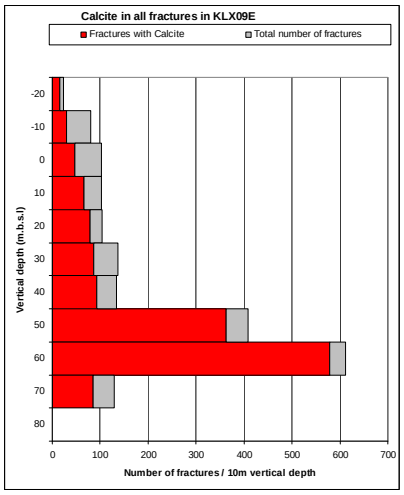
Calcite in all fractures in KLX09E
Fractures with Calcite
Total number of fractures
Vertical depth (m.b.s.l)
Number of fractures / 10m vertical depth

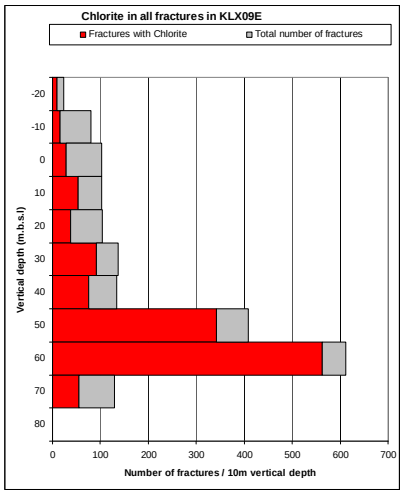
Chlorite in all fractures in KLX09E
Fractures with Chlorite
Total number of fractures
Vertical depth (m.b.s.l)
Number of fractures / 10m vertical depth

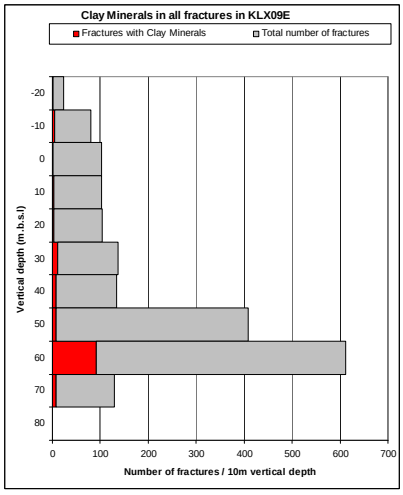
Clay Minerals in all fractures in KLX09E
Fractures with Clay Minerals
Total number of fractures
Vertical depth (m.b.s.l)
Number of fractures / 10m vertical depth

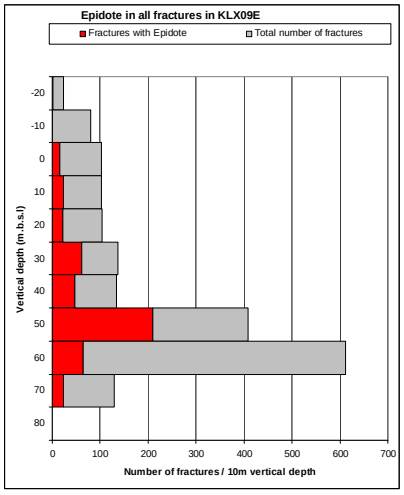
Epidote in all fractures in KLX09E
Fractures with Epidote
Total number of fractures
Vertical depth (m.b.s.l)
Number of fractures / 10m vertical depth

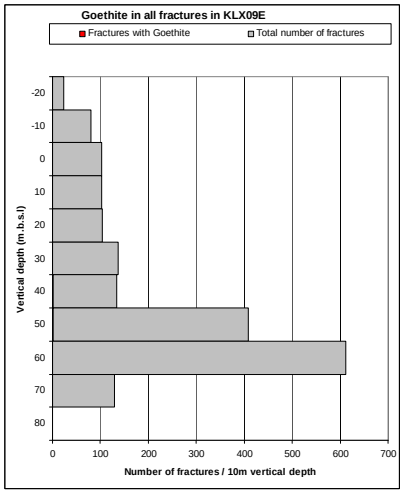
Goethite in all fractures in KLX09E
Fractures with Goethite
Total number of fractures
Vertical depth (m.b.s.l)
Number of fractures / 10m vertical depth

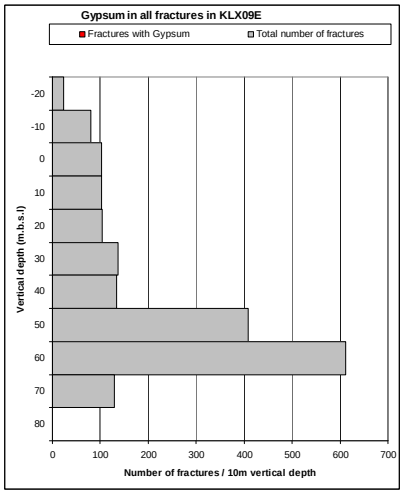
Gypsum in all fractures in KLX09E
Fractures with Gypsum
Total number of fractures
Vertical depth (m.b.s.l)
Number of fractures / 10m vertical depth

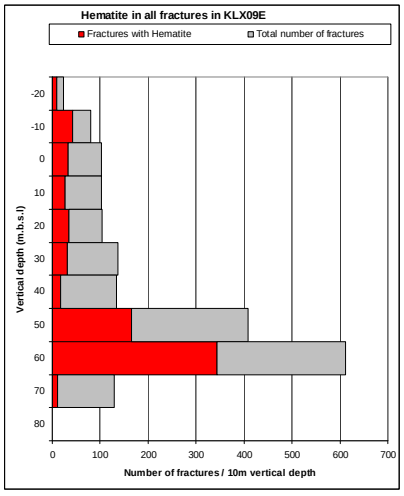
Hematite in all fractures in KLX09E
Fractures with Hematite
Total number of fractures
Vertical depth (m.b.s.l)
Number of fractures / 10m vertical depth

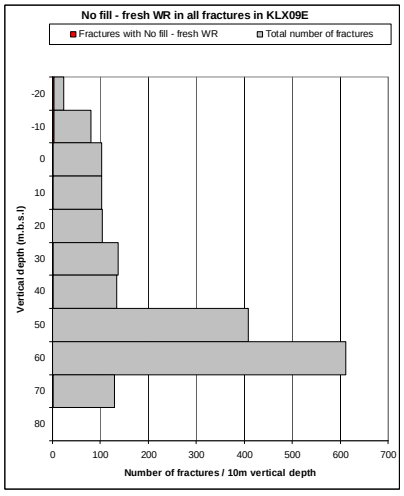
No fill - fresh WR in all fractures in KLX09E
Fractures with No fill - fresh WR
Total number of fractures
Vertical depth (m.b.s.l)
Number of fractures / 10m vertical depth

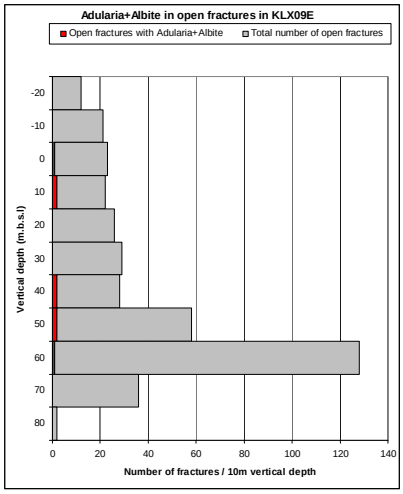
Adularia+Albite in open fractures in KLX09E
Open fractures with Adularia+Albite
Total number of open fractures
Vertical depth (m.b.s.l)
Number of fractures / 10m vertical depth

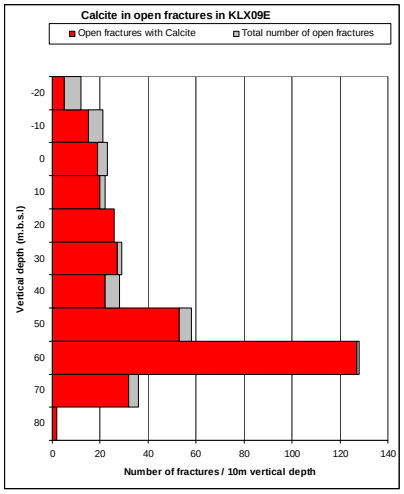
Calcite in open fractures in KLX09E
Open fractures with Calcite
Total number of open fractures
Vertical depth (m.b.s.l)
Number of fractures / 10m vertical depth

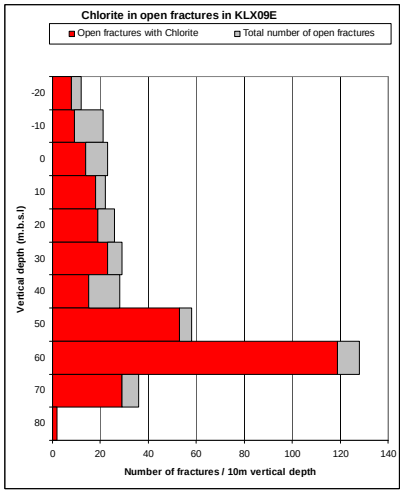
Chlorite in open fractures in KLX09E
Open fractures with Chlorite
Total number of open fractures
Vertical depth (m.b.s.l)
Number of fractures / 10m vertical depth

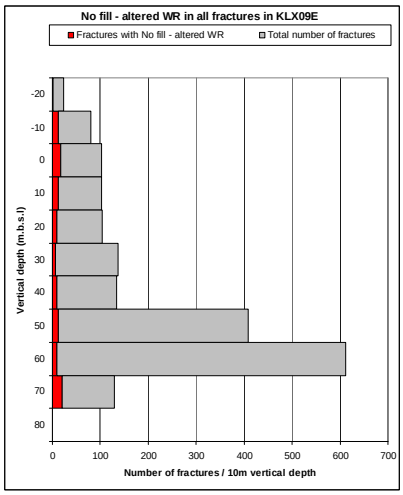
No fill - altered WR in all fractures in KLX09E
Fractures with No fill - altered WR
Total number of fractures
Vertical depth (m.b.s.l)
Number of fractures / 10m vertical depth

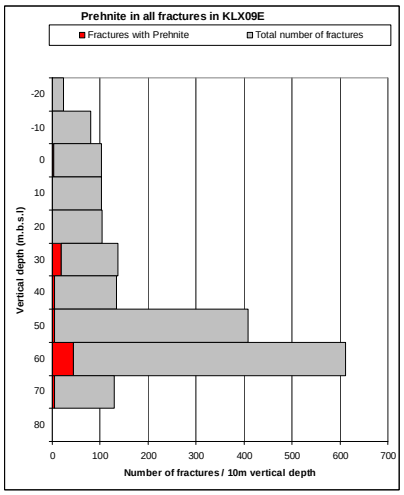
Prehnite in all fractures in KLX09E
Fractures with Prehnite
Total number of fractures
Vertical depth (m.b.s.l)
Number of fractures / 10m vertical depth

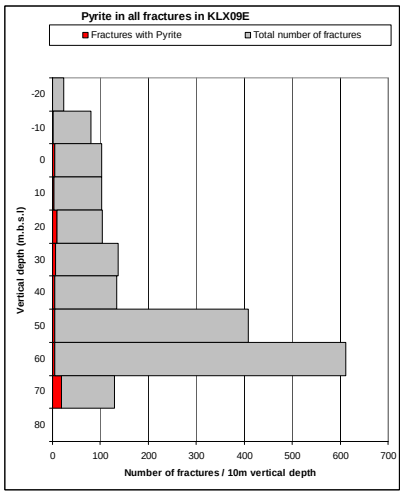
Pyrite in all fractures in KLX09E
Fractures with Pyrite
Total number of fractures
Vertical depth (m.b.s.l)
Number of fractures / 10m vertical depth

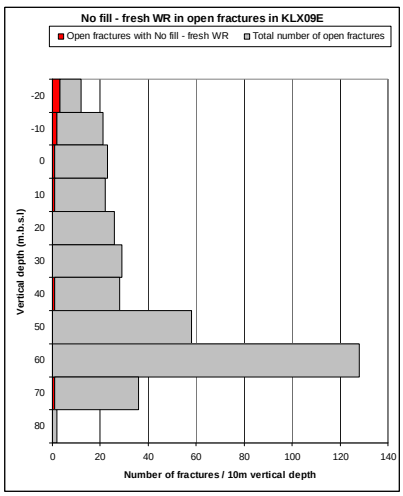
No fill - fresh WR in open fractures in KLX09E
Open fractures with No fill - fresh WR
Total number of open fractures
Vertical depth (m.b.s.l)
Number of fractures / 10m vertical depth

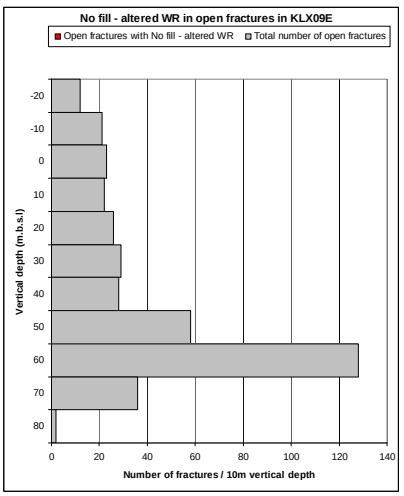
No fill - altered WR in open fractures in KLX09E
Open fractures with No fill - altered WR
Total number of open fractures
Vertical depth (m.b.s.l)
Number of fractures / 10m vertical depth

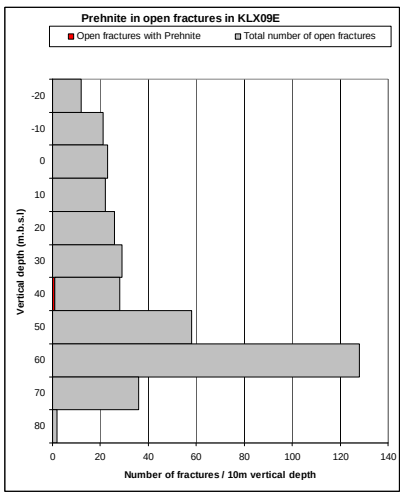
Prehnite in open fractures in KLX09E
Open fractures with Prehnite
Total number of open fractures
Vertical depth (m.b.s.l)
Number of fractures / 10m vertical depth

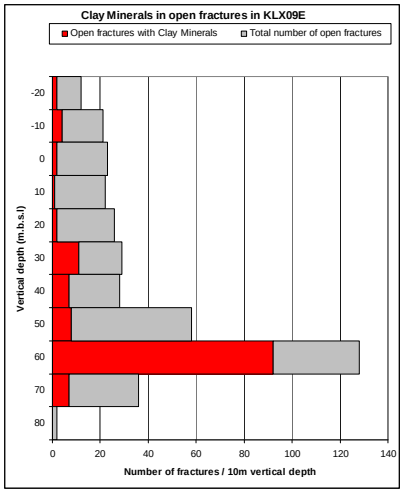
Clay Minerals in open fractures in KLX09E
Open fractures with Clay Minerals
Total number of open fractures
Vertical depth (m.b.s.l)
Number of fractures / 10m vertical depth

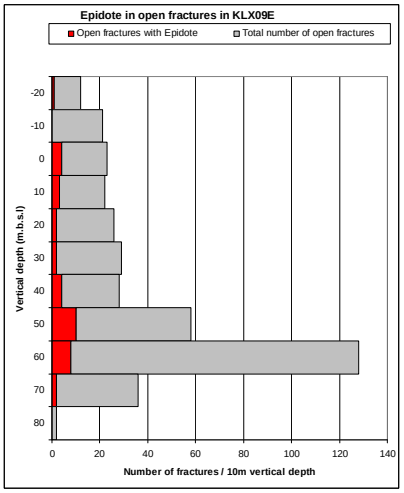
Epidote in open fractures in KLX09E
Open fractures with Epidote
Total number of open fractures
Vertical depth (m.b.s.l)
Number of fractures / 10m vertical depth

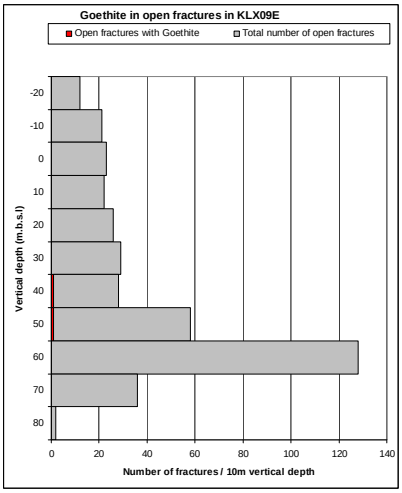
Goethite in open fractures in KLX09E
Open fractures with Goethite
Total number of open fractures
Vertical depth (m.b.s.l)
Number of fractures / 10m vertical depth

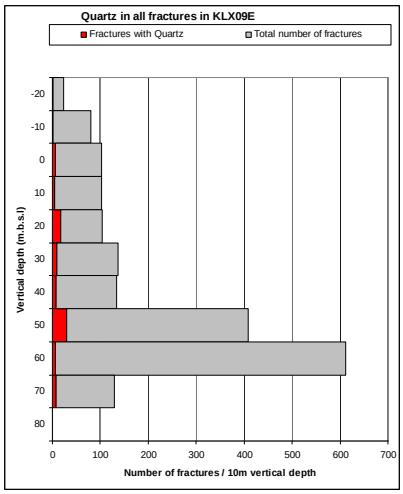
Quartz in all fractures in KLX09E
Fractures with Quartz
Total number of fractures
Vertical depth (m.b.s.l)
Number of fractures / 10m vertical depth

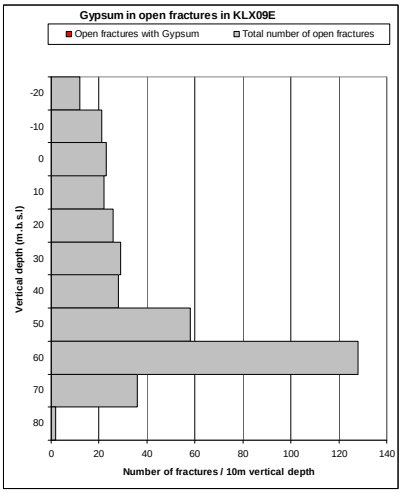
Gypsum in open fractures in KLX09E
Open fractures with Gypsum
Total number of open fractures
Vertical depth (m.b.s.l)
Number of fractures / 10m vertical depth

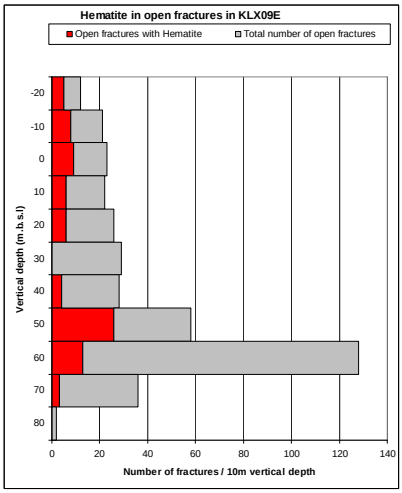
Hematite in open fractures in KLX09E
Open fractures with Hematite
Total number of open fractures
Vertical depth (m.b.s.l)
Number of fractures / 10m vertical depth

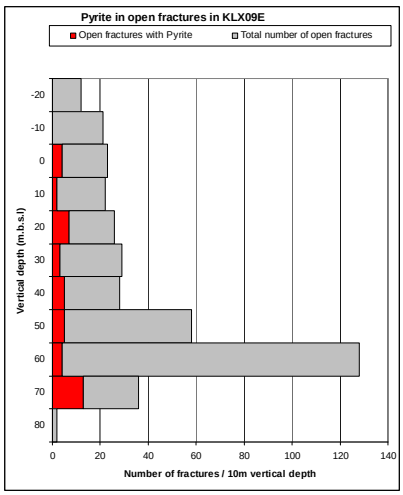
Pyrite in open fractures in KLX09E
Open fractures with Pyrite
Total number of open fractures
Vertical depth (m.b.s.l)
Number of fractures / 10m vertical depth

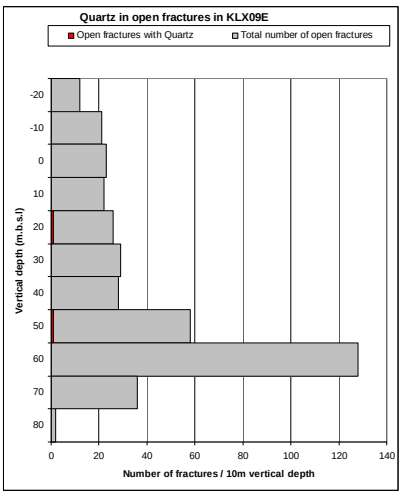
Quartz in open fractures in KLX09E
Open fractures with Quartz
Total number of open fractures
Vertical depth (m.b.s.l)
Number of fractures / 10m vertical depth

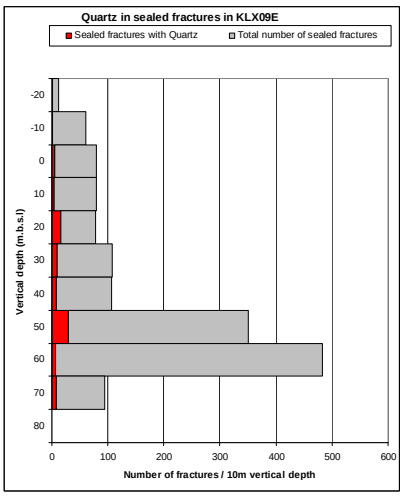
Quartz in sealed fractures in KLX09E
Sealed fractures with Quartz
Total number of sealed fractures
Vertical depth (m.b.s.l)
Number of fractures / 10m vertical depth

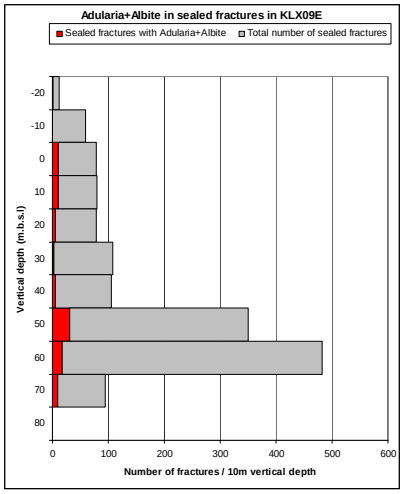
Adularia+Albite in sealed fractures in KLX09E
Sealed fractures with Adularia+Albite
Total number of sealed fractures
Vertical depth (m.b.s.l)
Number of fractures / 10m vertical depth

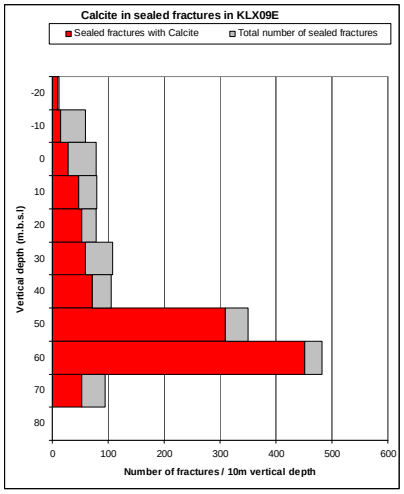
Calcite in sealed fractures in KLX09E
Sealed fractures with Calcite
Total number of sealed fractures
Vertical depth (m.b.s.l)
Number of fractures / 10m vertical depth

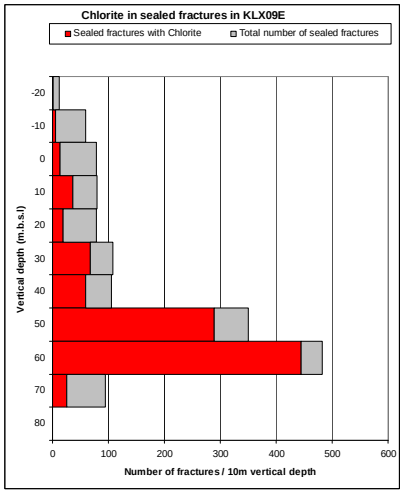
Chlorite in sealed fractures in KLX09E
Sealed fractures with Chlorite
Total number of sealed fractures
Vertical depth (m.b.s.l)
Number of fractures / 10m vertical depth

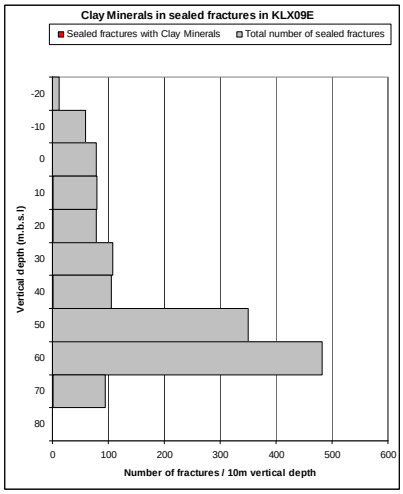
Clay Minerals in sealed fractures in KLX09E
Sealed fractures with Clay Minerals
Total number of sealed fractures
Vertical depth (m.b.s.l)
Number of fractures / 10m vertical depth

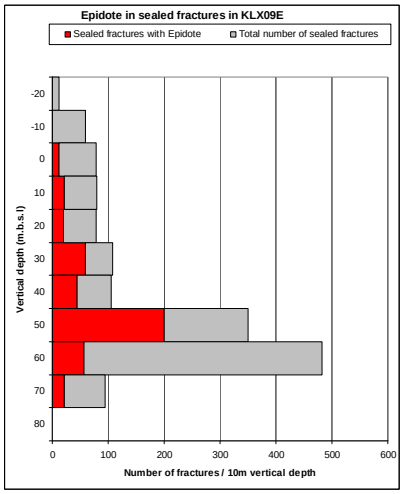
Epidote in sealed fractures in KLX09E
Sealed fractures with Epidote
Total number of sealed fractures
Vertical depth (m.b.s.l)
Number of fractures / 10m vertical depth

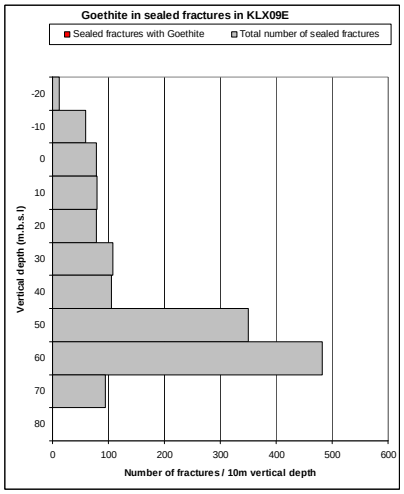
Goethite in sealed fractures in KLX09E
Sealed fractures with Goethite
Total number of sealed fractures
Vertical depth (m.b.s.l)
Number of fractures / 10m vertical depth

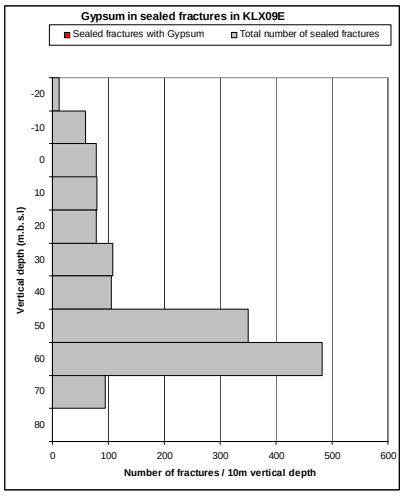
Gypsum in sealed fractures in KLX09E
Sealed fractures with Gypsum
Total number of sealed fractures
Vertical depth (m.b.s.l)
Number of fractures / 10m vertical depth

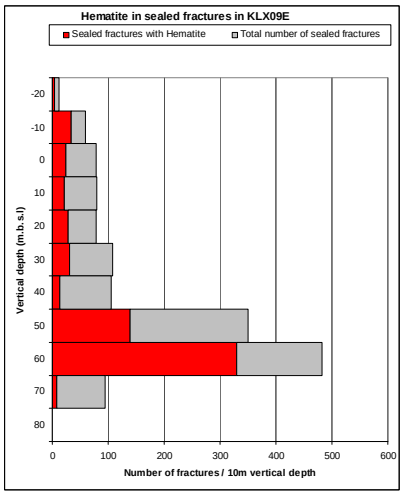
Hematite in sealed fractures in KLX09E
Sealed fractures with Hematite
Total number of sealed fractures
Vertical depth (m.b.s.l)
Number of fractures / 10m vertical depth

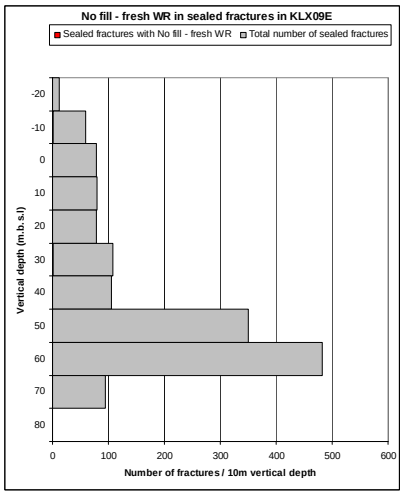
No fill - fresh WR in sealed fractures in KLX09E
Sealed fractures with No fill - fresh WR
Total number of sealed fractures
Vertical depth (m.b.s.l)
Number of fractures / 10m vertical depth

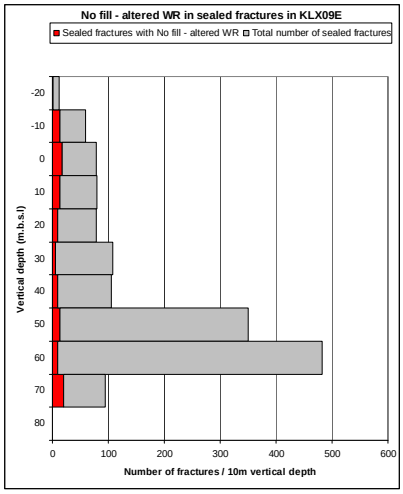
No fill - altered WR in sealed fractures in KLX09E
Sealed fractures with No fill - altered WR
Total number of sealed fractures
Vertical depth (m.b.s.l)
-20
-10
0
10
20
30
40
50
60
70
80
0
100
200
300
400
500
600
Number of fractures / 10m vertical depth

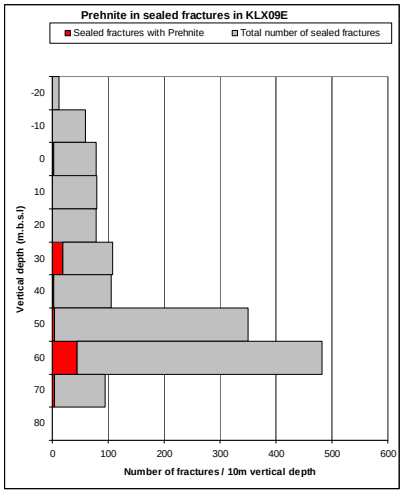
Prehnite in sealed fractures in KLX09E
Sealed fractures with Prehnite
Total number of sealed fractures
Vertical depth (m.b.s.l)
-20
-10
0
10
20
30
40
50
60
70
80
0
100
200
300
400
500
600
Number of fractures / 10m vertical depth

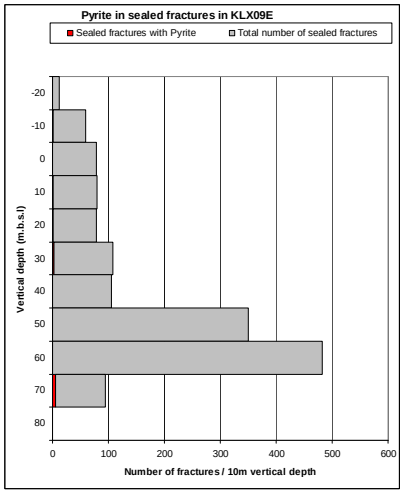
Pyrite in sealed fractures in KLX09E
Sealed fractures with Pyrite
Total number of sealed fractures
Vertical depth (m.b.s.l)
-20
-10
0
10
20
30
40
50
60
70
80
0
100
200
300
400
500
600
Number of fractures / 10m vertical depth

KLX09F

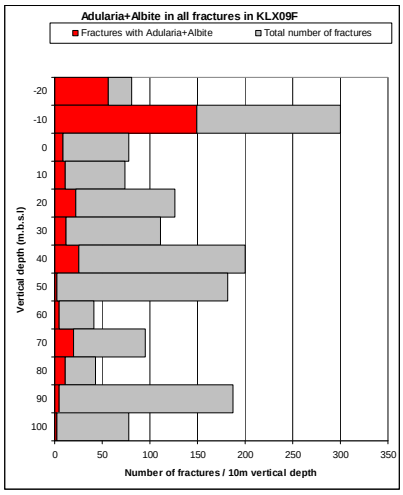
Adularia+Albite in all fractures in KLX09F
Fractures with Adularia+Albite
Total number of fractures
Vertical depth (m.b.s.l)
Number of fractures / 10m vertical depth

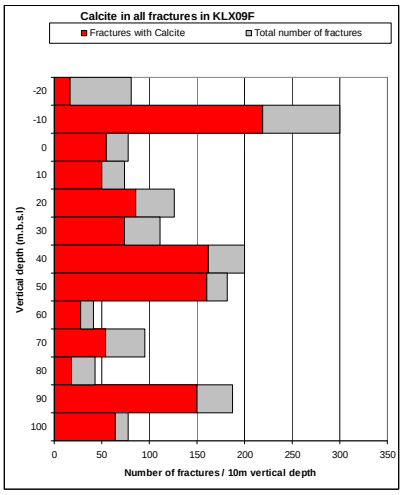
Calcite in all fractures in KLX09F
Fractures with Calcite
Total number of fractures
Vertical depth (m.b.s.l)
Number of fractures / 10m vertical depth

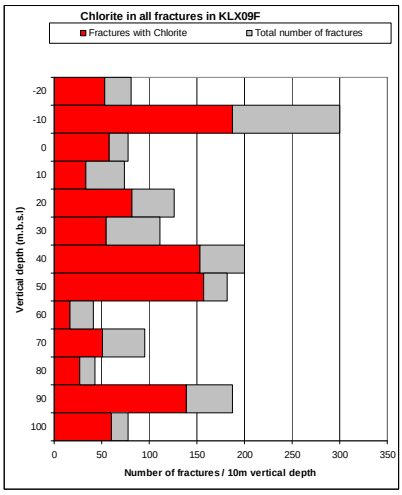
Chlorite in all fractures in KLX09F
Fractures with Chlorite
Total number of fractures
Vertical depth (m.b.s.l)
Number of fractures / 10m vertical depth

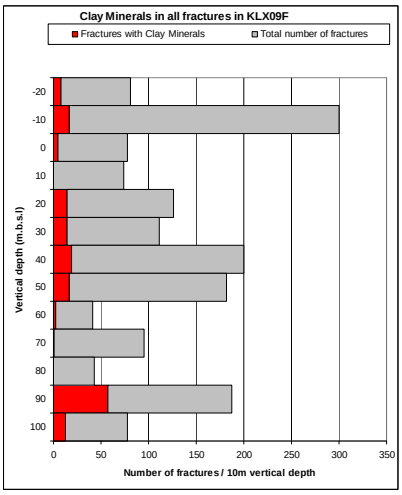
Clay Minerals in all fractures in KLX09F
Fractures with Clay Minerals
Total number of fractures
Vertical depth (m.b.s.l)
Number of fractures / 10m vertical depth

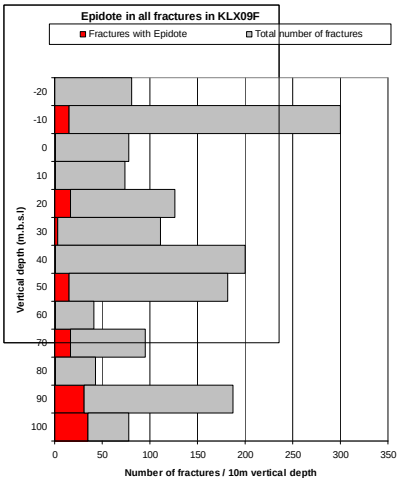
Epidote in all fractures in KLX09F
Fractures with Epidote
Total number of fractures
Vertical depth (m.b.s.l)
Number of fractures / 10m vertical depth

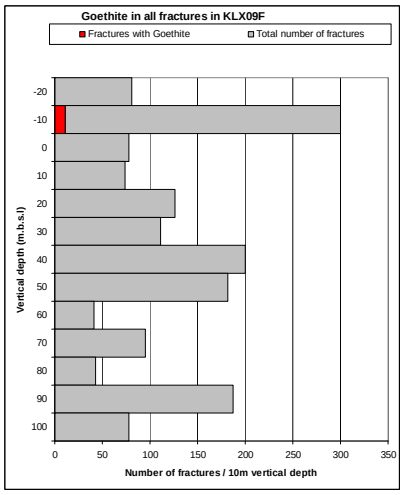
Goethite in all fractures in KLX09F
Fractures with Goethite
Total number of fractures
Vertical depth (m.b.s.l)
Number of fractures / 10m vertical depth

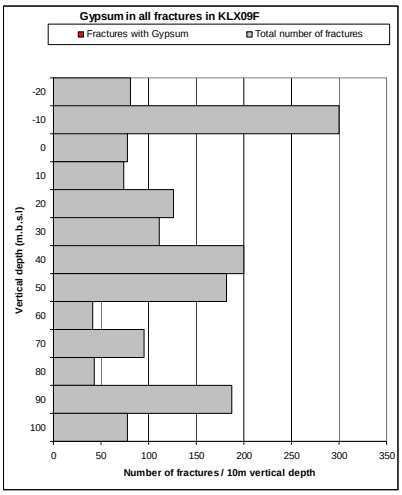
Gypsum in all fractures in KLX09F
Fractures with Gypsum
Total number of fractures
Vertical depth (m.b.s.l)
Number of fractures / 10m vertical depth

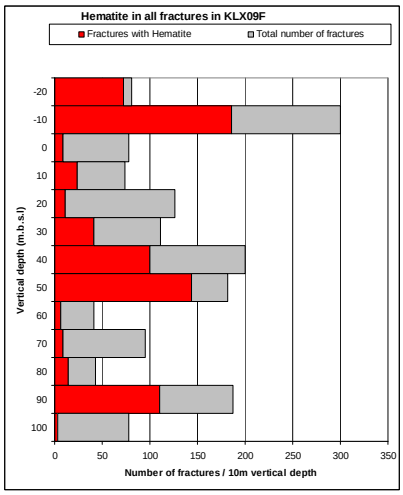
Hematite in all fractures in KLX09F
Fractures with Hematite
Total number of fractures
Vertical depth (m.b.s.l)
Number of fractures / 10m vertical depth

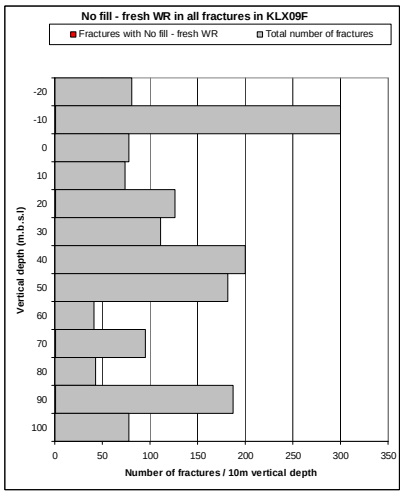
No fill - fresh WR in all fractures in KLX09F
Fractures with No fill - fresh WR
Total number of fractures
Vertical depth (m.b.s.l)
Number of fractures / 10m vertical depth

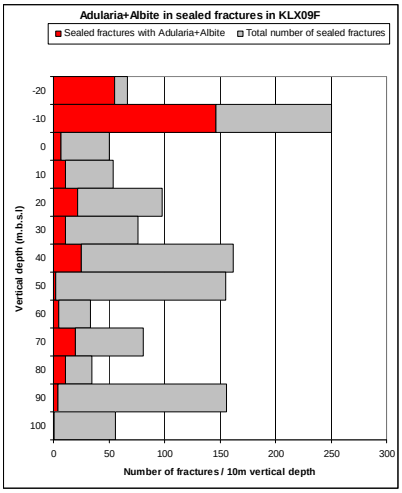
Adularia+Albite in sealed fractures in KLX09F
Sealed fractures with Adularia+Albite
Total number of sealed fractures
Vertical depth (m.b.s.l)
Number of fractures / 10m vertical depth

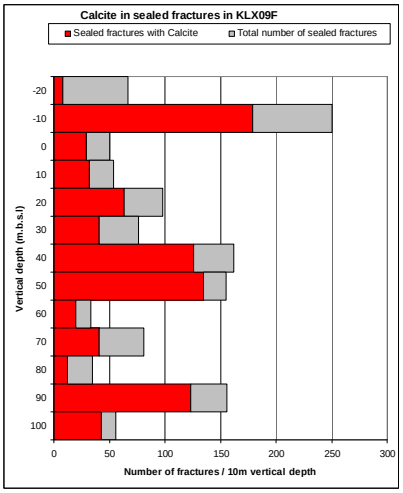
Calcite in sealed fractures in KLX09F
Sealed fractures with Calcite
Total number of sealed fractures
Vertical depth (m.b.s.l)
Number of fractures / 10m vertical depth

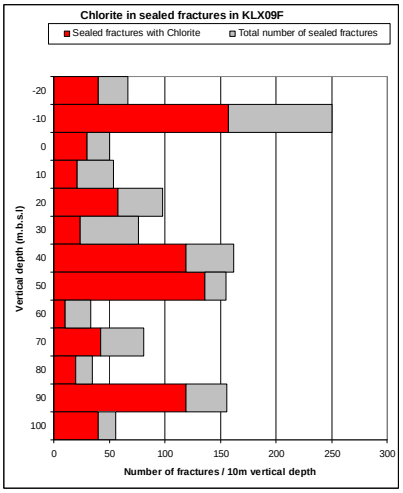
Chlorite in sealed fractures in KLX09F
Sealed fractures with Chlorite
Total number of sealed fractures
Vertical depth (m.b.s.l)
Number of fractures / 10m vertical depth

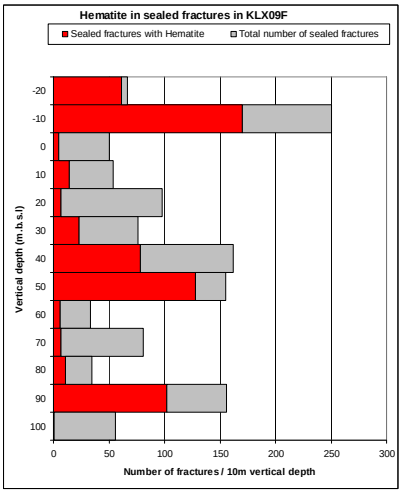
Hematite in sealed fractures in KLX09F
Sealed fractures with Hematite
Total number of sealed fractures
Vertical depth (m.b.s.l)
Number of fractures / 10m vertical depth

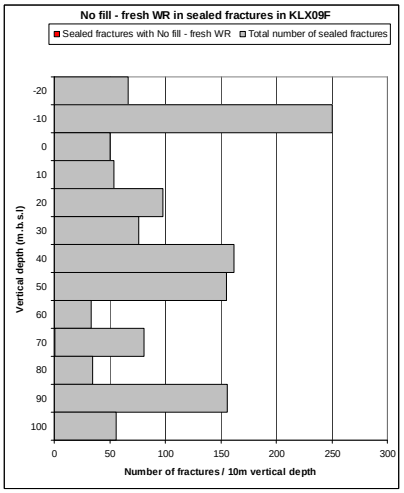
No fill - fresh WR in sealed fractures in KLX09F
Sealed fractures with No fill - fresh WR
Total number of sealed fractures
Vertical depth (m.b.s.l)
Number of fractures / 10m vertical depth

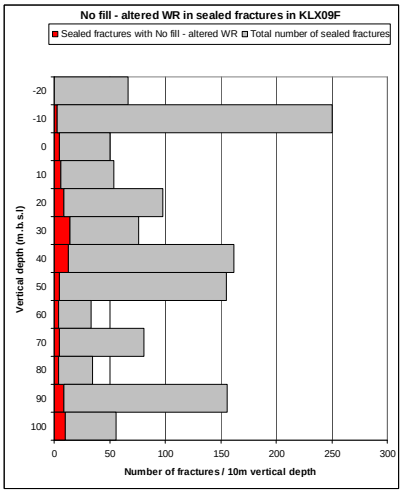
No fill - altered WR in sealed fractures in KLX09F
Sealed fractures with No fill - altered WR
Total number of sealed fractures
Vertical depth (m.b.s.l)
Number of fractures / 10m vertical depth

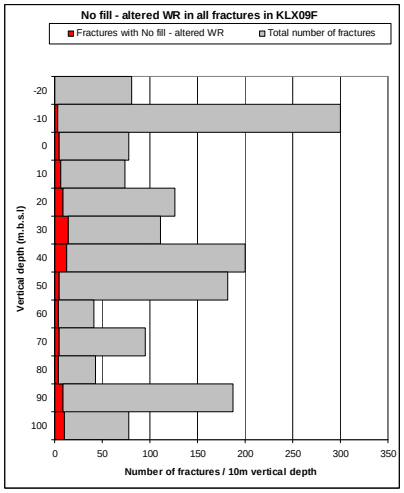
No fill - altered WR in all fractures in KLX09F
Fractures with No fill - altered WR
Total number of fractures
Vertical depth (m.b.s.l)
Number of fractures / 10m vertical depth

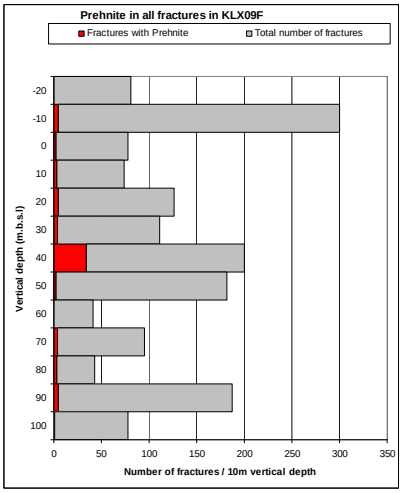
Prehnite in all fractures in KLX09F
Fractures with Prehnite
Total number of fractures
Vertical depth (m.b.s.l)
Number of fractures / 10m vertical depth

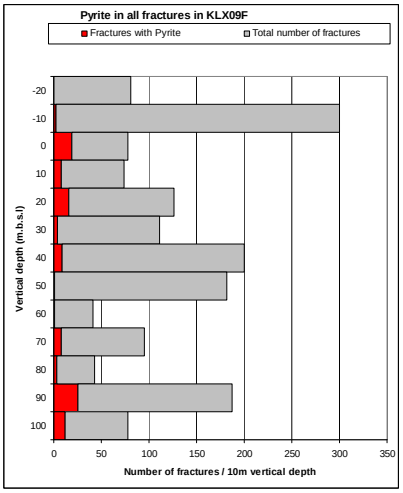
Pyrite in all fractures in KLX09F
Fractures with Pyrite
Total number of fractures
Vertical depth (m.b.s.l)
Number of fractures / 10m vertical depth

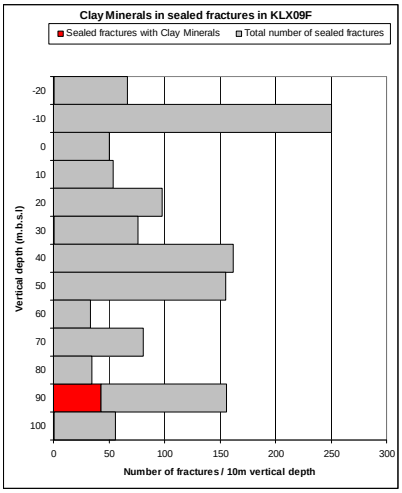
Clay Minerals in sealed fractures in KLX09F
Sealed fractures with Clay Minerals
Total number of sealed fractures
Vertical depth (m.b.s.l)
Number of fractures / 10m vertical depth

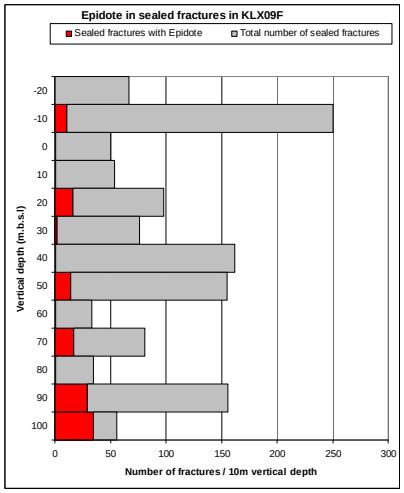
Epidote in sealed fractures in KLX09F
Sealed fractures with Epidote
Total number of sealed fractures
Vertical depth (m.b.s.l)
Number of fractures / 10m vertical depth

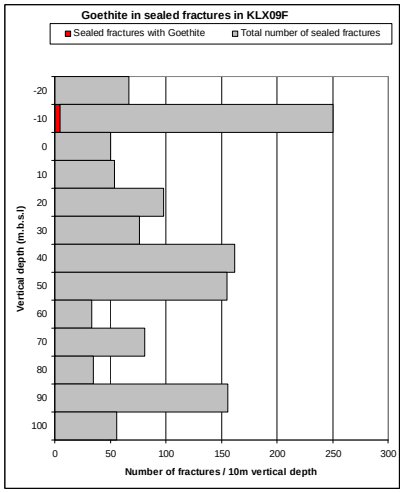
Goethite in sealed fractures in KLX09F
Sealed fractures with Goethite
Total number of sealed fractures
Vertical depth (m.b.s.l)
Number of fractures / 10m vertical depth

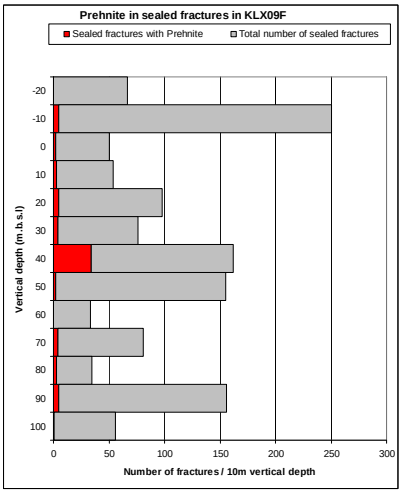
Prehnite in sealed fractures in KLX09F
Sealed fractures with Prehnite
Total number of sealed fractures
Vertical depth (m.b.s.l)
Number of fractures / 10m vertical depth

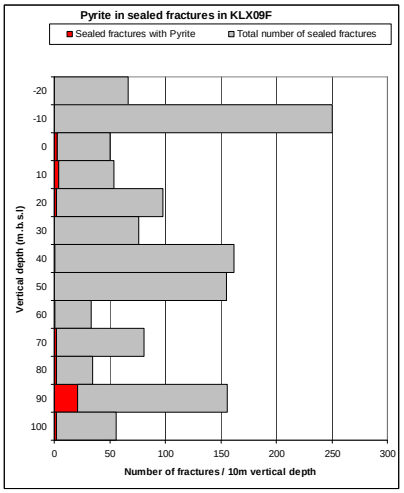
Pyrite in sealed fractures in KLX09F
Sealed fractures with Pyrite
Total number of sealed fractures
Vertical depth (m.b.s.l)
Number of fractures / 10m vertical depth

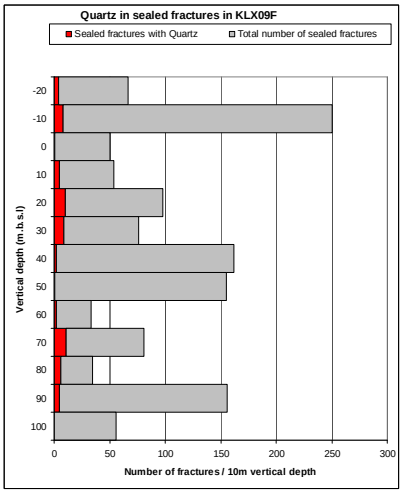
Quartz in sealed fractures in KLX09F
Sealed fractures with Quartz
Total number of sealed fractures
Vertical depth (m.b.s.l)
Number of fractures / 10m vertical depth

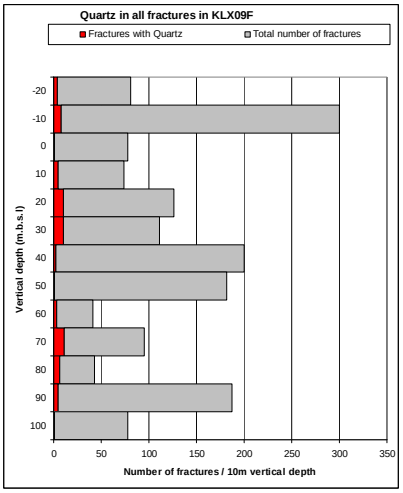
Quartz in all fractures in KLX09F
Fractures with Quartz
Total number of fractures
Vertical depth (m.b.s.l)
Number of fractures / 10m vertical depth

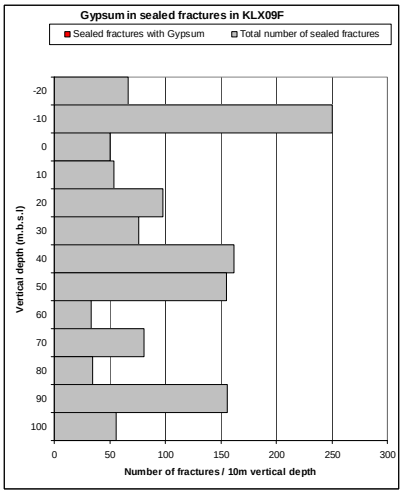
Gypsum in sealed fractures in KLX09F
Sealed fractures with Gypsum
Total number of sealed fractures
Vertical depth (m.b.s.l)
Number of fractures / 10m vertical depth

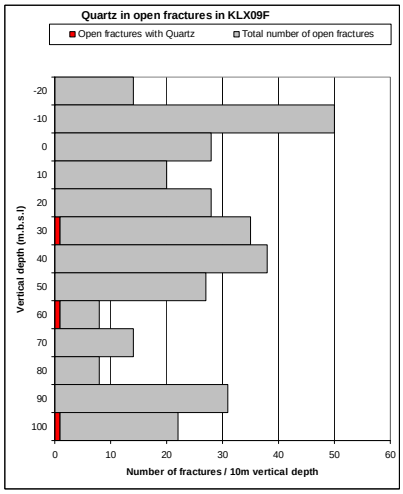
Quartz in open fractures in KLX09F
Open fractures with Quartz
Total number of open fractures
Vertical depth (m.b.s.l)
Number of fractures / 10m vertical depth

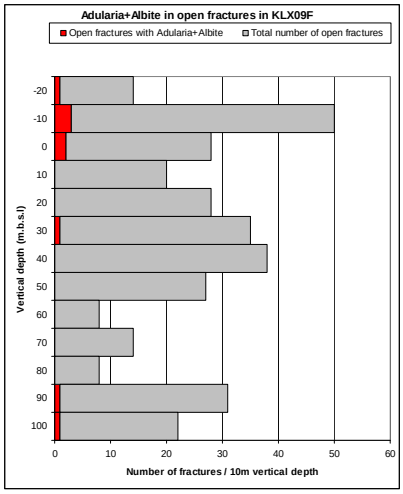
Adularia+Albite in open fractures in KLX09F
Open fractures with Adularia+Albite
Total number of open fractures
Vertical depth (m.b.s.l)
Number of fractures / 10m vertical depth

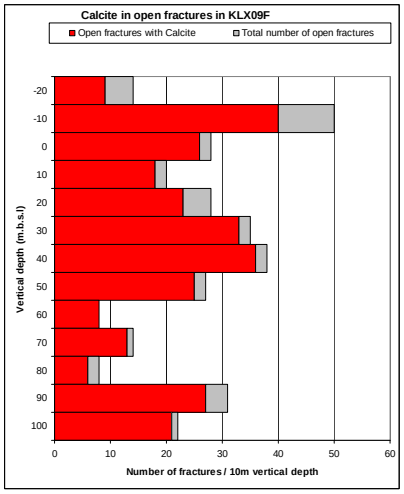
Calcite in open fractures in KLX09F
Open fractures with Calcite
Total number of open fractures
Vertical depth (m.b.s.l)
Number of fractures / 10m vertical depth

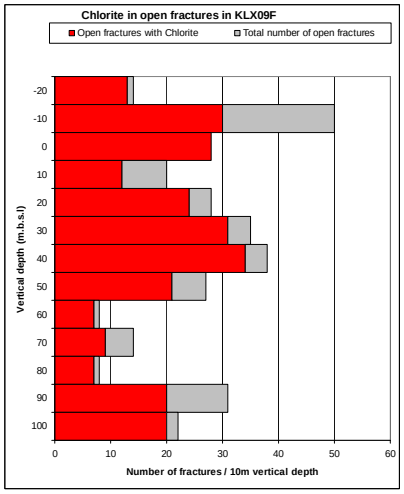
Chlorite in open fractures in KLX09F
Open fractures with Chlorite
Total number of open fractures
Vertical depth (m.b.s.l)
Number of fractures / 10m vertical depth

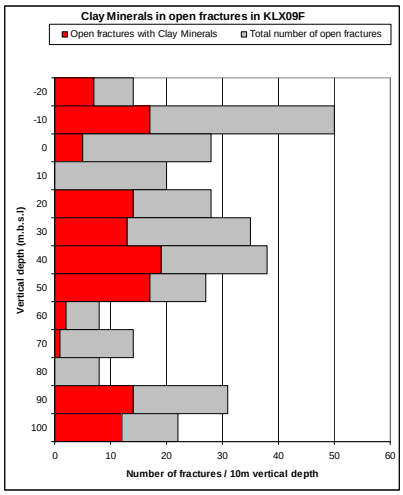
Clay Minerals in open fractures in KLX09F
Open fractures with Clay Minerals
Total number of open fractures
Vertical depth (m.b.s.l)
Number of fractures / 10m vertical depth

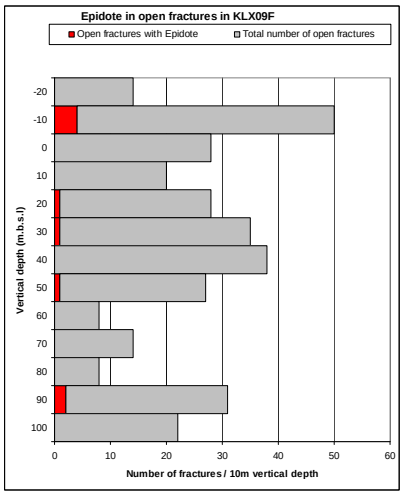
Epidote in open fractures in KLX09F
Open fractures with Epidote
Total number of open fractures
Vertical depth (m.b.s.l)
Number of fractures / 10m vertical depth

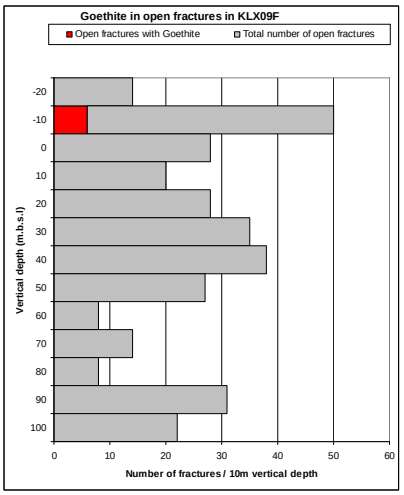
Goethite in open fractures in KLX09F
Open fractures with Goethite
Total number of open fractures
Vertical depth (m.b.s.l)
Number of fractures / 10m vertical depth

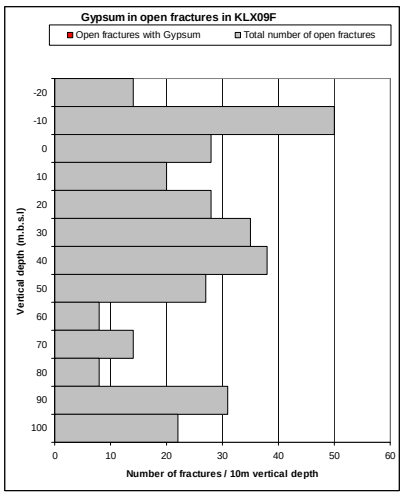
Gypsum in open fractures in KLX09F
Open fractures with Gypsum
Total number of open fractures
Vertical depth (m.b.s.l)
Number of fractures / 10m vertical depth

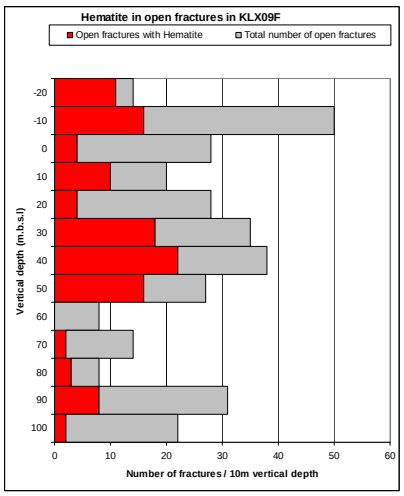
Hematite in open fractures in KLX09F
Open fractures with Hematite
Total number of open fractures
Vertical depth (m.b.s.l)
Number of fractures / 10m vertical depth

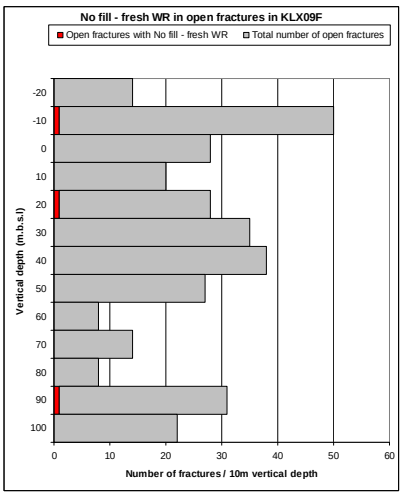
No fill - fresh WR in open fractures in KLX09F
Open fractures with No fill - fresh WR
Total number of open fractures
Vertical depth (m.b.s.l)
Number of fractures / 10m vertical depth

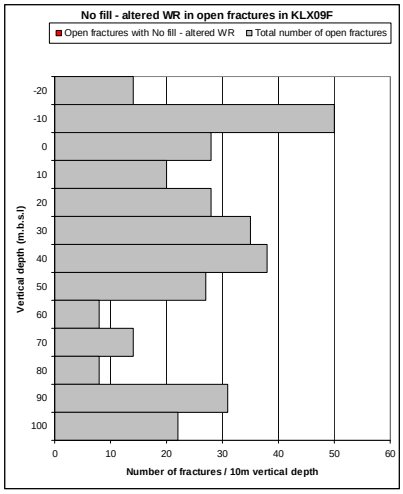
No fill - altered WR in open fractures in KLX09F
Open fractures with No fill - altered WR
Total number of open fractures
Vertical depth (m.b.s.l)
-20
-10
0
10
20
30
40
50
60
70
80
90
100
0
10
20
30
40
50
60
Number of fractures / 10m vertical depth

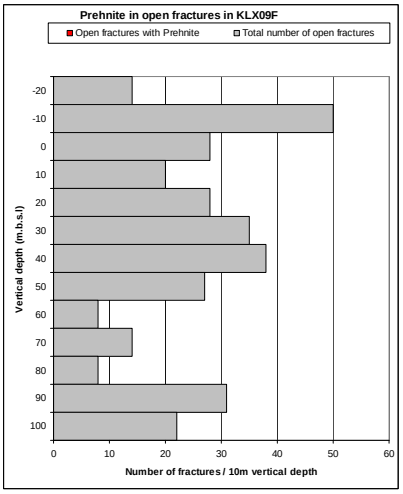
Prehnite in open fractures in KLX09F
Open fractures with Prehnite
Total number of open fractures
Vertical depth (m.b.s.l)
-20
-10
0
10
20
30
40
50
60
70
80
90
100
0
10
20
30
40
50
60
Number of fractures / 10m vertical depth

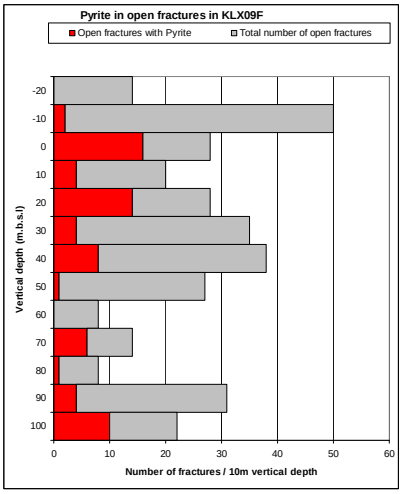
Pyrite in open fractures in KLX09F
Open fractures with Pyrite
Total number of open fractures
Vertical depth (m.b.s.l)
-20
-10
0
10
20
30
40
50
60
70
80
90
100
0
10
20
30
40
50
60
Number of fractures / 10m vertical depth

KLX09G

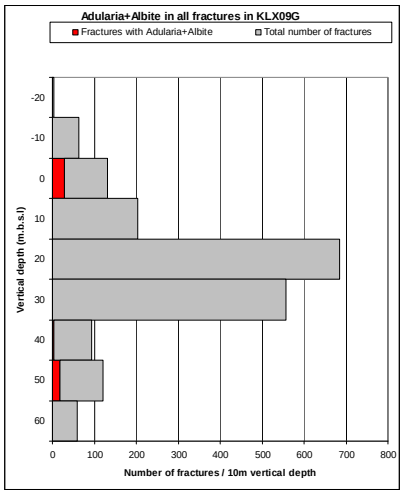
Adularia+Albite in all fractures in KLX09G
Fractures with Adularia+Albite
Total number of fractures
Vertical depth (m.b.s.l)
Number of fractures / 10m vertical depth

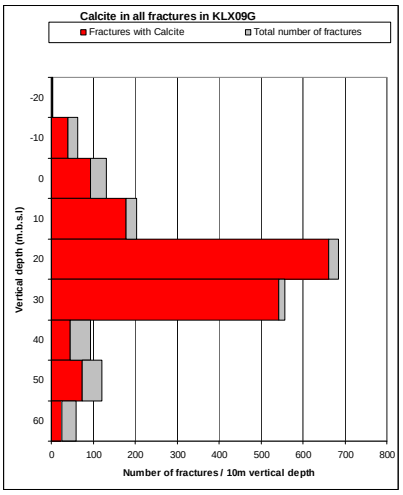
Calcite in all fractures in KLX09G
Fractures with Calcite
Total number of fractures
Vertical depth (m.b.s.l)
Number of fractures / 10m vertical depth

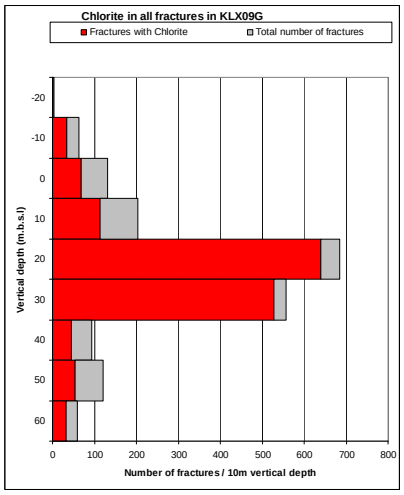
Chlorite in all fractures in KLX09G
Fractures with Chlorite
Total number of fractures
Vertical depth (m.b.s.l)
Number of fractures / 10m vertical depth

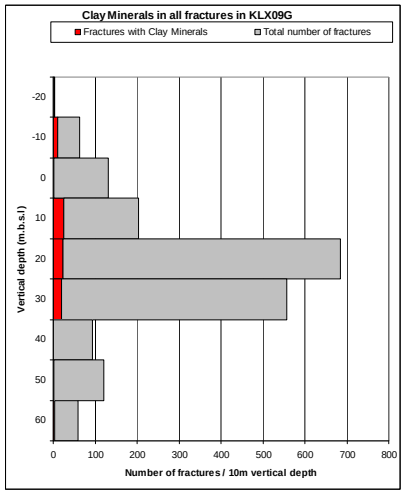
Clay Minerals in all fractures in KLX09G
Fractures with Clay Minerals
Total number of fractures
Vertical depth (m.b.s.l)
Number of fractures / 10m vertical depth

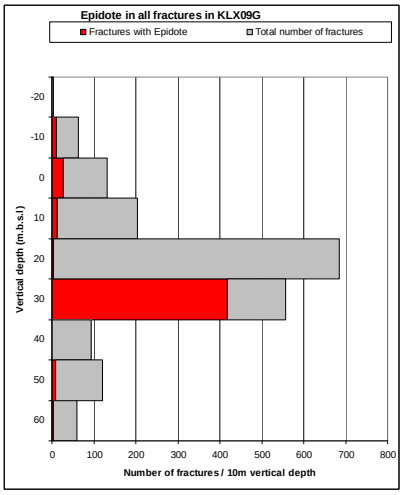
Epidote in all fractures in KLX09G
Fractures with Epidote
Total number of fractures
Vertical depth (m.b.s.l)
Number of fractures / 10m vertical depth

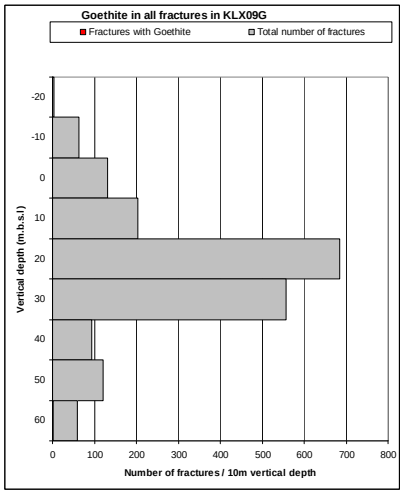
Goethite in all fractures in KLX09G
Fractures with Goethite
Total number of fractures
Vertical depth (m.b.s.l)
Number of fractures / 10m vertical depth

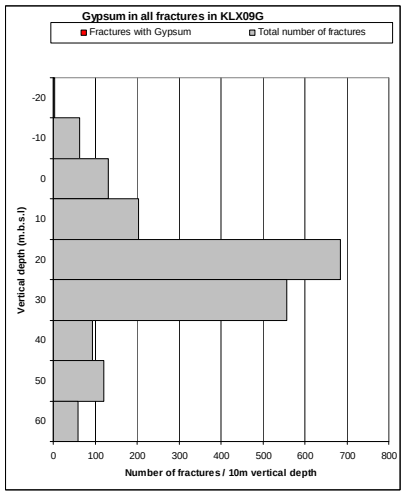
Gypsum in all fractures in KLX09G
Fractures with Gypsum
Total number of fractures
Vertical depth (m.b.s.l)
Number of fractures / 10m vertical depth

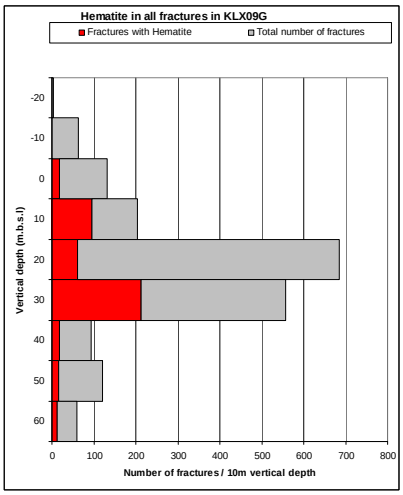
Hematite in all fractures in KLX09G
Fractures with Hematite
Total number of fractures
Vertical depth (m.b.s.l)
Number of fractures / 10m vertical depth

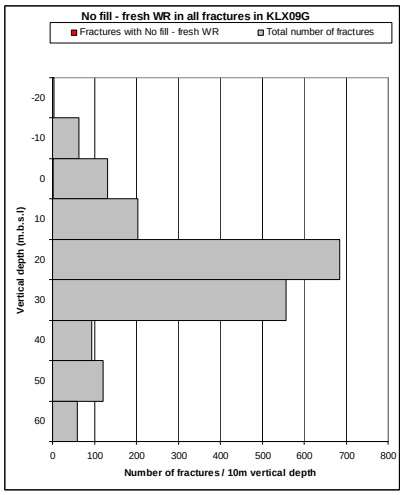
No fill - fresh WR in all fractures in KLX09G
Fractures with No fill - fresh WR
Total number of fractures
Vertical depth (m.b.s.l)
Number of fractures / 10m vertical depth

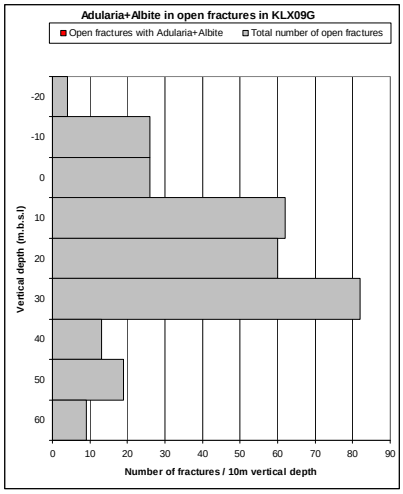
Adularia+Albite in open fractures in KLX09G
Open fractures with Adularia+Albite
Total number of open fractures
Vertical depth (m.b.s.l)
Number of fractures / 10m vertical depth

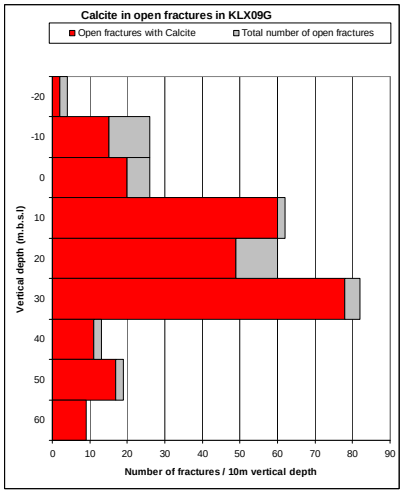
Calcite in open fractures in KLX09G
Open fractures with Calcite
Total number of open fractures
Vertical depth (m.b.s.l)
Number of fractures / 10m vertical depth

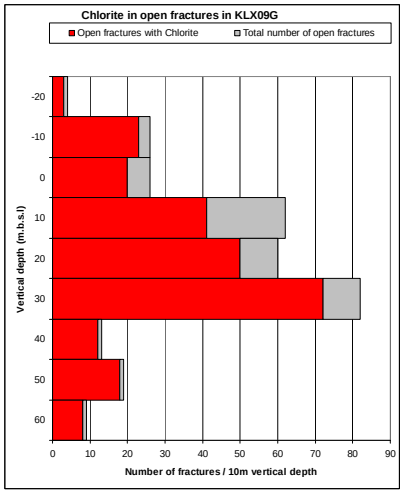
Chlorite in open fractures in KLX09G
Open fractures with Chlorite
Total number of open fractures
Vertical depth (m.b.s.l)
Number of fractures / 10m vertical depth

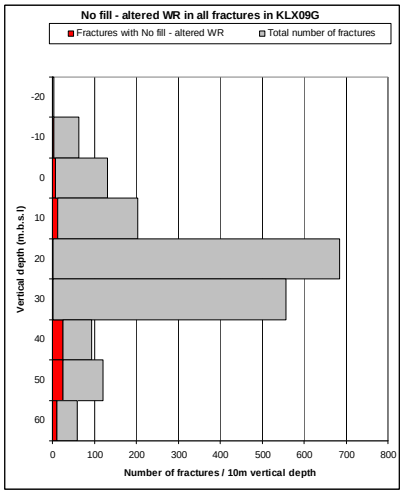
No fill - altered WR in all fractures in KLX09G
Fractures with No fill - altered WR
Total number of fractures
Vertical depth (m.b.s.l)
Number of fractures / 10m vertical depth

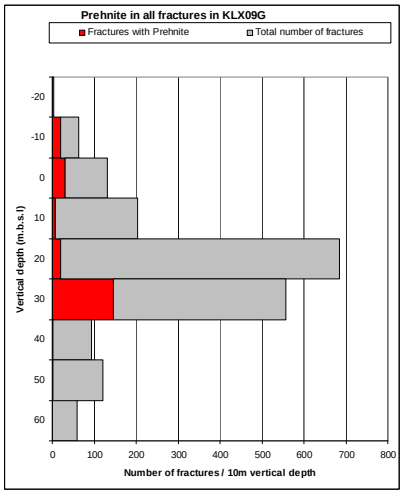
Prehnite in all fractures in KLX09G
Fractures with Prehnite
Total number of fractures
Vertical depth (m.b.s.l)
Number of fractures / 10m vertical depth

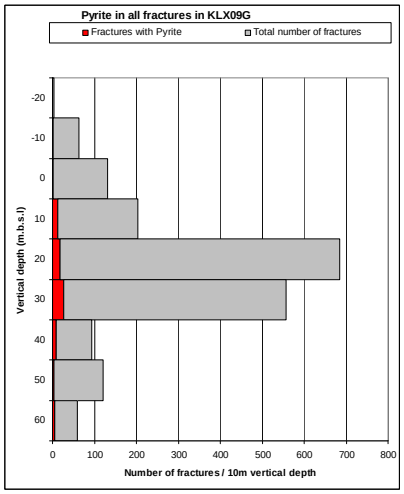
Pyrite in all fractures in KLX09G
Fractures with Pyrite
Total number of fractures
Vertical depth (m.b.s.l)
Number of fractures / 10m vertical depth

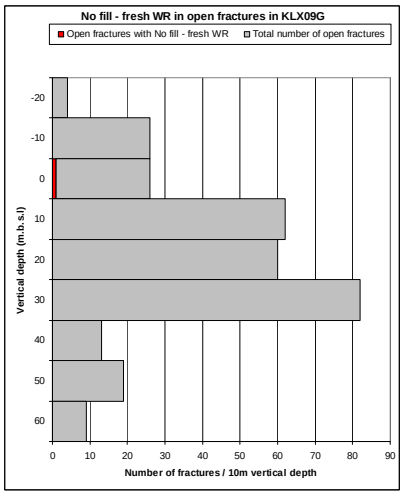
No fill - fresh WR in open fractures in KLX09G
Open fractures with No fill - fresh WR
Total number of open fractures
Vertical depth (m.b.s.l)
Number of fractures / 10m vertical depth

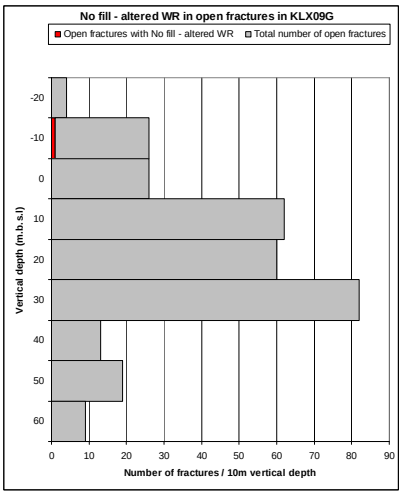
No fill - altered WR in open fractures in KLX09G
Open fractures with No fill - altered WR
Total number of open fractures
Vertical depth (m.b.s.l)
Number of fractures / 10m vertical depth

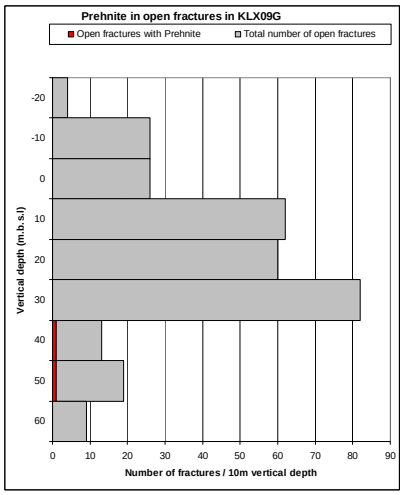
Prehnite in open fractures in KLX09G
Open fractures with Prehnite
Total number of open fractures
Vertical depth (m.b.s.l)
Number of fractures / 10m vertical depth

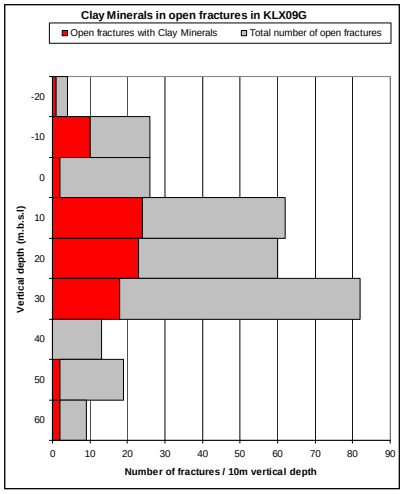
Clay Minerals in open fractures in KLX09G
Open fractures with Clay Minerals
Total number of open fractures
Vertical depth (m.b.s.l)
Number of fractures / 10m vertical depth

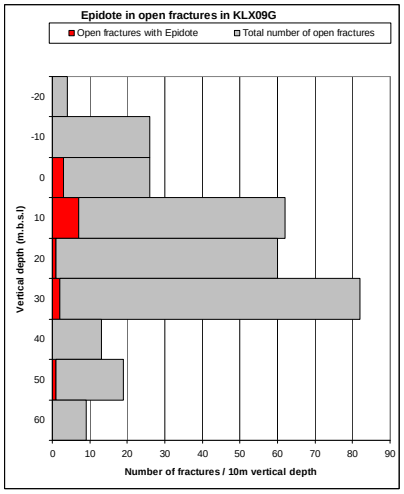
Epidote in open fractures in KLX09G
Open fractures with Epidote
Total number of open fractures
Vertical depth (m.b.s.l)
Number of fractures / 10m vertical depth

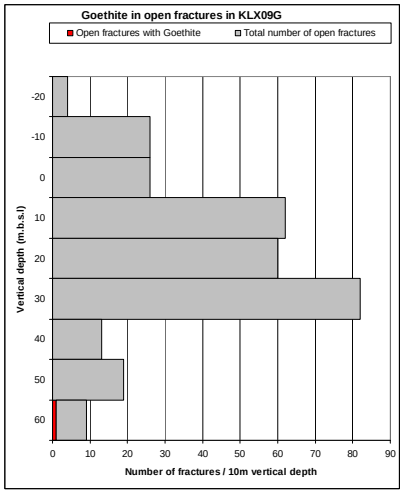
Goethite in open fractures in KLX09G
Open fractures with Goethite
Total number of open fractures
Vertical depth (m.b.s.l)
Number of fractures / 10m vertical depth

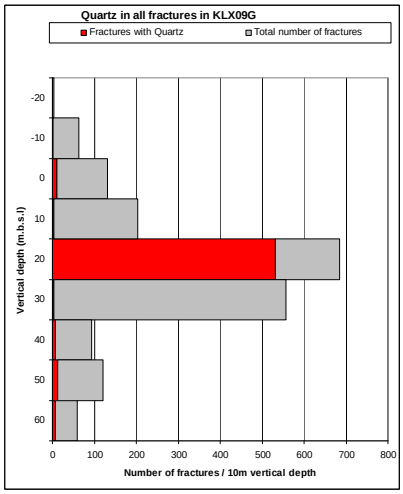
Quartz in all fractures in KLX09G
Fractures with Quartz
Total number of fractures
Vertical depth (m.b.s.l)
Number of fractures / 10m vertical depth

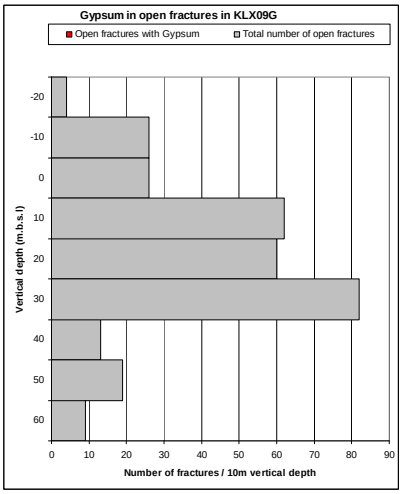
Gypsum in open fractures in KLX09G
Open fractures with Gypsum
Total number of open fractures
Vertical depth (m.b.s.l)
Number of fractures / 10m vertical depth

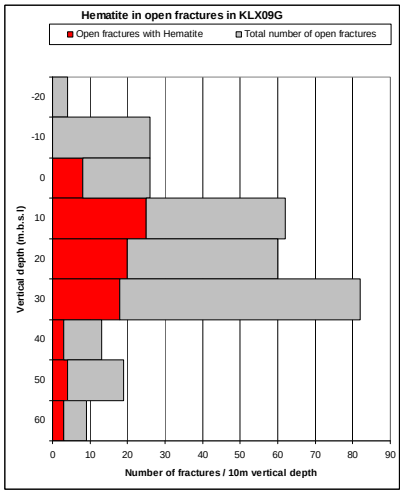
Hematite in open fractures in KLX09G
Open fractures with Hematite
Total number of open fractures
Vertical depth (m.b.s.l)
Number of fractures / 10m vertical depth

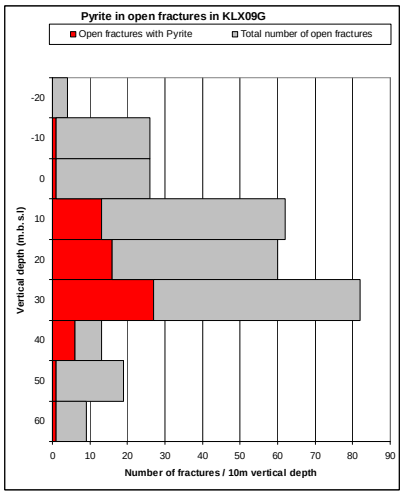
Pyrite in open fractures in KLX09G
Open fractures with Pyrite
Total number of open fractures
Vertical depth (m.b.s.l)
Number of fractures / 10m vertical depth

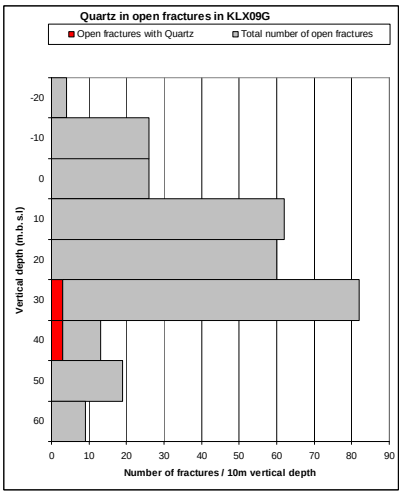
Quartz in open fractures in KLX09G
Open fractures with Quartz
Total number of open fractures
Vertical depth (m.b.s.l)
Number of fractures / 10m vertical depth

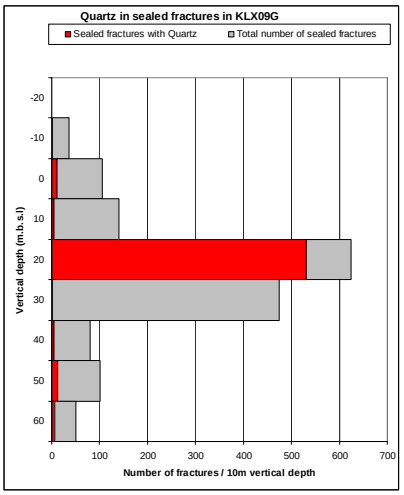
Quartz in sealed fractures in KLX09G
Sealed fractures with Quartz
Total number of sealed fractures
Vertical depth (m.b.s.l)
Number of fractures / 10m vertical depth

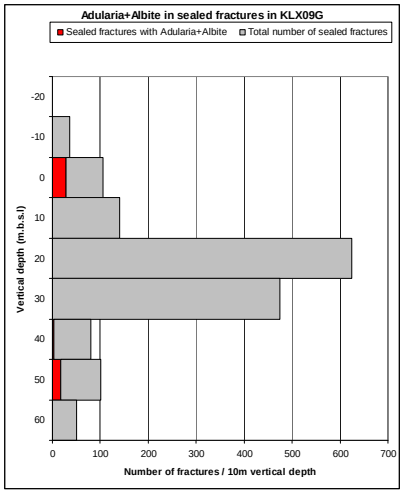
Adularia+Albite in sealed fractures in KLX09G
Sealed fractures with Adularia+Albite
Total number of sealed fractures
Vertical depth (m.b.s.l)
Number of fractures / 10m vertical depth

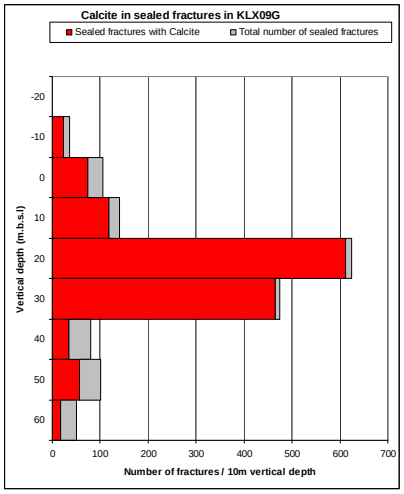
Calcite in sealed fractures in KLX09G
Sealed fractures with Calcite
Total number of sealed fractures
Vertical depth (m.b.s.l)
Number of fractures / 10m vertical depth

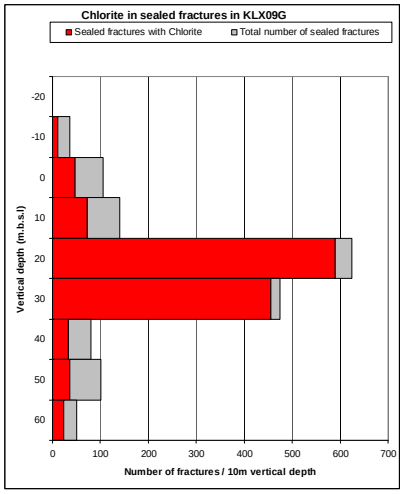
Chlorite in sealed fractures in KLX09G
Sealed fractures with Chlorite
Total number of sealed fractures
Vertical depth (m.b.s.l)
Number of fractures / 10m vertical depth

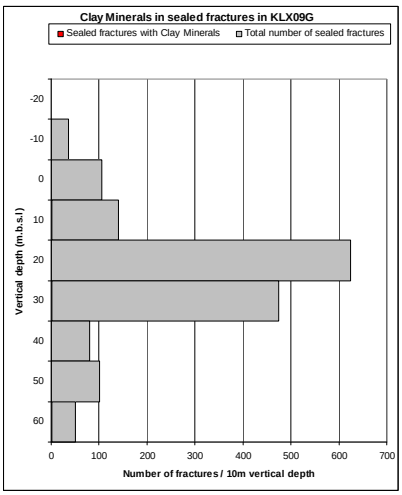
Clay Minerals in sealed fractures in KLX09G
Sealed fractures with Clay Minerals
Total number of sealed fractures
Vertical depth (m.b.s.l)
Number of fractures / 10m vertical depth

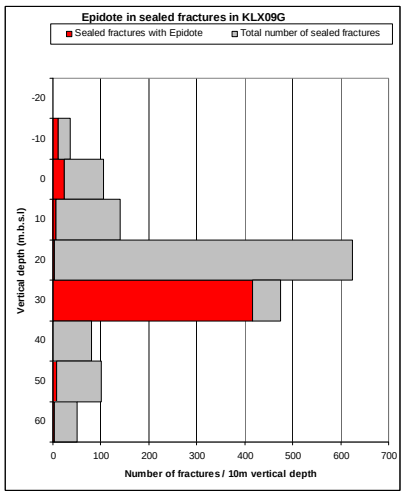
Epidote in sealed fractures in KLX09G
Sealed fractures with Epidote
Total number of sealed fractures
Vertical depth (m.b.s.l)
Number of fractures / 10m vertical depth

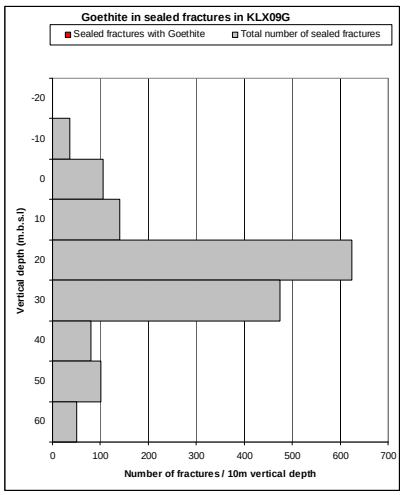
Goethite in sealed fractures in KLX09G
Sealed fractures with Goethite
Total number of sealed fractures
Vertical depth (m.b.s.l)
Number of fractures / 10m vertical depth

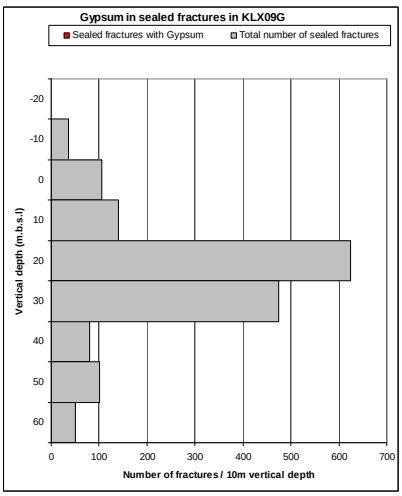
Gypsum in sealed fractures in KLX09G
Sealed fractures with Gypsum
Total number of sealed fractures
Vertical depth (m.b.s.l)
Number of fractures / 10m vertical depth

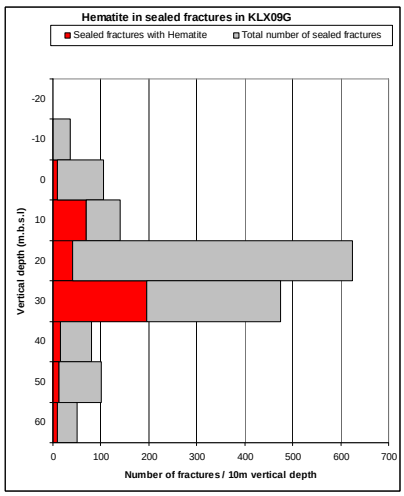
Hematite in sealed fractures in KLX09G
Sealed fractures with Hematite
Total number of sealed fractures
Vertical depth (m.b.s.l)
Number of fractures / 10m vertical depth

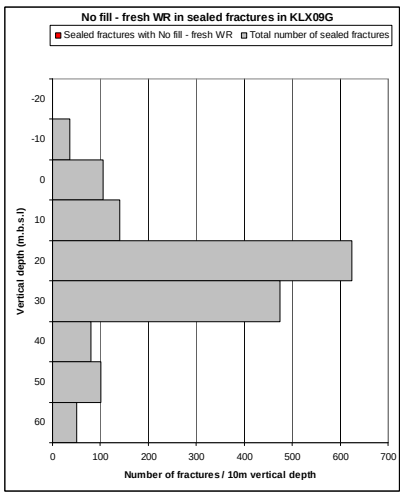
No fill - fresh WR in sealed fractures in KLX09G
Sealed fractures with No fill - fresh WR
Total number of sealed fractures
Vertical depth (m.b.s.l)
Number of fractures / 10m vertical depth

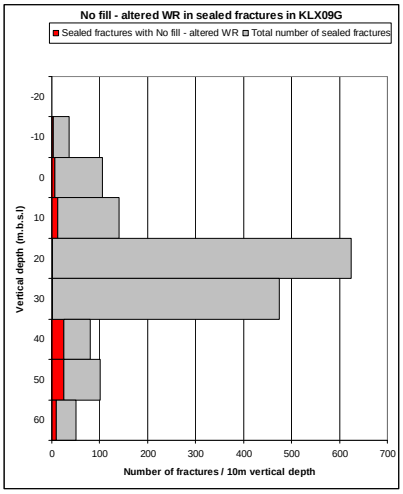
No fill - altered WR in sealed fractures in KLX09G
Sealed fractures with No fill - altered WR
Total number of sealed fractures
Vertical depth (m.b.s.l)
-20
-10
0
10
20
30
40
50
60
0
100
200
300
400
500
600
700
Number of fractures / 10m vertical depth

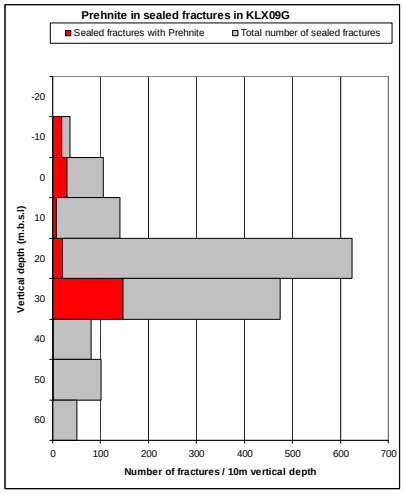
Prehnite in sealed fractures in KLX09G
Sealed fractures with Prehnite
Total number of sealed fractures
Vertical depth (m.b.s.l)
-20
-10
0
10
20
30
40
50
60
0
100
200
300
400
500
600
700
Number of fractures / 10m vertical depth

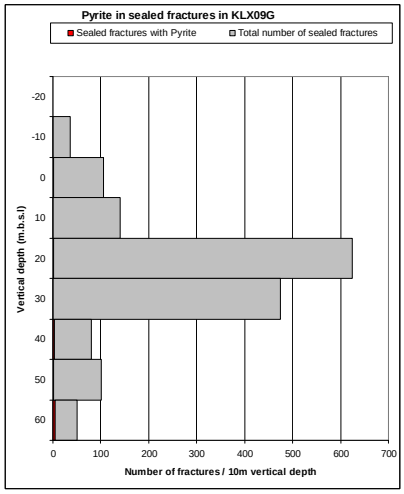
Pyrite in sealed fractures in KLX09G
Sealed fractures with Pyrite
Total number of sealed fractures
Vertical depth (m.b.s.l)
-20
-10
0
10
20
30
40
50
60
0
100
200
300
400
500
600
700
Number of fractures / 10m vertical depth

KLX10

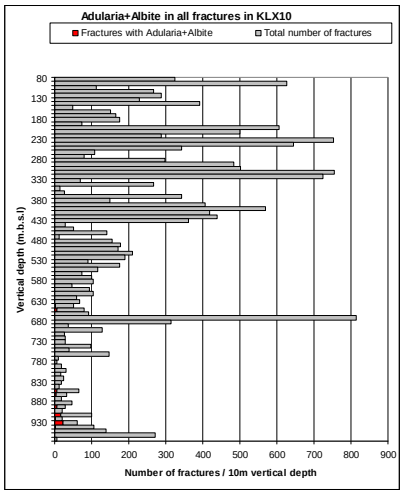
Adularia+Albite in all fractures in KLX10
Fractures with Adularia+Albite
Total number of fractures
Vertical depth (m.b.s.l)
Number of fractures / 10m vertical depth

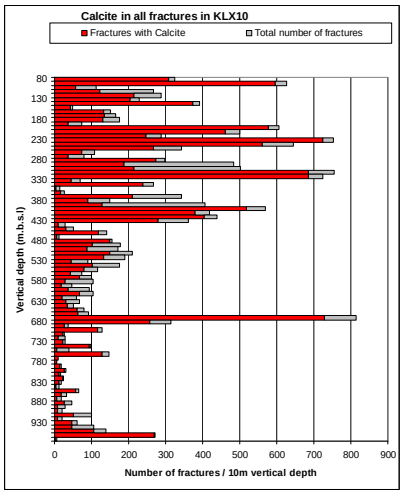
Calcite in all fractures in KLX10
Fractures with Calcite
Total number of fractures
Vertical depth (m.b.s.l)
Number of fractures / 10m vertical depth

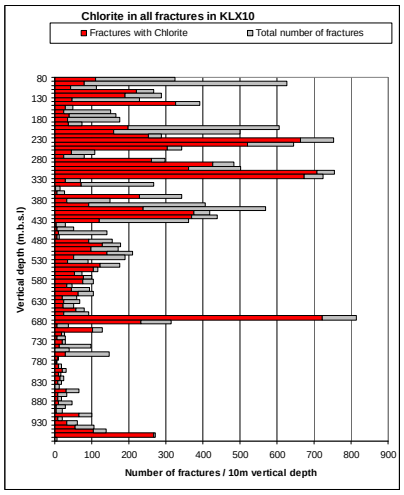
Chlorite in all fractures in KLX10
Fractures with Chlorite
Total number of fractures
Vertical depth (m.b.s.l)
Number of fractures / 10m vertical depth

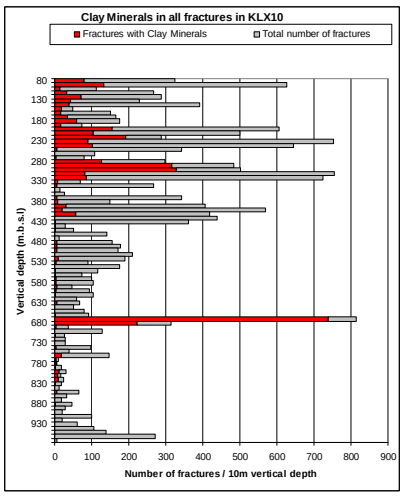
Clay Minerals in all fractures in KLX10
Fractures with Clay Minerals
Total number of fractures
Vertical depth (m.b.s.l)
Number of fractures / 10m vertical depth

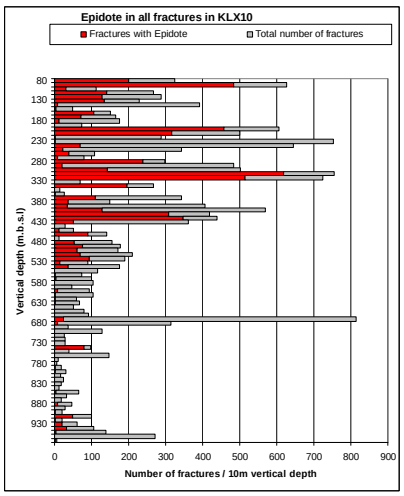
Epidote in all fractures in KLX10
Fractures with Epidote
Total number of fractures
Vertical depth (m.b.s.l)
Number of fractures / 10m vertical depth

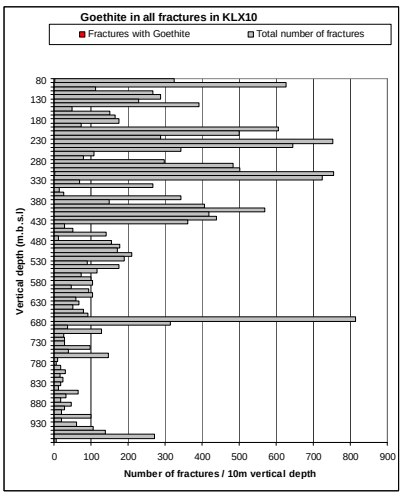
Goethite in all fractures in KLX10
Fractures with Goethite
Total number of fractures
Vertical depth (m.b.s.l)
Number of fractures / 10m vertical depth

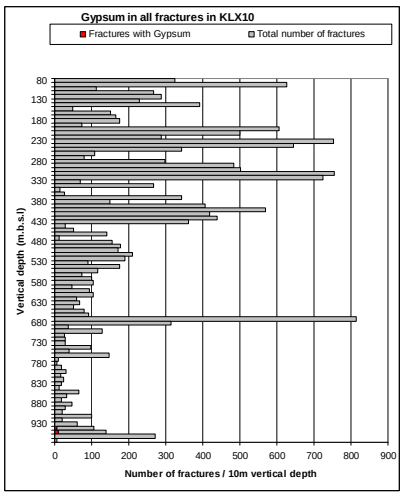
Gypsum in all fractures in KLX10
Fractures with Gypsum
Total number of fractures
Vertical depth (m.b.s.l)
Number of fractures / 10m vertical depth

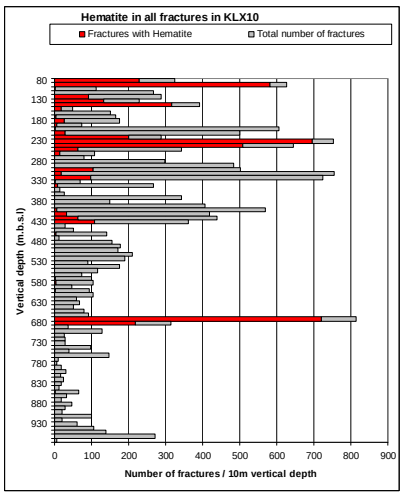
Hematite in all fractures in KLX10
Fractures with Hematite
Total number of fractures
Vertical depth (m.b.s.l)
Number of fractures / 10m vertical depth

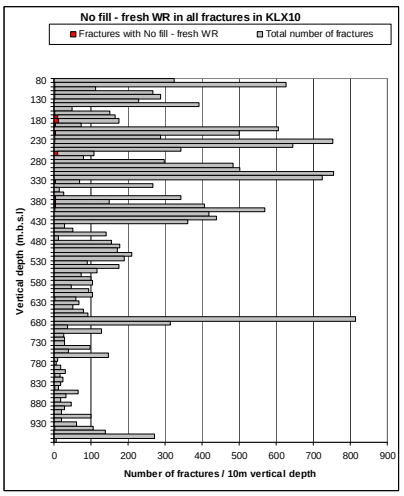
No fill - fresh WR in all fractures in KLX10
Fractures with No fill - fresh WR
Total number of fractures
Vertical depth (m.b.s.l)
Number of fractures / 10m vertical depth

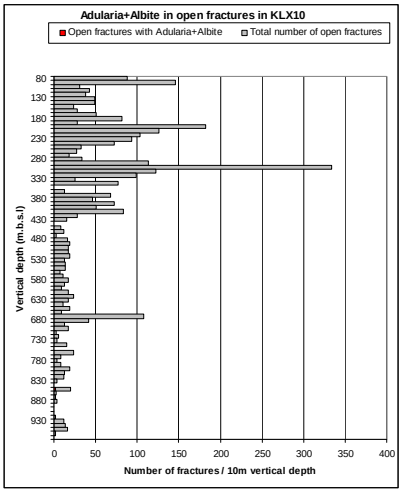
Adularia+Albite in open fractures in KLX10
Open fractures with Adularia+Albite
Total number of open fractures
Vertical depth (m.b.s.l)
Number of fractures / 10m vertical depth

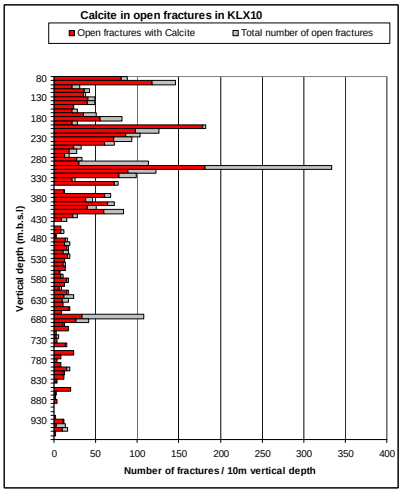
Calcite in open fractures in KLX10
Open fractures with Calcite
Total number of open fractures
Vertical depth (m.b.s.l)
Number of fractures / 10m vertical depth

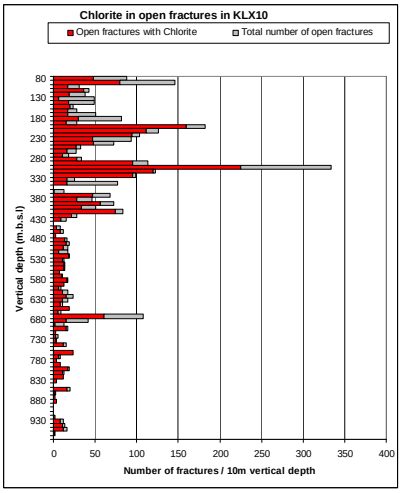
Chlorite in open fractures in KLX10
Open fractures with Chlorite
Total number of open fractures
Vertical depth (m.b.s.l)
Number of fractures / 10m vertical depth

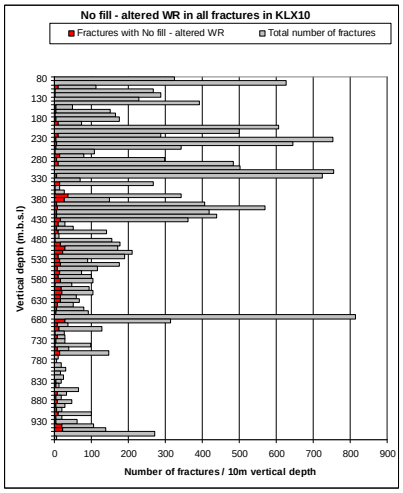
No fill - altered WR in all fractures in KLX10
Fractures with No fill - altered WR
Total number of fractures
Vertical depth (m.b.s.l)
Number of fractures / 10m vertical depth

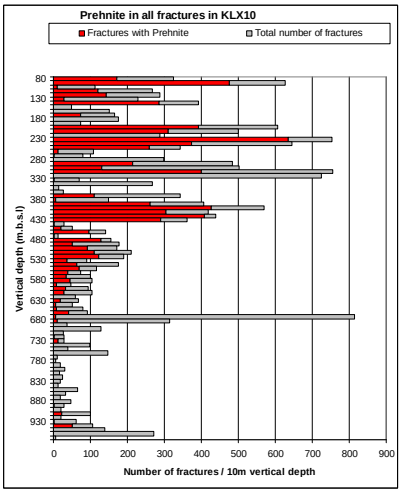
Prehnite in all fractures in KLX10
Fractures with Prehnite
Total number of fractures
Vertical depth (m.b.s.l)
Number of fractures / 10m vertical depth

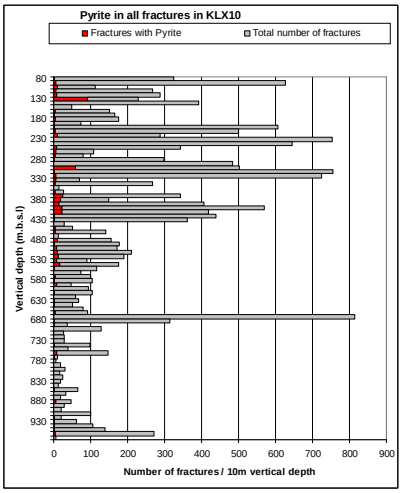
Pyrite in all fractures in KLX10
Fractures with Pyrite
Total number of fractures
Vertical depth (m.b.s.l)
Number of fractures / 10m vertical depth

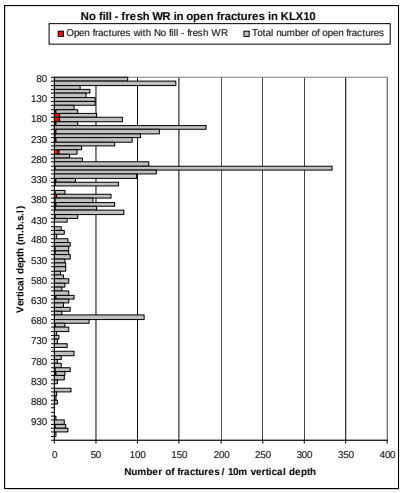
No fill - fresh WR in open fractures in KLX10
Open fractures with No fill - fresh WR
Total number of open fractures
Vertical depth (m.b.s.l)
Number of fractures / 10m vertical depth

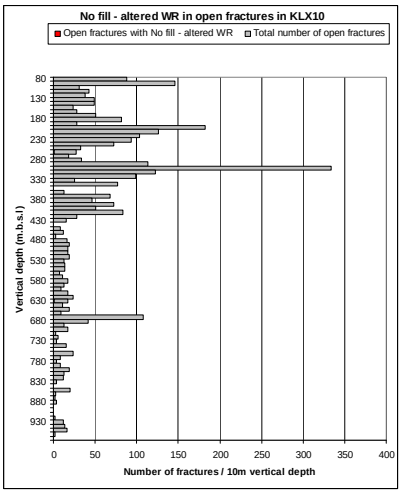
No fill - altered WR in open fractures in KLX10
Open fractures with No fill - altered WR
Total number of open fractures
Vertical depth (m.b.s.l)
Number of fractures / 10m vertical depth

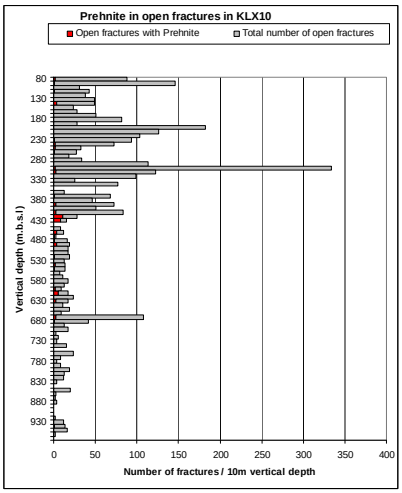
Prehnite in open fractures in KLX10
Open fractures with Prehnite
Total number of open fractures
Vertical depth (m.b.s.l)
Number of fractures / 10m vertical depth

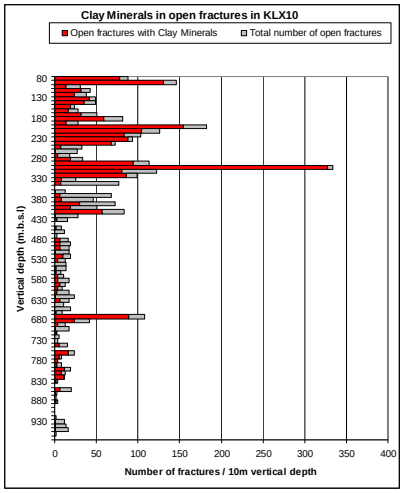
Clay Minerals in open fractures in KLX10
Open fractures with Clay Minerals
Total number of open fractures
Vertical depth (m.b.s.l)
Number of fractures / 10m vertical depth

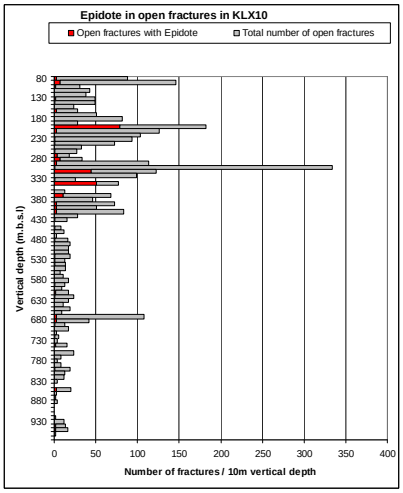
Epidote in open fractures in KLX10
Open fractures with Epidote
Total number of open fractures
Vertical depth (m.b.s.l)
Number of fractures / 10m vertical depth

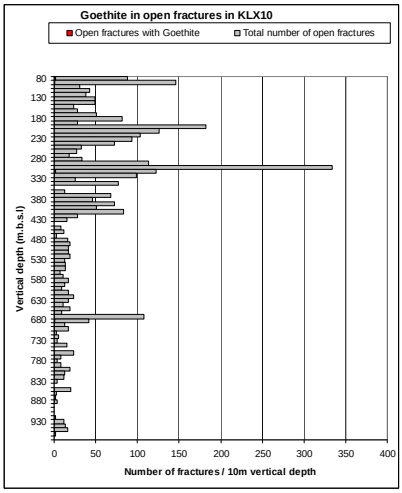
Goethite in open fractures in KLX10
Open fractures with Goethite
Total number of open fractures
Vertical depth (m.b.s.l)
Number of fractures / 10m vertical depth

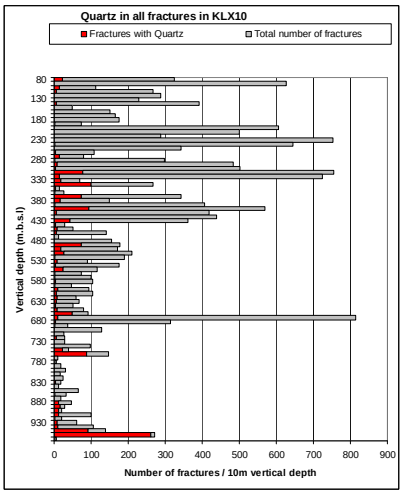
Quartz in all fractures in KLX10
Fractures with Quartz
Total number of fractures
Vertical depth (m.b.s.l)
Number of fractures / 10m vertical depth

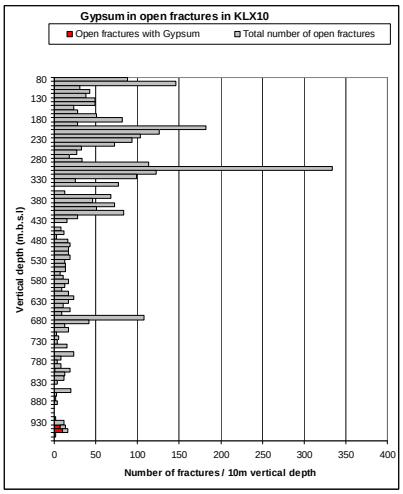
Gypsum in open fractures in KLX10
Open fractures with Gypsum
Total number of open fractures
Vertical depth (m.b.s.l)
Number of fractures / 10m vertical depth

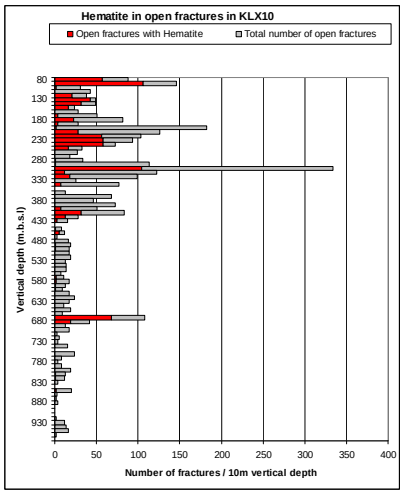
Hematite in open fractures in KLX10
Open fractures with Hematite
Total number of open fractures
Vertical depth (m.b.s.l)
Number of fractures / 10m vertical depth

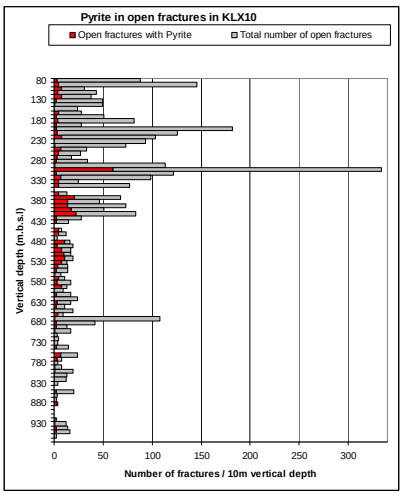
Pyrite in open fractures in KLX10
Open fractures with Pyrite
Total number of open fractures
Vertical depth (m.b.s.l)
Number of fractures / 10m vertical depth

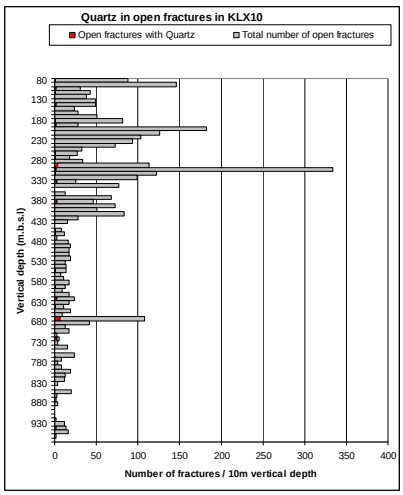
Quartz in open fractures in KLX10
Open fractures with Quartz
Total number of open fractures
Vertical depth (m.b.s.l)
Number of fractures / 10m vertical depth

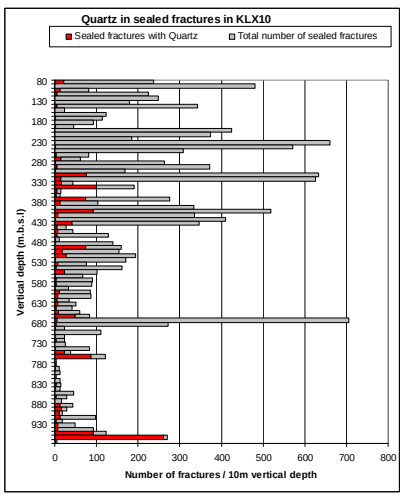
Quartz in sealed fractures in KLX10
Sealed fractures with Quartz
Total number of sealed fractures
Vertical depth (m.b.s.l)
Number of fractures / 10m vertical depth

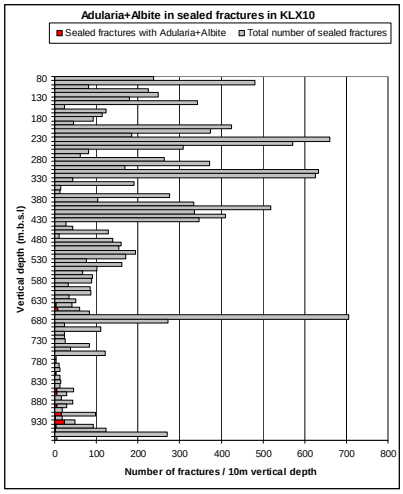
Adularia+Albite in sealed fractures in KLX10
Sealed fractures with Adularia+Albite
Total number of sealed fractures
Vertical depth (m.b.s.l)
Number of fractures / 10m vertical depth

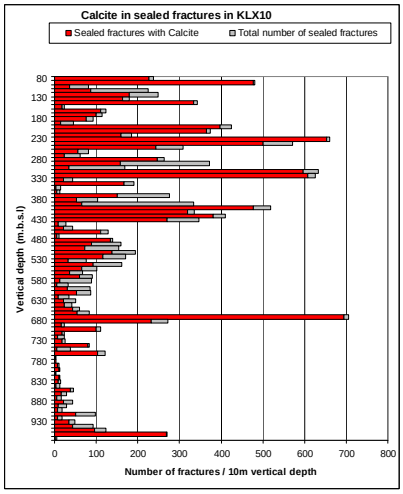
Calcite in sealed fractures in KLX10
Sealed fractures with Calcite
Total number of sealed fractures
Vertical depth (m.b.s.l)
Number of fractures / 10m vertical depth

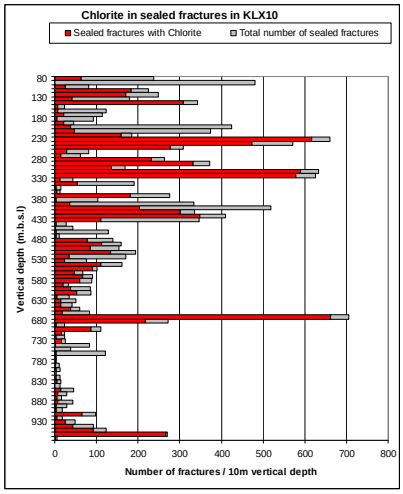
Chlorite in sealed fractures in KLX10
Sealed fractures with Chlorite
Total number of sealed fractures
Vertical depth (m.b.s.l)
Number of fractures / 10m vertical depth

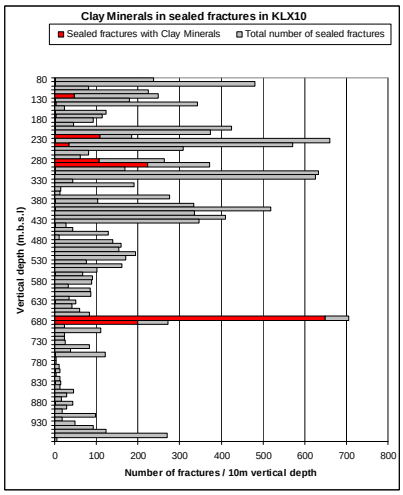
Clay Minerals in sealed fractures in KLX10
Sealed fractures with Clay Minerals
Total number of sealed fractures
Vertical depth (m.b.s.l)
Number of fractures / 10m vertical depth

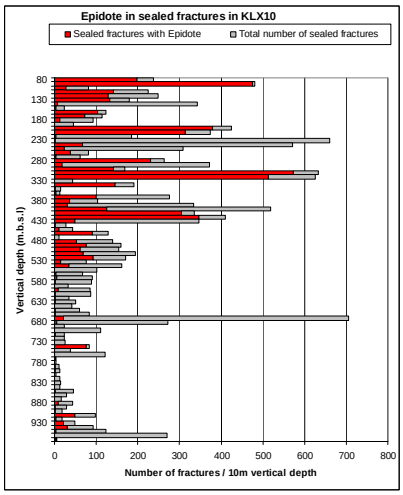
Epidote in sealed fractures in KLX10
Sealed fractures with Epidote
Total number of sealed fractures
Vertical depth (m.b.s.l)
Number of fractures / 10m vertical depth

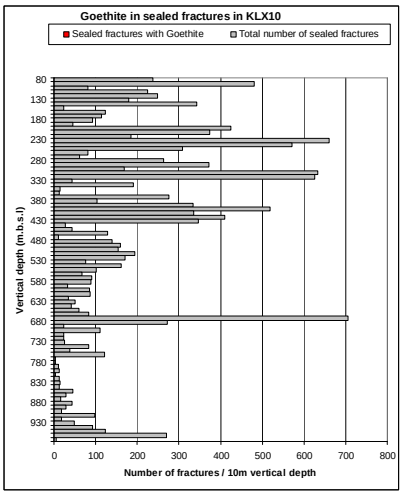
Goethite in sealed fractures in KLX10
Sealed fractures with Goethite
Total number of sealed fractures
Vertical depth (m.b.s.l)
Number of fractures / 10m vertical depth

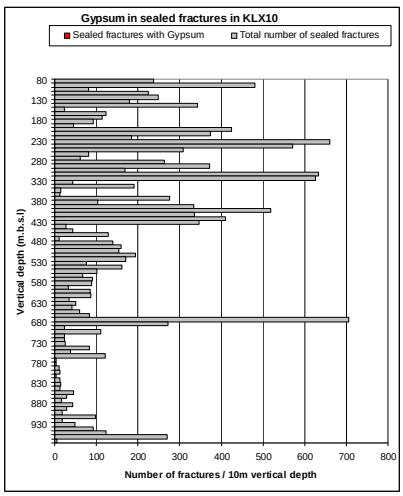
Gypsum in sealed fractures in KLX10
Sealed fractures with Gypsum
Total number of sealed fractures
Vertical depth (m.b.s.l)
Number of fractures / 10m vertical depth

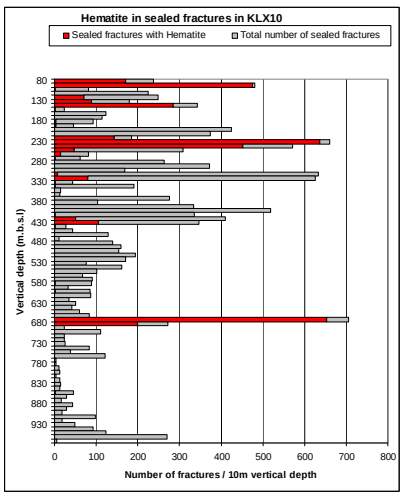
Hematite in sealed fractures in KLX10
Sealed fractures with Hematite
Total number of sealed fractures
Vertical depth (m.b.s.l)
Number of fractures / 10m vertical depth

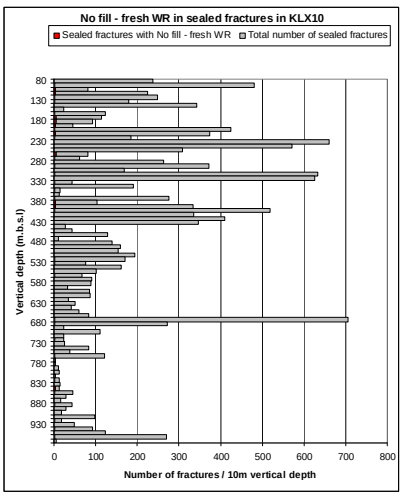
No fill - fresh WR in sealed fractures in KLX10
Sealed fractures with No fill - fresh WR
Total number of sealed fractures
Vertical depth (m.b.s.l)
Number of fractures / 10m vertical depth

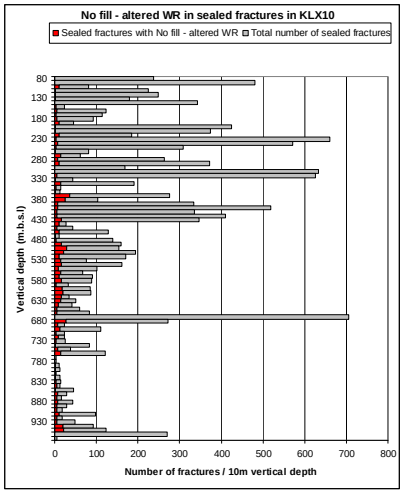
No fill - altered WR in sealed fractures in KLX10
Sealed fractures with No fill - altered WR
Total number of sealed fractures
Vertical depth (m.b.s.l)
Number of fractures / 10m vertical depth

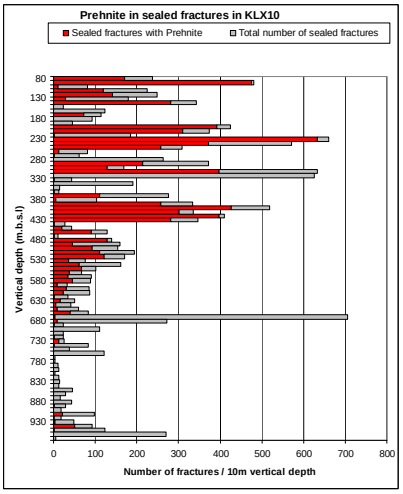
Prehnite in sealed fractures in KLX10
Sealed fractures with Prehnite
Total number of sealed fractures
Vertical depth (m.b.s.l)
Number of fractures / 10m vertical depth

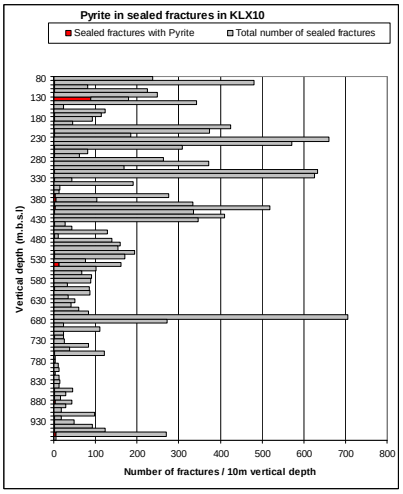
Pyrite in sealed fractures in KLX10
Sealed fractures with Pyrite
Total number of sealed fractures
Vertical depth (m.b.s.l)
Number of fractures / 10m vertical depth

KLX10B

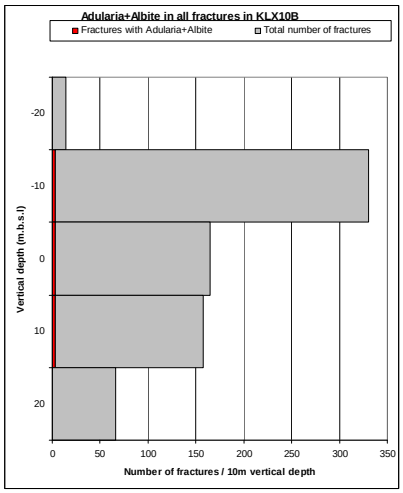
Adularia+Albite in all fractures in KLX10B
Fractures with Adularia+Albite
Total number of fractures
Vertical depth (m.b.s.l)
-20
-10
0
10
20
0
50
100
150
200
250
300
350
Number of fractures / 10m vertical depth

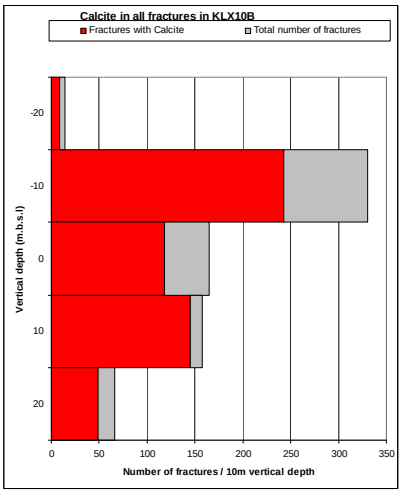
Calcite in all fractures in KLX10B
Fractures with Calcite
Total number of fractures
Vertical depth (m.b.s.l)
-20
-10
0
10
20
0
50
100
150
200
250
300
350
Number of fractures / 10m vertical depth

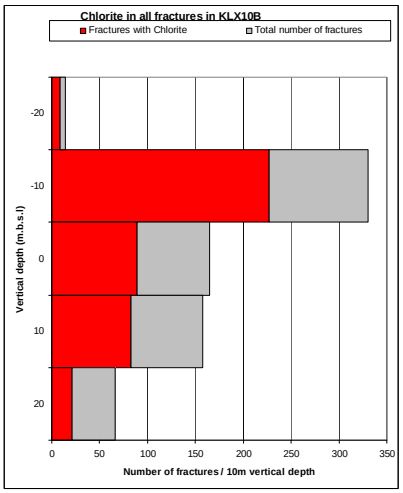
Chlorite in all fractures in KLX10B
Fractures with Chlorite
Total number of fractures
Vertical depth (m.b.s.l)
-20
-10
0
10
20
0
50
100
150
200
250
300
350
Number of fractures / 10m vertical depth

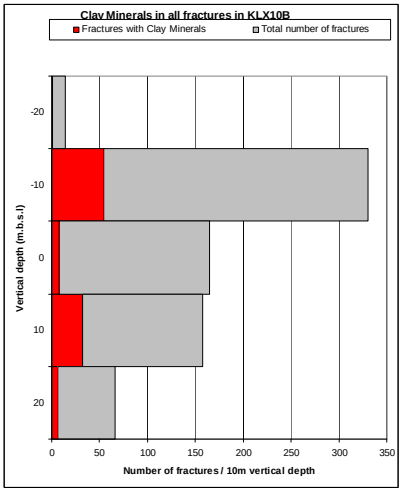
Clay Minerals in all fractures in KLX10B
Fractures with Clay Minerals
Total number of fractures
Vertical depth (m.b.s.l)
-20
-10
0
10
20
0
50
100
150
200
250
300
350
Number of fractures / 10m vertical depth

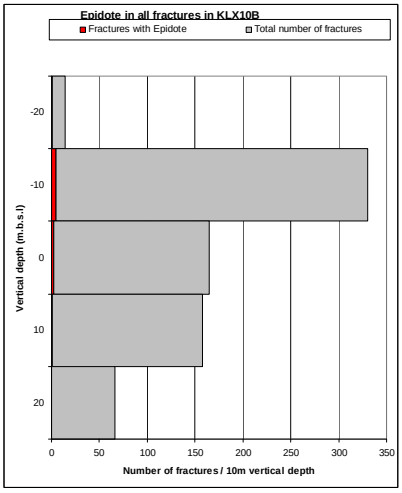
Epidote in all fractures in KLX10B
Fractures with Epidote
Total number of fractures
Vertical depth (m.b.s.l)
-20
-10
0
10
20
0
50
100
150
200
250
300
350
Number of fractures / 10m vertical depth

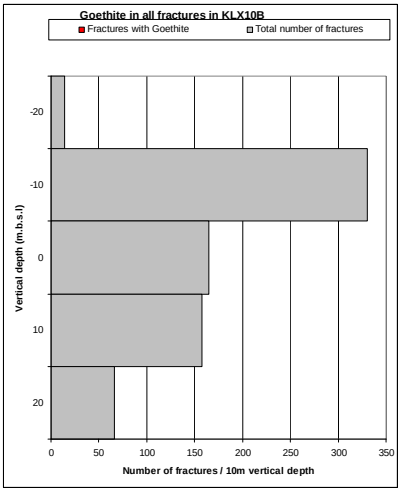
Goethite in all fractures in KLX10B
Fractures with Goethite
Total number of fractures
Vertical depth (m.b.s.l)
-20
-10
0
10
20
0
50
100
150
200
250
300
350
Number of fractures / 10m vertical depth

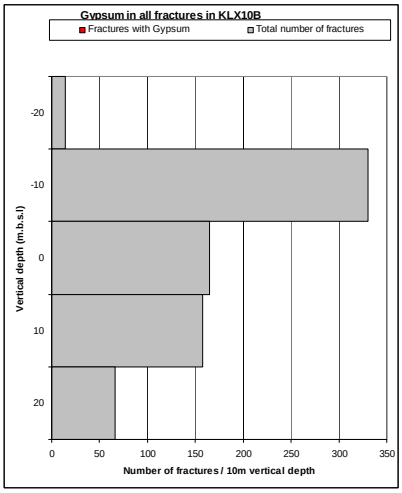
Gypsum in all fractures in KLX10B
Fractures with Gypsum
Total number of fractures
Vertical depth (m.b.s.l)
-20
-10
0
10
20
0
50
100
150
200
250
300
350
Number of fractures / 10m vertical depth

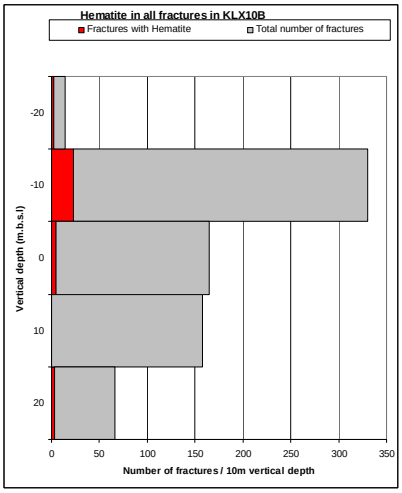
Hematite in all fractures in KLX10B
Fractures with Hematite
Total number of fractures
Vertical depth (m.b.s.l)
-20
-10
0
10
20
0
50
100
150
200
250
300
350
Number of fractures / 10m vertical depth

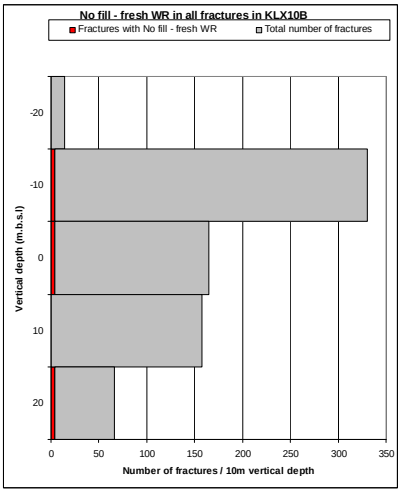
No fill - fresh WR in all fractures in KLX10B
Fractures with No fill - fresh WR
Total number of fractures
Vertical depth (m.b.s.l)
-20
-10
0
10
20
0
50
100
150
200
250
300
350
Number of fractures / 10m vertical depth

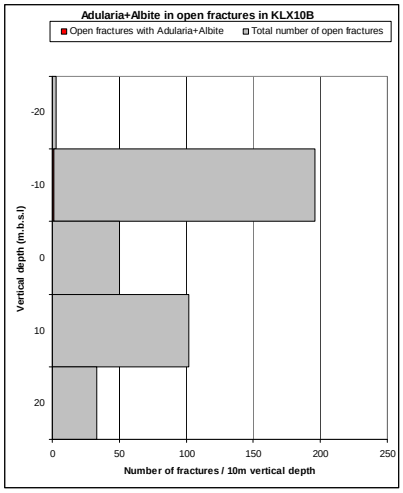
Adularia+Albite in open fractures in KLX10B
Open fractures with Adularia+Albite
Total number of open fractures
Vertical depth (m.b.s.l)
-20
-10
0
10
20
0
50
100
150
200
250
Number of fractures / 10m vertical depth

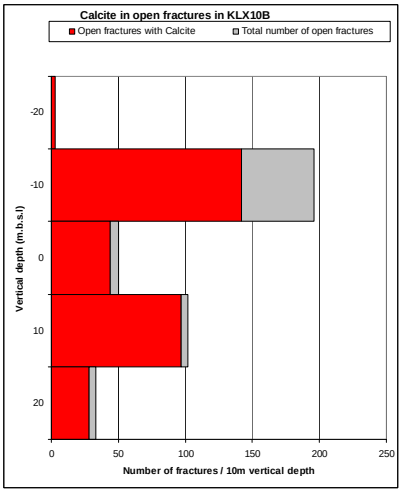
Calcite in open fractures in KLX10B
Open fractures with Calcite
Total number of open fractures
Vertical depth (m.b.s.l)
-20
-10
0
10
20
0
50
100
150
200
250
Number of fractures / 10m vertical depth

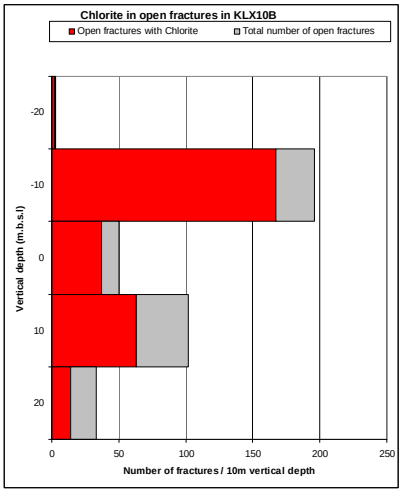
Chlorite in open fractures in KLX10B
Open fractures with Chlorite
Total number of open fractures
Vertical depth (m.b.s.l)
-20
-10
0
10
20
0
50
100
150
200
250
Number of fractures / 10m vertical depth

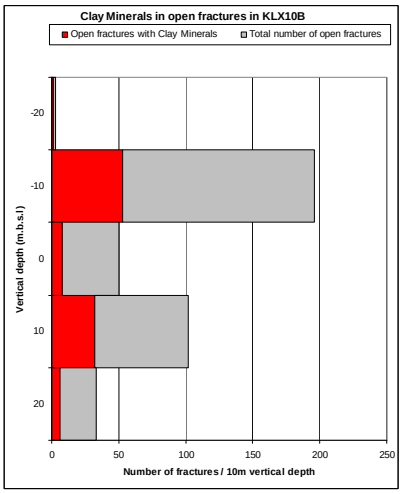
Clay Minerals in open fractures in KLX10B
Open fractures with Clay Minerals
Total number of open fractures
Vertical depth (m.b.s.l)
-20
-10
0
10
20
0
50
100
150
200
250
Number of fractures / 10m vertical depth

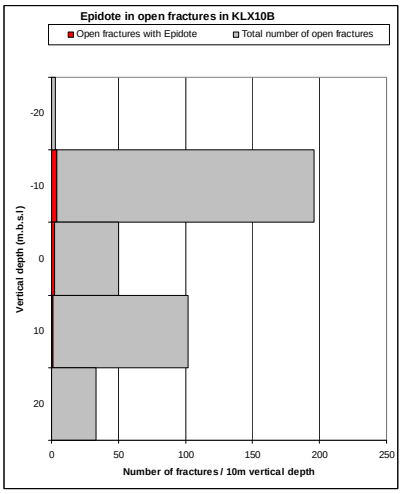
Epidote in open fractures in KLX10B
Open fractures with Epidote
Total number of open fractures
Vertical depth (m.b.s.l)
-20
-10
0
10
20
0
50
100
150
200
250
Number of fractures / 10m vertical depth

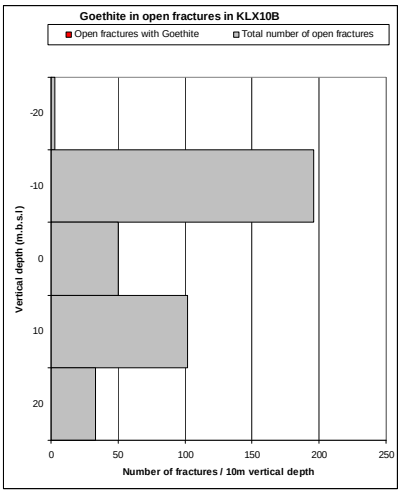
Goethite in open fractures in KLX10B
Open fractures with Goethite
Total number of open fractures
Vertical depth (m.b.s.l)
-20
-10
0
10
20
0
50
100
150
200
250
Number of fractures / 10m vertical depth

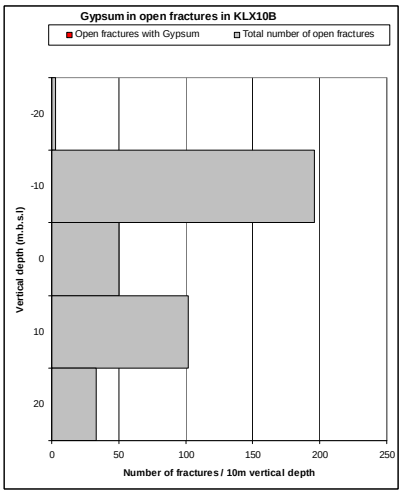
Gypsum in open fractures in KLX10B
Open fractures with Gypsum
Total number of open fractures
Vertical depth (m.b.s.l)
-20
-10
0
10
20
0
50
100
150
200
250
Number of fractures / 10m vertical depth

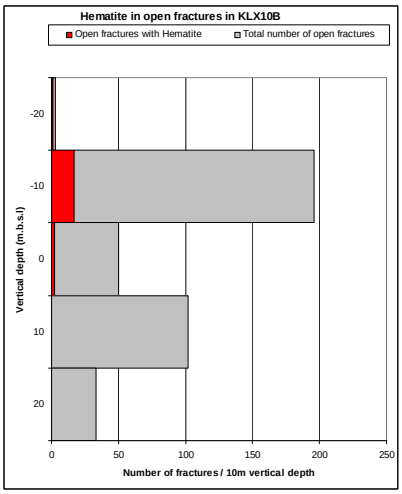
Hematite in open fractures in KLX10B
Open fractures with Hematite
Total number of open fractures
Vertical depth (m.b.s.l)
-20
-10
0
10
20
0
50
100
150
200
250
Number of fractures / 10m vertical depth

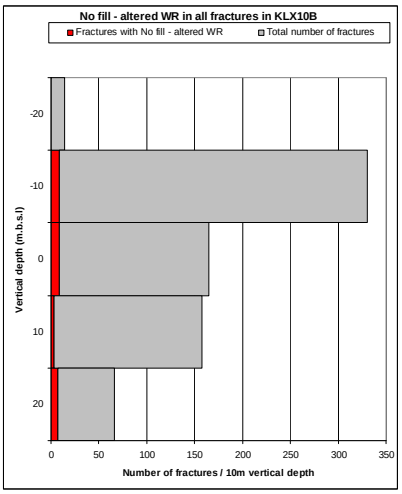
No fill - altered WR in all fractures in KLX10B
Fractures with No fill - altered WR
Total number of fractures
Vertical depth (m.b.s.l)
-20
-10
0
10
20
0
50
100
150
200
250
300
350
Number of fractures / 10m vertical depth

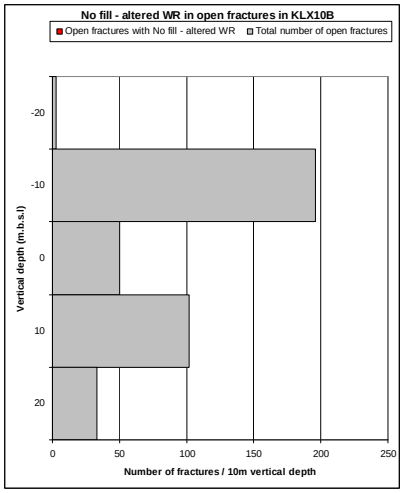
No fill - altered WR in open fractures in KLX10B
Open fractures with No fill - altered WR
Total number of open fractures
Vertical depth (m.b.s.l)
-20
-10
0
10
20
0
50
100
150
200
250
Number of fractures / 10m vertical depth

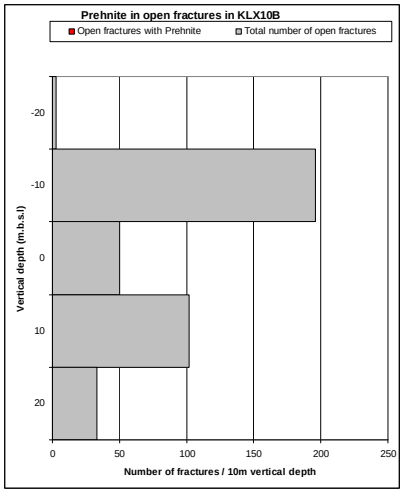
Prehnite in open fractures in KLX10B
Open fractures with Prehnite
Total number of open fractures
Vertical depth (m.b.s.l)
-20
-10
0
10
20
0
50
100
150
200
250
Number of fractures / 10m vertical depth

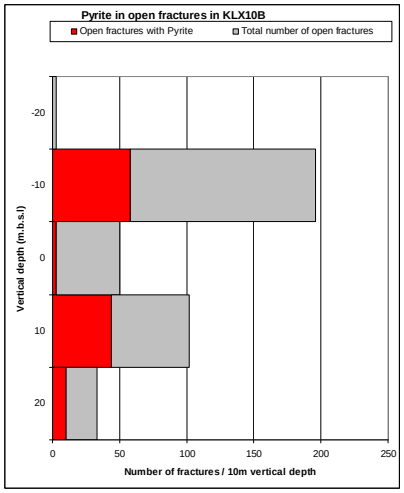
Pyrite in open fractures in KLX10B
Open fractures with Pyrite
Total number of open fractures
Vertical depth (m.b.s.l)
-20
-10
0
10
20
0
50
100
150
200
250
Number of fractures / 10m vertical depth

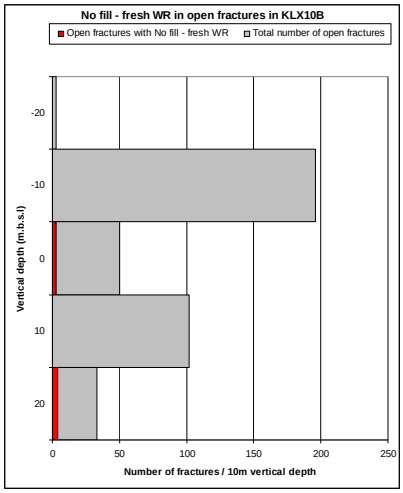
No fill - fresh WR in open fractures in KLX10B
Open fractures with No fill - fresh WR
Total number of open fractures
Vertical depth (m.b.s.l)
-20
-10
0
10
20
0
50
100
150
200
250
Number of fractures / 10m vertical depth

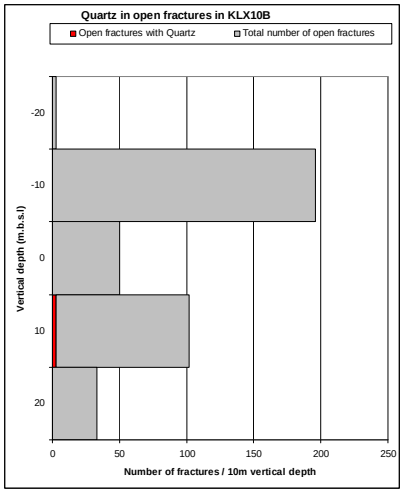
Quartz in open fractures in KLX10B
Open fractures with Quartz
Total number of open fractures
Vertical depth (m.b.s.l)
-20
-10
0
10
20
0
50
100
150
200
250
Number of fractures / 10m vertical depth

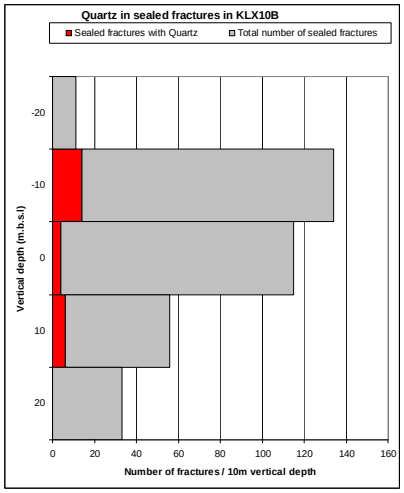
Quartz in sealed fractures in KLX10B
Sealed fractures with Quartz
Total number of sealed fractures
Vertical depth (m.b.s.l)
-20
-10
0
10
20
0
20
40
60
80
100
120
140
160
Number of fractures / 10m vertical depth

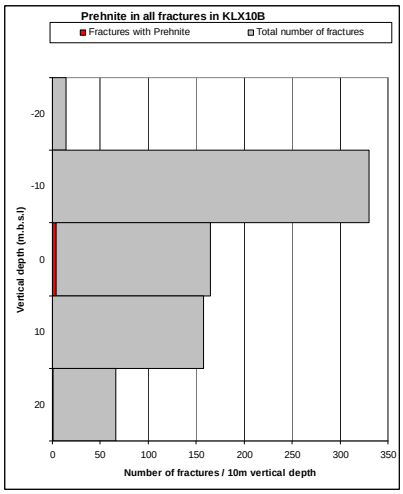
Prehnite in all fractures in KLX10B
Fractures with Prehnite
Total number of fractures
Vertical depth (m.b.s.l)
-20
-10
0
10
20
0
50
100
150
200
250
300
350
Number of fractures / 10m vertical depth

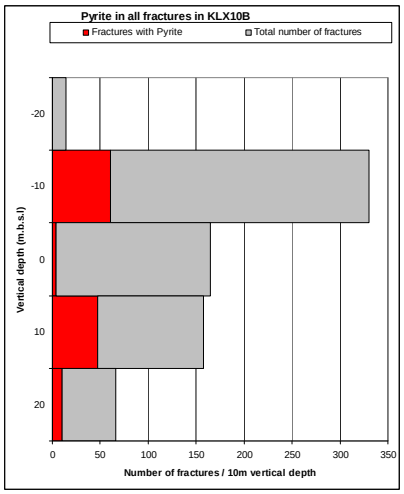
Pyrite in all fractures in KLX10B
Fractures with Pyrite
Total number of fractures
Vertical depth (m.b.s.l)
-20
-10
0
10
20
0
50
100
150
200
250
300
350
Number of fractures / 10m vertical depth

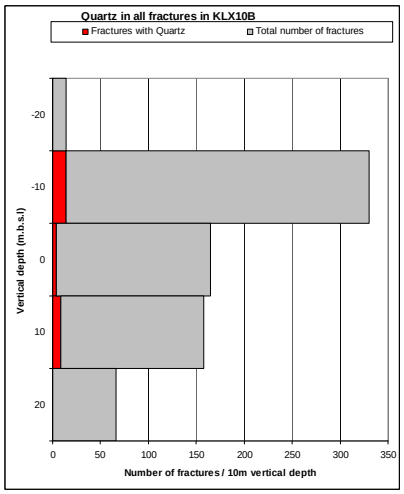
Quartz in all fractures in KLX10B
Fractures with Quartz
Total number of fractures
Vertical depth (m.b.s.l)
-20
-10
0
10
20
0
50
100
150
200
250
300
350
Number of fractures / 10m vertical depth

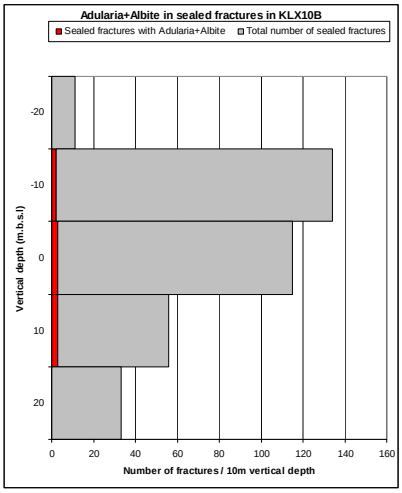
Adularia+Albite in sealed fractures in KLX10B
Sealed fractures with Adularia+Albite
Total number of sealed fractures
Vertical depth (m.b.s.l)
-20
-10
0
10
20
0
20
40
60
80
100
120
140
160
Number of fractures / 10m vertical depth

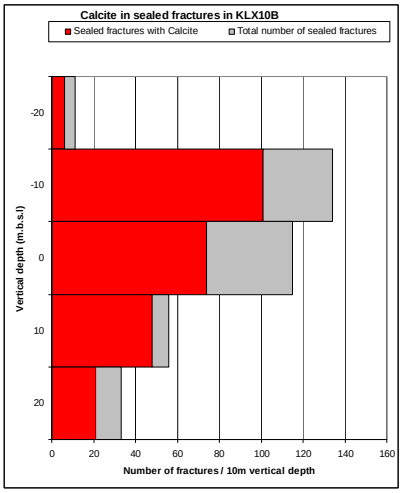
Calcite in sealed fractures in KLX10B
Sealed fractures with Calcite
Total number of sealed fractures
Vertical depth (m.b.s.l)
-20
-10
0
10
20
0
20
40
60
80
100
120
140
160
Number of fractures / 10m vertical depth

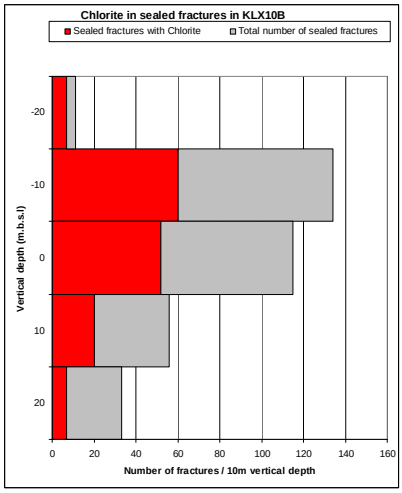
Chlorite in sealed fractures in KLX10B
Sealed fractures with Chlorite
Total number of sealed fractures
Vertical depth (m.b.s.l)
-20
-10
0
10
20
0
20
40
60
80
100
120
140
160
Number of fractures / 10m vertical depth

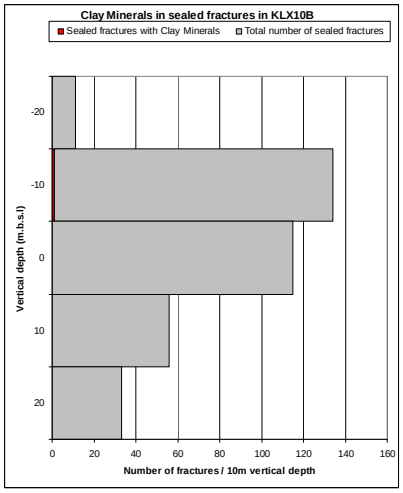
Clay Minerals in sealed fractures in KLX10B
Sealed fractures with Clay Minerals
Total number of sealed fractures
Vertical depth (m.b.s.l)
-20
-10
0
10
20
0
20
40
60
80
100
120
140
160
Number of fractures / 10m vertical depth

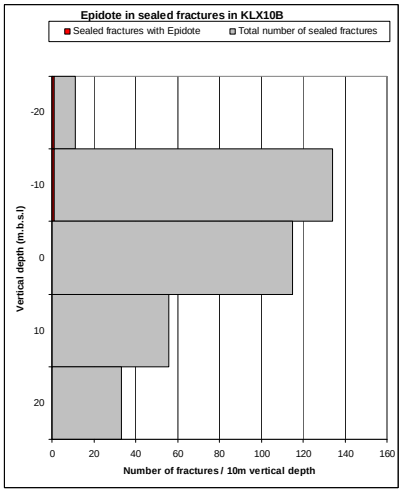
Epidote in sealed fractures in KLX10B
Sealed fractures with Epidote
Total number of sealed fractures
Vertical depth (m.b.s.l)
-20
-10
0
10
20
0
20
40
60
80
100
120
140
160
Number of fractures / 10m vertical depth

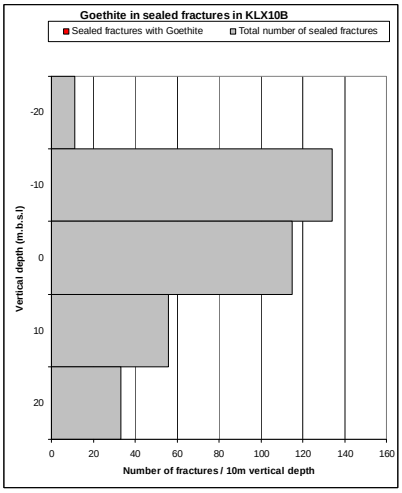
Goethite in sealed fractures in KLX10B
Sealed fractures with Goethite
Total number of sealed fractures
Vertical depth (m.b.s.l)
-20
-10
0
10
20
0
20
40
60
80
100
120
140
160
Number of fractures / 10m vertical depth

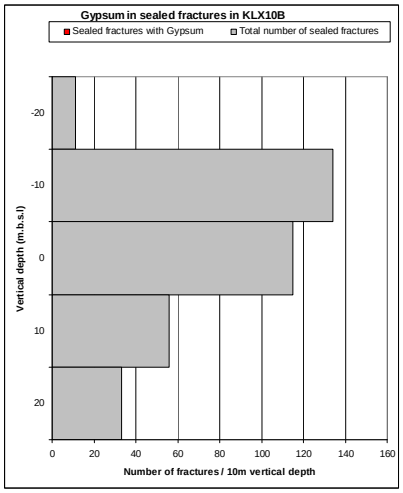
Gypsum in sealed fractures in KLX10B
Sealed fractures with Gypsum
Total number of sealed fractures
Vertical depth (m.b.s.l)
-20
-10
0
10
20
0
20
40
60
80
100
120
140
160
Number of fractures / 10m vertical depth

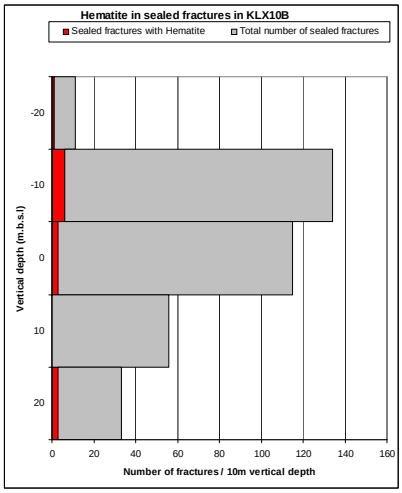
Hematite in sealed fractures in KLX10B
Sealed fractures with Hematite
Total number of sealed fractures
Vertical depth (m.b.s.l)
-20
-10
0
10
20
0
20
40
60
80
100
120
140
160
Number of fractures / 10m vertical depth

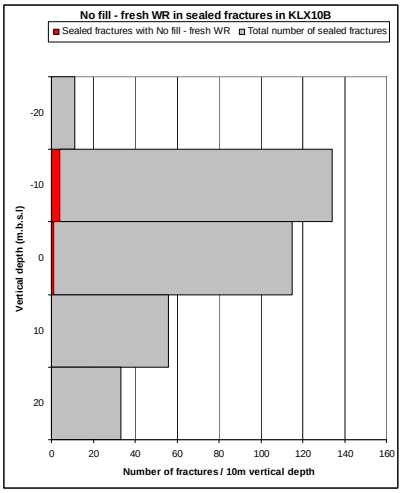
No fill - fresh WR in sealed fractures in KLX10B
Sealed fractures with No fill - fresh WR
Total number of sealed fractures
Vertical depth (m.b.s.l)
-20
-10
0
10
20
0
20
40
60
80
100
120
140
160
Number of fractures / 10m vertical depth

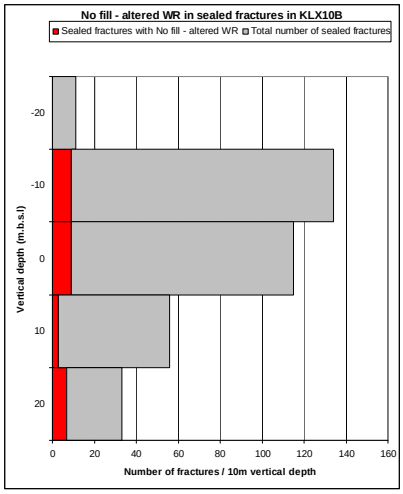
No fill - altered WR in sealed fractures in KLX10B
Sealed fractures with No fill - altered WR
Total number of sealed fractures
Vertical depth (m.b.s.l)
-20
-10
0
10
20
0
20
40
60
80
100
120
140
160
Number of fractures / 10m vertical depth

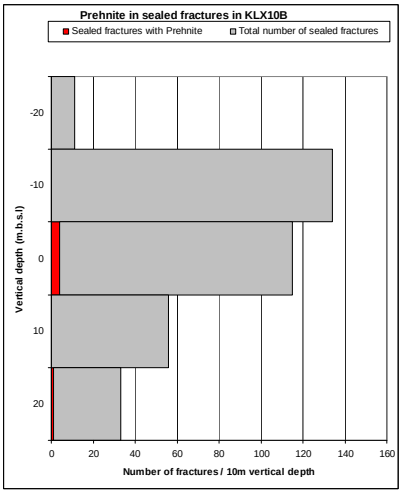
Prehnite in sealed fractures in KLX10B
Sealed fractures with Prehnite
Total number of sealed fractures
Vertical depth (m.b.s.l)
-20
-10
0
10
20
0
20
40
60
80
100
120
140
160
Number of fractures / 10m vertical depth

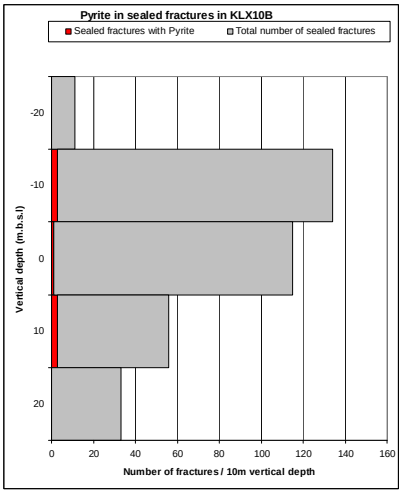
Pyrite in sealed fractures in KLX10B
Sealed fractures with Pyrite
Total number of sealed fractures
Vertical depth (m.b.s.l)
-20
-10
0
10
20
0
20
40
60
80
100
120
140
160
Number of fractures / 10m vertical depth

KLX10C

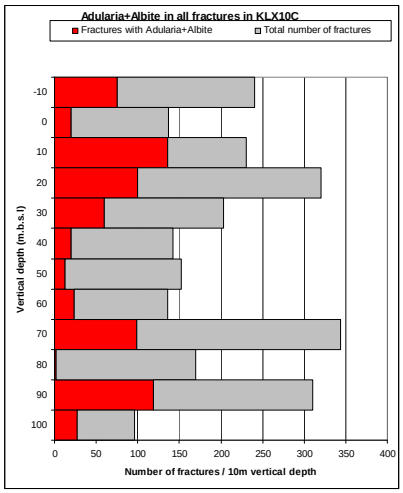
Adularia+Albite in all fractures in KLX10C
Fractures with Adularia+Albite
Total number of fractures
Vertical depth (m.b.s.l)
Number of fractures / 10m vertical depth

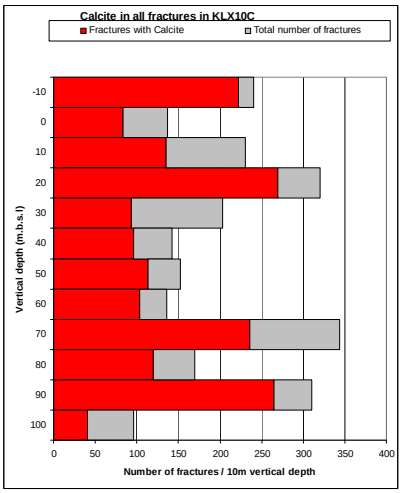
Calcite in all fractures in KLX10C
Fractures with Calcite
Total number of fractures
Vertical depth (m.b.s.l)
Number of fractures / 10m vertical depth

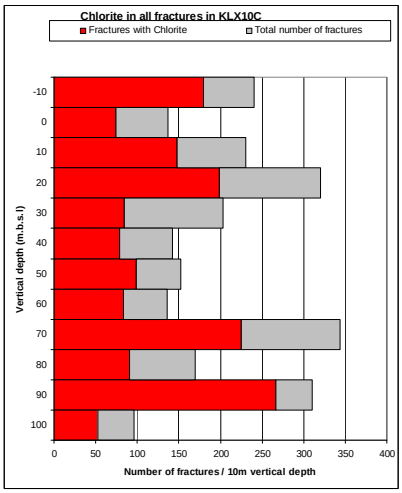
Chlorite in all fractures in KLX10C
Fractures with Chlorite
Total number of fractures
Vertical depth (m.b.s.l)
Number of fractures / 10m vertical depth

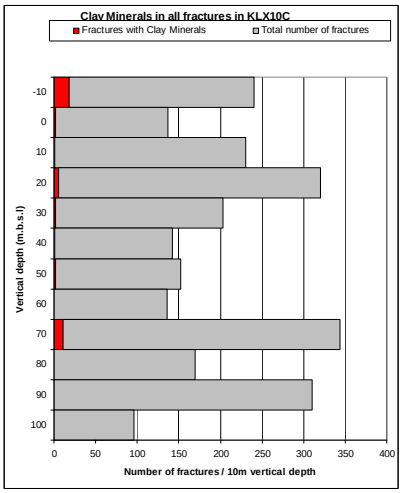
Clay Minerals in all fractures in KLX10C
Fractures with Clay Minerals
Total number of fractures
Vertical depth (m.b.s.l)
Number of fractures / 10m vertical depth

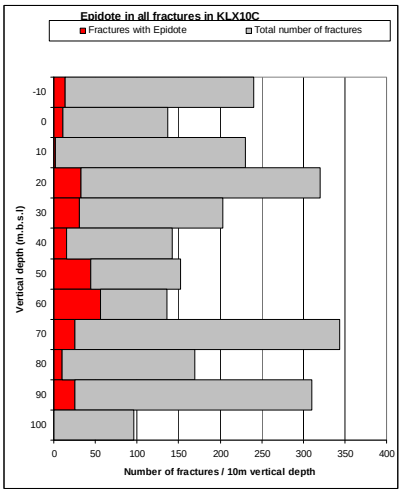
Epidote in all fractures in KLX10C
Fractures with Epidote
Total number of fractures
Vertical depth (m.b.s.l)
Number of fractures / 10m vertical depth

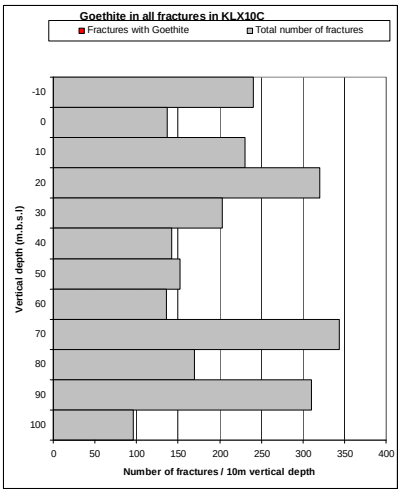
Goethite in all fractures in KLX10C
Fractures with Goethite
Total number of fractures
Vertical depth (m.b.s.l)
Number of fractures / 10m vertical depth

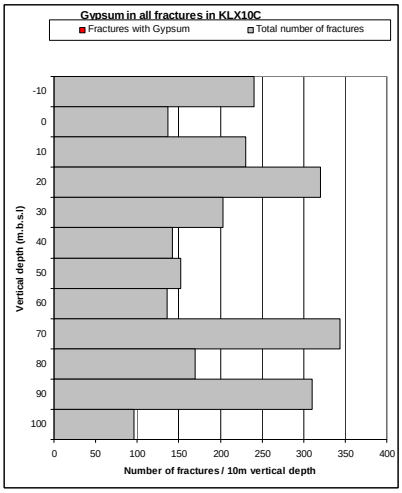
Gypsum in all fractures in KLX10C
Fractures with Gypsum
Total number of fractures
Vertical depth (m.b.s.l)
Number of fractures / 10m vertical depth

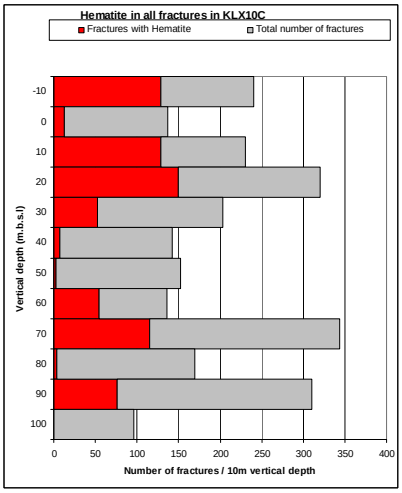
Hematite in all fractures in KLX10C
Fractures with Hematite
Total number of fractures
Vertical depth (m.b.s.l)
Number of fractures / 10m vertical depth

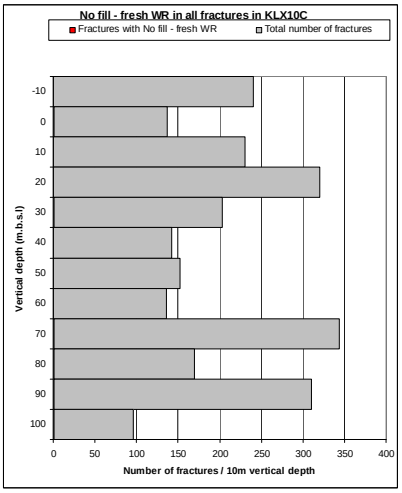
No fill - fresh WR in all fractures in KLX10C
Fractures with No fill - fresh WR
Total number of fractures
Vertical depth (m.b.s.l)
Number of fractures / 10m vertical depth

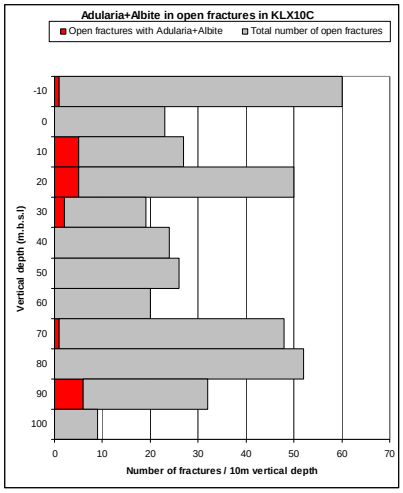
Adularia+Albite in open fractures in KLX10C
Open fractures with Adularia+Albite
Total number of open fractures
Vertical depth (m.b.s.l)
Number of fractures / 10m vertical depth

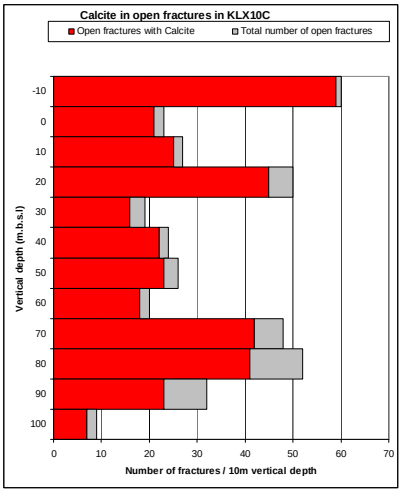
Calcite in open fractures in KLX10C
Open fractures with Calcite
Total number of open fractures
Vertical depth (m.b.s.l)
Number of fractures / 10m vertical depth

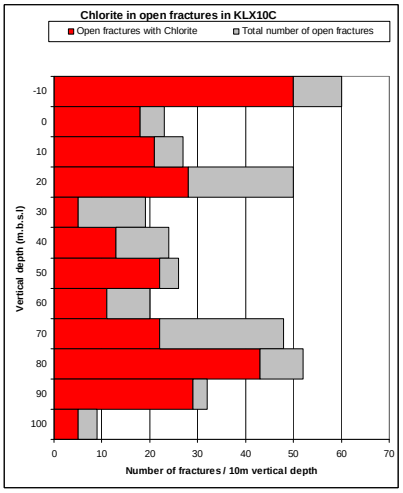
Chlorite in open fractures in KLX10C
Open fractures with Chlorite
Total number of open fractures
Vertical depth (m.b.s.l)
Number of fractures / 10m vertical depth

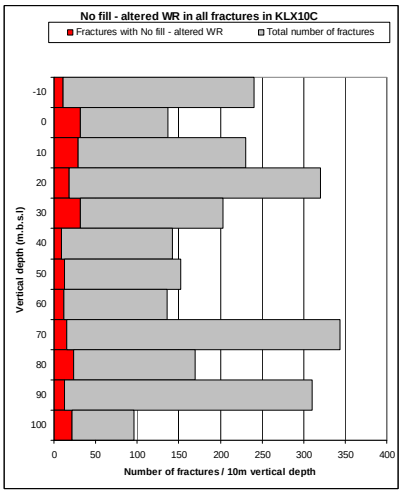
No fill - altered WR in all fractures in KLX10C
Fractures with No fill - altered WR
Total number of fractures
Vertical depth (m.b.s.l)
Number of fractures / 10m vertical depth

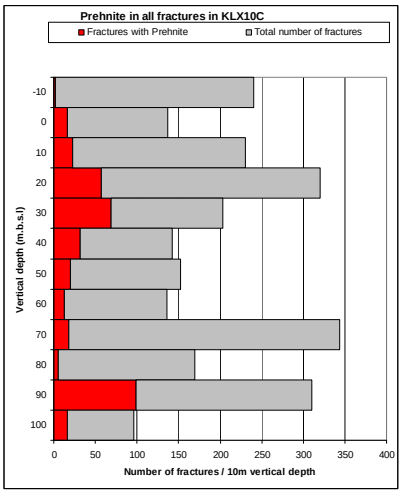
Prehnite in all fractures in KLX10C
Fractures with Prehnite
Total number of fractures
Vertical depth (m.b.s.l)
Number of fractures / 10m vertical depth

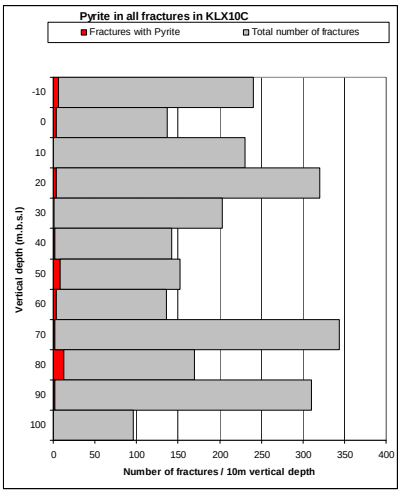
Pyrite in all fractures in KLX10C
Fractures with Pyrite
Total number of fractures
Vertical depth (m.b.s.l)
Number of fractures / 10m vertical depth

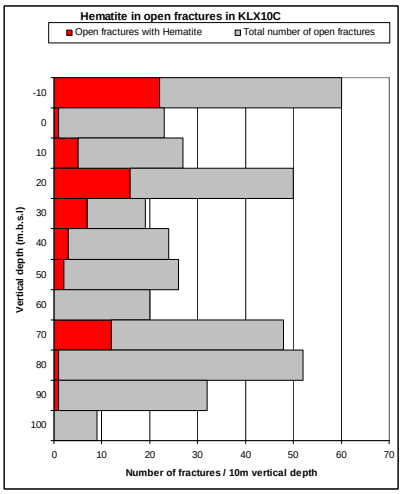
Hematite in open fractures in KLX10C
Open fractures with Hematite
Total number of open fractures
Vertical depth (m.b.s.l)
Number of fractures / 10m vertical depth

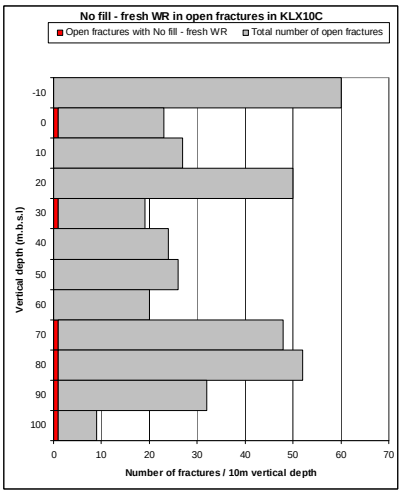
No fill - fresh WR in open fractures in KLX10C
Open fractures with No fill - fresh WR
Total number of open fractures
Vertical depth (m.b.s.l)
Number of fractures / 10m vertical depth

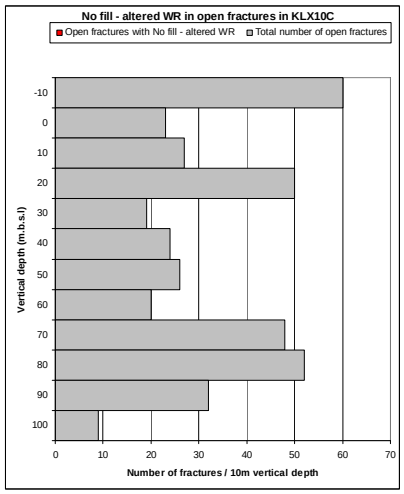
No fill - altered WR in open fractures in KLX10C
Open fractures with No fill - altered WR
Total number of open fractures
Vertical depth (m.b.s.l)
Number of fractures / 10m vertical depth

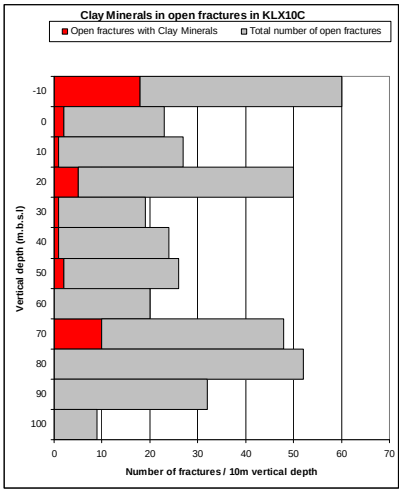
Clay Minerals in open fractures in KLX10C
Open fractures with Clay Minerals
Total number of open fractures
Vertical depth (m.b.s.l)
Number of fractures / 10m vertical depth

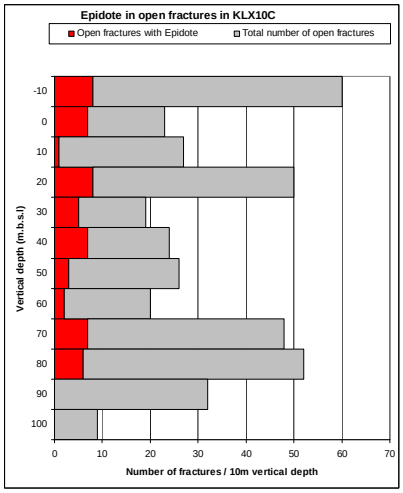
Epidote in open fractures in KLX10C
Open fractures with Epidote
Total number of open fractures
Vertical depth (m.b.s.l)
Number of fractures / 10m vertical depth

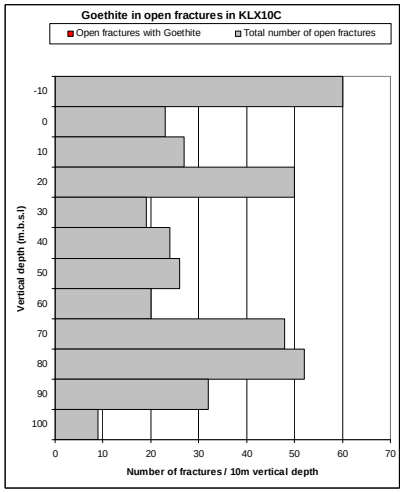
Goethite in open fractures in KLX10C
Open fractures with Goethite
Total number of open fractures
Vertical depth (m.b.s.l)
Number of fractures / 10m vertical depth

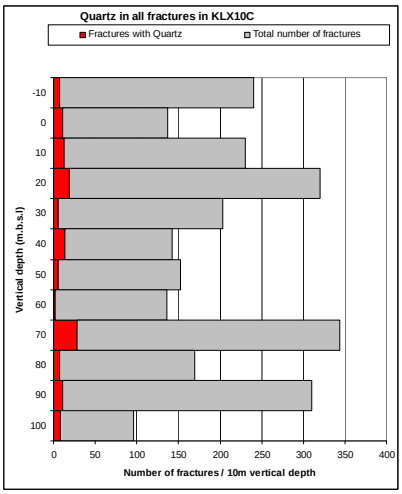
Quartz in all fractures in KLX10C
Fractures with Quartz
Total number of fractures
Vertical depth (m.b.s.l)
Number of fractures / 10m vertical depth

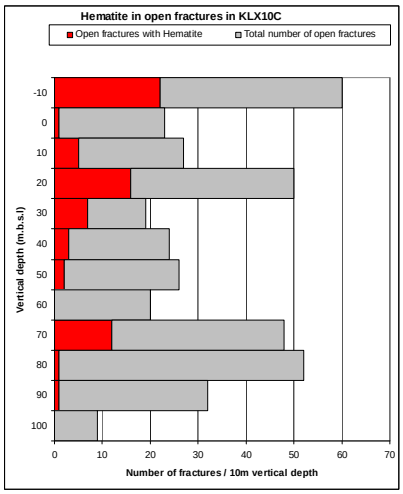
Hematite in open fractures in KLX10C
Open fractures with Hematite
Total number of open fractures
Vertical depth (m.b.s.l)
Number of fractures / 10m vertical depth

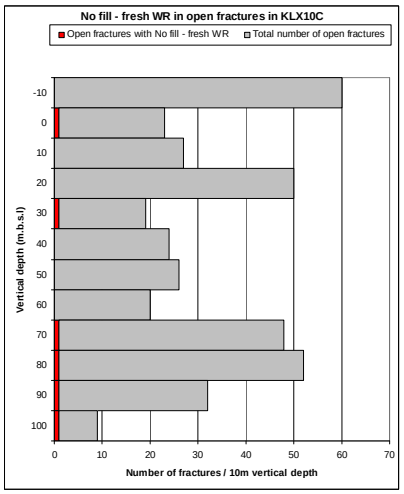
No fill - fresh WR in open fractures in KLX10C
Open fractures with No fill - fresh WR
Total number of open fractures
Vertical depth (m.b.s.l)
Number of fractures / 10m vertical depth

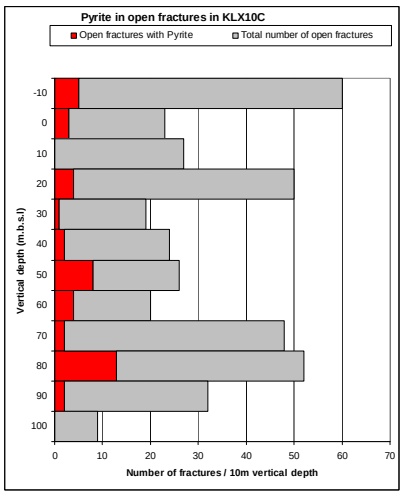
Pyrite in open fractures in KLX10C
Open fractures with Pyrite
Total number of open fractures
Vertical depth (m.b.s.l)
Number of fractures / 10m vertical depth

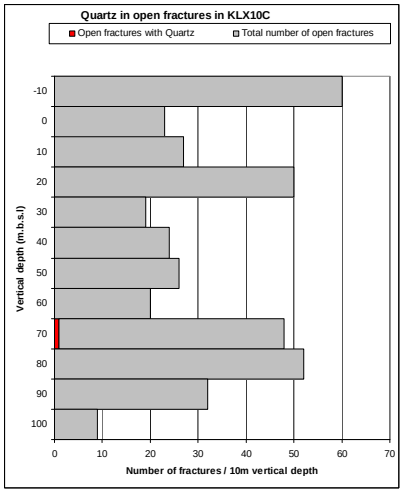
Quartz in open fractures in KLX10C
Open fractures with Quartz
Total number of open fractures
Vertical depth (m.b.s.l)
Number of fractures / 10m vertical depth

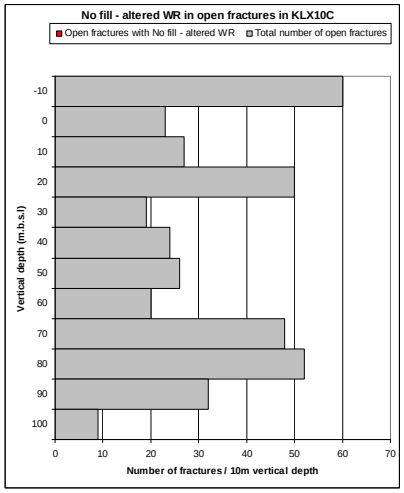
No fill - altered WR in open fractures in KLX10C
Open fractures with No fill - altered WR
Total number of open fractures
Vertical depth (m.b.s.l)
Number of fractures / 10m vertical depth

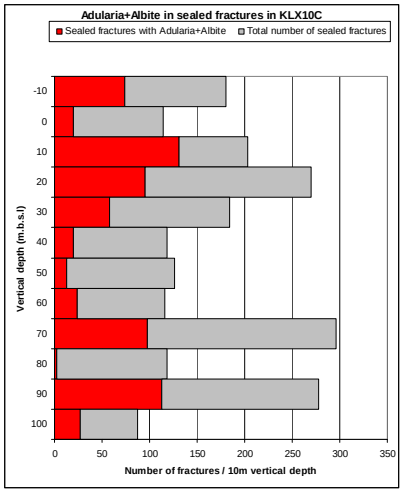
Adularia+Albite in sealed fractures in KLX10C
Sealed fractures with Adularia+Albite
Total number of sealed fractures
Vertical depth (m.b.s.l)
-10
0
10
20
30
40
50
60
70
80
90
100
0
50
100
150
200
250
300
350
Number of fractures / 10m vertical depth

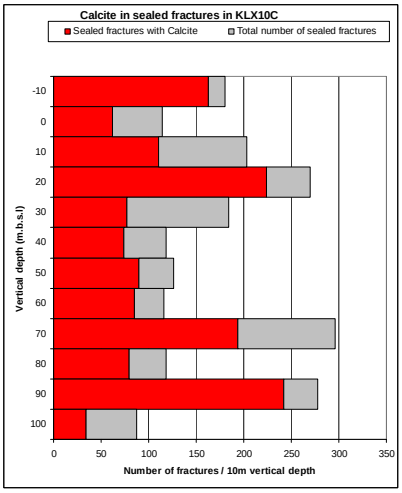
Calcite in sealed fractures in KLX10C
Sealed fractures with Calcite
Total number of sealed fractures
Vertical depth (m.b.s.l)
-10
0
10
20
30
40
50
60
70
80
90
100
0
50
100
150
200
250
300
350
Number of fractures / 10m vertical depth

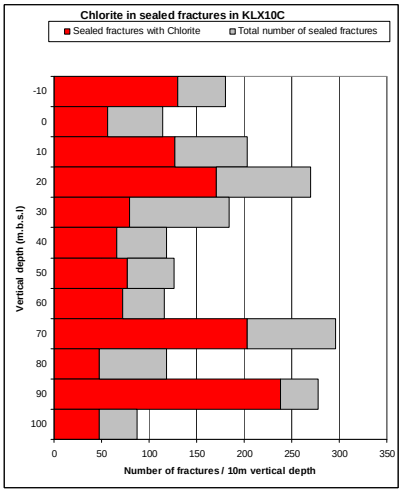
Chlorite in sealed fractures in KLX10C
Sealed fractures with Chlorite
Total number of sealed fractures
Vertical depth (m.b.s.l)
-10
0
10
20
30
40
50
60
70
80
90
100
0
50
100
150
200
250
300
350
Number of fractures / 10m vertical depth

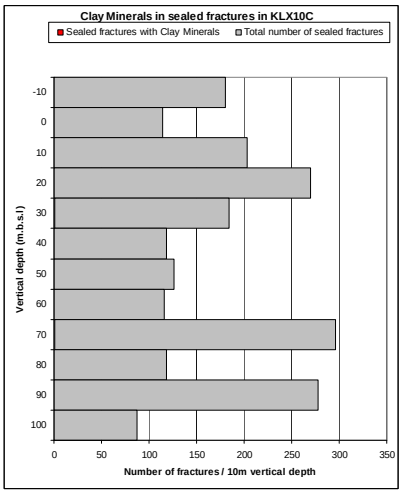
Clay Minerals in sealed fractures in KLX10C
Sealed fractures with Clay Minerals
Total number of sealed fractures
Vertical depth (m.b.s.l)
-10
0
10
20
30
40
50
60
70
80
90
100
0
50
100
150
200
250
300
350
Number of fractures / 10m vertical depth

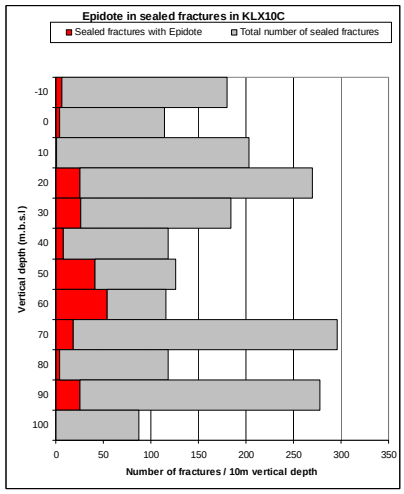
Epidote in sealed fractures in KLX10C
Sealed fractures with Epidote
Total number of sealed fractures
Vertical depth (m.b.s.l)
-10
0
10
20
30
40
50
60
70
80
90
100
0
50
100
150
200
250
300
350
Number of fractures / 10m vertical depth

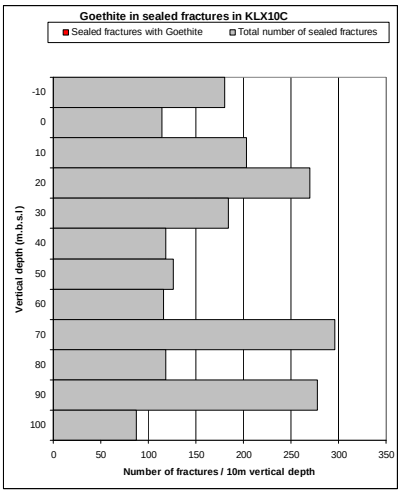
Goethite in sealed fractures in KLX10C
Sealed fractures with Goethite
Total number of sealed fractures
Vertical depth (m.b.s.l)
-10
0
10
20
30
40
50
60
70
80
90
100
0
50
100
150
200
250
300
350
Number of fractures / 10m vertical depth

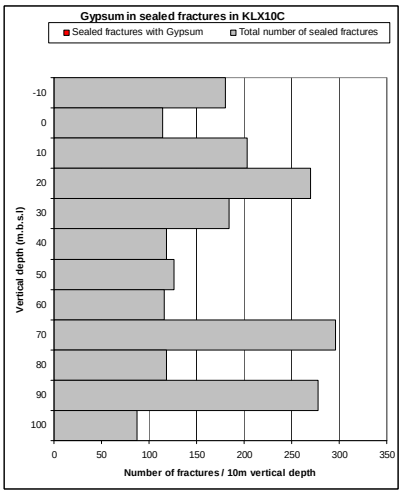
Gypsum in sealed fractures in KLX10C
Sealed fractures with Gypsum
Total number of sealed fractures
Vertical depth (m.b.s.l)
-10
0
10
20
30
40
50
60
70
80
90
100
0
50
100
150
200
250
300
350
Number of fractures / 10m vertical depth

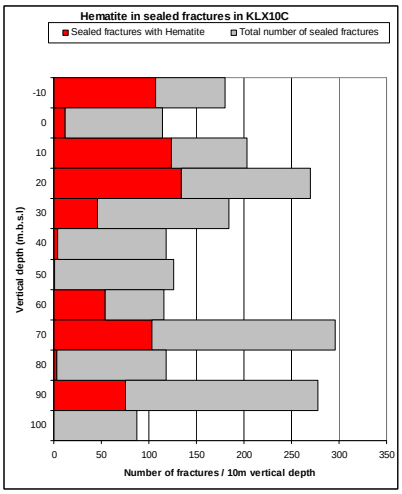
Hematite in sealed fractures in KLX10C
Sealed fractures with Hematite
Total number of sealed fractures
Vertical depth (m.b.s.l)
-10
0
10
20
30
40
50
60
70
80
90
100
0
50
100
150
200
250
300
350
Number of fractures / 10m vertical depth

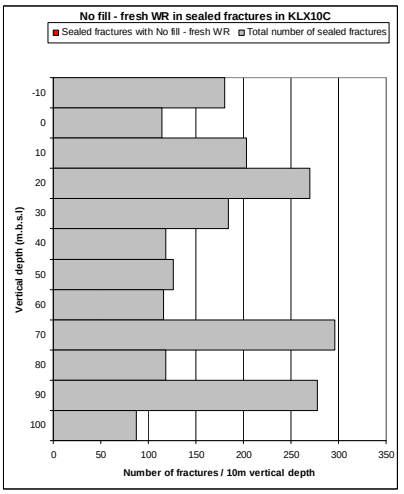
No fill - fresh WR in sealed fractures in KLX10C
Sealed fractures with No fill - fresh WR
Total number of sealed fractures
Vertical depth (m.b.s.l)
-10
0
10
20
30
40
50
60
70
80
90
100
0
50
100
150
200
250
300
350
Number of fractures / 10m vertical depth

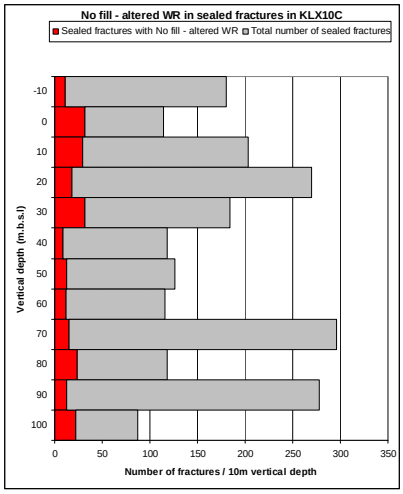
No fill - altered WR in sealed fractures in KLX10C
Sealed fractures with No fill - altered WR
Total number of sealed fractures
Vertical depth (m.b.s.l)
-10
0
10
20
30
40
50
60
70
80
90
100
0
50
100
150
200
250
300
350
Number of fractures / 10m vertical depth

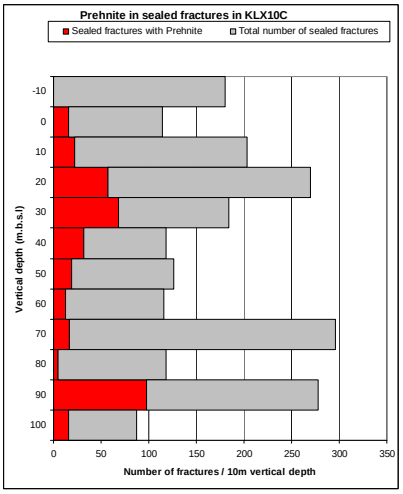
Prehnite in sealed fractures in KLX10C
Sealed fractures with Prehnite
Total number of sealed fractures
Vertical depth (m.b.s.l)
-10
0
10
20
30
40
50
60
70
80
90
100
0
50
100
150
200
250
300
350
Number of fractures / 10m vertical depth

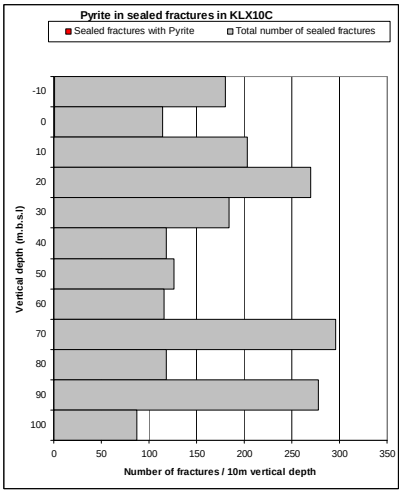
Pyrite in sealed fractures in KLX10C
Sealed fractures with Pyrite
Total number of sealed fractures
Vertical depth (m.b.s.l)
-10
0
10
20
30
40
50
60
70
80
90
100
0
50
100
150
200
250
300
350
Number of fractures / 10m vertical depth

KLX11A

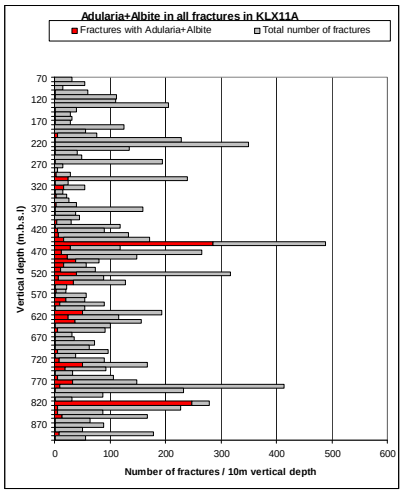
Adularia+Albite in all fractures in KLX11A
Fractures with Adularia+Albite
Total number of fractures
Vertical depth (m.b.s.l)
Number of fractures / 10m vertical depth

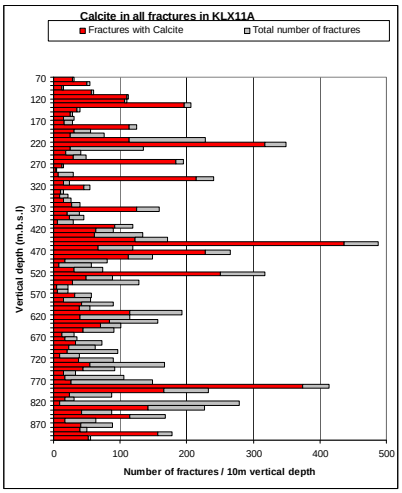
Calcite in all fractures in KLX11A
Fractures with Calcite
Total number of fractures
Vertical depth (m.b.s.l)
Number of fractures / 10m vertical depth

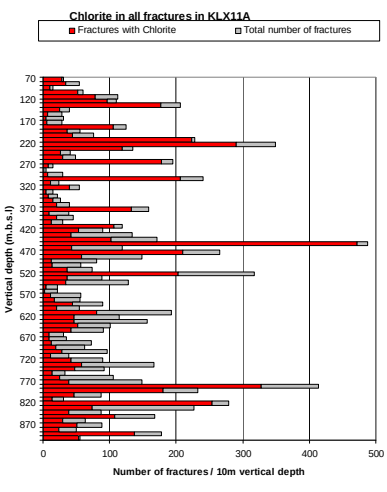
Chlorite in all fractures in KLX11A
Fractures with Chlorite
Total number of fractures
Vertical depth (m.b.s.l)
Number of fractures / 10m vertical depth

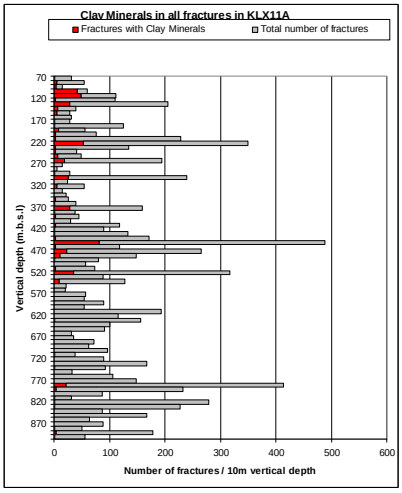
Clay Minerals in all fractures in KLX11A
Fractures with Clay Minerals
Total number of fractures
Vertical depth (m.b.s.l)
Number of fractures / 10m vertical depth

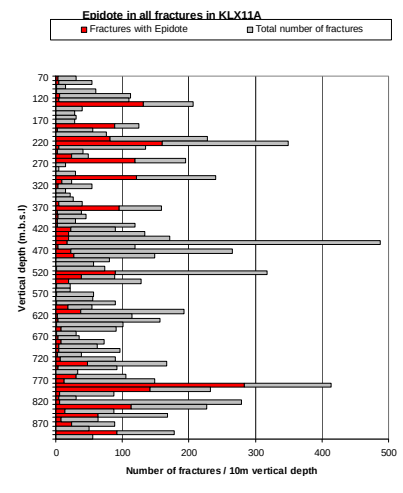
Epidote in all fractures in KLX11A
Fractures with Epidote
Total number of fractures
Vertical depth (m.b.s.l)
Number of fractures / 10m vertical depth

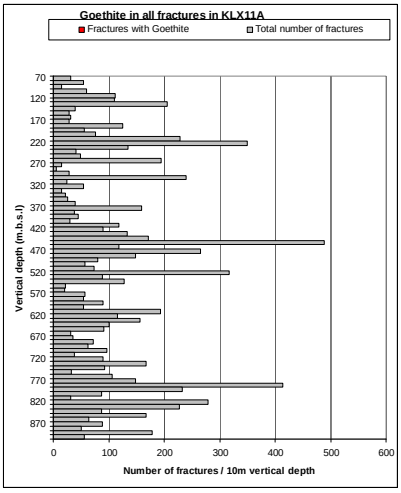
Goethite in all fractures in KLX11A
Fractures with Goethite
Total number of fractures
Vertical depth (m.b.s.l)
Number of fractures / 10m vertical depth

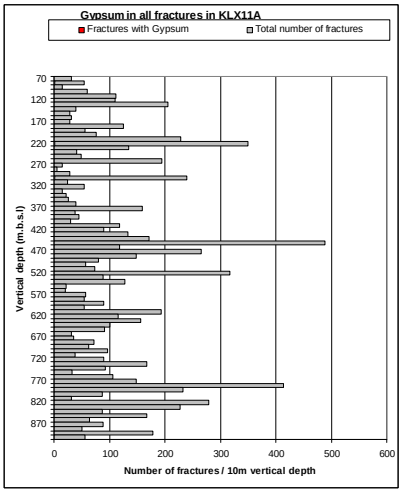
Gypsum in all fractures in KLX11A
Fractures with Gypsum
Total number of fractures
Vertical depth (m.b.s.l)
Number of fractures / 10m vertical depth

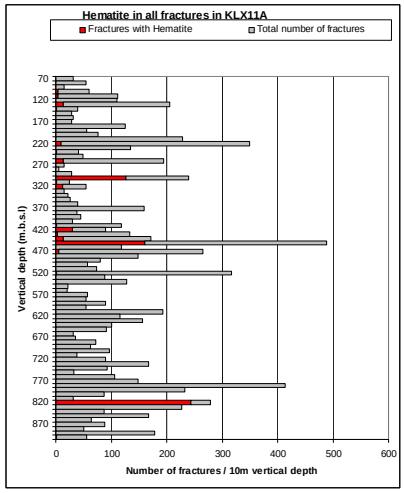
Hematite in all fractures in KLX11A
Fractures with Hematite
Total number of fractures
Vertical depth (m.b.s.l)
Number of fractures / 10m vertical depth

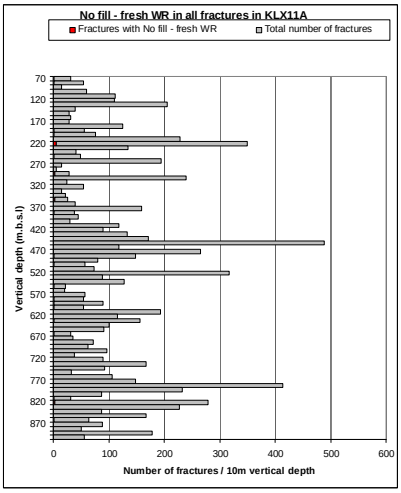
No fill - fresh WR in all fractures in KLX11A
Fractures with No fill - fresh WR
Total number of fractures
Vertical depth (m.b.s.l)
Number of fractures / 10m vertical depth

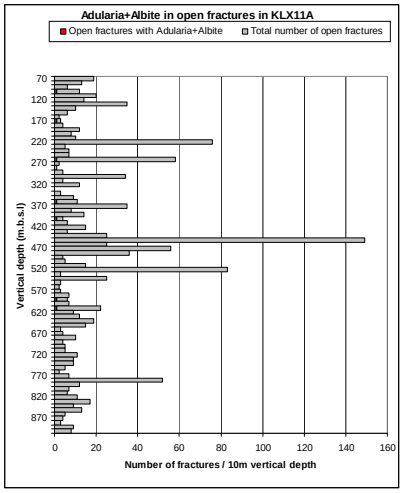
Adularia+Albite in open fractures in KLX11A
Open fractures with Adularia+Albite
Total number of open fractures
Vertical depth (m.b.s.l)
Number of fractures / 10m vertical depth

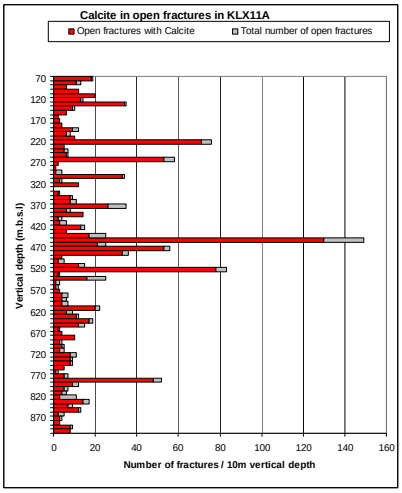
Calcite in open fractures in KLX11A
Open fractures with Calcite
Total number of open fractures
Vertical depth (m.b.s.l)
Number of fractures / 10m vertical depth

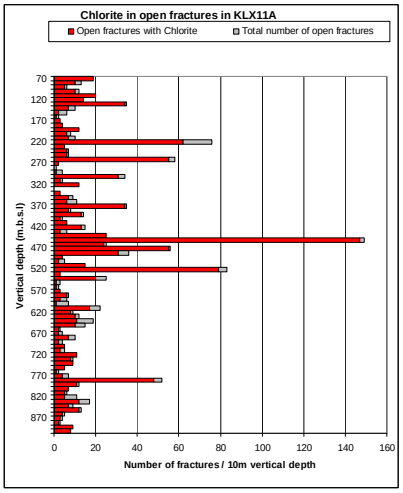
Chlorite in open fractures in KLX11A
Open fractures with Chlorite
Total number of open fractures
Vertical depth (m.b.s.l)
Number of fractures / 10m vertical depth

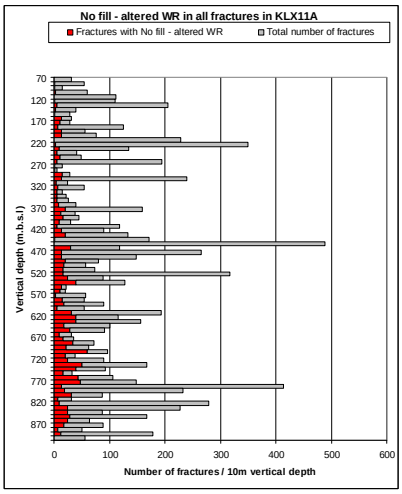
No fill - altered WR in all fractures in KLX11A
Fractures with No fill - altered WR
Total number of fractures
Vertical depth (m.b.s.l)
Number of fractures / 10m vertical depth

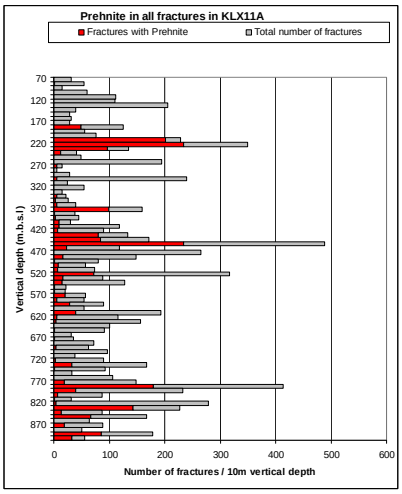
Prehnite in all fractures in KLX11A
Fractures with Prehnite
Total number of fractures
Vertical depth (m.b.s.l)
Number of fractures / 10m vertical depth

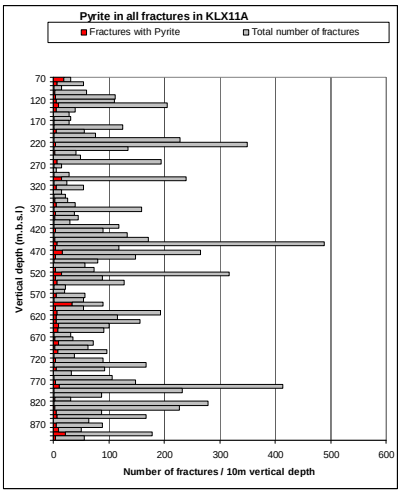
Pyrite in all fractures in KLX11A
Fractures with Pyrite
Total number of fractures
Vertical depth (m.b.s.l)
Number of fractures / 10m vertical depth

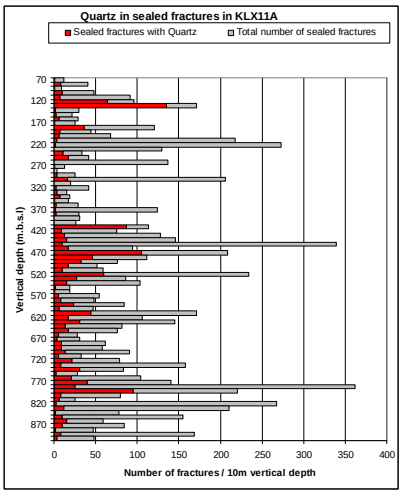
Quartz in sealed fractures in KLX11A
Sealed fractures with Quartz
Total number of sealed fractures
Vertical depth (m.b.s.l)
Number of fractures / 10m vertical depth

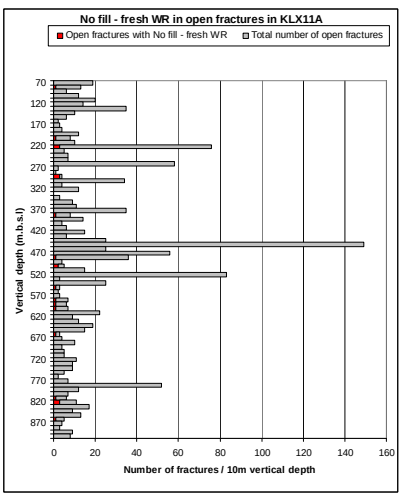
No fill - fresh WR in open fractures in KLX11A
Open fractures with No fill - fresh WR
Total number of open fractures
Vertical depth (m.b.s.l)
Number of fractures / 10m vertical depth

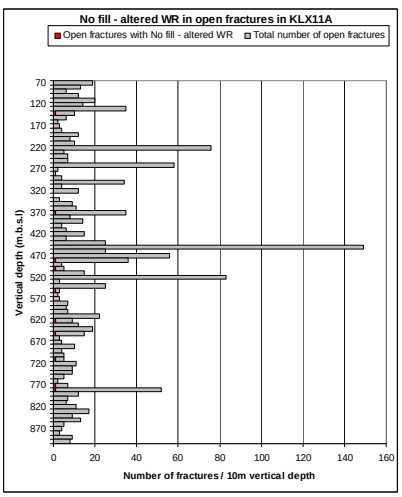
No fill - altered WR in open fractures in KLX11A
Open fractures with No fill - altered WR
Total number of open fractures
Vertical depth (m.b.s.l)
Number of fractures / 10m vertical depth

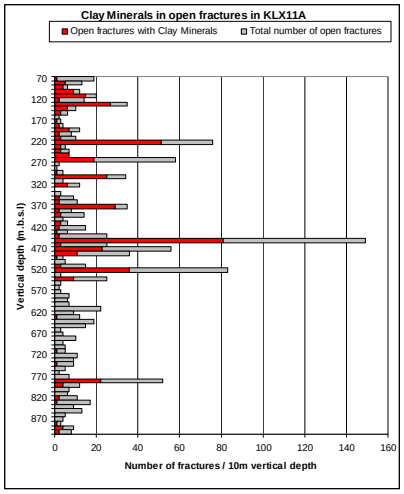
Clay Minerals in open fractures in KLX11A
Open fractures with Clay Minerals
Total number of open fractures
Vertical depth (m.b.s.l)
Number of fractures / 10m vertical depth

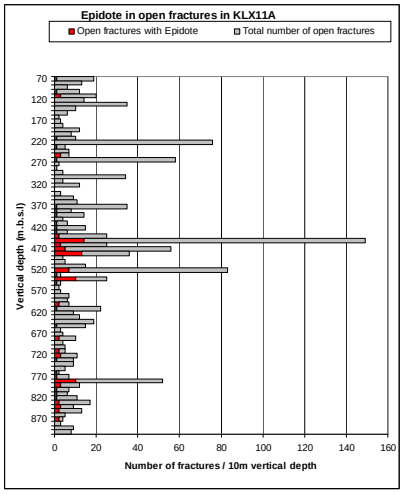
Epidote in open fractures in KLX11A
Open fractures with Epidote
Total number of open fractures
Vertical depth (m.b.s.l)
Number of fractures / 10m vertical depth

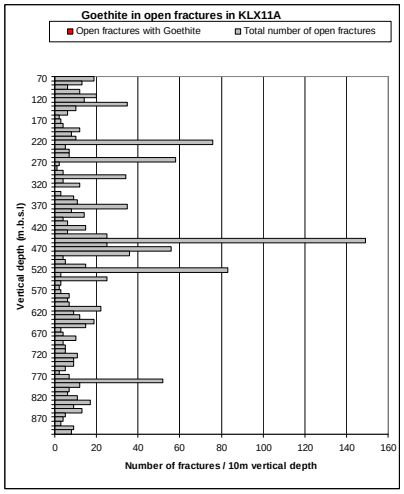
Goethite in open fractures in KLX11A
Open fractures with Goethite
Total number of open fractures
Vertical depth (m.b.s.l)
Number of fractures / 10m vertical depth

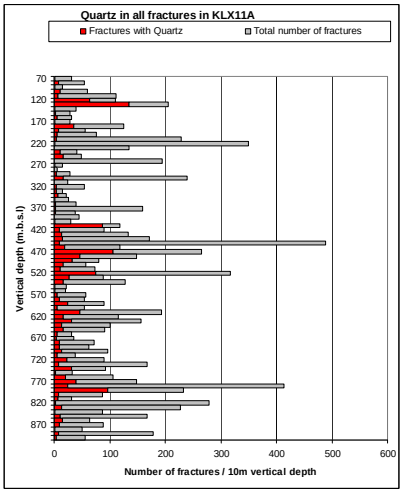
Quartz in all fractures in KLX11A
Fractures with Quartz
Total number of fractures
Vertical depth (m.b.s.l)
Number of fractures / 10m vertical depth

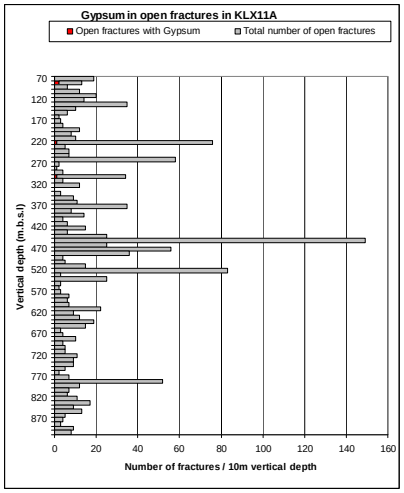
Gypsum in open fractures in KLX11A
Open fractures with Gypsum
Total number of open fractures
Vertical depth (m.b.s.l)
Number of fractures / 10m vertical depth

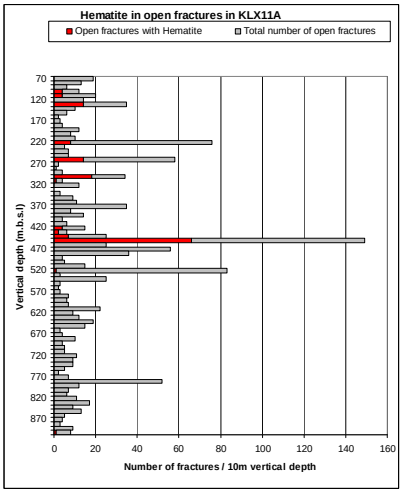
Hematite in open fractures in KLX11A
Open fractures with Hematite
Total number of open fractures
Vertical depth (m.b.s.l)
Number of fractures / 10m vertical depth

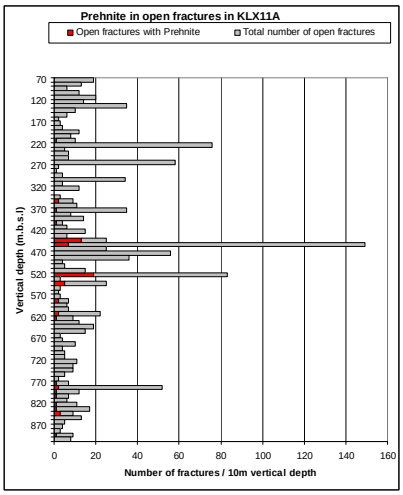
Prehnite in open fractures in KLX11A
Open fractures with Prehnite
Total number of open fractures
Vertical depth (m.b.s.l)
Number of fractures / 10m vertical depth

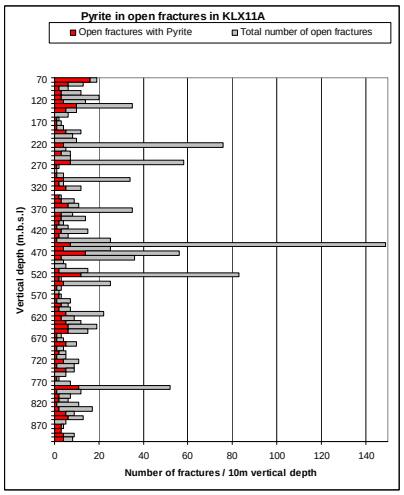
Pyrite in open fractures in KLX11A
Open fractures with Pyrite
Total number of open fractures
Vertical depth (m.b.s.l)
Number of fractures / 10m vertical depth

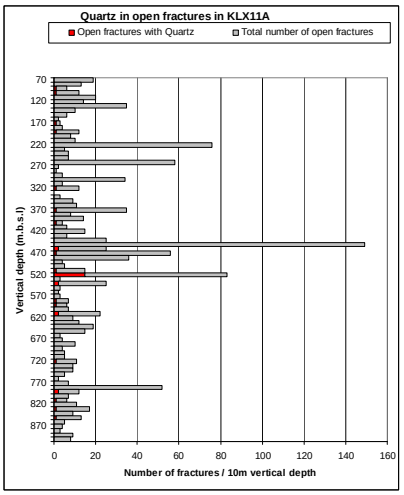
Quartz in open fractures in KLX11A
Open fractures with Quartz
Total number of open fractures
Vertical depth (m.b.s.l)
Number of fractures / 10m vertical depth

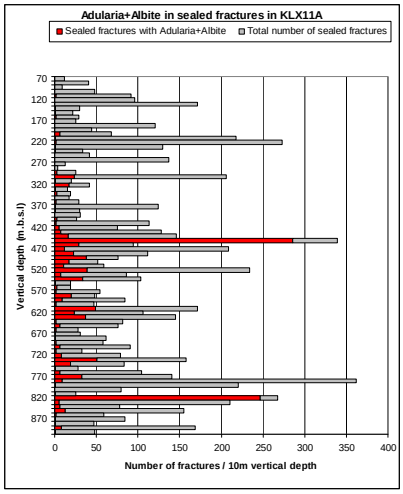
Adularia+Albite in sealed fractures in KLX11A
Sealed fractures with Adularia+Albite
Total number of sealed fractures
Vertical depth (m.b.s.l)
Number of fractures / 10m vertical depth

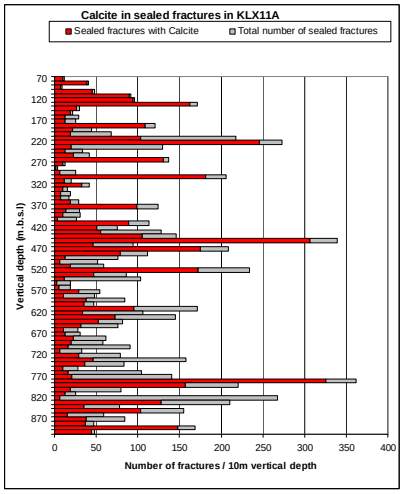
Calcite in sealed fractures in KLX11A
Sealed fractures with Calcite
Total number of sealed fractures
Vertical depth (m.b.s.l)
Number of fractures / 10m vertical depth

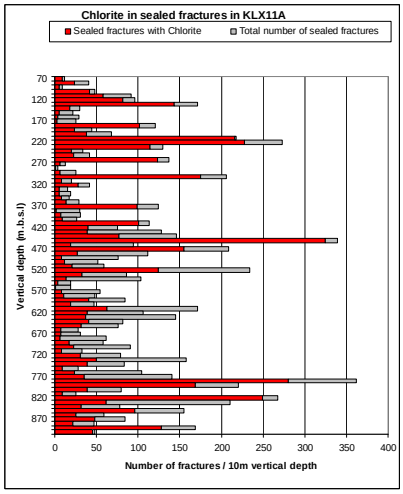
Chlorite in sealed fractures in KLX11A
Sealed fractures with Chlorite
Total number of sealed fractures
Vertical depth (m.b.s.l)
Number of fractures / 10m vertical depth

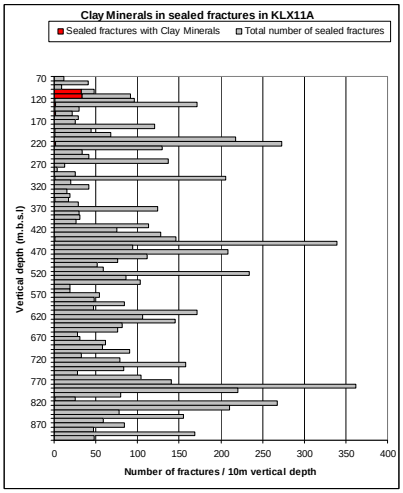
Clay Minerals in sealed fractures in KLX11A
Sealed fractures with Clay Minerals
Total number of sealed fractures
Vertical depth (m.b.s.l)
Number of fractures / 10m vertical depth

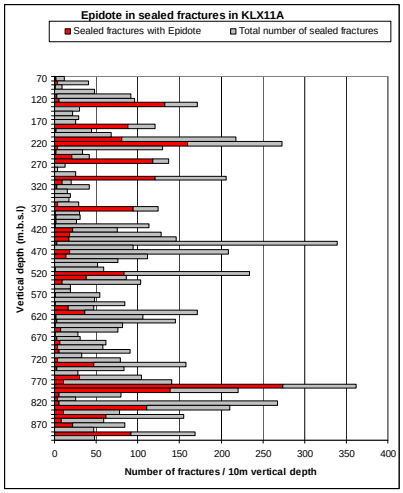
Epidote in sealed fractures in KLX11A
Sealed fractures with Epidote
Total number of sealed fractures
Vertical depth (m.b.s.l)
Number of fractures / 10m vertical depth

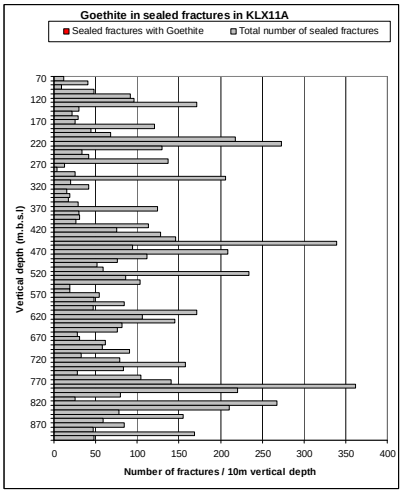
Goethite in sealed fractures in KLX11A
Sealed fractures with Goethite
Total number of sealed fractures
Vertical depth (m.b.s.l)
Number of fractures / 10m vertical depth

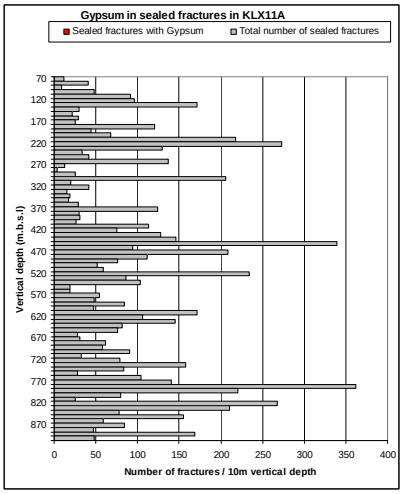
Gypsum in sealed fractures in KLX11A
Sealed fractures with Gypsum
Total number of sealed fractures
Vertical depth (m.b.s.l)
Number of fractures / 10m vertical depth

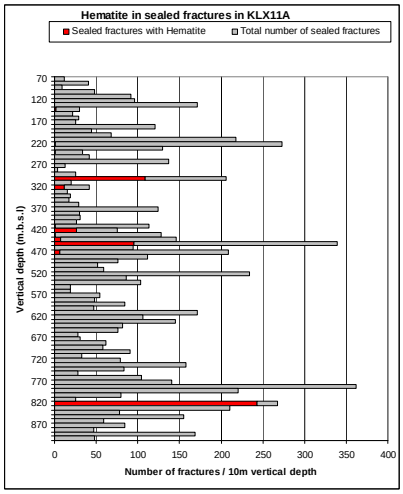
Hematite in sealed fractures in KLX11A
Sealed fractures with Hematite
Total number of sealed fractures
Vertical depth (m.b.s.l)
Number of fractures / 10m vertical depth

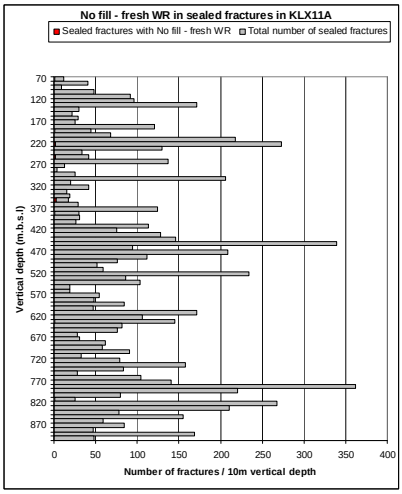
No fill - fresh WR in sealed fractures in KLX11A
Sealed fractures with No fill - fresh WR
Total number of sealed fractures
Vertical depth (m.b.s.l)
Number of fractures / 10m vertical depth

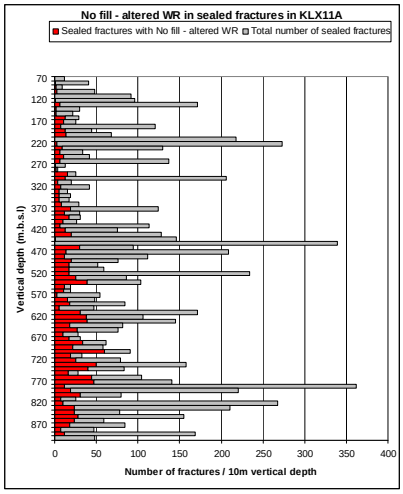
No fill - altered WR in sealed fractures in KLX11A
Sealed fractures with No fill - altered WR
Total number of sealed fractures
Vertical depth (m.b.s.l)
70
120
170
220
270
320
370
420
470
520
570
620
670
720
770
820
870
0
50
100
150
200
250
300
350
400
Number of fractures / 10m vertical depth

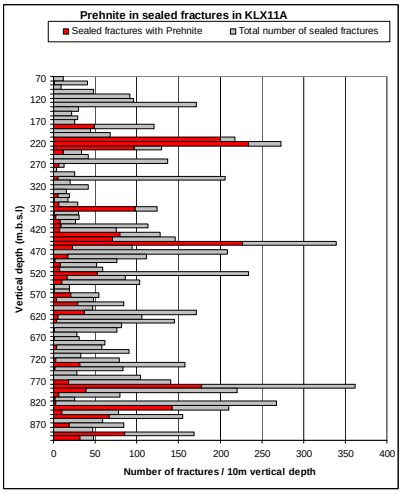
Prehnite in sealed fractures in KLX11A
Sealed fractures with Prehnite
Total number of sealed fractures
Vertical depth (m.b.s.l)
70
120
170
220
270
320
370
420
470
520
570
620
670
720
770
820
870
0
50
100
150
200
250
300
350
400
Number of fractures / 10m vertical depth

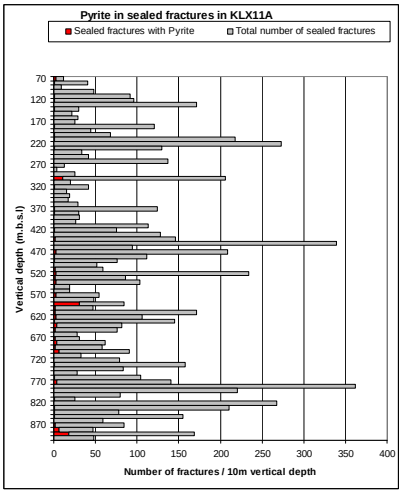
Pyrite in sealed fractures in KLX11A
Sealed fractures with Pyrite
Total number of sealed fractures
Vertical depth (m.b.s.l)
70
120
170
220
270
320
370
420
470
520
570
620
670
720
770
820
870
0
50
100
150
200
250
300
350
400
Number of fractures / 10m vertical depth

KLX11B

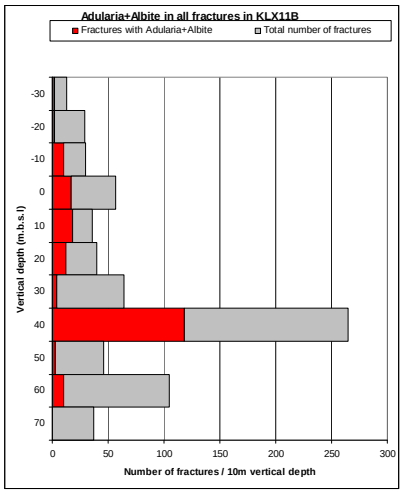
Adularia+Albite in all fractures in KLX11B
Fractures with Adularia+Albite
Total number of fractures
Vertical depth (m.b.s.l)
Number of fractures / 10m vertical depth

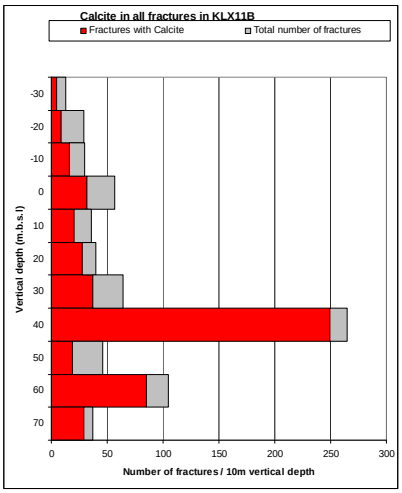
Calcite in all fractures in KLX11B
Fractures with Calcite
Total number of fractures
Vertical depth (m.b.s.l)
Number of fractures / 10m vertical depth

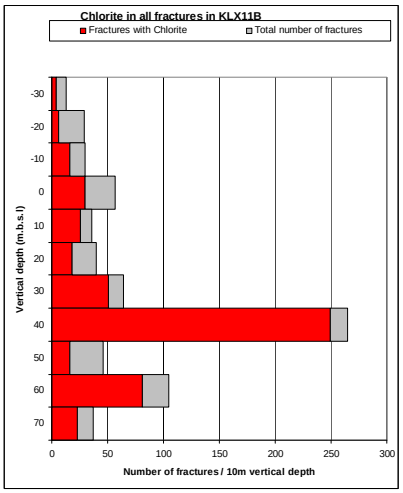
Chlorite in all fractures in KLX11B
Fractures with Chlorite
Total number of fractures
Vertical depth (m.b.s.l)
Number of fractures / 10m vertical depth

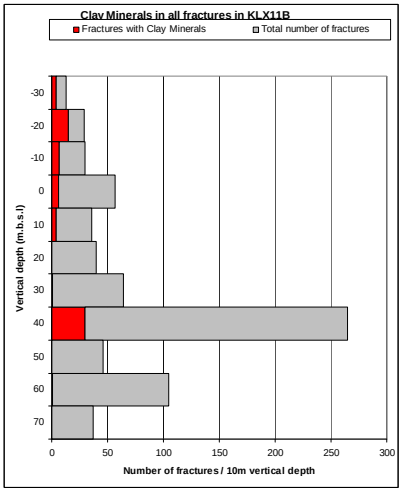
Clay Minerals in all fractures in KLX11B
Fractures with Clay Minerals
Total number of fractures
Vertical depth (m.b.s.l)
Number of fractures / 10m vertical depth

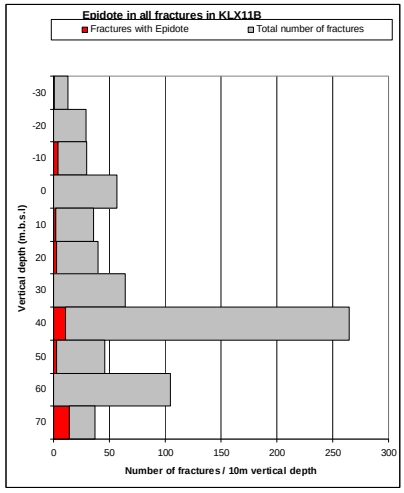
Epidote in all fractures in KLX11B
Fractures with Epidote
Total number of fractures
Vertical depth (m.b.s.l)
Number of fractures / 10m vertical depth

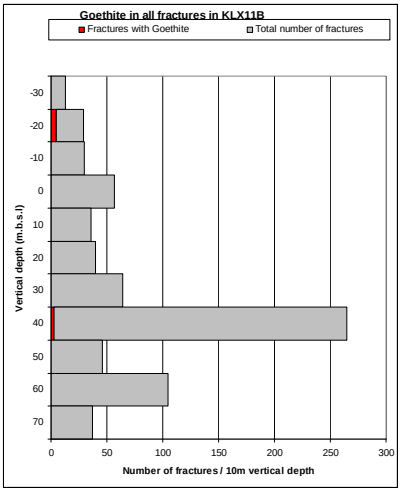
Goethite in all fractures in KLX11B
Fractures with Goethite
Total number of fractures
Vertical depth (m.b.s.l)
Number of fractures / 10m vertical depth

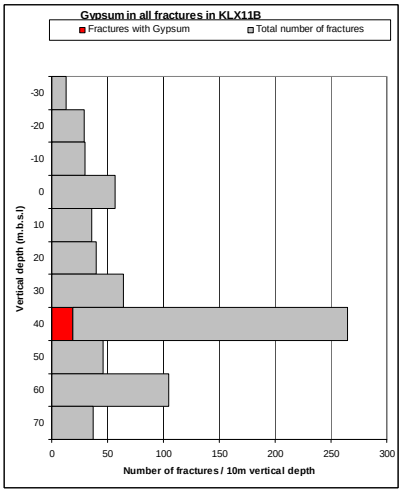
Gypsum in all fractures in KLX11B
Fractures with Gypsum
Total number of fractures
Vertical depth (m.b.s.l)
Number of fractures / 10m vertical depth

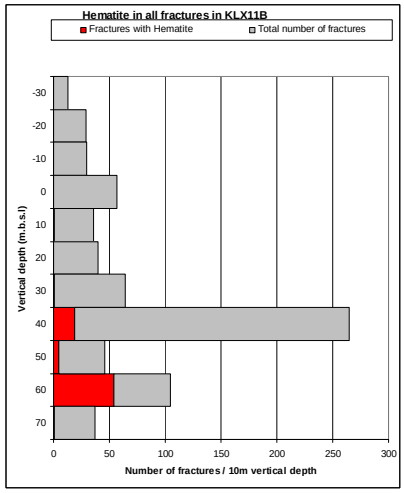
Hematite in all fractures in KLX11B
Fractures with Hematite
Total number of fractures
Vertical depth (m.b.s.l)
Number of fractures / 10m vertical depth

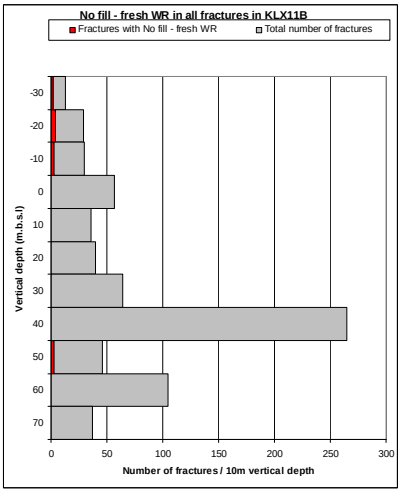
No fill - fresh WR in all fractures in KLX11B
Fractures with No fill - fresh WR
Total number of fractures
Vertical depth (m.b.s.l)
Number of fractures / 10m vertical depth

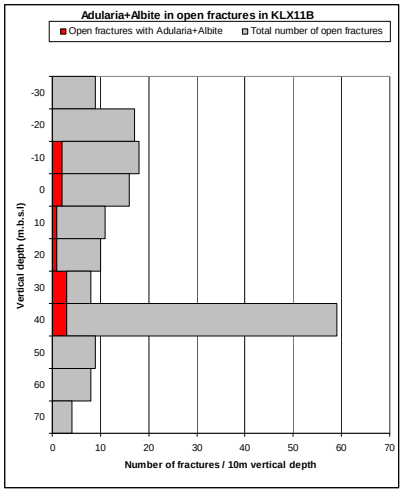
Adularia+Albite in open fractures in KLX11B
Open fractures with Adularia+Albite
Total number of open fractures
Vertical depth (m.b.s.l)
Number of fractures / 10m vertical depth

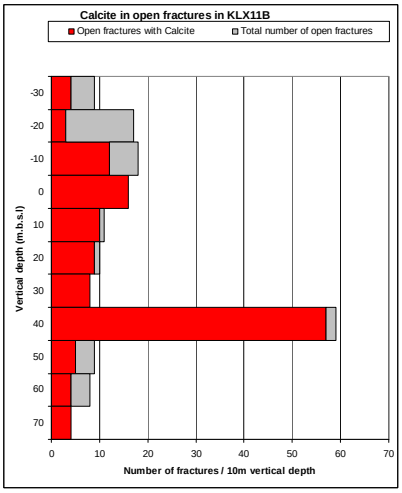
Calcite in open fractures in KLX11B
Open fractures with Calcite
Total number of open fractures
Vertical depth (m.b.s.l)
Number of fractures / 10m vertical depth

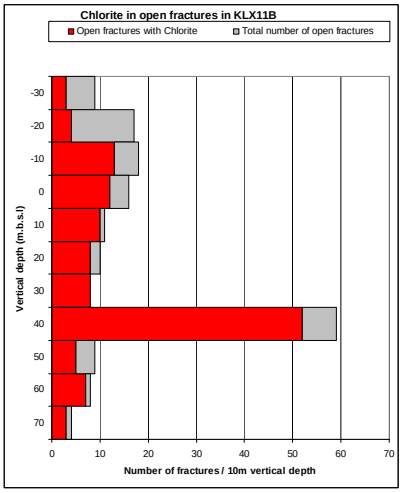
Chlorite in open fractures in KLX11B
Open fractures with Chlorite
Total number of open fractures
Vertical depth (m.b.s.l)
Number of fractures / 10m vertical depth

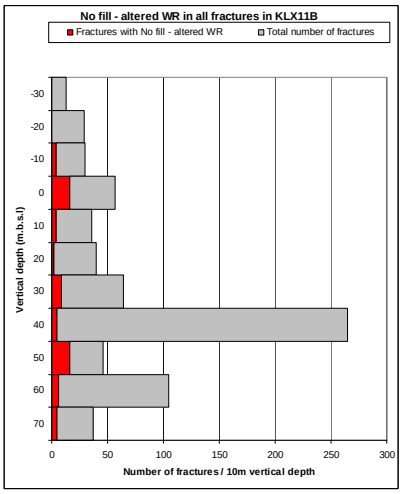
No fill - altered WR in all fractures in KLX11B
Fractures with No fill - altered WR
Total number of fractures
Vertical depth (m.b.s.l)
Number of fractures / 10m vertical depth

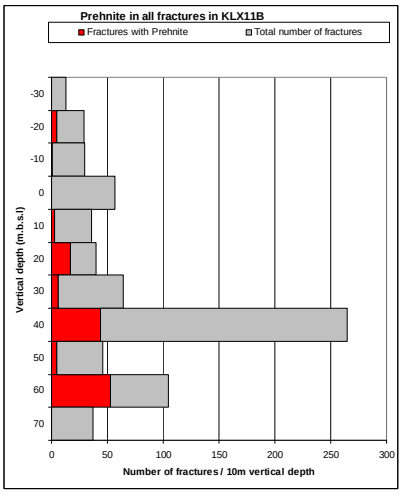
Prehnite in all fractures in KLX11B
Fractures with Prehnite
Total number of fractures
Vertical depth (m.b.s.l)
Number of fractures / 10m vertical depth

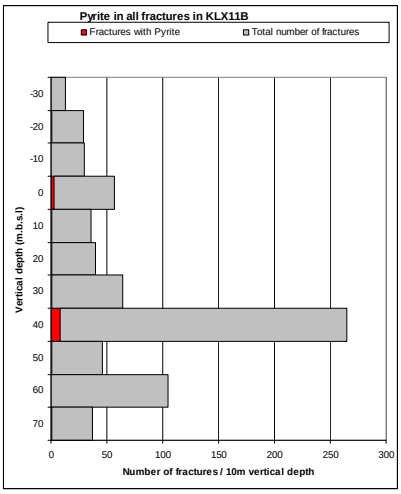
Pyrite in all fractures in KLX11B
Fractures with Pyrite
Total number of fractures
Vertical depth (m.b.s.l)
Number of fractures / 10m vertical depth

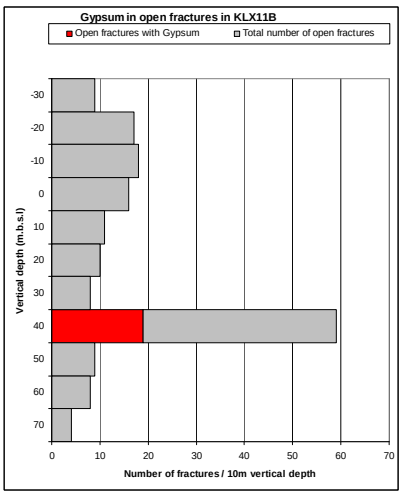
Gypsum in open fractures in KLX11B
Open fractures with Gypsum
Total number of open fractures
Vertical depth (m.b.s.l)
Number of fractures / 10m vertical depth

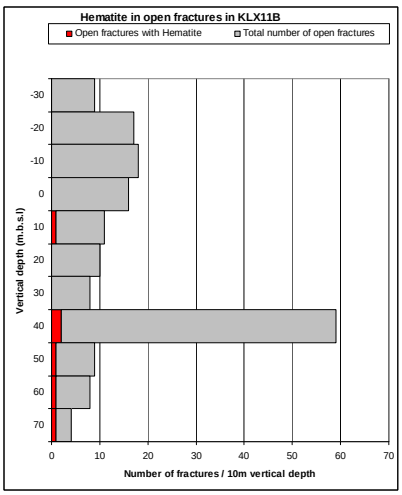
Hematite in open fractures in KLX11B
Open fractures with Hematite
Total number of open fractures
Vertical depth (m.b.s.l)
Number of fractures / 10m vertical depth

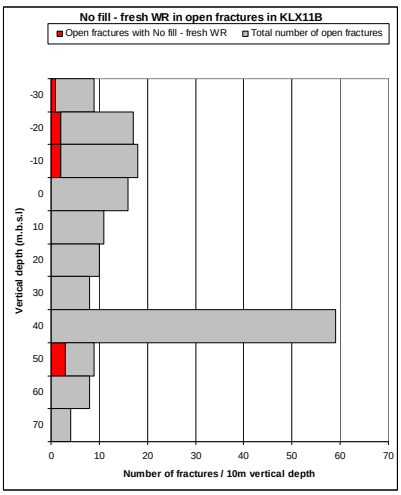
No fill - fresh WR in open fractures in KLX11B
Open fractures with No fill - fresh WR
Total number of open fractures
Vertical depth (m.b.s.l)
Number of fractures / 10m vertical depth

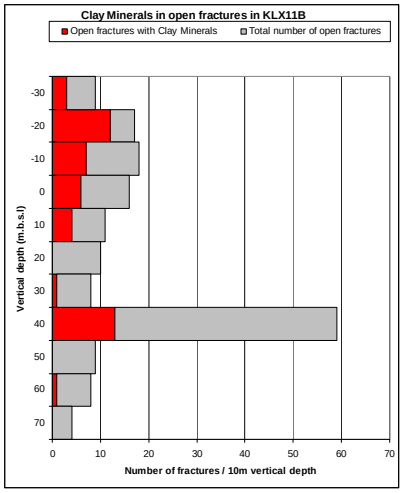
Clay Minerals in open fractures in KLX11B
Open fractures with Clay Minerals
Total number of open fractures
Vertical depth (m.b.s.l)
Number of fractures / 10m vertical depth

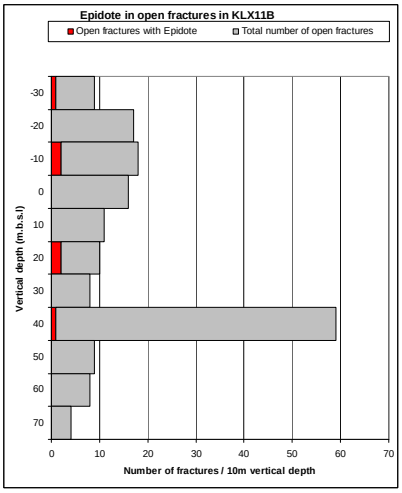
Epidote in open fractures in KLX11B
Open fractures with Epidote
Total number of open fractures
Vertical depth (m.b.s.l)
Number of fractures / 10m vertical depth

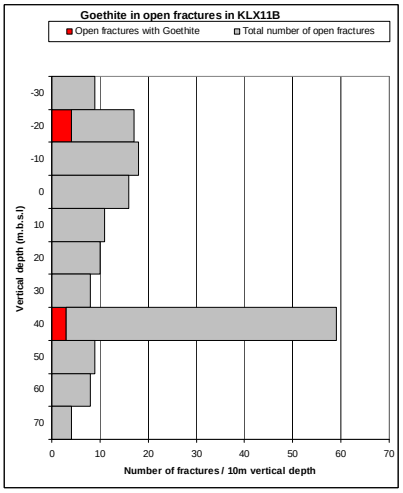
Goethite in open fractures in KLX11B
Open fractures with Goethite
Total number of open fractures
Vertical depth (m.b.s.l)
Number of fractures / 10m vertical depth

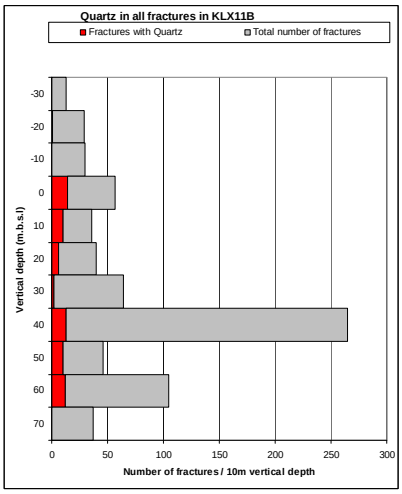
Quartz in all fractures in KLX11B
Fractures with Quartz
Total number of fractures
Vertical depth (m.b.s.l)
Number of fractures / 10m vertical depth

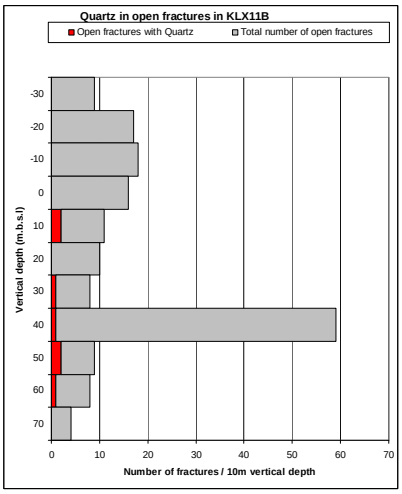
Quartz in open fractures in KLX11B
Open fractures with Quartz
Total number of open fractures
Vertical depth (m.b.s.l)
Number of fractures / 10m vertical depth

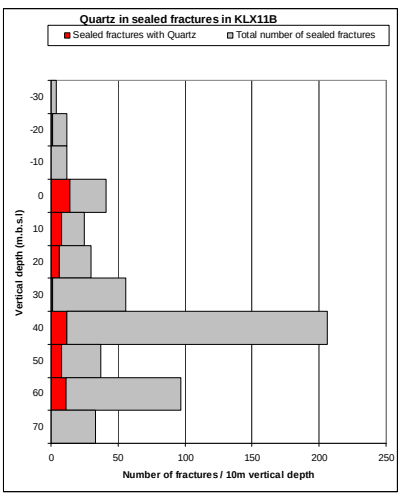
Quartz in sealed fractures in KLX11B
Sealed fractures with Quartz
Total number of sealed fractures
Vertical depth (m.b.s.l)
Number of fractures / 10m vertical depth

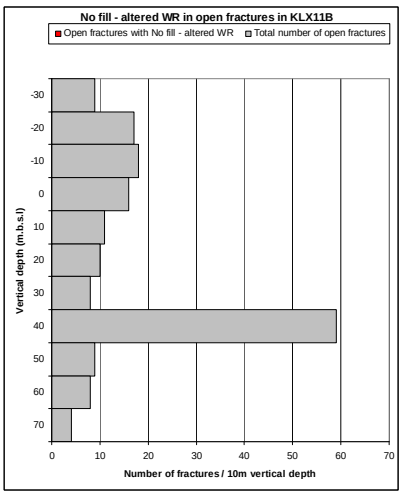
No fill - altered WR in open fractures in KLX11B
Open fractures with No fill - altered WR
Total number of open fractures
Vertical depth (m.b.s.l)
Number of fractures / 10m vertical depth

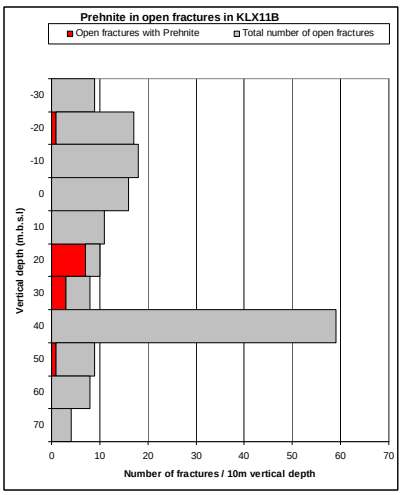
Prehnite in open fractures in KLX11B
Open fractures with Prehnite
Total number of open fractures
Vertical depth (m.b.s.l)
Number of fractures / 10m vertical depth

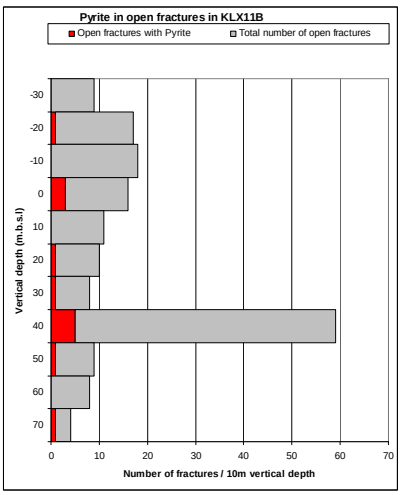
Pyrite in open fractures in KLX11B
Open fractures with Pyrite
Total number of open fractures
Vertical depth (m.b.s.l)
Number of fractures / 10m vertical depth

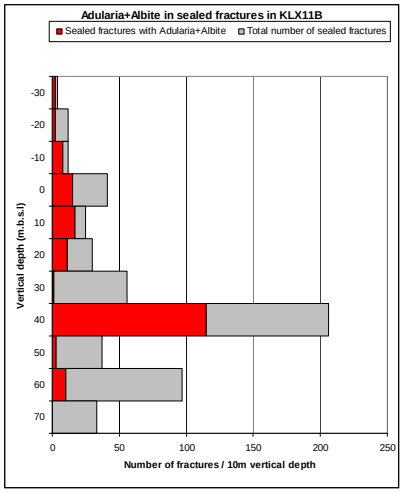
Adularia+Albite in sealed fractures in KLX11B
Sealed fractures with Adularia+Albite
Total number of sealed fractures
Vertical depth (m.b.s.l)
Number of fractures / 10m vertical depth

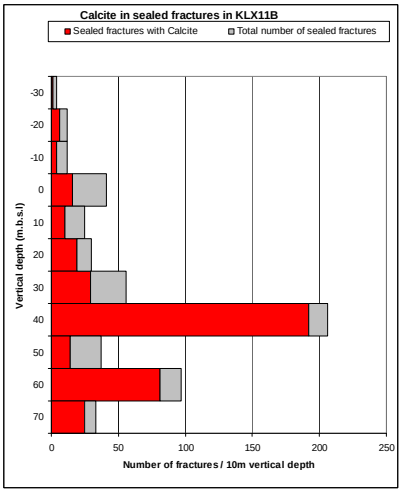
Calcite in sealed fractures in KLX11B
Sealed fractures with Calcite
Total number of sealed fractures
Vertical depth (m.b.s.l)
Number of fractures / 10m vertical depth

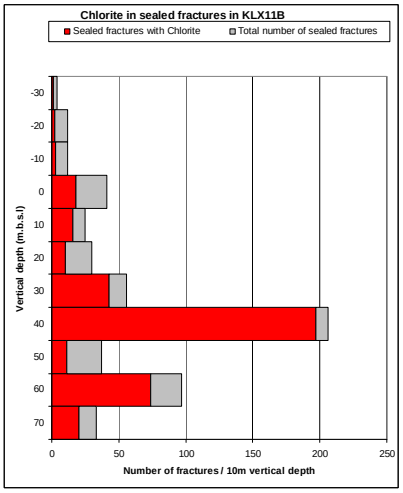
Chlorite in sealed fractures in KLX11B
Sealed fractures with Chlorite
Total number of sealed fractures
Vertical depth (m.b.s.l)
Number of fractures / 10m vertical depth

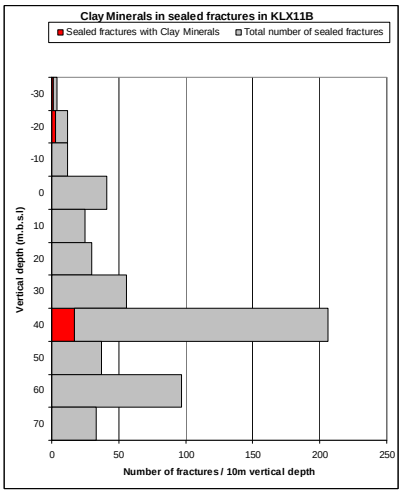
Clay Minerals in sealed fractures in KLX11B
Sealed fractures with Clay Minerals
Total number of sealed fractures
Vertical depth (m.b.s.l)
Number of fractures / 10m vertical depth

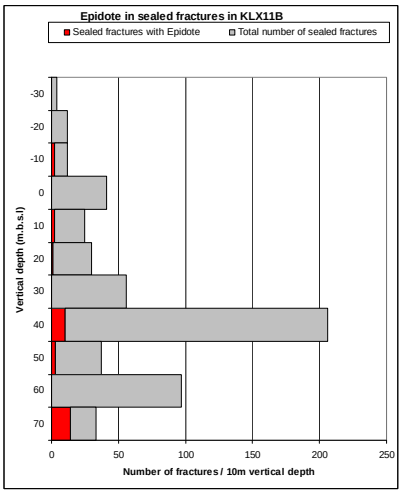
Epidote in sealed fractures in KLX11B
Sealed fractures with Epidote
Total number of sealed fractures
Vertical depth (m.b.s.l)
Number of fractures / 10m vertical depth

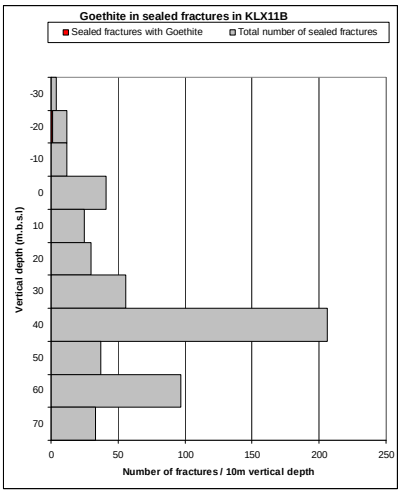
Goethite in sealed fractures in KLX11B
Sealed fractures with Goethite
Total number of sealed fractures
Vertical depth (m.b.s.l)
Number of fractures / 10m vertical depth

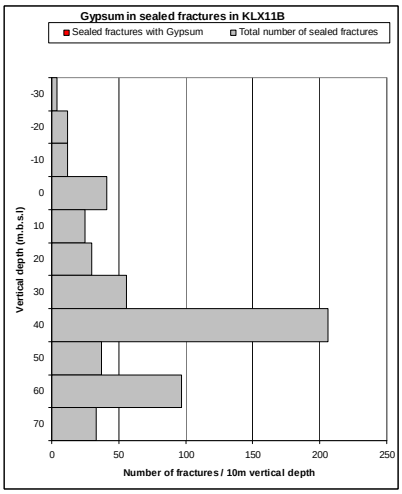
Gypsum in sealed fractures in KLX11B
Sealed fractures with Gypsum
Total number of sealed fractures
Vertical depth (m.b.s.l)
Number of fractures / 10m vertical depth

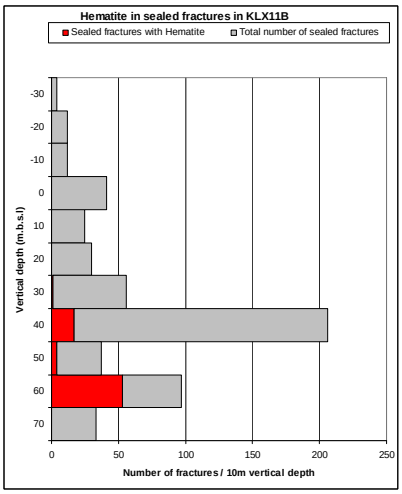
Hematite in sealed fractures in KLX11B
Sealed fractures with Hematite
Total number of sealed fractures
Vertical depth (m.b.s.l)
Number of fractures / 10m vertical depth

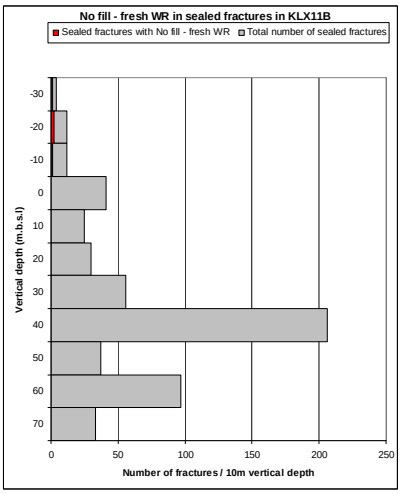
No fill - fresh WR in sealed fractures in KLX11B
Sealed fractures with No fill - fresh WR
Total number of sealed fractures
Vertical depth (m.b.s.l)
Number of fractures / 10m vertical depth

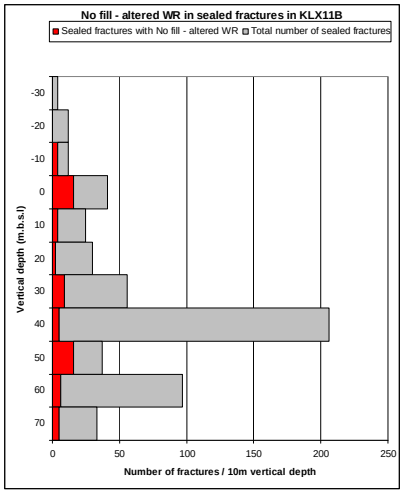
No fill - altered WR in sealed fractures in KLX11B
Sealed fractures with No fill - altered WR
Total number of sealed fractures
Vertical depth (m.b.s.l)
-30
-20
-10
0
10
20
30
40
50
60
70
0
50
100
150
200
250
Number of fractures / 10m vertical depth

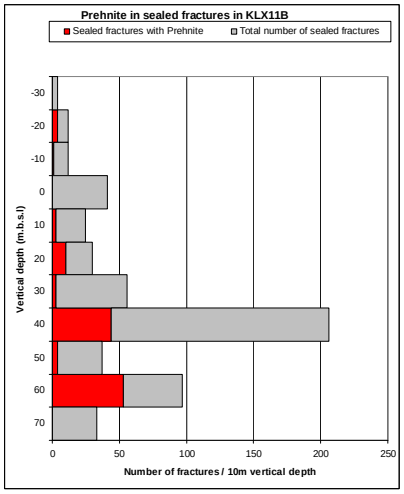
Prehnite in sealed fractures in KLX11B
Sealed fractures with Prehnite
Total number of sealed fractures
Vertical depth (m.b.s.l)
-30
-20
-10
0
10
20
30
40
50
60
70
0
50
100
150
200
250
Number of fractures / 10m vertical depth

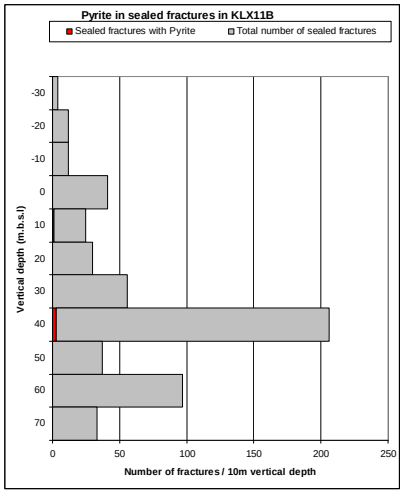
Pyrite in sealed fractures in KLX11B
Sealed fractures with Pyrite
Total number of sealed fractures
Vertical depth (m.b.s.l)
-30
-20
-10
0
10
20
30
40
50
60
70
0
50
100
150
200
250
Number of fractures / 10m vertical depth

KLX11C

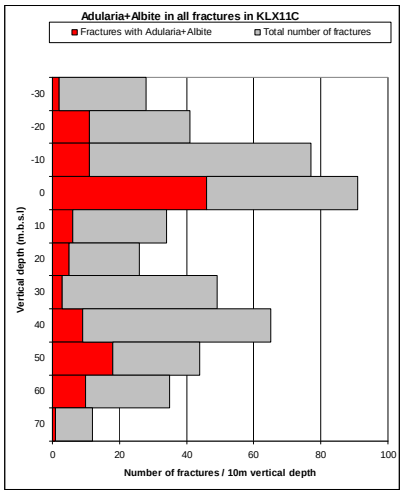
Adularia+Albite in all fractures in KLX11C
Fractures with Adularia+Albite
Total number of fractures
Vertical depth (m.b.s.l)
Number of fractures / 10m vertical depth

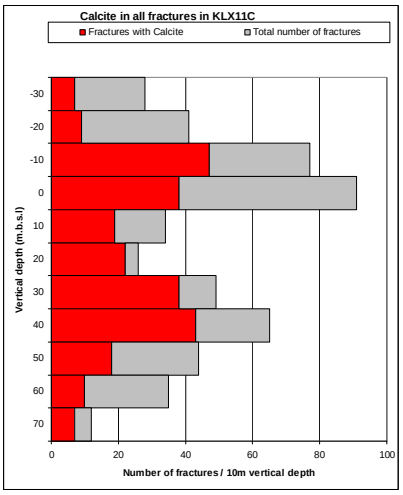
Calcite in all fractures in KLX11C
Fractures with Calcite
Total number of fractures
Vertical depth (m.b.s.l)
Number of fractures / 10m vertical depth

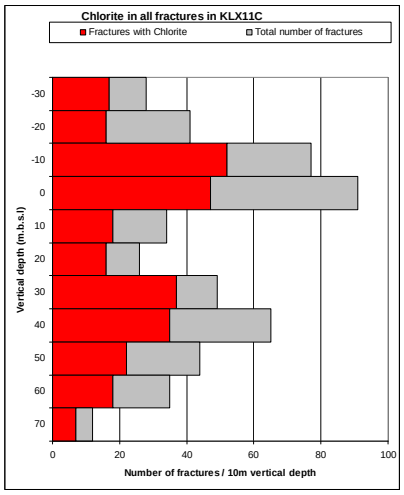
Chlorite in all fractures in KLX11C
Fractures with Chlorite
Total number of fractures
Vertical depth (m.b.s.l)
Number of fractures / 10m vertical depth

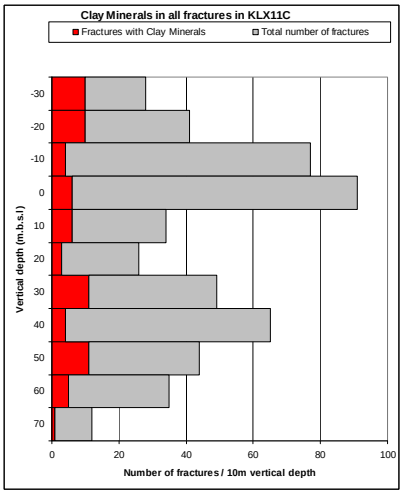
Clay Minerals in all fractures in KLX11C
Fractures with Clay Minerals
Total number of fractures
Vertical depth (m.b.s.l)
Number of fractures / 10m vertical depth

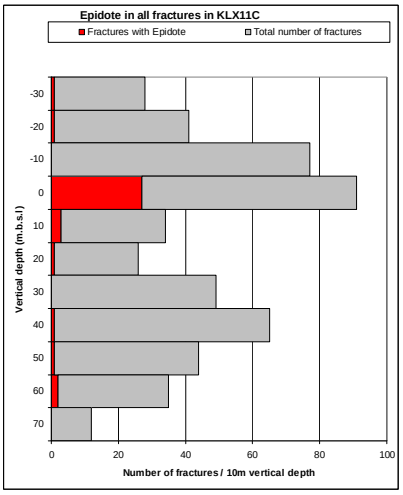
Epidote in all fractures in KLX11C
Fractures with Epidote
Total number of fractures
Vertical depth (m.b.s.l)
Number of fractures / 10m vertical depth

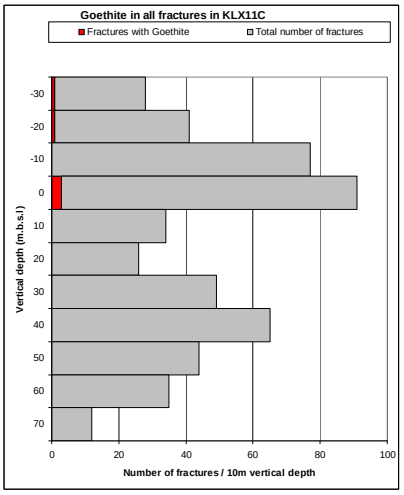
Goethite in all fractures in KLX11C
Fractures with Goethite
Total number of fractures
Vertical depth (m.b.s.l)
Number of fractures / 10m vertical depth

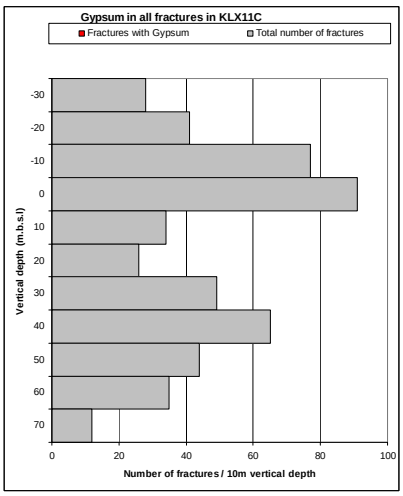
Gypsum in all fractures in KLX11C
Fractures with Gypsum
Total number of fractures
Vertical depth (m.b.s.l)
Number of fractures / 10m vertical depth

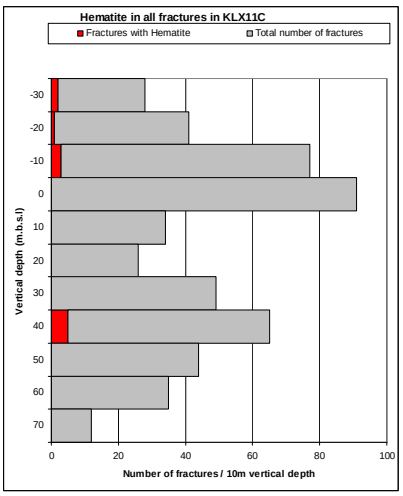
Hematite in all fractures in KLX11C
Fractures with Hematite
Total number of fractures
Vertical depth (m.b.s.l)
Number of fractures / 10m vertical depth

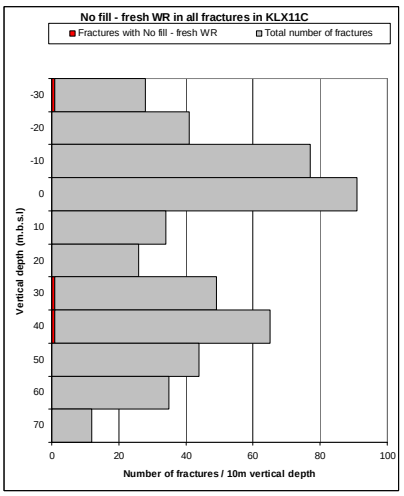
No fill - fresh WR in all fractures in KLX11C
Fractures with No fill - fresh WR
Total number of fractures
Vertical depth (m.b.s.l)
Number of fractures / 10m vertical depth

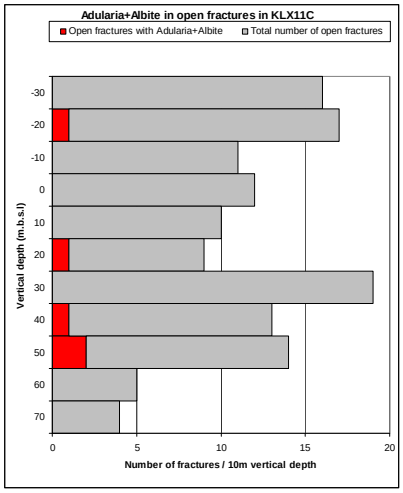
Adularia+Albite in open fractures in KLX11C
Open fractures with Adularia+Albite
Total number of open fractures
Vertical depth (m.b.s.l)
Number of fractures / 10m vertical depth

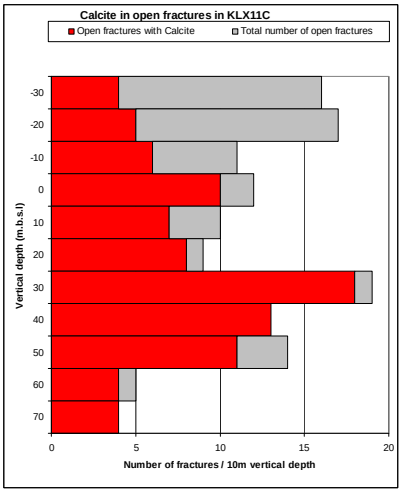
Calcite in open fractures in KLX11C
Open fractures with Calcite
Total number of open fractures
Vertical depth (m.b.s.l)
Number of fractures / 10m vertical depth

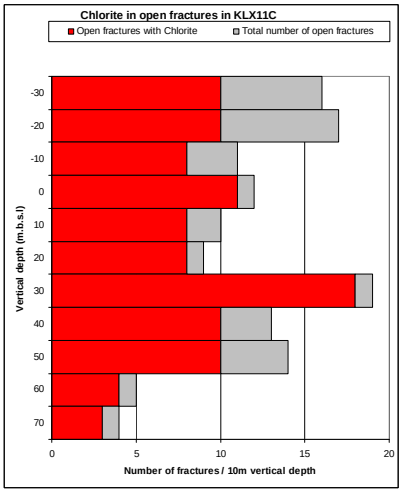
Chlorite in open fractures in KLX11C
Open fractures with Chlorite
Total number of open fractures
Vertical depth (m.b.s.l)
Number of fractures / 10m vertical depth

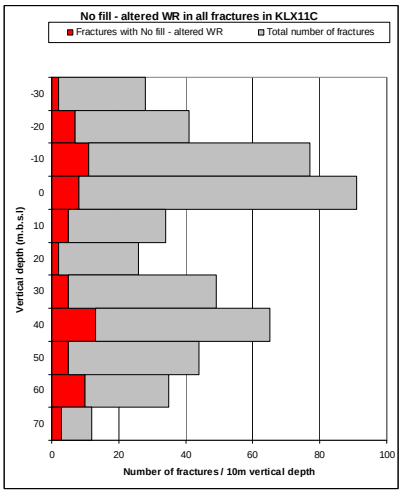
No fill - altered WR in all fractures in KLX11C
Fractures with No fill - altered WR
Total number of fractures
Vertical depth (m.b.s.l)
Number of fractures / 10m vertical depth

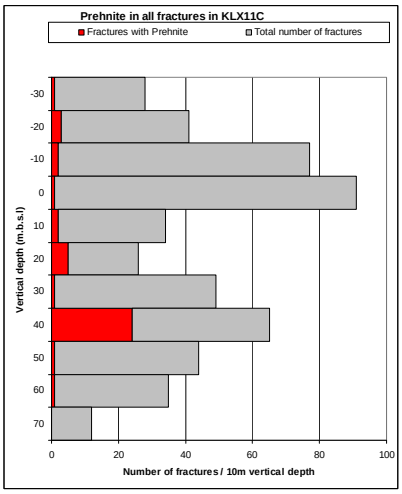
Prehnite in all fractures in KLX11C
Fractures with Prehnite
Total number of fractures
Vertical depth (m.b.s.l)
Number of fractures / 10m vertical depth

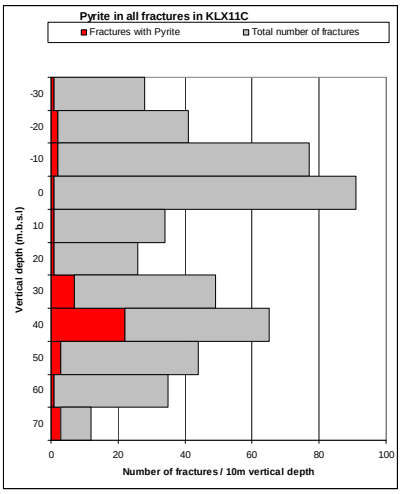
Pyrite in all fractures in KLX11C
Fractures with Pyrite
Total number of fractures
Vertical depth (m.b.s.l)
Number of fractures / 10m vertical depth

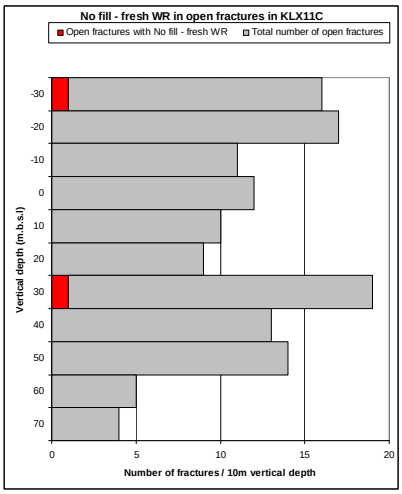
No fill - fresh WR in open fractures in KLX11C
Open fractures with No fill - fresh WR
Total number of open fractures
Vertical depth (m.b.s.l)
Number of fractures / 10m vertical depth

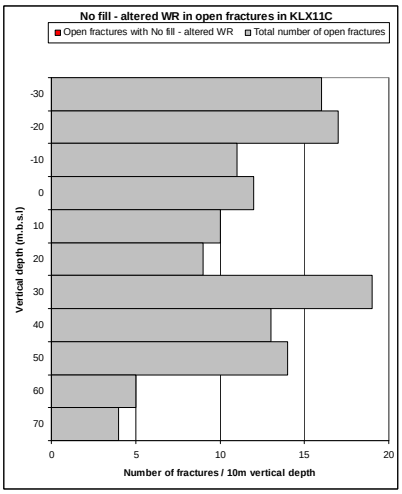
No fill - altered WR in open fractures in KLX11C
Open fractures with No fill - altered WR
Total number of open fractures
Vertical depth (m.b.s.l)
Number of fractures / 10m vertical depth

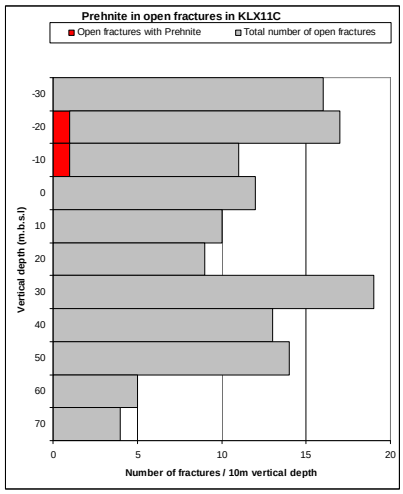
Prehnite in open fractures in KLX11C
Open fractures with Prehnite
Total number of open fractures
Vertical depth (m.b.s.l)
Number of fractures / 10m vertical depth

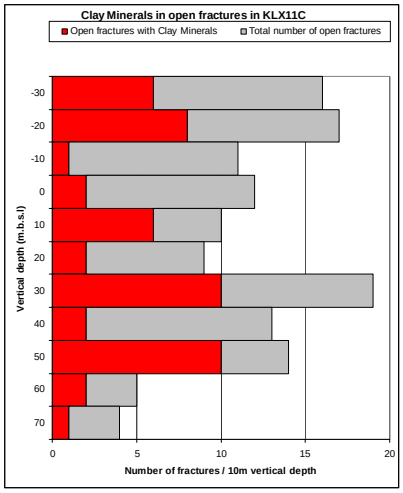
Clay Minerals in open fractures in KLX11C
Open fractures with Clay Minerals
Total number of open fractures
Vertical depth (m.b.s.l)
Number of fractures / 10m vertical depth

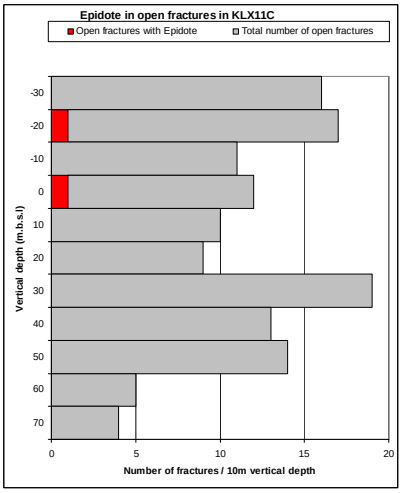
Epidote in open fractures in KLX11C
Open fractures with Epidote
Total number of open fractures
Vertical depth (m.b.s.l)
Number of fractures / 10m vertical depth

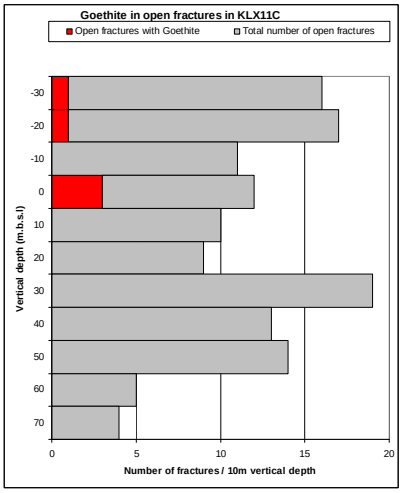
Goethite in open fractures in KLX11C
Open fractures with Goethite
Total number of open fractures
Vertical depth (m.b.s.l)
Number of fractures / 10m vertical depth

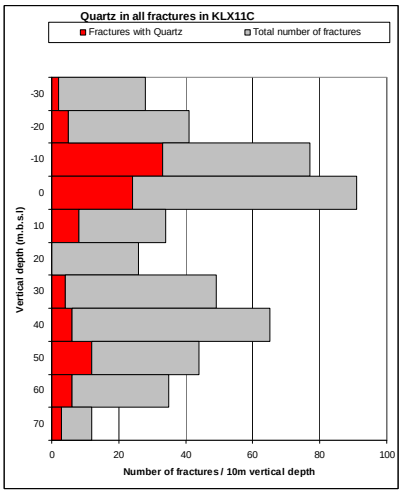
Quartz in all fractures in KLX11C
Fractures with Quartz
Total number of fractures
Vertical depth (m.b.s.l)
Number of fractures / 10m vertical depth

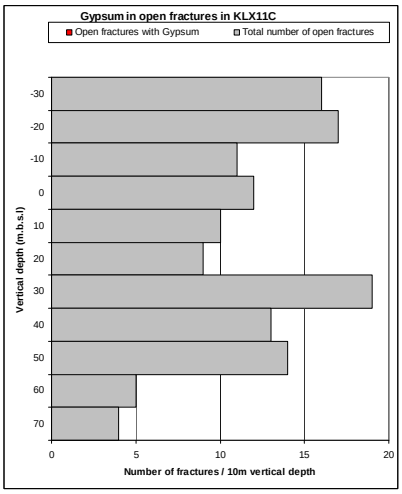
Gypsum in open fractures in KLX11C
Open fractures with Gypsum
Total number of open fractures
Vertical depth (m.b.s.l)
Number of fractures / 10m vertical depth

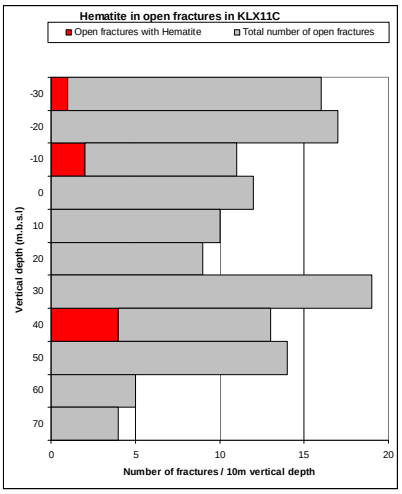
Hematite in open fractures in KLX11C
Open fractures with Hematite
Total number of open fractures
Vertical depth (m.b.s.l)
Number of fractures / 10m vertical depth

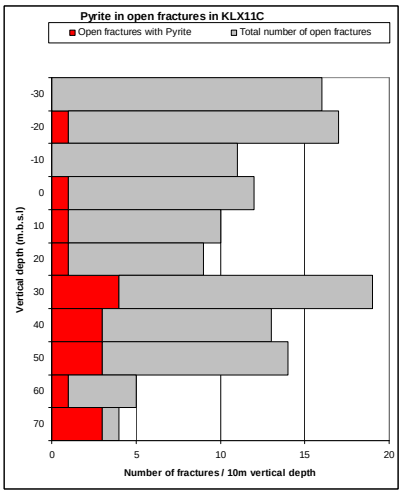
Pyrite in open fractures in KLX11C
Open fractures with Pyrite
Total number of open fractures
Vertical depth (m.b.s.l)
Number of fractures / 10m vertical depth

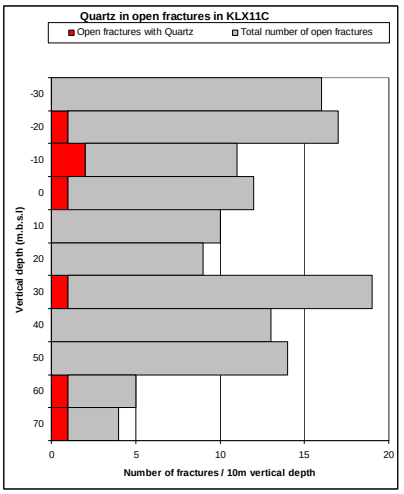
Quartz in open fractures in KLX11C
Open fractures with Quartz
Total number of open fractures
Vertical depth (m.b.s.l)
Number of fractures / 10m vertical depth

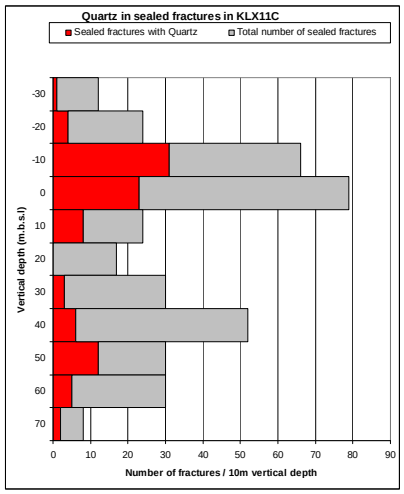
Quartz in sealed fractures in KLX11C
Sealed fractures with Quartz
Total number of sealed fractures
Vertical depth (m.b.s.l)
Number of fractures / 10m vertical depth

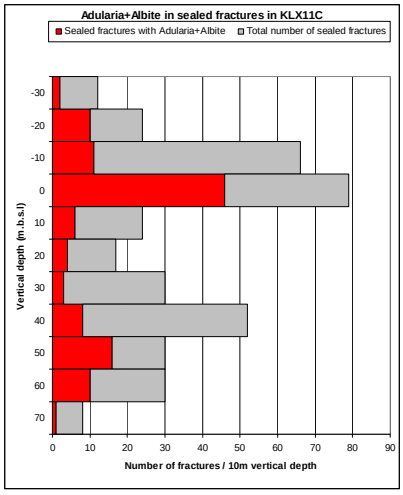
Adularia+Albite in sealed fractures in KLX11C
Sealed fractures with Adularia+Albite
Total number of sealed fractures
Vertical depth (m.b.s.l)
Number of fractures / 10m vertical depth

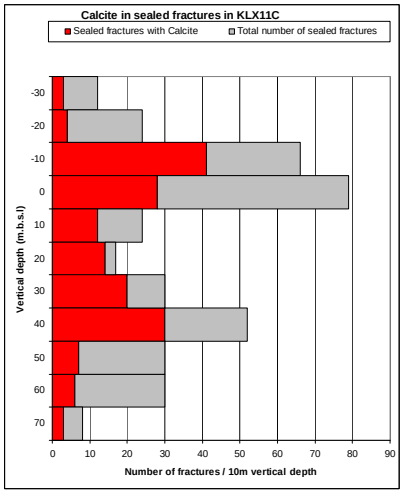
Calcite in sealed fractures in KLX11C
Sealed fractures with Calcite
Total number of sealed fractures
Vertical depth (m.b.s.l)
Number of fractures / 10m vertical depth

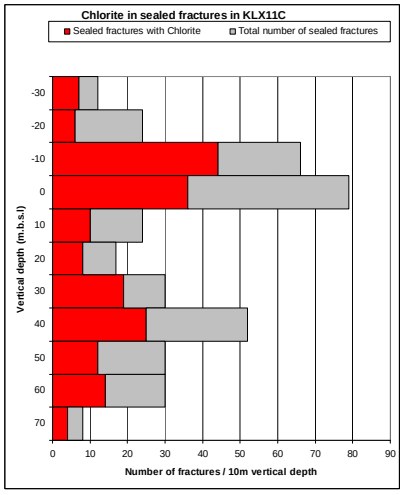
Chlorite in sealed fractures in KLX11C
Sealed fractures with Chlorite
Total number of sealed fractures
Vertical depth (m.b.s.l)
Number of fractures / 10m vertical depth

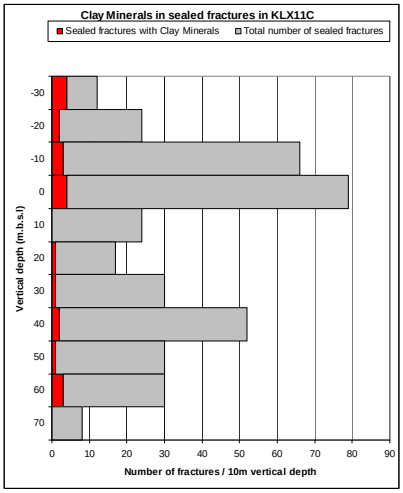
Clay Minerals in sealed fractures in KLX11C
Sealed fractures with Clay Minerals
Total number of sealed fractures
Vertical depth (m.b.s.l)
Number of fractures / 10m vertical depth

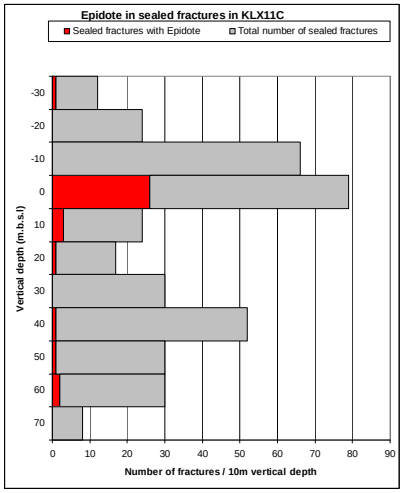
Epidote in sealed fractures in KLX11C
Sealed fractures with Epidote
Total number of sealed fractures
Vertical depth (m.b.s.l)
Number of fractures / 10m vertical depth

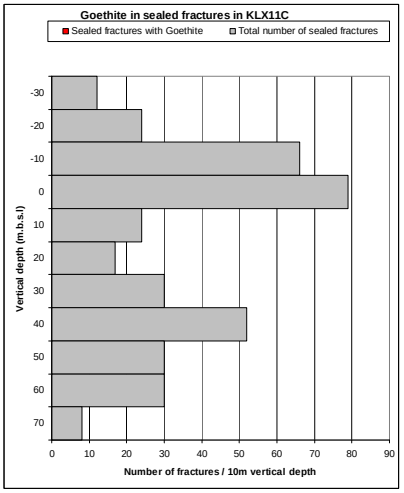
Goethite in sealed fractures in KLX11C
Sealed fractures with Goethite
Total number of sealed fractures
Vertical depth (m.b.s.l)
Number of fractures / 10m vertical depth

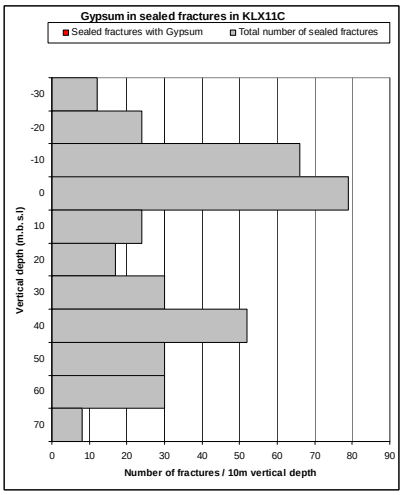
Gypsum in sealed fractures in KLX11C
Sealed fractures with Gypsum
Total number of sealed fractures
Vertical depth (m.b.s.l)
Number of fractures / 10m vertical depth

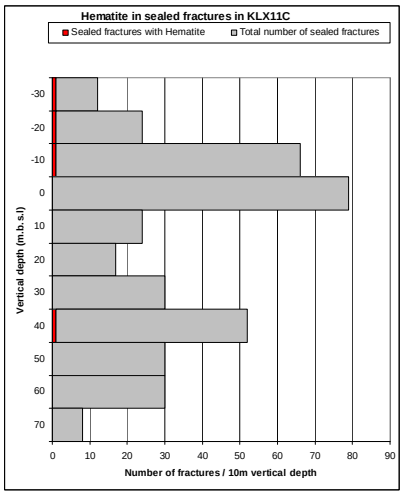
Hematite in sealed fractures in KLX11C
Sealed fractures with Hematite
Total number of sealed fractures
Vertical depth (m.b.s.l)
Number of fractures / 10m vertical depth

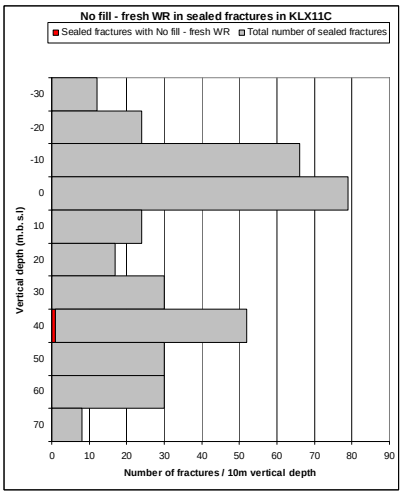
No fill - fresh WR in sealed fractures in KLX11C
Sealed fractures with No fill - fresh WR
Total number of sealed fractures
Vertical depth (m.b.s.l)
Number of fractures / 10m vertical depth

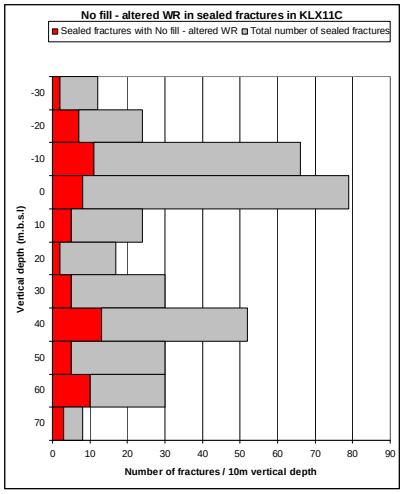
No fill - altered WR in sealed fractures in KLX11C
Sealed fractures with No fill - altered WR
Total number of sealed fractures
Vertical depth (m.b.s.l)
-30
-20
-10
0
10
20
30
40
50
60
70
0
10
20
30
40
50
60
70
80
90
Number of fractures / 10m vertical depth

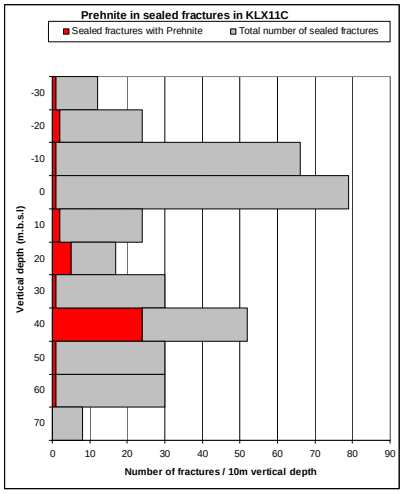
Prehnite in sealed fractures in KLX11C
Sealed fractures with Prehnite
Total number of sealed fractures
Vertical depth (m.b.s.l)
-30
-20
-10
0
10
20
30
40
50
60
70
0
10
20
30
40
50
60
70
80
90
Number of fractures / 10m vertical depth

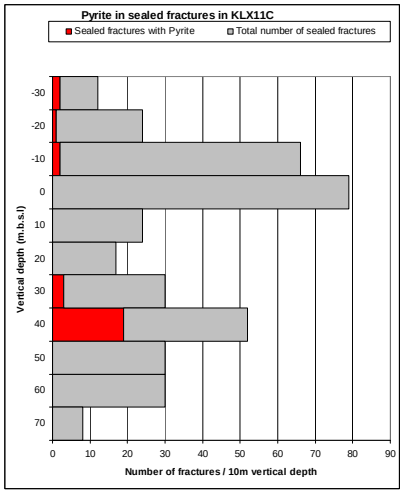
Pyrite in sealed fractures in KLX11C
Sealed fractures with Pyrite
Total number of sealed fractures
Vertical depth (m.b.s.l)
-30
-20
-10
0
10
20
30
40
50
60
70
0
10
20
30
40
50
60
70
80
90
Number of fractures / 10m vertical depth

KLX11D

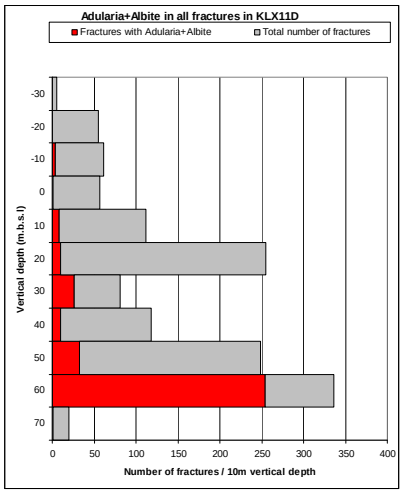
Adularia+Albite in all fractures in KLX11D
Fractures with Adularia+Albite
Total number of fractures
Vertical depth (m.b.s.l)
Number of fractures / 10m vertical depth

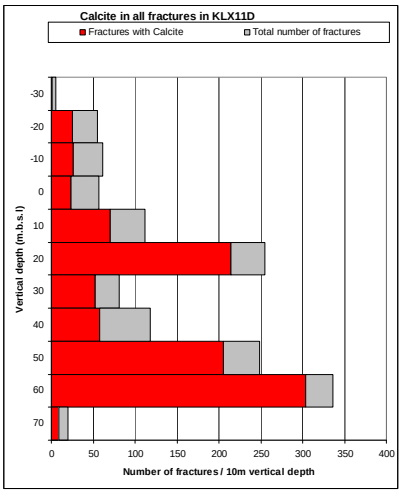
Calcite in all fractures in KLX11D
Fractures with Calcite
Total number of fractures
Vertical depth (m.b.s.l)
Number of fractures / 10m vertical depth

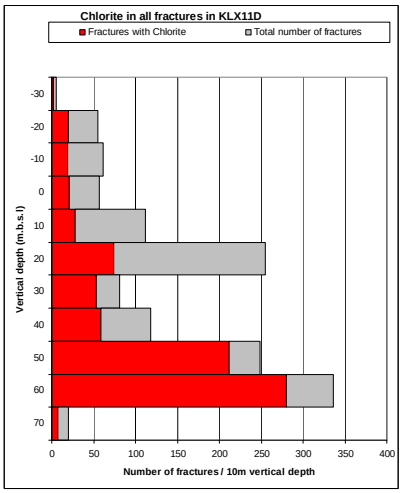
Chlorite in all fractures in KLX11D
Fractures with Chlorite
Total number of fractures
Vertical depth (m.b.s.l)
Number of fractures / 10m vertical depth

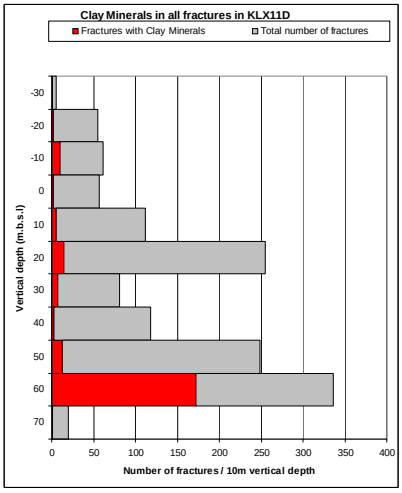
Clay Minerals in all fractures in KLX11D
Fractures with Clay Minerals
Total number of fractures
Vertical depth (m.b.s.l)
Number of fractures / 10m vertical depth

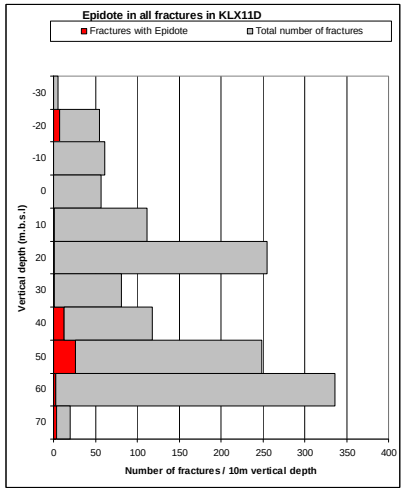
Epidote in all fractures in KLX11D
Fractures with Epidote
Total number of fractures
Vertical depth (m.b.s.l)
Number of fractures / 10m vertical depth

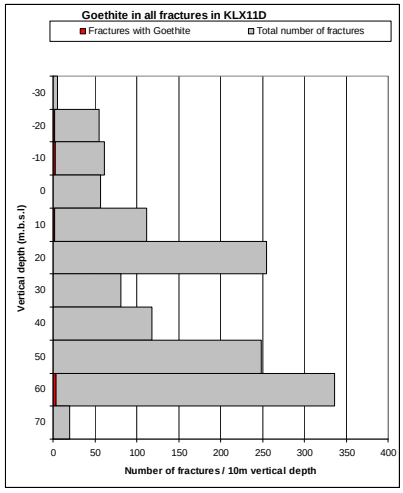
Goethite in all fractures in KLX11D
Fractures with Goethite
Total number of fractures
Vertical depth (m.b.s.l)
Number of fractures / 10m vertical depth

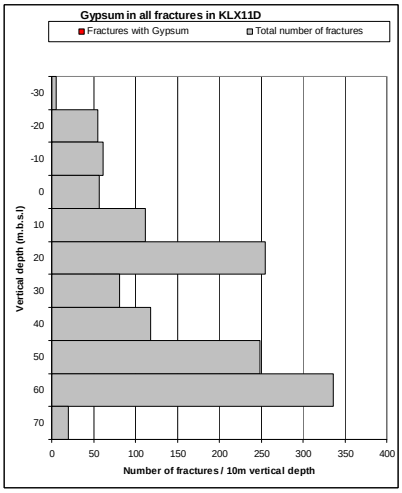
Gypsum in all fractures in KLX11D
Fractures with Gypsum
Total number of fractures
Vertical depth (m.b.s.l)
Number of fractures / 10m vertical depth

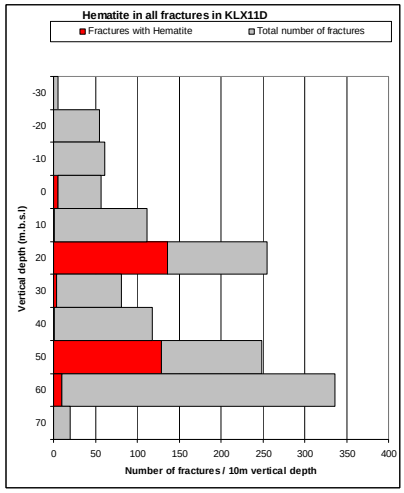
Hematite in all fractures in KLX11D
Fractures with Hematite
Total number of fractures
Vertical depth (m.b.s.l)
Number of fractures / 10m vertical depth

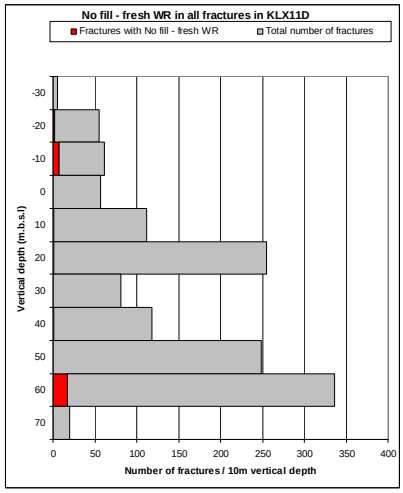
No fill - fresh WR in all fractures in KLX11D
Fractures with No fill - fresh WR
Total number of fractures
Vertical depth (m.b.s.l)
Number of fractures / 10m vertical depth

i

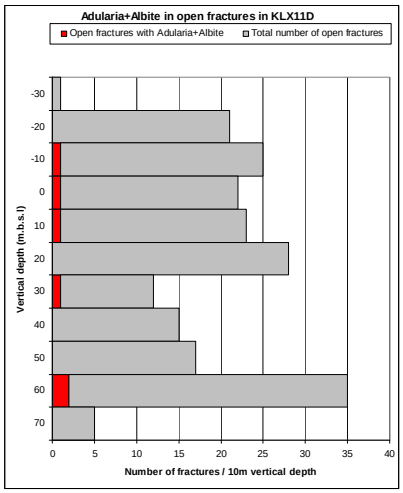
Adularia+Albite in open fractures in KLX11D
Open fractures with Adularia+Albite
Total number of open fractures
Vertical depth (m.b.s.l)
Number of fractures / 10m vertical depth

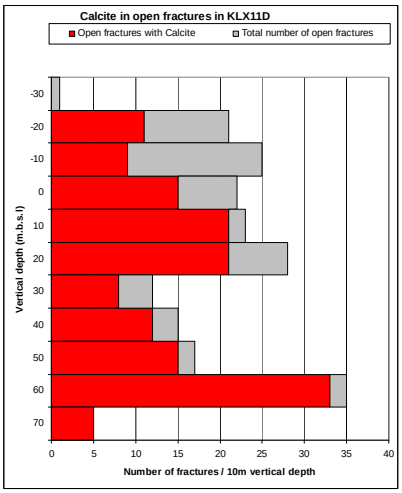
Calcite in open fractures in KLX11D
Open fractures with Calcite
Total number of open fractures
Vertical depth (m.b.s.l)
Number of fractures / 10m vertical depth

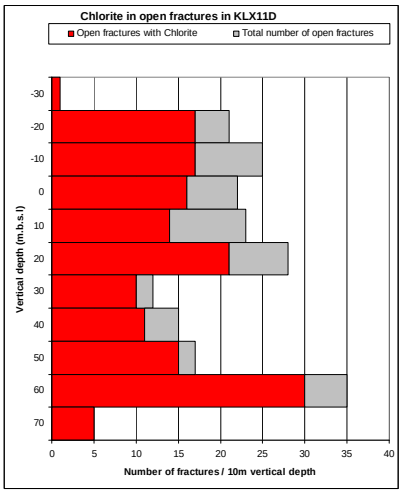
Chlorite in open fractures in KLX11D
Open fractures with Chlorite
Total number of open fractures
Vertical depth (m.b.s.l)
Number of fractures / 10m vertical depth

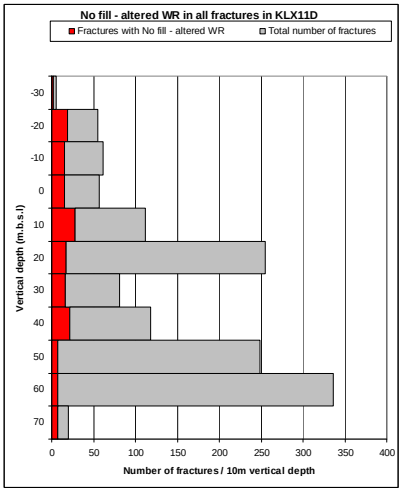
No fill - altered WR in all fractures in KLX11D
Fractures with No fill - altered WR
Total number of fractures
Vertical depth (m.b.s.l)
Number of fractures / 10m vertical depth

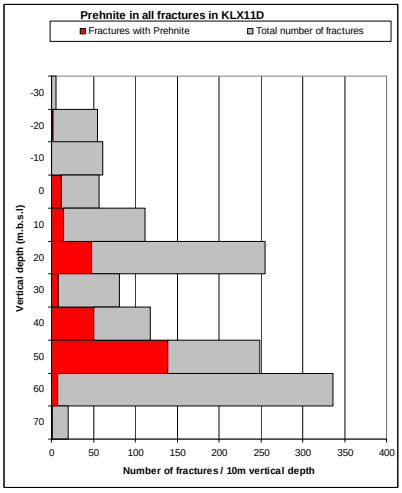
Prehnite in all fractures in KLX11D
Fractures with Prehnite
Total number of fractures
Vertical depth (m.b.s.l)
Number of fractures / 10m vertical depth

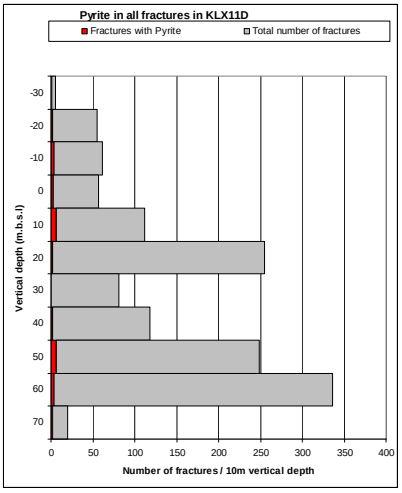
Pyrite in all fractures in KLX11D
Fractures with Pyrite
Total number of fractures
Vertical depth (m.b.s.l)
Number of fractures / 10m vertical depth

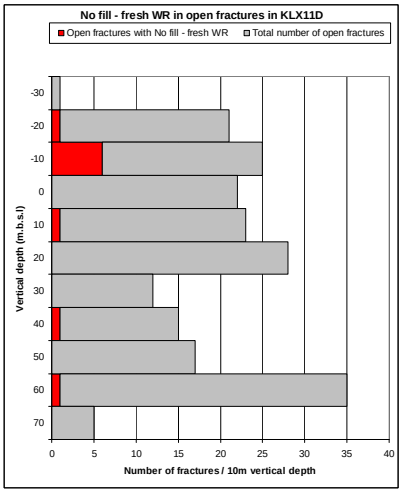
No fill - fresh WR in open fractures in KLX11D
Open fractures with No fill - fresh WR
Total number of open fractures
Vertical depth (m.b.s.l)
Number of fractures / 10m vertical depth

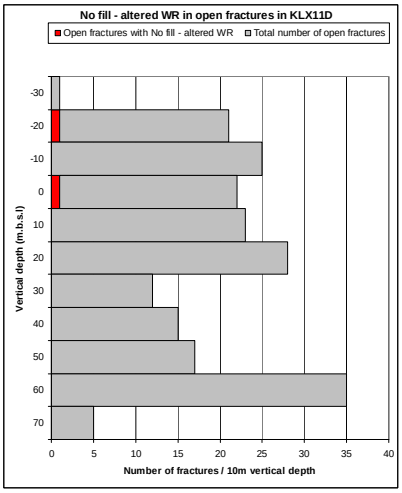
No fill - altered WR in open fractures in KLX11D
Open fractures with No fill - altered WR
Total number of open fractures
Vertical depth (m.b.s.l)
Number of fractures / 10m vertical depth

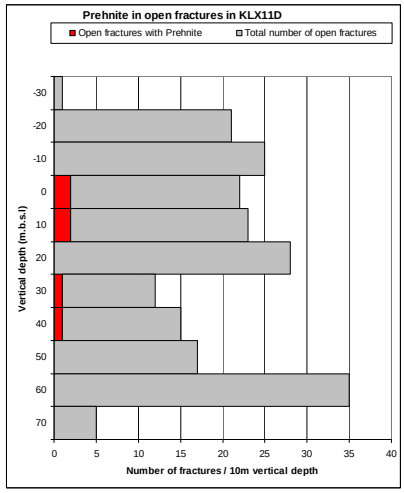
Prehnite in open fractures in KLX11D
Open fractures with Prehnite
Total number of open fractures
Vertical depth (m.b.s.l)
Number of fractures / 10m vertical depth

i

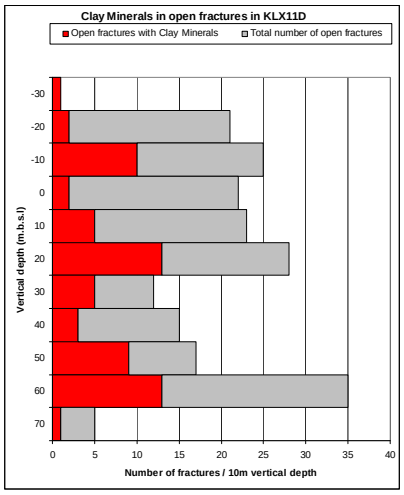
Clay Minerals in open fractures in KLX11D
Open fractures with Clay Minerals
Total number of open fractures
Vertical depth (m.b.s.l)
Number of fractures / 10m vertical depth

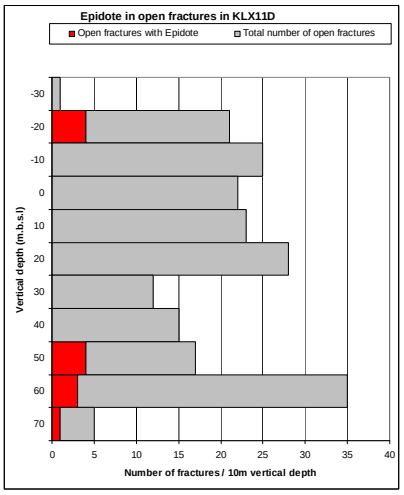
Epidote in open fractures in KLX11D
Open fractures with Epidote
Total number of open fractures
Vertical depth (m.b.s.l)
Number of fractures / 10m vertical depth

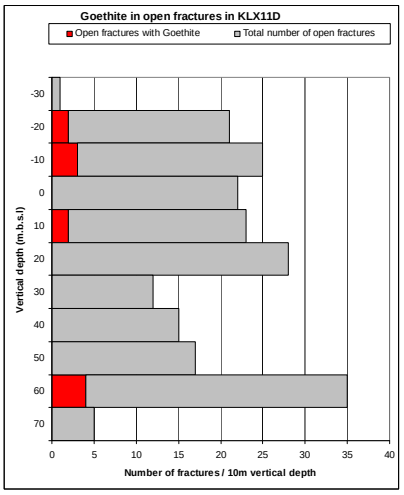
Goethite in open fractures in KLX11D
Open fractures with Goethite
Total number of open fractures
Vertical depth (m.b.s.l)
Number of fractures / 10m vertical depth

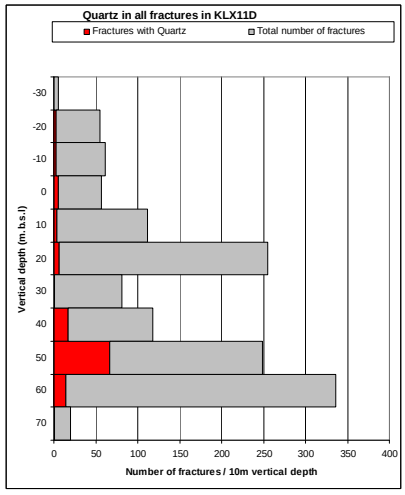
Quartz in all fractures in KLX11D
Fractures with Quartz
Total number of fractures
Vertical depth (m.b.s.l)
Number of fractures / 10m vertical depth

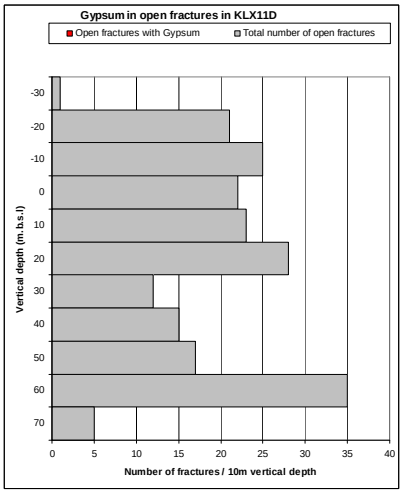
Gypsum in open fractures in KLX11D
Open fractures with Gypsum
Total number of open fractures
Vertical depth (m.b.s.l)
Number of fractures / 10m vertical depth

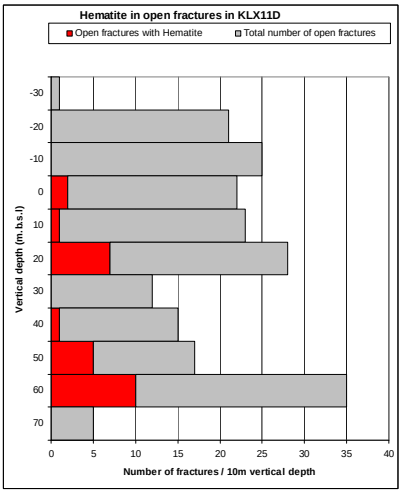
Hematite in open fractures in KLX11D
Open fractures with Hematite
Total number of open fractures
Vertical depth (m.b.s.l)
Number of fractures / 10m vertical depth

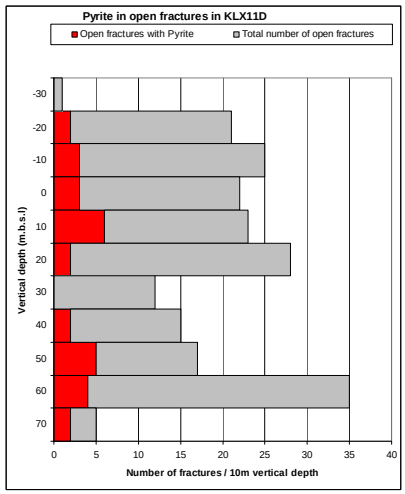
Pyrite in open fractures in KLX11D
Open fractures with Pyrite
Total number of open fractures
Vertical depth (m.b.s.l)
Number of fractures / 10m vertical depth

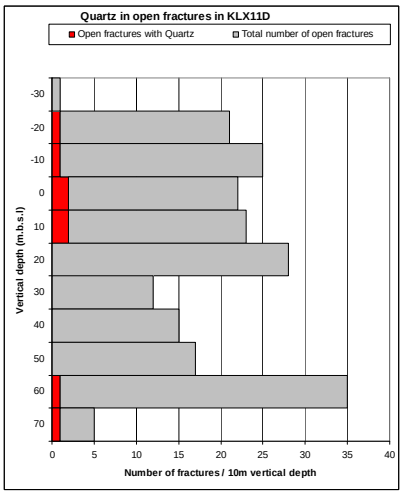
Quartz in open fractures in KLX11D
Open fractures with Quartz
Total number of open fractures
Vertical depth (m.b.s.l)
Number of fractures / 10m vertical depth

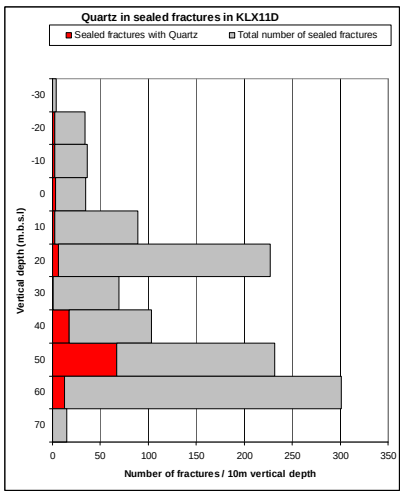
Quartz in sealed fractures in KLX11D
Sealed fractures with Quartz
Total number of sealed fractures
Vertical depth (m.b.s.l)
Number of fractures / 10m vertical depth

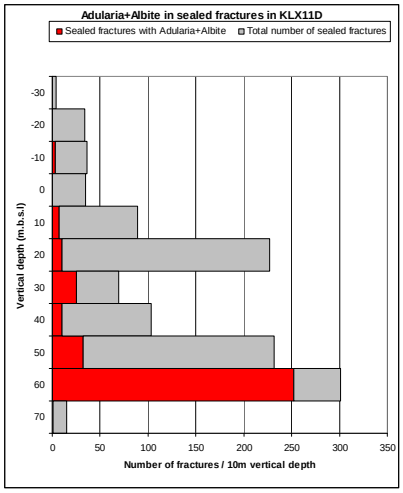
Adularia+Albite in sealed fractures in KLX11D
Sealed fractures with Adularia+Albite
Total number of sealed fractures
Vertical depth (m.b.s.l)
Number of fractures / 10m vertical depth

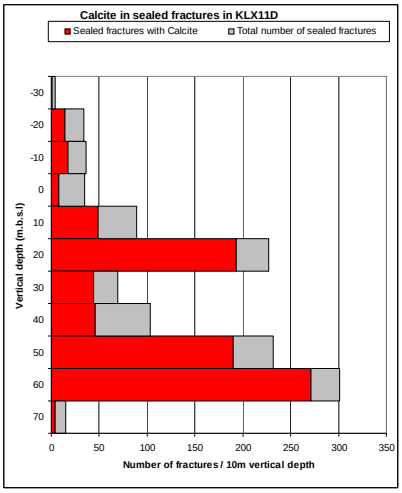
Calcite in sealed fractures in KLX11D
Sealed fractures with Calcite
Total number of sealed fractures
Vertical depth (m.b.s.l)
Number of fractures / 10m vertical depth

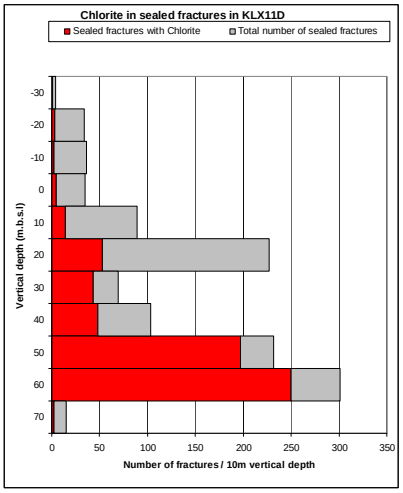
Chlorite in sealed fractures in KLX11D
Sealed fractures with Chlorite
Total number of sealed fractures
Vertical depth (m.b.s.l)
Number of fractures / 10m vertical depth

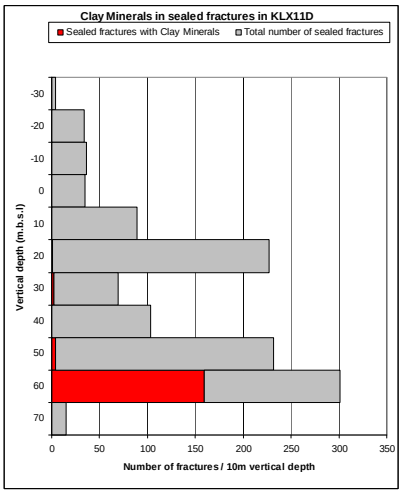
Clay Minerals in sealed fractures in KLX11D
Sealed fractures with Clay Minerals
Total number of sealed fractures
Vertical depth (m.b.s.l)
Number of fractures / 10m vertical depth

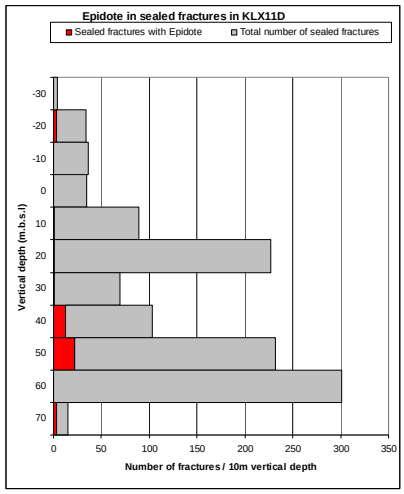
Epidote in sealed fractures in KLX11D
Sealed fractures with Epidote
Total number of sealed fractures
Vertical depth (m.b.s.l)
Number of fractures / 10m vertical depth

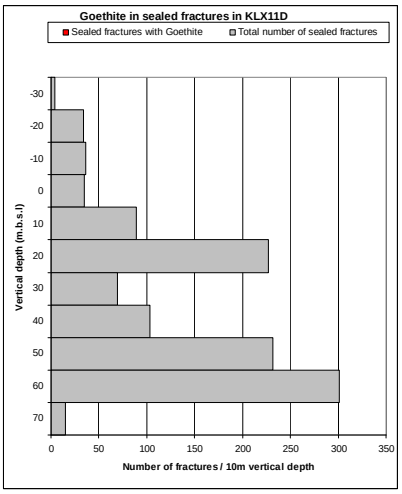
Goethite in sealed fractures in KLX11D
Sealed fractures with Goethite
Total number of sealed fractures
Vertical depth (m.b.s.l)
Number of fractures / 10m vertical depth

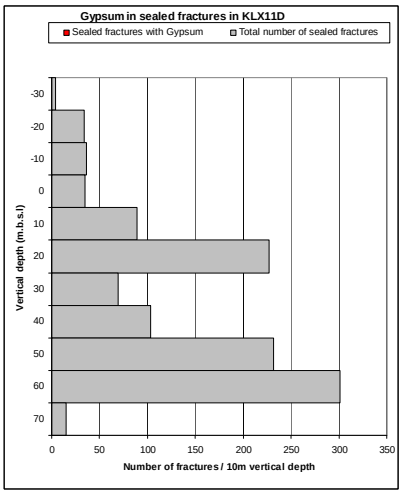
Gypsum in sealed fractures in KLX11D
Sealed fractures with Gypsum
Total number of sealed fractures
Vertical depth (m.b.s.l)
Number of fractures / 10m vertical depth

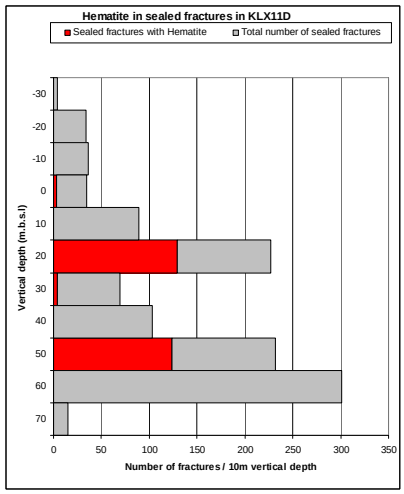
Hematite in sealed fractures in KLX11D
Sealed fractures with Hematite
Total number of sealed fractures
Vertical depth (m.b.s.l)
Number of fractures / 10m vertical depth

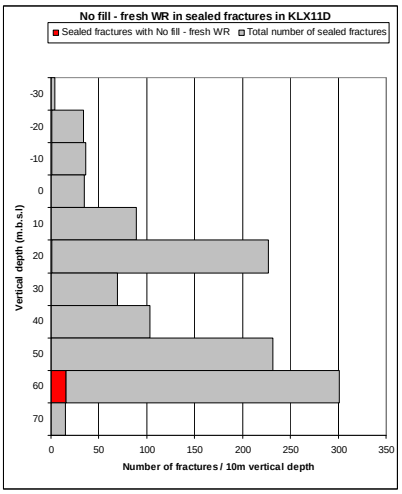
No fill - fresh WR in sealed fractures in KLX11D
Sealed fractures with No fill - fresh WR
Total number of sealed fractures
Vertical depth (m.b.s.l)
Number of fractures / 10m vertical depth

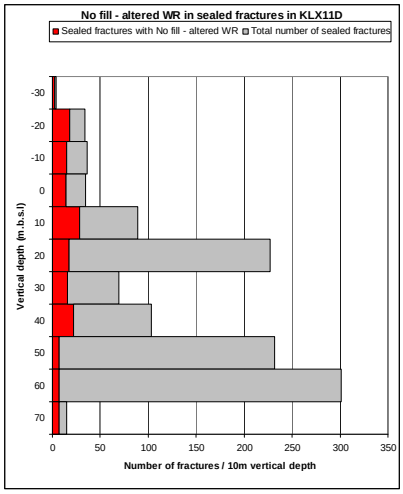
No fill - altered WR in sealed fractures in KLX11D
Sealed fractures with No fill - altered WR
Total number of sealed fractures
Vertical depth (m.b.s.l)
-30
-20
-10
0
10
20
30
40
50
60
70
0
50
100
150
200
250
300
350
Number of fractures / 10m vertical depth

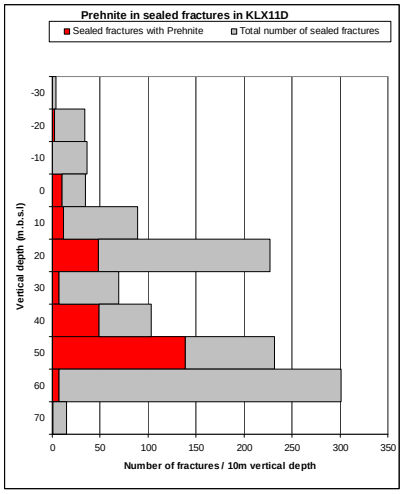
Prehnite in sealed fractures in KLX11D
Sealed fractures with Prehnite
Total number of sealed fractures
Vertical depth (m.b.s.l)
-30
-20
-10
0
10
20
30
40
50
60
70
0
50
100
150
200
250
300
350
Number of fractures / 10m vertical depth

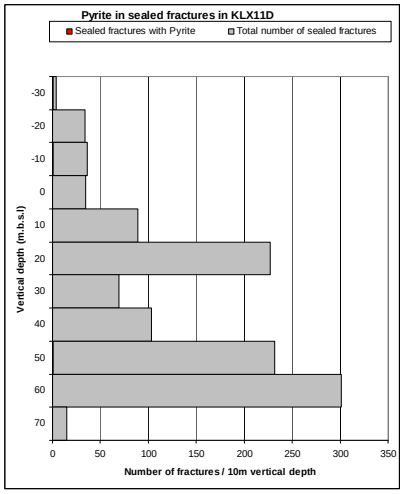
Pyrite in sealed fractures in KLX11D
Sealed fractures with Pyrite
Total number of sealed fractures
Vertical depth (m.b.s.l)
-30
-20
-10
0
10
20
30
40
50
60
70
0
50
100
150
200
250
300
350
Number of fractures / 10m vertical depth

KLX11E

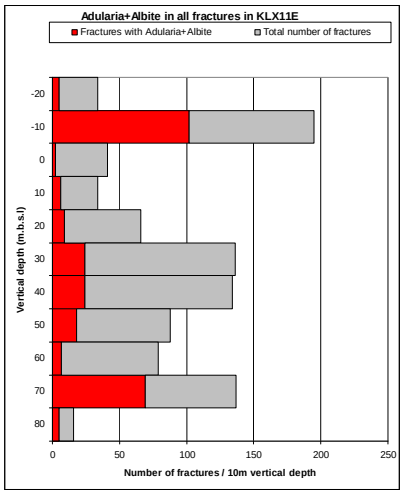
Adularia+Albite in all fractures in KLX11E
Fractures with Adularia+Albite
Total number of fractures
Vertical depth (m.b.s.l)
Number of fractures / 10m vertical depth

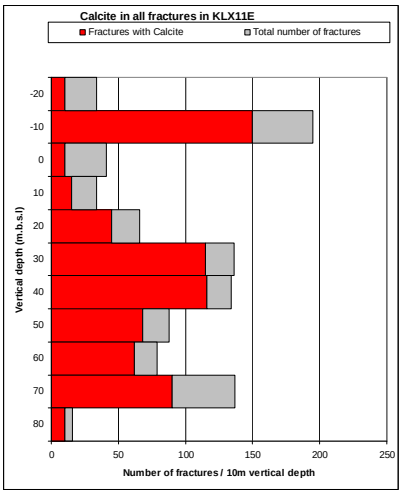
Calcite in all fractures in KLX11E
Fractures with Calcite
Total number of fractures
Vertical depth (m.b.s.l)
Number of fractures / 10m vertical depth

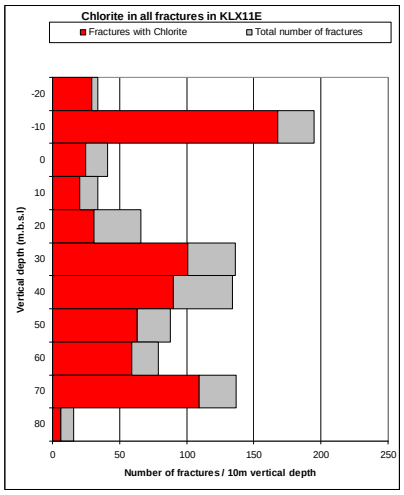
Chlorite in all fractures in KLX11E
Fractures with Chlorite
Total number of fractures
Vertical depth (m.b.s.l)
Number of fractures / 10m vertical depth

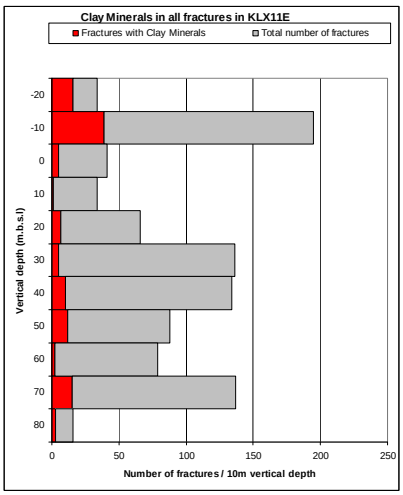
Clay Minerals in all fractures in KLX11E
Fractures with Clay Minerals
Total number of fractures
Vertical depth (m.b.s.l)
Number of fractures / 10m vertical depth

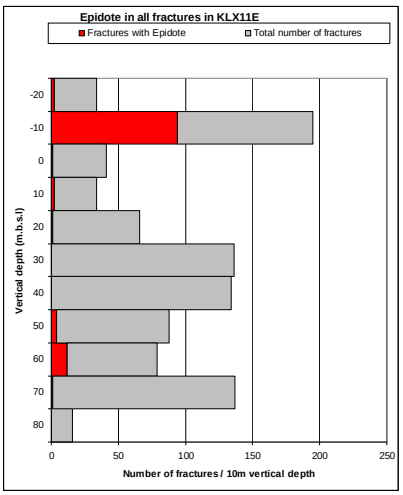
Epidote in all fractures in KLX11E
Fractures with Epidote
Total number of fractures
Vertical depth (m.b.s.l)
Number of fractures / 10m vertical depth

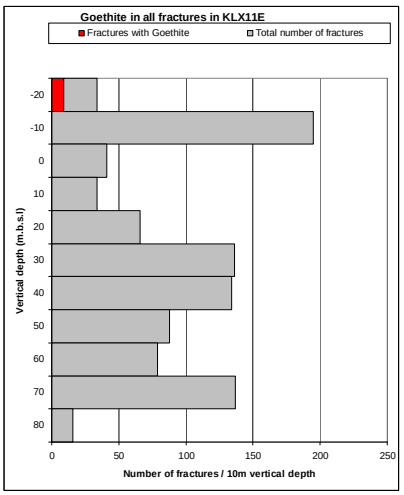
Goethite in all fractures in KLX11E
Fractures with Goethite
Total number of fractures
Vertical depth (m.b.s.l)
Number of fractures / 10m vertical depth

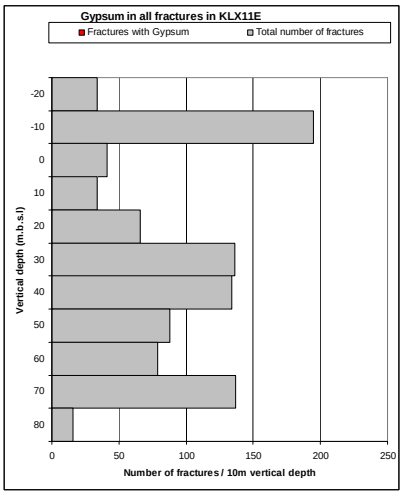
Gypsum in all fractures in KLX11E
Fractures with Gypsum
Total number of fractures
Vertical depth (m.b.s.l)
Number of fractures / 10m vertical depth

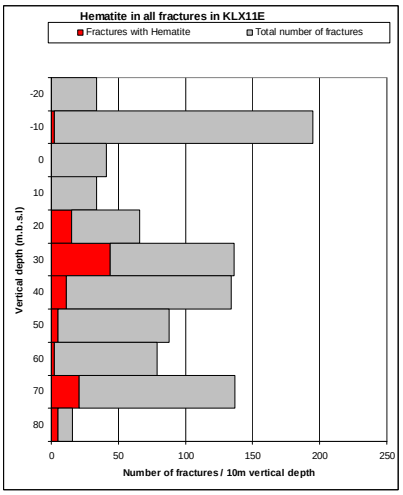
Hematite in all fractures in KLX11E
Fractures with Hematite
Total number of fractures
Vertical depth (m.b.s.l)
Number of fractures / 10m vertical depth

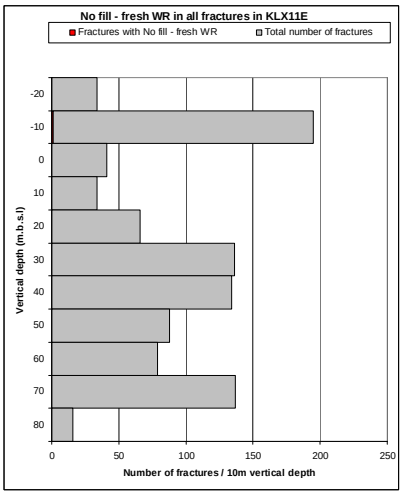
No fill - fresh WR in all fractures in KLX11E
Fractures with No fill - fresh WR
Total number of fractures
Vertical depth (m.b.s.l)
Number of fractures / 10m vertical depth

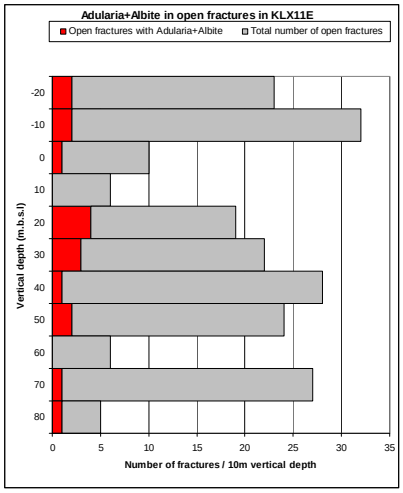
Adularia+Albite in open fractures in KLX11E
Open fractures with Adularia+Albite
Total number of open fractures
Vertical depth (m.b.s.l)
Number of fractures / 10m vertical depth

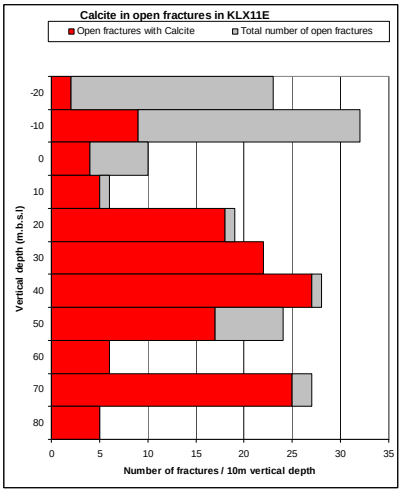
Calcite in open fractures in KLX11E
Open fractures with Calcite
Total number of open fractures
Vertical depth (m.b.s.l)
Number of fractures / 10m vertical depth

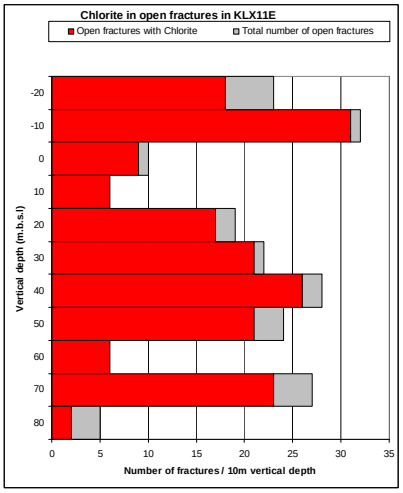
Chlorite in open fractures in KLX11E
Open fractures with Chlorite
Total number of open fractures
Vertical depth (m.b.s.l)
Number of fractures / 10m vertical depth

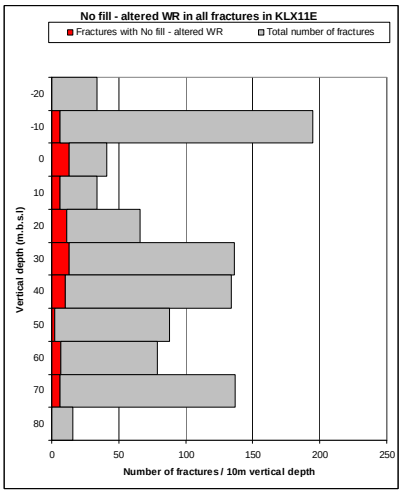
No fill - altered WR in all fractures in KLX11E
Fractures with No fill - altered WR
Total number of fractures
Vertical depth (m.b.s.l)
Number of fractures / 10m vertical depth

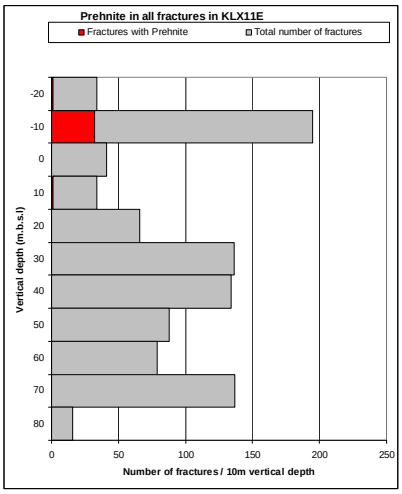
Prehnite in all fractures in KLX11E
Fractures with Prehnite
Total number of fractures
Vertical depth (m.b.s.l)
Number of fractures / 10m vertical depth

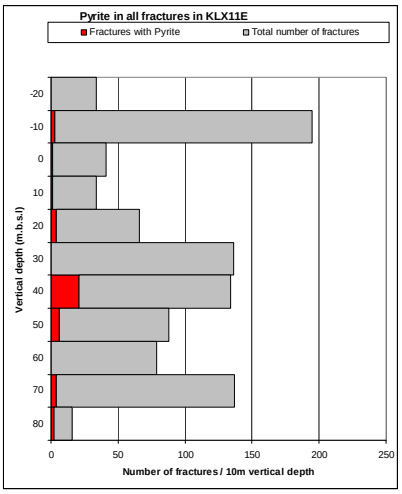
Pyrite in all fractures in KLX11E
Fractures with Pyrite
Total number of fractures
Vertical depth (m.b.s.l)
Number of fractures / 10m vertical depth

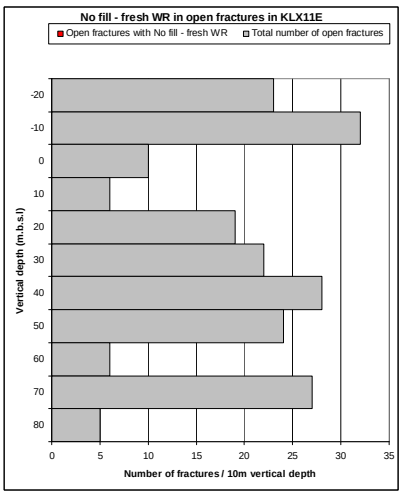
No fill - fresh WR in open fractures in KLX11E
Open fractures with No fill - fresh WR
Total number of open fractures
Vertical depth (m.b.s.l)
Number of fractures / 10m vertical depth

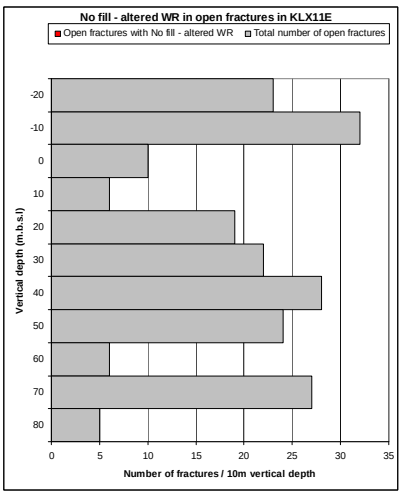
No fill - altered WR in open fractures in KLX11E
Open fractures with No fill - altered WR
Total number of open fractures
Vertical depth (m.b.s.l)
Number of fractures / 10m vertical depth

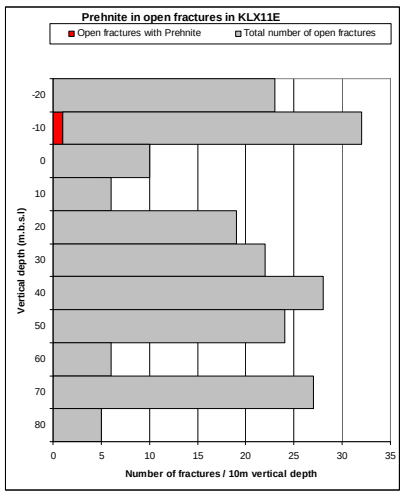
Prehnite in open fractures in KLX11E
Open fractures with Prehnite
Total number of open fractures
Vertical depth (m.b.s.l)
Number of fractures / 10m vertical depth

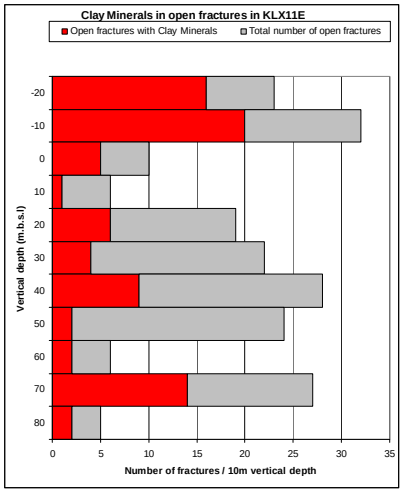
Clay Minerals in open fractures in KLX11E
Open fractures with Clay Minerals
Total number of open fractures
Vertical depth (m.b.s.l)
Number of fractures / 10m vertical depth

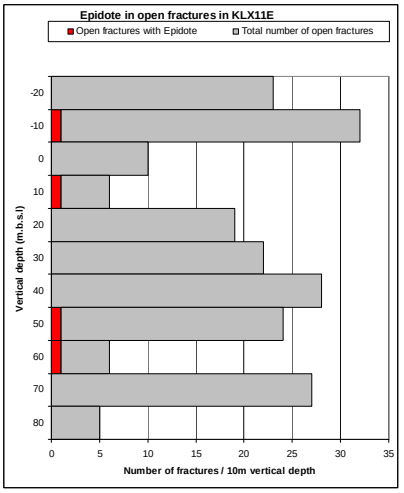
Epidote in open fractures in KLX11E
Open fractures with Epidote
Total number of open fractures
Vertical depth (m.b.s.l)
Number of fractures / 10m vertical depth

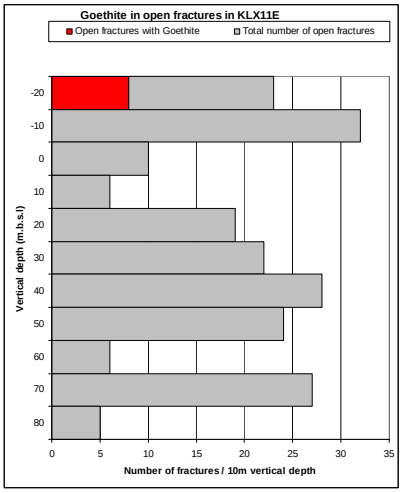
Goethite in open fractures in KLX11E
Open fractures with Goethite
Total number of open fractures
Vertical depth (m.b.s.l)
Number of fractures / 10m vertical depth

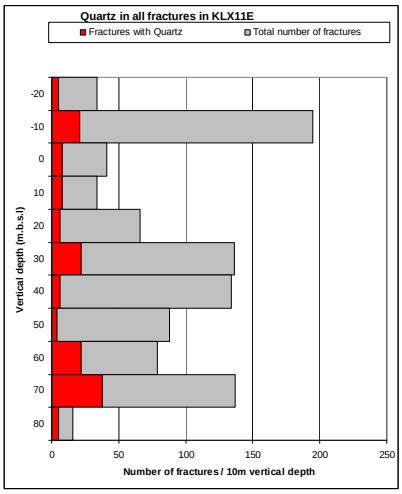
Quartz in all fractures in KLX11E
Fractures with Quartz
Total number of fractures
Vertical depth (m.b.s.l)
Number of fractures / 10m vertical depth

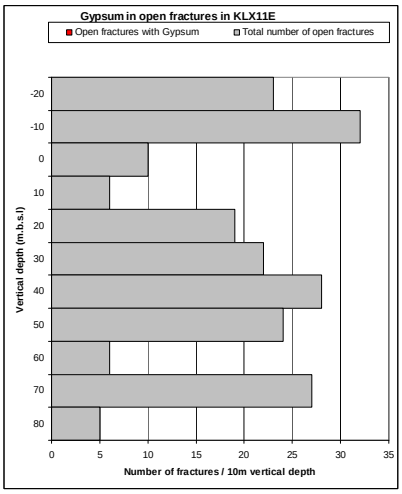
Gypsum in open fractures in KLX11E
Open fractures with Gypsum
Total number of open fractures
Vertical depth (m.b.s.l)
Number of fractures / 10m vertical depth

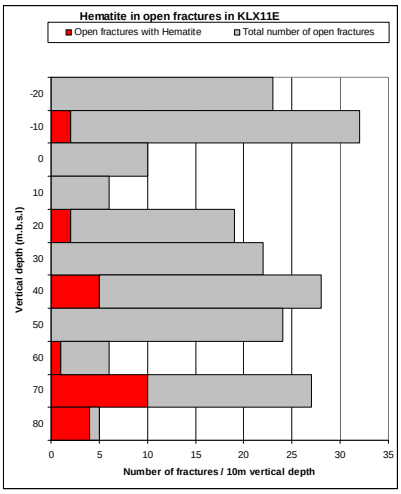
Hematite in open fractures in KLX11E
Open fractures with Hematite
Total number of open fractures
Vertical depth (m.b.s.l)
Number of fractures / 10m vertical depth

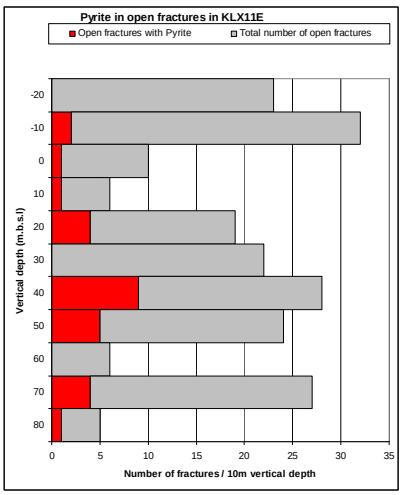
Pyrite in open fractures in KLX11E
Open fractures with Pyrite
Total number of open fractures
Vertical depth (m.b.s.l)
Number of fractures / 10m vertical depth

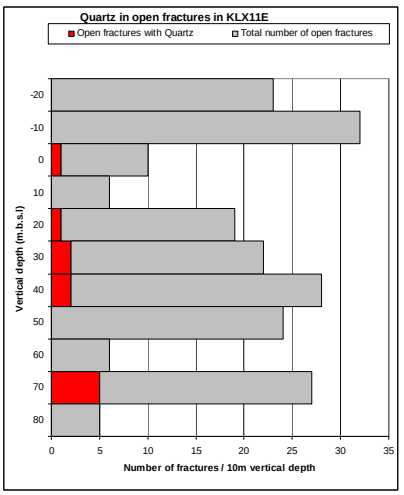
Quartz in open fractures in KLX11E
Open fractures with Quartz
Total number of open fractures
Vertical depth (m.b.s.l)
Number of fractures / 10m vertical depth

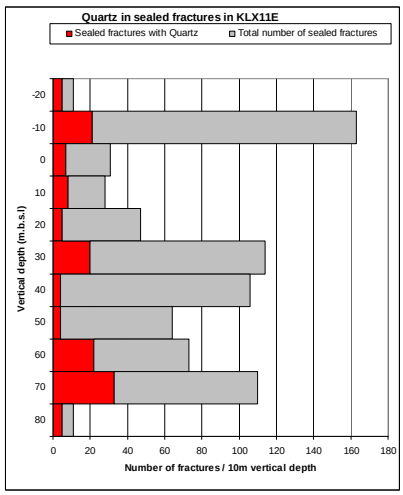
Quartz in sealed fractures in KLX11E
Sealed fractures with Quartz
Total number of sealed fractures
Vertical depth (m.b.s.l)
Number of fractures / 10m vertical depth

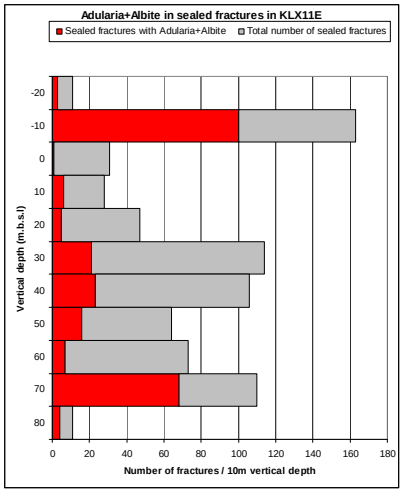
Adularia+Albite in sealed fractures in KLX11E
Sealed fractures with Adularia+Albite
Total number of sealed fractures
Vertical depth (m.b.s.l)
Number of fractures / 10m vertical depth

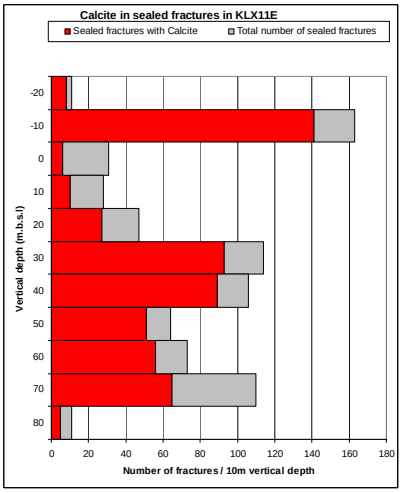
Calcite in sealed fractures in KLX11E
Sealed fractures with Calcite
Total number of sealed fractures
Vertical depth (m.b.s.l)
Number of fractures / 10m vertical depth

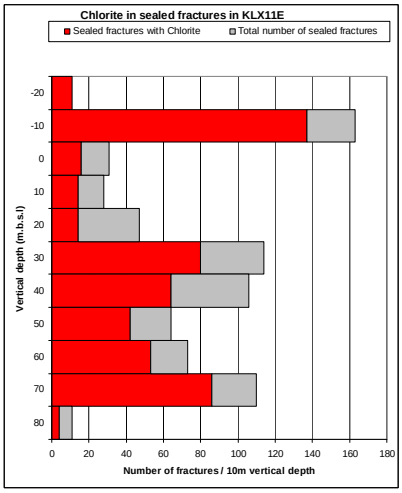
Chlorite in sealed fractures in KLX11E
Sealed fractures with Chlorite
Total number of sealed fractures
Vertical depth (m.b.s.l)
Number of fractures / 10m vertical depth

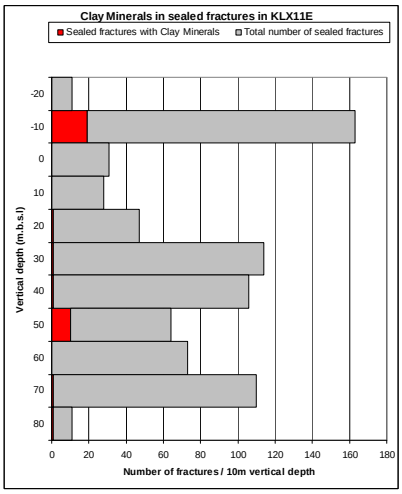
Clay Minerals in sealed fractures in KLX11E
Sealed fractures with Clay Minerals
Total number of sealed fractures
Vertical depth (m.b.s.l)
Number of fractures / 10m vertical depth

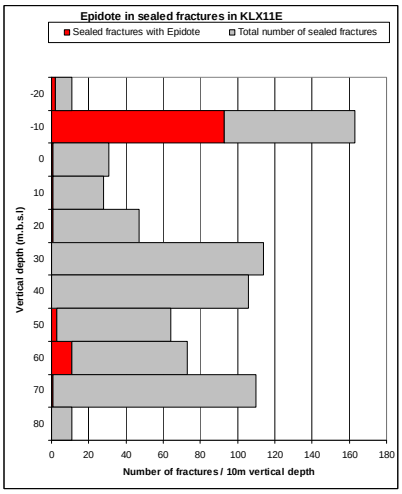
Epidote in sealed fractures in KLX11E
Sealed fractures with Epidote
Total number of sealed fractures
Vertical depth (m.b.s.l)
Number of fractures / 10m vertical depth

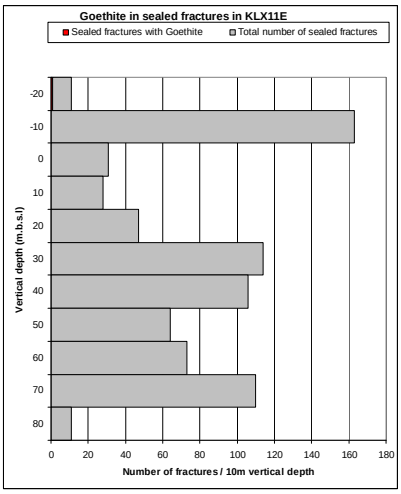
Goethite in sealed fractures in KLX11E
Sealed fractures with Goethite
Total number of sealed fractures
Vertical depth (m.b.s.l)
Number of fractures / 10m vertical depth

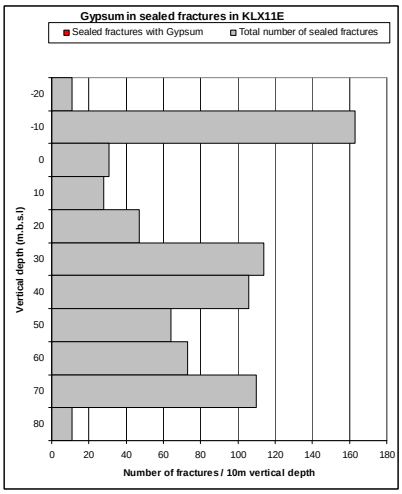
Gypsum in sealed fractures in KLX11E
Sealed fractures with Gypsum
Total number of sealed fractures
Vertical depth (m.b.s.l)
Number of fractures / 10m vertical depth

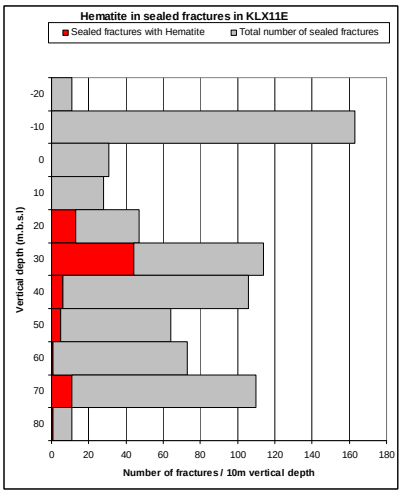
Hematite in sealed fractures in KLX11E
Sealed fractures with Hematite
Total number of sealed fractures
Vertical depth (m.b.s.l)
Number of fractures / 10m vertical depth

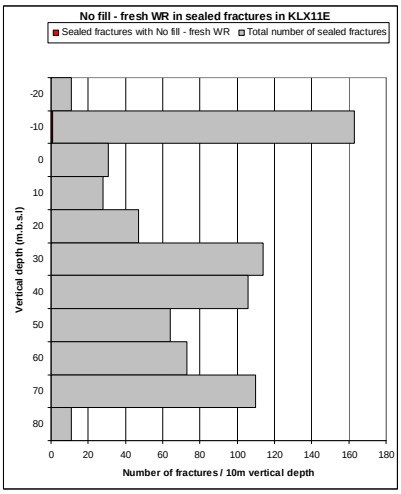
No fill - fresh WR in sealed fractures in KLX11E
Sealed fractures with No fill - fresh WR
Total number of sealed fractures
Vertical depth (m.b.s.l)
Number of fractures / 10m vertical depth

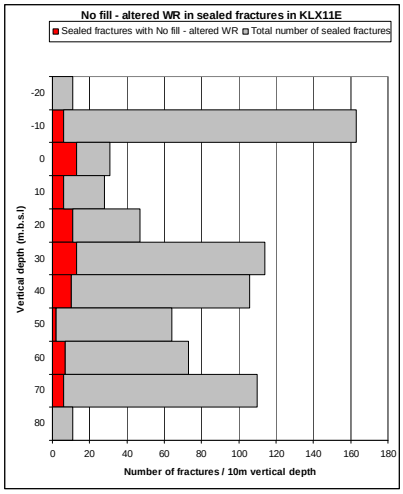
No fill - altered WR in sealed fractures in KLX11E
Sealed fractures with No fill - altered WR
Total number of sealed fractures
Vertical depth (m.b.s.l)
-20
-10
0
10
20
30
40
50
60
70
80
0
20
40
60
80
100
120
140
160
180
Number of fractures / 10m vertical depth

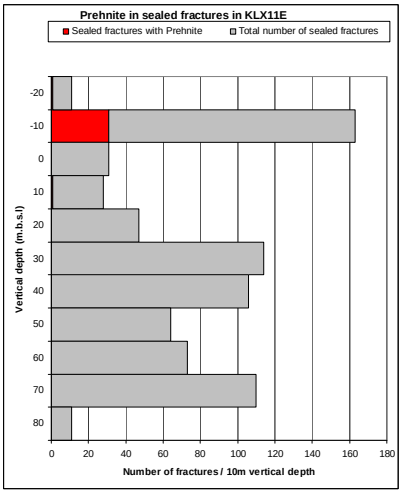
Prehnite in sealed fractures in KLX11E
Sealed fractures with Prehnite
Total number of sealed fractures
Vertical depth (m.b.s.l)
-20
-10
0
10
20
30
40
50
60
70
80
0
20
40
60
80
100
120
140
160
180
Number of fractures / 10m vertical depth

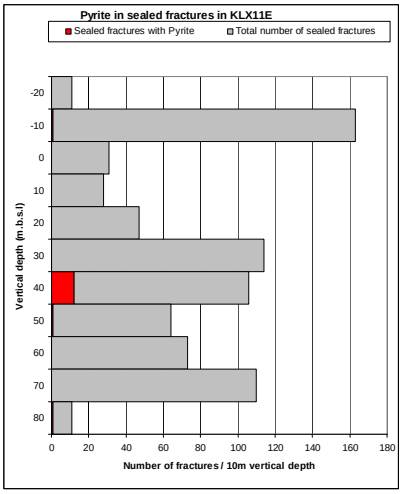
Pyrite in sealed fractures in KLX11E
Sealed fractures with Pyrite
Total number of sealed fractures
Vertical depth (m.b.s.l)
-20
-10
0
10
20
30
40
50
60
70
80
0
20
40
60
80
100
120
140
160
180
Number of fractures / 10m vertical depth

KLX11F

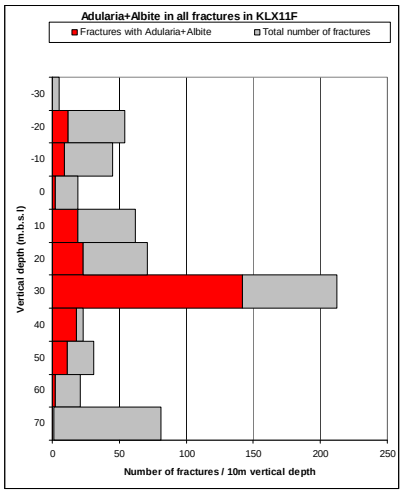
Adularia+Albite in all fractures in KLX11F
Fractures with Adularia+Albite
Total number of fractures
Vertical depth (m.b.s.l)
Number of fractures / 10m vertical depth

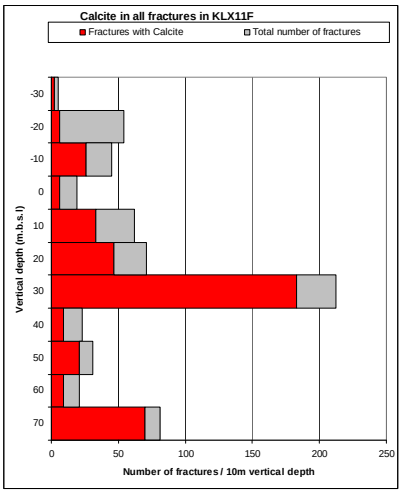
Calcite in all fractures in KLX11F
Fractures with Calcite
Total number of fractures
Vertical depth (m.b.s.l)
Number of fractures / 10m vertical depth

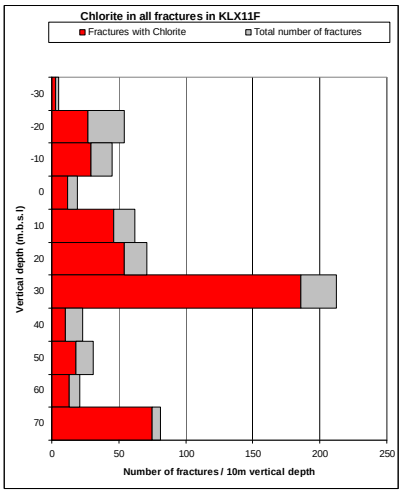
Chlorite in all fractures in KLX11F
Fractures with Chlorite
Total number of fractures
Vertical depth (m.b.s.l)
Number of fractures / 10m vertical depth

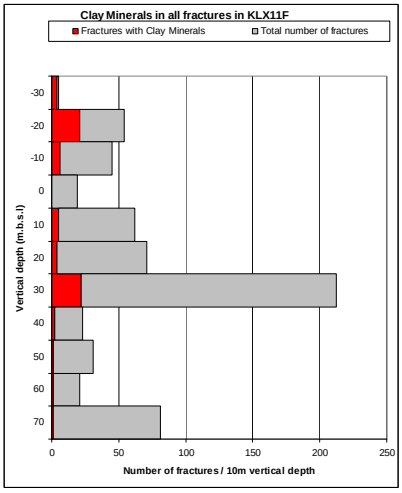
Clay Minerals in all fractures in KLX11F
Fractures with Clay Minerals
Total number of fractures
Vertical depth (m.b.s.l)
Number of fractures / 10m vertical depth

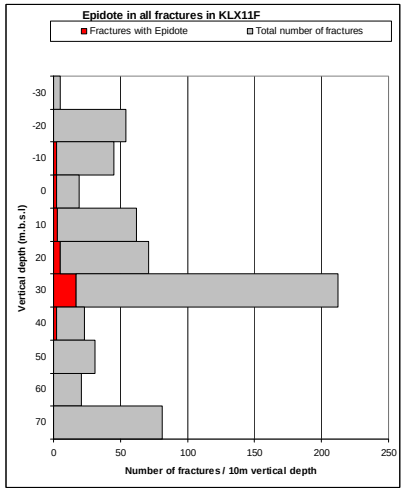
Epidote in all fractures in KLX11F
Fractures with Epidote
Total number of fractures
Vertical depth (m.b.s.l)
Number of fractures / 10m vertical depth

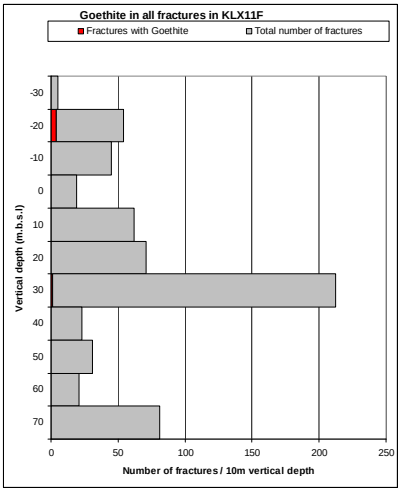
Goethite in all fractures in KLX11F
Fractures with Goethite
Total number of fractures
Vertical depth (m.b.s.l)
Number of fractures / 10m vertical depth

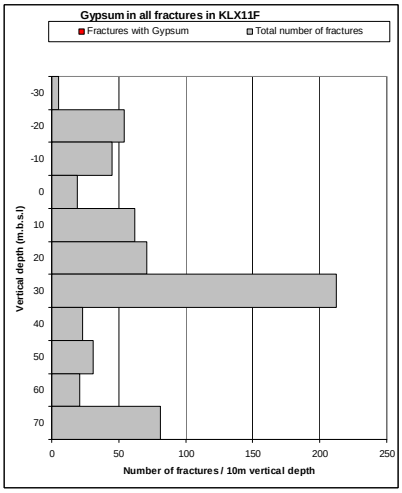
Gypsum in all fractures in KLX11F
Fractures with Gypsum
Total number of fractures
Vertical depth (m.b.s.l)
Number of fractures / 10m vertical depth

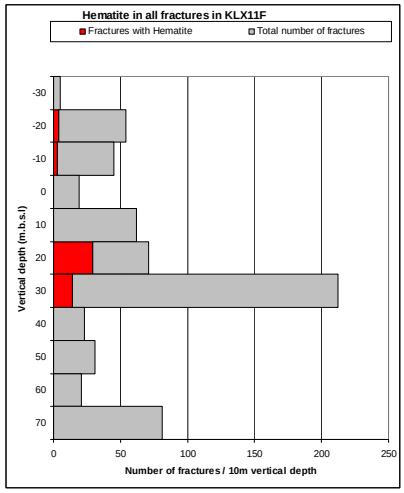
Hematite in all fractures in KLX11F
Fractures with Hematite
Total number of fractures
Vertical depth (m.b.s.l)
Number of fractures / 10m vertical depth

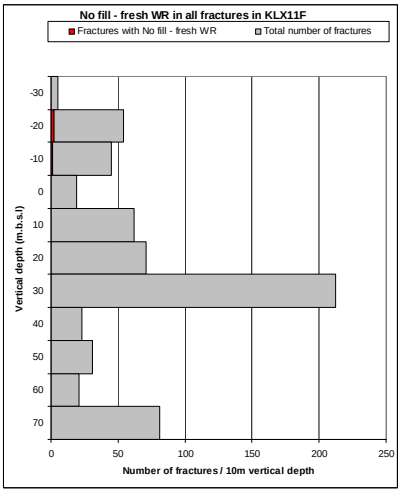
No fill - fresh WR in all fractures in KLX11F
Fractures with No fill - fresh WR
Total number of fractures
Vertical depth (m.b.s.l)
Number of fractures / 10m vertical depth

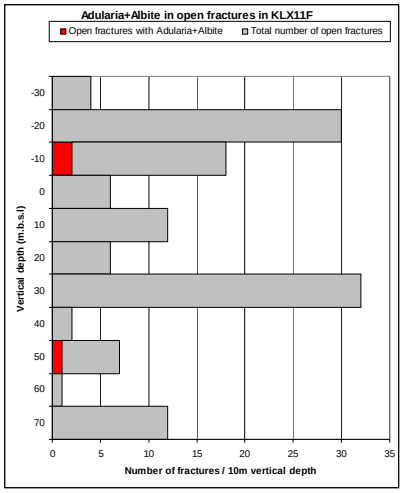
Adularia+Albite in open fractures in KLX11F
Open fractures with Adularia+Albite
Total number of open fractures
Vertical depth (m.b.s.l)
Number of fractures / 10m vertical depth

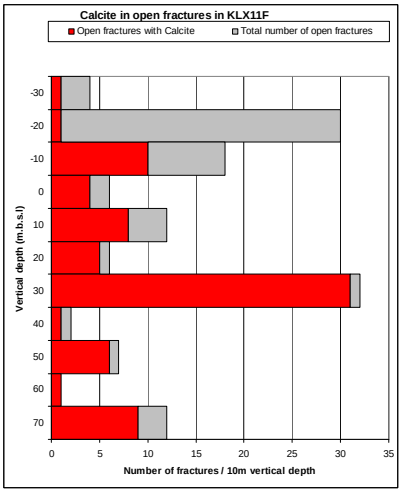
Calcite in open fractures in KLX11F
Open fractures with Calcite
Total number of open fractures
Vertical depth (m.b.s.l)
Number of fractures / 10m vertical depth

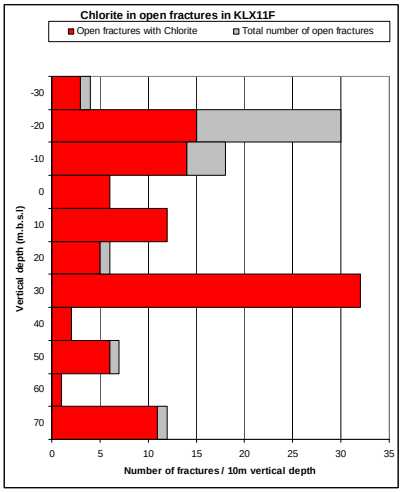
Chlorite in open fractures in KLX11F
Open fractures with Chlorite
Total number of open fractures
Vertical depth (m.b.s.l)
Number of fractures / 10m vertical depth

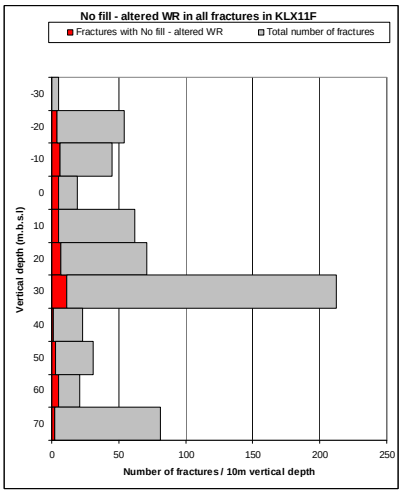
No fill - altered WR in all fractures in KLX11F
Fractures with No fill - altered WR
Total number of fractures
Vertical depth (m.b.s.l)
Number of fractures / 10m vertical depth

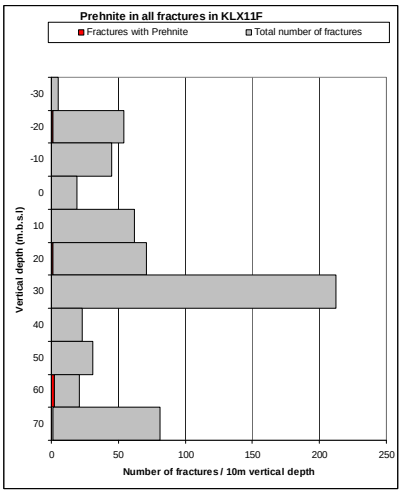
Prehnite in all fractures in KLX11F
Fractures with Prehnite
Total number of fractures
Vertical depth (m.b.s.l)
Number of fractures / 10m vertical depth

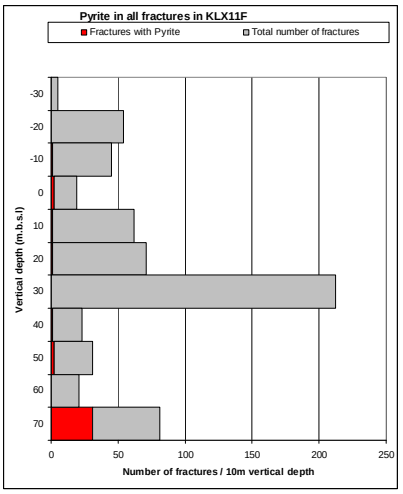
Pyrite in all fractures in KLX11F
Fractures with Pyrite
Total number of fractures
Vertical depth (m.b.s.l)
Number of fractures / 10m vertical depth

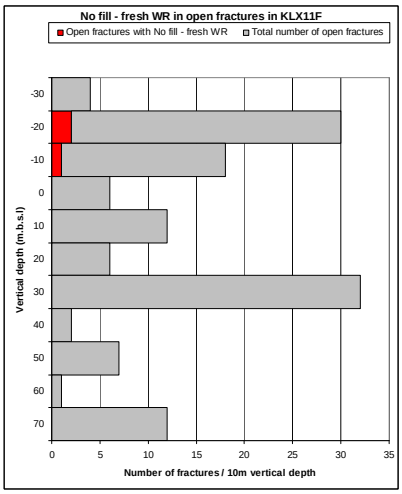
No fill - fresh WR in open fractures in KLX11F
Open fractures with No fill - fresh WR
Total number of open fractures
Vertical depth (m.b.s.l)
Number of fractures / 10m vertical depth

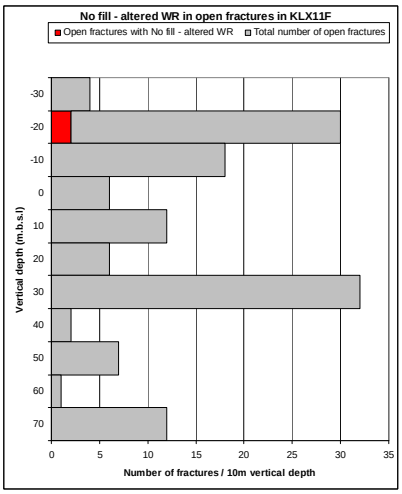
No fill - altered WR in open fractures in KLX11F
Open fractures with No fill - altered WR
Total number of open fractures
Vertical depth (m.b.s.l)
Number of fractures / 10m vertical depth

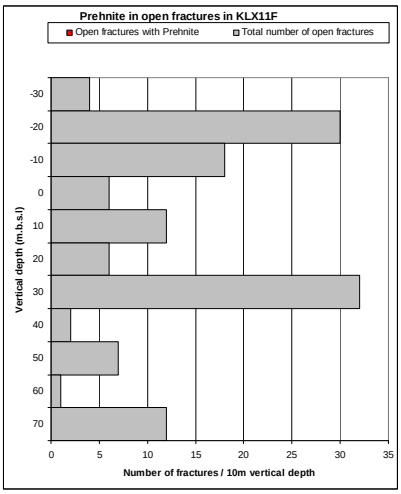
Prehnite in open fractures in KLX11F
Open fractures with Prehnite
Total number of open fractures
Vertical depth (m.b.s.l)
Number of fractures / 10m vertical depth

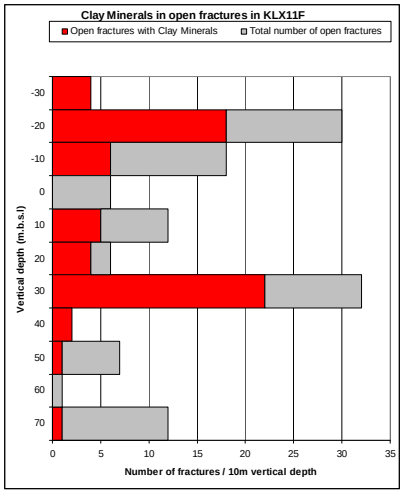
Clay Minerals in open fractures in KLX11F
Open fractures with Clay Minerals
Total number of open fractures
Vertical depth (m.b.s.l)
Number of fractures / 10m vertical depth

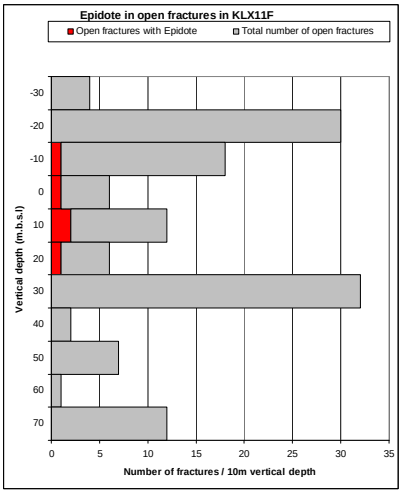
Epidote in open fractures in KLX11F
Open fractures with Epidote
Total number of open fractures
Vertical depth (m.b.s.l)
Number of fractures / 10m vertical depth

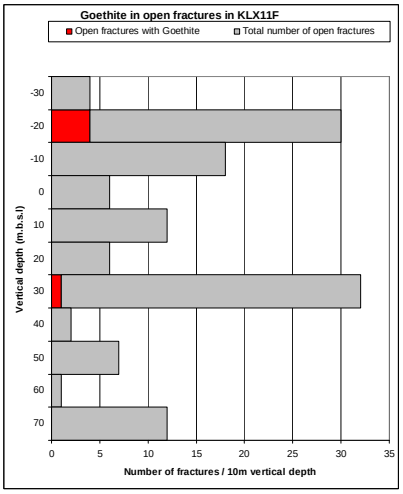
Goethite in open fractures in KLX11F
Open fractures with Goethite
Total number of open fractures
Vertical depth (m.b.s.l)
Number of fractures / 10m vertical depth

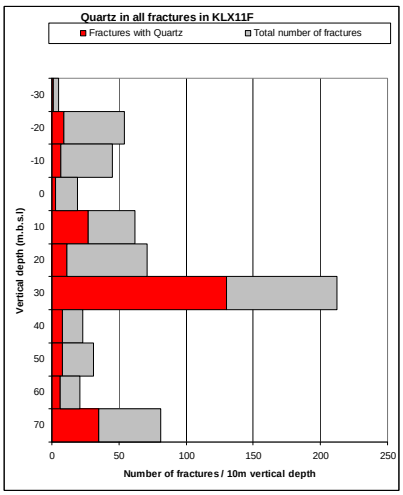
Quartz in all fractures in KLX11F
Fractures with Quartz
Total number of fractures
Vertical depth (m.b.s.l)
Number of fractures / 10m vertical depth

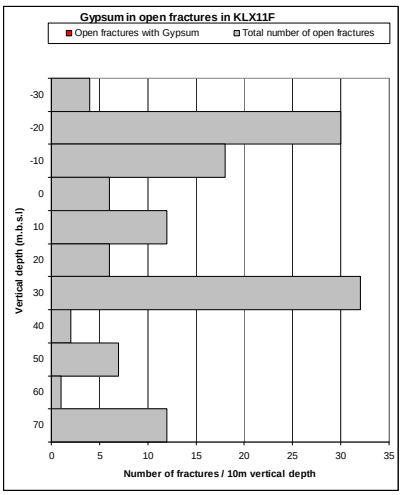
Gypsum in open fractures in KLX11F
Open fractures with Gypsum
Total number of open fractures
Vertical depth (m.b.s.l)
Number of fractures / 10m vertical depth

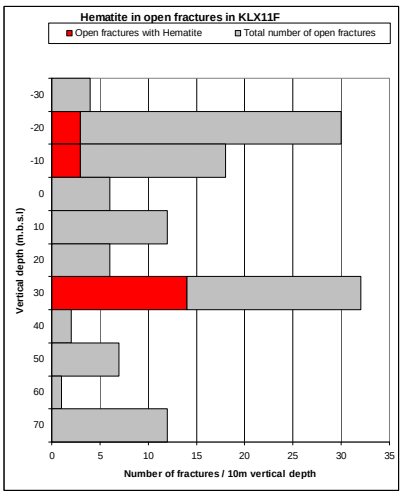
Hematite in open fractures in KLX11F
Open fractures with Hematite
Total number of open fractures
Vertical depth (m.b.s.l)
Number of fractures / 10m vertical depth

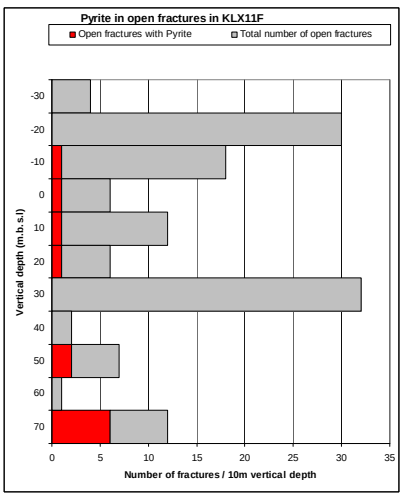
Pyrite in open fractures in KLX11F
Open fractures with Pyrite
Total number of open fractures
Vertical depth (m.b.s.l)
Number of fractures / 10m vertical depth

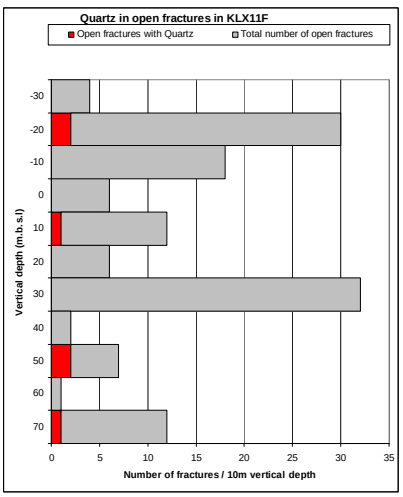
Quartz in open fractures in KLX11F
Open fractures with Quartz
Total number of open fractures
Vertical depth (m.b.s.l)
Number of fractures / 10m vertical depth

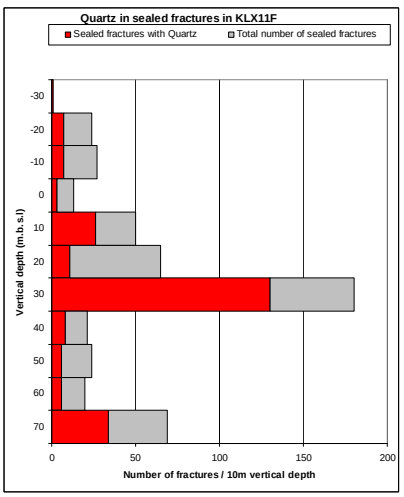
Quartz in sealed fractures in KLX11F
Sealed fractures with Quartz
Total number of sealed fractures
Vertical depth (m.b.s.l)
Number of fractures / 10m vertical depth

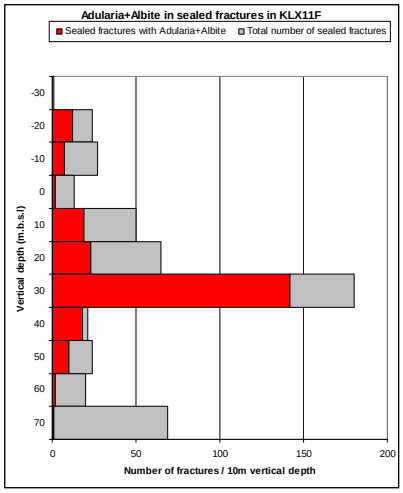
Adularia+Albite in sealed fractures in KLX11F
Sealed fractures with Adularia+Albite
Total number of sealed fractures
Vertical depth (m.b.s.l)
Number of fractures / 10m vertical depth

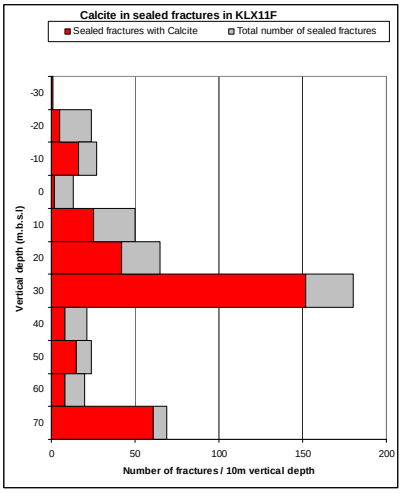
Calcite in sealed fractures in KLX11F
Sealed fractures with Calcite
Total number of sealed fractures
Vertical depth (m.b.s.l)
Number of fractures / 10m vertical depth

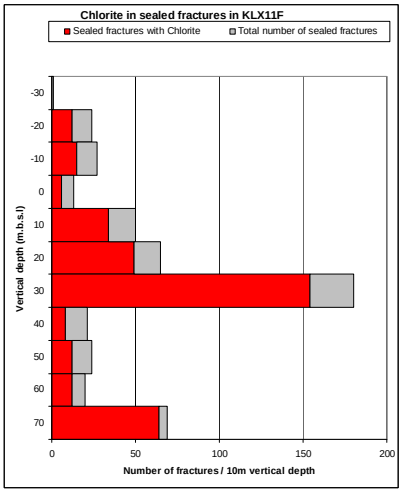
Chlorite in sealed fractures in KLX11F
Sealed fractures with Chlorite
Total number of sealed fractures
Vertical depth (m.b.s.l)
Number of fractures / 10m vertical depth

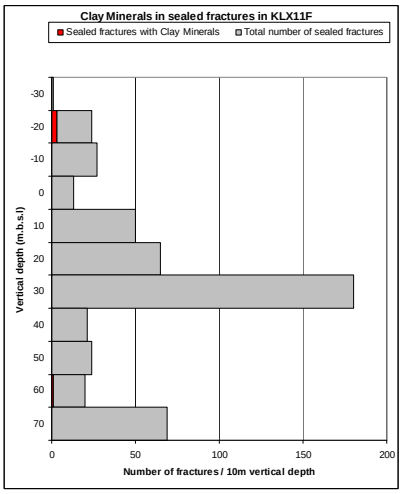
Clay Minerals in sealed fractures in KLX11F
Sealed fractures with Clay Minerals
Total number of sealed fractures
Vertical depth (m.b.s.l)
Number of fractures / 10m vertical depth

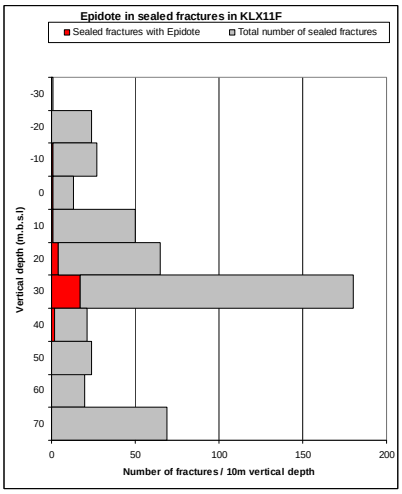
Epidote in sealed fractures in KLX11F
Sealed fractures with Epidote
Total number of sealed fractures
Vertical depth (m.b.s.l)
Number of fractures / 10m vertical depth

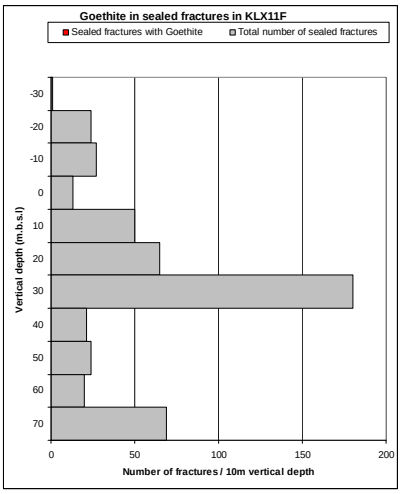
Goethite in sealed fractures in KLX11F
Sealed fractures with Goethite
Total number of sealed fractures
Vertical depth (m.b.s.l)
Number of fractures / 10m vertical depth

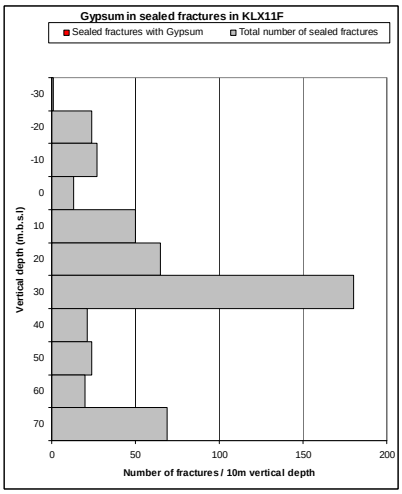
Gypsum in sealed fractures in KLX11F
Sealed fractures with Gypsum
Total number of sealed fractures
Vertical depth (m.b.s.l)
Number of fractures / 10m vertical depth

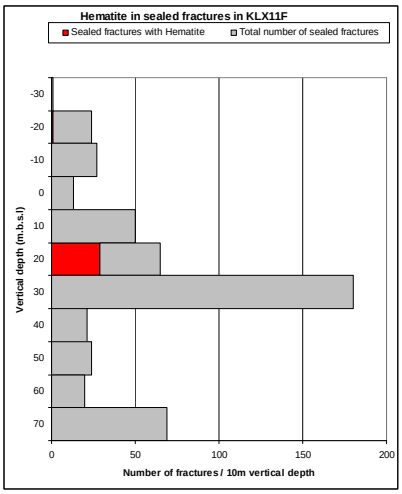
Hematite in sealed fractures in KLX11F
Sealed fractures with Hematite
Total number of sealed fractures
Vertical depth (m.b.s.l)
Number of fractures / 10m vertical depth

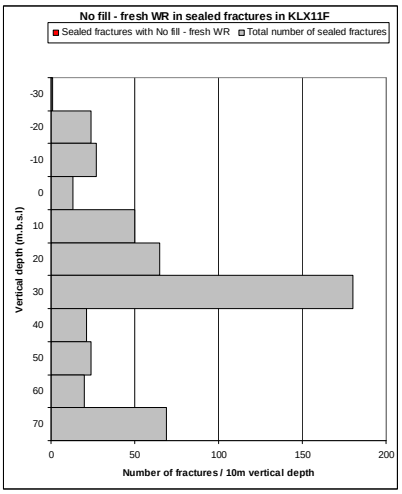
No fill - fresh WR in sealed fractures in KLX11F
Sealed fractures with No fill - fresh WR
Total number of sealed fractures
Vertical depth (m.b.s.l)
Number of fractures / 10m vertical depth

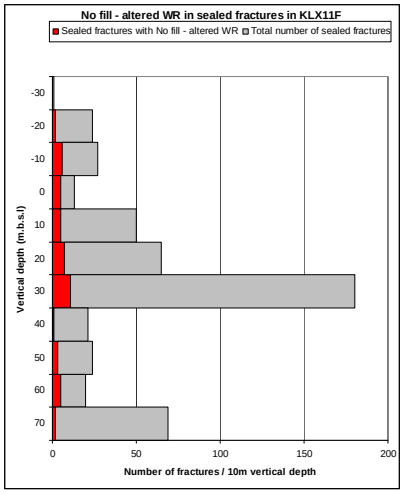
No fill - altered WR in sealed fractures in KLX11F
Sealed fractures with No fill - altered WR
Total number of sealed fractures
Vertical depth (m.b.s.l)
-30
-20
-10
0
10
20
30
40
50
60
70
0
50
100
150
200
Number of fractures / 10m vertical depth

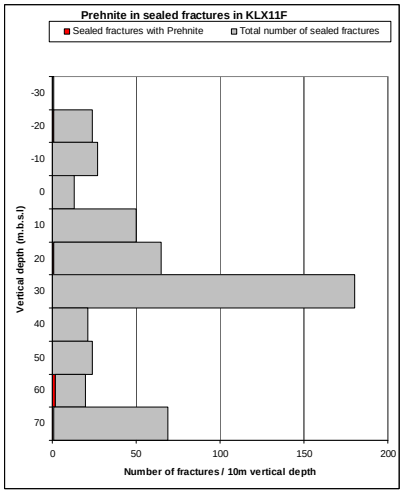
Prehnite in sealed fractures in KLX11F
Sealed fractures with Prehnite
Total number of sealed fractures
Vertical depth (m.b.s.l)
-30
-20
-10
0
10
20
30
40
50
60
70
0
50
100
150
200
Number of fractures / 10m vertical depth

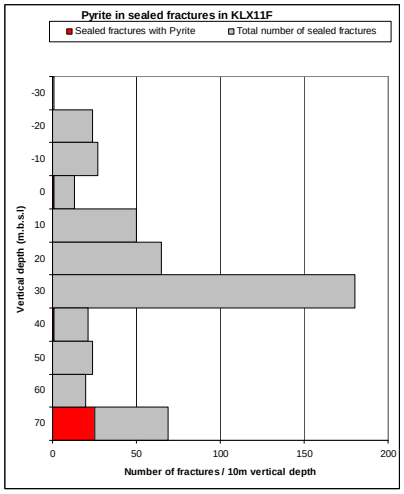
Pyrite in sealed fractures in KLX11F
Sealed fractures with Pyrite
Total number of sealed fractures
Vertical depth (m.b.s.l)
-30
-20
-10
0
10
20
30
40
50
60
70
0
50
100
150
200
Number of fractures / 10m vertical depth

KLX12A

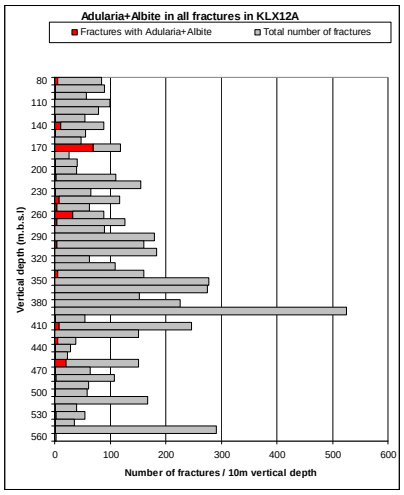
Adularia+Albite in all fractures in KLX12A
Fractures with Adularia+Albite
Total number of fractures
Vertical depth (m.b.s.l)
Number of fractures / 10m vertical depth

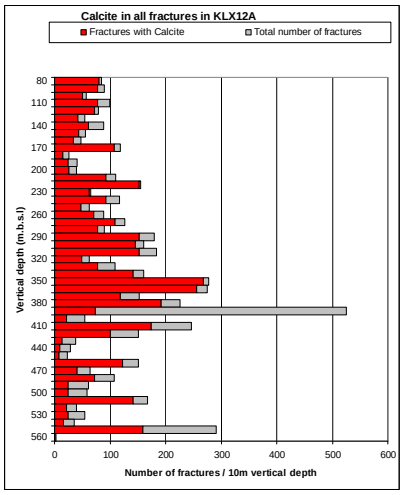
Calcite in all fractures in KLX12A
Fractures with Calcite
Total number of fractures
Vertical depth (m.b.s.l)
Number of fractures / 10m vertical depth

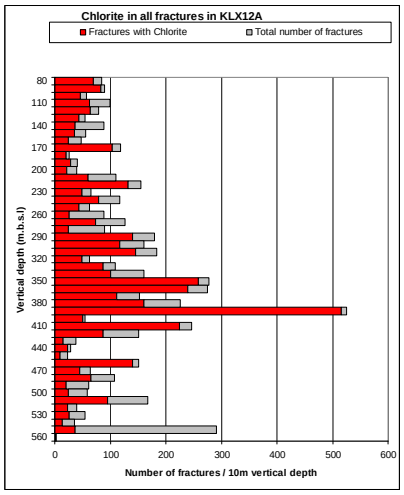
Chlorite in all fractures in KLX12A
Fractures with Chlorite
Total number of fractures
Vertical depth (m.b.s.l)
Number of fractures / 10m vertical depth

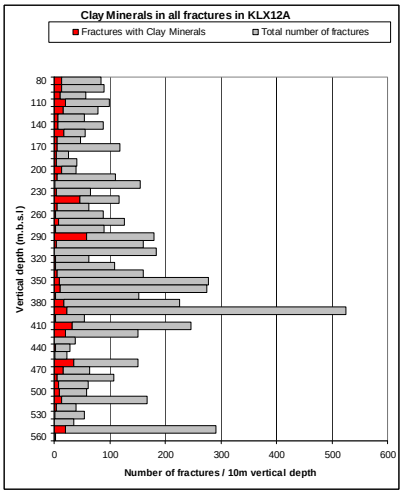
Clay Minerals in all fractures in KLX12A
Fractures with Clay Minerals
Total number of fractures
Vertical depth (m.b.s.l)
Number of fractures / 10m vertical depth

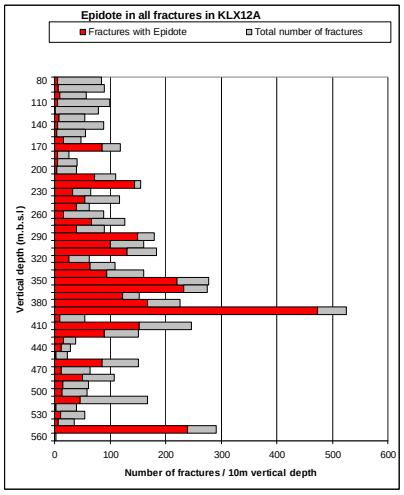
Epidote in all fractures in KLX12A
Fractures with Epidote
Total number of fractures
Vertical depth (m.b.s.l)
Number of fractures / 10m vertical depth

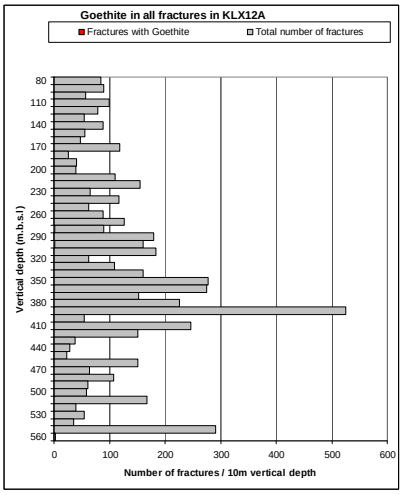
Goethite in all fractures in KLX12A
Fractures with Goethite
Total number of fractures
Vertical depth (m.b.s.l)
Number of fractures / 10m vertical depth

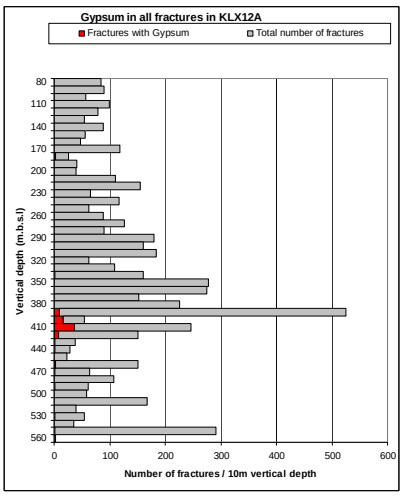
Gypsum in all fractures in KLX12A
Fractures with Gypsum
Total number of fractures
Vertical depth (m.b.s.l)
Number of fractures / 10m vertical depth

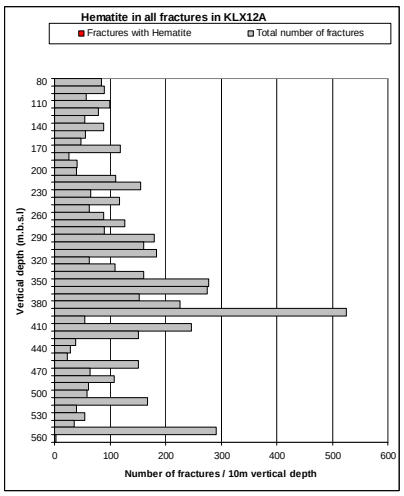
Hematite in all fractures in KLX12A
Fractures with Hematite
Total number of fractures
Vertical depth (m.b.s.l)
Number of fractures / 10m vertical depth

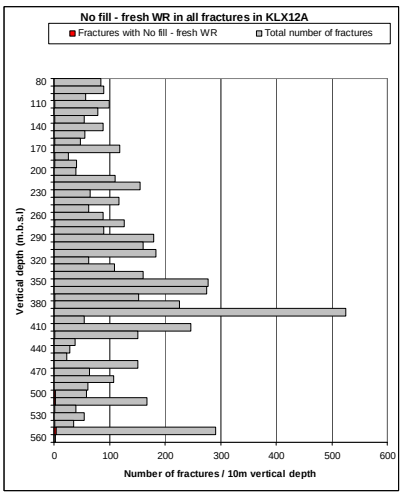
No fill - fresh WR in all fractures in KLX12A
Fractures with No fill - fresh WR
Total number of fractures
Vertical depth (m.b.s.l)
Number of fractures / 10m vertical depth

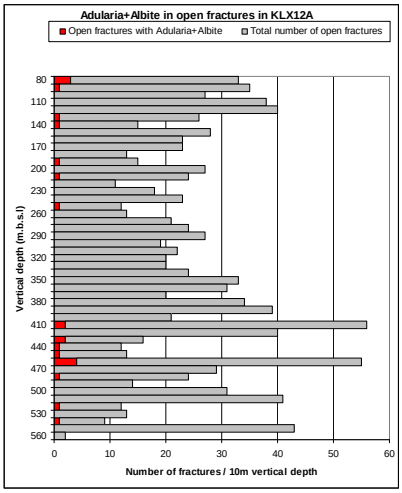
Adularia+Albite in open fractures in KLX12A
Open fractures with Adularia+Albite
Total number of open fractures
Vertical depth (m.b.s.l)
Number of fractures / 10m vertical depth

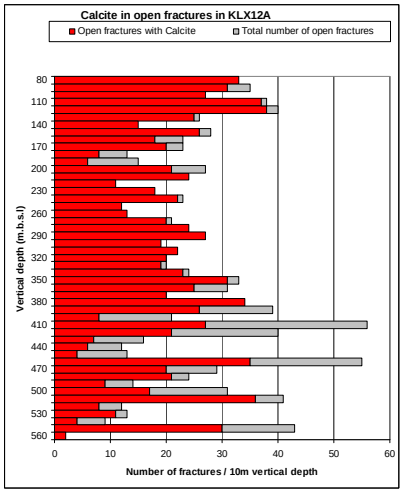
Calcite in open fractures in KLX12A
Open fractures with Calcite
Total number of open fractures
Vertical depth (m.b.s.l)
Number of fractures / 10m vertical depth

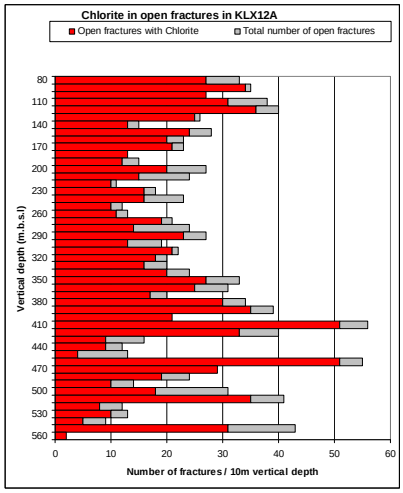
Chlorite in open fractures in KLX12A
Open fractures with Chlorite
Total number of open fractures
Vertical depth (m.b.s.l)
Number of fractures / 10m vertical depth

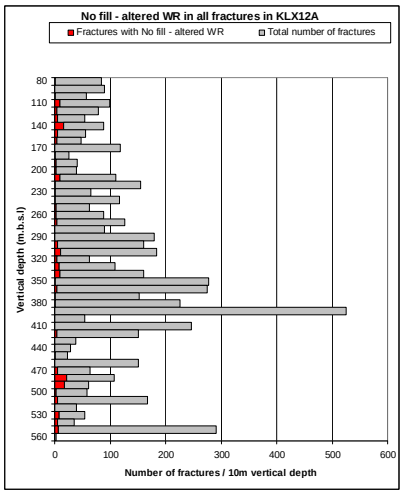
No fill - altered WR in all fractures in KLX12A
Fractures with No fill - altered WR
Total number of fractures
Vertical depth (m.b.s.l)
Number of fractures / 10m vertical depth

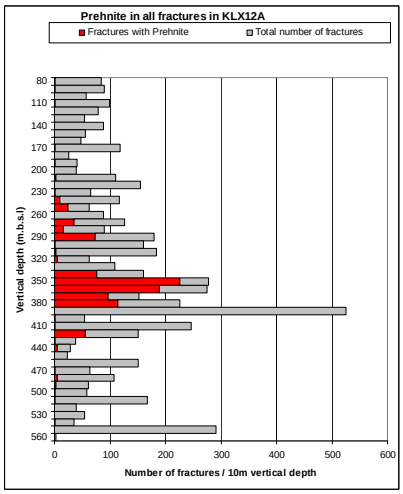
Prehnite in all fractures in KLX12A
Fractures with Prehnite
Total number of fractures
Vertical depth (m.b.s.l)
Number of fractures / 10m vertical depth

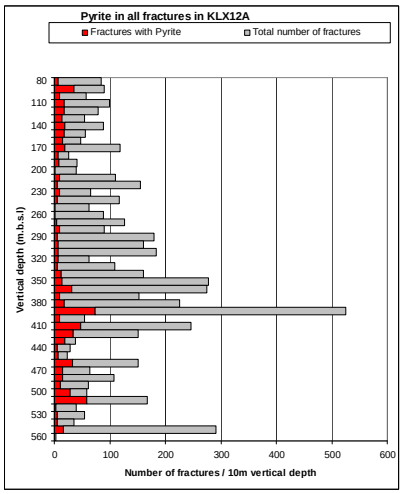
Pyrite in all fractures in KLX12A
Fractures with Pyrite
Total number of fractures
Vertical depth (m.b.s.l)
Number of fractures / 10m vertical depth

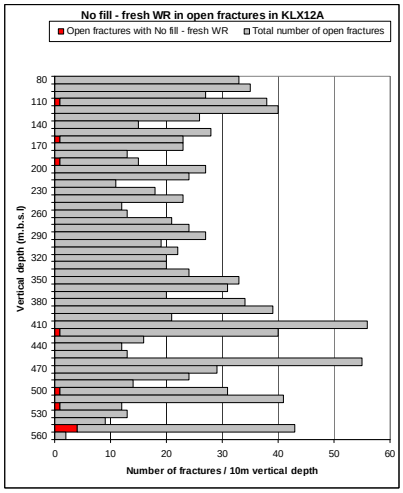
No fill - fresh WR in open fractures in KLX12A
Open fractures with No fill - fresh WR
Total number of open fractures
Vertical depth (m.b.s.l)
Number of fractures / 10m vertical depth

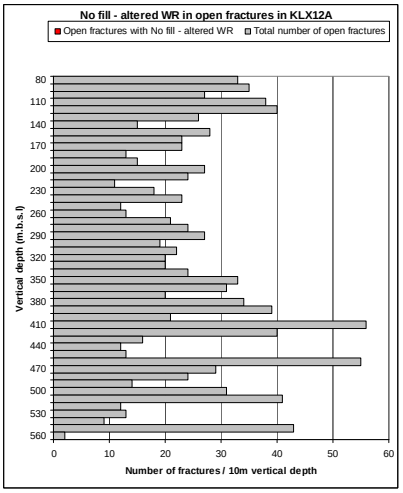
No fill - altered WR in open fractures in KLX12A
Open fractures with No fill - altered WR
Total number of open fractures
Vertical depth (m.b.s.l)
Number of fractures / 10m vertical depth

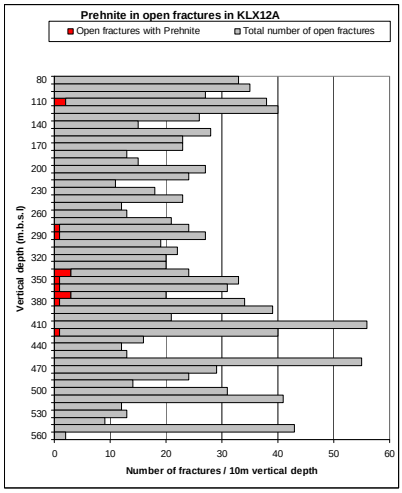
Prehnite in open fractures in KLX12A
Open fractures with Prehnite
Total number of open fractures
Vertical depth (m.b.s.l)
Number of fractures / 10m vertical depth

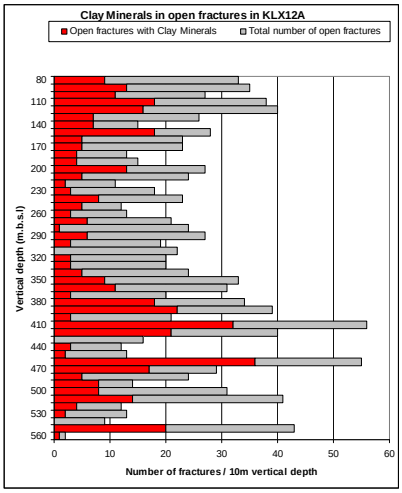
Clay Minerals in open fractures in KLX12A
Open fractures with Clay Minerals
Total number of open fractures
Vertical depth (m.b.s.l)
Number of fractures / 10m vertical depth

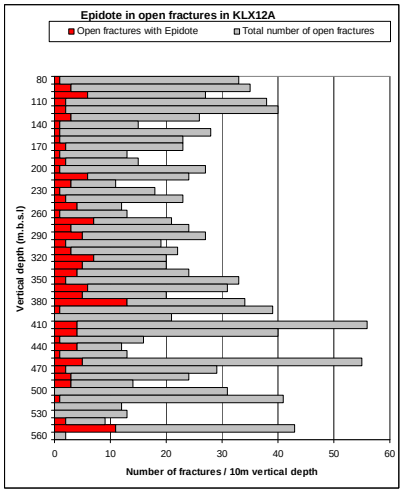
Epidote in open fractures in KLX12A
Open fractures with Epidote
Total number of open fractures
Vertical depth (m.b.s.l)
Number of fractures / 10m vertical depth

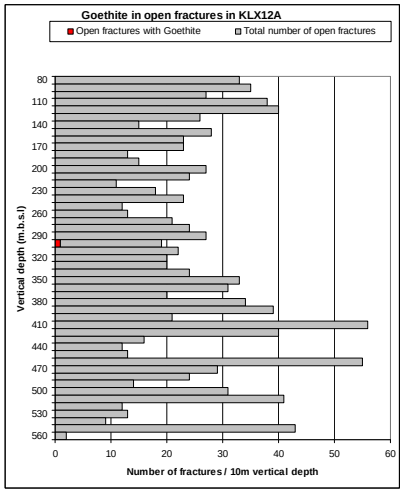
Goethite in open fractures in KLX12A
Open fractures with Goethite
Total number of open fractures
Vertical depth (m.b.s.l)
Number of fractures / 10m vertical depth

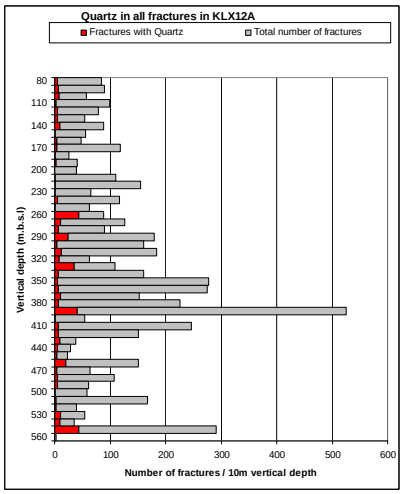
Quartz in all fractures in KLX12A
Fractures with Quartz
Total number of fractures
Vertical depth (m.b.s.l)
Number of fractures / 10m vertical depth

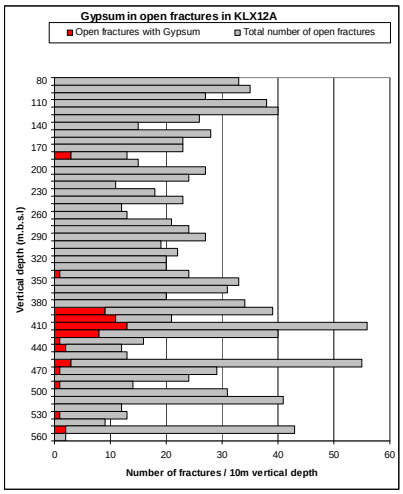
Gypsum in open fractures in KLX12A
Open fractures with Gypsum
Total number of open fractures
Vertical depth (m.b.s.l)
Number of fractures / 10m vertical depth

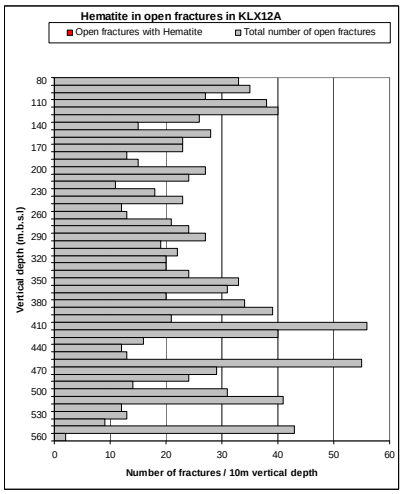
Hematite in open fractures in KLX12A
Open fractures with Hematite
Total number of open fractures
Vertical depth (m.b.s.l)
Number of fractures / 10m vertical depth

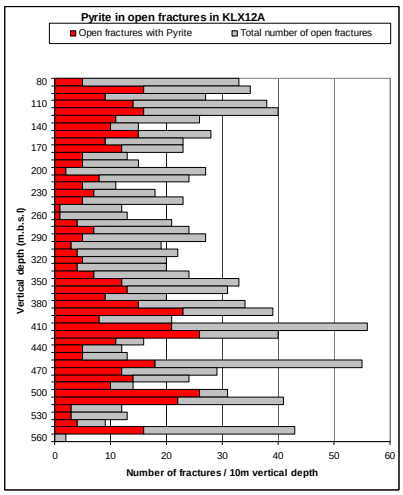
Pyrite in open fractures in KLX12A
Open fractures with Pyrite
Total number of open fractures
Vertical depth (m.b.s.l)
Number of fractures / 10m vertical depth

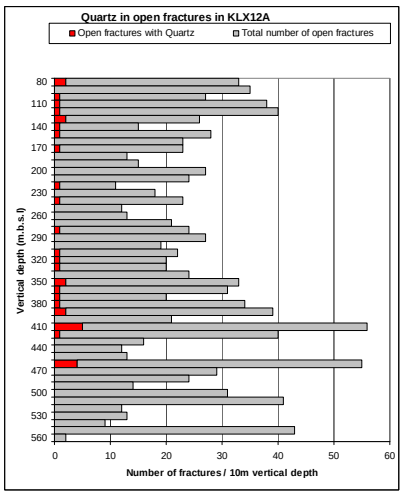
Quartz in open fractures in KLX12A
Open fractures with Quartz
Total number of open fractures
Vertical depth (m.b.s.l)
Number of fractures / 10m vertical depth

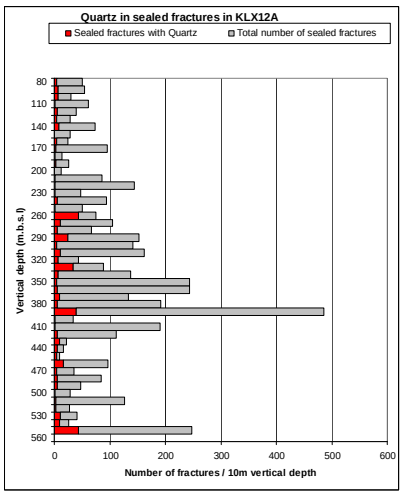
Quartz in sealed fractures in KLX12A
Sealed fractures with Quartz
Total number of sealed fractures
Vertical depth (m.b.s.l)
Number of fractures / 10m vertical depth

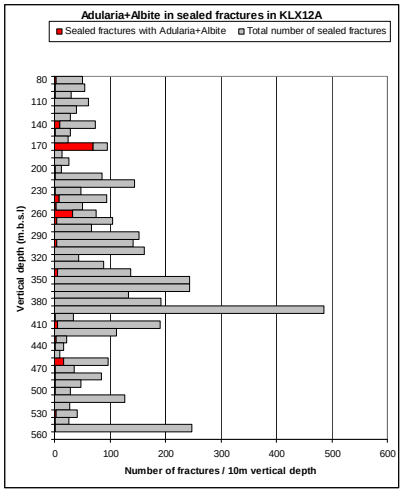
Adularia+Albite in sealed fractures in KLX12A
Sealed fractures with Adularia+Albite
Total number of sealed fractures
Vertical depth (m.b.s.l)
Number of fractures / 10m vertical depth

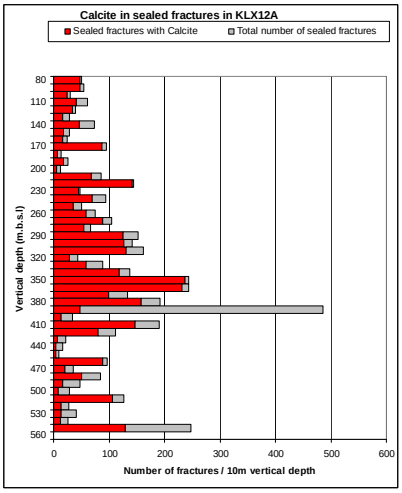
Calcite in sealed fractures in KLX12A
Sealed fractures with Calcite
Total number of sealed fractures
Vertical depth (m.b.s.l)
Number of fractures / 10m vertical depth

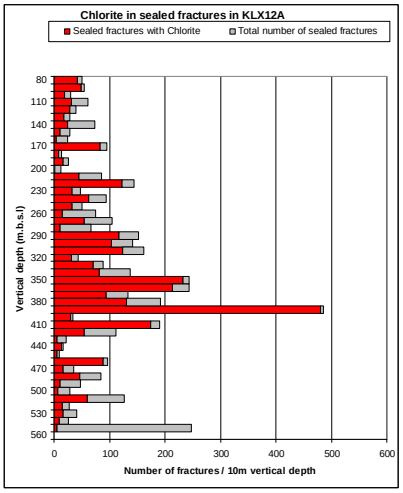
Chlorite in sealed fractures in KLX12A
Sealed fractures with Chlorite
Total number of sealed fractures
Vertical depth (m.b.s.l)
Number of fractures / 10m vertical depth

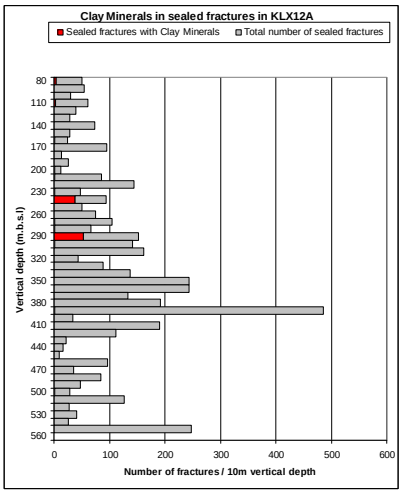
Clay Minerals in sealed fractures in KLX12A
Sealed fractures with Clay Minerals
Total number of sealed fractures
Vertical depth (m.b.s.l)
Number of fractures / 10m vertical depth

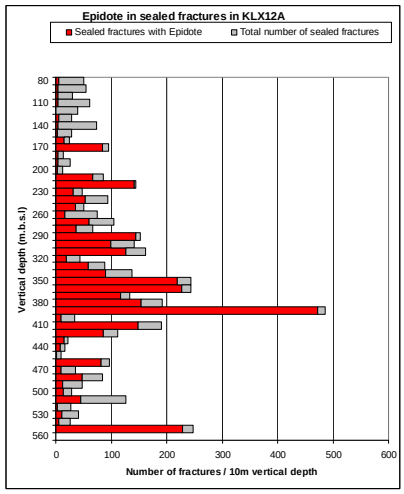
Epidote in sealed fractures in KLX12A
Sealed fractures with Epidote
Total number of sealed fractures
Vertical depth (m.b.s.l)
Number of fractures / 10m vertical depth

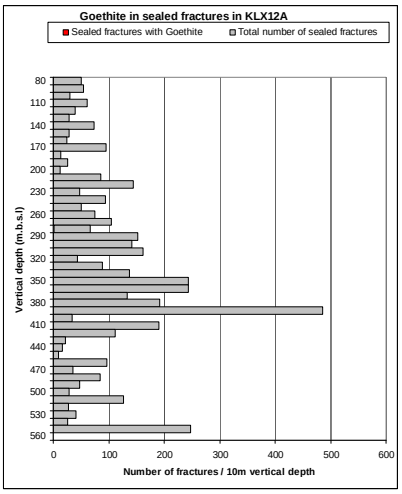
Goethite in sealed fractures in KLX12A
Sealed fractures with Goethite
Total number of sealed fractures
Vertical depth (m.b.s.l)
Number of fractures / 10m vertical depth

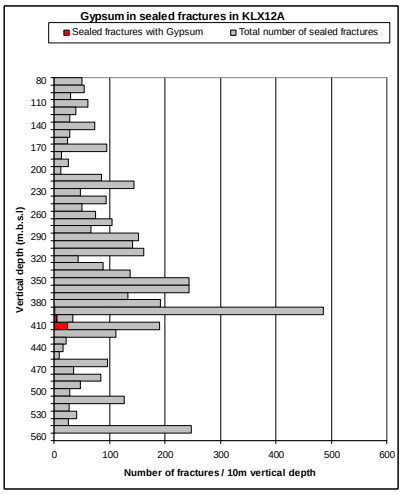
Gypsum in sealed fractures in KLX12A
Sealed fractures with Gypsum
Total number of sealed fractures
Vertical depth (m.b.s.l)
Number of fractures / 10m vertical depth

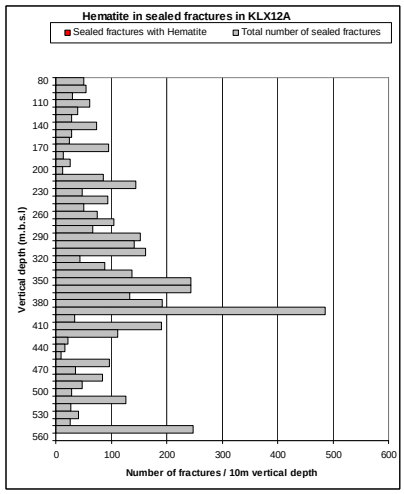
Hematite in sealed fractures in KLX12A
Sealed fractures with Hematite
Total number of sealed fractures
Vertical depth (m.b.s.l)
Number of fractures / 10m vertical depth

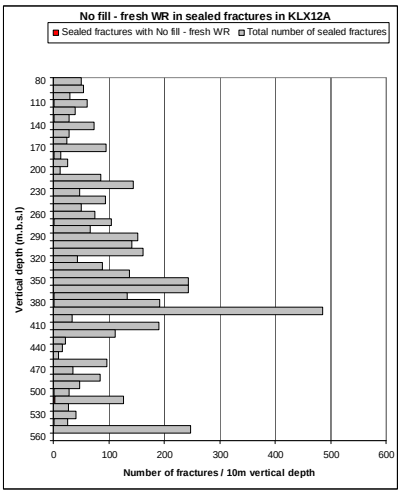
No fill - fresh WR in sealed fractures in KLX12A
Sealed fractures with No fill - fresh WR
Total number of sealed fractures
Vertical depth (m.b.s.l)
Number of fractures / 10m vertical depth

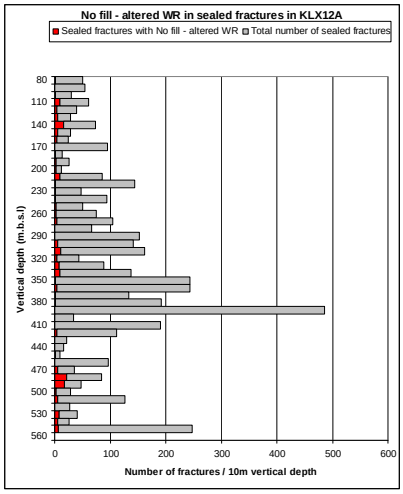
No fill - altered WR in sealed fractures in KLX12A
Sealed fractures with No fill - altered WR
Total number of sealed fractures
Vertical depth (m.b.s.l)
Number of fractures / 10m vertical depth

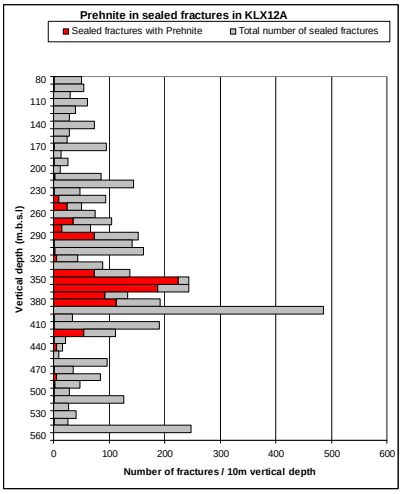
Prehnite in sealed fractures in KLX12A
Sealed fractures with Prehnite
Total number of sealed fractures
Vertical depth (m.b.s.l)
Number of fractures / 10m vertical depth

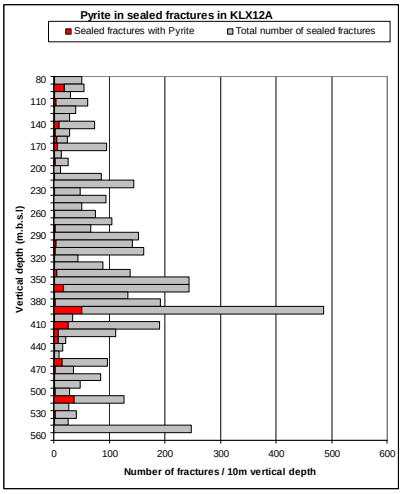
Pyrite in sealed fractures in KLX12A
Sealed fractures with Pyrite
Total number of sealed fractures
Vertical depth (m.b.s.l)
Number of fractures / 10m vertical depth

KLX13A

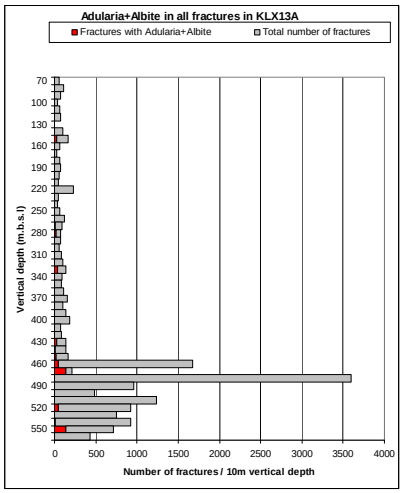
Adularia+Albite in all fractures in KLX13A
Fractures with Adularia+Albite
Total number of fractures
Vertical depth (m.b.s.l)
Number of fractures / 10m vertical depth

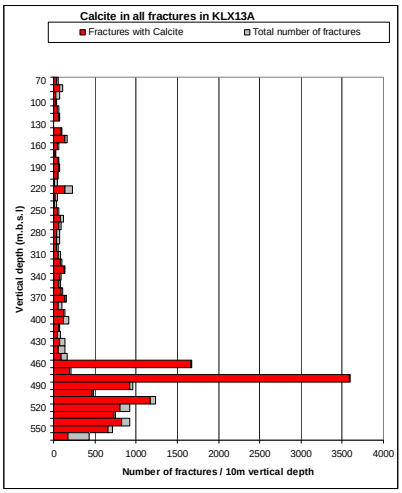
Calcite in all fractures in KLX13A
Fractures with Calcite
Total number of fractures
Vertical depth (m.b.s.l)
Number of fractures / 10m vertical depth

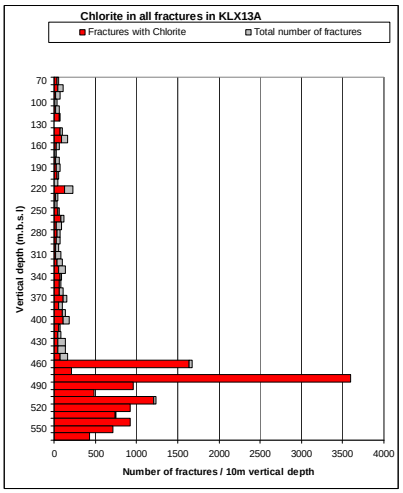
Chlorite in all fractures in KLX13A
Fractures with Chlorite
Total number of fractures
Vertical depth (m.b.s.l)
Number of fractures / 10m vertical depth

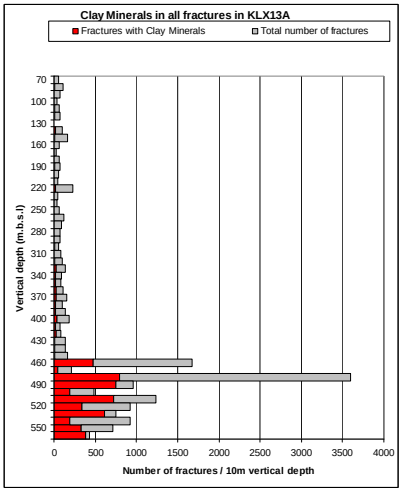
Clay Minerals in all fractures in KLX13A
Fractures with Clay Minerals
Total number of fractures
Vertical depth (m.b.s.l)
Number of fractures / 10m vertical depth

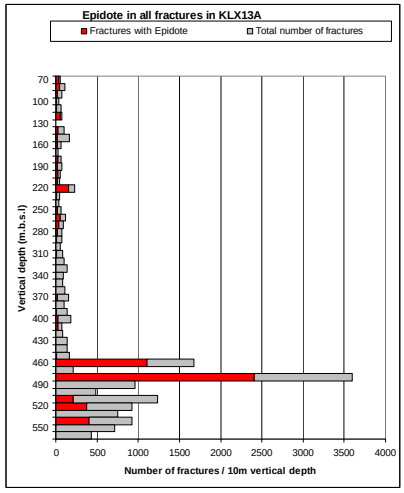
Epidote in all fractures in KLX13A
Fractures with Epidote
Total number of fractures
Vertical depth (m.b.s.l)
Number of fractures / 10m vertical depth

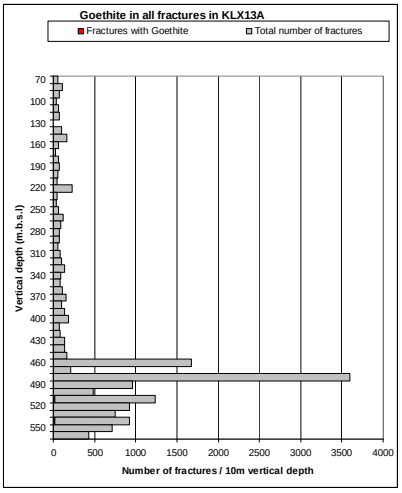
Goethite in all fractures in KLX13A
Fractures with Goethite
Total number of fractures
Vertical depth (m.b.s.l)
Number of fractures / 10m vertical depth

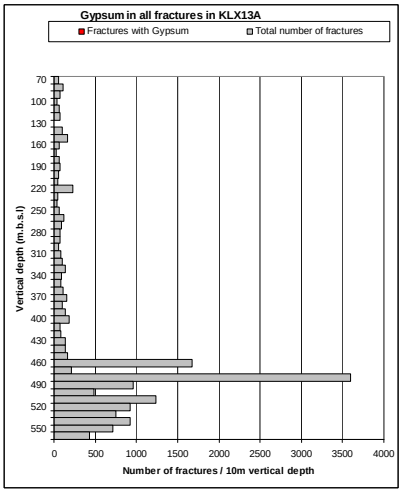
Gypsum in all fractures in KLX13A
Fractures with Gypsum
Total number of fractures
Vertical depth (m.b.s.l)
Number of fractures / 10m vertical depth

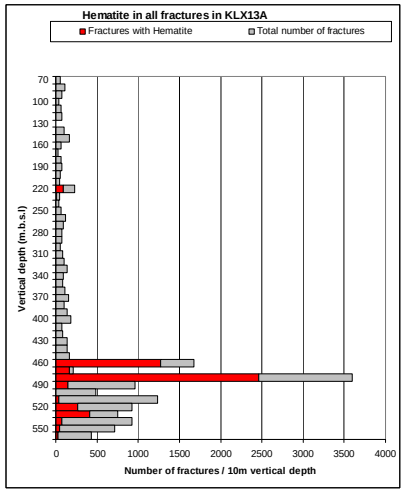
Hematite in all fractures in KLX13A
Fractures with Hematite
Total number of fractures
Vertical depth (m.b.s.l)
Number of fractures / 10m vertical depth

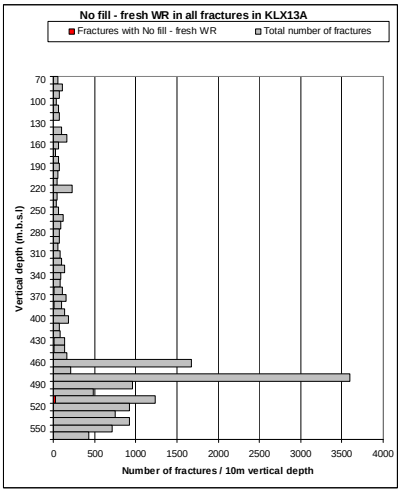
No fill - fresh WR in all fractures in KLX13A
Fractures with No fill - fresh WR
Total number of fractures
Vertical depth (m.b.s.l)
Number of fractures / 10m vertical depth

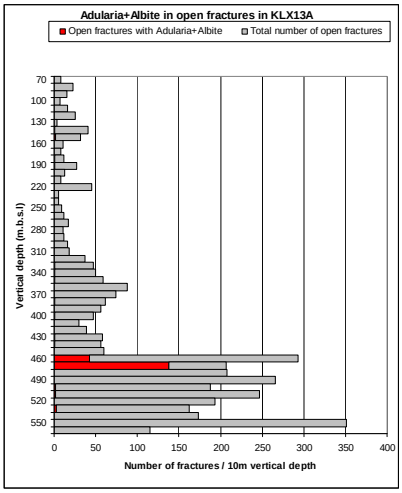
Adularia+Albite in open fractures in KLX13A
Open fractures with Adularia+Albite
Total number of open fractures
Vertical depth (m.b.s.l)
Number of fractures / 10m vertical depth

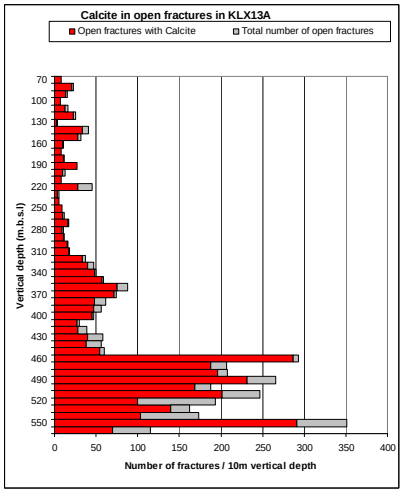
Calcite in open fractures in KLX13A
Open fractures with Calcite
Total number of open fractures
Vertical depth (m.b.s.l)
Number of fractures / 10m vertical depth

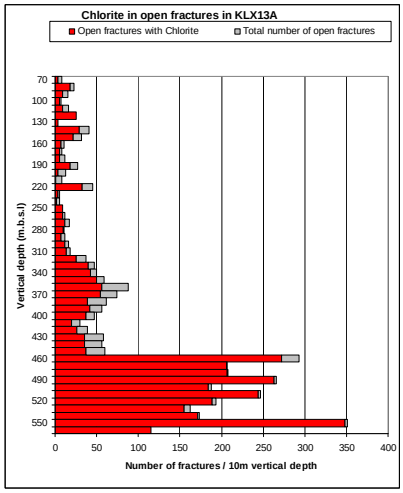
Chlorite in open fractures in KLX13A
Open fractures with Chlorite
Total number of open fractures
Vertical depth (m.b.s.l)
Number of fractures / 10m vertical depth

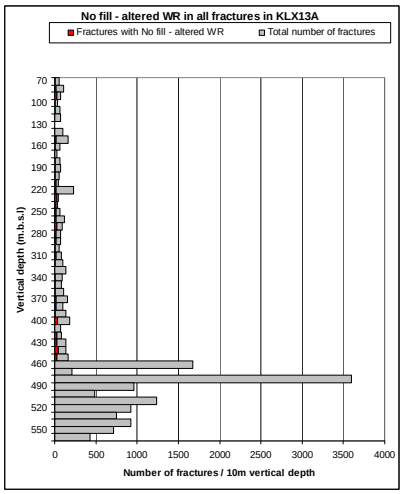
No fill - altered WR in all fractures in KLX13A
Fractures with No fill - altered WR
Total number of fractures
Vertical depth (m.b.s.l)
Number of fractures / 10m vertical depth

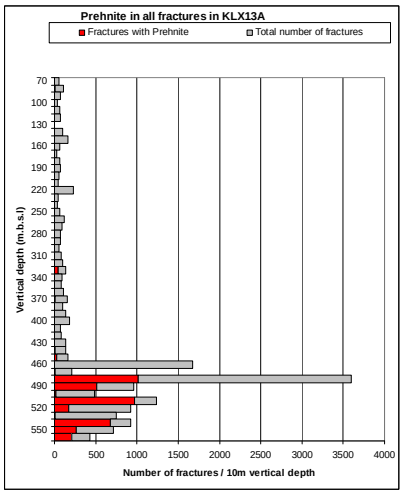
Prehnite in all fractures in KLX13A
Fractures with Prehnite
Total number of fractures
Vertical depth (m.b.s.l)
Number of fractures / 10m vertical depth

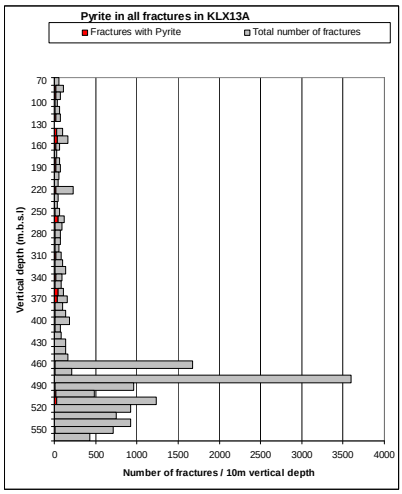
Pyrite in all fractures in KLX13A
Fractures with Pyrite
Total number of fractures
Vertical depth (m.b.s.l)
Number of fractures / 10m vertical depth

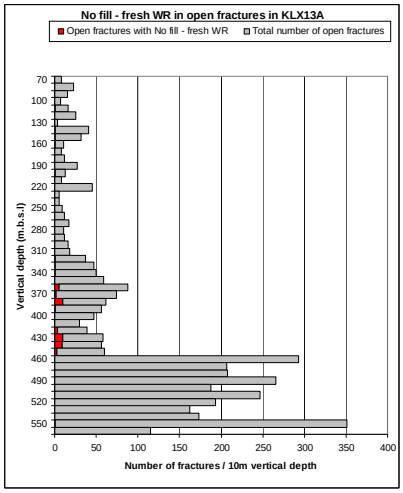
No fill - fresh WR in open fractures in KLX13A
Open fractures with No fill - fresh WR
Total number of open fractures
Vertical depth (m.b.s.l)
Number of fractures / 10m vertical depth

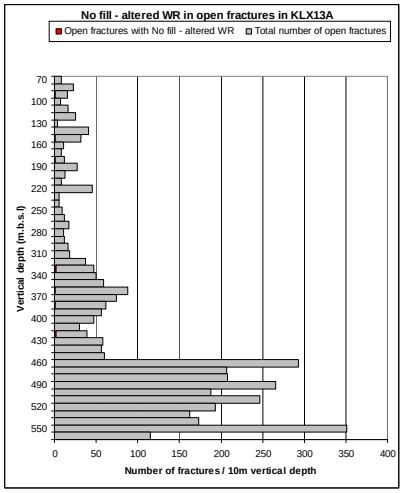
No fill - altered WR in open fractures in KLX13A
Open fractures with No fill - altered WR
Total number of open fractures
Vertical depth (m.b.s.l)
Number of fractures / 10m vertical depth

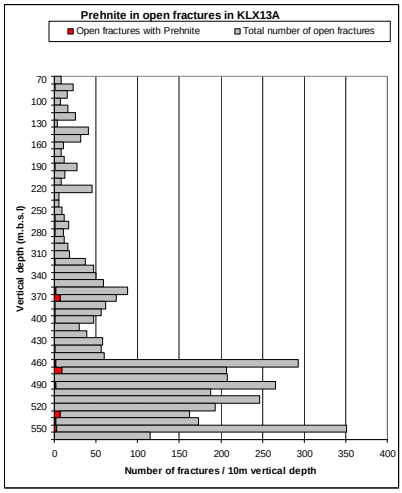
Prehnite in open fractures in KLX13A
Open fractures with Prehnite
Total number of open fractures
Vertical depth (m.b.s.l)
Number of fractures / 10m vertical depth

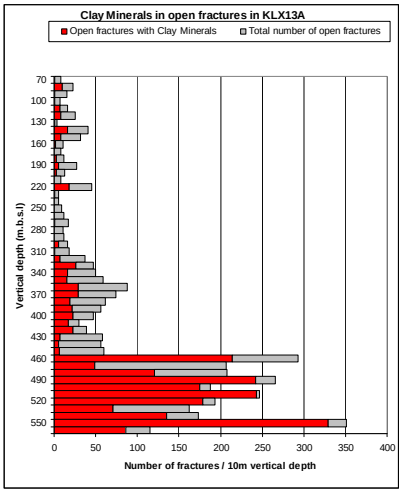
Clay Minerals in open fractures in KLX13A
Open fractures with Clay Minerals
Total number of open fractures
Vertical depth (m.b.s.l)
Number of fractures / 10m vertical depth

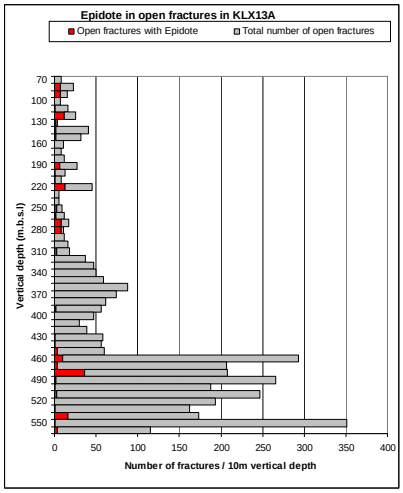
Epidote in open fractures in KLX13A
Open fractures with Epidote
Total number of open fractures
Vertical depth (m.b.s.l)
Number of fractures / 10m vertical depth

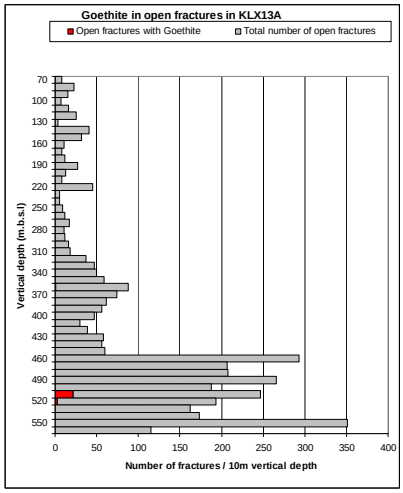
Goethite in open fractures in KLX13A
Open fractures with Goethite
Total number of open fractures
Vertical depth (m.b.s.l)
Number of fractures / 10m vertical depth

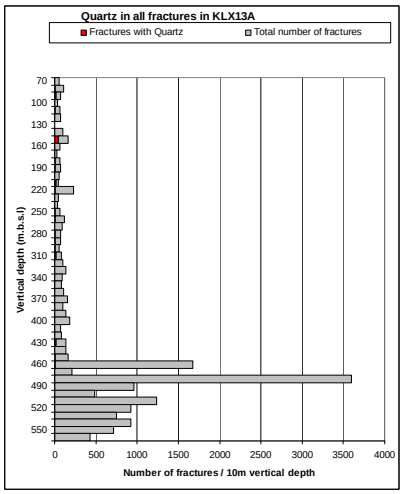
Quartz in all fractures in KLX13A
Fractures with Quartz
Total number of fractures
Vertical depth (m.b.s.l)
Number of fractures / 10m vertical depth

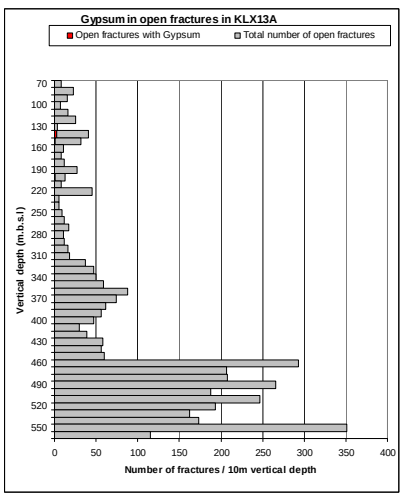
Gypsum in open fractures in KLX13A
Open fractures with Gypsum
Total number of open fractures
Vertical depth (m.b.s.l)
Number of fractures / 10m vertical depth

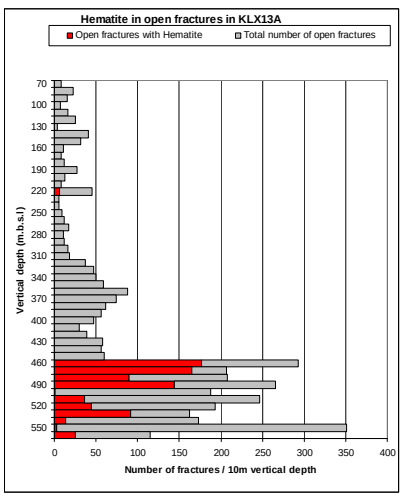
Hematite in open fractures in KLX13A
Open fractures with Hematite
Total number of open fractures
Vertical depth (m.b.s.l)
Number of fractures / 10m vertical depth

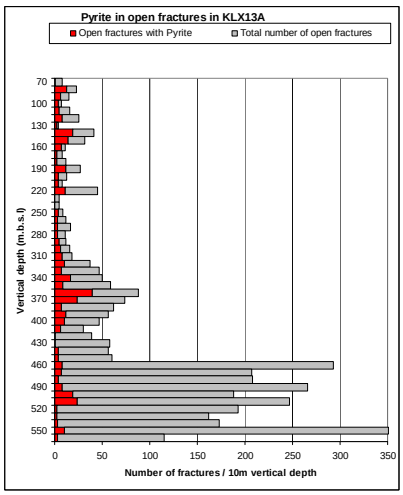
Pyrite in open fractures in KLX13A
Open fractures with Pyrite
Total number of open fractures
Vertical depth (m.b.s.l)
Number of fractures / 10m vertical depth

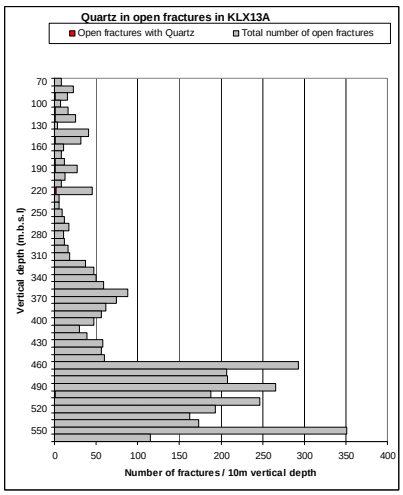
Quartz in open fractures in KLX13A
Open fractures with Quartz
Total number of open fractures
Vertical depth (m.b.s.l)
Number of fractures / 10m vertical depth

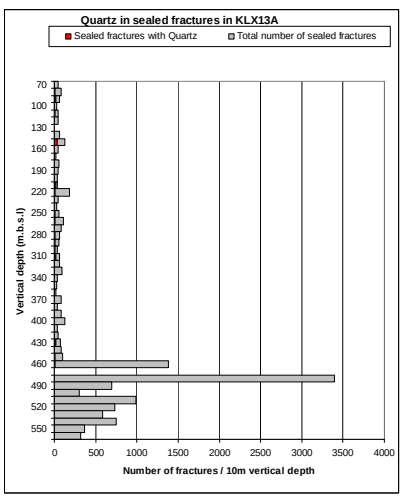
Quartz in sealed fractures in KLX13A
Sealed fractures with Quartz
Total number of sealed fractures
Vertical depth (m.b.s.l)
Number of fractures / 10m vertical depth

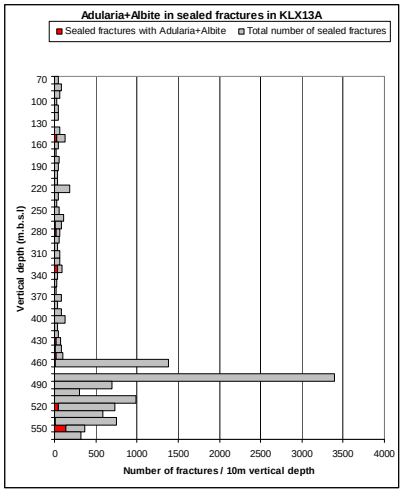
Adularia+Albite in sealed fractures in KLX13A
Sealed fractures with Adularia+Albite
Total number of sealed fractures
Vertical depth (m.b.s.l)
Number of fractures / 10m vertical depth

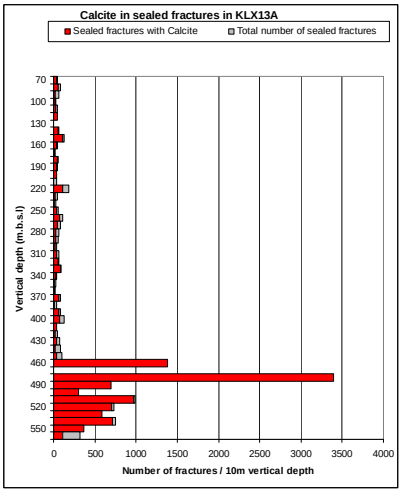
Calcite in sealed fractures in KLX13A
Sealed fractures with Calcite
Total number of sealed fractures
Vertical depth (m.b.s.l)
Number of fractures / 10m vertical depth

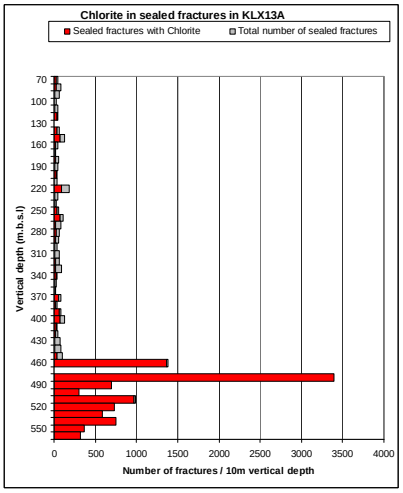
Chlorite in sealed fractures in KLX13A
Sealed fractures with Chlorite
Total number of sealed fractures
Vertical depth (m.b.s.l)
Number of fractures / 10m vertical depth

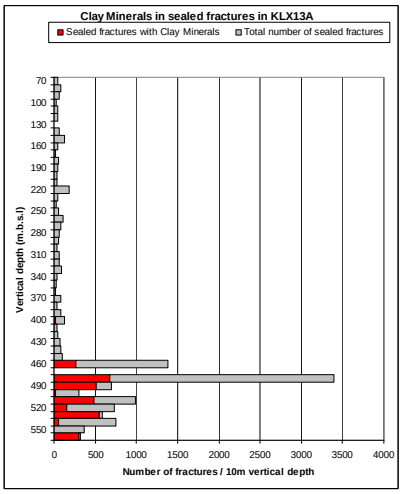
Clay Minerals in sealed fractures in KLX13A
Sealed fractures with Clay Minerals
Total number of sealed fractures
Vertical depth (m.b.s.l)
Number of fractures / 10m vertical depth

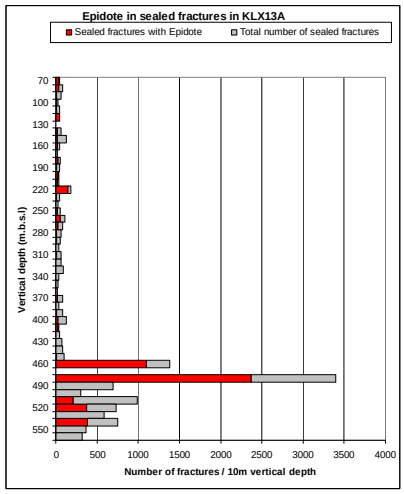
Epidote in sealed fractures in KLX13A
Sealed fractures with Epidote
Total number of sealed fractures
Vertical depth (m.b.s.l)
Number of fractures / 10m vertical depth

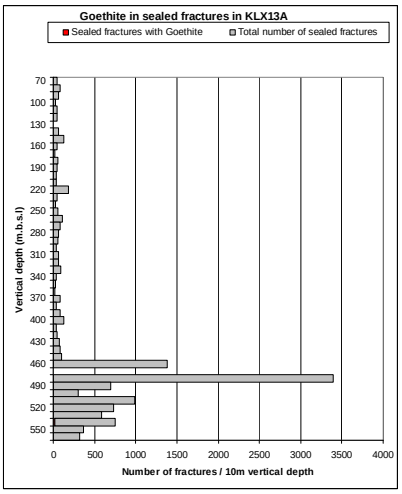
Goethite in sealed fractures in KLX13A
Sealed fractures with Goethite
Total number of sealed fractures
Vertical depth (m.b.s.l)
Number of fractures / 10m vertical depth

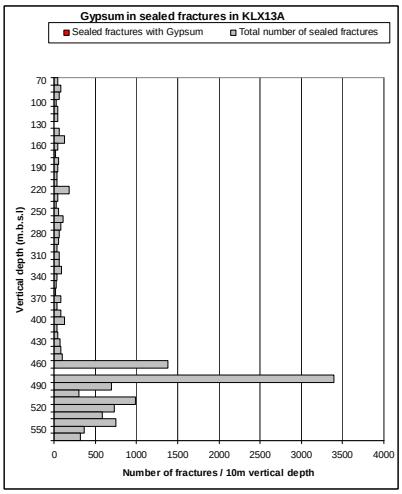
Gypsum in sealed fractures in KLX13A
Sealed fractures with Gypsum
Total number of sealed fractures
Vertical depth (m.b.s.l)
Number of fractures / 10m vertical depth

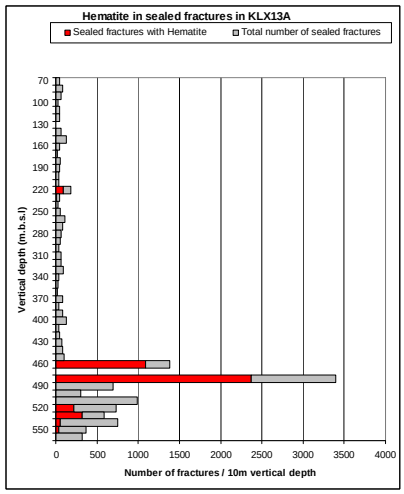
Hematite in sealed fractures in KLX13A
Sealed fractures with Hematite
Total number of sealed fractures
Vertical depth (m.b.s.l)
Number of fractures / 10m vertical depth

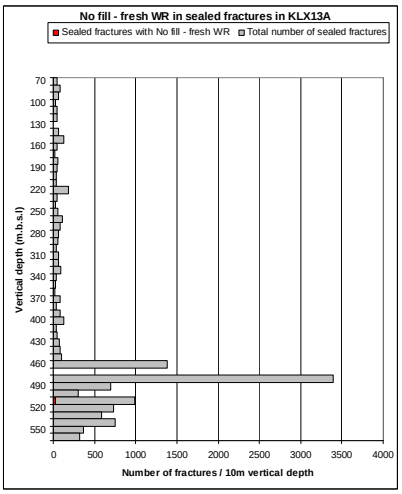
No fill - fresh WR in sealed fractures in KLX13A
Sealed fractures with No fill - fresh WR
Total number of sealed fractures
Vertical depth (m.b.s.l)
Number of fractures / 10m vertical depth

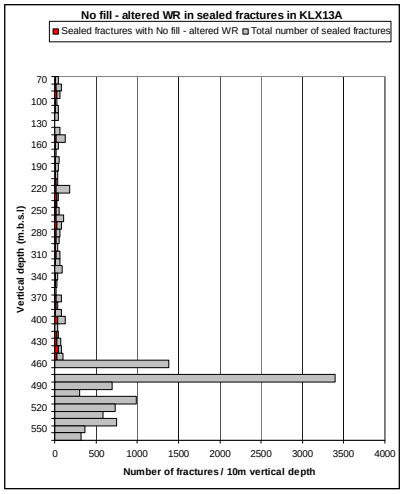
No fill - altered WR in sealed fractures in KLX13A
Sealed fractures with No fill - altered WR
Total number of sealed fractures
Vertical depth (m.b.s.l)
70
100
130
160
190
220
250
280
310
340
370
400
430
460
490
520
550
0
500
1000
1500
2000
2500
3000
3500
4000
Number of fractures / 10m vertical depth

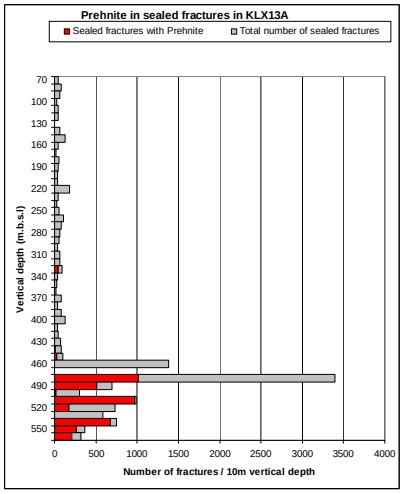
Prehnite in sealed fractures in KLX13A
Sealed fractures with Prehnite
Total number of sealed fractures
Vertical depth (m.b.s.l)
70
100
130
160
190
220
250
280
310
340
370
400
430
460
490
520
550
0
500
1000
1500
2000
2500
3000
3500
4000
Number of fractures / 10m vertical depth

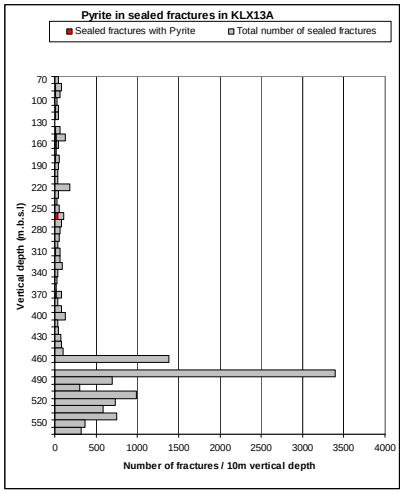
Pyrite in sealed fractures in KLX13A
Sealed fractures with Pyrite
Total number of sealed fractures
Vertical depth (m.b.s.l)
70
100
130
160
190
220
250
280
310
340
370
400
430
460
490
520
550
0
500
1000
1500
2000
2500
3000
3500
4000
Number of fractures / 10m vertical depth

KLX14A

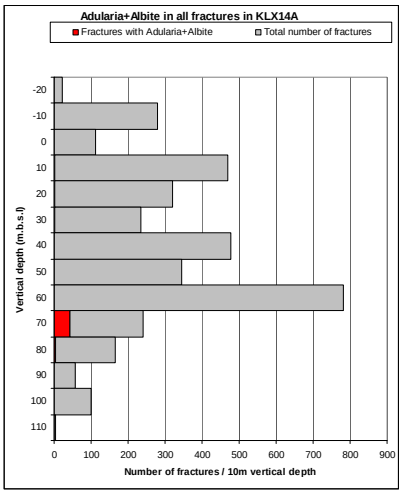
Adularia+Albite in all fractures in KLX14A
Fractures with Adularia+Albite
Total number of fractures
Vertical depth (m.b.s.l)
Number of fractures / 10m vertical depth

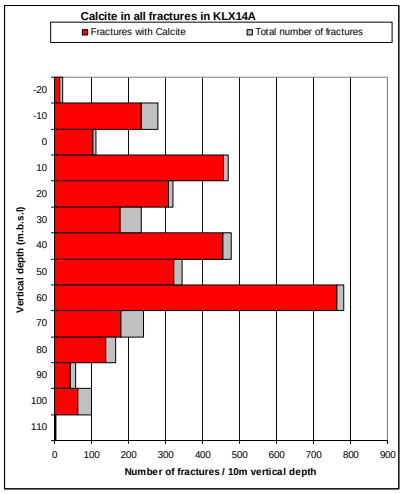
Calcite in all fractures in KLX14A
Fractures with Calcite
Total number of fractures
Vertical depth (m.b.s.l)
Number of fractures / 10m vertical depth

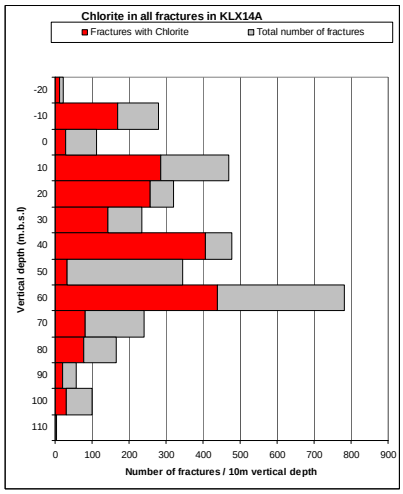
Chlorite in all fractures in KLX14A
Fractures with Chlorite
Total number of fractures
Vertical depth (m.b.s.l)
Number of fractures / 10m vertical depth

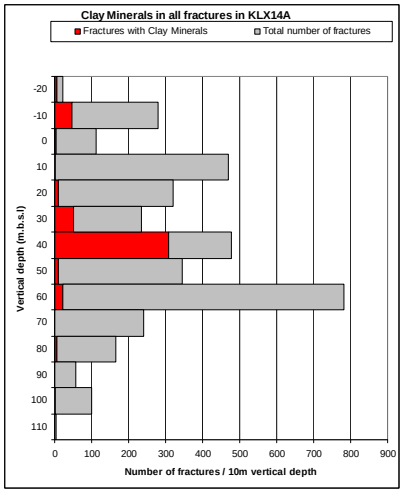
Clay Minerals in all fractures in KLX14A
Fractures with Clay Minerals
Total number of fractures
Vertical depth (m.b.s.l)
Number of fractures / 10m vertical depth

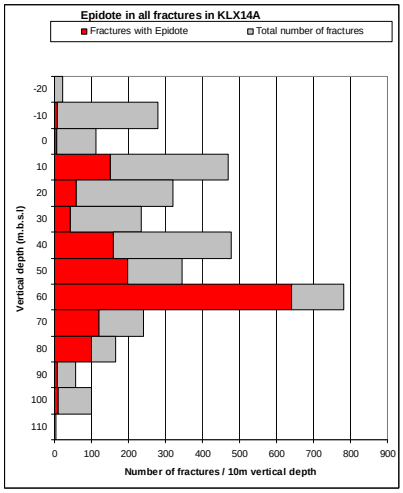
Epidote in all fractures in KLX14A
Fractures with Epidote
Total number of fractures
Vertical depth (m.b.s.l)
Number of fractures / 10m vertical depth

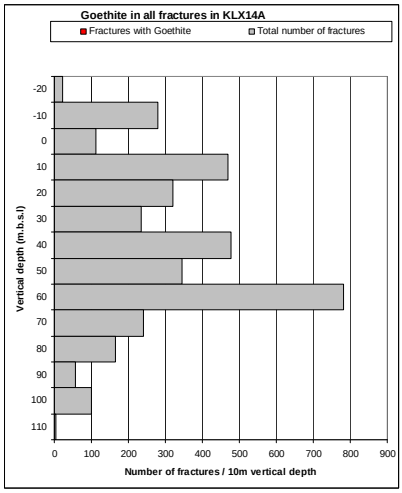
Goethite in all fractures in KLX14A
Fractures with Goethite
Total number of fractures
Vertical depth (m.b.s.l)
Number of fractures / 10m vertical depth

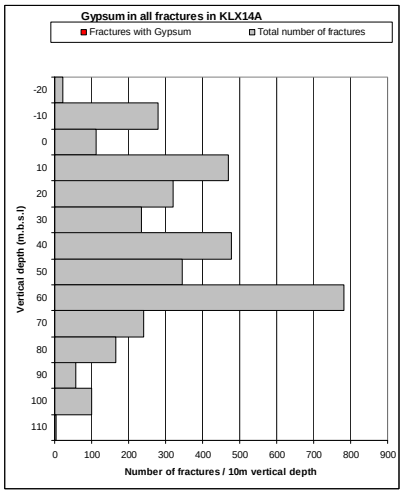
Gypsum in all fractures in KLX14A
Fractures with Gypsum
Total number of fractures
Vertical depth (m.b.s.l)
Number of fractures / 10m vertical depth

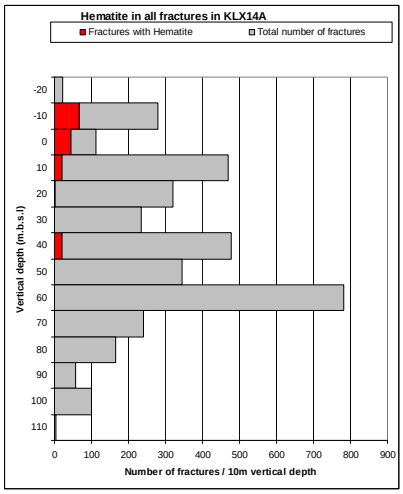
Hematite in all fractures in KLX14A
Fractures with Hematite
Total number of fractures
Vertical depth (m.b.s.l)
Number of fractures / 10m vertical depth

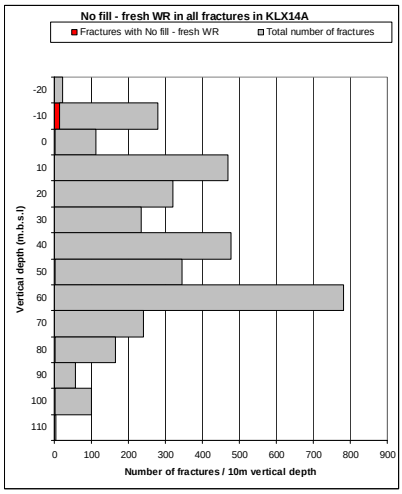
No fill - fresh WR in all fractures in KLX14A
Fractures with No fill - fresh WR
Total number of fractures
Vertical depth (m.b.s.l)
Number of fractures / 10m vertical depth

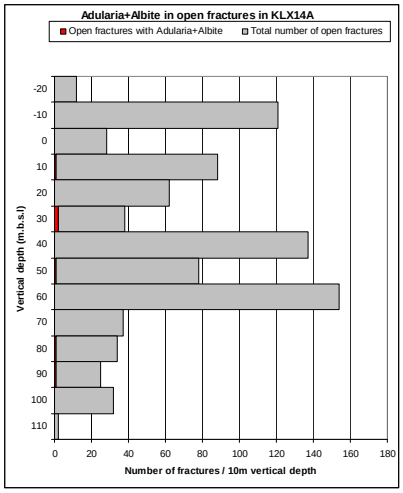
Adularia+Albite in open fractures in KLX14A
Open fractures with Adularia+Albite
Total number of open fractures
Vertical depth (m.b.s.l)
Number of fractures / 10m vertical depth

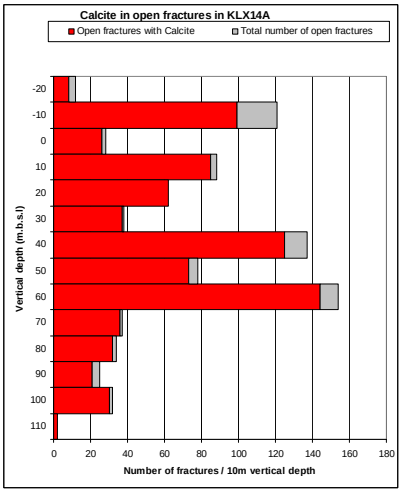
Calcite in open fractures in KLX14A
Open fractures with Calcite
Total number of open fractures
Vertical depth (m.b.s.l)
Number of fractures / 10m vertical depth

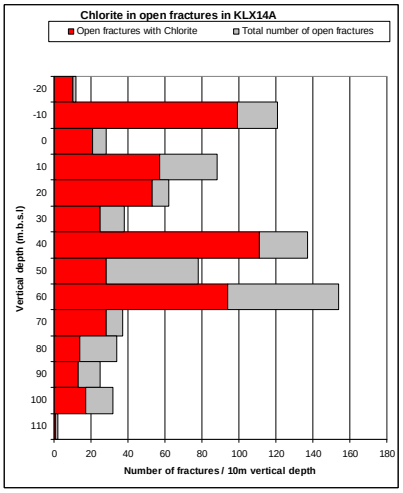
Chlorite in open fractures in KLX14A
Open fractures with Chlorite
Total number of open fractures
Vertical depth (m.b.s.l)
Number of fractures / 10m vertical depth

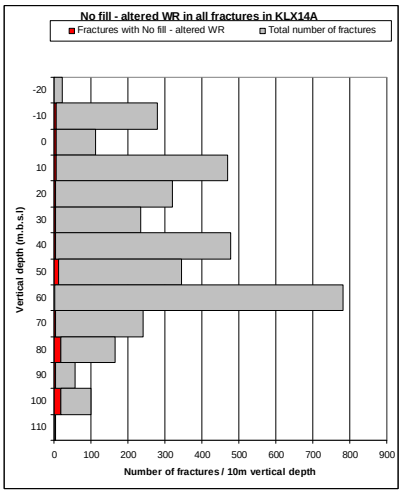
No fill - altered WR in all fractures in KLX14A
Fractures with No fill - altered WR
Total number of fractures
Vertical depth (m.b.s.l)
Number of fractures / 10m vertical depth

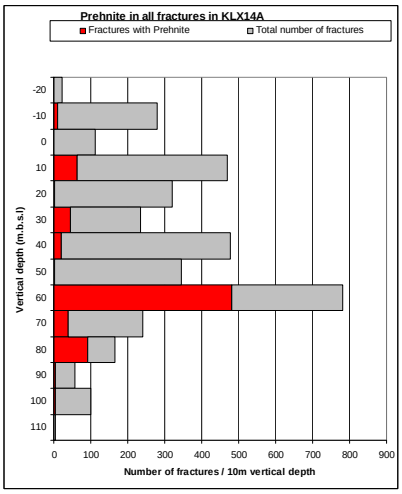
Prehnite in all fractures in KLX14A
Fractures with Prehnite
Total number of fractures
Vertical depth (m.b.s.l)
Number of fractures / 10m vertical depth

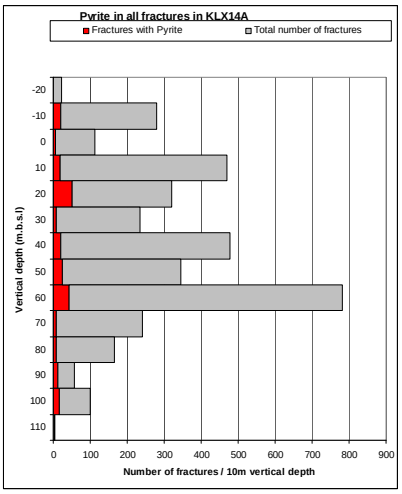
Pyrite in all fractures in KLX14A
Fractures with Pyrite
Total number of fractures
Vertical depth (m.b.s.l)
Number of fractures / 10m vertical depth

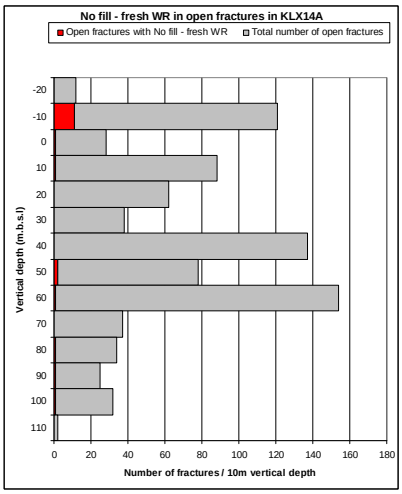
No fill - fresh WR in open fractures in KLX14A
Open fractures with No fill - fresh WR
Total number of open fractures
Vertical depth (m.b.s.l)
Number of fractures / 10m vertical depth

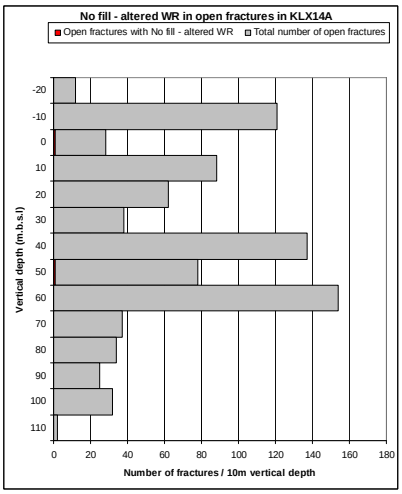
No fill - altered WR in open fractures in KLX14A
Open fractures with No fill - altered WR
Total number of open fractures
Vertical depth (m.b.s.l)
Number of fractures / 10m vertical depth

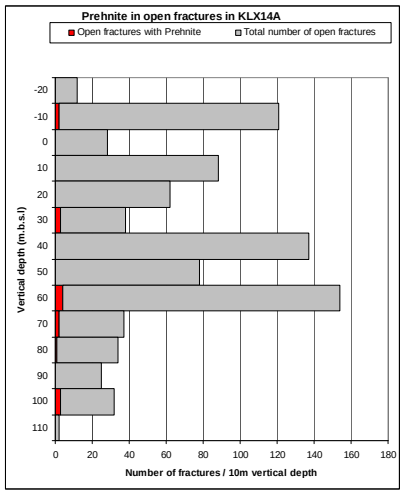
Prehnite in open fractures in KLX14A
Open fractures with Prehnite
Total number of open fractures
Vertical depth (m.b.s.l)
Number of fractures / 10m vertical depth

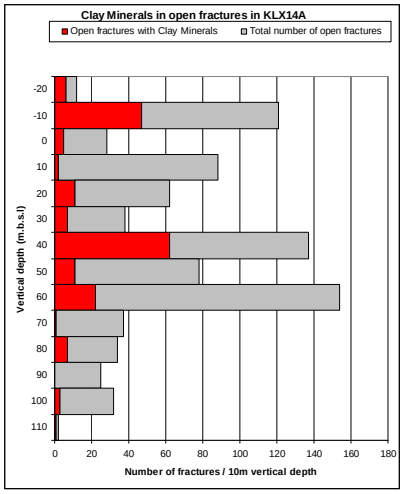
Clay Minerals in open fractures in KLX14A
Open fractures with Clay Minerals
Total number of open fractures
Vertical depth (m.b.s.l)
Number of fractures / 10m vertical depth

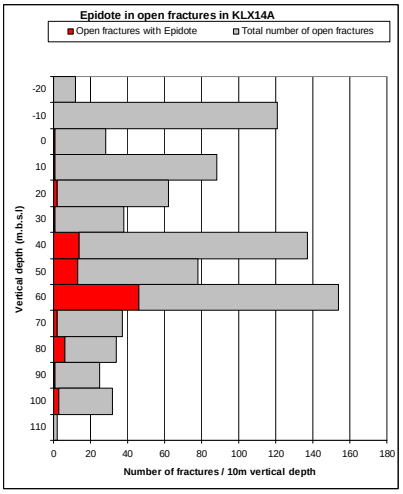
Epidote in open fractures in KLX14A
Open fractures with Epidote
Total number of open fractures
Vertical depth (m.b.s.l)
Number of fractures / 10m vertical depth

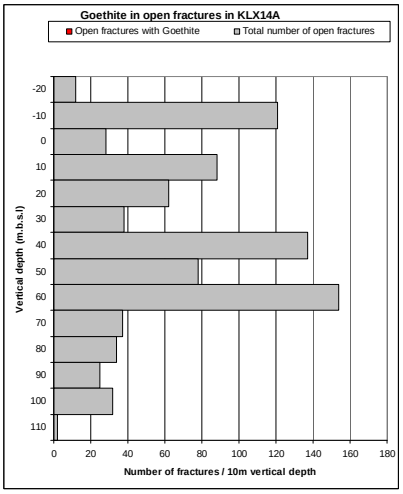
Goethite in open fractures in KLX14A
Open fractures with Goethite
Total number of open fractures
Vertical depth (m.b.s.l)
Number of fractures / 10m vertical depth

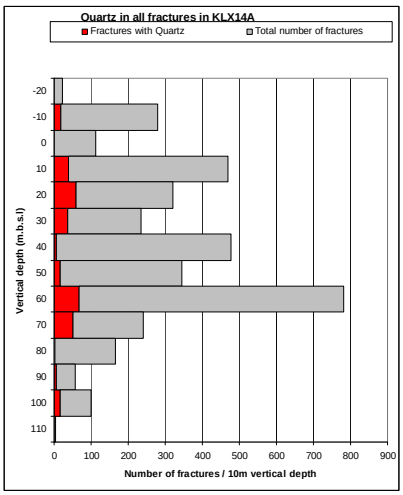
Quartz in all fractures in KLX14A
Fractures with Quartz
Total number of fractures
Vertical depth (m.b.s.l)
Number of fractures / 10m vertical depth

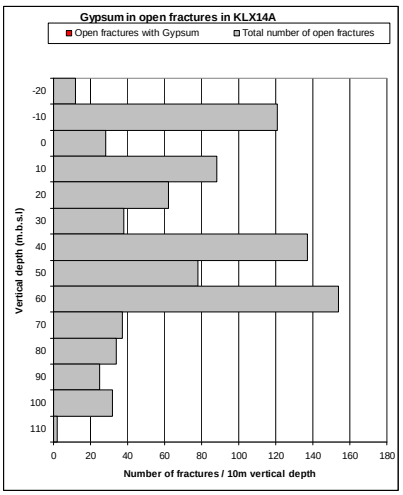
Gypsum in open fractures in KLX14A
Open fractures with Gypsum
Total number of open fractures
Vertical depth (m.b.s.l)
Number of fractures / 10m vertical depth

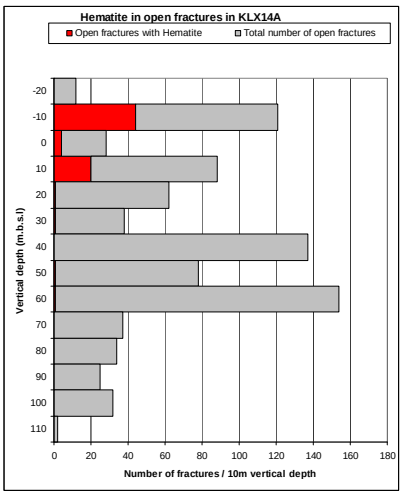
Hematite in open fractures in KLX14A
Open fractures with Hematite
Total number of open fractures
Vertical depth (m.b.s.l)
Number of fractures / 10m vertical depth

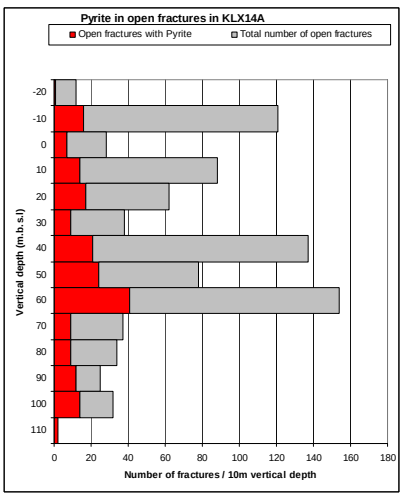
Pyrite in open fractures in KLX14A
Open fractures with Pyrite
Total number of open fractures
Vertical depth (m.b.s.l)
Number of fractures / 10m vertical depth

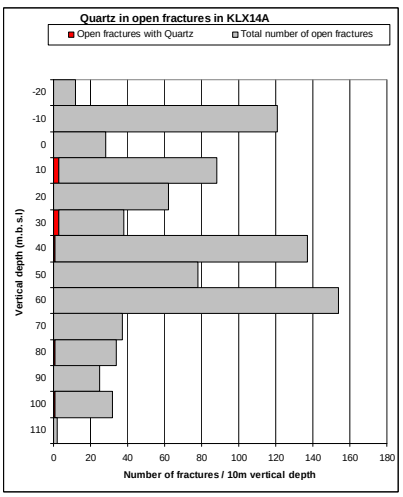
Quartz in open fractures in KLX14A
Open fractures with Quartz
Total number of open fractures
Vertical depth (m.b.s.l)
Number of fractures / 10m vertical depth

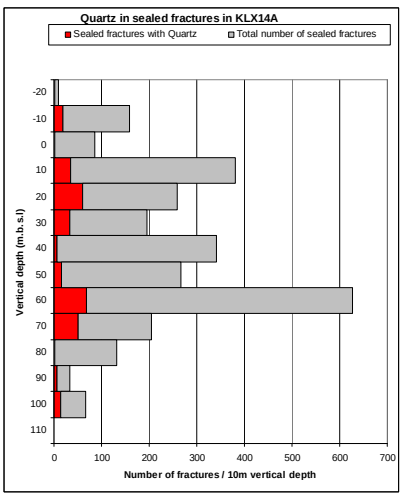
Quartz in sealed fractures in KLX14A
Sealed fractures with Quartz
Total number of sealed fractures
Vertical depth (m.b.s.l)
Number of fractures / 10m vertical depth

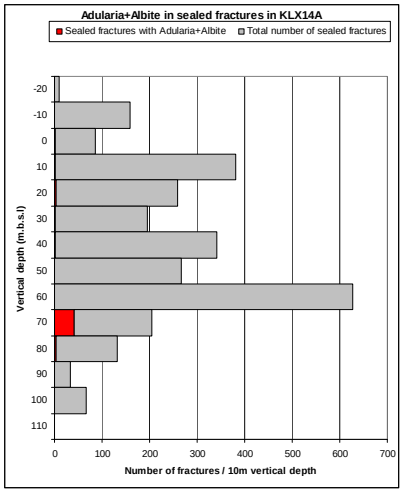
Adularia+Albite in sealed fractures in KLX14A
Sealed fractures with Adularia+Albite
Total number of sealed fractures
Vertical depth (m.b.s.l)
Number of fractures / 10m vertical depth

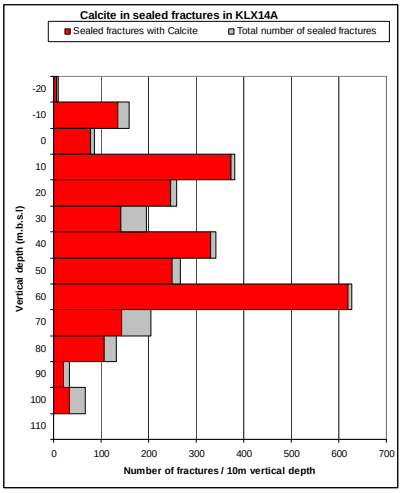
Calcite in sealed fractures in KLX14A
Sealed fractures with Calcite
Total number of sealed fractures
Vertical depth (m.b.s.l)
Number of fractures / 10m vertical depth

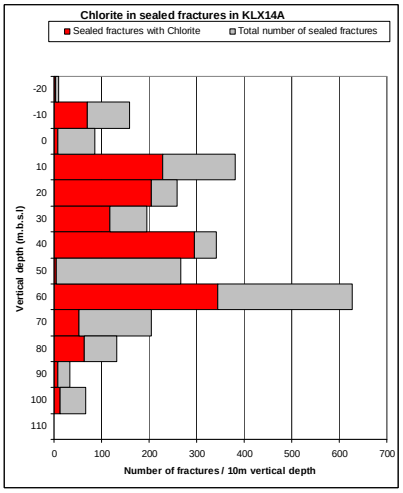
Chlorite in sealed fractures in KLX14A
Sealed fractures with Chlorite
Total number of sealed fractures
Vertical depth (m.b.s.l)
Number of fractures / 10m vertical depth

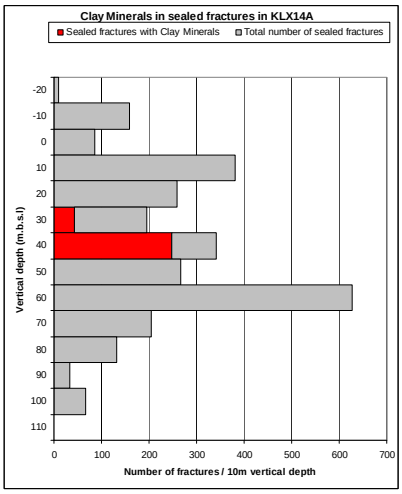
Clay Minerals in sealed fractures in KLX14A
Sealed fractures with Clay Minerals
Total number of sealed fractures
Vertical depth (m.b.s.l)
Number of fractures / 10m vertical depth

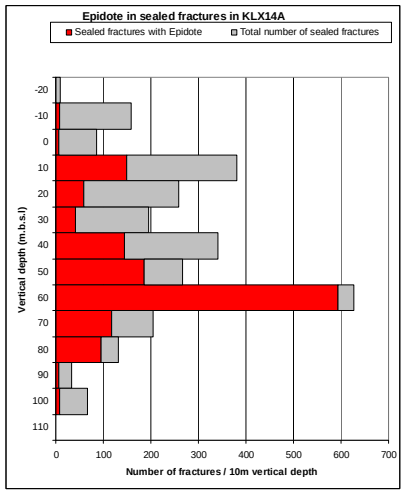
Epidote in sealed fractures in KLX14A
Sealed fractures with Epidote
Total number of sealed fractures
Vertical depth (m.b.s.l)
Number of fractures / 10m vertical depth

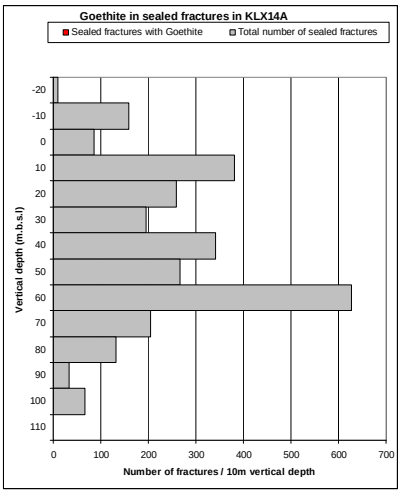
Goethite in sealed fractures in KLX14A
Sealed fractures with Goethite
Total number of sealed fractures
Vertical depth (m.b.s.l)
Number of fractures / 10m vertical depth

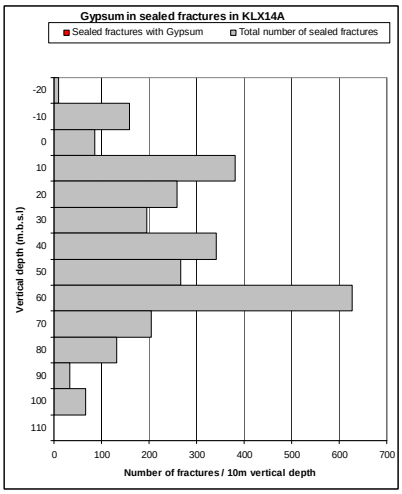
Gypsum in sealed fractures in KLX14A
Sealed fractures with Gypsum
Total number of sealed fractures
Vertical depth (m.b.s.l)
Number of fractures / 10m vertical depth

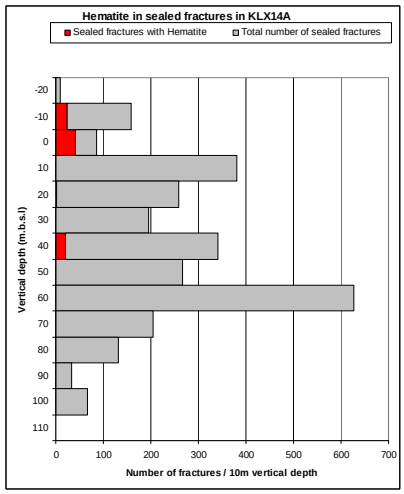
Hematite in sealed fractures in KLX14A
Sealed fractures with Hematite
Total number of sealed fractures
Vertical depth (m.b.s.l)
Number of fractures / 10m vertical depth

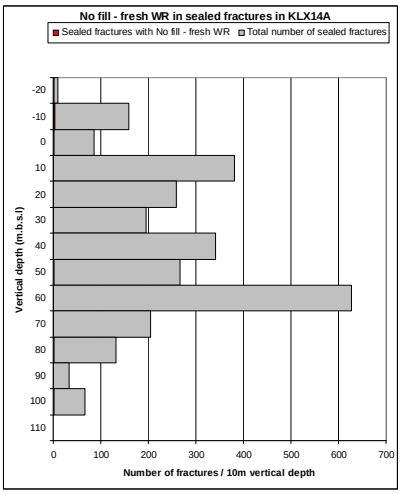
No fill - fresh WR in sealed fractures in KLX14A
Sealed fractures with No fill - fresh WR
Total number of sealed fractures
Vertical depth (m.b.s.l)
Number of fractures / 10m vertical depth

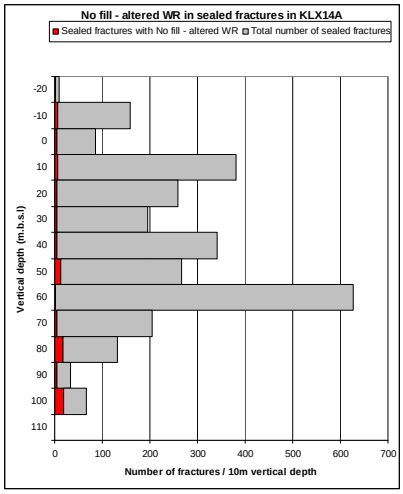
No fill - altered WR in sealed fractures in KLX14A
Sealed fractures with No fill - altered WR
Total number of sealed fractures
Vertical depth (m.b.s.l)
-20
-10
0
10
20
30
40
50
60
70
80
90
100
110
0
100
200
300
400
500
600
700
Number of fractures / 10m vertical depth

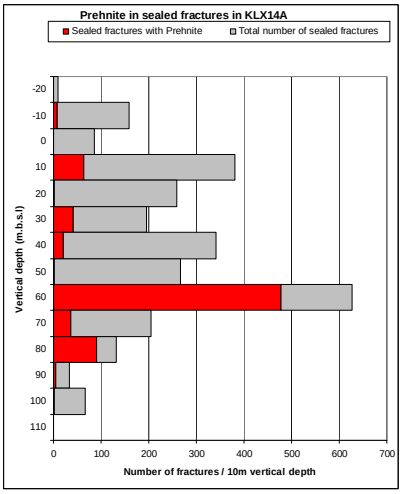
Prehnite in sealed fractures in KLX14A
Sealed fractures with Prehnite
Total number of sealed fractures
Vertical depth (m.b.s.l)
-20
-10
0
10
20
30
40
50
60
70
80
90
100
110
0
100
200
300
400
500
600
700
Number of fractures / 10m vertical depth

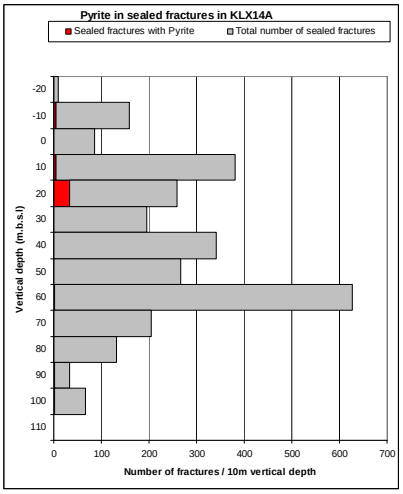
Pyrite in sealed fractures in KLX14A
Sealed fractures with Pyrite
Total number of sealed fractures
Vertical depth (m.b.s.l)
-20
-10
0
10
20
30
40
50
60
70
80
90
100
110
0
100
200
300
400
500
600
700
Number of fractures / 10m vertical depth

KLX15A

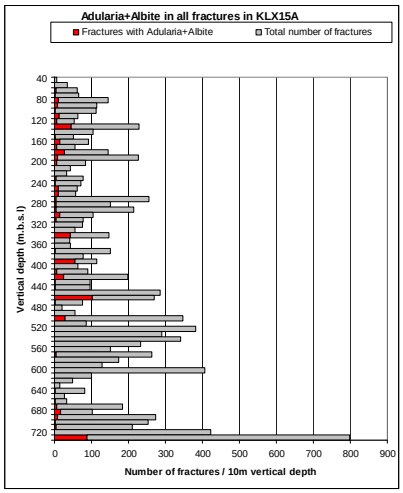
Adularia+Albite in all fractures in KLX15A
Fractures with Adularia+Albite
Total number of fractures
Vertical depth (m.b.s.l)
Number of fractures / 10m vertical depth

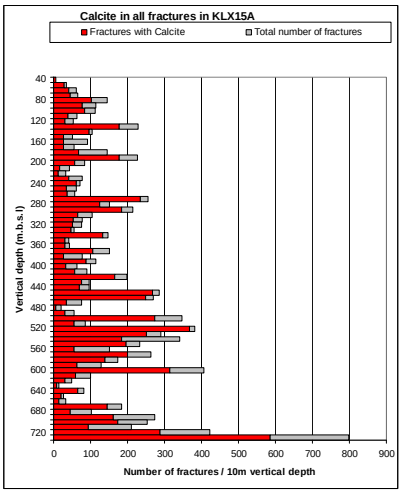
Calcite in all fractures in KLX15A
Fractures with Calcite
Total number of fractures
Vertical depth (m.b.s.l)
Number of fractures / 10m vertical depth

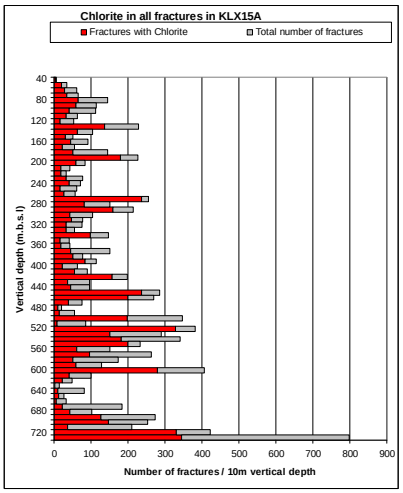
Chlorite in all fractures in KLX15A
Fractures with Chlorite
Total number of fractures
Vertical depth (m.b.s.l)
Number of fractures / 10m vertical depth

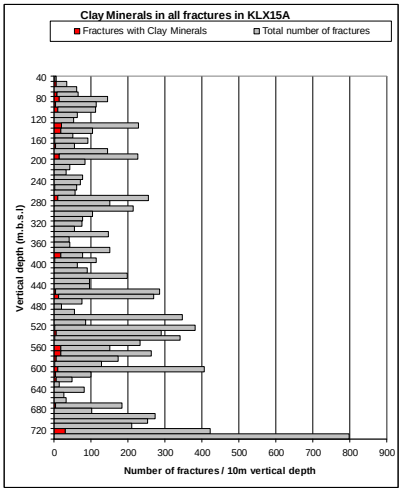
Clay Minerals in all fractures in KLX15A
Fractures with Clay Minerals
Total number of fractures
Vertical depth (m.b.s.l)
Number of fractures / 10m vertical depth

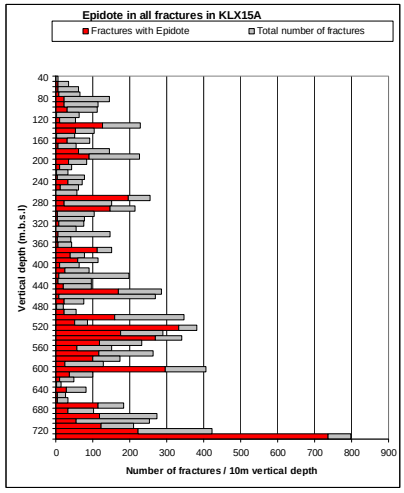
Epidote in all fractures in KLX15A
Fractures with Epidote
Total number of fractures
Vertical depth (m.b.s.l)
Number of fractures / 10m vertical depth

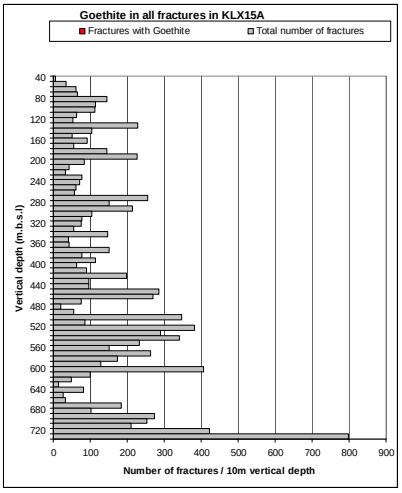
Goethite in all fractures in KLX15A
Fractures with Goethite
Total number of fractures
Vertical depth (m.b.s.l)
Number of fractures / 10m vertical depth

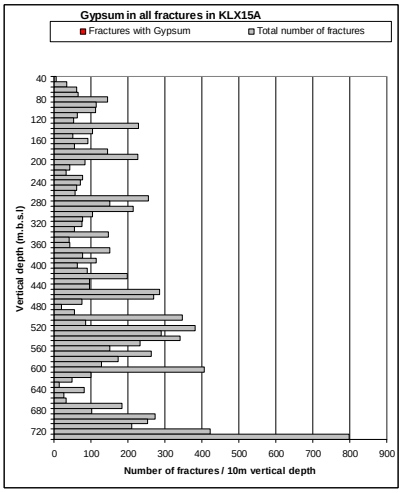
Gypsum in all fractures in KLX15A
Fractures with Gypsum
Total number of fractures
Vertical depth (m.b.s.l)
Number of fractures / 10m vertical depth

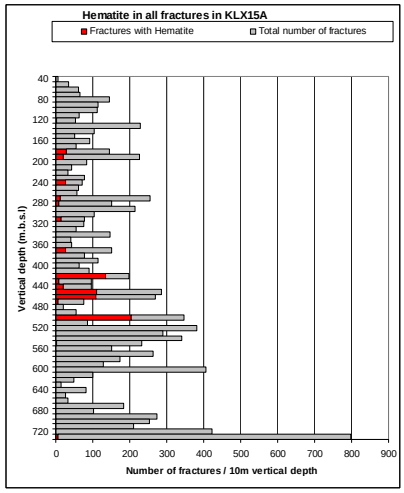
Hematite in all fractures in KLX15A
Fractures with Hematite
Total number of fractures
Vertical depth (m.b.s.l)
Number of fractures / 10m vertical depth

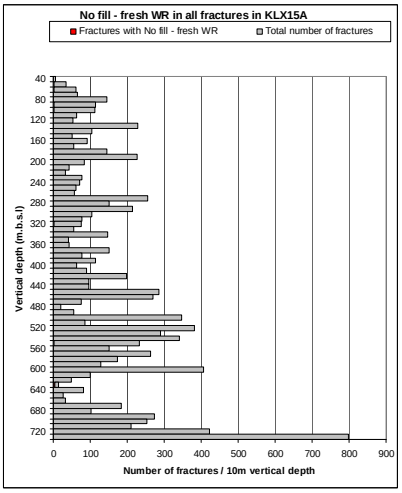
No fill - fresh WR in all fractures in KLX15A
Fractures with No fill - fresh WR
Total number of fractures
Vertical depth (m.b.s.l)
Number of fractures / 10m vertical depth

i

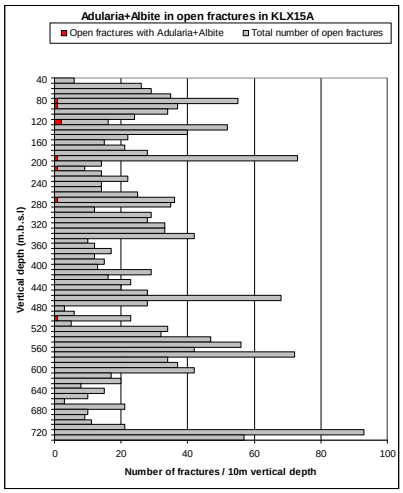
Adularia+Albite in open fractures in KLX15A
Open fractures with Adularia+Albite
Total number of open fractures
Vertical depth (m.b.s.l)
Number of fractures / 10m vertical depth

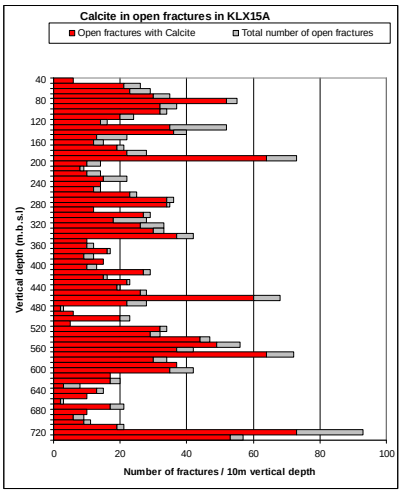
Calcite in open fractures in KLX15A
Open fractures with Calcite
Total number of open fractures
Vertical depth (m.b.s.l)
Number of fractures / 10m vertical depth

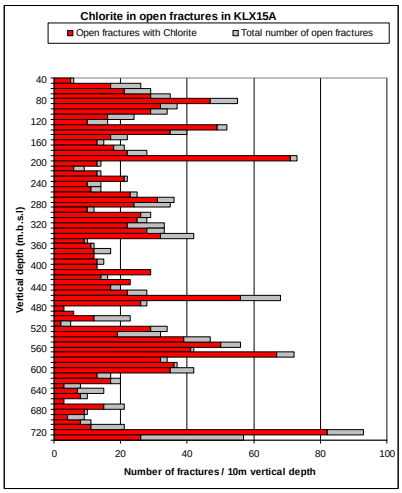
Chlorite in open fractures in KLX15A
Open fractures with Chlorite
Total number of open fractures
Vertical depth (m.b.s.l)
Number of fractures / 10m vertical depth

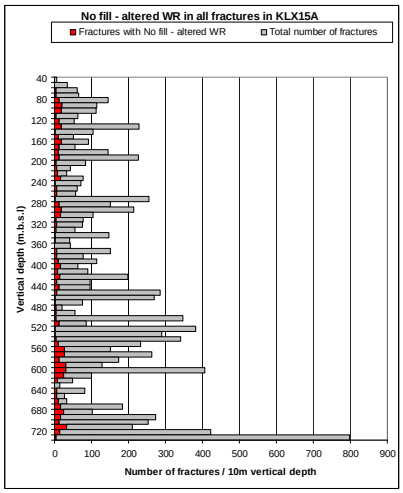
No fill - altered WR in all fractures in KLX15A
Fractures with No fill - altered WR
Total number of fractures
Vertical depth (m.b.s.l)
Number of fractures / 10m vertical depth

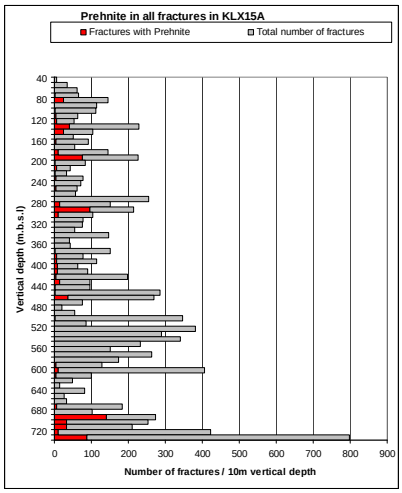
Prehnite in all fractures in KLX15A
Fractures with Prehnite
Total number of fractures
Vertical depth (m.b.s.l)
Number of fractures / 10m vertical depth

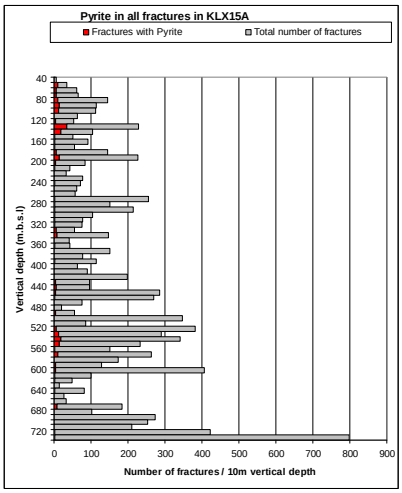
Pyrite in all fractures in KLX15A
Fractures with Pyrite
Total number of fractures
Vertical depth (m.b.s.l)
Number of fractures / 10m vertical depth

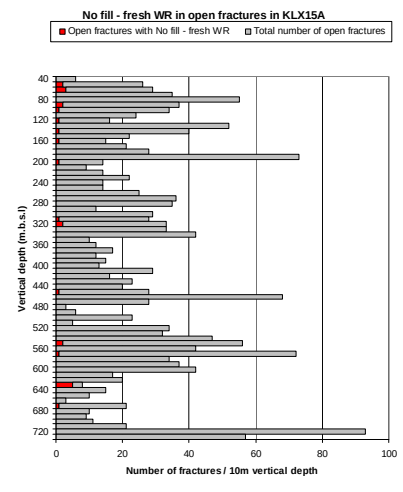
No fill - fresh WR in open fractures in KLX15A
Open fractures with No fill - fresh WR
Total number of open fractures
Vertical depth (m.b.s.l)
Number of fractures / 10m vertical depth

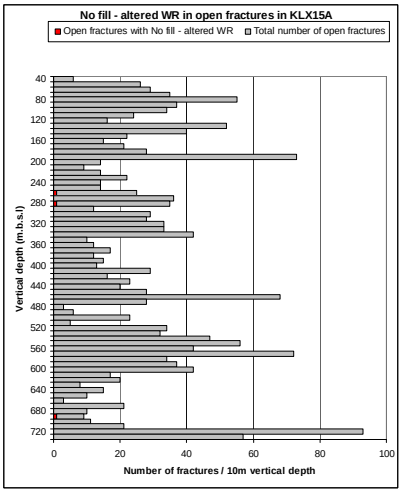
No fill - altered WR in open fractures in KLX15A
Open fractures with No fill - altered WR
Total number of open fractures
Vertical depth (m.b.s.l)
Number of fractures / 10m vertical depth

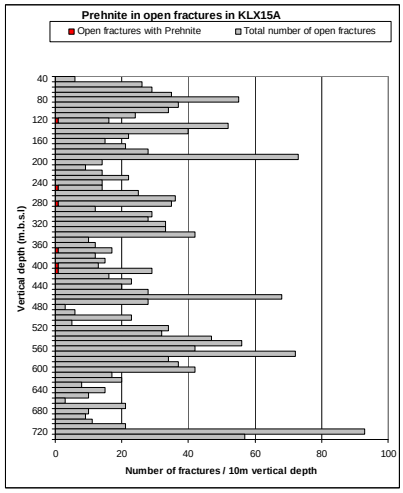
Prehnite in open fractures in KLX15A
Open fractures with Prehnite
Total number of open fractures
Vertical depth (m.b.s.l)
Number of fractures / 10m vertical depth

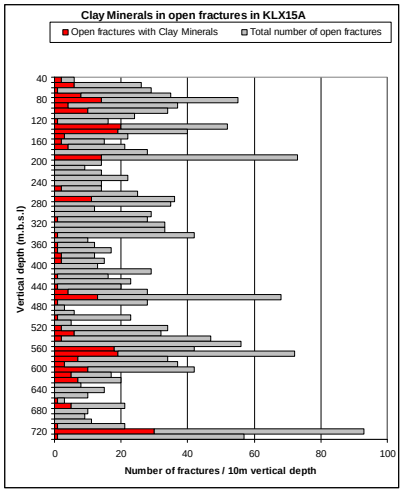
Clay Minerals in open fractures in KLX15A
Open fractures with Clay Minerals
Total number of open fractures
Vertical depth (m.b.s.l)
Number of fractures / 10m vertical depth

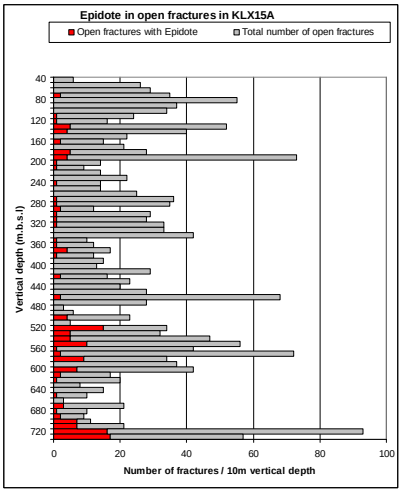
Epidote in open fractures in KLX15A
Open fractures with Epidote
Total number of open fractures
Vertical depth (m.b.s.l)
Number of fractures / 10m vertical depth

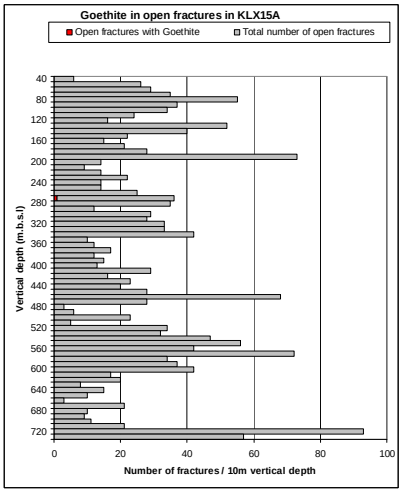
Goethite in open fractures in KLX15A
Open fractures with Goethite
Total number of open fractures
Vertical depth (m.b.s.l)
Number of fractures / 10m vertical depth

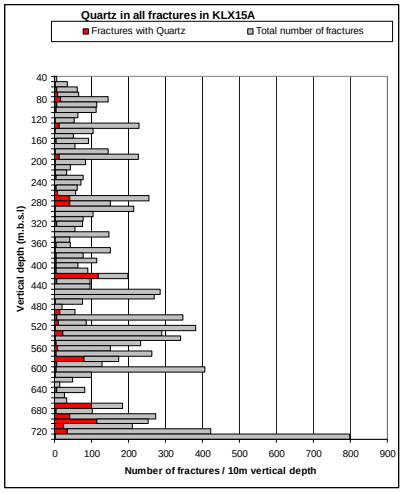
Quartz in all fractures in KLX15A
Fractures with Quartz
Total number of fractures
Vertical depth (m.b.s.l)
Number of fractures / 10m vertical depth

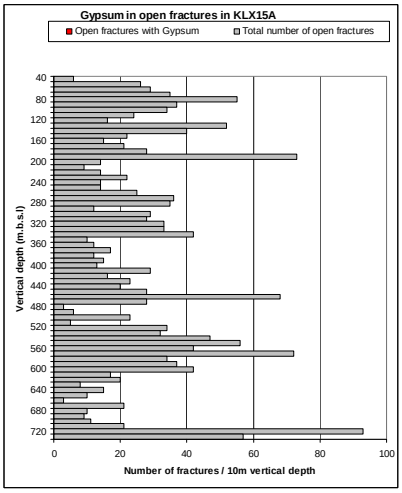
Gypsum in open fractures in KLX15A
Open fractures with Gypsum
Total number of open fractures
Vertical depth (m.b.s.l)
Number of fractures / 10m vertical depth

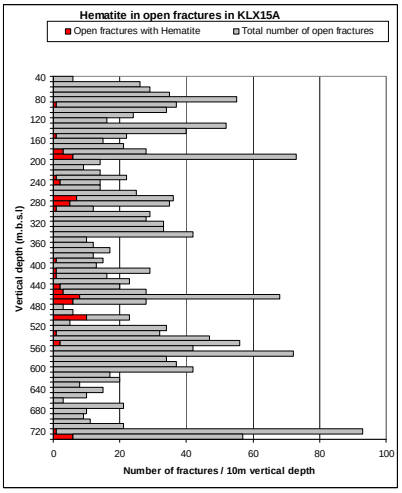
Hematite in open fractures in KLX15A
Open fractures with Hematite
Total number of open fractures
Vertical depth (m.b.s.l)
Number of fractures / 10m vertical depth

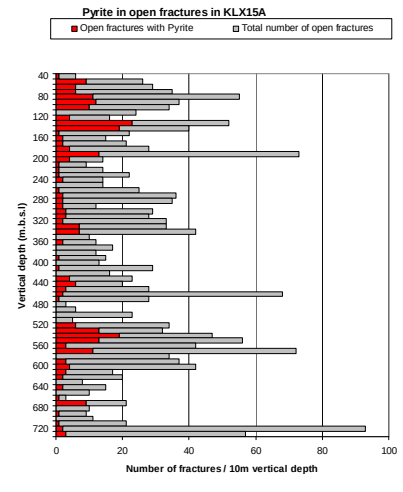
Pyrite in open fractures in KLX15A
Open fractures with Pyrite
Total number of open fractures
Vertical depth (m.b.s.l)
Number of fractures / 10m vertical depth

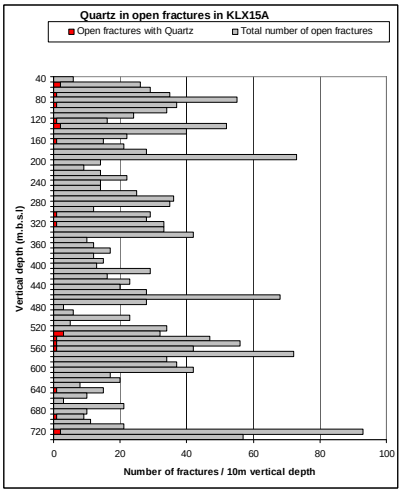
Quartz in open fractures in KLX15A
Open fractures with Quartz
Total number of open fractures
Vertical depth (m.b.s.l)
Number of fractures / 10m vertical depth

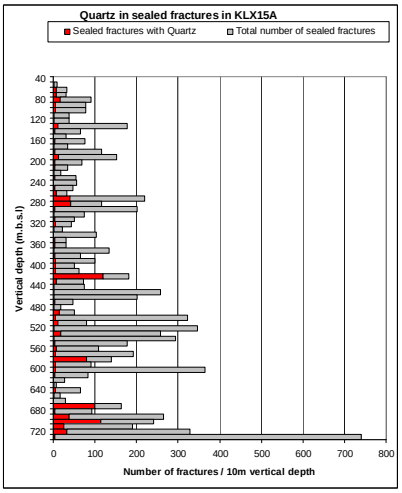
Quartz in sealed fractures in KLX15A
Sealed fractures with Quartz
Total number of sealed fractures
Vertical depth (m.b.s.l)
Number of fractures / 10m vertical depth

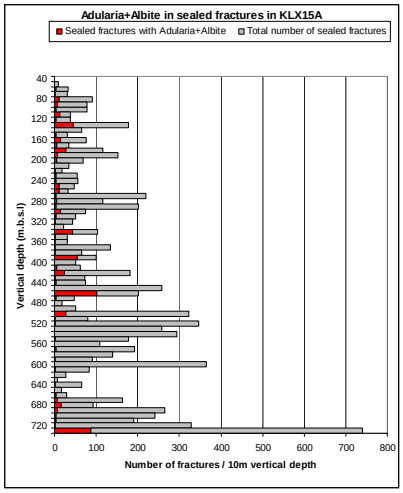
Adularia+Albite in sealed fractures in KLX15A
Sealed fractures with Adularia+Albite
Total number of sealed fractures
Vertical depth (m.b.s.l)
Number of fractures / 10m vertical depth

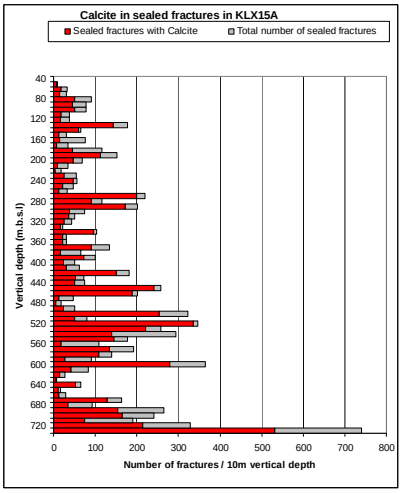
Calcite in sealed fractures in KLX15A
Sealed fractures with Calcite
Total number of sealed fractures
Vertical depth (m.b.s.l)
Number of fractures / 10m vertical depth

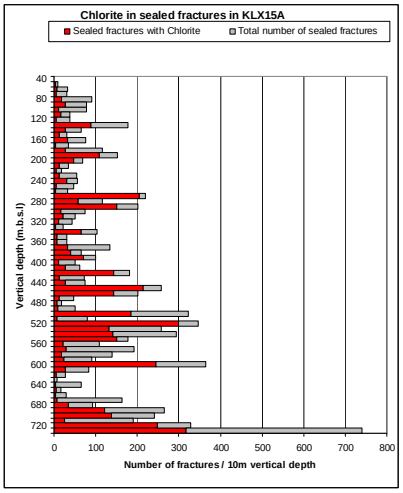
Chlorite in sealed fractures in KLX15A
Sealed fractures with Chlorite
Total number of sealed fractures
Vertical depth (m.b.s.l)
Number of fractures / 10m vertical depth

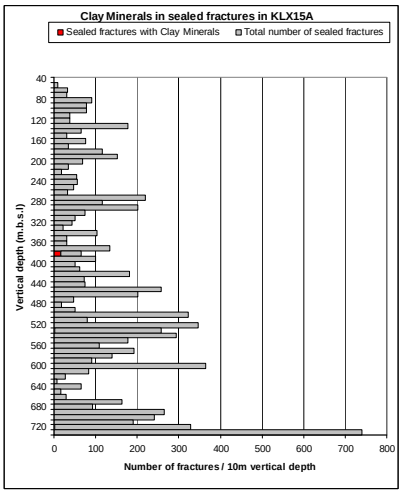
Clay Minerals in sealed fractures in KLX15A
Sealed fractures with Clay Minerals
Total number of sealed fractures
Vertical depth (m.b.s.l)
Number of fractures / 10m vertical depth

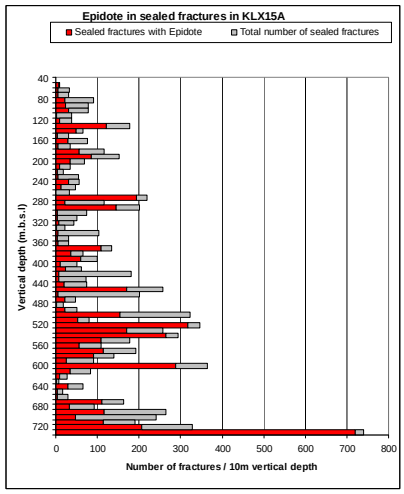
Epidote in sealed fractures in KLX15A
Sealed fractures with Epidote
Total number of sealed fractures
Vertical depth (m.b.s.l)
Number of fractures / 10m vertical depth

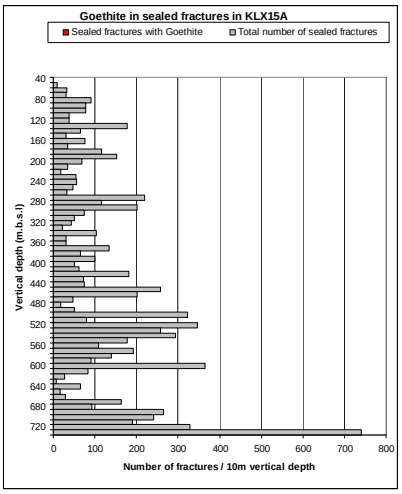
Goethite in sealed fractures in KLX15A
Sealed fractures with Goethite
Total number of sealed fractures
Vertical depth (m.b.s.l)
Number of fractures / 10m vertical depth

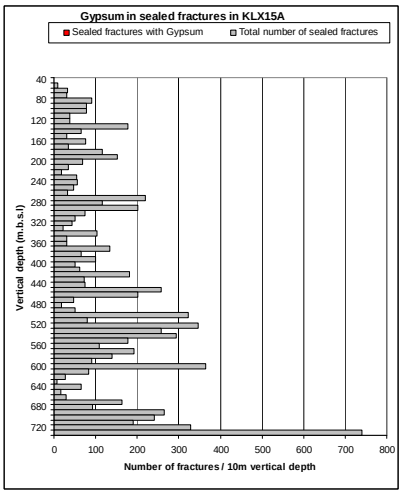
Gypsum in sealed fractures in KLX15A
Sealed fractures with Gypsum
Total number of sealed fractures
Vertical depth (m.b.s.l)
Number of fractures / 10m vertical depth

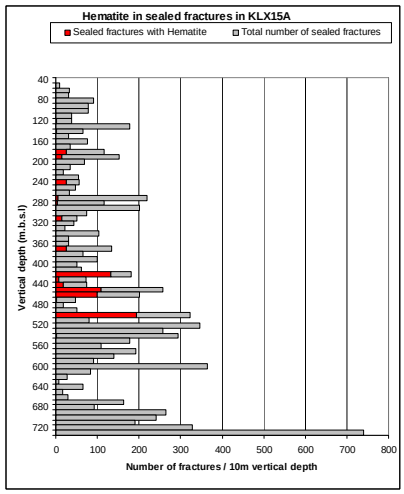
Hematite in sealed fractures in KLX15A
Sealed fractures with Hematite
Total number of sealed fractures
Vertical depth (m.b.s.l)
Number of fractures / 10m vertical depth

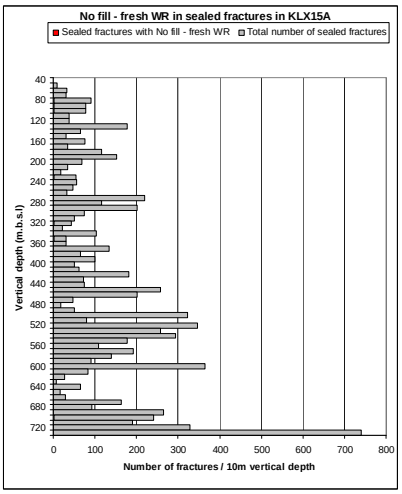
No fill - fresh WR in sealed fractures in KLX15A
Sealed fractures with No fill - fresh WR
Total number of sealed fractures
Vertical depth (m.b.s.l)
Number of fractures / 10m vertical depth

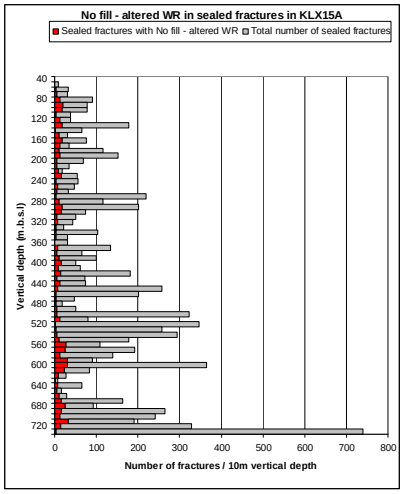
No fill - altered WR in sealed fractures in KLX15A
Sealed fractures with No fill - altered WR
Total number of sealed fractures
Vertical depth (m.b.s.l)
Number of fractures / 10m vertical depth

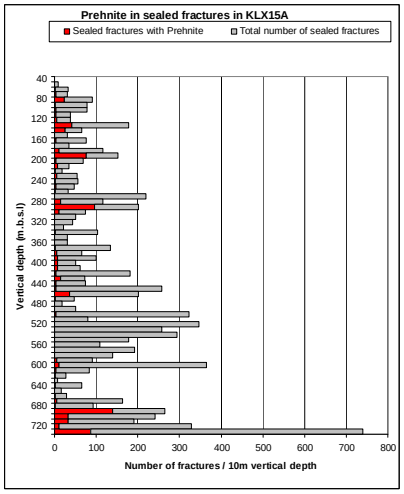
Prehnite in sealed fractures in KLX15A
Sealed fractures with Prehnite
Total number of sealed fractures
Vertical depth (m.b.s.l)
Number of fractures / 10m vertical depth

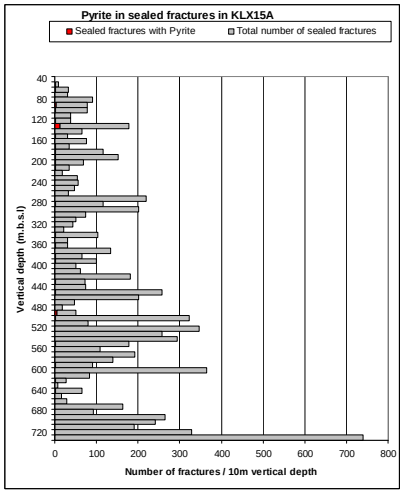
Pyrite in sealed fractures in KLX15A
Sealed fractures with Pyrite
Total number of sealed fractures
Vertical depth (m.b.s.l)
Number of fractures / 10m vertical depth

KLX16A

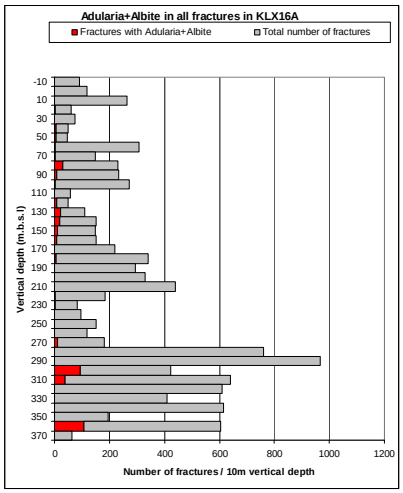
Adularia+Albite in all fractures in KLX16A
Fractures with Adularia+Albite
Total number of fractures
Vertical depth (m.b.s.l)
Number of fractures / 10m vertical depth

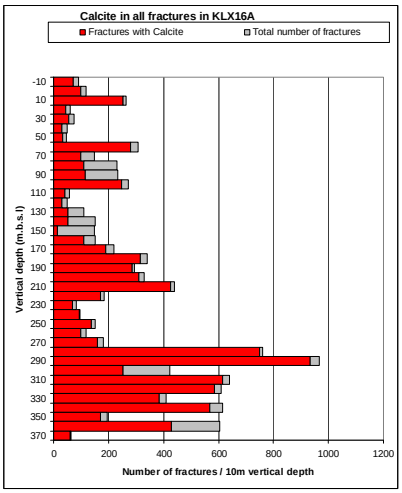
Calcite in all fractures in KLX16A
Fractures with Calcite
Total number of fractures
Vertical depth (m.b.s.l)
Number of fractures / 10m vertical depth

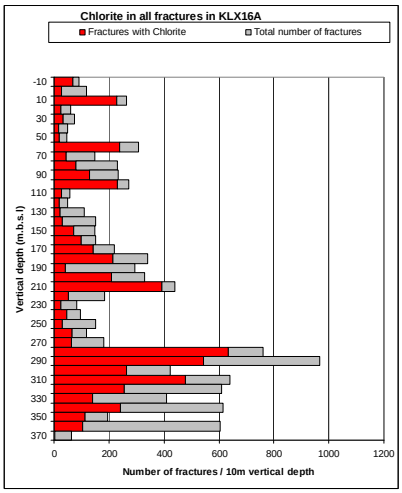
Chlorite in all fractures in KLX16A
Fractures with Chlorite
Total number of fractures
Vertical depth (m.b.s.l)
Number of fractures / 10m vertical depth

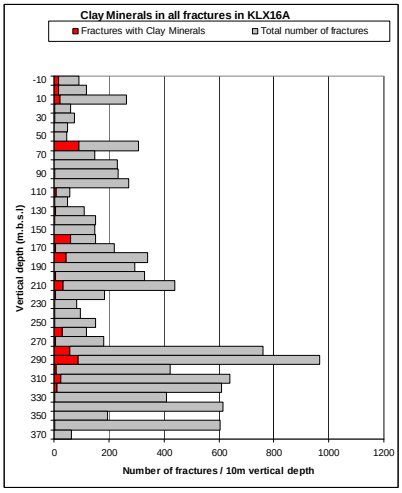
Clay Minerals in all fractures in KLX16A
Fractures with Clay Minerals
Total number of fractures
Vertical depth (m.b.s.l)
Number of fractures / 10m vertical depth

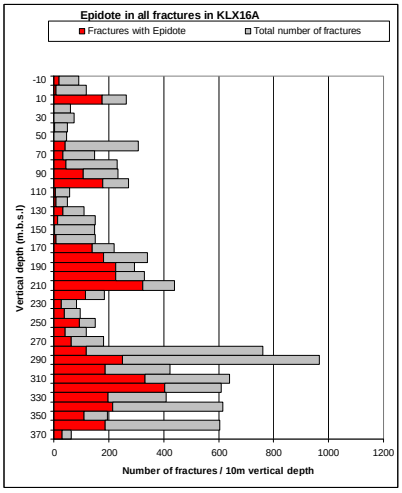
Epidote in all fractures in KLX16A
Fractures with Epidote
Total number of fractures
Vertical depth (m.b.s.l)
Number of fractures / 10m vertical depth

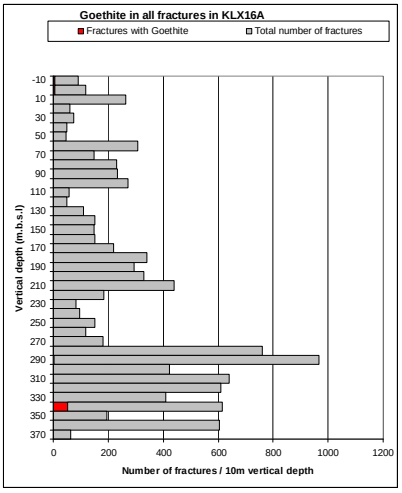
Goethite in all fractures in KLX16A
Fractures with Goethite
Total number of fractures
Vertical depth (m.b.s.l)
Number of fractures / 10m vertical depth

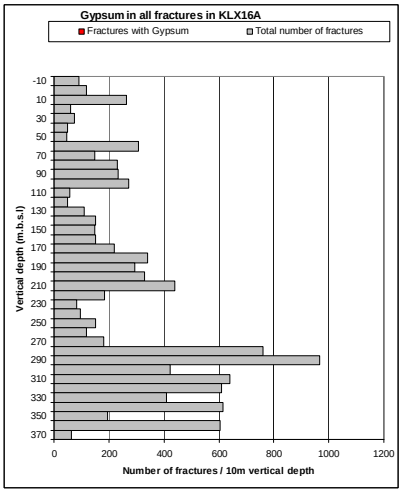
Gypsum in all fractures in KLX16A
Fractures with Gypsum
Total number of fractures
Vertical depth (m.b.s.l)
Number of fractures / 10m vertical depth

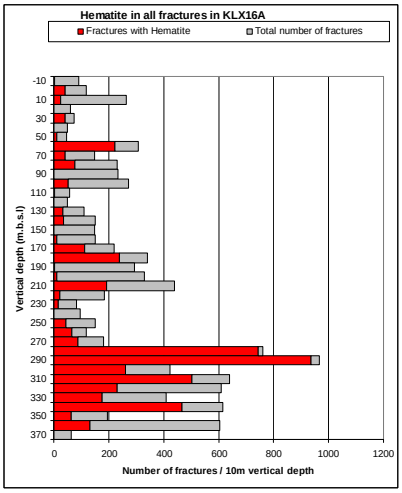
Hematite in all fractures in KLX16A
Fractures with Hematite
Total number of fractures
Vertical depth (m.b.s.l)
Number of fractures / 10m vertical depth

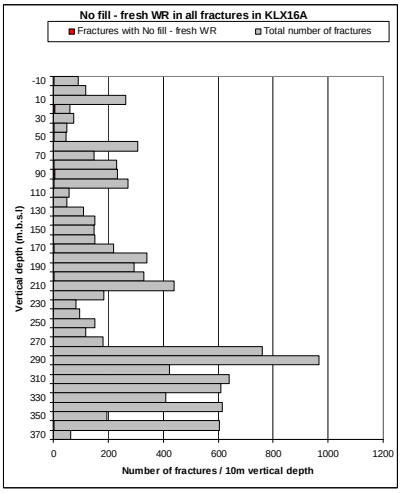
No fill - fresh WR in all fractures in KLX16A
Fractures with No fill - fresh WR
Total number of fractures
Vertical depth (m.b.s.l)
Number of fractures / 10m vertical depth

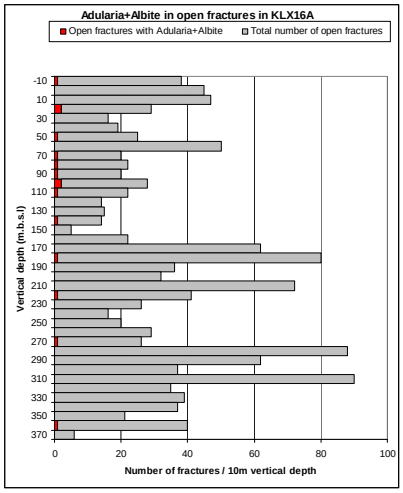
Adularia+Albite in open fractures in KLX16A
Open fractures with Adularia+Albite
Total number of open fractures
Vertical depth (m.b.s.l)
Number of fractures / 10m vertical depth

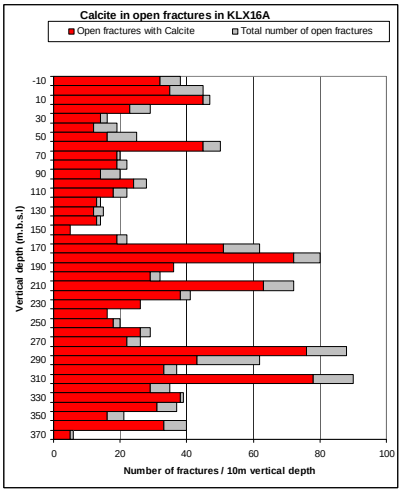
Calcite in open fractures in KLX16A
Open fractures with Calcite
Total number of open fractures
Vertical depth (m.b.s.l)
Number of fractures / 10m vertical depth

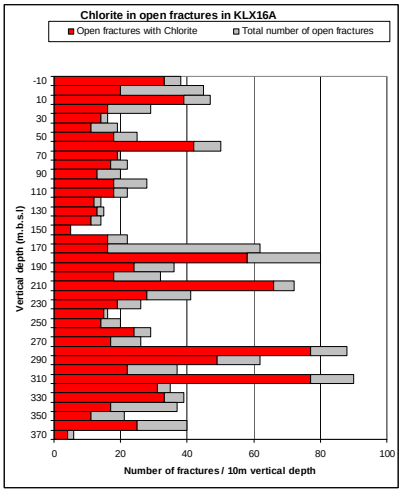
Chlorite in open fractures in KLX16A
Open fractures with Chlorite
Total number of open fractures
Vertical depth (m.b.s.l)
Number of fractures / 10m vertical depth

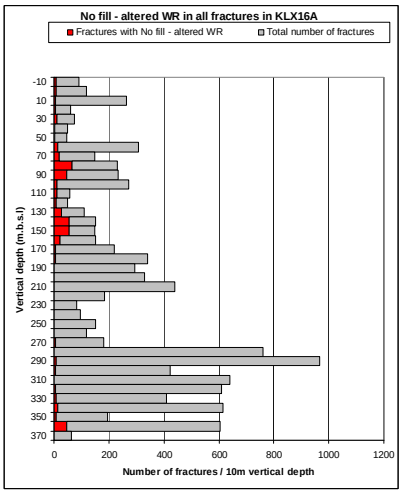
No fill - altered WR in all fractures in KLX16A
Fractures with No fill - altered WR
Total number of fractures
Vertical depth (m.b.s.l)
Number of fractures / 10m vertical depth

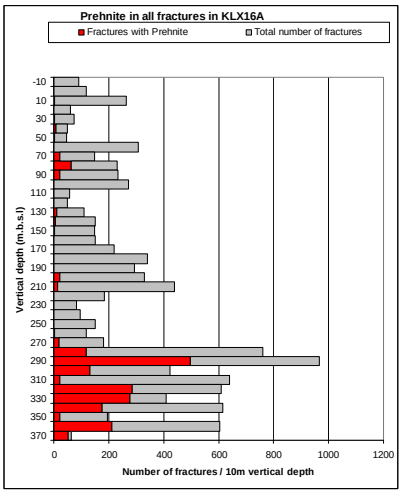
Prehnite in all fractures in KLX16A
Fractures with Prehnite
Total number of fractures
Vertical depth (m.b.s.l)
Number of fractures / 10m vertical depth

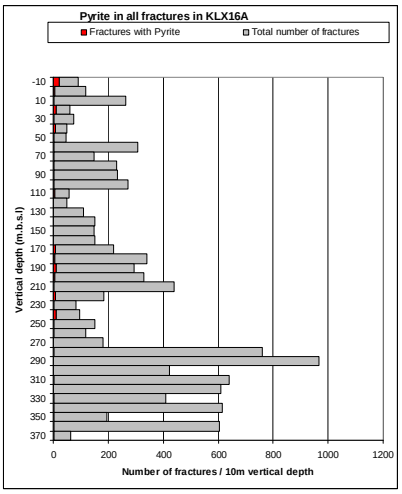
Pyrite in all fractures in KLX16A
Fractures with Pyrite
Total number of fractures
Vertical depth (m.b.s.l)
Number of fractures / 10m vertical depth

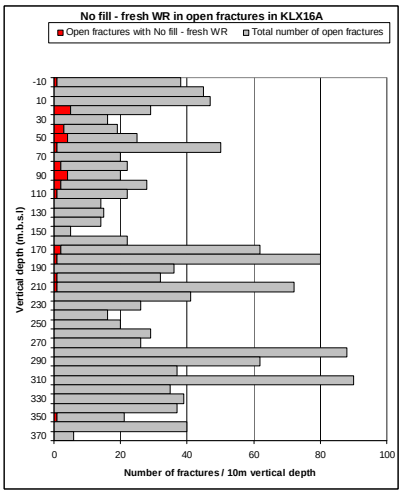
No fill - fresh WR in open fractures in KLX16A
Open fractures with No fill - fresh WR
Total number of open fractures
Vertical depth (m.b.s.l)
Number of fractures / 10m vertical depth

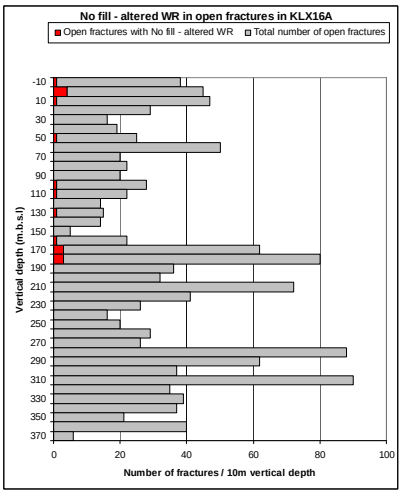
No fill - altered WR in open fractures in KLX16A
Open fractures with No fill - altered WR
Total number of open fractures
Vertical depth (m.b.s.l)
Number of fractures / 10m vertical depth

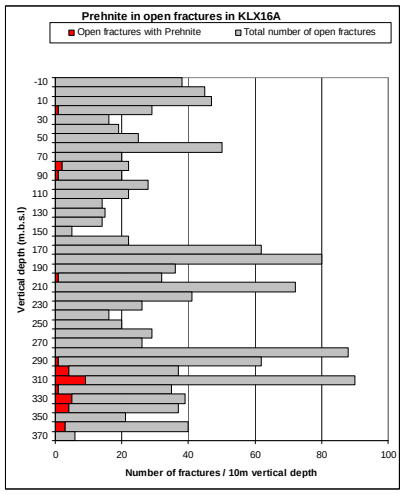
Prehnite in open fractures in KLX16A
Open fractures with Prehnite
Total number of open fractures
Vertical depth (m.b.s.l)
Number of fractures / 10m vertical depth

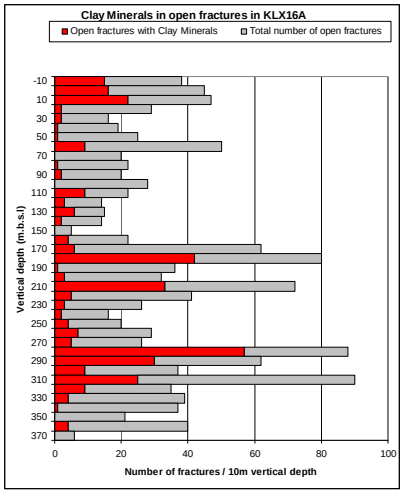
Clay Minerals in open fractures in KLX16A
Open fractures with Clay Minerals
Total number of open fractures
Vertical depth (m.b.s.l)
Number of fractures / 10m vertical depth

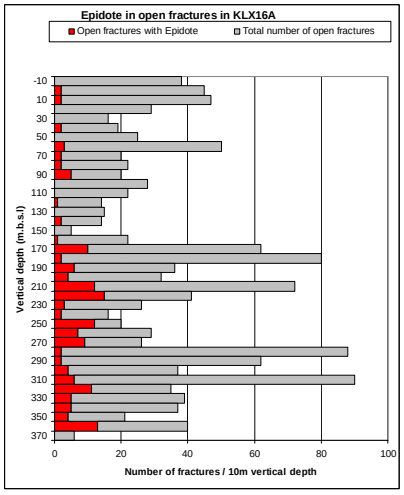
Epidote in open fractures in KLX16A
Open fractures with Epidote
Total number of open fractures
Vertical depth (m.b.s.l)
Number of fractures / 10m vertical depth

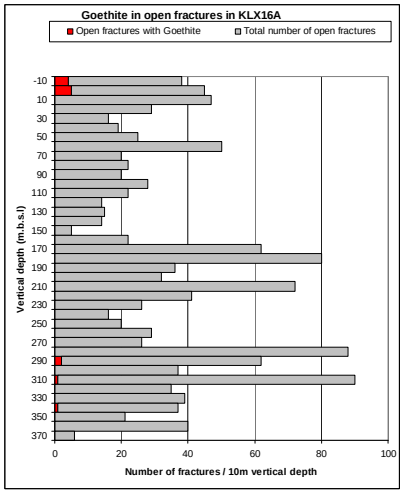
Goethite in open fractures in KLX16A
Open fractures with Goethite
Total number of open fractures
Vertical depth (m.b.s.l)
Number of fractures / 10m vertical depth

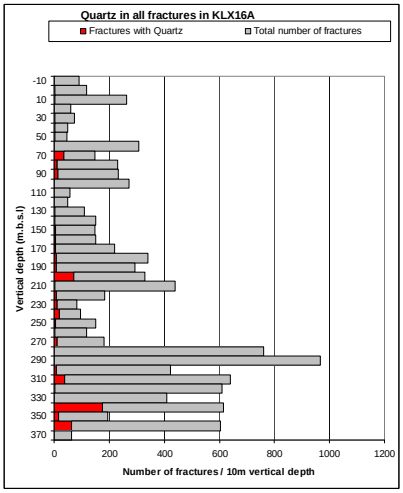
Quartz in all fractures in KLX16A
Fractures with Quartz
Total number of fractures
Vertical depth (m.b.s.l)
Number of fractures / 10m vertical depth

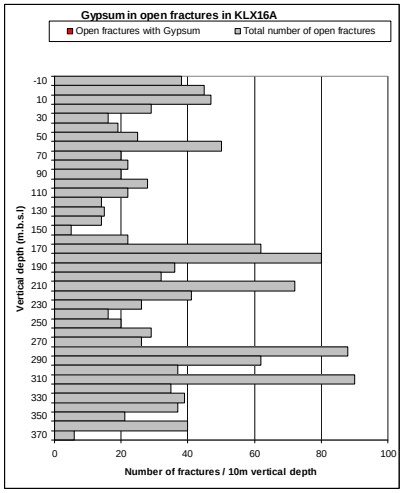
Gypsum in open fractures in KLX16A
Open fractures with Gypsum
Total number of open fractures
Vertical depth (m.b.s.l)
Number of fractures / 10m vertical depth

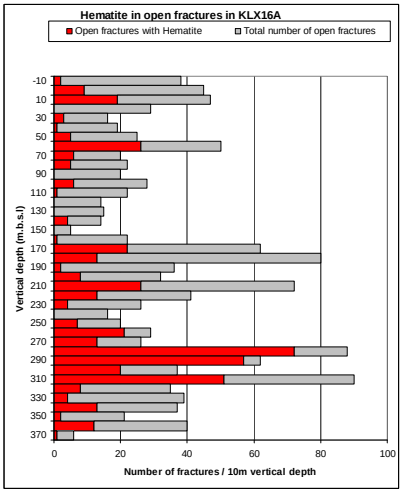
Hematite in open fractures in KLX16A
Open fractures with Hematite
Total number of open fractures
Vertical depth (m.b.s.l)
Number of fractures / 10m vertical depth

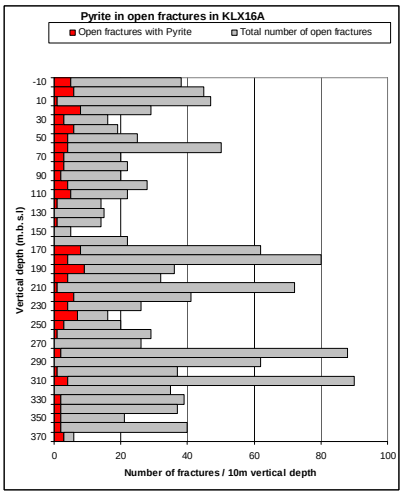
Pyrite in open fractures in KLX16A
Open fractures with Pyrite
Total number of open fractures
Vertical depth (m.b.s.l)
Number of fractures / 10m vertical depth

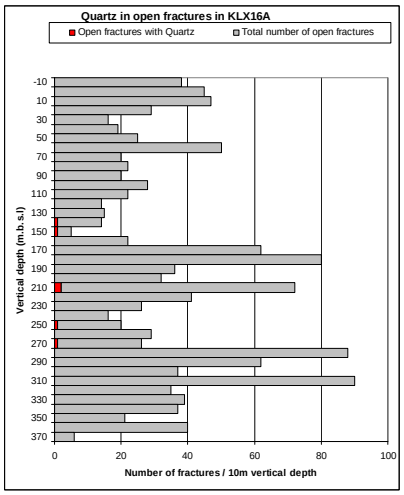
Quartz in open fractures in KLX16A
Open fractures with Quartz
Total number of open fractures
Vertical depth (m.b.s.l)
Number of fractures / 10m vertical depth

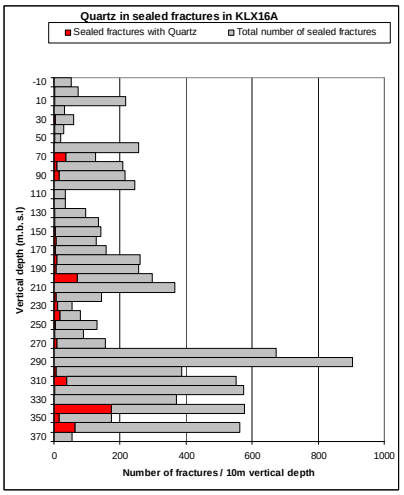
Quartz in sealed fractures in KLX16A
Sealed fractures with Quartz
Total number of sealed fractures
Vertical depth (m.b.s.l)
Number of fractures / 10m vertical depth

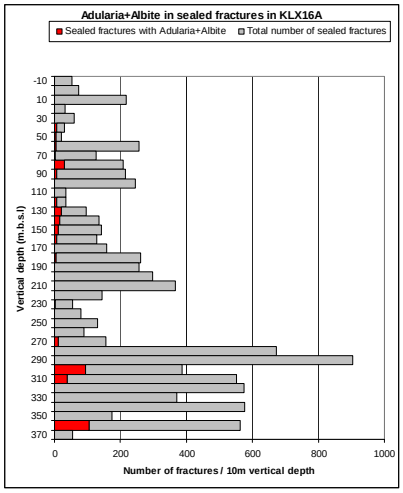
Adularia+Albite in sealed fractures in KLX16A
Sealed fractures with Adularia+Albite
Total number of sealed fractures
Vertical depth (m.b.s.l)
Number of fractures / 10m vertical depth

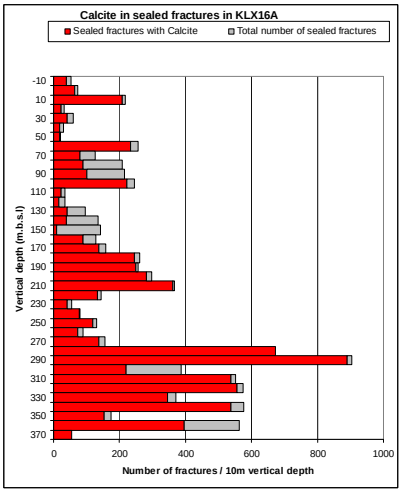
Calcite in sealed fractures in KLX16A
Sealed fractures with Calcite
Total number of sealed fractures
Vertical depth (m.b.s.l)
Number of fractures / 10m vertical depth

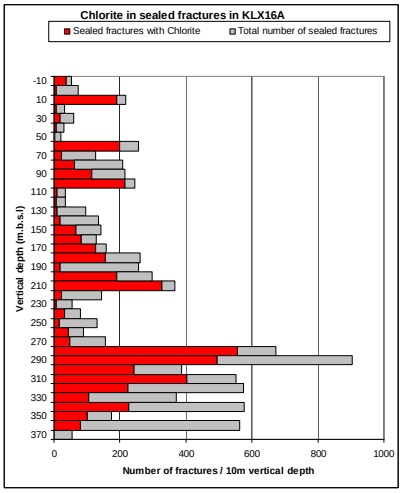
Chlorite in sealed fractures in KLX16A
Sealed fractures with Chlorite
Total number of sealed fractures
Vertical depth (m.b.s.l)
Number of fractures / 10m vertical depth

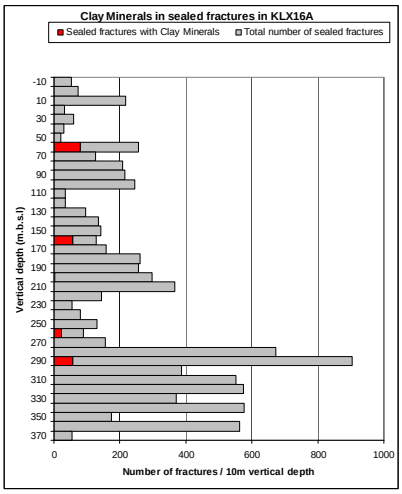
Clay Minerals in sealed fractures in KLX16A
Sealed fractures with Clay Minerals
Total number of sealed fractures
Vertical depth (m.b.s.l)
Number of fractures / 10m vertical depth

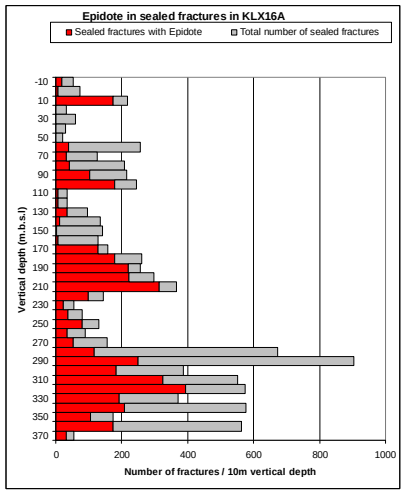
Epidote in sealed fractures in KLX16A
Sealed fractures with Epidote
Total number of sealed fractures
Vertical depth (m.b.s.l)
Number of fractures / 10m vertical depth

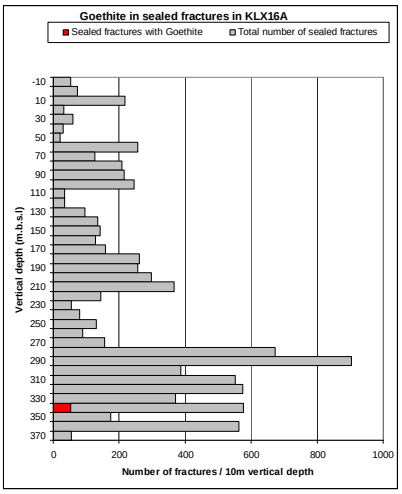
Goethite in sealed fractures in KLX16A
Sealed fractures with Goethite
Total number of sealed fractures
Vertical depth (m.b.s.l)
Number of fractures / 10m vertical depth

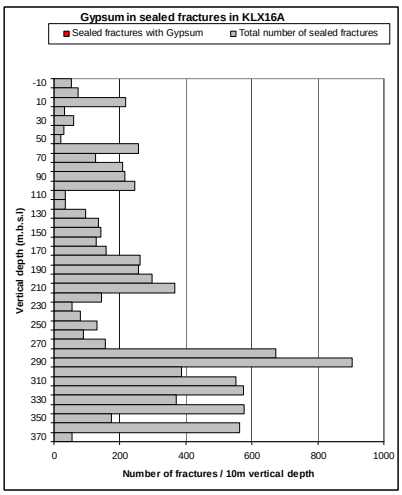
Gypsum in sealed fractures in KLX16A
Sealed fractures with Gypsum
Total number of sealed fractures
Vertical depth (m.b.s.l)
Number of fractures / 10m vertical depth

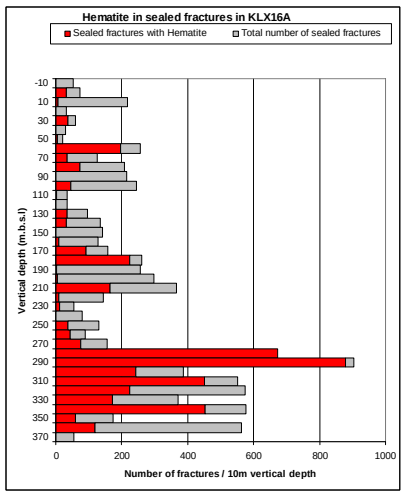
Hematite in sealed fractures in KLX16A
Sealed fractures with Hematite
Total number of sealed fractures
Vertical depth (m.b.s.l)
Number of fractures / 10m vertical depth

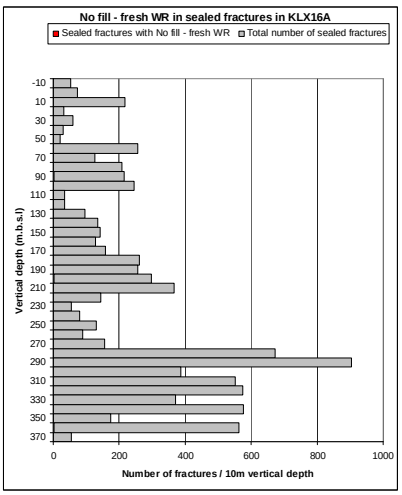
No fill - fresh WR in sealed fractures in KLX16A
Sealed fractures with No fill - fresh WR
Total number of sealed fractures
Vertical depth (m.b.s.l)
Number of fractures / 10m vertical depth

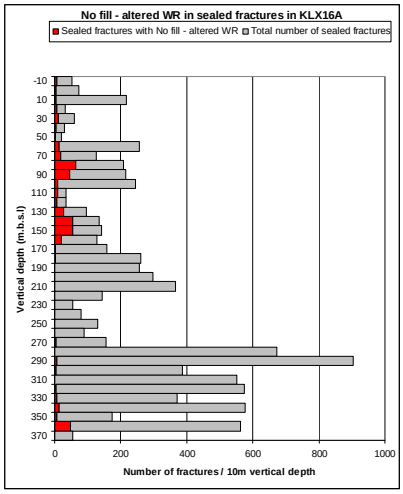
No fill - altered WR in sealed fractures in KLX16A
Sealed fractures with No fill - altered WR
Total number of sealed fractures
Vertical depth (m.b.s.l)
-10
10
30
50
70
90
110
130
150
170
190
210
230
250
270
290
310
330
350
370
0
200
400
600
800
1000
Number of fractures / 10m vertical depth

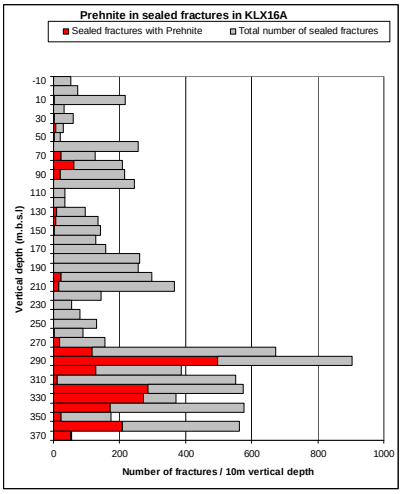
Prehnite in sealed fractures in KLX16A
Sealed fractures with Prehnite
Total number of sealed fractures
Vertical depth (m.b.s.l)
-10
10
30
50
70
90
110
130
150
170
190
210
230
250
270
290
310
330
350
370
0
200
400
600
800
1000
Number of fractures / 10m vertical depth

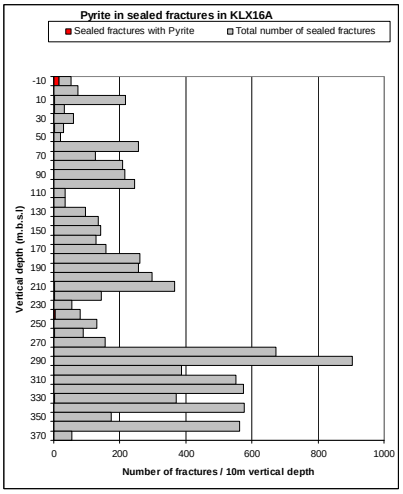
Pyrite in sealed fractures in KLX16A
Sealed fractures with Pyrite
Total number of sealed fractures
Vertical depth (m.b.s.l)
-10
10
30
50
70
90
110
130
150
170
190
210
230
250
270
290
310
330
350
370
0
200
400
600
800
1000
Number of fractures / 10m vertical depth

KLX17A

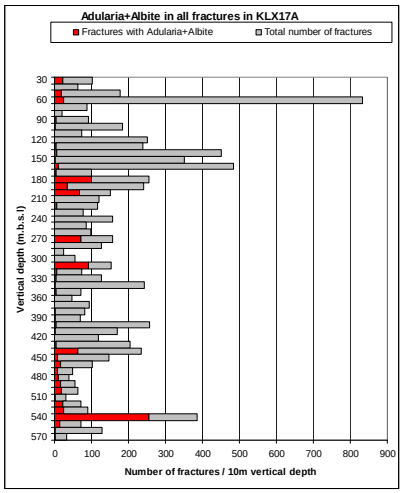
Adularia+Albite in all fractures in KLX17A
Fractures with Adularia+Albite
Total number of fractures
Vertical depth (m.b.s.l)
Number of fractures / 10m vertical depth

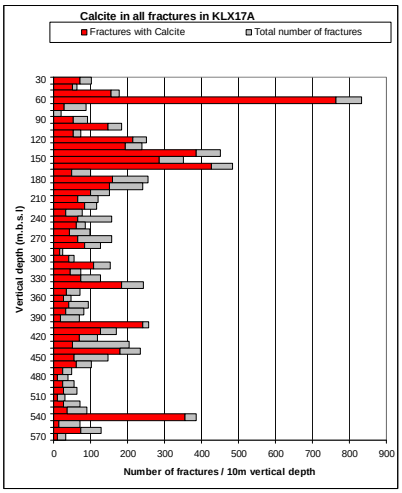
Calcite in all fractures in KLX17A
Fractures with Calcite
Total number of fractures
Vertical depth (m.b.s.l)
Number of fractures / 10m vertical depth

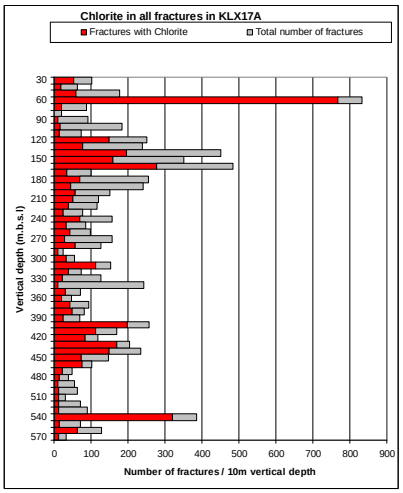
Chlorite in all fractures in KLX17A
Fractures with Chlorite
Total number of fractures
Vertical depth (m.b.s.l)
Number of fractures / 10m vertical depth

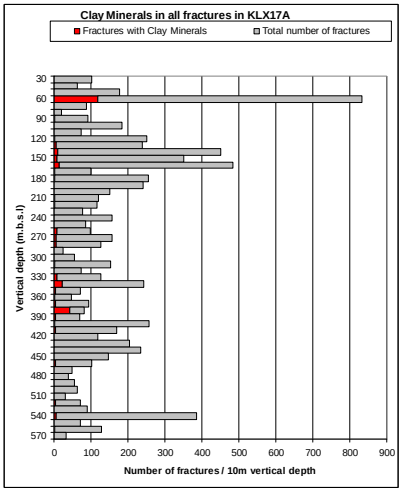
Clay Minerals in all fractures in KLX17A
Fractures with Clay Minerals
Total number of fractures
Vertical depth (m.b.s.l)
Number of fractures / 10m vertical depth

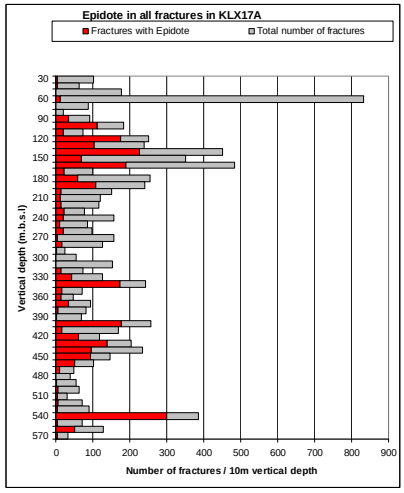
Epidote in all fractures in KLX17A
Fractures with Epidote
Total number of fractures
Vertical depth (m.b.s.l)
Number of fractures / 10m vertical depth

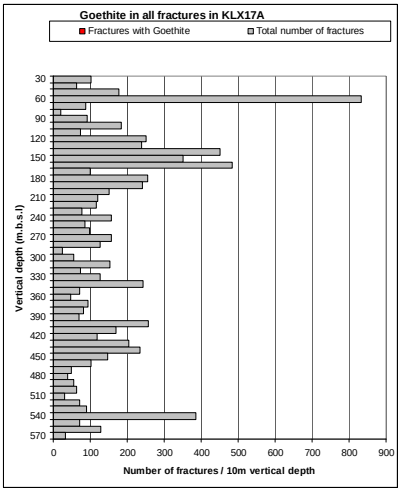
Goethite in all fractures in KLX17A
Fractures with Goethite
Total number of fractures
Vertical depth (m.b.s.l)
Number of fractures / 10m vertical depth

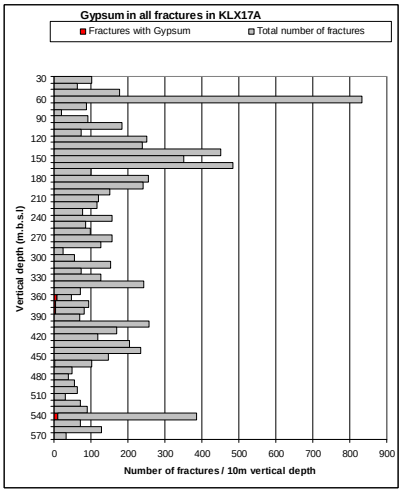
Gypsum in all fractures in KLX17A
Fractures with Gypsum
Total number of fractures
Vertical depth (m.b.s.l)
Number of fractures / 10m vertical depth

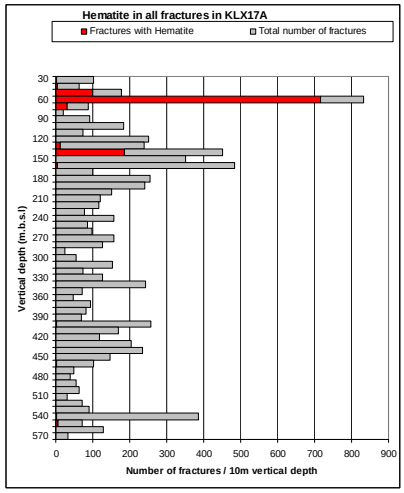
Hematite in all fractures in KLX17A
Fractures with Hematite
Total number of fractures
Vertical depth (m.b.s.l)
Number of fractures / 10m vertical depth

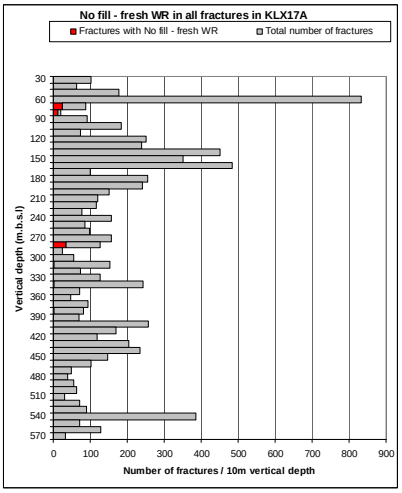
No fill - fresh WR in all fractures in KLX17A
Fractures with No fill - fresh WR
Total number of fractures
Vertical depth (m.b.s.l)
Number of fractures / 10m vertical depth

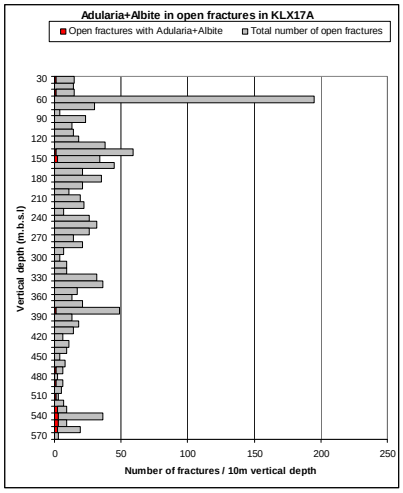
Adularia+Albite in open fractures in KLX17A
Open fractures with Adularia+Albite
Total number of open fractures
Vertical depth (m.b.s.l)
Number of fractures / 10m vertical depth

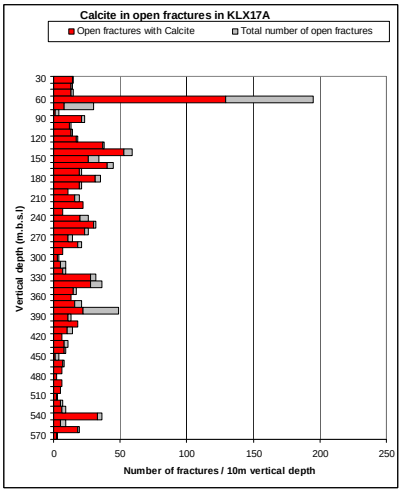
Calcite in open fractures in KLX17A
Open fractures with Calcite
Total number of open fractures
Vertical depth (m.b.s.l)
Number of fractures / 10m vertical depth

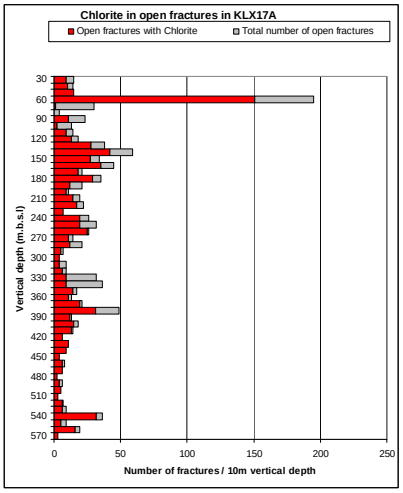
Chlorite in open fractures in KLX17A
Open fractures with Chlorite
Total number of open fractures
Vertical depth (m.b.s.l)
Number of fractures / 10m vertical depth

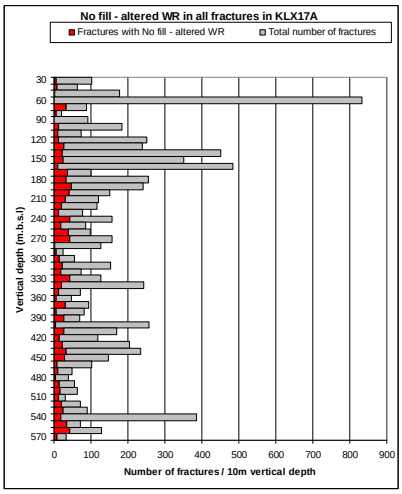
No fill - altered WR in all fractures in KLX17A
Fractures with No fill - altered WR
Total number of fractures
Vertical depth (m.b.s.l)
Number of fractures / 10m vertical depth

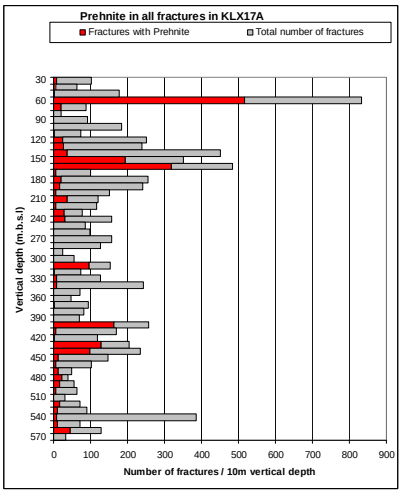
Prehnite in all fractures in KLX17A
Fractures with Prehnite
Total number of fractures
Vertical depth (m.b.s.l)
Number of fractures / 10m vertical depth

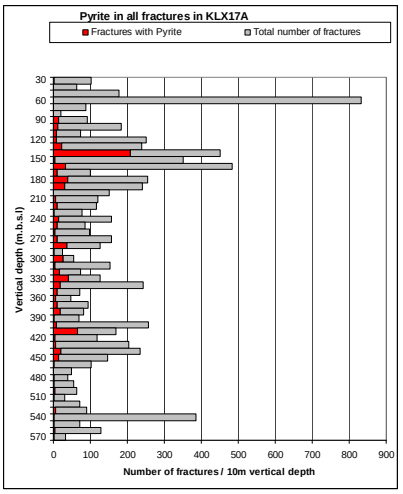
Pyrite in all fractures in KLX17A
Fractures with Pyrite
Total number of fractures
Vertical depth (m.b.s.l)
Number of fractures / 10m vertical depth

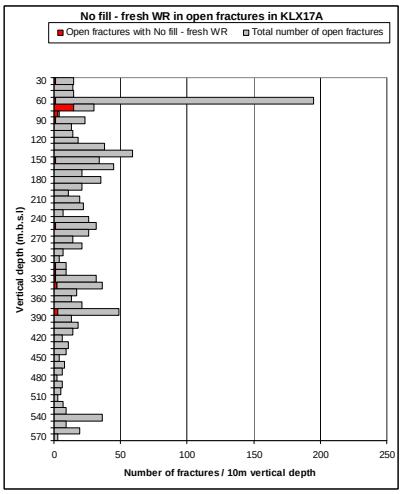
No fill - fresh WR in open fractures in KLX17A
Open fractures with No fill - fresh WR
Total number of open fractures
Vertical depth (m.b.s.l)
Number of fractures / 10m vertical depth

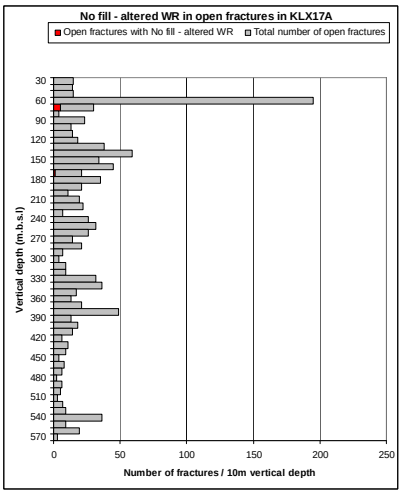
No fill - altered WR in open fractures in KLX17A
Open fractures with No fill - altered WR
Total number of open fractures
Vertical depth (m.b.s.l)
Number of fractures / 10m vertical depth

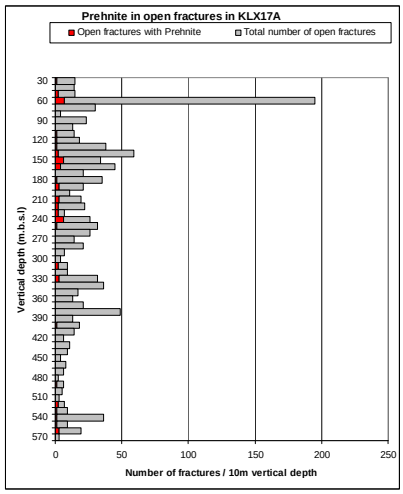
Prehnite in open fractures in KLX17A
Open fractures with Prehnite
Total number of open fractures
Vertical depth (m.b.s.l)
Number of fractures / 10m vertical depth

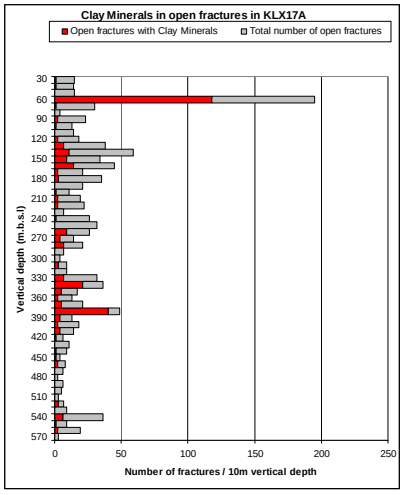
Clay Minerals in open fractures in KLX17A
Open fractures with Clay Minerals
Total number of open fractures
Vertical depth (m.b.s.l)
Number of fractures / 10m vertical depth

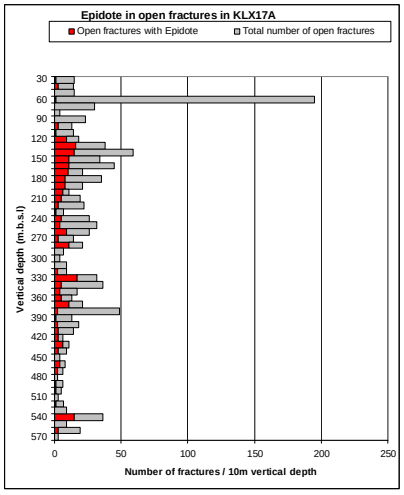
Epidote in open fractures in KLX17A
Open fractures with Epidote
Total number of open fractures
Vertical depth (m.b.s.l)
Number of fractures / 10m vertical depth

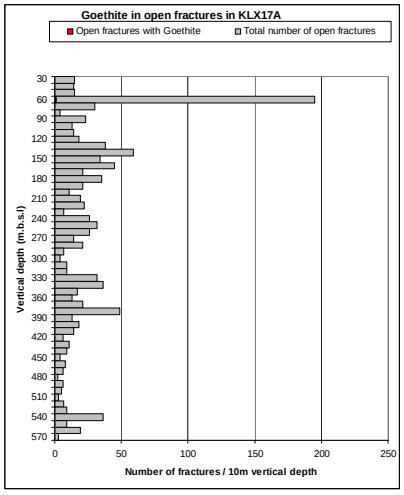
Goethite in open fractures in KLX17A
Open fractures with Goethite
Total number of open fractures
Vertical depth (m.b.s.l)
Number of fractures / 10m vertical depth

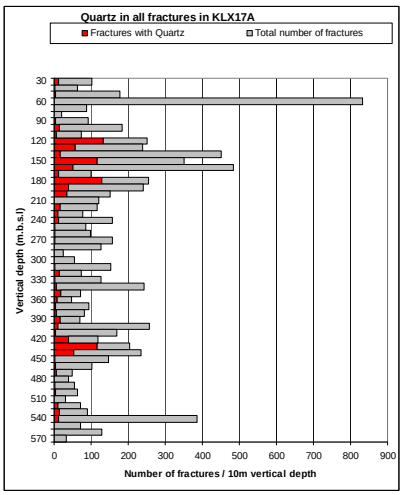
Quartz in all fractures in KLX17A
Fractures with Quartz
Total number of fractures
Vertical depth (m.b.s.l)
Number of fractures / 10m vertical depth

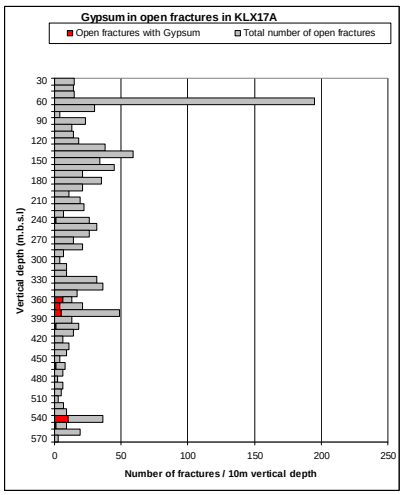
Gypsum in open fractures in KLX17A
Open fractures with Gypsum
Total number of open fractures
Vertical depth (m.b.s.l)
Number of fractures / 10m vertical depth

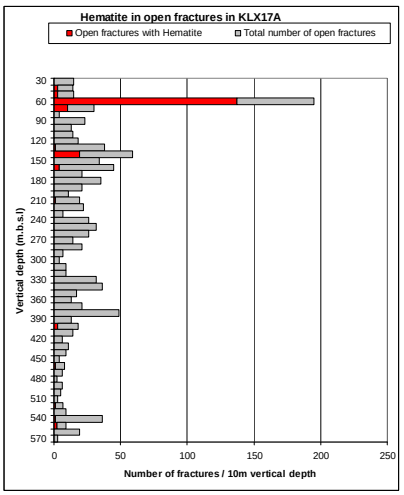
Hematite in open fractures in KLX17A
Open fractures with Hematite
Total number of open fractures
Vertical depth (m.b.s.l)
Number of fractures / 10m vertical depth

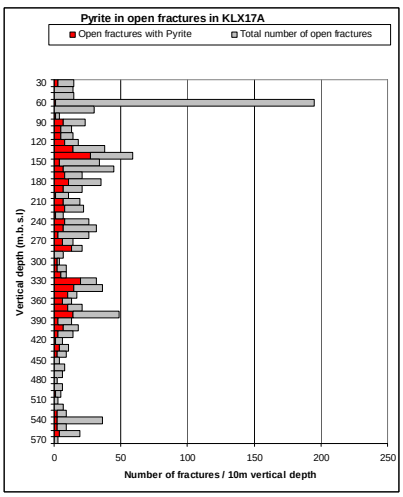
Pyrite in open fractures in KLX17A
Open fractures with Pyrite
Total number of open fractures
Vertical depth (m.b.s.l)
Number of fractures / 10m vertical depth

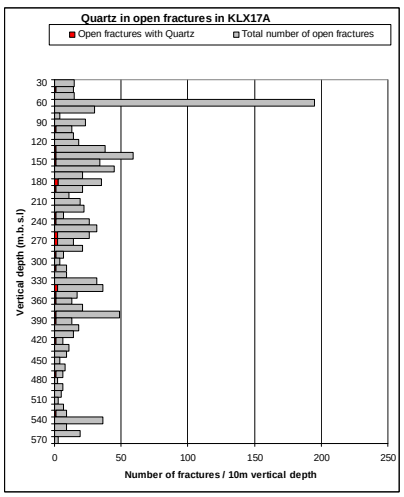
Quartz in open fractures in KLX17A
Open fractures with Quartz
Total number of open fractures
Vertical depth (m.b.s.l)
Number of fractures / 10m vertical depth

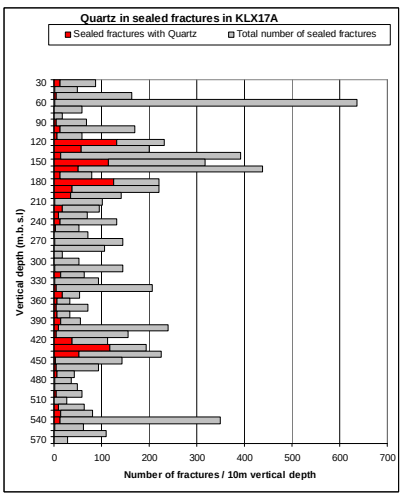
Quartz in sealed fractures in KLX17A
Sealed fractures with Quartz
Total number of sealed fractures
Vertical depth (m.b.s.l)
Number of fractures / 10m vertical depth

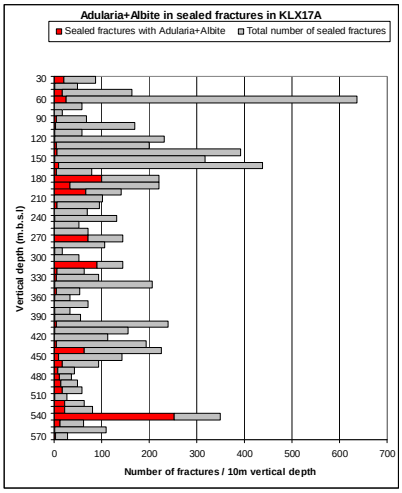
Adularia+Albite in sealed fractures in KLX17A
Sealed fractures with Adularia+Albite
Total number of sealed fractures
Vertical depth (m.b.s.l)
Number of fractures / 10m vertical depth

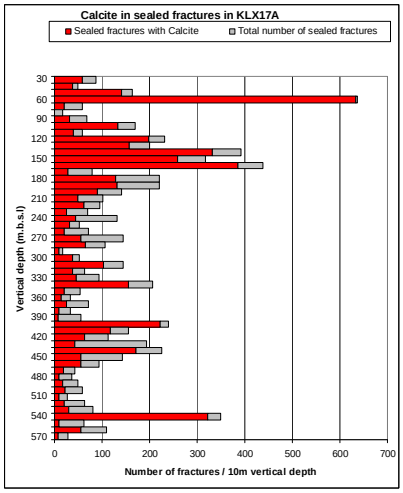
Calcite in sealed fractures in KLX17A
Sealed fractures with Calcite
Total number of sealed fractures
Vertical depth (m.b.s.l)
Number of fractures / 10m vertical depth

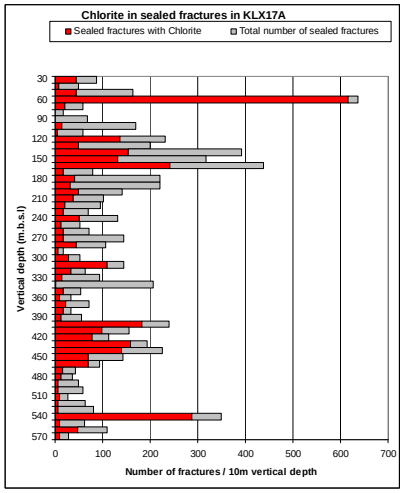
Chlorite in sealed fractures in KLX17A
Sealed fractures with Chlorite
Total number of sealed fractures
Vertical depth (m.b.s.l)
Number of fractures / 10m vertical depth

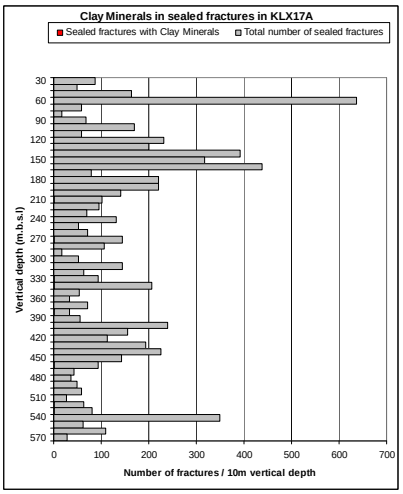
Clay Minerals in sealed fractures in KLX17A
Sealed fractures with Clay Minerals
Total number of sealed fractures
Vertical depth (m.b.s.l)
Number of fractures / 10m vertical depth

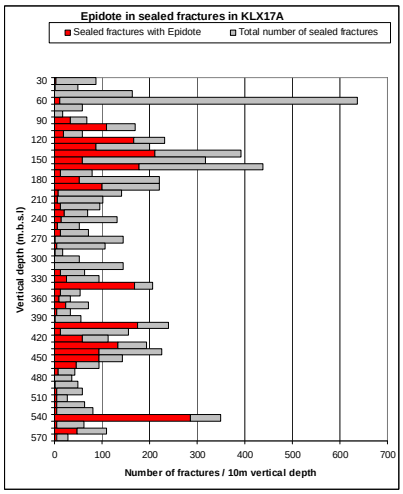
Epidote in sealed fractures in KLX17A
Sealed fractures with Epidote
Total number of sealed fractures
Vertical depth (m.b.s.l)
Number of fractures / 10m vertical depth

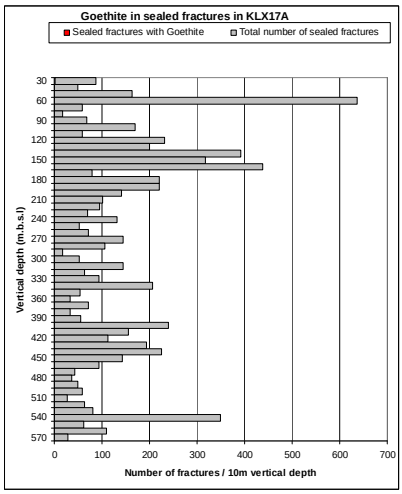
Goethite in sealed fractures in KLX17A
Sealed fractures with Goethite
Total number of sealed fractures
Vertical depth (m.b.s.l)
Number of fractures / 10m vertical depth

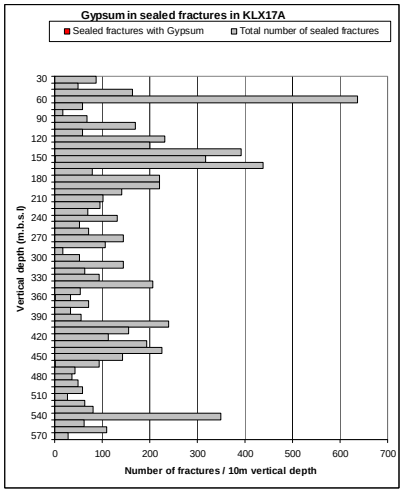
Gypsum in sealed fractures in KLX17A
Sealed fractures with Gypsum
Total number of sealed fractures
Vertical depth (m.b.s.l)
Number of fractures / 10m vertical depth

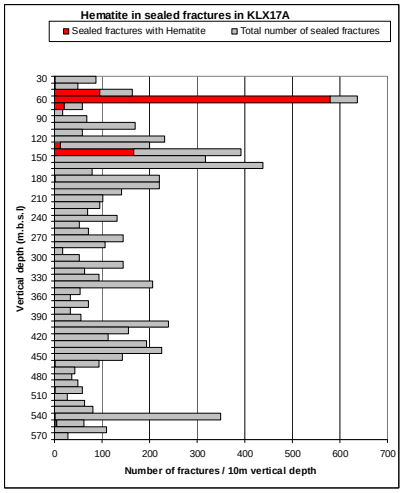
Hematite in sealed fractures in KLX17A
Sealed fractures with Hematite
Total number of sealed fractures
Vertical depth (m.b.s.l)
Number of fractures / 10m vertical depth

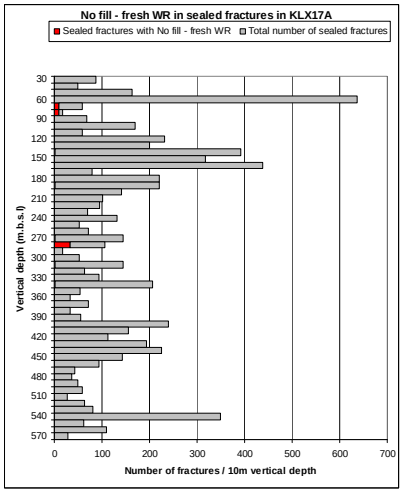
No fill - fresh WR in sealed fractures in KLX17A
Sealed fractures with No fill - fresh WR
Total number of sealed fractures
Verticel depth (m.b.s.l)
Number of fractures / 10m vertical depth

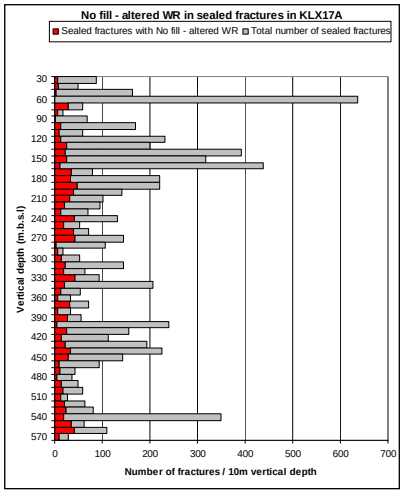
No fill - altered WR in sealed fractures in KLX17A
Sealed fractures with No fill - altered WR
Total number of sealed fractures
Vertical depth (m.b.s.l)
Number of fractures / 10m vertical depth

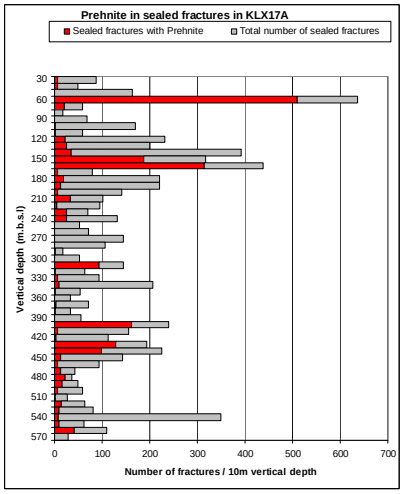
Prehnite in sealed fractures in KLX17A
Sealed fractures with Prehnite
Total number of sealed fractures
Vertical depth (m.b.s.l)
Number of fractures / 10m vertical depth

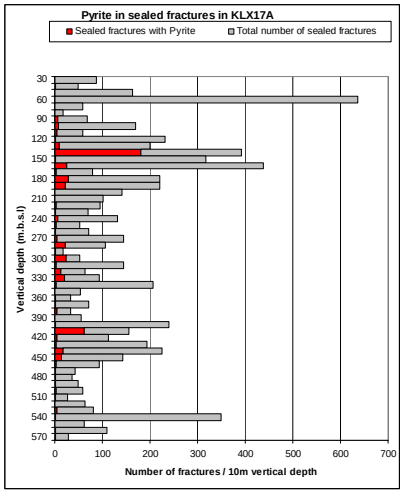
Pyrite in sealed fractures in KLX17A
Sealed fractures with Pyrite
Total number of sealed fractures
Vertical depth (m.b.s.l)
Number of fractures / 10m vertical depth

KLX18A

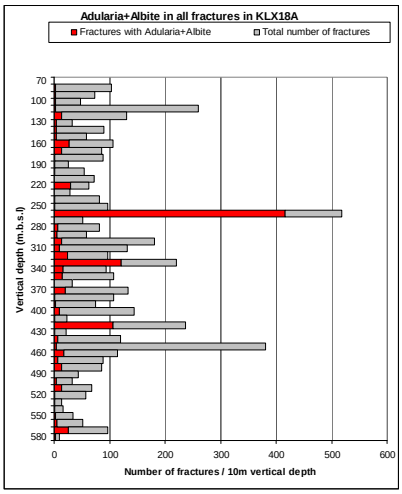
Adularia+Albite in all fractures in KLX18A
Fractures with Adularia+Albite
Total number of fractures
Vertical depth (m.b.s.l)
Number of fractures / 10m vertical depth

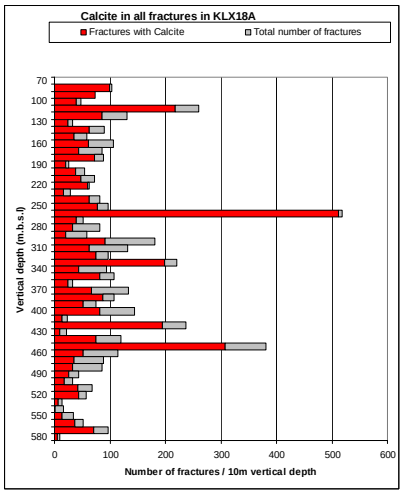
Calcite in all fractures in KLX18A
Fractures with Calcite
Total number of fractures
Vertical depth (m.b.s.l)
Number of fractures / 10m vertical depth

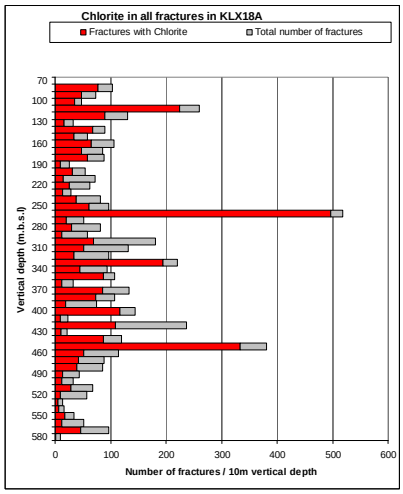
Chlorite in all fractures in KLX18A
Fractures with Chlorite
Total number of fractures
Vertical depth (m.b.s.l)
Number of fractures / 10m vertical depth

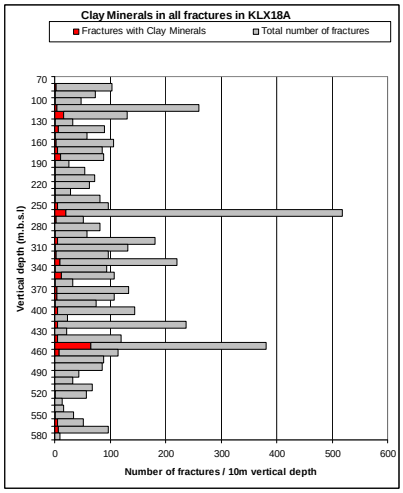
Clay Minerals in all fractures in KLX18A
Fractures with Clay Minerals
Total number of fractures
Vertical depth (m.b.s.l)
Number of fractures / 10m vertical depth

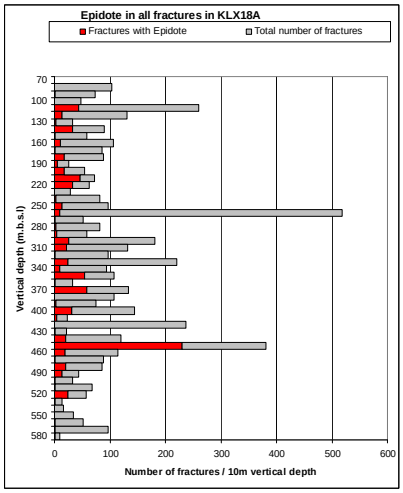
Epidote in all fractures in KLX18A
Fractures with Epidote
Total number of fractures
Vertical depth (m.b.s.l)
Number of fractures / 10m vertical depth

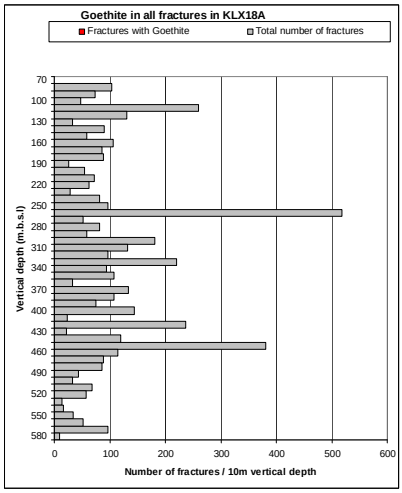
Goethite in all fractures in KLX18A
Fractures with Goethite
Total number of fractures
Vertical depth (m.b.s.l)
Number of fractures / 10m vertical depth

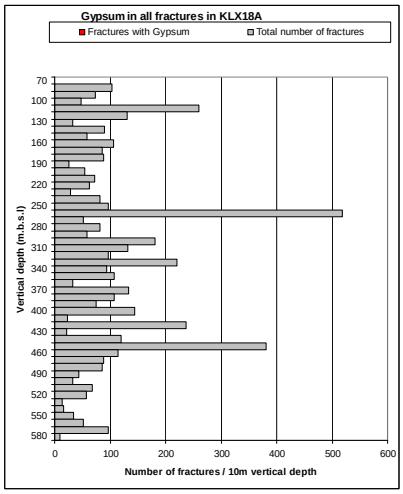
Gypsum in all fractures in KLX18A
Fractures with Gypsum
Total number of fractures
Vertical depth (m.b.s.l)
Number of fractures / 10m vertical depth

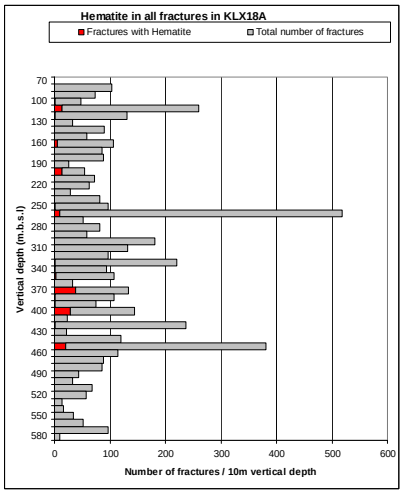
Hematite in all fractures in KLX18A
Fractures with Hematite
Total number of fractures
Vertical depth (m.b.s.l)
Number of fractures / 10m vertical depth

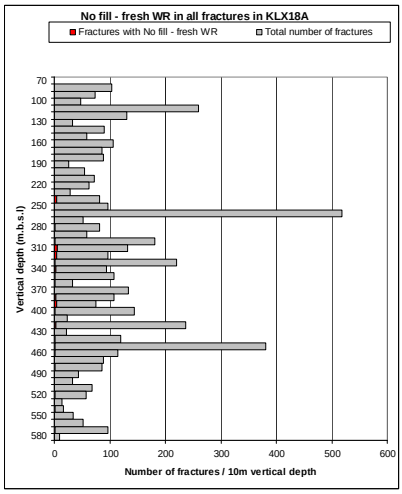
No fill - fresh WR in all fractures in KLX18A
Fractures with No fill - fresh WR
Total number of fractures
Vertical depth (m.b.s.l)
Number of fractures / 10m vertical depth

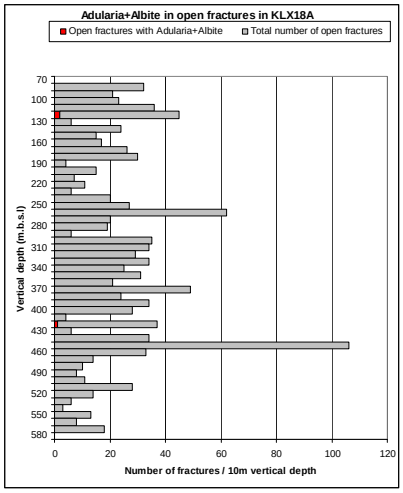
Adularia+Albite in open fractures in KLX18A
Open fractures with Adularia+Albite
Total number of open fractures
Vertical depth (m.b.s.l)
Number of fractures / 10m vertical depth

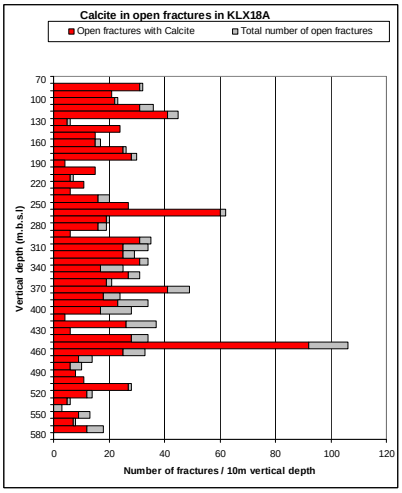
Calcite in open fractures in KLX18A
Open fractures with Calcite
Total number of open fractures
Vertical depth (m.b.s.l)
Number of fractures / 10m vertical depth

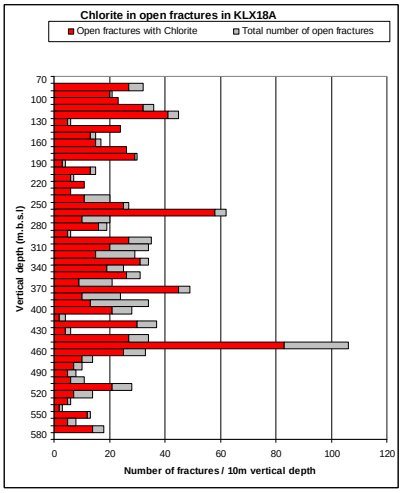
Chlorite in open fractures in KLX18A
Open fractures with Chlorite
Total number of open fractures
Vertical depth (m.b.s.l)
Number of fractures / 10m vertical depth

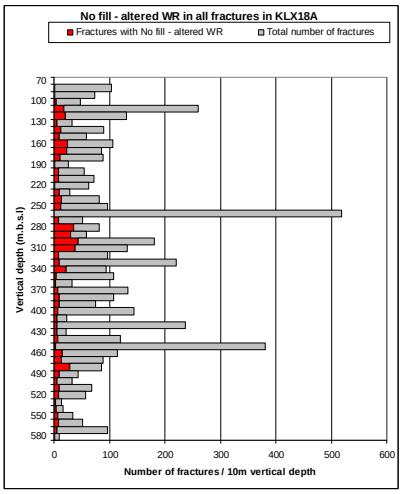
No fill - altered WR in all fractures in KLX18A
Fractures with No fill - altered WR
Total number of fractures
Vertical depth (m.b.s.l)
Number of fractures / 10m vertical depth

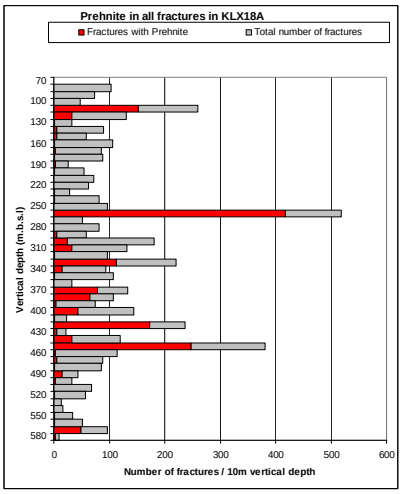
Prehnite in all fractures in KLX18A
Fractures with Prehnite
Total number of fractures
Vertical depth (m.b.s.l)
Number of fractures / 10m vertical depth

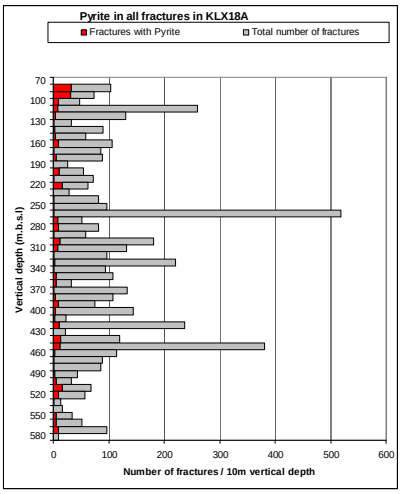
Pyrite in all fractures in KLX18A
Fractures with Pyrite
Total number of fractures
Vertical depth (m.b.s.l)
Number of fractures / 10m vertical depth

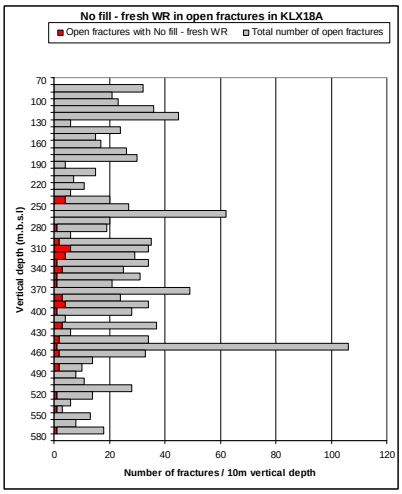
No fill - fresh WR in open fractures in KLX18A
Open fractures with No fill - fresh WR
Total number of open fractures
Vertical depth (m.b.s.l)
Number of fractures / 10m vertical depth

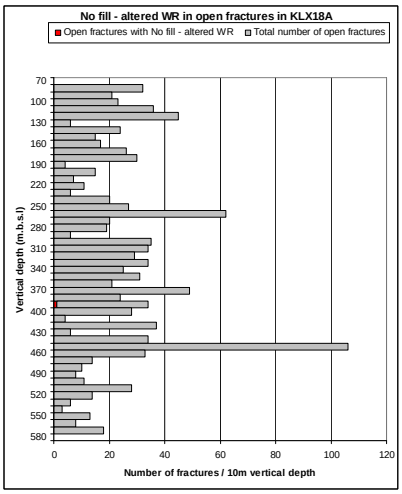
No fill - altered WR in open fractures in KLX18A
Open fractures with No fill - altered WR
Total number of open fractures
Vertical depth (m.b.s.l)
Number of fractures / 10m vertical depth

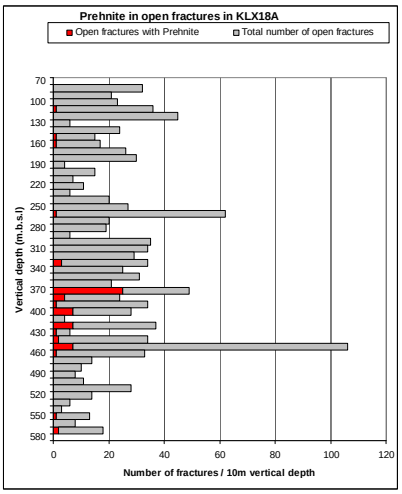
Prehnite in open fractures in KLX18A
Open fractures with Prehnite
Total number of open fractures
Vertical depth (m.b.s.l)
Number of fractures / 10m vertical depth

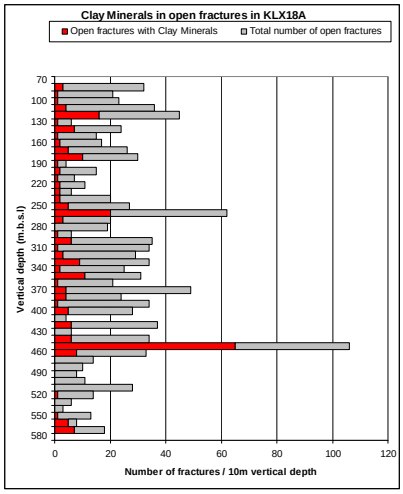
Clay Minerals in open fractures in KLX18A
Open fractures with Clay Minerals
Total number of open fractures
Vertical depth (m.b.s.l)
Number of fractures / 10m vertical depth

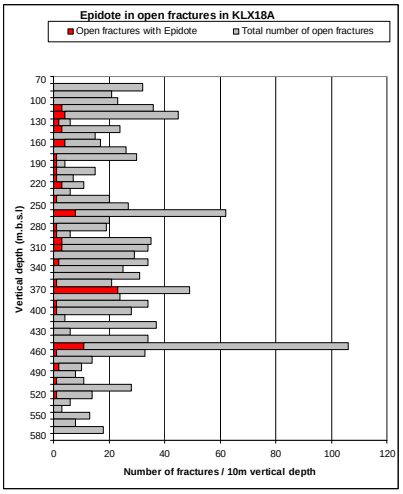
Epidote in open fractures in KLX18A
Open fractures with Epidote
Total number of open fractures
Vertical depth (m.b.s.l)
Number of fractures / 10m vertical depth

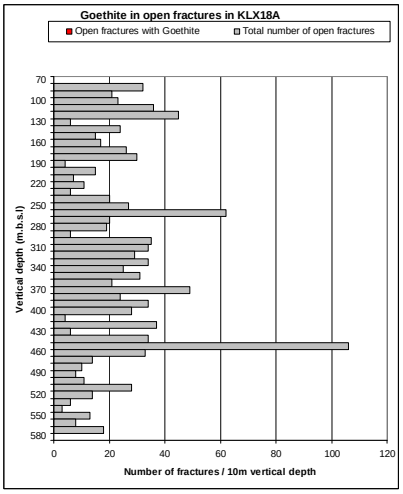
Goethite in open fractures in KLX18A
Open fractures with Goethite
Total number of open fractures
Vertical depth (m.b.s.l)
Number of fractures / 10m vertical depth

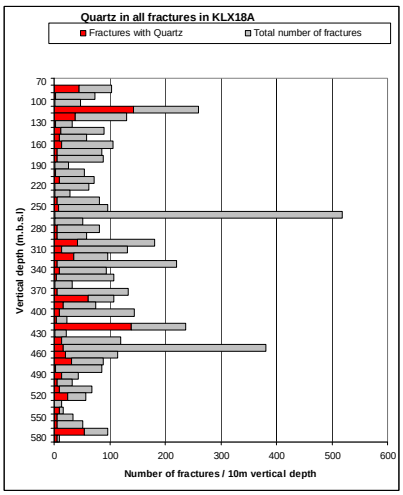
Quartz in all fractures in KLX18A
Fractures with Quartz
Total number of fractures
Vertical depth (m.b.s.l)
Number of fractures / 10m vertical depth

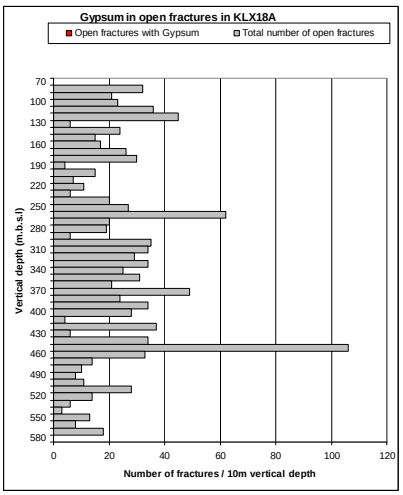
Gypsum in open fractures in KLX18A
Open fractures with Gypsum
Total number of open fractures
Vertical depth (m.b.s.l)
Number of fractures / 10m vertical depth

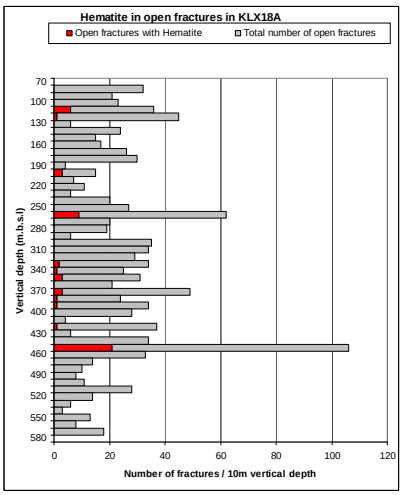
Hematite in open fractures in KLX18A
Open fractures with Hematite
Total number of open fractures
Vertical depth (m.b.s.l)
Number of fractures / 10m vertical depth

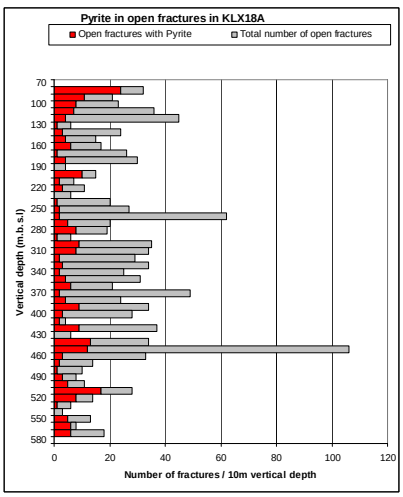
Pyrite in open fractures in KLX18A
Open fractures with Pyrite
Total number of open fractures
Vertical depth (m.b.s.l)
Number of fractures / 10m vertical depth

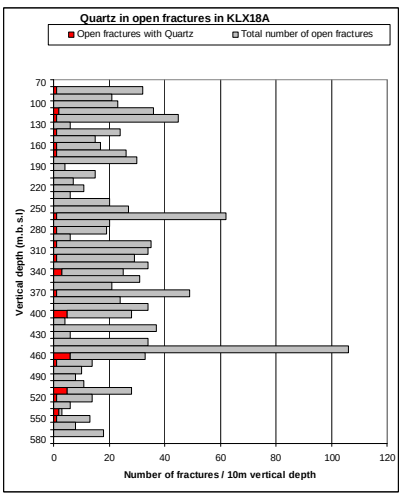
Quartz in open fractures in KLX18A
Open fractures with Quartz
Total number of open fractures
Vertical depth (m.b.s.l)
Number of fractures / 10m vertical depth

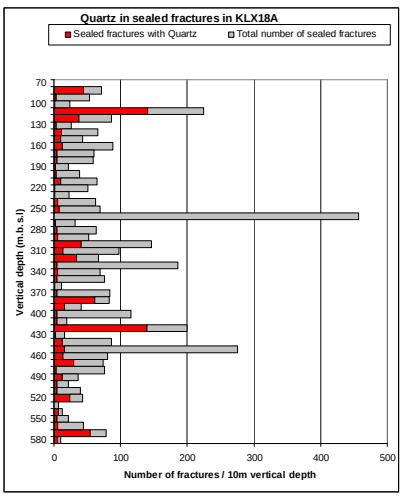
Quartz in sealed fractures in KLX18A
Sealed fractures with Quartz
Total number of sealed fractures
Vertical depth (m.b.s.l)
Number of fractures / 10m vertical depth

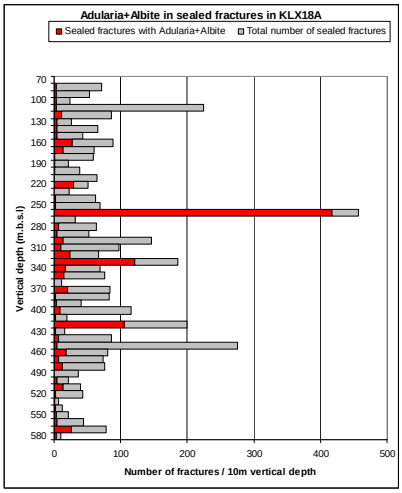
Adularia+Albite in sealed fractures in KLX18A
Sealed fractures with Adularia+Albite
Total number of sealed fractures
Vertical depth (m.b.s.l)
Number of fractures / 10m vertical depth

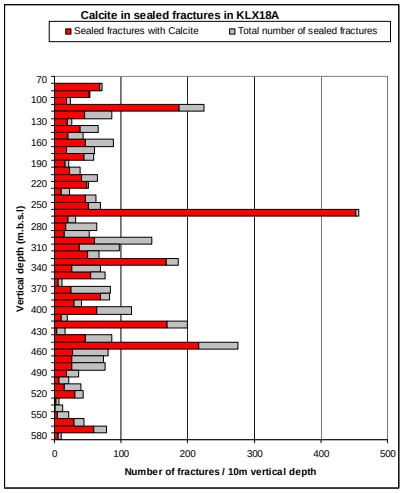
Calcite in sealed fractures in KLX18A
Sealed fractures with Calcite
Total number of sealed fractures
Vertical depth (m.b.s.l)
Number of fractures / 10m vertical depth

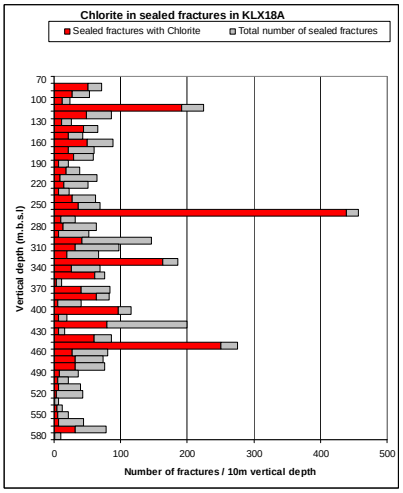
Chlorite in sealed fractures in KLX18A
Sealed fractures with Chlorite
Total number of sealed fractures
Vertical depth (m.b.s.l)
Number of fractures / 10m vertical depth

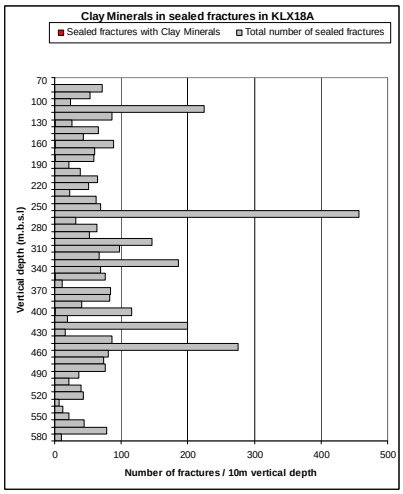
Clay Minerals in sealed fractures in KLX18A
Sealed fractures with Clay Minerals
Total number of sealed fractures
Vertical depth (m.b.s.l)
Number of fractures / 10m vertical depth

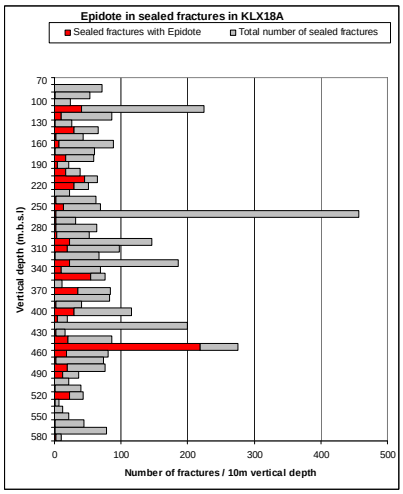
Epidote in sealed fractures in KLX18A
Sealed fractures with Epidote
Total number of sealed fractures
Vertical depth (m.b.s.l)
Number of fractures / 10m vertical depth

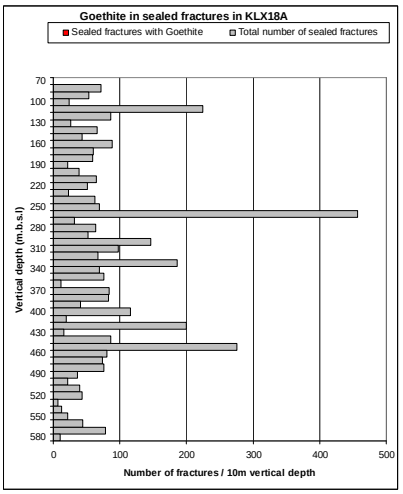
Goethite in sealed fractures in KLX18A
Sealed fractures with Goethite
Total number of sealed fractures
Vertical depth (m.b.s.l)
Number of fractures / 10m vertical depth

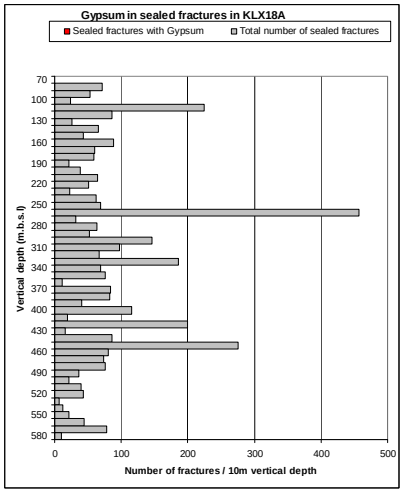
Gypsum in sealed fractures in KLX18A
Sealed fractures with Gypsum
Total number of sealed fractures
Vertical depth (m.b.s.l)
Number of fractures / 10m vertical depth

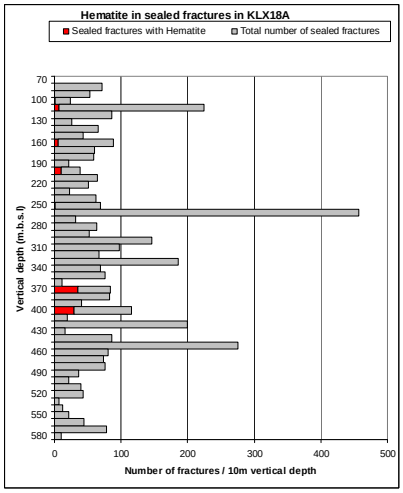
Hematite in sealed fractures in KLX18A
Sealed fractures with Hematite
Total number of sealed fractures
Vertical depth (m.b.s.l)
Number of fractures / 10m vertical depth

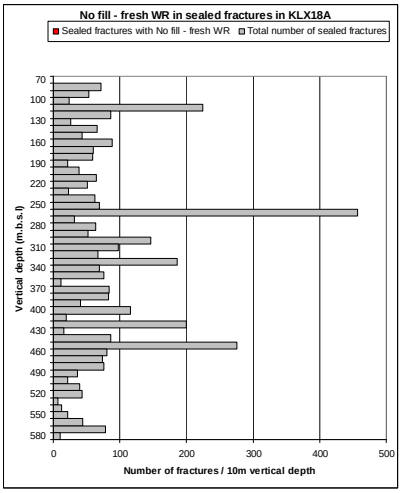
No fill - fresh WR in sealed fractures in KLX18A
Sealed fractures with No fill - fresh WR
Total number of sealed fractures
Vertical depth (m.b.s.l)
Number of fractures / 10m vertical depth

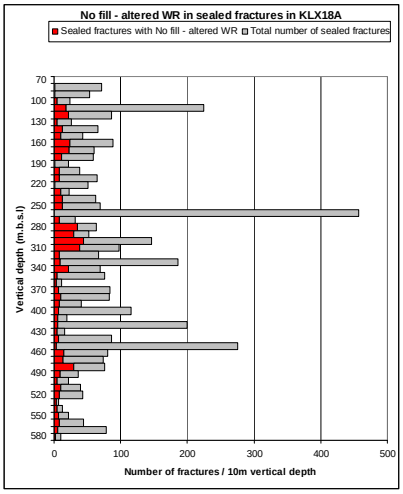
No fill - altered WR in sealed fractures in KLX18A
Sealed fractures with No fill - altered WR
Total number of sealed fractures
Vertical depth (m.b.s.l)
70
100
130
160
190
220
250
280
310
340
370
400
430
460
490
520
550
580
0
100
200
300
400
500
Number of fractures / 10m vertical depth

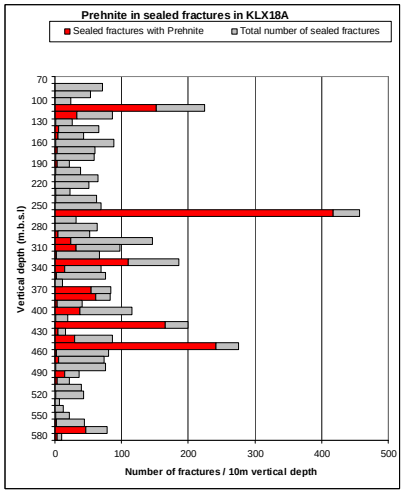
Prehnite in sealed fractures in KLX18A
Sealed fractures with Prehnite
Total number of sealed fractures
Vertical depth (m.b.s.l)
70
100
130
160
190
220
250
280
310
340
370
400
430
460
490
520
550
580
0
100
200
300
400
500
Number of fractures / 10m vertical depth

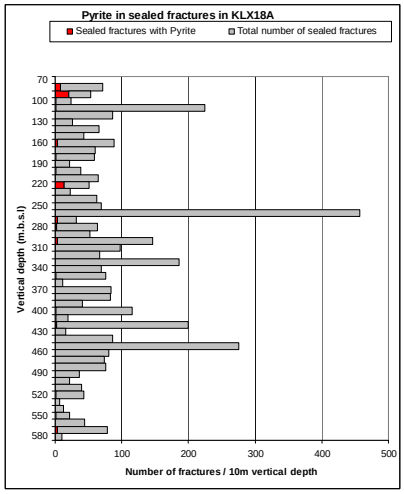
Pyrite in sealed fractures in KLX18A
Sealed fractures with Pyrite
Total number of sealed fractures
Vertical depth (m.b.s.l)
70
100
130
160
190
220
250
280
310
340
370
400
430
460
490
520
550
580
0
100
200
300
400
500
Number of fractures / 10m vertical depth

KLX19A

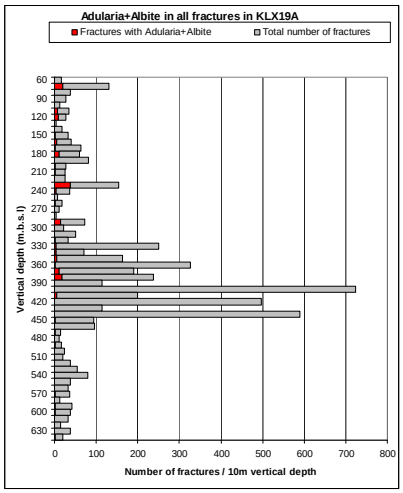
Adularia+Albite in all fractures in KLX19A
Fractures with Adularia+Albite
Total number of fractures
Vertical depth (m.b.s.l)
Number of fractures / 10m vertical depth

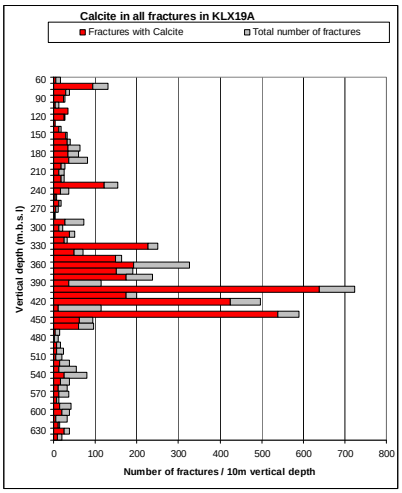
Calcite in all fractures in KLX19A
Fractures with Calcite
Total number of fractures
Vertical depth (m.b.s.l)
Number of fractures / 10m vertical depth

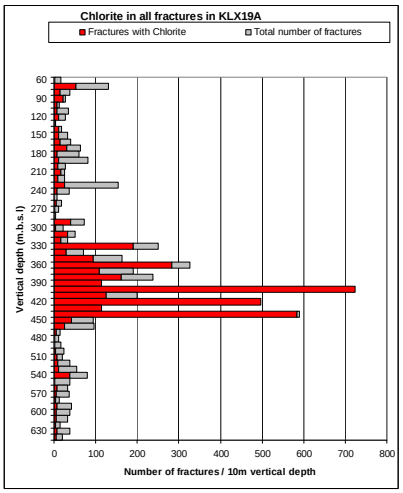
Chlorite in all fractures in KLX19A
Fractures with Chlorite
Total number of fractures
Vertical depth (m.b.s.l)
Number of fractures / 10m vertical depth

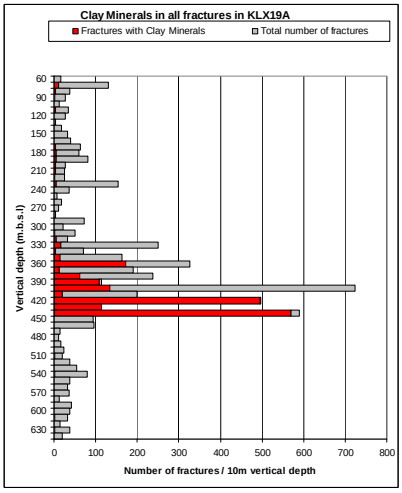
Clay Minerals in all fractures in KLX19A
Fractures with Clay Minerals
Total number of fractures
Vertical depth (m.b.s.l)
Number of fractures / 10m vertical depth

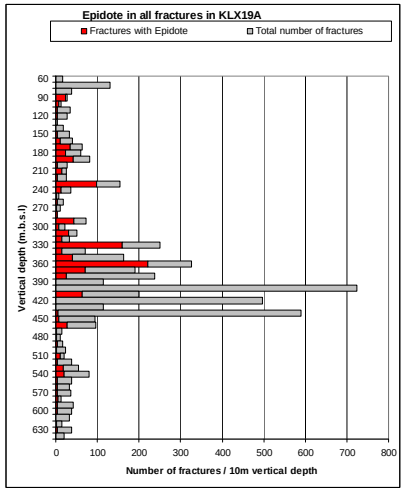
Epidote in all fractures in KLX19A
Fractures with Epidote
Total number of fractures
Vertical depth (m.b.s.l)
Number of fractures / 10m vertical depth

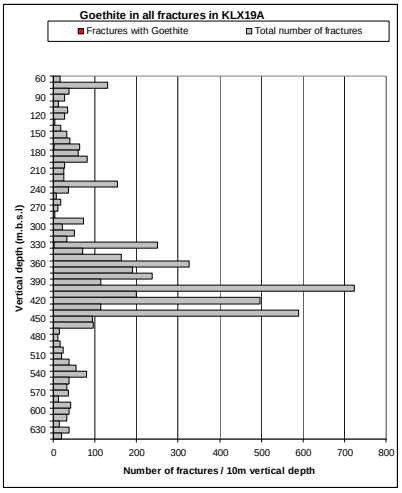
Goethite in all fractures in KLX19A
Fractures with Goethite
Total number of fractures
Vertical depth (m.b.s.l)
Number of fractures / 10m vertical depth

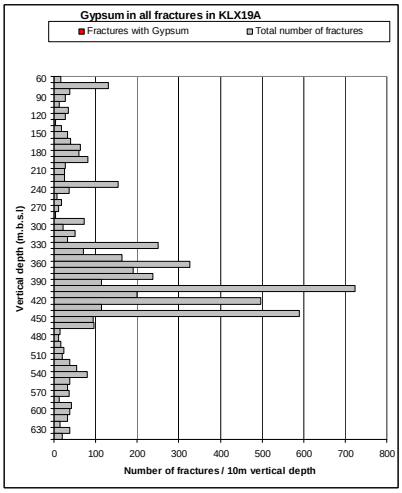
Gypsum in all fractures in KLX19A
Fractures with Gypsum
Total number of fractures
Vertical depth (m.b.s.l)
Number of fractures / 10m vertical depth

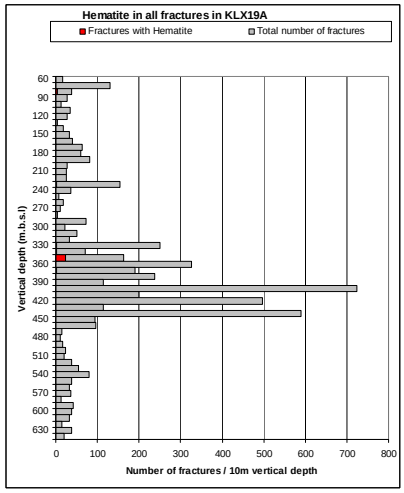
Hematite in all fractures in KLX19A
Fractures with Hematite
Total number of fractures
Vertical depth (m.b.s.l)
Number of fractures / 10m vertical depth

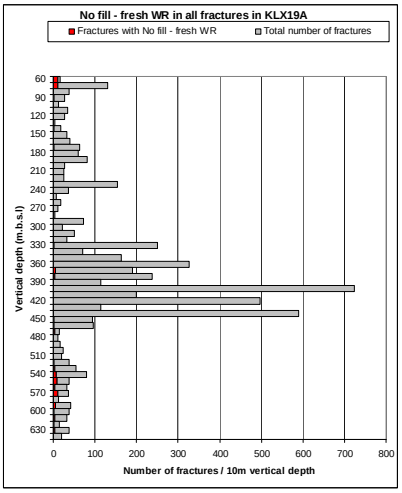
No fill - fresh WR in all fractures in KLX19A
Fractures with No fill - fresh WR
Total number of fractures
Vertical depth (m.b.s.l)
Number of fractures / 10m vertical depth

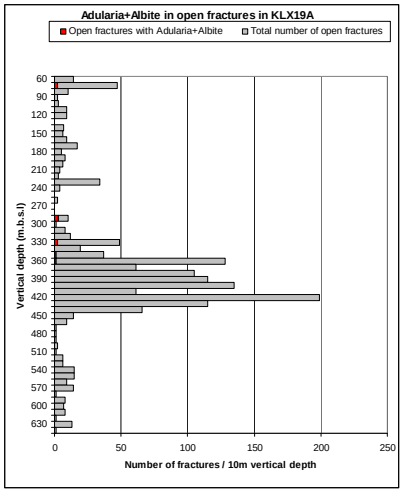
Adularia+Albite in open fractures in KLX19A
Open fractures with Adularia+Albite
Total number of open fractures
Vertical depth (m.b.s.l)
Number of fractures / 10m vertical depth

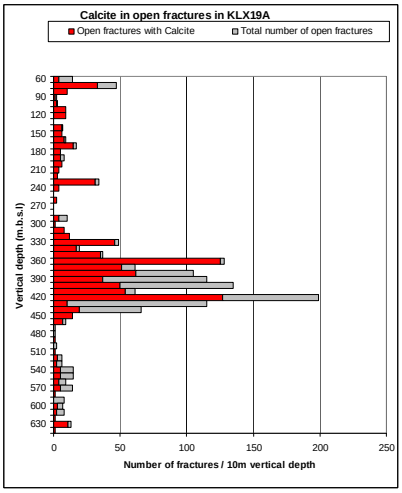
Calcite in open fractures in KLX19A
Open fractures with Calcite
Total number of open fractures
Vertical depth (m.b.s.l)
Number of fractures / 10m vertical depth

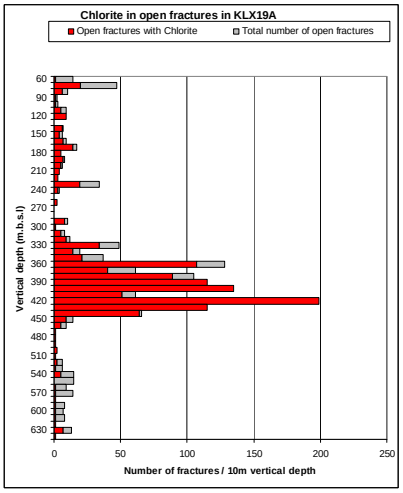
Chlorite in open fractures in KLX19A
Open fractures with Chlorite
Total number of open fractures
Vertical depth (m.b.s.l)
Number of fractures / 10m vertical depth

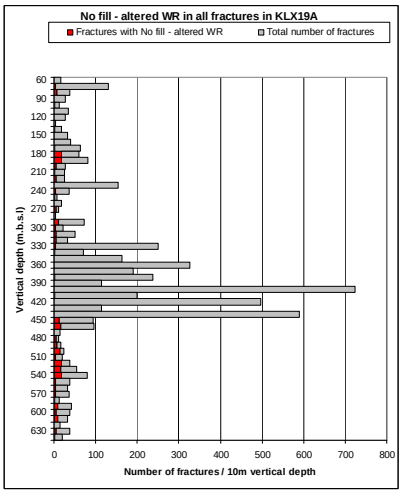
No fill - altered WR in all fractures in KLX19A
Fractures with No fill - altered WR
Total number of fractures
Vertical depth (m.b.s.l)
Number of fractures / 10m vertical depth

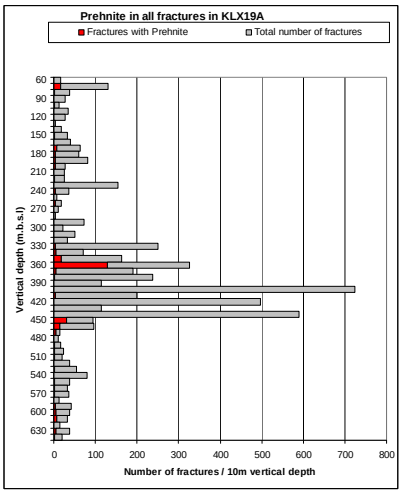
Prehnite in all fractures in KLX19A
Fractures with Prehnite
Total number of fractures
Vertical depth (m.b.s.l)
Number of fractures / 10m vertical depth

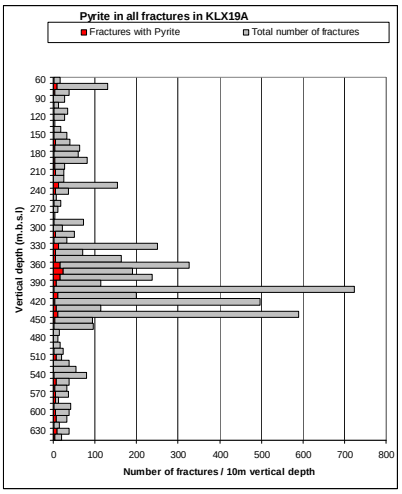
Pyrite in all fractures in KLX19A
Fractures with Pyrite
Total number of fractures
Vertical depth (m.b.s.l)
Number of fractures / 10m vertical depth

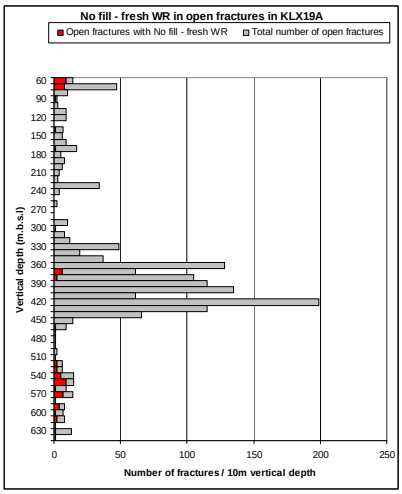
No fill - fresh WR in open fractures in KLX19A
Open fractures with No fill - fresh WR
Total number of open fractures
Vertical depth (m.b.s.l)
Number of fractures / 10m vertical depth

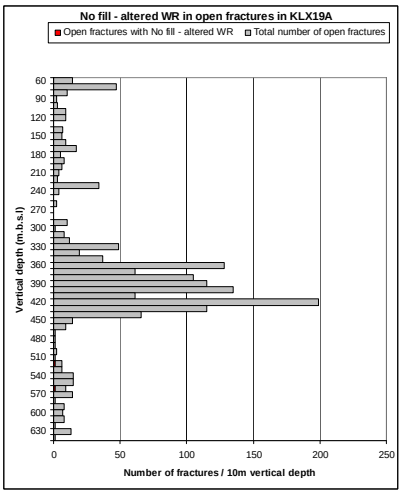
No fill - altered WR in open fractures in KLX19A
Open fractures with No fill - altered WR
Total number of open fractures
Vertical depth (m.b.s.l)
Number of fractures / 10m vertical depth

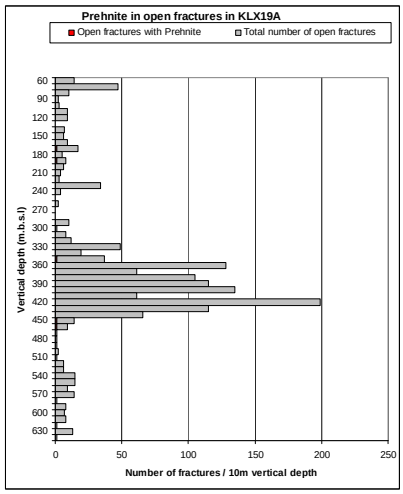
Prehnite in open fractures in KLX19A
Open fractures with Prehnite
Total number of open fractures
Vertical depth (m.b.s.l)
Number of fractures / 10m vertical depth

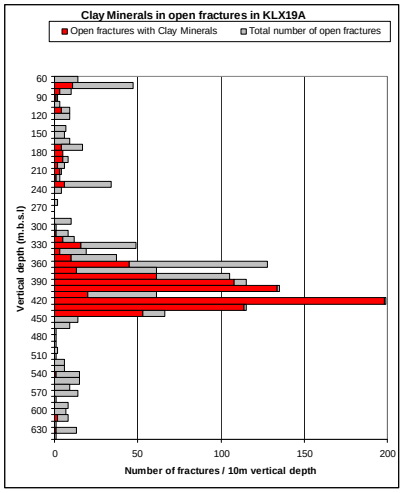
Clay Minerals in open fractures in KLX19A
Open fractures with Clay Minerals
Total number of open fractures
Vertical depth (m.b.s.l)
Number of fractures / 10m vertical depth

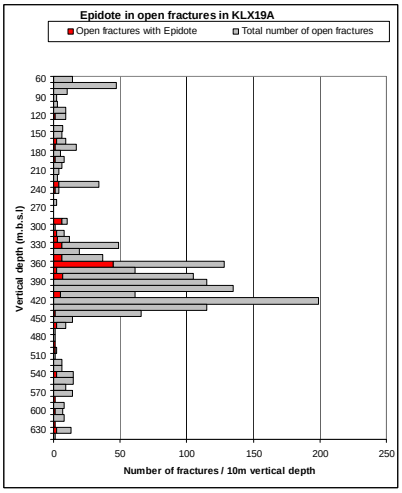
Epidote in open fractures in KLX19A
Open fractures with Epidote
Total number of open fractures
Vertical depth (m.b.s.l)
Number of fractures / 10m vertical depth

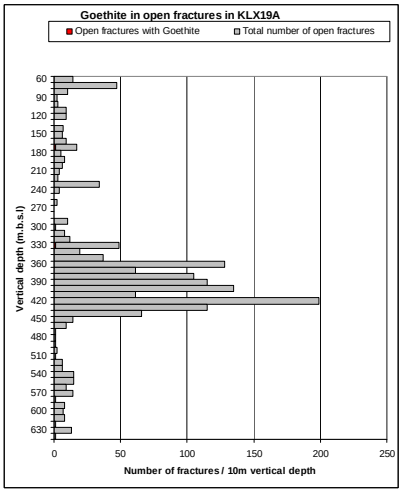
Goethite in open fractures in KLX19A
Open fractures with Goethite
Total number of open fractures
Vertical depth (m.b.s.l)
Number of fractures / 10m vertical depth

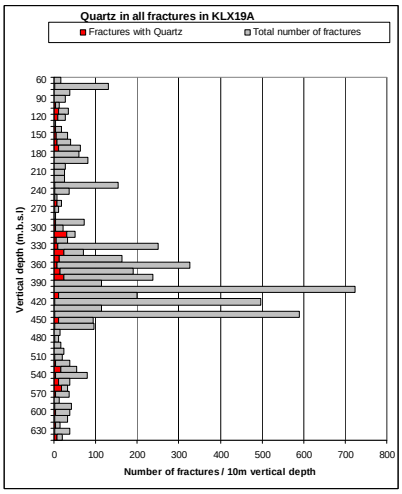
Quartz in all fractures in KLX19A
Fractures with Quartz
Total number of fractures
Vertical depth (m.b.s.l)
Number of fractures / 10m vertical depth

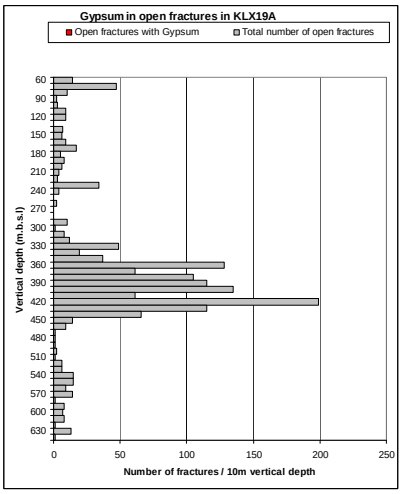
Gypsum in open fractures in KLX19A
Open fractures with Gypsum
Total number of open fractures
Vertical depth (m.b.s.l)
Number of fractures / 10m vertical depth

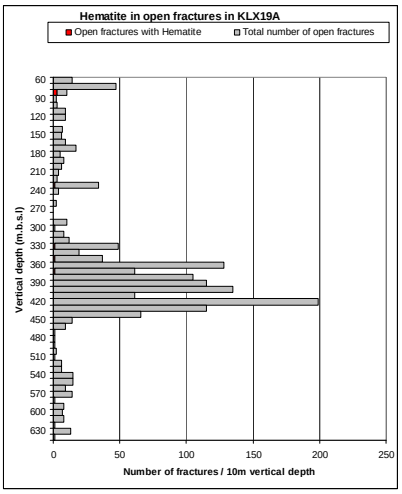
Hematite in open fractures in KLX19A
Open fractures with Hematite
Total number of open fractures
Vertical depth (m.b.s.l)
Number of fractures / 10m vertical depth

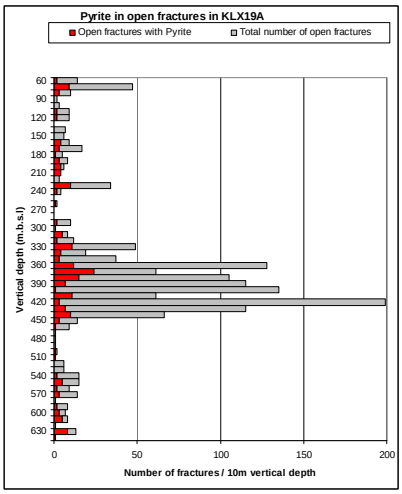
Pyrite in open fractures in KLX19A
Open fractures with Pyrite
Total number of open fractures
Vertical depth (m.b.s.l)
Number of fractures / 10m vertical depth

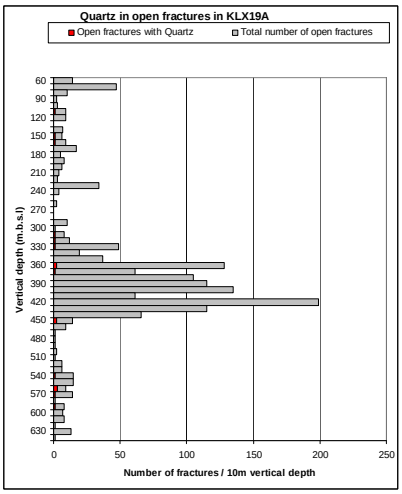
Quartz in open fractures in KLX19A
Open fractures with Quartz
Total number of open fractures
Vertical depth (m.b.s.l)
Number of fractures / 10m vertical depth

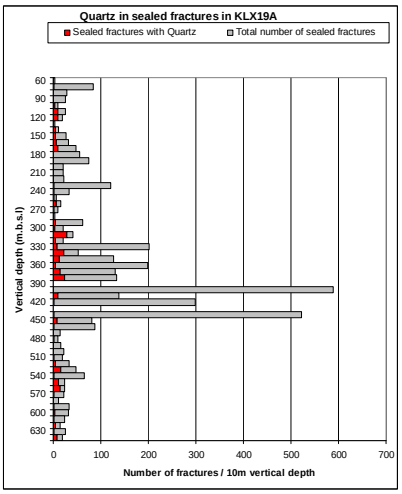
Quartz in sealed fractures in KLX19A
Sealed fractures with Quartz
Total number of sealed fractures
Vertical depth (m.b.s.l)
Number of fractures / 10m vertical depth

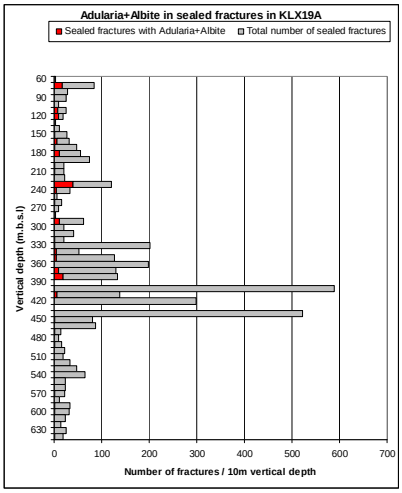
Adularia+Albite in sealed fractures in KLX19A
Sealed fractures with Adularia+Albite
Total number of sealed fractures
Vertical depth (m.b.s.l)
Number of fractures / 10m vertical depth

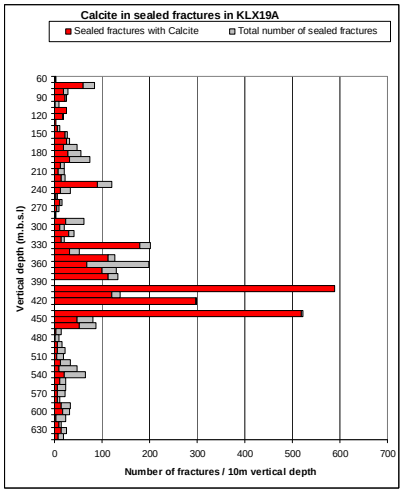
Calcite in sealed fractures in KLX19A
Sealed fractures with Calcite
Total number of sealed fractures
Vertical depth (m.b.s.l)
Number of fractures / 10m vertical depth

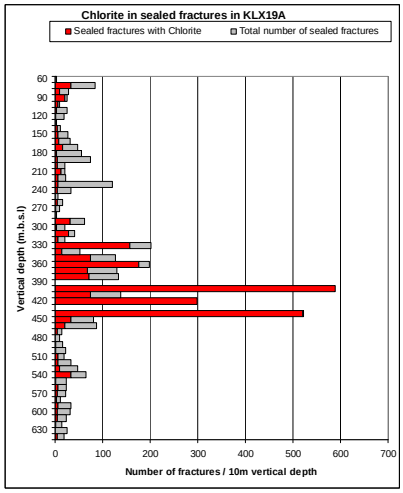
Chlorite in sealed fractures in KLX19A
Sealed fractures with Chlorite
Total number of sealed fractures
Vertical depth (m.b.s.l)
Number of fractures / 10m vertical depth

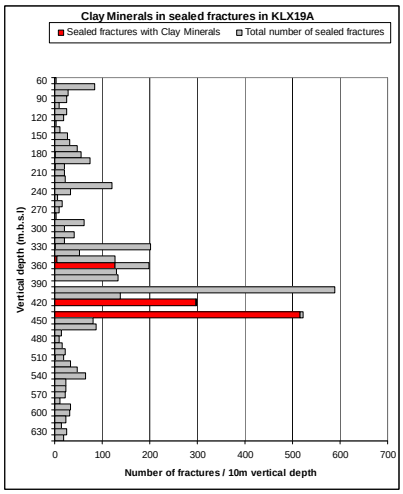
Clay Minerals in sealed fractures in KLX19A
Sealed fractures with Clay Minerals
Total number of sealed fractures
Vertical depth (m.b.s.l)
Number of fractures / 10m vertical depth

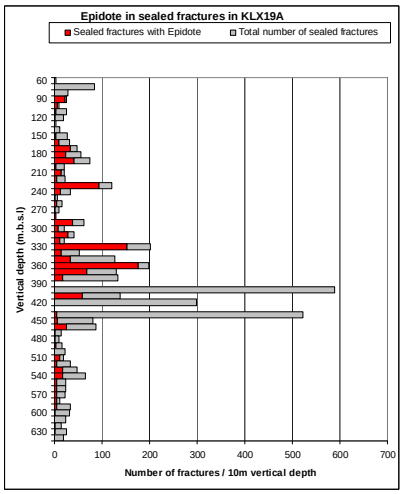
Epidote in sealed fractures in KLX19A
Sealed fractures with Epidote
Total number of sealed fractures
Vertical depth (m.b.s.l)
Number of fractures / 10m vertical depth

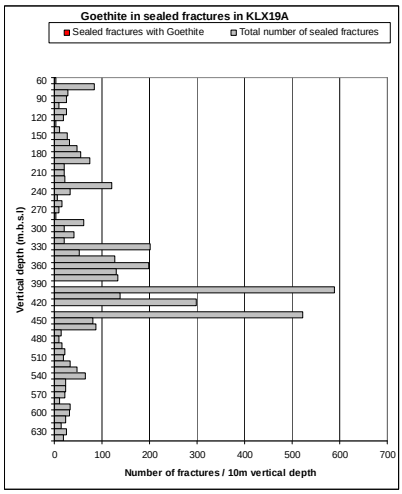
Goethite in sealed fractures in KLX19A
Sealed fractures with Goethite
Total number of sealed fractures
Vertical depth (m.b.s.l)
Number of fractures / 10m vertical depth

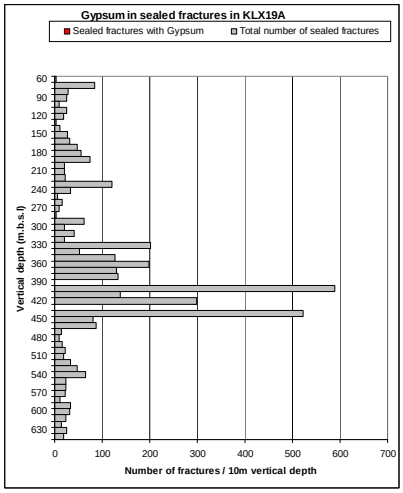
Gypsum in sealed fractures in KLX19A
Sealed fractures with Gypsum
Total number of sealed fractures
Vertical depth (m.b.s.l)
Number of fractures / 10m vertical depth

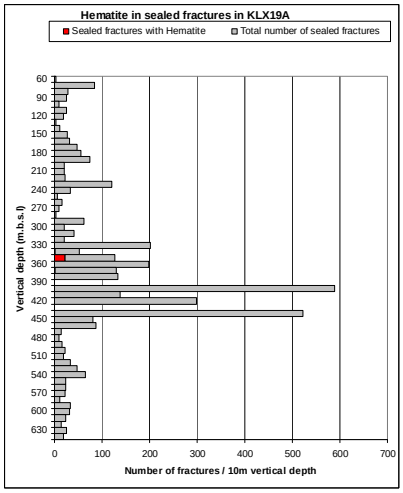
Hematite in sealed fractures in KLX19A
Sealed fractures with Hematite
Total number of sealed fractures
Vertical depth (m.b.s.l)
Number of fractures / 10m vertical depth

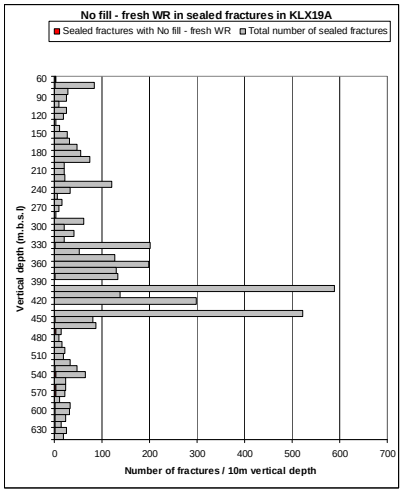
No fill - fresh WR in sealed fractures in KLX19A
Sealed fractures with No fill - fresh WR
Total number of sealed fractures
Verticel depth (m.b.s.l)
Number of fractures / 10m vertical depth

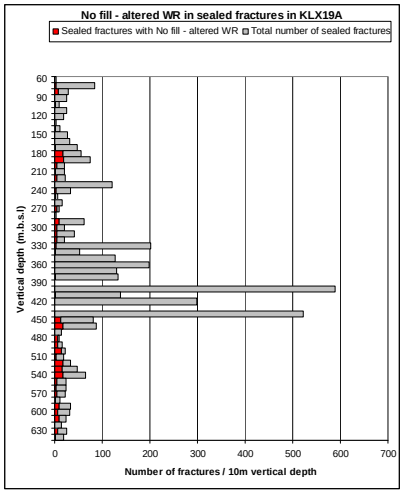
No fill - altered WR in sealed fractures in KLX19A
Sealed fractures with No fill - altered WR
Total number of sealed fractures
Vertical depth (m.b.s.l)
Number of fractures / 10m vertical depth

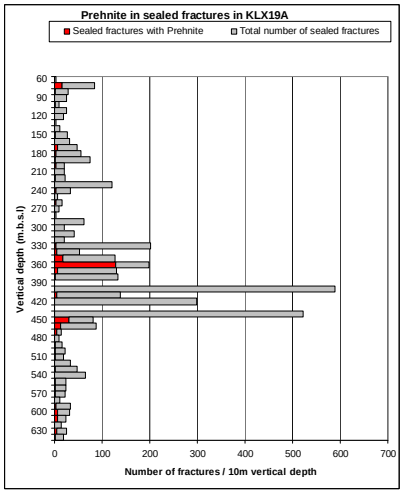
Prehnite in sealed fractures in KLX19A
Sealed fractures with Prehnite
Total number of sealed fractures
Vertical depth (m.b.s.l)
Number of fractures / 10m vertical depth

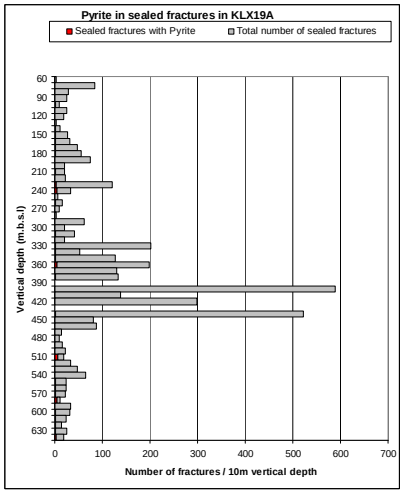
Pyrite in sealed fractures in KLX19A
Sealed fractures with Pyrite
Total number of sealed fractures
Vertical depth (m.b.s.l)
Number of fractures / 10m vertical depth

KLX20A

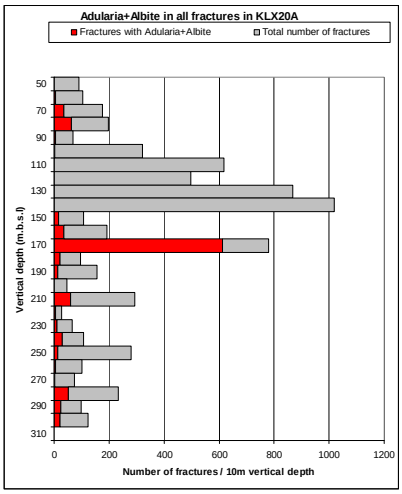
Adularia+Albite in all fractures in KLX20A
Fractures with Adularia+Albite
Total number of fractures
Vertical depth (m.b.s.l)
Number of fractures / 10m vertical depth

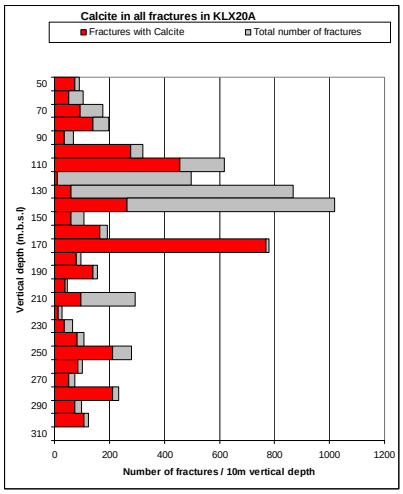
Calcite in all fractures in KLX20A
Fractures with Calcite
Total number of fractures
Vertical depth (m.b.s.l)
Number of fractures / 10m vertical depth

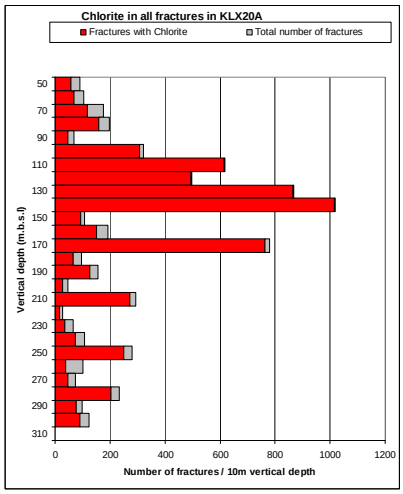
Chlorite in all fractures in KLX20A
Fractures with Chlorite
Total number of fractures
Vertical depth (m.b.s.l)
Number of fractures / 10m vertical depth

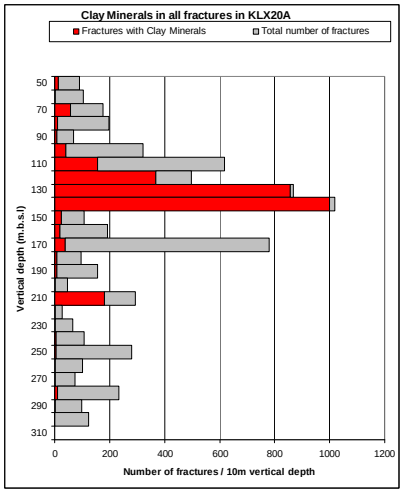
Clay Minerals in all fractures in KLX20A
Fractures with Clay Minerals
Total number of fractures
Vertical depth (m.b.s.l)
Number of fractures / 10m vertical depth

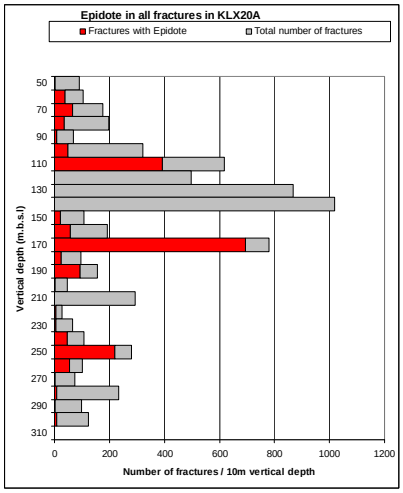
Epidote in all fractures in KLX20A
Fractures with Epidote
Total number of fractures
Vertical depth (m.b.s.l)
Number of fractures / 10m vertical depth

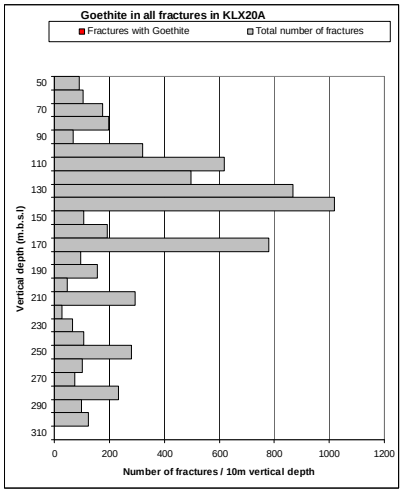
Goethite in all fractures in KLX20A
Fractures with Goethite
Total number of fractures
Vertical depth (m.b.s.l)
Number of fractures / 10m vertical depth

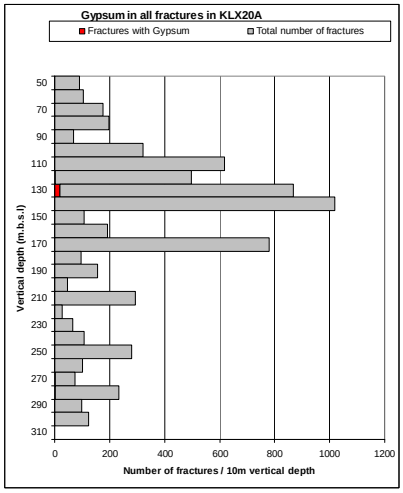
Gypsum in all fractures in KLX20A
Fractures with Gypsum
Total number of fractures
Vertical depth (m.b.s.l)
Number of fractures / 10m vertical depth

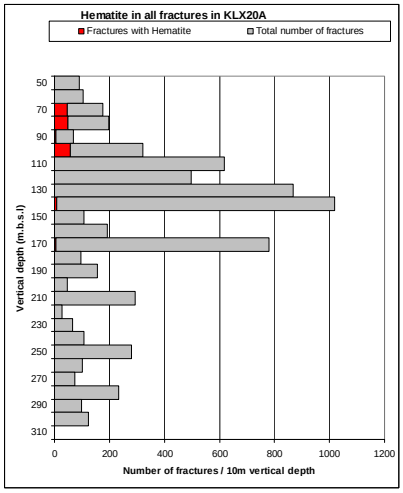
Hematite in all fractures in KLX20A
Fractures with Hematite
Total number of fractures
Vertical depth (m.b.s.l)
Number of fractures / 10m vertical depth

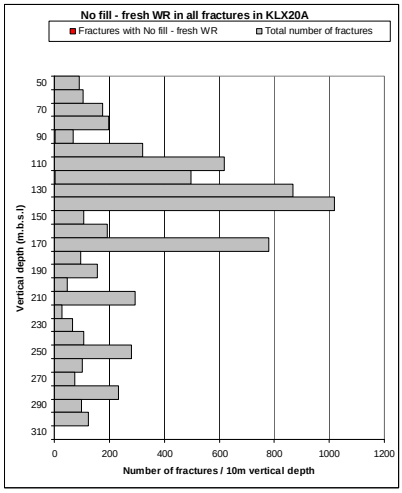
No fill - fresh WR in all fractures in KLX20A
Fractures with No fill - fresh WR
Total number of fractures
Vertical depth (m.b.s.l)
Number of fractures / 10m vertical depth

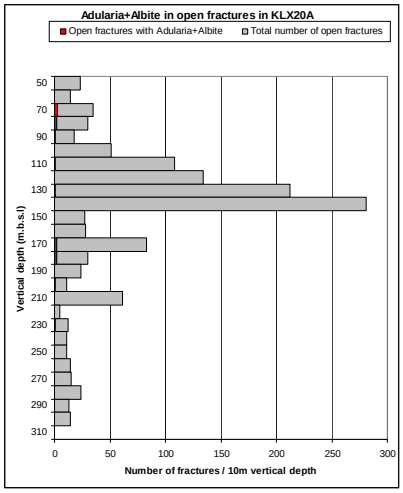
Adularia+Albite in open fractures in KLX20A
Open fractures with Adularia+Albite
Total number of open fractures
Vertical depth (m.b.s.l)
Number of fractures / 10m vertical depth

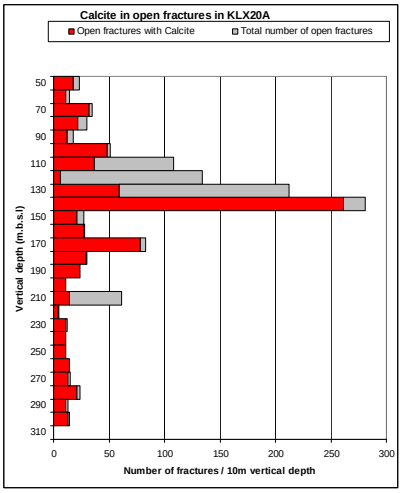
Calcite in open fractures in KLX20A
Open fractures with Calcite
Total number of open fractures
Vertical depth (m.b.s.l)
Number of fractures / 10m vertical depth

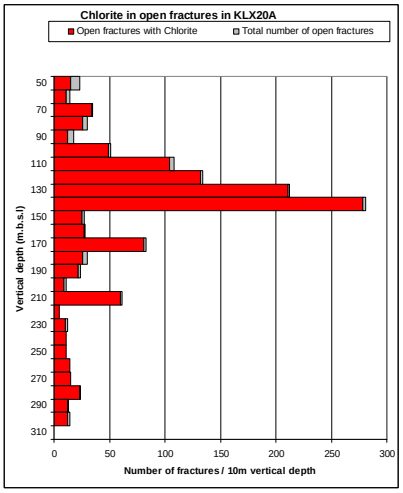
Chlorite in open fractures in KLX20A
Open fractures with Chlorite
Total number of open fractures
Vertical depth (m.b.s.l)
Number of fractures / 10m vertical depth

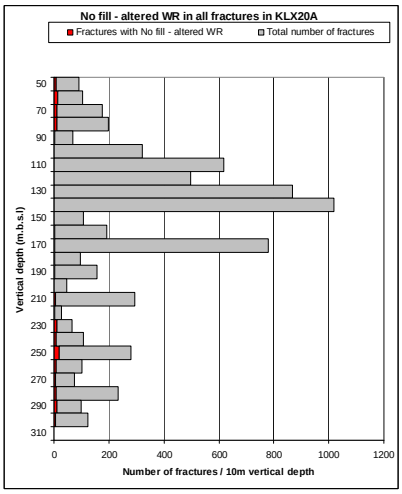
No fill - altered WR in all fractures in KLX20A
Fractures with No fill - altered WR
Total number of fractures
Vertical depth (m.b.s.l)
Number of fractures / 10m vertical depth

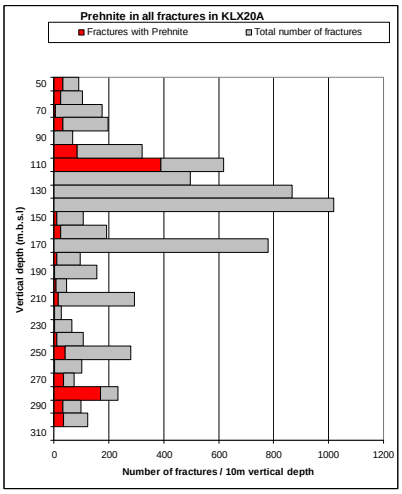
Prehnite in all fractures in KLX20A
Fractures with Prehnite
Total number of fractures
Vertical depth (m.b.s.l)
Number of fractures / 10m vertical depth

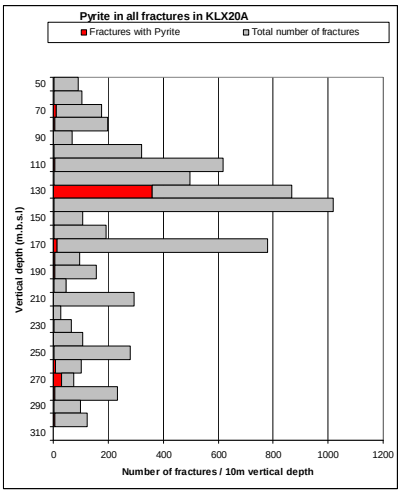
Pyrite in all fractures in KLX20A
Fractures with Pyrite
Total number of fractures
Vertical depth (m.b.s.l)
Number of fractures / 10m vertical depth

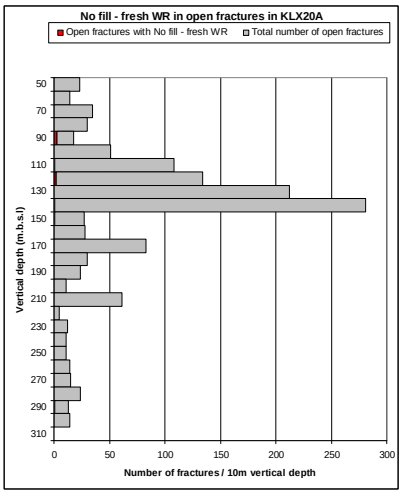
No fill - fresh WR in open fractures in KLX20A
Open fractures with No fill - fresh WR
Total number of open fractures
Vertical depth (m.b.s.l)
Number of fractures / 10m vertical depth

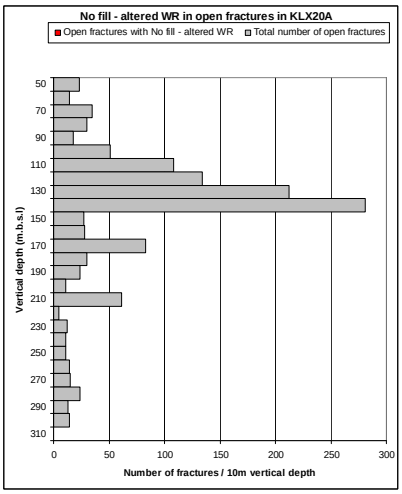
No fill - altered WR in open fractures in KLX20A
Open fractures with No fill - altered WR
Total number of open fractures
Vertical depth (m.b.s.l)
Number of fractures / 10m vertical depth

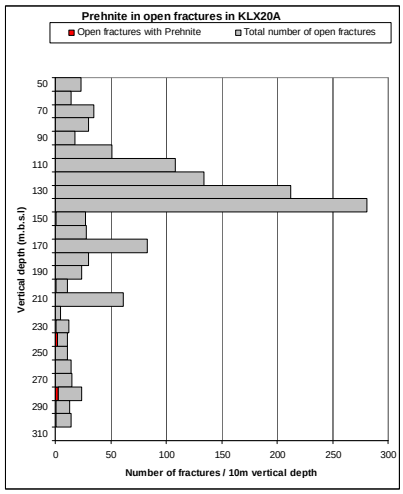
Prehnite in open fractures in KLX20A
Open fractures with Prehnite
Total number of open fractures
Vertical depth (m.b.s.l)
Number of fractures / 10m vertical depth

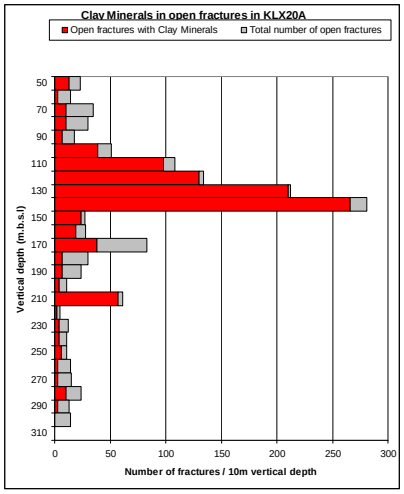
Clay Minerals in open fractures in KLX20A
Open fractures with Clay Minerals
Total number of open fractures
Vertical depth (m.b.s.l)
Number of fractures / 10m vertical depth

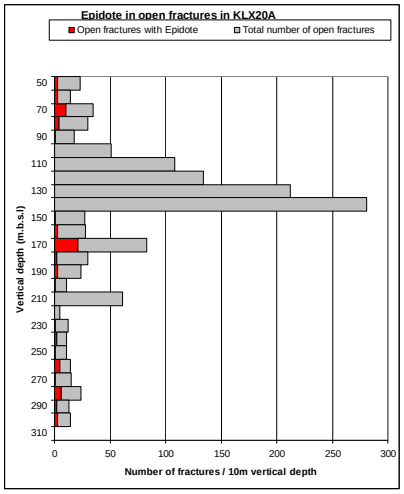
Epidote in open fractures in KLX20A
Open fractures with Epidote
Total number of open fractures
Vertical depth (m.b.s.l)
Number of fractures / 10m vertical depth

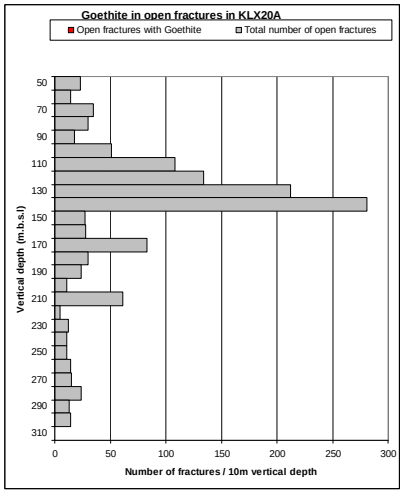
Goethite in open fractures in KLX20A
Open fractures with Goethite
Total number of open fractures
Vertical depth (m.b.s.l)
Number of fractures / 10m vertical depth

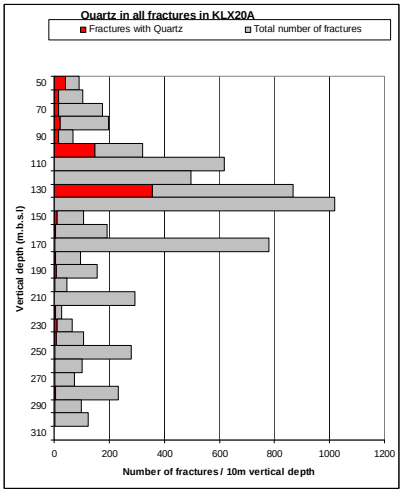
Quartz in all fractures in KLX20A
Fractures with Quartz
Total number of fractures
Vertical depth (m.b.s.l)
Number of fractures / 10m vertical depth

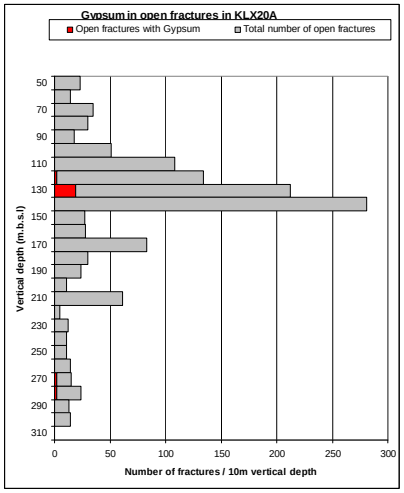
Gypsum in open fractures in KLX20A
Open fractures with Gypsum
Total number of open fractures
Vertical depth (m.b.s.l)
Number of fractures / 10m vertical depth

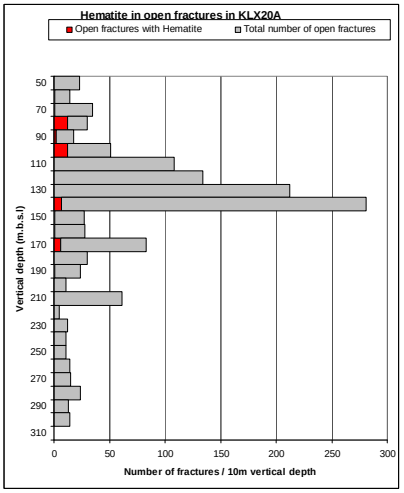
Hematite in open fractures in KLX20A
Open fractures with Hematite
Total number of open fractures
Vertical depth (m.b.s.l)
Number of fractures / 10m vertical depth

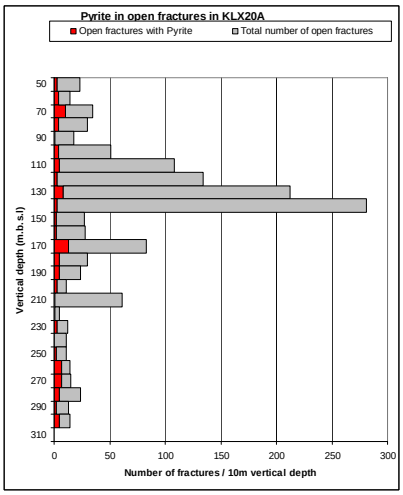
Pyrite in open fractures in KLX20A
Open fractures with Pyrite
Total number of open fractures
Vertical depth (m.b.s.l)
Number of fractures / 10m vertical depth

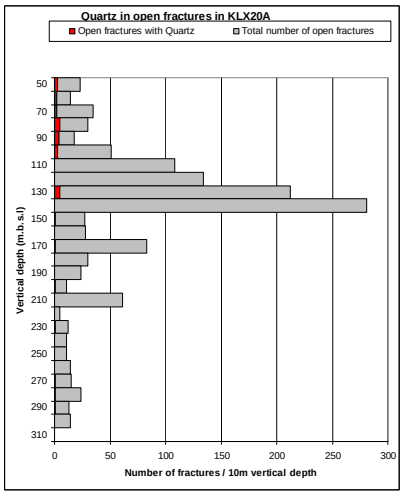
Quartz in open fractures in KLX20A
Open fractures with Quartz
Total number of open fractures
Vertical depth (m.b.s.l)
Number of fractures / 10m vertical depth

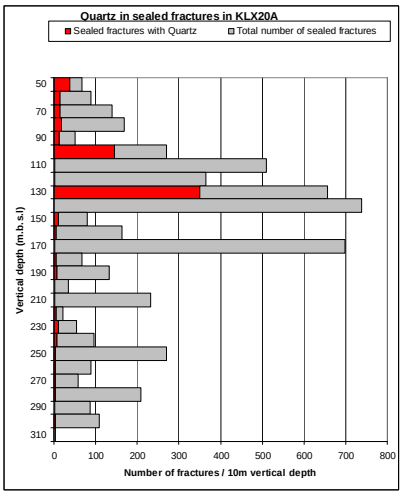
Quartz in sealed fractures in KLX20A
Sealed fractures with Quartz
Total number of sealed fractures
Vertical depth (m.b.s.l)
Number of fractures / 10m vertical depth

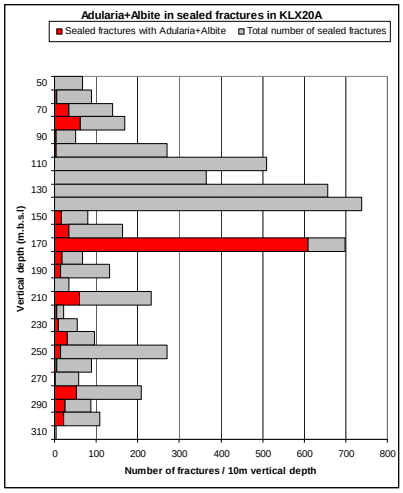
Adularia+Albite in sealed fractures in KLX20A
Sealed fractures with Adularia+Albite
Total number of sealed fractures
Vertical depth (m.b.s.l)
Number of fractures / 10m vertical depth

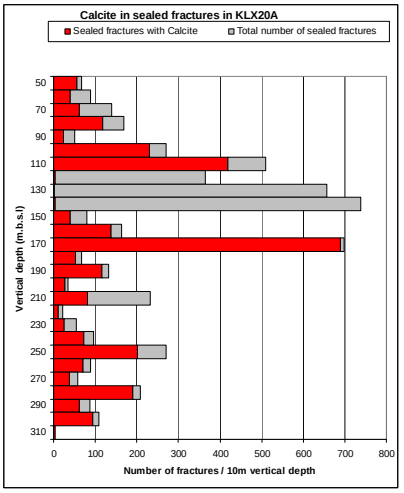
Calcite in sealed fractures in KLX20A
Sealed fractures with Calcite
Total number of sealed fractures
Vertical depth (m.b.s.l)
Number of fractures / 10m vertical depth

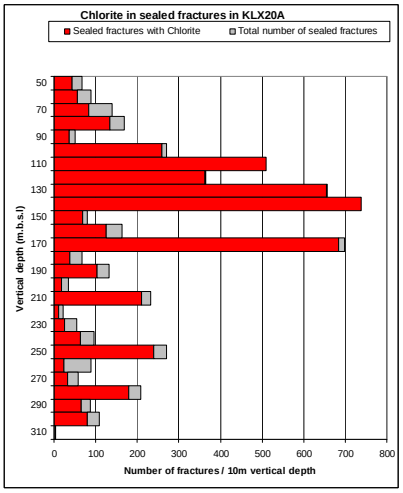
Chlorite in sealed fractures in KLX20A
Sealed fractures with Chlorite
Total number of sealed fractures
Vertical depth (m.b.s.l)
Number of fractures / 10m vertical depth

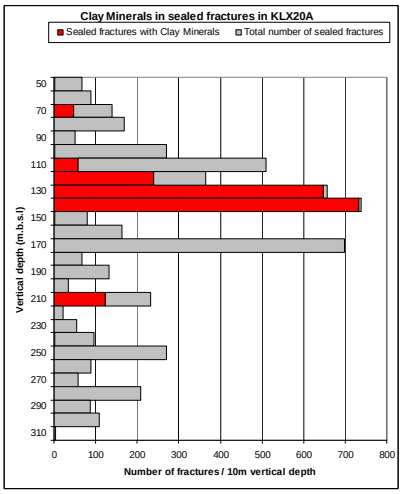
Clay Minerals in sealed fractures in KLX20A
Sealed fractures with Clay Minerals
Total number of sealed fractures
Vertical depth (m.b.s.l)
Number of fractures / 10m vertical depth

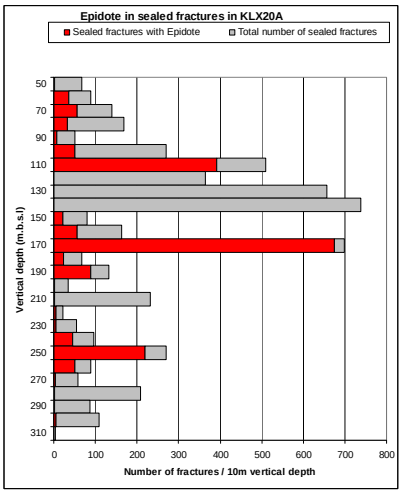
Epidote in sealed fractures in KLX20A
Sealed fractures with Epidote
Total number of sealed fractures
Vertical depth (m.b.s.l)
Number of fractures / 10m vertical depth

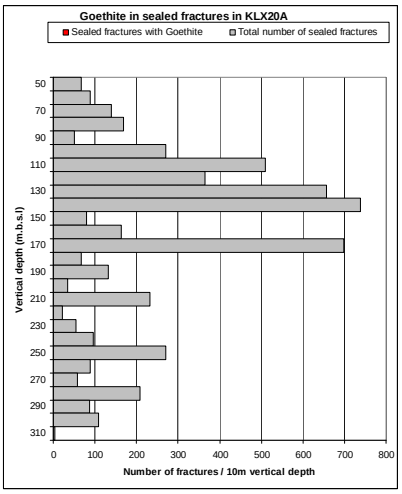
Goethite in sealed fractures in KLX20A
Sealed fractures with Goethite
Total number of sealed fractures
Vertical depth (m.b.s.l)
Number of fractures / 10m vertical depth

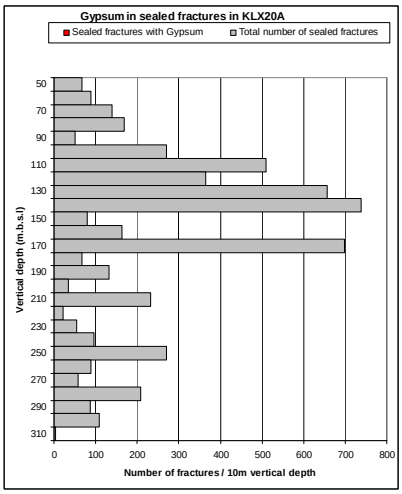
Gypsum in sealed fractures in KLX20A
Sealed fractures with Gypsum
Total number of sealed fractures
Vertical depth (m.b.s.l)
Number of fractures / 10m vertical depth

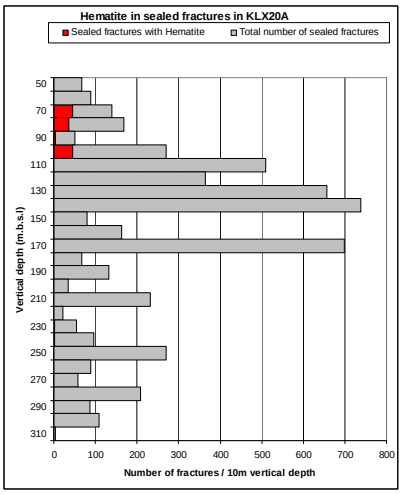
Hematite in sealed fractures in KLX20A
Sealed fractures with Hematite
Total number of sealed fractures
Vertical depth (m.b.s.l)
Number of fractures / 10m vertical depth

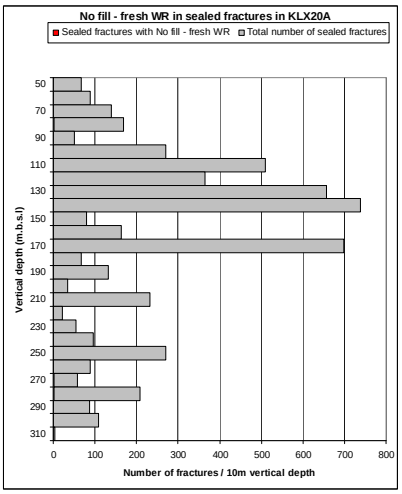
No fill - fresh WR in sealed fractures in KLX20A
Sealed fractures with No fill - fresh WR
Total number of sealed fractures
Vertical depth (m.b.s.l)
Number of fractures / 10m vertical depth

i

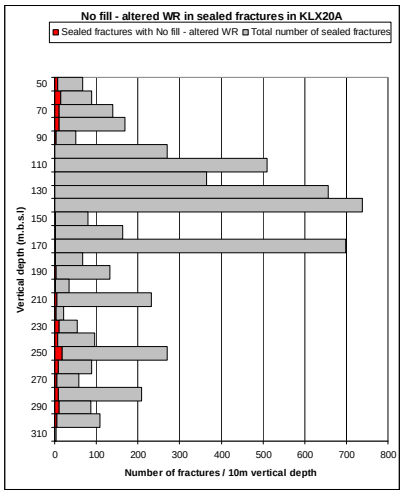
No fill - altered WR in sealed fractures in KLX20A
Sealed fractures with No fill - altered WR
Total number of sealed fractures
Vertical depth (m.b.s.l)
50
70
90
110
130
150
170
190
210
230
250
270
290
310
0
100
200
300
400
500
600
700
800
Number of fractures / 10m vertical depth

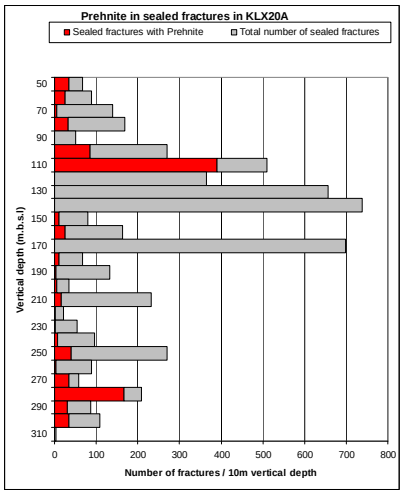
Prehnite in sealed fractures in KLX20A
Sealed fractures with Prehnite
Total number of sealed fractures
Vertical depth (m.b.s.l)
50
70
90
110
130
150
170
190
210
230
250
270
290
310
0
100
200
300
400
500
600
700
800
Number of fractures / 10m vertical depth

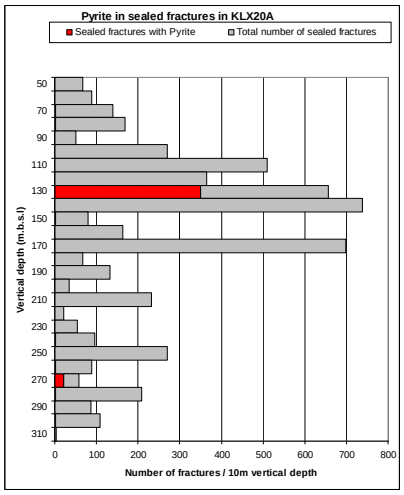
Pyrite in sealed fractures in KLX20A
Sealed fractures with Pyrite
Total number of sealed fractures
Vertical depth (m.b.s.l)
50
70
90
110
130
150
170
190
210
230
250
270
290
310
0
100
200
300
400
500
600
700
800
Number of fractures / 10m vertical depth

KLX21B

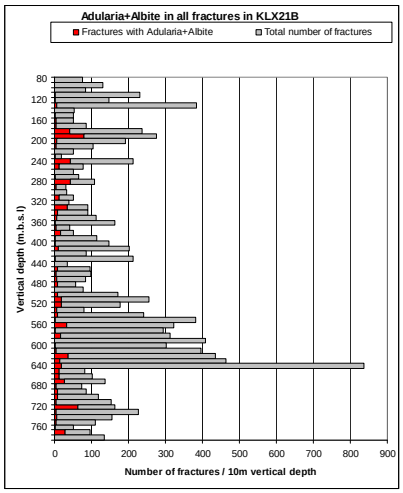
Adularia+Albite in all fractures in KLX21B
Fractures with Adularia+Albite
Total number of fractures
Vertical depth (m.b.s.l)
Number of fractures / 10m vertical depth

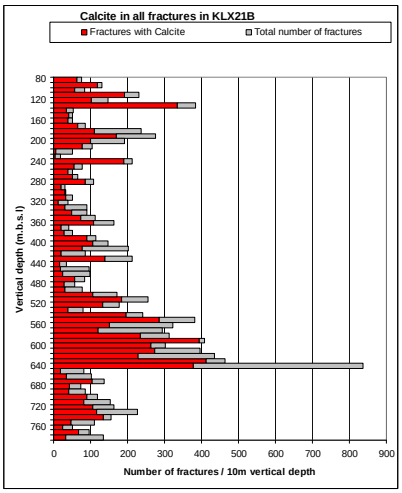
Calcite in all fractures in KLX21B
Fractures with Calcite
Total number of fractures
Vertical depth (m.b.s.l)
Number of fractures / 10m vertical depth

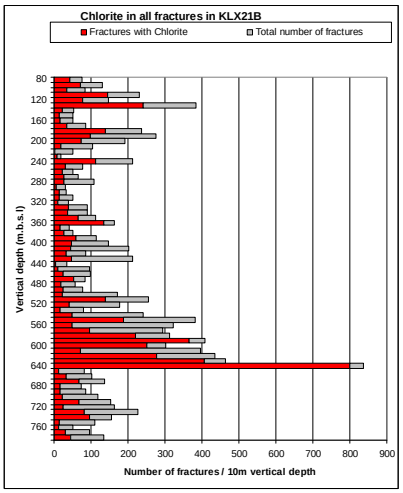
Chlorite in all fractures in KLX21B
Fractures with Chlorite
Total number of fractures
Vertical depth (m.b.s.l)
Number of fractures / 10m vertical depth

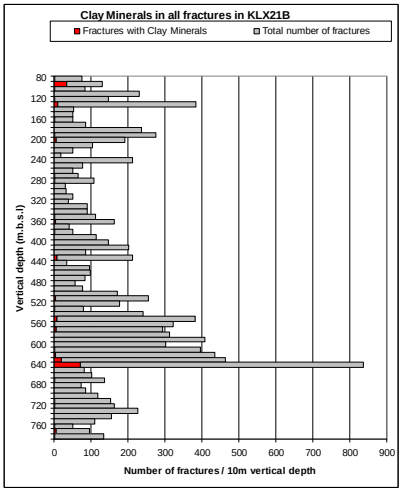
Clay Minerals in all fractures in KLX21B
Fractures with Clay Minerals
Total number of fractures
Vertical depth (m.b.s.l)
Number of fractures / 10m vertical depth

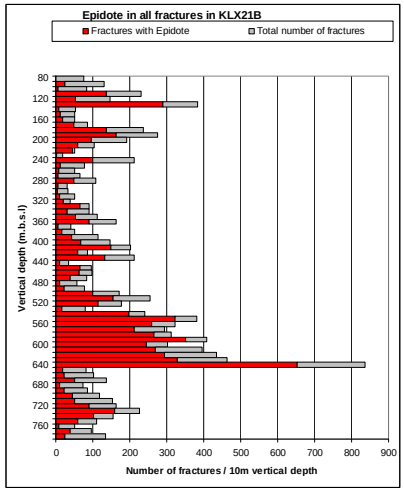
Epidote in all fractures in KLX21B
Fractures with Epidote
Total number of fractures
Vertical depth (m.b.s.l)
Number of fractures / 10m vertical depth

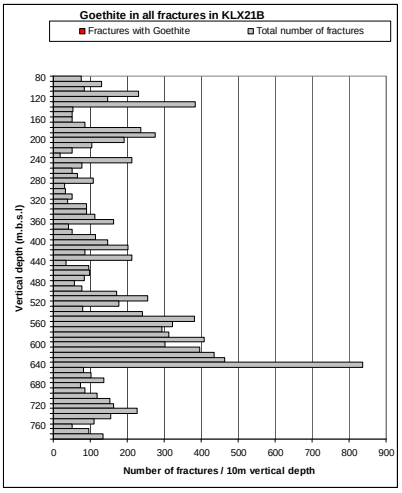
Goethite in all fractures in KLX21B
Fractures with Goethite
Total number of fractures
Vertical depth (m.b.s.l)
Number of fractures / 10m vertical depth

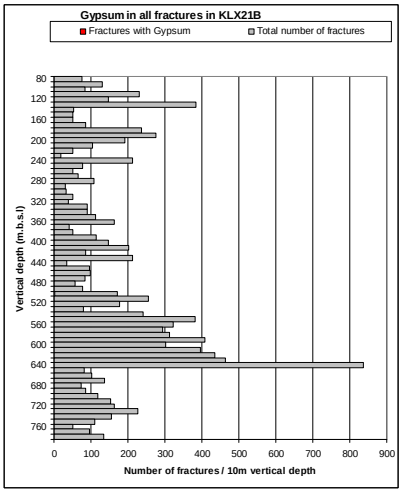
Gypsum in all fractures in KLX21B
Fractures with Gypsum
Total number of fractures
Vertical depth (m.b.s.l)
Number of fractures / 10m vertical depth

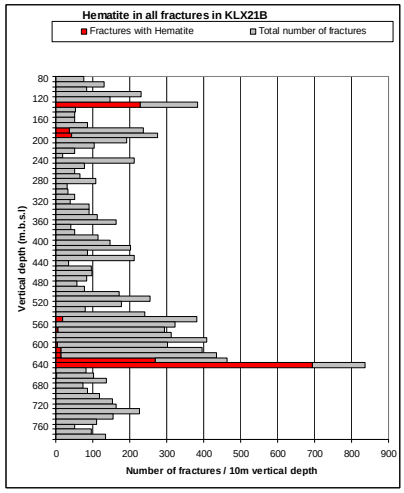
Hematite in all fractures in KLX21B
Fractures with Hematite
Total number of fractures
Vertical depth (m.b.s.l)
Number of fractures / 10m vertical depth

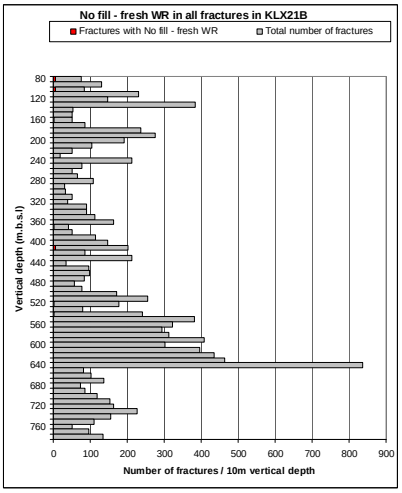
No fill - fresh WR in all fractures in KLX21B
Fractures with No fill - fresh WR
Total number of fractures
Vertical depth (m.b.s.l)
Number of fractures / 10m vertical depth

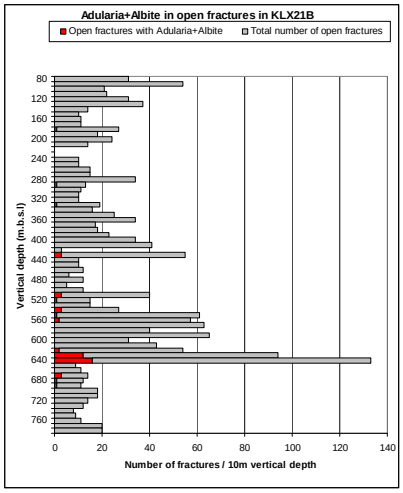
Adularia+Albite in open fractures in KLX21B
Open fractures with Adularia+Albite
Total number of open fractures
Vertical depth (m.b.s.l)
Number of fractures / 10m vertical depth

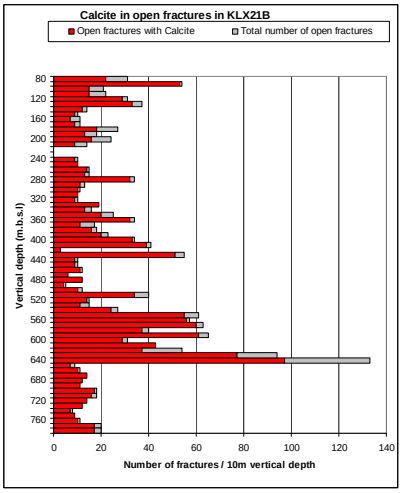
Calcite in open fractures in KLX21B
Open fractures with Calcite
Total number of open fractures
Vertical depth (m.b.s.l)
Number of fractures / 10m vertical depth

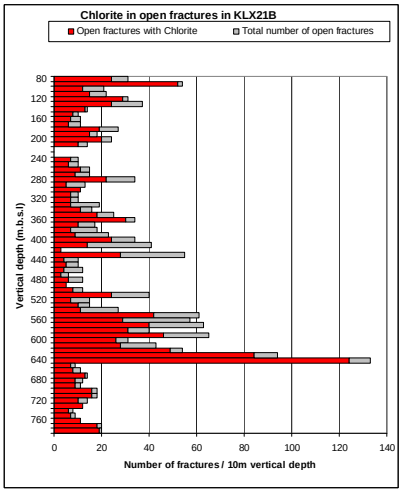
Chlorite in open fractures in KLX21B
Open fractures with Chlorite
Total number of open fractures
Vertical depth (m.b.s.l)
Number of fractures / 10m vertical depth

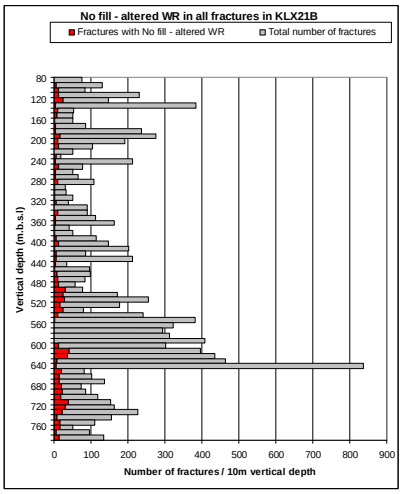
No fill - altered WR in all fractures in KLX21B
Fractures with No fill - altered WR
Total number of fractures
Vertical depth (m.b.s.l)
Number of fractures / 10m vertical depth

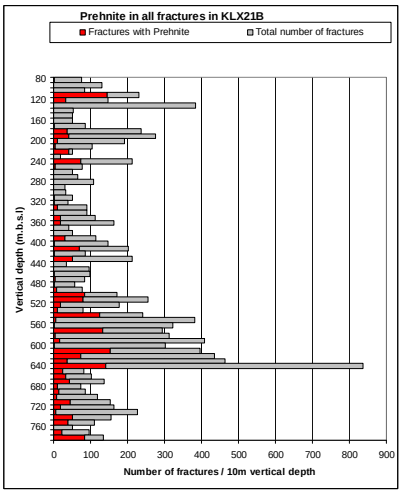
Prehnite in all fractures in KLX21B
Fractures with Prehnite
Total number of fractures
Vertical depth (m.b.s.l)
Number of fractures / 10m vertical depth

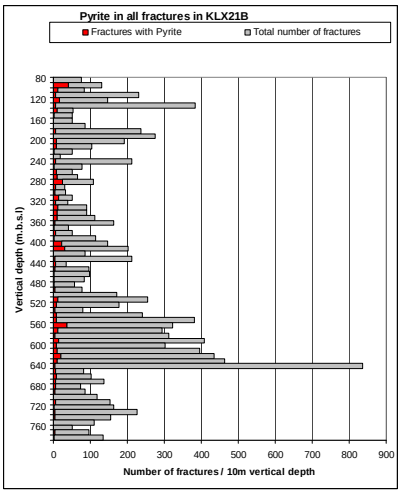
Pyrite in all fractures in KLX21B
Fractures with Pyrite
Total number of fractures
Vertical depth (m.b.s.l)
Number of fractures / 10m vertical depth

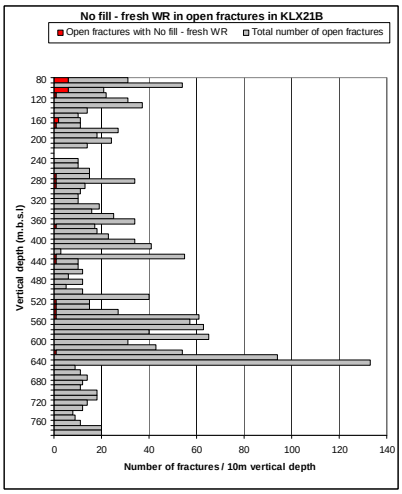
No fill - fresh WR in open fractures in KLX21B
Open fractures with No fill - fresh WR
Total number of open fractures
Vertical depth (m.b.s.l)
Number of fractures / 10m vertical depth

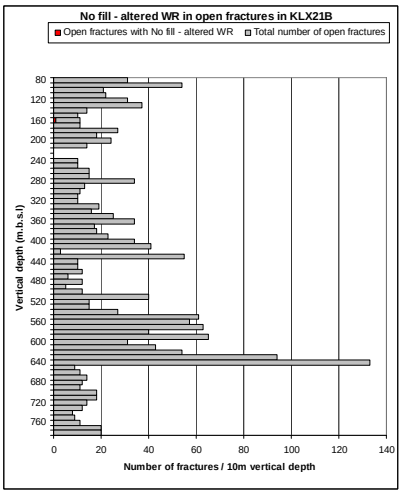
No fill - altered WR in open fractures in KLX21B
Open fractures with No fill - altered WR
Total number of open fractures
Vertical depth (m.b.s.l)
Number of fractures / 10m vertical depth

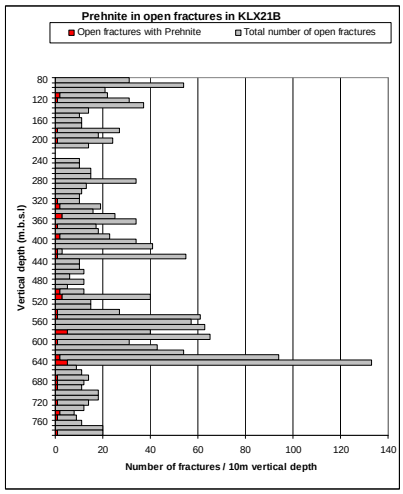
Prehnite in open fractures in KLX21B
Open fractures with Prehnite
Total number of open fractures
Vertical depth (m.b.s.l)
Number of fractures / 10m vertical depth

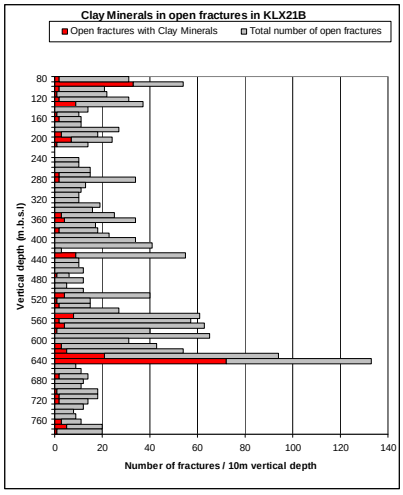
Clay Minerals in open fractures in KLX21B
Open fractures with Clay Minerals
Total number of open fractures
Vertical depth (m.b.s.l)
Number of fractures / 10m vertical depth

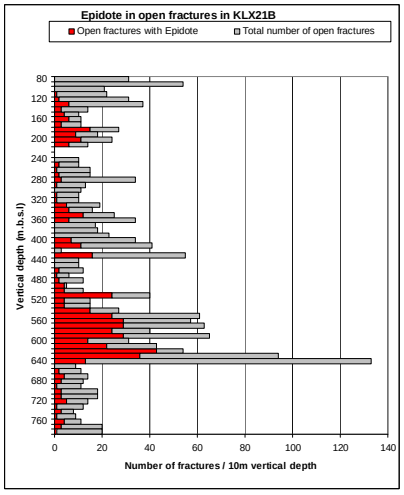
Epidote in open fractures in KLX21B
Open fractures with Epidote
Total number of open fractures
Vertical depth (m.b.s.l)
Number of fractures / 10m vertical depth

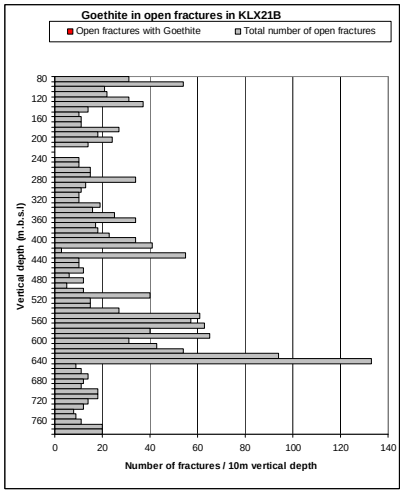
Goethite in open fractures in KLX21B
Open fractures with Goethite
Total number of open fractures
Vertical depth (m.b.s.l)
Number of fractures / 10m vertical depth

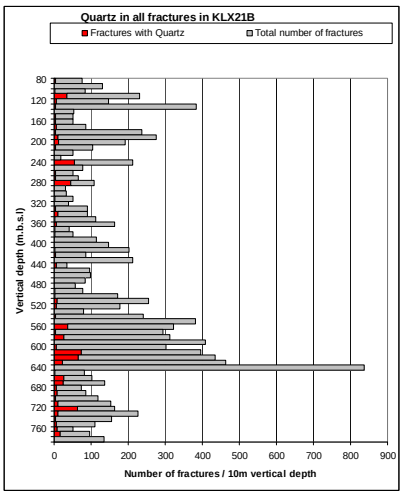
Quartz in all fractures in KLX21B
Fractures with Quartz
Total number of fractures
Vertical depth (m.b.s.l)
Number of fractures / 10m vertical depth

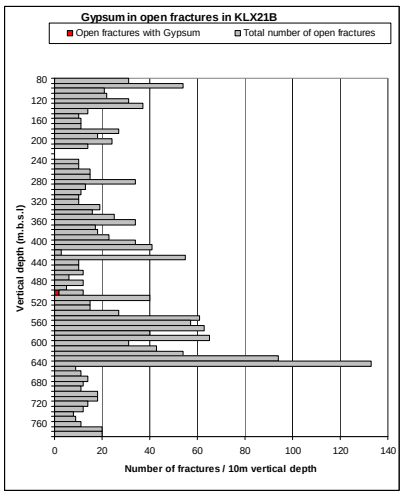
Gypsum in open fractures in KLX21B
Open fractures with Gypsum
Total number of open fractures
Vertical depth (m.b.s.l)
Number of fractures / 10m vertical depth

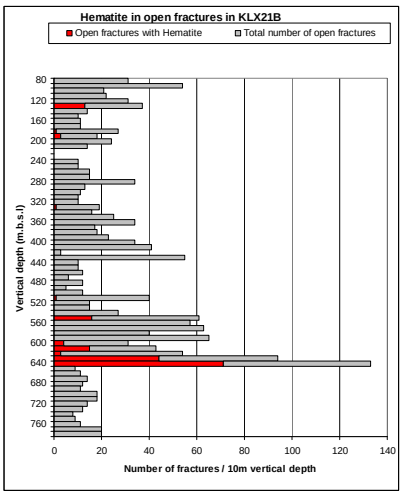
Hematite in open fractures in KLX21B
Open fractures with Hematite
Total number of open fractures
Vertical depth (m.b.s.l)
Number of fractures / 10m vertical depth

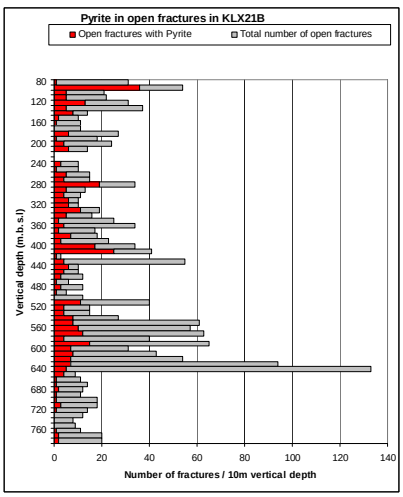
Pyrite in open fractures in KLX21B
Open fractures with Pyrite
Total number of open fractures
Vertical depth (m.b.s.l)
Number of fractures / 10m vertical depth

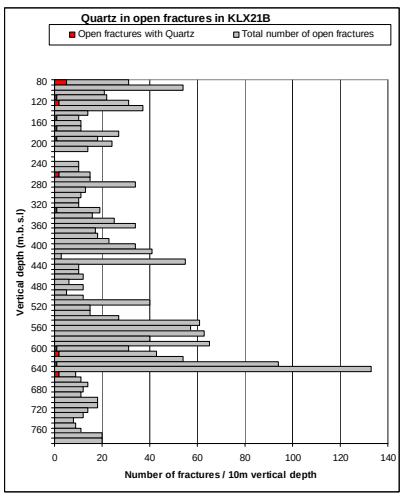
Quartz in open fractures in KLX21B
Open fractures with Quartz
Total number of open fractures
Vertical depth (m.b.s.l)
Number of fractures / 10m vertical depth

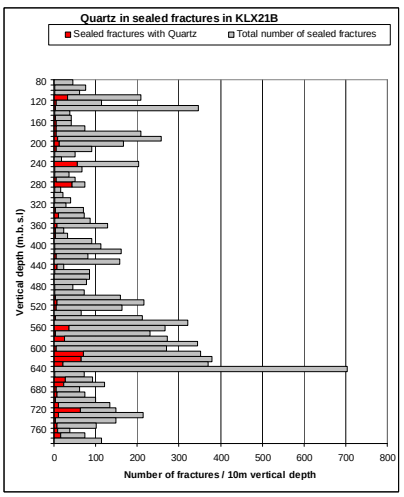
Quartz in sealed fractures in KLX21B
Sealed fractures with Quartz
Total number of sealed fractures
Vertical depth (m.b.s.l)
Number of fractures / 10m vertical depth

i

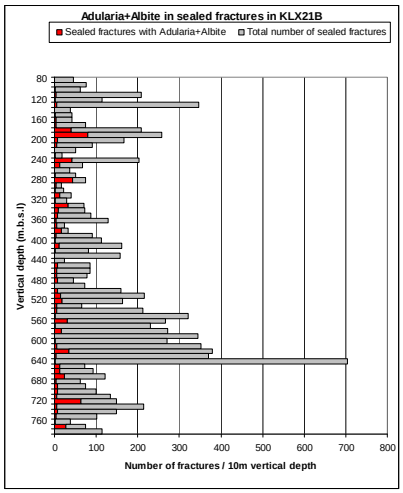
Adularia+Albite in sealed fractures in KLX21B
Sealed fractures with Adularia+Albite
Total number of sealed fractures
Vertical depth (m.b.s.l)
Number of fractures / 10m vertical depth

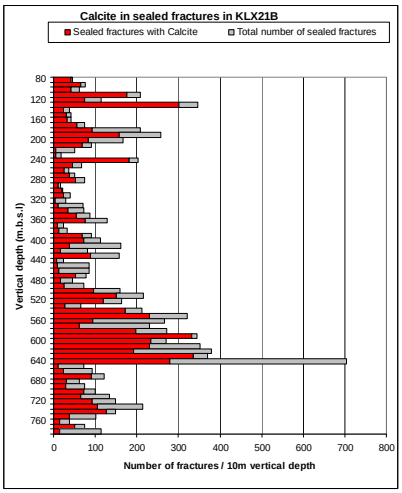
Calcite in sealed fractures in KLX21B
Sealed fractures with Calcite
Total number of sealed fractures
Vertical depth (m.b.s.l)
Number of fractures / 10m vertical depth

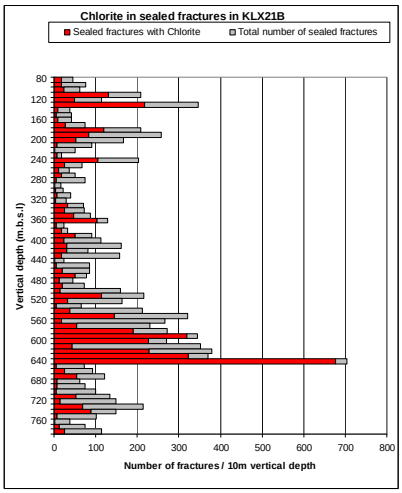
Chlorite in sealed fractures in KLX21B
Sealed fractures with Chlorite
Total number of sealed fractures
Vertical depth (m.b.s.l)
Number of fractures / 10m vertical depth

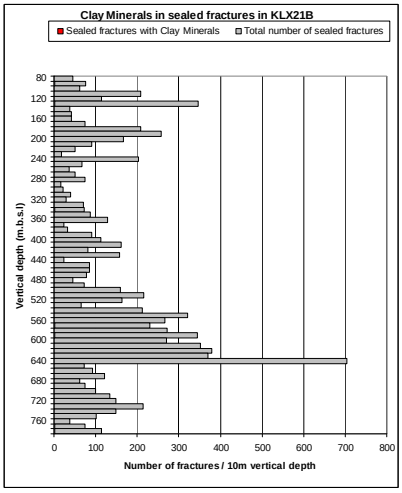
Clay Minerals in sealed fractures in KLX21B
Sealed fractures with Clay Minerals
Total number of sealed fractures
Vertical depth (m.b.s.l)
Number of fractures / 10m vertical depth

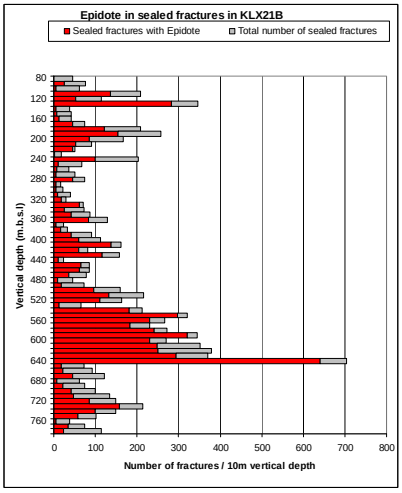
Epidote in sealed fractures in KLX21B
Sealed fractures with Epidote
Total number of sealed fractures
Vertical depth (m.b.s.l)
Number of fractures / 10m vertical depth

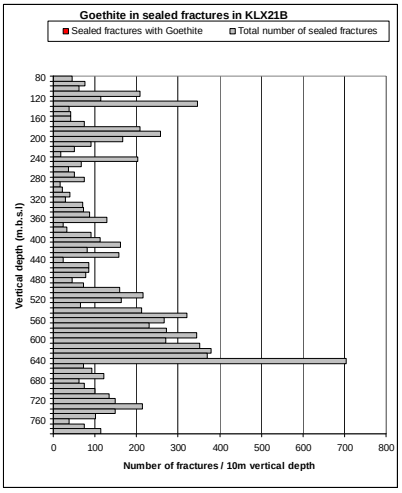
Goethite in sealed fractures in KLX21B
Sealed fractures with Goethite
Total number of sealed fractures
Vertical depth (m.b.s.l)
Number of fractures / 10m vertical depth

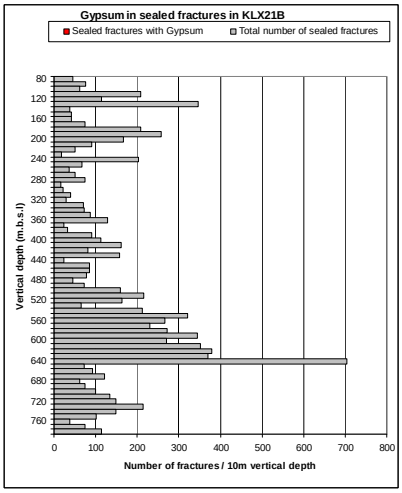
Gypsum in sealed fractures in KLX21B
Sealed fractures with Gypsum
Total number of sealed fractures
Vertical depth (m.b.s.l)
Number of fractures / 10m vertical depth

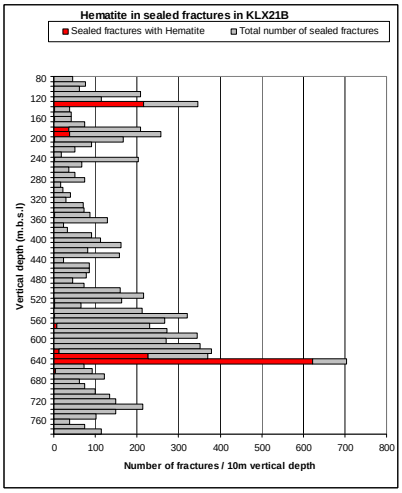
Hematite in sealed fractures in KLX21B
Sealed fractures with Hematite
Total number of sealed fractures
Vertical depth (m.b.s.l)
Number of fractures / 10m vertical depth

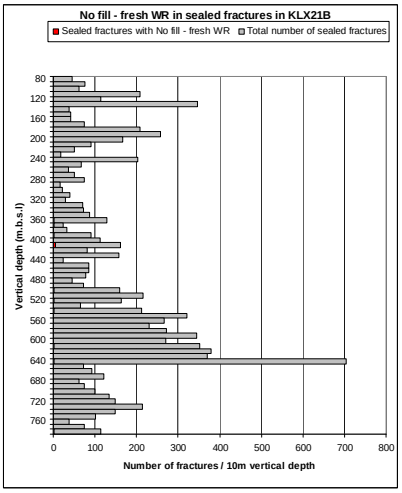
No fill - fresh WR in sealed fractures in KLX21B
Sealed fractures with No fill - fresh WR
Total number of sealed fractures
Vertical depth (m.b.s.l)
Number of fractures / 10m vertical depth

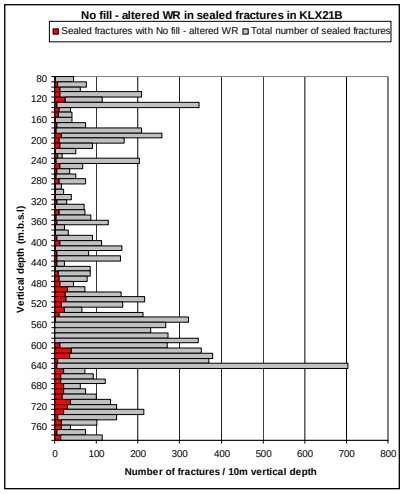
No fill - altered WR in sealed fractures in KLX21B
Sealed fractures with No fill - altered WR
Total number of sealed fractures
Vertical depth (m.b.s.l)
Number of fractures / 10m vertical depth

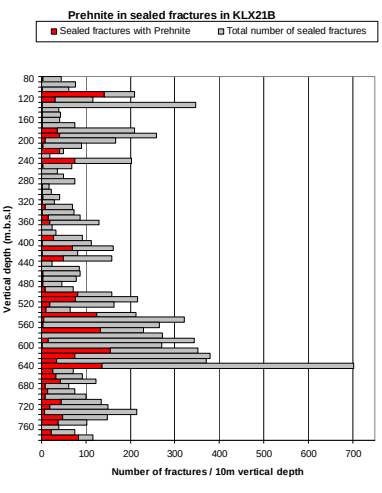
Prehnite in sealed fractures in KLX21B
Sealed fractures with Prehnite
Total number of sealed fractures
Vertical depth (m.b.s.l)
Number of fractures / 10m vertical depth

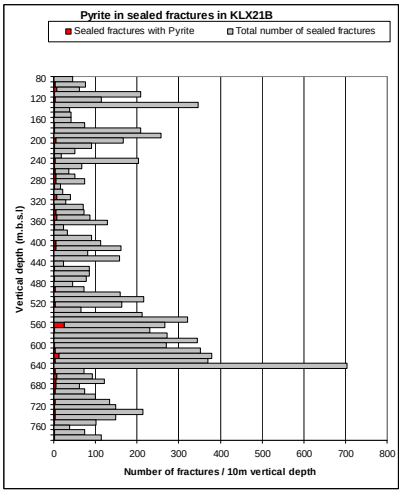
Pyrite in sealed fractures in KLX21B
Sealed fractures with Pyrite
Total number of sealed fractures
Vertical depth (m.b.s.l)
Number of fractures / 10m vertical depth

KLX22A

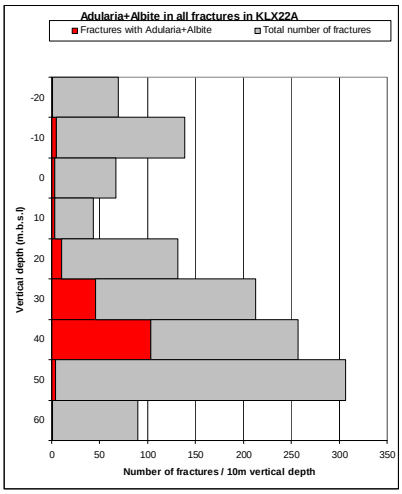
Adularia+Albite in all fractures in KLX22A
Fractures with Adularia+Albite
Total number of fractures
Vertical depth (m.b.s.l)
Number of fractures / 10m vertical depth

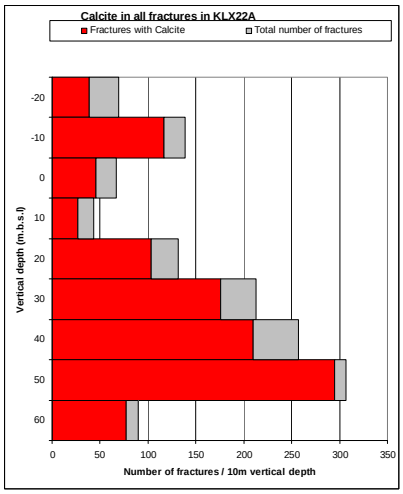
Calcite in all fractures in KLX22A
Fractures with Calcite
Total number of fractures
Vertical depth (m.b.s.l)
Number of fractures / 10m vertical depth

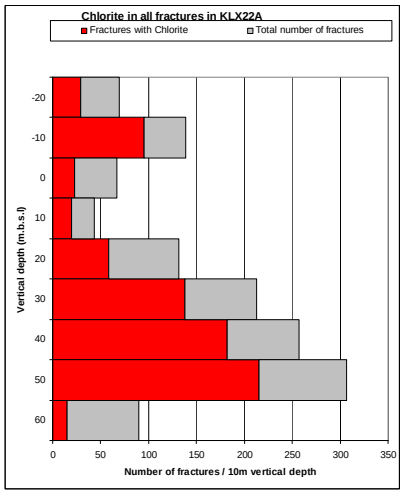
Chlorite in all fractures in KLX22A
Fractures with Chlorite
Total number of fractures
Vertical depth (m.b.s.l)
Number of fractures / 10m vertical depth

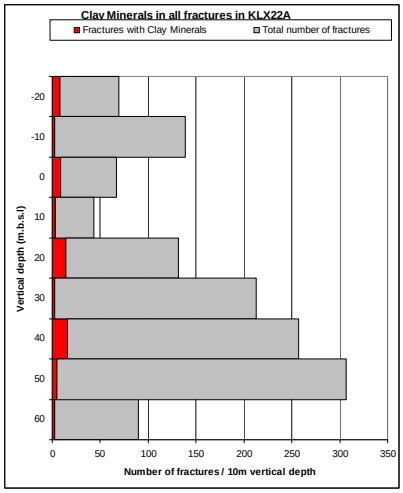
Clay Minerals in all fractures in KLX22A
Fractures with Clay Minerals
Total number of fractures
Vertical depth (m.b.s.l)
Number of fractures / 10m vertical depth

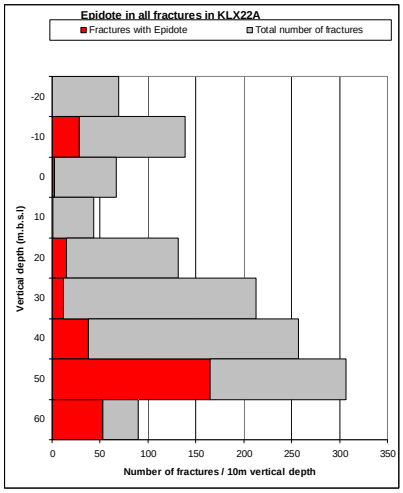
Epidote in all fractures in KLX22A
Fractures with Epidote
Total number of fractures
Vertical depth (m.b.s.l)
Number of fractures / 10m vertical depth

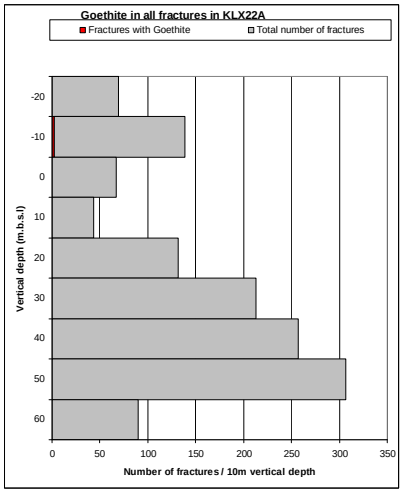
Goethite in all fractures in KLX22A
Fractures with Goethite
Total number of fractures
Vertical depth (m.b.s.l)
Number of fractures / 10m vertical depth

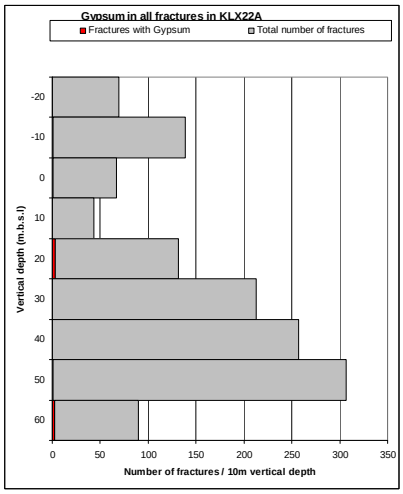
Gypsum in all fractures in KLX22A
Fractures with Gypsum
Total number of fractures
Vertical depth (m.b.s.l)
Number of fractures / 10m vertical depth

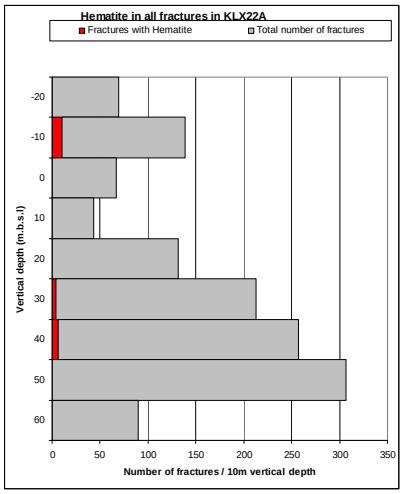
Hematite in all fractures in KLX22A
Fractures with Hematite
Total number of fractures
Vertical depth (m.b.s.l)
Number of fractures / 10m vertical depth

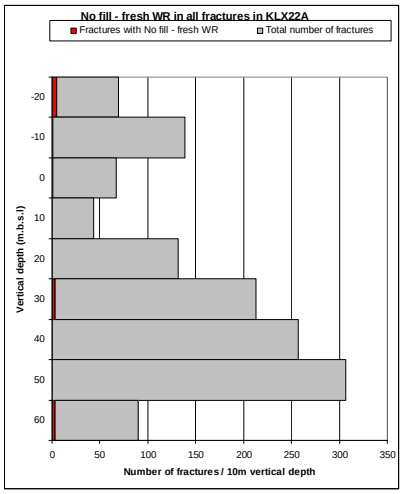
No fill - fresh WR in all fractures in KLX22A
Fractures with No fill - fresh WR
Total number of fractures
Vertical depth (m.b.s.l)
Number of fractures / 10m vertical depth

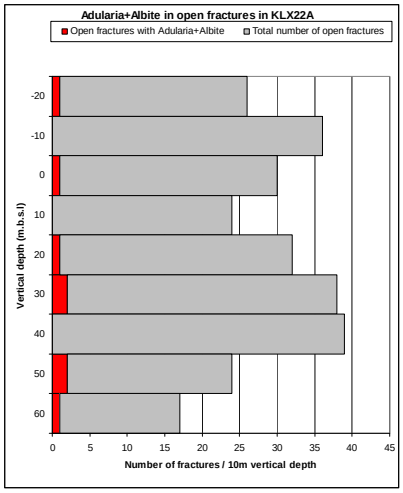
Adularia+Albite in open fractures in KLX22A
Open fractures with Adularia+Albite
Total number of open fractures
Vertical depth (m.b.s.l)
Number of fractures / 10m vertical depth

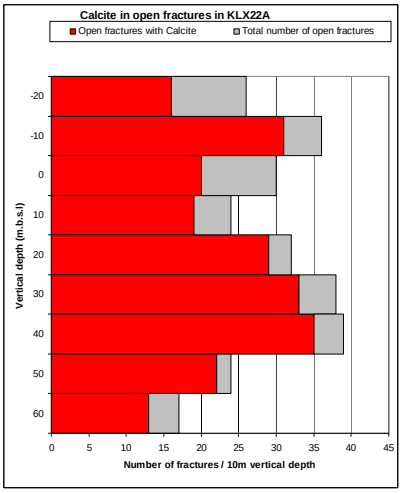
Calcite in open fractures in KLX22A
Open fractures with Calcite
Total number of open fractures
Vertical depth (m.b.s.l)
Number of fractures / 10m vertical depth

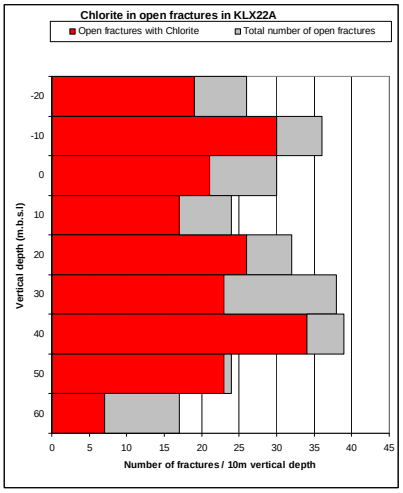
Chlorite in open fractures in KLX22A
Open fractures with Chlorite
Total number of open fractures
Vertical depth (m.b.s.l)
Number of fractures / 10m vertical depth

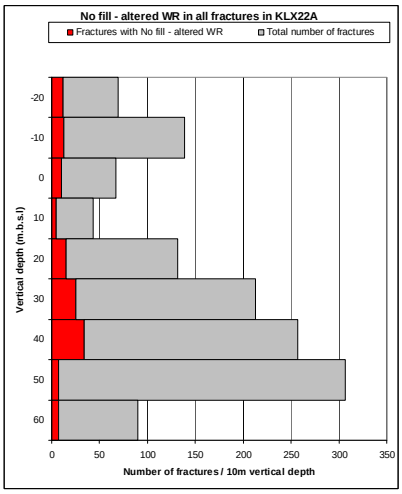
No fill - altered WR in all fractures in KLX22A
Fractures with No fill - altered WR
Total number of fractures
Vertical depth (m.b.s.l)
Number of fractures / 10m vertical depth

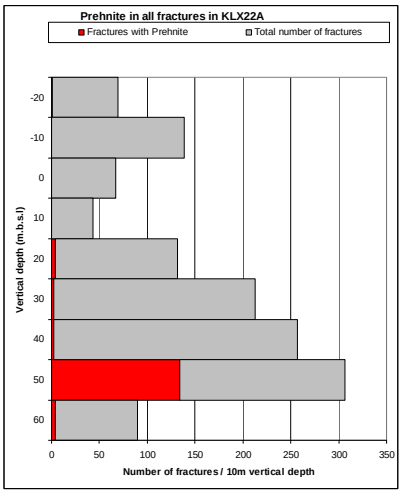
Prehnite in all fractures in KLX22A
Fractures with Prehnite
Total number of fractures
Vertical depth (m.b.s.l)
Number of fractures / 10m vertical depth

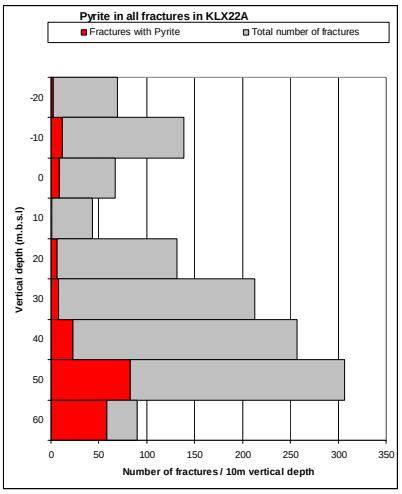
Pyrite in all fractures in KLX22A
Fractures with Pyrite
Total number of fractures
Vertical depth (m.b.s.l)
Number of fractures / 10m vertical depth

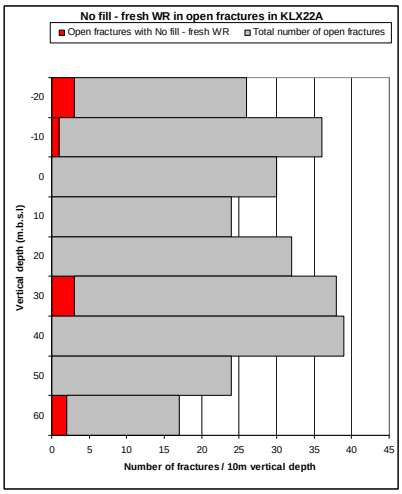
No fill - fresh WR in open fractures in KLX22A
Open fractures with No fill - fresh WR
Total number of open fractures
Vertical depth (m.b.s.l)
Number of fractures / 10m vertical depth

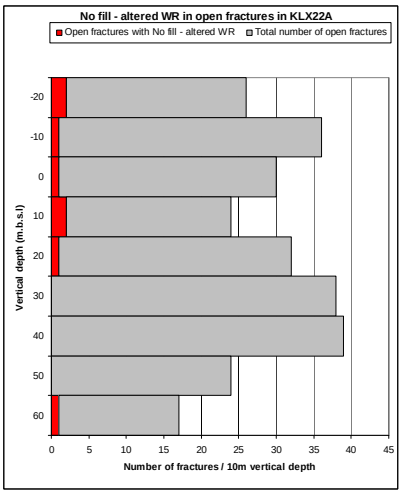
No fill - altered WR in open fractures in KLX22A
Open fractures with No fill - altered WR
Total number of open fractures
Vertical depth (m.b.s.l)
Number of fractures / 10m vertical depth

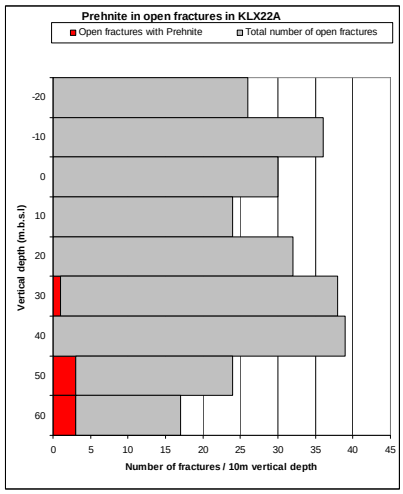
Prehnite in open fractures in KLX22A
Open fractures with Prehnite
Total number of open fractures
Vertical depth (m.b.s.l)
Number of fractures / 10m vertical depth

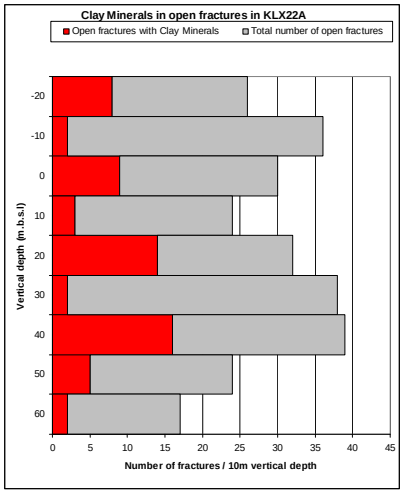
Clay Minerals in open fractures in KLX22A
Open fractures with Clay Minerals
Total number of open fractures
Vertical depth (m.b.s.l)
Number of fractures / 10m vertical depth

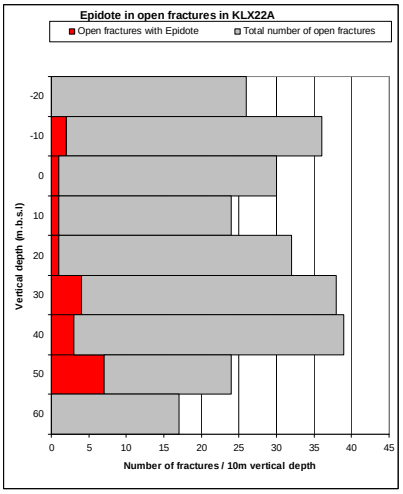
Epidote in open fractures in KLX22A
Open fractures with Epidote
Total number of open fractures
Vertical depth (m.b.s.l)
Number of fractures / 10m vertical depth

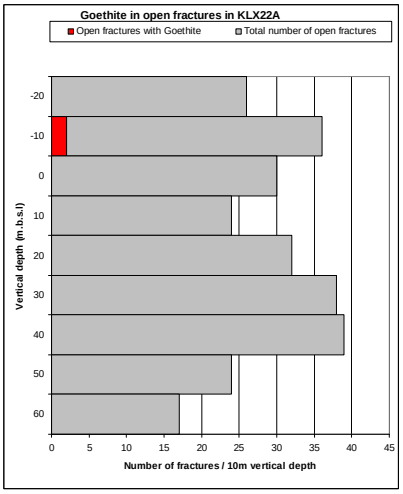
Goethite in open fractures in KLX22A
Open fractures with Goethite
Total number of open fractures
Vertical depth (m.b.s.l)
Number of fractures / 10m vertical depth

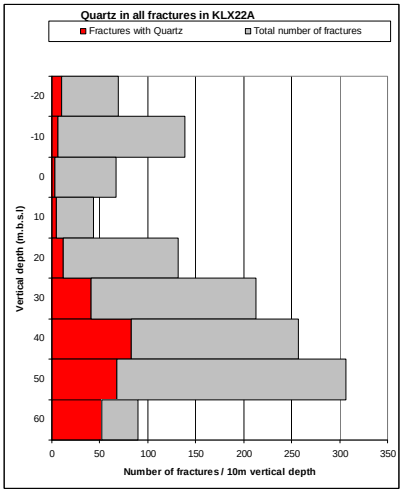
Quartz in all fractures in KLX22A
Fractures with Quartz
Total number of fractures
Vertical depth (m.b.s.l)
Number of fractures / 10m vertical depth

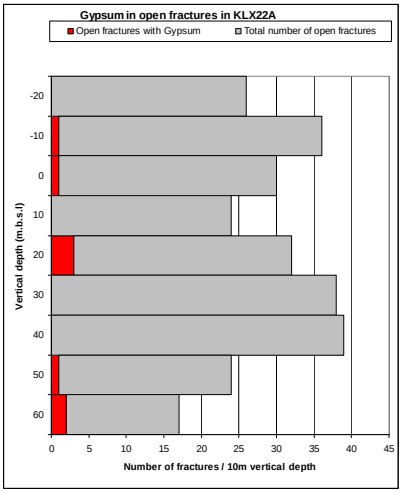
Gypsum in open fractures in KLX22A
Open fractures with Gypsum
Total number of open fractures
Vertical depth (m.b.s.l)
Number of fractures / 10m vertical depth

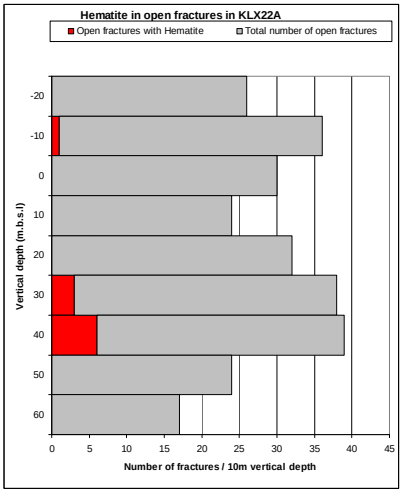
Hematite in open fractures in KLX22A
Open fractures with Hematite
Total number of open fractures
Vertical depth (m.b.s.l)
Number of fractures / 10m vertical depth

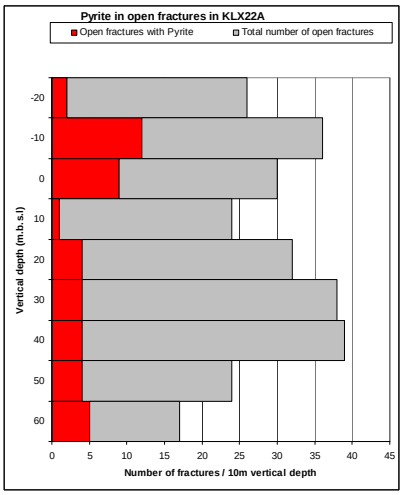
Pyrite in open fractures in KLX22A
Open fractures with Pyrite
Total number of open fractures
Vertical depth (m.b.s.l)
Number of fractures / 10m vertical depth

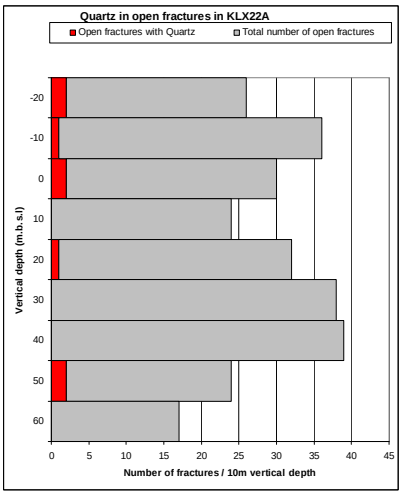
Quartz in open fractures in KLX22A
Open fractures with Quartz
Total number of open fractures
Vertical depth (m.b.s.l)
Number of fractures / 10m vertical depth

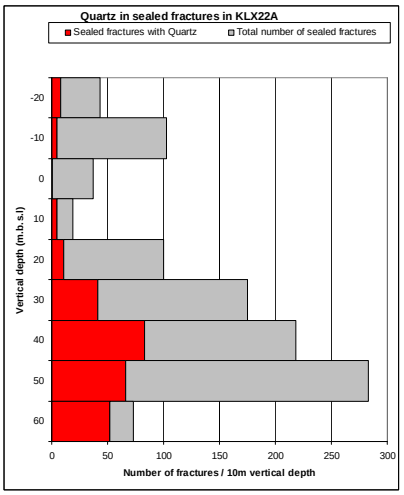
Quartz in sealed fractures in KLX22A
Sealed fractures with Quartz
Total number of sealed fractures
Vertical depth (m.b.s.l)
Number of fractures / 10m vertical depth

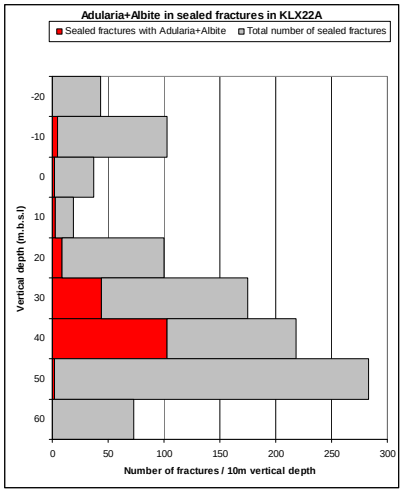
Adularia+Albite in sealed fractures in KLX22A
Sealed fractures with Adularia+Albite
Total number of sealed fractures
Vertical depth (m.b.s.l)
Number of fractures / 10m vertical depth

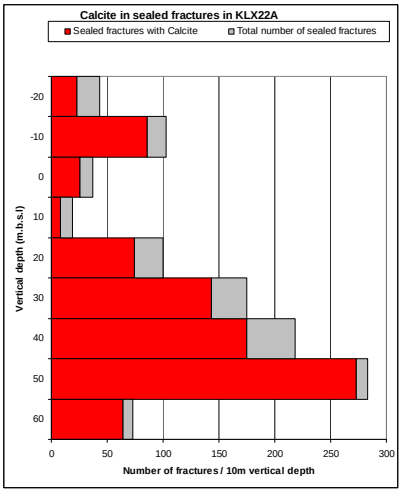
Calcite in sealed fractures in KLX22A
Sealed fractures with Calcite
Total number of sealed fractures
Vertical depth (m.b.s.l)
Number of fractures / 10m vertical depth

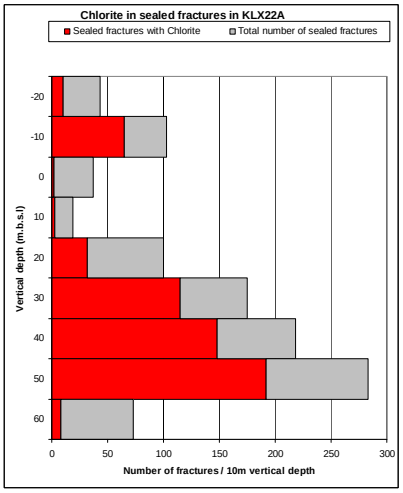
Chlorite in sealed fractures in KLX22A
Sealed fractures with Chlorite
Total number of sealed fractures
Vertical depth (m.b.s.l)
Number of fractures / 10m vertical depth

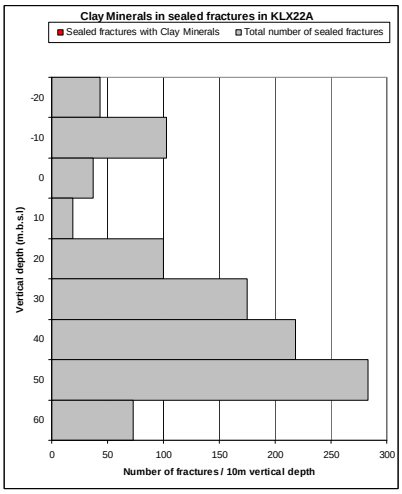
Clay Minerals in sealed fractures in KLX22A
Sealed fractures with Clay Minerals
Total number of sealed fractures
Vertical depth (m.b.s.l)
Number of fractures / 10m vertical depth

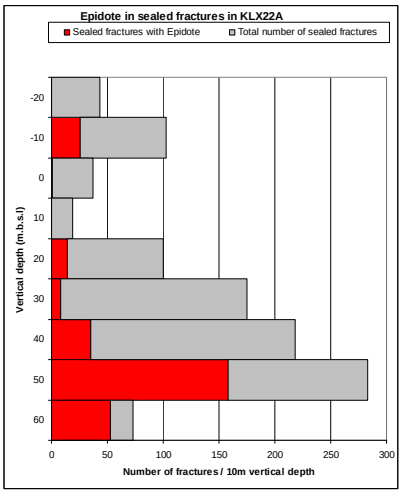
Epidote in sealed fractures in KLX22A
Sealed fractures with Epidote
Total number of sealed fractures
Vertical depth (m.b.s.l)
Number of fractures / 10m vertical depth

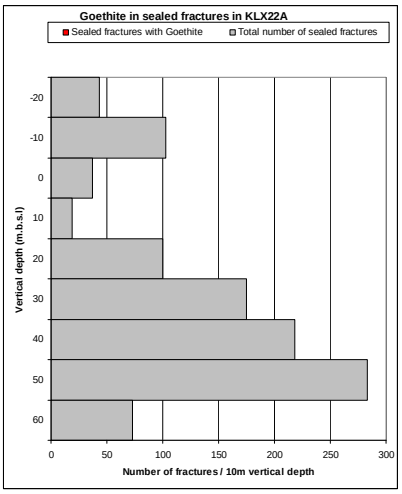
Goethite in sealed fractures in KLX22A
Sealed fractures with Goethite
Total number of sealed fractures
Vertical depth (m.b.s.l)
Number of fractures / 10m vertical depth

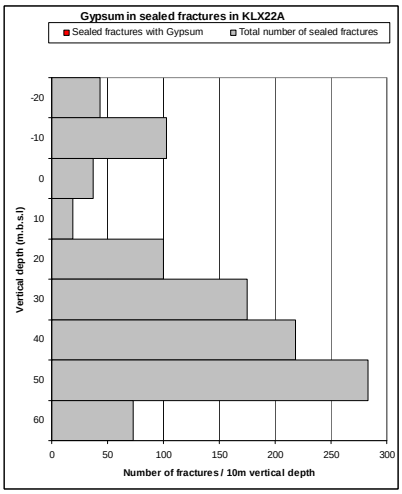
Gypsum in sealed fractures in KLX22A
Sealed fractures with Gypsum
Total number of sealed fractures
Vertical depth (m.b.s.l)
Number of fractures / 10m vertical depth

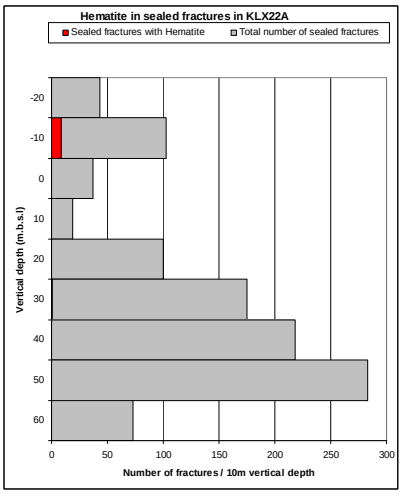
Hematite in sealed fractures in KLX22A
Sealed fractures with Hematite
Total number of sealed fractures
Vertical depth (m.b.s.l)
Number of fractures / 10m vertical depth

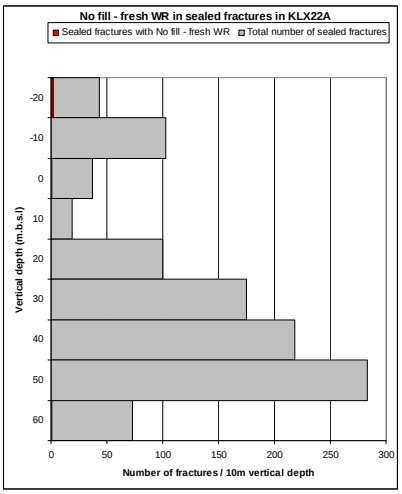
No fill - fresh WR in sealed fractures in KLX22A
Sealed fractures with No fill - fresh WR
Total number of sealed fractures
Vertical depth (m.b.s.l)
Number of fractures / 10m vertical depth

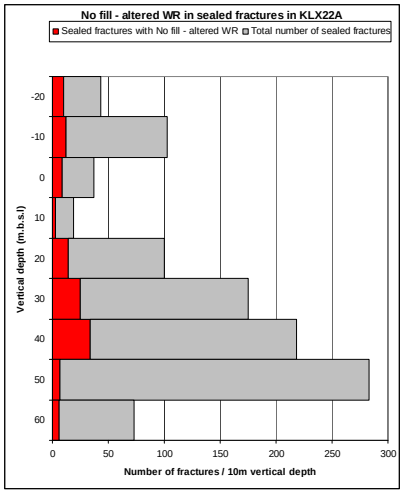
No fill - altered WR in sealed fractures in KLX22A
Sealed fractures with No fill - altered WR
Total number of sealed fractures
Vertical depth (m.b.s.l)
-20
-10
0
10
20
30
40
50
60
0
50
100
150
200
250
300
Number of fractures / 10m vertical depth

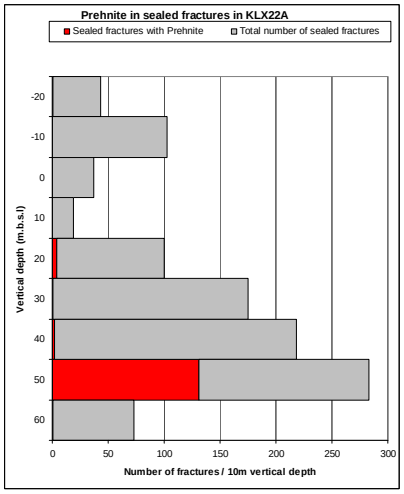
Prehnite in sealed fractures in KLX22A
Sealed fractures with Prehnite
Total number of sealed fractures
Vertical depth (m.b.s.l)
-20
-10
0
10
20
30
40
50
60
0
50
100
150
200
250
300
Number of fractures / 10m vertical depth

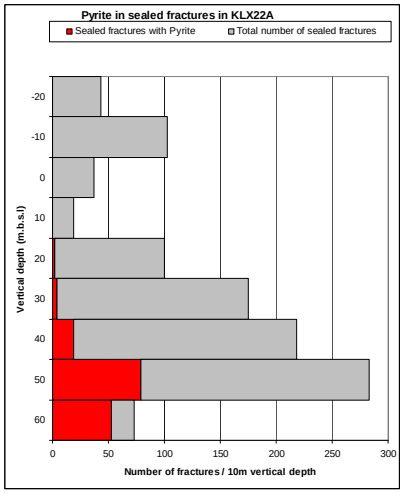
Pyrite in sealed fractures in KLX22A
Sealed fractures with Pyrite
Total number of sealed fractures
Vertical depth (m.b.s.l)
-20
-10
0
10
20
30
40
50
60
0
50
100
150
200
250
300
Number of fractures / 10m vertical depth

KLX22B

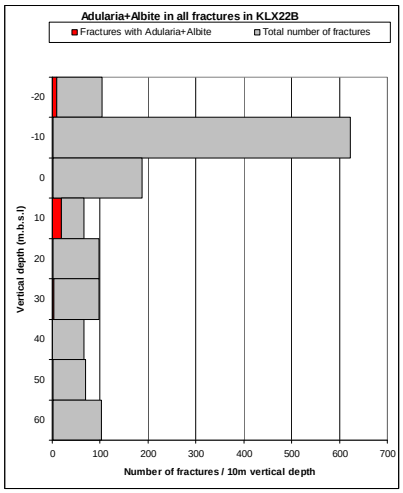
Adularia+Albite in all fractures in KLX22B
Fractures with Adularia+Albite
Total number of fractures
Vertical depth (m.b.s.l)
Number of fractures / 10m vertical depth

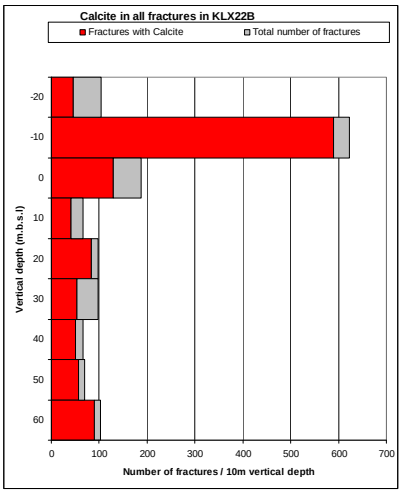
Calcite in all fractures in KLX22B
Fractures with Calcite
Total number of fractures
Vertical depth (m.b.s.l)
Number of fractures / 10m vertical depth

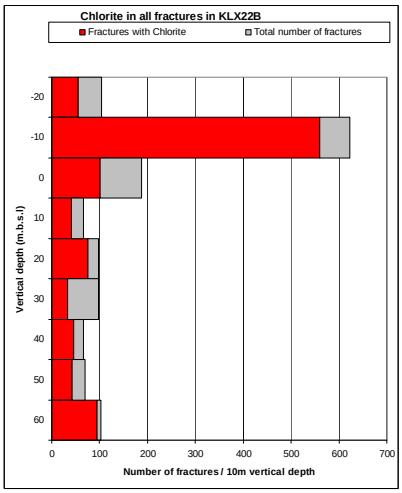
Chlorite in all fractures in KLX22B
Fractures with Chlorite
Total number of fractures
Vertical depth (m.b.s.l)
Number of fractures / 10m vertical depth

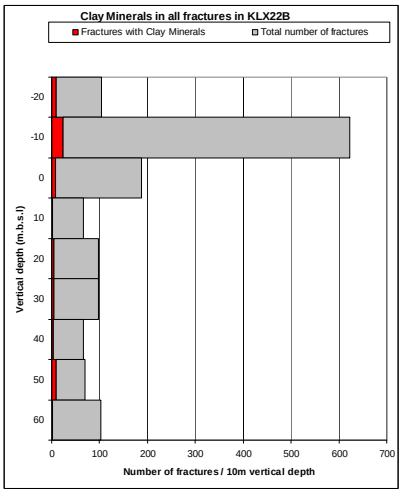
Clay Minerals in all fractures in KLX22B
Fractures with Clay Minerals
Total number of fractures
Vertical depth (m.b.s.l)
Number of fractures / 10m vertical depth

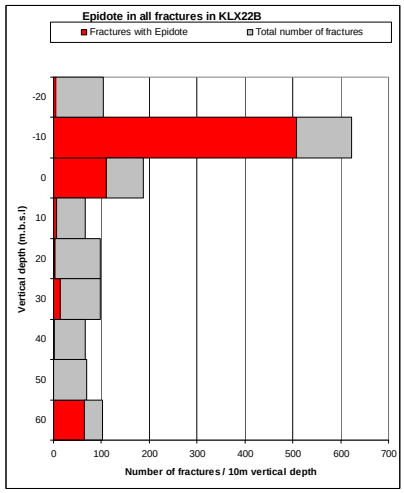
Epidote in all fractures in KLX22B
Fractures with Epidote
Total number of fractures
Vertical depth (m.b.s.l)
Number of fractures / 10m vertical depth

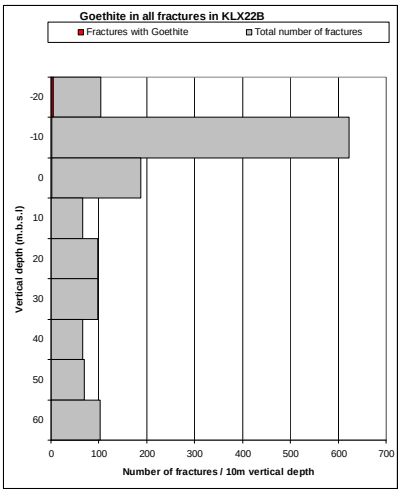
Goethite in all fractures in KLX22B
Fractures with Goethite
Total number of fractures
Vertical depth (m.b.s.l)
Number of fractures / 10m vertical depth

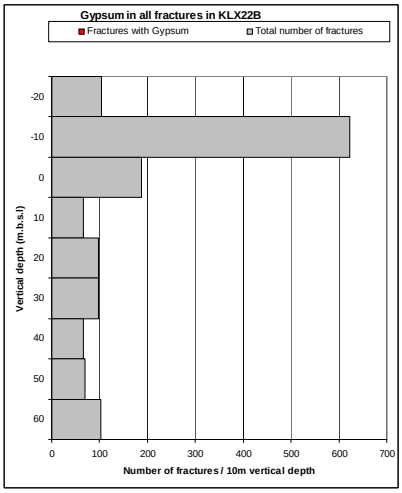
Gypsum in all fractures in KLX22B
Fractures with Gypsum
Total number of fractures
Vertical depth (m.b.s.l)
Number of fractures / 10m vertical depth

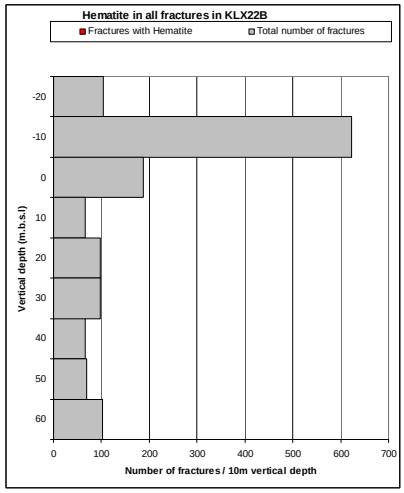
Hematite in all fractures in KLX22B
Fractures with Hematite
Total number of fractures
Vertical depth (m.b.s.l)
Number of fractures / 10m vertical depth

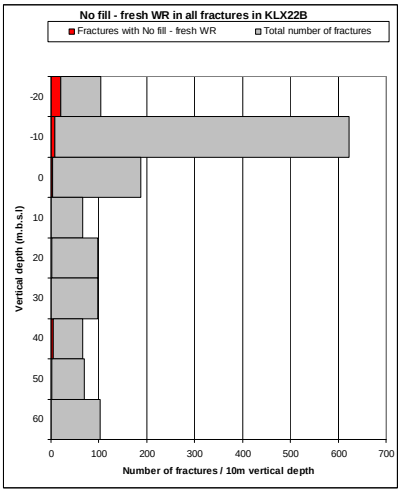
No fill - fresh WR in all fractures in KLX22B
Fractures with No fill - fresh WR
Total number of fractures
Vertical depth (m.b.s.l)
Number of fractures / 10m vertical depth

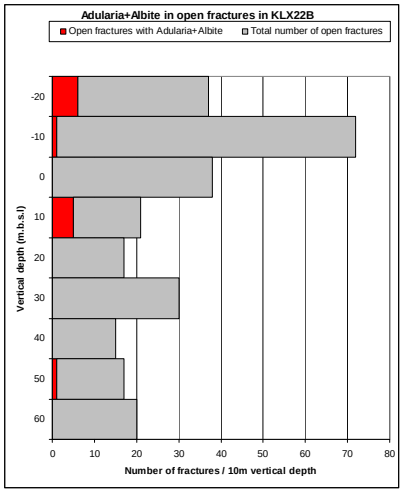
Adularia+Albite in open fractures in KLX22B
Open fractures with Adularia+Albite
Total number of open fractures
Vertical depth (m.b.s.l)
Number of fractures / 10m vertical depth

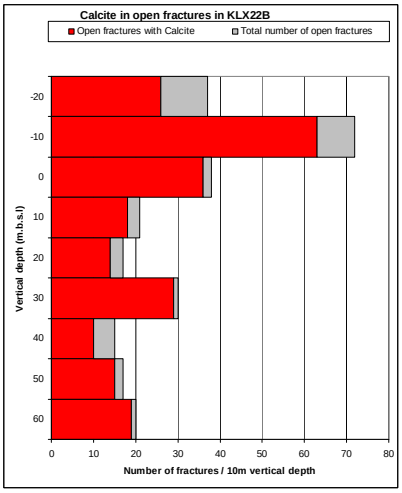
Calcite in open fractures in KLX22B
Open fractures with Calcite
Total number of open fractures
Vertical depth (m.b.s.l)
Number of fractures / 10m vertical depth

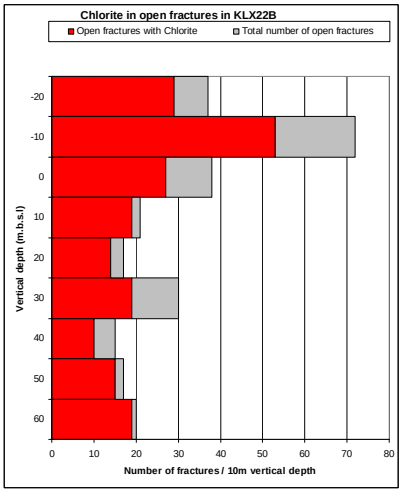
Chlorite in open fractures in KLX22B
Open fractures with Chlorite
Total number of open fractures
Vertical depth (m.b.s.l)
Number of fractures / 10m vertical depth

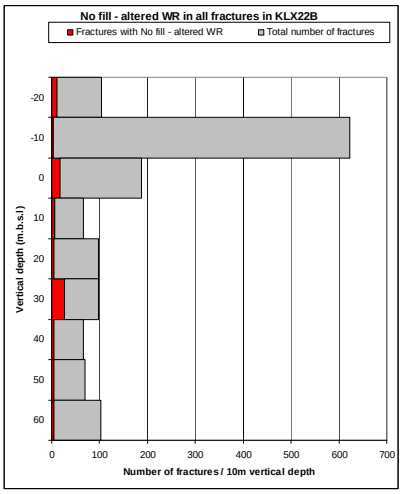
No fill - altered WR in all fractures in KLX22B
Fractures with No fill - altered WR
Total number of fractures
Vertical depth (m.b.s.l)
Number of fractures / 10m vertical depth

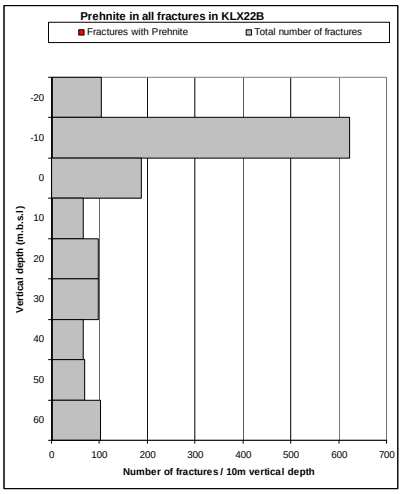
Prehnite in all fractures in KLX22B
Fractures with Prehnite
Total number of fractures
Vertical depth (m.b.s.l)
Number of fractures / 10m vertical depth

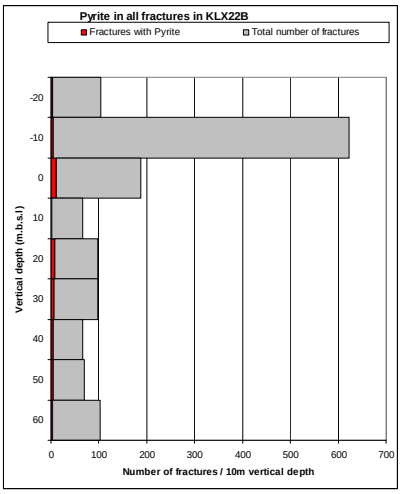
Pyrite in all fractures in KLX22B
Fractures with Pyrite
Total number of fractures
Vertical depth (m.b.s.l)
Number of fractures / 10m vertical depth

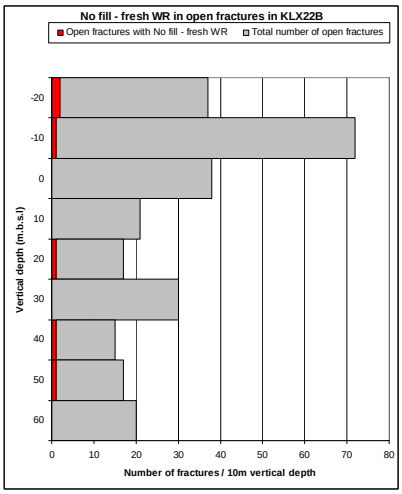
No fill - fresh WR in open fractures in KLX22B
Open fractures with No fill - fresh WR
Total number of open fractures
Vertical depth (m.b.s.l)
Number of fractures / 10m vertical depth

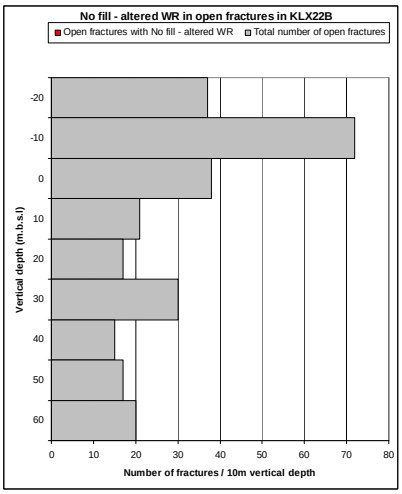
No fill - altered WR in open fractures in KLX22B
Open fractures with No fill - altered WR
Total number of open fractures
Vertical depth (m.b.s.l)
Number of fractures / 10m vertical depth

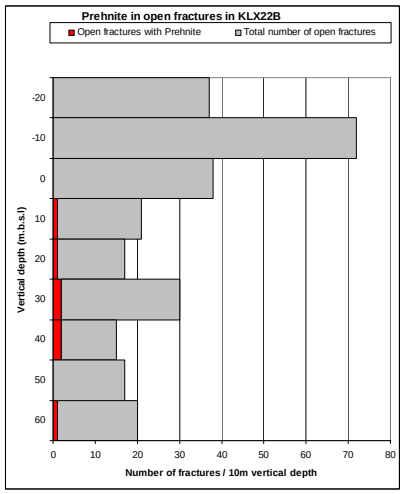
Prehnite in open fractures in KLX22B
Open fractures with Prehnite
Total number of open fractures
Vertical depth (m.b.s.l)
Number of fractures / 10m vertical depth

i

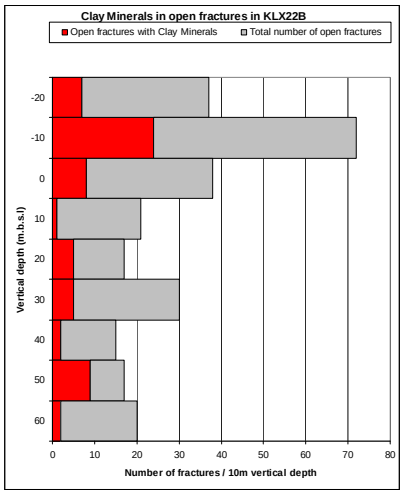
Clay Minerals in open fractures in KLX22B
Open fractures with Clay Minerals
Total number of open fractures
Vertical depth (m.b.s.l)
Number of fractures / 10m vertical depth

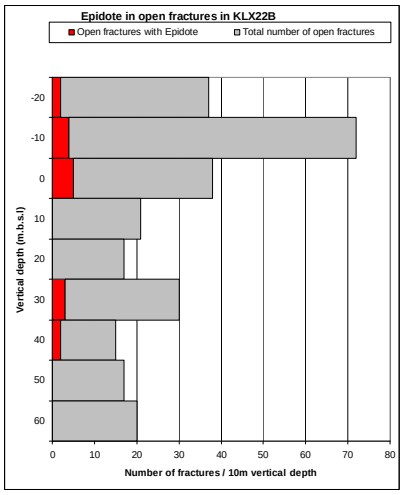
Epidote in open fractures in KLX22B
Open fractures with Epidote
Total number of open fractures
Vertical depth (m.b.s.l)
Number of fractures / 10m vertical depth

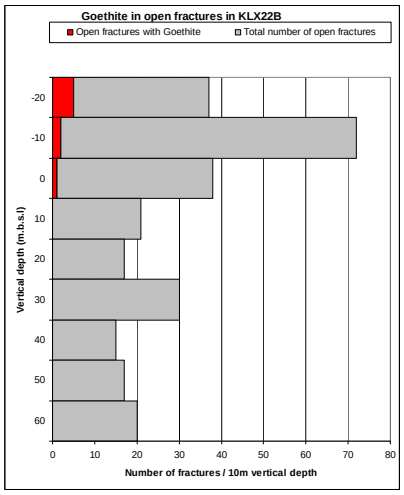
Goethite in open fractures in KLX22B
Open fractures with Goethite
Total number of open fractures
Vertical depth (m.b.s.l)
Number of fractures / 10m vertical depth

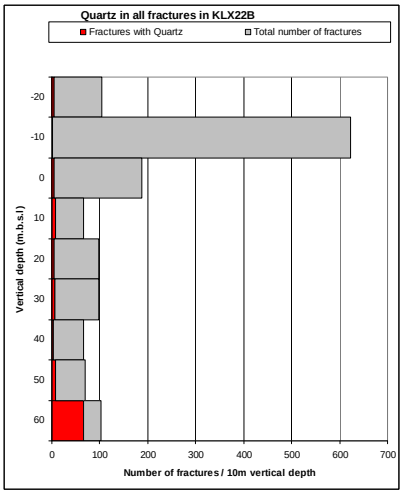
Quartz in all fractures in KLX22B
Fractures with Quartz
Total number of fractures
Vertical depth (m.b.s.l)
Number of fractures / 10m vertical depth

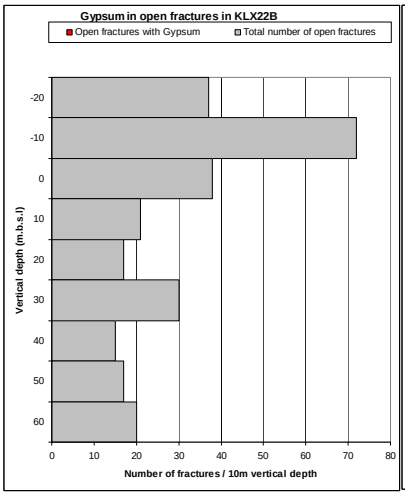
Gypsum in open fractures in KLX22B
Open fractures with Gypsum
Total number of open fractures
Vertical depth (m.b.s.l)
Number of fractures / 10m vertical depth

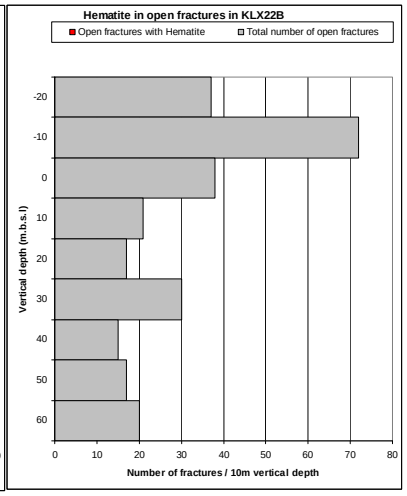
Hematite in open fractures in KLX22B
Open fractures with Hematite
Total number of open fractures
Vertical depth (m.b.s.l)
Number of fractures / 10m vertical depth

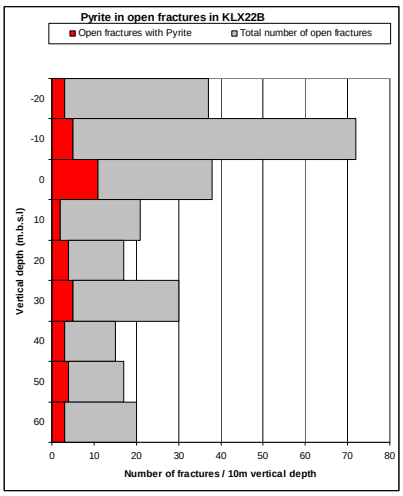
Pyrite in open fractures in KLX22B
Open fractures with Pyrite
Total number of open fractures
Vertical depth (m.b.s.l)
Number of fractures / 10m vertical depth

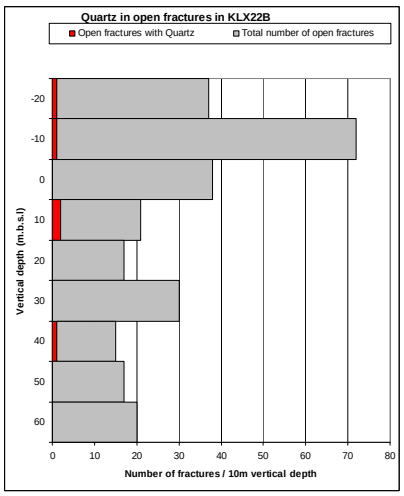
Quartz in open fractures in KLX22B
Open fractures with Quartz
Total number of open fractures
Vertical depth (m.b.s.l)
Number of fractures / 10m vertical depth

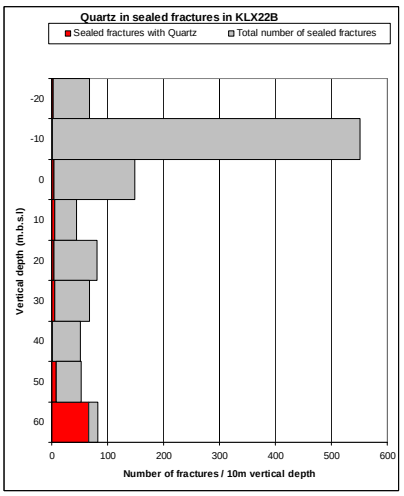
Quartz in sealed fractures in KLX22B
Sealed fractures with Quartz
Total number of sealed fractures
Vertical depth (m.b.s.l)
Number of fractures / 10m vertical depth

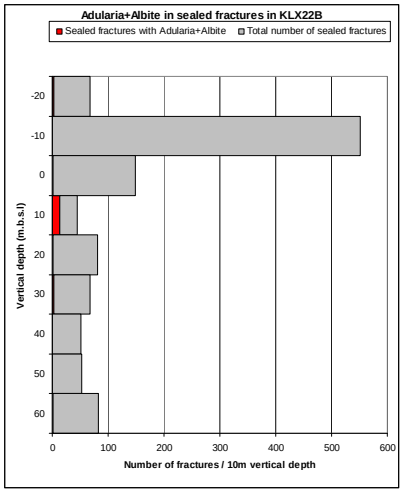
Adularia+Albite in sealed fractures in KLX22B
Sealed fractures with Adularia+Albite
Total number of sealed fractures
Vertical depth (m.b.s.l)
-20
-10
0
10
20
30
40
50
60
0
100
200
300
400
500
600
Number of fractures / 10m vertical depth

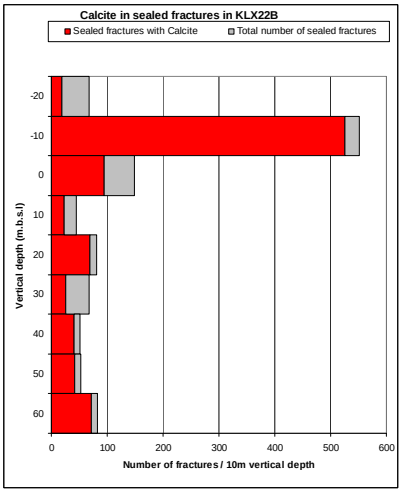
Calcite in sealed fractures in KLX22B
Sealed fractures with Calcite
Total number of sealed fractures
Vertical depth (m.b.s.l)
-20
-10
0
10
20
30
40
50
60
0
100
200
300
400
500
600
Number of fractures / 10m vertical depth

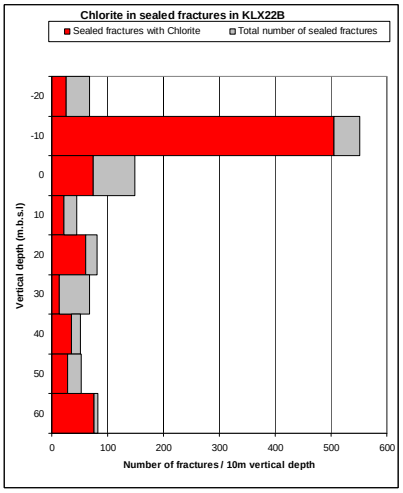
Chlorite in sealed fractures in KLX22B
Sealed fractures with Chlorite
Total number of sealed fractures
Vertical depth (m.b.s.l)
-20
-10
0
10
20
30
40
50
60
0
100
200
300
400
500
600
Number of fractures / 10m vertical depth

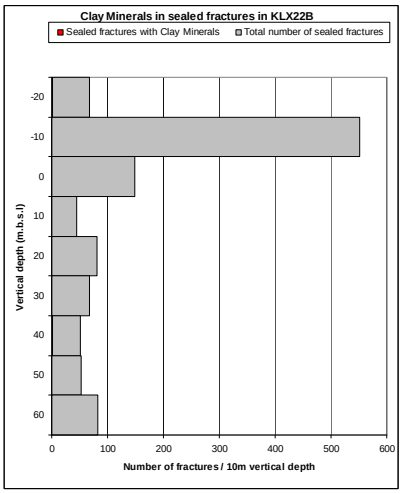
Clay Minerals in sealed fractures in KLX22B
Sealed fractures with Clay Minerals
Total number of sealed fractures
Vertical depth (m.b.s.l)
-20
-10
0
10
20
30
40
50
60
0
100
200
300
400
500
600
Number of fractures / 10m vertical depth

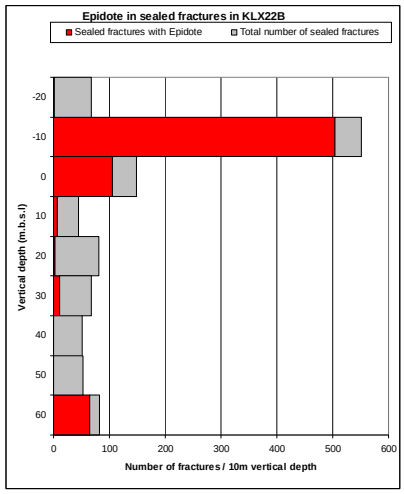
Epidote in sealed fractures in KLX22B
Sealed fractures with Epidote
Total number of sealed fractures
Vertical depth (m.b.s.l)
-20
-10
0
10
20
30
40
50
60
0
100
200
300
400
500
600
Number of fractures / 10m vertical depth

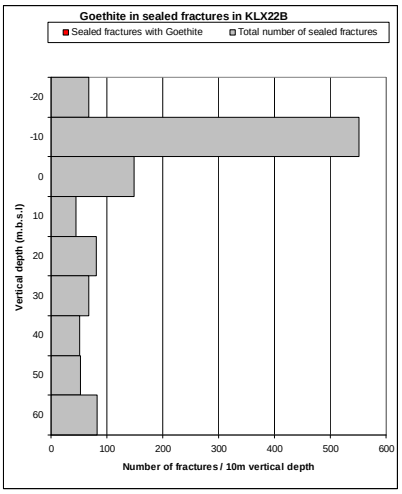
Goethite in sealed fractures in KLX22B
Sealed fractures with Goethite
Total number of sealed fractures
Vertical depth (m.b.s.l)
-20
-10
0
10
20
30
40
50
60
0
100
200
300
400
500
600
Number of fractures / 10m vertical depth

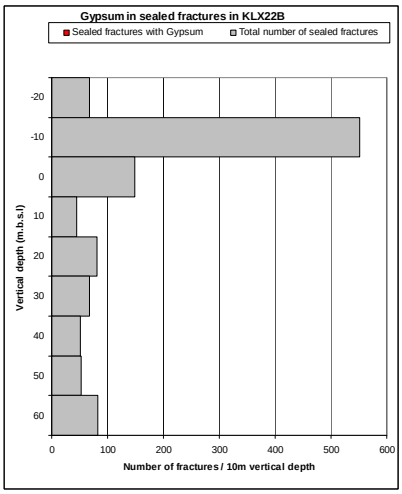
Gypsum in sealed fractures in KLX22B
Sealed fractures with Gypsum
Total number of sealed fractures
Vertical depth (m.b.s.l)
-20
-10
0
10
20
30
40
50
60
0
100
200
300
400
500
600
Number of fractures / 10m vertical depth

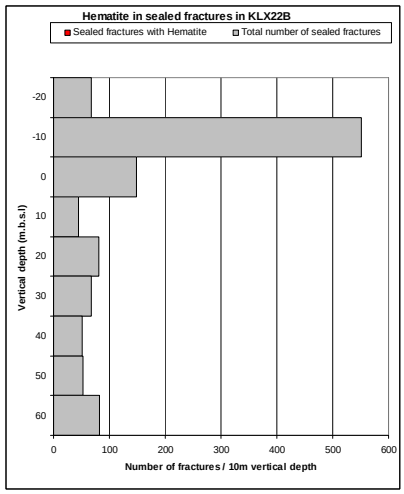
Hematite in sealed fractures in KLX22B
Sealed fractures with Hematite
Total number of sealed fractures
Vertical depth (m.b.s.l)
-20
-10
0
10
20
30
40
50
60
0
100
200
300
400
500
600
Number of fractures / 10m vertical depth

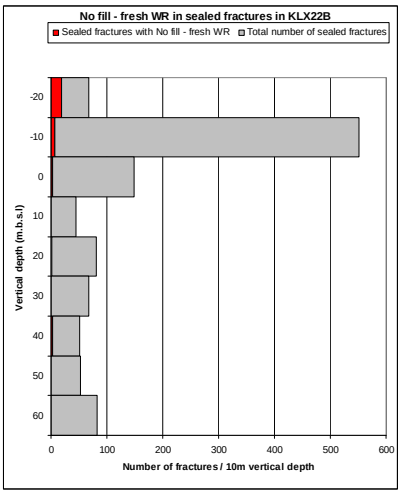
No fill - fresh WR in sealed fractures in KLX22B
Sealed fractures with No fill - fresh WR
Total number of sealed fractures
Vertical depth (m.b.s.l)
-20
-10
0
10
20
30
40
50
60
0
100
200
300
400
500
600
Number of fractures / 10m vertical depth

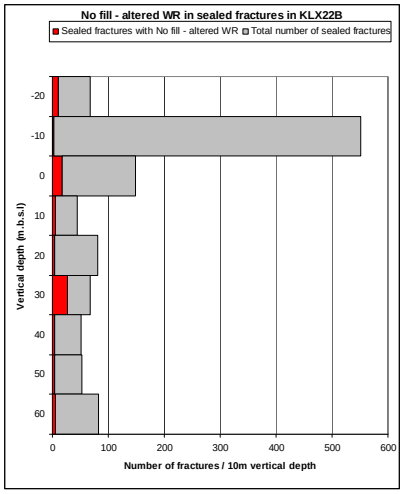
No fill - altered WR in sealed fractures in KLX22B
Sealed fractures with No fill - altered WR
Total number of sealed fractures
Vertical depth (m.b.s.l)
-20
-10
0
10
20
30
40
50
60
0
100
200
300
400
500
600
Number of fractures / 10m vertical depth

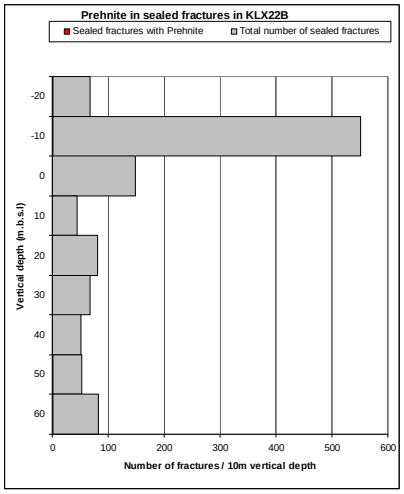
Prehnite in sealed fractures in KLX22B
Sealed fractures with Prehnite
Total number of sealed fractures
Vertical depth (m.b.s.l)
-20
-10
0
10
20
30
40
50
60
0
100
200
300
400
500
600
Number of fractures / 10m vertical depth

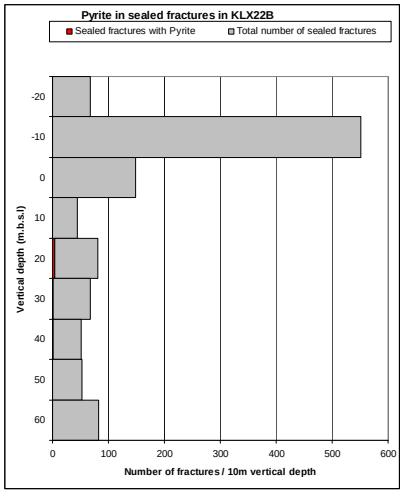
Pyrite in sealed fractures in KLX22B
Sealed fractures with Pyrite
Total number of sealed fractures
Vertical depth (m.b.s.l)
-20
-10
0
10
20
30
40
50
60
0
100
200
300
400
500
600
Number of fractures / 10m vertical depth

KLX23A

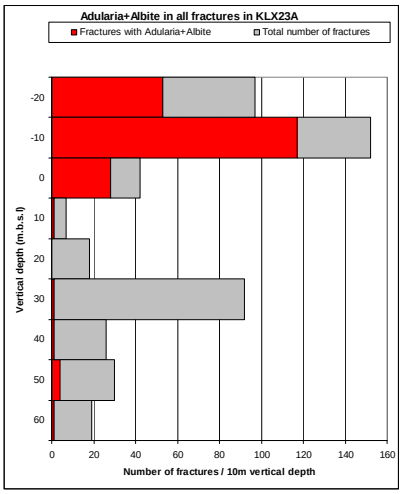
Adularia+Albite in all fractures in KLX23A
Fractures with Adularia+Albite
Total number of fractures
Vertical depth (m.b.s.l)
Number of fractures / 10m vertical depth

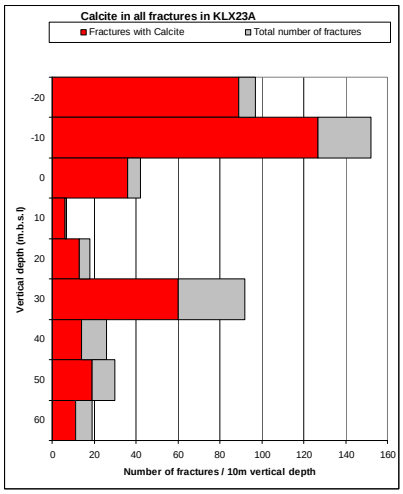
Calcite in all fractures in KLX23A
Fractures with Calcite
Total number of fractures
Vertical depth (m.b.s.l)
Number of fractures / 10m vertical depth

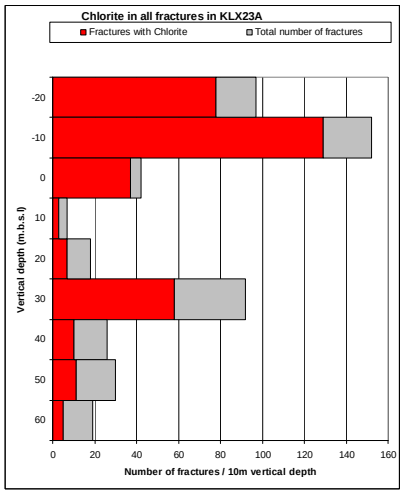
Chlorite in all fractures in KLX23A
Fractures with Chlorite
Total number of fractures
Vertical depth (m.b.s.l)
Number of fractures / 10m vertical depth

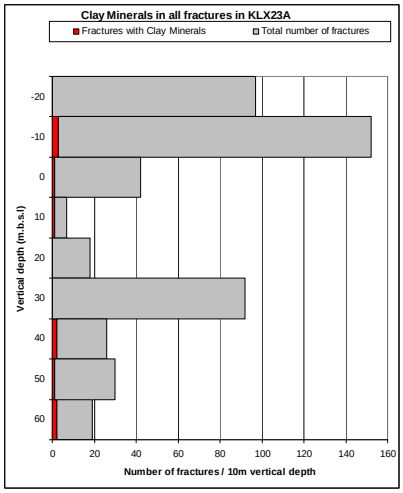
Clay Minerals in all fractures in KLX23A
Fractures with Clay Minerals
Total number of fractures
Vertical depth (m.b.s.l)
Number of fractures / 10m vertical depth

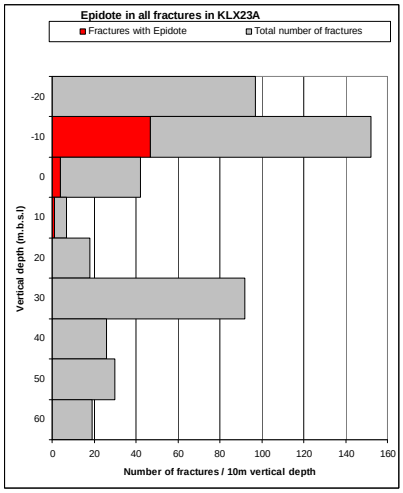
Epidote in all fractures in KLX23A
Fractures with Epidote
Total number of fractures
Vertical depth (m.b.s.l)
Number of fractures / 10m vertical depth

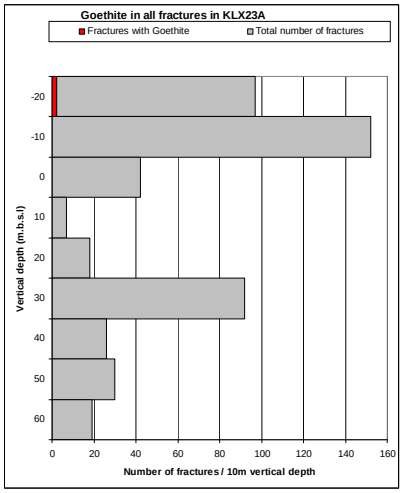
Goethite in all fractures in KLX23A
Fractures with Goethite
Total number of fractures
Vertical depth (m.b.s.l)
Number of fractures / 10m vertical depth

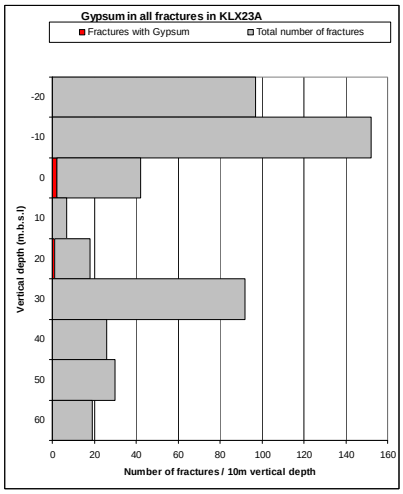
Gypsum in all fractures in KLX23A
Fractures with Gypsum
Total number of fractures
Vertical depth (m.b.s.l)
Number of fractures / 10m vertical depth

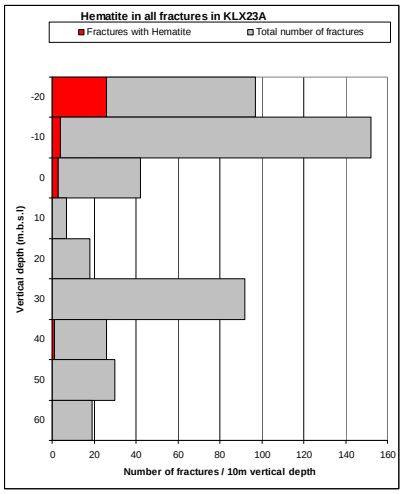
Hematite in all fractures in KLX23A
Fractures with Hematite
Total number of fractures
Vertical depth (m.b.s.l)
Number of fractures / 10m vertical depth

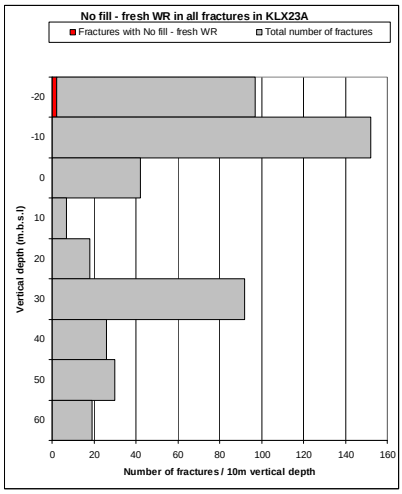
No fill - fresh WR in all fractures in KLX23A
Fractures with No fill - fresh WR
Total number of fractures
Vertical depth (m.b.s.l)
Number of fractures / 10m vertical depth

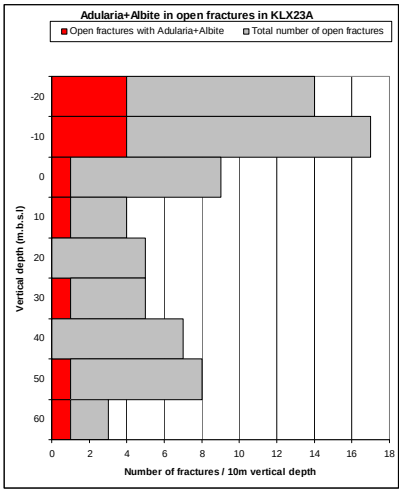
Adularia+Albite in open fractures in KLX23A
Open fractures with Adularia+Albite
Total number of open fractures
Vertical depth (m.b.s.l)
Number of fractures / 10m vertical depth

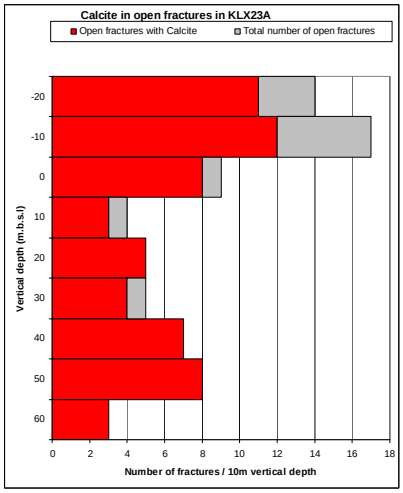
Calcite in open fractures in KLX23A
Open fractures with Calcite
Total number of open fractures
Vertical depth (m.b.s.l)
Number of fractures / 10m vertical depth

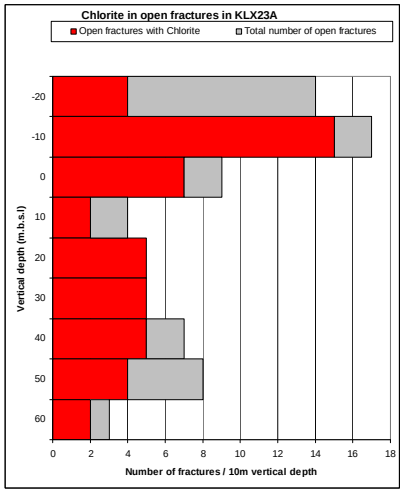
Chlorite in open fractures in KLX23A
Open fractures with Chlorite
Total number of open fractures
Vertical depth (m.b.s.l)
Number of fractures / 10m vertical depth

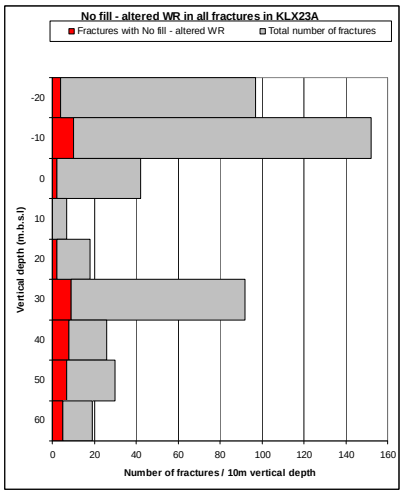
No fill - altered WR in all fractures in KLX23A
Fractures with No fill - altered WR
Total number of fractures
Vertical depth (m.b.s.l)
Number of fractures / 10m vertical depth

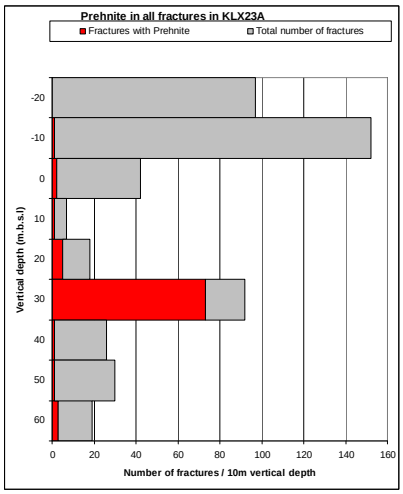
Prehnite in all fractures in KLX23A
Fractures with Prehnite
Total number of fractures
Vertical depth (m.b.s.l)
Number of fractures / 10m vertical depth

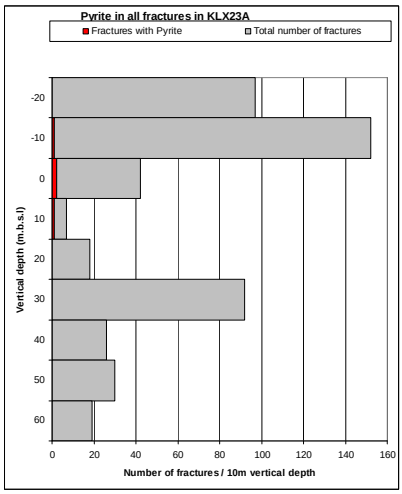
Pyrite in all fractures in KLX23A
Fractures with Pyrite
Total number of fractures
Vertical depth (m.b.s.l)
Number of fractures / 10m vertical depth

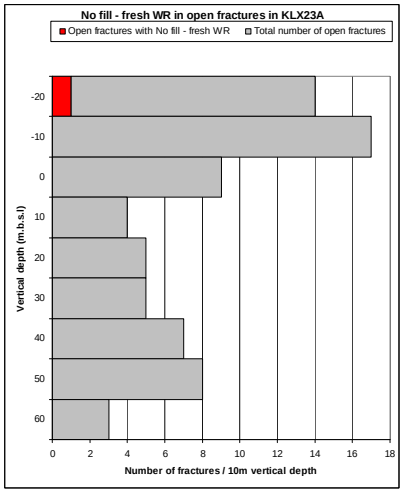
No fill - fresh WR in open fractures in KLX23A
Open fractures with No fill - fresh WR
Total number of open fractures
Vertical depth (m.b.s.l)
Number of fractures / 10m vertical depth

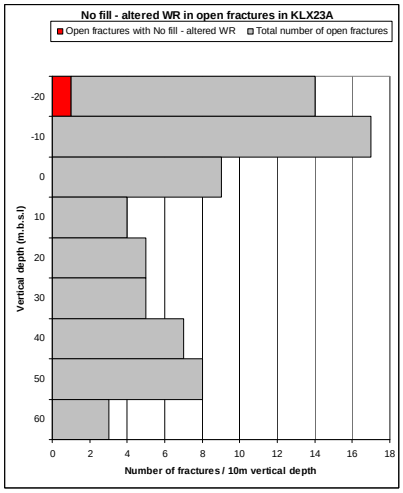
No fill - altered WR in open fractures in KLX23A
Open fractures with No fill - altered WR
Total number of open fractures
Vertical depth (m.b.s.l)
Number of fractures / 10m vertical depth

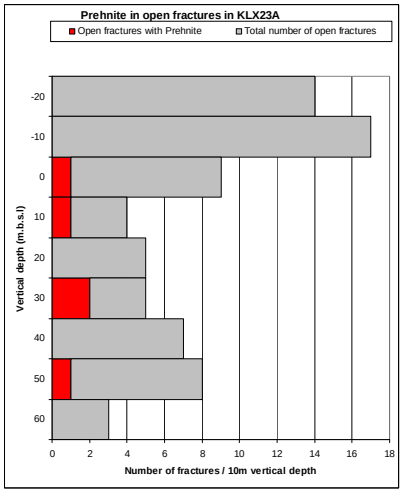
Prehnite in open fractures in KLX23A
Open fractures with Prehnite
Total number of open fractures
Vertical depth (m.b.s.l)
Number of fractures / 10m vertical depth

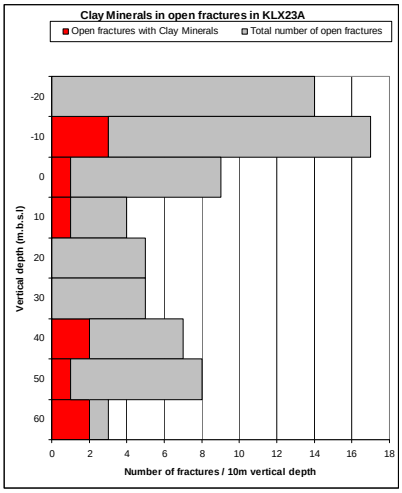
Clay Minerals in open fractures in KLX23A
Open fractures with Clay Minerals
Total number of open fractures
Vertical depth (m.b.s.l)
Number of fractures / 10m vertical depth

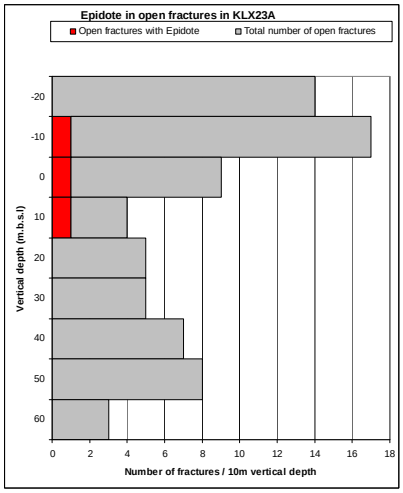
Epidote in open fractures in KLX23A
Open fractures with Epidote
Total number of open fractures
Vertical depth (m.b.s.l)
Number of fractures / 10m vertical depth

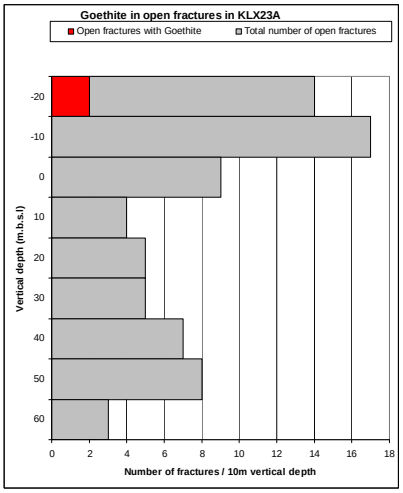
Goethite in open fractures in KLX23A
Open fractures with Goethite
Total number of open fractures
Vertical depth (m.b.s.l)
Number of fractures / 10m vertical depth

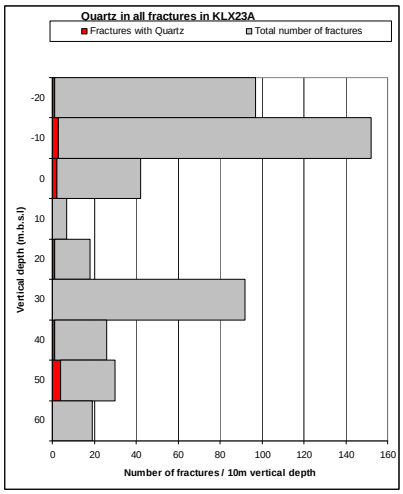
Quartz in all fractures in KLX23A
Fractures with Quartz
Total number of fractures
Vertical depth (m.b.s.l)
Number of fractures / 10m vertical depth

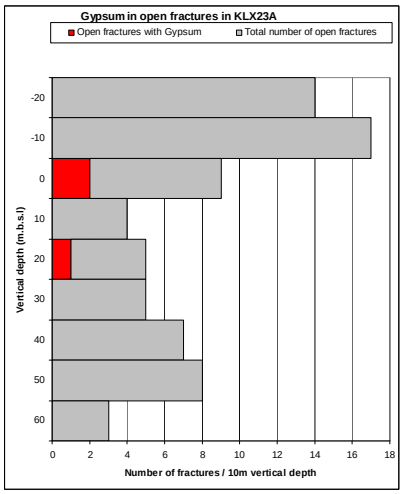
Gypsum in open fractures in KLX23A
Open fractures with Gypsum
Total number of open fractures
Vertical depth (m.b.s.l)
Number of fractures / 10m vertical depth

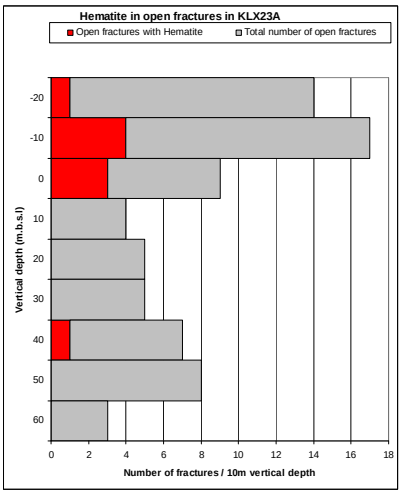
Hematite in open fractures in KLX23A
Open fractures with Hematite
Total number of open fractures
Vertical depth (m.b.s.l)
Number of fractures / 10m vertical depth

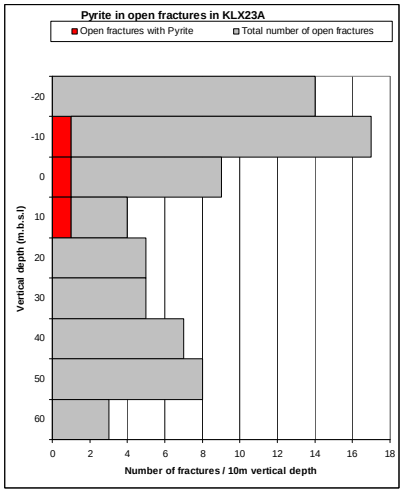
Pyrite in open fractures in KLX23A
Open fractures with Pyrite
Total number of open fractures
Vertical depth (m.b.s.l)
Number of fractures / 10m vertical depth

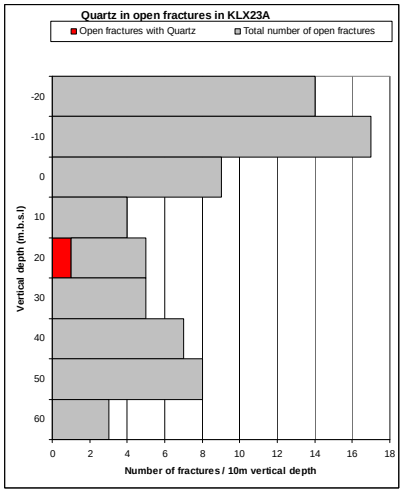
Quartz in open fractures in KLX23A
Open fractures with Quartz
Total number of open fractures
Vertical depth (m.b.s.l)
Number of fractures / 10m vertical depth

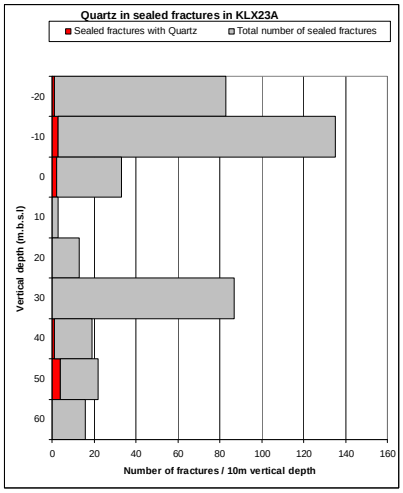
Quartz in sealed fractures in KLX23A
Sealed fractures with Quartz
Total number of sealed fractures
Vertical depth (m.b.s.l)
Number of fractures / 10m vertical depth

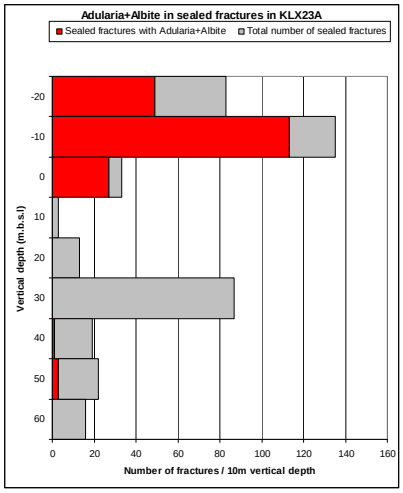
Adularia+Albite in sealed fractures in KLX23A
Sealed fractures with Adularia+Albite
Total number of sealed fractures
Vertical depth (m.b.s.l)
Number of fractures / 10m vertical depth

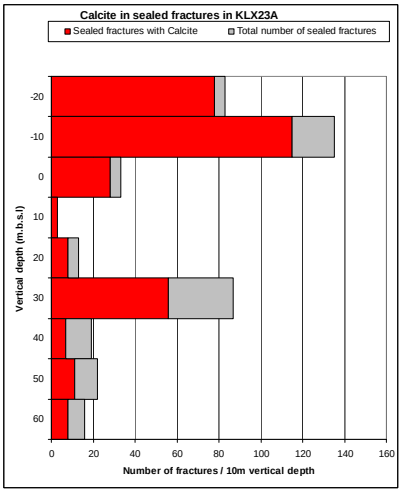
Calcite in sealed fractures in KLX23A
Sealed fractures with Calcite
Total number of sealed fractures
Vertical depth (m.b.s.l)
Number of fractures / 10m vertical depth

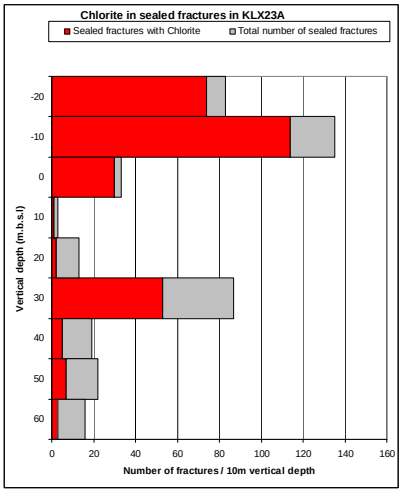
Chlorite in sealed fractures in KLX23A
Sealed fractures with Chlorite
Total number of sealed fractures
Vertical depth (m.b.s.l)
Number of fractures / 10m vertical depth

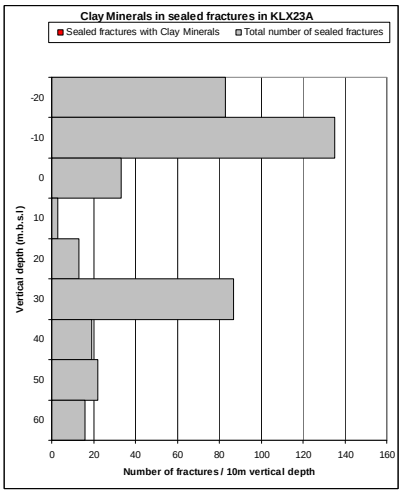
Clay Minerals in sealed fractures in KLX23A
Sealed fractures with Clay Minerals
Total number of sealed fractures
Vertical depth (m.b.s.l)
Number of fractures / 10m vertical depth

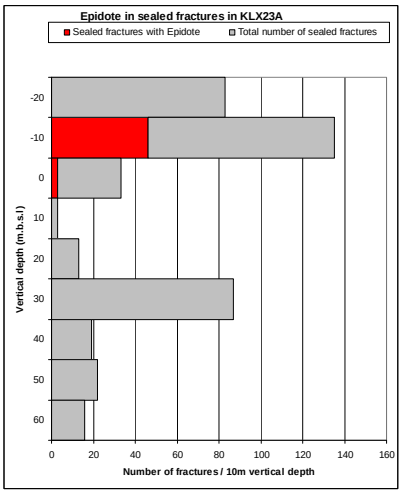
Epidote in sealed fractures in KLX23A
Sealed fractures with Epidote
Total number of sealed fractures
Vertical depth (m.b.s.l)
Number of fractures / 10m vertical depth

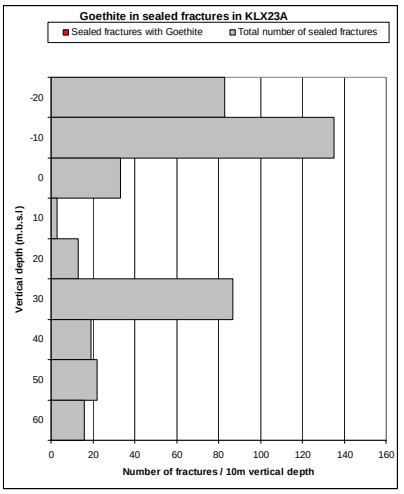
Goethite in sealed fractures in KLX23A
Sealed fractures with Goethite
Total number of sealed fractures
Vertical depth (m.b.s.l)
Number of fractures / 10m vertical depth

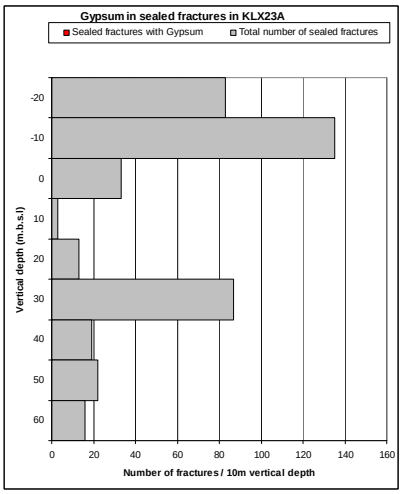
Gypsum in sealed fractures in KLX23A
Sealed fractures with Gypsum
Total number of sealed fractures
Vertical depth (m.b.s.l)
Number of fractures / 10m vertical depth

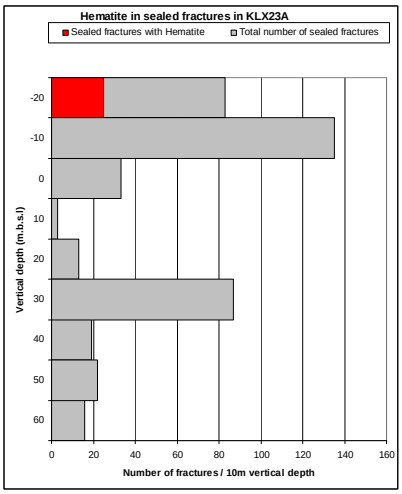
Hematite in sealed fractures in KLX23A
Sealed fractures with Hematite
Total number of sealed fractures
Vertical depth (m.b.s.l)
Number of fractures / 10m vertical depth

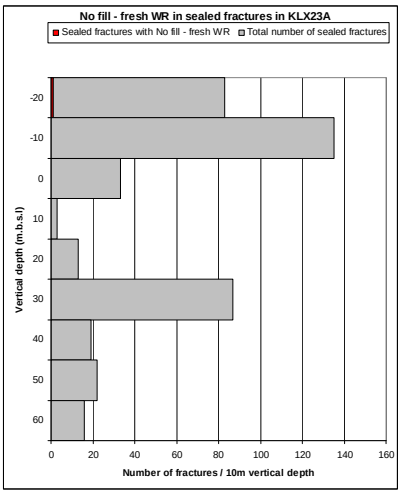
No fill - fresh WR in sealed fractures in KLX23A
Sealed fractures with No fill - fresh WR
Total number of sealed fractures
Vertical depth (m.b.s.l)
Number of fractures / 10m vertical depth

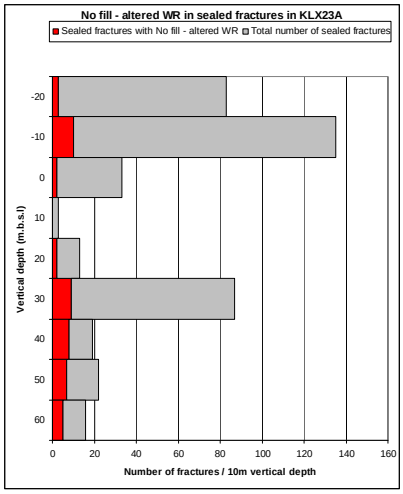
No fill - altered WR in sealed fractures in KLX23A
Sealed fractures with No fill - altered WR
Total number of sealed fractures
Vertical depth (m.b.s.l)
-20
-10
0
10
20
30
40
50
60
0
20
40
60
80
100
120
140
160
Number of fractures / 10m vertical depth

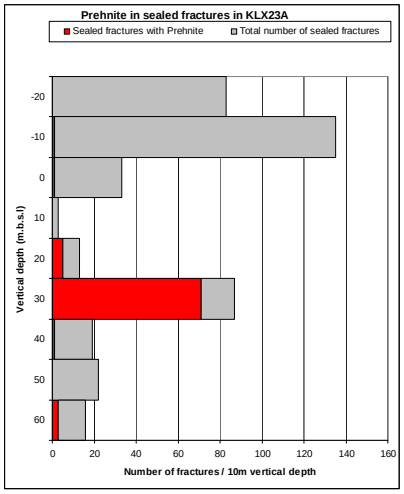
Prehnite in sealed fractures in KLX23A
Sealed fractures with Prehnite
Total number of sealed fractures
Vertical depth (m.b.s.l)
-20
-10
0
10
20
30
40
50
60
0
20
40
60
80
100
120
140
160
Number of fractures / 10m vertical depth

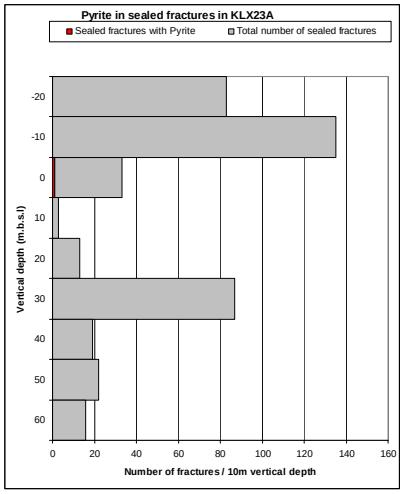
Pyrite in sealed fractures in KLX23A
Sealed fractures with Pyrite
Total number of sealed fractures
Vertical depth (m.b.s.l)
-20
-10
0
10
20
30
40
50
60
0
20
40
60
80
100
120
140
160
Number of fractures / 10m vertical depth

KLX23B

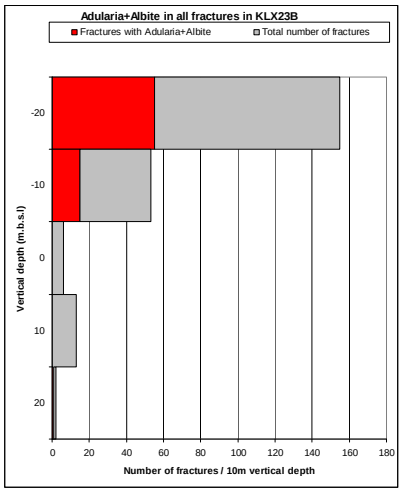
Adularia+Albite in all fractures in KLX23B
Fractures with Adularia+Albite
Total number of fractures
Vertical depth (m.b.s.l)
Number of fractures / 10m vertical depth

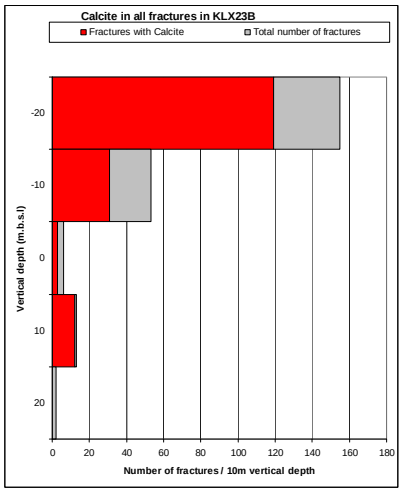
Calcite in all fractures in KLX23B
Fractures with Calcite
Total number of fractures
Vertical depth (m.b.s.l)
Number of fractures / 10m vertical depth

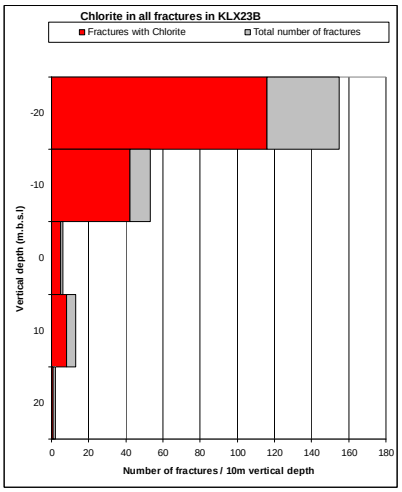
Chlorite in all fractures in KLX23B
Fractures with Chlorite
Total number of fractures
Vertical depth (m.b.s.l)
Number of fractures / 10m vertical depth

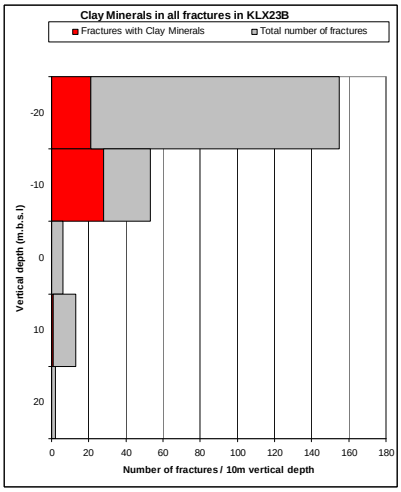
Clay Minerals in all fractures in KLX23B
Fractures with Clay Minerals
Total number of fractures
Vertical depth (m.b.s.l)
Number of fractures / 10m vertical depth

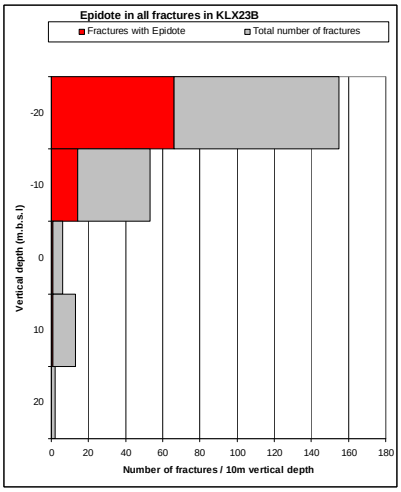
Epidote in all fractures in KLX23B
Fractures with Epidote
Total number of fractures
Vertical depth (m.b.s.l)
Number of fractures / 10m vertical depth

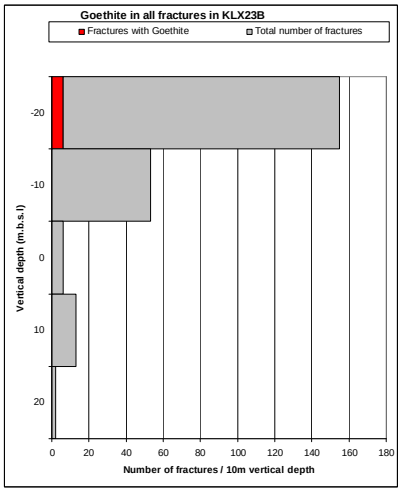
Goethite in all fractures in KLX23B
Fractures with Goethite
Total number of fractures
Vertical depth (m.b.s.l)
Number of fractures / 10m vertical depth

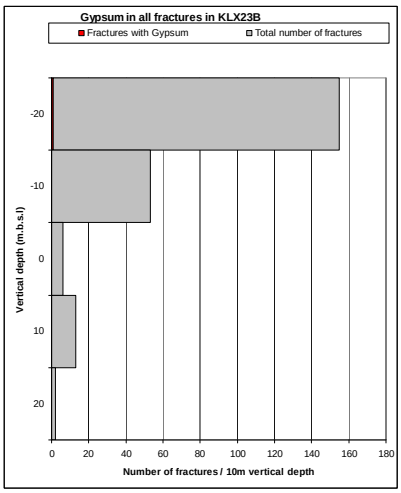
Gypsum in all fractures in KLX23B
Fractures with Gypsum
Total number of fractures
Vertical depth (m.b.s.l)
Number of fractures / 10m vertical depth

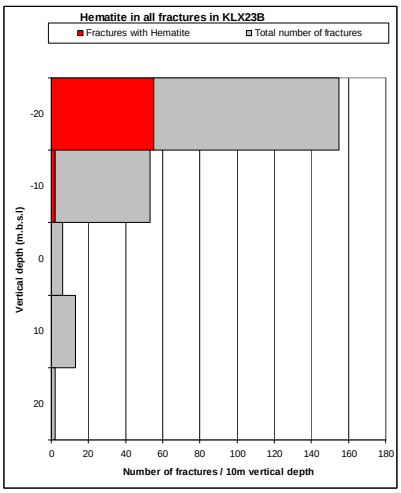
Hematite in all fractures in KLX23B
Fractures with Hematite
Total number of fractures
Vertical depth (m.b.s.l)
Number of fractures / 10m vertical depth

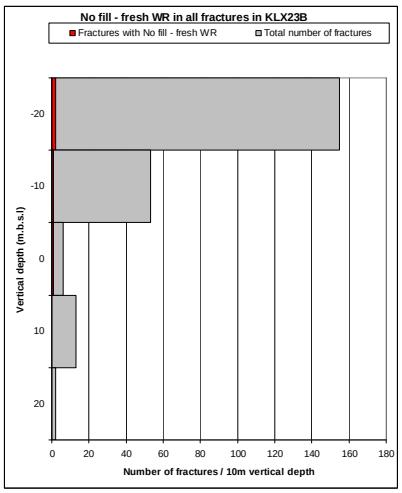
No fill - fresh WR in all fractures in KLX23B
Fractures with No fill - fresh WR
Total number of fractures
Vertical depth (m.b.s.l)
Number of fractures / 10m vertical depth

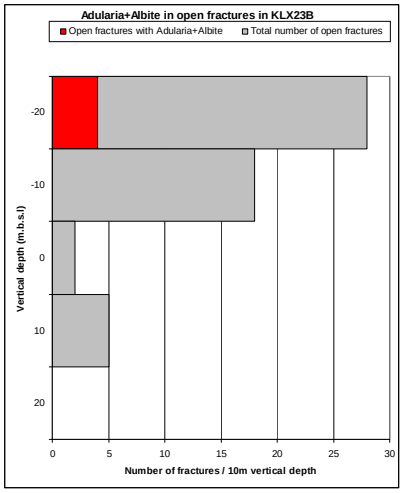
Adularia+Albite in open fractures in KLX23B
Open fractures with Adularia+Albite
Total number of open fractures
Vertical depth (m.b.s.l)
Number of fractures / 10m vertical depth

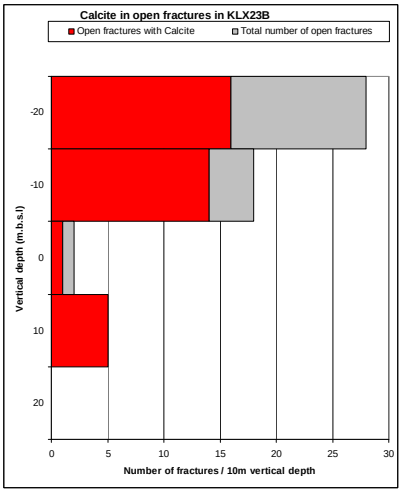
Calcite in open fractures in KLX23B
Open fractures with Calcite
Total number of open fractures
Vertical depth (m.b.s.l)
Number of fractures / 10m vertical depth

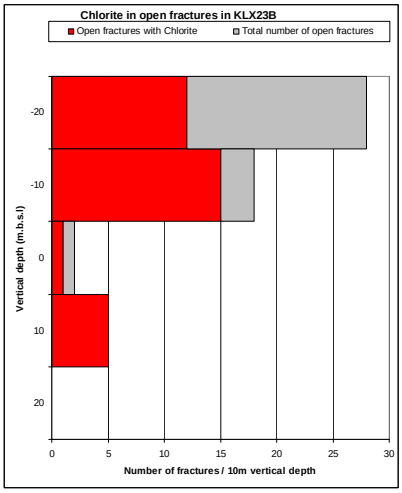
Chlorite in open fractures in KLX23B
Open fractures with Chlorite
Total number of open fractures
Vertical depth (m.b.s.l)
Number of fractures / 10m vertical depth

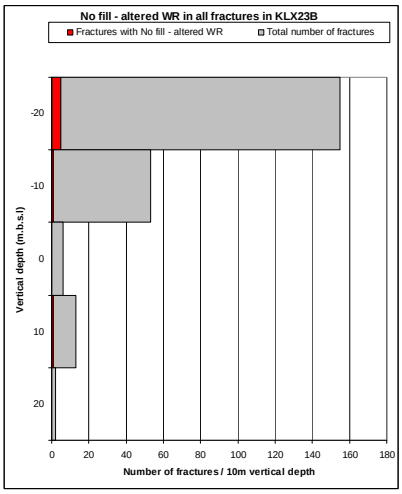
No fill - altered WR in all fractures in KLX23B
Fractures with No fill - altered WR
Total number of fractures
Vertical depth (m.b.s.l)
Number of fractures / 10m vertical depth

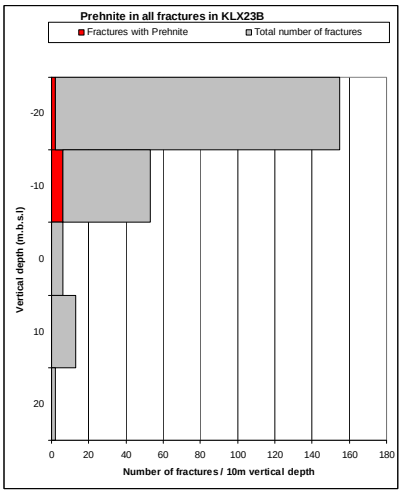
Prehnite in all fractures in KLX23B
Fractures with Prehnite
Total number of fractures
Vertical depth (m.b.s.l)
Number of fractures / 10m vertical depth

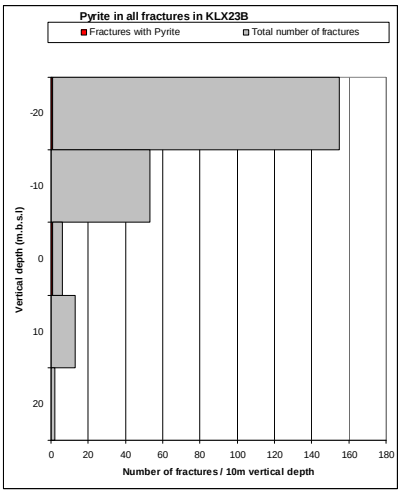
Pyrite in all fractures in KLX23B
Fractures with Pyrite
Total number of fractures
Vertical depth (m.b.s.l)
Number of fractures / 10m vertical depth

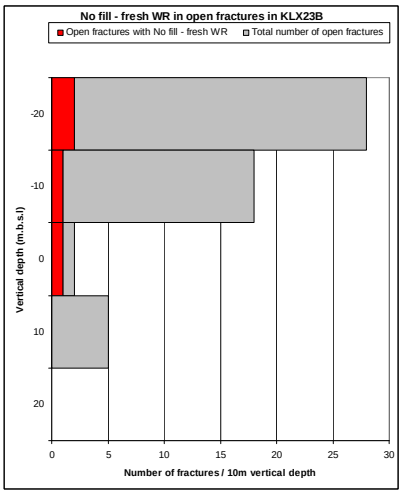
No fill - fresh WR in open fractures in KLX23B
Open fractures with No fill - fresh WR
Total number of open fractures
Vertical depth (m.b.s.l)
Number of fractures / 10m vertical depth

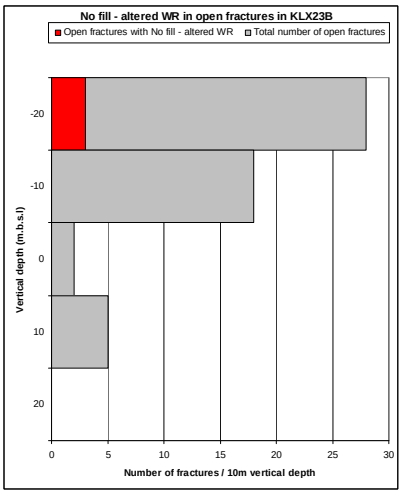
No fill - altered WR in open fractures in KLX23B
Open fractures with No fill - altered WR
Total number of open fractures
Vertical depth (m.b.s.l)
Number of fractures / 10m vertical depth

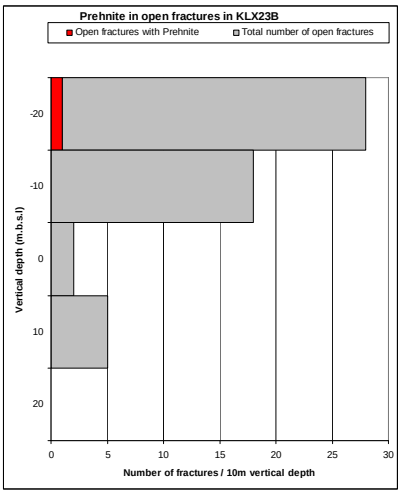
Prehnite in open fractures in KLX23B
Open fractures with Prehnite
Total number of open fractures
Vertical depth (m.b.s.l)
Number of fractures / 10m vertical depth

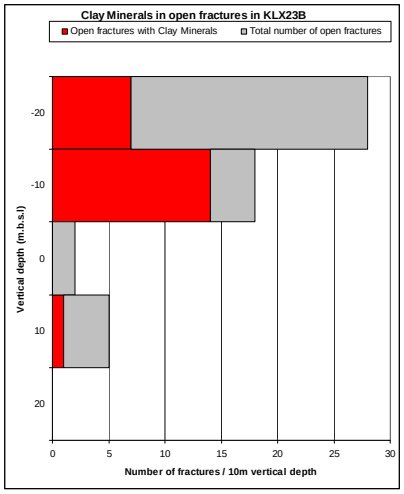
Clay Minerals in open fractures in KLX23B
Open fractures with Clay Minerals
Total number of open fractures
Vertical depth (m.b.s.l)
Number of fractures / 10m vertical depth

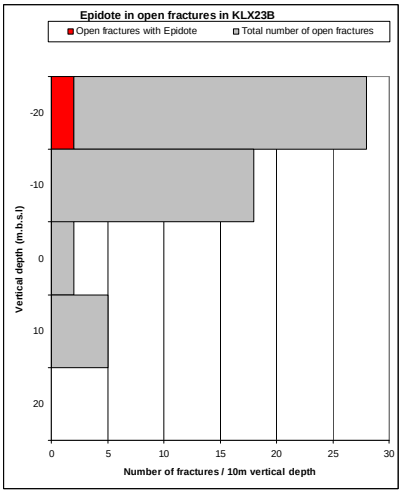
Epidote in open fractures in KLX23B
Open fractures with Epidote
Total number of open fractures
Vertical depth (m.b.s.l)
Number of fractures / 10m vertical depth

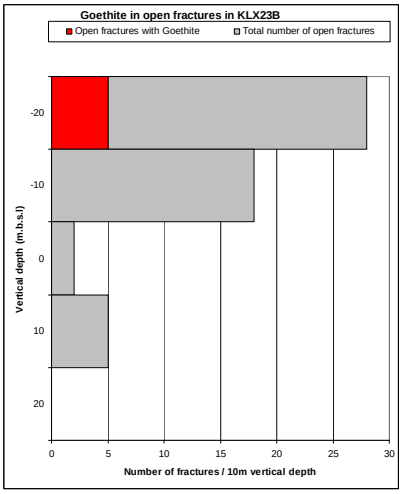
Goethite in open fractures in KLX23B
Open fractures with Goethite
Total number of open fractures
Vertical depth (m.b.s.l)
Number of fractures / 10m vertical depth

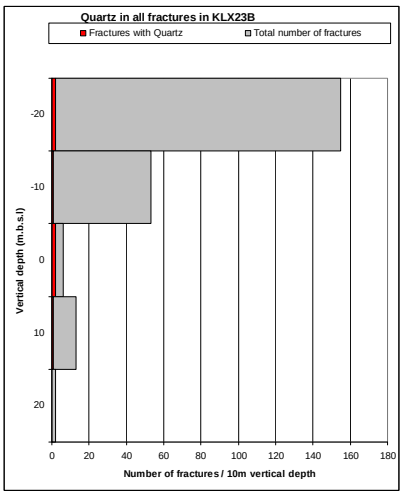
Quartz in all fractures in KLX23B
Fractures with Quartz
Total number of fractures
Vertical depth (m.b.s.l)
Number of fractures / 10m vertical depth

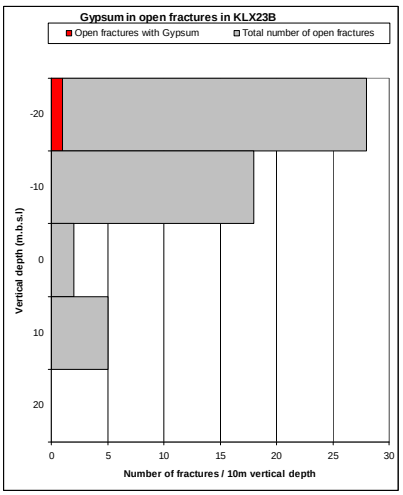
Gypsum in open fractures in KLX23B
Open fractures with Gypsum
Total number of open fractures
Vertical depth (m.b.s.l)
Number of fractures / 10m vertical depth

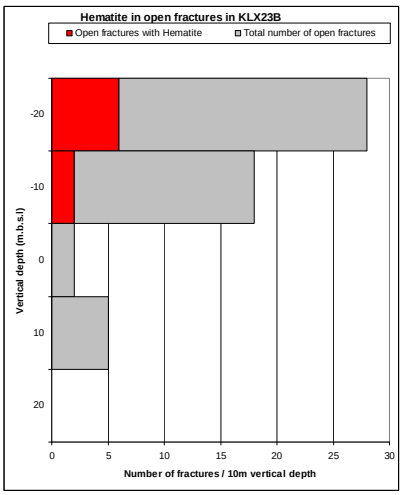
Hematite in open fractures in KLX23B
Open fractures with Hematite
Total number of open fractures
Vertical depth (m.b.s.l)
Number of fractures / 10m vertical depth

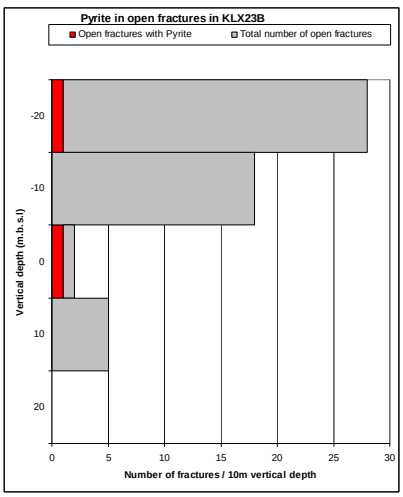
Pyrite in open fractures in KLX23B
Open fractures with Pyrite
Total number of open fractures
Vertical depth (m.b.s.l)
Number of fractures / 10m vertical depth

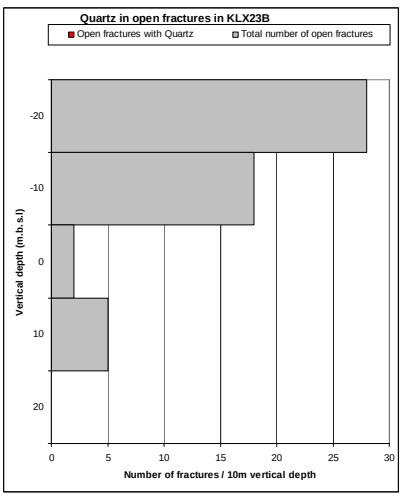
Quartz in open fractures in KLX23B
Open fractures with Quartz
Total number of open fractures
Vertical depth (m.b.s.l)
Number of fractures / 10m vertical depth

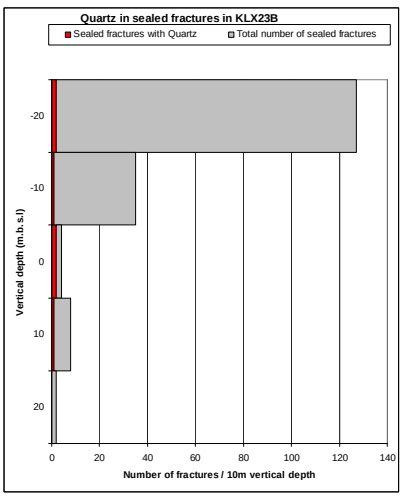
Quartz in sealed fractures in KLX23B
Sealed fractures with Quartz
Total number of sealed fractures
Vertical depth (m.b.s.l)
Number of fractures / 10m vertical depth

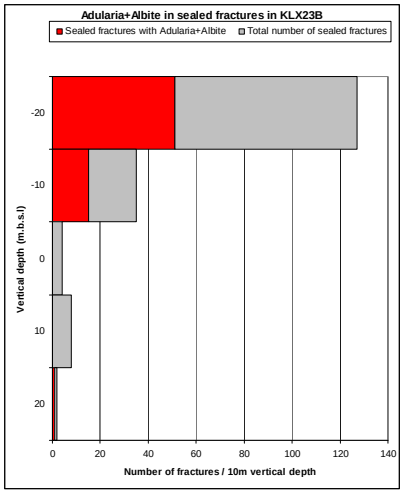
Adularia+Albite in sealed fractures in KLX23B
Sealed fractures with Adularia+Albite
Total number of sealed fractures
Vertical depth (m.b.s.l)
-20
-10
0
10
20
0
20
40
60
80
100
120
140
Number of fractures / 10m vertical depth

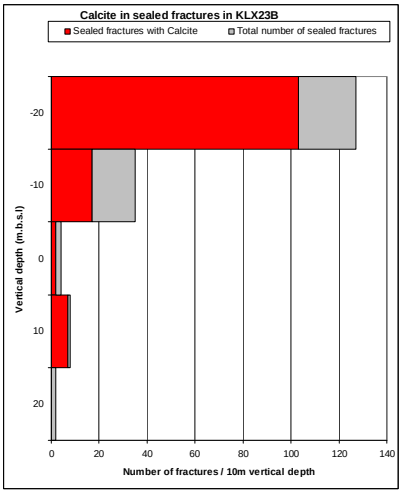
Calcite in sealed fractures in KLX23B
Sealed fractures with Calcite
Total number of sealed fractures
Vertical depth (m.b.s.l)
-20
-10
0
10
20
0
20
40
60
80
100
120
140
Number of fractures / 10m vertical depth

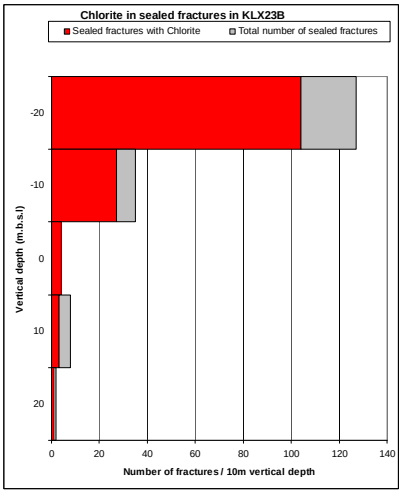
Chlorite in sealed fractures in KLX23B
Sealed fractures with Chlorite
Total number of sealed fractures
Vertical depth (m.b.s.l)
-20
-10
0
10
20
0
20
40
60
80
100
120
140
Number of fractures / 10m vertical depth

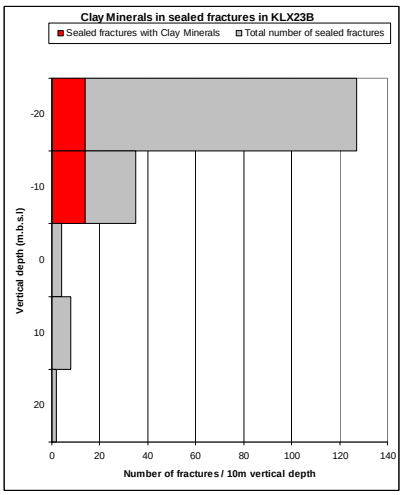
Clay Minerals in sealed fractures in KLX23B
Sealed fractures with Clay Minerals
Total number of sealed fractures
Vertical depth (m.b.s.l)
-20
-10
0
10
20
0
20
40
60
80
100
120
140
Number of fractures / 10m vertical depth

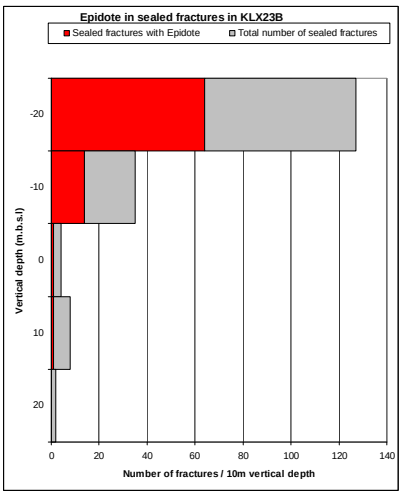
Epidote in sealed fractures in KLX23B
Sealed fractures with Epidote
Total number of sealed fractures
Vertical depth (m.b.s.l)
-20
-10
0
10
20
0
20
40
60
80
100
120
140
Number of fractures / 10m vertical depth

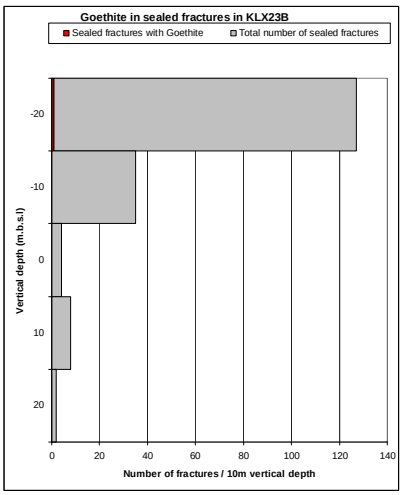
Goethite in sealed fractures in KLX23B
Sealed fractures with Goethite
Total number of sealed fractures
Vertical depth (m.b.s.l)
-20
-10
0
10
20
0
20
40
60
80
100
120
140
Number of fractures / 10m vertical depth

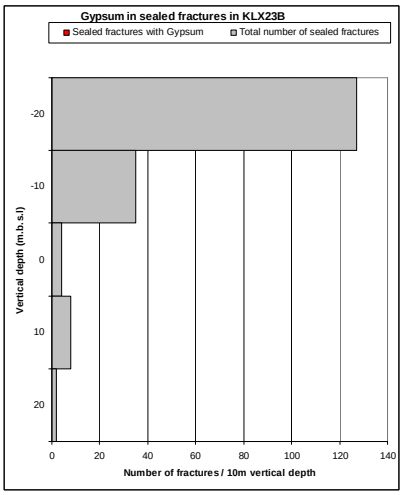
Gypsum in sealed fractures in KLX23B
Sealed fractures with Gypsum
Total number of sealed fractures
Vertical depth (m.b.s.l)
-20
-10
0
10
20
0
20
40
60
80
100
120
140
Number of fractures / 10m vertical depth

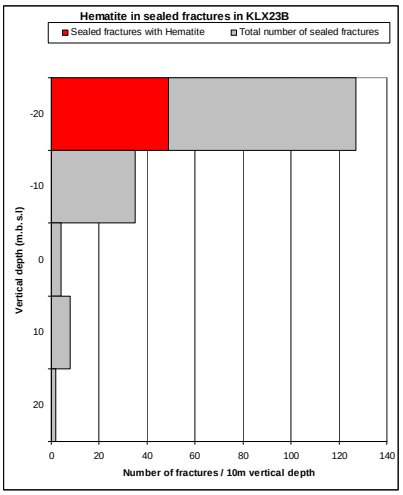
Hematite in sealed fractures in KLX23B
Sealed fractures with Hematite
Total number of sealed fractures
Vertical depth (m.b.s.l)
-20
-10
0
10
20
0
20
40
60
80
100
120
140
Number of fractures / 10m vertical depth

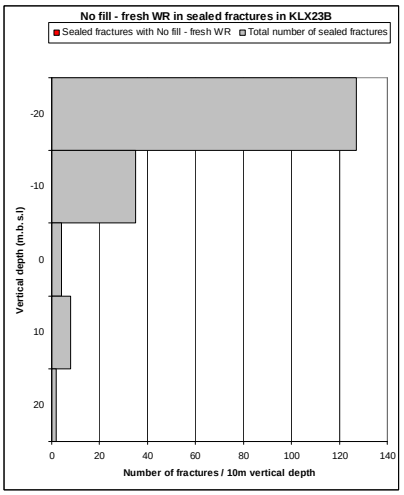
No fill - fresh WR in sealed fractures in KLX23B
Sealed fractures with No fill - fresh WR
Total number of sealed fractures
Vertical depth (m.b.s.l)
-20
-10
0
10
20
0
20
40
60
80
100
120
140
Number of fractures / 10m vertical depth

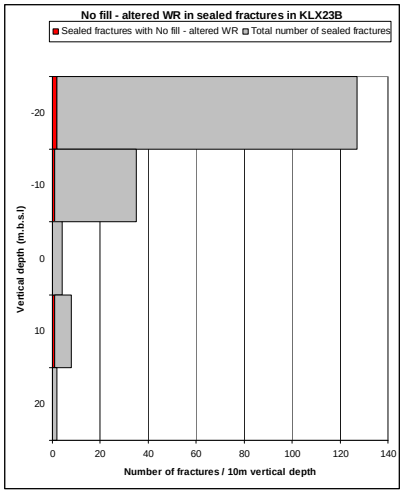
No fill - altered WR in sealed fractures in KLX23B
Sealed fractures with No fill - altered WR
Total number of sealed fractures
Vertical depth (m.b.s.l)
-20
-10
0
10
20
0
20
40
60
80
100
120
140
Number of fractures / 10m vertical depth

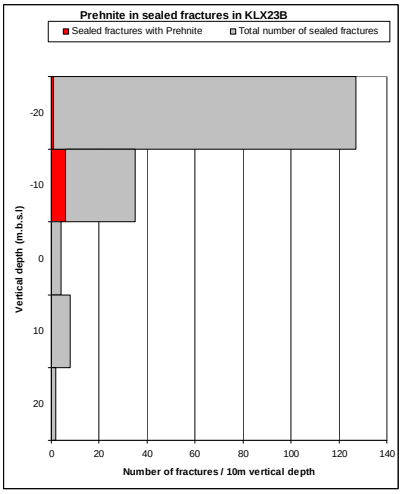
Prehnite in sealed fractures in KLX23B
Sealed fractures with Prehnite
Total number of sealed fractures
Vertical depth (m.b.s.l)
-20
-10
0
10
20
0
20
40
60
80
100
120
140
Number of fractures / 10m vertical depth

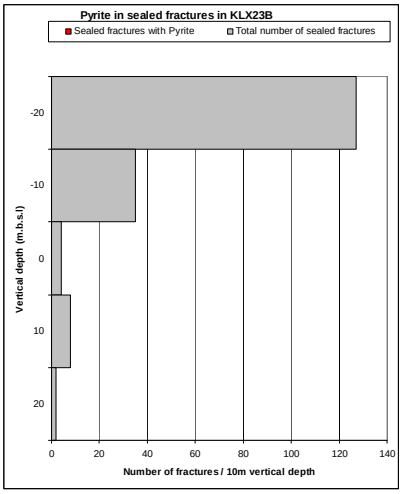
Pyrite in sealed fractures in KLX23B
Sealed fractures with Pyrite
Total number of sealed fractures
Vertical depth (m.b.s.l)
-20
-10
0
10
20
0
20
40
60
80
100
120
140
Number of fractures / 10m vertical depth

KLX24A

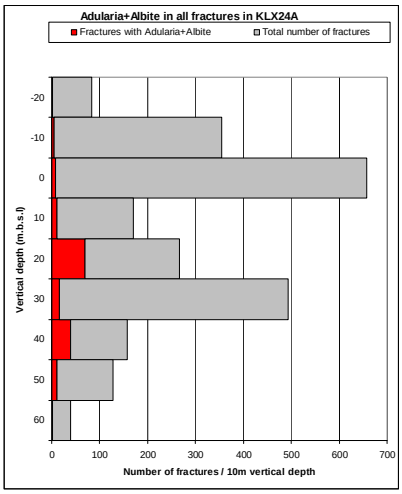
Adularia+Albite in all fractures in KLX24A
Fractures with Adularia+Albite
Total number of fractures
Vertical depth (m.b.s.l)
Number of fractures / 10m vertical depth

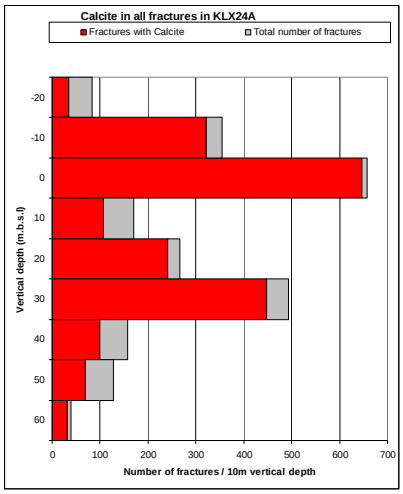
Calcite in all fractures in KLX24A
Fractures with Calcite
Total number of fractures
Vertical depth (m.b.s.l)
Number of fractures / 10m vertical depth

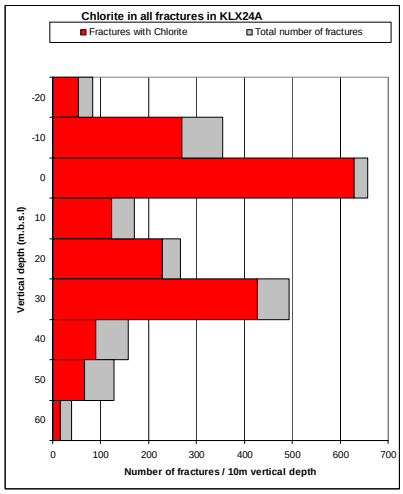
Chlorite in all fractures in KLX24A
Fractures with Chlorite
Total number of fractures
Vertical depth (m.b.s.l)
Number of fractures / 10m vertical depth

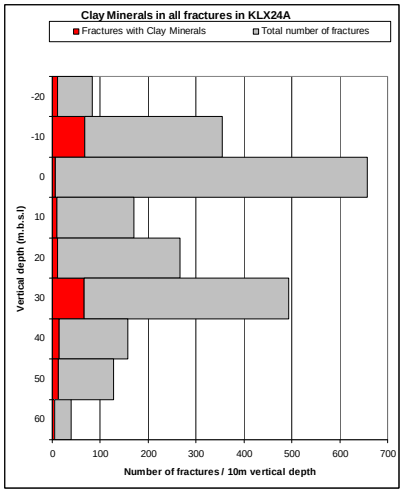
Clay Minerals in all fractures in KLX24A
Fractures with Clay Minerals
Total number of fractures
Vertical depth (m.b.s.l)
Number of fractures / 10m vertical depth

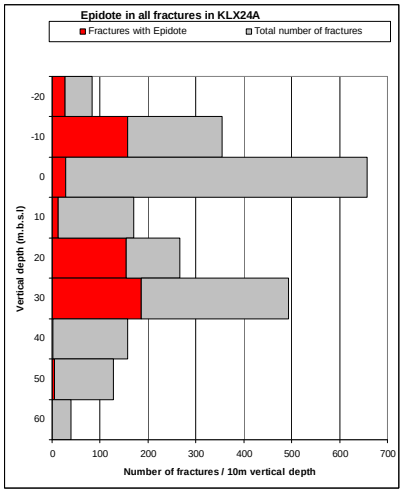
Epidote in all fractures in KLX24A
Fractures with Epidote
Total number of fractures
Vertical depth (m.b.s.l)
Number of fractures / 10m vertical depth

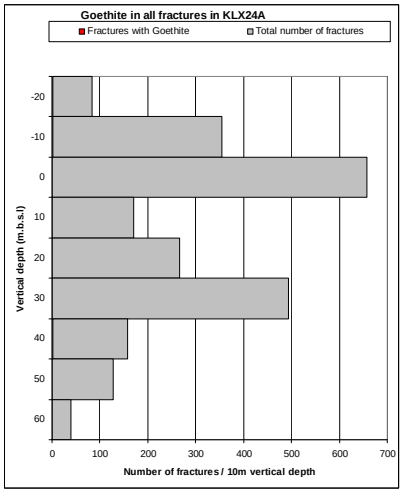
Goethite in all fractures in KLX24A
Fractures with Goethite
Total number of fractures
Vertical depth (m.b.s.l)
Number of fractures / 10m vertical depth

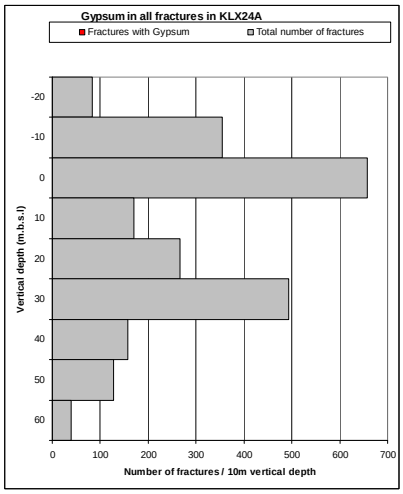
Gypsum in all fractures in KLX24A
Fractures with Gypsum
Total number of fractures
Vertical depth (m.b.s.l)
Number of fractures / 10m vertical depth

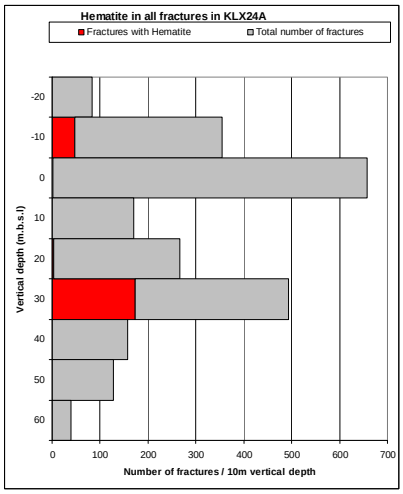
Hematite in all fractures in KLX24A
Fractures with Hematite
Total number of fractures
Vertical depth (m.b.s.l)
Number of fractures / 10m vertical depth

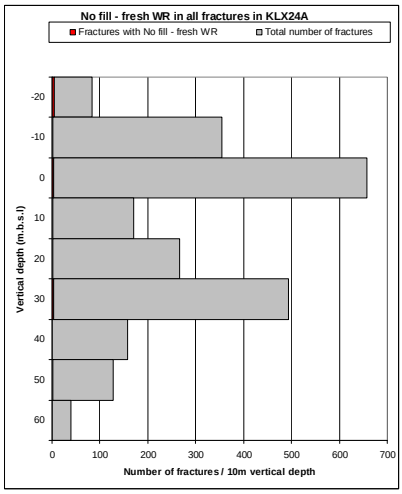
No fill - fresh WR in all fractures in KLX24A
Fractures with No fill - fresh WR
Total number of fractures
Vertical depth (m.b.s.l)
Number of fractures / 10m vertical depth

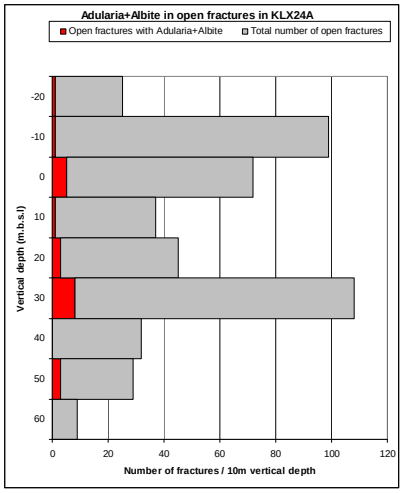
Adularia+Albite in open fractures in KLX24A
Open fractures with Adularia+Albite
Total number of open fractures
Vertical depth (m.b.s.l)
Number of fractures / 10m vertical depth

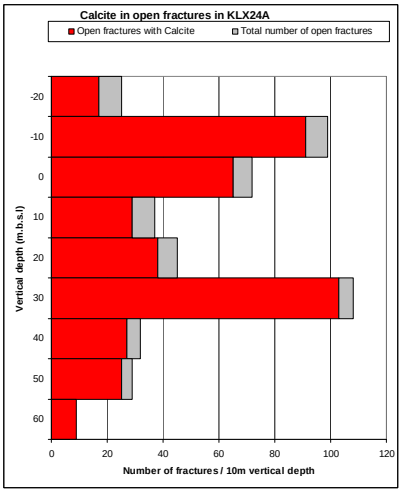
Calcite in open fractures in KLX24A
Open fractures with Calcite
Total number of open fractures
Vertical depth (m.b.s.l)
Number of fractures / 10m vertical depth

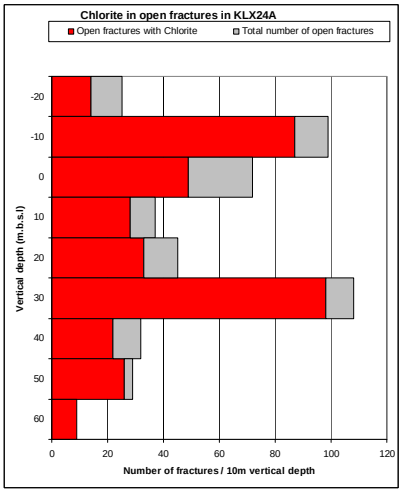
Chlorite in open fractures in KLX24A
Open fractures with Chlorite
Total number of open fractures
Vertical depth (m.b.s.l)
Number of fractures / 10m vertical depth

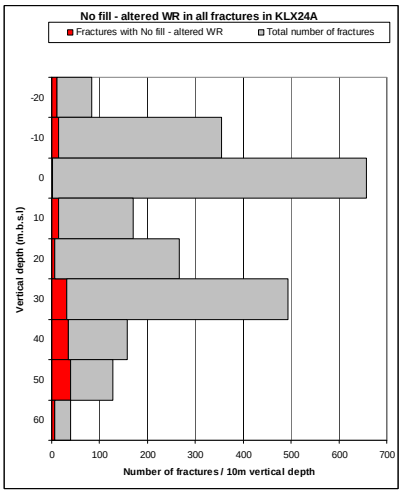
No fill - altered WR in all fractures in KLX24A
Fractures with No fill - altered WR
Total number of fractures
Vertical depth (m.b.s.l)
Number of fractures / 10m vertical depth

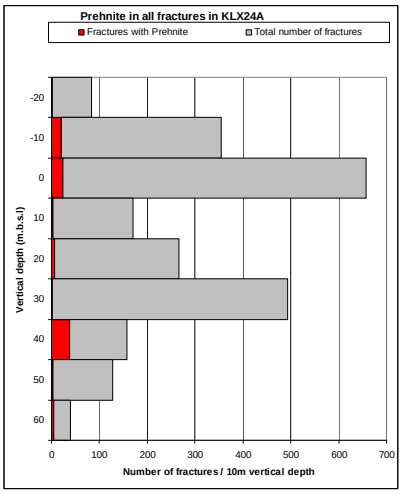
Prehnite in all fractures in KLX24A
Fractures with Prehnite
Total number of fractures
Vertical depth (m.b.s.l)
Number of fractures / 10m vertical depth

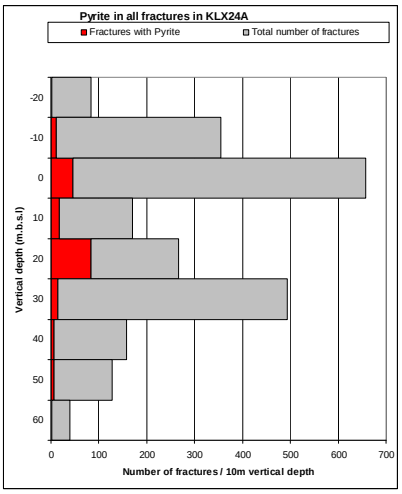
Pyrite in all fractures in KLX24A
Fractures with Pyrite
Total number of fractures
Vertical depth (m.b.s.l)
Number of fractures / 10m vertical depth

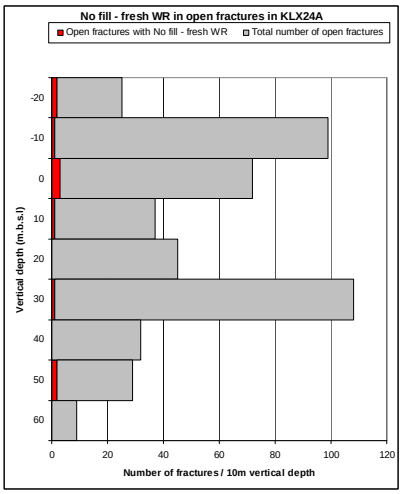
No fill - fresh WR in open fractures in KLX24A
Open fractures with No fill - fresh WR
Total number of open fractures
Vertical depth (m.b.s.l)
Number of fractures / 10m vertical depth

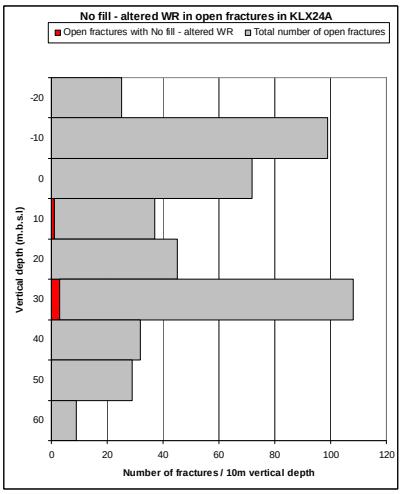
No fill - altered WR in open fractures in KLX24A
Open fractures with No fill - altered WR
Total number of open fractures
Vertical depth (m.b.s.l)
Number of fractures / 10m vertical depth

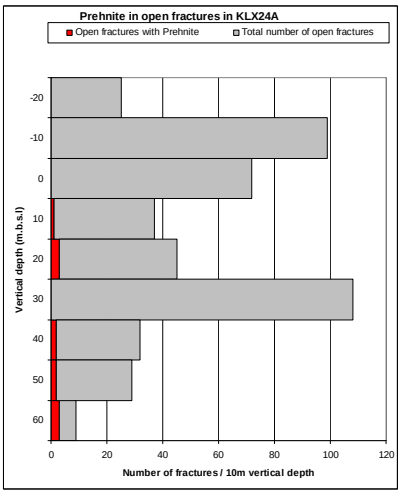
Prehnite in open fractures in KLX24A
Open fractures with Prehnite
Total number of open fractures
Vertical depth (m.b.s.l)
Number of fractures / 10m vertical depth

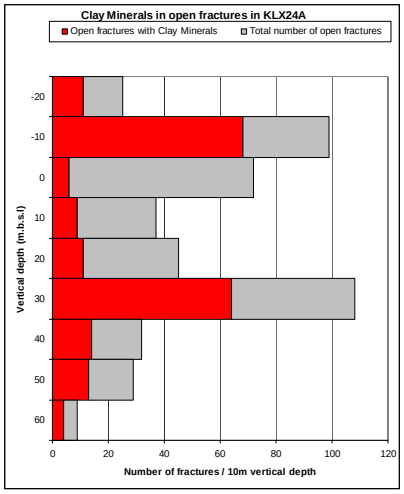
Clay Minerals in open fractures in KLX24A
Open fractures with Clay Minerals
Total number of open fractures
Vertical depth (m.b.s.l)
Number of fractures / 10m vertical depth

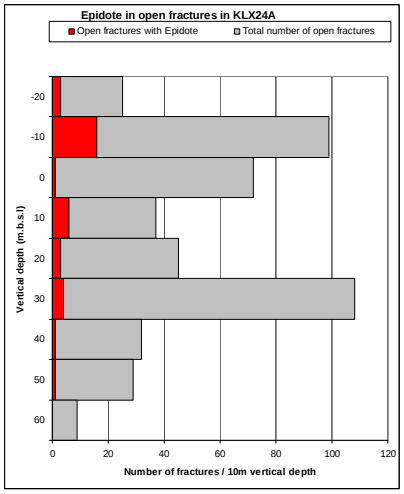
Epidote in open fractures in KLX24A
Open fractures with Epidote
Total number of open fractures
Vertical depth (m.b.s.l)
Number of fractures / 10m vertical depth

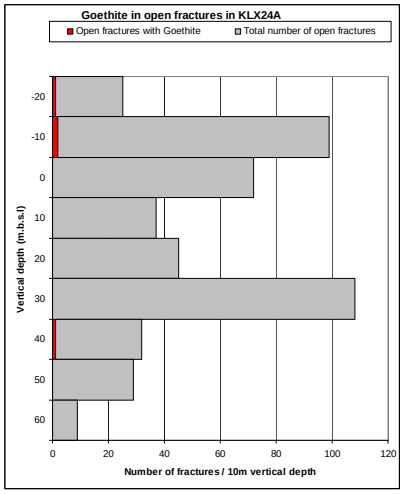
Goethite in open fractures in KLX24A
Open fractures with Goethite
Total number of open fractures
Vertical depth (m.b.s.l)
Number of fractures / 10m vertical depth

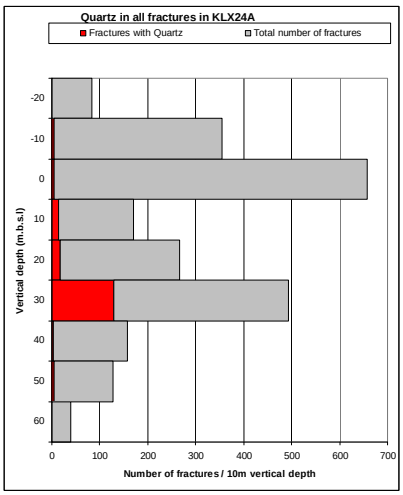
Quartz in all fractures in KLX24A
Fractures with Quartz
Total number of fractures
Vertical depth (m.b.s.l)
Number of fractures / 10m vertical depth

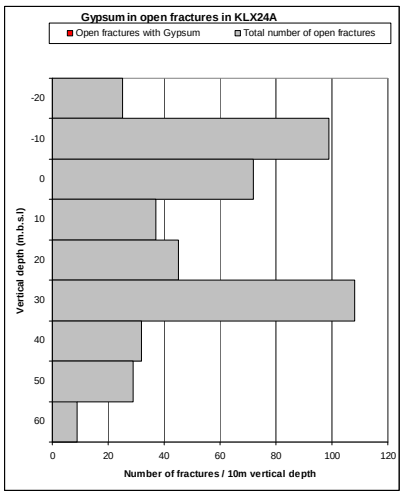
Gypsum in open fractures in KLX24A
Open fractures with Gypsum
Total number of open fractures
Vertical depth (m.b.s.l)
Number of fractures / 10m vertical depth

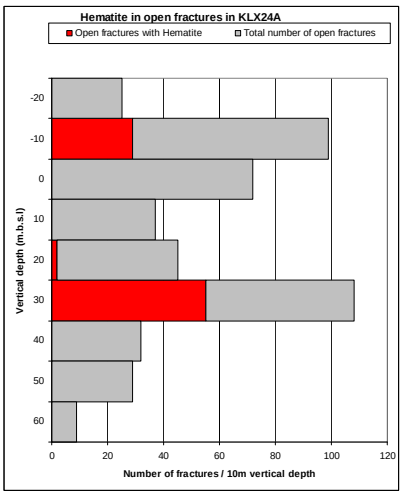
Hematite in open fractures in KLX24A
Open fractures with Hematite
Total number of open fractures
Vertical depth (m.b.s.l)
Number of fractures / 10m vertical depth

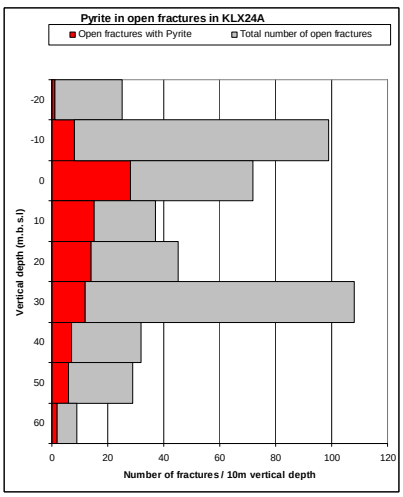
Pyrite in open fractures in KLX24A
Open fractures with Pyrite
Total number of open fractures
Vertical depth (m.b.s.l)
Number of fractures / 10m vertical depth

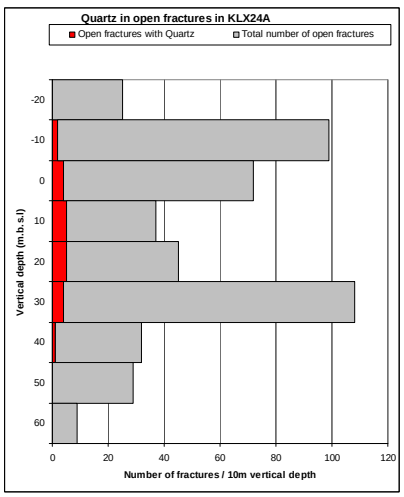
Quartz in open fractures in KLX24A
Open fractures with Quartz
Total number of open fractures
Vertical depth (m.b.s.l)
Number of fractures / 10m vertical depth

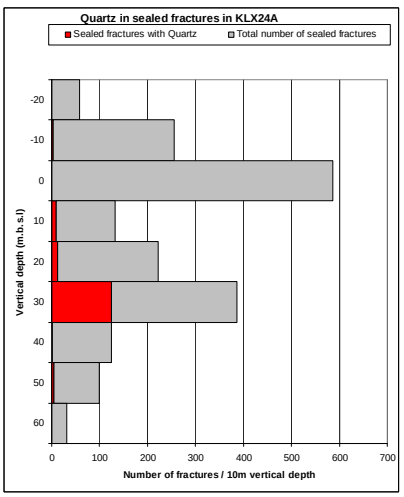
Quartz in sealed fractures in KLX24A
Sealed fractures with Quartz
Total number of sealed fractures
Vertical depth (m.b.s.l)
Number of fractures / 10m vertical depth

i

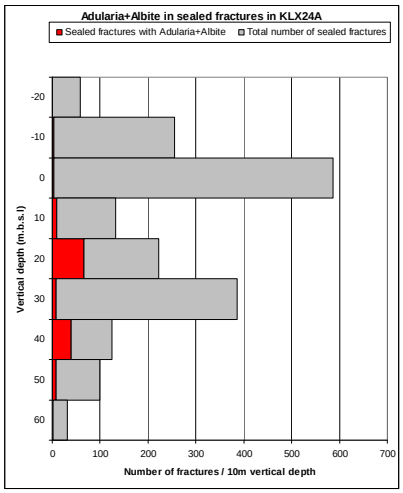
Adularia+Albite in sealed fractures in KLX24A
Sealed fractures with Adularia+Albite
Total number of sealed fractures
Vertical depth (m.b.s.l)
Number of fractures / 10m vertical depth

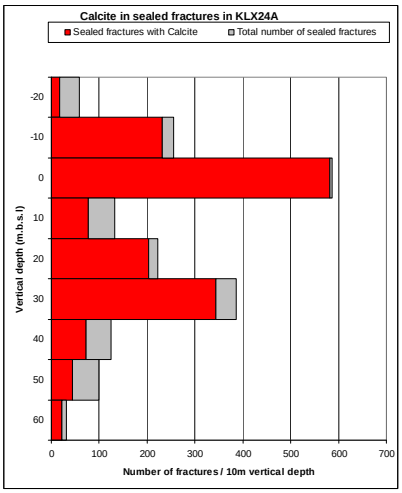
Calcite in sealed fractures in KLX24A
Sealed fractures with Calcite
Total number of sealed fractures
Vertical depth (m.b.s.l)
Number of fractures / 10m vertical depth

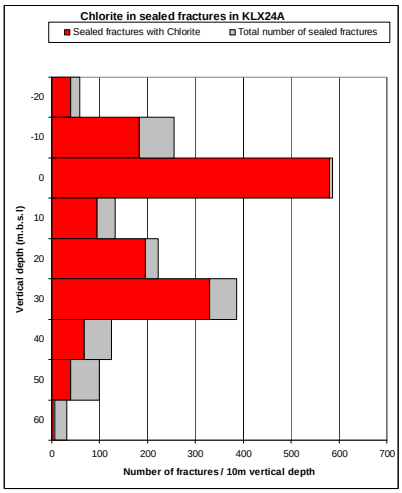
Chlorite in sealed fractures in KLX24A
Sealed fractures with Chlorite
Total number of sealed fractures
Vertical depth (m.b.s.l)
Number of fractures / 10m vertical depth

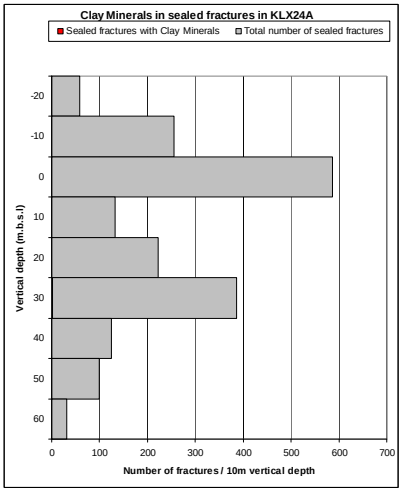
Clay Minerals in sealed fractures in KLX24A
Sealed fractures with Clay Minerals
Total number of sealed fractures
Vertical depth (m.b.s.l)
Number of fractures / 10m vertical depth

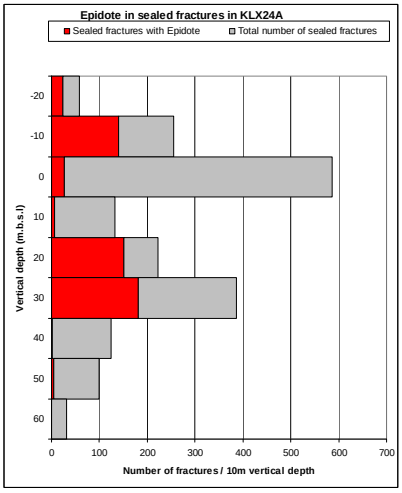
Epidote in sealed fractures in KLX24A
Sealed fractures with Epidote
Total number of sealed fractures
Vertical depth (m.b.s.l)
Number of fractures / 10m vertical depth

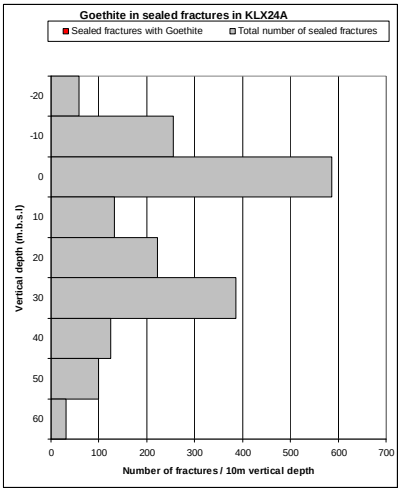
Goethite in sealed fractures in KLX24A
Sealed fractures with Goethite
Total number of sealed fractures
Vertical depth (m.b.s.l)
Number of fractures / 10m vertical depth

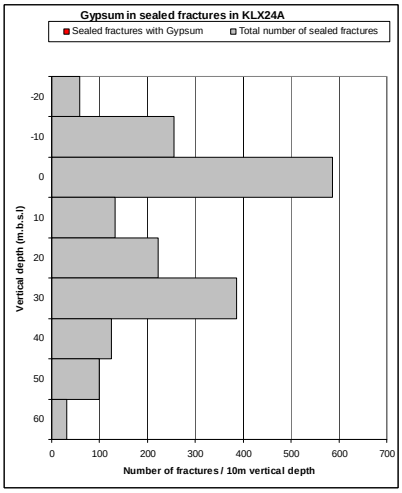
Gypsum in sealed fractures in KLX24A
Sealed fractures with Gypsum
Total number of sealed fractures
Vertical depth (m.b.s.l)
Number of fractures / 10m vertical depth

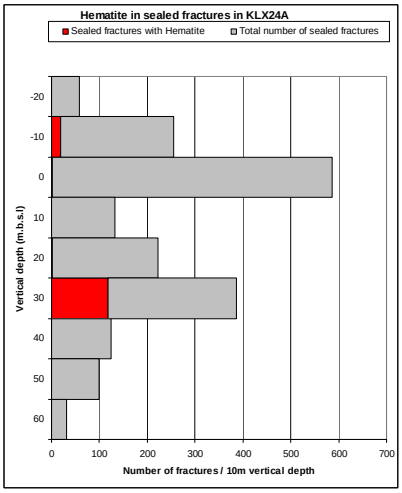
Hematite in sealed fractures in KLX24A
Sealed fractures with Hematite
Total number of sealed fractures
Vertical depth (m.b.s.l)
Number of fractures / 10m vertical depth

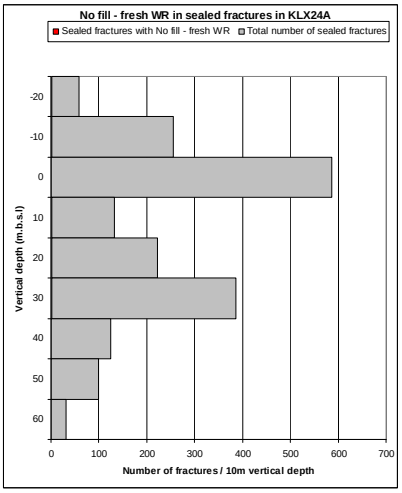
No fill - fresh WR in sealed fractures in KLX24A
Sealed fractures with No fill - fresh WR
Total number of sealed fractures
Vertical depth (m.b.s.l)
Number of fractures / 10m vertical depth

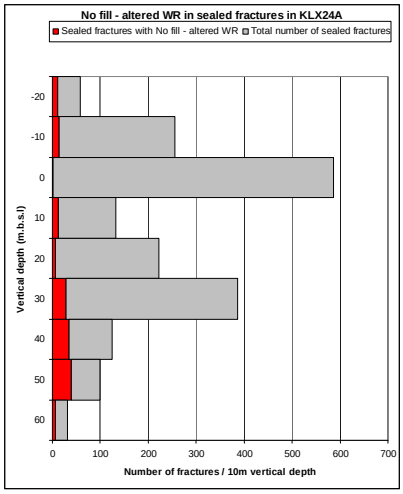
No fill - altered WR in sealed fractures in KLX24A
Sealed fractures with No fill - altered WR
Total number of sealed fractures
Vertical depth (m.b.s.l)
-20
-10
0
10
20
30
40
50
60
0
100
200
300
400
500
600
700
Number of fractures / 10m vertical depth

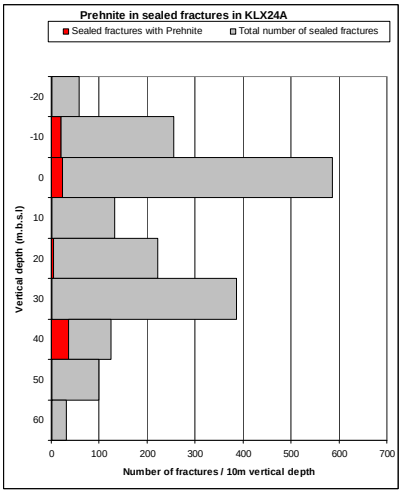
Prehnite in sealed fractures in KLX24A
Sealed fractures with Prehnite
Total number of sealed fractures
Vertical depth (m.b.s.l)
-20
-10
0
10
20
30
40
50
60
0
100
200
300
400
500
600
700
Number of fractures / 10m vertical depth

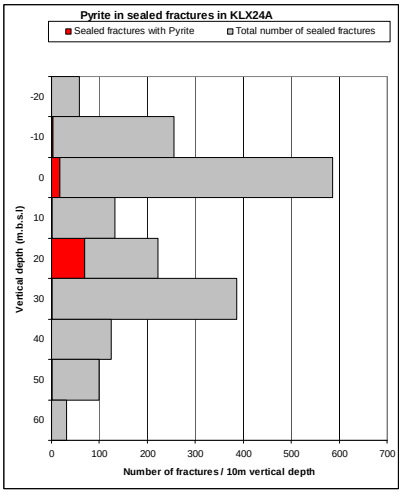
Pyrite in sealed fractures in KLX24A
Sealed fractures with Pyrite
Total number of sealed fractures
Vertical depth (m.b.s.l)
-20
-10
0
10
20
30
40
50
60
0
100
200
300
400
500
600
700
Number of fractures / 10m vertical depth

KLX25A

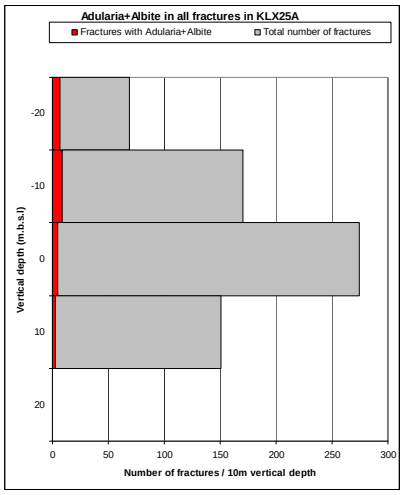
Adularia+Albite in all fractures in KLX25A
Fractures with Adularia+Albite
Total number of fractures
Vertical depth (m.b.s.l)
-20
-10
0
10
20
0
50
100
150
200
250
300
Number of fractures / 10m vertical depth

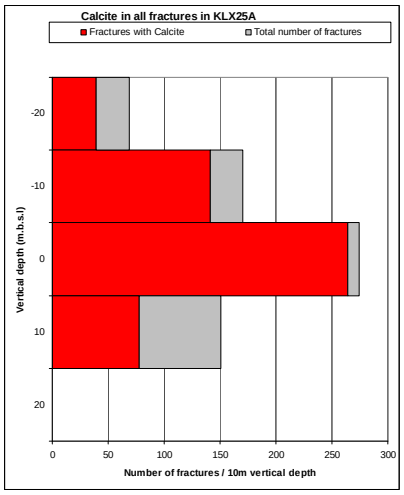
Calcite in all fractures in KLX25A
Fractures with Calcite
Total number of fractures
Vertical depth (m.b.s.l)
-20
-10
0
10
20
0
50
100
150
200
250
300
Number of fractures / 10m vertical depth

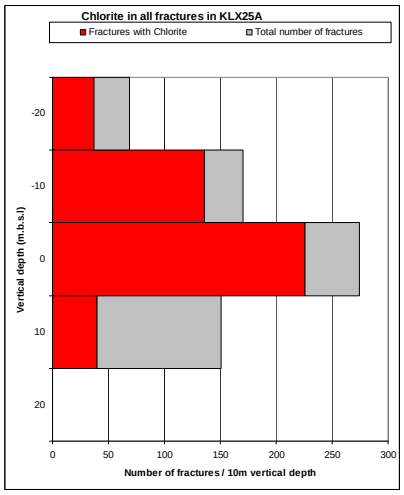
Chlorite in all fractures in KLX25A
Fractures with Chlorite
Total number of fractures
Vertical depth (m.b.s.l)
-20
-10
0
10
20
0
50
100
150
200
250
300
Number of fractures / 10m vertical depth

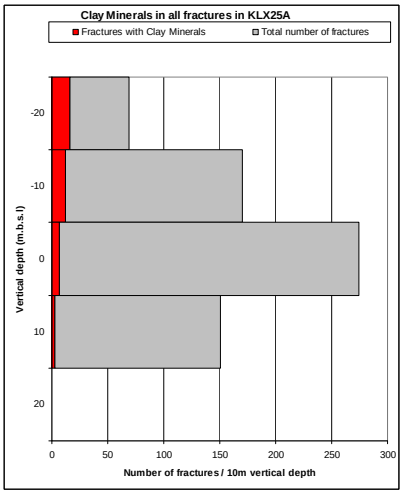
Clay Minerals in all fractures in KLX25A
Fractures with Clay Minerals
Total number of fractures
Vertical depth (m.b.s.l)
-20
-10
0
10
20
0
50
100
150
200
250
300
Number of fractures / 10m vertical depth

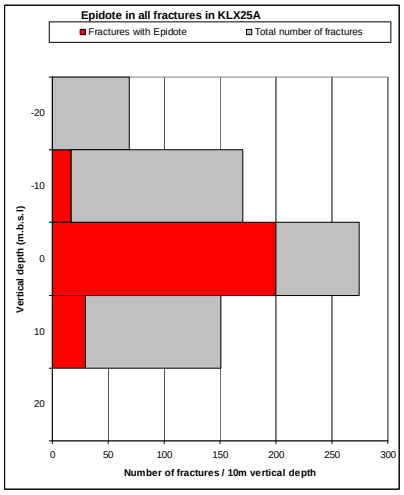
Epidote in all fractures in KLX25A
Fractures with Epidote
Total number of fractures
Vertical depth (m.b.s.l)
-20
-10
0
10
20
0
50
100
150
200
250
300
Number of fractures / 10m vertical depth

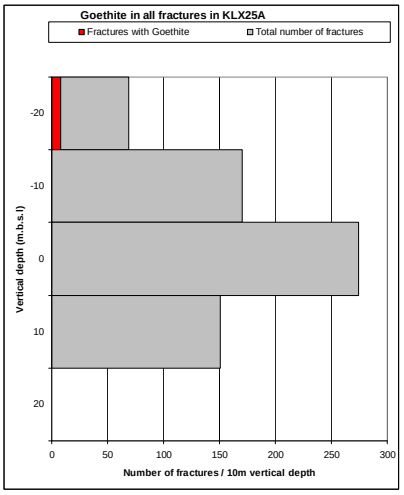
Goethite in all fractures in KLX25A
Fractures with Goethite
Total number of fractures
Vertical depth (m.b.s.l)
-20
-10
0
10
20
0
50
100
150
200
250
300
Number of fractures / 10m vertical depth

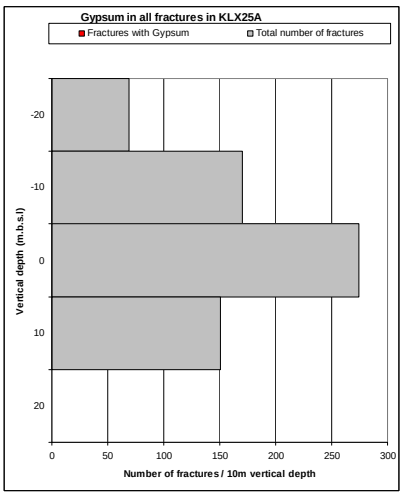
Gypsum in all fractures in KLX25A
Fractures with Gypsum
Total number of fractures
Vertical depth (m.b.s.l)
-20
-10
0
10
20
0
50
100
150
200
250
300
Number of fractures / 10m vertical depth

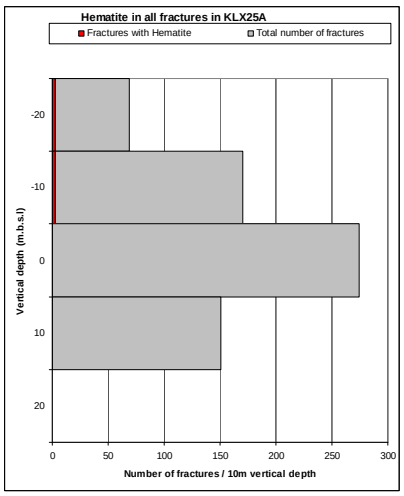
Hematite in all fractures in KLX25A
Fractures with Hematite
Total number of fractures
Vertical depth (m.b.s.l)
-20
-10
0
10
20
0
50
100
150
200
250
300
Number of fractures / 10m vertical depth

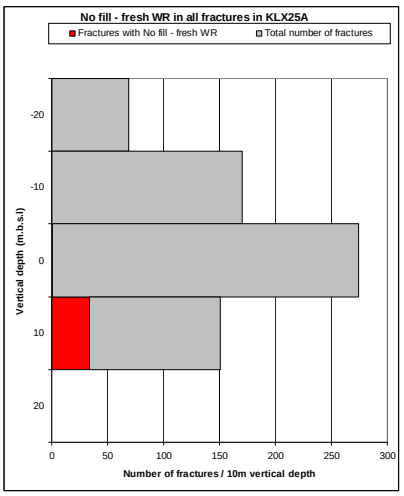
No fill - fresh WR in all fractures in KLX25A
Fractures with No fill - fresh WR
Total number of fractures
Vertical depth (m.b.s.l)
-20
-10
0
10
20
0
50
100
150
200
250
300
Number of fractures / 10m vertical depth

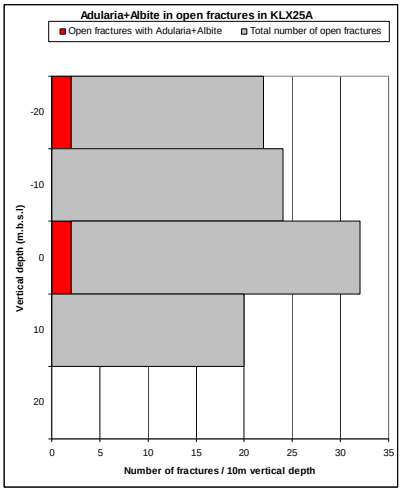
Adularia+Albite in open fractures in KLX25A
Open fractures with Adularia+Albite
Total number of open fractures
Vertical depth (m.b.s.l)
-20
-10
0
10
20
0
5
10
15
20
25
30
35
Number of fractures / 10m vertical depth

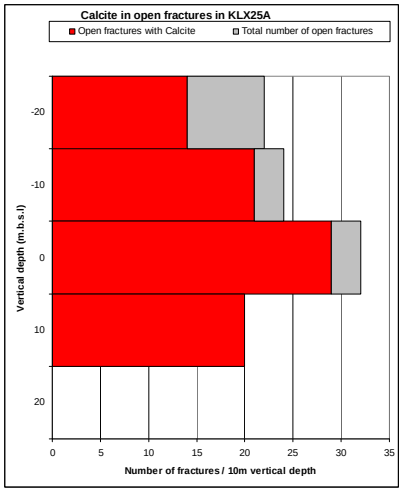
Calcite in open fractures in KLX25A
Open fractures with Calcite
Total number of open fractures
Vertical depth (m.b.s.l)
-20
-10
0
10
20
0
5
10
15
20
25
30
35
Number of fractures / 10m vertical depth

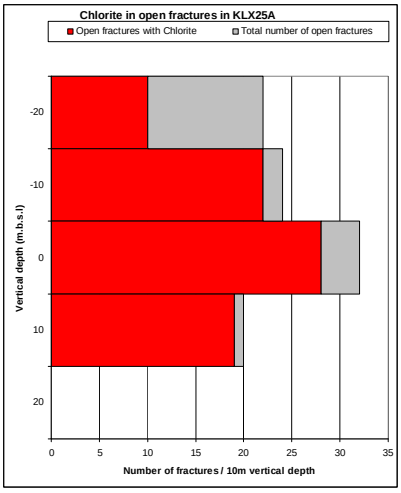
Chlorite in open fractures in KLX25A
Open fractures with Chlorite
Total number of open fractures
Vertical depth (m.b.s.l)
-20
-10
0
10
20
0
5
10
15
20
25
30
35
Number of fractures / 10m vertical depth

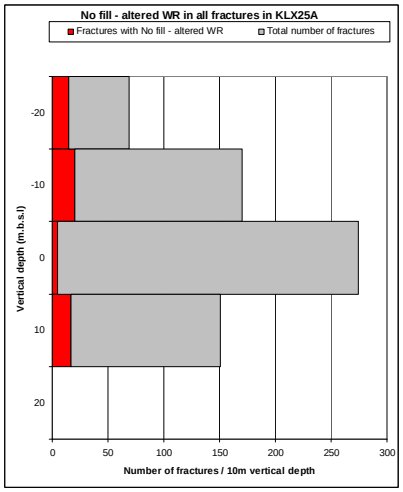
No fill - altered WR in all fractures in KLX25A
Fractures with No fill - altered WR
Total number of fractures
Vertical depth (m.b.s.l)
-20
-10
0
10
20
0
50
100
150
200
250
300
Number of fractures / 10m vertical depth

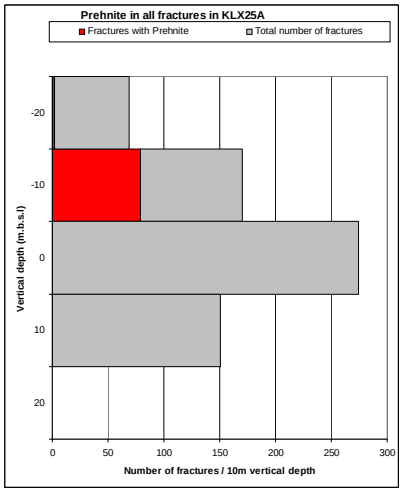
Prehnite in all fractures in KLX25A
Fractures with Prehnite
Total number of fractures
Vertical depth (m.b.s.l)
-20
-10
0
10
20
0
50
100
150
200
250
300
Number of fractures / 10m vertical depth

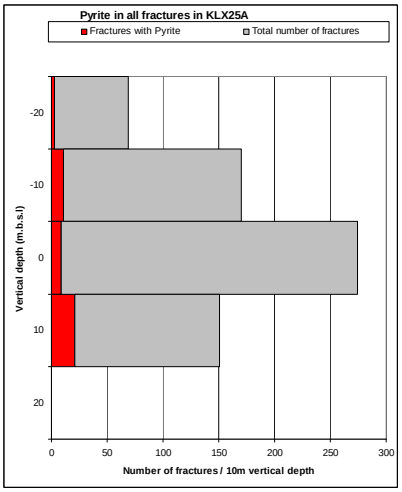
Pyrite in all fractures in KLX25A
Fractures with Pyrite
Total number of fractures
Vertical depth (m.b.s.l)
-20
-10
0
10
20
0
50
100
150
200
250
300
Number of fractures / 10m vertical depth

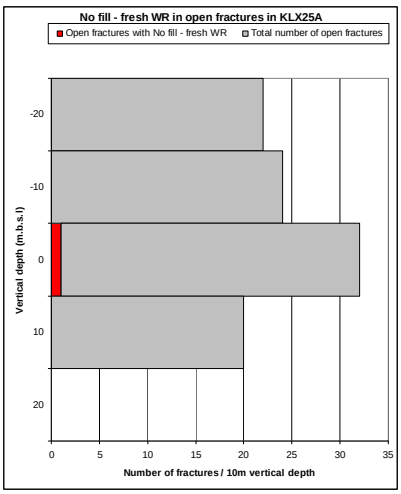
No fill - fresh WR in open fractures in KLX25A
Open fractures with No fill - fresh WR
Total number of open fractures
Vertical depth (m.b.s.l)
-20
-10
0
10
20
0
5
10
15
20
25
30
35
Number of fractures / 10m vertical depth

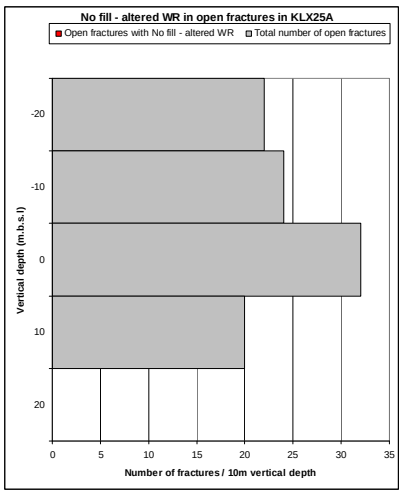
No fill - altered WR in open fractures in KLX25A
Open fractures with No fill - altered WR
Total number of open fractures
Vertical depth (m.b.s.l)
-20
-10
0
10
20
0
5
10
15
20
25
30
35
Number of fractures / 10m vertical depth

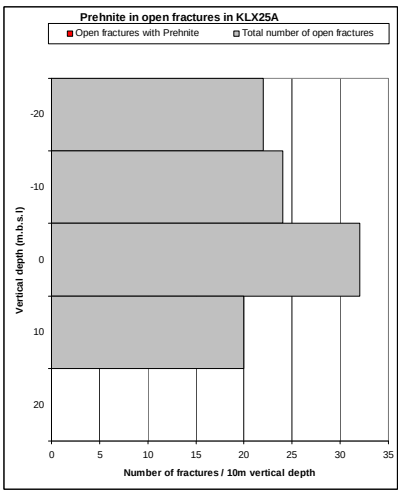
Prehnite in open fractures in KLX25A
Open fractures with Prehnite
Total number of open fractures
Vertical depth (m.b.s.l)
-20
-10
0
10
20
0
5
10
15
20
25
30
35
Number of fractures / 10m vertical depth

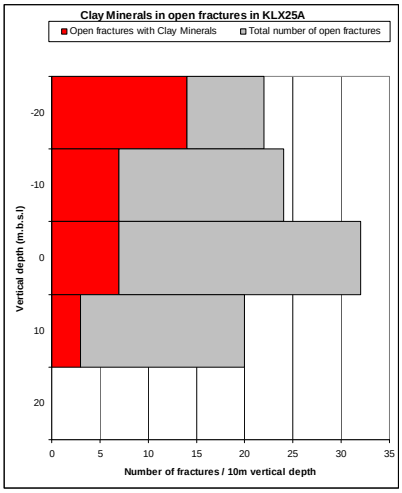
Clay Minerals in open fractures in KLX25A
Open fractures with Clay Minerals
Total number of open fractures
Vertical depth (m.b.s.l)
-20
-10
0
10
20
0
5
10
15
20
25
30
35
Number of fractures / 10m vertical depth

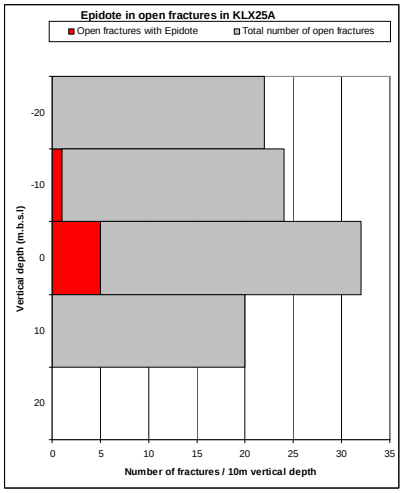
Epidote in open fractures in KLX25A
Open fractures with Epidote
Total number of open fractures
Vertical depth (m.b.s.l)
-20
-10
0
10
20
0
5
10
15
20
25
30
35
Number of fractures / 10m vertical depth

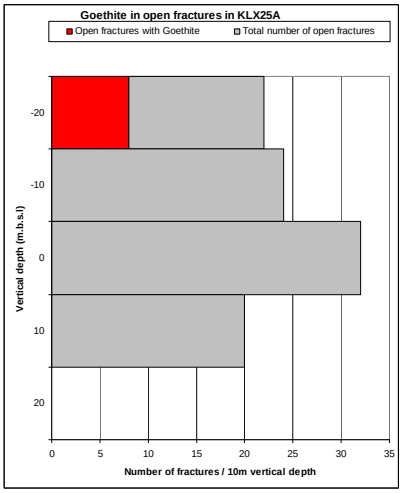
Goethite in open fractures in KLX25A
Open fractures with Goethite
Total number of open fractures
Vertical depth (m.b.s.l)
-20
-10
0
10
20
0
5
10
15
20
25
30
35
Number of fractures / 10m vertical depth

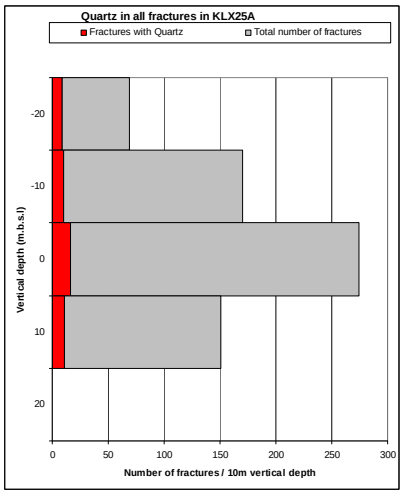
Quartz in all fractures in KLX25A
Fractures with Quartz
Total number of fractures
Vertical depth (m.b.s.l)
-20
-10
0
10
20
0
50
100
150
200
250
300
Number of fractures / 10m vertical depth

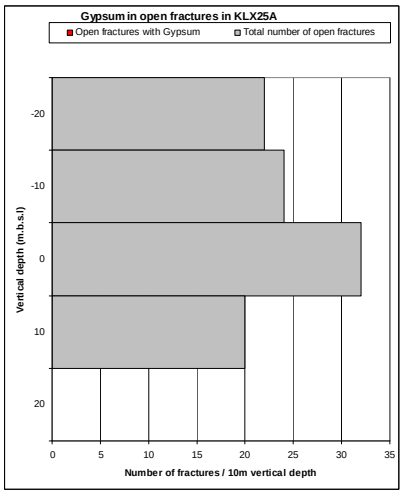
Gypsum in open fractures in KLX25A
Open fractures with Gypsum
Total number of open fractures
Vertical depth (m.b.s.l)
-20
-10
0
10
20
0
5
10
15
20
25
30
35
Number of fractures / 10m vertical depth

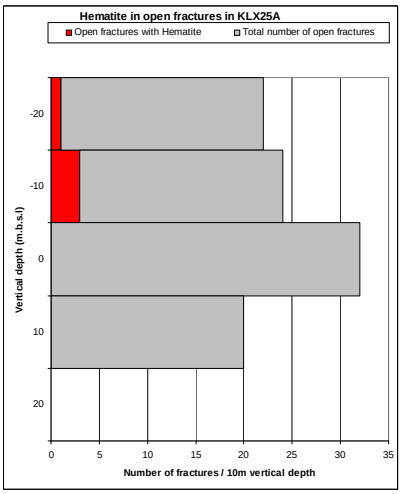
Hematite in open fractures in KLX25A
Open fractures with Hematite
Total number of open fractures
Vertical depth (m.b.s.l)
-20
-10
0
10
20
0
5
10
15
20
25
30
35
Number of fractures / 10m vertical depth

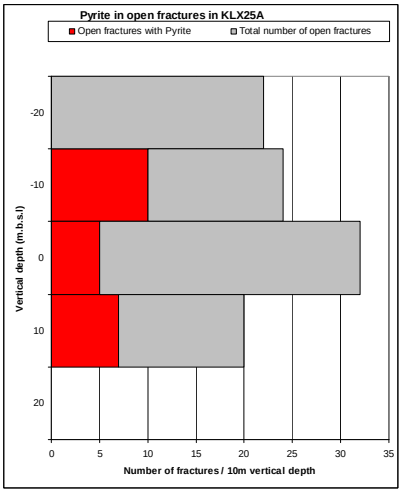
Pyrite in open fractures in KLX25A
Open fractures with Pyrite
Total number of open fractures
Vertical depth (m.b.s.l)
-20
-10
0
10
20
0
5
10
15
20
25
30
35
Number of fractures / 10m vertical depth

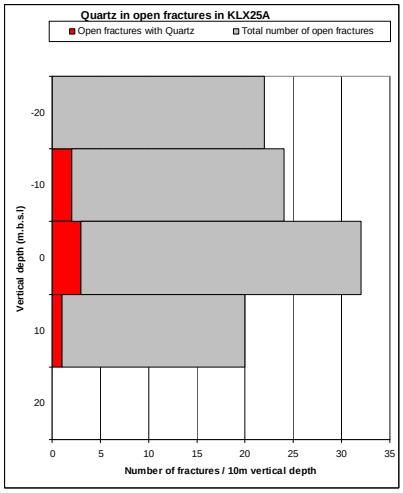
Quartz in open fractures in KLX25A
Open fractures with Quartz
Total number of open fractures
Vertical depth (m.b.s.l)
-20
-10
0
10
20
0
5
10
15
20
25
30
35
Number of fractures / 10m vertical depth

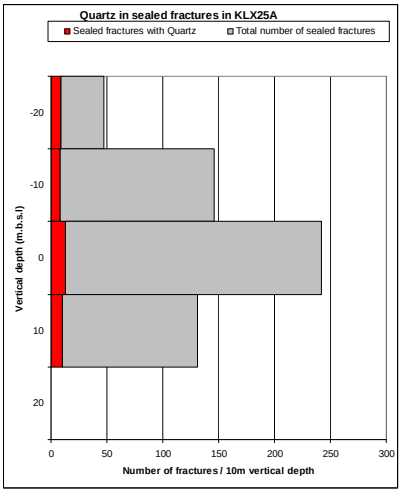
Quartz in sealed fractures in KLX25A
Sealed fractures with Quartz
Total number of sealed fractures
Vertical depth (m.b.s.l)
-20
-10
0
10
20
0
50
100
150
200
250
300
Number of fractures / 10m vertical depth

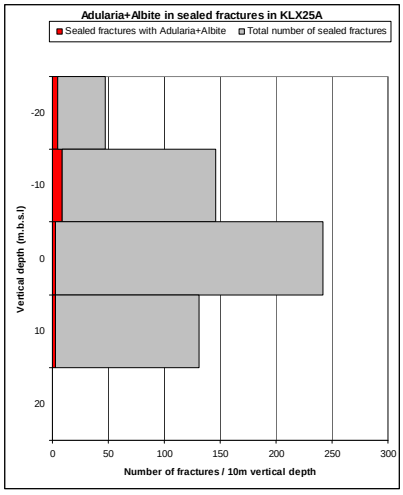
Adularia+Albite in sealed fractures in KLX25A
Sealed fractures with Adularia+Albite
Total number of sealed fractures
Vertical depth (m.b.s.l)
-20
-10
0
10
20
0
50
100
150
200
250
300
Number of fractures / 10m vertical depth

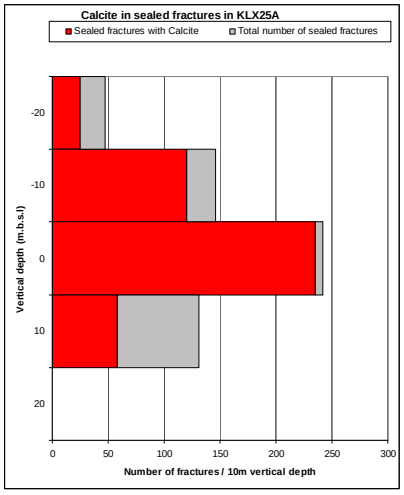
Calcite in sealed fractures in KLX25A
Sealed fractures with Calcite
Total number of sealed fractures
Vertical depth (m.b.s.l)
-20
-10
0
10
20
0
50
100
150
200
250
300
Number of fractures / 10m vertical depth

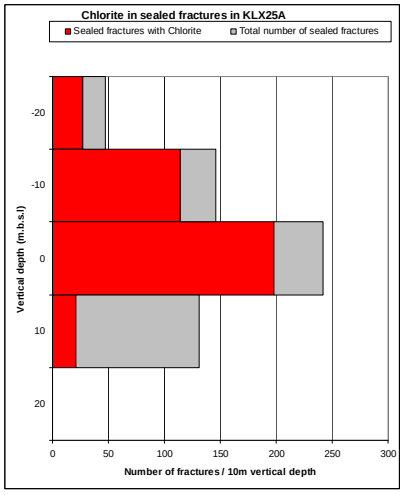
Chlorite in sealed fractures in KLX25A
Sealed fractures with Chlorite
Total number of sealed fractures
Vertical depth (m.b.s.l)
-20
-10
0
10
20
0
50
100
150
200
250
300
Number of fractures / 10m vertical depth

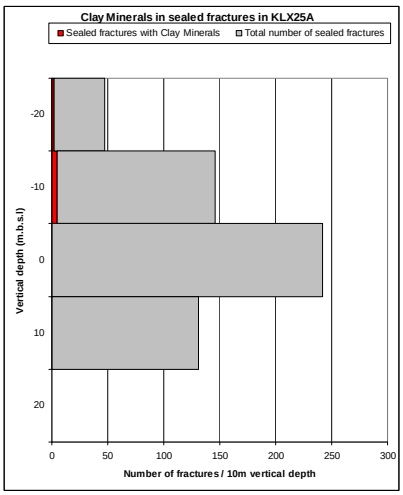
Clay Minerals in sealed fractures in KLX25A
Sealed fractures with Clay Minerals
Total number of sealed fractures
Vertical depth (m.b.s.l)
-20
-10
0
10
20
0
50
100
150
200
250
300
Number of fractures / 10m vertical depth

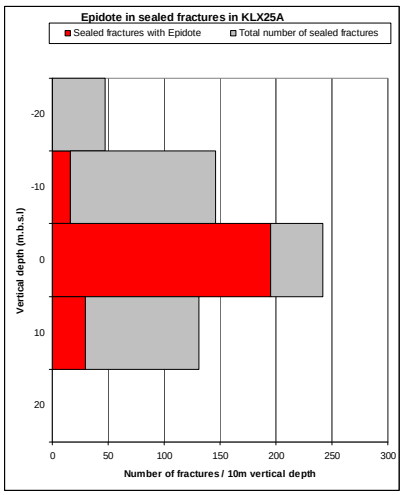
Epidote in sealed fractures in KLX25A
Sealed fractures with Epidote
Total number of sealed fractures
Vertical depth (m.b.s.l)
-20
-10
0
10
20
0
50
100
150
200
250
300
Number of fractures / 10m vertical depth

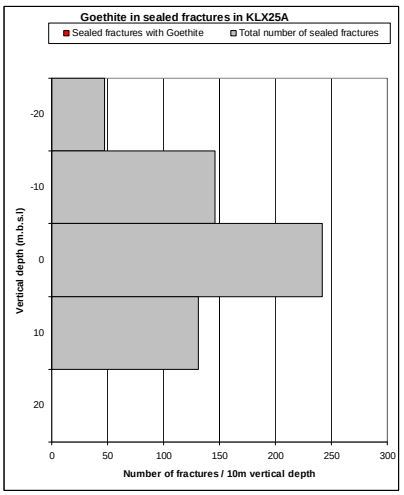
Goethite in sealed fractures in KLX25A
Sealed fractures with Goethite
Total number of sealed fractures
Vertical depth (m.b.s.l)
-20
-10
0
10
20
0
50
100
150
200
250
300
Number of fractures / 10m vertical depth

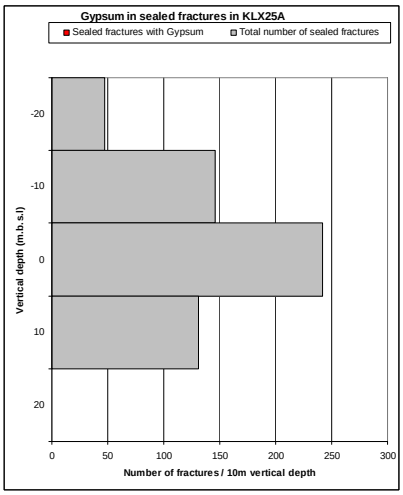
Gypsum in sealed fractures in KLX25A
Sealed fractures with Gypsum
Total number of sealed fractures
Vertical depth (m.b.s.l)
-20
-10
0
10
20
0
50
100
150
200
250
300
Number of fractures / 10m vertical depth

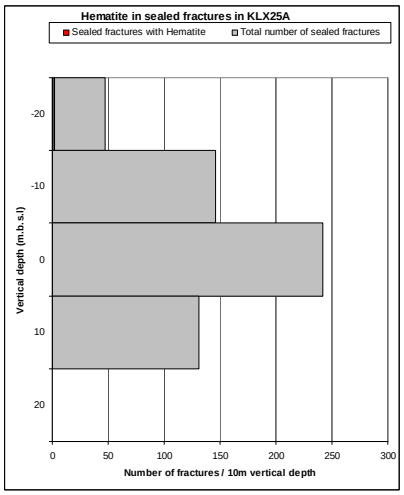
Hematite in sealed fractures in KLX25A
Sealed fractures with Hematite
Total number of sealed fractures
Vertical depth (m.b.s.l)
-20
-10
0
10
20
0
50
100
150
200
250
300
Number of fractures / 10m vertical depth

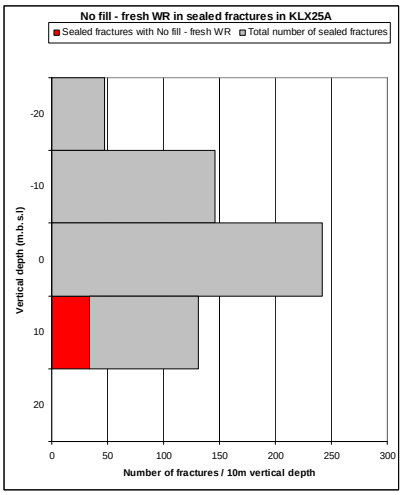
No fill - fresh WR in sealed fractures in KLX25A
Sealed fractures with No fill - fresh WR
Total number of sealed fractures
Vertical depth (m.b.s.l)
-20
-10
0
10
20
0
50
100
150
200
250
300
Number of fractures / 10m vertical depth

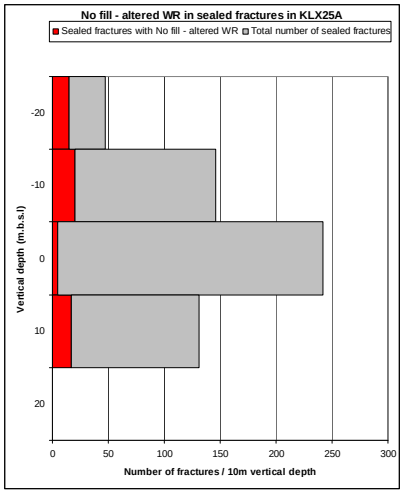
No fill - altered WR in sealed fractures in KLX25A
Sealed fractures with No fill - altered WR
Total number of sealed fractures
Vertical depth (m.b.s.l)
-20
-10
0
10
20
0
50
100
150
200
250
300
Number of fractures / 10m vertical depth

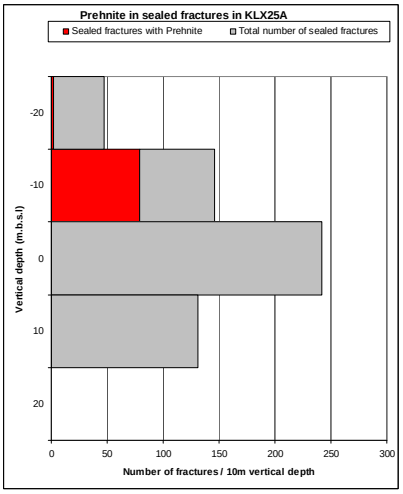
Prehnite in sealed fractures in KLX25A
Sealed fractures with Prehnite
Total number of sealed fractures
Vertical depth (m.b.s.l)
-20
-10
0
10
20
0
50
100
150
200
250
300
Number of fractures / 10m vertical depth

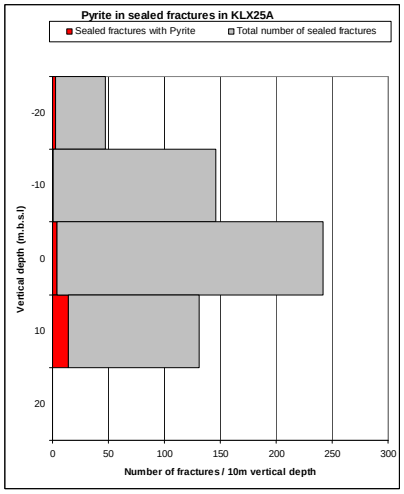
Pyrite in sealed fractures in KLX25A
Sealed fractures with Pyrite
Total number of sealed fractures
Vertical depth (m.b.s.l)
-20
-10
0
10
20
0
50
100
150
200
250
300
Number of fractures / 10m vertical depth

KLX26A

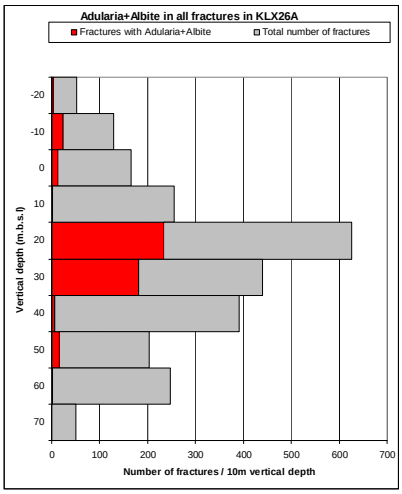
Adularia+Albite in all fractures in KLX26A
Fractures with Adularia+Albite
Total number of fractures
Vertical depth (m.b.s.l)
Number of fractures / 10m vertical depth

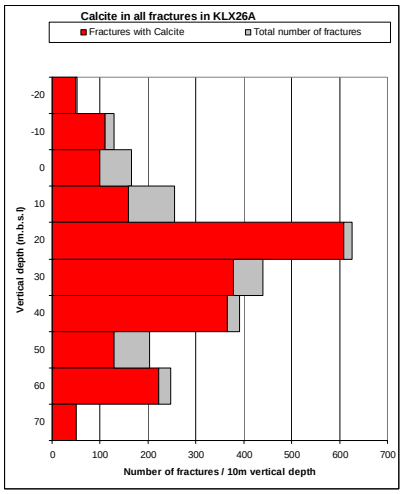
Calcite in all fractures in KLX26A
Fractures with Calcite
Total number of fractures
Vertical depth (m.b.s.l)
Number of fractures / 10m vertical depth

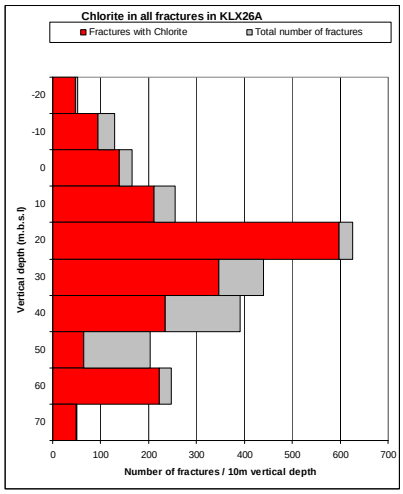
Chlorite in all fractures in KLX26A
Fractures with Chlorite
Total number of fractures
Vertical depth (m.b.s.l)
Number of fractures / 10m vertical depth

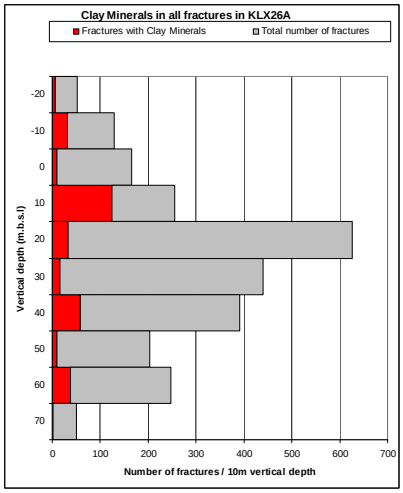
Clay Minerals in all fractures in KLX26A
Fractures with Clay Minerals
Total number of fractures
Vertical depth (m.b.s.l)
Number of fractures / 10m vertical depth

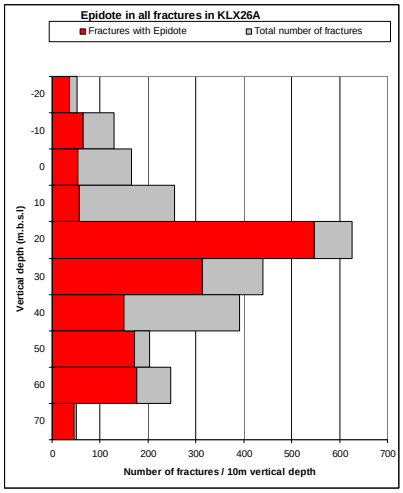
Epidote in all fractures in KLX26A
Fractures with Epidote
Total number of fractures
Vertical depth (m.b.s.l)
Number of fractures / 10m vertical depth

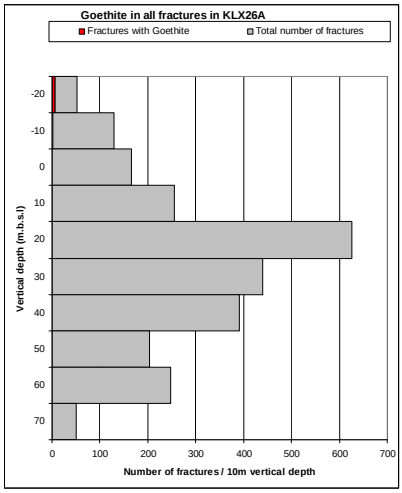
Goethite in all fractures in KLX26A
Fractures with Goethite
Total number of fractures
Vertical depth (m.b.s.l)
Number of fractures / 10m vertical depth

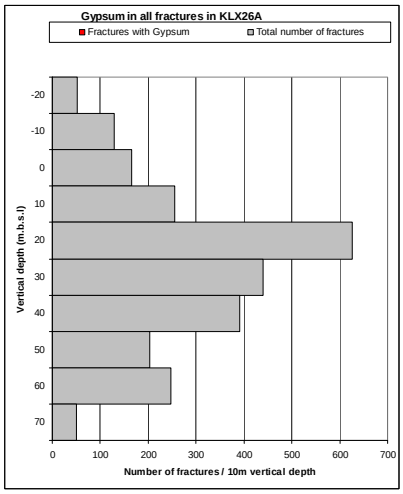
Gypsum in all fractures in KLX26A
Fractures with Gypsum
Total number of fractures
Vertical depth (m.b.s.l)
Number of fractures / 10m vertical depth

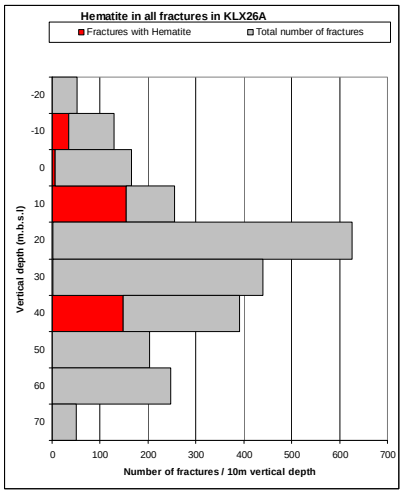
Hematite in all fractures in KLX26A
Fractures with Hematite
Total number of fractures
Vertical depth (m.b.s.l)
Number of fractures / 10m vertical depth

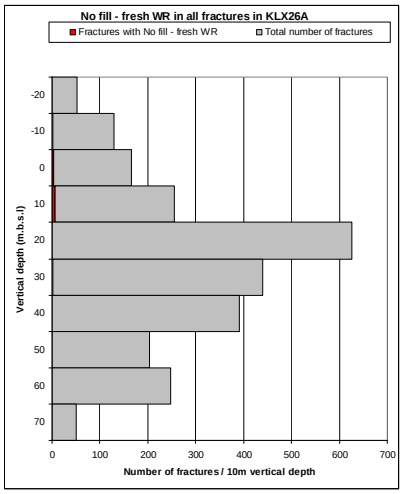
No fill - fresh WR in all fractures in KLX26A
Fractures with No fill - fresh WR
Total number of fractures
Vertical depth (m.b.s.l)
Number of fractures / 10m vertical depth

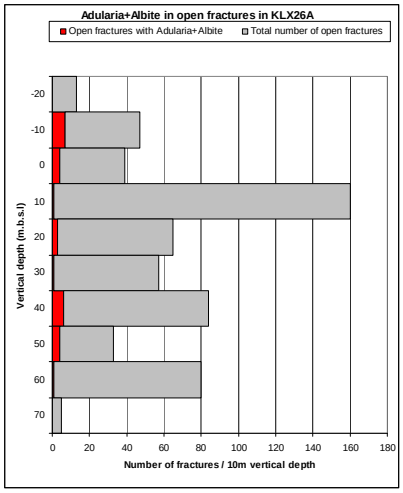
Adularia+Albite in open fractures in KLX26A
Open fractures with Adularia+Albite
Total number of open fractures
Vertical depth (m.b.s.l)
Number of fractures / 10m vertical depth

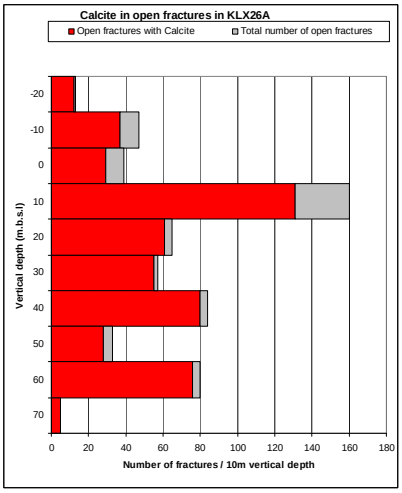
Calcite in open fractures in KLX26A
Open fractures with Calcite
Total number of open fractures
Vertical depth (m.b.s.l)
Number of fractures / 10m vertical depth

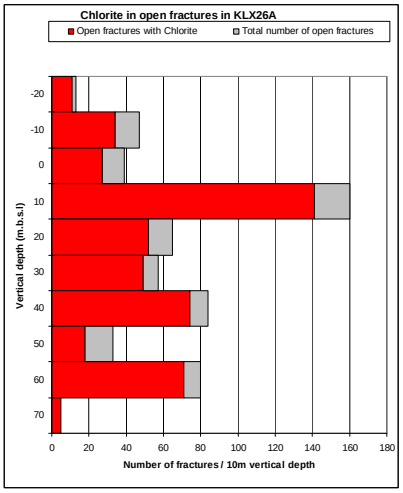
Chlorite in open fractures in KLX26A
Open fractures with Chlorite
Total number of open fractures
Vertical depth (m.b.s.l)
Number of fractures / 10m vertical depth

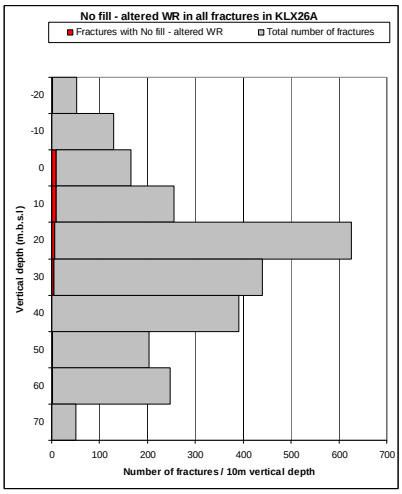
No fill - altered WR in all fractures in KLX26A
Fractures with No fill - altered WR
Total number of fractures
Vertical depth (m.b.s.l)
Number of fractures / 10m vertical depth

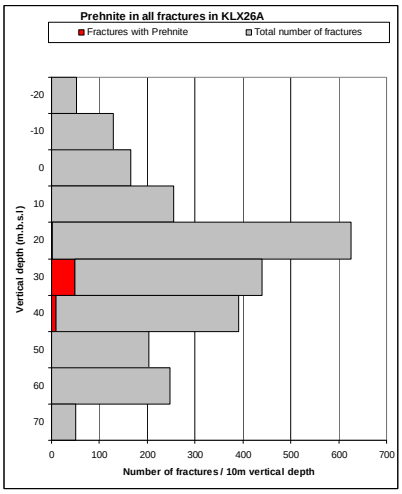
Prehnite in all fractures in KLX26A
Fractures with Prehnite
Total number of fractures
Vertical depth (m.b.s.l)
Number of fractures / 10m vertical depth

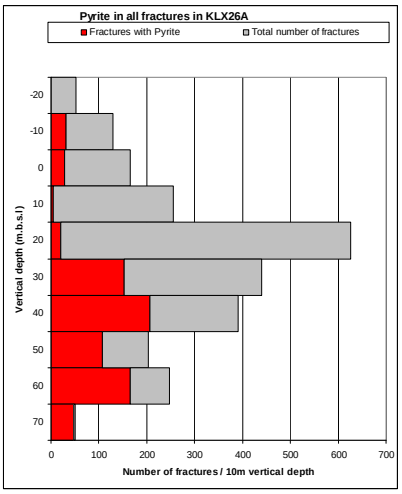
Pyrite in all fractures in KLX26A
Fractures with Pyrite
Total number of fractures
Vertical depth (m.b.s.l)
Number of fractures / 10m vertical depth

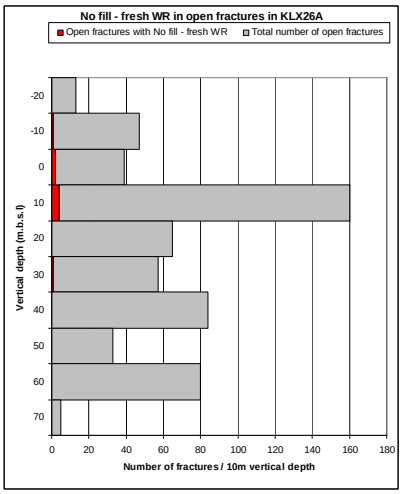
No fill - fresh WR in open fractures in KLX26A
Open fractures with No fill - fresh WR
Total number of open fractures
Vertical depth (m.b.s.l)
Number of fractures / 10m vertical depth

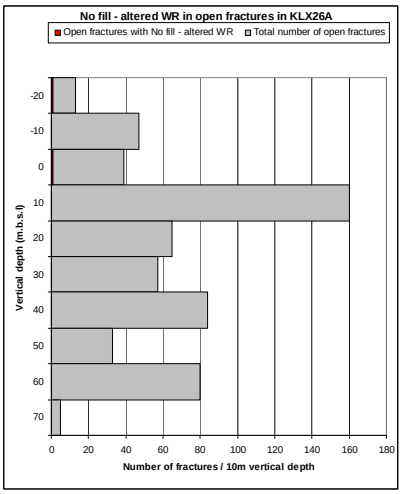
No fill - altered WR in open fractures in KLX26A
Open fractures with No fill - altered WR
Total number of open fractures
Vertical depth (m.b.s.l)
Number of fractures / 10m vertical depth

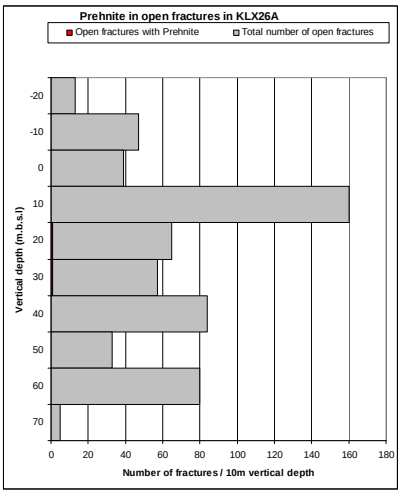
Prehnite in open fractures in KLX26A
Open fractures with Prehnite
Total number of open fractures
Vertical depth (m.b.s.l)
Number of fractures / 10m vertical depth

i

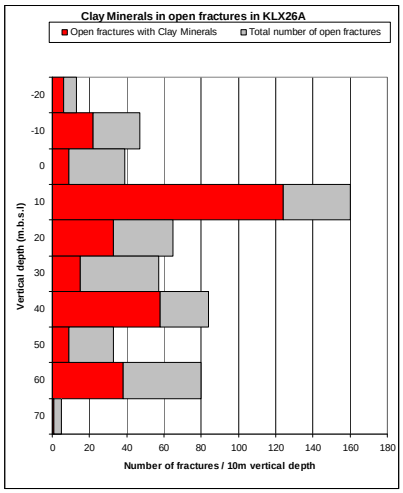
Clay Minerals in open fractures in KLX26A
Open fractures with Clay Minerals
Total number of open fractures
Vertical depth (m.b.s.l)
Number of fractures / 10m vertical depth

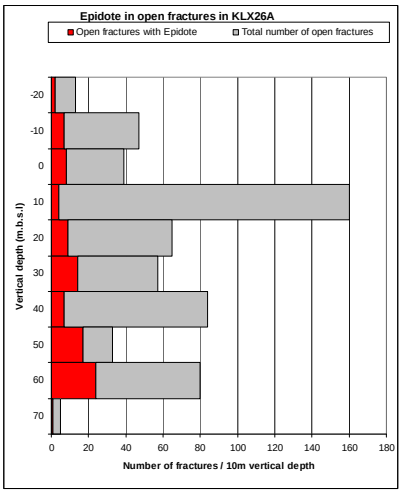
Epidote in open fractures in KLX26A
Open fractures with Epidote
Total number of open fractures
Vertical depth (m.b.s.l)
Number of fractures / 10m vertical depth

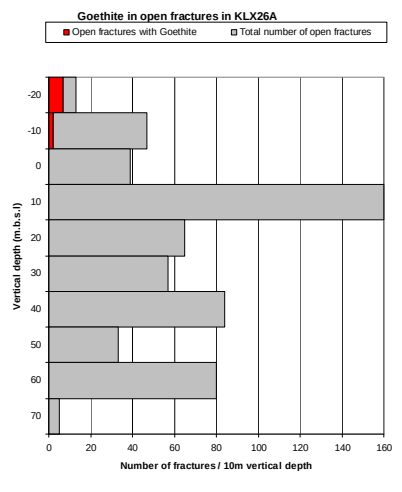
Goethite in open fractures in KLX26A
Open fractures with Goethite
Total number of open fractures
Vertical depth (m.b.s.l)
Number of fractures / 10m vertical depth

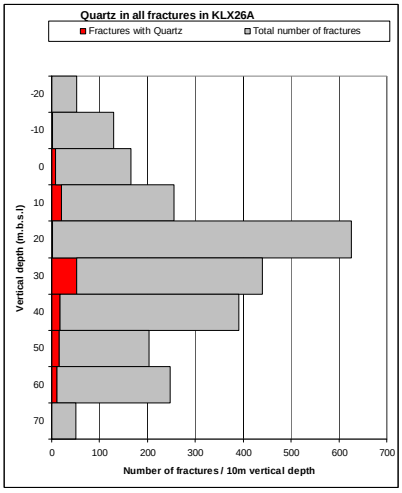
Quartz in all fractures in KLX26A
Fractures with Quartz
Total number of fractures
Vertical depth (m.b.s.l)
Number of fractures / 10m vertical depth

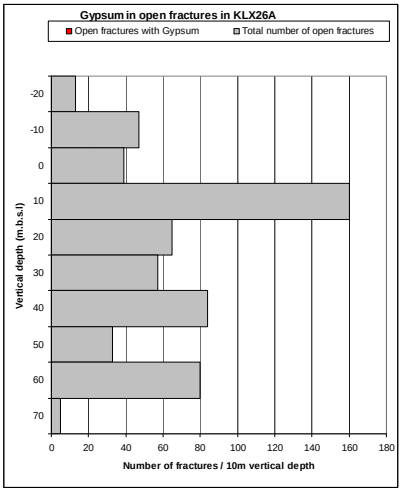
Gypsum in open fractures in KLX26A
Open fractures with Gypsum
Total number of open fractures
Vertical depth (m.b.s.l)
Number of fractures / 10m vertical depth

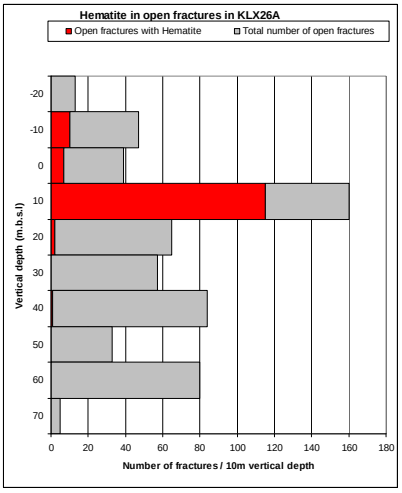
Hematite in open fractures in KLX26A
Open fractures with Hematite
Total number of open fractures
Vertical depth (m.b.s.l)
Number of fractures / 10m vertical depth

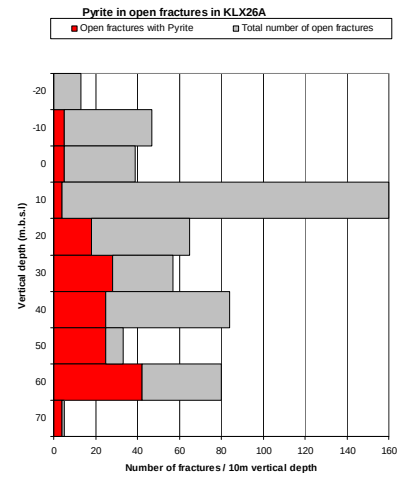
Pyrite in open fractures in KLX26A
Open fractures with Pyrite
Total number of open fractures
Vertical depth (m.b.s.l)
Number of fractures / 10m vertical depth

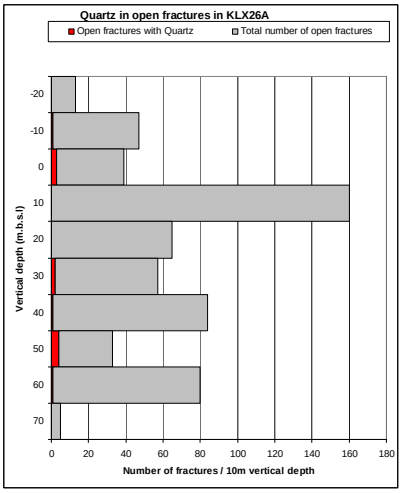
Quartz in open fractures in KLX26A
Open fractures with Quartz
Total number of open fractures
Vertical depth (m.b.s.l)
Number of fractures / 10m vertical depth

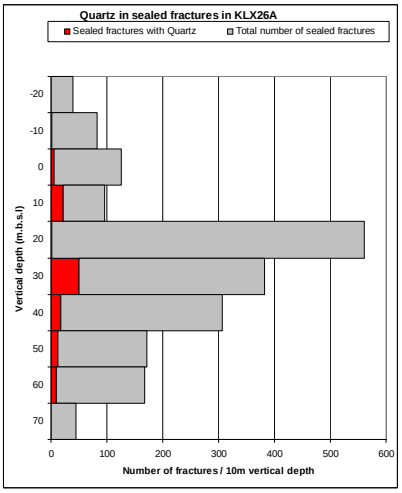
Quartz in sealed fractures in KLX26A
Sealed fractures with Quartz
Total number of sealed fractures
Vertical depth (m.b.s.l)
Number of fractures / 10m vertical depth

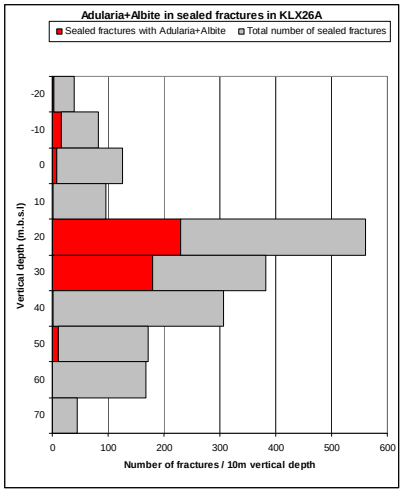
Adularia+Albite in sealed fractures in KLX26A
Sealed fractures with Adularia+Albite
Total number of sealed fractures
Vertical depth (m.b.s.l)
-20
-10
0
10
20
30
40
50
60
70
0
100
200
300
400
500
600
Number of fractures / 10m vertical depth

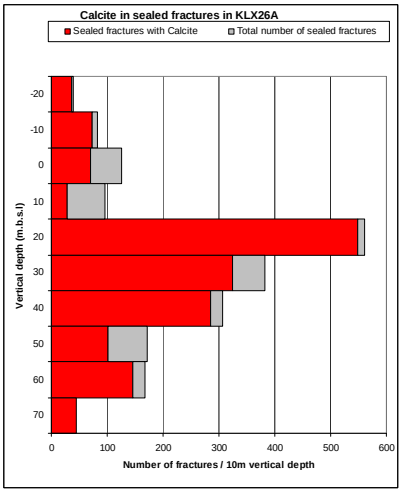
Calcite in sealed fractures in KLX26A
Sealed fractures with Calcite
Total number of sealed fractures
Vertical depth (m.b.s.l)
-20
-10
0
10
20
30
40
50
60
70
0
100
200
300
400
500
600
Number of fractures / 10m vertical depth

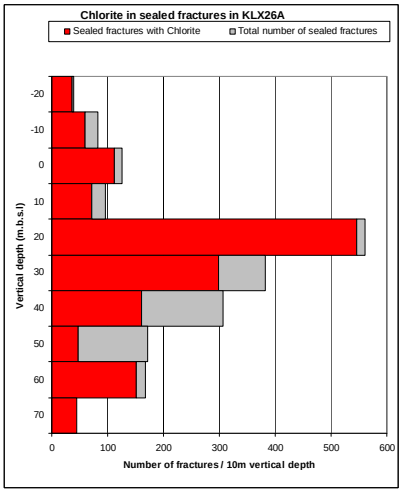
Chlorite in sealed fractures in KLX26A
Sealed fractures with Chlorite
Total number of sealed fractures
Vertical depth (m.b.s.l)
-20
-10
0
10
20
30
40
50
60
70
0
100
200
300
400
500
600
Number of fractures / 10m vertical depth

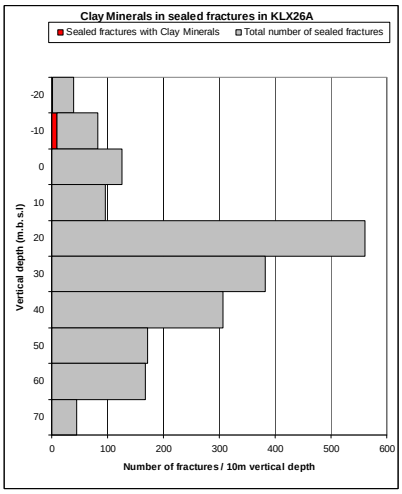
Clay Minerals in sealed fractures in KLX26A
Sealed fractures with Clay Minerals
Total number of sealed fractures
Vertical depth (m.b.s.l)
-20
-10
0
10
20
30
40
50
60
70
0
100
200
300
400
500
600
Number of fractures / 10m vertical depth

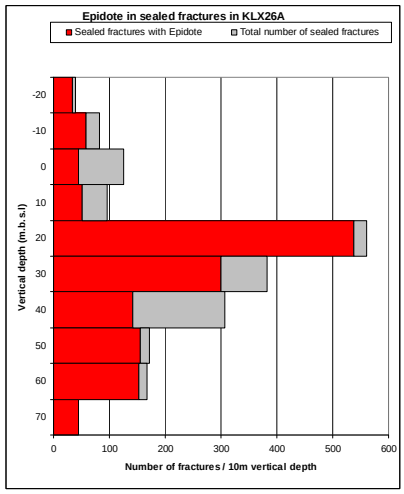
Epidote in sealed fractures in KLX26A
Sealed fractures with Epidote
Total number of sealed fractures
Vertical depth (m.b.s.l)
-20
-10
0
10
20
30
40
50
60
70
0
100
200
300
400
500
600
Number of fractures / 10m vertical depth

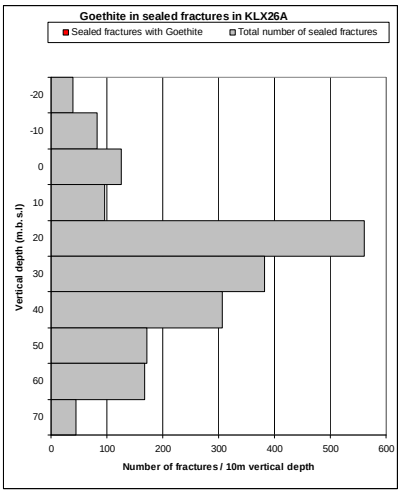
Goethite in sealed fractures in KLX26A
Sealed fractures with Goethite
Total number of sealed fractures
Vertical depth (m.b.s.l)
-20
-10
0
10
20
30
40
50
60
70
0
100
200
300
400
500
600
Number of fractures / 10m vertical depth

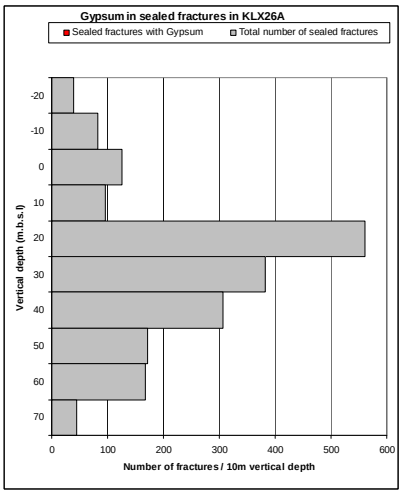
Gypsum in sealed fractures in KLX26A
Sealed fractures with Gypsum
Total number of sealed fractures
Vertical depth (m.b.s.l)
-20
-10
0
10
20
30
40
50
60
70
0
100
200
300
400
500
600
Number of fractures / 10m vertical depth

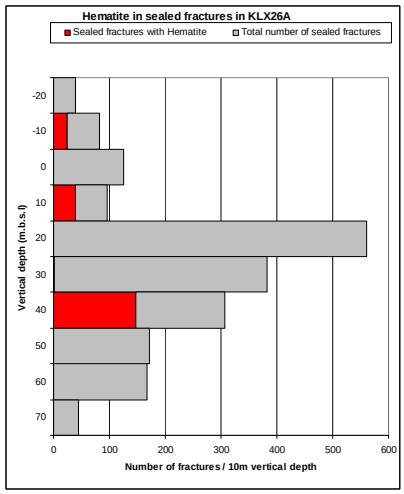
Hematite in sealed fractures in KLX26A
Sealed fractures with Hematite
Total number of sealed fractures
Vertical depth (m.b.s.l)
-20
-10
0
10
20
30
40
50
60
70
0
100
200
300
400
500
600
Number of fractures / 10m vertical depth

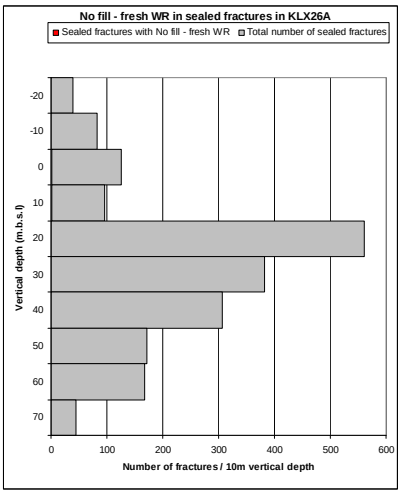
No fill - fresh WR in sealed fractures in KLX26A
Sealed fractures with No fill - fresh WR
Total number of sealed fractures
Vertical depth (m.b.s.l)
-20
-10
0
10
20
30
40
50
60
70
0
100
200
300
400
500
600
Number of fractures / 10m vertical depth

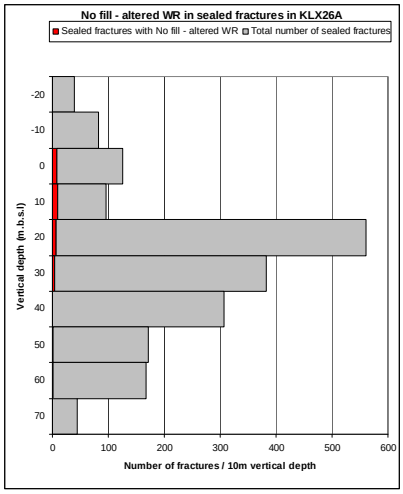
No fill - altered WR in sealed fractures in KLX26A
Sealed fractures with No fill - altered WR
Total number of sealed fractures
Vertical depth (m.b.s.l)
-20
-10
0
10
20
30
40
50
60
70
0
100
200
300
400
500
600
Number of fractures / 10m vertical depth

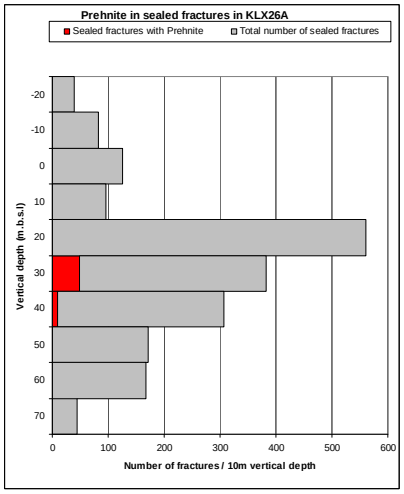
Prehnite in sealed fractures in KLX26A
Sealed fractures with Prehnite
Total number of sealed fractures
Vertical depth (m.b.s.l)
-20
-10
0
10
20
30
40
50
60
70
0
100
200
300
400
500
600
Number of fractures / 10m vertical depth

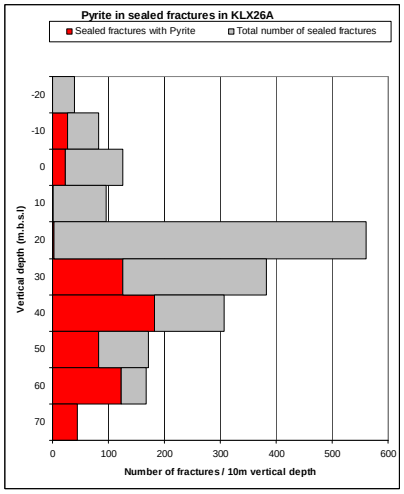
Pyrite in sealed fractures in KLX26A
Sealed fractures with Pyrite
Total number of sealed fractures
Vertical depth (m.b.s.l)
-20
-10
0
10
20
30
40
50
60
70
0
100
200
300
400
500
600
Number of fractures / 10m vertical depth

KLX26B

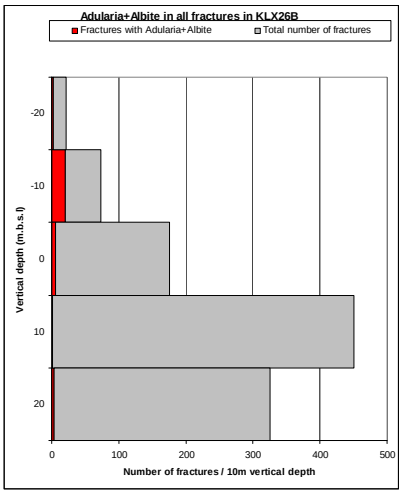
Adularia+Albite in all fractures in KLX26B
Fractures with Adularia+Albite
Total number of fractures
Vertical depth (m.b.s.l)
Number of fractures / 10m vertical depth

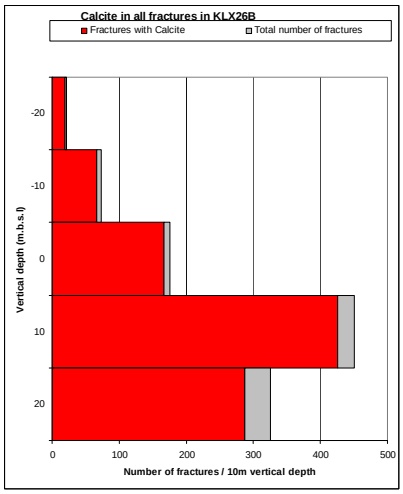
Calcite in all fractures in KLX26B
Fractures with Calcite
Total number of fractures
Vertical depth (m.b.s.l)
Number of fractures / 10m vertical depth

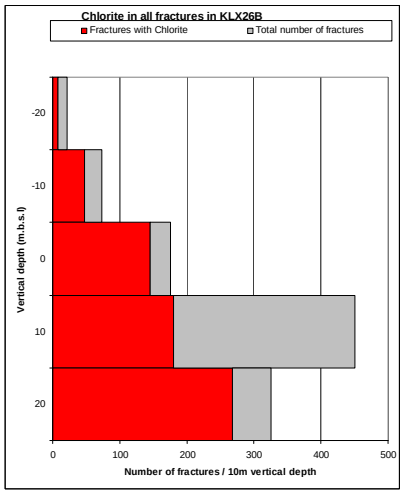
Chlorite in all fractures in KLX26B
Fractures with Chlorite
Total number of fractures
Vertical depth (m.b.s.l)
Number of fractures / 10m vertical depth

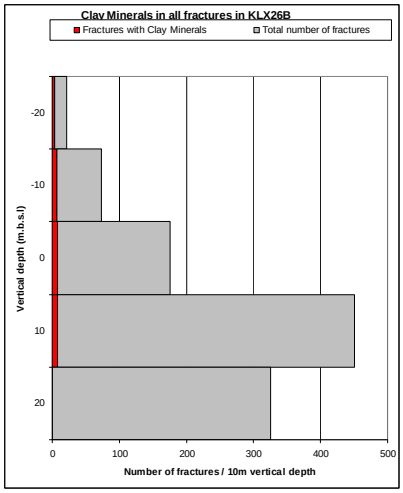
Clay Minerals in all fractures in KLX26B
Fractures with Clay Minerals
Total number of fractures
Vertical depth (m.b.s.l)
Number of fractures / 10m vertical depth

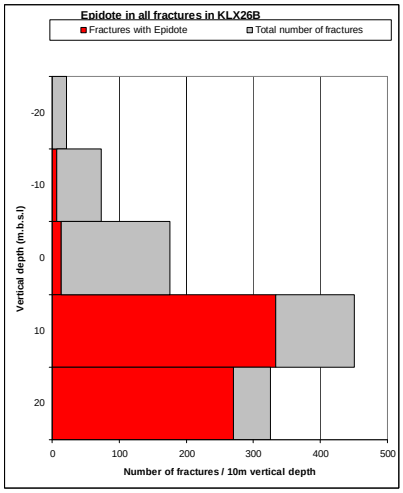
Epidote in all fractures in KLX26B
Fractures with Epidote
Total number of fractures
Vertical depth (m.b.s.l)
Number of fractures / 10m vertical depth

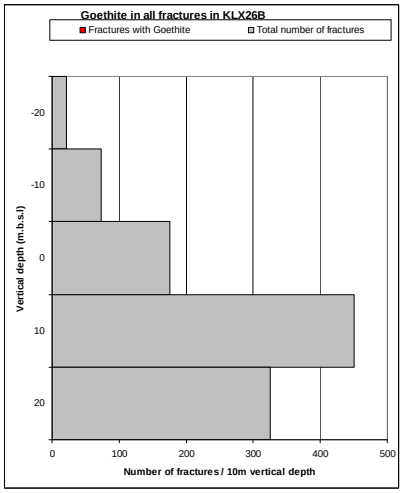
Goethite in all fractures in KLX26B
Fractures with Goethite
Total number of fractures
Vertical depth (m.b.s.l)
Number of fractures / 10m vertical depth

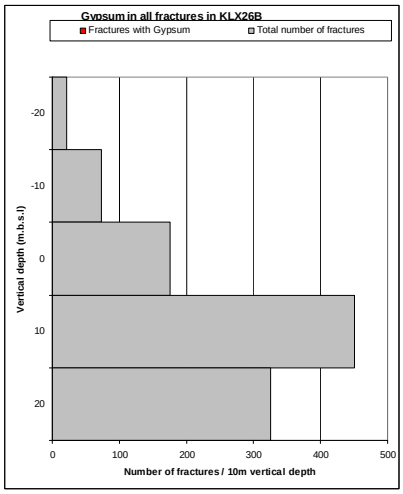
Gypsum in all fractures in KLX26B
Fractures with Gypsum
Total number of fractures
Vertical depth (m.b.s.l)
Number of fractures / 10m vertical depth

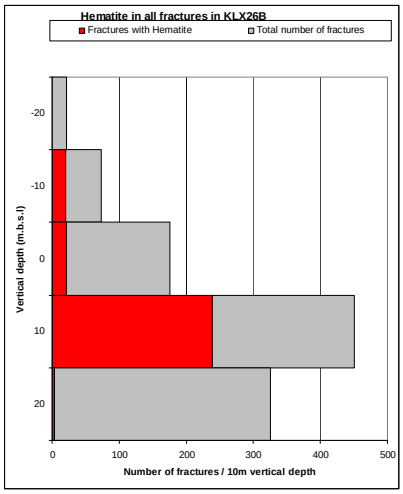
Hematite in all fractures in KLX26B
Fractures with Hematite
Total number of fractures
Vertical depth (m.b.s.l)
Number of fractures / 10m vertical depth

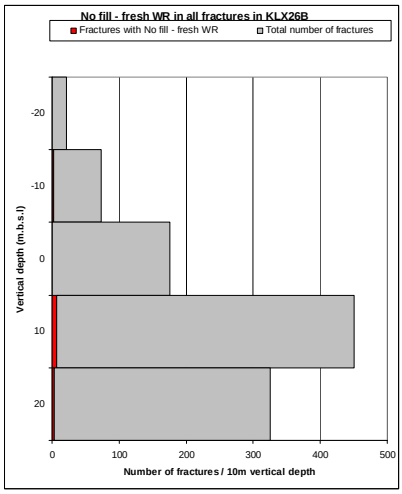
No fill - fresh WR in all fractures in KLX26B
Fractures with No fill - fresh WR
Total number of fractures
Vertical depth (m.b.s.l)
Number of fractures / 10m vertical depth

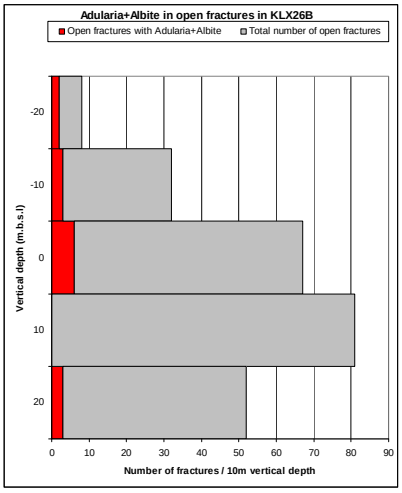
Adularia+Albite in open fractures in KLX26B
Open fractures with Adularia+Albite
Total number of open fractures
Vertical depth (m.b.s.l)
-20
-10
0
10
20
0
10
20
30
40
50
60
70
80
90
Number of fractures / 10m vertical depth

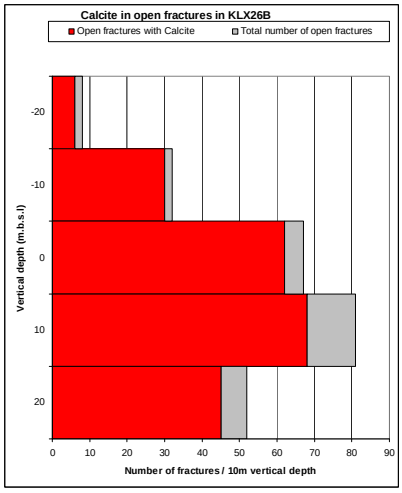
Calcite in open fractures in KLX26B
Open fractures with Calcite
Total number of open fractures
Vertical depth (m.b.s.l)
-20
-10
0
10
20
0
10
20
30
40
50
60
70
80
90
Number of fractures / 10m vertical depth

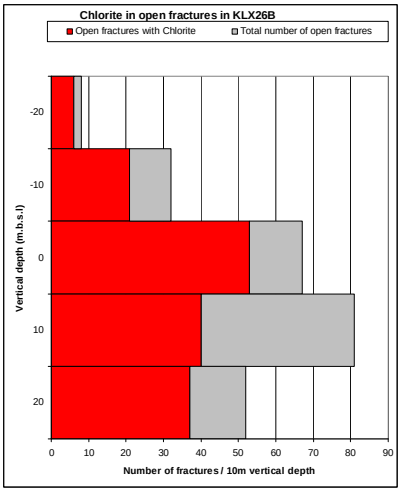
Chlorite in open fractures in KLX26B
Open fractures with Chlorite
Total number of open fractures
Vertical depth (m.b.s.l)
-20
-10
0
10
20
0
10
20
30
40
50
60
70
80
90
Number of fractures / 10m vertical depth

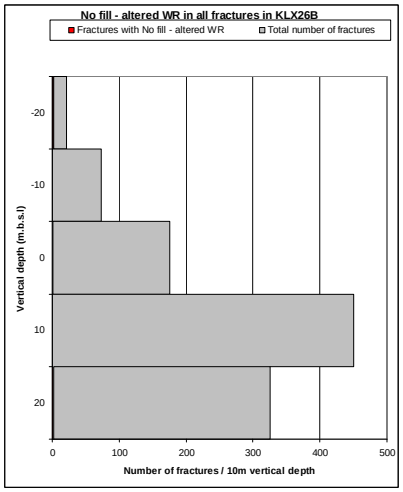
No fill - altered WR in all fractures in KLX26B
Fractures with No fill - altered WR
Total number of fractures
Vertical depth (m.b.s.l)
-20
-10
0
10
20
0
100
200
300
400
500
Number of fractures / 10m vertical depth

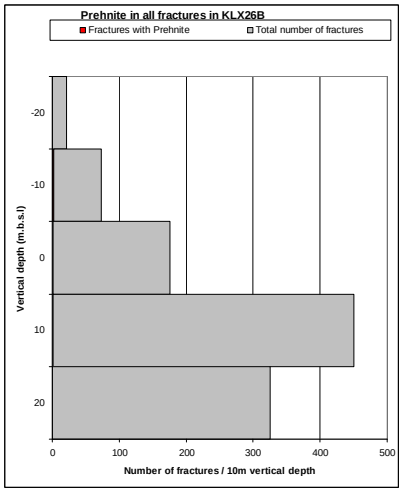
Prehnite in all fractures in KLX26B
Fractures with Prehnite
Total number of fractures
Vertical depth (m.b.s.l)
-20
-10
0
10
20
0
100
200
300
400
500
Number of fractures / 10m vertical depth

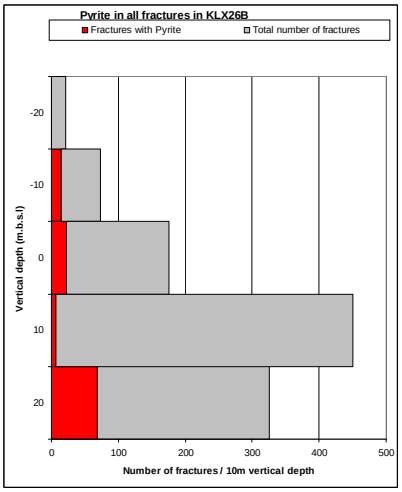
Pyrite in all fractures in KLX26B
Fractures with Pyrite
Total number of fractures
Vertical depth (m.b.s.l)
-20
-10
0
10
20
0
100
200
300
400
500
Number of fractures / 10m vertical depth

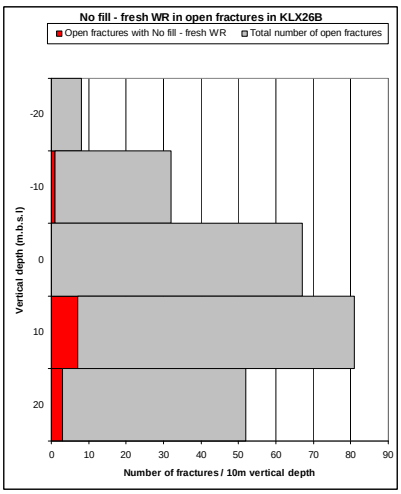
No fill - fresh WR in open fractures in KLX26B
Open fractures with No fill - fresh WR
Total number of open fractures
Vertical depth (m.b.s.l)
-20
-10
0
10
20
0
10
20
30
40
50
60
70
80
90
Number of fractures / 10m vertical depth

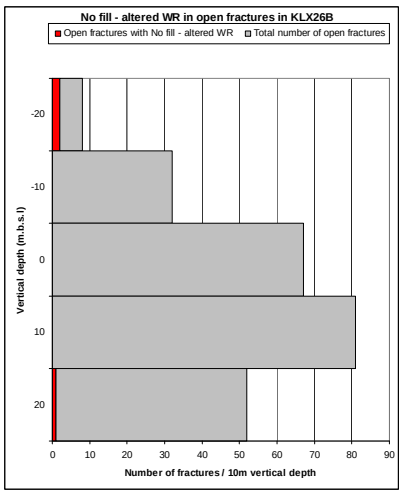
No fill - altered WR in open fractures in KLX26B
Open fractures with No fill - altered WR
Total number of open fractures
Vertical depth (m.b.s.l)
-20
-10
0
10
20
0
10
20
30
40
50
60
70
80
90
Number of fractures / 10m vertical depth

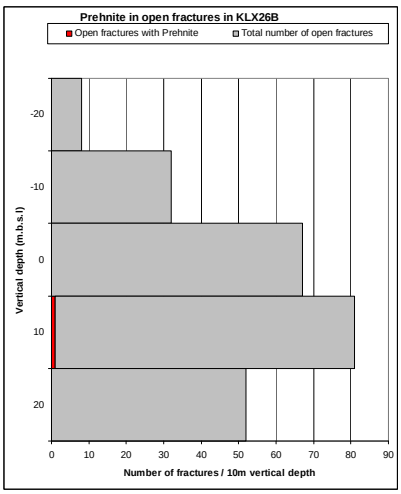
Prehnite in open fractures in KLX26B
Open fractures with Prehnite
Total number of open fractures
Vertical depth (m.b.s.l)
-20
-10
0
10
20
0
10
20
30
40
50
60
70
80
90
Number of fractures / 10m vertical depth

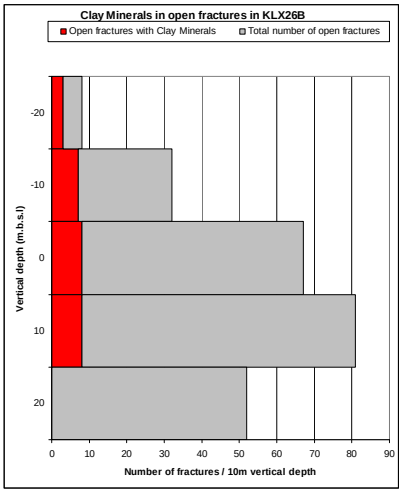
Clay Minerals in open fractures in KLX26B
Open fractures with Clay Minerals
Total number of open fractures
Vertical depth (m.b.s.l)
Number of fractures / 10m vertical depth

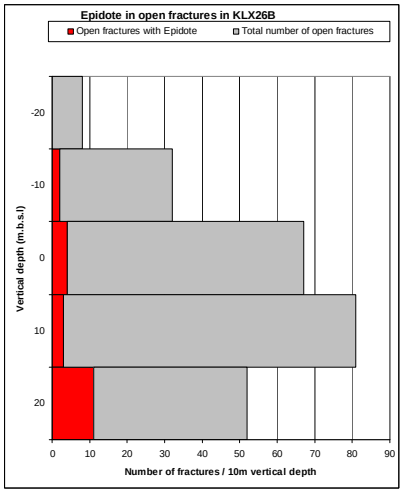
Epidote in open fractures in KLX26B
Open fractures with Epidote
Total number of open fractures
Vertical depth (m.b.s.l)
Number of fractures / 10m vertical depth

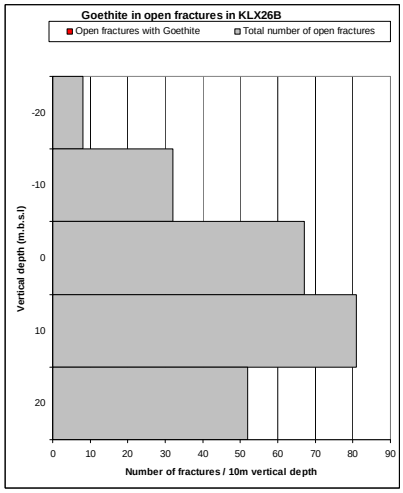
Goethite in open fractures in KLX26B
Open fractures with Goethite
Total number of open fractures
Vertical depth (m.b.s.l)
Number of fractures / 10m vertical depth

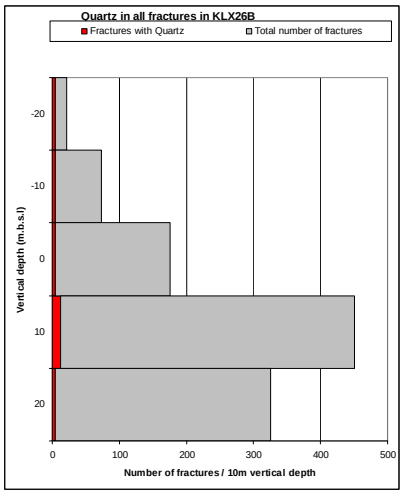
Quartz in all fractures in KLX26B
Fractures with Quartz
Total number of fractures
Vertical depth (m.b.s.l)
Number of fractures / 10m vertical depth

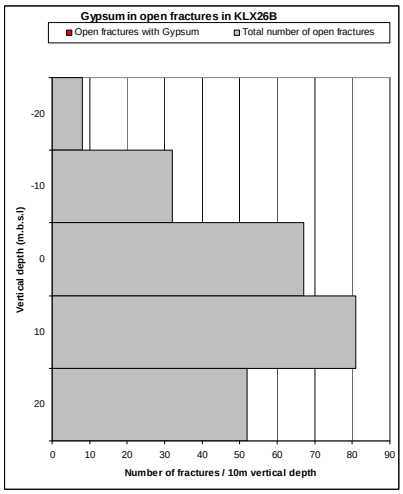
Gypsum in open fractures in KLX26B
Open fractures with Gypsum
Total number of open fractures
Vertical depth (m.b.s.l)
Number of fractures / 10m vertical depth

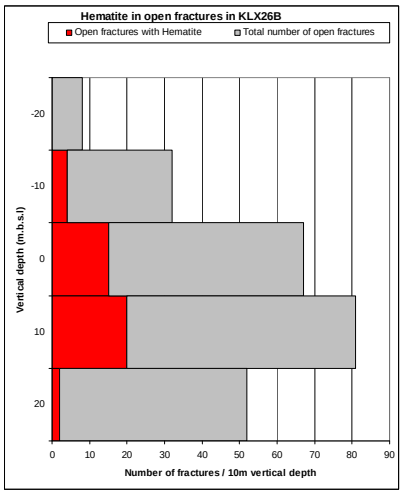
Hematite in open fractures in KLX26B
Open fractures with Hematite
Total number of open fractures
Vertical depth (m.b.s.l)
Number of fractures / 10m vertical depth

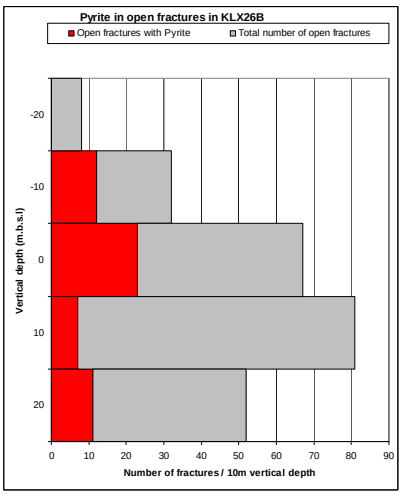
Pyrite in open fractures in KLX26B
Open fractures with Pyrite
Total number of open fractures
Vertical depth (m.b.s.l)
Number of fractures / 10m vertical depth

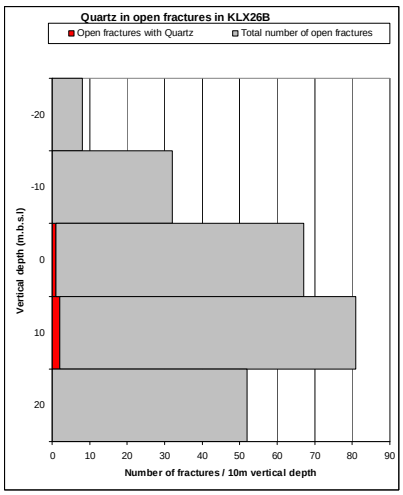
Quartz in open fractures in KLX26B
Open fractures with Quartz
Total number of open fractures
Vertical depth (m.b.s.l)
Number of fractures / 10m vertical depth

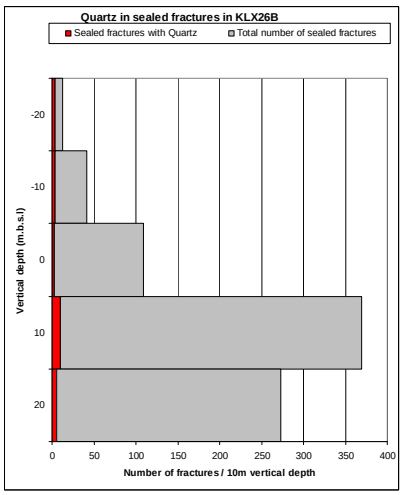
Quartz in sealed fractures in KLX26B
Sealed fractures with Quartz
Total number of sealed fractures
Vertical depth (m.b.s.l)
Number of fractures / 10m vertical depth

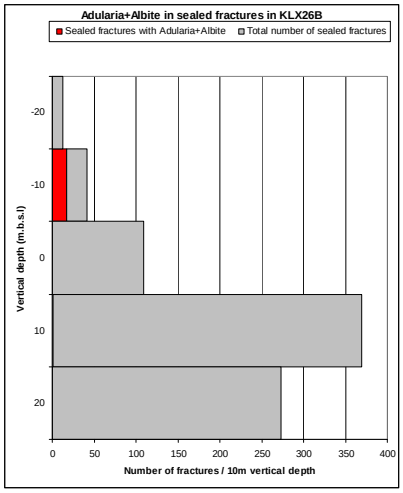
Adularia+Albite in sealed fractures in KLX26B
Sealed fractures with Adularia+Albite
Total number of sealed fractures
Vertical depth (m.b.s.l)
-20
-10
0
10
20
0
50
100
150
200
250
300
350
400
Number of fractures / 10m vertical depth

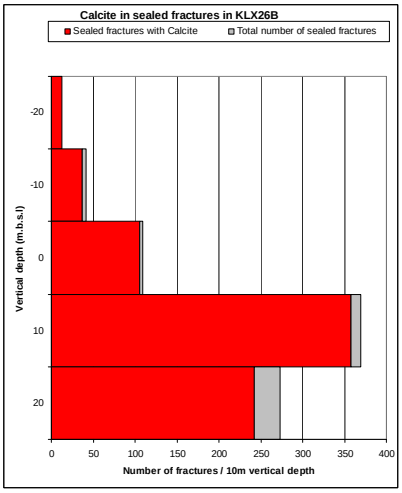
Calcite in sealed fractures in KLX26B
Sealed fractures with Calcite
Total number of sealed fractures
Vertical depth (m.b.s.l)
-20
-10
0
10
20
0
50
100
150
200
250
300
350
400
Number of fractures / 10m vertical depth

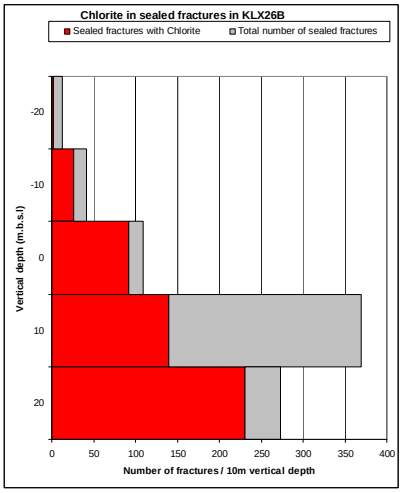
Chlorite in sealed fractures in KLX26B
Sealed fractures with Chlorite
Total number of sealed fractures
Vertical depth (m.b.s.l)
-20
-10
0
10
20
0
50
100
150
200
250
300
350
400
Number of fractures / 10m vertical depth

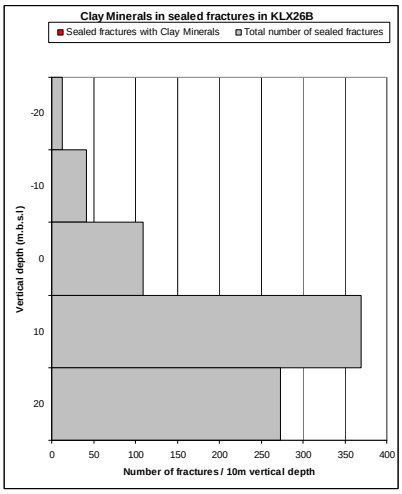
Clay Minerals in sealed fractures in KLX26B
Sealed fractures with Clay Minerals
Total number of sealed fractures
Vertical depth (m.b.s.l)
-20
-10
0
10
20
0
50
100
150
200
250
300
350
400
Number of fractures / 10m vertical depth

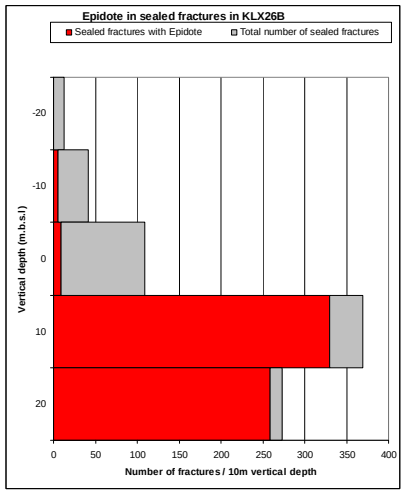
Epidote in sealed fractures in KLX26B
Sealed fractures with Epidote
Total number of sealed fractures
Vertical depth (m.b.s.l)
-20
-10
0
10
20
0
50
100
150
200
250
300
350
400
Number of fractures / 10m vertical depth

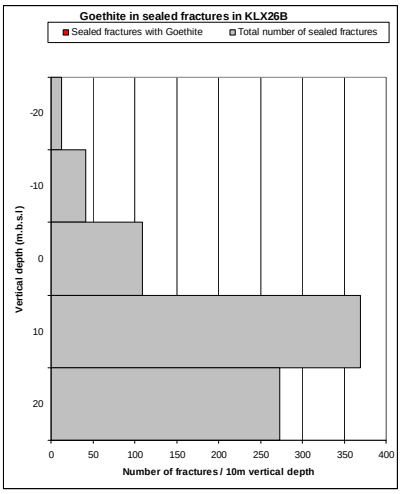
Goethite in sealed fractures in KLX26B
Sealed fractures with Goethite
Total number of sealed fractures
Vertical depth (m.b.s.l)
-20
-10
0
10
20
0
50
100
150
200
250
300
350
400
Number of fractures / 10m vertical depth

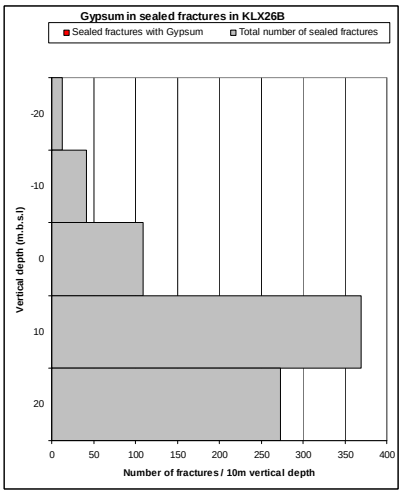
Gypsum in sealed fractures in KLX26B
Sealed fractures with Gypsum
Total number of sealed fractures
Vertical depth (m.b.s.l)
-20
-10
0
10
20
0
50
100
150
200
250
300
350
400
Number of fractures / 10m vertical depth

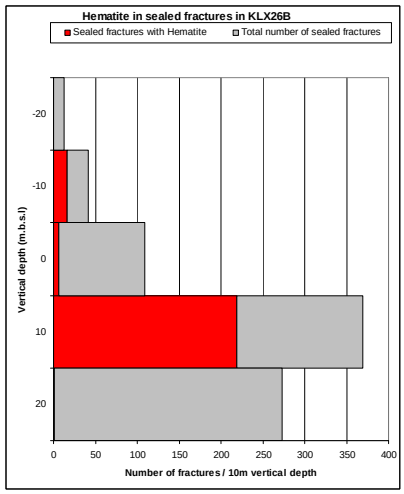
Hematite in sealed fractures in KLX26B
Sealed fractures with Hematite
Total number of sealed fractures
Vertical depth (m.b.s.l)
-20
-10
0
10
20
0
50
100
150
200
250
300
350
400
Number of fractures / 10m vertical depth

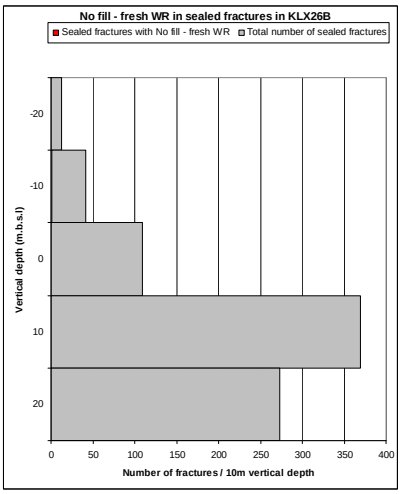
No fill - fresh WR in sealed fractures in KLX26B
Sealed fractures with No fill - fresh WR
Total number of sealed fractures
Vertical depth (m.b.s.l)
-20
-10
0
10
20
0
50
100
150
200
250
300
350
400
Number of fractures / 10m vertical depth

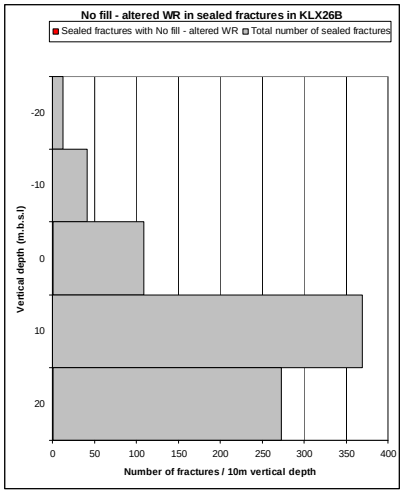
No fill - altered WR in sealed fractures in KLX26B
Sealed fractures with No fill - altered WR
Total number of sealed fractures
Vertical depth (m.b.s.l)
-20
-10
0
10
20
0
50
100
150
200
250
300
350
400
Number of fractures / 10m vertical depth

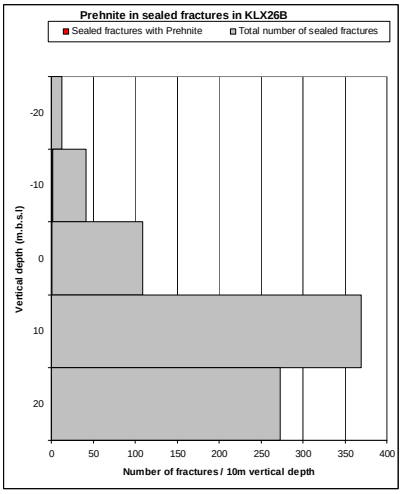
Prehnite in sealed fractures in KLX26B
Sealed fractures with Prehnite
Total number of sealed fractures
Vertical depth (m.b.s.l)
-20
-10
0
10
20
0
50
100
150
200
250
300
350
400
Number of fractures / 10m vertical depth

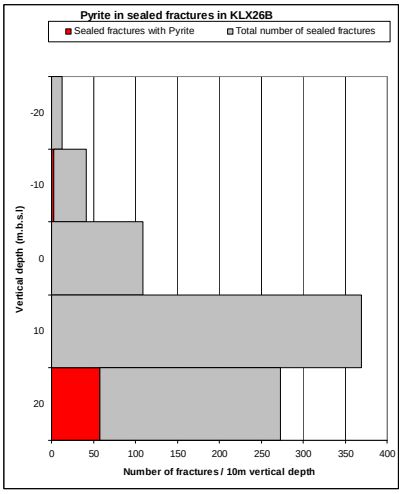
Pyrite in sealed fractures in KLX26B
Sealed fractures with Pyrite
Total number of sealed fractures
Vertical depth (m.b.s.l)
-20
-10
0
10
20
0
50
100
150
200
250
300
350
400
Number of fractures / 10m vertical depth

KLX27A

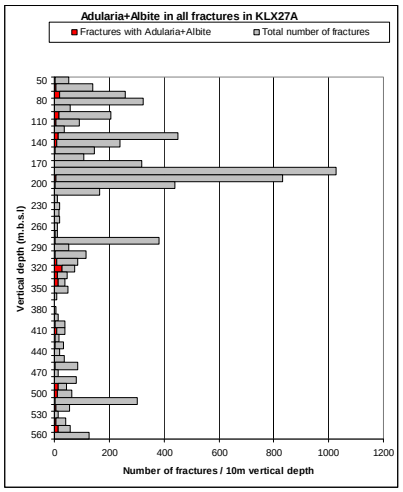
Adularia+Albite in all fractures in KLX27A
Fractures with Adularia+Albite
Total number of fractures
Vertical depth (m.b.s.l)
Number of fractures / 10m vertical depth

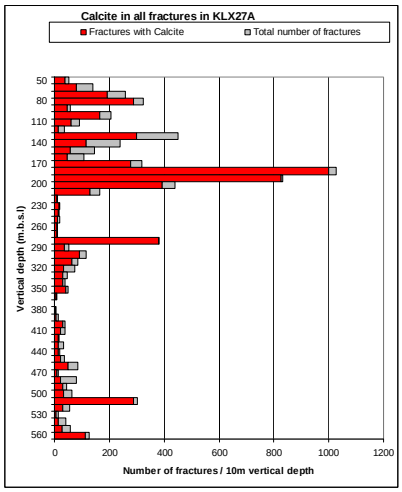
Calcite in all fractures in KLX27A
Fractures with Calcite
Total number of fractures
Vertical depth (m.b.s.l)
Number of fractures / 10m vertical depth

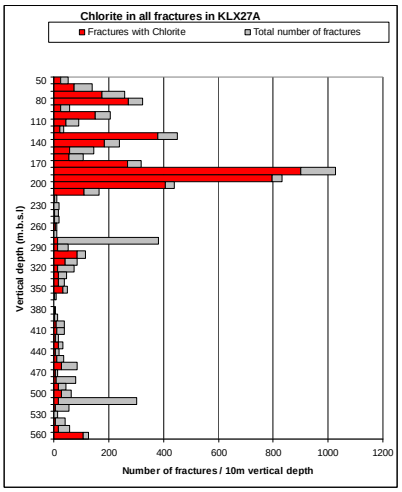
Chlorite in all fractures in KLX27A
Fractures with Chlorite
Total number of fractures
Vertical depth (m.b.s.l)
Number of fractures / 10m vertical depth

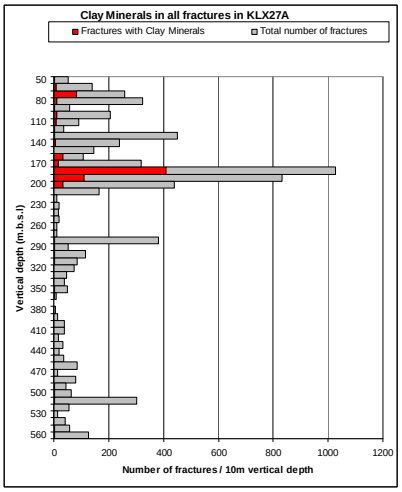
Clay Minerals in all fractures in KLX27A
Fractures with Clay Minerals
Total number of fractures
Vertical depth (m.b.s.l)
Number of fractures / 10m vertical depth

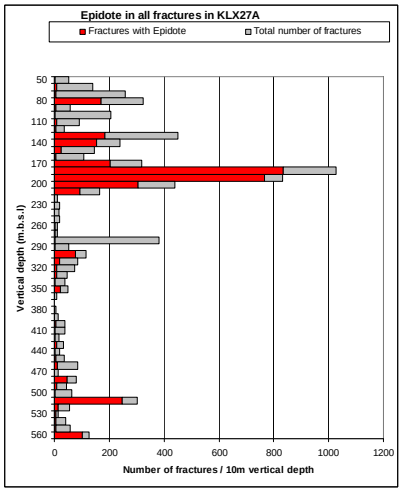
Epidote in all fractures in KLX27A
Fractures with Epidote
Total number of fractures
Vertical depth (m.b.s.l)
Number of fractures / 10m vertical depth

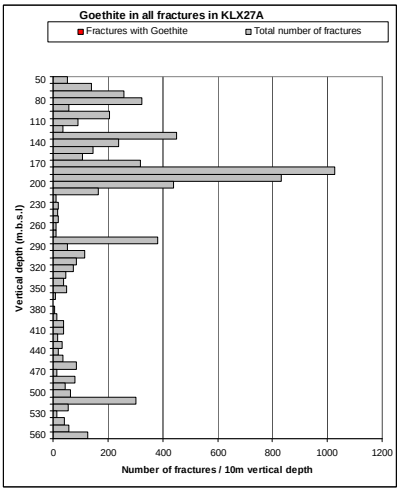
Goethite in all fractures in KLX27A
Fractures with Goethite
Total number of fractures
Vertical depth (m.b.s.l)
Number of fractures / 10m vertical depth

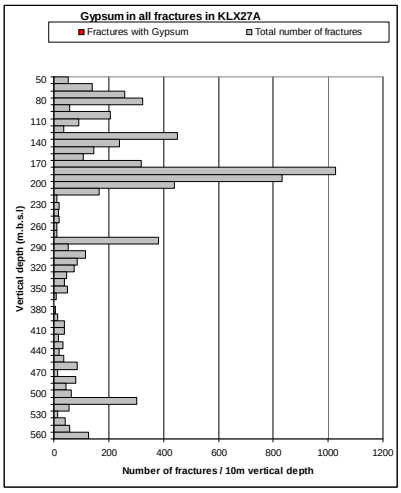
Gypsum in all fractures in KLX27A
Fractures with Gypsum
Total number of fractures
Vertical depth (m.b.s.l)
Number of fractures / 10m vertical depth

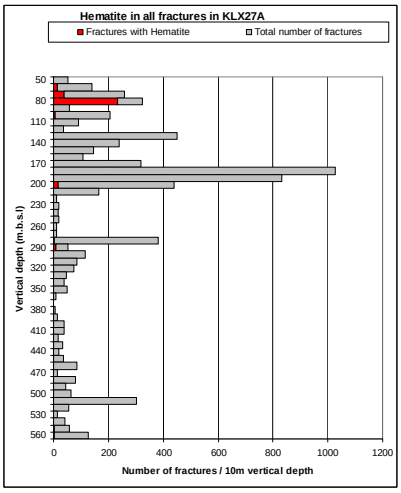
Hematite in all fractures in KLX27A
Fractures with Hematite
Total number of fractures
Vertical depth (m.b.s.l)
Number of fractures / 10m vertical depth

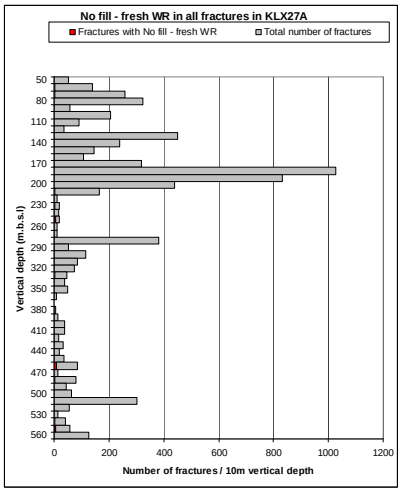
No fill - fresh WR in all fractures in KLX27A
Fractures with No fill - fresh WR
Total number of fractures
Vertical depth (m.b.s.l)
Number of fractures / 10m vertical depth

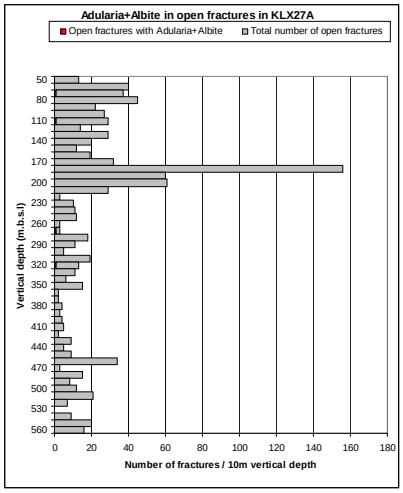
Adularia+Albite in open fractures in KLX27A
Open fractures with Adularia+Albite
Total number of open fractures
Vertical depth (m.b.s.l)
Number of fractures / 10m vertical depth

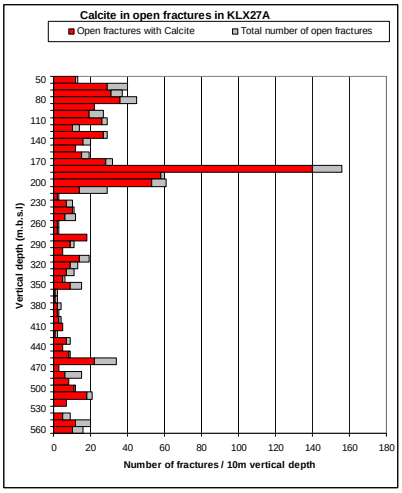
Calcite in open fractures in KLX27A
Open fractures with Calcite
Total number of open fractures
Vertical depth (m.b.s.l)
Number of fractures / 10m vertical depth

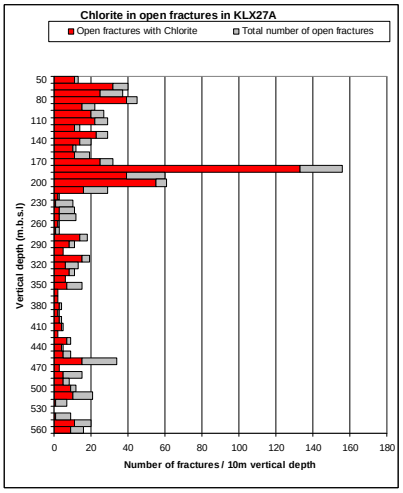
Chlorite in open fractures in KLX27A
Open fractures with Chlorite
Total number of open fractures
Vertical depth (m.b.s.l)
Number of fractures / 10m vertical depth

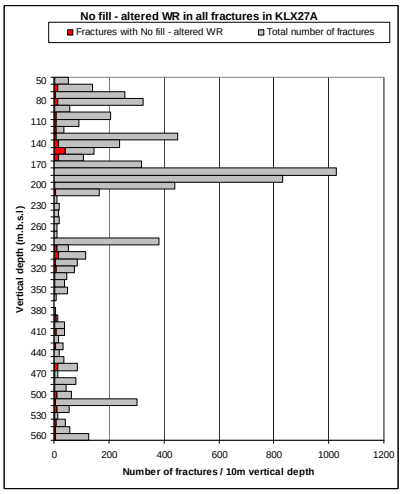
No fill - altered WR in all fractures in KLX27A
Fractures with No fill - altered WR
Total number of fractures
Vertical depth (m.b.s.l)
Number of fractures / 10m vertical depth

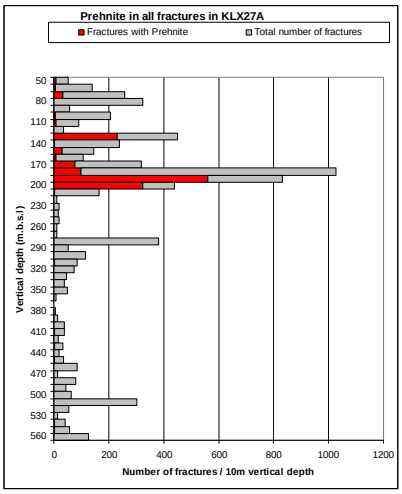
Prehnite in all fractures in KLX27A
Fractures with Prehnite
Total number of fractures
Vertical depth (m.b.s.l)
Number of fractures / 10m vertical depth

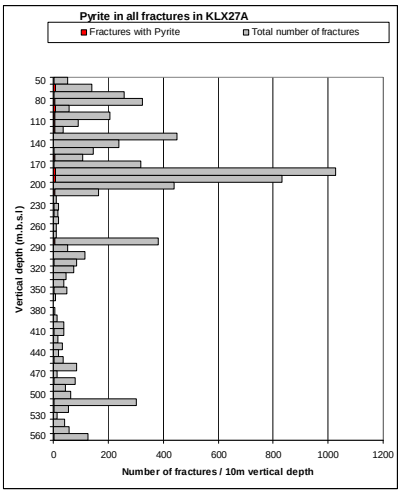
Pyrite in all fractures in KLX27A
Fractures with Pyrite
Total number of fractures
Vertical depth (m.b.s.l)
Number of fractures / 10m vertical depth

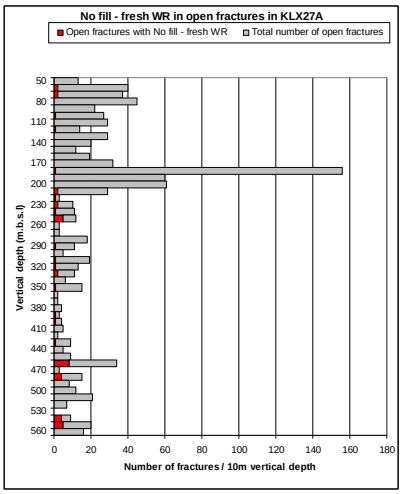
No fill - fresh WR in open fractures in KLX27A
Open fractures with No fill - fresh WR
Total number of open fractures
Vertical depth (m.b.s.l)
Number of fractures / 10m vertical depth

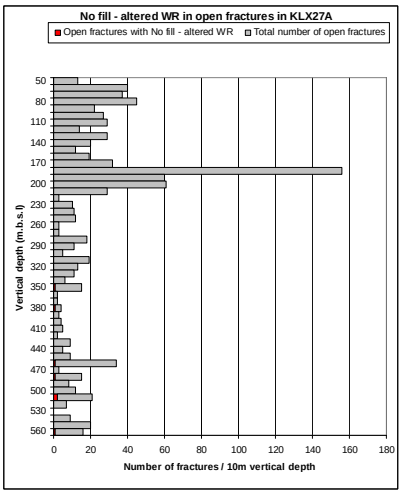
No fill - altered WR in open fractures in KLX27A
Open fractures with No fill - altered WR
Total number of open fractures
Vertical depth (m.b.s.l)
Number of fractures / 10m vertical depth

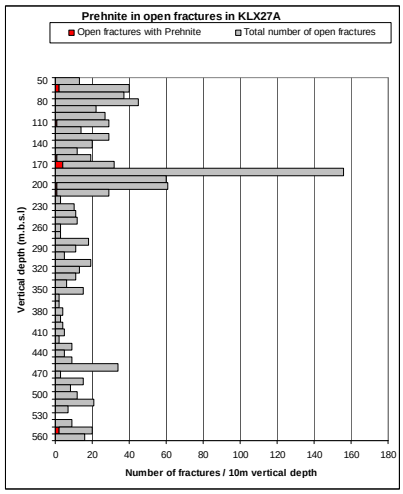
Prehnite in open fractures in KLX27A
Open fractures with Prehnite
Total number of open fractures
Vertical depth (m.b.s.l)
Number of fractures / 10m vertical depth

i

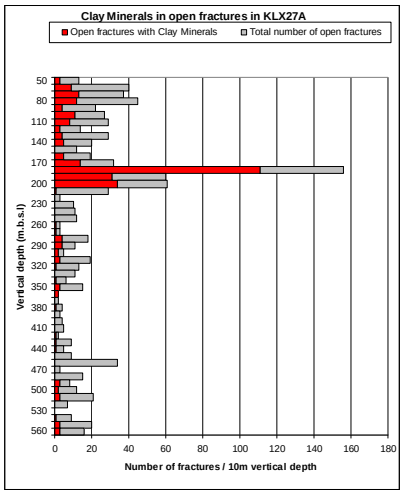
Clay Minerals in open fractures in KLX27A
Open fractures with Clay Minerals
Total number of open fractures
Vertical depth (m.b.s.l)
Number of fractures / 10m vertical depth

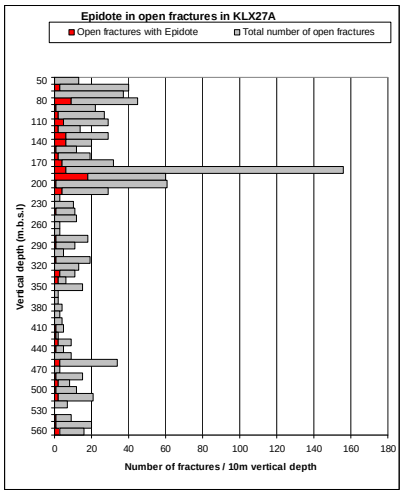
Epidote in open fractures in KLX27A
Open fractures with Epidote
Total number of open fractures
Vertical depth (m.b.s.l)
Number of fractures / 10m vertical depth

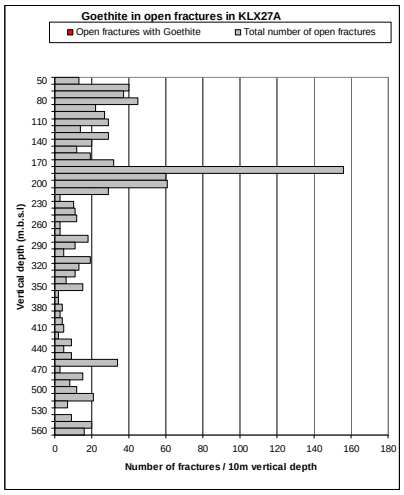
Goethite in open fractures in KLX27A
Open fractures with Goethite
Total number of open fractures
Vertical depth (m.b.s.l)
Number of fractures / 10m vertical depth

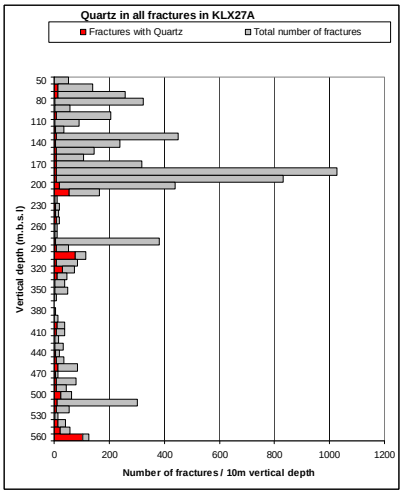
Quartz in all fractures in KLX27A
Fractures with Quartz
Total number of fractures
Vertical depth (m.b.s.l)
Number of fractures / 10m vertical depth

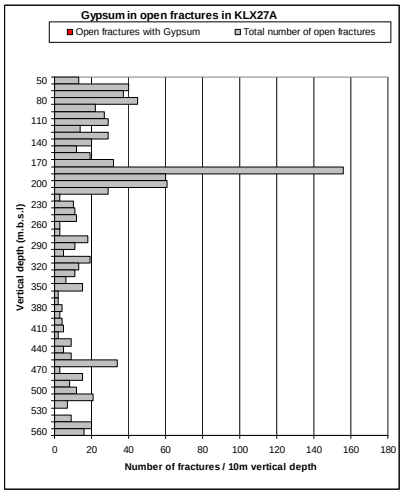
Gypsum in open fractures in KLX27A
Open fractures with Gypsum
Total number of open fractures
Vertical depth (m.b.s.l)
Number of fractures / 10m vertical depth

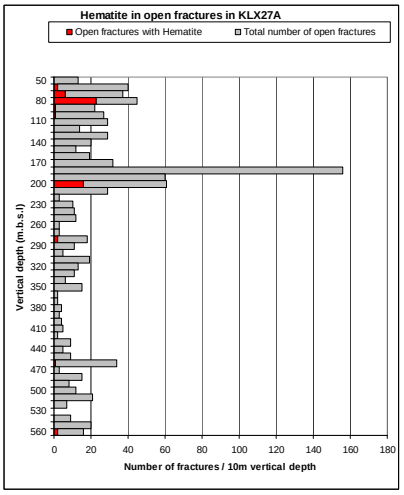
Hematite in open fractures in KLX27A
Open fractures with Hematite
Total number of open fractures
Vertical depth (m.b.s.l)
Number of fractures / 10m vertical depth

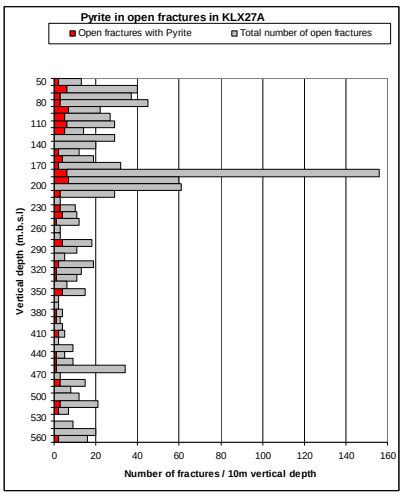
Pyrite in open fractures in KLX27A
Open fractures with Pyrite
Total number of open fractures
Vertical depth (m.b.s.l)
Number of fractures / 10m vertical depth

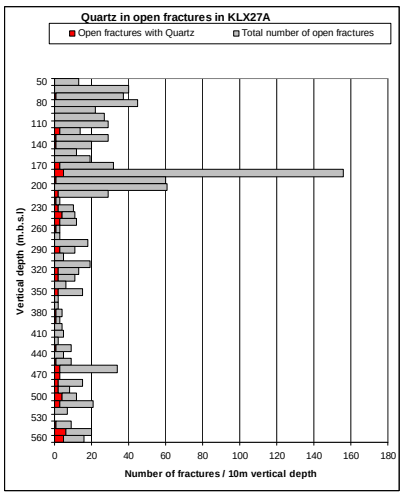
Quartz in open fractures in KLX27A
Open fractures with Quartz
Total number of open fractures
Vertical depth (m.b.s.l)
Number of fractures / 10m vertical depth

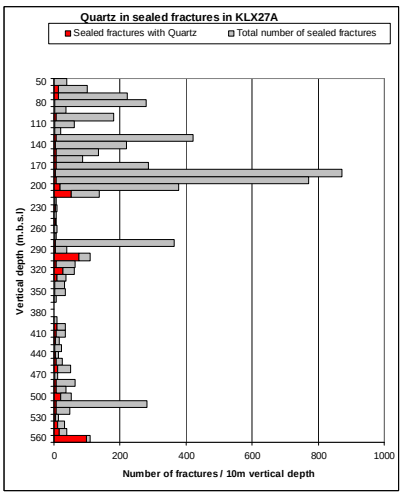
Quartz in sealed fractures in KLX27A
Sealed fractures with Quartz
Total number of sealed fractures
Vertical depth (m.b.s.l)
Number of fractures / 10m vertical depth

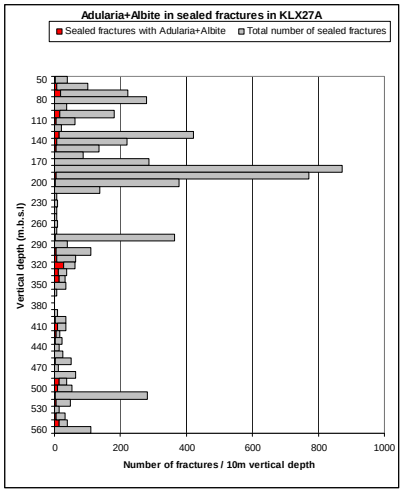
Adularia+Albite in sealed fractures in KLX27A
Sealed fractures with Adularia+Albite
Total number of sealed fractures
Vertical depth (m.b.s.l)
Number of fractures / 10m vertical depth

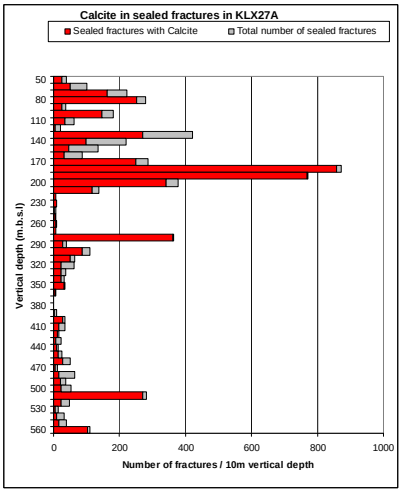
Calcite in sealed fractures in KLX27A
Sealed fractures with Calcite
Total number of sealed fractures
Vertical depth (m.b.s.l)
Number of fractures / 10m vertical depth

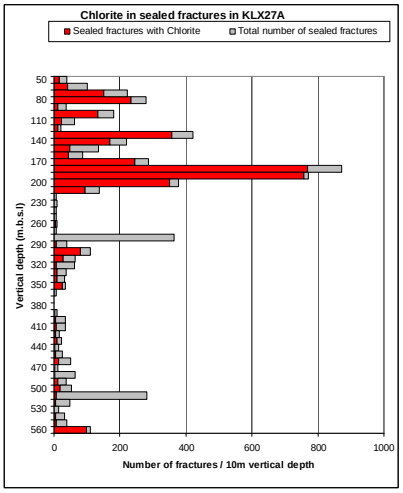
Chlorite in sealed fractures in KLX27A
Sealed fractures with Chlorite
Total number of sealed fractures
Vertical depth (m.b.s.l)
Number of fractures / 10m vertical depth

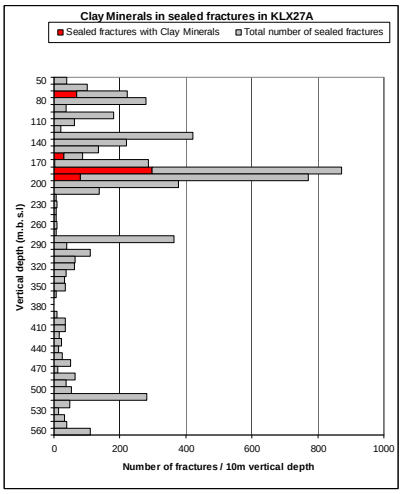
Clay Minerals in sealed fractures in KLX27A
Sealed fractures with Clay Minerals
Total number of sealed fractures
Vertical depth (m.b.s.l)
Number of fractures / 10m vertical depth

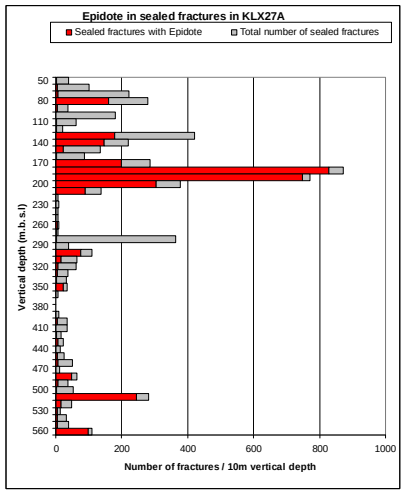
Epidote in sealed fractures in KLX27A
Sealed fractures with Epidote
Total number of sealed fractures
Vertical depth (m.b.s.l)
Number of fractures / 10m vertical depth

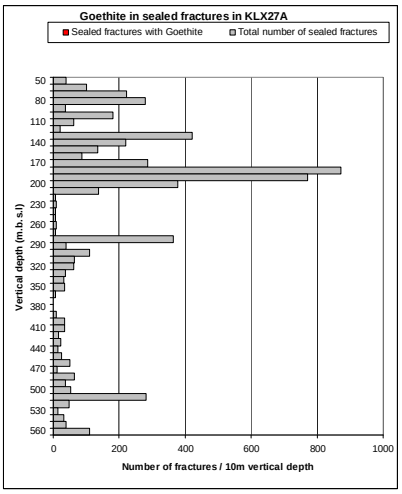
Goethite in sealed fractures in KLX27A
Sealed fractures with Goethite
Total number of sealed fractures
Vertical depth (m.b.s.l)
Number of fractures / 10m vertical depth

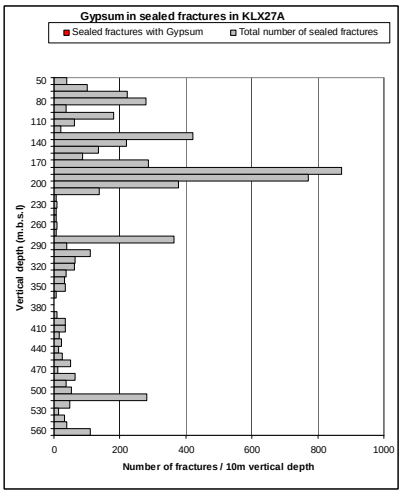
Gypsum in sealed fractures in KLX27A
Sealed fractures with Gypsum
Total number of sealed fractures
Vertical depth (m.b.s.l)
Number of fractures / 10m vertical depth

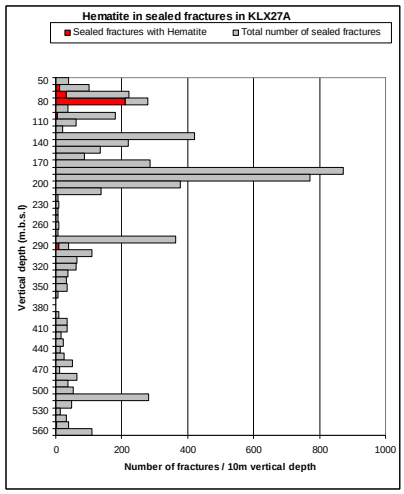
Hematite in sealed fractures in KLX27A
Sealed fractures with Hematite
Total number of sealed fractures
Vertical depth (m.b.s.l)
Number of fractures / 10m vertical depth

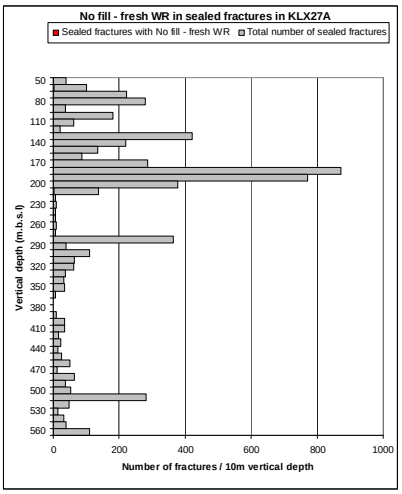
No fill - fresh WR in sealed fractures in KLX27A
Sealed fractures with No fill - fresh WR
Total number of sealed fractures
Vertical depth (m.b.s.l)
Number of fractures / 10m vertical depth

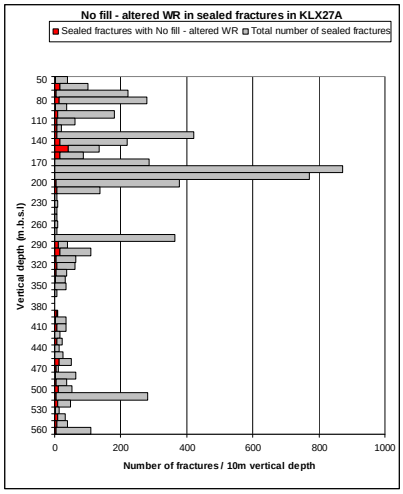
No fill - altered WR in sealed fractures in KLX27A
Sealed fractures with No fill - altered WR
Total number of sealed fractures
Vertical depth (m.b.s.l)
50
80
110
140
170
200
230
260
290
320
350
380
410
440
470
500
530
560
0
200
400
600
800
1000
Number of fractures / 10m vertical depth

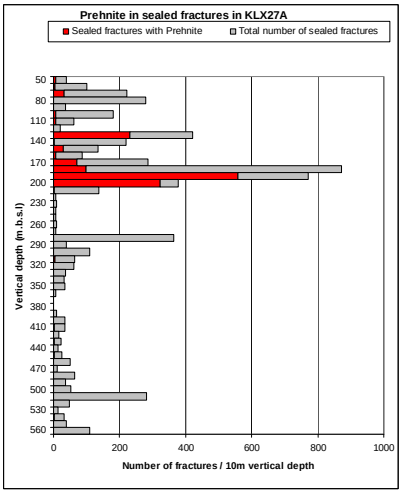
Prehnite in sealed fractures in KLX27A
Sealed fractures with Prehnite
Total number of sealed fractures
Vertical depth (m.b.s.l)
50
80
110
140
170
200
230
260
290
320
350
380
410
440
470
500
530
560
0
200
400
600
800
1000
Number of fractures / 10m vertical depth

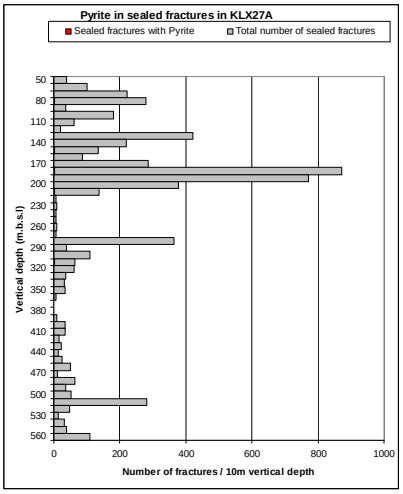
Pyrite in sealed fractures in KLX27A
Sealed fractures with Pyrite
Total number of sealed fractures
Vertical depth (m.b.s.l)
50
80
110
140
170
200
230
260
290
320
350
380
410
440
470
500
530
560
0
200
400
600
800
1000
Number of fractures / 10m vertical depth

KLX28A

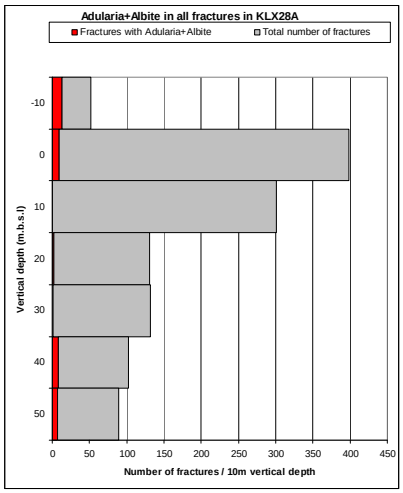
Adularia+Albite in all fractures in KLX28A
Fractures with Adularia+Albite
Total number of fractures
Vertical depth (m.b.s.l)
Number of fractures / 10m vertical depth

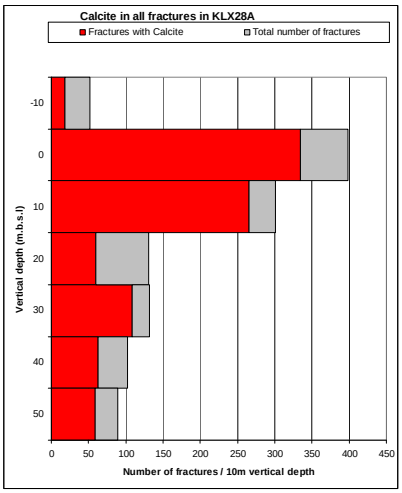
Calcite in all fractures in KLX28A
Fractures with Calcite
Total number of fractures
Vertical depth (m.b.s.l)
Number of fractures / 10m vertical depth

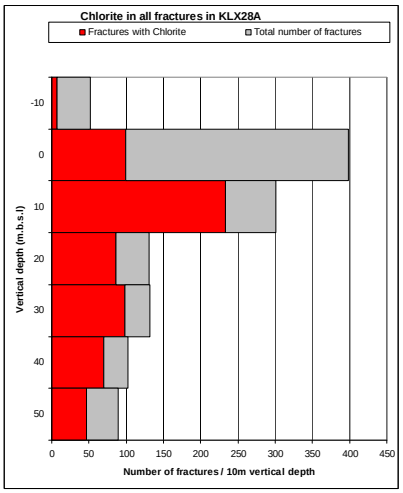
Chlorite in all fractures in KLX28A
Fractures with Chlorite
Total number of fractures
Vertical depth (m.b.s.l)
Number of fractures / 10m vertical depth

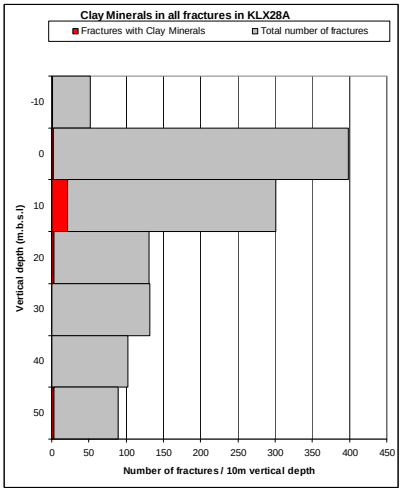
Clay Minerals in all fractures in KLX28A
Fractures with Clay Minerals
Total number of fractures
Vertical depth (m.b.s.l)
Number of fractures / 10m vertical depth

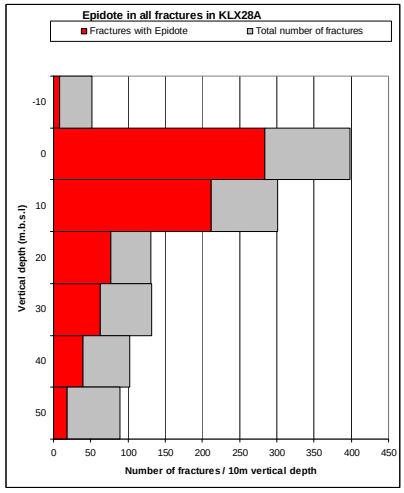
Epidote in all fractures in KLX28A
Fractures with Epidote
Total number of fractures
Vertical depth (m.b.s.l)
Number of fractures / 10m vertical depth

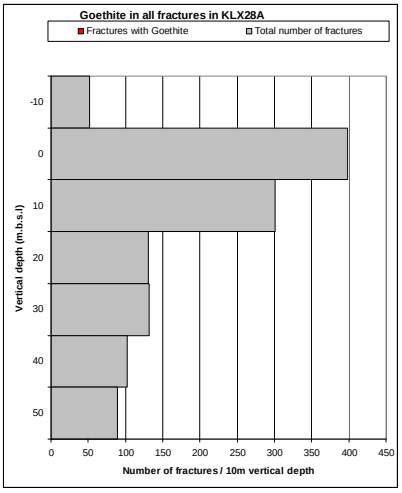
Goethite in all fractures in KLX28A
Fractures with Goethite
Total number of fractures
Vertical depth (m.b.s.l)
Number of fractures / 10m vertical depth

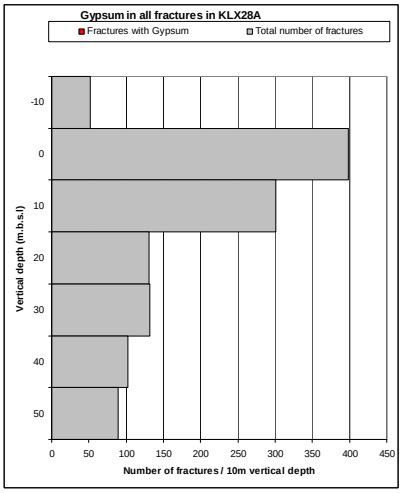
Gypsum in all fractures in KLX28A
Fractures with Gypsum
Total number of fractures
Vertical depth (m.b.s.l)
Number of fractures / 10m vertical depth

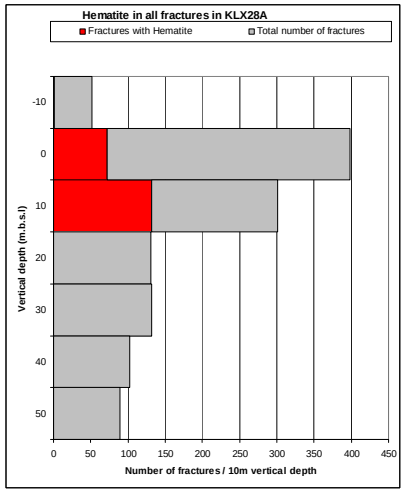
Hematite in all fractures in KLX28A
Fractures with Hematite
Total number of fractures
Vertical depth (m.b.s.l)
Number of fractures / 10m vertical depth

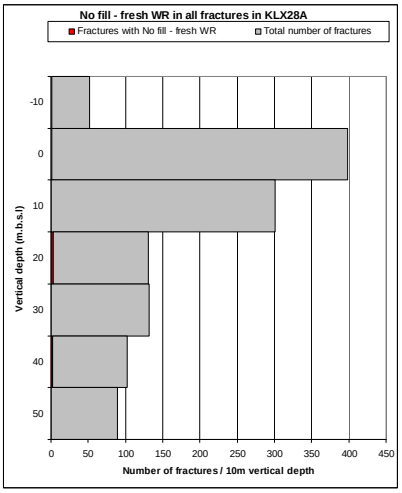
No fill - fresh WR in all fractures in KLX28A
Fractures with No fill - fresh WR
Total number of fractures
Vertical depth (m.b.s.l)
Number of fractures / 10m vertical depth

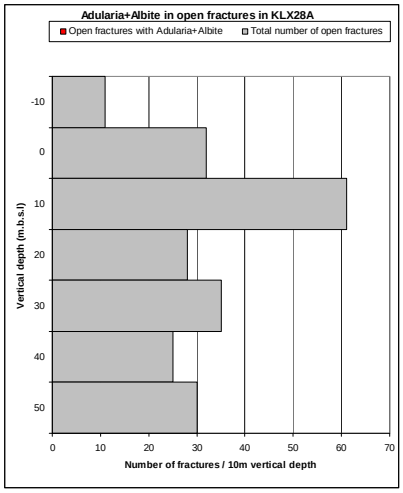
Adularia+Albite in open fractures in KLX28A
Open fractures with Adularia+Albite
Total number of open fractures
Vertical depth (m.b.s.l)
-10
0
10
20
30
40
50
0
10
20
30
40
50
60
70
Number of fractures / 10m vertical depth

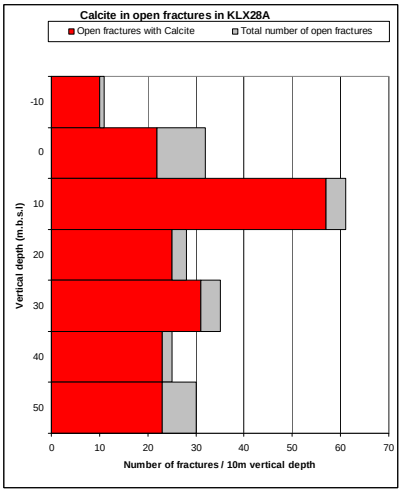
Calcite in open fractures in KLX28A
Open fractures with Calcite
Total number of open fractures
Vertical depth (m.b.s.l)
-10
0
10
20
30
40
50
0
10
20
30
40
50
60
70
Number of fractures / 10m vertical depth

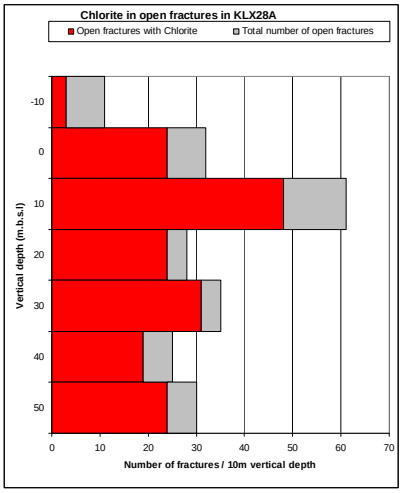
Chlorite in open fractures in KLX28A
Open fractures with Chlorite
Total number of open fractures
Vertical depth (m.b.s.l)
-10
0
10
20
30
40
50
0
10
20
30
40
50
60
70
Number of fractures / 10m vertical depth

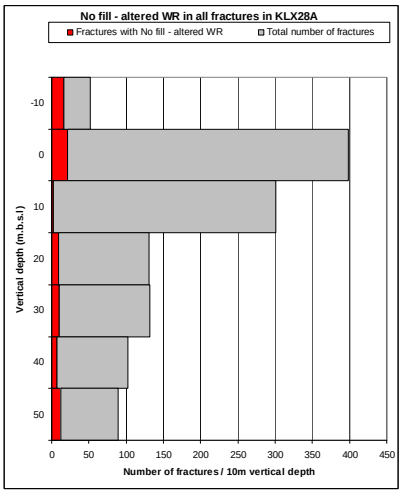
No fill - altered WR in all fractures in KLX28A
Fractures with No fill - altered WR
Total number of fractures
Vertical depth (m.b.s.l)
-10
0
10
20
30
40
50
0
50
100
150
200
250
300
350
400
450
Number of fractures / 10m vertical depth

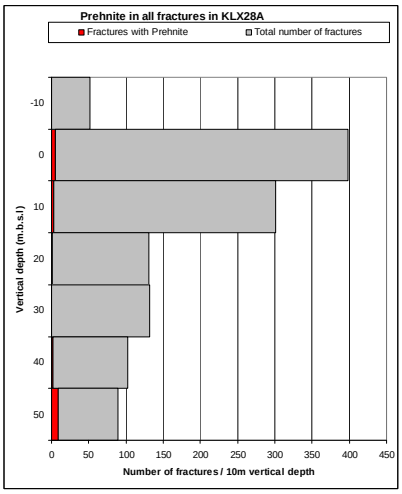
Prehnite in all fractures in KLX28A
Fractures with Prehnite
Total number of fractures
Vertical depth (m.b.s.l)
-10
0
10
20
30
40
50
0
50
100
150
200
250
300
350
400
450
Number of fractures / 10m vertical depth

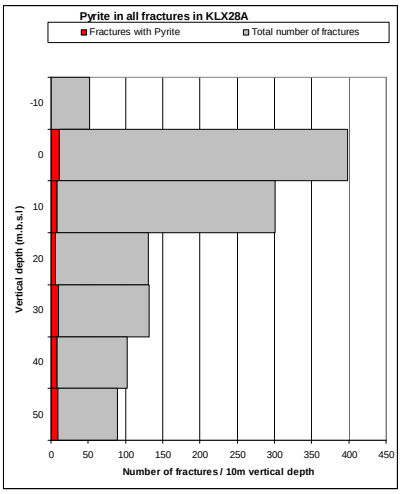
Pyrite in all fractures in KLX28A
Fractures with Pyrite
Total number of fractures
Vertical depth (m.b.s.l)
-10
0
10
20
30
40
50
0
50
100
150
200
250
300
350
400
450
Number of fractures / 10m vertical depth

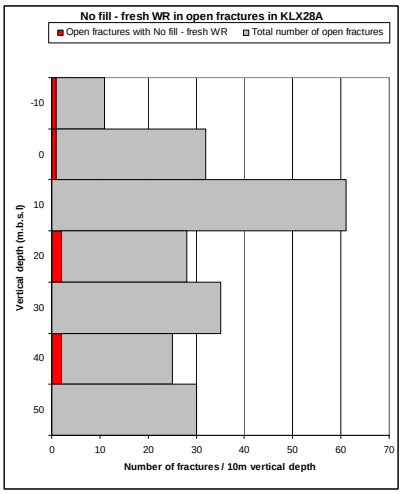
No fill - fresh WR in open fractures in KLX28A
Open fractures with No fill - fresh WR
Total number of open fractures
Vertical depth (m.b.s.l)
-10
0
10
20
30
40
50
0
10
20
30
40
50
60
70
Number of fractures / 10m vertical depth

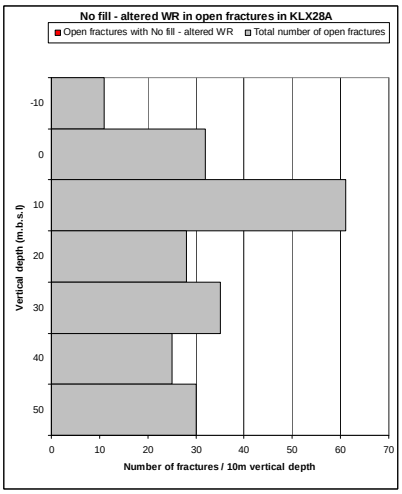
No fill - altered WR in open fractures in KLX28A
Open fractures with No fill - altered WR
Total number of open fractures
Vertical depth (m.b.s.l)
-10
0
10
20
30
40
50
0
10
20
30
40
50
60
70
Number of fractures / 10m vertical depth

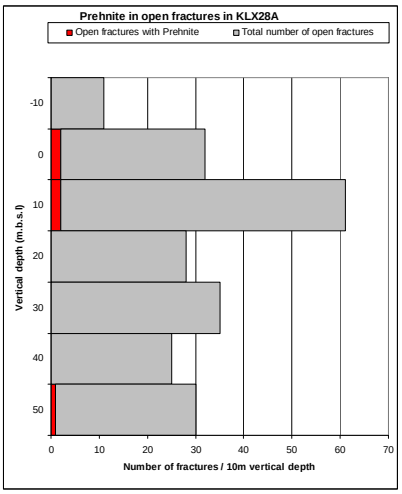
Prehnite in open fractures in KLX28A
Open fractures with Prehnite
Total number of open fractures
Vertical depth (m.b.s.l)
-10
0
10
20
30
40
50
0
10
20
30
40
50
60
70
Number of fractures / 10m vertical depth

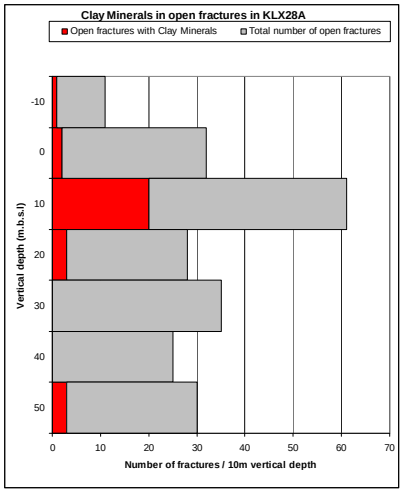
Clay Minerals in open fractures in KLX28A
Open fractures with Clay Minerals
Total number of open fractures
Vertical depth (m.b.s.l)
-10
0
10
20
30
40
50
0
10
20
30
40
50
60
70
Number of fractures / 10m vertical depth

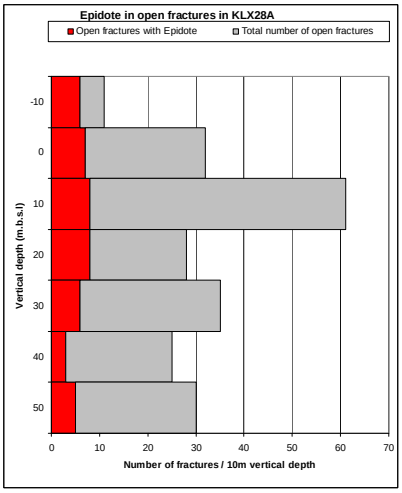
Epidote in open fractures in KLX28A
Open fractures with Epidote
Total number of open fractures
Vertical depth (m.b.s.l)
-10
0
10
20
30
40
50
0
10
20
30
40
50
60
70
Number of fractures / 10m vertical depth

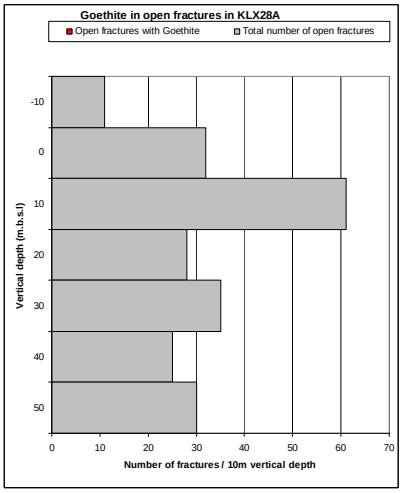
Goethite in open fractures in KLX28A
Open fractures with Goethite
Total number of open fractures
Vertical depth (m.b.s.l)
-10
0
10
20
30
40
50
0
10
20
30
40
50
60
70
Number of fractures / 10m vertical depth

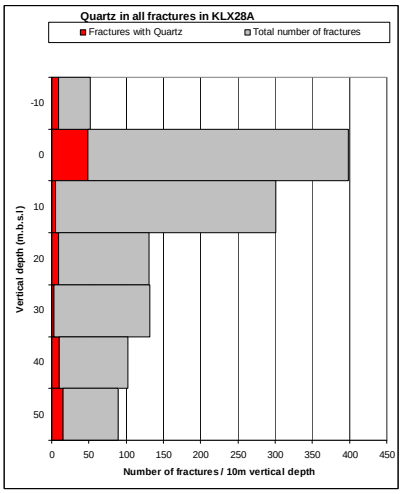
Quartz in all fractures in KLX28A
Fractures with Quartz
Total number of fractures
Vertical depth (m.b.s.l)
-10
0
10
20
30
40
50
0
50
100
150
200
250
300
350
400
450
Number of fractures / 10m vertical depth

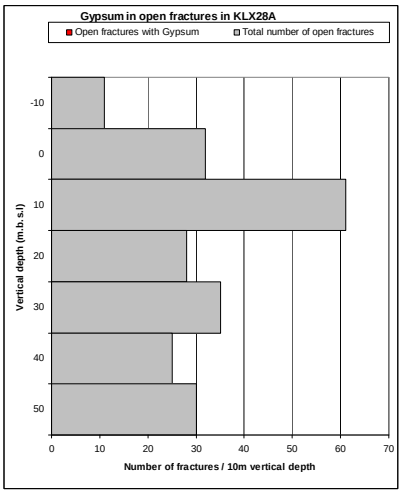
Gypsum in open fractures in KLX28A
Open fractures with Gypsum
Total number of open fractures
Vertical depth (m.b.s.l)
-10
0
10
20
30
40
50
0
10
20
30
40
50
60
70
Number of fractures / 10m vertical depth

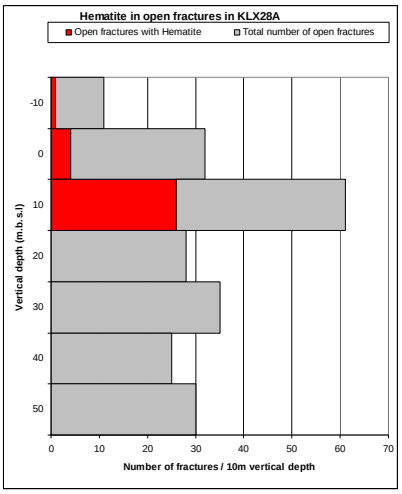
Hematite in open fractures in KLX28A
Open fractures with Hematite
Total number of open fractures
Vertical depth (m.b.s.l)
-10
0
10
20
30
40
50
0
10
20
30
40
50
60
70
Number of fractures / 10m vertical depth

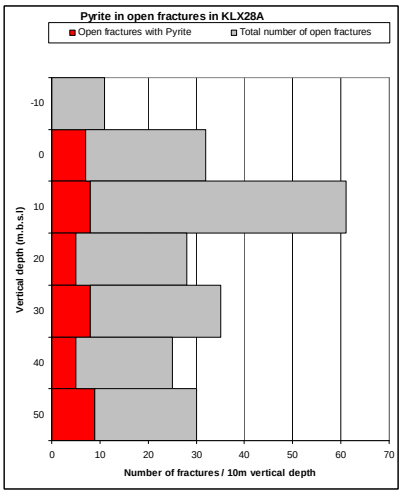
Pyrite in open fractures in KLX28A
Open fractures with Pyrite
Total number of open fractures
Vertical depth (m.b.s.l)
-10
0
10
20
30
40
50
0
10
20
30
40
50
60
70
Number of fractures / 10m vertical depth

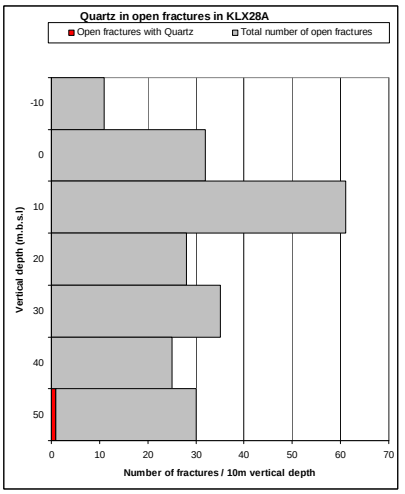
Quartz in open fractures in KLX28A
Open fractures with Quartz
Total number of open fractures
Vertical depth (m.b.s.l)
-10
0
10
20
30
40
50
0
10
20
30
40
50
60
70
Number of fractures / 10m vertical depth

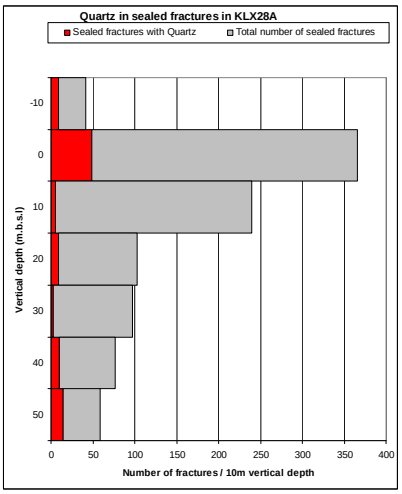
Quartz in sealed fractures in KLX28A
Sealed fractures with Quartz
Total number of sealed fractures
Vertical depth (m.b.s.l)
-10
0
10
20
30
40
50
0
50
100
150
200
250
300
350
400
Number of fractures / 10m vertical depth

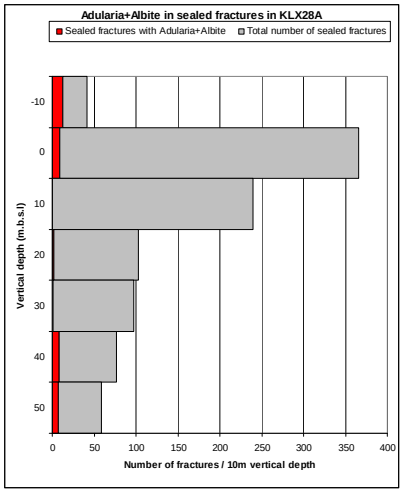
Adularia+Albite in sealed fractures in KLX28A
Sealed fractures with Adularia+Albite
Total number of sealed fractures
Vertical depth (m.b.s.l)
-10
0
10
20
30
40
50
0
50
100
150
200
250
300
350
400
Number of fractures / 10m vertical depth

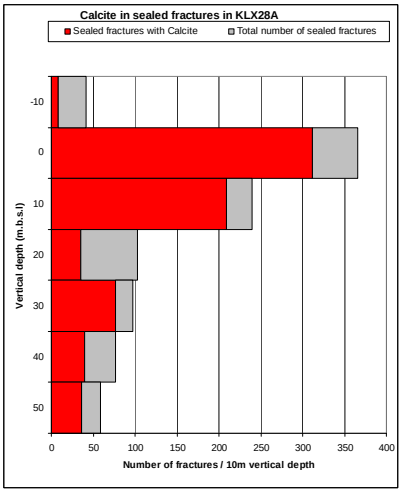
Calcite in sealed fractures in KLX28A
Sealed fractures with Calcite
Total number of sealed fractures
Vertical depth (m.b.s.l)
-10
0
10
20
30
40
50
0
50
100
150
200
250
300
350
400
Number of fractures / 10m vertical depth

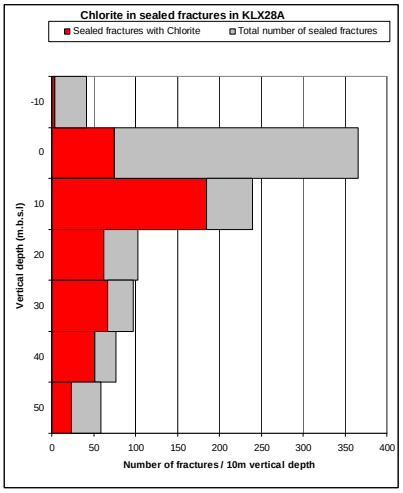
Chlorite in sealed fractures in KLX28A
Sealed fractures with Chlorite
Total number of sealed fractures
Vertical depth (m.b.s.l)
-10
0
10
20
30
40
50
0
50
100
150
200
250
300
350
400
Number of fractures / 10m vertical depth

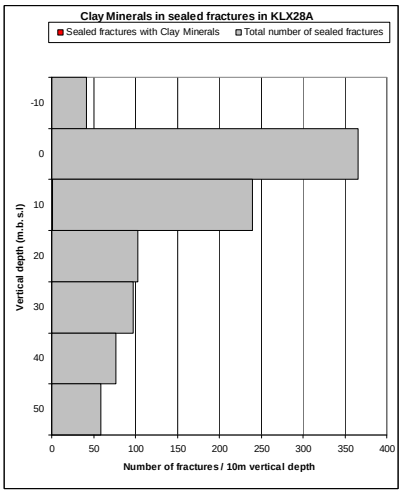
Clay Minerals in sealed fractures in KLX28A
Sealed fractures with Clay Minerals
Total number of sealed fractures
Vertical depth (m.b.s.l)
-10
0
10
20
30
40
50
0
50
100
150
200
250
300
350
400
Number of fractures / 10m vertical depth

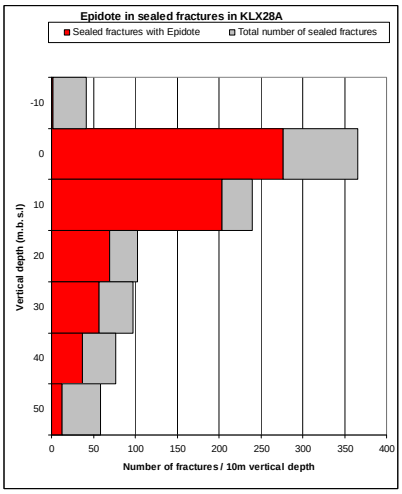
Epidote in sealed fractures in KLX28A
Sealed fractures with Epidote
Total number of sealed fractures
Vertical depth (m.b.s.l)
-10
0
10
20
30
40
50
0
50
100
150
200
250
300
350
400
Number of fractures / 10m vertical depth

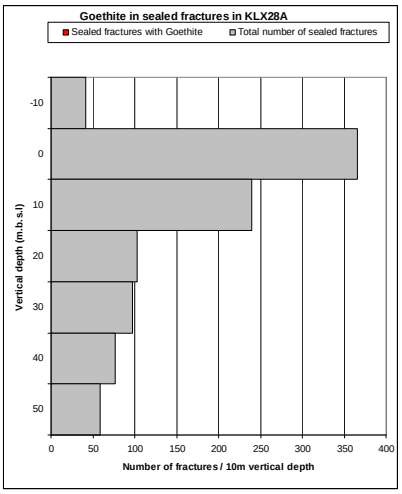
Goethite in sealed fractures in KLX28A
Sealed fractures with Goethite
Total number of sealed fractures
Vertical depth (m.b.s.l)
-10
0
10
20
30
40
50
0
50
100
150
200
250
300
350
400
Number of fractures / 10m vertical depth

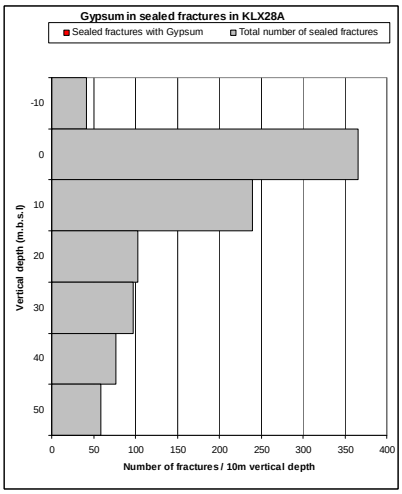
Gypsum in sealed fractures in KLX28A
Sealed fractures with Gypsum
Total number of sealed fractures
Vertical depth (m.b.s.l)
-10
0
10
20
30
40
50
0
50
100
150
200
250
300
350
400
Number of fractures / 10m vertical depth

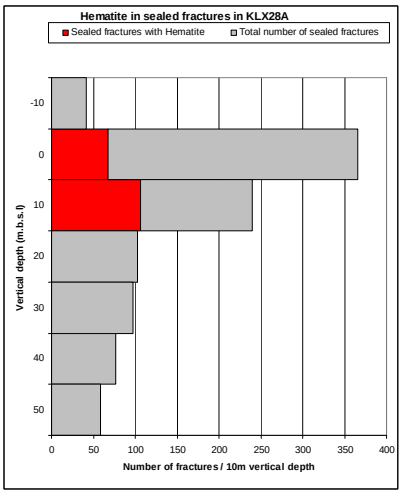
Hematite in sealed fractures in KLX28A
Sealed fractures with Hematite
Total number of sealed fractures
Vertical depth (m.b.s.l)
-10
0
10
20
30
40
50
0
50
100
150
200
250
300
350
400
Number of fractures / 10m vertical depth

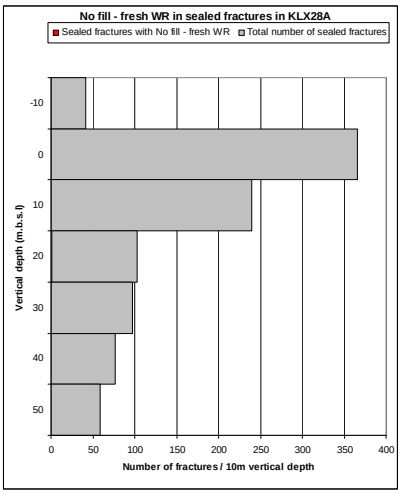
No fill - fresh WR in sealed fractures in KLX28A
Sealed fractures with No fill - fresh WR
Total number of sealed fractures
Vertical depth (m.b.s.l)
-10
0
10
20
30
40
50
0
50
100
150
200
250
300
350
400
Number of fractures / 10m vertical depth

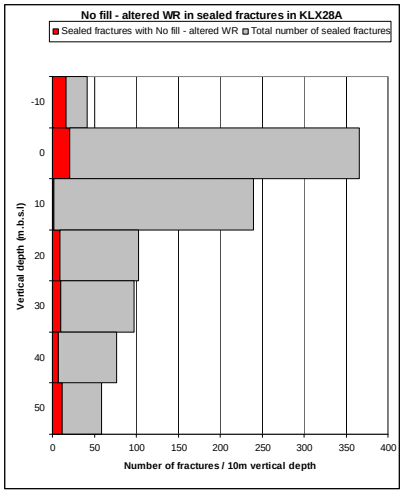
No fill - altered WR in sealed fractures in KLX28A
Sealed fractures with No fill - altered WR
Total number of sealed fractures
Vertical depth (m.b.s.l)
-10
0
10
20
30
40
50
0
50
100
150
200
250
300
350
400
Number of fractures / 10m vertical depth

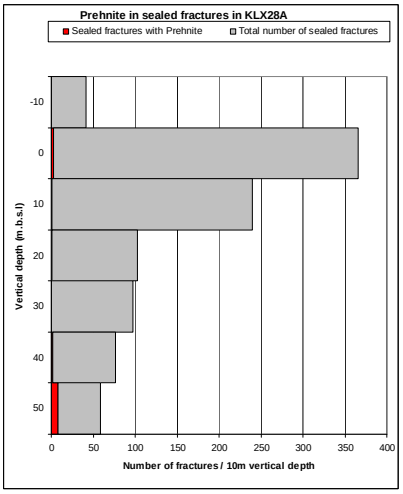
Prehnite in sealed fractures in KLX28A
Sealed fractures with Prehnite
Total number of sealed fractures
Vertical depth (m.b.s.l)
-10
0
10
20
30
40
50
0
50
100
150
200
250
300
350
400
Number of fractures / 10m vertical depth

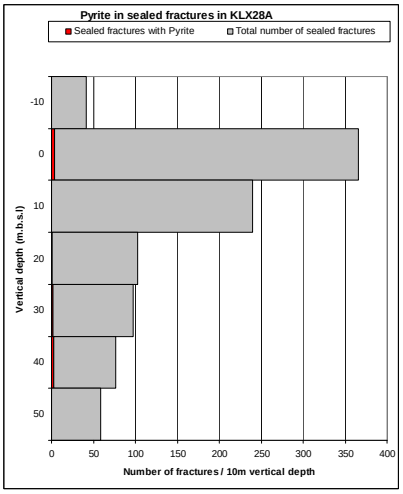
Pyrite in sealed fractures in KLX28A
Sealed fractures with Pyrite
Total number of sealed fractures
Vertical depth (m.b.s.l)
-10
0
10
20
30
40
50
0
50
100
150
200
250
300
350
400
Number of fractures / 10m vertical depth

KLX29A

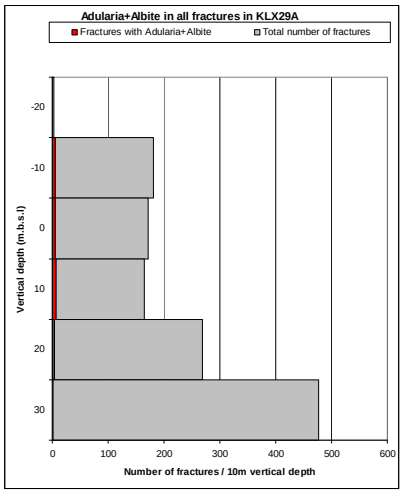
Adularia+Albite in all fractures in KLX29A
Fractures with Adularia+Albite
Total number of fractures
Vertical depth (m.b.s.l)
-20
-10
0
10
20
30
0
100
200
300
400
500
600
Number of fractures / 10m vertical depth

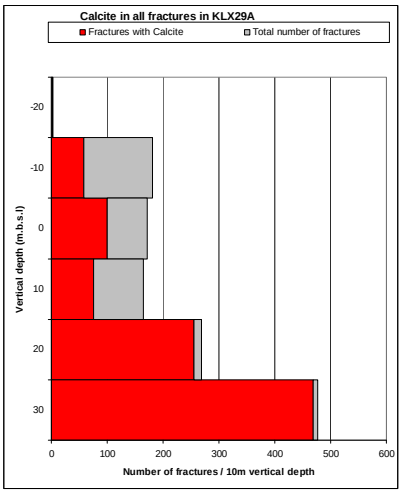
Calcite in all fractures in KLX29A
Fractures with Calcite
Total number of fractures
Vertical depth (m.b.s.l)
-20
-10
0
10
20
30
0
100
200
300
400
500
600
Number of fractures / 10m vertical depth

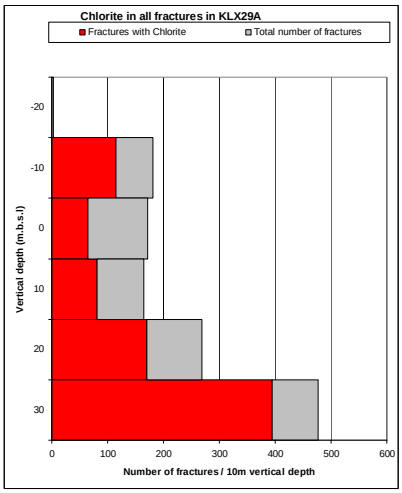
Chlorite in all fractures in KLX29A
Fractures with Chlorite
Total number of fractures
Vertical depth (m.b.s.l)
-20
-10
0
10
20
30
0
100
200
300
400
500
600
Number of fractures / 10m vertical depth

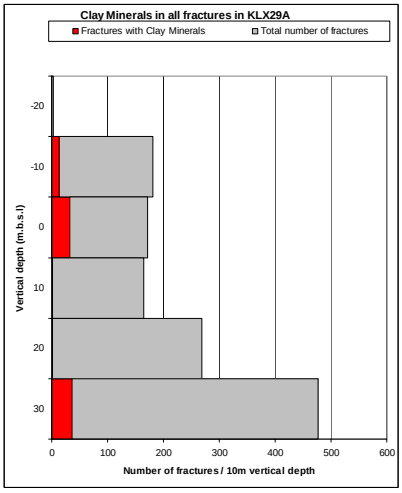
Clay Minerals in all fractures in KLX29A
Fractures with Clay Minerals
Total number of fractures
Vertical depth (m.b.s.l)
-20
-10
0
10
20
30
0
100
200
300
400
500
600
Number of fractures / 10m vertical depth

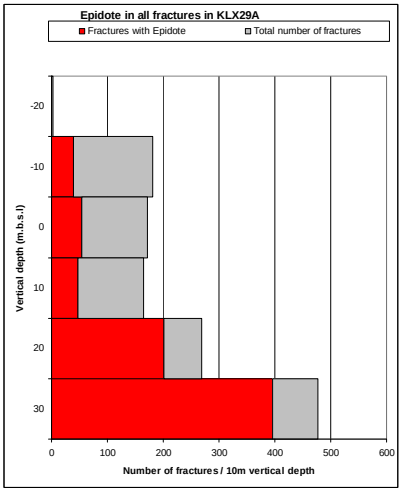
Epidote in all fractures in KLX29A
Fractures with Epidote
Total number of fractures
Vertical depth (m.b.s.l)
-20
-10
0
10
20
30
0
100
200
300
400
500
600
Number of fractures / 10m vertical depth

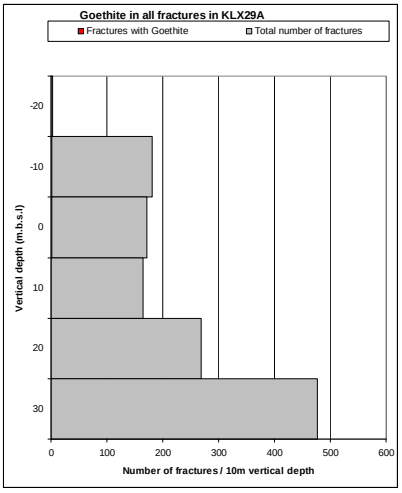
Goethite in all fractures in KLX29A
Fractures with Goethite
Total number of fractures
Vertical depth (m.b.s.l)
-20
-10
0
10
20
30
0
100
200
300
400
500
600
Number of fractures / 10m vertical depth

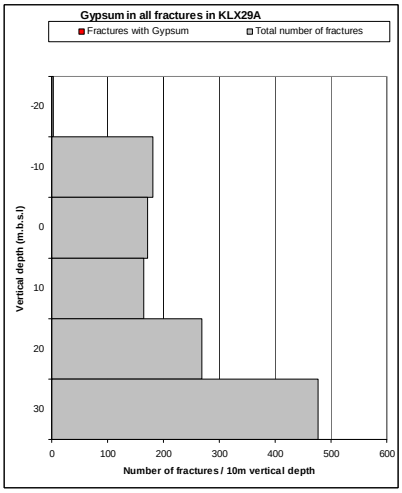
Gypsum in all fractures in KLX29A
Fractures with Gypsum
Total number of fractures
Vertical depth (m.b.s.l)
-20
-10
0
10
20
30
0
100
200
300
400
500
600
Number of fractures / 10m vertical depth

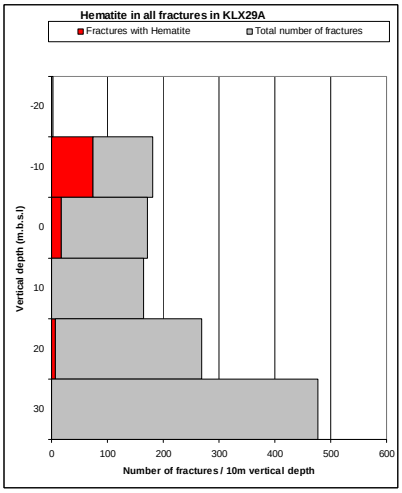
Hematite in all fractures in KLX29A
Fractures with Hematite
Total number of fractures
Vertical depth (m.b.s.l)
-20
-10
0
10
20
30
0
100
200
300
400
500
600
Number of fractures / 10m vertical depth

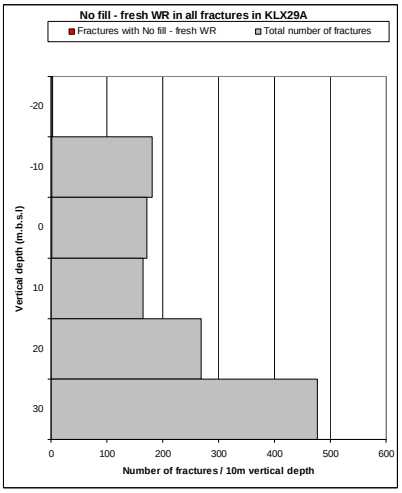
No fill - fresh WR in all fractures in KLX29A
Fractures with No fill - fresh WR
Total number of fractures
Vertical depth (m.b.s.l)
-20
-10
0
10
20
30
0
100
200
300
400
500
600
Number of fractures / 10m vertical depth

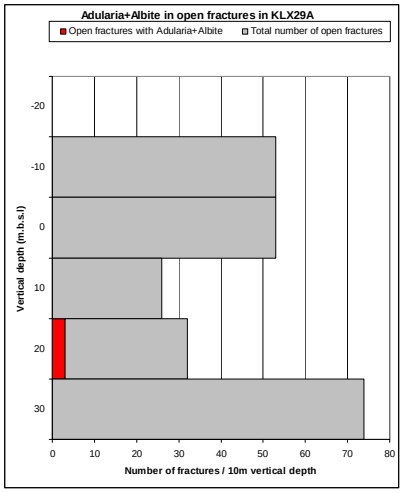
Adularia+Albite in open fractures in KLX29A
Open fractures with Adularia+Albite
Total number of open fractures
Vertical depth (m.b.s.l)
-20
-10
0
10
20
30
0
10
20
30
40
50
60
70
80
Number of fractures / 10m vertical depth

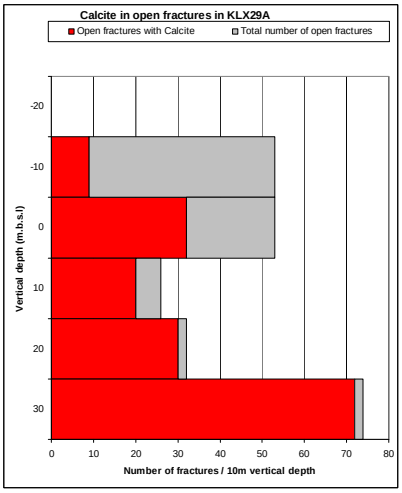
Calcite in open fractures in KLX29A
Open fractures with Calcite
Total number of open fractures
Vertical depth (m.b.s.l)
-20
-10
0
10
20
30
0
10
20
30
40
50
60
70
80
Number of fractures / 10m vertical depth

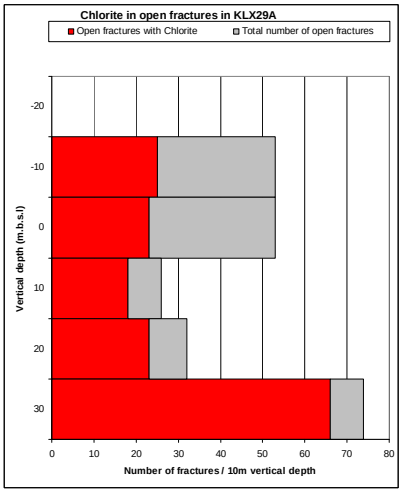
Chlorite in open fractures in KLX29A
Open fractures with Chlorite
Total number of open fractures
Vertical depth (m.b.s.l)
-20
-10
0
10
20
30
0
10
20
30
40
50
60
70
80
Number of fractures / 10m vertical depth

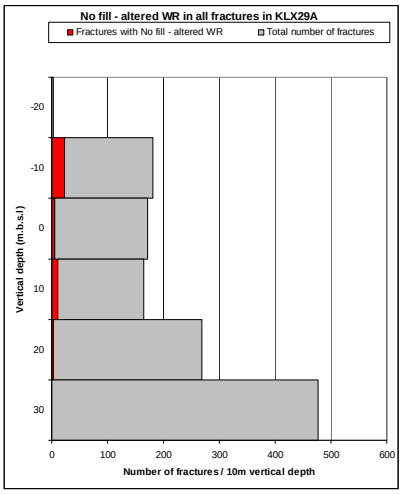
No fill - altered WR in all fractures in KLX29A
Fractures with No fill - altered WR
Total number of fractures
Vertical depth (m.b.s.l)
-20
-10
0
10
20
30
0
100
200
300
400
500
600
Number of fractures / 10m vertical depth

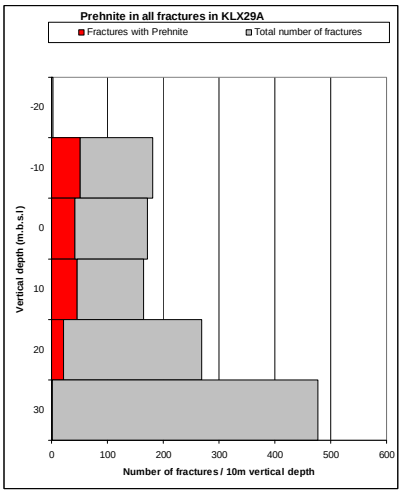
Prehnite in all fractures in KLX29A
Fractures with Prehnite
Total number of fractures
Vertical depth (m.b.s.l)
-20
-10
0
10
20
30
0
100
200
300
400
500
600
Number of fractures / 10m vertical depth

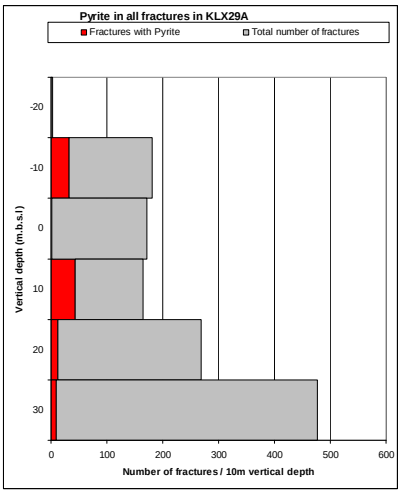
Pyrite in all fractures in KLX29A
Fractures with Pyrite
Total number of fractures
Vertical depth (m.b.s.l)
-20
-10
0
10
20
30
0
100
200
300
400
500
600
Number of fractures / 10m vertical depth

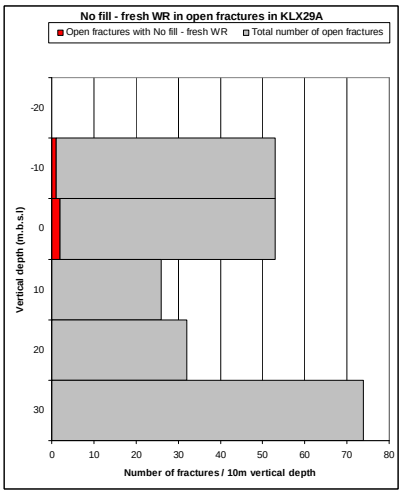
No fill - fresh WR in open fractures in KLX29A
Open fractures with No fill - fresh WR
Total number of open fractures
Vertical depth (m.b.s.l)
-20
-10
0
10
20
30
0
10
20
30
40
50
60
70
80
Number of fractures / 10m vertical depth

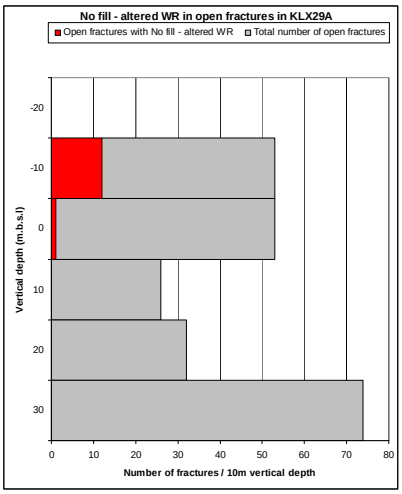
No fill - altered WR in open fractures in KLX29A
Open fractures with No fill - altered WR
Total number of open fractures
Vertical depth (m.b.s.l)
-20
-10
0
10
20
30
0
10
20
30
40
50
60
70
80
Number of fractures / 10m vertical depth

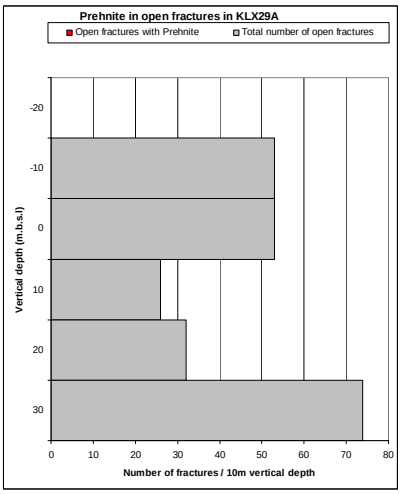
Prehnite in open fractures in KLX29A
Open fractures with Prehnite
Total number of open fractures
Vertical depth (m.b.s.l)
-20
-10
0
10
20
30
0
10
20
30
40
50
60
70
80
Number of fractures / 10m vertical depth

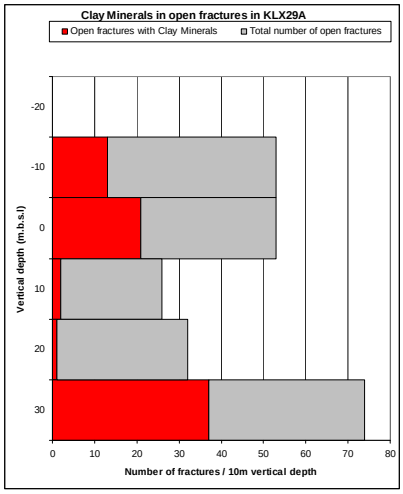
Clay Minerals in open fractures in KLX29A
Open fractures with Clay Minerals
Total number of open fractures
Vertical depth (m.b.s.l)
-20
-10
0
10
20
30
0 10 20 30 40 50 60 70 80
Number of fractures / 10m vertical depth

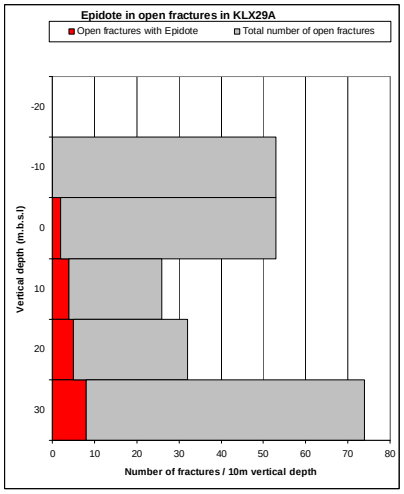
Epidote in open fractures in KLX29A
Open fractures with Epidote
Total number of open fractures
Vertical depth (m.b.s.l)
-20
-10
0
10
20
30
0 10 20 30 40 50 60 70 80
Number of fractures / 10m vertical depth

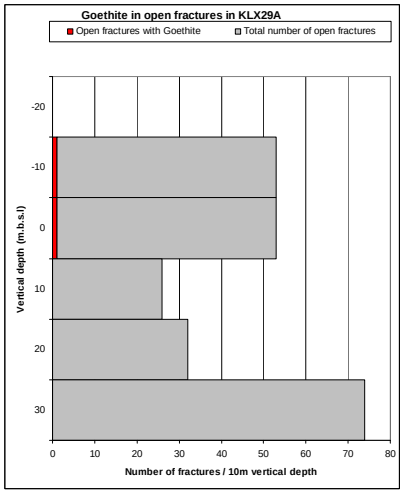
Goethite in open fractures in KLX29A
Open fractures with Goethite
Total number of open fractures
Vertical depth (m.b.s.l)
-20
-10
0
10
20
30
0 10 20 30 40 50 60 70 80
Number of fractures / 10m vertical depth

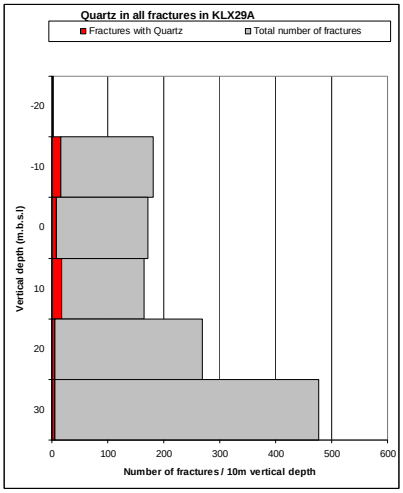
Quartz in all fractures in KLX29A
Fractures with Quartz
Total number of fractures
Vertical depth (m.b.s.l)
-20
-10
0
10
20
30
0 100 200 300 400 500 600
Number of fractures / 10m vertical depth

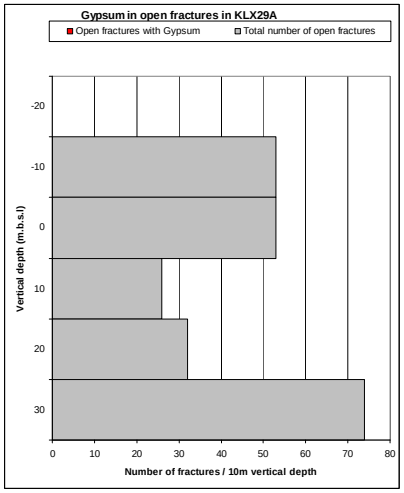
Gypsum in open fractures in KLX29A
Open fractures with Gypsum
Total number of open fractures
Vertical depth (m.b.s.l)
-20
-10
0
10
20
30
0 10 20 30 40 50 60 70 80
Number of fractures / 10m vertical depth

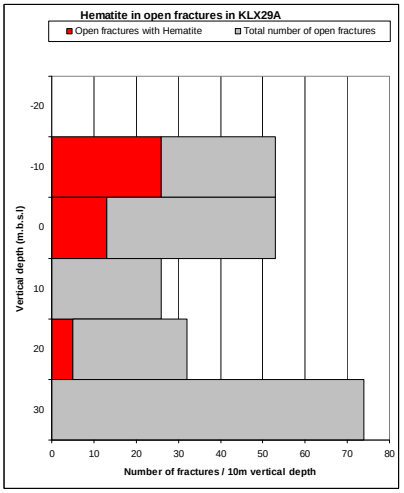
Hematite in open fractures in KLX29A
Open fractures with Hematite
Total number of open fractures
Vertical depth (m.b.s.l)
-20
-10
0
10
20
30
0 10 20 30 40 50 60 70 80
Number of fractures / 10m vertical depth

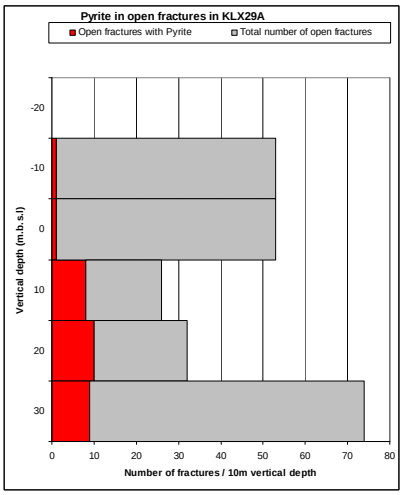
Pyrite in open fractures in KLX29A
Open fractures with Pyrite
Total number of open fractures
Vertical depth (m.b.s.l)
-20
-10
0
10
20
30
0 10 20 30 40 50 60 70 80
Number of fractures / 10m vertical depth

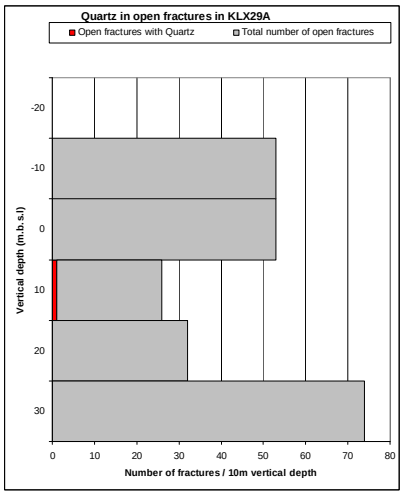
Quartz in open fractures in KLX29A
Open fractures with Quartz
Total number of open fractures
Vertical depth (m.b.s.l)
-20
-10
0
10
20
30
0 10 20 30 40 50 60 70 80
Number of fractures / 10m vertical depth

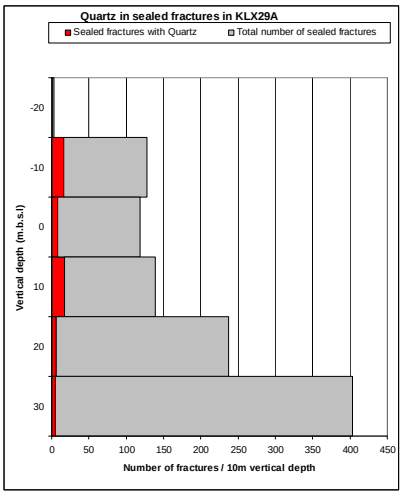
Quartz in sealed fractures in KLX29A
Sealed fractures with Quartz
Total number of sealed fractures
Vertical depth (m.b.s.l)
-20
-10
0
10
20
30
0 50 100 150 200 250 300 350 400 450
Number of fractures / 10m vertical depth

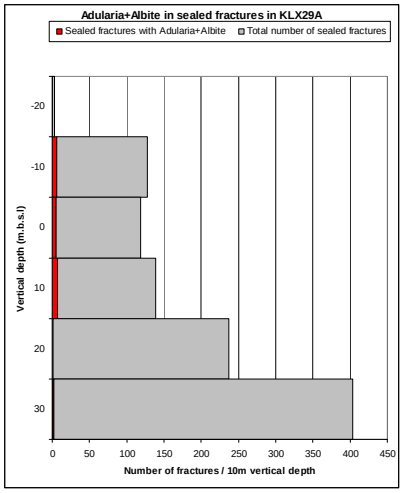
Adularia+Albite in sealed fractures in KLX29A
Sealed fractures with Adularia+Albite
Total number of sealed fractures
Vertical depth (m.b.s.l)
-20
-10
0
10
20
30
0
50
100
150
200
250
300
350
400
450
Number of fractures / 10m vertical depth

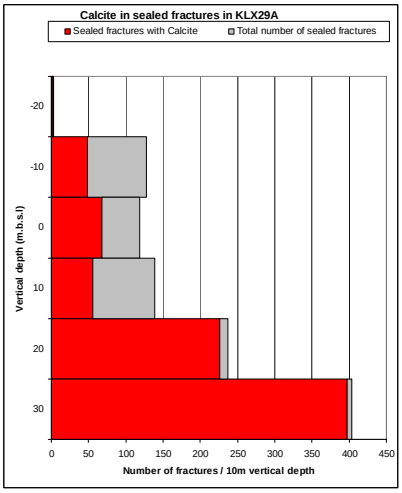
Calcite in sealed fractures in KLX29A
Sealed fractures with Calcite
Total number of sealed fractures
Vertical depth (m.b.s.l)
-20
-10
0
10
20
30
0
50
100
150
200
250
300
350
400
450
Number of fractures / 10m vertical depth

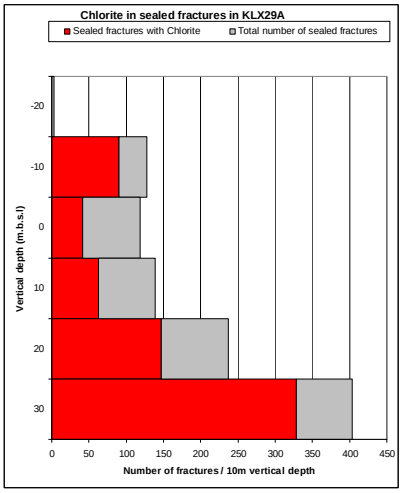
Chlorite in sealed fractures in KLX29A
Sealed fractures with Chlorite
Total number of sealed fractures
Vertical depth (m.b.s.l)
-20
-10
0
10
20
30
0
50
100
150
200
250
300
350
400
450
Number of fractures / 10m vertical depth

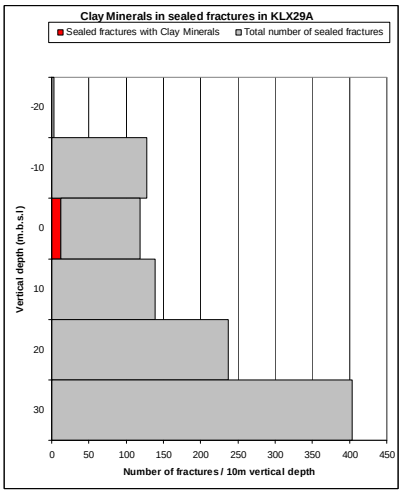
Clay Minerals in sealed fractures in KLX29A
Sealed fractures with Clay Minerals
Total number of sealed fractures
Vertical depth (m.b.s.l)
-20
-10
0
10
20
30
0
50
100
150
200
250
300
350
400
450
Number of fractures / 10m vertical depth

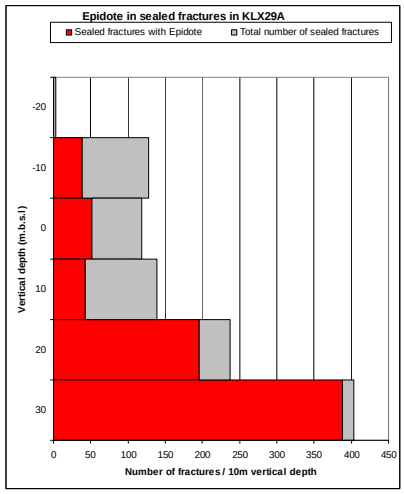
Epidote in sealed fractures in KLX29A
Sealed fractures with Epidote
Total number of sealed fractures
Vertical depth (m.b.s.l)
-20
-10
0
10
20
30
0
50
100
150
200
250
300
350
400
450
Number of fractures / 10m vertical depth

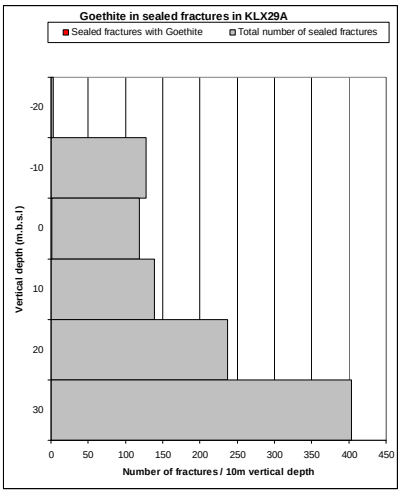
Goethite in sealed fractures in KLX29A
Sealed fractures with Goethite
Total number of sealed fractures
Vertical depth (m.b.s.l)
-20
-10
0
10
20
30
0
50
100
150
200
250
300
350
400
450
Number of fractures / 10m vertical depth

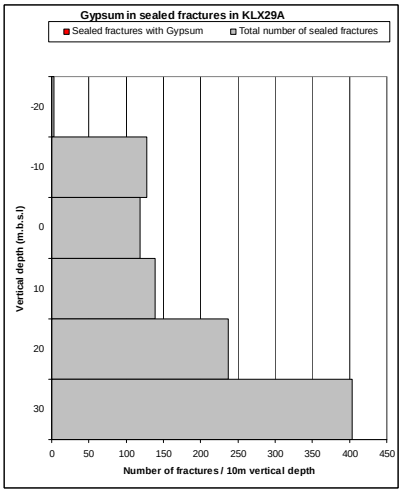
Gypsum in sealed fractures in KLX29A
Sealed fractures with Gypsum
Total number of sealed fractures
Vertical depth (m.b.s.l)
-20
-10
0
10
20
30
0
50
100
150
200
250
300
350
400
450
Number of fractures / 10m vertical depth

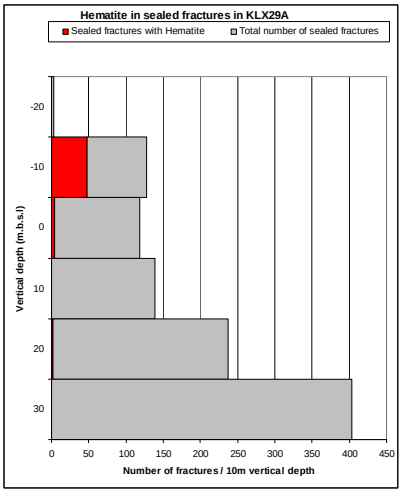
Hematite in sealed fractures in KLX29A
Sealed fractures with Hematite
Total number of sealed fractures
Vertical depth (m.b.s.l)
-20
-10
0
10
20
30
0
50
100
150
200
250
300
350
400
450
Number of fractures / 10m vertical depth

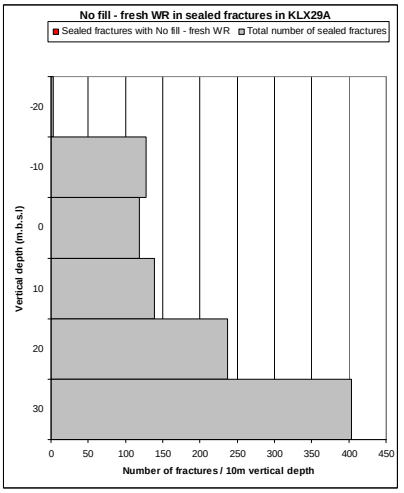
No fill - fresh WR in sealed fractures in KLX29A
Sealed fractures with No fill - fresh WR
Total number of sealed fractures
Vertical depth (m.b.s.l)
-20
-10
0
10
20
30
0
50
100
150
200
250
300
350
400
450
Number of fractures / 10m vertical depth

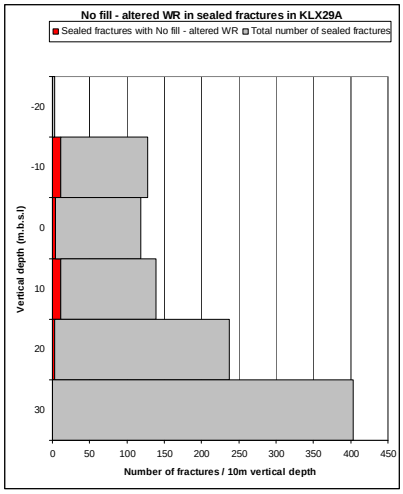
No fill - altered WR in sealed fractures in KLX29A
Sealed fractures with No fill - altered WR
Total number of sealed fractures
Vertical depth (m.b.s.l)
-20
-10
0
10
20
30
0
50
100
150
200
250
300
350
400
450
Number of fractures / 10m vertical depth

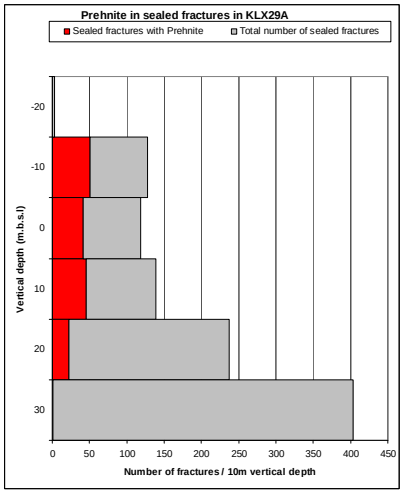
Prehnite in sealed fractures in KLX29A
Sealed fractures with Prehnite
Total number of sealed fractures
Vertical depth (m.b.s.l)
-20
-10
0
10
20
30
0
50
100
150
200
250
300
350
400
450
Number of fractures / 10m vertical depth

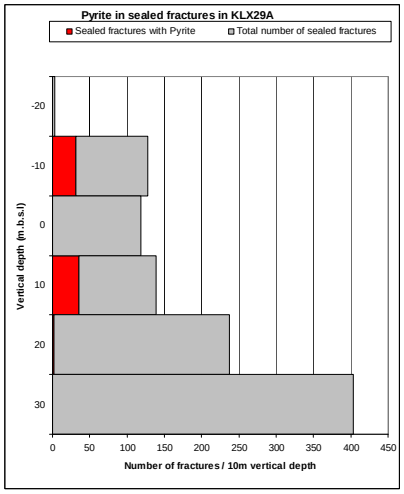
Pyrite in sealed fractures in KLX29A
Sealed fractures with Pyrite
Total number of sealed fractures
Vertical depth (m.b.s.l)
-20
-10
0
10
20
30
0
50
100
150
200
250
300
350
400
450
Number of fractures / 10m vertical depth

Appendix 4

Results of U-series analyses

Borehole		KLX09B	KLX09B	KLX09C	KLX09D	KLX09D	KLX09D	KLX09D	KLX09E	KLX09E	KLX09F	KLX09F	KLX09F	KLX09G	KLX11B
SecUp (m)		7.18	11.11	85.00	3.70	83.02	88.43	104.59	1.00	11.45	68.53	79.66	81.78	40.36	3.48
SecLow (m)		7.29	11.32	85.12	3.86	83.18	88.75	104.87	1.14	11.65	68.72	79.87	81.89	40.41	3.71
^{238}U	Bq/kg	117	76	75	36	321	119	53	76	60	39	180	460	592	126
	±	2	1	2	1	1	2	1	1	1	1	2	2	6	2
^{234}U	Bq/kg	155	88	87	42	396	128	60	79	67	48	239	677	964	136
	±	3	1	2	1	2	2	1	1	1	1	3	3	8	2
^{230}Th	Bq/kg	210	96	86	85	293	123	62	96	78	45	201	656	794	152
	±	10	5	6	3	13	5	2	9	3	1	5	21	10	3
^{232}Th	Bq/kg	68	53	56	19	53	61	57	61	45	31	59	45	36	130
	±	5	3	5	1	4	3	2	7	2	1	2	4	1	2
^{234}U/^{238}U	1.32	1.15	1.17	1.18	1.23	1.07	1.13	1.03	1.12	1.21	1.32	1.47	1.63	1.08	
±	0.04	0.02	0.03	0.03	0.01	0.02	0.02	0.02	0.03	0.04	0.02	0.01	0.02	0.02	
^{230}Th/^{234}U	1.36	1.09	0.99	2.01	0.74	0.96	1.03	1.21	1.16	0.95	0.84	0.97	0.82	1.11	
±	0.07	0.06	0.08	0.08	0.03	0.04	0.03	0.12	0.04	0.04	0.02	0.03	0.01	0.03	
^{230}Th/^{238}U	1.79	1.26	1.15	2.36	0.91	1.03	1.17	1.26	1.3	1.15	1.12	1.43	1.34	1.21	
±	0.07	0.07	0.1	0.06	0.05	0.06	0.05	0.11	0.06	0.05	0.04	0.04	0.02	0.04	

Borehole		KLX11B	KLX11D	KLX11D	KLX11D	KLX11E	KLX11E	KLX11E	KLX11F	KLX03	KLX03	KLX03	KLX03	KLX03	KLX03
SecUp (m)		13.24	2.02	64.34	108.60	4.40	19.53	42.34	2.35	168.47	195.36	326.94	397.79	409.83	743.98
SecLow (m)		13.50	2.06	64.89	108.81	4.53	19.97	42.45	2.58	168.54	195.36	327.04	397.89	410.13	744.06
^{238}U	Bq/kg	38	71	43	248	23	292	10	108	40	80	30	19	42	43
	±	1	1	1	2	1	3	1	1	1.3	1.4	2	1	1	2
^{234}U	Bq/kg	41	74	51	296	23	281	12	111	53	86	20	18	36	33
	±	1	1	1	2	1	3	1	1	1.4	1.4	2	1	1	2
^{230}Th	Bq/kg	70	80	76	324	37	447	28	107	52	92	54	18	41	43
	±	2	2	5	8	3	34	1	9	1.7	2.7	3	1	1	2
^{232}Th	Bq/kg	40	48	63	93	48	1115	15	43	21	56	41	8	55	13
	±	1	2	4	4	3	67	1	5	0.9	1.8	2	1	2	1
^{234}U/^{238}U		1.08	1.04	1.21	1.19	1.02	0.96	1.25	1.03	1.33	1.07	0.69	0.91	0.85	0.77
±		0.03	0.02	0.03	0.01	0.03	0.01	0.06	0.01	0.05	0.024	0.08	0.06	0.04	0.07
^{230}Th/^{234}U		1.68	1.08	1.48	1.09	1.57	1.59	2.23	0.96	1	1.07	2.67	1.03	1.14	1.30
±		0.05	0.03	0.1	0.03	0.12	0.12	0.09	0.08	0.04	0.04	0.26	0.06	0.06	0.11
^{230}Th/^{238}U		1.84	1.13	1.77	1.31	1.61	1.53	2.8	0.99	1.30	1.15	1.80	0.95	0.98	1.00
±	0.06	0.04	0.09	0.03	0.13	0.09	0.15	0.09	0.07	0.05	0.13	0.11	0.05	0.10	

Borehole		KLX03	KLX04	KLX04	KLX04	KLX04	KLX04	KLX06	KLX06	KLX06	KLX06	KLX07B	KLX07A	KLX08	KLX08
SecUp		904.38	139.08	193.74	216.66	352.69	513.53	214.11	383.93	383.93	388.27	4.85	782.64	106.33	121.57
SecLow		904.54	139.13	193.90	216.79	352.81	513.70	214.16	383.93	383.93	388.30	4.85	782.83	106.40	121.62
^{238}U	Bq/kg	48	113	35	56	133	54	109	214	212	56.5	146	85.4	64.7	84.2
	±	1	3	1	2	3	2	1	2	2	3	2	1.5	0.8	1.8
^{234}U	Bq/kg	44	102	41	70	119	161	152	230	228	49.4	152	86.1	65.8	83.5
	±	1	2	2	2	2	4	1	2	2	3	2	1.5	0.8	1.8
^{230}Th	Bq/kg	43	111	42	80	120	123	176	251	280	58.8	187	122	59.6	79.8
	±	2	3	2	3	3	5	4	13	38	3	9	12	5	8.1
^{232}Th	Bq/kg	275	55	30	20	53	14	10.9	81	66.1	106.8	56.2	59.5	28.3	42.8
	±	7	2	1	1	2	1	0.5	6	16	4	4.7	8.5	3.3	5.6
^{234}U/^{238}U		0.90	0.90	1.18	1.25	0.89	3.01	1.39	1.08	1.07	0.88	1.04	1.01	1.02	0.99
±		0.03	0.03	0.06	0.06	0.03	0.15	0.02	0.08	0.01	0.06	0.02	0.02	0.02	0.03
^{230}Th/^{234}U		0.99	1.08	1.03	1.14	1.01	0.76	1.16	1.09	1.23	1.19	1.23	1.42	0.91	0.96
±		0.06	0.04	0.06	0.05	0.04	0.03	0.03	0.06	0.17	0.08	0.07	0.15	0.08	0.09
^{230}Th/^{238}U		0.90	0.98	1.20	1.43	0.90	2.28	1.61	1.17	1.32	1.04	1.28	1.43	0.92	0.95
±	0.07	0.06	0.08	0.08	0.05	0.08	0.03	0.06	0.15	0.11	0.06	0.12	0.10	0.13	

Borehole		KLX08	KLX08	KLX08	KLX08	KLX08	KLX08	KLX08	KLX08	KLX08	KSH01B	KSH01B	KSH01B	KSH01B	KSH01B
SecUp (m)		218.80	408.11	465.10	478.44	478.44	614.47	614.47	772.34	772.34	3.70	8.6	8.70	67.8	82.2
SecLow (m)		218.83	408.17	465.14	478.59	478.59	614.71	614.72	772.49	772.50	3.87	8.6	8.75	67.9	82.2
^{238}U	Bq/kg	35.6	110	69.3	67	69.3	16	20.8	25.6	29	48.2	55.4	174	49.9	356
	±	0.5	2	5	2	3	1	0.5	0.7	1	1	1.7	6	1.4	11
^{234}U	Bq/kg	38.8	96.3	64.1	70	66.6	19	23.6	26.3	31	65.7	58.1	194	50.1	381
	±	0.5	2	5	2	3	1	0.5	0.7	1	1.2	1.7	6	1.4	11
^{230}Th	Bq/kg	46.9	103	156	88	104	22	17.7	17.7	48	41.6	65.2	265	63.2	283
	±	3.9	4.5	11	4	12	3	2.5	12	5	1.6	2.3	8	2.6	23
^{232}Th	Bq/kg	28.5	40.4	56.3	35	48.1	11	10.6	21.6	26	2.3	26.3	117	50.3	53.7
	±	2.9	2.4	6.2	2	7.9	2	1.9	6.1	4	0.3	1.3	5	2.2	5.6
^{234}U/^{238}U		1.09	0.88	0.93	1.05	0.96	1.15	1.13	1.03	1.06	1.36	1.05	1.11	1.00	1.07
±		0.02	0.02	0.1	0.05	0.05	0.06	0.03	0.04	0.04	0.05	0.06	0.08	0.06	0.07
^{230}Th/^{234}U		1.21	1.07	2.44	1.26	1.56	1.16	0.75	2.47	1.56	0.63	1.12	1.37	1.26	0.74
±		0.10	0.05	0.25	0.06	0.19	0.19	0.11	0.45	0.18	0.04	0.07	0.09	0.09	0.08
^{230}Th/^{238}U		1.32	0.94	2.25	1.31	1.50	1.38	0.85	0.69	1.66	0.86	1.18	1.52	1.27	0.79
±	0.10	0.06	0.15	0.08	0.17	0.21	0.17	0.73	0.14	0.06	0.07	0.07	0.07	0.12	

Borehole		KSH01A	KSH01A	KSH01A	KSH01A	KSH01A	KSH02	KSH02	KSH03A
SecUp		159.2	250.40	255.78	558.6	590.36	289.00	578.00	272.00
SecLow		159.3	250.45	255.93	558.6	590.52	289.05	578.05	272.50
^{238}U	Bq/kg	136	178	305	187	12.5	144	96	301
	±	2	3	7	4	0.4	1	0.78	2.6
^{234}U	Bq/kg	134	191	327	210	12	148	94.4	336
	±	2	3	8	5	0.4	1	0.77	2.78
^{230}Th	Bq/kg	102	176	285	209	14.2	170	112	377
	±	2	4	16	5	0.6	6.1	4.1	7.4
^{232}Th	Bq/kg	34.9	41	49	33	8.3	38	72	103
	±	0.9	1.3	3.9	1.4	0.4	2.4	3.1	2.9
$^{234}U/^{238}U$		0.99	1.07	1.07	1.12	0.96	1.03	0.98	1.12
±		0.03	0.04	0.05	0.05	0.06	0.01	0.01	0.01
$^{230}Th/^{234}U$		0.76	0.92	0.87	1.00	1.18	1.15	1.19	1.12
±		0.03	0.04	0.07	0.05	0.09	0.04	0.05	0.02
$^{230}Th/^{238}U$		0.75	0.99	0.93	1.12	1.14	1.18	1.17	1.25
±	0.03	0.04	0.08	0.05	0.08	0.04	0.05	0.03	